Indexes

ENGINEERING-TRANSPORTATION
LIBRARY

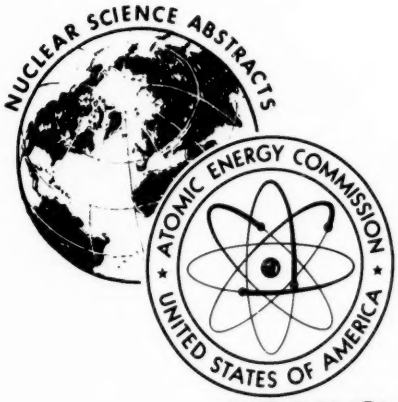

THE UNIVERSITY OF MICHIGAN
DEC 6 1966
ENGINEERING LIBRARY

NUCLEAR SCIENCE ABSTRACTS

Volume 20 Number 21

Abstracts 38542–40492

November 15, 1966

UNITED STATES ATOMIC ENERGY COMMISSION
Division of Technical Information

DEPOSITED BY THE
UNITED STATES OF AMERICA

UNITED STATES ATOMIC ENERGY COMMISSION

NUCLEAR SCIENCE ABSTRACTS

Volume 20
Numbers ~~19~~ 21-24

38542
Abstracts ~~35192~~-47096

October-December
1966

Division of Technical Information

STAFF OF NUCLEAR SCIENCE ABSTRACTS

MANAGING EDITOR

John W. Norris

ASSISTANT MANAGING EDITOR

Donald D. Davis

ASSOCIATE EDITORS

Lawrence T. Whitehead
David E. Bost
Robert C. Kelly
Lee M. Thompson

SUBJECT INDEX EDITOR

Everett J. Hoffman

EVALUATORS

William D. Matheny
John H. Mitchell
Mary H. Newman

ABSTRACTORS

F. S. Armstrong (AECL)
Jane G. Buchanan
D. Lamar Cason
Bennie G. Di Bona
Helen G. Donald
James R. Dulaney
Wells L. Green
Mary Catherine Grissom
Fernando J. Hamilton
Phyllis C. Hansen
Carolyn D. Houston
Rose V. Jermain
Betty L. McDowell
Jean F. Peckham
Mona H. Raridon
Julia S. Redford
Francis L. Sachs
Lila B. Smith
Charles E. Stuber
Martha J. Thomas
Anne G. Ward
David C. West
Milton O. Whitson
Gabriel O. Ycaza

SUBJECT HEADING SPECIALIST

Robert E. Upchurch

CORPORATE AUTHOR SPECIALIST

Clara L. Fox

DESCRIPTIVE CATALOGING SPECIALIST

J. Paul Meredith

SCHEDULING AND PUBLISHING COORDINATOR

Brainard L. Patton

Communication concerning the editorial policy and content of *NSA* should be addressed to the Managing Editor, *Nuclear Science Abstracts*, AEC Division of Technical Information Extension, P. O. Box 62, Oak Ridge, Tennessee 37830.

Use of funds for printing this publication approved by the Director of the Bureau of the Budget, June 28, 1966.

USAEC DEPOSITORY LIBRARIES

Collections of USAEC reports are maintained in the libraries of the organizations listed below for reference use by the general public. Facilities for making photocopies are available. The USAEC also makes available through these libraries atomic energy reports of countries other than the U. S. that are abstracted in *Nuclear Science Abstracts*.

ALABAMA
Auburn, Auburn University
ALASKA
College, University of Alaska
ARIZONA
Tucson, University of Arizona
ARKANSAS
Fayetteville, University of Arkansas
CALIFORNIA
Berkeley, University of California
Davis, University of California
Los Angeles, University of California
San Diego, Public Library
Stanford, Stanford University
COLORADO
Boulder, University of Colorado
Denver, Public Library
CONNECTICUT
New Haven, Yale University
DELAWARE
Newark, University of Delaware
DISTRICT OF COLUMBIA
Washington, Library of Congress
FLORIDA
Coral Gables, University of Miami
Gainesville, University of Florida
Tallahassee, The Florida State University
GEORGIA
Atlanta, Georgia Institute of Technology
HAWAII
Honolulu, University of Hawaii
ILLINOIS
Chicago, John Crerar Library
Chicago, University of Chicago
Evanston, Northwestern University
Urbana, University of Illinois
INDIANA
Bloomington, Indiana University
Lafayette, Purdue University
IOWA
Ames, Iowa State University
KANSAS
Manhattan, Kansas State University
KENTUCKY
Lexington, University of Kentucky
Louisville, University of Louisville
LOUISIANA
Baton Rouge, Louisiana State University
New Orleans, Tulane University
MARYLAND
Baltimore, Johns Hopkins University
College Park, University of Maryland
MASSACHUSETTS
Cambridge, Harvard University
Cambridge, Massachusetts Institute of Technology
MICHIGAN
Ann Arbor, University of Michigan
Detroit, Public Library
East Lansing, Michigan State University
MINNESOTA
Minneapolis, University of Minnesota
MISSISSIPPI
State College, Mississippi State University
MISSOURI
Kansas City, Linda Hall Library
Rolla, University of Missouri School of Mines and Metallurgy
St. Louis, Washington University
MONTANA
Bozeman, Montana State College
NEVADA
Las Vegas, Nevada Southern University
Reno, University of Nevada
NEW JERSEY
Princeton, Princeton University
Teaneck, Fairleigh Dickinson University
NEW MEXICO
Albuquerque, University of New Mexico
NEW YORK
Albany, The University of the State of New York
Buffalo, State University of New York at Buffalo
Ithaca, Cornell University
New York, Atomic Industrial Forum, Inc.
New York, Columbia University
New York, New York University
Rochester, University of Rochester
Schenectady, Union College
Syracuse, Syracuse University
Troy, Rensselaer Polytechnic Institute
NORTH CAROLINA
Charlotte, Public Library of Charlotte and Mecklenburg County
Durham, Duke University
Raleigh, North Carolina State College
NORTH DAKOTA
Grand Forks, University of North Dakota
OHIO
Cincinnati, University of Cincinnati
Cleveland, Public Library
OHIO (CONT.)
Columbus, Ohio State University
Toledo, University of Toledo
Youngstown, Youngstown University
OKLAHOMA
Norman, University of Oklahoma
Stillwater, Oklahoma State University
OREGON
Corvallis, Oregon State University
Portland, Reed College
PENNSYLVANIA
Philadelphia, University of Pennsylvania
Pittsburgh, Carnegie Library
University Park, Pennsylvania State University
PUERTO RICO
Rio Piedras, University of Puerto Rico
RHODE ISLAND
Providence, Brown University
SOUTH CAROLINA
Columbia, University of South Carolina
TENNESSEE
Knoxville, University of Tennessee
Memphis, Public Library
Nashville, Joint University Libraries
Oak Ridge, Oak Ridge Associated Universities
TEXAS
Austin, University of Texas
College Station, Texas A & M University
Dallas, Southern Methodist University
Houston, Rice University
Lubbock, Texas Technological College
San Antonio, Public Library
UTAH
Salt Lake City, University of Utah
VIRGINIA
Blacksburg, Virginia Polytechnic Institute
Charlottesville, University of Virginia
Norfolk, Old Dominion College
WASHINGTON
Pullman, Washington State University
Seattle, University of Washington
WEST VIRGINIA
Morgantown, West Virginia University
WISCONSIN
Madison, University of Wisconsin
Milwaukee, Public Library
WYOMING
Laramie, University of Wyoming

DEPOSITED BY THE
UNITED STATES OF AMERICA

Volume 20, Number 21, November 15, 1966

NUCLEAR SCIENCE ABSTRACTS

A semimonthly publication of the USAEC Division of Technical Information, Edward J. Brunenkant, Director. Published by the USAEC Division of Technical Information Extension, Robert L. Shannon, Extension Manager.

Nuclear Science Abstracts covers the international literature on nuclear science and technology and provides the only comprehensive abstracting and indexing of this body of information. Published twice each month since 1947, *NSA* covers technical reports of the U. S. Atomic Energy Commission and its contractors, technical reports of U. S. Government agencies and other governments, universities, industrial and research organizations, as well as patents, books, and journal literature on a world-wide basis. Nearly 350,000 abstracts have appeared in *NSA* through Volume 19. The subject matter covered in *NSA* is described in issue Number 1 and in TID-4552, *Subject Scope of Nuclear Science Abstracts*, available free from the U. S. Atomic Energy Commission, Division of Technical Information Extension, P. O. Box 62, Oak Ridge, Tennessee 37830.

Abstracts are arranged according to a number of subject categories and subcategories. Definitions of categories appear in issues Number 1 and 13. If the language of the original item is not English, the language will be indicated. Translations are not abstracted where an abstract of the original item has appeared in *NSA*.

INDEXES TO NSA

Corporate author, personal author, subject, and report number indexes appear in each issue and are cumulated quarterly, semiannually, and annually. Multi-volume cumulations have been issued as indicated on the following page. Report number indexes for all volumes (1–18) were issued at the end of Vol. 18. At the end of Vol. 19, the indexes for Vols. 1–15 were reissued to include additional public availability information. This cumulation will be a permanent shelf item and will not be reissued. Report number indexes for Vol. 19 are included as a cumulation beginning with Vol. 16.

AVAILABILITY OF PUBLICATIONS ABSTRACTED

The public availability of all U. S. Atomic Energy Commission reports is indicated in the report number indexes. The availability of other reports, when known, is also indicated. The availability of some unnumbered reports is given in the abstract.

Dissertations abstracted in *Dissertation Abstracts* and included in *NSA* are available from University Microfilms, Inc., 315 N. First Street, Ann Arbor, Michigan 48103.

Most of the published literature abstracted in *NSA* is on deposit at the Library, Oak Ridge Associated Universities, Oak Ridge, Tennessee, (a USAEC depository library) and is available through interlibrary loan. When requesting papers from this source, it is important that *NSA* volume and abstract number be cited.

HOW TO OBTAIN NUCLEAR SCIENCE ABSTRACTS

NSA is available on an exchange basis to universities, research institutions, industrial firms, and publishers of scientific information. Inquiries should be directed to the U. S. Atomic Energy Commission, Division of Technical Information Extension, P. O. Box 62, Oak Ridge, Tennessee 37830.

Government agencies may obtain *NSA* free of charge.

NSA is available to the general public on a subscription basis from the Superintendent of Documents, U. S. Government Printing Office, Washington, D. C. 20402, as follows:

For the 24 regular issues, $30.00 domestic, $37.00 foreign. A single issue costs $1.75, plus 25 per cent for foreign mailing. Domestic rates apply to the United States, Canada, Mexico, and Central and South American countries except Argentina, Brazil, Guyana and French Guiana, Surinam, and British Honduras. Foreign rates apply to the countries excepted above and to all other countries throughout the world.

For the quarterly, semiannual, and annual indexes, $22.00 domestic, $25.00 foreign.

Multivolume subject and author indexes are available as follows:

Vols. 1–4 (1948–1950) Johnson Reprint Corporation, 111 Fifth Avenue, New York, N. Y. 10003, $30.00.

Vols. 5–10 (1951–1956) Superintendent of Documents, U. S. Government Printing Office, Washington, D. C. 20402, $5.25.

Vols. 11–15, Subjects, Superintendent of Documents, U. S. Government Printing Office, Washington, D. C. 20402, $19.00.

Vols. 11–15, Personal Authors, Superintendent of Documents, U. S. Government Printing Office, Washington, D. C. 20402, $14.25.

Vols. 11–15, Corporate Authors, Superintendent of Documents, U. S. Government Printing Office, Washington, D. C. 20402, $2.50.

Cumulative Report Number Index, Vols. 1–15, Revised, is available from the Superintendent of Documents, U. S. Government Printing Office, Washington, D. C. 20402, $4.00.

Cumulative Report Number Index, Vols. 16–19, is available from the Superintendent of Documents, U. S. Government Printing Office, Washington, D. C. 20402, $2.50.

Annual Indexes are available separately from the U. S. Government Printing Office as follows:

Vol. 16, Subject and Authors, $9.75.
Vol. 17, Subject and Authors, $12.25.
Vol. 18, Subject and Authors, $12.50.
Vol. 19, Subject and Authors, $12.50.

ACKNOWLEDGMENTS

Agreements between the United States Atomic Energy Commission and the following organizations with regard to providing continuing services and specific literature coverage for *Nuclear Science Abstracts* are gratefully acknowledged:

American Institute of Physics; Atomic Energy of Canada Limited; Atomic Energy Research Establishment, United Kingdom; European Atomic Energy Community (EURATOM); Gmelin Institute; International Atomic Energy Agency; Japan Atomic Energy Bureau — Japan Atomic Energy Research Institute; Netherlands Patent Office; Reactor Centrum Nederland.

TABLE OF CONTENTS

Volume 20, Number 21, November 15, 1966

Category	Page
BIOLOGY AND MEDICINE	4675
General	4675
Metabolism, Tissue Distribution, and Toxicology	4675
Radiation Effects on Biochemicals	4679
Radiation Effects on Tissues	4681
Radiation Effects Therapy and Countermeasures	4699
Radiation Hazards and Protection	4703
Radiotherapy and Radiodiagnosis	4704
CHEMISTRY	4713
General	4713
Analytical Procedures	4713
Inorganic and Physical Chemistry	4719
Organic Chemistry	4727
Radiation Chemistry	4728
Radiochemistry	4734
Separation Processes and Procedures	4735
ENGINEERING	4738
General	4738
Applications of Nuclear Explosions	4739
Facilities and Equipment	4739
Heat Transfer and Fluid Flow	4742
Materials Testing	4743
Protective Structures	4743
Space Propulsion	4746
Vacuum Engineering	4747
GEOLOGY, METEOROLOGY, AND MINERALOGY	4748
General	4748
Meteorology	4748
Natural Radioactivity and Fallout	4749
Techniques and Equipment	4751
Thorium and Uranium Minerals	4754
HEALTH AND SAFETY	4755
INSTRUMENTATION	4758
General	4758
Radiation Detection	4760
Radiation Effects	4768
ISOTOPE TECHNOLOGY	4769
General	4769
Industrial Applications	4769
Power Application	4772
Separation and Production	4773
MATHEMATICS AND COMPUTERS	4775
METALS, CERAMICS, AND OTHER MATERIALS	4776
General	4776
Corrosion	4777
Fabrication	4778
Properties and Structure	4781
Radiation Effects	4789
PHYSICS	4793
General	4793
Accelerators	4793
Astrophysics and Cosmology	4801
Atomic Physics	4804
Cosmic Radiation	4809
Direct Energy Conversion	4810
Elementary Particles and Radiations	4832
Field Theory, Scattering Theory, and Symmetries	4844
Fluid Physics and Thermodynamics	4852
Geophysics	4854
Gravitation, Quantum Mechanics, and Relativity Theory	4861
Low Temperature Physics	4863
Neutron Physics	4868
Nuclear Properties and Reactions	4870
Plasma Physics and Thermonuclear Processes	4882
Shielding	4897
Solid State Physics	4898
REACTOR TECHNOLOGY	4907
General	4907
Auxiliaries and Components	4908
Criticality Studies	4909
Fuels	4910
Power and Power-Breeder Reactors	4911
Propulsion and Space	4916
Research and Test Reactors	4917
WASTE DISPOSAL AND PROCESSING	4921
GENERAL AND MISCELLANEOUS	4923
CORPORATE AUTHOR INDEX	INDEX-1
PERSONAL AUTHOR INDEX	INDEX-9
SUBJECT INDEX	INDEX-50
REPORT NUMBER INDEX	INDEX-128

STAFF OF NUCLEAR SCIENCE ABSTRACTS

MANAGING EDITOR

John W. Norris

ASSISTANT MANAGING EDITOR

Donald D. Davis

ASSOCIATE EDITORS

Lawrence T. Whitehead
David E. Bost
Robert C. Kelly
Lee M. Thompson

SUBJECT INDEX EDITOR

Everett J. Hoffman

EVALUATORS

William D. Matheny
John H. Mitchell
Mary H. Newman

ABSTRACTORS

F. S. Armstrong (AECL)
Jane G. Buchanan
D. Lamar Cason
Bennie G. Di Bona
Helen G. Donald
James R. Dulaney
Wells L. Green
Mary Catherine Grissom
Fernando J. Hamilton
Phyllis C. Hansen
Carolyn D. Houston
Rose V. Jermain
Betty L. McDowell
Jean F. Peckham
Mona H. Raridon
Julia S. Redford
Francis L. Sachs
Lila B. Smith
Charles E. Stuber
Martha J. Thomas
Anne G. Ward
David C. West
Milton O. Whitson
Gabriel O. Ycaza

SUBJECT HEADING SPECIALIST

Robert E. Upchurch

CORPORATE AUTHOR SPECIALIST

Clara L. Fox

DESCRIPTIVE CATALOGING SPECIALIST

J. Paul Meredith

SCHEDULING AND PUBLISHING COORDINATOR

Brainard L. Patton

Communication concerning the editorial policy and content of *NSA* should be addressed to the Managing Editor, *Nuclear Science Abstracts*, AEC Division of Technical Information Extension, P. O. Box 62, Oak Ridge, Tennessee 37830.

Use of funds for printing this publication approved by the Director of the Bureau of the Budget, June 28, 1966.

A-30 - OP. 2422.

Volume 20, Number 21 November 15, 1966

NUCLEAR SCIENCE ABSTRACTS

BIOLOGY AND MEDICINE

General

Refer also to abstract 39030.

38542 (UCRL-Trans-10029) MOLECULAR MECHANISMS OF MUTAGENESIS AND THE NATURE OF MUTATIONS. Heslot, H. Translated for Univ. of California Lawrence Radiation Lab., Livermore, from Ann. Amelior. Plantes, 15: 111-57(1965). 94p. Dep. mn. CFSTI $3.00 cy, $0.75 mn. JCL $8.60 fs, $3.02 mf.

The nature and structure of DNA and RNA are reviewed and the molecular mechanisms of mutagenesis in bacteriophages are discussed. Results are reported from tracer studies of protein biosynthesis. Models are proposed to explain both the origin of mutations and their consequences on enzymes. Data are included from studies on the mutagenic effects of nitrous acid, hydroxylamine, alkylating agents, acridines, uv radiation, and x radiation on DNA. The effects of mutagenesis on proteins are discussed. Emphasis was placed on mutagenesis induced by acridines since this permitted the determination of the genetic code. (150 references). (C.H.)

38543 ADSORPTION AND ELUTION OF TRACE ELEMENTS ON HUMAN HAIR. Bate, L. C. (Oak Ridge National Lab., Tenn.). Int. J. Appl. Radiat. Isotop., 17: 417-23(July 1966). (ORNL-P-1764).

Since 1962 the trace element content of human hair has been studied as a possible means of comparing physical-evidence hair samples. It is recognized that for hair to be of wide value in this application, its trace element content must not change rapidly with time. Limited studies have indicated, however, that changes do occur over relatively long periods of time. These changes may be due to natural growth processes and/or environmental contamination. This study was made to see how extensively the trace element content of hair might be modified by the adsorption of environmental trace elements and to see if solvents could be found that would remove the adsorbed elements. The procedure used was to place a sample of hair in a solution containing measured quantities of an element and a radiotracer. After 16 hr, the sample was removed from the solution, rinsed, and then washed. The radioactivity that remained after the wash was a measure of the quantity of adsorbed element. All solutions were prepared to approximate the composition and pH(3.5 to 5.5) of perspiration. The elements studied were Na, K, Cl, Br, Cu, Zn, Au, Se, Cr, I, As, Ag, Sb, Co, Fe, Mn, Ca, Ba, and Sr. All elements except Na and K were found to absorb, and the extent of adsorption was pH dependent. The elements Zn, Fe, Ba, Co, Mn, and Sb were removed by solutions containing EDTA, but no solvent was found that would remove Au, Ag, and Se. (auth)

38544 ELEMENTARY RADIATSIONNOI BIOLOGII I BIOKHIMII. (Elements of Radiation Biology and Biochemistry). Lipkan, N. F. Kiev, State Publishing House of Medical Literature, 1963. 165p.

Effects of various types of radiation on animal organisms are reviewed. The sensitivity of animals to internal and external and to whole-body and local irradiations are considered. Genetic effects are analyzed. Data are given on radioinduced metabolic changes and on disturbed biochemical processes. Mechanisms in radioinduced processes and uses of isotopic labeling are also discussed. (R.V.J.)

38545 PARTICLE SEPARATOR (Engineering Materials). (Los Alamos Scientific Lab., Univ. of California, N. Mex.). (CAPE-1417).

13 drawings.

Biological or nonbiological particles may be separated by volume according to electronically measurable characteristics such as optical density or reflectivity. The separator can analyze 500 to 1000 cells/sec, 50% of which may be separated. (For details see TID-4100) (F.S.)

38546 NEUROSPORA COLONY COUNTER /Q-2768/ (Engineering Materials). (Oak Ridge National Lab., Tenn.). (CAPE-1393).

1 drawing.

The number of Neurospora colonies in samples of a culture solution may be counted with an average error of ~1.0%. The detector cell is optimized for random size colonies ranging between 0.020 and 0.080 in. in diameter. (For details see TID-4100) (F.S.)

Metabolism, Tissue Distribution, and Toxicology

Refer also to abstracts 38585, 38669, 38841, 38848, and 39150.

38547 (NYO-918-15) PROGRESS REPORT [ON STEROID SYNTHESIS, ANALYSIS, AND METABOLISM], MAY 1, 1965-APRIL 30, 1966. Pincus, Gregory (Worcester Foundation for Experimental Biology, Shrewsbury, Mass.). June 13, 1966. Contract AT(30-1)-918. 25p. Dep. mn. CFSTI $1.00 cy, $0.50 mn.

Developments are reported for studies on: synthesis of steroid labeled radioisotopes; application of methods for automation of steroid analysis; steroid biogenesis and metabolism; and effects of radiation on steroid metabolism. (P.C.H.)

38548 (ORO-2410-1) ANNUAL PROGRESS REPORT [ON CESIUM AND STRONTIUM UPTAKE AND ASSIMILATION BY HIGHER PLANTS], MAY 1, 1965-FEBRUARY 1, 1966. Jackson, William A.; Craig, Doris L. (North Carolina State Univ., Raleigh. Dept. of Soil Science). Jan. 1966. Contract AT(40-1)-2410. 46p. Dep. mn. CFSTI $2.00 cy, $0.50 mn.

Progress is reported in tracer studies of factors influ-

encing the uptake of Cs and Sr by plants. Data are included from studies in wheat seedlings. Emphasis was placed on the effects of nitrogen on the uptake and transport of Cs and Sr. Data are included from a comparative study of the effects of Ca and K on nitrate uptake and reduction in seedlings and the effects of phosphates, carbohydrate level, NH_4, and selected cations on the uptake of nitrate nitrogen and Cs and Sr. The changes in metabolic patterns within short time periods indicate a large number of ways in which plant metabolism is altered when exposed to ammonium or nitrate nitrogen. (C.H.)

38549 (UCLA-12-592) A FORTRAN IV PROGRAM FOR EVALUATION OF THYROIDAL ASSIMILATION OF RADIOIODINE. French, Norman R. (California Univ., Los Angeles. Lab. of Nuclear Medicine and Radiation Biology). June 1966. Contract AT-04-1-GEN-12. 13p. Dep. mn. CFSTI $1.00 cy, $0.50 mn.

A fortran IV program was developed for the computer reduction of data on the thyroid uptake and effective half-life of ingested ^{131}I in different mammalian species and of members of the same species on different diets. Experimental animals were given a measured quantity of ^{131}I solution orally and the radioactivity from the thyroid was counted by means of a scintillation counter twice in the first 24 hr and daily thereafter for 14 days. The animals were sacrificed and the thyroid was counted in a well-type scintillation detector. The counting data were used to calculate the effective half-life of ^{131}I in the thyroid of each animal and the mean, standard deviation, the sum of deviations squared for each group of animals, and the effects of diet on ^{131}I uptake by the thyroid gland. (C.H.)

38550 METHOD OF ASSAYING ^{36}Cl IN STUDIES ON THE KINETICS OF CHLORINE METABOLISM IN THE BODY. Lipinski, Stanislaw; Lipski, Slawomir. Acta Physiol. Pol., 17: 341-6(1966). (In Polish).

A method of assaying ^{36}Cl in aqueous tissue extracts was developed, and its yield of extraction determined. The method was applied in studies on the metabolism of the chlorine ion. (auth)

38551 EFFECT OF ^{137}Cs AND ^{90}Sr ON THE GROWTH AND REPRODUCTION OF MICE. III. Nishio, Kazuo; Megumi, Tsuneo. Ann. Rep. Radiat. Center Osaka Prefect., 6: 119-21(1965).

The effects of ^{90}Sr and ^{137}Cs administered in drinking water on reproduction and life span in mice were studied after continuous exposure for five generations. It was observed that accumulated bad effects on life span as well as reproduction appeared after one generation in mice administered large doses of the isotopes. The lower doses of isotopes appeared to induce prolonging life span throughout some generations. (auth)

38552 METABOLISM OF RADIUM IN DAIRY COWS. Sansom, B. F.; Garner, R. J. (Agricultural Research Council Inst. for Research on Animal Diseases, Compton, Eng.). Biochem. J., 99: 677-81(June 1966).

The isotopes ^{45}Ca and ^{224}Ra were administered simultaneously, both orally and intravenously, to two pairs of cows. The first pair of animals received large doses of ^{224}Ra and ^{45}Ca, which produced clinical and metabolic disturbances. The second pair of animals received much smaller doses and showed no clinical disturbances. The mean recoveries in these animals of ^{45}Ca and ^{224}Ra in the 8 days after the oral administration were respectively: from feces, 63.2 and 103.8%; from urine, 0.26 and 0.44%; from milk, 15.8 and 0.35% of the dose; and in the 8 days after intravenous administration: from feces, 20.5 and 36.5%; from urine, 1.56 and 17.6%; from milk, 49.3 and 11.8% of the dose. Calculation of discrimination factors shows that absorptive discrimination played the most important part in the overall discrimination between the calcium and radium in their passage from diet to milk, but that mammary discrimination plays a more important role than in the overall discrimination between calcium and strontium or barium. In its treatment by the kidney radium is more like strontium than barium, but radium is actively secreted by the gut in the same way as barium. In its skeletal metabolism radium is indistinguishable from calcium and strontium except in its rate of resorption, which is similar to that of barium. (auth)

38553 THYROIDAL ^{131}I UPTAKE, TURNOVER AND BLOCKING IN ADULTS AND ADOLESCENTS. Cuddihy, Richard G. (Univ. of Rochester, N. Y.). Health Phys., 12: 1021-5(Aug. 1966).

From an investigation of thyroidal uptake of radioactive ^{131}I in seven adolescents and four adults, several observations have been made. First, the per cent uptake over a 14-day ingestion period was identical for both groups of subjects, being about 23%. Secondly, the turnover rate was more rapid in the adolescent group of subjects. Finally the per cent of uptake can be reduced to about 4% with a pharmacological dosage of 10 mg of stable iodine. (auth)

38554 CASE OF ACCIDENTAL INHALATION OF ^{227}Ac. Newton, D. (Atomic Energy Research Establishment, Harwell, Eng.). Health Phys., 12: 1129-38(Aug. 1966). (AERE-R-4955).

The retention of ^{227}Ac in a case of accidental inhalation was studied for more than 800 days after intake, by the technique of body radioactivity measurement using scintillation gamma-ray spectrometry. During this period the activity remained largely confined to the chest region and it is concluded that the biological half-life for clearance from the thorax was at least 10 years. (auth)

38555 IMPROVED METHOD FOR THE SIMULTANEOUS DETERMINATION OF ^{55}Fe AND ^{59}Fe IN BLOOD BY LIQUID SCINTILLATION COUNTING. Eakins, J. D.; Brown, D. A. (Atomic Energy Research Establishment, Harwell, Eng.). Int. J. Appl. Radiat. Isotop., 17: 391-7 (July 1966).

A method for the simultaneous determination of ^{55}Fe and ^{59}Fe in blood is described. After wet oxidation of the blood sample the iron is precipitated as ferric hydroxide. It is then converted to an insoluble white ferriphosphate complex by dissolving the hydroxide in phosphoric acid and adding a solution of ammonium chloride in absolute ethanol. The resulting precipitate is counted as a gel in a two-channel, liquid-scintillation spectrometer, set to count ^{59}Fe alone in one channel and ^{55}Fe plus a small percentage of ^{59}Fe in the other channel. The counting efficiencies obtained are 19.4 percent for ^{55}Fe and 33.4 percent for ^{59}Fe with chemical yields of 95 percent. The counting efficiency for ^{55}Fe is greater by a factor 3 than the best value previously reported for liquid scintillation counting, with sources, containing comparable amounts of inactive iron. The nature of the ferriphosphate complex is discussed. The results of an analysis of the compound suggest that it is an ammonium salt of a ferriphosphoric acid with formula $NH_4H_2[Fe(PO_4)_2]2H_2O$. The procedure described may be used for the analysis of materials other than blood. It is currently being used for the determination of ^{55}Fe and ^{59}Fe in bread samples doubly labeled with these isotopes. (auth)

38556 EXCRETION OF ^{65}Zn-DTPA IN THE RAT. Harmuth-Hoene, Anna-Elisabeth; Catsch, Alexander; Nigrovic, Vladimir; Bohne, Felicitas (Kernforschungszentrum, Karlsruhe, Ger.). Int. J. Radiat. Biol., 10: 479-83(1966).

Doubly labeled $^{65}Zn-DTPA-^{14}C$ was injected into rats and the urine assayed for Zn, ^{65}Zn, and ^{14}C. A simple quantitative method is proposed which allows the metabolic fate of ^{65}Zn to be derived. It has been shown that the retention of ^{65}Zn is mainly due to isotopic exchange whereas the Zn balance remains virtually unchanged. The exchangeable endogenous Zn pool was estimated to be 5.5 $\mu moles \cdot kg^{-1}$, i.e., 1 per cent of the total-body Zn. The implication of these findings for the therapeutic usage of Zn-DTPA is stressed. (auth)

38557 DIMINUTION OF RADIOCESIUM BODY-BURDEN IN DOGS AND HUMAN BEINGS BY PRUSSIAN BLUE. Madshus, K. (Norsk Hydro's Inst. for Cancer Research, Montebello, Norway); Stroemme, A.; Bohne, F.; Nigrovic, V. Int. J. Radiat. Biol., 10: 519-20(1966).

Dogs were given ^{137}Cs orally over a period of 10 days and

some of the dogs were treated with daily doses of Prussian Blue (ferric cyanoferrate II). The ^{137}Cs body burden was measured by whole-body counting for 11 days. The biological half-time of ^{137}Cs was found to be 11 days in control dogs and 6.5 days in treated dogs. The ^{137}Cs content of two men was determined by whole-body counting over a period of several months after the ingestion of approximately 1 μC of carrier-free ^{137}Cs. The biological half-life was found to be 110 and 115 days. Ten months after the ingestion of ^{137}Cs treatment with daily 3 g doses of Prussian Blue was begun. In both cases the biological half-life of ^{137}Cs was markedly reduced. No significant side effects were observed. (C.H.)

38558 SHIELDED COIL FOR CONTINUOUS SCINTILLATION MONITORING OF CIRCULATING RADIOACTIVITY. Threefoot, Sam A. (Tulane Univ., New Orleans). Invest. Radiol., 1: 184-7(May-June 1966).

A simple shielded coil was developed for use with any suitable pumping apparatus that can circulate fluid around a scintillation crystal and return it to the container. The basic components of the system are a coil support, plastic tubing for the coil, and Pb housing. The system was developed for the continuous extracorporeal measurement of circulating radioactivity in the blood of dogs. The method can be used, however, for prolonged continuous monitoring and recording of radioactivity from either veins or arteries of living animals, simultaneous sampling from multiple site using duplicate equipment, and either in a circuit or as an open-end sampling method for any circulating fluid. The necessity for quantitative calibration depends on the particular use to which the system is applied. (C.H.)

38559 PERFUSION IN SITU WITH TRITIUM OXIDE TO MEASURE HEPATIC LIPOGENESIS AND LIPID SECRETION: NORMAL AND OROTIC ACID-FED RATS. Windmueller, H. G.; Spaeth, Albert E. (National Insts. of Health, Bethesda, Md.). J. Biol. Chem., 241: 2891-9 (June 1966).

From measurements of tritium incorporation following the perfusion in situ of livers with blood enriched in ^3H_2O, the rate of hepatic fatty acid and cholesterol biosynthesis in young nonfasted rats was found to be 7.0 and 0.09 μmoles per g of liver per hour, respectively. Newly synthesized fatty acids were utilized by liver in the same manner as has been shown by others for preformed fatty acids arriving in liver via plasma; at the end of 3 hours, 37% were found in liver phospholipids, 34% in liver neutral lipids, and 29% had been released into the perfusate, nearly all as triglycerides. At least two pools of liver triglycerides could be shown. Depriving a rat of food for 48 hours reduced hepatic fatty acid and cholesterol synthesis to less than 2% the rate in nonfasted controls. Feeding rats 1% orotic acid reduced hepatic fatty acid synthesis, stimulated cholesterolgenesis, and almost completely blocked the transfer of hepatic lipids into perfusate. From whole animal studies with Triton, the block in lipid secretion was found to increase in severity during the first week of orotic acid feeding, and could be rapidly reversed by inclusion of 0.25% dietary adenine sulfate. Accumulated liver triglyceride was seen only after 3 days of continuous orotic acid feeding. (auth)

38560 GAMMA EMITTERS IN MARINE ORGANISMS. I. CONCENTRATION OF GAMMA EMITTING NUCLIDES IN THE FIN WHALE. Sachithananthan, C.; Hiyama, Yoshio (Tokyo Univ.). J. Radiat. Res. (Jap.), 6: 141-7(Sept.-Dec. 1966).

Fin whales from three geographically different regions were examined for accumulated radioactive nuclides by the gamma spectrometric method. The gamma spectra showed prominent peaks for radioactive zinc, manganese, and cesium, apart from the naturally occurring radioisotope of potassium. Concentrations of these accumulated radionuclides by tissues and by regions were compared. Other nuclides noticed in the spectra are ruthenium-103 -106, and cerium-141 -144. Specific tissues examined revealed that ^{54}Mn is greatly lodged in the liver and ^{137}Cs in the muscle. The bone showed affinity for ^{65}Zn and ^{137}Cs and less for ^{54}Mn. The Hokkaido bone sample for the same year (1964), however, showed exceptionally high values for ^{54}Mn. The Arctic fin whales showed larger accumulation of the radionuclides than the Antarctic fin whales, confirming heavier contamination of the northern hemisphere waters. (auth)

38561 ARE IODOTYROSINES NORMAL CONSTITUENTS OF PLASMA? Rhodes, Buck A.; Wagner, Henry N. Jr. (John Hopkins Medical Institutions, Baltimore). Nature, 210: 647-8(May 7, 1966).

Rats were maintained for 3 to 6 months on a diet containing 86% of I content as ^{129}I. Plasma samples were analyzed and ^{131}I-labeled mono- and di-iodotyrosine, triiodothyronine, and thyroxine were added to the proteins. The iodoamino acids were extracted and identified by autoradiography of paper chromatograms. The spots from paper chromatograms that contained doubly purified substances were exposed for 16 hr in a thermal neutron flux of approximately 10^{13} n/cm^2/sec. The iodine was purified and counted in a scintillation counter. The γ spectrum and half-life of each sample was determined and after the ^{130}I activity had decayed the ^{131}I activity was compared with the activity of the original carrier chromatograms. Control experiments and analysis of standards were also carried out. Data are tabulated. It was concluded that iodotyrosines are normally present in the circulating blood of rats. (C.H.)

38562 PATTERNS OF NUCLEIC ACID AND PROTEIN SYNTHESIS DURING MODIFICATION OF LETHAL ULTRAVIOLET LESION. Kos, E.; Drakulic, M.; Brdar, B. (Inst. Ruder Boskovic, Zagreb). Photochem. Photobiol., 5: 231-41(Mar. 1966).

It was shown previously that the viability of Escherichia coli B.U.$^-$ and E. coli B. try$^-$ could be restored after uv irradiation if postirradiation incubation took place in the presence of chloramphenicol or in the absence of an essential metabolite. In contrast, the viability of the uv-irradiated E. coli K.$_{12}$ meth$^-$ decreased rapidly during postirradiation incubation in the presence of chloramphenicol or in the absence of methionine. A study was made of the biosynthesis of nucleic acids and protein in these strains. Protein synthesis was permanently inhibited in both amino acid-requiring strains during postirradiation incubation in the absence of the respective essential metabolite. In E. coli B.U.$^-$ a slow synthesis of protein could be observed even if postirradiation incubation took place in the absence or uracil. DNA synthesis was completely and permanently inhibited in both E. coli B. try$^-$ and E. coli K.$_{12}$ meth$^-$ during postirradiation incubation in the absence of the respective essential amino acid. In E. coli B.U.$^-$, however, DNA synthesis resumed after a prolonged lag even if the bacteria were incubated after uv irradiation in the absence of uracil. RNA synthesis was completely and permanently inhibited in both E. coli B. mutants (uracil-requiring and tryptophan-requiring) if they were incubated after irradiation in the absence of uracil and tryptophan respectively. In E. coli K.$_{12}$ meth$^-$ a small amount of RNA is synthesized during postirradiation incubation in the absence of the essential amino acid. (BBB)

38563 COMPARISON OF SURVIVAL OF A UV-IRRADIATED URACIL-REQUIRING STRAIN OF ESCHERICHIA COLI B IN THE PRESENCE OF CHLORAMPHENICOL AND IN THE ABSENCE OF THE ESSENTIAL METABOLITE. Drakulic, M.; Kos, E.; Brdar, B. (Inst. Ruder Boskovic, Zagreb). Photochem. Photobiol., 5: 265-7(Mar. 1966).

Postirradiation inhibition of protein synthesis in E. coli B and in some of its auxotrophic mutants increases the colony-forming ability of the uv-irradiated bacteria. This occurs if chloramphenicol (CAM) is added to the cultures of microorganisms, or if essential amino acids are omitted from the incubation media after irradiation. Restoration of viability of E. coli B U$^-$ after a total dose of 900 erg/mm^2 uv in the presence of CAM and in the absence of uracil was studied. Both treatments resulted in the recovery of the same fraction of the irradiated bacterial population. There was no additive effect if both treatments are applied to the same irradiated culture. Inhibition of protein synthesis in

uv-irradiated E. coli B U⁻ by preventing RNA synthesis, that is by omitting uracil from the liquid medium, enhanced the colony-forming ability of the bacteria after plating on agar. The effect on survival was comparable to that obtained by CAM, which does not inhibit RNA synthesis, but interferes only with the function of ribosomes. Thus inhibition of protein synthesis seems to enhance the viability of uv-irradiated E. coli B and its auxotrophic mutants, regardless of the metabolic level through which this inhibition is brought about. Both uracil-less growth and CAM treatment seem to have an effect on the viability of the same fraction of the irradiated bacterial suspension. It is concluded that only a definite fraction of the uv-irradiated population is accessible to recovery by inhibition of protein synthesis. This might mean that only cells which suffered a particular type of damage (depending, possibly, on their physiological state at the moment of irradiation) are sensitive to a given restorative treatment. (BBB)

38564 NEUTRON ACTIVATION ANALYSIS STUDIES OF ^{129}I IN THE BIOSPHERE. Koch, R. C.; Keisch, B. (Nuclear Science and Engineering Corp., Pittsburgh). pp 47-68 of Radioactivation Analysis and Its Applications in Biological Sciences. Paris, Presses Universitaires de France, 1964.

Results are reported for studies on the distribution of ^{129}I among the several physical states and chemical forms in which it occurs in nuclear debris arriving at ground level, and determination of the concentrations of ^{129}I in human and animal thyroid tissues and its temporal behavior throughout the nuclear age. Leaching studies were performed and the behavior of ^{129}I and 8.05-day ^{131}I was studied in some of the samples. Increased values for ^{129}I levels in more recent thyroid specimens serve as an index of the rate at which this fission product is accumulating in the biosphere. Since this array also spans the entire group (prenatal to geriatric), statistical studies of current biospheric addition rates and of variations with subject age have been possible. Typical radiation dose rates and integrated doses were estimated for various categories of subjects. (P.C.H.)

38565 STUDIES ON THE CONCENTRATION OF VANADIUM IN SOME BIOLOGICAL SPECIMENS. Soeremark, Rune (Univ., Umea, Sweden). pp 223-38 of Radioactivation Analysis and Its Applications in Biological Sciences. Paris, Presses Universitaires de France, 1964.

Activation analyses were carried out for vanadium in several different types of biological specimens as well as in drinking water from various geographical areas in Sweden. Radiochemical procedures coupled with gamma spectrometry permitted determination of submicrogram amounts of this element in the samples. (P.C.H.)

38566 HIGH-STRONTIUM DIET AND RADIOSTRONTIUM RETENTION IN RATS. Depczyk, D.; Domanski, T.; Liniecki, J. (Inst. of Occupational Medicine, Lodz, Poland). Radiobiol. Radiotherap., 7: 185-98(1966).

The retention of intravenously injected ^{85}Sr, ^{90}Sr, and ^{133}Ba was followed for 100 days in rats of varying age after feeding different types of diet: a control diet with 12.5 and 16 mM % of calcium and phosphorus, respectively, a high-Ca diet (30 mM %), and a diet with high concentration of stable strontium (20 mM %). The effect of corresponding diets with lowered phosphorus content (3 mM %) was also investigated. High Sr diet reduced the body content of the Sr tracer in all age groups (1.5, 2.5, 7.5, and 13.5 month old rats), the resulting retention in these animals becoming almost identical and independent of age. The reduction of radiostrontium retention was apparent after one day of feeding a high Sr diet, and practically no further effect was attained by giving this type of food for periods longer than 10 days. Elevated calcium content of the diet had no effect upon radiostrontium retention in rats; lower phosphorus concentration in food reduced retention of radiostrontium by some twenty per cent regardless of the age. High Sr diet was equally effective when the tracer was introduced with food. Retention of radiobarium in rats was similarly influenced by feeding the diet with high concentration of stable strontium. (auth)

38567 SOME DATA ON LIVER CIRRHOSIS DEVELOPMENT UNDER THE INFLUENCE OF RADIOACTIVE CERIUM. Lebedeva, G. A. Radiobiologiya, 6: 55-8 (1966). (In Russian).

Studies were carried out in rats on the morphological changes of the liver during the development of cirrhosis induced by ^{144}Ce. Necrotic changes, as well as changes of the regeneration process in liver parenchyma, usually preceded the growth of connective tissue. The development of the cirrhotic changes proceeded according to the morphological origin of the cirrhosis. Very diffuse growth of the connective tissue structure was observed. (tr-auth)

38568 TOXICITY OF TRITIUM OXIDE IN MICE AND RATS SUBJECTED TO INTRAPERITONEAL INJECTION. Zhuravlev, V. F.; Bugryshev, P. F.; Istomina, A. G. Radiobiologiya, 6: 59-64(1966). (In Russian).

Tritium oxide at doses of 2.4 and 1.2 mc/g intraperitoneal injections caused a clinical picture of acute radiation sickness in rats and mice while the injection of 1.0, 0.8, and 0.6 mc/g caused one of only moderate gravity. The $LD_{50/30}$ was 1.03 mc/g for rats and 0.34 mc/g for mice. Rats received the maximum dose of tissue irradiation two weeks after the intraperitoneal injection of the isotope. (tr-auth)

38569 ABSORPTION OF VARIOUS CALCIUM COMPOUNDS FROM THE STOMACH AND INTESTINES AND THEIR EFFECTS ON ASSIMILATION OF RADIOACTIVE STRONTIUM IN RATS. Dubrovina, Z. V. Radiobiologiya, 6: 78-80(1966). (In Russian).

The protective effects of different calcium salts against the gastrointestinal absorption of ^{90}Sr in rats were dissimilar. They were correlated with the assimilability of calcium from the various compounds. (tr-auth)

38570 ACCUMULATION OF RADIOACTIVE STRONTIUM, YTTRIUM, AND CERIUM ISOTOPES BY FILAMENTOUS ALGAE IN THE PRESENCE OF EDTA AND DISSOLVED ORGANIC COMPOUNDS. Khmeleva, N. N.; Lavrent'eva, G. M. (Inst. of Biology of South Seas, Academy of Sciences, Sevastopol SSR. State Research Inst. of Lake and River Fishing Industry, Leningrad). Radiobiologiya, 6: 117-21(1966). (In Russian).

In the presence of EDTA ^{144}Ce and ^{91}Y were accumulated by filamentous algae very slowly from aqueous solutions. This complex did not affect the up-take of ^{90}Sr and the coefficient of accumulation was kept much higher than in the controls. The maximum depression of the coefficient of accumulation of the radioisotopes by the filamentous algae occurred with introduction of EDTA in quantity with equal molar salt composition of the water. Dissolved organic substances in the form of aqueous tinctures at a pH of 7.5 did not complex the radioisotopes of cerium and strontium and did not affect their accumulation by the filamentous algae. During massive growth of the filamentous algae, capable of intensive accumulation of the radioisotopes of cerium and yttrium, the transfer of the latter to very high trophic levels across this chain can be restricted by the use of EDTA. In the case of accumulation of ^{90}Sr by the filamentous algae the use of these complexes is ineffective. (tr-auth)

38571 MATHEMATICAL MODEL OF ACCUMULATION AND ELIMINATION OF RADIOACTIVE ISOTOPES. Grinev, V. S.; Kalinina, E. V.; Korolev, G. K.; Moskalev, Yu. I.; Parfenov, Yu. D. Radiobiologiya, 6: 122-7(1966). (In Russian).

A proposed 5-chambered model of the accumulation and elimination of ^{144}Ce, introduced once intratracheally, describes the behavior of this isotope with time. Tests on the intratracheal method of introduction to predict the behavior of ^{144}Ce introduced by other methods give satisfactory results for blood, skeleton, and liver. The theoretical results coincided with the experimental results only for long periods after the introduction. With significant changes in the mechanical program the proposed calculation method can be used for model behavior of radioactive isotopes with different methods of intake into the organism. (tr-auth)

38572 ACTION OF RETICULIN ON THE ACCUMULATION OF RADIOPHOSPHORUS (^{32}P) IN VARIOUS ORGANS

AND ENDOCRINE GLANDS IN INTACT AND HEPATECTOMIZED SUBTOTALLY ANIMALS. Sterescu, N.; Tanko, P.; Stancu-Ardeleanu, Alexandra; Sauvard, Sandra. Studii Cercet. Fiziol., 10: 43-7(1965). (In Rumanian).

Radiophosphorus was used as a tracer to determine the biological action of reticulin, a hormonal by-product of injured cells in reticulo-endothelial tissues of intact and partially hepatectomized rats. The subtotal hepatectomy involved 70 to 80% of the hepatic parenchyma. The animals were injected subcutaneously for seven days with 0.5 ml of reticulin per 100 g of body weight, using a corresponding isotonic saline solution for the comparison series. On the eighth day, the animals were injected intraperitoneally, before killing with 5μC per 100 g of body weight of ^{32}P in the form of Na_2HPO_4. After bleeding, the liver, thyroid, spleen, kidneys, heart, pancreas, and testicles were subjected to radiobiological analysis. It was found that the reticulin stimulates the accumulation of ^{32}P in the liver of both intact and hepatectomized animals; a similar effect was noted in the adrenal and thyroid glands but only for the hepatectomized animals. The results did not allow the differentiation between the stimulation of the reticulo-endothelial and of hepatic tissue. (TTT)

38573 KINETIC STUDIES WITH RADIOACTIVE (^{59}Fe) AND NONRADIOACTIVE (^{56}Fe) IRON IN SERUM. Gladtke, E.; Scholz, A. (Univ.-Kinderklinik, Giessen, Ger.). Verhandl. Deut. Ges. Inn. Med., 70: 390-3(1964). (In German).

The authors compared the serum transfer rates obtained with ^{59}Fe and ^{56}Fe injected into three small groups of humans. In the first group 10 to 20 μC of ^{59}Fe was administered followed by 6 to 10 mg of ^{56}Fe, administered intravenously. The calculated transfer of Fe ranged from ~12 to 52 μg/kg/hr. The half value time of elimination ranged from 68 to 125 min. When the ^{56}Fe was given, the serum disappearance curve flattened slightly, suggesting alteration of the steady state. This was not observed when ^{59}Fe and ^{56}Fe were given simultaneously in the second group, where the calculated transfer rate ranged from ~16 to 81 μg/kg/hr and the half value time of disappearance ranged between 66 and 140 min. In the third group where the amounts of ^{56}Fe given were greater than in the first group but also were given after the ^{59}Fe, the transfer rates ranged from ~13 to 46 μg/kg/hr, and the serum disappearance values ranged from 37 to 150 min. In this group the values calculated on the basis of the ^{59}Fe present were altered by the greater amounts of ^{56}Fe given. As long as the two Fe isotopes were not given simultaneously or the sp act. of the ^{59}Fe was high similar kinetic transfer rates were formed when calculated on the basis of either ^{56}Fe or ^{59}Fe. (BBB)

Radiation Effects on Biochemicals

See also CHEMISTRY — Radiation Chemistry

38574 (NYO-3449-1) THE MOLECULAR BASIS FOR THE MUTAGENIC AND LETHAL EFFECTS OF ULTRAVIOLET IRRADIATION. Progress Report, September 1, 1965–June 1966. Grossman, Lawrence (Brandeis Univ., Waltham, Mass. Graduate Dept. of Biochemistry). Contract AT(30-1)-3449. 9p. Dep. mn. CFSTI $1.00 cy, $0.50 mn.

Results are reported from tracer studies of reaction mechanisms involved in the effects of ultraviolet radiation or the powerful chemical mutagen, hydroxylamine, on the RNA polymerase system from Micrococcus lysodeikticus. It was concluded that the effective reduction of the 5,6-double bond of cytosine residues by either uv or hydroxylamine results in the formation of uracil. The effects of analogous modification of the uracil ring, such as reduction, photohydration, and dimerization, and the effect of uv or hydroxylamine on the synthesis of DNA and RNA and the relation between changes at substrate levels and those that take place at the template level were followed in nucleoside triphosphate systems using ^{14}C-labeled precursors. (C.H.)

38575 (ORNL-P-2267) REPAIR OF MOLECULAR DAMAGE TO DNA. Setlow, R. B. (Oak Ridge National Lab., Tenn.). [1966]. Contract W-7405-eng-26. 24p. (CONF-660614-2). Dep. mn. CFSTI $1.00 cy, $0.50 mn.

From 3rd International Congress on Radiation Research, Cortina, Italy.

Macromolecular changes in DNA induced by x radiation are reviewed and recovery processes that nullify the initial damage to DNA in E. coli are discussed. (28 references.) (C.H.)

38576 (TID-22103) THE VARIATION OF TOTAL RADIATION DOSE, DOSE RATE AND THE DURATION OF RADIATION AND ITS RELATIONSHIP TO THE DEPRESSION OF DNA SYNTHESIS. Looney, W. B.; Chang, L. O. (Virginia Univ., Charlottesville. Radiobiology and Biophysics Lab.). [1965]. Contract AT(40-1)-2889. 19p. Dep. mn. CFSTI $1.00 cy, $0.50 mn.

The depression of the rate of DNA synthesis was evaluated in vivo in semisynchronous populations of radioresistant regenerating rat liver cells and asynchronous populations of radiosensitive intestinal cells following local x radiation to the liver and adjacent intestines. The duration of radiation was varied from less than 1 min to 120 min, the dose rates, from 0.78 R/min to 300 R/min and the total radiation doses from 94 R to 1500 R. Primarily all the depression of DNA synthesis occurred during the first 15 min and the major part occurred during the first few minutes of radiation (3.75 min). The principal depression of DNA synthesis occurred between dose rates of 300 to 25 R/min; lowering the dose rates from 25 R/min to 0.78 R/min has little further effect on the lowering of the rate of DNA synthesis. There was little change in the depression of the rate of DNA synthesis between a total dose of 94 R and a total dose of 750 R. However, there is a correlation between depression and total radiation dose. The data indicate that DNA synthesis is not radioresistant when the three parameters, total dose, dose rate, and duration of radiation are taken into consideration. DNA depression can be produced by as little as 12 R of radiation when low radiation dose rates are used. The results of this study and preliminary results from dose fractionation studies suggest that the critical time period of the radiation depressing the rate of DNA synthesis is in the order of a few minutes. The demonstration of the importance of the temporal relationship between the delivery of the radiation and the depression of DNA synthesis will lead to a better understanding of the mechanism of action of radiation on DNA synthesis. More important, it offers promise in further attempts to better understand the temporal relationship between the initial physical effects on biological systems following radiation and the subsequent chemical, biochemical, and biological reactions to the initial physical insult. (auth)

38577 RELEASE OF ENZYMES FROM LYSOSOMES BY IRRADIATION AND THE RELATION OF LIPID PEROXIDE FORMATION TO ENZYME RELEASE. Wills, E. D.; Wilkinson, A. E. (Medical Coll. of St. Bartholomew's Hospital, London). Biochem. J., 99: 657-66(June 1966).

Acid phosphatase, cathepsin, and β-glucuronidase was released from rat-liver lysosomes by electron beams and x irradiation in vitro. Enzyme release was detectable after a dose of 1 krad and increased with dose up to 100 krads. Maximum radiation effects were observed when the lysosomes were kept for 20 hr at 4° or 20° after irradiation. An atmosphere of nitrogen considerably decreases enzyme release from lysosomes. Enzyme release was enhanced by ascorbic acid and decreased by vitamin E. Irradiation caused formation of lipid peroxides in lysosomes, and enzyme release increased with lipid peroxide formation. It is suggested that lipid peroxide formation leads to rupture of the lysosome membrane and allows release of the contained hydrolytic enzymes. (auth)

38578 INCREASE IN RNase AND DPNase ACTIVITIES IN ASCITES TUMOR CELLS INDUCED BY VARIOUS CYTOSTATIC AGENTS. Erbe, W.; Preiss, J.; Seifert, R.; Hilz, H. (Univ., Hamburg). Biochim. Biophys. Res. Commun., 23: 392-7(May 25, 1966).

Inhibition of ascites tumor cells from mice by a variety of cytostatic agents having different action mechanisms (x rays, tris ethyleniminobenzoquinone, colchicine, 5-fluorouracil, and actinomycin) leads to cells with elevated RNase and DPNase activities. The increase is correlated with the degree of proliferation inhibition and reaches values >15 times normal. Elevated DPNase activity mainly concerns the microsomal enzyme, whereas the nuclear (nucleolar) isoenzyme shows but a minor response. The increase in RNase comprises both free and latent RNase, higher doses leading to a shift much in favor of free RNase. (auth)

38579 CHANGES IN ANTIINSULIN ANTIBODIES SUBJECTED TO RADIOACTIVITY. Pellegrini, G.; Rodari, T.; Maggi, G.; Tirella, G.; Fratino, P.; Foschi, G. C. (Univ., Pavia). Boll. Soc. Ital. Biol. Sper., 41: 1342-5 (Dec. 31, 1965). (In Italian).

Earlier studies have shown that ^{131}I-labeled insulin in buffer or plasma undergoes partial or complete inactivation. This would have to be taken into account in radioimmunoassays of plasma insulin. The possible effect of ^{131}I-insulin on its corresponding rabbit antibody was evaluated in the present experiments. It was shown that rabbit antiinsulin antibody is inactivated when a solution of $K^{131}I$ is added to antiserum at a level of 0.03 mC/ml. When incubated at 4°C, no loss of antibody activity (tested by the Boyden passive hemagglutination technique) was noted after 24 hr, but by 48 hr 55% of activity was lost and by 72 hr, 100%. Other tests showed that when complexes of insulin and its antibody were incubated in the presence of ^{131}I (0.03 mC/ml), within 24 hr insulin was completely liberated from the complex. These results indicated a progressive inactivation of the ability of the antibody to bind its antigen in the presence of radioactivity from ^{131}I. (BBB)

38580 EFFECTS OF GAMMA RAYS ON VITAMIN B_6. Galatzeanu, I.; Antoni, F. Int. J. Appl. Radiat. Isotop., 17: 369-90(July 1966). (In French).

The effects of ^{60}Co gamma irradiation on pyridoxine and pyridoxal were studied with respect to structural changes and biological behavior. Irradiation of the substances in aqueous solutions leads to their partial or complete destruction depending on dose. Irradiation of pyridoxine in the solid state leads mainly to dehydrogenation and formation of free radicals. By dissolving irradiated samples in acid solutions, it was observed that the irradiated molecule reconstitutes itself by replacing its eliminated hydrogen atoms in a manner proportional to the pH of the solution. A complex of pyridoxine and ascorbic acid was obtained in the solid state which was more stable to irradiation (sterilization) than the pyridoxine itself in liquid state. (auth)

38581 EFFECT OF β-IRRADIATION ON DEOXYRIBONUCLEOPROTEIN. Yoshii, Giichi (Kyoto Univ.); Tchoe, Yuong-Tchel. Int. J. Radiat. Biol., 10: 485-93(1966).

The infra-red absorption spectrum, ^{45}Ca uptake, and dielectric increment of calf thymus deoxyribonucleoprotein (DNP) solution was measured after or during irradiation with β rays from ^3H_2O. With 600 rads, a shoulder at 6.17 μ appeared and the absorption at 7.09 μ increased. $Ca_3(PO_4)_2$ also showed absorption peaks at these wavelengths. Uptake of ^{45}Ca in DNP increased by 13 to 27 per cent with 600 rads. The dielectric increment decreased gradually with increasing doses after 300 rads. When Ca^{++} was added to the DNP solution prior to irradiation, the dielectric increment began to decrease with smaller doses. All these observations can be explained by complex formation between Ca^{++} and two neighboring phosphates of the DNA moiety, which are exposed on dissociation of DNP into DNA and protein due to ionizing radiation. (auth)

38582 RADIOLYTIC DECOMPOSITION AND RADIATION SENSITIVITY OF AMINO ACIDS IN AQUEOUS SOLUTION BY GAMMA IRRADIATION. Ohara, Akira (Kyoto Coll. of Pharmacy). J. Radiat. Res. (Jap), 6: 130-40(Sept.-Dec. 1965).

Radiation sensitivity of amino acids in aqueous solution to γ rays was investigated by determining a rate of decomposition of amino acids on exposure to various doses of γ irradiation. From the results the first order rate constants of the decomposition of amino acids were determined to refer the radiation sensitivities. In the aqueous solution, methionine, cystine, threonine, histidine, and arginine were proved to be more radiosensitive while cysteic acid, tyrosine, alanine, and proline were relatively radioresistant. Tryptophan, cystine, methionine, phenylalanine, and tyrosine were more easily decomposed in mixture than in the free solution. Among other amino acids a reciprocal protection was found in the mixture and they were less easily decomposed in mixture than in the free solution. A protective effect of tryptophan, cystine, methionine, tyrosine, and phenylalanine was proposed to other amino acids which were more radioresistant, in the γ irradiated amino acids mixture. (auth)

38583 VARIATIONS IN ASCORBIC ACID CONTENT OF GRAMINEAE DURING GERMINATION AND THE EFFECT OF β- AND γ-RADIATION. Barakat, M. Z.; Abdel-Wahab, M. F.; Megahed, Y. M. J. Sci. Food Agr., 17: 205-7(May 1966).

The ascorbic acid content of seeds of three types of Gramineae, viz, Triticum vulgare, Hordeum vulgare, and Zea mays and the average variations in the seeds during germination were determined. The effects on the seedlings of β irradiation emitted from small doses of $H_3{}^{32}PO_4$ or ^{131}I were also investigated. Results showed that radiation may either inhibit the biosynthesis or accelerate the degradation of vitamin C during the germination of seeds. (C.H.)

38584 INACTIVATION OF TOBACCO MOSAIC VIRUS BY ULTRAVIOLET LIGHT. Goddard, Judy; Streeter, David; Weber, Celia; Gordon, Milton P. (Univ. of Washington, Seattle). Photochem. Photobiol., 5: 213-22(Feb. 1966).

In the inactivation of tobacco mosaic virus (TMV) by uv light, the basic mechanism remains obscure. Unlike the action spectrum of many viruses, such as T_1 and T_2 phages, tobacco necrosis virus and influenza virus A, the action spectrum for the uv inactivation of TMV does not resemble the absorption spectrum of its nucleic acid, but appears to involve its protein component as well. Since a dose-dependent binding between cellular DNA and protein was seen in irradiated E. coli cells, it was of interest to determine whether this type of effect could be demonstrated for TMV. The irradiation of TMV with uv light (2537 Å) was found to result in the binding of protein subunits to the RNA. These bound subunits were stable toward warm sodium dodecylsulfate solution; however, the binding was not covalent since the subunits were removed by 66% acetic acid, guanidine hydrochloride, or phenol. Approximately one protein subunit was bound per lethal biological hit. The virus and the nucleic acid extracted from irradiated virus showed virtually identical rates of inactivation. (BBB)

38585 MECHANISM OF INHIBITION OF NUCLEIC ACID SYNTHESIS IN IRRADIATED ANIMALS. Libinzon, R. E.; Tseveleva, I. A. Radiobiologiya, 6: 9-12(1966). (In Russian).

The dependence of the inclusion of radioactive phosphate in DNA and RNA of the bone marrow and lymphoid tissues of the appendix on the radiation dose was studied in animals exposed to ^{60}Co γ radiation. The synthesis of nucleic acids was most radiosensitive in the dose range from 30 to 135 R. The suppression of the inclusion of ^{32}P in the DNA of the bone marrow after 135 R was 43.5%, and for the lymphoid tissue of the appendix 29%. With increase of the dose the effect significantly decreased and in the dose range from 500 to 1000 R the reduction of inclusion into the DNA of bone marrow was 2.2% and into the DNA of the appendix was 13.5%. The stationary concentration of ribonucleoside polyphosphates of the lymphoid tissue after irradiation at doses of 135 and 250 R was significantly increased. Only irradiation at a dose of 1000 R causes significant decrease of the concentration of ribonucleoside polyphosphates and some inhibition of the inclusion of radioactive phosphate in these compounds. (tr-auth)

38586 EFFECT OF IRRADIATION AND BRUCELLA INFECTION ON THE MALIC DEHYDROGENASE ACTIVITY OF RABBIT PERITONEAL MACROPHAGES. Tenoso, Harold John. Los Angeles, Univ. of California, 1966. 92p.

Thesis.

A metabolic approach was used to study the host-parasite relation between B. abortus and rabbit peritoneal mononuclear cells. The malate dehydrogenase activities of mononuclear cells from normal, Brucella-infected, and irradiated rabbits were examined and an attempt was made to correlate these differences with ability of the cells to survive Brucella infection. Findings showed that by using inhibitory concentrations of malate specific differences in malate dehydrogenase activity could be found among mononuclear cells from normal, immune, and irradiated rabbits. Mononuclear cells from rabbits infected with Brucella had an increase (relative to cells from normal rabbits) in MDH activity from the third post-infection day onward. Agglutinating antibody was demonstrable in the circulation of these rabbits on the fifth day. In the irradiated rabbits a reduction in MDH activity could be detected on the fourth through the sixth day. When rabbits were both irradiated and infected with Brucella it was possible to detect increases in MDH activity in the absence of agglutinating antibody. The evidence suggests that the malate dehydrogenase activity was specific for Brucella and that there was no direct correlation between agglutinating antibody and changes in MDH activity. There are two possible explanations for the change in MDH activity. One is that some part of the bacterial cell remains for long periods of time exerting a constant effect on the enzyme directly (on an allosteric site) or through some intermediate. The other explanation is that some part of the bacterial cell induces a precursor cell to start producing an isomer of malate dehydrogenase with different activity. The suggestion is implicit that a heightened enzymatic response in peritoneal macrophages of an infected animal may be of some significance in assessing the animal's ability to survive specific bacterial invaders. (Dissertation Abstr.)

Radiation Effects on Tissues

Refer also to abstracts 38780 and 38783.

38587 (CEA-R-2909) VARIATION DE L'HEMATOCRITE APRES IRRADIATION GAMMA CHEZ LE RAT. (Variation in the Hematocrit of the Rat After Gamma Irradiation). Marble, Georges; Breuil, Lucien; Berthelet, Jacqueline (Commissariat a l'Energie Atomique, Fontenay-aux-Roses (France). Centre d'Etudes Nucleaires). Mar. 1966. 12p. Dep. mn.

Statistical analysis of results of hematocrit measurement was carried out for twenty batches of rats with a view to studying the variation in the hematocrit as a function of the irradiation dose during the first four days after γ irradiation. A significant increase in the hematocrit was observed on the third day for 750 and 1000 rads and on the fourth day for 1000 rads only. (auth)

38588 (COO-1400-10) FACTORS RESPONSIBLE FOR CHANGES IN RADIOSENSITIVITY OF EMBRYONIC TISSUES. Technical Progress Report, 1965-66. Mericle, L. W.; Mericle, R. P. (Michigan State Univ., East Lansing. Dept. of Botany and Plant Pathology). May 31, 1966. Contract AT(11-1)-1400. 20p. Dep. mn. CFSTI $1.00 cy, $0.50 mn.

Factors responsible for changes in radiosensitivity of embryonic tissues were studied in barley and Tradescantia. Results are summarized from studies of the normal pattern of floral bud development in hybrid Tradescantia plants; the occurrence of spontaneous color mutants in Tradescantia; the influence of environmental factors and influorescence age on the radiosensitivity of Tradescantia bud clusters exposed to 60 R x radiation; the genetic effects of uv, visible light, chronic, low-level ^{60}Co γ irradiation, and diurnal temperature variations in Tradescantia; the effects of a single acute exposure to 450 R x radiation on barley embryo material, and the biological effects of ^{60}Co γ radiation in the first 3 to 5 mm of tissue depth in barley heads containing embryos and in Tradescantia. (C.H.)

38589 (EUR-2761.f) MISE AU POINT ET ETUDES DES EFFETS DE SUBSTANCES MUTAGENES CHIMIQUES, EN COMPARAISON AVEC LES AGENTS MUTAGENES PHYSIQUES. Rapport Annuel 1.10.1964-30.9.1965. (Preparation and Study of the Effects of Chemical Mutagenic Substances as Compared With Physical Mutagenic Agents. Annual Report, January 10, 1964-September 30, 1965). (Institut for Teoretisk Fysik, Copenhagen (Denmark)). May 1966. 8p. Dep. mn.

The basic and applied research on the preparation and effects of chemical mutagenic substances is summarized. Progress is reported on the synthesis of purines and histidine, genetic and biochemical studies on Schizosaccharomyces pombe, a comparative study of the cytological effects of γ radiation and of radiomimetic substances, the effect of chemical mutagenic agents on DNA, and mutations produced by chemical and γ radiation in barley, roses, and Rose of India. (J.S.R.)

38590 (NYO-1979-13) QUANTITATIVE POPULATION GENETICS OF MICE UNDER IRRADIATION. Progress Report, July 1, 1965-May 31, 1966. Green, Earl L.; Roderick, Thomas H.; Schlager, Gunther (Jackson Lab., Bar Harbor, Maine). June 24, 1966. Contract AT(30-1)-1979. 46p. Dep. mn. CFSTI $2.00 cy, $0.50 mn.

Progress is reported on studies of the biological effects of whole-body or spermatogonial exposure to doses of 50 or 100 R x radiation in mice followed through the 16th generation of irradiation. Data are included on the reproductive performance, body weight, life span, embryonic mortality, and genetics of irradiated populations. Three mutations that occurred during the studies were propagated for further study and analysis. A list is included of publications during the period covered by this report. (C.H.)

38591 (NYO-3445-7) BIOCHEMICAL AND HISTOCHEMICAL STUDIES IN AN ATTEMPT TO DEMONSTRATE LYSOSOMES AND LYSOSOMAL ENZYMES IN NORMAL AND BETA-IRRADIATED ALBINO GUINEA PIG EPIDERMIS. Second Year Progress Report, August 14, 1965-April 15, 1966. (Albert Einstein Medical Center, Philadelphia, Pa.). Contract AT(30-1)-3445. 28p. Dep. mn. CFSTI $2.00 cy, $0.50 mn.

Guinea pigs were given a single skin-surface dose of 3000 rep β radiation from a ^{90}Sr-^{90}Y source and killed 30 days later. Indirect evidence was obtained in support of the hypothesis that the increase in epidermal extracellular DNase I after ionizing radiation injury, or other skin trauma, is due to increased diffusion of a DNase I-inhibitor complex from the blood into the epidermis, where it accumulates with subsequent loss of the inhibitor. There was relatively high latent DNase I in epidermal washings from both control and irradiated tissue and this may be the postulated DNase I-inhibitor complex. However, there was no direct relation between latent DNase I content and the heightened DNase activity in the interstitial fluid of irradiated epidermis (i.e., greater enzyme activity was not associated with lower latent DNase content). Latent DNase I was released in epidermal washings by aging at 18 hrs at 37°C or heating 10 min at 55 or 60°C. Only traces of free DNase I are present in guinea pig plasma or sera and, as yet, the DNase I-inhibitor complex could not be demonstrated in these fluids. The inability to detect free inhibitor may be due to the high DNase I activator content found in these humoral fluids. (auth)

38592 (ORNL-P-2158) FUNCTIONAL AND MORPHOLOGICAL CHARACTERIZATION OF STEM CELLS: THE UNIPOTENTIAL ROLE OF "LYMPHOCYTES" OF MOUSE MARROW. Bennett, Michael; Cudkowicz, Gustavo (Roswell Park Memorial Inst., Buffalo, N. Y. Dept. of Experimental Biology. Oak Ridge National Lab., Tenn.). [1966]. Contract W-7405-eng-26. 29p. (CONF-660423-1). Dep. mn. CFSTI $2.00 cy, $0.50 mn.

From International Symposium on Lymphocyte in Immunology and Haemopoiesis, Bristol, Eng.

The growth of hematopoietic cells derived from grafted

marrow was estimated in the spleens of x irradiated recipient mice by labeling dividing cells with the radioactive DNA precursor 5-iodo-2′-deoxyuridine-^{131}I. Erythropoiesis is suppressed in marrow recipients made polycythemic by hypertransfusion with erythrocytes; in this case the dividing cells are non-erythroid in nature, i.e., they do not synthesize hemoglobin. Erythropoiesis was estimated separately by labeling the recipient spleens also with $^{59}FeCl_3$. Polycythemia induced either at the time of marrow transplantation or three days later reduced the pool of dividing hematopoietic cells by an amount clearly related to the suppression of erythropoiesis. There was no evidence for the shunting of pluripotent stem cells from or into the production of nonerythroid cells as a consequence of the induced changes in erythropoiesis. Filtration of marrow through columns of glass wool increased the concentration of colony-forming cells and of cells capable of establishing erythropoiesis in irradiated recipients; the procedure, however, did not concentrate precursors of leukocytic elements. The results indicate that primitive, independent hematopoietic cells with limited potential, as opposed to pluripotent stem cells, were assayed by transplantation of marrow from adult donor mice. The data also suggest that colony-forming cells are not all pluripotent but, rather, that under these conditions most of them are unrelated to the production of non-erythroid hematopoietic cells. The frequency of marrow lymphocytes was increased in the effluent from glass wool columns and was consistently correlated with erythroid precursor function. This correlation was observed without exception in the twenty-three separate experiments described. The concentration of other cell types in marrow decreased upon filtration. Hence, marrow cells, resembling the peripheral lymphocyte morphologically but not functionally may be the primitive erythropoietic cells assayed by transplantation and filtration technique. (24 references.) (auth)

38593 (ORNL-P-2175) CYTOGENETIC METHODS: SOMATIC CHROMOSOME ABERRATIONS IN OCCUPATIONALLY IRRADIATED HUMANS. Bender, M. A.; Gooch, P. C. (Oak Ridge National Lab., Tenn.). [1965]. Contract W-7405-eng-26. 14p. (CONF-660412-2). Dep. mn. CFSTI $1.00 cy, $0.50 mn.

From Symposium on Accidental Irradiation at Place of Work, Nice.

Results are reviewed from studies of radioinduced chromosome aberrations in occupationally exposed humans. Chromosome breaks increase as a linear function of radiation dose and may be induced in either somatic or germinal cells. The peripheral leukocytes and their precursors have been studied extensively in cultures and data from cytogenetic studies are summarized. It is concluded that aberration analysis of peripheral leukocytes is a useful tool for the diagnosis of radiation exposure. (C.H.)

38594 (ORO-2066-10) ECOLOGICAL SIGNIFICANCE OF NEUTRON AND GAMMA RADIATION ON DORMANT AND PHYSIOLOGICALLY ACTIVE SEED AND SEEDLINGS OF TREE SPECIES NATIVE TO THE EASTERN DECIDUOUS FOREST. Progress Report. Heaslip, Margaret B. (Morehead State Univ., Ky.). June 23, 1966. Contract AT(40-1)-2066. 35p. Dep. mn. CFSTI $2.00 cy, $0.50 mn.

The relative biological effectiveness of γ radiation and neutrons on dormant and physiologically active seed and seedlings of 18 tree species native to the Eastern Deciduous Forest Area was determined. Data are included on the effects of physiological activity and water content on the radiosensitivity of seed as measured by the percent germination and survival of seedlings. The ecological significance of the data is discussed. (85 references.) (C.H.)

38595 (ORO-3295-2) STUDIES OF THE EFFECTS OF HORMONES, X RAYS, AND CERTAIN CERIUM COMPOUNDS ON RAT LIVER CELLS AND SUBCELLULAR FRACTIONS FROM THE ZONAL ULTRACENTRIFUGE. Progress Report, October 1, 1965–September 30, 1966. Tipton, Samuel R. (Tennessee Univ., Knoxville. Dept. of Zoology and Entomology). Contract AT(40-1)-3295. 13p. Dep. mn. CFSTI $1.00 cy, $0.50 mn.

Progress is reported in studies on the effects of x radiation, certain hormones, and cerium compounds on rat liver cells. Data are included on the distribution patterns of β-glucuronidase and acid phosphatase in subcellular fractions of rat liver brei; the effects of 1,500 R x radiation on protein synthesis in rat liver; and the effects of thyroid hormone level and x radiation on the rate of polyribosome formation in rat liver and muscle. (C.H.)

38596 (SAN-590-1) IDENTIFICATION OF THE PROPOSAL: X-RAY INDUCED CHANGES IN DROSOPHILA GERM CELLS. Progress Report, September 1, 1965–August 31, 1966. Rinehart, Robert R. (San Diego State Coll., Calif.). Contract AT(04-3)-590. 18p. Dep. mn. CFSTI $1.00 cy, $0.50 mn.

Progress is reported in studies on the effects of x radiation on germ cells in Drosophila, with emphasis on metabolic and physiological influences on mutation processes. Results are included from studies of mutations from Drosophila males and females cultured on food exposed to 150, 500, or 3000 kR x radiation; measurements of frequencies of detached and attached X-chromosomes from females given helium treatments, the effects of helium treatments on spermatogenesis, and detachments in eggs from irradiated single females. (C.H.)

38597 (TID-23057) STUDIES OF THE EFFECT OF IONIZING RADIATIONS ON THE PROCESSES OF CELLULAR PROLIFERATION, MEGASPOROGENESIS, AND EMBRYO-SAC DEVELOPMENT. Progress Report. (Hawaii Univ., Honolulu). May 16, 1966. Contract AT(04-3)-235. 8p. Dep. mn. CFSTI $1.00 cy, $0.50 mn.

Fruits set on Dendrobium phalaenopsis were exposed to 5,000 R or 7,500 R x radiation at weekly intervals from 1 to 9 weeks after pollination. Smears and tissue sections were examined at intervals of 2 weeks and morphological findings are described. (C.H.)

38598 (TID-22955) ELECTROPHORETIC AND HISTOCHEMICAL STUDIES OF TISSUES AND BODY FLUIDS OF X-IRRADIATED HAMSTERS. Progress Report. (Oregon Univ., Eugene). [nd]. Contract AT(45-1)-1926. 6p. Dep. mn. CFSTI $1.00 cy, $0.50 mn.

The effects of 100-R whole-body x irradiation on blood serum proteins and albumin-globulin-ratios in blood from female hamsters sampled during the course of gestation were determined by chromatographic and electrophoretic techniques. Results indicate that the percentage drop in α-globulin is proportional to the number of viable implants and the difference between α-globulin in irradiated and control animals is reflected in the serum α-1 globulin. (C.H.)

38599 (TID-22968) FINAL REPORT [ON EFFECT OF RADIATION ON METABOLISM OF ASCITES TUMOR CELLS]. Ontko, Joseph A. (Tennessee Univ., Memphis. Dept. of Biochemistry). Apr. 22, 1966. Contract AT (40-1)-2748. 55p. Dep. mn. CFSTI $3.00 cy, $0.50 mn.

Results are summarized from studies on the effect of x irradiation on the metabolism of Ehrlich ascites tumor cells. These cells offer many advantages in the study of acute radiation damage and in the exploration of the mechanism of this injury in biochemical terms. The data indicate that a non-lethal dose of radiation increases the endogenous oxygen consumption of ascites tumor cells. It was found that the increase in oxygen consumption induced by 1250 R of x irradiation is observed in hypertonic but not isotonic systems, and that the irradiated cells were more resistant to hypertonic injury and that they also retained their morphological integrity for longer periods of incubation in hypertonic media. In an extensive series of experiments on the fundamental difference in ion balance which is responsible for the depressed oxygen consumption of normal cells in the hypertonic saline-phosphate system, it was found that magnesium is the key constituent which can reverse the inability of normal ascites tumor cells to respire for prolonged periods in the hypertonic saline-phosphate system. The methodology, experimental design, statistical treatments, results, and discussion of these data are compiled. (C.H.)

38600 (TID-23034) EFFECTS OF X RADIATION ON METABOLISM OF ^{15}N FROM AMMONIUM CITRATE AND

GLYCINE, IN RATS. Technical Progress Report, September 1, 1965–April 30, 1966. Gaebler, Oliver H. (Edsel B. Ford Inst. for Medical Research, Detroit, Mich.). Contract AT(11-1)-1522. 4p. Dep. mn. CFSTI $1.00 cy, $0.50 mn.

Progress is reported in studies on the effects of 400 R whole-body x irradiation on the metabolism of ammonia and glycine in rats. Nitrogen-15 was used as a tracer for both ammonium citrate and glycine. (C.H.)

38601 (UCLA-12-567) RADIATION EFFECTS ON LIZARDS IN A PUERTO RICAN FOREST. Turner, Frederick B. (California Univ., Los Angeles. Lab. of Nuclear Medicine and Radiation Biology). [Aug. 5, 1965]. Contract AT(04-1)-Gen-12. 11p. Dep. mn. CFSTI $1.00 cy, $0.50 mn.

Three months exposure to gamma radiation from a 10,000 curie ^{137}Cs source caused approximately a 50% reduction in the number of Anolis gundlachi occupying 0.7 acres of Puerto Rican forest. The reduction was most evident within 15 m of the source. The proportion of older animals in the irradiated population may have been reduced. Accumulated doses of over 9,000 R were survived by some lizards. No departures from normal weight-length relationships were noted among survivors. (auth)

38602 (UCLA-34P60-1) IRRADIATION EFFECTS ON BRAIN WAVE CORRELATES OF CONDITIONED BEHAVIOR. Final Report. Adey, W. R.; Schoenbrun, R. L. (California Univ., Los Angeles). May 25, 1966. Contract AT(11-1)-34. 72p. Dep. mn. CFSTI $3.00 cy, $0.75 mn.

The effects of low doses of x irradiation on brain wave activity recorded from temporal lobe structures during conditioned behavior in the cat were studied. A major effort was directed to evaluation of several behavioral training techniques with concurrent EEG recording. Initial studies utilized 250 kv x rays in doses ranging from 100 to 1,500 R delivered to the whole head. Later studies involved a technique of focal brain irradiation with 910 Mev γ particles that permitted selective irradiation of discrete regions. A novel stereotaxic alignment frame was designed for precision placement in focal irradiations. Data are presented on electrophysiological behavioral and morphological changes induced by whole head or focal exposure. (C.H.)

38603 (AD-629422) RADIATION SAFETY. Grigor'ev, Yu.; Kovalev, E. Translated from Med. Gaz., 3(Sept. 21, 1965). 9p. (FTD-TT-65-1682). CFSTI $1.00 cy, $0.50 mn. JCL $1.10 fs, $0.80 mf.

The problems of radiation protection of astronauts during space flight are reviewed. Information obtained at astrophysical observatories, by space probes and artificial earth satellites on radiation conditions in space, is summarized. It is pointed out that the crew of Voskhod II, and in particular A.A. Leonov during his space walk, were not subjected to the danger of radiation by the protons of solar flares since calculations of solar flare activity were made in advance of the flight. Calculations showed that even if solar flares had occurred during the 20 min a man was in free cosmic space, the dose of radiation he would receive would not exceed 30 m Rem. It is concluded that the successful radiation protection of astronauts during prolonged space flights will depend on how accurately the basic criteria of radiation danger are determined and on how effectively problems of radiation protection such as shielding parameters, dosimetry, prophylaxis of radiation sickness, and the peculiarities of the biological effects of cosmic radiation in combination with other factors of space flight are solved. (C.H.)

38604 RADIATION-INDUCED PROTEIN LEAKAGE INTO THE SMALL INTESTINE OF THE RAT. Zenklusen, G. (Univ., Bern). Acta Isotop., 5: 141-52(Oct. 31, 1965). (In German).

One to seven days after a short exposure of the whole-body with 500 to 800 R x radiation, polyvinylpyrrolidone (^{131}I-PVP), which may be used as a substitute for plasma-protein, was given intravenously to a breed of swiss-albino rats. Immediately after the injection of the compound, its excretion into the upper part of the small intestine, which was perfused with a solution of Tyrode, was measured continuously over a period of four hours. The excretion rate of ^{131}I-PVP into the intestinal perfusate plotted against time was linear in radiated animals and non-radiated ones used for comparison. The radiated animals showed an increase in the activity of the intestinal perfusate compared to the non-radiated four to seven days after irradiation. The maximal excretory rate was found five to six days after exposure to 800 R. The hypoproteinemia, observed repeatedly after total-body irradiation, is caused, at least partially, by an enteric loss of protein due to an increase in the permeability of the intestinal wall for macromolecules. (auth)

38605 GENETIC STUDIES ON RADIO-RESISTANT STRAIN OF CHLORELLA ELLIPSOIDEA. I. RADIOSENSITIVITY AND A RADIO-RESISTANT STRAIN INDUCED BY REPEATED γ-IRRADIATION IN CHLORELLA ELLIPSOIDEA. Ujihara, Akio; Mori, Shigeyuki; Hori, Shiro. Ann. Rep. Radiat. Center Osaka Prefect., 6: 90-2 (1965).

The radiosensitivity of Chlorella ellipsoidea to γ rays, and the effects of γ rays on the process of cell division were investigated. It was recognized that the LD_{50} value at 240 hours after irradiation was between 25 to 50 kR, and the cell division of irradiated cells lagged extremely. A radio-resistant strain was obtained by repeated exposure to γ rays of a cell population derived from a single cell. It was considered that this strain was induced by the accumulation of polygenic mutations. (auth)

38606 OBSERVATIONS ON THYMUS OF MICE AFTER X IRRADIATION. Takeda, Atsuhiko; Hori, Yasuharu; Nishio, Kazuo. Ann. Rep. Radiat. Center Osaka Prefect., 6: 122-5(1965).

After whole-body x irradiation of mice with doses of 150 to 1000 R, DNA content, proteolytic activity, and lactic dehydrogenase activity of the thymus were measured. DNA content of two fractions with different solubility for saline was measured and a rate of protein-free DNA (soluble in saline) to total DNA was determined. While the rate amounted to 3.0% in non-irradiated control, the values in irradiated groups indicated remarkable increase. When the thymus was extirpated immediately after irradiation with 1000 R and incubated in O_2 at 37°C for 3 hrs, a similar increase in the rate was found. The change in proteolytic activity after irradiation did not occur except for slight increase after 1000 R. Lactic dehydrogenase activities at 4.5 hrs after 300 R and 1000 R irradiation were notably decreased. (auth)

38607 MUTATIONAL RESPONSE OF THE PREMEIOTIC GERM-CELL STAGES OF ADULT DROSOPHILA MELANOGASTER MALES TO X IRRADIATION. Puro, Jaakko (Univ. of Turku, Finland). Ann. Zool. Fenn., 3: 99-126(1966).

The mutagenic effect of a single 3000-R dose of x irradiation on spermatogenesis in adult flies was studied by the brood pattern technic. Irradiation caused a period of low fertility on the 6th to 9th days; almost complete sterility occurred on the 8th day. Restoration of fertility took place in two steps, with a secondary decline during the 11th to 12th days. Control level was reached on the 13th or 14th day. Recessive 3rd chromosome lethal mutations, Y:3 translocations, and male sterility mutations (probably arising from damage to the Y chromosome) showed the familiar brood patterns with gradually increasing mutation rates in the first three successive 2- or 3-day broods, corresponding to progressively earlier postmeiotic germ-cell stages at the time of irradiation. The mutant frequencies in the poststerile broods were lower than in any of the presterile broods. There were, however, essential differences between the brood pattern of different types of genetic damage. While no Y:3 translocations were found in about 4000 offspring, the frequency of sterile male offspring was almost as high in the 8th to 10th day broods as in the first brood, but it gradually decreased to about the control level in the last broods. A more irregular pattern was observed for recessive lethal and visible mutations, and there was no indication of a progressive decrease towards the last broods. Clusters of 3rd chromosome crossovers and recessive mutations provided evidence that germ cell renewal occurs in

Drosophila by means of a stem-cell mechanism. The relative size of the continuing clusters suggested that only about five stem cells per male survived 3000-R irradiation, but repopulation may occur by dichotomous divisions of the survivors. (BBB)

38608 ANTIBODY PRODUCTION IN CORNEAL HYPERSENSITIVITY. Leibowitz, Howard M.; Elliott, James H. (Harvard Univ., Boston). Arch. Opthalmol. (Chicago), 73: 687-95(May 1965).

An immunosupressive dose of total-body x irradiation given to rabbits prior to antigen administration inhibited corneal response to the antigen. Humoral antibody production and invasion of the limbus by plasma cells was also inhibited. Irradiation of the eye, with the body shielded produced none of these inhibitions. It was concluded that the cornea plays no significant role in the etiology of primary corneal hypersensitivity. (C.H.)

38609 EFFECT OF RADIOMIMETICS AND X RAYS ON THE PERMEABILITY OF THE BLOOD-BRAIN BARRIER. Zipf, K.; Roessner, W.; Tempel, K. (Tierarztlichen Fakultaet, Munich). Arch. Pharmakol. Exper. Pathol., 254: 83-90(1966). (In German).

Albino rats received whole-body irradiation of either 367 or 734 R, or were treated with the radiomimetic drugs, trichlorotriethylamine (HN_3) and triethylenemelamine (TEM). The effects of the irradiation exposures were generally greater than those of the drugs. Within 12 hr after irradiation the concentrations of Evans blue in the animals' brains were increased significantly. The recovery phases in the sublethally irradiated animals required ~6 weeks, while the recovery phase with the drugs was ~2 weeks. At ~3 weeks the Evans blue concentration of the brain increased somewhat in the sublethally irradiated animals. An increase in permeability of the blood-brain barrier for Evans blue during the lethal dose of whole-body irradiation was reversible. This may have been a primary reaction to irradiation. (BBB)

38610 EFFECT OF 19-NOR-TESTOSTERONE PHENYLPROPIONATE ON POSTIRRADIATION SYNDROME AND SOME OTHER KINDS OF STRESS. Jelinek, J. M.; Dienstbier, Z.; Hava, M. (Research Inst. for Natural Drugs, Prague. Charles Univ., Prague). Atompraxis, 12: 303-5(June 1966).

In experiments on male mice it was found that combined administration of 19-nor-testosterone phenylpropionate (=NPP) before and after x irradiation significantly decreased the survival of animals. In experiments with shock or stress, caused by traumatization in the Noble-Collip drum, by scalding and by starvation, the survival of mice was not influenced by treatment with NPP. Possible differences in mechanism, occurring in survival of animals in various shock and stress conditions, are discussed. (auth)

38611 ACRIFLAVINE INHIBITION OF DARK REPAIR AND LATE GENERATION DEATH. Davies, D. Roy (Wantage Research Lab., Eng.). Biochem. Biophys. Res. Commun., 23: 652-9(June 13, 1966).

Wild type haploid strains of Chlamydomonas reinhardi of + and – mating type were maintained and diploid spores were produced. The cultures were exposed to 125 ergs/mm^2/sec ultraviolet radiation or 17,500 rads/min ^{60}Co γ radiation. The organisms were grown under daylight conditions and photoreactivation was carried out using fluorescent tubes that delivered 1000 ft-C/hr. The criterion of survival was the production of a 100-cell colony from a single irradiated cell. Acriflavine was incorporated in the post-irradiation agar at concentrations that had no effect on the viability of controls. Results showed that acriflavine had no effect on cells exposed to γ radiation. The response of cells exposed to uv indicated that acriflavine acts by inhibiting repair in these cells. Possible reaction mechanisms are discussed. (C.H.)

38612 DESTRUCTIVE EFFECT OF RADIATION ON LYMPHATIC TISSUE. Congdon, Charles C. (Oak Ridge National Lab., Tenn.). Cancer Res., 26: 1211-20(June 1966). (ORNL-P-1542).

The destructive effect of x radiation on lymphatic tissues is influenced in variable ways and to different extents depending on the physical factors concerned with the radiation itself and on biologic factors concerning the exposed organism. In this context the major physical factor is radiation dose and the major biologic factor is local versus whole-body exposure. Presence of non-neoplastic pathologic changes in lymphatic tissue could conceivably also alter radiation effects as well as the subsequent ability of the lymphatic tissues to regenerate. Regeneration in the exposed tissue is interesting from the normal physiology point of view, and the observation that granulopoiesis usually precedes reaccumulation of lymphocytes requires further consideration. Potentiation of radiation effects by graft-versus-host and graft-versus-tumor reactions is of great interest because clinical trials utilizing immunotherapy of cancer as a supplement to standard therapeutic measures are now worth serious consideration. The idea that tumor cells of lymphatic tissue origin might cause graft-versus-host reactions could form the basis for additional experiments. (57 references.) (auth)

38613 SYNERGETIC EFFECT OF X RAYS AND OF VINCALEUCOBLASTINE ON A SOLID ISOLOGOUS TUMOR OF THE MOUSE C^3H. Girard, V.; Oth, D.; Robert, J.; Burg, C. (Faculte de Medecine, Nancy. Faculte des Sciences, Nancy). Compt. Rend. Soc. Biol., 159: 1404-7 (Dec. 1965). (In French).

The synergetic action of vincaleucoblastine with x rays was studied by determinating the radiosensitivity of a solid isologous tumor of the C^3H mouse and following the tumor modification when the pharmacological agent is administered before and after irradiation. After tumor fixation the mice were exposed to whole-body irradiation of 2250 R. The results showed that the tumor receiving no treatment has a take rate of 100% and kills the animal within 90 days. The administration of vincaleucoblastine alone either before or after the grafting does not modify this result. X irradiation has a moderating effect. The combined effect of x irradiation and vincaleucoblastine causes a significant decrease in the rate of take and in the mortality. (J.S.R.)

38614 EFFECTS OF ULTRAVIOLET MICROBEAM IRRADIATIONS ON MITOSIS STUDIED IN TRADESCANTIA CELLS IN VIVO. Wada, Bungo (Shizuoka Univ., Japan); Izutsu, Kosaku. Cytologia (Tokyo), 26: 480-91(1961).

The effect of uv microbeam irradiation on mitosis in Tradescantia cells was studied with regard to the development of the polar caps and the karyokinetic spindles and to their roles during the mitosis of plant cells. The irradiation area with the instrument used was about 2μ in dia. The time of irradiation ranged from 3 to 30 min. A complete suppression of the spindle development occurred when a polar cap was irradiated at an early stage and partial suppression appeared when a polar cap was irradiated at a slightly later stage after its appearance. With complete suppression of spindle development, a restitution nucleus appeared, while with partial suppression of the spindle a half spindle developed at the intact pole side, inducing blocking and sticking of the chromosomes on the irradiated pole side. When the half spindle transformed into a phragmoplast, both daughter chromosome groups were pushed by the growing of the phragmoplast to the irradiated pole side. Other mitotic aberrations, such as daughter nuclei unequal in size, nuclei with vacuoles, reversion of prophase nuclei into resting ones, and occurrence of sticky chromosome bridges, were obtained in cells irradiated at various mitotic stages. From the results of uv microbeam irradiation of the polar caps and spindle poles, their roles and submicroscopic structure are discussed in relation to the mechanism of mitosis. (BBB)

38615 CHROMOSOME ANOMALIES AFTER RADIATION EXPOSURE. Marsch, W.; Niederalt, G.; Gropp, A. (Univ., Bonn). Deut. Med. Wochschr., 90: 2205-8(Dec. 3, 1965). (In German).

Lymphocytes from patients irradiated previously for various clinical conditions were examined for evidence of structural anomalies after three days of in vitro culturing.

No significant variations from the normal diploid number of 46. However, several structural anomalies were observed. These included color defects of chromosomes or chromatids without dislocation, corresponding to the "gaps" or "isogaps" reported previously, chromosomal or chromatid breaks with dislocation of the broken sections or fragments (acentric sections), anisomorphia, and pathological chromosomes, with immediately identifiable structural changes such as ring chromosomes, dicentric chromosomes, abnormally long chromosomes, recombinations, and translocations. Study of the distribution of the chromosome anomalies among the patients observed indicated that infrequent x-ray studies made for diagnostic purposes did not result in significant chromosome changes, while numerous irradiations administered in the course of tumor therapy, at high dose levels damaged the genetic material of the lymphocytes severely. Most of the chromosomal anomalies observed were not related to the time interval since the last irradiation received, but upon the total irradiation dose. (BBB)

38616 RADIOBIOLOGICAL ACTION MECHANISMS. **Dittrich, Wolfgang (Univ., Muenster, Ger.). Fortschr. Kiefer- Gesichtschir., 8: 9-20(1962). (In German).**

The nature of primary and secondary reactions in the cell occurring as a result of various kinds of ionizing radiations is reviewed, and various hypotheses which have been proposed to explain cellular injury to such irradiation are examined. The primary chemical reaction resulting from irradiation in therapeutic doses involves an extraordinarily small number of molecules. The physical basis underlying the absorption of ionizing radiation is therefore treated in a statistical manner. In addition to the energy absorbed, the topography of the biological primary effects are of importance, namely, ionization, initiation, and paramagnetic centers (e.g., water radicals). This is true for direct and indirect radiation effects and explains the low biological effect of fast electrons and ultrahard x rays observed at a given dose level. Oxygen and radioprotective substances can intervene at one of several independent stages during the course of a radiation reaction. Hypoxic and consequently radiation-resistant groups of cells in a tumor may determine the success or failure of radiation treatment. Ways in which hypoxia may be overcome during irradiation are considered. Under suitable conditions it is possible to observe the development of resistance to irradiation among a population of tumor cells. The hypothesis of close correlation between resistance to radiation and catalase in tumor cells suggested by Warburg is not supported experimentally. The selectivity of tumor cell damage with the use of ultrahard radiation is discussed. (BBB)

38617 THE PROPERTIES, ORIGIN, AND MECHANISM OF CONVERSION-TYPE INHERITANCE AT THE B LOCUS IN MAIZE. **Coe, E. H. Jr. (Univ. of Missouri, Columbia). Genetics, 53: 1035-63(June 1966).**

A regular, conversion-type (paramutation) system at the B locus was examined with experiments designed to discriminate among plasmid (gene-extrinsic), enforced copying (gene-intrinsic), and episomic (combination) bases for the phenomenon. The effect of the system is to cause reduced function of B, represented by B′; the capacity for this reduction is conferred on B in heterozygotes, since all gametes from B′B hybrids are B′. From B′b hybrids, however, half the gametes are B′ and half b, demonstrating Mendelian segregation of the system. Selection and repetitive induction do not influence the expression of B′. The phenotypes of reciprocal hybrids, B′/B and B/B′, are equal, but both of these heterozygotes are darker in color than B′B′ and B′b. Functional capacity and mutability are independent of paramutability and paramutagenicity; basic functional properties of inducing alleles are not transferred to induced alleles. No chromosomal aberrancies have been found, but a significant reduction in crossing over is found in B′-bearing heterozygotes, and coincidence may be lowered in B′B heterozygotes. Segregation of B′ from b is regular; B′ is consistent in inducing the change of B to B′ and is stable. X rays and ultraviolet light produce no gross effects on B′ expression, but x ray induced deletion of B′ effect is concurrent with chromosomal deletion. Deletion of the B′ chromosome in B′/B heterozygotes uncovers unchanged B through the 10-leaf stage. Artificial infection trials using B′ and unstable-B sources were unsuccessful, and maternal haploids and sectorial plants do not show infectious transmission of B′ under natural conditions. Two chromosome aberrations that were tested had no gross effects on B′ or B. New B′ mutations arise somatically, and are expressed in sectors. The instability that gives rise to new B′ mutations could be maternally inherited, but since no completely stable lines have been found this is in doubt; BB plants are much more unstable than Bb. New B′ mutations are suspected to arise in time clusters, but tests for environmental induction of B′ were negative. Interpreting these observations, a model is formulated that represents B′ as a combination of B plus an appended or inserted element, E, symbolized B · E. The element is viewed as transferred to B without error, probably at meiosis; b is considered incapable of receiving the element. The action of B in the B · E combination is interfered with but not completely inhibited, and the action of B in B/B · E heterozygotes is suppressed. The possibility is considered that E represents a mutant linker-regulator element. (auth)

38618 THE MECHANISM OF THE EFFECT OF POST-IRRADIATION CENTRIFUGATION ON THE YIELD AND THE KINETICS OF RADIATION-INDUCED CHROMOSOME ABERRATIONS IN BARLEY. **Kumar, Sushil; Natarajan, A. T. (Indian Agricultural Research Inst., New Delhi). Genetics, 53: 1065-9(June 1966).**

An effect of centrifugation on the yield of chromosome exchanges was demonstrated by measuring the frequency of dicentrics and rings at first mitosis in root meristems of barley grown from γ irradiated seeds. The increase after centrifugation is highly significant after allowance has been made for any oxygen effect arising from centrifugation, is dependent on the dose of radiation, and is accompanied by an increase in the number of chromosome exchange sites. (auth)

38619 HEREDITARY HYPOCHROMIC MICROCYTIC ANEMIA IN THE LABORATORY RAT. **Sladic-Simic, D.; Zivkovic, N.; Pavic, D.; Marinkovic, D.; Martinovic, J.; Martinovitch, P. N. (Boris Kidrich Inst. of Nuclear Sciences Belgrade). Genetics, 53: 1079-89(June 1966).**

A hereditary severe hypochromic and microcytic anemia in the rat is described. The anemia appeared in the offspring of one of 17 female animals of our random bred rat colony exposed to 50 R of total-body x irradiation at eight days of age. The disease is caused by an autosomal recessive mutation. The basic phenotypic characteristics of the recessive homozygotes are hypochromia, microcytosis, reticulocytosis, and extreme osmotic resistance of red blood cells. The hemoglobin and hematocrit values and the number of red blood cells which are far below normal undergo further decrease with the process of aging, while the calculated mean corpuscular hemoglobin remains unchanged. The anemia responds favorably to iron treatment. In nontreated animals the anemia usually leads to death at various ages prior to six months. Iron treatment prolongs the life of anemic animals indefinitely, but the pathological forms of erythrocytes remain in large numbers in the peripheral blood throughout and after the treatment. (auth)

38620 THREE LOCI IN ESCHERICHIA COLI K-12 THAT CONTROL THE EXCISION OF PYRIMIDINE DIMERS AND CERTAIN OTHER MUTAGEN PRODUCTS FROM DNA. **Howard-Flanders, Paul; Boyce, Richard P.; Theriot, Lee (Yale Univ. School of Medicine, New Haven). Genetics, 53: 1119-36(June 1966).**

Twenty-three mutants of Escherichia coli, sensitive to ultraviolet light (uv), were isolated that plate T1 phage normally but form abnormally few plaques when used to plate uv-irradiated phage. These mutants are defective in their ability to repair either their own DNA or that of infecting phage. All the mutants map at one of three loci designated uvrA, uvrB and uvrC, as determined from the time of entry of markers in crosses with various Hfr donor strains. The loci are cotransducible as follows: uvrA with

met 4%; uvrB with bio 80% and gal 20%; uvrC with supH 17% and his 0.3%. Double uvr mutants of types A, B; B, C and C, A are no more than about 20% more sensitive to uv than the most sensitive single mutants. uvrA, uvrB and uvrC mutants are phenotypically similar in all respects so far tested, and there is no evidence of sequential action, or specificity in acting on particular types of defects. A convenient test to distinguish between the A, B, and C mutants depends upon the development of uv resistance in the zygotes in crosses with Hfr strains that carry a complementary uvr mutation. The development of such resistance indicates that in all three loci the wild-type allele is probably dominant in the zygote. The mutants were also labeled with H^3-thymidine, exposed to uv and tested for ability to excise thymine dimers. None of the fully uv sensitive uvrA, B or C mutants were able to excise detectable amounts of thymine dimer during incubation. Certain mutants that were not so sensitive to uv showed an intermediate level of dimer excision, as if some residual activity was retained, but uv sensitivity did not show a strict relationship to the level of dimer release, while uvr mutations, at all three loci, had little effect on the sensitivity to ionizing radiation, but they affected control of the sensitivity of E. coli to certain other mutagens, including bifunctional alkylating agents, nitrous acid and mitomycin C, as well as the DNA degradation that occurred after treatment with uv or mitomycin C. Mutations uvrA, uvrB, and uvrC may thus control an excision nuclease, specific for certain types of defect in DNA while the observed breakdown of DNA may be secondary to excision. (auth)

38621 MUTANTS OF ESCHERICHIA COLI K-12 DEFECTIVE IN DNA REPAIR AND IN GENETIC RECOMBINATION. Howard-Flanders, Paul; Theriot, Lee (Yale Univ. School of Medicine, New Haven). Genetics, 53: 1137-50 (June 1966).

Five x ray sensitive mutants were isolated from a genetically marked F^- strain of E. coli K-12 following treatment with nitrosoguanidine and testing survivors by replica plating for sensitivity to radiation. Each one of the five most x-ray sensitive mutants was found to be defective in ability to form recombinants in suitable crosses. These mutants are able to conjugate with F-gal^+ donors to form Gal^+ recipient strains with almost normal frequency. However, in crosses with Hfr H or Hfr J2 in which transmission of the early markers thr and leu was required, the numbers of recombinants was less than 1% of that formed in comparable crosses with the original strain. In crosses with Hfr 313 that transmitted the chromosome from mtl to his, the number of recombinants formed was between 1 and 10% of those formed with the original strain. These results suggest that the wild-type allele for the recombination defect in these mutants lies between mtl and his, and that the entry of the wild-type allele is able to promote the formation of some of the recombinants which would otherwise be lost. These mutants are able to reactivate ultraviolet (uv)-irradiated T1 bacteriophage (Hcr^+) and carry out the repair of uv-induced pyrimidine dimers in their own DNA with a reduced efficiency. When labeled in their DNA by growth with ^3H-thymidine and then irradiated, the mutants show both a spontaneous release of radioactivity during incubation and a greatly increased release if exposed to uv. Unlabeled log phase mutants exposed to uv show an immediate and prolonged inhibition of ability to incorporate radioactive thymidine. These Rec^- mutants appear to be defective in their ability to terminate DNA breakdown and initiate repair synthesis correctly, following single-strand interruption. The finding that certain recombination-defective mutants are highly sensitive to radiation and that certain mutants selected for high sensitivity to x rays are also defective in genetic recombination, supports the idea that common enzyme mediated steps are involved in the two processes. These steps may include the widening of single-strand gaps DNA repair synthesis, and joining phospho-diester bonds. (auth)

38622 SOME PROTECTIVE MEASURES FOR MEDICAL PERSONNEL AND PATIENTS DURING THE OPERATION OF SUPERHIGHFREQUENCY PHYSIOTHERAPY APPARATUS. Karelin, O. N.; Mishina, I. M. Gig. Sanit., No. 5, 46-51(May 1966). (In Russian).

The Luch-58 and Luch-2 superhighfrequency (shf) generators have recently found wide application in physiotherapy. Medical personnel working with these generators often suffer from headache, rapid fatigability, and disrupted sleep patterns. Since working conditions around these generators have been little studied, the authors used a PO-1 dosimeter to measure power densities in the vicinity of shf generators used for medical purposes. Three tables show the power density values in the vicinity of the control panel of a Luch-58 generator, in the vicinity of a table situated 3m from the generator, in the area of the eyes when the torso is irradiated, and in the gonad area when the lower body is irradiated. All values were expressed in mw/cm^2. It was found that the maximum power density was 0.17 mw/cm^2 in the vicinity of a Luch-58 control panel. At a distance of 4.5m from the generator, power densities did not exceed the maximum permissible level (10 $\mu w/cm^2$). It was therefore concluded that the working table for medical personnel should not be placed closer than 4.5m, or that it should be screened. It was found that the power density in the area of the gonads and eyes could reach 8.7 mw/cm^2 during various therapeutic procedures and cause irreversible lesions in these organs. Patients should also be protected from possible harm from irradiation. The study showed that power density in the vicinity of irradiated body areas could reach 120 to 600 mw/cm^2, which could produce a thermal effect. (auth)

38623 STUDY OF INTERNAL CONTAMINATION WITH ^{90}Sr AND ^{226}Ra IN MAN IN RELATION TO CLINICAL FINDINGS. Mueller, J.; Klener, V.; Tuscany, R.; Thomas, J.; Brezikova, D.; Houskova, M. (Inst. of Radiation Hygiene, Prague). Health Phys., 12: 993-1006(Aug. 1966).

The results of a follow up of a group of fifty-two persons carrying body burdens of ^{90}Sr and ^{226}Ra for a period of about 2500 days are given. The body burdens vary in the group from less than 10 per cent of the maximum permissible to somewhat more than 100 per cent of the maximum permissible burden. The urinary ^{90}Sr excretion data observed up to now do not differ significantly from a power function model with the exponent b = 0.215. The three-exponential model described by other authors is, however, no longer valid and a fourth exponential with a half-life of about 700 days had to be added. A fifth exponential with a still longer half-life was predicted by extrapolation. The large fluctuation in the ^{90}Sr excretion observed from day to day and at different times of the day could be greatly diminished by relating it to calcium excretion. No significant clinical changes could be observed in the exposed group except the signs of radiation dermatitis in some cases. A small but statistically significant increase in the number of red cells, hemoglobin, and hematocrit values could be detected, when comparing the whole group to a group of healthy prospective blood donors. There was, however, no significant difference in these indicators when comparing persons with different levels of body burdens within the group. Karyological investigation of bone marrow cells showed a statistically significant increase in the occurrence of aneuploid cells as compared to healthy controls. Differences in the occurrence of aneuploid cells found in groups with different levels of body burden are at this stage of the study not statistically significant. A significant increase in the rate of chromosomal aberrations could be demonstrated in cases with cumulative body burdens higher then 10 per cent of the maximum permissible. A single cell with a haploid set of chromosomes was found in a female patient with the highest body burden. An increased rate of nonagglutinable red cells was a frequent but not regular finding in the exposed group and no relation to the size of the body burden could be established. (auth)

38624 INTRANUCLEAR ^3H THYMIDINE: DOSIMETRIC, RADIOBIOLOGICAL AND RADIATION PROTECTION ASPECTS. Bond, V. P.; Feinendegen, L. E. (Brookhaven National Lab., Upton, N. Y.). Health Phys., 12: 1007-20 (Aug. 1966). (BNL-9435).

It appears from a study of available data that the degree of early somatic biological effect from intranuclear ^3H is that anticipated on the basis of calculated average absorbed dose to the cell nucleus, at least down to doses of 5 rad or less. This result indicates that the absorbed dose concept holds down to the order of 10^{-11} g or less, and somatic effects can be predicted on this basis; the distribution of ^3H atoms incorporated into DNA as ^{3}HTdR (and ion pairs from the beta particles) are randomly distributed as far as dose calculations for the purpose of predicting somatic effects are concerned; every part of the cell nucleus lies within one ^3H beta range of some part of a chromatid, and the nucleus contains no sizeable contiguous insensitive volume of a radius exceeding the effective range of ^3H beta rays ($1-2\ \mu$); the origin of ^3H beta tracks in, or their close juxtaposition to the DNA molecule does not appear to enhance the degree of somatic effect. Transmutation effects of the disintegrating ^3H nuclide in DNA appear to have been demonstrated to produce genetic mutations in microorganisms, and data suggestive of this mechanism in Drosophila are available. The degree to which this factor in addition to absorbed dose must be taken into account in estimating possible genetic effects in the mammal cannot be assessed adequately at this time, but appears to be small. From available data, it appears that the degree of genetic effect in mammalian cells can be approximated closely from the average absorbed dose to the nucleus. The intrinsic RBE of ^3H beta particles appears to be 1.0 (compared to 250 kvp x rays), rather than the value of 1.7 currently used for radiation protection. (auth)

38625 DOSIMETRY FOR LARGE ANIMAL EXPERIMENTS USING MULTIPLE ^{60}Co SOURCES AND 1 mvp X-RAYS. Menkes, Cirel K. (Naval Radiological Defense Lab., San Francisco). Health Phys., 12: 1115-23(Aug. 1966).

A quadrilateral configuration of four movable uncollimated ^{60}Co sources with a total activity of 9000°C was used to obtain exposure measurements in air and depth doses in a masonite phantom for radiation experiments involving sheep. The depth dose distribution in the phantom in the four source exposure is compared to distributions obtained using a single collimated ^{60}Co source four times in succession to simulate the four source array and exposure geometry, and to 1 Mvp x rays in a bilateral exposure. Distributions of the quadrilateral gamma and x ray exposures differed quantitatively by no more than 5% throughout the phantom thickness. Ionization measurements were made in outdoor pens built to house 100 sheep individually during chronic low-level exposures ranging from 500 mR/hr to 4 R/hr. Exposure rates at the two rows of pens were varied by using several source arrangements. Bilateral depth dose distributions in a sheep phantom exposed in the pens showed that the radiation from the uncollimated sources at the distances of the pens was less penetrating than from a collimated ^{60}Co source at a closer distance (corrected for inverse square effect), and more penetrating than from 1 Mvp x rays except at the phantom surfaces. (auth)

38626 RELATIVE BIOLOGICAL EFFECTIVENESS OF 14 Mev NEUTRONS TO GAMMA-RAYS FOR INDUCING MUTATIONS IN MATURE SPERM OF THE SILKWORM. Murakami, Akio (National Inst. of Genetics, Misima, Japan). Idengaku Zasshi, 41: 17-26(Feb. 1966).

Mature sperm of the silkworm were exposed to fast neutrons or ^{137}Cs γ radiation at late pupal stage. A series of ^{137}Cs γ ray irradiation experiments were run in parallel with those 14 Mev neutrons. For the determination of mutation frequency visible recessive egg color mutations were used as markers. Dose-frequency curves for recovered mutations increased linearly with the increasing dose for both radiations, which indicates that they are due to single-hit events. The frequency curves for mosaics increased non-linearly, indicating that they are of multi-hit nature. Neutrons of 14 Mev energy were approximately 6 times as efficient as γ rays in producing recessive visible mutations in mature sperm of the silkworm. Hence, RBE values of 14 Mev neutrons are larger in mature sperm than in spermatogonia. For the production of mosaics RBE of 14 Mev neutrons relative to ^{137}Cs γ rays was about 5. (auth)

38627 FURTHER INVESTIGATIONS OF THE RESPONSE OF IRRADIATED MOUSE SKIN. Denekamp, J.; Fowler, J. F. (Hammersmith Hospital, London). Int. J. Radiat. Biol., 10: 435-41(1966).

Closely similar skin reactions after doses of 250 kv x rays were found in SAS/4 and C_3H male mice. The comparison of the skin reactions of anaesthetized and non-anaesthetized mice was difficult, and was carried out most satisfactorily on hairless mice. No effect of the anaesthetic was seen. A variation of skin reaction with time of day was sought, but none was found. No difference in single-dose or split-dose skin reactions was observed after 100 or 6000 rad/min of 8 Mev electrons. It was shown that the skin reactions of a second leg in the same mouse irradiated 24 hours after the first were the same as those on the first leg, showing that no systemic protective substance was present to reduce the skin reaction 24 hours after irradiation. (auth)

38628 X-RAY INACTIVATION OF LAMBDA PHAGES. I. DAMAGE ON ADSORPTION AND INJECTION. Hradecna, Zdenka (Univ. of Geneva). Int. J. Radiat. Biol., 10: 443-9(1966).

X-ray-inactivated lambda phages carry about 80% of all lethal damage in the DNA and about 10 to 20% in the adsorption apparatus. On the adsorbed phages, 5 to 10% of the damage prevent the DNA injection. No significantly selective protection is found after irradiation in the presence of protective substances like cysteine, cysteamine or glycerol, which act simply as dose reducers. (auth)

38629 CLINICAL AND PATHOLOGICAL RESPONSE OF GOATS TO WHOLE-BODY IRRADIATION BY GAMMA-RAYS AND FISSION NEUTRONS. Edmondson, P. W.; Batchelor, A. L. (Medical Research Council, Harwell, Eng.). Int. J. Radiat. Biol., 10: 451-78(1966).

Fifty adult male British Saanen goats in equal numbers were given acute whole-body irradiation with either fission neutrons or gamma rays of 2.5 Mev mean energy. The LD 50/30 was about 505 rad for neutrons and 395 R for gamma rays, giving an RBE of 0.8. Higher doses resulted in a fatal gastrointestinal syndrome characterized by severe to absolute anorexia, fluid intake greatly reduced to absent, progressive hemoconcentration from 48 hours and diarrhea from 4 days after exposure. At post-mortem there were mucus casts within the lumen of the small intestine. Deaths in the third and fourth weeks were commonly the result of widespread hemorrhage with severe thrombocytopenia following bone marrow damage. Severe anemia was seen only once and that in a survivor. Although few deaths could be confidently attributed to infection and blood cultures were sterile, bacterial aggregates were nearly always found in the tissues, most commonly in the intestines, liver, and lungs, and fever occurred invariably in the few days before death. Blood urea, proteins, glucose, chloride, and electrolyte measurements showed no radiation-induced changes. No deaths were seen after 30 days in a one-year follow-up. Platelet recovery when it began was usually rapid. The most reliable prognostic sign was a progressive rise in platelet count. Blood lymphocytes began to increase in number at the end of the first week, even in animals which were going to die, but recovery was so slow that even after one year, values were only about half the pre-irradiation mean. The response to the two kinds of radiation was qualitatively very similar. However, epilation was common after neutrons and rare after gamma radiation, and in survivors platelet recovery was distinctly faster after neutron than after gamma radiation. (auth)

38630 COMPARATIVE LETHAL ACTION OF X AND β OF TRITIUM ON E. COLI. Apelgot, Sonia (Institut du Radium, Paris). Int. J. Radiat. Biol., 10: 495-508(1966). (In French).

Bacteria of two strains of E. coli having different radiosensitivities were either labeled with tritiated thymidine or irradiated with x rays. The influences of temperature and of a radioprotector (cysteamine) on the inactivation were studied. The results obtained showed that the survival

curves are exponential after x ray irradiation or tritium disintegrations. In both cases, the slope of the survival curves is similarly affected by temperature or radioprotection. In the experiments with tritium, probability of action of one disintegration and the corresponding one-hit doses were evaluated and compared with those of x rays. The results point to the conclusion that the lethal action of tritium disintegration is due only to the internal β self-irradiation. (auth)

38631 PARTIAL-BODY RADIATION OF QUEEN HONEYBEES. Lee, W. R. (Univ. of New Hampshire, Durham). J. Apicult. Res., 3: 113-16(1964).

The queen honeybee (Apis mellifera) is particularly useful for studying the effect of ionizing radiation. She contains both male and female gametes within her body for several years; can be instrumentally inseminated; and produces both haploid and diploid eggs in large numbers. Methods were developed for high-dose irradiation of either the spermatozoa in the queen's spermatheca, or the oögonia in the anterior region of her ovary without killing the queen. A lead shield was equipped with an air hose, which prevented the queen from crawling further into the lead block, and cellophane tape, which prevented more than the last two visible segments protruding. It was verified that segments VI and VII (the last two visible segments), which contain the spermatheca, could be given excessive doses with a collimated beam of x rays without appreciably reducing the length of life of a queen, provided that the remainder of the queen's body was shielded. Thus, by shielding abdominal segments III to V, queen honeybees survived otherwise lethal doses of radiation; in contrast, irradiating only segments III to V with 10,000 R killed all queens within three weeks, as did whole-body irradiation. After irradiation, four queens given doses as high as 10,000 R laid a normal number of eggs, but all fertilized eggs contained dominant lethals (the only eggs to hatch were those that developed parthenogenetically); this was also true when drones were given 10,000 R before their semen was used for insemination. The spermathecae of five queens were treated with 6000 R and those of three queens with 4000 R, and except for one in the second group who died upon being re-introduced into her colony, all these queens continued egg laying at their normal rate after treatment. Irradiation of oögonia in the anterior part of the ovary of two queens at 13,500 R while shielding the remainder of the abdomen caused death within three weeks. Six queens irradiated with 5400 R laid normally for the following 2 to 4 days, and then their egg-laying rate dropped by 90%. From the low point on the fourth day following irradiation, there was a gradual rise until the end of the season one month later. Nine days after the first irradiation two of the queens were given a second irradiation of 5400 R; this produced permanent sterility after 4 days. (TCO)

38632 THE EFFECTS OF GAMMA RADIATION ON MATING COMPETITIVENESS AND FECUNDITY OF HIPPELATES PUSIO LOEW. Flint, H. M. (State Univ. Station, Fargo, N. D.). J. Econ. Entomol., 59: 96-9 (Feb. 1966).

Studies were conducted on the eye gnat, a pestiferous insect throughout the Southeastern States and other parts of the United States, to determine the effects of γ radiation on its biology and the possible use of radiation in control. Radiation studies have shown that eye gnats of either sex are sterilized by a dose of 5000 R applied to freshly emerged adults or by a dose of 4500 R applied to late-stage pupae, without drastically altering the life span of treated gnats. The effects of sterilizing doses on mating competitiveness, observations on the testes of treated males, and fecundity of treated females are reported. Irradiation was accomplished with a ^{60}Co source which delivered 2200 R/min in air. All gnats were treated either as adults 24–36 hr after emergence or as pupae 2 days prior to emergence. Male gnats which had been sterilized as adults were found to be fully competitive with untreated males in fertilizing females in lab tests. When males were sterilized in the pupal stage, there was a significant reduction in their ability to compete with untreated males. Observations on the testes indicated a significant reduction in the size of testes of males treated in the pupal stage, while testes of males irradiated as adults were similar in size to untreated controls. When females were treated with a sterilizing dose as adults, initial oviposition was 1.6- and 2.3-fold greater than untreated females during the first and second days of oviposition, respectively. Thereafter the untreated females laid greater numbers of eggs to the end of the test period. (BBB)

38633 AGENTS INFLUENCING GRANULOCYTE OUTPUT AND PRODUCTION IN IRRADIATED RABBITS. Feher, Imre; Gidali, Julia; Varteresz, Vilmos. J. Lab. Clin. Med., 67: 966-72(June 1966).

It was demonstrated that an agent stimulating granulocyte output from the bone marrow is produced in rabbits x irradiated with 800 R upon the administration of colloids. However, due to the radiation damage of the bone marrow, no granulocytosis develops in irradiated rabbits. Sera from rabbits irradiated with 600 or 800 R, but not normal sera, when added to normal bone marrow cells in vitro decreased ^{14}C-formate incorporation. This is attributed to the deficiency of a myelopoietic agent possibly produced in the bone marrow. The agent controlling granulocyte output from the bone marrow and the myelopoietic agent are possibly not identical. (auth)

38634 CURRENT CONCEPTS OF RADIATION BIOLOGY AS RELEVANT TO RADIATION THERAPY. Maruyama, Yosh (Univ. of Minnesota Hospitals, Minneapolis). J.-Lancet, 86: 169-76(Apr. 1966).

The response of mammalian cells to ionizing irradiation is reviewed. Evidence indicates that the response of single mammalian cells in vitro and in vivo is characterized by a nearly exponential survival curve, similar to that of all other single cell systems studied. Radioresponse is a function of the intrinsic radiosensitivity, local tissue and cell oxygenation, mode of cell death, and mitotic rate of the cells. Local irradiation control of a tumor in vivo represents the sum of at least two major and three minor components. The two major components are cell killing, that is, the loss of reproductive integrity or proliferative capacity, and growth inhibition. The latter is due to mitotic suppression, division delay and, in some cases, to alteration in the cell growth kinetics. Division inhibition may be associated with the formation of giant cells. The three minor components are immunological, due in part to the release of lethally damaged cells to incite the immunological responses in the host, implying antigenic dissimilarities between normal and tumor cells, vascular, due to alterations to the vascular supply, and abscopal effects, acting through complex factors and possibly humoral agents from remote sites in the host animal. Radioresponse, as viewed by the radiotherapist, is the gross response of tumors and is the commonly used criterion of radiosensitivity. Neither term is related to radiocurability, which is dependent on the inherent biological behavior of the tumor. It is anticipated that with further understanding of basic radiobiological mechanisms, a decreased primary failure rate will be observed and extension of radiotherapy to tumors hitherto considered radioresistant will be possible. (BBB)

38635 QUANTITATIVE RADIOSENSITIVITY STUDIES OF SOLID CARCINOMAS IN VIVO: METHODOLOGY AND EFFECT OF ANOXIA. Clifton, Kelly H.; Briggs, Russell C.; Stone, Helen B. (Univ. of Wisconsin, Madison). J. Nat. Cancer Inst., 36: 965-74(May 1966).

A transplantation assay method was developed for studies of cell survival in solid adenocarcinomas of mice irradiated in vivo. The assay depends on the inverse relationship between the time from grafting until tumors are first palpable and the logarithm of the volume of viable tumor cells inoculated. Sources of variation in the procedure were examined, and LD_{37} values were determined for adenocarcinoma–755 and adenocarcinoma–MTG-B irradiated in vivo with ^{137}Cs γ rays. The D_{37} of MTG-B tumor cells irradiated in situ in dead mice was also determined. The

data suggest that D_{37} values for such tumor cells irradiated in vivo reflect the sensitivity of a relatively resistant, anoxic fraction which comprises a minority of the tumor cell population. Radiation damage to the larger fraction of cells that were more sensitive and presumably better oxygenated was not reflected in the observed D_{37} values, but was interpreted as affecting the lower extrapolation number of the mixed cell population. These studies demonstrate that the kinetics of the acute cytolethal response of solid carcinoma cells irradiated in vivo are similar to those of free cell tumor and culture systems. (auth)

38636 SHIFT IN THE RELATIVE DISTRIBUTION OF BODY NITROGEN BETWEEN SKIN AND CARCASS IN MOUSE RADIATION CHIMERAS. Kretchmar, A. L.; McArthur, W. H.; Congdon, C. C. (Oak Ridge Associated Universities, Tenn. Knoxville Coll., Tenn. Oak Ridge National Lab., Tenn.). J. Nutr., 87: 261-6(Nov. 1965).

Earlier work on nitrogen balance of radiation chimeras suggested the possibility that the relative distribution of kinds of body nitrogen in tissues of these animals might be altered. The purpose of this study was to determine whether measurable changes in nitrogen content of tissues occur in radiation chimeras. A total of 108 male mice was used. The experimental group, 36 mice, were given 950 R total-boxy x irradiation and then 20×10^6 bone marrow cells by intravenous injection; the cells were taken from normal, unirradiated mice of a different strain (homologous bone marrow cells). The 2 control groups were: 36 normal untreated mice; and, 36 mice that were given 950 R x-irradiation and then injected with 20×10^6 bone marrow cells from donors of the same strain (isologous bone marrow cells). The irradiated mice treated with homologous bone marrow cells had a decreased fraction of total-body nitrogen in the carcass and an increased fraction in skin. This shift in nitrogen distribution was detectable as early as 4 days after treatment, but was more definite after 25 days. The results are biochemical evidence that some integumentary structure or structures may be a major target of the graft-versus-host reaction in radiation chimeras. (auth)

38637 EFFECTS OF PULSED FISSION SPECTRUM NEUTRON IRRADIATION. Quaife, M. A. (Veterans Administration Hospital, Omaha); Odland, L. T. J. Occup. Med., 8: 120-6(Mar. 1966).

Sheep were given uniform whole-body exposure to varying doses of pulsed fission spectrum neutrons (neutron to gamma ratio, 5:1) to define the response of the hematopoietic system to this form of ionizing radiation. Four groups of 12 subjects each (with 4 controls) were given 218, 359, 476, and 518 rad, respectively, after which the classic parameters of hematopoiesis were assayed for a period of 60 days. Results of this study suggest that neutrons are less damaging to the blood-forming organs than equal exposure doses of x or gamma rays. This is most probably the result of their inability to penetrate tissue and bone to the same extent. (Pub. Health Abstr.)

38638 ALTERATIONS IN THE FUNCTIONAL STATE OF RAT ADRENAL FOLLOWING THE LETHAL AND SUB-LETHAL, WHOLE-BODY X-IRRADIATIONS. Ichii, Shogo; Kobayashi, Shigeru; Omata, Saburo (National Inst. of Radiological Sciences, Chiba, Japan). J. Radiat. Res. (Jap.), 6: 97-104(Sept.-Dec. 1965).

The effects of whole-body irradiation with lethal and sub-lethal doses (1000 and 600 R) of x ray on the adrenal function of rats were studied by estimating corticosterone and sterol biosynthesis from ^{14}C-acetate in vitro to assess a functional state of adrenals. At 24 hours post-irradiation, the elevated corticosterone biosynthesis was observed in the adrenals obtained from both 600 and 1000 R x irradiated rats, while the accelerated incorporation of ^{14}C-acetate into free sterol was noticed in 600 R irradiated adrenals but not in the 1000 R irradiated. At 48 hours after irradiation, the elevated function of 600 R irradiated adrenals was maintained, while in the 1000 R irradiated adrenals, both the corticosterone and sterol formation in vitro were observed to be depressed markedly. The relationship between lethality and adrenal function in irradiated animals is discussed. (auth)

38639 EFFECT OF WHOLE BODY X-IRRADIATION ON THE SWELLING OF RAT LIVER MITOCHONDRIA. Kawasaki, Shoji (Yamaguchi Univ., Ube, Japan). J. Radiat. Res. (Jap.), 6: 111-21(Sept.-Dec. 1965).

Swelling phenomena of the liver mitochondria were investigated in rats subjected to x irradiation of 1000 R. The rats were killed at 4.5, 6, 17, 22, and 52 hours after irradiation. The rate of swelling of the mitochondria in reaction to various agents decreased after irradiation, reaching its lowest level at 6 hours, but gradually recovering the normal level after 22 hours. Swellings of mitochondria induced by ferrous and ferric ions in a KCl–Tris–HCl medium were accelerated by x irradiation, reaching the maximum at 22 hours. A large amount of lipid peroxide, measured by the degree of formation of thiobarbiturate color matter, was formed in mitochondria treated by ferrous and ferric ions. This formation showed remarkable correlation with the mitochondrial swelling. Irradiation shortened the lag period for the formation of lipid peroxide with Fe^{2+}, as was also observed in the case of mitochondrial swelling. (auth)

38640 MODIFICATION OF PERIVASCULAR SUBCUTANEOUS CONNECTIVE TISSUE REACTION FOLLOWING X-RAY IRRADIATION BY SEVERAL VASOCONSTRICTING AGENTS. Nakatsuka, Haruo; Sakai, Masako; Fujino, Moriji (Osaka City Univ. Medical School). J. Radiat. Res. (Jap.), 6: 122-9(Sept.-Dec. 1965).

The rabbits' subcutaneous connective tissue reaction following x irradiation and inhibitory effects of several vasoconstricting agents against this reaction were studied by means of supravital staining of the stretch preparation of the subcutaneous connective tissue. In irradiated connective tissue perivascular granulocytic emigration was observed at the beginning of the process. They increased in number till 8 to 12 hours, and then degenerated and were devoured by monocytes or histiocytes disappearing in 1 to 3 days. In addition the monocytes increased in number in 1 to 3 days. This tissue reaction was inhibited for 3 post-irradiation hours, when the epinephrine, norepinephrine, phenylephrine, naphazoline, or atropine were administered locally 5 minutes before or immediately after irradiation. Following non-local administration of the phenylephrine or naphazoline 5 minutes before or immediately after irradiation the tissue reaction was inhibited for 5 post-irradiation hours. The post-irradiation treatment by phenylephrine produced less inhibitory effect as compared with pre-irradiation treatment. As the mechanisms of this inhibitory action, the antagonism to the radiation induced vasodilatation and the hypoxia caused by vasoconstriction were discussed. (auth)

38641 CHARACTERISTICS OF THE REACTION TO BACTERIAL ANTIGENS AFTER IRRADIATION. Malʹsev, V. N. Med. Radiol., 11: No. 2, 70-5(Feb. 1966). (In Russian).

Experiments were performed on 40 rabbits subjected to whole-body x irradiation with a dose of 700 R (LD-30/30); the capacity of the dose being 254 R/min and the time of irradiation, 2 minutes and 45 seconds. The reactogenic nature and effectiveness of intravenous and subcutaneous routes of introduction of the vaccine to the irradiated animals were studied. It was found that irradiation enhances the organism's sensitivity to the toxic action of typhoid vaccine. This was substantiated by the sharp aggravation of the general state, hemorrhages and necrosis at the site of the antigen injection, protracted postvaccinal leukopenia, and an acutely marked hypo- or hyperthermic reaction of the irradiated organisms to the administration of the vaccine. Vaccination aggravates the course of radiation sickness and often leads to death of animals of the experimental group. Simultaneously with this the efficacy of vaccination of the irradiated organisms is reduced. (auth)

38642 INFLUENCE OF GASEOUS MEDIA ON THE INJURIES INDUCED IN MICE BY VARIOUS RADIATION DOSES. Smirnov, O. P. Med. Radiol., 11: No. 2, 75-80(Feb. 1966). (In Russian).

The oxygen effect during ^{60}Co gamma irradiation with different dose levels was investigated in mice. The value of the protective action of the oxygen reduction in a dose of 51 R/sec is greater than in irradiation with a dose of 4.68 R/sec. A supposition is made on the diverse participation of oxygen in primary processes of interaction of radiation with the substance during different levels of irradiation. (auth)

38643 STATE OF MEGAKARYOCYTES OF THE BONE MARROW IN PATIENTS WITH MILK-DUCT AND LUNG CARCINOMA DURING RADIOACTIVE COLLOIDAL GOLD THERAPY. Agamova, K. A.; Brin, M. L. Med. Radiol., 11: No. 2, 81-4(Feb. 1966). (In Russian).

The state of megakaryocytes of the bone marrow was investigated in 26 patients treated with radioactive colloidal gold for milk-duct (15 persons) and pulmonary (11 cases) carcinoma. The treatment is attended by the appearance in megakaryocytes of manifestations of dystrophy and phagocytosis. This makes it possible to use elements of the megakaryocytogram as a test-object for assessing the influence of ^{198}Au on the thrombocytes. No profound changes of thrombocytopoiesis were revealed. (auth)

38644 AUTOFLORA AS A TEST OF CLINICAL STUDY OF THE IMMUNOLOGICAL REACTIVITY IN RADIATION INJURIES. Klemparskaya, N. N. Med. Radiol., 11: No. 2, 85-91(Feb. 1966). (In Russian).

Immunological reactivity is one of the most radiosensitive functions of the human and animal organism and by its alteration one could establish the presence of the injurious action of different types of emitters. Under the influence of ionizing radiation a significant (8 to 10 times) increase was observed of the total quantity of microorganisms on the skin and all mucous membranes; an elevation among this microflora of the percentage content of forms capable of hemolyzing human and rabbit erythrocytes, and of strains with a marked enzymatic activity; distribution of B. coli far beyond the limits of the intestinal tract with its appearance in the oral cavity, on the skin, and in the vagina. An increase in the microbial autoflora content occurs in the latent period long before the development of clinical symptoms of radiation injury. Observation of the growth of the quantity of autoflora is of prognostic importance and may serve as a good test for assessing the effectiveness of treatment and it is also suitable for estimating the degree of restoration after radiation injuries. (auth)

38645 RBE OF FAST NEUTRONS BY THE RELEASE OF MUTATIONS IN DROSOPHILA MELANOGASTER. Dauch, Fritz; Apitzsch, Ursula; Catsch, Alexander; Zimmer, Karl G. (Kernforschungszentrum, Karlsruhe, Ger.). Mutat. Res., 3: 185-93(June 1966). (In German).

The RBE of fast neutrons (as compared with x rays) was determined in Drosophila melanogaster for various broods (stages of germ cells) and for sex-linked recessive lethals as well as for translocations between 2nd and 3rd chromosome. A pronounced dependence of RBE on the stage of the germ cells was shown to occur and to account for most of the discrepancies reported in earlier work. Moreover, the RBE was demonstrated to be lower for recessive lethals than for translocations at all stages of spermatogenesis tested. These findings are discussed briefly as to their implications for problems of protection from radiation damage. (auth)

38646 NATURAL AND RADIATION-INDUCED CHROMOSOMAL POLYMORPHISM IN DROSOPHILA. Wallace, Bruce (Cornell Univ., Ithaca, N. Y.). Contract AT-(30-1)-2139. Mutat. Res., 3: 194-200(June 1966).

The retention of x radiation-induced inversions in small populations of Drosophila pseudoobscura whose parental flies were from different geographic origins is discussed. Fifty populations were studied; 5 were found to be polymorphic for newly induced autosomal inversions 6 months to one year later; 3 of these polymorphisms persisted for another 2 years when the experiment was terminated; 3 of the 5 original polymorphisms involved chromosome-two, a chromosome that is generally monomorphic in natural populations. The restriction of naturally occurring polymorphisms in this species to chromosome-three cannot be explained, then, by the absence of fitness heterosis in individuals heterozygous for genes on other chromosomes. Nor can such a lack of fitness heterosis explain the tendency for closely related species (such as D. pseudoobscura and D. persimilis) to utilize homologous chromosomes for adaptive polymorphisms. Alternative possibilities are discussed. (auth)

38647 COMPARISON OF THE MUTAGENIC EFFECTIVENESS OF CHRONIC NEUTRON AND γ IRRADIATION OF MOUSE SPERMATOGONIA. Batchelor, A. L.; Phillips, R. J. S.; Searle, A. G. (Medical Research Council Radiobiological Research Unit, Harwell, Eng.). Mutat. Res., 3: 218-29(June 1966).

Hybrid male mice were given a dose of 214 rad fast fission neutrons (plus 93 rad γ contamination) over twelve weeks, while brothers were given 606 rad γ radiation (plus 2.5 rad neutron contamination) over the same period. Six weeks later they were mated to females homozygous for recessive alleles at seven specific loci. Neutron irradiated mice remained sterile for a further four weeks but γ irradiated mice showed no sterile period. Testis weight fell to less than 20% during neutron irradiation, but to about half normal during the γ irradiation. The frequency of specific locus mutations was $22.9 \cdot 10^{-5}$/locus in the neutron series and $3.9 \cdot 10^{-5}$/locus in the γ series, from which induced mutation rates of $100.6 \cdot 10^{-8}$/rad for neutrons and $4.4 \cdot 10^{-8}$/rad for γ rays were derived, after allowing for spontaneous mutations. Thus the RBE for neutrons is about 23 in these circumstances. A figure of about 20 was arrived at by analysing data on dominant visible mutations. There were indications that chronic neutron exposures were also much more effective than chronic γ for the induction of reciprocal translocations and other chromosomal changes. However, the sex ratio was very similar in the two series. Most of the dominant and recessive mutations tested proved to be homozygous lethals; there were also signs that carriers of newly arisen specific locus mutations were more likely to die before weaning age than non-carriers. The true specific locus mutation frequencies are probably higher than those given here. (auth)

38648 LONGEVITY AND BODY WEIGHTS OF MICE WITH ANCESTRAL SPERMATOGONIAL X IRRADIATION. Schlager, Gunther; Roderick, Thomas H.; Storer, John B. (Jackson Lab., Bar Harbor, Maine). Mutat. Res., 3: 230-6(June 1966).

No consistent effect of ancestral spermatogonial x irradiation on lifespan was found with 50 and 100 R exposure for 7 to 10 generations in genetically homogeneous mouse populations, or with 900 R exposure for as many as 6 generations in genetically heterogeneous populations. The 900 R given in each of 6 generations is the highest x ray exposure of spermatogonia reported to date. Environmental factors of unknown nature reduced lifespan of the males in the homogeneous populations and appeared to interact with the effects of low-dose irradiation to produce a life shortening as ancestral exposure increased. Body weights at maturity decreased significantly with increased ancestral exposure in two of the three generations studied in the 900 R experiment. Pre-weaning body weights also tended to decrease, but the differences were statistically significant in only one of the three generations. No effect of ancestral irradiation on post-weaning body weights was evident in the 50 and 100 R experiment. (auth)

38649 EVIDENCE FOR NONRANDOM REJOINING OF CHROMATID BREAKS AND ITS RELATION TO THE ORIGIN OF SISTER-CHROMATID EXCHANGES. Olivieri, G.; Brewen, J. G. (Oak Ridge National Lab., Tenn.). Mutat. Res., 3: 237-48(June 1966). (ORNL-P-1673).

Studies were made of the relative frequencies of sister-strand exchanges, isochromatid deletions, and symmetrical and asymmetrical interchanges involving daughter endoreduplicated chromosomes (diplochromosomes) in tritiated thymidine-labeled aneuploid Chinese hamster and diploid human cells. It was found that the reunion of broken ends in the endoreduplicated chromosomes was not random and that the ratio of symmetrical to asymmetrical inter-

changes was about the same as the ratio of sister-strand exchanges to isochromatid deletions. These data are interpreted to mean that sister-strand exchanges may be radiation-induced exchanges resulting from isolocus breaks that do not rejoin in the expected random fashion. The very high frequency of interchanges in daughter endoreduplicated chromosomes is taken as evidence in support of site hypothesis. (auth)

38650 COMPARISON OF FREQUENCY PATTERNS BETWEEN WHOLE-BODY AND FRACTIONAL MUTATIONS INDUCED BY X RAYS IN DROSOPHILA MELANOGASTER. Inagaki, Eiichi; Nakao, Yoshio (National Inst. of Radiological Sciences, Chiba, Japan). Mutat. Res., 3: 268-72(June 1966).

Male Drosophila melanogaster were exposed to 1000, 2000, 3000, or 4000 R x radiation and mated two days later with virgin females carrying four visible sex-linked recessive mutations. Careful examination of the F1 generation was made to assess the frequencies of whole-body and fractional-appearing mutations. The data indicate an increase in the frequency of whole-body mutations with increase in radiation dose. There did not appear to be a statistically observable change in the relative frequency of fractional mutations with increase in radiation dose. The ratio of fractional to whole-body mutations tended to decrease with increasing dose in the ranges studied. (C.H.)

38651 EXPERIMENTAL CRITERIA TO STUDY THE RELATION OF INTERNAL β IRRADIATION AND BIOCHEMICAL EFFECTS IN THE CNS. I. DOSIMETRY STUDIES. Valderas, Ramon; Egana, Enrique (Univ. of Chile, Santiago). Nucl. Energy, 152-62(June 1966).

An experimental criterion is presented for the quantitative analysis of β internal irradiation of the CNS. The dose-rate and total-dose from ^{32}P absorbed by different CNS levels: brain cortex, diencephalon, hypothalamus, cerebellum, olfactory bulbs, mesencephalon (midbrain), pons/medulla, and spinal cord, and also whole encephalon and neuro-axis were studied. The radiation depends on the ^{32}P uptake by the nervous tissue itself (studied as CNS levels and as whole encephalon and whole neuro-axis); the CNS levels have a very similar uptake of ^{32}P, except during the first day, during which the olfactory bulbs and hypothalamus show greater uptake. This is valid for all types of experiments one single dose, one month, and four doses. The blood (encephalic blood flow) adds a negligible percentage to the absorbed dose and although its dose-rate is high during the first hours, the blood actually included in the encephalon is in a proportion of 2%, a fact which minimizes its importance as an irradiation factor. The skull bones constitute major contributions in the irradiation of the CNS levels which are contiguous. It is established that the dose-rate is relatively moderate, as in the 90 to 100 days one single dose and one month experiments at 12 days, 50% of the dose is absorbed; in the four dose treatment, 50% at approximately forty days. This happens in spite of the fact that the maximum irradiation velocity occurs during the first days, or remains practically constant as in the one month experiments. The increase in the isotope injected and its form of administration do not influence the ^{32}P uptake and consequently the dose-rate, this latter thus being a simple and additive function. With the dose-rate and total-dose established by means of this study, a relation between the metabolic effects of CNS induced by β-internal irradiation was established. From this relation there may arise the concept of CNS radioresistance (of metabolic character). (auth)

38652 STUDIES ON CHANGES IN BLOOD LIPIDS INDUCED BY ROENTGEN IRRADIATION. Koike, Hiroyuki; Koike, Nobuyuki (Osaka Univ.). Osaka City Med. J., 11: 175-223(1965).

Micro methods are described for the determinations of total lipid, total fatty acid, total cholesterol, total phosphatide, and iodine in blood. The method is easily standardized for routine use in clinical and research studies, and can be subjected to quantitative analysis of lipids in blood of irradiated animals. From the results obtained on rabbits, it seems possible to determine the prognosis of a patient treated with high doses of x rays by measuring total lipid, total fatty acid, total phosphatide, total cholesterol, and iodine values in the blood. (C.H.)

38653 SOME RESULTS OF EXPERIMENTAL STUDY OF RADIATION PATHOLOGY AND APPROACHES FOR THE FURTHER RESOLUTION OF THE PROBLEM. Gorizontov, P. D. pp 5-21 of Patogenez, Eksperimental'naya Profilaktika i Terapiya Luchevykh Porazhenii. Lebedinskii, A. V. (ed.). Moscow, Izdatel'stvo Meditsina, 1964. (In Russian).

The radiation response of living tissues is reviewed. In noting the importance of the nervous system in radiation pathology, it is emphasized that in radiobiology the concept of radiosensitivity and susceptibility of animals must not be confused. The role of the endocrine system in control of functions of the irradiated organism was examined; in particular, it was pointed out that the reaction of the frontal lobe of the hypophysis and the adrenal cortex, resulting from the effect of radiation on the central nervous system at early periods of acute radiation injury, has a protective effect. As to the blood system, reliable information on the hematopoietic function was lacking. Radiation injuries to connective tissue and the role of the humoral component in the development of radiation pathology are also discussed. (H.G.D.)

38654 MECHANISMS OF DISTURBANCE OF CENTRAL REGULATION OF AUTOMATIC FUNCTIONS IN IRRADIATED ANIMALS. Klimovskaya, L. D.; Maslova, A. F. pp 35-9 of Patogenez, Eksperimental'naya Profilaktika i Terapiya Luchevykh Porazhenii. Lebedinskii, A. V. (ed.). Moscow, Izdatel'stvo Meditsina, 1964. (In Russian).

After x irradiation at a dose of 800 rads, the threshold of pupillary reaction of rabbits to electrical stimulation of the Westphal-Edinger nucleus was substantially increased in 1 to 3 days. It was not possible to detect the relationship between change in adrenaline and noradrenaline content in the adrenals under conditions of stimulated hypothalamus (H) characteristic of the reaction in the controls. When H was stimulated, the acetylcholine (I) level in the upper cervical sympathetic ganglion increased in 1 to 3 hours after x-irradiation of 2.5 to 32 micrograms/gram of bodyweight. At one day post-irradiation the acetylcholine level was sharply reduced, but the concentration of cathechinamines (II) gradually rose. Upon stimulation of H during the first hour post-irradiation the content of acetylcholine was reduced, but the level of cathechinamines remained unchanged. In unirradiated animals stimulation of the hypothalamus induced an increase in acetylcholine level (by 90%) and the almost total disappearance of II from the ganglion. After a day following irradiation the reaction to stimulation of H was normalized. The quantitative changes in I and II noted above confirmed the hypothesis of the reciprocal relationships of these compounds in the synaptic transmission of impulses to ganglia. (ATD)

38655 CONDITIONED REFLEX DURING ^{60}Co γ IRRADIATION OF FISH AND RABBITS. Tsypin, A. B. pp 46-9 of Patogenez, Eksperimental'naya Profilaktika i Terapiya Luchevykh Porazhenii. Lebedinskii, A. V. (ed.). Moscow, Izdatel'stvo Meditsina, 1964. (In Russian).

Total ^{60}Co gamma radiation at a dose rate of 0.1 to 0.5 R/sec over a period of 5 to 10 seconds for fish and 3 to 4 seconds for rabbits was used as a conditioned stimulus. Electric skin shock was used as the unconditioned stimulus. After 4 to 13 combinations of irradiation with electric shock the fish began to respond with a motor reactor only to irradiation. The conditioned reflex appeared in the rabbits after 15 to 50 combinations of irradiations with electric shock. The percentage of conditioned reactions to the total number of conditioned stimuli varied from 31 to 51% for the fish, and from 26 to 48% for the rabbits. When the total dose exceeded 250 to 500 R, sometimes a decrease in the strength of the conditioned reflex was observed. Removal of the hypothalamus eliminated completely the possibility of the appearance of a conditioned reflex to gamma irradiation. Radiation also served to stimulate various receptor systems such as the olfactory tract and the splanchnic nerve. (TTT)

38656 ROLE OF AUTOINFECTION IN DEVELOPMENT OF THE HEMORRHAGIC SYNDROME DURING

ACUTE RADIATION SICKNESS. Kiselev, P. N.; Nikitina, K. I.; Cheng, Shao-chang; Karmanova, Z. P. pp 49-61 of Patogenez, Eksperimental'naya Profilaktika i Terapiya Luchevykh Porazhenii. Lebedinskii, A. V. (ed.). Moscow, Izdatel'stvo Meditsina, 1964. (In Russian).

Guinea pigs were given an x-ray dose of 200 R, and then killed daily over a period of 15 days. The presence of bleeding in various organs was determined by visual observation and these observations were related to the number of bacteria per 0.1 ml of blood or per 100 mg of tissue. It was found that autoinfection always preceded the appearance of bleeding. The endotoxin of E. coli was given to irradiated and control animals at a dose of 0.1 to 0.3 mg/kg of body weight over a period of 10 days. The endotoxin caused heavy bleeding in the unirradiated animals. All the other signs of severe radiation sickness were present. The blood clotting time decreased. Strong leucopenia was observed. A daily endotoxin dose of 1 mg/kg of body weight simulated the effects of an x ray dose of 200 R. A maximum in hematopoietic suppression was noted on the 10th day after irradiation or after initial administration of the endotoxin. The administration of 0.3 mg/kg of endotoxin to guinea pigs given an x ray dose of 200 R resulted in stronger bleeding, greater fragility of the blood vessels, and higher bacteria counts in the blood and tissues as compared with the guinea pigs who were given only an x ray dose of 200 R. The maximum in leucopoietic depression was observed on the 4th day instead of the 7th day with irradiation alone. The administration of endotoxin increased the blood clotting time by 40% in comparison with the animals which were irradiated without being given any endotoxin. (TTT)

38657 PULMONARY CIRCULATION DURING ACUTE AND CHRONIC RADIATION SICKNESS. Amosov, I. S. pp 61-9 of Patogenez, Eksperimental'naya Profilaktika i Terapiya Luchevykh Porazhenii. Lebedinskii, A. V. (ed.). Moscow, Izdatel'stvo Meditsina, 1964. (In Russian).

Impairment of pulmonary circulation was studied by the method of experimental angiography. The method made it possible to examine the same animal repeatedly without injury. The effectiveness and safety of the method was tested in 50 control rabbits. Roentgenography was carried out by means of fast exposures (15 in succession at 0.5 and 1 sec intervals). The rabbits (180) were irradiated with 1,000 R (dose rate 25 R/min) either once or several times, 25 R daily and then subjected to a clinical-roentgenological examination. Angiography was used to determine the rate of blood flow in individual phases of pulmonary circulation (arterial, capillary, venous) and length of time it took for the contrast substance to move from the orifices of the venae cavae to the aorta. Hemodynamic disorders in the lungs during radiation sickness in relation to individual peculiarities may reflect the pattern characteristic of the dystonic, hypertonic, or hypotonic syndrome. The latter two types of disorders are unfavorable from the standpoint of prognosis. Acute radiation sickness is characterized by general hemodynamic disorders; chronic radiation sickness, by lesions of the small blood vessels of the lungs. (ATD)

38658 CHANGES IN THE BLOOD VESSELS DURING ACUTE RADIATION SICKNESS. Il'inskii, D. A.; Kuznetsov, V. I.; Mozzhukhin, A. S. pp 70-8 of Patogenez, Eksperimental'naya Profilaktika i Terapiya Luchevykh Porazhenii. Lebedinskii, A. V. (ed.). Moscow, Izdatel'stvo Meditsina, 1964. (In Russian).

The blood vessel tonus of irradiated dogs was determined by measuring the rate of propagation of a wave along an artery or vein. The tonus is characterized by the modules of elasticity for the blood vessel wall. It was found that the modulus of elasticity or the tonus of muscular arteries increased with irradiation. On the other hand, the change in tonus of elastic arteries such as the aorta was much smaller, or even fell off somewhat (the modulus of elasticity decreased). After allowing for the contraction in blood vessel size and a drop in blood pressure, it is concluded that the tonus of the fine arterial vessels is increased. The data indicated a decrease in the tonus of the veins. A decrease in the volume of circulating blood was noted. (TTT)

38659 FUNCTIONAL AND MORPHOLOGICAL ALTERATIONS IN THE BRONCHIO-PULMONARY SYSTEM AND GASTRO-INTESTINAL TRACT DURING CHRONIC RADIATION SICKNESS. Kishkovskii, A. N. pp 79-85 of Patogenez, Eksperimental'naya Profilaktika i Terapiya Luchevykh Porazhenii. Lebedinskii, A. V. (ed.). Moscow, Izdatel'stvo Meditsina, 1964. (In Russian).

A total of 218 rabbits was given daily x ray dose of 5, 10, and 25 R, or total doses of 800, 1000, and 1500 R. X ray studies of the thoracic cage including bronchography, and also contrast studies of the stomach and intestine, were carried out over a period of three years and more. Disturbances in the tonus of the bronchi in the form of dystonia and dyskinesia were noted from the x ray studies. The lumen of the large bronchi were frequently widened while the smaller bronchi had contracted sometimes to the point of spasm. The evacuatory function of the bronchi was lowered significantly so that the contrast substance after bronchography was retained for a long time in the alveoli and bronchi. Respiratory disturbances and secondary infections were noted. Serious disturbances were observed in the evacuatory function of the gastro-intestinal tract. The tonus tended to be low, peristalsis was weakened, and the stomach and intestine tended to evacuate slowly. (TTT)

38660 FORMATION OF ORGANIC PEROXIDES AS ONE OF THE FIRST BIOCHEMICAL REACTIONS TO RADIATION. Zhulanova, Z. I.; Romantsev, E. F. pp 93-8 of Patogenez, Eksperimental'naya Profilaktika i Terapiya Luchevykh Porazhenii. Lebedinskii, A. V. (ed.). Moscow, Izdatel'stvo Meditsina, 1964. (In Russian).

Mice were given a lethal x ray dose of 1500 R, and the content of organic peroxy compounds (OPC) was determined. The OPC content increased 30 to 60 seconds after irradiation, fell back to normal, and increased again by 75% on the 3rd day after irradiation. A study of OPC formation in separate tissues showed the formation of OPC in the spleen immediately after irradiation, and an accumulation of OPC in the spleen, kidneys, and liver on the 3rd day after irradiation. The amount of organic peroxy compounds (OPC) increased by a factor of 1.4 to 4 in the neutral fat fraction. Special in vitro experiments showed that no OPC compounds were formed on irradiating the phospholipid fraction. It was found that 1 g/kg of cysteine, 0.15 g/kg of beta-mercaptoethylamine (MEA), and 0.30 g/kg of beta-mercaptopropylamine (MPA) as protective substances decreased the amount of organic peroxy compounds formed during irradiation. On maintaining the animals under oxygen deficiency (10% oxygen in the air) it was found that a smaller amount of OPC tended to form. (TTT)

38661 BIOCHEMICAL ASPECTS OF IONIZING RADIATION EFFECTS ON THE HYPOPHYSIS-SUPRARENAL SYSTEM. Grozdenskii, D. E.; Bagramyan, E. R.; Ivanenko, T. I. pp 98-105 of Patogenez, Eksperimental'naya Profilaktika i Terapiya Luchevykh Porazhenii. Lebedinskii, A. V. (ed.). Moscow, Izdatel'stvo Meditsina, 1964. (In Russian).

The ACTH content in the front part of the hypophysis of rats given a lethal x ray dose was determined by collecting the hypophysis 3 hours after the irradiation and noting the decrease in concentration of ascorbic acid in the adrenals of 5 to 7 day rats. The rat adrenal reacted to the administered ACTH. No difference from the controls could be observed 3 hours after the irradiation. In addition, no ACTH could be found in the peripheral blood. ACTH was injected into hypophysectomized rats with and without a lethal x ray dose. The decrease in ascorbic acid content of the right adrenal as compared with the left adrenal did not depend on whether or not the rat was irradiated. The disappearance of exogenous ACTH from the peripheral blood was found to go at the same rate in irradiated and in control animals. It was concluded that radiation did not damage the ferment systems responsible for the biosynthesis of the corticosteroid. (TTT)

38662 CHANGES IN BIOCHEMICAL AND PHYSIOLOGICAL INDICIES IN GUINEA PIGS DURING INTERNAL

CHRONIC IRRADIATION. Balmukhanov, S. B.; Kazaeva, F. M.; Servetnik-Chalaya, G. K.; Aitabaev, T. Kh.; Saibekov, T.; Arykova, M. A. pp 115-20 of Patogenez, Eksperimental'naya Profilaktika i Terapiya Luchevykh Porazhenii. Lebedinskii, A. V. (ed.). Moscow, Izdatel'stvo Meditsina, 1964. (In Russian).

Guinea pigs were given a daily dose of 0.0002 mC of ^{90}Sr by mouth. The ^{90}Sr distribution in the organs and tissues was determined by autoradiography and by counting the ashed residue on an end-window counter. The bone was the critical organ, and the integral dose to this organ was calculated. Changes in biochemical and physiological indexes were followed for 30 days after administration of ^{90}Sr. (C.H.)

38663 RESTORATION OF BONE MARROW TISSUE IN ACUTE RADIATION SICKNESS. Gruzdev, G. P.; Fedotova, M. I.; Shcherbova, E. N. pp 120-3 of Patogenez, Eksperimental'naya Profilaktika i Terapiya Luchevykh Porazhenii. Lebedinskii, A. V. (ed.). Moscow, Izdatel'stvo Meditsina, 1964. (In Russian).

A total of 140 Wistar rats was given a ^{60}Co γ dose of 700 R. The total number of bone marrow cells in the femur (by the method of Mantz), the mitotic index, the duration of a mitosis, and the morphological composition of the peripheral blood cells were determined on the 6th and 7th days after the irradiation. During this time there was no discharge of regular cell elements from the bone marrow to the peripheral blood. Bone marrow recovery was determined primarily by mitotic cell division. The average durations of a mitosis were found to be 18.8 and 18.3 minutes by two different methods. This behavior indicated that bone marrow recuperation was due to mitotic cell division and that there was no extensive cell death during recuperation. The average interphase of the bone marrow cells in the irradiated rats on the 6th to 7th day after irradiation was 40 hours, which was long compared to an interphase of 18 hours in the controls. The duration of a mitosis for different cellular elements of the bone marrow such as reticular, erythroid, or myeloid elements was the same or very close in value. (TTT)

38664 ROLE OF TOXINS IN RADIATION-INDUCED CELL INJURY. Kuzin, A. M. pp 131-47 of Patogenez, Eksperimental'naya Profilaktika i Terapiya Luchevykh Porazhenii. Lebedinskii, A. V. (ed.). Moscow, Izdatel'stvo Meditsina, 1964. (In Russian).

The thesis is developed that toxic metabolites are formed as a result of cell irradiation, and these new compounds have a profound effect on the cell. It is noted that 1.5×10^6 excitations per cell arise on administering a lethal dose of 500 R. If the cell nucleus is irradiated in the absence of the cytoplasm, no visible damage is observed. On the other hand, toxic products from the irradiated cytoplasm cause damage to the nucleus. Local leaf irradiation of young Vicia faba plants result in a slowdown in mitoses in the upper parts of the plant which were protected from radiation. A water extract containing antimitotic substances can be isolated from the irradiated plants, and can be used to stunt plant growth. These toxic substances not only slow down cell division but also cause chromosomal aberrations. The uptake of phosphorus and adenine tagged with ^{14}C is slowed down. The evidence indicates that these toxic intermediates have a quinoid or semiquinoid structure. Numerous observations show that toxic substances can be detected in the blood stream after irradiation. Blood transfusions from an irradiated animal to a control can result in leucopenia, for example. The data show that anomalous irradiation products have toxic effects on various life processes. (TTT)

38665 INBORN RADIATION SYNDROME INDUCED EXPERIMENTALLY. Piontkovskii, I. A.; Gol'dberg, M. B. pp 147-53 of Patogenez, Eksperimental'naya Profilaktika i Terapiya Luchevykh Porazhenii. Lebedinskii, A. V. (ed.). Moscow, Izdatel'stvo Meditsina, 1964. (In Russian).

Data are given on postnatal manifestations of radiation sickness (RS) in animals irradiated at different periods (P) of intrauterine development (P of preimplantation-I; P of main organogenesis-II; fetal P-III). With irradiation and P-I, the prenatal mortality of the embryos was high, but the surviving offspring were born without any symptoms of RS. With irradiation and P II, high radiosensitivity of the embryo was characteristic, but the inborn radiation syndrome did not appear. The newborn animals exhibited no changes in composition of the peripheral blood due to the marked reparative capacity of elements of the embryo, particularly the hematopoietic. After P II was completed, resistance of the embryo to irradiation increased. Irradiation in P III caused symptoms to arise in the newborn that were characteristic of RS, chiefly changes in the blood (anemia, leukopenia, subcutaneous hemorrhages, etc.). One of the manifestations of inborn RS after irradiation in P III was the high mortality rate in the postnatal period (rabbits - 37%, rats - 33%, dogs - 60%). It is believed that the cause of RS of the fetus may be either the direct or indirect effect (due to the mother becoming sick) of radiation. (ATD)

38666 MECHANISM OF DEATH OF ANIMALS WITH THE MOST ACUTE FORM OF RADIATION SICKNESS. Domshlak, M. P.; Sedov, V. V.; Nevskaya, G. F.; Petrov, R. V. pp 153-62 of Patogenez, Eksperimental'naya Profilaktika i Terapiya Luchevykh Porazhenii. Lebedinskii, A. V. (ed.). Moscow, Izdatel'stvo Meditsina, 1964. (In Russian).

A total of 575 mice, 50 rats, and 45 rabbits was investigated to study the mechanism of death in 3½ days after exposure to x-ray doses of 1,000-15,000 R. It was concluded that injury to the intestine is a leading factor in the mechanism of death of the animals with the most acute form of radiation sickness. Shielding the intestine during irradiation completely blocked the effect of the dose plateau and the mortality curve assumed its ordinary form for acute radiation sickness. With doses ranging from 1,500 to 13,000 R the survival time of the mice increased from 4.3 to 6.3 days. However, intestinal lesions are not the only cause of death of animals with the most acute form of radiation sickness. Significant changes were found in the cardiovascular system and liver. It was found that autoinfection, impairment of adrenal function, and disruption of the oxidation-reduction processes do not play a decisive role in the death of animals in 3½ days. (ATD)

38667 DYNAMICS OF ALTERATIONS IN MICROFLORA OF ORAL CAVITY MUCUS MEMBRANE IN DOGS SUFFERING FROM ACUTE RADIATION SICKNESS. Shal'nova, G. A.; Sosova, V. F. pp 287-9 of Patogenez, Eksperimental'naya Profilaktika i Terapiya Luchevykh Porazhenii. Lebedinskii, A. V. (ed.). Moscow, Izdatel'stvo Meditsina, 1964. (In Russian).

Dogs were given a ^{60}Co γ dose of 350 R, and apes were given a ^{60}Co γ dose of 300 to 630 R. The presence of intestinal bacilli in the mouth was tested with the use of paper smears and subsequent growth of bacterial colonies on Petri dishes. The unirradiated dogs did not show any intestinal bacteria in the mouth. The irradiated dogs showed the presence of E. coli in 23.6% of the cases, especially near the end of the animal's life. The number of coccal forms increased. The irradiated apes showed the presence of E. coli in 18.3% of the cases compared to 8.8% in the controls which should be due to fecal contamination. It was surprising to find 91.3% of the control apes showed the presence of E. coli after being treated with massive doses of antibiotics compared to 90.9% in the irradiated apes treated with antibiotics. The spread of the intestinal bacilli indicate a breakdown in natural immunity. (TTT)

38668 ETIOLOGY OF CHILDHOOD LEUKEMIA: EPIDEMIOLOGIC EVIDENCE. Miller, Robert W. (National Inst. of Health, Bethesda, Md.). Pediat. Clin. N. Amer., 13: 267-77 (May 1966).

The possible role of ionizing radiations, chemical compounds, viruses, and genetic factors on leukemogenesis in children is reviewed. The leukemogenic capacity of ionizing radiation was first accurately evaluated as a result of the atomic-bomb explosions in Hiroshima and Nagasaki which exposed large numbers of people to a wide range of radiation dose. There is now convincing evidence that radiation in sufficient dose is leukemogenic in man. The re-

sponse was proportionate to the dose, and, unlike hospital series of patients exposed to x ray for medical purposes, can be attributed to no variable except radiation. This is consistent with results of animal experimentation. The 7-yr post-exposure peak in the occurrence of leukemia among atomic bomb survivors is of interest with respect to a similar pronounced peak in United States leukemia mortality rates at four years of age among white children only. There is no peak at this age among nonwhite children. The implication is that the high rate at four years of age among white children occurs because of some event before conception, in utero, or soon after birth, and that the nonwhite population is either not exposed or not susceptible to its leukemogenic effect. The most convincing evidence that partial-body irradiation in sufficient dose can induce leukemia in man comes from the study of x-ray-treated ankylosing spondylitis patients. The results were similar to those from the study of Japanese atomic-bomb survivors. Fetal tissues are unusually susceptible to the leukemogenic effect of radiation as two large studies indicate on the basis of in utero exposure to diagnostic irradiation. Exposures of mothers or fathers to diagnostic x-ray before conception of their children also appears to increase the risk of childhood leukemia. In a study of 319 leukemic children as compared with a randomly selected control group it was found that such parental exposure occurred 30 to 100% more often among the cases than among the controls. In this study as in others there is the problem of differences in the accuracy of reporting histories by parents of children with cancer as compared with other parents and the possibility that the primary relation is to ill health and not to the diagnostic x-ray exposures. (60 references.) (BBB)

38669 ACTION SPECTRA FOR PHOTOREACTIVATION OF MUTATION TO PROTOTROPHY IN STRAINS OF ESCHERICHIA COLI POSSESSING AND LACKING PHOTOREACTIVATING-ENZYME ACTIVITY. Kondo, S. (Osaka Univ.).; Jagger, J. Photochem. Photobiol., 5: 189-200 (Feb. 1966). (ORNL-P-1081).

There are two types of damage induced in Escherichia coli by far uv (2537 Å) radiation that can be distinguished by their patterns of response to recovery treatments. The first class, represented by killing and by mutation to streptomycin resistance, is photoreactivable in the usual E. coli strains but under various conditions may or may not show photoreactivation in strains that lack photoreactivating-enzyme activity. The second class is represented by certain mutations from auxotrophy to prototrophy that are photoreactivable in all strains and for all conditions so far tested. The action spectrum and dose-rate dependence for photoreactivation of mutation to prototrophy in late lag-phase cultures of E. coli ^{3}Hr30 (which lacks active photoreactivating enzyme) are roughly similar to those for photoprotection from killing in other strains. It is suggested that photoreactivation of this mutation in H/r30 is an indirect effect, similar in mechanism to photoprotection. The action spectrum and dose-rate dependence for photoreactivation of mutation to prototrophy in late lag-phase cultures of E. coli ^{3}Hr30-R (which possesses active photoreactivating enzyme) are roughly similar to those for photoreactivation of killing in most other strains. It is suggested that photoreactivation of this mutation in H/r30-R is a direct effect at long wavelengths, but that there is an indirect component at short wavelengths. It was found that, under the conditions of these experiments, indirect photoreactivation of killing in H/r30 and H/r30-R is weak or nonexistent. (BBB)

38670 MIXED CLONES OF UV-INDUCED MUTANTS IN KAPPA PHAGE. Kaplan, R. W. (Univ., Frankfurt am Main). Photochem. Photobiol., 5: 261-4(Mar. 1966). (In German).

Clear-plaque mutations of phage κ of Serratia marcescens are induced by extracellular uv irradiation in a 2-hit process. The 2-hit-nature cannot be due to induction of one hit in each of the two DNA strands since replating the contents of 97 wild-type plaques of uv survivors (uv dose = 4.5 min) revealed only 1 case of heterozygosity; at least 20 cases would have been expected if phage with 1-hit-mutations formed phages looking like the wild type. On the other hand, only one case of heterozygosity was observed among replatings of 94 c-mutants induced by the uv dose of 4.5 min (survival 10^{-3}); most of the plaques contained pure c-type. The pure c-mutant clones are probably due to recessive lethal lesions in the nonpremutated DNA strand. This is indicated by the dose dependence of the frequency of heterozygotes; at a dose of 3 min uv (survival 1.2×10^{-2}) 9 heterozygotes were observed among 95 mutants tested. From these numbers the rate of induction by uv of the recessive lesions can be calculated. The data at the higher dose are in satisfactory agreement with the calculated rate. Other types of plaque mutations (e, t, b) also showed heterozygosity. Two cases of abnormal heterozygosity were observed; one contained 2 stable mutant types (c and b), another one wild type, c-type, and l-type. (BBB)

38671 POSSIBILITIES OF USE OF RADIATIONS IN THE CONTROL OF INSECTS. Nardon, P. (Inst. National des Sciences Appliquees, Lyon). Phytoma, 15: 7-12(Jan. 1963). (In French).

Use of ionizing radiation to control insect populations of economic interest is discussed in terms of direct techniques and indirect ones. Direct means include the irradiation of stored food stocks, such as the use of radiation to control Sitophilus oryzae in stored grain. Use of radiation for parasitized cereals is preferred to chemical insecticides because of the presumed absence of toxic residues after acceptable doses of radiation. Data are given on the radiosensitivity of some Sitophilus species exposed to ^{60}Co. The threshold of sensitivity of adult S. sasakii was found to be 5000 R for males and 6000 to 8000 R for females. After a dose of 2000 R, which does not modify longevity of the insect, its fertility is halved. Thus, 2000 R irradiated and nonirradiated females produced an average of 101 and 249 offspring, respectively. A 4000-R dose reduced fertility to $1/25$ of normal for 27 days, and after two months the insects were almost completely sterile. A dose of 5000 R caused transient sterility, from the 7th to 12th day. Practical methods of using ionizing radiations to eradicate cereal pests are stated. The indirect use of radiation in insect control, particularly the sterile-male technique, is also considered. Data applicable to Musca domestica, Ephestia kuehniella, and Anthonomus grandis are discussed. (BBB)

38672 EFFECT OF X-RADIATION ON SPORE GERMINATION AND STABILITY OF VIRULENCE IN USTILAGO AVENAE. Holton, C. S. (Dept. of Agriculture, Pullman, Wash.); Nilan, R. A. Phytopathology, 56: 265-8(Mar. 1966).

Two kinds of spore populations (of known homozygous virulence restricted in range to a single host variety and a pedigreed line known to carry genes for total avirulence on a series of varieties) were used in an attempt to induce mutation for virulence in U. avenae by x rays. Spore forms in both the diploid and the haploid nuclear stages were used. The spores were irradiated with x rays produced at 300 kv and a dose rate of 1100 R/min, and the doses delivered were 75, 150, 200, 250, and 300 kR. Although radiation at all doses reduced spore viability, the percentage reduction did not follow an orderly, downward trend with each dosage increase. Thus, germination was reduced least at 150 kR and most at 200 kR. The effect of x radiation on germination type in U. avenae reflects interference with growth processes related to meiosis. Although the basic effect is the same at all exposure doses, the impact is least at the lowest and most pronounced at the highest exposure doses. The first and most consistent visible symptom of radiation damage in the germinating spores of U. avenae is the increased length of the promycelium. In the germination of irradiated spores, only occasionally does the mother spore function as a promycelial cell. Variable functioning of the promycelial cells, ranging from sporidial production and mycelial branching to fusion and segmentation, is another symptom of radiation damage in germinating spores. Radiation failed to alter the basic apparent monogenic virulence of the spore population used. The spore lots from all radiation dosages exhibited the same virulence pattern as the original line. Compatible combinations of monosporidial cultures derived from

irradiated spores failed to exhibit any degree of deviation from the original virulence pattern, nor did x radiation induce mutation to virulence in a pedigreed compatible pair of monosporidial lines apparently nonpathogenic on any variety. The radiation effect on growth type was only temporary, and the progeny of the surviving irradiated sporidia retained the avirulence of their progenitor lines. (BBB)

38673 EFFECT OF GAMMA IRRADIATION ON RESPONSE TO ERYTHROPOIETIN OF NON-FASTED RATS. Eskuche, Irma; Hodgson, George (Univ., Chile, Santiago). Proc. Soc. Exp. Biol. Med., 122: 440-2(June 1966).

The effect of gamma irradiation on the erythropoietic response to erythropoietin (EP) in non-fasted rats depends on the time of irradiation in relation to EP injection. There is maximum sensitivity to irradiation when it is given 3 hours before or 24 hours after EP. Radiosensitivity is at a minimum when irradiation is given 1 to 3 hours after EP injection. Fractional depression of erythropoiesis by varying doses of gamma rays is less in animals injected with EP, when it is given before irradiation. There is no effect of EP on fractional depression produced by irradiation given 6 hours before EP. (auth)

38674 ASTROGLIAL REACTIONS TO IONIZING RADIATION - WITH EMPHASIS ON GLYCOGEN ACCUMULATION. Miquel, J.; Haymaker, W. (Ames Research Center, Moffett Field, Calif.). Progr. Brain Res., 15: 89-114(1965).

A description is given of the effects of α particle and x irradiation on cerebral astroglial cells and blood vessels. The materials and methods are reviewed, in which young rats received various dosages of x-irradiation in the head. A constant-potential x-ray therapy unit was the source of the irradiation, and the 60-in. cyclotron at Berkeley and Heavy Ion Linear Accelerator (HILAC) were the sources of α particles. Shortly after exposure of the brains of rats to x-ray of α particles, disturbances in vascular permeability, glial mitosis and edema of the white matter were observed. Accumulation of glycogen in the astroglial cells was especially noted. The glycogen increase is observed in the absence of morphological changes in the brain cells, and is found to be maximal in the gray matter. It is concluded that the disturbances in the glycogen metabolism appear to be associated with a derangement of the aerobic metabolism of the astroglia-neuron metabolic unit. (auth)

38675 TOLERANCE OF THE HEART TO IONIZING RADIATIONS. Beltrami, Mario (Consorzio Provinciale Antitubercolare, La Spezia, Italy). Progr. Med., 21: 52-8(Jan. 31, 1965). (In Italian).

This review considers the relative radiosensitivity of various tissues, particularly of myocardium. Myocardium and muscle tissue in general are among the least radiosensitive in the body. Clinical reports of myocardial injury as a result of radiotherapy are surveyed, and an attempt made to estimate the dose threshold for cardiac damage. Electrocardiographic evidence of myocardial injury is described. Doses higher than 5000 R delivered in a short period of time appear to sometimes result in heart damage as a direct response to irradiation. More frequently indirect effects on the vascular system of the heart may be responsible for myocardial injury. Pericardial changes can also be implicated in some cases, and pulmonary fibrosis or pneumonitis may be superimposed on heart damage. Proposed recommendations for avoiding heart injury include, excluding the heart from the tissue volume receiving the maximum therapeutic dose, cardiac pathology observed before radiotherapy is not an absolute contraindication to thoracic irradiation; nor are such complications developing in the course of therapy to be considered as a reason for terminating therapy, and cardiac conditions present before radiotherapy should receive appropriate treatment before irradiation of the thorax is commenced. (BBB)

38676 CONTRIBUTION TO THE ESTIMATION OF RADIOSENSITIVITY IN DOMESTIC FOWL (GALLUS DOMESTICUS). Prochazka, Z.; Hampl, J. (Research Inst. of Veterinary Medicine, Brno). Radiobiol. Radiotherap., 7: 231-5(1966).

An attempt was made to determine the $LD_{50/14}$ in adult hens and cocks of the New Hampshire breed, 6 to 12 months of age, exposed to irradiation by an x ray apparatus under the following conditions: 175 kV, 15 mA, 1.0 Al, 0.5 Cu, focal distance 55 cm, dose rate 40 R/min. The measured dose rate was checked by measurements performed on a paraffin dummy. The $LD_{50/14}$ was found to be 1265 R, in range of 1113 and 1427 R, resp. ($P = 0.05$). These results were compared with those obtained by probit analysis and two-dose interpolation method. (auth)

38677 CONTRIBUTION TO THE QUESTION OF BREED-SPECIFIC RADIOSENSITIVITY. Mach, P.; Vinkler, A. (Research Inst. for Veterinary Medicine, Brno). Radiobiol. Radiotherap., 7: 237-40(1966).

Breed-specific radiosensitivity to a single whole-body dose of 800 R x radiation was studied using chickens of 5 various breeds and one group of crossbred birds. A high percentage of mortality was found in breeds of extreme characteristics ($LW_{\bar{c}s}$ and CW) with extremely unbalanced metabolism. It appears, therefore, that breed-specific radiosensitivity may be related not to the amount of irradiated mass with respect to its total volume but to the balance of metabolic processes. This hypothesis applies only to purebred birds where the intensity of metabolism is determined on the genetic basis as a breed characteristic. (auth)

38678 INFLUENCE OF X-IRRADIATION ON THE COURSE OF ADRENALIN-LYMPHOCYTOSIS. Szasz, Gy.; Voeroes, I.; Lakos, J. (Korvin Otto Krankenhauses, Budapest). Radiobiol. Radiotherap., 7: 241-7(1966). (In German).

The course of the lymphocyte curve following the administration of adrenaline changed typically after x irradiation with high radiation doses, 2 to 3000 R skin dose in the case of local irradiation. Mobilization of lymphocytic reserves and the consecutive lymphocytosis did not occur. The cause of this phenomenon possibly is an immediate damage of the lymphoreticular system. It was concluded that the adrenaline test is valuable for establishing an eventual radiation injury and that in the case of a normal result of the adrenaline test the suspicion of a radiation injury may be dropped with absolute certainty. A further advantage of this method is that it is very simple; it may be done in every routine laboratory. (auth)

38679 CHANGES OF THE CONTENT OF ASCORBIC ACID, DEHYDROASCORBIC ACID, AND REDUCED GLUTATHIONE IN THE BRAIN OF IRRADIATED RATS. Tomana, M. (Charles Univ., Hradec Kralove, Czechoslovakia). Radiobiol. Radiotherap., 7: 249-57(1966). (In German).

Changes of the content of ascorbic acid, glutathione, dehydroascorbic acid, and diketogulonic acid in the brain of Wistar rats were studied following an x irradiation with a dose of 600 R. Irradiation was done to the whole body as well as with the head screened. Determinations were performed after one and two hours and the 3rd, 6th, and 9th day after irradiation. Changes in the concentration of the tested substances with time depending on the way of irradiation first of all occurred in their rate of increase on the first three days. In those rats who were whole-body irradiated an increase of AS- and GSH-values, having a maximum 24 hours after irradiation, was observed following an initial decrease. In those rats who were irradiated with the head screened the decrease of concentration of AS after irradiation was slower, the slowest values being measured after 24 hours. An increase above the control value did not occur before the third day after irradiation. After the maximum values had been reached, a permanent decrease of AS- and GSH-values occurred again in both ways of irradiation. Changes of the sum of dehydroascorbic acid and diketogulonic acid showed an extreme course, the course of both kinds of oxidation of AS. (auth)

38680 X-IRRADIATION EFFECTS ON CYTOCHROME SYSTEMS OF YEAST ORGANISMS. Pomoshnikova, N. A.;

Mokhova, E. N.; Leonova, V. G. (Inst. of Microbiology, Academy of Sciences, USSR. Inst. of Radiation and Physico-Chemical Biology, Moscow). Radiobiologiya, 6: 13-16 (1966). (In Russian).

The cytochrome systems of yeast cultures are stable to the effects of radiation. The retardation of the work of the respiratory chain is begun at sublethal doses, reducing the survival by only a tenth of a percent. Injury to the cytochrome chain was observed at lower doses of x radiation in radiosensitive cultures than in radioresistant cultures of Saccharomyces. Comparison of the data obtained with the determination of the number of yeast cells dying immediately after irradiation lead to the conclusion that a disturbance of the respiratory chain occurs only during immediate death of the cells. (tr-auth)

38681 CONTENTS OF GLYCOGEN AND RIBONUCLEIC ACID AND PHAGOCYTIC ACTIVITY OF LEUKOCYTES DURING X IRRADIATION OF RABBITS. Savitskii, I. V.; Zaretskaya, I. V.; Shafran, L. M. (Pirogov State Medical Inst., Odessa). Radiobiologiya, 6: 17-19(1966). (In Russian).

Under an x radiation dose of 900 R, the phagocytic activity of the leukocytes of rabbits decreased, and the glycogen content of the cytoplasmic neutrophils showed complete disappearance on the seventh day after irradiation. The quantity of RNA was also modified. A quantitative alteration of the cell structure of the leukocytes was observed that included hypersegmentation of the nucleus, appearance of uncolored granules in the protoplasm, decrease of the granularity, and incapacity to bond dyes. The decrease of the phagocytic activity of the leukocytes is connected probably with the decrease of glycogen and RNA concentration. (tr-auth)

38682 X-RAY EFFECTS ON ESTERASE ACTIVITY IN WHITE RAT BLOOD SERUM. Bulatskii, N. P. (Pirogov Medical Inst., Odessa). Radiobiologiya, 6: 27-9(1966). (In Russian).

The esterase activity of blood serum decreased more than 40% in the rat given whole-body x radiation at a dose of 600 R. (tr-auth)

38683 EFFECTS OF γ IRRADIATION INFLUENCE ON SYNTHESIS AND DECAY OF RNA IN HeLa CELLS. Kuzin, A. M.; Kalendo, G. S. (Inst. of Biophysics, Moscow). Radiobiologiya, 6: 30-8(1966). (In Russian).

Autoradiography was used to study the distribution of ^{3}H-uridine in cultures of HeLa cells exposed to γ radiation. The dynamics of the synthesis and decomposition of RNA in the nucleus, nucleolus, and cytoplasm were followed during the first 5 hrs after irradiation. Pulse labeling with ^{3}H-uridine made it possible to calculate the comparative speed of the RNA synthesis in the nucleus and the speed of its decay and yield in the cytoplasm. The mean cycle of the RNA in the nucleus was found to be only 6 min, which agrees with the literature data. The speed of accumulation of labeled RNA in the cytoplasm was approximately 3% of the speed of the synthesis of the labeled RNA in the nucleus. The γ irradiation of Hela cells at doses of 10 kR did not cause significant changes in the velocity of RNA synthesis for 3 hrs after the irradiation. In the irradiated cells the level of labeled RNA in the nucleus underwent regular changes with a period of 2 hrs in contrast with normal cells where the level stabilized rapidly after 1 hr, and remained unchanged for 5 hrs after the introduction of the labeled compound. In the cytoplasm of normal cells within 20 to 30 min after the introduction of labeled compounds, a uniform increase of the quantity of the RNA was observed. In the irradiated cells, this quantity both in the cytoplasm and in the nucleus has an oscillating character with a gradual increase with time. The oscillation of the level of labeled RNA in the cytoplasms of the irradiated cells was synchronized with the oscillations in the nucleus. It was concluded that under the effects of γ irradiation the system of self regulation of the RNA levels in the nucleus and cytoplasm is changed as the result of the periodic increase of the decomposition processes of the RNA. This increase of decomposition can be the result of changes in the activity of the ribonuclease or the albumin-protected RNA. The phenomena observed agrees well with the hypothesis of the synthesis of RNA of two types; of quickly produced RNA, which has a high speed synthesis and periodically decomposes and the other that has a significantly higher stability but which limits the increase of the mean level of RNA in the cytoplasm. (tr-auth)

38684 WHOLE-BODY X-IRRADIATION EFFECTS ON THE CONTENT OF 17-OXYCORTICOSTEROIDS IN PERIPHERAL BLOOD OF DOGS. Shkhinek, E. K. (Inst. of Experimental Medicine, Leningrad). Radiobiologiya, 6: 46-9(1966). (In Russian).

The whole-body irradiation of dogs with x rays at lethal doses caused an increase of the concentration of 17-oxycorticosteroids in the blood in the first hrs after irradiation. There was then a decrease of the concentration to normal or almost normal within three days after irradiation followed by a new abrupt increase some days before death. The reaction of the suprarenals to irradiation was indicated to a smaller degree by the severity of the radiation sickness. (tr-auth)

38685 EXPERIMENTAL DATA ON THYMUS STATE DURING ACUTE RADIATION SYNDROME. Kholin, V. V. (Kirov Medical Graduate School, Leningrad). Radiobiologiya, 6: 65-8(1966). (In Russian).

After whole-body x radiation of animals, there is an inter-relationship between the degree of radiation sickness and the degree of morphological changes of the thymus. In whole-body x radiation the most serious impairment of the thymus was observed in sexually immature animals aged 25 to 30 days and the least serious in sexually mature animals. (tr-auth)

38686 ADRENALINE INFLUENCE ON THE LEUKOCYTIC AND GLYCEMIC REACTIONS IN RABBITS EXPOSED TO SINGLE OR MULTIPLE IRRADIATION DOSES. Remizova, I. V. (Central Scientific-Research Inst. of Roentgen-Radiology, Leningrad). Radiobiologiya, 6: 69-72 (1966). (In Russian).

The leukocytic and glycemic reactions of x irradiated rabbits following the introduction of adrenaline depends on the distribution of the radiation dose with time. Soon after a single irradiation a sharply increasing leukocytic reaction to the adrenaline was observed and at the climax of radiation sickness it had a leukopenic character. With fractional doses the leukocytic reaction proceeded without significant increase of the leukocytes. The glycemic reaction to adrenaline significantly increased under fractionated radiation doses, especially soon after the total dose was administered. (tr-auth)

38687 INVESTIGATION OF REFLECTORY STIMULATION OF SOLAR PLEXUS GANGLIONS FOLLOWING X IRRADIATION. Maiorova, N. F. (Inst. of Experimental Medicine, Leningrad. Central Scientific Research Inst. or Roentgen-Radiology, Leningrad). Radiobiologiya, 6: 73-8(1966). (In Russian).

The effects of x radiation on the functional state of solar plexus ganglions were detected from 5 to 10 min up to 1.5 hrs after irradiation. The changes of the excitability of the ganglions with respect to the threshold and intensity of the vasomotor reaction had a heterodirectional character (increase and decrease of the excitability and the wave-like character of the change). In the case of a decrease of the excitability, a reduction of the response threshold took place in proportion to the range of the frequency parameter of the current causing the vasomotor effect. (tr-auth)

38688 EFFECTS OF FUNCTIONAL CONDITION OF THE HYPOTHALAMUS ON THE COURSE OF RADIATION SICKNESS. Petelina, V. V. (Inst. of Experimental Medicine, Leningrad). Radiobiologiya, 6: 81-3 (1966). (In Russian).

The functional state of the hypothalamus has a significant effect on the development and outcome of radiation sickness in dogs and rabbits. With weak electric irradiation of the hypothalamus (0.5 v and 6 hertz) under whole-body x irradiation the lightest case of radiation sickness was noted

with a subsequent decrease of the survival of the animals to 40 to 47% with respect to the controls. (tr-auth)

38689 MORPHOLOGICAL AND FUNCTIONAL CHANGES OF RETINA DURING RADIATION SYNDROME IN RABBITS. Melik-Musyan, A. B. (Lab. of Biophysics, Erevan). Radiobiologiya, 6: 88-92(1966). (In Russian).

Radiation sickness begins during the x irradiation of the head of rabbits at doses of 1000 to 5000 R. At 3000 to 5000 R conjunctivitis occurred, an abrupt decrease of the intraoptical pressure developed, and death occurred. Morphological changes in the retina after irradiation are described. After exposure to ionizing radiation, displacements in the distribution of acid phosphatases occur. The radiation affects the visual cells of the retina which lead to its destruction. Changes in the functional state of the retina were observed soon after irradiation. (tr-auth)

38690 INFLUENCE OF X IRRADIATION ON THE YIELD AND CHEMICAL COMPOSITION OF POTATOES. Avakyan, V. A.; Gukasyan, L. A.; Sisakyan, I. Sh.; Avakyan, S. O. (Lab. of Radiation Hygiene, Erevan). Radiobiologiya, 6: 128-30(1966). (In Russian).

Irradiation of potato tubers of the Lorkh variety before sprouting with doses of 0.1 and 0.5 kr stimulates the aging of the potato plants. The irradiation of both sprouting and and non-sprouting tubers at doses of 0.1, 0.5, 1, and 2 kR x radiation lead to a decrease of the harvest. Irradiation caused a decrease of the concentration of starch and an increase of the concentration of vitamin C in the tubers. Some increase of the albumin concentration was also noticed. The efficiency of the irradiation of potatoes depends on, in addition to the irradiation dose, the physiological state of the tubers and the cultivation conditions after irradiation. (tr-auth)

38691 CHANGES IN BARLEY PLANT GROWTH AND LEAF-FORMING RATE FOLLOWING γ IRRADIATION OF SEED. Savin, V. N.; Shutov, A. A. (Agrophysical Research Inst., Leningrad). Radiobiologiya, 6: 131-3 (1966). (In Russian).

Gamma irradiation of barley seeds produced an inhibition of the growth of new leaves which caused a reduction of the concentration of dry materials. In plants from irradiated seeds the tempo of leaf formation was increased, a stimulation of the growth of the leaves of the upper section was observed, and the quantity of lateral shoots was increased. The greatest quantity of productive sprouts was formed at irradiation doses of 5 kR which moderately inhibited the growth process. Possible mechanisms for the observed changes in the growth of leaves and stems are discussed. (tr-auth)

38692 CYTOLOGICAL DISTURBANCES IN APPLE-TREE ROOTS FOLLOWING IRRADIATION OF SEEDS. Dryagina, I. V.; Kalinichenko, I. M.; Lozhkina, V. G. (Moscow State Univ.). Radiobiologiya, 6: 134-9(1966). (In Russian).

Small doses of from 10 to 500 R γ radiation stimulated the process of division of the cells of apple rootlets and at these doses an increased number of interferences in the anaphase and telephase (2 to 9 times) was observed with respect to the controls. With increased radiation dose, the number of different types of interferences in the mitotic path was increased. During the irradiation of the apple seed with doses of 0.5 to 10 kR, a great difference was observed in effect of fast neutrons and γ rays from ^{60}Co. A larger number of aberrations were observed with fast neutrons than with γ rays. The events and character of these disturbances are described. Irradiation led to some morphological changes in the apple seedlings. At doses higher than 0.5 kR the number of bifurcated plants sharply increased, especially after irradiation of the seed with neutrons. (tr-auth)

38693 METHOD OF CALCULATION OF ABSORBED DOSES IN PLANT SEEDS DURING THEIR IRRADIATION WITH FAST NEUTRONS. Isaev, B. M.; Bregadze, Yu. I. (Inst. of Biological Physics, Moscow). Radiobiologiya, 6: 140-2(1966). (In Russian).

The calculation of the absorbed dose in fast neutron irradiation of seeds can be carried out only with knowledge of the chemical composition of the seeds. The determination of the absorbed dose can be determined by use of a homogeneous ionization chamber made of polyethylene and polystyrene. (tr-auth)

38694 HEMATOLOGICAL CHANGES AFTER IRRADIATION OF NORMAL AND DAMAGED LIVER TISSUE. Schneider, Rudolf; Schmidt, Juergen; Stender, Hans-Stephan (Univ., Marburg, Ger. Medizinische Hochschule, Hanover). Strahlentherapie, 130: 116-30(May 1966). (In German).

The influence of local fractionated x irradiation (5 × 600 R or 5 × 300 R) on blood formation in normal rat liver and spleen as well as liver and spleen damaged by thioacetamide was investigated. Local irradiation of healthy liver caused only a slight temporary change in the blood picture. X irradiation of liver damaged by thioacetamide resulted in changes in erythropoiesis which were more severe and prolonged than caused by thioacetamide alone. Simultaneous irradiation of the liver and spleen with a total dose of 1.500 R (5 × 300 R) and 3.000 R (5 × 600 R) per organ caused very severe and long lasting disturbances in erythro- and leukopoiesis. (auth)

38695 INFLUENCING PROPERDIN AND AGGLUTININ FORMATION BY WHOLE-BODY IRRADIATION. Thueringen, Guenther; Janssen, Norbert; Stender, Hans-Stephan (Univ., Marburg, Ger.). Strahlentherapie, 130: 131-8(May 1966). (In German).

The changes in properdin and in Brucella agglutinins in serum were investigated in rats after whole-body irradiation with ^{60}Co (500, 800, 900 rad, and 3 × 300 rad, respectively). The properdin level was decreased for about 3 weeks after 500 rad. A greater decrease was observed after fractionated irradiation with 3 × 300 rad than with a single dose of 500 or 900 rad. Administration of Brucella antigen 3 and 5 days prior to irradiation decreases the fall of the serum properdin. The rise of the properdin level was observed at the same time at which production of agglutinin could also be found. Properdin, a system of heterologous effective and polyvalent antibodies, showed the same behavior as Brucella agglutinin after whole-body irradiation. (auth)

38696 RADIOGENIC RADIATION PROTECTION EFFECT. Krokowski, Ernst; Taenzer, Volker (Freie Univ., Berlin). Strahlentherapie, 130: 139-45(May 1966). (In German).

Published data concerning radiation response of animals after whole-body irradiation were organized in a uniform dose-time-effect scheme for use in general evaluations. A radioprotective effect was shown about 10 days after a total-body pre-irradiation that lasted for slightly longer than 6 months. The mechanism is discussed. An adaptation effect seemed to be responsible for the response to small total-body pre-irradiation doses (about 5% of the LD_{50}), while an immunization effect seemed to be prevailant at higher doses. This immunization process exceeded considerably the biological events called recovery. Absolutely lethal radiation doses were tolerated without recognizable damages if a total-body irradiation was done longer than 10 days prior to the radiation application. (auth)

38697 INFLUENCE OF IONIZING RADIATIONS ON THE CORTICO-SUPRARENAL SYSTEM EVALUATED ON THE BASIS OF POTASSEMIA IN RABBITS. Petrescu, D.; Boros, I.; Schiau, S.; Stonescu, R.; Corneci, I. Studii Cercet. Fiziol., 10: 89-95(1965). (In Rumanian).

Whole-body x irradiation at 800 R in a single session, intramuscular injection of serum from normal or irradiated rabbits, and intravenous injection of dead Proteus $X_{19}O$ bacterial suspension was found to cause a general increase of the serum potassium of rabbits. These tests were carried out in order to examine the potential role of the cortico-suprarenal system on immunological reactions under the influence of ionizing radiations. The increase of the K content of the serum is more noticeable after irradiation or injection of normal serum than after injection of serum of irradiated rabbits. If it is assumed that increase of the K content indicates a certain insuffi-

ciency of the cortico-suprarenal system, the results obtained may be taken as indicating that the serum of the irradiated animals contains factors which exert an action on the functions of the cortico-suprarenal system, counteracting the inhibiting effect of direct radiation and of the above-mentioned injections. A 6.5 R/minute x-ray source was used in the experiments. (TTT)

38698 EFFECTS OF LOW-LEVEL CHRONIC IRRADIATION OF CHINOOK AND COHO SALMON EGGS AND ALEVINS. Donaldson, Lauren R.; Bonham, Kelshaw (Univ. of Washington, Seattle). Contract AT(45-1)-1385. Trans. Amer. Fish. Soc., 93: 333-41(Oct. 1964).

Chinook and coho salmon eggs were subjected to about 0.5 roentgen per day of the gamma radiation from cobalt-60 from shortly after fertilization until the alevins swam, resulting in a total dose to the chinooks of from 33 to 37 roentgens and to the cohos of 40 roentgens. Irradiated, and similarly treated but unirradiated controls, were compared for survival, growth, vertebral numbers and anomalies, opercular defects, and sex ratios. Significant differences were observed only in the more frequent occurrence of opercular defects among irradiated than among control coho salmon smolt. In some phases of growth the controls and in others the irradiated groups showed superiority without a discernible pattern. As late as the time of release of the smolt for their seaward migration, little if any difference appeared between experimental and control groups. Differences will be sought in the F_1 generation from these fish. (auth)

38699 LEUKEMIC CELL GROWTH, HOST DEATH, AND THE RESPONSE TO X-IRRADIATION. Maruyama, Yosh. Univ. Minn. Med. Bull., 36: 258-60(Mar. 1965).

When cells of an isogenic lymphoma were injected intravenously into normal isogenic mice the animals died following certain intervals of time, dependent upon the number of cells given. X radiation exposure of the recipients before transplantation or at intervals following transplantation increased the survival time of the mice as a function of x ray dose. When dilutions containing known numbers of tumor cells irradiated in ascitic mice, in tissue cultures under conditions of full oxygenation, or in N_2-asphyxiated mice shortly after sacrifice were inoculated intravenously into recipient mice, cells were found to be most radiosensitive under oxygenated conditions, intermediate in response in the ascitic fluid of living mice, and least radiosensitive under the conditions of anoxia encountered in dead mice. (C.H.)

38700 THE ACUTE WHOLE-BODY IRRADIATION SYNDROME: SOME BASIC FACTORS IN ITS MODE OF ORIGIN. Cottier, H. (Univ., Bern). Vierteljahresschr. Schweiz. Sanitaetsoff., 42: 36-40(May 1965). (In German).

The acute whole-body irradiation syndrome is defined as the totality of changes that appear in the organism after short-term exposure to ionizing radiation. The pathogenetic mechanisms leading to death are very dose dependent. Midlethal doses of 400 to 500 rad produces the bone marrow syndrome, while after a lethal or supralethal dose of ~700 rad the gastrointestinal syndrome also appears. The severity of the bone marrow syndrome depends on the radiosensitivity and the mitotic activity of the immature precursors of the blood cells, and radiosensitivity of these new cells produced. The average lifetime of the highly radiosensitive erythroblasts, their short generation times, great radioresistance and long survival, and the radiosensitivity of granulopoiesis, thrombopoiesis, and lymphopoiesis are also considered as variables in the bone marrow syndrome. Because of the continuous circulation of hematopoietic stem cells in blood, the bone marrow can be renewed by transfusion from an intact hematopoietic source. (TCO)

38701 LIPOID CHANGES IN VARIOUS RAT ORGANS AFTER WHOLE-BODY IRRADIATION WITH LETHAL X RAY DOSES. III. Eberhagen, Dietrich; Plette, Gisela (Univ., Munich). Z. Physiol. Chem., 343: 17-26(1965). (In German).

Rays were irradiated with 1500 R of whole-body x irradiation. The fatty acid composition of the adrenal lipids were separated by column chromatography at 0.5, 3, 6, 12, 24, 48, and 60 hr after irradiation, and analyzed gas-chromatographically. There was a considerable accumulation of highly unsaturated fatty acids in all classes of lipids. Within 24 hr after irradiation the arachidonic acid content of the phosphatides had increased threefold, and represented ~40% of the fatty acids. By 60 hr after irradiation when the animals had died the tetraenoic acid values in the cholesterol esters were almost doubled. Arachidonic acid was also increased in the triglycerides after irradiation. The cholesterol esters could be separated into two fractions, but it was not possible to characterize these on the basis of their fatty acid composition or sterol components. The ester concentrations in these fractions varied in a complementary manner over the time periods when they were measured. (BBB)

38702 RADIOBIOLOGICAL AND BIOCHEMICAL INVESTIGATIONS OF POLYOMA VIRUS-CELL INTERACTIONS. Benjamin, Thomas Livingston. Pasadena, Calif., California Inst. of Tech., 1966. 87p.

Thesis.

The cytologic interaction of Polyoma virus with mouse embryo cells was studied by radiobiological methods known to distinguish temperate from virulent bacteriophage. No evidence for temperate properties of Polyoma was found. It was observed that the curve of inactivation of Polyoma virus by ultraviolet light had two components – a more sensitive one at low doses, and a less sensitive one at higher doses. Virus that survives a low dose has an eclipse period similar to that of unirradiated virus, while virus surviving higher doses shows a significantly longer eclipse period. If Puromycin is present during the early part of the eclipse period, the survival curve becomes a single exponential with the sensitivity of the less sensitive component. These results suggest a repair mechanism in mouse cells, which operates more effectively if virus development is delayed. A comparison of the rates of inactivation of the cytolytic and transforming abilities of Polyoma by ultraviolet light, x rays, nitrous acid treatment, or the decay of incorporated ^{32}P showed that the transforming ability has a target size roughly 60% of that of the plaque-forming ability. It is thus concluded that only a fraction of the viral genes are necessary for causing transformation. The appearance of virus-specific RNA in productively infected mouse kidney cells was followed by means of hybridization between pulse-labeled RNA from the infected cells and the purified virus DNA. The results show a sharp increase in the amount of virus-specific RNA around the time of virus DNA synthesis. The presence of a small amount of virus-specific RNA in virus-free transformed cells was also shown. This result offers strong evidence for the persistence of at least part of the viral genome in transformed cells. (Dissertation Abstr.)

38703 EFFECT OF IRRADIATION ON RESPONSE OF THE DOG TO A STANDARDIZED HEMORRHAGIC STRESS. Knott, David Howard. [Knoxville], Tenn., Univ. of Tennessee, 1965. 166p.

Thesis.

In an attempt to delineate the general response of the irradiated dog to superimposed trauma, the combined insults of whole-body irradiation and hemorrhagic shock were employed. A single episode of hemorrhagic shock was effected in dogs subsequent to receiving acute lethal (500 R) and supralethal (1500 R) doses of x irradiation. The hemorrhage procedure was applied on a serial basis (weekly for six weeks) in animals exposed to (a) an acute sublethal dose of 265 R or to (b) a chronic low-level dose of 966 R at 1 R per hour. The serial bleeding technique was instituted both during the course of radiation sickness and also subsequent to the hematologic recovery from irradiation. The volumetric, hemodynamic, and hematologic responses to hemorrhage in nonirradiated and irradiated dogs were measured. The irradiated animals (500 R) bled at two days and five days after exposure exhibited a greater tendency toward posthemorrhage intravascular volume replacement, but these animals expired earlier than similarly irradiated, non-hemorrhaged dogs. Hemodynamic studies

revealed that the response in the acutely irradiated dog (500 R and 1500 R) to hemorrhagic shock was marked by less evidence of vasoconstriction than that noted in control animals. Application of the hemorrhagic stress on a serial basis in acutely (265 R) and chronically irradiated dogs decreased survival time when compared with hemorrhaged, nonirradiated controls. The pathophysiologic state indigenous to hemorrhagic shock was much more severe in the irradiated dogs as evidenced by signs of more extensive functional and morphological deterioration. However, the data suggest that hematologic recovery from irradiation is coincident with a partial restoration in the capacity of the irradiated dog to respond to hemorrhagic shock. (Dissertation Abstr.)

38704 THE PHOTOCHEMISTRY OF IODOURACIL AS RELATED TO THE SURVIVAL OF ULTRAVIOLET-IRRADIATED T1 BACTERIOPHAGE SUBSTITUTED WITH 5-IODO-2'-DEOXYURIDINE. Rupp, W. Dean. New Haven, Yale Univ., 1965. 104p.

Thesis.

The photochemistry of 5-iodouracil (IU) was studied as a model system for reactions that may occur in DNA substituted with a halogenated pyrimidine. A scheme in which the 5-uracilyl radical is a common intermediate explains the various photoproducts obtained from IU. The subsequent reaction of this intermediate determines the nature of the final products. Experiments with T1 phage that have about 60% of the DNA-thymine replaced by IU indicate that the presence of cysteamine during uv irradiation had a marked protective effect on substituted T1 phage but had no effect on control phage. Irradiated phage were assayed on a uvr^- mutant strain of E. coli K-12 that is deficient in enzymatic repair of uv lesions. In this case, cysteamine again protects only the IU-substituted phage and raises the survival of these phage to a level significantly higher than that of the unsubstituted control phage. Other compounds (ethanol, cysteine, and 2-mercaptoethanol) that acted as hydrogen donors in the photochemical studies of IU also protect IU-substituted phage but do not protect normal unsubstituted phage. The protection of these compounds can be explained if a 5-uracilyl radical is an intermediate in the photochemical alteration of IU in DNA. (TCO)

38705 EFFECTS OF SUB-LETHAL GAMMA RADIATION ON THE BIOLOGY AND BEHAVIOR OF THE ANGOUMOIS GRAIN MOTH, SITOTROGA CEREALELLA OLIVIER. Qureshi, Zafar Ahmad. Manhattan, Kan., Kansas State Univ., 1966. 138p.

Thesis.

Effects of irradiation of eggs, first, third, and last instar, prepupae, pupae and adults as determined by hatch, emergency pattern, length of developmental period, and fecundity, fertility, longevity and body weights are reported. Insects were irradiated with gamma rays, using a 10-curie cobalt-60 source. Data were obtained on hatching of eggs irradiated with 2 to 18 kR at different ages. Early and late first instar were irradiated at doses of from 2 to 20 kR; third and last instars, and early and late pupae, from 5 to 25 kR; prepupae, from 3 to 24 kR. Fecundity and fertility were determined by mating irradiated females with normal males and vice versa. Results following irradiation of eggs of different ages showed that sensitivity declines with age. Adult emergence after irradiation of early and late first instar, third instar, and last instar, prepupae, and early pupae revealed that irradiation delayed emergence and reduced the number emerged. Earlier stages were more sensitive than older ones. Fecundity and fertility studies indicate that 20 kR may cause complete sterility of both sexes when irradiated as first instar, third instar, last instar, and early pupae. Generally, females were more sensitive to radiation than males. Fecundity and fertility of females in one-day old irradiated adults was significantly different from the controls under various crosses. Adult longevity following irradiation of early and late first instar, third instar, and last instar, prepupae, early and late pupae, and one-day old adults was not significantly different from the controls. Emerged adults irradiated as early and late first instar and last instar showed a significant reduction in body weight. (TCO)

38706 EFFECTS OF WHOLE-BODY GAMMA IRRADIATION ON SOME BLOOD CONSTITUENTS AND HEMOPOIETIC ORGANS OF THE CALF. Olsen, Raymond Edgar. [Urbana], Ill., Univ. of Illinois, 1965. 269p.

Thesis.

Sixty percent of ten female Holstein calves exposed to 150 R whole-body gamma irradiation died between the seventh and thirty-fifth days after irradiation, and 70% of ten calves died between the fourth and twenty-fifth days after exposure to 250 R whole-body gamma irradiation. These calves averaged three days of age when exposed to gamma-irradiation from a cobalt-60 source at the rate of 5 R/minute. At post-mortem examination, the gross lesions most frequently observed were pneumonia in the cardiac and apical lobes of the lung, serosal hemorrhages along the intestinal tract, gastritis, enteritis, and hemorrhages in the kidneys, lymph nodes, and intestine. Microscopically, there was acute to chronic pneumonia, catarrhal to necrotic gastroenteritis, and in some calves, thickening of the arteriolar walls with occasional occlusion of the lumen. Tubular degeneration and glomerulonephritis were frequently seen. In the pancreas, the islets of Langerhans were numerous and enlarged. Kupffer cells in the liver were numerous. In about 50% of the calves, there was a marked infiltration of eosinophils in the intestine. The thymus, spleen, and lymph nodes were hypocellular, and lymph follicles were absent or few in number. Bone marrow was very hypocellular and, in one case, acellular. Serum sodium of calves exposed to 150 R gamma irradiation was consistently higher than that of unexposed calves or calves exposed to 250 R. Serum potassium decreased with advancing age. The irradiated calves had higher serum calcium values than the unexposed calves. There was an increase in the serum albumin/globulin ratio of irradiated calves caused by a decrease in albumin and an increase in alpha-globulin. Irradiation caused a rapid fall of lymphocytes in the peripheral blood within 24 hours. Low counts were reached in two days and persisted for 23 days. Neutrophils were increased the first post-irradiation day and then declined to a low value on day 5. This persisted until day 28. Irradiation caused a hypoplasia of the bone marrow. (TCO)

38707 RADIATION STUDIES OF LARGE RNA VIRUSES AND CHICK EMBRYO CELLS. Levinson, Warren Edward. Berkeley, Calif., Univ. of California, 1965. 194p.

Thesis.

The finding that the infectivity of Rous sarcoma virus (RSV) is 10 times more resistant to inactivation by uv radiation than Newcastle disease virus (NDV) is confirmed and extended. The cause of the high resistance of RSV and Rous associated virus (RAV) to uv irradiation is unknown. The suspending medium was shown not to be responsible for the resistance. Three procedures failed to demonstrate the presence of an intracellular repair mechanism for uv damage: lengthening the latent period of NDV, exposure of cells to acridines, and infection of cells with unirradiated or uv-irradiated RAV and NDV prior to assay of uv-irradiated RSV and NDV. Several procedures designed to alter the chemical structure of RSV failed to change the resistance. The rates of inactivation of NDV and RSV increased with increases in x-ray dose. X-irradiated medium can damage chick embryo cells as evidenced by the inhibition of the spreading and growth of the cells and of their capacity to synthesize RSV. The death of the cells is caused by the H_2O_2 generated in the medium upon x irradiation. Sodium pyruvate, serum, and a substance produced by cells can protect cells from the lethal effects of irradiated medium. (TCO)

Radiation Effects Therapy and Countermeasures

Refer also to abstracts 38562 and 38563.

38708 (IAEA–3173–5) THE APPLICATION OF CLONED HAEMOPOIETIC CELLS IN RADIATION PROTECTION. Final Report, 1965–66. Feldman, Michael

(International Atomic Energy Agency, Vienna (Austria)). Contract 196/R2/US. 6p. Dep. mn. CFSTI $1,00 cy, $0,50 mn.

Macroscopic cell colonies of bone marrow origin formed in the spleens of lethally irradiated mice after the injection of bone marrow cells were used for a quantitative analysis of the in vivo regulation of proliferation and differentiation of erythroid, granuloid, and megakariocytic cells in populations derived from single cells. Emphasis was placed on the effects of polycythemic conditions, hypoxia, erythropoietin, and transfusion with red blood cells on the formation of erythroid clones. (C.H.)

38709 RADIOPROTECTION OF SULFURATED MINERAL WATERS. Di Carlo, R.; Pagnini, G. (Univ., Naples). Arch. Ital. Sci. Farmacol., 13: 4p.(Apr. 1963). (In Italian).

When adult mice were given Vanacore mineral water high in sulfur (from Castellammare di Stabia) for 12 days before 700-R irradiation, a slight radioprotective action was observed, as seen by a significant reduction in mortality rate. Experiments were conducted on the radioprotective action of the water when supplied to the animals for longer periods. It was provided as drinking water ad libidum for 75 days before irradiation. Irradiation of the male Swiss mice was then carried out with whole-body doses of 700 R of x rays. The mortality rates of the control mice (provided with Naples fountain water) and mineral water-supplied mice were as follows at the stated times post-irradiation: at 10 days, 14.3%, 17.9%; 13 days, 57.1%, 17.9%; 16 days, 60.7%, 32.2%; 19 days, 64.3%, 32.2%; 30 days, 71.4%, 39.3%; and 60 days, 82.1%, 50%. These differences in mortality rate were significantly higher for the control mice at the $P < 0.01$ level on the 13th and 19th postirradiation day and at the $P < 0.05$ level on the 16th, 30th, and 60th day. These results confirm the radioprotective action of this sulfurated mineral water. (BBB)

38710 EFFECTS OF SOME METABOLIC INHIBITORS ON X-RAY DOSE-RESPONSE CURVES FOR THE SURVIVAL OF MAMMALIAN CELLS IN VITRO, AND ON EARLY RECOVERY BETWEEN FRACTIONATED X-RAY DOSES. Berry, Roger J. (Churchill Hospital, Oxford). Brit. J. Radiol., 39: 458-63(June 1966).

The rapid (0 to 8 hour) recovery from sub-lethal x ray damage in HeLa $S\text{-}3_{oxf}$ cells in vitro is neither delayed nor reduced in magnitude by incubating the cells in media containing high concentrations of 2—4 Dinitrophenol, which deprives the cells of a major energy source by uncoupling oxidative phosphorylation. In fact, cells surviving 100 μg/ml concentrations of DNP showed somewhat increased recovery between fractionated x ray doses. 5-Fluorouracil in high concentrations sensitizes the cells to single x ray exposures, but the steeper dose-response curve retains a marked shoulder and no significant modification of the two-dose recovery curve is seen even with drug concentrations that are high enough to reduce cell survival drastically on their own. The antibiotics Puromycin and Cycloheximide, although inhibiting protein synthesis and sensitizing cells to the effects of single doses of x rays, do not decrease early recovery even when the drug under study is added to the cell cultures as much as 20 hours prior to the first x ray dose. The folic acid antagonist Methotrexate, when added to the growth medium, sensitizes cells to the effects of single doses of x rays, producing an almost shoulderless survival curve. No measurable recovery is observed when fractionated doses of x rays are delivered at times greater than 16 hours after addition of the drug to the medium. The possible inferences to be drawn from these results for combined courses of radiotherapy and chemotherapy are discussed. (auth)

38711 THE EFFECTIVENESS OF TRANSPLANTATIONS OF ISOLOGOUS BONE MARROW IN EXPERIMENTAL HYPOPLASTIC ANEMIA INDUCED BY MULTIPLE IRRADIATION. Muksinova, K. N. (Inst. of Medical Radiology, Moscow). Med. Radiol., 11: No. 1, 36-42(Jan. 1966). (In Russian).

Isologous bone marrow (1×10^8 and 5×10^8 cells) was introduced to rats with hypoplastic anemia induced by multiple gamma-irradiation (^{60}Co), the daily dose amounting to 60 R. In the control group only 11.9% survived. After the administration of 1×10^8 and 5×10^8 bone marrow cells the survival of rats increased up to 30.7 and 60% respectively. In the treated animals, as compared to the controls, there was noted an earlier and more intensive restoration of the content of myelokaryocytes and other blood elements. The temporary survival of the introduced medullary elements was shown by cytological and immunological methods of identification of donor cells. (auth)

38712 MECHANISM OF X-RAY SENSITIZATION OF BACTERIOPHAGE T_7 BY 5-BROMOURACIL. Freifelder, David; Freifelder, Dorothy Read (Univ. of California, Berkeley). Mutat. Res., 3: 177-84(June 1966).

Coliphage T7 suspended in protective media are inactivated by x rays more rapidly when the DNA contains 5-bromouracil (5-BU) replacing thymine. The percentage of the total number of inactivated phages which were killed by the production of double-strand breaks in the DNA was measured by means of an ultracentrifugal technique which yields the ratio of broken to unbroken DNA molecules. It was found that the sensitization by 5-BU substitution resulted only partially from an increase in the rate of strand breakage. If the phage were irradiated in a N_2 atmosphere and in the presence of cysteine, all non-breakage damage was eliminated. From this it is hypothesized that 5-BU phage are more sensitive than normal phage because 5-BU is more easily damaged than thymine. (auth)

38713 INHIBITION OF OXYGEN CONSUMPTION OF LIVER HOMOGENATES FROM MICE INJECTED WITH RADIOPROTECTORS IN THE PRESENCE OF PYRUVATE. Ciccarone, P. (CSN, Rome); Bacq, Z. M. Nature, 210: 648-9(May 7, 1966).

An inhibition of oxygen consumption in the presence of pyruvate was observed in the livers of mice killed 20 min after the intravenous injection of cystamine or serotonin. The possible effects of the biochemical shock induced by the injection of radioprotective compounds on the mechanism of action of these compounds are discussed. (C.H.)

38714 THE PROTECTIVE EFFECT OF GLYCINE IN X-RAY IRRADIATION IN RELATION TO THE AMOUNT OF GLYCINE ADMINISTERED. Capalna, Simion; Stefan, Maria; Ghizari, Eugenia (Inst. for Physiology, Bucharest). Naturwissenschaften, 53: 254-5(1966). (In German).

The protective effect of glycine on x irradiated white mice was determined with respect to the amount of glycine administered before the irradiation. The results are tabulated and show the increase of the ATP-ase and the PP-ase when glycine was injected before irradiation. The probable mechanism of radiation injury and the probability that as a result of the irradiation each organic compound in living materials is dissociated into radicals is discussed. (J.S.R.)

38715 CHEMICAL PREVENTION OF RADIATION-INDUCED LEUKEMIA IN MICE. Pollard, Morris; Matsuzawa, Taiju (Univ. of Notre Dame, Ind.). Proc. Soc. Exp. Biol. Med., 122: 539-42(June 1966).

Mice which were subjected to repeated treatments of endotoxin plus 150 R x rays developed leukemia to the same extent as the drug-free irradiated controls. Treatments of mice with AET prior to each exposure to 150 R x rays reduced the incidence of leukemia in them. Mice which had been inoculated with endotoxin were thereby immunized against the radioprotective and leukemia-sparing benefits of the drug. When AET replaced endotoxin in the above scheme, the radioprotective and leukemia-sparing benefits of AET were sustained. (auth)

38716 EFFECT OF CYSTEAMINE ON ULTRASTRUCTURAL MODIFICATIONS OF THE LIVER OF RABBITS EXPOSED TO WHOLE-BODY X IRRADIATION. Birarelli, B.; Levis, F. Radiobiol. Radioterap. Fis. Med., 21: 73-85(Mar.-Apr. 1966). (In Italian).

The radioprotective effects of cysteamine on the ultrastructure of rabbit liver cells were studied. Rabbits were exposed to 600 R whole-body irradiation. Thirty minutes before the exposure the animals received an intraperitoneal

injection of cysteamine at the rate of 150 mg/k. The radioprotective activity of cysteamine was very slight in the irradiated animals over the untreated controls. The use of cysteamine however seemed to induce a delay in the chronological evolution of ultrastructural changes. Some hypotheses to explain the phenomenon are advanced. The inactivation of the sulfhydryl and disulphide groups in the liver cells is a probable explanation. This conclusion was confirmed by cysteamine-^{35}S studies. (tr-auth)

38717 INVESTIGATIONS ON BIOLOGICAL RADIATION PROTECTION. PART LXX. TAURINE EXCRETION IN WHITE MICE AFTER WHOLE-BODY IRRADIATION AND ITS INFLUENCING BY RADIOPROTECTIVE SUBSTANCES. Streffer, Christian; Melching, Hans-Joachim; Mattausch, Herbert (Univ., Freiburg i. B.). Strahlentherapie, 130: 146-56(May 1966). (In German).

The taurine excretion in female white mice was determined after total-body x irradiation with doses from 2.5 to 690 R. The first significant increase in excretion of this amino acid was observed after a radiation dose of 75 R; the same dose also resulted in the first significant decrease in a second phase. The excretion rate of taurine increased up to 200 R. The average value remained constant for higher doses; scattering decreased; thus, the P-value for the statistical significance decreased. Cysteine and AET, administered prophylactically, did not influence the radio-induced increase in taurine excretion within the first few days after irradiation. However, the decrease between the 4th and 9th day after irradiation was normalized. Cysteamine had only a small effect on this second phase of the induced changes. (auth)

38718 PATOGENEZ, EKSPERIMENTAL'NAYA PROFILAKTIKA I TERAPIYA LUCHEVYKH PORAZHENII. (Pathogenesis, Experimental Prophylaxis and Therapy of Radiation Injuries). Lebedinskii, A. V. (ed.). Moscow, Izdatel'stvo Meditsina, 1964. 292p.

Thirty-five articles are included; separate abstracts were prepared for 31. (P.C.H.)

For abstracts of individual papers see: 38653–38667 and 38719–38734.

38719 FUNCTIONAL AND MORPHOLOGICAL CHANGES OF KIDNEYS IN ANIMALS DURING RADIATION SICKNESS (^{210}Po) WHEN TREATED WITH UNITHIOL. Poluboyarinova, Z. I.; Strel'tsova, V. N. pp 85-92 of Patogenez, Eksperimental'naya Profilaktika i Terapiya Luchevykh Porazhenii. Lebedinskii, A. V. (ed.). Moscow, Izdatel'stvo Meditsina, 1964. (In Russian).

Acute radiation sickness (RS) was induced in dogs and rats by subcutaneous administration of ^{210}Po in doses of 0.05 and 0.075 millicurie/kg of bodyweight. In some dogs, the ureters were brought to the skin. Treatment with unithiol (I; 25-100 mg/kg) increased the lifespan of the animals given ^{210}Po by 50-200%. In dogs treated with I, and in untreated dogs as well, a substantial disturbance of functional activity of the kidneys took place. Glomerular filtration was enhanced, tubule reabsorption was intensified, and diarrhea retarded. However, at early periods of RS, kidney function in treated animals was disturbed more slowly than in untreated, with the development of temporary compensation. In animals treated with I the phase of destructive changes was shortened; and processes of regeneration were accelerated. Intensification of restorative processes in kidneys under the effect of I is possibly related to the observed translocation of ^{210}Po from the cortical layer to the intermediate and medullary. The total absorbed dose after 21 days in the kidney tissues of rats exposed to ^{210}Po was 2,059, and in rats exposed to ^{210}Po and treated with I, 2,987 rads. (ATD)

38720 CHANGES IN THE THYMUS DURING ACUTE RADIATION SICKNESS IN ANIMALS PROTECTED BY CYSTAMINE AND ETHYLNORANTIFFEINE. Khussar, Yu. P. pp 105-10 of Patogenez, Eksperimental'naya Profilaktika i Terapiya Luchevykh Porazhenii. Lebedinskii, A. V. (ed.). Moscow, Izdatel'stvo Meditsina, 1964. (In Russian).

A total of 69 white rats was given an x-ray dose of 1000 R after administration of 100 mg/kg of a 1% cystamine solution. The animals were also given 25 to 50 μ/kg of a 1.5% IDED solution singly or in combination with the cystamine. The rats were killed 1, 2, 3, 5, 7, 10, 14, and 21 days after irradiation. The thymus was fixed, and paraffin sections were stained to determine the mitoses. The mitotic coefficient (the number of mitoses per 1000 non-dividing cells) was calculated. The value of the mitotic coefficient (MC) fell from 1.9 to 0.8 with the use of cystamine and IDED, and from 1.9 to 0.4 without any protective agent 1 day after the irradiation. The MC value was a maximum of 7.0 for the controls at seven days after irradiation. With the use of cystamine the MC value reached a maximum of 9.0 at 3 days after the irradiation. With the use of cystamine and IDED, the MC value was a maximum of 4.8 at 5 days after the irradiation. The use of IDED decreased the number of aberrant mitoses. It is thought that IDED or ethylnorantifein has a neuro-humoral stimulatory effect through the hypophysis and adrenal gland. (TTT)

38721 EFFECT OF SOME VITAMINS OF THE B GROUP AND PHOSPHATIDES ON RESISTANCE TO IONIZING RADIATION. Bukhman, N. D.; Danetskaya, E. V.; Kadykov, B. I.; Lebedeva, M. A.; Pogorelko, M. A.; Yurtaev, G. I.; Yazeva, L. I. pp 110-15 of Patogenez, Eksperimental'naya Profilaktika i Terapiya Luchevykh Porazhenii. Lebedinskii, A. V. (ed.). Moscow, Izdatel'stvo Meditsina, 1964. (In Russian).

White male rats were exposed to whole-body x irradiation in doses of 50-100 R or to chronic gamma irradiation in doses of 0.05 R daily for 500 days. Two months before irradiation (IR) the animals were kept on synthetic diets with varying contents of vitamins B_1, B_2, and B_6 (I), folic acid (II), and phosphatide concentrate (III). Several biochemical indexes were studied. It was found that prolonged addition of I and II to the diet mitigated the injurious effect of IR. Liver function and lipid metabolism gradually returned to normal, the ascorbic acid content of the blood decreased less, the survival time lengthened, and there was more efficient use of the substances in intermediary metabolism in experiments with partial starvation. I, II, (150 micrograms per rat daily), and III (100 mg/kg), i.e., in amounts three times greater than the physiological norm, had a particularly favorable effect. The combined use of I for prophylactic purposes was effective only with certain dosages. It was concluded that the selection of special diets containing I, III, and other biologically active substances is of great value in working out preventive nutrition for persons exposed to radiation. (ATD)

38722 EFFECT OF SOME RADIOPROTECTIVE AGENTS ON THE FREQUENCY OF LEUKEMIA INDUCED BY IONIZING RADIATION. Svyatukhin, M. V.; Zherebchenko, P. G.; Sorokina, Yu. D. pp 123-31 of Patogenez, Eksperimental'naya Profilaktika i Terapiya Luchevykh Porazhenii. Lebedinskii, A. V. (ed.). Moscow, Izdatel'stvo Meditsina, 1964. (In Russian).

Black mice of the C_{57} strain 2-3 months old were injected intraperitoneally with propamine (150 mg/kg) and 5-methoxytryptamine (75 mg/kg) 15-30 min before exposure to whole-body irradiation (I) with 550 R. Only one of 185 non-irradiated mice developed leukemia (L). After I, L developed much more frequently (the peak occurred 6 months after I). The generalized L with tumorous enlargement of the thymus characteristic of this strain of mice was predominant (16 cases). Myelosis and reticulosis were much less frequent. 5-Methoxytryptamine greatly reduced the frequency of L induced by I. Propamine in this respect was less effective. The chemical radioprotective agents did not reduce the frequency of myeloid leukemia in stockbred white mice after I. (ATD)

38723 SOME ASPECTS OF THE MECHANISM OF THE PROTECTIVE ACTION OF AMINOTHIOLS. Dzharak'yan, T. K.; Berlin, L. B.; Vladimirov, V. G.; Il'inskii, D. A.; Smirnov, A. D. pp 162-70 of Patogenez, Eksperimental'naya Profilaktika i Terapiya Luchevykh Porazhenii. Lebedinskii, A. V. (ed.). Moscow, Izdatel'stvo Meditsina, 1964. (In Russian).

A study was made of the influence of one of the most effective radiation protectors from the aminothioles group — cystamine — on the mitotic activity of the epithelium of the cornea, intestine, and tissue cultures of the spleen of white rats. The concept that protective substances do not prevent damage to cells from radiation but only facilitate the more intensive course of restorative processes was rejected. The effects of cystamine on adrenalin action and the adrenolytic effect of cystamine were studied. The results demonstrated that the principal mechanism in the protective action of aminothioles and their disulfides is the blocking of adrenoreactive systems. Nevertheless the facts showed that in the mechanism of action of protective substances it is necessary to consider their effect not only on the primary radiation-chemical processes in the cells of radiosensitive organs but also on the functional condition of the regulatory systems of the organism. (ATD)

38724 RELATION BETWEEN THE CHEMICAL STRUCTURE AND RADIOPROTECTIVE PROPERTIES IN A SERIES OF AMINOTHIOLS AND CERTAIN OF THEIR DERIVATIVES. Mozzhukhin, A. S.; Rachinskii, F. Yu.; Slavachevskaya, N. M.; Tank, L. I. pp 170-8 of Patogenez, Eksperimental'naya Profilaktika i Terapiya Luchevykh Porazhenii. Lebedinskii, A. V. (ed.). Moscow, Izdatel'stvo Meditsina, 1964. (In Russian).

During the course of a search for new radiation-protection agents considerable numbers of mercaptoamines and mercaptoguanidines and a much smaller number of disulfides of mercaptoamines and thiazolidines were synthesized and studied. The results of tests performed on white mice are presented in five tables. It was concluded that the functional groups that provide the protective action in the mercaptoamine molecule are the mercapto and amino groups with the optimum distance between functional groups not exceeding 2 to 3 carbon atoms. Similar results were obtained with the aminosulfides. Derivatives of aminothioles, aminodisulfides, and mercaptoguanides were no more effective with respect to radiation protection than the original compounds. (ATD)

38725 MECHANISM OF THE RADIOPROTECTIVE ACTION OF INDOLYLALKYLAMINES AND CERTAIN OTHER COMPOUNDS. Zherebchenko, P. G.; Airapetyan, G. M.; Krasnykh, I. G.; Suvorov, N. N.; Shevchenko, A. N. pp 193-211 of Patogenez, Eksperimental'naya Profilaktika i Terapiya Luchevykh Porazhenii. Lebedinskii, A. V. (ed.). Moscow, Izdatel'stvo Meditsina, 1964. (In Russian).

An investigation was made involving the use of new compounds to determine the significance of the position and nature of substitutions in the manifestation of the radiation-protective properties of amines of the indole series. The previously discovered relation of the anti-radiation action of indolylalkylamines to their chemical structure was confirmed. The introduction of substitutions in the fifth position of the indole ring of the tryptamine molecule is accompanied by reinforcement and in the other positions by weakening of the radioprotective activity. The ability of indole compounds to compete for free radicals was practically unrelated to the presence of substitutions, but was based on the specific properties of the indole ring. The vessel-constricting action of amines of the indole series depended on the chemical structure, indicating a causal link between it and the radiation protection effect. Indolylalkylamines that were effective for radiation protection caused a reduction in the accumulation of a neutral red in the blood-forming organs, skin, and testes of rats and mice. Adrenalin had about the same action. Of the aminothiols, cystamine caused the clearest changes in blood formation. The combined use of cystamine with 5-methoxytryptamine or unithiol increased the survival rate of irradiated mice. This was not observed if 5-methoxytryptamine was given to the animals together with unithiol. (ATD)

38726 PROPHYLAXIS OF DISEASES CAUSED BY MULTIPLE EXTERNAL GAMMA IRRADIATION. Saksonov, P. P.; Vasil'ev, P. V.; Belai, V. E.; Vedernikov, A. N.; Chernenko, G. T. pp 211-19 of Patogenez, Eksperimental'naya Profilaktika i Terapiya Luchevykh Porazhenii. Lebedinskii, A. V. (ed.). Moscow, Izdatel'stvo Meditsina, 1964. (In Russian).

Tests were made on white mice and white rats to determine the effectiveness of certain antiradiation agents in different variants of multiple irradiation. The prophylactic agents were cystamine, cystaphen-cystamine in combination with phenatine, and isotyphen-β-aminoethylisothiuronium in combination with phenatine. The protective compounds had a prophylactic effect both in single and in multiple irradiation of animals, and increased the survival rate by 8 to 25%. In the case of prior repeated administration of protective agents and subsequent one-time irradiation, the antiradiation action of the preparations was preserved; however, the percentage of survival of the animals was less than in the case of a single administration of the protective agent. (ATD)

38727 INVESTIGATION OF THE EFFECT OF NOVOCAINE ON THE COURSE OF ACUTE RADIATION SICKNESS AND IMMUNOGENESIS. Klemparskaya, N. N.; Raeva, N. V. pp 219-27 of Patogenez, Eksperimental'naya Profilaktika i Terapiya Luchevykh Porazhenii. Lebedinskii, A. V. (ed.). Moscow, Izdatel'stvo Meditsina, 1964. (In Russian).

Studies were made on the effects of prophylactic and therapeutic oral administration of novocaine in acute radiation sickness of animals and also certain aspects of the mechanism of action of novocaine that are important for understanding its therapeutic effect in radiation sickness. Mice, rats, rabbits, and dogs were used. It was found that oral administration of novocaine prior to or after irradiation lessened the severity of radiation sickness, and, according to the data of the tests on mice and rats, increased the survival rate of the animals. The administration of a novocaine solution in immunized animals lessened the formation of agglutinins, hemolysins, and precipitins. Subcutaneous administration had a stronger and longer effect than oral administration. Novocaine solutions also had an inhibiting effect on the formation of anti-infection immunity in both non-irradiated and irradiated mice. (ATD)

38728 USE OF GALLIC ACID IN PROPHYLAXIS AND THERAPY OF ACUTE RADIATION SICKNESS. Gorodetskii, A. A.; Baraboi, V. A. pp 228-33 of Patogenez, Eksperimental'naya Profilaktika i Terapiya Luchevykh Porazhenii. Lebedinskii, A. V. (ed.). Moscow, Izdatel'stvo Meditsina, 1964. (In Russian).

A 50% survival of rats or mice given an x-ray dose of 600 to 750 R is obtained with the use of 300 mg/kg of sodium gallate, or with the use of 150 mg/kg of propylgallate. On increasing the amount of sodium gallate to 500 mg/kg, a survival of 15 to 25% is obtained even on administering the compound 2 to 4 hours after the irradiation. Repeated use of sodium gallate improves the therapeutic effect. Even with a high irradiation dose of 1000 R the protective effects of sodium gallate are evident by increasing the survival time from 5.6 days for the controls to 8.0 days for the protected mice. In addition, 3 to 7% of the protected mice survived. Dogs given a 600 R radiation dose showed a 40% survival on being protected with an intravenous injection of sodium gallate immediately after irradiation. (TTT)

38729 COMPARATIVE EVALUATION OF CERTAIN MODELS FOR THE INITIAL SELECTION OF RADIOPROTECTIVE COMPOUNDS. Rachinskii, F. Yu.; Kushakovskii, M. S.; Matveev, B. V.; Potapenko, T. G.; Slavachevskaya, N. M.; Tank, L. I.; Titov, A. V.; Yampol'skaya, L. I. pp 233-47 of Patogenez, Eksperimental'naya Profilaktika i Terapiya Luchevykh Porazhenii. Lebedinskii, A. V. (ed.). Moscow, Izdatel'stvo Meditsina, 1964. (In Russian).

Assuming that the antioxidant and reducing properties of radioprotective compounds of bivalent sulfur are related to their ability to decrease the severity of radiation sickness, models using these properties were compared. It was established that not a single model, taken separately, was

adequate for a biological method of selecting antiradiation agents; however, the results of tests of substances on several models can serve as an initial test for the selection of active substances. (ATD)

38730 RELATION BETWEEN THE EFFECTS OF THERAPEUTIC MARROW TRANSFUSION DURING RADIATION SICKNESS AND THE NUMBER OF TRANSPLANTED CELLS. **Muksinova, K. N.** pp 247-54 of Patogenez, Eksperimental'naya Profilaktika i Terapiya Luchevykh Porazhenii. **Lebedinskii, A. V. (ed.).** Moscow, Izdatel'stvo Meditsina, 1964. **(In Russian).**

A total of 25 dogs was given a ^{60}Co dose of 800 R. A suspension of bone marrow cells was then transplanted into the animals on the 3rd (Group I), 7th (Group II), or 12th (Group III) day after irradiation. Each group of six dogs was given 0.3×10^9 or 0.6×10^9 bone marrow cells per 1 kg of body weight. All the animals treated on the 3rd day after irradiation survived. No survivals were obtained in the animals treated on the 7th and 12th days after irradiation and treatment with 0.3×10^9 cell/kg. Two out of three dogs survived on being treated with 0.6×10^9 cells/kg on the 7th and 12th days after irradiation. A larger number of homologous bone marrow cells was required because of the lag in treatment time. The survival of Wistar rats given a ^{60}Co dose of 1200 R was only 10% on being treated with 5×10^7 bone marrow cells per rat. The survival increased to 32.5% on increasing the number of bone marrow cells to 5×10^8 per rat. A larger number of transplanted cells was required to obtain the maximum therapeutic effect, especially at high radiation doses. (TTT)

38731 THERAPEUTIC EFFECTS OF SELACHYL ALCOHOL DURING EXPERIMENTAL RADIATION SICKNESS. **Sviridov, N. K.; Abaturova, E. A.; Shubina, A. V.; Elpat'evskaya, G. N.** pp 254-8 of Patogenez, Eksperimental'naya Profilaktika i Terapiya Luchevykh Porazhenii. **Lebedinskii, A. V. (ed.).** Moscow, Izdatel'stvo Meditsina, 1964. **(In Russian).**

Dogs were given an x ray dose of 600 R (severe radiation sickness); rabbits were given an x ray dose of 700 R (light and average radiation sickness); rats were given an x ray dose of 800 R (average and severe radiation sickness). The dogs were given 10 mg of selachyl alcohol twice a day for 4 weeks, and the rabbits and rats were given 1 mg of compound once a day for 4 weeks. The selachyl alcohol moderated the course of the radiation sickness. The number of rat deaths decreased by a factor of 2.5 with the use of selachyl alcohol, and the average lifetime was prolonged by 4 days. Selachyl alcohol significantly increased oxygen absorption in the tissues of the irradiated animals. (TTT)

38732 USE OF TETOXACIN AND UNITHIOL IN RADIATION SICKNESS CAUSED BY ^{144}Ce. PRELIMINARY REPORT. **Vissonov, Yu. V.** pp 267-75 of Patogenez, Eksperimental'naya Profilaktika i Terapiya Luchevykh Porazhenii. **Lebedinskii, A. V. (ed.).** Moscow, Izdatel'stvo Meditsina, 1964. **(In Russian).**

Unithiol given one hour prior to intraperitoneal injection of ^{144}Ce only slightly accelerated its excretion, reducing inclusion of the isotope into the liver. However, unithiol in a dose of 100 mg/g proved very toxic for rats. Tetoxacin substantially accelerated excretion of ^{144}Ce. In the first 2 weeks after its use, up to 80% of the isotope was excreted from the organism. The preparation is of low toxicity and it is recommended that it be tested in clinics for ^{144}Ce-caused disorders. (ATD)

38733 INVESTIGATION OF PREPARATIONS CONDUCIVE TO THE REMOVAL OF CERTAIN RADIOACTIVE ISOTOPES FROM AN ORGANISM. **Il'in, L. A.; Arkhangel'skaya, G. V.; Horets, T. A.; Bokk, M. I.; Turkevich, E. A.; Lukash, N. I.** pp 275-81 of Patogenez, Eksperimental'naya Profilaktika i Terapiya Luchevykh Porazhenii. **Lebedinskii, A. V. (ed.).** Moscow, Izdatel'stvo Meditsina, 1964. **(In Russian).**

A total of 800 male rats and 100 mice were inoculated a single time by mouth or intraperitoneally with ^{144}Ce, ^{204}Tl, ^{65}Zn, ^{131}I and also with a radioisotope mixture (RM) containing, Ce, Sr, Y, I, La and other radioisotopes. Pectin was not effective in decreasing the accumulation of isotopes in the tissues. Zirconium phosphate was effective in absorbing ^{204}Tl in the stomach. DTPA was the most effective complexing agent in removing ^{65}Zn, ^{204}Tl, and the radioisotope mixture from the organism. The use of tyrosine decreased the accumulation of ^{131}I in the thyroid gland by 98% as compared to the controls. The decrease in accumulated dose with elimination of the radioisotope from the body is calculated for ^{65}Zn and for $^{144}Ce-^{144}Pr$. (TTT)

38734 INFLUENCE OF CERTAIN PHARMACOLOGICAL PREPARATIONS ON THE ABSORPTION AND REMOVAL OF ^{131}I FROM THE THYROID GLAND. **Fakhrutdinov, G. F.** pp 281-6 of Patogenez, Eksperimental'naya Profilaktika i Terapiya Luchevykh Porazhenii. **Lebedinskii, A. V. (ed.).** Moscow, Izdatel'stvo Meditsina, 1964. **(In Russian).**

The experiments were carried out on 90 white mice, 420 white rats, and 30 dogs with ^{131}I and other stable compounds being introduced by the stomach. A 5 mg/kg dose of KI administered shortly after the ^{131}I gave only a 0.3% absorption of ^{131}I by the thyroid. A KI dose <0.05 mg/kg had no effect on the accumulation of ^{131}I by the thyroid. A considerable time after ^{131}I had entered the body it was found that the administration of 0.04, 0.2 and 1 mg/kg of KI decreased the thyroid absorption of ^{131}I by a factor of 3 to 15. These amounts of KI have no effect on the hormone synthesis of the thyroid. It was found that 6-methylthiouracil (6-MTU) was effective in removing ^{131}I which had already been absorbed by the thyroid. The effectiveness of 6-MTU was significantly increased on using potassium thiocyanate along with the 6-MTU. (TTT)

Radiation Hazards and Protection

See also HEALTH AND SAFETY

Refer also to abstracts 39064 and 39218.

38735 (NYO-1704-13) THE MEASUREMENT OF ENVIRONMENTAL RADIATION. Annual Report, September 1, 1965-August 31, 1966. (New York Univ., N. Y. Dept. of Physics). July 1, 1966. Contract AT(30-1)-1704. 60p. Dep. mn. CFSTI $3.00 cy, $0.75 mn.

Environmental studies are reported on: cosmic ray ionization in the first 10,000 ft, ultralow ionization intensities from terrestrial sources, and the beta component on the ground. New instruments for the cosmic ray laboratory are mentioned which include a large analytical balance, a large (130 liter) spherical monitoring chamber on the roof, special data recording equipment, provision for eventual data handling by computer, and new small spherical chambers. On field trips laboratory instrumentation was compared with the HASL scintillation spectrometer and ionization chamber. (W.E.B.)

38736 RELATION BETWEEN THE MODIFICATIONS OF THE WATER CONTENT OF BARLEY SEEDS AND THE RADIOPROTECTION INDUCED BY SALINE SOLUTIONS WITH INCREASING OSMOTIC POTENTIAL. **Gillet, C.** Bull. Cl. Sci., Acad. Roy. Belg. (5), 51: 1074-81(1965). **(In French).**

The length of seedlings from x irradiated barley seeds presoaked in water for increasing periods of time or in $CaCl_2$ solutions with increasing osmotic potential were compared. The radioprotective effect of saline solutions was shown and its limits were defined with respect to the water content of the seed. It appears that the action of $CaCl_2$ solutions are only effective during the enzymatic activation period that characterizes the initial stages of germination. In post treatment, $CaCl_2$ has no favorable effect except at high sublethal doses. Different mechanisms such as the modifications in the physiochemical state of the macromolecules and the reduction of leaching of some substances were proposed to explain the radioprotective effect of $CaCl_2$ solutions. (tr-auth)

38737 RADIATION PROTECTION DURING OPERATION OF X-RAY DEVICES. **Safronova, M. V.** (Inst. of

Radiation Protection, Leningrad). Gig. Truda Prof. Zabolev., 9: No. 9, 22-7(1965). (In Russian).

The effectiveness of protection provided to personnel servicing industrial x ray equipment was evaluated. Measures ensuring safety of the service personnel from radiation hazards are suggested. A check-up on the effectiveness of the protection provided for in the units under discussion disclosed certain defects in their design. Dosage rates of scattered radiation recorded at a number of installation sites accessible for the staff reach tens and, in some cases, several thousand milliroentgens per hour. The available protection brings radiation levels down by 3 to 4 orders. The energy of scattered radiation conforms to the characteristic radiation coming from the material comprising the scattering surface and, when scattered from copper, brass, and lead, amounts to 8.4, 8.6, and 11.2 kev, respectively. (auth)

38738 MECHANISM OF THE PROTECTIVE EFFECT OF THIOPENTAL. Vacek, A.; Tacev, T. (Inst. of Biophysics, Czechoslovak Academy of Sciences, Brno). Int. J. Radiat. Biol., 10: 509-17(1966).

The relation between change in oxygen tension in the tissue and survival after administration of thiopental was studied in mice exposed to 525 or 720 R x radiation. A decrease in oxygen tension in all tissues was found. The speed of the decrease in oxygen-tension was dependent on the manner of administration of thiopental and the extent of the reduction on the quantity administered. A reduction in oxygen consumption and a fall in rectal temperature occurred at the same time as the decrease in oxygen tension. After intraperitoneal injection of thiopental, the decrease in oxygen-tension reached a peak in 10 min and thereafter returned to its initial level. During irradiation of the mice at various times after administration of thiopental, radioresistance increased as oxygen tension was reduced, then decreased as oxygen tension returned to the initial level. The authors conclude that the radioprotective effect of thiopental is due to the reduction in oxygen tension. (auth)

38739 CORRELATION BETWEEN THE MORTALITY DUE TO TUMORS AND THE DIETARY RADIOACTIVITY IN MAN. Pincet, J. (Travail du Centre Anticancereux, Rennes, France). J. Radiol., Electrol. Med. Nucl., 47: 249-51(May 1966). (In French).

A comparative study was made on cancer mortality in two communities identical in social environment and dietary habits but differing in geology in that one community had numerous uranium deposits. Mortality due to carcinoma was much higher in the community with uranium deposits than in the control community. Analysis of water samples for Ra, Rn, and U showed a relation between the amount of these elements ingested and tumor mortality. (C.H.)

38740 EFFECTIVENESS OF BONE MARROW TRANSPLANTATION IN RELATION TO TIME OF ADMINISTRATION. Muksinova, K. N.; Klyzhuk, K. N. Med. Radiol., 11: No. 4, 42-7(Apr. 1966). (In Russian).

The possibility of elevating the curative effect of late bone marrow transfusions by increasing the quantity of transplanted cells was studied. Experiments were performed on mongrel dogs and rats of the Wistar line. The dogs were subjected to ^{60}Co total gamma irradiation in a dose of 800 R (intensity of radiation 3.5 to 4 R/min) and rats, in a dose of 900 R (intensity of radiation 22 R/min). The authors compared the curative effect of different quantities of bone marrow administered at various times after the irradiation. It was found that by transfusion of large quantities of bone marrow at late periods after irradiation one could obtain almost the same effect as in instances of treatment at early periods. There was noted a distinct relation between the restoration of hematopoiesis in the treated animals and the quantity of cells introduced. (auth)

38741 RADIATION DOSES FOR SOME TYPES OF MARINE BIOTA UNDER PRESENT-DAY CONDITIONS. Fedorov, Anatol F. (IAEA, Monaco). Radioact. Sea, No. 14, 1-28(1965).

General considerations regarding the specific nature of the distribution of radiation doses received from natural sources under marine conditions are discussed. It is suggested that the most critical form of marine life from the point of view of radiation damage will be the eggs of different organisms. Some mathematical calculations are made and formulas derived for determining the radiation dose received by individual eggs, as independently developing organisms, in a radiocontaminated medium. A working formula is derived for calculating the dose rate to individual eggs in water contaminated by beta-emitting isotopes. A general formula is derived for calculating the dose rate received by various organs and tissues adjoining the integument of fish from the beta radiation emitted by a mixture of long-lived radioactive substances adsorbed on the skin. (auth)

38742 MONITORING STREAMS FOR RADIOACTIVE WASTES. Robinson, Loyd R. Jr. (Mississippi State Univ., State College). Water Sewage Works, No. 112, R152-R60(Nov. 30, 1965).

The monitoring of a stream for radioactivity and the fate of radionuclides in streams are discussed. Samples of water, biota, and silt are required for adequate monitoring of a stream. Water below a nuclear installation should be continuously monitored. As biological and silt samples are cumulative, monthly or even seasonal samples give a good indication of concentration buildup. (D.H.M.)

38743 HEARINGS BEFORE THE SUBCOMMITTEE ON RESEARCH, DEVELOPMENT, AND RADIATION OF THE JOINT COMMITTEE ON ATOMIC ENERGY, CONGRESS OF THE UNITED STATES, EIGHTY-NINTH CONGRESS, FIRST SESSION ON FEDERAL RADIATION COUNCIL PROTECTIVE ACTION GUIDES, JUNE 29 AND 30, 1965. Washington, D. C.. Joint Committee on Atomic Energy, 1965. 701p. GPO.

The Subcommittee on Research, Development, and Radiation of the Joint Committee on Atomic Energy, Eighty-ninth Congress of the United States held hearings on June 29 and June 30, 1965, on the Federal Radiation Council Protective Action Guides, as set forth in FRC Reports Nos. 5 and 7. Emphasis was placed on information on fallout that had accrued since 1963, and particularly the FRC Protective Action Guides for ^{137}Cs, ^{131}I, ^{89}Sr and ^{90}Sr, published in 1964 and 1965. Topics discussed included the radioactive half life, biological half life, and affinity for specific body organs of these isotopes; the world-wide inventory of environmental ^{90}Sr in 1965; food chain pathways to man, dietary levels, and content in specific foods such as milk and wheat during 1965; content in whole-body or specific tissues of man; the types of action taken for the protection of populations; monitoring and sampling equipment used for protective programs, and the cost of protective actions. (C.H.)

Radiotherapy and Radiodiagnosis

Refer also to abstracts 38615, 38634, and 38675.

38744 (DP-1066(Vol.1), pp IV.47-66) RADIOTHERAPY. Bruner, H. D. (Division of Biology and Medicine (AEC), Washington, D. C.).

Radiotherapy practices are reviewed. Radiation sources of ^{60}Co, ^{226}Ra, and ^{137}Cs are described and their applications in radiotherapy explained. The use of beads of ^{90}Y in the pituitary gland and the proposed uses of ^{252}Cf are discussed. (F.S.)

38745 (NYO-3267-3) USE OF ISOTOPES AND SLOW NEUTRONS IN DIAGNOSIS AND TREATMENT OF NEOPLASMS. Technical Progress Report, June 1, 1965-May 31, 1966. Sweet, William H. (Massachusetts General Hospital, Boston. Physics Research Lab. Massachusetts General Hospital, Boston. Neurosurgical Service). May 25, 1966. Contract AT(30-1)-3267. 19p. Dep. mn. CFSTI $1.00 cy, $0.50 mn.

I. Progress is reported in studies of applications of thermal and epithermal neutrons and appropriate isotopes for the treatment of brain neoplasms. Radiation dosimetry

for neutron capture therapy was investigated in tissue equivalent phantoms containing Au wires and LiF powder in capsules. The activities of the Au wires were measured in a scintillation spectrometer and the flux was calculated from the measured activities while the γ absorbed dose was measured using the LiF dosimeters read in a thermoluminescent readout meter. Semiconductor detectors were used to estimate the dose contribution from background radiations. Efforts to obtain and evaluate boron compounds for use in ^{10}B thermal neutron capture were continued. Two sulfhydryl-containing boron hydride anions were evaluated in mice and rabbits as to tumor-blood boron ratios and pharmacological effects. Antigens were prepared from normal human cortical gray matter and tumor tissues for use in studies of brain tumor proteins. Preliminary results of immunological studies in rabbits are reported. Attempts to synthesize boron analogues of biologically-active compounds led to the preparation of boron containing nitrogen mustards known to have anti-cancer activity. II. Progress is reported in the use of positron emitting radioisotopes in the diagnosis and localization of neoplastic and non-neoplastic brain tumors. The development of a positron camera, that uses a large NaI detector viewed by a chain of image intensifier tubes to determine the geometric relation of annihilation γ pairs, the development of a multi-crystal mechanical positron scanner, and the computer processing of scan data are discussed. Applications of the positron-emitting ^{15}O for studies of cerebral blood flow are reported. A list is included of 24 publications during the period covered by this report. (C.H.)

38746 (NYO-3364-19) RADIATION EXPOSURE OF THE GONADS DURING BETATRON THERAPY AT 31 Mev. Stroemme, Aksel (Statens Radiologisk-Fysiske Laboratorium, Oslo (Norway)). [1965]. Contract AT(30-1)-3364. 4p. Dep. mn. CFSTI $1.00 cy, $0.50 mn.

Small cylindrical ionization chambers attached to the skin or inserted in the rectum were used to measure the radiation dose to the gonads during radiotherapy of tumors using 31 Mev x radiation. During exposure of a 12 × 15 cm field on the thorax to 6000 R given in 30 seances of 200 R the dose to the ovaries averaged 2.2 to 2.8 R and the dose to the testes averaged 1.6 to 2.1 R. Possible genetic consequences of radiation exposure during radiotherapy are discussed. (C.H.)

38747 MYOMETRIAL BLOOD FLOW IN PREGNANCY MEASURED WITH XENON. Lysgaard, H.; Lefevre, H. (Glostrup Hospital, Copenhagen). Acta Obstet. Gynecol. Scand., 44: 401-7(1965).

Advantages and disadvantages of the ^{24}Na and ^{133}Xe methods for measuring myometrial blood flow (MyBF) in pregnancy are contrasted, results with the ^{133}Xe technic are described, and radiation doses to mother and fetus with this technic are estimated. The range of values of ^{24}Na clearance in the myometrium is wide. A direct determination of placental clearance is possible only when the placenta is situated anteriorly in the uterus. As ^{24}Na is not freely diffusible in the tissues, the values found by a ^{24}Na clearance test are inapplicable as a measure of the absolute blood flow in the placenta or in the myometrium. The inert radioactive gas ^{133}Xe is well-suited for measuring the blood flow in skeletal muscle, and its use for determining myometrial blood flow was therefore explored. As with ^{24}Na, preliminary results showed a marked scatter, but a considerably reduced MyBF was evident in abnormal pregnancies. To carry out the technic, 0.1 ml isotonic NaCl, containing about 50 μC ^{133}Xe, was injected through the abdominal wall into the myometrium of pregnant women in the last trimester. A scintillation detector, coupled to an automatic scaler and printer, was placed about 10 cm above the site of injection, thus covering an abdominal area having a diameter of about 20 cm. The rate at which Xe disappeared from the tissue was measured. In 46 tests on 34 normal pregnant women the mean MyBF was found to be 12.7 ml/100 g/min, with a range from 2 to 32 ml. Eight patients with pre-eclampsia gave a value of 12.7 ml/100 g/min, with a range from 3 to 26 ml. The average of the 45 measurements in abnormal pregnancies is 10 ml/100 g/min. The radiation dose to the fetus and the gonads was calculated as ~0.2 mrad, which is about 0.2% of the dose received in a general x-ray survey of the abdomen and ~0.5% of the radioactivity to which the fetus and gonads are exposed when the investigation is performed with ^{24}Na. (BBB)

38748 VETERINARY MEDICINE AND NUCLEAR SCIENCE: INTRODUCTION TO RADIOBIOLOGY AND RADIOISOTOPE TECHNICS. Bruyere, P. (Ecole de Medecine Veterinaire, Brussels). Ann. Med. Vet., 107: 383-430(Oct. 1963). (In French).

An extensive account is given of the physical bases of the use of radioisotopes in veterinary medicine. Numerous tables are provided showing the physical characteristics of isotopes used in this field. Theory, practice, and instrumentation for measurement of radioactivity are described in detail and examples are cited. Data are given for synthesis of the artificial radionuclides, and for the preparation of labeled compounds. Nuclear reactions involved in the formation of radionuclides are explained and illustrated by numerous examples. Characteristics of the various types of radiation (α, β, and γ) are described and specific applications to veterinary research and medicine are presented. (BBB)

38749 THYROID CANCER AFTER ^{131}I THERAPY FOR THYROTOXICOSIS. Staffurth, J. S. (St. Thomas's Hospital, London). Brit. J. Radiol., 39: 471-3(June 1966).

The case history is presented on a thyroid cancer that developed six years after ^{131}I therapy of toxic nodular goiter. The ^{131}I dose was 13.5 mc estimated to deliver 10,000 rads to the thyroid. (C.H.)

38750 NOTATION AND FORMULAE FOR DOSE SPECIFICATION AND CALCULATIONS IN RADIOTHERAPY. Karzmark, C. J.; Deubert, Angela; Loevinger, R.; Steed, Patricia R. (Stanford Univ., Palo Alto, Calif.). Brit. J. Radiol., 39: 476-8(June 1966).

Notations and formulae are presented that were developed to simplify radiotherapy records and dose calculations. Tables are included for symbols and subscripts for dose specification and calculation, notation and formulae for source-skin-distance techniques, and notation and formulae for source-tumor-distance techniques. The need is stressed for standardized conventions and symbols for the communication of information on radiation dose calculations. (C.H.)

38751 CARCINOMA OF THE CERVIX. MacLean, Margaret A. (Vancouver General Hospital, Can.). Can. Nurse, 61: 968-71(Dec. 1965).

Radiotherapy for cervical cancer is explained in terms of technique, dosage, and clinical results. Nursing hazards with Ra-implanted patients are discussed and a case of radiation injury to a patient receiving combined Ra and conventional x-ray therapy is given. In the invasive stage, the best treatment is radium and cobalt-60 therapy. The radium is used in three consecutive insertions over a 3 week period. This is followed by external irradiation using cobalt-60 therapy to prevent spread to the lymph drainage area. Necessary precautions against the loss of radioactive material are described. Using the inverse square law, at two ft the nurse would receive 200 mR/hr while at 8 ft she would receive 12.5 mR/hr. The radiation the nurse receives should be measured on a dose meter, and the amount of radiation should be minimized by careful planning. The case history is reported of a patient who developed a radio-induced ulcer as a result of Ra and x-ray treatments. Four months after completion of treatment, the superior fornix showed a necrotic area. Symptomatic treatment was instituted and continued although the necrotic area appeared improved. The following month, radiation necrosis was apparent, and a biopsy was done. Antibiotic cream was used to treat the chronic inflammation which was secondary to irradiation. Nine months following initial therapy the area appeared improved and four months later treatment was discontinued. (TCO)

38752 CANCER OF THE LOWER LIP. Elfenbaum, Arthur. Dent. Dig., 71: 550-3(Dec. 1965).

Design and construction of protective device for radium irradiation of lip cancer are explained with reference to a patient with squamous cell carcinoma of the lower lip. Irradiation is often the preferred treatment because of its high rate of cure in lip cancer, its easy accessibility, and to avoid surgical mutilation of tissue which would require further surgical correction later. The appliances recommended in textbooks for placing radium needles around the tumor are too clumsy. A new approach in constructing a radiation device that would protect healthy tissues was developed. Two acrylic rims were constructed for the edentulous jaws, the lower one with a curved extension so that when the radium needles were placed in it they would virtually be wrapped around the tumor. Guided by dummy needles, slots were cut in the extension according to a mathematically calculated dosage formula. The upper and lower rims were then luted together with self-curing acrylic and the patient was taught how to manage the entire carrier which was unavoidedly bulky. Pieces of sheet lead were shaped and glued to the appliance as shields to protect the upper lip and tongue against the radiation. After the needles were placed in the slots, they were locked in with carding wax securely held in undercuts. (BBB)

38753 MOBILE SHADOW-SHIELD WHOLE-BODY MONITOR FOR MEDICAL RESEARCH. Boddy, K. (Scottish Research Reactor Centre, East Kilbride, Scotland). Health Phys., 12: 1148-9(Aug. 1966).

Design criteria are presented for a shadow-shield whole-body counter for use in medical research. A single large scintillation detector is used close to the patient. The construction is simplified and less shielding is required by providing for mobility of the patient. (C.H.)

38754 RADIOTHERAPY IN TREATMENT OF CARCINOMA OF THE CERVIX AND ITS COMPLICATIONS. Roy, D. K. (Chittaranjan Cancer Hospital, Calcutta). Indian J. Cancer, 2: 153-8(Sept. 1965).

Early and late side-effects of irradiation are reported in this survey of 3056 cases of gynecologic cancer, consisting of 2597 cases of carcinoma of the cervix (85%). Of these, 297 belonged to Stage I (11.5%), 391 to Stage II (15.1%), 1490 to Stage III (57.4%), and 389 to Stage IV (15%). Of these, 153 were treated by surgery (usually Stage I or II) and 1231 by radiotherapy. The results of radiotherapy and the complications arising from this treatment were studied in 951 cases which had completed either full course of radium or full course of deep x rays. By a modified Stockholm method, three applications of radium were usually given, each application consisting of 50 mg radium inside the uterus and 50 mg in the vagina. The interval between the 1st and 2nd applications was 1 week. External radiation was usually given in the 3-wk interval between the 2nd and 3rd radium applications or in some cases after the completion of the radium treatment. Radiation-induced complications were divided into immediate and late types. The immediate complications were anorexia, nausea, vomiting, diarrhea, dysuria, anemia, leucopenia, infection, and moist desquamation of the skin. Only the late complications were studied statistically. Of 951 cases treated, 165 complained of pain (17.4%), the commonest being sciatic pain and backache. Rectal complications occurred in 98 (10.3%). Of these, 85 had proctitis and bleeding with or without ulcer (8.9%) and 13 had rectovaginal fistula (1.4%). Bladder complications were seen in 47 cases (4.9%). Of these 31 had cystitis and hematuria with or without ulcer (3.3%); 16 cases developed vesicovaginal fistula (1.6%) and all were in Stage III. Other complications included 4 cases of pyrometra (0.5%), two cases of intestinal obstruction, 13 cases of edema of legs, fracture of femoral neck, hydroureter, and hydronephrosis. The incidence of these complications was higher in advanced stages of the disease. Of 951 cases treated, 292 had symptoms within 1 year (30.7%), 49 between 1 to 2 years (5.2%), 27 between 2 to 5 years (2.8%) and only 8 after 5 years (0.8%). A total of 39.5% of patients had some complications after treatment. (TCO)

38755 RATIONALE AND BENEFIT OF PREOPERATIVE IRRADIATION IN LUNG CANCER. Bloedorn, Fernando G. (Univ. of Maryland, Baltimore). J. Amer. Med. Ass., 196: 340-1(Apr. 25, 1966).

Use of preoperative irradiation for lung cancer is founded on the principle that the periphery of the tumor is more sensitive than its core, the sensitivity of the tumor to irradiation is in inverse ratio to its volume or number of cells, blood and oxygen supply are indispensable for proper radiation effect on the tumor, lymph-node metastases can be controlled by radiation, radiation prior to surgical manipulation can diminish the number of malignant cells shed into the operative fields and circulatory stream, and a waiting period between irradiation and surgery is important when high doses of irradiation have been used to allow the tumor to regress and the radiation reaction to subside. The main objection to this therapy is the delay in healing, which is always present in heavily irradiated tissues. These delays can be reduced to a minimum. The area of irradiation should include the whole mediastinum and primary tumor and when indicated, the supraclavicular areas are added to the volume of irradiation. Results in 200 patients show that irradiation is well tolerated by most patients. Sterilization of the lymph nodes is higher than the sterilization of the primary tumor, and the rate of sterilization in both the primary tumor (35%) and the lymph nodes (77%) is higher than was expected. There is a higher percentage of cases made operable after preoperative irradiation. The rate of complications was high at the beginning of the study, but improved considerably in the last two years with proper changes in the technique and the selection of patients for postirradiation surgery. (TCO)

38756 THE THOROTRAST KIDNEY. Verhaak, R. (St. Ignatius Ziekenhuis, Breda, Netherlands). J. Belge Radiol., 48: 711-29(1965).

By an examination of case histories and follow-up studies, 8 patients were found in whom pyelo-renal backflow had occurred during Thorotrast pyelography in 1932-1934. Pyelo-interstitial backflow was found in 10, and pyelo-tubular backflow on 3 occasions. A control group of patients was also studied in whom no pyelo-renal backflow had occurred. Where no pyelo-renal backflow was seen in the retrograde pyelogram in 19 kidneys a subsequent x ray showed no Thorotrast deposits in this kidney. In 3 kidneys the site where the retrograde pyelogram showed a pyelo-tubular backflow, no Thorotrast residue was subsequently visible. When, however, the retrograde pyelogram showed a pyelo-interstitial backflow, a subsequent x ray disclosed Thorotrast deposits in the kidney (11 kidneys in 9 patients). Invariably ThO_2 deposits were found around the calyces where the pyelo-interstitial backflow had previously been visible. Thorotrast residues sometimes remain in the renal pelvis when drainage from the renal pelvis is impeded but these deposits apparently disappear after a few months. In subsequent x rays of two patients with moderate hydronephrosis in whom Thorotrast pyelography had previously been carried out, no deposits of the contrast medium were seen. Small quantities of Thorotrast deposits in kidney are drained by the lymph channels. After a few years punctiform deposits are found at the sites of the regional lymph nodes of the kidney. These deposits grow larger in the course of time. Linear opacities were also frequently seen in this region, caused by lymph vessels filled with Thorotrast. The quantity of Thorotrast in the kidney does not appreciably diminish in the course of 25 years. In one case the quantity of thorium was chemically determined to be 75 mg, as thorium. The 5 kidneys found to contain appreciable quantities of Thorotrast were found to be diminished in size as compared with the size 20-25 years earlier. In 8 cases, no suggestion of the existence of a malignant process in the Thorotrast kidney was found but in another case renal pelvis carcinoma was found 27 years after retrograde pyelography. (TCO)

38757 ISOTOPE PLACENTAL LOCALIZATION. Kretzschmar, Robert M. J. Iowa Med. Soc., 55: 628-9(Nov. 1965).

An evaluation is made of fetal and maternal hazards when radioisotopes are used to visualize the placenta. Fifteen years of progress have brought about refinements of instrumentation and isotopes, with reduction of radiation exposure and increased accuracy of localization. Isotope placental localization is simply another indirect technique for the localization of the placenta. It is necessary to use an indirect technique since a direct examination of the cervix carries with it hazards of hemorrhage. The principle behind the isotope technique is explained. The selected radioactive compound is one that remains in the blood stream; since the placenta had the largest volume of blood in the uterine area, it can be located by means of a suitable scanning device. The heart is used as a reference pool of blood, and measurements are expressed in terms of per cent of radioactivity of the heart. Any radiation exposure of the mother and fetus must be scrutinized carefully. In using small doses of radioactivity, e.g., 10 μC RISA, it is calculated that the total radiation exposure to the fetus is 4 Mrad or less. This represents 5% of the radiation that might be administered during the taking of a single x-ray film of the maternal abdomen. The low dose of radiation is made possible through the use of extremely sensitive external counting devices. With the use of the newer chromium-tagged products, the theoretical hazard to the fetal and maternal thyroids can be eliminated. In general, it is concluded that the isotope technique of placental localization is safe, and is as accurate as any presently used indirect method. (BBB)

38758 TRANS-SPHENOIDAL HYPOPHYSECTOMY. Bateman, G. H. J. Oto-Laryngol. Soc. Austral., 1: 256-60 (Sept. 1964).

Use of ^{90}Y and ^{198}Au in radiohypophysectomy is described, along with clinical results and complications. Seven of 18 cases of metastatic breast cancer showed clinical remission of symptoms following trans-sphenoidal implantation of ^{198}Au. However, serious complications were noted, namely blindness in both eyes in one patient and blindness in one eye in another. By use of ^{90}Y, replacing ^{198}Au, it was felt that the shorter range of β radiation, compared with the γ radiation of radiogold, might help avoid such damage to adjacent structures, particularly in optic chiasma or nerves. Eleven of 22 cases of breast cancer treated by ^{90}Y hypophysectomy showed clinical improvement. Effectiveness of hypophysectomy by this method was demonstrated by reduction of ^{131}I uptake by the thyroid and adrenal steroid secretion. These radioisotope methods were contrasted to the surgical procedure in simplicity of technique, results, and complications. Treatment of complications is also considered. Hormone replacement is provided by three 25-mg doses of cortisone acetate per day orally and 1 g thyroid extract per day orally. Polyuria may be treated by Pitressin. Cerebrospinal fluid leak may be managed by muscle graft. (BBB)

38759 PREGNANCY COMPLICATED BY CARCINOMA OF THE CERVIX: A CASE REPORT. Klauber, William A. J. S. Carolina Med. Ass., 61: 340-2 (Nov. 1965).

The case report of a 26-year-old woman with pregnancy complicated by carcinoma of the cervix is reviewed. The diagnosis was made at the early part of the last trimester of pregnancy at which time it was felt that the fetus was nonviable. Consequently, a novel approach was devised to permit radiation therapy to the mother without harm to the fetus. By an abdominal x-ray film it was demonstrated that the fetal buttocks could be displaced at least 10 cm above and to the right of the cervical os by external pressure on the fetus during x-ray filming. The cervix was then treated locally with intracavitary cone x-ray therapy directed obliquely toward the left side while the fetus was being displaced upward and toward the right side. Calculations and diagrams revealed that the fetus received an insignificant amount of radiation during this procedure. The local x-ray therapy to the cervix would perform a delaying action with respect to the primary cervical tumor and would attenuate any cells which might tend to escape from the primary lesion while awaiting viability of the fetus. A dose of 3000 R (in air) delivered obliquely to the cervix, was given in two fractions at a one-week interval. Eleven days after the last x-ray treatment the patient was delivered of a normal male premature infant by cesarean section. Following delivery, external x-ray therapy was given in two courses. During the interval between courses of x-ray therapy, intracavitary radium treatment was initiated. The total depth doses are given. Following radiation therapy no complications or untoward effects on the baby were noted. At present the child is a normal healthy male 10 years of age and the mother is well. (TCO)

38760 LONG-TERM RESULTS OF TREATMENT OF BASEDOW'S DISEASE WITH RADIOACTIVE IODINE. Linquette, M.; Swyngedauw, J.; May, J. P. (Centre Oscar Lambret, Lille). Lille Med., 9: 903-5 (Dec. 1964). (In French).

Clinical results and complications resulting from the therapeutic use of ^{131}I in hyperthyroidism are discussed. Clinical and biologic criteria of improvement resulting from ^{131}I treatment are defined. In 86% of the 91 cases examined, euthyroidism was established, 6% remained hyperthyroid, and 8% became hypothyroid. Body weight was maintained or increased in most of the patients. The volume of the goitrous gland did not increase in any case. Ocular symptoms became worse in two cases, while residual exophthalmos was seen in a few cases. Tachycardia was reduced in most cases, but in five patients complete arrhythmia persisted. The cure rate of 86% after use of ^{131}I compares favorably with results in two other large studies (80 and 84.5%). The problem of development of hypothyroidism as a late complication of radioiodine treatment is discussed. The rate observed here (8%) is rather high but lower than in some earlier studies. By giving relatively low doses (6 to 8 mC) it is possible to minimize this complication. However it is not possible to foresee undue radiosensitivity of the thyroid in individual cases. At present, hypothyroidism remains a drawback of the radioiodine treatment of hyperthyroidism, but with improved dose calculation and measurement its incidence can be reduced. (BBB)

38761 DOSIMETRIC SUBSTANTIATION OF THE ROENTGENOTHERAPEUTIC METHODS IN DEALING WITH HYPOPHYSEAL TUMORS. Stavitskii, R. V.; Slavin, L. G. Med. Radiol., 11: No. 1, 6-12 (Jan. 1966). (In Russian).

Experimental data are presented that define more accurately dosimetric characteristics of methods for teleroentgentherapy of hypophyseal tumors with due account of absorption by the bone tissue. Dosimetric investigations showed that both qualitative and quantitative characteristics of the radiation tend to undergo certain changes because the latter undergoes some changes due to its absorption by the bone tissues. This leads to variations occurring in relative radiation depth doses. The obtained data enabled true values to be obtained for the radiation doses in hypophysis, while the appraisal of the quality of the radiation permitted a more appropriate approach to the estimation of absorbed doses on the basis of the known exposure doses. (auth)

38762 A METHOD FOR DETERMINING DOSE DISTRIBUTIONS IN A HOMOLOGOUS PHANTOMS IN DISTANCE GAMMA THERAPY INVOLVING THE USE OF WEDGE-LIKE FILTERS. Pavlov, A. S.; Ermolaeva, E. V.; Pavlova, T. G. (Central Clinical Hospital, Ministry of Public Health and Scientific Research, USSR. Inst. of Roentgen-Radiology, Ministry of Public Health, USSR). Med. Radiol., 11: No. 2, 3-11 (Feb. 1966). (In Russian).

A method is described of determining isodoses in the tissue in distance gamma therapy using ^{60}Co sources that employs the use of wedge-like lead filters. Tissue isodoses for irradiation fields of 4×4, 6×4, and 8×6 cm, the skin-focus distance of 55 cm, for angles of wedge-like lead filters of 10, 13, and 18° are given. The authors obtained a diagram of dependence between the angle of inclination of isodoses in the central part of the irradiation field and the value of the filter angle. The paper describes the method of determining the filter profile at any distance from the irradiated surface and gives one of the possible designs of the wedge-like filter, which may be fastened to the pro-

tective casing of the apparatus charging device. The data presented make it possible to supplement the existing dosimetric characteristics of the gamma apparatus and to enhance the choice of optimal conditions of irradiation in distance gamma therapy. (auth)

38763 X-RAY THERAPY OF CARCINOMA OF THE STOMACH THROUGH A LEAD GRATING. Karibov, Yu. I. Med. Radiol., 11: No. 2, 15-19(Feb. 1966). (In Russian).

A method is described of x ray therapy through a lead grating (screen) by means of which it is possible to enlarge the absorbed dose in the focus during irradiation from several fields and results in maximal sparing of the surrounding organs and tissues. This method of irradiation was used in the treatment of 19 patients suffering from inoperable carcinoma of the cardial region of the stomach. The irradiation was effected from two skin fields (anterior and posterior). The single absorbed focal dose on the average comprised 230 rad in the open areas and 160 rad in the closed ones. The total absorbed focal dose comprised correspondingly 9,300 rad in the open areas and 6,500 rad in the closed ones. Good results of palliative treatment of inoperable carcinoma of the stomach in comparison with other modes of therapy were obtained. (auth)

38764 RADIOSENSITIVITY OF MALIGNANT MELANOMA. Nivinskaya, M. M.; Parshikova, S. M. Med. Radiol., 11: No. 2, 20-6(Feb. 1966). (In Russian).

On the basis of a meticulous clinico-morphological analysis of 72 patients who were subjected to preoperative x irradiation with the subsequent removal of malignant melanoma, the authors revealed signs of dystrophy of the tumor in 52 cases. In 26 patients there were noted marked changes in the tumorous tissue, frequently with complete necrosis of tumorous cells and replacement of the tumorous focus by cicatricial connective tissue. The degree of radiation injury does not directly depend on the value of the dose, this making it unnecessary to utilize doses over 13,000 to 15,000 rad. In the authors' opinion, the absence of morphological signs of degeneration could not be considered as absolute proof of the radioresistance of malignant melanoma, since the clinical regression of the tumor, as well as a number of radiometric and biochemical investigations, point to profound alterations occurring under the influence of irradiation in the malignant melanoma. (auth)

38765 ABSORBED RADIATION DOSES IN ORGANS AND TISSUES OF THE HEAD IN SHORT-DISTANCE X-RAY THERAPY OF CANCER OF THE FACIAL SKIN. Novikova, L. V.; Konnov, B. A. Med. Radiol., 11: No. 2, 62-70(Feb. 1966). (In Russian).

On the basis of complex clinical examination of 226 patients before short-distance x ray therapy, directly thereafter, and at different periods following recovery, the authors established that a mild total radiation reaction occurs in a number of patients. The occurrence of the latter is explained by the fact that the institution of short-distance x ray therapy of cancer of the facial skin is attended by absorption of ionizing radiation in organs and tissues of the head. Measurement of the absorbed doses was carried out on a bone-paraffin phantom of the head by means of a chemical method of dosimetry. Dosimetric investigations showed that when the median absorbed dose in the tumor comprises 3.744 rad the mean absorbed radiation dose varies within the following limits, depending on the localization of the irradiation field, its size, and direction of the central ray: in the hypophysis, 15.3 to 80.5 rad; in the region of the lateral ventricle and corpus callosum, a 14.8 to 73.0 rad; in the temporal lobe, 12.0 to 51.0 rad; in the cerebellum, 10.0 to 32.0 rad; in the medulla oblongata, 17.5 to 53.0 rad; and in the bulbus oculi, 9.2 to 73.0 rad. When the technique of simultaneous treatment of several neoplasms of the facial skin is employed the absorbed radiation doses in vital organs and tissues of the brain may reach 500 to 700 rad and more. (auth)

38766 HEMATOPOIETIC CHANGES IN PATIENTS WITH MALIGNANT TUMORS FOLLOWING BEAM THERAPY. Kozlova, A. V.; Klimenko, A. A. (State Scientific-Research Inst., Ministry of Public Health, USSR). Med. Radiol., 11: No. 3, 27-35(Mar. 1966). (In Russian).

The dynamics of hematological changes in the peripheral blood picture following ^{60}Co γ beam therapy were followed in patients with malignant tumors. The effects of the extent of the neoplastic process, irradiation dose, and the intensity of the local and general response to irradiation were considered. Instances of nonconformance between the peripheral blood and bone marrow indices were found. The possibility of such a nonconformance necessitates examination of the bone marrow in patients with marked leukopenia during radiation treatment with a view to ascertain the actual condition of hemopoietic organs and deciding upon the continuation of the beam therapy. (auth)

38767 ROENTGENO-MORPHOLOGICAL INVESTIGATION OF THE SKELETON SUBSEQUENT TO RADIATION THERAPY OF PELVIC TUMORS. Cherkasskii, L. A.; Shimanovskii, K. B. (Central Scientific Research Inst., Ministry of Public Health, USSR). Med. Radiol., 11: No. 3, 35-9(Mar. 1966). (In Russian).

In 20 deceased patients with radiation treatment in their past history, roentgenological and morphological investigations were done on the proximal portion of the femur (in 12) and of the pubic bone (in 8 cases). The patients were irradiated for carcinoma of the cervix (in 18 cases) and for cancer of the urinary bladder (in 2 cases). The cumulative dose encompassing the skin in the region of the bones under study varied from 6,000 up to 10,000 R. Radiation injury of the bone was established by radiography. The histological examination of the irradiated bone demonstrated the presence of a whole series of pathological changes in the form of osseous plates, fibrosis, and proliferation of the periosteum and fibrosis of the bone marrow. In osseous necrosis evidence was obtained of disintegration and styloid prominences on the bone. (auth)

38768 SYSTEMATIC TRANSFUSIONS OF FRESHLY PRESERVED BLOOD AND OF LEUKOCYTES TO GYNECOLOGICAL CANCER PATIENTS FOR PREVENTION OF LEUKOPENIA IN THE COURSE OF RADIATION THERAPY. Zhavoronkova, L. A.; Katulkina, N. N.; Kovalevskaya, T. N.; Litvina, N. M.; Makarova, I. A.; Tregubova, N. N.; Khait, M. M.; Yastrebenetskaya, M. M. (District Oncological Clinic of the Stavropol Region, USSR). Med. Radiol., 11: No. 3, 40-4(Mar. 1966). (In Russian).

Transfusions of freshly preserved blood to cancer patients undergoing radiation therapy, started prior to the initiation of the treatment or in the first days after its commencement and practiced once a week for 7 to 10 weeks as a general rule prevented the development of leukopenia, and ensured the regular rhythm of the treatment and its proper conclusion. In most of the patients phagocytic activity and the production of leukocytes were stimulated. The transfusion of leukocytic mass was found to have no advantages over that of the freshly preserved blood. When analyzing the blood of patients in the course of radiation therapy, account is to be taken not only of the quantitative and morphological composition of the white blood but also its capacity for phagocytosis. Considering the possibility of complications due to isosensibilization the blood should be taken each time from different donors. Since there were cases of leukopenia after termination of hemotransfusions with radiation therapy still going on the hemotransfusion is to be continued up to the termination of the treatment. (auth)

38769 THE STATE OF CELLULAR ELEMENTS IN PARAMETRIAL AND PARACERVICAL CELLULAR TISSUE DURING PREOPERATIVE BEAM THERAPY IN CARCINOMA OF THE CERVIX. Kolesnikova, G. S. (Kharkov Inst. Medical Radiology). Med. Radiol., 11: No. 3, 44-50 (Mar. 1966). (In Russian).

The state of cells in the parametrial and paracervical cellular tissue of patients undergoing radiation therapy was studied. An appreciable reduction of the cellular composition of the tissue, as distinct from patients not subjected to roentgen and radium beam therapy, prevailed. Degenerated cellular forms (old and degenerated fibroblasts and macrophages), along with a large number of stripped nuclei were observed. Patients who received radioactive isotopes into the parametrial cellular tissue

demonstrated a complete disappearance of cambium cells, nearly complete absence of macrophages, and an increased number of fibroblasts presenting signs of degeneration. All these phenomena are, apparently, due to a more powerful radiation effect of isotopes produced directly on the cellular tissue. (auth)

38770 DETERMINATION OF THE TRACER DEPOSITION DEPTH BY A METHOD INVOLVING SIMULTANEOUS MEASUREMENT OF TWO VALUES. Denisenko, A. N.; Lyapidevskii, V. K. Med. Radiol., 11: No. 3, 62-5(Mar. 1966). (In Russian).

A procedure is proposed to determine the depth of tracer radioisotope deposition by a simultaneous measurement of two values dependent upon the γ spectral composition of the radiation. The method permits gaining information about the depth of the tracer deposition directly on a scanogram during isotopic scanning. Application of the method for measurements of ^{198}Au deposition is described. (auth)

38771 SOME DOSIMETRIC SPECIFICATIONS OF THE GAMMA THERAPY UNIT "LUCH-1". Ostretsov, L. A.; Galina, L. S.; Vasil'eva, E. D.; Partolin, O. F. Med. Radiol., 11: No. 3, 77-81(Mar. 1966). (In Russian).

Isodose curves for a new ^{60}Co gamma therapy unit, Luch-1, were plotted for skin-source distances of 50 and 75 cm. The dosage rate is shown to depend upon the extent of the field. The dosage rate is noted to go up parallel with the increase in the extent of the field and, for this reason, the qualitative characteristics of the unit can be established only when the dosage rate is measured for a definite size of the field. An estimation of the backscattering contribution from the phantom was made. The maximum of ionization for E-1.25 Mev in a tissue equivalent medium was determined. Evidence was obtained proving that for relative measurements it is possible to use semiconductor CdS detectors, with a corresponding provision for energy dependence compensation. The essential advantage of the method are simplicity of the measuring circuit and small dimensions of the detector. (auth)

38772 TECHNIQUE OF RADIUM THERAPY OF CANCER OF THE CARDIAL REGION OF THE STOMACH WITH A 25-Mev BETATRON. Tsybul'skii, B. A.; Kornev, I. I. Med. Radiol., 11: No. 4, 3-8(Apr. 1966). (In Russian).

The authors propose a new method of irradiation of patients suffering from cancer of the cardia by means of 25 Mev betatron involving inflation of the stomach. This method makes it possible to maintain the required focal dose in the tumor and to avoid, to a great extent, irradiation of vital organs. The authors discuss the favorable immediate results of treatment instituted in 11 patients suffering from cancer of the cardia. (auth)

38773 IMMEDIATE AND REMOTE REACTIONS IN BEAM THERAPY OF CERVICAL MALIGNANT NEOPLASMS. Kozlova, A. V.; Merkova, M. A. Med. Radiol., 11: No. 4, 8-15(Apr. 1966). (In Russian).

Examination of 60 patients with malignant cervical new growths at various dates after ^{60}Co γ therapy demonstrated the consequences to be dependent on the conditions attending irradiation course, distribution of the radiation energy in the cervical tissues, and on the magnitude of the dosage. In teletherapy of cancer of the larynx there are seen mildly pronounced and reversible vegetative vascular disorders, whose emergence is explained by the fact that the neurovascular bundle gets less than 50% of the focal dose, i.e., about 3,000 to 35,000 rad. Similar changes are noted also to occur in the application of gamma therapy to the cervical lymph node metastases, where the dosage in the neurovascular bundle region does not surpass 3,000 rad. In the gamma-ray teletherapy of the cervical lymph node metastases, when a dosage comprising 6,000 to 7,000 rad is absorbed in the region of sympathetic cervical nodes and in the sinocarotid reflexogenic area, there appear persistent vegetative vascular disturbances. (auth)

38774 ON THE CORRELATION OF LOCAL TISSUE CHANGES AND GENERAL REACTIONS AT DIFFERENT STAGES OF ACUTE RADIATION SICKNESS IN MAN. Kurshakov, N. A.; Baisogolov, G. D.; Guskova, A. K.; Shtukkenberg, Yu. M.; Drutman, R. D.; Malysheva, M. S. Med. Radiol., 11: No. 4, 15-42(Apr. 1966). (In Russian).

A survey was made of the pertinent literature and personal data concerning 11 patients suffering from acute radiation sickness. The importance of the distribution of irradiation doses in separate segments of the body for the character of the clinical effect is discussed. The authors also give an assessment of the diagnostic and prognostic significance of individual symptoms of the disease and the influence of therapeutic measures on the clinical picture of acute radiation sickness. (auth)

38775 SEPARATE DETERMINATION OF DAUGHTER PRODUCTS OF RADON AND THORON DURING ALPHA THERAPY. Andreev, S. V.; Tadzhikov, M. M. Med. Radiol., 11: No. 4, 50-8(Apr. 1966). (In Russian).

A precise and simple method of separate determination of daughter products of radon and thoron, based on an analysis of the curves of alpha activity, is presented. (C.H.)

38776 SUBSTANTIATION OF PERORAL INGESTION OF RADON WATER IN ALPHA THERAPY. Lebedeva, D. A. Med. Radiol., 11: No. 4, 58-64(Apr. 1966). (In Russian).

In experiments staged on animals the author studied the influence of peroral administration of radon water (1 to 200 μC) on electrical parameters (ohmic resistance and polarization capacity) of skeletal muscles. It was found that in the employed quantities of radon the ohmic resistance rises with a drop of the polarization capacity; this may testify to the stimulating effect of the radiation doses utilized. The value of shifts grows with the increase of absorbed doses of radiation. The shifts are of a reversible nature. The data derived may be conducive to the biophysical substantiation of alpha therapy. (auth)

38777 SCINTILLATION DOSIMETER FOR RATING BETA APPLICATORS. Timofeev, L. V.; Bochkarev, V. V. Med. Radiol., 11: No. 4, 67-72(Apr. 1966). (In Russian).

A scintillation dosimeter was designed which enables the measurement of the distribution of doses in the depth of the tissue from flat beta-applicators, to determine the degree of irregularity of isotope distribution along the surface of the applicator, and to record bremsstrahlung from soft beta-applicators. The authors recorded experimentally the curves of dose distribution in polyethylene from beta-applicators with ^{32}P and ^{147}Pm, and assessed the participation of ^{147}Pm in the dose of bremsstrahlung. (auth)

38778 EXACT MEASUREMENT OF GAMMA-RAY DOSES IN THE URETER. Widholm, O.; Unnerus, C-E.; Kiviniitty, K. (Univ. Central Hospital, Helsinki). Nature, 210: 1076-7(June 4, 1966).

A small rod-shaped piece of metaphosphate glass fitted into a ureteral catheter was used to measure the radiation dose received by the ureter during radium therapy. Results were compared with those obtained by the isodose method. The glass dosimeter was also used during ^{60}Co γ therapy. (C.H.)

38779 PARTIAL AMYGDALO-HIPPOCAMPAL DESTRUCTION BY ^{90}Y IN THE TREATMENT OF CERTAIN RHINENCEPHALIC TYPES OF EPILEPSY. Talairach, J.; Szikla, G. (Hopital Sainte-Anne, Paris). Neuro-Chir., 11: 233-40(1965). (In French).

A new treatment for epilepsy, employing radioisotopes, was explored, and some side-effects of its use in 15 patients are described. Stereotactic introduction of ^{90}Y in multiple sources in brain to produce a necrotic zone in an epileptogenic focus was attempted. Usually 12 to 18 grains of ^{90}Y were introduced, each containing 0.20 to 1 mC. All epileptic patients treated had severe attacks not controlled by other means. In some cases lobectomy was additionally performed. In 9 out of the 15 cases, ^{90}Y-induced partial destruction of the epileptogenic focus was effective in preventing attacks. Complications of a serious nature developed in some patients. In three cases transitory confusion states

developed, probably as a result of local brain edema during the ^{90}Y-induced necrotic reaction. Serious memory disturbances developed in two cases, and less seriously in 10 other cases. Further clinical studies are required to demonstrate the value of radioisotope treatment of epilepsy. (BBB)

38780 TUMORICIDAL EFFECT OF LASER ENERGY ON EXPERIMENTAL AND HUMAN MALIGNANT TUMORS. McGuff, Paul E.; Deterling, Ralpha A. Jr.; Gottlieb, Leonard S. (Tufts New England Medical Center, Boston). New Eng. J. Med., 273: 490-2(Aug. 26, 1965).

Effects of ruby laser energy were studied on tumors implanted in the cheek pouch or flank of Syrian hamsters. Eleven tumors of human origin, 3 of induced origin, and 6 of autogenous hamster origin were subjected to laser energy ranging from 50 to 1500 J. All treated animals with tumors were cured grossly and no viable tumor cells were seen on histologic examination. A summary of results in patients receiving laser energy to malignant tumors is also presented. Tumor dissolution varied, depending upon factors such as the absorption capability of the tumor, ratio of dose to tumor mass, and laser-energy density utilized. Deeper lesions require a surgical exposure for laser use, unless they can be approached by means of modified endoscopes. Laser energy is unique because it has a selective effect upon certain malignant tumors in that it causes their progressive regression and eventual complete dissolution while it causes only slight injury to normal tissues excluding the retina. The mechanism of laser-energy action on certain malignant tumors is still unsolved although thermal effects have been observed, recorded, and analyzed. However, the principal biologic effect of laser-energy action on malignant tumors may not be that of heat alone. Enzymes may be altered or lose their specificity. High electric fields may cause the breaking of molecular bonds. (BBB)

38781 BLOOD AND BONE MARROW DISORDERS OCCURRING IN RADIOLOGY-SERVICE PERSONNEL. Micu, D. (Inst. of Internal Medicine, Bucharest); Maximilian, Stefania; Dumitrescu, Rodica; Pillat, L. Nucl. Energy, 166-9(June 1966).

Results are reported from a 12-year study of the blood picture of 296 individuals between 20 and 50 years of age who worked in medical radiology services. Of this group, 161 were radiologists and 135 were technical assistants. Complete blood and bone marrow studies were made of 10 individuals. Results of the bone marrow studies indicated the iliac crest was superior to the sternal area for the aspiration of active bone marrow. Evaluation of the results of the blood studies have shown that these studies have definite value for indicating radiation exposure of radiology services personnel. (C.H.)

38782 MANAGEMENT OF GLOTTIC CARCINOMA OF THE LARYNX. Harrison, Kenneth (Royal Infirmary, Manchester, Eng.). Practitioner, 196: 23-6(Jan. 1966).

Relative advantages of radiotherapy and surgery in treatment of larynx cancer are examined. The early case is more suitable for radiotherapy and the advanced one for surgery. An accepted method of radiotherapy is so-called beam-directed x-ray therapy and at present megavoltage radiation is used. The primary tumor must be accurately defined by clinical examination, direct laryngoscopy, and tomography before any therapy is initiated. As a result of this treatment more than 80% of early cases are alive and well five years after treatment. In many of these patients the function of the larynx is maintained within normal limits. Some complications occur due to perichondritis of laryngeal cartilages with possible radionecrosis. This may be a very painful condition and cause great distress to the patient. It may resolve satisfactorily on antibiotic treatment. Sometimes recurrence of the growth occurs and may be associated with radioinduced necrosis. It is important to have a regular follow-up examination by both the radiotherapist and the surgeon, so that any radioinduced complications or recurrence may be diagnosed at an early date. Laryngectomy may be a secondary procedure following failure of radiotherapy recurrence, or radionecrosis. Primary laryngectomy is indicated when the growth is advanced and impairment of the airway exists. (TCO)

38783 MANAGEMENT OF CEREBRAL TUMORS. Crawford, J. V. (London Hospital). Practitioner, 196: 72-5(Jan. 1966).

Use of radiation in treatment of brain tumors is reviewed, and an assessment is given of the radiosensitivity of various neural tumors. The medulloblastoma is the most radiosensitive intracranial tumor. It is a highly malignant tumor occurring mainly in young children. This tumor characteristically disseminates throughout the brain and spinal cord by sending off tumor cells into the cerebrospinal fluid. It is essential to irradiate the whole of the brain and spinal cord to avoid distant recurrence. Pituitary adenomas are radiosensitive and radiotherapy is the first line of treatment. Careful watch is required at the start of treatment, as the adenoma may swell and cause chiasmal compression. Patients showing visual field cuts are better treated by surgery. The gliomas vary in radiosensitivity, the more malignant the tumor histologically, the more likely it is that a definite response to radiation will be seen. In glioblastoma the immediate response may be marked, but symptoms usually recur within a year, and many cases show no response. Of the benign gliomas, hemangioblastomas of the cerebellum, ependymomas, and atypical teratomas of the pineal body show impressive clinical improvement, but the natural course of these neoplasms is so unpredictable that it is difficult to assess whether the long-term prognosis of any given patient is materially affected. Angiomatous malformations are usually treated by radiation. Angiomatous meningiomas respond well to irradiation, but these are the rarest variety of meningioma and the other types are completely radioresistant. Metastases occurring from radiosensitive primary sources, e.g., thyroid or kidney, sometimes show temporary relief of symptoms after irradiation. (TCO)

38784 MANAGEMENT OF MALIGNANT TUMORS OF BONE. Eyre-Brook, A. L. (United Bristol Hospitals, Eng.). Practitioner, 196: 76-8(Jan. 1966).

Radiosensitivity of various types of bone tumor is outlined, with remarks on some radioinduced complications of therapy. In the treatment of osteogenic sarcoma supervoltage radiotherapy has recently provided results as satisfactory as those obtained by amputation and is being used widely. Osteogenic sarcoma is not radiosensitive and so radiotherapy was not very effective until the last decade; massive doses are called for. Pain is relieved and the tumor slowly gets smaller, but there may be severe secondary radioinduced changes such as fibrosis of muscle, leathering of skin, and stiffening of joints. Radiotherapy is effective in shrinking giant-cell tumors of bone, but there is a strong body of opinion that such irradiated tumors may later develop fibrosarcoma. Such cases are the outcome of radiotherapy applied 15 to 20 years ago, and radiotherapists claim that there is no similar risk from radiotherapy as applied in the present decade. Most radiotherapists, however, prefer giant-cell tumor to be treated by surgical means. Chondrosarcoma, a slow-growing tumor of cartilage, is unamenable to radiotherapy, and treatment is excision. For primary reticulum cell sarcoma treatment should be radiotherapy, all such tumor tissue being very radiosensitive. Tumors of the notochord, or chordomas, occur in the spine, more commonly in the sacro-coccygeal or upper cervical region, but can occur anywhere in the vertebral column. These tumors are radioresistant and surgery is difficult to apply effectively. There are reports of plasmacytoma treated by radiotherapy and resulting in five- or ten-year cure. but the more common event is that the lesion, though amenable to radiotherapy, is but the first evidence of multiple myelomatosis. (BBB)

38785 PHYSICAL AND BIOLOGICAL PRINCIPLES FOR AN IMPROVEMENT IN THE TECHNIQUES OF METABOLIC RADIOTHERAPY OF THYROID DISORDERS. Buraggi, G. L. (Univ., Milan). Radiobiol. Radioterap. Fis. Med., 21: 86-98(Mar.-Apr. 1966). (In Italian).

The analysis of the variability of the parameters for ^{131}I

dose evaluation and studies of the modification of thyroid metabolic pathways produced by some anti-thyroid drugs lead to the supposition, from a theoretical viewpoint, that there is a possibility of treating hyperthyroidism with a smaller amount of radioiodine than is usually employed. The physical and biological principles of this hypothesis are discussed. (tr-auth)

38786 RADIOTHERAPY OF THE CARCINOMA OF THE UTERINE NECK. Madonia, G.; Coucourde, F.; Bandirali, G. R.; Zanolla, W. (Univ., Pavia, Italy). Radiobiol. Radioterap. Fis. Med., 21: 112-25(Mar.-Apr. 1966). (In Italian).

One-hundred and forty patients suffering from cancer of the uterine neck were examined. All the patients received deep x-ray therapy as a supplement to endocavity radiotherapy or to a previous operation. The survival percentages for all stages were 56% at 3 years, 48% at 5 years, and 41% at 10 years from the beginning of the x ray therapy. After a brief review of the different methods of radiotherapy, it is concluded that the present deep x ray therapy is the most efficient treatment for malignant tumors of the neck of the uterus and is a valid alternative to surgery. (tr-auth)

38787 LONG-TERM RESULTS AND COMPLICATIONS AFTER THE IRRADIATION OF HAEMANGIOMAS IN CHILDREN. Hliniak, A.; Czownicki, Z.; Medynska, A.; Wojcieszek, Z. (Inst. of Oncology, Gliwice, Poland). Radiobiol. Radiotherap., 7: 141-4(1966).

Two hundred and eight cases (out of 645 treated) of hemangiomas in children irradiated with radium at least ten years ago were examined. Good cosmetic results were obtained in 121 children. In 30 per cent of cases late complications were observed, among them one case of carcinoma developed in the post-irradiation scar. In 27 children the bone underlying the lesion was damaged, in 10 asymmetry of the face was observed. This asymmetry was in the majority of cases due to the underdevelopment of soft tissues. In one case the underdevelopment of the facial skeleton was radiologically observed. The underdevelopment of muscles and mammary gland was also seen. In six cases of hemangiomas treated in the frontal and parietal region, some degree of mental underdevelopment was recorded. The number of complications and the risk of serious damages seem to be a sufficient reason for a complete abandoning of irradiation of hemangiomas in children with radium wax applicators. (auth)

38788 SQUAMOUS-CELL CARCINOMA OF THE SKIN IN A CHILD TREATED BY RADIUM-GAMMA-RAYS. Niepolomska, W. (Inst. of Oncology, Gliwice, Poland). Radiobiol. Radiotherap., 7: 145-6(1966).

A case of squamous cell carcinoma of the skin occurring in a young girl, aged 12, who had received a gamma ray treatment for a hemangioma of the skin of the chest wall is presented. The lesion developed 11 years after therapy near the postirradiation scar in skin showing no irradiation injury. (auth)

38789 COMPARATIVE SCINTIGRAPHIC DETERMINATIONS OF THYROID WEIGHT FOR DOSE DETERMINATION IN RADIOIODINE THERAPY. Deckart, H.; Tautz, M. (Staedtische Klinikum, Berlin). Radiobiol. Radiotherap., 7: 147-53(1966). (In German).

Because the exact dose determination for radioiodine therapy of thyroid diseases is mainly burdened by the difficult determination of thyroid weight, we have determined the weight from the scintigram according to different formulas given in literature and on pathological material, and have statistically compared it with the results of postoperative glandular weighing. It is pointed out that each investigator has to determine the proportionality factor k used in the calculation for the respectively valid reproducible measuring conditions and the nuclide used. The error in determining the weight will increase with increasing volume of the thyroid as well as with inhomogeneous activity distribution. (auth)

38790 CONSIDERATIONS AS TO THE ESTIMATION OF VOLUME AND NUMBER OF DECONTAMINATION VESSELS FOR CONTAMINATED SEWAGE OF A WARD FOR RADIOISOTOPE PATIENTS TAKING IDEALIZED PREMISES AS A BASE. Kirsch, M.; Koenig, W. (Medizinsche Akademie, Erfurt, Ger.). Radiobiol. Radiotherap., 7: 165-83(1966). (In German).

Methods are described for estimating the activity in a body, in sewage, and in the daily excrements of patients who have undergone therapy with unsealed radioactive isotopes (^{131}I, ^{198}Au, or ^{32}P). The activity for one application is assumed to be 100 mCi or 10 mCi for ^{131}I, 150 mCi for ^{198}Au, and 7 mCi for ^{32}P. The necessary residence time of patients at the isotope ward is determined by the requirements of radiation protection. Equations are presented for use in the estimation of activities, physical, and biological half-life. The volume and number of decontamination vessels needed were determined for different idealized plans of treatment and sewage volume, for an isotope ward having a total of 16 beds for therapy patients based on the regulations of radiation protection. The volume of the containers depends on the mean contaminated amount of sewage daily per patient. The stationary time of the vessels, and hence the number, is determined by the maximum permissible concentrations. (C.H.)

38791 COMPARISON OF THE THEORETICAL AND EXPERIMENTAL INVESTIGATIONS OF INFLUENCE OF BONE ON THE DEPTH DOSE DISTRIBUTION IN IRRADIATED MEDIUM. Lobodziec, W.; Lubas, B. (Inst. of Oncology, Gliwice, Poland). Radiobiol. Radiotherap., 7: 225-9(1966).

Experimental results are presented from an analysis of the influence of both transverse dimensions and thickness of bone on the dose distribution below the bone. The measurements were carried out in a water phantom, with plates of Al as the equivalent of bone for chosen qualities of x radiation and γ radiation from a ^{60}Co unit. (auth)

38792 ORTHOVOLTAGE RADIATION THERAPY: FUNDAMENTAL, VERSATILE, AND STILL INDISPENSABLE. Scott, W. P. (Charlotte Memorial Hospital, N. C.); Mastillo, J. A. Radiol. Technol., 37: 257-9(1966).

Increasing use of cobalt-60 teletherapy units has curtailed further development of, or investment in, the conventional 200- to 300-kv x-ray therapy generators. The superiority of supervoltage over orthovoltage technique is well established in certain respects, however, the conventional unit is capable of producing excellent results. From both clinical and economic points of view, conventional units are still the most practical for treatment of primary lesions requiring up to 4000 R tumor dose, cutaneous and subcutaneous lesions, mucosal lesions, lesions requiring precise shielding of adjacent structures (e.g., eyes), benign disease, and most metastatic and palliative disease. Previously, tumor doses in excess of 4000 R were attained with nonrotating orthovoltage equipment by adhering rigidly to the Curie Foundation single or split-dose technique. For extraordinarily high skin doses (up to 7000 R per port) and multiple fields, (up to eight in carcinoma of the uterine cervix), it has been found desirable to augment the dose directly with radioactive materials, or indirectly with chemotherapeutic agents. Direct augmentation of the external source dose is achieved with interstitial or intercavitary radium, radioactive iridium, gold, and phosphorus. With the advent of ^{60}Co supervoltage units, it became possible to realize a high tumor dose with this modality alone. However, facilities and number of curies in the source may limit the volume of cases that can be handled. A program was developed for initially treating the patient with orthovoltage x radiation to skin tolerance (usually resulting in 3000-R tumor dose) and then transferring the patient to the cobalt-60 unit for completion of therapy to achieve a total tumor dose of 5000 to 6000 R. Three cases are cited to illustrate successful examples of this co-operative radiation therapy. There have been no complications from combining the two radiation energies. The skin response had not progressed beyond that produced by the orthovoltage radiation alone. These modalities can be combined to augment the skin and subcutaneous doses, which are considerably reduced in the cobalt-60 isodose curves for the first 0.5

cm of tissue. The per cent cobalt-60 skin dose is compensated by the orthovoltage back-scatter factor. This augmentation can also be produced by superimposing bolus material to bring the skin surface dose up to 100%. Depth dose curves for orthovoltage, cobalt-60, and an equal mixture of each are shown. (TCO)

38793 RADIATION AND DENTISTRY. Barros, Ramon E. (Univ. of Buenos Aires). Rev. Asoc. Odontol. Argent., 53: 397(Nov. 1965). (In Spanish).

The problem of radiation protection in the use of radiography in dentistry is discussed, with an examination of conflicting views as to the hazards and innocuousness of x-ray procedures in dental practice. By standard precautions and routine checks on the operating efficiency of the x-ray equipment, exposure of patients and personnel can be kept well within the max permissible limits without sacrificing the essential diagnostic information provided by radiography. Only in exceptional cases will relatively high exposures be necessary. All exposures should be minimized by limiting the radiation to the oral area to be examined. This can best be done by use of collimators which reduce scattered radiation and narrow the primary beam to the field under study. It is especially important to maintain beam limitation in pregnant women and young children. With these precautions, the benefits of oral radiography will outweigh any possible hazards. (BBB)

38794 COMPARISON OF THE EFFECT OF WHOLE BODY IRRADIATION AND METHYL-HYDRAZINE WITH WHOLE BODY IRRADIATION ALONE IN ERADICATING TRANSPLANT LEUKAEMIA 1210 TREATED BY IMMUNOTHERAPY. Choquet, Claudine; Rosenkovitch, Emma; Halle-Pannenko, Olga; Crochet, Marie-Francoise; Florentin, Irene (Hopital Paule-Brousse, Villejuif, France). Rev. Franc. Etud. Clin. Biol., 11: 298-301(Mar. 1966). (In French).

Mice F_1 (DBA/2 × C57 Bl/6) bearing the transplanted leukemia L 1210 were treated with total-body irradiation followed by isogenic bone marrow grafts. The combination of the irradiation with methyl-hydrazine therapy did not appear to cause any improvement of the eradication of the leukemia compared to that following irradiation alone. The methyl-hydrazine did not appear to enhance the effects of immunotherapy of the L 1210 leukemia in these animals by grafts of allogeneic hematopoietic cells from C57 Bl/6 mice. (auth)

CHEMISTRY

General

Refer also to abstract 39724.

Analytical Procedures

See also Separation Processes and Procedures

Refer also to abstracts 38555, 38565, 38859, 39025, 39044, 39110, 39143, 39191, and 39300.

38795 (BNWL-265) SULFUR DETERMINATION SUPPORTING THE WASTE SOLIDIFICATION PROGRAM. Lust, L. F.; Van der Cook, B. P. (Battelle-Northwest, Richland, Wash. Pacific Northwest Lab.). July 1966. Contract AT(45-1)-1830. 9p. Dep. mn. CFSTI $1.00 cy, $0.50 mn.

Combustion with vanadium pentoxide proved to be an effective method of separating sulfur from a complex matrix such as the solid product from the solidification of fission product wastes. After the sulfur has been volatilized from the sample in the form of sulfur trioxide, it is reduced to sulfur dioxide by hot copper turnings, removed from the off-gas stream, and quantitatively determined by titration or colorimetry. Absorption in an iodine solution and back-titration of the excess iodine is used in the range of 1 to 5 mg of sulfur. The error is approximately ±5%. A colorimetric determination employing pararosaniline hydrochloride and formaldehyde is used in the range 5 μg to 1 mg of sulfur with ±10% error. (P.C.H.)

38796 (CEA-R-2968) DOSAGE DU CARBONE PAR COULOMETRIE DANS LE PLUTONIUM ET LES ALLIAGES URANIUM-MOLYBDENE. (Coulometric Determination of Carbon in Plutonium and in Uranium-Molybdenum Alloys). Pichotin, Bernard; Chasseur, Philippe (Commissariat a l'Energie Atomique, Saclay (France). Centre d'Etudes Nucleaires). June 1966. 19p. Dep. mn.

A rapid and reliable coulometric method for the determination of carbon is described. Analysis time for the uranium alloy is 10 minutes; for plutonium it is 45 minutes. The limit of sensitivity is about 5 ppM for a sample of 1 g. (J.G.B.)

38797 (MSAR-66-150) DEVELOPMENT OF TECHNIQUES FOR MEASUREMENT OF IMPURITIES IN SODIUM. Quarterly Progress Report, April-June 1966. (MSA Research Corp., Evans City, Pa.). July 1966. Contract AT(11-1)-765. 31p. Dep. mn. CFSTI $2.00 cy, $0.50 mn.

Surface tension measurements of pure sodium as well as sodium contaminated with 43 ppm oxygen at 300 to 1400°F, were completed. Reaction of sodium-sodium oxide systems with naphthalene in tetrahydrofuran, with subsequent titration of the oxide, gave high values. Measurements are being completed on the 304 SS and 316 SS tabs exposed up to 5500 hr in sodium contaminated with carbon and oxygen. Sampling for sodium oxide determination by electric potential concentration is discussed. Hydrogen measurements using a "diffusion tube" proved successful. (M.C.G.)

38798 (NIJS-R-465) THE FLAME PHOTOMETRIC DETERMINATION OF Li, Na, K, Ca, Mg AND Sr IN NATURAL AND MINERAL WATERS. Podobnik, B.; Dular, M.; Korosin, J. (Nuklearni Institut Jozef Stefan, Ljubljana (Yugoslavia)). Sept. 1965. 8p. Dep. mn.

A method which enables rapid, sensitive, and accurate flame photometric analysis of Li, Na, K, Mg, Ca, and Sr in various kinds of waters is described. Taking into consideration anionic interferences with the emission of some elements the dissolved salts are transformed into chlorides by passing through the anion exchanger. Mutual interelemental effects are eliminated by applying the dilution and standard-addition techniques. Using the monochromator, providing high line-to-background ratios, very high sensitivities are obtained. Analyzing the sample with high salt concentration, the spectral lines, which do not show bending of calibration curves, are used (K404 mμ, Na 330 mμ, etc.). The variation of the standard error of determination by changing the concentration was studied. Experimentally obtained mathematical relations are given for each element. The positional interference of strontium with lithium is discussed, and the possibility of its mathematical elimination is suggested. (auth)

38799 (NLCO-980) SUMMARY TECHNICAL REPORT FOR THE PERIOD APRIL 1, 1966 TO JUNE 30, 1966. Burgett, R. (National Lead Co. of Ohio, Cincinnati). July 1966. Contract AT(30-1)-1156. 29p. Dep. mn. CFSTI $2.00 cy, $0.50 mn.

In studies of backscatter and secondary electrons in the microprobe analyzer it was demonstrated that the composition of a binary alloy is linearly related to the electron backscatter yield. Therefore, by measuring sample current alone the alloy composition can be determined. An infrared spectral study was made of the complexes formed by various metal nitrates, especially thorium nitrate, with diamylamylphosphonate (DAAP). A test lot of uranium fuel cores 2.430 in. OD, by 1.395 in. ID, by 8 in. long were rolled, drilled, and machined to finished size. (auth)

38800 (PAEC(C)RE-652) PRR-1 WATER ANALYSIS, DECEMBER 1963-NOVEMBER 1964. Yoshisaki, M. B.; Penas, N. P. Jr.; Sabina, A. C. (Philippine Atomic Energy Commission, Manila). Feb. 1965. 23p. Dep. mn.

Pool-water samples from PRR-1 were subjected to chemical and neutron activation analysis in order to establish standards for the pool-water characteristics, as well as to determine any corrosive effects on the fuel element aluminum cladding and on the pool aluminum lining. Results obtained show that the total solids content was approximately 17 ppM with trace amounts of Fe and Al and practically nothing of chlorides. The pH ranged from 6.10 to 6.66. Conductivity of the pool water was found to be between 0.41 and 1.45 μmho/cm. Results by activation analysis show that ^{24}Na and ^{38}Cl, which are known corrosive agents, were among the main radionuclides detected. A study of the water coolant activity during high power operation was also conducted as a possible means of detecting the occurrence of failure in the fuel cladding. Generally, the coolant water activity was more or less observed to remain the same, corresponding to a given kw-hr of operation. (auth)

38801 (PG-Report-729) ANALYTICAL METHOD FOR THE ABSORPTIOMETRIC DETERMINATION OF IRON IN HIGH PURITY PLUTONIUM METAL (BATHOPHENANTHROLINE METHOD). (Production Group, United Kingdom Atomic Energy Authority, Sellafield (England)). 1966. 8p. Dep. BIS $0.30. HMSO 1s. 3d.

Iron is extracted into chloroform as the tris-bathophenanthroline ferrous complex from a solution of the sample containing EDTA. The absorbancy of the complex is measured on an absorptiometer. The bias is less than 2% at the 10-μg level. Three times the coefficient of variation is 10% at the 10-μg level, based on 20 determinations. The limit of detection is 0.5 μg. The method as written applies to high-purity plutonium metal, but could be applied to less pure metal and plutonium nitrate solutions with minor modifications. (auth)

38802 DETERMINATION OF RHENIUM BY NEUTRON ACTIVATION. Ishida, Koji (Univ. of Chiba, Japan); Kuroda, Rokuro; Kawabuchi, Kazuaki. Anal. Chim. Acta, 36: 18-24(Sept. 1966).

A neutron activation method is proposed for the determination of rhenium in rocks and ores. After irradiation, the radiochemical separation consists of a one-step anion

exchange; β-activities of radiochemically pure ^{188}Re or ^{186}Re are counted. The chemical yield averaged 75% and there was a considerable saving of time in the radiochemical work. Results are quoted for the rhenium contents of the standard rock W-I, several molybdenites, and pyrolusites. (auth)

38803 ATTEMPT TO DETERMINE THE BORON NATURAL ABUNDANCE RATIO, $^{11}B/^{10}B$, BY ATOMIC ABSORPTION SPECTROPHOTOMETRY. Goleb, Joseph A. (Argonne National Lab., Ill.). Anal. Chim. Acta, 36: 130-31(Sept. 1966).

The determination of the natural abundance ratio of the boron isotopes, $^{11}B/^{10}B$, by atomic absorption spectrophotometry, using water-cooled absorption tubes, was not possible. The percentage of $^{11}B/^{10}B$ light absorbed was the same even though the samples in the absorption tube contained approximately 4 times as much ^{11}B as ^{10}B. (D.H.M.)

38804 DETERMINATION OF MAGNESIUM IN ALUMINUM BY NEUTRON ACTIVATION. APPLICATION BEFORE IRRADIATION OF A CHEMICAL TREATMENT FOLLOWED WITH ^{27}Mg AND ^{28}Al AS TRACERS. Sabbioni, Enrico; Pauly, Jules; Girardi, Francesco (EURATOM, Ispra, Italy). Bull. Soc. Chim. France, No. 6, 1924-6 (June 1966). (In French).

In order to avoid nuclear interferences, a chemical separation of Mg and Al is made before activation analysis. This operation is controlled by the isotopic indicators ^{27}Mg and ^{28}Al, prepared by irradiation of the sample to be analyzed. (tr-auth)

38805 DETERMINATION OF SURFACE CARBOXYLIC AND HYDROXYL GROUPS OF CARBON BLACK BY A RADIOCHEMICAL METHOD. Papirer, Eugene; Donnet, Jean-Baptiste (Ecole Superieure de Chimie, Mulhouse, France). Bull. Soc. Chim. France, No. 6, 2033-6(June 1966). (In French).

The carboxyl and hydroxyl groups of carbon black are determined by exhaustive methylation with diazomethane followed by determination of the esters and methyl ethers formed. However, when the ratio of these functions becomes low, the chemical method becomes imprecise. This can be remedied by using diazomethane labeled with ^{14}C in mixture with ordinary diazomethane, which increases the sensitivity of the method. (tr-auth)

38806 RADIOMETRIC TITRATION OF TRACE AMOUNTS OF COBALT USING EDTA. Ishibashi, Nobuhiko; Kohara, Hitoshi; Fukuda, Makoto (Kyushu Univ., Fukuoka). Bunseki Kagaku, 15: 637-42(July 1966). (In Japanese).

The radiometric titration of trace amounts of cobalt with EDTA was investigated. After known amounts of EDTA are added to a series of aliquots of the sample solution containing ^{60}Co, the free metal ion is separated from the EDTA complex by the chelating resin or cation exchange resin. The radioactivity of the supernatant solution that contains the complex is measured to determine the end point of the titration. The optimum pH and lowest determinable concentration are discussed. The experimental results show that 10^{-6} or 10^{-7} M of cobalt can be determined. The titration of both ferric and cobaltous ions in the mixture is possible. The mixture of cobaltous and zinc ions is analyzed by a replacement titration. After adding EDTA equivalent to the total amount of the both ions and ^{65}Zn as an indicator, the Co(II)-EDTA complex is oxidized to the Co(III) complex. Finally Zn-EDTA complex is titrated with the Fe(III) standard solution. Zinc in the EDTA complex is replaced by ferric ion and separated from the cobalt(III) and iron (III) complexes using a cation exchange resin. The end point of the titration is determined from the radioactivity of ^{65}Zn in the supernatant solution. (auth)

38807 RADIOISOTOPIC DILUTION ANALYSIS OF TRACE AMOUNT OF COBALT USING COMPLEX FORMATION AND PAPER CHROMATOGRAPHY. Kohara, Hitoshi; Ishibashi, Nobuhiko (Kyushu Univ., Fukuoka). Bunseki Kagaku, 15: 642-6(July 1966). (In Japanese).

The complex formation of a portion of cobalt present in a sample and the paper chromatographic separation of the complex for excess free cobalt were investigated for the radioisotopic dilution analysis of the trace amount of cobalt. β-nitroso-α-naphthol as the complexing reagent and acetone-isoamyl alcohol mixed solvent (4:1) as the developer were found to be effective for the separation. To the standard cobalt solution containing ^{60}Co as tracer, less complexing reagent is added than corresponds to the stoichiometric ratio of the complex. After formation of the complex, the solution is chromatographed by the ascending method. The amount of cobalt in the solution to be analyzed is obtained by comparing the activity of the separated complex from the standard solution with that from the sample. The effects of ferric, cupric, and nickel ions are relatively small, and the determination of 10 μg/l of cobalt is possible by this dilution analysis. (auth)

38808 THIOCYANATE IONS IN COLORIMETRIC ANALYSIS. Rozycki, Cezary (Politechnika, Warsaw). Chem. Anal. (Warsaw), 11: 447-72(1966).

A review is presented on the properties of thiocyanate complexes in solutions and their application in colorimetric analysis. Formation and stability, spectra, and extraction of thiocyanate complexes are discussed. Special attention is given to extraction of thiocyanate complexes of Co, Cu, Fe, Mo, Nb, Pd, Re, Ru, Tc, Ti, W, U, and V. 194 references are given for the period 1960 through August 1965. (P.C.H.)

38809 SPECTROPHOTOMETRIC DETERMINATION OF URANIUM(VI) IN SOLUTIONS OF TRI-N-OCTYLAMINE SULPHATE. Deptula, Czeslaw. Chem. Anal. (Warsaw), 11: 589-93(1966). (In Polish).

A new spectrophotometric method was developed for determining uranium(VI) in solutions of tri-n-octylamine sulfate obtained by extraction of uranium(VI) from solutions of uranyl sulfate and also from solutions obtained by etching of ores with sulfuric acid. (auth)

38810 AMPEROMETRY WITH TWO POLARIZABLE ELECTRODES. X. INVESTIGATION OF THE CONCENTRATION RATIOS IN CHELATE FORMATION. Vydra, F.; Stulik, K. (Czechoslovak Akademie der Wissenschaften, Prague). Collect. Czech. Chem. Commun., 31: 2518-24(June 1966). (In German).

The possibilities for the use of biamperometric titrations for the determination of the ratios of the reacting components in complex formation in solutions are shown using Fe, Th, Ga, and UO_2 as examples. Nitrilotriacetic acid and some polyamino polycarboxylic acids (substances of the EDTA type) were used as complexing agents. (tr-auth)

38811 OSCILLOGRAPHIC DETERMINATION OF THE SUM OF RARE-EARTH ELEMENTS ON A SOLID ELECTRODE BY MEANS OF PRECIPITATION. Skobets, E. M.; Chornii, V. A. (Agricultural Academy, Academy of Sciences, Ukrainian SSR). Dopov. Akad. Nauk Ukr. RSR, No. 6, 779-82(1966). (In Russian).

An oscillographic determination of Ce on an amalgamated Ag electrode using lead oxalate precipitant in salt solutions was carried out; it is shown that the relative error of the determination averages 5.1%. The uses of a solid amalgamated Ag microelectrode and the solid phase (precipitates) in oscillopolarographic analysis are shown. (auth)

38812 CONTROLLED-POTENTIAL COULOMETRIC DETERMINATION OF THE RARE EARTHS IN ACETONITRILE. Cokal, E. J.; Wise, E. N. (Univ. of Arizona, Tucson). J. Electroanal. Chem., 12: 136-47(Aug. 1966).

Controlled-potential coulometry was examined as a means of determining the lanthanide series of rare earth elements. It was found possible to reduce quantitatively, europium, ytterbium, and samarium from the tri- to the di-positive state in acetonitrile solutions of the perchlorates, using tetraethylammonium perchlorate as the supporting electrolyte salt. The method suffers from lack of a convenient method of sample preparation. The attempted determination of neodymium failed. (auth)

38813 SOME OBSERVATIONS ON THE CONTROLLED-POTENTIAL ELECTROLYSIS OF EUROPIUM, YTTER-

BIUM, AND SAMARIUM AND THEIR MIXTURES IN ACETONITRILE SOLUTIONS. Cokal, E. J.; Wise, E. N. (Univ. of Arizona, Tucson). J. Electroanal. Chem., 12: 170-1 (Aug. 1966).

During an investigation of controlled-potential coulometry of the rare earths in acetonitrile, intense colors were observed when rare earth ions in two different oxidation states were present. For example, during reduction of europium(III), a yellow green coloration was produced, the intensity of which was approximately proportional to the concentration of europium(II) present. The color gradually disappeared upon subsequent controlled-potential oxidation of europium(II). (J.G.B.)

38814 SUBSTOICHIOMETRIC DETERMINATION OF AMOUNT OF CARRIER IN A "CARRIER-FREE" ^{65}Zn PREPARATION. Benes, Petr; Ruzicka, Jaromir (CVUT, Prague). Jad. Energ., 12: 179-80(1966). (In Czech).

Two samples of "carrier-free" ^{65}Zn, with activities of 0.04 and 0.4 mC/ml, according to scintillation counter readings, were analyzed for their carrier content by a reverse isotopic dilution method, in which inactive carrier is added, and substoichiometric separation is carried out (NSA 19: 40424). Dithizone was used as the reagent (log of extraction constant of $Zn(HDz)_2 = 2.3$), and triply distilled water was used for dilution. Each analysis took about 20 min, and approximately 1% of the sample was expended in the procedure. The unknown amount of carrier was calculated from the relation $y = xa_2/(a_1 - a_2)$, where x is the milligrams of inert carrier added and a_1 and a_2 are the specific activities (counts per minute) of the separated fractions before and after dilution, respectively. (TTT)

38815 APPLICATION OF A HIGH SENSITIVE INTEGRATOR IN GAS CHROMATOGRAPHY. Feist, Ivan; Sojka, Bohumil (Inst. of Nuclear Research, Czechoslovak Academy of Sciences, Rez). Jad. Energ., 12: 301(1966). (In Czech).

An integral supplement to the gas chromatograph is described. The apparatus gives accurate quantitative reading and it is especially suitable for repeated analyses, in which a constant composition of the mixture analyzed is maintained and only the content of separate components is in question. The original apparatus was modified for chromatographic measurements, but it will also do well in the same construction for other purposes. (auth)

38816 USE OF NEUTRON ACTIVATION IN THE CHARACTERIZATION OF SMALL QUANTITIES OF NUCLEIC ACIDS. Murray, K.; Offord, R. E. (Medical Research Council, Cambridge, Eng.). Nature, 211: 376-8 (July 23, 1966).

A procedure is described for the location of oligonucleotide and other phosphorus-containing spots by neutron activation of the completed chromatogram and subsequent autoradiography. The particular application discussed is the mapping of digests of DNA from higher animals. After two-dimensional ionophoretic separation, neutron activation of nuclease digests may be used to obtain nucleotide maps on small quantities (100 to 200 μg) of nucleic acids from sources that cannot conveniently be labeled biosynthetically. (D.H.M.)

38817 PROGRESS IN NUCLEAR ENERGY. SERIES IX. ANALYTICAL CHEMISTRY. VOLUME 6. Stewart, D. C.; Elion, H. A. (eds.). Progr. Nucl. Energy, Ser. IX, 6: 1-260(1966).

Separate abstracts were prepared on each of the five chapters. Author and subject indexes are included. (J.G.B.)

For abstracts of individual chapters see: 38818—38822.

38818 ION EXCHANGE IN MIXED AND NON-AQUEOUS MEDIA. Korkisch, Johann (Univ., Vienna). Progr. Nucl. Energy, Ser. IX, 6: 1-94(1966).

Studies were made on the behavior of electrolytes in mixed and non-aqueous media as applied to inorganic analytical chemistry. The effects of solvent uptake and swelling of the resin, dissociation, solvation, and complex formation, as well as ionic and molecular interactions on ion exchange equilibria in mixed solvents were investigated. The effects of solvent dielectric constant on resin swelling and adsorption were also studied. 156 references are included. (J.G.B.)

38819 SOME NEUTRAL BIFUNCTIONAL ORGANOPHOSPHORUS COMPOUNDS AS SOLVENT EXTRACTANTS. O'Laughlin, Jerome W. (Ames Lab., Ames, Iowa). Progr. Nucl. Energy, Ser. IX, 6: 95-146(1966). (IS-1126).

The syntheses and solvent extraction properties of a number of neutral bifunctional organophosphorus compounds which act as bidentate ligands are reviewed. Comparison with monofunctional extractants are made. Semitheoretical treatments of the extraction process and the probable nature of the adducts formed are discussed. It appears that a number of bifunctional extractants of the type described will be valuable additions to the arsenal of extractants already available. (J.G.B.)

38820 ANION EXCHANGE IN NITRATE SOLUTIONS. Faris, John; Buchanan, Robert F. (Argonne National Lab., Ill.). Progr. Nucl. Energy, Ser. IX, 6: 147-80(1966).

Anion exchange in a nitric acid medium and its applications, which range from low-level radiochemical separations to large scale purification or recovery processes, are reviewed. Results of recent studies on adsorption of 70 elements in nitric acid solutions are given. Anion exchange separations from mixtures containing a high proportion of a water-miscible organic solvent and the use of anion exchange in spectrochemical analysis are discussed. References (233) to literature published through most of 1964 are included. (J.G.B.)

38821 ANALYTICAL CHEMISTRY OF NEPTUNIUM. Burney, G. A.; Dukes, E. K.; Groh, H. J. (E. I. du Pont de Nemours and Co., Aiken, S. C.). Progr. Nucl. Energy, Ser. IX, 6: 181-211(1966). (TID-21529).

The discovery, occurrence, synthesis, properties, and methods for separation of neptunium are discussed. Various qualitative and quantitative methods for its determination are reviewed. (103 references) (J.G.B.)

38822 ANALYTICAL CHEMISTRY OF POLONIUM. Lange, Robert C. (Monsanto Research Corp., Miamisburg, Ohio). Progr. Nucl. Energy, Ser. IX, 6: 213-39(1966).

The chemistry of polonium, including methods for its detection, determination, and separation, is reviewed. (133 references) (J.G.B.)

38823 SIMULTANEOUS DETERMINATION OF ^{3}H AND ^{14}C IN PROPORTIONAL COUNTERS. Jordan, P.; Lykourezos, A. P. (Eidgenoessische Technische Hochschule, Zurich). Radiochim. Acta, 5: 137-40(June 1966). (In German).

38824 THE EXTRACTION OF MOLYBDENUM INTO ACETYLACETONE AND ITS USE IN THE ANALYSIS OF FISSION PRODUCTS. Fritze, K. (McMaster Univ., Hamilton, Ont.). Radiochim. Acta, 5: 164-6(June 1966).

The extraction of molybdenum into acetylacetone was investigated as a function of pH value, for the anions SO_4^{2-}, NO_3^-, and Cl^-. From the results a process was derived for the separation of molybdenum from mixtures of fission products. (auth)

38825 DETERMINATION BY NEUTRON ACTIVATION OF GALLIUM AND GERMANIUM IN IRON METEORITES. Wasson, John T.; Kimberlin, Jerome (Univ. of California, Los Angeles). Radiochim. Acta, 5: 170-4(June 1966).

A procedure is given for the simultaneous determination by neutron activation of gallium and germanium in iron meteorites or other similar materials. Germanium is separated from interfering activities by solvent extraction from 8N HCl into carbon tetrachloride followed by distillation as $GeCl_4$. The chemical yield is determined colorimetrically using phenylfluorone. Gallium is separated by repeated solvent extractions into isopropyl ether, and the yield is determined by flame photometry. Above 12 man hours are necessary to process six to eight samples, not including the time necessary to reduce the counting data. The detection limits for a thermal-neutron flux of 10^{12} cm^{-2} sec^{-1} are about 0.02 ppM germanium and 0.0001 ppM gallium. (auth)

38826 PAPER ELECTROPHORESIS OF PROTACTINIUM IN SULFURIC ACID MEDIUM. Venkateswarlu, K. S.; Subramanyan, V. (Atomic Energy Establishment, Trombay, India). Radiochim. Acta, 5: 174-5(June 1966).

A study of paper electrophoretic behavior of protactinium in sulfuric acid medium was made. Ninety percent of the protactinium activity remains immobile in 0.05M sulfuric acid, even though liquid anion exchange studies from 0.1M sulfuric acid show that more than 90% of protactinium exists as mononegative charged species. The effects of fluoride and oxalate complexing on protactinium mobility at 0.05M sulfuric acid was reported. (D.H.M.)

38827 CHEMICAL AND RADIOCHEMICAL PURITY OF THE RADIOACTIVE CALCIUM OBTAINED AT THE INSTITUTE FOR ATOMIC PHYSICS-BUCHAREST. Chiotan, C.; Zamfir, I.; Ciplea, I. Teh. Nucl., No. 1, 57-61 (Jan.-Mar. 1965). (In Rumanian).

Chromatographic and radiochromatographic analyses were performed for determining the comparative purity of samples of ^{45}Ca and ^{47}Ca prepared from imported and native raw materials. It was found that the ^{45}Ca compounds obtained by irradiation from indigenous raw material are sufficiently pure for medical purposes. It was also found that ^{47}Ca obtained from the I.F.A. (Institute for Atomic Physics) reactor by short time irradiation still contained traces of radioactive impurities ^{24}Na and ^{42}K. However, as these impurities decay rapidly, the ^{47}Ca left is sufficiently pure to be used in certain applications with good results. (Abstr. Rum. Tech. Lit. Vol. 1, No. 2, 1965)

38828 THE USE OF ALKYL PHOSPHORIC ACIDS IN ANALYTICAL CHEMISTRY. COMMUNICATION 4. EXTRACTION OF BISMUTH WITH ALKYL PHOSPHORIC ACIDS AND ITS SEPARATION FROM ACCOMPANYING ELEMENTS. Levin, I. S.; Shatalova, A. A.; Azarenko, T. G. (Inst. of Physical-Chemical Principles of the Treatment of Raw Mineral Material, Novosibirsk, USSR). Zh. Anal. Khim., 21: 276-9(1966). (In Russian).

Methods were developed for separating bismuth from the majority of accompanying elements, including Sn, Sb, As, and Pb, by the extraction of bismuth with alkyl phosphoric acids from sulfuric, nitric, and perchloric acid solutions. Bismuth is back extracted with solutions of hydrochloric and hydrobromic acids and their salts. (auth)

38829 DETERMINATION OF PRASEODYMIUM, NEODYMIUM, HOLMIUM, AND ERBIUM IN FLUORITE MONOCRYSTALS. Krotova, L. V. (Lebedev Inst. of Physics, Moscow). Zh. Anal. Khim., 21: 789-92(1966). (In Russian).

A spectrophotometric method was developed for determining Pr, Nd, Ho, and Er in fluorite monocrystals with an accuracy of 10 to 20%. (auth)

38830 ANALYSIS OF ALLOYS OF RARE EARTH ELEMENTS WITH MAGNESIUM IN NONAQUEOUS SOLUTIONS. Kreshkov, A. P.; Yarovenko, A. N.; Milaev, S. M. (Mendeleev Chemical-Technological Inst., Moscow). Zh. Anal. Khim., 21: 813-16(1966). (In Russian).

A study was made of the behavior of rare earth chlorides, bromides, and nitrates in non-aqueous solutions in the presence of tetraethylammonium hydroxide. A rapid method was developed for analysis of alloys of rare earth elements with magnesium. The method is based on successive potentiometric titration of rare earth and magnesium bromides in non-aqueous solutions. The method was also applied to the analysis of certain magnesium alloys. The results obtained are reasonably accurate. (auth)

38831 MEASUREMENT OF DIFFERENCE IN ISOTOPIC RATIOS IN SMALL VOLUMES OF GASES AND POSSIBILITIES FOR THE MASS-SPECTROGRAPHIC DETERMINATION OF MICROAMOUNTS OF OXYGEN AND NITROGEN IN SOLID SUBSTANCES. Chupakhin, M. S. (Vernadskii Inst. of Geochemistry and Analytical Chemistry, Moscow). Zh. Anal. Khim., 21: 817-25(1966). (In Russian).

A method for determining difference in the isotopic ratios by diluting small volumes of the gas analyzed with large amounts of a standard gas is discussed. The possibility of developing a highly sensitive method for determining nitrogen and oxygen in solid substances using mass spectrographic precision recording of the isotopic shifts, vacuum fusion, and isotopic balancing was found. A design is suggested for extracting gases from the samples and introducing them into the mass spectrometer. Conditions for highly sensitive recording of oxygen and nitrogen in solid samples, sources of errors, and the total instrumental errors observed using the method suggested are considered. (auth)

38832 SPARK METHOD FOR SPECTROGRAPHIC DETERMINATION OF RARE EARTHS IN SOLUTIONS. Karpenko, L. I.; Fadeeva, L. A.; Beltyukova, S. V. (Inst. of General and Inorganic Chemistry, Odessa). Zh. Anal. Khim., 21: 864-7(1966). (In Russian).

A spectrographic method was suggested for the direct analysis of solutions obtained during chromatographic separation of rare earths. A high-voltage condensed spark is used as an excitation source. The method permits the determination of Eu, Gd, Tb, Dy, Ho, Er, Tm, Yb, Lu, and Y in solutions with a sensitivity of hundredths and thousandths parts of a milligram in 1 milliliter. The standard experimental error is 6 to 8%. (auth)

38833 DETERMINATION OF DYSPROSIUM IN SAMPLES OF YTTRIUM OXIDE AND FERRITE GARNETS BY A RADIOACTIVATION METHOD. Lobanov, E. M.; Dutov, A. G.; Leushkina, G. V. (Inst. of Nuclear Physics, Tashkent). Zh. Anal. Khim., 21: 867-70(1966). (In Russian).

A rapid method was developed for determining dysprosium in samples of yttrium oxide and ferrite garnets by ^{165m}Dy, $T_{1/2}$ = 1.3 min. The sensitivity of determinations is 10^{-4} to 10^{-5}% of Dy. The mean experimental error is 9%. (auth)

38834 SEPARATION OF IONIUM (^{230}Th) FROM URANIUM, PROTACTINIUM, IRON, MANGANESE, AND EUROPIUM BY CATION EXCHANGE. Palei, P. N.; Karalova, Z. K.; Shibaeva, N. P.; Pyzhova, Z. I. Zh. Anal. Khim., 21: 874-6(1966). (In Russian).

A method was suggested for separating ionium (^{230}Th) from U, Pa, Fe, Mn, and Eu from a 0.1N H_2SO_4 solution by means of a KY-2 cation exchange resin. The method is based on separate elution of absorbed elements: at first U, Fe, Mn, Eu, and Pa are eluted by a 2N solution of HNO_3, then the resin is washed with 1N H_2SO_4 to remove protactinium completely. Ionium is extracted by a saturated ammonium carbonate solution and determined radiometrically. The mean yield of ^{230}Th is 88%. (auth)

38835 THERMOGRAVIMETRIC BALANCE (Engineering Materials). (Rocky Flats Div., Dow Chemical Co., Golden, Colo.). (CAPE-1411).

6 drawings.

The balance is used with samples of Pu in an atmosphere of HF in a glove box. Helium protects the balance from HF. Drawings are also included for a fluorination reactor and a furnace. (For details see TID-4100). (F.S.)

38836 L'ANALYSE PAR RADIOACTIVATION ET SES APPLICATIONS AUX SCIENCES BIOLOGIQUES. 3e COLLOQUE INTERNATIONAL DE BIOLOGIE DE SACLAY, SEPTEMBRE 1963. (Radioactivation Analysis and Its Applications in Biological Sciences. Third International Conference on Biology, Saclay, September 1963). Paris, Presses Universitaires de France, 1964. 416p. (CONF-384).

Twenty-two articles are included; separate abstracts were prepared for 18. The remaining 4 articles were previously abstracted in NSA as 18: 9818, 13414, 37086, and 20: 7046. (P.C.H.)

For abstracts of individual papers see: 38564, 38565, and 38837–38852.

38837 THE DETERMINATION OF TRACES OF Se, V, Sr, AND As IN BIOLOGICAL SAMPLES BY NEUTRON-ACTIVATION ANALYSIS (WITH SPECIAL REFERENCE TO THE INSTRUMENTAL DETECTION OF 17-SECOND

^{77m}Se. Guinn, Vincent P. (General Atomic Div., General Dynamics Corp., San Diego, Calif.). pp 69-82 of Radioactivation Analysis and Its Applications in Biological Sciences. Paris, Presses Universitaires de France, 1964.

Techniques used in analyzing biological samples for trace levels of Se, V, Sr, and As are described. These illustrate several different methods: a purely instrumental pneumatic-tube method (^{77m}Se); a purely instrumental method with a long-lived activity (^{75}Se); a rapid radiochemical separation method with a 3.8-min activity (^{52}V); and the more conventional radiochemical separation procedures with longer-lived activities (^{75}Se, ^{87m}Sr, and ^{76}As). Some involve pre-irradiation sample ashing. Samples and standards are activated, for appropriate lengths of time, in a 250-kw TRIGA Mark I reactor, at a thermal neutron flux of 1.8×10^{12} n/cm^2/sec. Final counting is done by multichannel gamma spectrometry. With longer-lived activities, as many as 40 samples (including one standard) can be activated at the same time, all at exactly the same flux. Results for individual elements are given. (P.C.H.)

38838 FAST NEUTRONS IN ACTIVATION ANALYSIS. Schulze, Werner (Freie Univ., Berlin). pp 85-118 of Radioactivation Analysis and Its Applications in Biological Sciences. Paris, Presses Universitaires de France, 1964.

The analytical difficulties arising from the presence of fast neutrons as admixture to a thermal flux are discussed for several special cases. In an example on the determination of magnesium and aluminium in a silicon-matrix it is shown how a distinction between the amounts of one radionuclide produced by several reactions is possible if the thresholds of these reactions are different. Then two irradiations with different neutron spectra are necessary. In a discussion of the radionuclides formed by (n,γ)-, (n,2n)-, (n,p)-, and (n,α)-reactions it is shown that for many elements with the exception of 23 there exists some characteristic radionuclides that are produced from one element only. 14 Mev neutron cross sections are known for only ⅓ of the possible 850 reactions. New cross section values are extrapolated from published data for 25 (n,γ)-reactions. Cross sections for (n,2n)-, (n,p)- and (n,α)-reactions were calculated applying nuclear laws in empirical formulas. A tabulation of nearly all experimental and calculated 14 Mev neutron cross sections is given for the stable elements beginning with lithium. A series of graphs shows saturation-activity and half life for the activation products of each stable element. The evaluation for different irradiation time is described. A figure φ is introduced to characterize the analytical usefulness of a nuclear reaction. It contains essentially the difference of log saturation-activity and log half life counted from an appropriate reference-line. (auth)

38839 HIGH-OUTPUT NEUTRON TUBE FOR ACTIVATION ANALYSIS. Wood, J. D. L. H.; Lomer, P. D.; Bounden, J. E. (Services Electronics Research Lab., Baldock, Eng.). pp 119-22 of Radioactivation Analysis and Its Applications in Biological Sciences. Paris, Presses Universitaires de France, 1964.

Sealed-off neutron tubes in which the ion source and accelerating gap are at uniform pressure and with the advantage of being able to use a mixture of D and T in both ion source and target so that a continuous circulation of the gas mixture occurs with proportions of D and T maintained constant in ion source and target are discussed. A tube using such a mixture has been shown to have a life of hundreds of hours at 10^8 neutrons per second. (P.C.H.)

38840 RADIOACTIVATION ANALYSIS BY MEANS OF 14-Mev NEUTRONS. Laverlochere, J. (CEN, Grenoble, France). pp 123-9 of Radioactivation Analysis and Its Applications in Biological Sciences. Paris, Presses Universitaires de France, 1964. (In French).

Preliminary experiments made on the detection of oxygen, boron, fluorine, and nitrogen in metals with 14-Mev neutrons are reported. Typical determination curves are given for each element. (J.S.R.)

38841 ANALYSIS BY NUCLEAR REACTION. Marmier, P. (Eidgenoessisches Technische Hochschule, Zurich). pp 131-43 of Radioactivation Analysis and Its Applications in Biological Sciences. Paris, Presses Universitaires de France, 1964. (In French).

Some techniques of microanalysis by nuclear reactions are described. The use of radioactivation analysis of ^{18}O in the problem of turnover of ATP and of 2,3-diphosphoglyceric acid (2,3-DPG) in erythrocytes showed that the rate of exchange of ATP is small (0.7×10^{-3}/sec) with relation to that of the 2,3-DPG (7×10^{-3}/sec) which seems to play an important role in the glycolytic cycle. (tr-auth)

38842 APPLICATION OF RAPID RADIOCHEMICAL SEPARATIONS TO THE ACTIVATION ANALYSIS OF BIOLOGICAL SAMPLES. Meinke, W. Wayne (National Bureau of Standards, Washington, D. C.). pp 145-55 of Radioactivation Analysis and Its Applications in Biological Sciences. Paris, Presses Universitaires de France, 1964.

Rapid radiochemical separations are discussed in relation to the determination of such elements as Na and Mg in biological samples by activation analysis. An isotopic exchange technique is described for use in the determination of Mg in a drop of blood, water, urine, and tissues by activation. (P.C.H.)

38843 USE OF HIGH-SPEED COMPUTER-COUPLED AUTOMATIC SYSTEMS FOR NON-DESTRUCTIVE MEDICAL AND BIOLOGIC NUCLEAR ACTIVATION ANALYSIS. Wainerdi, Richard E.; Fite, Lloyd E.; Steele, Edgar L. (Texas A and M Univ., College Station). pp 171-98 of Radioactivation Analysis and Its Applications in Biological Sciences. Paris, Presses Universitaires de France, 1964.

The development of high-speed automatic nuclear activation analysis systems, coupled to both versatile activating sources and computers is discussed for medical and biological applications. Such machines as the Mark I and Mark II systems reduce the time and cost requirements per analysis to the point where large scale medical and biological surveying can be undertaken in many previously prohibitively expensive and time-consuming situations. Results reported on the determination of Mg, Na, Te, Dy, Se, and Ag in biological samples are indicative of the kind of information that can be obtained with systems of this type. (P.C.H.)

38844 NECESSITY OF BIOLOGICAL STANDARDS FOR ACTIVATION ANALYSIS. Bowen, H. J. M. (Atomic Energy Research Establishment, Wantage, Eng.). pp 199-210 of Radioactivation Analysis and Its Applications in Biological Sciences. Paris, Presses Universitaires de France, 1964. (In French).

Biological materials suitable for use as standards in activation analysis are discussed in detail. These include such materials as blood, algae, and muscles. (P.C.H.)

38845 ASSESSMENT OF THE TRACE ELEMENTS OF BLOOD AND TISSUES BY NEUTRON RADIOACTIVATION AND GAMMA SPECTROSCOPY. Plantin, Lars-Olof (Konung Gustaf V:s, Stockholm). pp 211-22 of Radioactivation Analysis and Its Applications in Biological Sciences. Paris, Presses Universitaires de France, 1964.

Some difficulties in the application of activation analysis to the determination of trace elements in human tissues are discussed. Results of methods for determination of Cu, Zn, Mn, I, and Au in blood and Cd in kidney tissue are reported for healthy people and for patients with rheumatoid arthritis. The copper content in whole blood in patients with rheumatoid arthritis is neither correlated to the clinical state of the patient nor to any of the other investigated parameters of the blood. Standardization of procedures to obtain a gamma spectrum of the trace elements of blood is proposed. (auth)

38846 THE USE OF NEUTRON ACTIVATION ANALYSIS IN THE DETERMINATION OF TRACE ELEMENTS IN TOBACCO MOSAIC VIRUS AND NUCLEIC ACIDS OF TOBACCO PLANTS. Altmann, Hans; Stehlik, Gerhard; Kaindl, Karl (Institut fuer Biologie und Landwirtschaft, Vienna). pp 243-50 of Radioactivation Analysis and Its Applications in Biological Sciences. Paris, Presses Universitaires de France, 1964.

In experiments done with tobacco-mosaic-virus (TMV)-infected tobacco plants the host's nucleic acid decreased with time after infection while the TMV-RNA (ribonucleic acid) increased with time. Similar trends were detected in the trace element content of these nucleic acids. The role

of the trace elements in stabilizing TMV-RNA in the host cell is discussed. For the determination of trace elements, neutron activation analysis was used. (auth)

38847 TRACE ELEMENTS IN HUMAN DISEASE. Lenihan, J. M. A. (Western Regional Hospital Board, Glasgow). pp 251-65 of Radioactivation Analysis and Its Applications in Biological Sciences. Paris, Presses Universitaires de France, 1964.

The role of activation analysis in the study of trace element metabolism, with particular reference to human diseases of nutrition and of occupation is reviewed. The list of elements recognized as essential in the nutrition of the higher animals, including man has steadily grown through refinement of techniques in analytical and biochemical assay. Studies discussed include: the significance of dietary and environmental exposure to arsenic in cancer (including the case of Napoleon Bonaparte); strontium metabolism in bone diseases; occupational hazards of arsenic; and animal diseases and human medicine. (P.C.H.)

38848 BIOLOGICAL APPLICATION OF ACTIVATION ANALYSIS OF ^{18}O. Fleckenstein, A.; Janke, J. (Univ., Freiburg i. B.). pp 267-85 of Radioactivation Analysis and Its Applications in Biological Sciences. Paris, Presses Universitaires de France, 1964. (In French).

A new method based on the principle of analysis of ^{18}O by radioactivation by transforming the stable ^{18}O into radioactive ^{18}F by bombardment with protons was used for measuring the incorporation of ^{18}O coming from $H_2{}^{18}O$ under different physiological conditions in molecules of ATP, phosphocreatine, mineral phosphate, and other phosphorus compounds contained in the cardiac and skeletal muscle. The results obtained showed the advantages of this new method with respect to the traditional use of radiophosphate. Primarily the incorporation of radiophosphate in the intracellular phosphorus compounds is strongly inhibited by the membrane of the muscular fiber whereas $H_2{}^{18}O$ rapidly arrives at all the intercellular sites where the metabolism reactions of the phosphoryl compounds are produced. For this reason the acceleration of the metabolism of ATP and phosphocreatine provoked by an electric stimulation can be detected only with $H_2{}^{18}O$. (P.C.H.)

38849 DETERMINATION OF IODINE BY MEANS OF RADIOACTIVATION ANALYSIS AND ITS APPLICATIONS IN THYROIDAL PHYSIOPATHOLOGY. Comar, D.; Riviere, R.; Kellershohn, C. (CEN, Saclay, France). pp 307-36 of Radioactivation Analysis and Its Applications in Biological Sciences. Paris, Presses Universitaires de France, 1964. (In French).

Partial automation of these iodine measurements under development for thyroid function tests is described. This partial automation makes it possible to measure continuously samples containing iodine between 0.1 and 0.001 ppM. A statistical study of the total and organic iodine rate found in the blood of normal and pathological subjects was undertaken and the results are discussed. With the possibility of measuring precisely the food iodine rate and iodine excreted by patients examined, it is possible, because of the measurement of the specific activity in the different media of the organism after a single injection of radioactive iodine, to measure important parameters aiding in the comprehension of certain aspects of thyroid metabolism. Some examples are given of measurements of iodine contained in the thyroid, measurements of the rate of hormonal secretion, and measurement of different pools in the organism. (P.C.H.)

38850 ISOTOPIC ANALYSIS OF ^{48}Ca BY NEUTRON ACTIVATION. Junod, E.; Laverlochere, J. (CEN, Grenoble, France). pp 337-60 of Radioactivation Analysis and Its Applications in Biological Sciences. Paris, Presses Universitaires de France, 1964. (In French).

With the object of studying the possibilities of using ^{48}Ca as a tracer in a medium containing natural calcium, studies were made on neutron activation analysis of the isotope, by means of the reaction $^{48}Ca(n,\gamma)^{49}Ca$ ($T^{1/2}$ = 8.8 min, E_γ = 3 Mev). Straight lines of standardization were established to be in the area of 1 to 12 μg of ^{48}Ca by three methods of computing. Interferences were also studied. Enrichment of ^{48}Ca was determined in samples of calcium carbonate from tracer experience. From the straight lines of standardization, the sensitivity of dosage of natural calcium was calculated by ^{49}Ca, which is of the microgram order. The irradiation facilities are described. (tr-auth)

38851 DETERMINATION OF Cu, Cr, Zn, Co, Na, AND K IN BLOOD SERUM. Pijck, J.; Hoste, J. (Faculteit der Wetenschappen, Instituut voor Analytische Chemie, Ghent). pp 361-78 of Radioactivation Analysis and Its Applications in Biological Sciences. Paris, Presses Universitaires de France, 1964. (In French).

The results of experiments made with a view of determining the behavior of the elements Sb, As, Cr, Au, Fe, Cu, Hg, Pb, Mo, Mn, V, Ag, and Zn during the process of mineralization demonstrated that the combustion method generally involves considerable waste. Use of a concentrated acid mixture $H_2SO_4-HClO_4-HNO_3$ in the ratio of 1:1:3, on the other hand, permitted quantitative recovery of the elements considered with the exception of Fe, Hg, As, Au, and Sb. The trace elements Cu, Cr, Zn, Co, Na, and K were determined in serum by radioactivation. Cu, Cr, and Co were isolated quantitatively by selective procedures. Zinc required a more complex separation, from which the product was determined by gravimetry and titrimetry. For K and Na, two techniques were elaborated, with and without chemical separation. All the analyses were controlled by comparison with the results obtained by classic methods (spectrophotometry) on the same samples. These proved to be reproducible and quantitative. The advantage of the proposed methods lies in the reduction of the sample, which varies between 250 and 1 μl. (tr-auth)

38852 THE USE OF NEUTRON ACTIVATION ANALYSIS FOR THE QUANTITATION OF SELECTED CATIONS IN HUMAN BLOOD. Bethard, W. F.; Olehy, D. A.; Schmitt, R. A. (General Atomic Div., General Dynamics Corp., San Diego, Calif.). pp 379-93 of Radioactivation Analysis and Its Applications in Biological Sciences. Paris, Presses Universitaires de France, 1964.

Using neutron activation analysis, concentrations of magnesium, manganese, copper, and zinc were measured in plasma and erythrocytes of normal adult human blood. Errors arising from the use of heparin as an anticoagulant prior to neutron irradiation of blood are pointed out. It is emphasized that when using neutron activation analysis, addition for extraneous materials to the samples prior to neutron irradiation should be eliminated whenever possible. Preliminary data on the concentrations of magnesium, manganese, copper, and zinc in normal adult human erythrocytes after three weeks of blood bank storage are presented. Data on the concentrations of these cations in leukocytes from patients having chronic myelocytic leukemia and acute monocytic leukemia are also included. (auth)

38853 PRECISION NEUTRON ACTIVATION ANALYSIS OF ZINC AND TITANIUM OXIDES IN ORGANIC COATING PIGMENTS. Eggebraaten, V. L.; Miller, L. E. (Boeing Co., Seattle). 9p. (CONF-650809-2). ORAU. Gmelin, AED-CONF-65-229-3.

From Society for Applied Spectroscopy, 4th National Meeting, Denver.

Description is given of an activation analysis system that was set up in order to study the performance of precise quantitative determinations of selective elements in various materials along with maintaining the expedience in the analysis that is typical of analytical instrumentation. A typical quality control application is given that involves the analysis of zinc and titanium, both present as the oxides, in organic coating pigments. The analysis of both elements requires only one neutron irradiation. The zinc samples are allowed to set 40 min before counting for ^{63}Zn to allow for the decay of ^{13}N. The reaction $^{48}Ti(n,p)^{48}Sc$ is used for the quantitative determination of Ti. Requirements for obtaining maximum precision in activation analysis using a 150-kv accelerator are listed. (P.C.H.)

38854 DETERMINATION OF AMERICIUM BY CONTROLLED-POTENTIAL COULOMETRY. Koehly, G.; Berger, R. (Commissariat a l'Energie Atomique, Fontenay-

aux-Roses, France). 17p. (CONF-651004-16). ORAU. Gmelin, AED-CONF-65-287-3.

From 9th Conference on Analytical Chemistry in Nuclear Technology, Gatlinburg, Tenn.

Equipment and conditions are described for the determination of Am by controlled-potential coulometry. Selectivity, reliability, and sensitivity are also discussed. The chemical yield of the quantitative oxidation of Am^{3+} to AmO_2^{2+} in sulfate solution, followed by coulometric reduction to AmO_2^{2+} and the current yields of the reduction were investigated. The procedure used is described. (P.C.H.)

Inorganic and Physical Chemistry

Refer also to abstracts 38835, 39333, 39354, and 39387.

38855 (BNL-10350) MIXED β-DIKETONES. Newman, L.; Klotz, P. (Brookhaven National Lab., Upton, N. Y.). June 30, 1966. Contract AT(30-2)-Gen-16. 17p. (CONF-660805-1). Dep. mn. CFSTI $1.00 cy, $0.50 mn.

From International Conference on Solvent Extraction, Goteborg, Sweden.

The increased extraction of metals (M) by a benzene solution containing two β-diketones as compared with the sum of the extraction due to each of the β-diketones was interpreted as arising from the formation of a mixed β-diketone complex. All possible combinations of the following were studied: thenoyltrifluoroacetone (TTA), benzoyltrifluoroacetone (BTA), thenoylacetone (TA), acetylacetone (AA), benzoylacetone (BA), and dibenzoylmethane (DBM). Formation constants, K_m, were measured in benzene for the reaction $\frac{1}{2} MX_2 + \frac{1}{2} MY_2 = MXY$, where X^- and Y^- are the enolate ions of the different β-diketones. The systems UO_2^{2+}/BTA + TTA, UO_2^{2+}/AA + BA, Cu^{2+}/BTA + TTA, and Cu^{2+}/AA + BA all give log K_m values equal to the statistically predicted value of 0.3. These systems can be classified as containing strong + strong or weak + weak β-diketones. The systems which contain weak + strong β-diketones, UO_2^{2+}/AA + TTA, and Cu^{2+}/AA + TTA, give log K_m values of 1.0 and 0.5, respectively, which indicate a somewhat more favorable formation of the mixed species. (auth)

38856 (BNL-10372) PHYSICAL AND CHEMICAL PROPERTIES OF DILUTE ALLOYS OF Cd IN Na. Weeks, John R.; Davies, Hywel A. (Brookhaven National Lab., Upton, N. Y.). [1964]. Contract AT(30-2)-Gen-16. 23p. (CONF-660712-1). Dep. mn. CFSTI $1.00 cy, $0.50 mn.

From International Conference on the Alkali Metals, Nottingham, England.

The Na–Cd liquidus was reinvestigated at the Na-rich end at temperatures between 100 and 400°C by the method of sampling and chemical analysis. Partial molar thermodynamic properties of Cd in liquid Na were calculated from the low-temperature portion of this curve. The densities and surface tensions of Na–Cd alloys were determined from 200 to 400°C by the maximum bubble pressure technique. The molal volumes behave abnormally at low concentrations of Cd and become strongly negative at higher concentrations. The surface tension of sodium decreases initially upon the addition of Cd, reaches a minimum at approximately 3 to 4 at. % Cd, and then increases. (auth)

38857 (BNWL-235-3) PACIFIC NORTHWEST LABORATORY ANNUAL REPORT FOR 1965 IN THE PHYSICAL SCIENCES. VOLUME 3. EARTH SCIENCES. Pearce, D. W.; Green, J. K. (Battelle-Northwest, Richland, Wash. Pacific Northwest Lab.). May 1966. Contract AT(45-1)-1830. 76p. Dep. mn. CFSTI $3.00 cy, $0.75 mn.

Results are reported for studies on geology and hydrology, mineral chemistry, and particles and gases. Separate abstracts were prepared for each of the three sections. (P.C.H.)

For abstracts of individual sections see: 38858, 39099, and 39103.

38858 (BNWL-235-3, pp 23-51) MINERAL CHEMISTRY. (Battelle-Northwest, Richland, Wash. Pacific Northwest Lab.).

Results are reported for studies on: montmorillonite exchange equilibria with Sr–Na–Cs; self-diffusion of Na in vermiculite; exchange of alkali metal cations on a natural stilbite; alkali metal cation equilibria with chabazite; unit cell size and Cs loading on Type A and Type X zeolites; cation exchange properties of wairakite and analcime; radionuclide migration in soil columns-development of a computer program; dispersion characteristics of Sr in soil columns; and Cs and Sr distribution beneath liquid waste disposal sites. (P.C.H.)

38859 (CEA-R-2895) CONTRIBUTION A L'ETUDE ANALYTIQUE DES FERRATES. (Contribution to the Analytic Study of Ferrates). Becarud, Nicole (Commissariat a l'Energie Atomique, Fontenay-aux-Roses (France). Centre d'Etudes Nucleaires). 1966. 52p. Dep. mn. Thesis. Submitted to Univ., Paris.

The preparation and chemical properties of potassium, strontium and barium ferrates are described. Separation by glass-paper chromatography, electrochemical studies, and infrared spectra are discussed. A polarographic determination of ferrate ion was developed. The stability of these compounds was studied with differential thermal analysis. (auth)

38860 (COO-1297-6) CHEMICAL EFFECTS OF LEAD IONS ON POSITRONIUM. Leeson, Jeffrey Sanford (Western Reserve Univ., Cleveland, Ohio. Dept. of Physics). June 1966. Contract AT(11-1)-1297. 24p. Dep. mn. CFSTI $1.00 cy, $0.50 mn.

Thesis.

When lead perchlorate was added to a solution in which a positron had been added, it was found that something was competing with positronium formation. Measurements with lead acetate showed the same result. Therefore, studies were made to determine how positronium is affected by Pb^{2+} by measuring the intensity, I_2, as a function of Pb^{2+} concentration. Mechanisms are proposed for the decrease in I_2 that was observed. The only conclusion made was that the effects observed in NO_3^- solutions and Pb^{2+} solutions may be quite similar, and neither requires that one postulate the formation of any positron compounds. (P.C.H.)

38861 (COO-1109-22) THE SOLID-STATE CHEMISTRY OF RARE EARTH OXIDES. Technical Progress Report, 1965–1966. Caro, Paul; Eyring, Leroy; Kordis, J.; Burnham, D. Arthur; Felmlee, Theron L.; Stone, G. Duane; Warmkessel, Joyce M.; Weber, Gary R.; Sawyer, James O. (Arizona State Univ., Tempe). July 1, 1966. Contract AT(11-1)-1109. 415p. Dep. mn. CFSTI $7.15 cy, $2.00 mn.

Research progress is reported in 8 sections. A separate abstract was prepared for each section. (M.C.G.)

For abstracts of individual sections see: 38862–38869.

38862 (COO-1109-22, Paper 1) SOME TENSIMETRIC STUDIES IN THE MIXED CERIA–TERBIA SYSTEM. (Arizona State Univ., Tempe). 46p.

Tensimetric studies were made of the $(Ce,Tb)O_x$ system at temperatures below ~1050°C and oxygen dissociation pressures from ~1 to ~760 mm Hg both isobarically and isothermally. The sensitivity of the oxygen dissociation pressures to variations in structural makeup is illustrated. In this system there was little evidence of valence stabilization of one oxide by the other. In the terbia-rich region the behavior resembled pure terbia except for the appearance of a disordered phase at low temperatures and the change in equilibrium oxygen pressures. X-ray-diffraction analysis indicated a solid solution over the entire composition range even though the tensimetric curves indicated a large deviation from ideal behavior. (M.C.G.)

38863 (COO-1109-22, Paper 2) A TENSIMETRIC STUDY OF THE TERBIA AND PRASEODYMIA SYSTEM AND THE MIXED PRASEODYMIA–TERBIA SYSTEM. (Arizona State Univ., Tempe). 33p.

Tensimetric studies of high-purity (99.999%) Pr_2O_3 and Tb_2O_3 systems are reported. The mutually modifying influences of these oxides in the mixed state on their individually complex phase relations, which arise from the presence of discrete ordered phases, were investigated. In the system there was an obliteration of many of the ordered intermedi-

of the trace elements in stabilizing TMV-RNA in the host cell is discussed. For the determination of trace elements, neutron activation analysis was used. (auth)

38847 TRACE ELEMENTS IN HUMAN DISEASE. Lenihan, J. M. A. (Western Regional Hospital Board, Glasgow). pp 251-65 of Radioactivation Analysis and Its Applications in Biological Sciences. Paris, Presses Universitaires de France, 1964.

The role of activation analysis in the study of trace element metabolism, with particular reference to human diseases of nutrition and of occupation is reviewed. The list of elements recognized as essential in the nutrition of the higher animals, including man has steadily grown through refinement of techniques in analytical and biochemical assay. Studies discussed include: the significance of dietary and environmental exposure to arsenic in cancer (including the case of Napoleon Bonaparte); strontium metabolism in bone diseases; occupational hazards of arsenic; and animal diseases and human medicine. (P.C.H.)

38848 BIOLOGICAL APPLICATION OF ACTIVATION ANALYSIS OF ^{18}O. Fleckenstein, A.; Janke, J. (Univ., Freiburg i. B.). pp 267-85 of Radioactivation Analysis and Its Applications in Biological Sciences. Paris, Presses Universitaires de France, 1964. (In French).

A new method based on the principle of analysis of ^{18}O by radioactivation by transforming the stable ^{18}O into radioactive ^{18}F by bombardment with protons was used for measuring the incorporation of ^{18}O coming from $H_2{}^{18}O$ under different physiological conditions in molecules of ATP, phosphocreatine, mineral phosphate, and other phosphorus compounds contained in the cardiac and skeletal muscle. The results obtained showed the advantages of this new method with respect to the traditional use of radiophosphate. Primarily the incorporation of radiophosphate in the intracellular phosphorus compounds is strongly inhibited by the membrane of the muscular fiber whereas $H_2{}^{18}O$ rapidly arrives at all the intercellular sites where the metabolism reactions of the phosphoryl compounds are produced. For this reason the acceleration of the metabolism of ATP and phosphocreatine provoked by an electric stimulation can be detected only with $H_2{}^{18}O$. (P.C.H.)

38849 DETERMINATION OF IODINE BY MEANS OF RADIOACTIVATION ANALYSIS AND ITS APPLICATIONS IN THYROIDAL PHYSIOPATHOLOGY. Comar, D.; Riviere, R.; Kellershohn, C. (CEN, Saclay, France). pp 307-36 of Radioactivation Analysis and Its Applications in Biological Sciences. Paris, Presses Universitaires de France, 1964. (In French).

Partial automation of these iodine measurements under development for thyroid function tests is described. This partial automation makes it possible to measure continuously samples containing iodine between 0.1 and 0.001 ppM. A statistical study of the total and organic iodine rate found in the blood of normal and pathological subjects was undertaken and the results are discussed. With the possibility of measuring precisely the food iodine rate and iodine excreted by patients examined, it is possible, because of the measurement of the specific activity in the different media of the organism after a single injection of radioactive iodine, to measure important parameters aiding in the comprehension of certain aspects of thyroid metabolism. Some examples are given of measurements of iodine contained in the thyroid, measurements of the rate of hormonal secretion, and measurement of different pools in the organism. (P.C.H.)

38850 ISOTOPIC ANALYSIS OF ^{48}Ca BY NEUTRON ACTIVATION. Junod, E.; Laverlochere, J. (CEN, Grenoble, France). pp 337-60 of Radioactivation Analysis and Its Applications in Biological Sciences. Paris, Presses Universitaires de France, 1964. (In French).

With the object of studying the possibilities of using ^{48}Ca as a tracer in a medium containing natural calcium, studies were made on neutron activation analysis of the isotope, by means of the reaction $^{48}Ca(n,\gamma)^{49}Ca$ ($T^{1/2}$ = 8.8 min, E_γ = 3 Mev). Straight lines of standardization were established to be in the area of 1 to 12 μg of ^{48}Ca by three methods of computing. Interferences were also studied. Enrichment of ^{48}Ca was determined in samples of calcium carbonate from tracer experience. From the straight lines of standardization, the sensitivity of dosage of natural calcium was calculated by ^{49}Ca, which is of the microgram order. The irradiation facilities are described. (tr-auth)

38851 DETERMINATION OF Cu, Cr, Zn, Co, Na, AND K IN BLOOD SERUM. Pijck, J.; Hoste, J. (Faculteit der Wetenschappen, Instituut voor Analytische Chemie, Ghent). pp 361-78 of Radioactivation Analysis and Its Applications in Biological Sciences. Paris, Presses Universitaires de France, 1964. (In French).

The results of experiments made with a view of determining the behavior of the elements Sb, As, Cr, Au, Fe, Cu, Hg, Pb, Mo, Mn, V, Ag, and Zn during the process of mineralization demonstrated that the combustion method generally involves considerable waste. Use of a concentrated acid mixture H_2SO_4–$HClO_4$–HNO_3 in the ratio of 1:1:3, on the other hand, permitted quantitative recovery of the elements considered with the exception of Fe, Hg, As, Au, and Sb. The trace elements Cu, Cr, Zn, Co, Na, and K were determined in serum by radioactivation. Cu, Cr, and Co were isolated quantitatively by selective procedures. Zinc required a more complex separation, from which the product was determined by gravimetry and titrimetry. For K and Na, two techniques were elaborated, with and without chemical separation. All the analyses were controlled by comparison with the results obtained by classic method[s] (gravimetry) on the same samples. These prove[d] [re]producible and quantitative. The advantage of the[se] final methods lies in the reduction of the sample, which varies between 250 and 1 μl. (tr-auth)

38852 THE USE OF NEUTRON ACTIVATION ANALYSIS FOR THE QUANTITATION OF SELECTED CATIONS IN HUMAN BLOOD. Bethard, W. F.; Olehy, D. A.; Schmitt, R. A. (General Atomic Div., General Dynamics Corp., San Diego, Calif.). pp 379-93 of Radioactivation Analysis and Its Applications in Biological Sciences. Paris, Presses Universitaires de France, 1964.

Using neutron activation analysis, concentrations of magnesium, manganese, copper, and zinc were measured in plasma and erythrocytes of normal adult human blood. Errors arising from the use of heparin as an anticoagulant prior to neutron irradiation of blood are pointed out. It is emphasized that when using neutron activation analysis, addition for extraneous materials to the samples prior to neutron irradiation should be eliminated whenever possible. Preliminary data on the concentrations of magnesium, manganese, copper, and zinc in normal adult human erythrocytes after three weeks of blood bank storage are presented. Data on the concentrations of these cations in leukocytes from patients having chronic myelocytic leukemia and acute monocytic leukemia are also included. (auth)

38853 PRECISION NEUTRON ACTIVATION ANALYSIS OF ZINC AND TITANIUM OXIDES IN ORGANIC COATING PIGMENTS. Eggebraaten, V. L.; Miller, L. E. (Boeing Co., Seattle). 9p. (CONF-650809-2). ORAU. Gmelin, AED-CONF-65-229-3.

From Society for Applied Spectroscopy, 4th National Meeting, Denver.

Description is given of an activation analysis system that was set up in order to study the performance of precise quantitative determinations of selective elements in various materials along with maintaining the expedience in the analysis that is typical of analytical instrumentation. A typical quality control application is given that involves the analysis of zinc and titanium, both present as the oxides, in organic coating pigments. The analysis of both elements requires only one neutron irradiation. The zinc samples are allowed to set 40 min before counting for ^{65}Zn to allow for the decay of ^{13}N. The reaction $^{48}Ti(n,p)^{48}Sc$ is used for the quantitative determination of Ti. Requirements for obtaining maximum precision in activation analysis using a 150-kv accelerator are listed. (P.C.H.)

38854 DETERMINATION OF AMERICIUM BY CONTROLLED-POTENTIAL COULOMETRY. Koehly, G.; Berger, R. (Commissariat a l'Energie Atomique, Fontenay-

aux-Roses, France). 17p. (CONF-651004-16). ORAU. Gmelin, AED-CONF-65-287-3.

From 9th Conference on Analytical Chemistry in Nuclear Technology, Gatlinburg, Tenn.

Equipment and conditions are described for the determination of Am by controlled-potential coulometry. Selectivity, reliability, and sensitivity are also discussed. The chemical yield of the quantitative oxidation of Am^{3+} to AmO_2^{2+} in sulfate solution, followed by coulometric reduction to AmO_2^{+} and the current yields of the reduction were investigated. The procedure used is described. (P.C.H.)

Inorganic and Physical Chemistry

Refer also to abstracts 38835, 39333, 39354, and 39387.

38855 (BNL-10350) MIXED β-DIKETONES. Newman, L.; Klotz, P. (Brookhaven National Lab., Upton, N. Y.). June 30, 1966. Contract AT(30-2)-Gen-16. 17p. (CONF-660805-1). Dep. mn. CFSTI $1.00 cy, $0.50 mn.

From International Conference on Solvent Extraction, Goteborg, Sweden.

The increased extraction of metals (M) by a benzene solution containing two β-diketones as compared with the sum of the extraction due to each of the β-diketones was interpreted as arising from the formation of a mixed β-diketone complex. All possible combinations of the following were studied: thenoyltrifluoroacetone (TTA), benzoyltrifluoroacetone (BTA), thenoylacetone (TA), acetylacetone (AA), benzoylacetone (BA), and dibenzoylmethane (DBM). Formation constants, K_m, were measured in benzene for the reaction $\frac{1}{2} MX_2 + \frac{1}{2} MY_2 = MXY$, where X^- and Y^- are the enolate ions of the different β-diketones. The systems UO_2^{2+}/BTA + TTA, UO_2^{2+}/AA + BA, Cu^{2+}/BTA + TTA, and Cu^{2+}/AA + BA all give log K_m values equal to the statistically predicted value of 0.3. These systems can be classified as containing strong + strong or weak + weak β-diketones. The systems which contain weak + strong β-diketones, UO_2^{2+}/AA + TTA, and Cu^{2+}/AA + TTA, give log K_m values of 1.0 and 0.5, respectively, which indicate a somewhat more favorable formation of the mixed species. (auth)

38856 (BNL-10372) PHYSICAL AND CHEMICAL PROPERTIES OF DILUTE ALLOYS OF Cd IN Na. Weeks, John R.; Davies, Hywel A. (Brookhaven National Lab., Upton, N. Y.). [1964]. Contract AT(30-2)-Gen-16. 23p. (CONF-660712-1). Dep. mn. CFSTI $1.00 cy, $0.50 mn.

From International Conference on the Alkali Metals, Nottingham, England.

The Na–Cd liquidus was reinvestigated at the Na-rich end at temperatures between 100 and 400°C by the method of sampling and chemical analysis. Partial molar thermodynamic properties of Cd in liquid Na were calculated from the low-temperature portion of this curve. The densities and surface tensions of Na–Cd alloys were determined from 200 to 400°C by the maximum bubble pressure technique. The molal volumes behave abnormally at low concentrations of Cd and become strongly negative at higher concentrations. The surface tension of sodium decreases initially upon the addition of Cd, reaches a minimum at approximately 3 to 4 at. % Cd, and then increases. (auth)

38857 (BNWL-235-3) PACIFIC NORTHWEST LABORATORY ANNUAL REPORT FOR 1965 IN THE PHYSICAL SCIENCES. VOLUME 3. EARTH SCIENCES. Pearce, D. W.; Green, J. K. (Battelle-Northwest, Richland, Wash. Pacific Northwest Lab.). May 1966. Contract AT(45-1)-1830. 76p. Dep. mn. CFSTI $3.00 cy, $0.75 mn.

Results are reported for studies on geology and hydrology, mineral chemistry, and particles and gases. Separate abstracts were prepared for each of the three sections. (P.C.H.)

For abstracts of individual sections see: 38858, 39099, and 39103.

38858 (BNWL-235-3, pp 23-51) MINERAL CHEMISTRY. (Battelle-Northwest, Richland, Wash. Pacific Northwest Lab.).

Results are reported for studies on: montmorillonite exchange equilibria with Sr–Na–Cs; self-diffusion of Na in vermiculite; exchange of alkali metal cations on a natural stilbite; alkali metal cation equilibria with chabazite; unit cell size and Cs loading on Type A and Type X zeolites; cation exchange properties of wairakite and analcime; radionuclide migration in soil columns-development of a computer program; dispersion characteristics of Sr in soil columns; and Cs and Sr distribution beneath liquid waste disposal sites. (P.C.H.)

38859 (CEA-R-2895) CONTRIBUTION A L'ETUDE ANALYTIQUE DES FERRATES. (Contribution to the Analytic Study of Ferrates). Becarud, Nicole (Commissariat a l'Energie Atomique, Fontenay-aux-Roses (France). Centre d'Etudes Nucleaires). 1966. 52p. Dep. mn.

Thesis. Submitted to Univ., Paris.

The preparation and chemical properties of potassium, strontium and barium ferrates are described. Separation by glass-paper chromatography, electrochemical studies, and infrared spectra are discussed. A polarographic determination of ferrate ion was developed. The stability of these compounds was studied with differential thermal analysis. (auth)

38860 (COO-1297-6) CHEMICAL EFFECTS OF LEAD IONS ON POSITRONIUM. Leeson, Jeffrey Sanford (Western Reserve Univ., Cleveland, Ohio. Dept. of Physics). June 1966. Contract AT(11-1)-1297. 24p. Dep. mn. CFSTI $1.00 cy, $0.50 mn.

Thesis.

When lead perchlorate was added to a solution in which a positron had been added, it was found that something was competing with positronium formation. Measurements with lead acetate showed the same result. Therefore, studies were made to determine how positronium is affected by Pb^{2+} by measuring the intensity, I_2, as a function of Pb^{2+} concentration. Mechanisms are proposed for the decrease in I_2 that was observed. The only conclusion made was that the effects observed in NO_3^- solutions and Pb^{2+} solutions may be quite similar, and neither requires that one postulate the formation of any positron compounds. (P.C.H.)

38861 (COO-1109-22) THE SOLID-STATE CHEMISTRY OF RARE EARTH OXIDES. Technical Progress Report, 1965-1966. Caro, Paul; Eyring, Leroy; Kordis, J.; Burnham, D. Arthur; Felmlee, Theron L.; Stone, G. Duane; Warmkessel, Joyce M.; Weber, Gary R.; Sawyer, James O. (Arizona State Univ., Tempe). July 1, 1966. Contract AT(11-1)-1109. 415p. Dep. mn. CFSTI $7.15 cy, $2.00 mn.

Research progress is reported in 8 sections. A separate abstract was prepared for each section. (M.C.G.)

For abstracts of individual sections see: 38862–38869.

38862 (COO-1109-22, Paper 1) SOME TENSIMETRIC STUDIES IN THE MIXED CERIA–TERBIA SYSTEM. (Arizona State Univ., Tempe). 46p.

Tensimetric studies were made of the $(Ce,Tb)O_x$ system at temperatures below ~1050°C and oxygen dissociation pressures from ~1 to ~760 mm Hg both isobarically and isothermally. The sensitivity of the oxygen dissociation pressures to variations in structural makeup is illustrated. In this system there was little evidence of valence stabilization of one oxide by the other. In the terbia-rich region the behavior resembled pure terbia except for the appearance of a disordered phase at low temperatures and the change in equilibrium oxygen pressures. X-ray-diffraction analysis indicated a solid solution over the entire composition range even though the tensimetric curves indicated a large deviation from ideal behavior. (M.C.G.)

38863 (COO-1109-22, Paper 2) A TENSIMETRIC STUDY OF THE TERBIA AND PRASEODYMIA SYSTEM AND THE MIXED PRASEODYMIA–TERBIA SYSTEM. (Arizona State Univ., Tempe). 33p.

Tensimetric studies of high-purity (99.999%) Pr_2O_3 and Tb_2O_3 systems are reported. The mutually modifying influences of these oxides in the mixed state on their individually complex phase relations, which arise from the presence of discrete ordered phases, were investigated. In the system there was an obliteration of many of the ordered intermedi-

ate phases found in the individual oxides. The most prominent feature was the appearance of two disordered phases of wide nonstoichiometry with a miscibility gap between them. The question of why the addition of Tb_2O_3 to Pr_2O_3, and vice-versa, obscures or destroys the isobaric habits of the pure phases is discussed. (M.C.G.)

38864 (COO–1109-22, Paper 3) HIGH-TEMPERATURE X-RAY DIFFRACTION STUDIES IN SELECTED RARE EARTH OXIDE–OXYGEN SYSTEMS. (Arizona State Univ., Tempe). 91p.

Phase studies were made on PrO_x-O_2, TbO_x-O_2, and Tb–Ce–O systems in oxidation-reduction cycles. The stability regions of the various phases were determined. All the single-phase regions proposed were clearly seen by high-temperature x-ray studies. The existence of hysteresis is manifest by a delay in the appearance of the new second phase between reduction and oxidation. All hysteresis loops are two-phase with essentially stoichiometric end members where the amounts of each is appropriate to the over-all composition. Data are presented in tables and graphs. (M.C.G.)

38865 (COO–1109-22, Paper 4) ANION DIFFUSION IN SAMARIUM SESQUIOXIDE. (Arizona State Univ., Tempe). 57p.

The exchange of ^{18}O in the gas phase with an oxide having only ^{16}O was studied to determine the migration of reacting species into and away from the surface and the reaction zone. The exchange study on Sm_2O_3 was carried out at 700 to 1000°C and 45 to 200 mm to yield diffusion rate coefficients, rate constants for the surface exchange, and activation energies for both processes. Self-diffusion coefficients were also determined for La_2O_3 and Nd_2O_3. An activation energy for diffusion in Sm_2O_3 was found to be 33 kcal/mole. The activation energy for the surface process was 40 kcal/mole. (M.C.G.)

38866 (COO-1109-22, Paper 5) SPECTROSCOPIC AND X-RAY STUDIES IN THE REGION PrO_x $1.5 \leq x \leq 1.714$. (Arizona State Univ., Tempe). 29p.

The phase diagram of the PrO_x-O_2 system in the region PrO_x, $1.5 \leq x \leq 1.714$ was studied. Changes in splitting of the free ion level as the composition of the oxide was changed were monitored. It was concluded that for the sesquioxide the bands in the near infrared are due to the $4f^2$ configuration and the bands in the visible region are covered due to the presence of the +4 ion, which probably has a configuration of $4f^1$. There was an electric conductivity maximum at $PrO_{1.725}$, which suggests that the $4f^2$-state praseodymium is at the center of a slightly irregular octahedron. As the composition was changed there was a change from C_2 symmetry to seven coordination symmetry. (M.C.G.)

38867 (COO–1109-22, Paper 6) ON THE LOWER OXIDES OF THE RARE EARTHS. (Arizona State Univ., Tempe). 33p.

Efforts were made to prepare pure SmO and Sm_2O. It was demonstrated that "SmO" is actually $Sm_2O_xN_{1-x}$, where x is near $\frac{1}{2}$, and that while solutions with $x < \frac{1}{2}$ can be prepared, those with $x \geq \frac{1}{2}$ disproportionate. These results are discussed in terms of the nature of the bonding in these ternary systems. A phase that appeared to be the same as the Sm_2O previously reported was found to be SmH_2. Ytterbium and Yb_2O_3 were heated together and no phase that could be attributed to a lower oxide was observed. Direct combination of Sm and Si at 1400°C gave Sm_5Si_3. (M.C.G.)

38868 (COO–1109-22, Paper 7) THE RARE EARTH CARBONATE SYSTEM. (Arizona State Univ., Tempe). 73p.

Methods are described for preparation of rare earth carbonates with $CO_2 : Ln_2O_3$ ratios of 3 and 2. Their optical properties were investigated from the far infrared to the ultraviolet. It was found that the absorption of CO_2 by rare earth oxides in suspension in water is unique to each. (M.C.G.)

38869 (COO–1109-22, Paper 8) X-RAY DIFFRACTION STUDIES ON RARE EARTH CARBONATES FORMED UNDER CONDITIONS OF GRADUALLY INCREASING pH AND CARBON DIOXIDE CONCENTRATION, FROM HOT Ln^{3+} NITRATE SOLUTIONS CONTAINING UREA. (Arizona State Univ., Tempe). 42p.

X-ray-diffraction studies of rare earth carbonates are described and structures are proposed for $(SmO)_2CO_3$ and $Pr_2(CO_3)_3 \cdot 8H_2O$. (M.C.G.)

38870 (IS–1356) HEATS OF DILUTION OF SOME AQUEOUS RARE-EARTH CHLORIDE SOLUTIONS AT 25 DEG C. De Kock, C. W.; Spedding, F. H. (Ames Lab., Iowa State Univ. of Science and Tech.). Feb. 1965. Contract W-7405-eng-82. 166p. Dep. mn. CFSTI $5.00 cy, $1.00 mn.

The heats of dilution of aqueous $PrCl_3$, $TbCl_3$, and $YbCl_3$ solutions were determined from zero molal to saturation, and aqueous $LaCl_3$ and $HoCl_3$ solutions from 0.25 molal to saturation at 25°C. In addition, aqueous heats of solution of $TbCl_3 \cdot 6H_2O$ and $HoCl_3 \cdot 6H_2O$ were determined at 25°C. From these data empirical least square equations for the relative apparent molal heat contents, ϕ_L, were determined as a function of $m^{\frac{1}{2}}$ using an IBM-7074 computer. Expressions for the relative partial molal heat content of the water, $\overline{L}_1$, and of the salt, $\overline{L}_2$, were determined from these empirical equations. The relative partial molal excess entropies of the water $(\overline{S}_1 - \overline{S}_1^0)$ and of the salt $(\overline{S}_2 - \overline{S}_2^0)$ were determined from the $\overline{L}_1$ and $\overline{L}_2$ data and from the activity coefficient data of these electrolytes. Values for $\overline{L}_1$, $\overline{L}_2$, $T(\overline{S}_1 - \overline{S}_1^0)$, and $T(\overline{S}_2 - \overline{S}_2^0)$ were calculated at rounded concentrations. The data show that aqueous $PrCl_3$ and $TbCl_3$ solutions obey the Debye-Hückel limiting law and there is strong indication that aqueous $YbCl_3$ solutions also obey the limiting law. It is postulated that the heat of dilution data below 0.15 molal for all the aqueous rare-earth chloride solutions which have been studied can be understood in terms of two series within the rare earths. (P.C.H.)

38871 (NYO–1769-54) INVESTIGATION OF PROPERTIES AND STRUCTURE OF MOLTEN SALTS. Annual Progress Report, 1964–1965. Bockris, John O'M. (Pennsylvania Univ., Philadelphia. Electrochemistry Lab.). July 30, 1965. Contract AT(30-1)-1769. 107p. Dep. mn. CFSTI $4.00 cy, $0.75 mn.

Developments are reported for studies on: diffusion process in molten salts at constant volume; apparatus for simultaneous measurement of viscosity and density of molten salts at high pressure; calibration of oscillating bob viscometer at room temperature; pressure vessel design for viscosity determination in molten salts; self-diffusion in molten Group II chlorides; Raman spectra of liquid $MgCl_2$, $MgCl_2-KCl$ system, and $ZnCl_2$. (P.C.H.)

38872 (NYO–1769-68) INVESTIGATION OF PROPERTIES AND STRUCTURE OF MOLTEN SALTS. Annual Progress Report, 1965–1966. Bockris, John O'M. (Pennsylvania Univ., Philadelphia. Electrochemistry Lab.). June 14, 1966. Contract AT(30-1)-1769. 83p. Dep. mn. CFSTI $3.00 cy, $0.75 mn.

Viscosity, Raman spectroscopy, and diffusion in molten salts were studied. The first viscometer capable of use at high pressure and high temperatures was developed. Measurements were made on constant-volume diffusion of ^{134}Cs ions in cesium nitrate. The data obtained confirm and extend the findings that the formation of holes constitutes the rate-determining step in the diffusion process at constant pressure. Further, as the size of the diffusing ion increases, compared with the hole volume in the diffusion medium, a corresponding increase occurs in both the activation energy at constant volume and in the activation volume for jumping. These results can be interpreted very satisfactorily in terms of the Density Fluctuation Hole Model for liquids. The use of laser-excited Raman spectroscopy was extended to fused salts (where its special characteristics offer considerable advantages). Determinations were made in the system sodium nitrate and stannous chloride. The laser Raman apparatus was developed to a point at which any limitations are those set by the salt sample itself rather than by the equipment. In general terms, an increase of some 30 times in sensitivity was

achieved together with a great increase in quality of the picture. (P.C.H.)

38873 (NYO-2269-9) STUDIES IN SOLUTION AND NUCLEAR CHEMISTRY. Progress Report, October 1, 1965–September 30, 1966. Marinsky, Jacob A.; Clarke, George A. (State Univ. of New York, Buffalo, Dept. of Chemistry). July 1, 1966. Contract AT(30-1)-2269. 117p. Dep. mn. CFSTI $4.00 cy, $0.75 mn.

Research to elucidate ion-exchange phenomenon and to study the solution chemistry of the alkali metals, the alkaline earths, the transition elements, and the rare earths is reported. Various ion-forms of polystyrene sulfonate, the polyelectrolyte analog of commercially produced ion-exchange resins, Dowex-50 and Amberlite IR-120, and polymethacrylic acid, and analog of the commercially produced ion-exchange resin, Amberlite IRC-50, were employed. Ion-exchange as well as polarographic and potentiometric techniques were employed to study solution chemistry. In continuing the study of heavy atom effects on the energy transfer processes in analogs of well-characterized rare earth chelates emphasis was shifted from the β-diketone ligands investigated earlier to uncharged heterocyclic ligands. These latter systems employ nitrogen rather than oxygen bonding. The nuclear portion of the program was enhanced by reactor pulse operation. (auth)

38874 (ORNL-TM-1540) OXIDATION OF HYDROGEN AND CARBON MONOXIDE IN A HELIUM STREAM BY COPPER OXIDE. ANALYSIS OF COMBINED FILM AND PORE DIFFUSION WITH RAPID IRREVERSIBLE REACTION FOR TWO COMPONENTS IN A FIXED-BED PROCESS. Scott, Charles D. (Oak Ridge National Lab., Tenn.). Aug. 1966. Contract W-7405-eng-26. 304p. Dep. mn. CFSTI $7.00 cy, $1.50 mn.

Thesis. Submitted to Univ. of Tennessee, Knoxville.

The reaction of hydrogen and carbon monoxide as contaminants in a stream of helium with fixed beds of copper oxide pellets was investigated in tests with both differential and deep beds and with both a single reacting species and two reacting species. Differential-bed tests were used to establish transport properties of the contaminants within the porous solids, and deep beds were evaluated by considering the effluent concentration history of the contaminants. The ranges of experimental conditions investigated were: temperature, 400 to 600°C; pressure, 10.2 to 30.0 atm; mass flow rate of gas, 0.0058 to 0.050 g/cm²-sec; and inlet concentration of reacting species, 0.0008 to 1.21%. The results indicated that, under the conditions studied, the reaction system can be represented by two rate-limiting steps: external diffusion of the contaminant gas through a stagnant gas film surrounding the copper oxide pellet and molecular diffusion of the contaminant through the pores in the porous solid to the reaction site. There was no apparent interaction between the two contaminant gases. Differential equations were developed to describe the mathematical model of the system, and the mathematical solution was extended to the generalized case, which is usable for other systems. The equations were also used as design equations for fixed-bed copper oxide oxidizers. Finite-difference solutions of the differential equations were obtained, and computer codes were written and used for these solutions. Correlation of the experimental data and results from the differential equations of the mathematical model are shown in graphic form. A series of curves that show reacting gas breakthrough as a function of the system parameters are presented, and their use as design correlations is demonstrated. (auth)

38875 (UCRL-14703-T) STUDY OF THE ISOTOPIC DISPROPORTIONATION REACTION BETWEEN LIGHT AND HEAVY WATER USING A PULSED-MOLECULAR-BEAM MASS SPECTROMETER. Pyper, J. W.; Newbury, R. S.; Barton, G. W. Jr. (Lawrence Radiation Lab., Univ. of California, Livermore). [1965]. Contract W-7405-eng-48. 5p. (CONF-660537-1). Dep. mn. CFSTI $1.00 cy, $0.50 mn.

From 14th Annual Conference on Mass Spectrometry and Allied Topics, Dallas.

Disagreement in calculated values of the equilibrium constant (K) for the disproportionation reaction $H_2O + D_2O \rightarrow 2HDO$ led to attempts to determine K precisely by direct experiment. A pulsed-molecular-beam mass spectrometer was devised to minimize errors caused by "memory effect" and background encountered in previous work with mass spectrometers. Values of K are compared with those determined by other means. (J.G.B.)

38876 (UJV-1598) VYPAROVANI AKTINIDU A JEJICH SLOUCENIN. I. ZAKLADNI PROBLEMY STUDIA VYPAROVANTI VYPAROVANI AKTINIDU. (Vaporization of the Actinides and their Compounds. Part I. Basic Problems of Vaporization Studies. Vaporization of Actinides). Krivy, I. (Ustav Jaderneho Vyzkumu, Ceskoslovenska Akademie Ved, Rez). May 1966. 40p. Dep. mn.

Individual stages of vaporization studies are discussed, including: establishment of the general behavior of the system, identification of the gaseous species, formulation of the net reaction(s), vapor-pressure measurement, and study of the kinetics and the mechanism of vaporization processes. The general principles of the theory of vaporization and usual treatment of experimental results are also given. Earlier studies in the field of vaporization of actinide elements (Th, U, Np, Pu, Am, and Cm) are reviewed. The best approximations for temperature dependence of the pressure of monoatomic vapor, the standard free energy, enthalpy, and entropy of vaporization (sublimation) are presented separately for each actinide metal. In addition estimated values of normal boiling point are included for individual actinides as well as the appropriate values of standard heat and entropy of vaporization at normal boiling point. Partial correlation and comparison of the thermodynamic data characterizing the vaporization of actinides were made with those for lanthanides. (auth)

38877 (JPRS-35594) SOME PROBLEMS OF RARE EARTHS CATALYSIS. P'eng, Pi-hsien. Translated from Hua Hsueh Tung Pao, No. 11, 1-8(1966). 19p. (TT-66-32029). CFSTI $1.00 cy, $0.50 mn.

Physical and chemical properties of rare earths relative to catalysis are discussed. Certain structural factors and magnetic properties of the rare earths and the relations between electronic and catalytic properties are considered. Uses of rare earth catalysts are reviewed. (M.C.G.)

38878 (ORNL-tr-1257) INVESTIGATION OF THE COMPLEXING OF TRIVALENT ACTINIDES AND LANTHANIDES IN PHOSPHORIC ACID SOLUTIONS. Birisov, M. S.; Elesin, A. A.; Lebedev, I. A.; Filimonov, V. T.; Yakovlev, G. N. Translated for Oak Ridge National Lab., Tenn., from Radiokhimiya, 8: 42-8(1966). 11p. Dep. mn. CFSTI $1.00 cy, $0.50 mn. JCL $1.60 fs, $0.80 mf.

An investigation was made of the sorption of indicator quantities of Am^{3+}, Ce^{3+}, Pm^{3+}, and Y^{3+} by Dowex 50 × 8 cationite from acid phosphate solutions. It was established that phosphate concentrations of 3×10^{-4} to 0.1 M and pH values of 2 to 4 complex ions with the composition $MH_2PO_4^{2+}$ are present in the solution. The concentration (=0.2) and thermodynamic stability constants of phosphate complex ions of americium, cerium, promethium, and ytterium were calculated. The strength of the phosphate complexes of trivalent actinides and lanthanides exceeds that of other complexes of those elements with single-charged inorganic additives and is comparable with that of weak organic complexes. (auth)

38879 (UCRL-Trans-1325) ON THE POLARIZATION CAPACITY OF CERTAIN IONS. Mickevicius, V. V. Translated by Maria Kassatkin (Univ. of California Lawrence Radiation Lab., Berkeley), from Lietuvos Fiz. Rinkinys, Lietuvos TSR Aukstosios Mokylos, 4: 81-5(1964). 8p. Dep. mn. CFSTI $1.00 cy, $0.50 mn. JCL $1.10 fs, $0.80 mf.

Application of the variational method to calculations of the polarization capacities of certain ions with completed electronic shells is discussed. The polarization capacities of ions of alkali metals were calculated using the latest experimental data on spectral terms. Results of calculations of the polarization capacities of various researchers are discussed. (auth)

38880 ADVANCES IN INORGANIC CHEMISTRY AND RADIOCHEMISTRY. VOLUME 8. Emeleus, H. J.; Sharpe, A. G. (eds.). Advances Inorg. Chem. Radiochem., 8: 1-365(1966).

Six chapters are included; separate abstracts were prepared for two. The remaining four chapters contain information on: substitution products of the Group VIB metal carbonyls; perchloric acid; nuclear quadrupole resonance and its application in inorganic chemistry; and the chemistry of complex aluminohydrides. (P.C.H.)

For abstracts of individual chapters see: 38881 and 38882.

38881 TRANSITION METAL CYANIDES AND THEIR COMPLEXES. Chadwick, B. M.; Sharpe, A. G. (Cambridge Univ., Eng.). Advances Inorg. Chem. Radiochem., 8: 83-176(1966).

A critical review is given of the preparation, characterization, and properties of cyanide complexes of the transition metals. Special attention is given to structural, thermodynamic, and kinetic data where these exist. 544 references are given to mid-1965. (P.C.H.)

38882 NEUTRON DIFFRACTION AND ITS APPLICATIONS IN INORGANIC CHEMISTRY. Bacon, G. E. (Univ. of Sheffield, Eng.). Advances Inorg. Chem. Radiochem., 8: 225-56(1966).

The present position of neutron diffraction as it relates to inorganic chemistry is reviewed, concentrating on accounts of investigations published within the last 3 or 4 years. The detection of light elements and magnetic scattering in paramagnetic materials, which has been used to deduce direct information on the valence states of certain atoms, is discussed. (74 references). (P.C.H.)

38883 PHOSPHATES AND POLYPHOSPHATES OF THE LANTHANIDE ELEMENTS. VIII. PRASEODYMIUM, TERBIUM, HOLMIUM, ERBIUM, THULIUM, YTTERBIUM, AND LUTETIUM TRIPHOSPHATES. Melardi, Ebe Barbieri; Giesbrecht, Ernesto (Univ., Sao Paulo, Brazil). An. Acad. Brasil. Cienc., 37: 221-8(1965).

Potentiometric and conductometric titrations of praseodymium, terbium, holmium, erbium, thulium, ytterbium, and lutetium chloride solutions with sodium triphosphate solutions or vice-versa showed the formation of compounds in which the ratio $Ln^{3+}: P_3O_{10}^{5-}$ is 3:2 (insoluble), 1:1 (soluble), and 1:2 (soluble), respectively. The compounds $Ln_3(P_3O_{10})_2 \cdot$ water were isolated and analyzed. The change of the absorption spectrum of Pr^{3+} ions in the ultraviolet region when complexed with $P_3O_{10}^{5-}$ ions is presented and the influence of the ratio $Pr^{3+}: P_3O_{10}^{5-}$ and pH values are discussed. (auth)

38884 SELENIDES ML_4Se_7 OF STRUCTURAL TYPE Y_5S_7 (L = RARE EARTH AND M = Mg, Cr^{2+}, Mn, Fe^{2+}). Souleau, Charles; Guittard, Micheline; Wintenberger, Micheline (Faculte de Pharmacie, Paris). Bull. Soc. Chim. France, No. 5, 1644-5(May 1966). (In French).

Among the rare earths the selenides ML_4Se_7 exist only with dysprosium and with M as Cr^{2+}, Mn, or Fe^{2+}. These compounds are monoclinic of the Y_5S_7 type. They have a paramagnetic behavior between −196 and 400°C. Comparison of the selenides and sulfides belonging to the same crystalline type permits a definition of the structural conditions for their formations. (tr-auth)

38885 SYSTEM As_2O_5–ThO_2. Le Flem, Gilles; Lamic, Jacques; Hagenmuller, Paul (CNRS, Talence, France). Bull. Soc. Chim. France, No. 6, 1880-3(June 1966). (In French).

By thermally treating precipitates of thorium salts, in solution, with arsenic acid, some new thorium arsenates were prepared and isolated: a metaarsenate, $Th(AsO_3)_4$, in both α and β forms, a pyroarsenate, $ThAs_2O_7$, with two allotropic varieties α and β; a hexaarsenate, $Th_4As_6O_{23}$; and an orthoarsenate, $Th_3(AsO_4)_4$. Some crystallographic data and the areas of thermal stability were defined. The thorium arsenates, although thermally less stable, seemed more to resemble the phosphates more than the vanadates. (tr-auth)

38886 PREPARATION AND PROPERTIES OF THE DOUBLE SALT $2Th(C_2O_4)_2 \cdot (NH_4)_2C_2O_4 \cdot 7H_2O$. Bressat, Rene (Institut de Recherches sur la Catalyse, Villeurbanne, France); Trambouze, Yves; Claudel, Bernard; Lang, Gerard; Navarro, Alain. Bull. Soc. Chim. France, No. 6, 2094-9(June 1966). (In French).

The salt $(NH_4)_2[Th_2(C_2O_4)_5] \cdot 7H_2O$ was prepared. Its complex nature was established, its crystal structure determined, and the scheme for its thermal decomposition given. (tr-auth)

38887 IONIZATION, DISSOCIATION, AND INTRAMOLECULAR REARRANGEMENTS IN ALIPHATIC AMINES UNDER ELECTRON BOMBARDMENT. CASE OF METHYLAMINE AND METHYLAMINE–Nd_2. Collin, J. E.; Franskin, M. J. (Univ., Liege). Bull. Soc. Roy. Sci. Liege, 35: 267-84(1966). (In French).

The mass spectra of methylamine and deuterated methylamine–Nd_2 were investigated by means of a high resolution mass spectrometer. Rearrangement processes, including exchange between deuterium and hydrogen atoms, are discussed with the help of isotopic labeling and the use of high resolution. Dissociative mechanisms are considered, and it is shown that the removal of one hydrogen atom mainly refers to a C−H bond breakage; the removal of two hydrogen atoms is due mostly to departure of a H_2 molecule by simultaneous rupture of a C−H and a N−H bond, whereas in the removal of three hydrogen atoms, two atoms come from the methyl group and one from the amino group. Heats of formation of various ions were deduced from appearance potentials data, and ionization potentials were estimated for different species. The following values for ionization potentials are proposed: CH_2NH_2 = 6.05 ev; CN_3NH = 7.49v; CH_3 = NH = 11.9 ev and $\cdot CH$ = NH = 10.9 ev. (auth)

38888 IONIZATION, DISSOCIATION, AND INTRAMOLECULAR REARRANGEMENTS IN ALIPHATIC AMINES UNDER ELECTRON BOMBARDMENT. CASE OF DIETHYLAMINE AND DIETHYLAMINE–Nd. Collin, J. E.; Franskin, M. J. (Univ., Liege). Bull. Soc. Roy. Sci. Liege, 35: 285-305(1966). (In French).

The mass spectra of diethylamine and monodeuterated diethylamine–Nd were obtained by means of a high resolution mass spectrometer. The dissociation rearrangement processes are discussed, taking advantage of deuteration and high resolution. It is shown that an exchange between hydrogen and deuterium atoms occurs after ionization, in addition to the usual rearrangement processes by addition of atoms; this has to be taken into account for a proper discussion of the observed ion abundances, particularly when discussing complicated fragmentation mechanisms. It is shown that rearranged ions with or without the nitrogen atom occur. Numerous metastable transitions in both compounds are observed, and help in the identification of the dissociative sequences of the parent ion. It is also shown that the parent −1 ion results almost only from the loss of a hydrogen atom from the hydrocarbon part of the molecule, rather than from the amino group. No useful information was drawn from the appearance potentials, except for the ionization potential of the molecule itself. (auth)

38889 AN IMPROVED METHOD OF HYDROGEN ISOTOPIC EXCHANGE WITH DEUTERIUM SULFATE, AND THE PREPARATION OF 9,10-ANTHRAQUINONE-d_8. Lunelli, Bruno; Pecile, Cesare (Univ. of Padua). Can. J. Chem., 44: 1633-6(July 15, 1966).

An apparatus and improved conditions are described for using easily and efficiently sulfuric acid-d_2 as a deuterating agent. The preparation of 9, 10-anthraquinone-d_8 with a high deuterium content is reported. (auth)

38890 CONTRIBUTION TO THE STUDY OF PROTACTINIUM PEROXIDE COMPOUNDS IN BASIC MEDIA. Stchouzkoy, Tatiana; Muxart, Roland; Bouissieres, Georges (Institut de Physique Nucleaire, Arcueil, France). Compt. Rend., Ser. C, 262: 1845-7(June 27, 1966). (In French).

The conditions for the formation of peroxide compounds

of protactinium in basic media were examined. An insoluble sodium perprotactinate was isolated and analyzed. (tr-auth)

38891 SULFIDES AND OXYSULFIDES OF URANIUM AND POTASSIUM. Padiou, Jean; Lucas, Jacques, Prigent, Jacques (Faculte des Sciences, Rennes, France). Compt. Rend., Ser. C, 262: 1869-71(June 27, 1966). (In French).

When gaseous CS_2 reacts with potassium diuranate, there are obtained in succession $K_2U_2O_2S_5$ and then potassium thiouranite KUS_2. Treatment of $K_2U_2O_2S_5$ under hydrogen leads to the oxysulfides $K_2U_2O_2S_3$ and KUOS. (tr-auth)

38892 SYNTHESIS OF A NEW DOUBLE OXIDE OF NIOBIUM AND URANIUM. Gasperin, Madeleine (CNRS, Paris). Compt. Rend., Ser. C, 263: 135-6(July 11, 1966). (In French).

A new double oxide of niobium and uranium was obtained as a monocrystal by synthesis. It is a cubic substance of the pyrochlore type and with the formula $U_{\frac{1}{3}}Nb_2O_7$. This synthesis is related to the problem of the betafites. (tr-auth)

38893 RELAXATION OF PROTONS AND DEUTERONS IN AQUEOUS SOLUTIONS OF PENTAVALENT MOLYBDENUM. Mazitov, R. K. (Kazan State Univ.). Dokl. Akad. Nauk SSSR, 166: 1158-61(Feb. 11, 1966). (In Russian).

The longitudinal and transversal times of magnetic relaxation of protons and deuterons in aqueous solutions containing pentavalent Mo ions were determined by means of the nuclear spin echo method and by electron paramagnetic resonance measurements. The proton resonances were observed in 6730 and 1030, the deuteron resonances in 6730 oersted fields; the EPR spectra were measured at about 3200 oersted. In order to eliminate the effect of possible differential behavior of Mo^{5+} in HCl and DCl solutions, identical 12.5N HCl and DCl mixtures containing 22 and 78 at. % of protons and deuterons, respectively, were prepared by dissolving HCl in D_2O. The results indicated that the lowest limit of the existence of H within the paramagnetic complex is 10^{-8} sec. The effect of the acidity of the medium on the relaxation time of protons and deuterons was investigated with solutions containing 0.2M Mo^{5+}. It was found that within the 12.5 to 5N range the longitudinal time of relaxation was not affected but at lower concentrations the time of relaxation increased rapidly. The transverse time of relaxation decreased with decreasing acidity, passed through a minimum, and increased suddenly. (TTT)

38894 COMPARATIVE OXIDATION RATE OF ^{234}U AND ^{238}U ATOMS IN CERTAIN MINERALS. Chalov, P. I.; Merkulova, K. I. (Inst. of Physics and Mathematics, Academy of Sciences, USSR). Dokl. Akad. Nauk SSSR, 167: 669-71(Mar. 21, 1966). (In Russian).

Oxidation rates of ^{234}U and ^{238}U in various minerals were studied with specimens of uraninite, black uranite, and other minerals. The problem was resolved by separation of uranium into fractions of various valences followed by determination of the ratio of $^{234}U/^{238}U$ in the fractions. Faster oxidation of ^{234}U was observed in uraninite and black uranite while in minerals containing hexavalent uranium and in tantalum-niobium minerals, the rates of oxidation were identical. The partial separation of ^{234}U and ^{238}U during uranium migration from minerals into natural solutions took place at the expense of faster oxidation of ^{234}U, when uranium was leached from minerals containing uranium oxides and tetravalent uranium. The role played by radioactive yield should be considered because the formation of ^{234}U atoms led to a more rapid oxidation of ^{234}U in comparison to ^{238}U. (R.V.J.)

38895 ORGANIC PHOSPHORUS COMPOUNDS. XXVI. ^{31}P CHEMICAL SHIFTS IN PRIMARY PHOSPHINES. Maier, Ludwig (Monsanto Research SA, Zurich). Helv. Chim. Acta, 49: 1718-19(1966). (In German).

An empirical equation is given, which allows the calculation of the ^{31}P-chemical shifts of primary phosphines. (auth)

38896 STABILITY CONSTANTS OF LANTHANIDE PHTHALATES FROM POTENTIOMETRIC DATA. Krishnamurthy, M.; Krishna Prasad, N. S. (Atomic Energy Establishment, Trombay, India). Indian J. Chem., 4: 316-17(July 1966).

Stability constants (log β_2) of lanthanide phthalates determined potentiometrically were found to lie in the range from 7.12 to 8.37 and not to conform to any particular order. The shape of the formation curves indicated that chelate formation does not take place in distinct steps; the 1:2 complex is formed appreciably before the formation of 1:1 complex is completed. Among the ceria group lanthanides a reversal in the order of the stability constants was observed between lanthanum and cerium. The yttria group lanthanides also showed a similar anomalous behavior. (auth)

38897 MEAN AMPLITUDES OF THERMAL MOTION AND SHRINKAGES OF CHEMICAL BONDS: OCTAHEDRAL HEXAFLUORIDES. Nagarajan, G. (Univ. of Maryland, College Park). Indian J. Pure Appl. Phys., 4: 237-43 (June 1966).

Mean amplitudes of vibration at the temperatures 0 and 298°K were computed using the recent vibrational and molecular structural data for the hexafluorides of sulfur, selenium, tellurium, molybdenum, tungsten, technetium, rhenium, ruthenium, osmium, rhodium, iridium, platinum, uranium, neptunium, and plutonium possessing an octahedral symmetry, and the results discussed in relation to other ionic systems having similar chemical bonds. Linear as well as non-linear Bastiansen-Morino shrinkages were computed at 0 and 298°K. The results showed that the replacement of the central atom with one of slightly higher atomic weight causes no significant variation in the mean amplitude of vibration, and the replacement of peripheral atoms of the system with atoms of higher atomic weights results in higher values of mean amplitudes of vibration. The computed values of the mean amplitudes of vibration and of the Bastiansen-Morino shrinkages will be useful in the interpretation of the experimental results of the electron diffraction studies of these molecules when available. (auth)

38898 LATTICE CONSTANTS OF 7:6 SODIUM-ACTINIDE(IV) FLUORIDES. Keenan, Thomas K. (Los Alamos Scientific Lab., N. Mex.). Inorg. Nucl. Chem. Lett., 2: 211-14(Aug. 1966). (LA-DC-8019).

The compounds $Na_7Np_6F_{31}$, $Na_7Pu_6F_{31}$, $Na_7Am_6F_{31}$, and $Na_7Cm_6F_{31}$ were prepared and their lattice constants were determined. All of these compounds are isostructural, hexagonal (rhombohedral), space group R-3, with three molecules per unit cell. Molecular volume decreases throughout the series. These structures are distinctly different from those of the $LiThF_5-LiCmF_5$ series of actinide(IV) complex fluorides in which the combining ratio of lithium:actinide is 1:1. (D.H.M.)

38899 SUBSOLIDUS FORMATION IN TERNARY COMPOUNDS OF THE SYSTEM $BaO-ZrO_2-SiO_2$. Galkin, Yu. M.; Chukhlantsev, V. G. (Kirov Ural Polytechnic Inst., USSR). Izv. Akad. Nauk SSSR, Neorg. Mater., 2: 529-36(1966). (In Russian).

The subsolidus structure of the system $BaO-ZrO_2-SiO_2$ was investigated. The existence of the barium zirconosilicates, $2BaO \cdot 3SiO_2$ and $BaO \cdot ZrO_2 \cdot 3SiO_2$, was discovered. The x-ray characteristics are reported and some properties of these compounds are described. A complete triangulation was made of the system. (tr-auth)

38900 HEAT OF FORMATION OF LANTHANUM SELENITES. Maier, A. I.; Suponitskii, Yu. L.; Karapetyants, M. Kh. (Mendeleev Inst. of Chemistry and Tech., Moscow). Izv. Akad. Nauk SSSR, Neorg. Mater., 2: 775-7 (Apr. 1966). (In Russian).

The heats of solution of lanthanum sulfate and sodium selenite were measured, and the heat of formation of lanthanum selenite was found to be $\Delta H^0_{298} = -705.4$. (R.V.J.)

38901 HEAT OF FORMATION OF PRASEODYMIUM SELENITES. Maier, A. I.; Suponitskii, Yu. L.; Karapetyants, M. Kh. (Mendeleev Inst. of Chemistry and Tech., Moscow). Izv. Akad. Nauk SSSR, Neorg. Mater., 2: 778-80(Apr. 1966). (In Russian).

The heats of solution of $PrCl_3$, Na_2SeO_3, and $PrCl_3 \cdot 7H_2O$ in water, producing concentrations of 1:3000, were measured. The heat of formation of $Pr_2(SeO_3)_3$ was found to be $\Delta H^0_{298^0} = -701.51$. (R.V.J.)

38902 ION-CYCLOTRON DOUBLE RESONANCE. Anders, L. R.; Beauchamp, J. L.; Dunbar, R. C.; Baldeschwieler, John D. (Stanford Univ., Calif.). J. Chem. Phys., 45: 1062-3(Aug. 1, 1966).

The single-resonance ion-cyclotron spectrum of a mixture of CD_4 and N_2 is shown. In addition to the parent ions CD_4^+ and N_2^+, the fragment CD_3^+ and the products of various ion-molecule reactions CD_5^+, N_2D^+, and $C_2D_5^+$ are apparent. These reaction products disappear as the total pressure is reduced. However, N_2D^+ does not disappear even when the ionizing electron energy is reduced below the threshold for N_2^+ production. This suggests that the reaction $N_2 + CD_4^+ \rightarrow N_2D^+ + CD_3$ is important for the production of N_2D^+. A double-resonance effect for this reaction and the N_2D^+ single resonance observed with $\omega_1 \cong 285.5$ kc/sec are shown. The N_2D^+ cyclotron resonance observed with strong irradiation of the CD_4^+ ion with $\omega_2 \cong 425.5$ kc/sec and a series of field sweep spectra of the CD_4-N_2 mixture for various fixed values of ω_2/ω_1 are shown. It is evident that multiple resonance methods will be useful in identifying specific ion-molecule reactions in complex mixtures. (W.D.M.)

38903 HEATS OF DILUTION OF AQUEOUS RARE EARTH CHLORIDE SOLUTIONS AT 25 DEG. Spedding, F. H.; Csejka, D. A.; DeKock, C. W. (Ames Lab., Ames, Iowa). Contract W-7405-eng-42. J. Phys. Chem., 70: 2423-9(Aug. 1966). (IS-1291).

The heats of dilution of aqueous $PrCl_3$, $SmCl_3$, $GdCl_3$, $TbCl_3$, $DyCl_3$, $HoCl_3$, $TmCl_3$, and $YbCl_3$ were measured for concentrations up to about 0.25M. Relative apparent molal heat contents, ϕ_L, were calculated for these solutions, and empirical equations were obtained for the concentration dependence of ϕ_L. The data showed that all of the salts, with the possible exception of $YbCl_3$, obey the Debye-Hückel limiting law. A qualitative interpretation is given for the behavior of ϕ_L across the rare earth series. (auth)

38904 RELATIVE VISCOSITIES OF SOME AQUEOUS RARE EARTH CHLORIDE SOLUTIONS AT 25 DEG. Spedding, F. H.; Pikal, M. J. (Ames Lab., Ames, Iowa). Contract W-7405-eng-42. J. Phys. Chem., 70: 2430-40(Aug. 1966). (IS-1294).

The relative viscosities of aqueous solutions of $LaCl_3$, $NdCl_3$, $SmCl_3$, $TbCl_3$, $DyCl_3$, $HoCl_3$, and $ErCl_3$ were determined at 25°C over a concentration range of about 0.05M to saturation. The B coefficients of the Jones-Dole equation were determined for these salts. The relative viscosities of several dilute $PrCl_3$ solutions were also measured to allow the B coefficient for this salt to be determined. The concentration dependence of the relative viscosity of a rare earth chloride solution is discussed in terms of the Vand theory for large nonelectrolyte molecules. It is proposed that the major contribution to the viscosity of a rare earth chloride solution at moderate to high concentration arises from the interference of large hydrated rare earth ions with the stream lines in the solvent. The B coefficients and the relative viscosities at "iso-molalities" are studied as a function of the ionic radius of the rare earth ion, and irregularities are noted near the middle of the rare earth series. These irregularities are discussed in terms of a change in preferred water coordination number of the rare earth ion. (auth)

38905 APPARENT MOLAL VOLUMES OF SOME AQUEOUS RARE EARTH CHLORIDE AND NITRATE SOLUTIONS AT 25 DEG. Spedding, F. H.; Pikal, M. J.; Ayers, B. O. (Ames Lab., Ames, Iowa). Contract W-7405-eng-42. J. Phys. Chem., 70: 2440-9(Aug. 1966). (IS-1292).

The specific gravities and apparent molal volumes of aqueous solutions of 14 rare earth salts were determined over a concentration range of about 0.002 to 0.2M. A magnetically controlled float apparatus was used to determine the specific gravities with an accuracy of about $\pm 5 \times 10^{-7}$. The apparent molal volumes showed significant deviations from the simple limiting law at low concentrations. However, it was shown that, except for $Nd(NO_3)_3$, these deviations are consistent with interionic attraction theory, provided the effect of the distance of closest approach parameter, a, is recognized. The partial molal volumes at infinite dilution, $\overline{V}_2^0$, do not vary smoothly with ionic radius of the cation for either anion series. The $\overline{V}_2^0$ values decrease with decreasing ionic radius from La to Nd and from Tb to Yb, but from Nd to Tb the $\overline{V}_2^0$ values increase with decreasing ionic radius. A change in preferred coordination number of the $R^{3+}-H_2O$ species at a critical cation radius is postulated to account for this behavior. (auth)

38906 HEAT CAPACITIES OF AQUEOUS RARE EARTH CHLORIDE SOLUTIONS AT 25 DEG. Spedding, F. H.; Jones, K. C. (Ames Lab., Ames, Iowa). Contract W-7405-eng-42. J. Phys. Chem., 70: 2450-5(Aug. 1966). (IS-1290).

Specific heats were measured for aqueous solutions of $LaCl_3$, $NdCl_3$, $DyCl_3$, $ErCl_3$, and $YbCl_3$ at 25°C over the concentration range from 0.1M to saturation. Apparent molal heat capacities, ϕ_{cp}, were calculated for each solution and empirical equations were derived for the concentration dependence of ϕ_{cp}. From these equations, partial molal heat capacities of the solute and solvent were calculated. The data indicated that at moderate concentrations the heavy rare earths have a lower water coordination number than the light rare earths. An adiabatic solution calorimeter, employing a thermistor thermometer, is described. (auth)

38907 GIBBS FREE ENERGIES OF FORMATION OF THORIUM PHOSPHIDES FROM SOLID-STATE ELECTROMOTIVE FORCE MEASUREMENTS. Gingerich, K. A. (Battelle Memorial Inst., Columbus, Ohio); Aronson, S. Contract AT(30-2)-Gen-16. J. Phys. Chem., 70: 2517-23 (Aug. 1966). (BNL-9951).

Thermodynamic information in the thorium–phosphorus system was obtained from measurements on solid electrochemical cells from 800 to 950°C. The following cells were employed: (I) Th, $ThF_4|CaF_2|ThF_4$, ThP, Th_3P_4; and (II) Th, $ThF_4|CaF_2|ThF_4$, Th_α, $ThP_{0.55}$. The measured emf values at 900°C were 582.2 ± 30 mv for cell I and 8.9 ± 8 mv for cell II. From the data on cell I, the following thermodynamic properties were calculated for the reaction Th + Th_3P_4 = 4ThP at 1173°K: a free-energy value of −53.7 ± 2.8 kcal/g-atom of Th, an entropy value of −9.3 ± 3.7 cal/°K g-atom of Th, and an enthalpy value of −64.6 ± 7.1 kcal/g-atom of Th. Free energies of formation at 1173°K of ThP of −71.5 ± 4.8 kcal and of Th_3P_4 of −232 ± 15 kcal were calculated using the emf data and information on the P_2 partial pressures over Th_3P_4. An enthalpy of formation of ThP of −106 ± 10 kcal at 1173°K was also estimated. (auth)

38908 HYDROGENATION OF ETHYLENE AND PROPYLENE OVER PALLADIUM HYDRIDE. Rennard, R. J. Jr.; Kokes, R. J. (Johns Hopkins Univ., Baltimore). J. Phys. Chem., 70: 2543-9(Aug. 1966).

The rate of ethylene hydrogenation as a function of hydrogen concentration, temperature, ethylene pressure, and hydrogen pressure was studied over palladium hydride and palladium deuteride. Similar (but less extensive) studies were carried out with propylene. The rate of hydrogenation at −78°C was found to be nearly zero order in ethylene and hydrogen pressure but first-order in the hydride concentration. Although the first-order rate constant decreased with hydride concentration, the activity increased. There was an inverse isotope effect with deuterium, and the principal deuterated product was $C_2H_4D_2$. Analysis of the data suggested that the slow step is the addition of adsorbed hydrogen atoms to adsorbed ethylene or adsorbed ethyl radicals. (auth)

38909 APPLICATION OF IRREVERSIBLE THERMODYNAMICS TO ELECTROLYTE SOLUTIONS. I. DETERMINATION OF IONIC TRANSPORT COEFFICIENTS l_{ij} FOR ISOTHERMAL VECTOR TRANSPORT PROCESSES IN BINARY ELECTOLYTE SYSTEMS. Miller, Donald G.

(Univ. of California, Livermore). Contract W-7405-eng-48. J. Phys. Chem., 70: 2639-59(Aug. 1966). (UCRL-14571-T).

Irreversible thermodynamics was applied to binary electrolyte solutions undergoing isothermal vector transport processes. Rigorous expressions for the conductance Λ, diffusion coefficient $(D)_0$, and cell and Hittorf transference numbers t_i^c and t_i^h were derived systematically in terms of the Onsager transport coefficients l_{ij}. Conversely, expressions for the l_{ij} were derived in terms of the experimental quantities t_i, Λ, and $(D)_0$. Values of l_{ij} calculated from experimental data are given for HCl, LiCl, NaCl, KCl, $CaCl_2$, $BaCl_2$, and $LaCl_3$ at 25°C from c = 0 to 3N. Aspects of their relative sizes and concentration dependences are discussed. Insights into ionic properties are possible because the l_{ij} are more fundamental than usual transport quantities (which are composites of the l's). Curie's theorem is used to show that no rigorous quantitative connection can exist between the viscosity and D or Λ. Friction coefficients are also presented and aspects of that formalism are discussed. (auth)

38910 NATURAL ORBITAL BASED ENERGY CALCULATION FOR HELIUM HYDRIDE AND LITHIUM HYDRIDE. Bender, Charles F.; Davidson, Ernest R. (Univ. of Washington, Seattle). J. Phys. Chem., 70: 2675-85 (Aug. 1966).

An iterative procedure for simultaneous calculation of the natural orbitals and energy was developed. This was applied to the determination of the wave function for the ground electronic state of HeH and LiH near an internuclear separation of 3.0 bohrs. The energies obtained were −3.38280 hartrees for HeH (experimental approximately −3.3849) and −8.0606 hartrees for LiH (experimental −8.0705). (auth)

38911 THERMODYNAMIC PROPERTIES OF PLUTONIUM MONONITRIDE FROM ELECTROMOTIVE FORCE MEASUREMENTS. Campbell, G. M.; Leary, J. A. (Los Alamos Scientific Lab., N. Mex.). Contract W-7405-eng-36. J. Phys. Chem., 70: 2703-5(Aug. 1966). (LA-DC-7747).

The emf of the cell $Pu(s)|Pu^{+3}(x_1)$, LiCl-KCl||LiCl-KCl, $Ag^+(x_2 = 0.000568)|Ag$ over the temperature range from 685 to 729°K and composition range $x_1 = 0.000594$ to 0.0215 mole fraction was determined. Potentials were determined for four cells of the type $N_2(g,p_1)$, $PuN(s)|Pu^{+3}(x_1)$ LiCl-K-Cl||LiCl-KCl, $Ag^+(x_2 = 0.000568)|Ag$ over the temperature range from 695 to 716°K and the composition range $x_1 = 0.0177$ to 0.0193. The cells behaved in a reversible manner. The emf was independent of the direction of temperature approach and obeyed the Nernst equation with respect to nitrogen pressure and the Pu^{+3} concentration. The emf was independent of time after an initial 24 hour cell equilibration period for cells of the second type. The free energy of formation of PuN at 700°K was determined to be −60 ± 1 kcal/mole. (D.H.M.)

38912 DEUTERIUM AND TRITIUM ISOTOPE EFFECTS IN THE METHOXIDE-PROMOTED ELIMINATION REACTION OF 2,2-DIPHENYLETHYL BENZENESULFONATE. Willi, A. V. (Brookhaven National Lab., Upton, N. Y. Columbia Univ., New York). Contract AT(30-2)-Gen-16. J. Phys. Chem., 70: 2705-7(Aug. 1966). (BNL-10111).

A kinetic study of the primary deuterium and tritium isotope effects at different temperatures was made with special interest in the problem of tunneling. The reaction chosen for this purpose was the elimination of 2,2-diphenylethyl benzenesulfonate under the action of sodium methoxide in Methyl Cellosolve solution. The main product, 1,1-diphenylethylene, was identified by ultraviolet and NMR spectra of the ether-soluble fraction. There was less than 0.1% stilbene in the product. In the kinetic experiments with the tritium-labeled compound, the radioactivity of the toluene-soluble fraction did not decrease to normal background. It appears that there are large differences in the transition state and barrier dimensions for different proton-transfer reactions. (D.H.M.)

38913 CHEMICAL BEHAVIOR OF A NEW ELEMENT. Zvara, Ivo. pp 22-6 of Perspektivy Sinteza Transuranovykh Elementov. Moscow, Izdatel'stvo Znanie, 1965. (In Russian).

It was found that the chemical properties of neptunium, plutonium, and in part, americium, resemble those of uranium; the elements discovered later, curium, berkelium, californium, etc., exhibited properties similar to those of the lanthanide series. There is a close correlation between the electron-shell structure of curium and gadolinium, berkelium and terbium and the following elements in the two series. The recently discovered 101st, 102nd, and 103rd elements are the next members of the actinides; the elements Nos. 104, 105, etc., should be the chemical analogs of hafnium, tantalum, etc.; Mendeleeff would have called them ekahafnium and ekatantalum. The chemical properties of the transuranium elements were studied up to those of mendelevium but not beyond because only a few tons of atoms with half lives of a few seconds, have been available. An experimental setup, based on rapid gas-phase reactions was proposed to compare the properties of Element 104 with those of hafnium. The new atoms, knocked out of the ^{242}Pu target by interaction with ^{22}Ne were collected in the gas stream. (TTT)

38914 TEMPERATURE VARIATION AND SEPARATION DEPENDENCE OF EXCHANGE INTERACTIONS OF Gd^{3+} PAIRS IN $LaCl_3$. Birgeneau, R. J.; Hutchings, M. T.; Wolf, W. P. (Yale Univ., New Haven). Phys. Rev. Lett., 17: 308-12(Aug. 8, 1966).

Gd^{3+} pairs in $LaCl_3$ provide examples of comparable magnetic and exchange interactions for which precise values of the interaction constants can be found from microwave resonance fields. The separation dependence of the exchange is estimated from the observed temperature variation and found to be anomalous. (auth)

38915 CRYSTALLIZATION OF DOUBLE AMMONIUM LANTHANIDE NITRATES. Golinski, Marek. Przem. Chem., 45: 301-3(1966). (In Polish).

Fractional crystallization of double ammonium lanthanide nitrates of the cerium group was studied. The crystallization scheme applied made it possible to obtain concentrates of lanthanum containing about 97% of La_2O_3 with a 30 per cent yield. From the mother liquor a concentrate of samarium containing 16% Sm_2O_3 was obtained with a 70% yield. It was observed that measurement of the boiling point of the evaporating solution could be utilized in obtaining optimum (50 per cent) yield of crystallization. (auth)

38916 KINETICS OF THE ISOTOPIC EXCHANGE BETWEEN 1-IODO-2,4-DINITRONAPHTHALENE AND IODIDES IN ACETONE. Marcopoulos, Christos A. (Democritus Nuclear Research Center, Athens). Radiochim. Acta, 5: 121-3(June 1966).

The isotopic exchange reaction between 1-iodo-2,4-dinitronaphthalene and potassium iodide was followed in acetone solution using ^{131}I as tracer, at various temperatures and over a wide range of concentration of iodide ion. To separate the organic from the inorganic compound a toluene-water extraction method was applied and to follow the increasing activity of the organic compound, a liquid scintillator technique was adopted. Specific rates and the Arrhenius parameters were calculated. (auth)

38917 THE EXISTENCE OF CURIUM(VI). Bagnall, K. W.; Easey, J. F. (Atomic Energy Research Establishment, Harwell, Eng.). Radiochim. Acta, 5: 180(June 1966).

A study was made to determine if solvent extraction and ion exchange results obtained with ozonized solutions of curium(III) was evidence of oxidation of curium(III) to curium(IV). In solvent extraction with diisooctylamine the absorption spectra of the aqueous phase remained that of curium(III) throughout the ozonization. Samples of the extractant were examined by thin-layer chromatography and it was found that diisooctylamine was completely destroyed by the ozone in aqueous phase. It was concluded that curium(III) is not oxidized by ozone in aqueous medium. (D.H.M.)

38918 RELATIONSHIP BETWEEN THE DIFFUSION RATE OF ^{90}Sr AND SOIL MOISTURE CONTENT. Prok-

horov, V. M. Soviet Soil Sci. (Eng. Transl.), No. 10, 1184-6(May 1966).

^{90}Sr diffusion in three soils belonging to the same group (Sod-Podzolic clay loam) but differing in certain properties is compared. The properties considered are exchange capacity, specific surface area, humus content, and pH of aqueous suspension. In texture, samples 1 and 3 were coarse clay loams, while sample 2 was medium clay loam. Relations between the ^{90}Sr diffusion coefficient and the volume moisture content of the three soil samples are shown. It was evident that the ^{90}Sr diffusion coefficients for samples 1 and 2 coincided within large moisture contents. There was a distinct difference only in the region of about 20% moisture. In sample 3 the rate of ^{90}Sr diffusion with the same moisture content was 1.5 to 2 times less than in sample 1. A comparison of the samples showed that according to all the properties investigated, except pH, the diffusion of ^{90}Sr in sample 3 should have occurred more slowly than in samples 1 and 2. This was confirmed by experiments. The difference in pH in the samples was insignificant. Thus, the effect of the pH was probably less than that of the other factors. The values of the exchange capacity and specific surface area of sample 2 were 1.23 and 1.65 times greater, respectively, than in sample 1. Judged solely by these values, the diffusion rate in sample 1 should have been greater. However, sample 1 contained 1.52 times (1.5%) more humus than did sample 2. This was sufficient for the diffusion rate in sample 1 to be equal to or less than that in sample 2. According to these data, the humus content has a great effect on the ^{90}Sr diffusion rate in soil. It is concluded that the ^{90}Sr diffusion rate is lowest in soils with the highest exhange capacity, specific surface area, and humus content. (BBB)

38919 INVESTIGATION OF THE COMPOSITION OF VAPOR IN THE $ErCl_3$–CsCl AND $NdCl_3$–CsCl SYSTEMS. Gavryuchenkov, F. G.; Novikov, G. I. Vestn. Leningr. Univ., Ser. Fiz. Khim. (4), No. 1, 106-12(1966). (In Russian).

The tensimetrical and mass-spectrometrical investigation of the $ErCl_3-CsCl$ and $NdCl_3-CsCl$ systems was performed. The existence of the $CsErCl_4$ and $CsNdCl_4$ species in vapor was established. The thermodynamical parameters of the dissociation process of this compound were calculated. (auth)

38920 AMMONOLYSIS OF URANIUM HALIDES. I. AMMONOLYSIS OF URANIUM TETRACHLORIDE AND TETRABROMIDE. Burk, W.; Naumann, D. (Zentralinstitut fuer Kernforschung, Rossendorf, Ger.). Z. Anorg. Allg. Chem., 344: 306-15(June 1966). (In German).

The reactions of UCl_4 and UBr_4 with ammonia, which was investigated between 20 and 700°C, led to the formation of ammoniates, amidohalides, imidohalides, and nitridohalides and nitrides of uranium according to the reaction temperature. (auth)

38921 BOILING TEMPERATURES AND VAPOR PRESSURE OF H_2O–D_2O MIXTURES AND THEIR AZEOTROPES. Zieborak, K. (Inst. of General Chemistry, Warsaw). Z. Phys. Chem. (Leipzig), 231: 248-58(1966). (In German).

The boiling temperatures and vapor pressures of H_2O and D_2O and their mixtures were determined by boiling measurements in the temperature range from 74 to 222°C. In this temperature range small negative deviations from the Raoult law were detected. Between 220 and 222°C an azeotrope was formed with a very small boiling temperature increase, ≥0.003°C at 221.00°C, when the boiling temperatures of both substances are equal. A special apparatus for boiling temperature measurements with an over pressure up to 25 atm was constructed. (tr-auth)

38922 POLAROGRAPHY OF URANIUM IN HYDROCHLORIC ACID SOLUTIONS. Stabrovskii, A. I. Zh. Neorg. Khim., 11: 76-85(Jan. 1966). (In Russian).

During a study of the effects of additions of thymol and gelatin to hydrochloric acid solutions on electrode processes in the reduction of uranyl ions at dropping electrodes, it was established that the optimum concentration is 0.002 to 0.005% for thymol and 0.005% for gelatin. By increasing the concentration of thymol to 0.01% and that of gelatin to 0.1%, the electrode reactions in uranyl ion reduction were inhibited. There was a reduction of the limiting current and a change in the size of the potential half-wave. The potential half-wave changes from +0.067 to 0.041 v with variation of the HCl concentration from 0.001 to 1.0 mol/l. The reduction waves of U(IV) to U(III) with different concentrations of HCl and KCl in the solution were studied. It was established that increases in the concentration at first increased the limiting current of the reduction, but then decreased it. The half-wave potential depended on the concentration of both the HCl and the KCl and changed under the conditions studied from –0.636 to –0.685 v. The electrode reaction for the reduction of U(IV) to U(III) in hydrochloric acid solution is reversed. With increasing solution pH and formation of the hydrolyzed ion form of U(IV), its reduction wave was reduced. The oxidation wave of U(IV) to U(VI) appeared during this reduction. The oxidation half-wave potential of U(IV) depended on the hydrochloric acid solution and was equal to +0.285 v at pH 2.45. U(IV) ions, subjected to hydrolysis, lost the capacity of being reduced on the dropping electrode and became capable of being oxidized. Tests were made to verify and explain the possibility of reducing U(III) to the metallic state on the dropping electrode in the hydrochloric acid solution. With the potential of the dropping electrode up to –1.7 v, during which reduction of potassium ions was initiated, the reduction wave of U(III) was not formed on the polarogram. (tr-auth)

38923 EUROPIUM AND GADOLINIUM HYDROXIDES AND PRODUCTS OF THEIR THERMAL DECOMPOSITION. Ambrozhii, N. M.; Dvornikova, L. M.; Lazareva, L. S. (Saratov State Univ., USSR). Zh. Neorg. Khim., 11: 86-9(Jan. 1966). (In Russian).

Thermographic characteristics of decomposition processes of hydroxides of Eu and Gd are given. The composition of the freshly prepared europium hydroxide and the products of its thermal dissociation were determined more precisely on the basis of a study of the hydroxide–water–sodium chloride system, using the third-component method and the thermogravimetric method. The decomposition of the hydroxides of europium and gadolinium proceeded with formation of the trihydrate, monohydrate, and oxide anhydride according to the scheme $Ln_2O_3 \cdot \underline{n}H_2O \rightarrow Ln_2O_3 \cdot 3H_2O \rightarrow Ln_2O_3 \cdot H_2O \rightarrow Ln_2O_3$, where $\underline{n} > 3$. (tr-auth)

38924 COMPLEXES OF LANTHANUM, YTTRIUM, LUTETIUM, AND SCANDIUM WITH XYLENOL ORANGE. Kumok, V. N.; Serebrennikov, V. V. (Tomsk State Univ., USSR). Zh. Neorg. Khim., 11: 90-2(Jan. 1966). (In Russian).

The composition, spectra, and stability of the complex ions $LaHX^{2-}$, YHX^{2-}, $LuHX^{2-}$, $ScHX^{2-}$, and ScH_2X^{-} (X^{6-} is Xylenol Orange anion) were investigated. (tr-auth)

38925 SCANDIUM HYDROLYSIS AS MEASURED BY CHELATE SOLVENT EXTRACTION. Winkley, Donald Charles. [Knoxville], Tenn., Univ. of Tennessee, 1965. 86p.

Thesis.

The first hydrolysis constant of scandium was measured utilizing the chelate solvent extraction technique. The distribution of scandium between 4-methyl-2-pentanone and water 0.1M in sodium perchlorate was measured as a function of pH and concentration of the reagent 3,5-dinitrobenzoic acid. The results were subjected to computer (least-squares) analysis and various constants describing the system were solved for. The value of the first hydrolysis constant for scandium, K_1, for the reaction $Sc^{+3} + H_2O \rightarrow Sc(OH)^{+2} + H^+$, was found to be 1.5×10^{-4}. This value is compared with previous measurements made by potentiometric titration. Several different reagent-solvent systems were employed in preliminary experiments to determine the best one for determination of the hydrolysis constant for scandium. The criteria for the best reagent-solvent system are examined in detail. Also some of the factors that cause solvent extraction results to be errone-

ous, namely, impure reagent or solvent, nonequilibrium, inaccurate pH measurements, incomplete phase separation, and assumptions made in the derivation of solvent extraction equations are discussed. Possible ways of avoiding some of these difficulties are examined. (Dissertation Abstr.)

38926 PROPERTIES OF COLLOIDAL THORIA. PARTS I-V. Chun, Byong Doo. Salt Lake City, Univ. of Utah, 1964. 129p.

Thesis.

Thoria gel was fired in nitrogen atmosphere in the temperature region from 786°C to 1122°C. The grain size was determined by means of electron microscopy. From 860°C to 1000°C normal grain growth was observed to occur. Above 1000°C erratic grain growth took place and resulted in the formation of isolated large grains which grew at an accelerated rate. The large erratic grains would recrystallize forming a matrix of smaller grains, which again would repeat erratic grain growth and recystallization. This behavior was observed repeatedly and was found to be influenced by presoaking temperature, presoaking time, and atmospheres used. Following the initial erratic grain growth period it was observed that the grain growth patterns followed the normal grain growth equations from which it was possible to determine the activation energy for the grain growth process. The activation energy was determined to be 35.6 kcal/mole. The validity of the Rayleigh light scattering law was tested for thoria sol. The relation between the wavelength and the turbidity showed good agreement with the theory. The effects of various parameters on particle growth rates of colloidal thoria prepared from a nitrate medium was studied. It was found by x-ray diffraction that the colloidal thoria converts to another compound at a low pH upon heating for a long time. The compound was separated from the mother liquid, and the formula of the compound was determined as $ThOCl_2 \cdot 14H_2O$. The absorption of ultra-violet light by nitric acid and nitrates in general was used to determine the concentration of nitrates contained in thoria gel. Equilibria and kinetics studies of thoria gel dehydration indicated that water adsorbed in the temperature range room temperature to about 140°C is hydrogen-bonded in a state very similar to liquid water. The bulk of the dehydration at temperatures up to about 140°C was first order. (TCO)

38927 SELENIDY I TELLURIDY REDKOZEMEL'NYKH METALLOV I AKTINOIDOV. (Selenides and Tellurides of Rare Earth Metals and Actinides). Obolonchik, V. A.; Lashkarev, G. V. Kiev, Naukova Dumka, 1966. 164p.

Results of investigations of the crystal structure and properties of selenides and tellurides of rare earths and actinides and the possibilities for their use are reported. The crystal structure, physical properties, chemical properties, methods of preparation, and methods of analytical determination and analysis of the rare earth and actinide selenides and tellurides are described. Possible future uses of the selenides and tellurides and safety precautions for work with these compounds are also discussed. (J.S.R.)

38928 PRECIPITATION AND HYDROLYSIS OF URANIUM (VI) IN AQUEOUS SYSTEMS. IV. THE MECHANISM OF PRECIPITATION AND COPRECIPITATION OF URANIUM IN THE SYSTEMS URANYL NITRATE–SODIUM CARBONATE–ALKALINE EARTH CHLORIDES. Fueredi, H.; Devide, Z.; Wrischer, M.; Tezak, B. (Institute Ruder Boskovic, Zagreb). 26p. (CONF-650902-36). ORAU. Gmelin, AED-CONF-65-235-91.

From American Chemical Society, 150th National Meeting, Atlantic City.

Uranium-bearing precipitates, which were most frequently observed in the precipitation systems uranyl nitrate–sodium carbonate–barium, strontium, calcium and magnesium chlorides were investigated. The distribution of characteristic precipitates in the system with barium chloride as revealed by means of microscopy and electron microscopy is given in a plane of barium chloride and sodium carbonate concentrations at constant concentration of uranyl nitrate. Crystalline aggregates of $Ba_2UO_2(CO_3)_3 \cdot 6H_2O$ were found to precipitate in the region of sodium carbonate and uranyl nitrate concentration ratios between 3 and 10. The results of chemical analyses of the precipitates occurring in the concentration maxima of all investigated systems are also given. The molar percentage of coprecipitated uranium in strontium and calcium carbonate was calculated and coprecipitation systems were investigated by means of microscopy, electron microscopy, and x-ray powder patterns. The mechanism of coprecipitation of uranium with alkaline earth carbonates is discussed accordingly. (auth)

38929 PROCESS FOR THE PRODUCTION OF ZIRCONIA. Clearfield, Abraham (to National Lead Co.). U. S. Patent 3,254,949. June 7, 1966. Filed Oct. 8, 1962.

A process for the preparation of crystalline hydrated ZrO_2 includes the following steps: forming an essentially dry mixture of an alkali metal hydroxide with a Zr compound selected from the group consisting of $ZrCl_4$, hydrolysis products of $ZrCl_4$ which have a Cl : Zr atomic ratio of at least 2 : 1, and mixtures of these; heating at least a portion of the mixture to initiate a reaction between the materials; washing from the reaction product the alkali metal chloride formed by the reaction; and drying the residual zirconia product. (B.L.M.)

Organic Chemistry

Refer also to abstracts 38887, 38888, and 38941.

38930 (TID–23264) THERMAL DEGRADATION OF STYRENE AND METHYLMETHACRYLATE COPOLYMERS WITH PURE m- AND p- DIVINYLBENZENE ISOMERS. Martin, Frank E. (Louisville Univ., Ky. Dept. of Chemistry). 1966. Contract AT(40-1)-2055. 162p. Dep. mn. CFSTI $5.00 cy, $1.00 mn.

Thesis.

The high temperature degradation of styrene copolymerized with 8 mole per cent m- or p-divinylbenzene was studied in order to further establish differences in the copolymer networks dependent on the nature of the divinyl units. It is supposed that if polystyrene degrades predominantly by reverse polymerization, i.e., stepwise terminal monomer unit cleavage, then the amount of para-related products in the copolymer pyrolyzates should be negligible at low conversions but should increase rapidly as depolymerization proceeds toward the copolymer nuclei. On the other hand, m-DVB related products should be observed early in the degradations and regularly. Degradation of the isomerically crosslinked copolymers at 552 and 627°C tends to confirm this hypothesis. The results tend to confirm not only the differences postulated in divinylbenzene unit distribution, but also that polystyrene does degrade to an appreciable extent by stepwise terminal monomer unit cleavage. The postulated differences between m- and p-divinylbenzene distributions in the copolymers of both styrene and methyl methacrylate were additionally confirmed by comparing the rates of formation of individual degradation products, the rates of volatilization, and the activation energies for volatilization. Nearly all of the volatile degradation products for the various polymers and copolymers were identified by vapor phase chromatographic analysis. Mechanisms for the formation of many of the secondary products are proposed. (P.C.H.)

38931 SYNTHESIS OF MALATHION LABELED WITH ^{35}S OR ^{32}P AND DIPTEREX-^{32}P. Jezdic, Vojislav; Skakun, Miroslava; Konstantinovic, Stanimir Bull. Boris Kidrich Inst. Nucl. Sci., 17: 29-37 (Jan. 1966).

Malathion and Dipterex are two of the group of organophosphorus compounds that are widely applied in agriculture as insecticides. In order to study the effect of Malathion and Dipterex as insecticides, methods were worked out for their synthesis with incorporated radioactive isotopes ^{32}P and ^{35}S. The synthesis described are simple and give greater yields than those previously reported. (auth)

38932 STUDIES ON THE PREPARATION OF SOME ISOTOPICALLY LABELLED ORGANIC IODO COMPOUNDS FOR MEDICAL USE. Mani, R. S. (Atomic Energy Establishment, Trombay, India). Curr. Sci. (India), 35: 401-3 (Aug. 20, 1966).

A study was made of the impurities present in the ^{131}I solution used for labeling compounds for medical use. It was found that ^{131}I used for the preparation of labeled compounds should be free from reducing agents and preservatives to ensure high yields. Methods are given for the preparation of the pure labeled compounds. (D.H.M.)

38933 ON THE LABELING OF INSULIN WITH IODINE-131. Barakat, M. F.; El-Asrag, H. A. (Atomic Energy Establishment, Cairo). Indian J. Chem., 4: 362-64(1966).

Iodination of insulin at pH 8 using radioactive iodine monochloride prepared in situ from radioactive sodium iodide solution was studied. The purity of the labeled preparation is followed by ascending paper chromatography using butanol–acetic acid–water (4:5:1) as the solvent and ninhydrin as the spray reagent. Use of excess potassium iodide in the in situ preparation of iodine monochloride, increases the extent of labeling. This labeling technique is relatively simple and losses inherent in other techniques are avoided. (auth)

38934 PHOTOSENSITIZED POLYMERIZATION OF METHYL METHACRYLATE USING URANYL, VANADYL, AND MOLYBDENYL SALTS WITH PARTICULAR REFERENCE TO END GROUPS. Pramanick, Dinabandhu; Saha, Mihir K. (Indian Association for the Cultivation of Science, Calcutta). Indian J. Chem., 4: 253-5(June 1966).

Uranyl, vanadyl, and molybdenyl salts in combination with different anions were used as photosensitizers for the aqueous polymerization of methyl methacrylate under varying conditions of acidity. The resulting polymers were subjected to end group analysis by the application of the "dye techniques" developed earlier by Ghosh and coworkers (J. Polymer Sci., A2: 4433 (1964)). The polymers obtained at higher pH were found to incorporate about two hydroxyl end groups per chain while the end group content of the polymers at lower pH decreased sharply to a very low value. On the basis of the results of end group analysis, the mechanism of initiation of polymerization by such metal salts was explained from a consideration of the nature and identity of the initiating species involved in such a process. (auth)

38935 NEUTRON-DIFFRACTION DETERMINATION OF THE STRUCTURE OF $CH_3CN.2HCl$. Peterson, S. W.; Williams, Jack M. (Washington State Univ., Pullman). J. Amer. Chem. Soc., 88: 2866(June 20, 1966).

The structure of $CH_3CN \cdot 2HCl$ was investigated by single-crystal neutron diffraction methods. The structure was solved from the three-dimensional neutron Patterson function with some assistance from an x-ray projection. All atoms except two methyl hydrogens lie in mirror planes. The basic molecular structure was found to be that of the imino hydrohalide model. The Cl^- ion was involved as an acceptor in two hydrogen bonds that lie in the molecular plane and serve to tie together the planar acetimino groups. After two cycles of full matrix anisotropic least-squares refinement the weighted $R = [\Sigma w(F_o - F_c)^2]^{1/2} / [\Sigma w F_o^2]^{1/2}$ was 0.083 for all reflections. (D.H.M.)

38936 SOLVENT EFFECTS IN ISOTOPE EXCHANGE REACTIONS. VI. INFLUENCE OF AZA-AROMATICS ON THE RATE OF THE IODINE EXCHANGE BETWEEN ELEMENTARY IODINE AND 1-PHENYL-2,3-DIMETHYL-4-IODOPYRAZOLONE. Koroes, Endre; Orban, Miklos; Ladanyi, Laszlo; Buxbaum, Piroska. Magyar Kem. Foly., 72: 260-7(June 1966). (In Hungarian).

The influence of some azine aromatics (pyridine, α-picoline, γ-collidine, quinoline, and isoquinoline) on iodine exchange was investigated in benzene, chloroform, and ethanol. Linear relationship between the rate-inhibiting effect, characterized by the "retardation" coefficient, and the stability of the iodine–azine aromatic donor-acceptor complex could be established. The kinetics of the reaction were measured in pyridine-containing benzene; the enthalpy, the entropy, and the free energy of activation were calculated and the thermodynamic data analyzed. (auth)

Radiation Chemistry

See also BIOLOGY AND MEDICINE — Radiation Effects on Biochemicals Radiation Effects on Tissues

Refer also to abstracts 38581, 38994, and 40364.

38937 (AD-635655) APPLICATION OF FAST NEUTRON ACTIVATION ANALYSIS TO POLYMER DOSIMETRY. Coates, Arthur D.; Swisher, Joe A. (Ballistic Research Labs., Aberdeen Proving Ground, Md.). Mar. 1966. 18p. (BRL-R-1312). CFSTI $1.00 cy, $0.50 mn.

Fast neutron activation analysis was used to measure the gamma dose absorbed by a polymer. A series of low density polyethylene films was irradiated by cobalt-60 gamma rays in the presence of air. The gamma doses ranged from 1×10^5 to 4.7×10^7 rads. The oxygen content of the polymer films increased with increasing dose. The increase in oxygen content of each film was monitored at 1720 cm^{-1} by infrared spectroscopy. The oxygen increase also was monitored by measuring the activation of oxygen-16. This latter method employs fast neutron activation of oxygen-16 and the measurement of the emitted radiation to determine gamma dose. The results of both methods of dosimetry are presented, and the improvements offered by the neutron activation technique are indicated. (auth)

38938 (IA-1074) H/D ISOTOPE EFFECTS IN THE FORMATION OF HYDROGEN FROM THE COMBINATION OF TWO RADICALS IN AQUEOUS SOLUTIONS. Anbar, M.; Meyerstein, D. (Israel Atomic Energy Commission, Yavne, Soreq Nuclear Research Center). Mar. 1966. 21p. Dep. mn.

The H/D isotope effects of the reactions $e^-_{aq} + e^-_{aq}$ (a), $e^-_{aq} + H$ (b), and $H + H$ (c) were determined using high intensity pulse radiolysis. In 1:1 mixtures of H_2O: D_2O at room temperature the following H/D isotope effects were observed: $\alpha_a = 4.7 \pm 0.2$, $\alpha_b = 1.5 - 1.9 \pm 0.3$ (depending on the pH), and $\alpha_c = 2.6 - 3.5 \pm 0.2$ (depending on the pH). The isotope effect of the molecular hydrogen formed in the radiolysis of water, $\alpha_M = 2.2 \pm 0.1$, was found to be independent of pH. In view of the isotope effects, reaction (a) was interpreted in terms of the formation of a $(e^-_{aq})_2$ center as an intermediate, and reaction (b) as involving the formation of a hydride ion. The results indicate that the molecular and residual hydrogen produced in neutral radiolyzed aqueous solution are formed via reactions different from those assumed in the diffusion model for the radiolysis of water. Most probably these species are formed from excited water molecules. (auth)

38939 (NYO-2668-13) PRIMARY CHEMICAL PROCESSES IN THE RADIOLYSIS OF LIQUIDS. Annual Progress Report, September 15, 1965–September 14, 1966. Trumbore, C. N. (Delaware Univ., Newark. Dept. of Chemistry). June 11, 1966. Contract AT(30-1)-2668. 14p. Dep. mn. CFSTI $1.00 cy, $0.50 mn.

Studies were continued on the detection in liquids of chemical and physical precursors ultimately responsible for radiolytic damage. Continuing studies on the aqueous p-nitrosodimethylaniline (RNO) system provided some results that may not be accounted for by the commonly invoked radiolytic intermediates, •H, •OH and e^-_{aq}. These studies were carried out at low RNO concentrations where quantitative studies are made of G(–RNO) as a function of RNO concentration, pH, and added solute concentration. Several pieces of evidence point to some kind of excited water molecule such as the H•, OH•, and/or e^-_{aq} precursor, which is scavenged at high solute concentrations. An oxygen concentration effect cannot be explained by the usual competition mechanism invoked in radiation chemistry and an energy transfer mechanism that possibly activates dissolved oxygen is suggested. Pulse radiolysis studies of aqueous solutions were carried out in which the absorption

of laser radiation during the pulse of x rays occurs and is detected with a rise time in the nanosecond region. Studies on the gamma radiolysis of the cyclopentanone–benzene system demonstrated a benzene triplet scavenging action, which is in quantitative agreement with photolysis studies on the same system. A yield of G(benzene triplet) = 0.4 is reported. (auth)

38940 (NYO–3410-2) THE EFFECTS OF GAMMA IRRADIATION ON TWO CYCLIC CARBONATES. Mazda, Rumi N. (Rhode Island Univ., Providence). 1966. Contract AT(30-1)-3410. 70p. Dep. mn. CFSTI $3.00 cy, $0.75 mn.

Thesis.

Tetraphenylethylene carbonate was irradiated in two facilities. In the rabbit tube, it received a total dose of 2.8×10^7 rads and in the gamma irradiation facility, a dose of 5.9×10^7 rads. In both cases, the weights of the products obtained were approximately the same, indicating fairly constant G values for tetraphenylethylene carbonate radiolysis. These results are parallel to those obtained from irradiation of esters. Hence, the G values for cyclic carbonates undergoing much larger doses may vary inversely with the total dose, as is the case with ester radiolysis. Ethylene carbonate was subjected to a total dose of 6.1×10^7 rads in the gamma irradiation facility. No solid products were obtained from this irradiation. In addition, an attempt to show the presence of gaseous products by infrared spectroscopy was unsuccessful. (P.C.H.)

38941 (RRL–2310–182) QUARTERLY REPORT [ON RADIATION RESEARCH], APRIL 1–JUNE 30, 1966. Fundamental Research No. 6041. (Radiation Research Labs., Mellon Inst., Pittsburgh, Pa.). July 15, 1966. Contract AT(30-1)-2310. 12p. Dep. mn. CFSTI $1.00 cy, $0.50 mn.

Results are reported on the following studies: ESR spectra of some isotopically substituted hydrocarbon radicals and fluorine-containing radicals, PF_4 and SF_4^+; liquid phase argon-sensitized radiolysis of ethylene; effects of hydrogen iodide on hydrogen and radical yields in irradiated hexane; identification of radicals and measurements of their yields by ESR and scavenger methods; and decolorization of blue cellophane films by high LET radiations. Preliminary results are also given for studies on: radiolytic dissociation of methyl iodide in cyclohexane solutions; competition between N_2O and C_2F_4 for electrons in the radiolysis of propylene; spectroscopic studies of alkali hydroxide glasses; effects of added gases in the Hg photosensitized decomposition of cyclobutane, a high intensity lamp for vacuum ultraviolet photochemical studies; and oxygen-18 isotopic dilution studies of oxygen body stores. (J.G.B.)

38942 (UJV–1457) RADIATION-INDUCED OXIDATION OF METHANOL. Habersbergerova, A.; Janovsky, I.; Teply, J. (Ustav Jaderneho Vyzkumu, Ceskoslovenska Akademie Ved, Rez). May 1966. 17p. Dep. mn.

Radioinduced oxidation of methanol resulted in hydrogen, methane, formaldehyde, ethylene glycol, hydrogen peroxide, hydroxymethylhydroperoxide, formic acid, and carbon dioxide yields. A reaction scheme is proposed to account for dependence of yields of hydroxymethylhydroperoxide, hydrogen peroxide, formaldehyde, and of oxygen consumption on the inverse value of the square root of the gamma dose rate and the independence of hydrogen yield on the dose rate. At high doses due to secondary reactions carbon dioxide is formed and formic acid decomposed. (J.G.B.)

38943 CALCULATION OF EFFICIENCY OF RADIATION-CHEMICAL APPARATUS WITH PLANE BETA SOURCES. Dzhagatspanyan, R. V.; Lyaskin, Yu. G. At. Energ. (USSR), 20: 485-8(June 1966). (In Russian).

A method was given for the calculation of the efficiency of radiation-chemical apparatus with plain α sources of finite thickness in the general case where the speed of the radiation chemical process depends on the dose output. Formulas were obtained for the calculation of the efficiency per unit surface of the source containing the integral $\int_0^{\nu x} [f(\nu h, \nu x)]^{1-\epsilon} d(\nu x)$. The value of this integral for different νh, νx, and ϵ is given in the form of graphs. For comparison of this method of calculating the efficiency with the calculation method by mean absorptive capacity of the dose, the relation of the value of the efficiencies calculated by these two methods was found. The results show that in the case when the velocity of the radiation chemical process depends on the dose output the method of calculation by mean dose output for liquid phase processes gives large errors. The method proposed in the present study can be used for the calculation of the efficiency of different radiation chemical apparatus with plain β sources for liquid and gaseous phase processes. (tr-auth)

38944 ENERGY TRANSFER MECHANISM IN THE RADIOLYSIS OF AMMONIA ADSORBED ON ZEOLITES. Kotov, A. G.; Sorokin, Yu. A.; Pshezhetskii, S. Ya. (Karpov Inst. of Physics and Chemistry, USSR). Dokl. Akad. Nauk SSSR, 166: 1386-9(Feb. 21, 1966). (In Russian).

In studying the radiolysis of adsorbed ammonia, A-type Na, Ca, and mixed zeolites were exposed to γ radiation from a ^{60}Co source and the electron paramagnetic resonance (EPR) of the paramagnetic systems determined. The EPR spectrum was found to consist of the superposition of the spectrum of the aluminosilicate base and of a singlet belonging to the paramagnetic center related to the cations. It may be assumed that paramagnetic F- or V-centers are formed near the cations. The results suggest the following energy transfer scheme: when the ammonia molecule, which possesses high affinity toward protons, is adsorbed, a donor-acceptor bond is formed between nitrogen and the surface ion. As the result of the irradiation, the holes localized at the surface strengthen the bond with the ammonia molecule. The electron level of the adsorbed ammonia may lie within the forbidden zone and the electron may recombine with the ammonia + hole system. The energy released thereby may be sufficiently large to dissociate the N–H bond, forming the NH_2 radical. The surface concentration of the radicals was found to be close to the calculated value. (TTT)

38945 SOME ASPECTS OF THE RADIATION CHEMISTRY OF POLYPROPYLENE. Veselovskii, R. A.; Leshchenko, S. S.; Karpov, V. L. (Karpov Inst. of Physics and Chemistry, Moscow). Dokl. Akad. Nauk SSSR, 167: 339-41(Mar. 11, 1966). (In Russian).

Structural changes occurring in isotactic polypropylene (intrinsic viscosity of 5.3) under the influence of ^{60}Co gamma irradiation were studied. The contribution of radical and ionic reactions to the crosslinking process was found to be negligible, presumably because the side methyl groups cause steric hindrance effects which do not permit the polypropylene chain to come sufficiently close to one another. Vinylidene-type double bonds were found to be responsible for the formation of cross-linkages in polypropylene. The cross-linking is thought to result from the interaction between an excited double bond and the polymer chain, and the energy required for the excitation must be propagated along this chain. The rate of formation of vinylidene groups, determined by ir spectrometry, is much faster below the gelation dose (6.5 Mrad) than above it; this is explained by a higher rate of consumption of vinylidene groups after the gelation dose. The decomposition of oxygen-containing groups follows a radical mechanism followed by rupture of the main polymer chain. Introduction of radical acceptors into the polymer prevents such ruptures and thus shifts the start of gelation toward lower doses. (ATD)

38946 RADIATION-INDUCED POLYMERIZATION OF FLUOROOLEFINS. Volkova, E. V.; Zimakov, P. V.; Fokin, A. V. Dokl. Akad. Nauk SSSR, 167: 1057-9 (Apr. 11, 1966). (In Russian).

A study was made of the kinetics of the radioinduced polymerization of certain fluoroölefins in the gaseous, liquid, and solid phases at −196 to 80°C, at dose rates of 6 to 600 rad/sec and doses of 0.012 to 250 Mrad. The results are given in graphic and tabular form. Studies on temperature effects showed that the reaction rate in-

creases only up to a certain temperature, after which it decreases. (ATD)

38947 NEW APPARATUS FOR IRRADIATING LIQUIDS AND GASES BY MEANS OF ACCELERATED ELECTRONS. Huyskens, P. (Univ., Louvain, Belg.). Ind. Chim. Belg., 30: 693-700(June-July 1965). (In Dutch).

An apparatus was built for irradiating liquids and gases by means of electrons from 10 to 100 kev, in which the dose rate reaches approximately 10^7 rad/sec. The apparatus was designed with a view to continuous irradiation. It made it possible to note intensity effects in the irradiation of hydrocarbons and aqueous solutions. (auth)

38948 TRIPLET STATES IN RADIATION CHEMISTRY. RADIOCHEMICAL CIS-TRANS ISOMERIZATION. Caldwell, Richard A.; Whitten, David G.; Hammond, George S. (California Inst. of Tech., Pasadena). J. Amer. Chem. Soc., 88: 2659-63(June 20, 1966).

Radioinduced cis-trans isomerization of three pairs of olefins was studied by determination of both initial rates of isomerization and the composition of radiostationary states. The data correlated well with data obtained in sensitized photoisomerization reactions of the same substrates. Consequently, it was inferred that isomerization involves formation and decay of excited triplet states of the olefins. The sum of the G values for the trans → cis and cis → trans reactions was taken as the value of G for formation of olefin triplets. Except in very concentrated solutions most of the excitation had to be first absorbed by the solvent and then transferred to the solute. The highest yield of triplets measured in benzene was 9.9, and a value of 20 was estimated in an experiment in which pure cis-stilbene was irradiated. The very high G values for triplets were attributed to the fact that reactive energy acceptors can compete effectively with triplet-triplet annihilation reactions in regions of high excitation density within spurs. (auth)

38949 ELECTRON SPIN RESONANCE SPECTRUM AND ELECTRONIC STRUCTURE OF THE PO_3^{2-} RADICAL IN AN X-RAY IRRADIATED SINGLE CRYSTAL OF AMMONIUM FLUOROPHOSPHATE. Herring, F. G.; Hwang, J. H.; Lin, W. C.; McDowell, C. A. (Univ. of British Columbia, Vancouver). J. Phys. Chem., 70: 2487-92(Aug. 1966).

The electron spin resonance spectrum of an x-irradiated single crystal of ammonium fluorophosphate ($NH_4)_2PO_3F \cdot H_2O$ is most easily interpreted by assuming that the main paramagnetic species formed is the PO_3^{2-} radical. For this particular case equations were derived, which permit the eigenvalues of the appropriate spin Hamiltonian to be calculated for an arbitrary set of coordinates. From the theoretical expressions developed it was calculated by an iterative method that the principal values of the ^{31}P hyperfine interaction tensor are 1822.3, 1419.7, and 1408.6 Mc/sec. The probable electronic structure of the PO_3^{2-} radical is discussed in terms of the semiempirical LCAO extended Hückel molecular orbital method and it was calculated that the eigenfunction for the orbital containing the odd electron is $\psi = -0.422\phi^P_{3s} + 0.696\phi^P_{3p_z} + [(0.133/\sqrt{3})\lambda^0_{2s}] + [(0.206/\sqrt{3})\lambda^0_{2p_z}] - [(0.635/\sqrt{3})\lambda^0_{2p_z}]$ where ϕ^P_{3s} and ϕ^P_{3p} are the phosphorus 3s and $3p_z$ orbitals and $\lambda^0_{2s} \equiv (2s^1 + 2s^2 + 2s^3)$, $\lambda^0_{2p_z} \equiv (2p^1_x + 2p^2_y + 2p^3_z)$, $\lambda^0_{2p_z} \equiv (2p^1_z + 2p^2_z + 2p^3_z)$, where the superscripts refer to oxygen atoms in the PO_3^{2-} radical. This eigenfunction leads to theoretical estimates for the principal values of the ^{31}P hyperfine interaction tensor, namely, 2088, 1674, and 1674 Mc/sec, which are in reasonably good agreement with the experimental results. (auth)

38950 RADIOLYSIS OF FROZEN SOLUTIONS. VI. ELECTRON AND EXCITED WATER REACTIONS IN NITRATE ICES. Kevan, Larry (Univ. of Kansas, Lawrence). Contract AT(11-1)-1528. J. Phys. Chem., 70: 2529-34 (Aug. 1966). (COO-1528-4).

The γ radiolysis of frozen nitrate solutions irradiated at 77°K was studied. Nitrite yields were measured as a function of nitrate concentration, pH, radiation dose, and cation type. The data were compared with EPR and aqueous solution results from which it was concluded that NO_2^- is mainly produced by reactions of electrons and of electronically excited water with nitrate. The latter is responsible for the enhanced NO_2^- yields above pH 11. The results in aqueous and frozen solutions showed very close parallels and strongly implied that the same radiation-produced intermediates are formed and react similarly in both phases. (auth)

38951 ACETYLENE PRODUCTION IN THE RADIOLYSIS OF METHANE. Hummel, R. W. (Wantage Research Lab., Eng.). J. Phys. Chem., 70: 2685-6(Aug. 1966).

Experiments were conducted to measure acetylene produced by the radiolysis of methane at various dose rates. Methane was irradiated with ^{60}Co γ rays at 1.7×10^{17} ev min^{-1} g^{-1}; total dose 4.6×10^{20} ev g^{-1}. Acetylene could not be detected. When 1% propylene was added to methane under the same conditions and using the same methods, peaks were obtained at the elution time corresponding to that of acetylene. Pure methane was irradiated with 4-Mev electrons from a linear accelerator at a pulse dose rate of 3×10^{23} ev min^{-1} g^{-1}. After corrections for ethane, propane, and isobutane, the remaining peaks compared well with the pattern obtained on the spectrometer using pure acetylene. Further experiments with 4-Mev electrons at pulse dose rates of 1.4×10^{23} and 9×10^{23} ev min^{-1} g^{-1} showed that more acetylene was produced from irradiated methane at higher dose rates than from the higher dose total given at the lower dose rate. (D.H.M.)

38952 AN APPARENTLY ANOMALOUS EFFECT ON HYDROGEN PEROXIDE YIELDS IN THE RADIOLYSIS OF AERATED 0.8 N SULFURIC ACID SOLUTIONS OF POTASSIUM BROMIDE WITH ~15-Mev ELECTRONS. Farhataziz (Univ. of Notre Dame, Ind.). J. Phys. Chem., 70: 2696-9(Aug. 1966).

A study of the suppression of hydrogen peroxide yields by potassium bromide in aerated 0.8N sulfuric acid solutions was made using 15.2-Mev pulsed electrons, 1.3-Mev pulsed electrons, and ^{60}Co γ rays. The results demonstrated that the behavior of hydrogen peroxide yields was not significantly affected by the pulse conditions used, but a real difference did exist between the effect of 15.2-Mev electrons and that of 1.3-Mev electrons or ^{60}Co γ rays on the behavior of hydrogen peroxide yields. (D.H.M.)

38953 POLYMERIZATION OF CYCLIC ETHERS IN THE PRESENCE OF MALEIC ANHYDRIDE. PART I. POLYMERIZATION OF TRIOXANE AND 3,3-BIS(CHLOROMETHYL)OXETANE BY γ RAYS, ULTRAVIOLET LIGHT, AND BENZOYL PEROXIDE. Takakura, Koichi; Hayashi, Koichiro; Okamura, Seizo (Japanese Association for Radiation Research on Polymers, Osaka). J. Polym. Sci., Pt. A-1, 4: 1731-45(July 1966).

Cyclic ethers such as trioxane and 3,3-bis(chloromethyl)-oxetane were polymerized in the presence of maleic anhydride by irradiation with γ rays and ultraviolet light. The polymer formed is a homopolymer of cyclic ether. The rate of polymerization is accelerated by suitable amounts of oxygen, which is required to form some active species at the initiation step. The polymerization is inhibited by the addition of a small amount of radical scavenger, thus suggesting a radical initiating mechanism. In addition, the polymerization is easily initiated by benzoyl peroxide even in vacuo at or above 50°C. Diaroyl and diacyl peroxides are also effective, and polymerization also proceeds in the presence of chloromaleic anhydride, exactly in the same manner as in maleic anhydride. On the other hand, polymerization of these cyclic monomers rarely occurs with radical catalysts and easily with cationic catalysts in the absence of maleic anhydride. From these results, it may be concluded that the polymerization is brought about by means of a radical–cationic species. (auth)

38954 THE ROOM-TEMPERATURE ESR SPECTRUM OF IRRADIATED POLYPROPYLENE: A REINTERPRETATION. Ayscough, P. B.; Munari, S. (Univ. of Leeds, Eng. Univ., Genoa). J. Polym. Sci., Pt. B, 4: 503-6 (July 1966).

Samples of stretched and unstretched Montecatini isotactic polypropylene were irradiated in vacuo using either ^{60}Co gamma irradiation or 3-Mev electrons. The ESR

spectra were then compared with that observed in a model hydrocarbon, 2,4-dimethyl-3-heptene which is thought to give an allylic radical during gamma irradiation. It is suggested that the configuration is asymmetric with respect to the $C-CH_3$ bond. Reasons for this are given. (P.C.H.)

38955 EFFECTS OF IONIZING RADIATION AND OTHER FACTORS ON RATE OF TOPOCHEMICAL DECOMPOSITION OF VARIOUS INORGANIC COMPOUNDS. Gordeeva, V. A.; Zhabrova, G. M.; Kadenatsi, B. M.; Mikhlin, V. E. (Inst. of Chemical Physics, Academy of Sciences, USSR). Kinet. Kataliz, 7: 62-8 (Jan.-Feb. 1966). (In Russian).

Ionizing radiation and the composition of the gaseous medium exert different effects on the rate of decomposition of magnesium hydroxide, aluminum hydroxide, lead oxalate, and nickel oxalate. The decomposition processes of magnesium and aluminum hydroxides were characterized by an apparent induction period and were insensitive to the oxidation-reduction properties of the gaseous medium. Preliminary γ and β irradiation caused an insignificant effect on the subsequent thermal decomposition of the hydroxides. The decomposition of the oxalates of lead and nickel were characterized by the presence of a conspicuous induction period and were sensitive to the oxidation-reduction properties of the gaseous medium. Preliminary irradiation led to a reduction of the induction period and a significant increase of the speed of the subsequent thermal decomposition of the oxalates. On the basis of the data obtained, hypothesis on the electron (acceptor-donor) character of the decomposition of the lead and nickel oxalates is proposed and considerations on the limited stage of the hydroxide decomposition are reported. (tr-auth)

38956 ANALYSIS OF THE KINETICS OF RADIATION-INDUCED ALLYL POLYMERIZATION. III. Dolmatov, S. A. (Topchiev Inst. of Petroleum Chemical Synthesis, Academy of Sciences, USSR). Kinet. Kataliz, 7: 214-18 (Mar.-Apr. 1966). (In Russian).

A scheme for radioinduced polymerization of allyl monomers was proposed. Allyl alcohol was investigated as an example. The initiation and growth of the chain, both in the monomer and polymer, and the rupture of the chain, as a result of the degradation transfer of the chain on the monomer, were considered. The equations for rate of conversion and polymerization in mass, in solution, and in the presence of inhibitors agreed with experimental data. (tr-auth)

38957 DIFFUSION OF TRIPLET EXCITONS PRODUCED BY IONIZING RADIATION IN AROMATIC MATERIALS. Voltz, R. (Centre de Recherches Nucleaires, Strasbourg); Dupont, H.; King, T. A. Nature, 211: 405-6 (July 23, 1966).

It is demonstrated that analysis of experimental radioluminescence decay curves provides estimates of the diffusion coefficient of triplet excitons produced by ionizing particles in aromatic materials. Using a single photoelectron technique, the luminescence decay pulse shapes for liquid scintillators, 5-phenyl-2-biphenylyloxadiazole and terphenyl in toluene, excited by α particles were measured. Analysis of the values measured with liquid toluene and those obtained from other sources for crystalline anthracene and t-stilbene gave estimates of the triplet state diffusion coefficient in the crystals that were in good agreement with those calculated using the hopping model. (D.H.M.)

38958 EFFECT OF DEUTERIUM SUBSTITUTION ON RADIATION-LESS DECAY OF ANTHRACENE TRIPLET. Beckett, A. (Univ. of California, Los Angeles). Nature, 211: 410-11 (July 23, 1966).

The decay kinetics of both perprotonated and perdeuterated triplet anthracene in room temperature and 77°K glasses were monitored. Decays of the transients were strictly exponential and no difference in transient lifetime was observed over many successive flashes. The mean lifetimes for the triplets of perprotonated anthracene were 0.025 sec at room temperature and 0.048 sec at 77°K. The mean lifetimes for the triplets of perdeuterated anthracene were 0.073 sec at room temperature and 0.153 at 77°K. Deuterium substitution caused a threefold reduction in the transition probability for radiationless decay of the triplet. (D.H.M.)

38959 RADIATION-INDUCED WATER DECOMPOSITION. Draganic, Zorica; Draganic, Ivan. Nukl. Energ., 1: 11-19 (1966). (In Yugoslavian).

The free-radical model of water radiolysis was investigated. The choice of convenient scavengers for free radicals and accurate measurement of radiolysis products permitted quantitative data to be obtained for pH effects. Values are given for samples in which oxygen and oxalic acid were used as the free radicals scavengers. It was found that change in pH practically does not affect the molecular products H_2 and H_2O_2 formed by diffusion controlled recombination reactions. A laboratory source of 300 C ^{60}Co and a radiation unit of 1.000 C were used as radiation sources. For quantitative measurements of stable radiolysis products, a number of standard physicochemical methods were developed. In some cases, when these were insufficient, electrochemical measurements were made during irradiation. Radioactive ^{14}C was used to follow the re-formation of oxalic acid in irradiated oxalic-oxalate solutions. Data are given for rate constant ratios and reactions between ions or molecules and free radicals formed in water radiolysis. Calorimetric devices were designed so that they can be used simultaneously for measuring the absorbed energy and as irradiation vessels. For routine dosimetry of large absorbed doses especially in nuclear reactors, a chemical dosimeter was realized. It consists of oxalic acid aqueous solution in a quartz vessel. Radiation causes decomposition of oxalate ions and changes in concentration are used to determine the absorbed dose. (P.C.H.)

38960 ^{36}Cl AND ^{82}Br ISOTOPIC EXCHANGE IN SOLID Co AND Rh DIHALOBIS(ETHYLENEDIAMINE) HALOGENIDES AND THE INFLUENCE OF X AND γ RADIATION. Schmidt, G. B.; Roessler, K. (Univ., Cologne). Radiochim. Acta, 5: 123-6 (June 1966). (In German).

The ^{36}Cl and ^{82}Br isotopic exchange, respectively, of covalent and ionic-bound halogen atoms was investigated in crystalline cis-and trans-$[Co(en)_2Cl_2]$ Cl and trans-$[Co(en)_2Br_2]$ Br from 100 to 170°C and in trans-$[Rh(en)_2Cl_2]$ Cl from 170 to 300°C. The activation energy of these exchange reactions was determined to be 30 to 34 kcal/mol. By pre-irradiation with x or ^{60}Co γ rays, the rate of isotopic exchange increased strongly with dose in solid trans-$[Co(en)_2Cl_2]$ Cl. Irradiation with bremsstrahlung was more effective than with ^{60}Co γ rays. It was assumed that the exchange occurs by a jump-mechanism on lattice defects. (auth)

38961 DISTRIBUTION OF RADIOACTIVE SELENIUM BETWEEN THE MODIFICATIONS OF SELENIUM IN NEUTRON-IRRADIATED RED CRYSTALLINE SELENIUM. Cifka, J. (Nuclear Research Inst., Czechoslovak Academy of Sciences, Rez, Czech.). Radiochim. Acta, 5: 140-3 (June 1966).

Red crystalline selenium was irradiated with neutrons and the distribution of radioactive selenium between the red and gray allotropic modifications was investigated. Approximately 2% of activity was stabilized in the gray modification with an enrichment of about ten, which decreased during thermal annealing. (auth)

38962 ON THE SZILARD-CHALMERS RECOIL OF ^{60}Co AND ^{60m}Co IN $[Co(NH_3)_6]$ $(NO_3)_3$ AND TRANS-$[Co\ en_2\ (NO_2)_2]$ NO_3. Gorla, P.; Lazzarini, E.; Sangiust, V. (Politecnico, Milan). Radiochim. Acta, 5: 146-8 (June 1966).

The possibility of different behaviors of ^{60}Co and ^{60m}Co in Szilard-Chalmers recoil was investigated and proved in $[Co(NH_3)_6]$ $(NO_3)_3$ and trans-$[Co\ en_2(NO_2)_2]$ NO_3. It was found that the retentions of ^{60}Co and ^{60m}Co atoms in the original compounds, for irradiation time approaching zero, are different. The ratio of ^{60m}Co to ^{60}Co retentions at zero irradiation time is 0.90 ± 0.02 for $[Co(NH_3)_6] \cdot (NO_3)_3$ and 1.26 ± 0.04 for trans-$[Co\ en_2(NO_2)]$ NO_3. The annealing

kinetics of recoiled ^{60}Co and ^{60m}Co atoms under fast-neutron and γ irradiations at a temperature of 40°C are also different. (auth)

38963 CHEMICAL EFFECTS OF ISOMERIC TRANSITION AND (n,γ) ACTIVATION OF BROMINE ATOMS IN n-PROPYL BROMIDE. Katsanos, Nicholas A.; Stamouli, Maria I. (Democritus Nuclear Research Center, Athens). Radiochim. Acta, 5: 148-55(June 1966).

A method is described by means of which the chemical effects of $^{81}Br(n,\gamma)^{82m}Br$ and $^{82m}Br \xrightarrow{IT} {}^{82}Br$ in n-propyl bromide can be determined separately. In the latter case effects due to the decay of $n\text{-}C_3H_7\text{-}^{82m}Br$ and to the decay of inorganic ^{82m}Br can also be separated, not only in the pure system but also in solutions of n-propyl bromide in methyl alcohol containing Br^-. The results showed that (n,γ) activation produces much lower organic retention than activation by isomeric transition. Moreover the organic yield of ^{82}Br is much higher when it is born from $n\text{-}C_3H_7 - {}^{82m}Br$ than when it is born from inorganic ^{82m}Br. These are explained by assuming that the probability of recombination of ^{82}Br with the parent radical, after bond rupture, is very high in isomeric transition activation but lower in (n,γ) activation, owing probably to the different recoil energies of the two processes. Retentions as parent compound are high and their ratio to total organic yield is constant in all cases. The half life of ^{82m}Br was determined through its chemical effects but this shows a small variation with change in temperature. (auth)

38964 REACTIONS OF ENERGETIC CARBON ATOMS IN METHYLAMINE. Cacace, Fulvio; Stoecklin, Gerhard; Wolf, Alfred P. (Brookhaven National Lab., Upton, N. Y.). Radiochim. Acta, 5: 155-61(June 1966).

The reactions of recoiling carbon atoms produced via the $^{14}N(p,\alpha)^{11}C$ process were studied in gaseous and liquid methylamine, with and without scavenger. The product-forming mechanisms in this system seemed to follow the general pattern of the chemistry of energetic carbon atoms in simple hydrocarbons. The major products resulting from fragmentation of excited intermediates were acetylene and ethylene. Ethylamine and dimethylamine were found as the synthesis products. A small yield of acetonitrile, which remained unaffected by the presence of scavenger or the change of phase, was also found. In agreement with the deexcitation-fragmentation hypothesis the yield of the fragmentation products acetylene and ethylene decreased while the yield of the synthesis products ethylamine and dimethylamine increased in the condensed phases. The formation of the products is explained on the basis of insertion reactions. From comparison of the acetylene and ethylene yields in methylamine with those in the ethane system it seemed that C–H bonds are much more reactive towards insertion reactions than N–H bonds. Whether this is due to a lower reaction probability or to a more easily stabilized intermediate could be decided on the basis of the evidence. The comparison with alkane systems showed no effect of the "leaving group" on the postulated acetylene and ethylene producing fragmentation process. It is suggested that the formation of acetonitrile takes place via decomposition of an excited ethyleneimine molecule, since the activity is equally distributed between the two carbon atoms. (auth)

38965 INFLUENCE OF ELECTRON-ACCEPTING AND DONATING AMBIENT ATMOSPHERES ON THE THERMAL ANNEALING OF RECOIL DAMAGE IN COBALT CHELATES bis-SALICYLALDEHYDE-TRIETHYLENE-TETRAMINE Co(III) CHLORIDE, HYDRATE. Rao, K. A.; Nath, Amar (Atomic Energy Establishment, Trombay, India). Radiochim. Acta, 5: 162-4(June 1966).

The ambient atmosphere was found to influence the thermal annealing behavior of neutron-irradiated bis-salicylaldehyde-triethylenetetramine Co(III) chloride, hydrate. Electron-donors, acetone and ethyl alcohol vapors, accelerate the annealing process, while electron-acceptors like oxygen and nitric oxide gas retard it. Evidently, a donor-acceptor electron transfer takes place between the crystallite and the adsorbed molecules of the ambient gas or vapor. It supports an annealing mechanism invoking participation of free electrons. (auth)

38966 CARBOXYLATION OF FORMATE UNDER THE RADIATION EFFECTS OF RADON. Getoff, N.; Hernegger, F. (Oesterreichische Akademie der Wissenschaften, Vienna). Radiochim. Acta, 5: 166-9(June 1966). (In German).

Carboxylation of formate under action of radiation from radon is reported. Yields of oxalate were relatively high and amounted to G (oxalate) = 22.1 at p_H 9. In the presence of n-butanol or glycerine as a competitive partner during the carboxylation the yield of oxalate decreased considerably. For radon and its decay products a value of $G(Fe^{3+}) = 10.5$ was calculated taking into account a series of factors. (auth)

38967 REDUCTION OF CERIC SULFATE IN PRESENCE OF THALLOUS IONS BY 5-Mev α PARTICLES. INTRATRACK DISTRIBUTION OF PRIMARY PRODUCTS OF RADIOLYSIS. Mariano, Maria Helena; Novais, Horacio Maggiolli (Junta de Energia Nuclear, Lisbon). Rev. Port. Quim. (Lisbon), 7: 198-204(1965). (In Portuguese).

The maximum sensitization value of the radiolytic reduction of ceric sulfate, induced by Tl^+ ions, is far below the theoretical one. The difference is ascribed to competition of reaction $OH + Tl^+ \rightarrow OH^- + Tl^{2+}$ with reserve reaction of OH radicals, in the α-ray track, along with a partial reduction of Tl^{2+} ions formed, before diffusing to the bulk of the solution. A mean OH radical concentration $\approx 3.10^{-1}$ M, in the intratrack region of pairwise recombination, is deduced; the region where reverse reactions of the radiolytic products take place has a volume one hundredfold greater than the zone first considered. (auth)

38968 KINETIC INVESTIGATION OF GAMMA RADIOLYSIS OF 5-BROMOURACIL IN AQUEOUS SOLUTIONS. Reuschl, H. (Kernforschungszentrum, Karlsruhe, Ger.). Z. Naturforsch., 21b: 643-6(July 1966). (In German).

Kinetics of the decomposition of 5-bromouracil in aqueous solutions at pH = 6.5 by irradiation with gamma rays were investigated under N_2, O_2, and N_2O. The results are discussed on the basis of the radical theory of aqueous solutions and a hypothesis was derived for the origin of the radiosensitization of living cells with bromouracil. (tr-auth)

38969 RADIATION CHEMISTRY OF CARBOHYDRATES, VII. RADIOLYSIS OF AQUEOUS SOLUTIONS OF SOME DERIVATIVES OF GLUCOSAMINE. Kochetov, N. K.; Kudryashov, L. I.; Senchenkova, T. M.; Nedoborova, L. I. Zh. Obshch. Khim., 36: 1020-5(June 1966). (In Russian).

The radiolysis of glucosamine and some of its derivatives was investigated. It was found that the radiolysis of aminosaccharides has a series of characteristics distinguishing them from their neutral monosaccharides. The radiation-chemical yield for N-acetylglucosamine is proportionally dependent on the concentration in the interval studied and at concentrations of 5×10^{-2} M it is 18.2 ± 4.5. The radiation-chemical yield for α-methyl-N-acetylglucosamine at concentrations of 10^{-2} M is 2.57 ± 0.34 and 3.96 ± 0.024 for the β isomer which indicates the effects of the configuration of the glucosamine center on the stability with respect to radiation. (tr-auth)

38970 REACTIONS OF HOT TRITIUM ATOMS PRODUCED BY ELECTRON IMPACT ON T_2 WITH SOLID PROPENE AND PROPANE. Shores, Richard Dale. Manhattan, Kan., Kansas State Univ., 1966. 82p.
Thesis.

Hot tritium atoms were produced by electronic excitation of molecular tritium to the $^3\Sigma_u$ state by electron impact. This state dissociates into two tritium atoms each possessing an energy of about 3.7 ev. The products of the reactions were separated by gas chromatography and the tritiated compounds were counted in an ionization chamber connected to a vibrating reed electrometer. The reaction of tritium atoms with solid propene at 77°K resulted in formation of the following products that contained tritium: HT, propane propene, 2,3-dimethylbutane, 2-methyl-pentane, 4-methyl-pentene-1, n-hexane, 1-hexene, methane, and ethene. Small amounts of ethane, isobutane, and n-butane were also formed. The distribution of products gave indication that hot tritium atoms react primarily with solid films of pro-

pene at 77°K in three ways: tritium atom addition to form isopropyl or n-propyl radicals or hydrogen atom abstraction to form allyl radicals. These propyl radicals disproportionate to form propane and propene or the C_3 radicals combine to form the C_6 compounds. Decomposition of vibrationally excited n-propyl radicals was proposed to explain the formation of methane and ethene. The reaction of energetic tritium atoms with thin films of propane at 77°K resulted in the formation of the following compounds that contained tritium: HT, methane, and propane with lesser amounts of ethane, ethene, propene, isobutene, and n-butane. A two-step process was proposed as predominant in the formation of products. The first step is abstraction of a hydrogen atom from propane to form propyl radicals and HT. A second hot tritium adds to the propyl radical to form excited propane. The excited propane dissociates into methyl and ethyl radicals or else it becomes stabilized by the matrix. The products can be explained by methyl, ethyl, and propyl radical reactions. Evidence for energetic, displacement reactions of tritium atoms was obtained when labeled propane was observed as a product from mixtures of propane and 2-methylpropene. (TCO)

38971 THE EFFECT OF RADIATION ON ELECTRIC CONDUCTION IN n-HEXANE. Kao, K. C.; Phahle, A. M.; Calderwood, J. H. (Royal Coll. of Advanced Technology, Salford, Eng.). 5p. (CONF-650962-2). ORAU. Gmelin, AED-CONF-65-240-3.

From 6th Electrical Insulation Conference, New York.

At fields up to 80 kv/cm, the dark conduction obeys Ohm's law, and the gamma induced and ultraviolet photoinjected currents do not saturate for a wide range of temperatures. The induced and injected currents are proportional to the intensity of radiation. It is suggested that the dark conduction is associated with the presence of irremovable impurities, and that the small fluctuation of conduction current is attributed in the electrons being irregularly trapped and thermally released during their drift toward the anode. The factors influencing the mobilities of positive and negative charge carriers are discussed. (auth)

38972 METHOD OF PERFORMING A RADIATION-INDUCED CHEMICAL REACTION. Hentz, Robert R. (to Socony Mobil Oil Co., Inc.). U. S. Patent 3,258,404. June 28, 1966. Filed Sept. 14, 1962.

A method of performing a chemical reaction in the presence of a solid contact material, which may or may not have catalytic activity, comprises impregnating a contact material with 1 to 25 wt % of an element with a stable inactive nuclide having an abundance of at least 2% and a thermal neutron activation cross section of at least 50 barns, subjecting the mixture to thermal neutron activation to yield a nuclide which emits purely beta radiation, and then removing the activated material to a conventional chemical reaction zone where the material is contacted with a reactant characterized by having C–C and C–H bonds. The reactants are converted to a desired product by the aid of the radiation while absorbing substantially all of the radiation in the activated material–reactant system, and the conversion step affects only the C–C and C–H. (B.L.M.)

38973 RADIATION RESISTANT LUBRICANTS. Gupta, Sharda Das; Slobodian, James Theodore (to Atomic Energy of Canada Ltd.). U. S. Patent 3,262,882. July 26, 1966. Filed Apr. 22, 1963.

An invention is described relating to lubricating oils and greases for use in areas where they are subjected to large doses of high energy radiation of the order of 10^9 rads and greater and which can maintain their lubricating properties with little or no deterioration. New lubricants for high radiation were developed and a description of the invention is given in which comparisons are made between the properties of the new lubricants exposed to high radiation doses and conventional lubricants which were not irradiated. A comparison of the effects of radiation on the new and conventional lubricants is also made. (J.R.D.)

38974 IRRADIATION OF OIL SHALE–POLYOLEFIN ARTICLES. Carr, Donald E. (to Phillips Petroleum Co.). U. S. Patent 3,258,412. June 28, 1966. Filed Apr. 28, 1960.

A process is described for producing molded articles, such as floor tiles, road surfacing strips, preformed or continuous piling for buildings, or heavy structure supports for warfs and docks by intimately admixing oil shale and a solid polyolefin, subjecting the mixture to a molding temperature and molding pressure, removing the molded article from the mold, and irradiating the molded article with high energy ionizing radiation. Colored pigments may be incorporated into the materials during the admixing to form products having a wide spectrum of color. (B.L.M.)

38975 PROCESS OF MODIFYING CELLULOSIC MATERIALS WITH IONIZING RADIATION. Munzel, Fritz (to Herberlein and Co. AG.). U. S. Patent 3,254,939. June 7, 1966. Filed Feb. 1, 1965.

A process is described for enhancing crease resistance and some other properties of cellulosic textiles by irradiating the textile with ionizing radiation to a total dose in the range of about 10^5 to 10^7 rad in the presence of a sensitizer at ambient moisture conditions and without subsequent heating. The sensitizer is an organic compound that contains molecular groups capable of absorbing ionizing radiation and transferring excitation energy to cellulose molecules of the textile to effect the crosslinking of the cellulose polymers. The preferred sensitizer is 1, 4 diphenylbenzene. Excellent wet crease resistance is imparted to the textile if after the irradiation treatment at least one graftable organic finishing chemical is grafter onto the cellulose molecule. (B.L.M.)

38976 IONIZING RADIATION OF WATER SOLUTION OF POLYALKYLENE OXIDE AND PRODUCT THEREOF. King, Paul A. (to Union Carbide Corp.). U. S. Patent 3,264,202. Aug. 2, 1966. Filed June 13, 1961.

An invention is described relating to a new class of polymeric compounds containing C-to-C crosslinking bonds and a new process utilizing ionizing radiation for preparation of such compounds, using polymers as starting material. The invention provides polymeric materials containing C-to-C crosslinking bonds to the O_2 in an ether linkage. The invention also provides macro-molecular polymeric materials which are insoluble in water and organic liquids and which contain intra and inter molecular C-to-C crosslinking bonds and which polymeric materials are stable in the presence of O_2. The invention also provides gel-like materials comprising a matrix which is stable in the presence of O_2 and which consists of polymeric materials containing intra and inter molecular C-to-C crosslinking bonds and wherein the matrix reversibly holds large amounts of water. (J.R.D.)

38977 METHOD FOR PRODUCING KETENE POLYMER WITH IONIZING RADIATION. Tashiro, Shigeki (to Japanese Association for Radiation Research on Polymers). Japanese Patent 1965-9966. May 21, 1965. Filed Feb. 27, 1962.

A new method is proposed for producing ketene polymer with ionizing radiation. Ketene is usually not polymerized with the radical initiator, and the polymer cannot be obtained at a high yield even by the use of metallic compounds. In the method proposed the polymer is obtained, without catalysts, by irradiating ketene with an ionizing radiation in the liquid phase or solid phase below –41°C (b.p. of ketene) either in the presence or absence of the unreactive solvent. The yield increases in proportion to the first order of the dose or the dose rate, and the saturation value is reached at several tens of per cent. (NSA of Japan)

38978 METHOD FOR PRODUCING THERMOPLASTIC RESINS OF TERNARY COPOLYMERS. Harada, Yoshishige (to Sumitomo Bakelite Co., Ltd.). Japanese Patent 1965-17150. Aug. 4, 1965. Filed Feb. 9, 1963.

A method for producing resins with high impact strength

on an industrial scale includes the following steps: emulsifying in the aqueous system a mixture of three components; (1) polyisobutylene, isobutylene copolymers, or their mixture, (2) at least one of the aromatic vinyl monomers, and (3) at least one of the acrylic monomers and then irradiating the emulsified mixture with a high-energy ionizing radiation. (NSA of Japan)

38979 METHOD FOR PREPARATION OF ADHESIVE FILMS. Iwashita, Fumio (to Tokyo Shibaura Electric Co., Ltd.). Japanese Patent 1965-17662. Aug. 11, 1965. Filed Dec. 26, 1962.

A method is proposed for the preparation of an adhesive film in which a resin containing hydroxyl group is combined with graft-copolymers of epoxy and polyamide resins. A hydroxyl group-containing resin is painted on one side or both sides of the polyamide film onto which an unsaturated epoxy compound has been graft-copolymerized by irradiation. For the graft-copolymerization, at least one of the compounds is admixed beforehand with a hydroxyl group-containing resin. This adhesive film has high adhesion and thermal stability, as well as accelerated curability. (NSA of Japan)

38980 METHOD FOR PRODUCING TETRAFLUOROETHYLENE POLYMERS. Hori, Yoshimichi (to Industrial Research Institute). Japanese Patent 1965-18430. Aug. 19, 1965. Filed Feb. 8, 1963.

In the proposed method for producing tetrafluoroethylene polymers by irradiation, the tetrafluoroethylene partially polymerized by means of an ionizing radiation is again polymerized in the condensed system below 0°C without using radiation. The tetrafluoroethylene polymer can be produced continuously on an industrial scale, the economy with respect to the radiation dose is being improved, and the properties of the polymer are easily controllable. (TSS)

38981 METHOD FOR PRODUCING FOAMED PLASTICS. Ueno, Jiroo (to Sekisui Chemical Co., Ltd.). Japanese Patent 1965-19192. Aug. 27, 1965. Filed July 18, 1962.

Foamed bodies of poly(acrylic acid), poly(methacrylic acid), poly(acrylamide) and poly(methacrylamide), hitherto considered unsuitable as materials for such foamed plastics, have been obtained. The foamed plastics obtained have been found to be usable at high temperatures such as above 200°C. The plastics are formed by mixing homogeneously with a foaming agent, one or more kinds of monomers selected from the group consisting of acrylamide, acrylic acid, methacrylamide, and methacrylic acid then polymerizing the monomers by irradiating with an ionizing radiation to give polymeric resins capable of softening when heated; and then heating the polymerized bodies so that the foaming and the crosslinking between the polymer molecules take place. (NSA of Japan)

Radiochemistry

See also Separation Processes and Procedures

Refer also to abstracts 38991, 39336, and 39337.

38982 (PAEC(D)IS–652) THE PREPARATION OF HIGH SPECIFIC ACTIVITY ^{51}Cr AT THE PHILIPPINE ATOMIC RESEARCH CENTER. Berbano, Mario C.; Lumba, Linda G. (Philippine Atomic Energy Commission, Manila). May 1965. 12p. Dep. mn.

The Szilard-Chalmers reaction was used in the production of ^{51}Cr of high specific activity. With reagent grade K_2CrO_4 as target material, irradiations were carried out for 3 to 18 hr at approximately 1×10^{11} to 6×10^{11} n/cm^2/sec in the PRR pool-type reactor. The irradiated K_2CrO_4 was treated with dilute NH_3 and passed through a column of chromatographic-grade alumina conditioned with dilute NH_3 to retain the active trivalent Cr which was subsequently eluted with dilute HCl, finally converted to Na_2CrO_4 using Na_2O_2 as oxidizing agent. Cr content was estimated colorimetrically. Results indicated that the yield varied from 2 to 37%, with maximum specific activity of about 5 mC/mg Cr, and an enrichment factor greater than 4,000. Radiochemical analysis was carried out by gamma spectrometry and paper chromatography. The former method was also used in the absolute activity determination. (auth)

38983 (SGAE-SS-3/1966) EIN VERGLEICH ZWISCHEN EXISTIERENDEN METHODEN ZUR MESSUNG RADIOAKTIVER PROBEN BEI BERUECKSICHTIGUNG DER EMPFINDLICHKEIT UND DER GESAMTMESSZEIT. (Comparison Between Existing Methods for the Measurement of Radioactive Samples with Consideration of the Sensitivity and the Total Measurement Time). Kambourov, Christo (Oesterreichische Studiengesellschaft fuer Atomenergie G.m.b.H., Seibersdorf. Institut fuer Strahlenschutz). Nov. 1965. 17p. Dep. mn.

A comparison was made between existing methods for measurement of radioactive materials. The comparison was made with respect to the statistical accuracy and total measurement time. The formulas derived for the calculation of the lowest possible detection limits permit a determination of the sensitivity in all cases. (tr-auth)

38984 FORMATION OF XeO_3 IN β DECAY OF ^{131}I IN THE COMPOSITION OF ALKALI METAL IODATES. Kirin, I. S.; Gusev, Yu. K. (Ioffe Inst. of Physics and Tech., Leningrad). Dokl. Akad. Nauk SSSR, 167: 1090-3(Apr. 11, 1966). (In Russian).

Studies were made of properties of xenon oxide compounds formed in β decay of ^{131}I in alkali metal iodates, $LiIO_3$, $NaIO_3$, KIO_3, $RbIO_3$, and $CsIO_3$. ^{131m}Xe, ^{131m}XeO, $^{131m}XeO_2$, and $^{131m}XeO_3$ are formed. XeO and XeO_2 are unstable and disintegrate to elementary xenon and oxygen. Products of the ^{131}I β decay are studied using the radioactive ^{131m}Xe formed during the decay process. Tabulated data are given of the yield of bound xenon in β decay of ^{131}I in iodates and periodates during various steps of the experiment. (R.V.J.)

38985 PREPARATION OF DIIODO-^{131}I FLUORESCEIN AND TETRAIODO-^{131}I PHENOLPHTHALEIN FOR DIAGNOSTIC PURPOSES. Hallaba, E.; Abdullah, E. (Atomic Energy Establishment, Cairo). Int. J. Appl. Radiat. Isotop., 17: 425-6(July 1966).

Procedures are described for the preparation of ^{131}I-labeled-diiodofluorescein and ^{131}I-labeled-tetraiodophenolphthalein for use as tracers in diagnostic studies. (C.H.)

38986 COMMENTS ON ^{99m}Tc. Richards, P. (Brookhaven National Lab., Upton, N. Y.). Int. J. Appl. Radiat. Isotop., 17: 427(July 1966). (BNL-9624).

A ^{99m}Tc generator for medical applications is discussed. Carrier-free fission product ^{99}Mo is used as source and ^{99m}Tc is milked from the generator directly using physiological saline solution as the eluent. (C.H.)

38987 SYNTHESIS AND CHARACTERIZATION OF 3-KETOHEXADECANOIC ACID-1-^{14}C, DL-3-HYDROXYHEXADECANOIC ACID-1-^{14}C, AND TRANS-2-HEXADECENOIC ACID-1-^{14}C. Jones, John A.; Blecher, Melvin (Georgetown Univ., Washington, D. C.). J. Lipid Res., 7: 422-6(May 1966).

The procedure of Stallberg-Stenhagen was adapted to synthesize pure methyl 3-ketohexadecanoate-1-^{14}C in adequate yield, and the method of Mitz et al. was utilized to obtain the free 3-keto acid without decomposition. Melting point, ir data, and elemental analysis confirmed the purity and identity of the products, and thin-layer chromatography (TLC) indicated their radiochemical purity. The Reformatsky reaction was used to prepare 3-hydroxyhexadecanoic acid-1-^{14}C in adequate yield. Optical rotatory data confirmed that the product was a racemic mixture composed of equal parts of the D- and L-optical isomers. 2-Hexadecanoic acid-1-^{14}C resulted from the dehydration of DL-3-hydroxyhexadecanoic acid-1-^{14}C in the presence of boric anhydride. Gas-liquid chromatography indicated the presence of about 6% of the 3-hexadecanoic acid. In addition, ir and TLC data indicated that the unsaturated acid was of the trans configuration. The three radioactive fatty acid derivatives described may be of value in elucidating mitochondrial mechanism of oxidation, interconversions, synthesis, and transport of long-chain fatty acids. (TCO)

38988 ENRICHMENT OF ^{64}Cu BY THE SZILARD-CHALMERS PROCESS. Lin, Tsing Ko; Yeh, Si Jung (National Tsing Hua Univ., Hsinchu, Taiwan). J. Nucl. Sci. Technol. (Tokyo), 3: 289-93(July 1966).

Bisacetylacetone–ethylenediimino–Cu(II) was used as target material for an investigation of the enrichment of ^{64}Cu by the Szilard-Chalmers process. The recoiling radioactive copper was extracted from the target with aqueous solutions of various electrolytes in different concentrations. An enrichment factor as high as about 720 was observed under optimum conditions. It was found that the enrichment factor decreases with increasing irradiation time. The effect of cooling time on the enrichment factor of ^{64}Cu was also investigated. (auth)

38989 METHOD FOR DETERMINING γ RADIATION OF A SPHERICAL SOURCE WITH A CYLINDRICAL CHANNEL AT SYMMETRICAL AXES. Abrams, I. A.; Kalis, Kh. E.; Pelekis, L. L.; Taure, I. Ya. (Inst. of Physics, Academy of Sciences, Latv. SSR). Latv. PSR Zinat. Akad. Vestis, Fiz. Teh. Zinat. Ser., No. 2, 32-6 (1966). (In Russian).

A method was developed for counting the dose rate and flux of γ rays from a spherical source with a cylindrical channel at the symmetrical axes. The counting was conducted by an electronic computer and the results are given in diagrams. The results of computation were compared with the experimental ones, being obtained by the help of photoactivation of the metastable level (335 kev) from ^{115}In by the reaction $^{115}In\ (\gamma,\gamma')\ ^{115m}In$. (auth)

38990 PREPARATION OF SOURCES FOR ALPHA SPECTROMETRY. Kirby, H. W.; Dauby, J. J. (Monsanto Research Corp., Miamisburg, Ohio). Radiochim. Acta, 5: 133-7(June 1966).

A method is presented for the preparation of alpha sources to be analyzed by an alpha spectrometer equipped with a semiconductor detector. The procedure consists of evaporating to dryness an aqueous solution of the alpha emitter, redissolving the residue in situ with 0.1N HNO_3, precipitating with 3N NH_4OH. and drying. The residual NH_4NO_3 is redissolved in 3N NH_4OH, dried again, and sublimed at a higher temperature. The deposit is washed with distilled water, after which the plate is dried and ignited at red heat. Dramatic improvement is illustrated with several alpha emitters of different chemical properties, including $^{208/209}Po$, ^{230}Th, ^{231}Pa, $^{232/234}U$, and $^{238/239}Pu$. By providing better distribution of the alpha-emitting nuclides and by removing alpha-absorbing impurities, the same procedure significantly increases the gross alpha counting rate and is recommended for use in improving the accuracy and reproducibility of routine alpha counting. (auth)

38991 PREPARATION OF SELENOUREA-^{75}Se BY NEUTRON ACTIVATION AND ITS RADIOLYTIC DECOMPOSITION. Badiello, Roberto; Breccia, Alberto (Univ., Bologna. CNR, Bologna). Ric. Sci. Riv., 36: 335-7(May 1966). (In Italian).

Selenourea-^{75}Se was prepared by the neutron activation procedure. Its radiolysis was investigated for determining colorimetrically the elementary selenium sol stabilized with a new type of suspendent (hyamine). The radiolytic decomposition was about 6%, and no autoradiolytic effect was observed. (auth)

38992 PREPARATION OF RADIO-IODINATED TYROSINES AND THYROXINE AND SEPARATION ON SEPHADEX G 25. Abdel-Wahab, M. F.; El-Kinawy, S. A. (Middle Eastern Regional Radioisotope Centre for Arab Countries, Cairo. Research and Control Centre, Giza, Egypt). Z. Anal. Chem., 219: 425-31(1966).

Iodination of tyrosines was carried out easily by interaction between nascent ^{131}I and the amino acid. The labeling of thyroxine follows the same route but with less yield. Fractionation of the iodinated compounds reveals the predominance of 3.5-diiodotyrosine (3.5-DIT) when tyrosine is iodinated. Labeling of thyroxine gives pure ^{131}I-thyroxine. All separated fractions obtained from the Sephadex column were confirmed by means of paper chromatography and identified by the use of authentic samples. (auth)

38993 PROCESS FOR IMPREGNATING AN ADSORBENT CATALYST WITH A RADIOACTIVE METAL ISOTOPE. Wilson, William A.; Herrington, Arthur C. (to Standard Oil Co.). U. S. Patent 3,252,916. May 24, 1966. Filed Sept. 13, 1962.

As a basis for catalyst retention or loss studies in processes for the conversion of hydrocarbons, a process is described for impregnating an absorbent catalyst with either ^{95}Zr, ^{181}Hf, or ^{46}Sc. The finely divided absorbent solid such as a silica-alumina cracking catalyst is slurried with an inert volatile organic liquid, and a solution containing the radioactive metal isotope in the form of the soluble coordination compound of thenoyltrifluoroacetone dissolved in the inert organic solvent is added to the slurry. The slurry and solution are intimately mixed at the boiling point of the organic liquid to obtain rapid but uniform impregnation of the catalyst with the isotope. The excess liquid is removed, and the resultant impregnated solid is dried. (B.L.M.)

Separation Processes and Procedures

See *also* Analytical Procedures
ISOTOPE TECHNOLOGY — Separation and Production

Refer also to abstract 40081.

38994 (AE–232) NUCLEAR CHEMISTRY. Progress Report, 1965. Carleson, G. (Aktiebolaget Atomenergi, Stockholm (Sweden)). Apr. 1966. 26p. Dep. mn.

Isotopic hydrogen-deuterium effects down to eutectic temperatures in saturated halide and nitrate solutions were investigated by means of Rayleigh distillations and solubility determinations. A thorough study of the fission-fragment-induced emission of uranium atoms from uranium metal and dioxide was concluded. Supplementary and new experiments were performed in various atmospheres and at different pressures, and the results and mechanism theoretically interpreted. In order to study the energy transfer mechanism the heterogeneous system n-hexane/silica gel was irradiated with a γ source. The products formed were identified by gas chromatography and ESR spectroscopy and their G-values determined. New and efficient methods of separating mixed fission products from an acid and highly active waste solution containing large amounts of uranyl nitrate are required for the reprocessing of plutonium-enriched fuel elements by amine extraction. As part of a project to achieve this separation by eutectic freezing the ternary phase diagram of simulated waste solution was studied and solubilities were determined at low temperatures. Work on the separation of fission products of interest by means of inorganic ion exchangers was also carried out. The properties and affinities of zirconium phosphates and zirconium silicate phosphates were studied. It was found that high loads of cesium may be selectively sorbed on partially dehydrated zirconium phosphate gels. (auth)

38995 (BM-RI–6809) EXTRACTION AND SEPARATION OF SELECTED LANTHANIDES WITH A TERTIARY AMINE. Bauer, D. J. (Bureau of Mines, Reno Metallurgy Research Center). Feb. 1966. 15p.

The feasibility of fractionating lanthanide nitrates with a tertiary amine on lanthanum-cerium and thulium-ytterbium pairs was demonstrated. Optimum values were determined for pH, phase concentration, and percent chelation of metal ions in the aqueous phase. Percent extraction is markedly dependent on the concentration of lithium nitrate in the aqueous phase. Selective masking of the heavier element in each extraction system with DTPA or EDTA aqueous-phase chelating agents resulted in lanthanum-cerium separation factors of 8.5 and thulium-ytterbium separation factors of 3.4. (auth)

38996 (DP–1066(Vol.2), pp II.79-102) THE LARGE SCALE SEPARATION OF ^{210}Po FROM BISMUTH. Jenn-

ings, A. S.; Proctor, J. F.; Fernandez, L. P. (Du Pont de Nemours (E. I.) and Co., Aiken, S. C. Savannah River Lab.).

A vacuum distillation process and related equipment are described for large-scale separation of ^{210}Po from irradiated bismuth. Polonium is concentrated to greater than 95 wt % from bismuth feed containing 25 to 75 ppM polonium. Advantages are high throughput in equipment of modest size and ready purification of both polonium and bismuth products, while avoiding the reduction of polonium and bismuth back to the metallic form. (auth)

38997 (NLJS-R-483) SEPARATION OF ^{99m}Tc FROM ^{99}Mo SORBED ON ALUMINUM OXIDE BY PHYSIOLOGIC SOLUTION. Ravnik, V.; Gorenc, B.; Novak, J. (Nuklearni Institut Jozef Stefan, Ljubljana (Yugoslavia)). May 1966. 5p. Dep. mn.

The partition of technetium-99m and molybdenum-99 between aluminum oxide and solutions of hydrochloric acid and sodium chloride was investigated. Distribution coefficients were determined, as well as the elution curves for technetium-99m. The results prove that physiological solution can be used besides acids for preparation of technetium-99m solutions for medical purposes. (auth)

38998 (ORNL-3958) UNIT OPERATIONS SECTION QUARTERLY PROGRESS REPORT, OCTOBER-DECEMBER 1965. Whatley, M. E.; Haas, P. A.; Horton, R. W.; Ryon, A. D.; Suddath, J. C.; Watson, C. D. (Oak Ridge National Lab., Tenn.). July 1966. Contract W-7405-eng-26. 60p. Dep. mn. CFSTI $3.00 cy, $0.75 mn.

Studies are reported on stacked-clone solvent extraction contactor; shear-leach processing of power reactor fuels; grind-leach processing of graphite fuels; engineering separation of macromolecular biological substances; urania-sol preparation; thorium microsphere preparation; pulse-column tests; berkelium extraction-rack tests; and waste processing. (P.C.H.)

38999 (TID-23229) ION EXCHANGE SEPARATION OF URANIUM AND THORIUM IN MIXED AND NON-AQUEOUS SOLVENTS. Korkisch, J. (Vienna Univ. (Austria). Analytisches Institut). Dec. 1965. Contract AT(30-1)-2623. 13p. Dep. mn. CFSTI $1.00 cy, $0.50 mn.

From a medium consisting of 90% tetrahydrofuran and 10% 6N nitric acid, uranium(VI) is much less strongly retained (Kd-value = 40) on Dowex 50 (hydrogen form) than most other metal ions (Kd values > 10^3 to 10^4) so that its ready separation can be effected from these as well as from elements which are practically non-adsorbable under these conditions (Kd values of about 1 to 2). The group of elements strongly retained includes the alkaline earth metals, the rare earths, titanium, zirconium, thorium, iron(III), cobalt, nickel, copper etc., whereas phosphate, vanadium(V), molybdenum(VI), and gold(III) are taken up by the resin to a negligible extent only. On the basis of this fact uranium in amounts ranging from micrograms to grams can be completely separated from practically all elements except bismuth. This peculiar behavior of uranium, which is not observed in either pure aqueous or other mixed aqueous-organic solvent systems containing nitric acid, is explained by an effect which was termed combined ion exchange-solvent extraction or CIESE. This is assumed to be based on a competition for the uranyl ion by the cation exchange resin and the tetrahydrofuran-nitric acid mixture acting as a liquid anion exchanger. (auth)

39000 INORGANIC CHROMATOGRAPHY ON IMPREGNATED ION-EXCHANGE PAPERS. Sherma, Joseph (Lafayette Coll., Easton, Pa.). Anal. Chim. Acta, 36: 138-41(Sept. 1966).

A study was made to compare the separation of 26 ions on commercial ion-exchange paper, impregnated with a reagent, with that of unimpregnated ion-exchange paper and with Whatman No. 1 paper, impregnated with reagent. Results demonstrated that it can be advantageous to use ion-exchange paper rather than conventional chromatographic paper as the support in paper extraction chromatography. When the effect of a stationary complexing reagent is added to the effect of a stationary phase capable of ion exchange, chromatographic systems with greater or altered selectivity may result. (D.H.M.)

39001 RADIOCHEMICAL SEPARATION AND PURIFICATION OF ^{140}Ba AND RAPID MILKING OF ^{140}La FROM ^{140}Ba. Bhatki, K. S.; Ephraim, D. C. (Tata Inst. of Fundamental Research, Bombay). Indian J. Chem., 4: 261-2(June 1966).

A quick cation exchange procedure for purifying ^{140}Ba from its daughter ^{140}La using dilute nitric acid (2.14N) and the hydrogen form of Dowex-50W-X8 resin is described. As nitric acid can be removed easily, the separation is clean and fast. Milking of ^{140}La was also effected at a fast rate when 0.5M lactic acid solution (pH 3.95) and Dowex-50W-X8 (ammonium form) were employed. (auth)

39002 EXCHANGE ADSORPTION OF CATIONS ON TiO_2.aq. Levi, H. W.; Schiewer, E. (Hahn-Meitner-Institut fuer Kernforschung, Berlin). Radiochim. Acta, 5: 126-33(June 1966). (In German).

The exchange of Cs and Sr ions on very pure $TiO_2 \cdot aq$ was investigated. The TiO_2 was prepared by hydrolysis of the tetraethyl ester of orthotitanic acid. When the exchange capacity of $TiO_2 \cdot aq$ is determined by titration with CsOH or $Sr(OH)_2$, one, two or three inflection points are obtained (depending on the experimental conditions), corresponding to 0.1, 0.2 and 0.3 gram atoms of metal ion per mole $TiO_2 \cdot aq$. At any p_H value between 5 and 12 Sr is better adsorbed from carrier-free radionuclide solutions than Cs. The Cs adsorption is repressed by other monovalent cations. The ion activities that influence the Cs adsorption equally strong are $Cs : K : Na : Li : N(CH_3)_4 = 1 : 2.2 : 12.5 : 37 : 490$. The Cs adsorption can be quantitatively described as Cs-H-exchange. Sr is partially exchanged as monovalent ion, partially as divalent ion, therefore the Sr adsorption can also be explained as Sr-H exchange. At constant p_H value the exchange adsorption on $TiO_2 \cdot aq$ can be described by the Langmuir adsorption isotherm. (auth)

39003 EXTRACTION OF PROTACTINIUM BY LONG-CHAIN AMINES FROM HYDROCHLORIC ACID SOLUTIONS. Venkateswarlu, K. S.; Subramanyan, V.; Dhaneshwar, M. R. (Atomic Energy Establishment, Trombay, India). Radiochim. Acta, 5: 175-6(June 1966).

A liquid anion exchange study of the extraction of ^{233}Pa from hydrochloric acid solutions using tri-n-nonyl amine and Amberlite LA-2 (a highly branched secondary amine) with benzene as extractants was made. Tracer ^{233}Pa, obtained from neutron irradiation of thorium nitrate followed by ion exchange, was used in the experiments. The effect of variation of HCl concentration on the distribution coefficient and the effect of independent variation of H^+ and Cl^- on the distribution coefficient are reported. (D.H.M.)

39004 EFFECT OF TEMPERATURE ON RARE EARTH SEPARATIONS ON CATION RESIN COLUMNS WITH LACTATE. Schonfeld, Ernest; Stewart, D. C. (Argonne National Lab., Ill.). Radiochim. Acta, 5: 176-7 (June 1966).

A study was made to determine if higher column operating temperatures of the lactate-cation resin system would improve the separation of the individual ions of the rare earths. Data for curium, europium, and terbium at temperatures from 24 to 89°C show that when the temperature was increased there was an improvement in the separation of the ions studied. (D.H.M.)

39005 APPROACH TO THE THEORY OF SEPARATING COLUMNS WITH SUCCESSIVE EXCHANGE BETWEEN THREE FLUIDS. Palibroda, N. (Inst. for Atomic Physics, Cluj). Z. Naturforsch., 21a: 745-9(June 1966).

Cohen's method was used to develop the theory of continuous separating columns with successive exchange among three fluids. The equations of the column were solved for stationary state and small concentrations. The general solutions representing the dependence of the mole fractions of the desired isotope in the three fluids on the column height involve the following particular cases: concurrent and countercurrent exchange between two fluids and two limiting cases of exchange between three fluids in which the intermediate fluid is at isotopic equilibrium with one of the other two fluids. As a general feature of the col-

umns with successive exchange among three fluids, it was found that the ratio of the driving forces corresponding to the fluid pairs, between which the mass transfer takes place, has a constant value along the column, excepting a zone situated at the bottom. Methods to calculate the rate constants from experimental data are given. (auth)

39006 PROGRESS ON THE PCUT PROGRAM. Orsenigo, Giuseppe; Cambi, Silvano (Comitato Nazionale per l'Energia Nucleare, Rome, Italy). 42p. (CONF-660524-9). ORAU. Gmelin, AED-CONF-66-104-10.

From 2nd International Thorium Fuel Cycle Symposium, Gatlinburg, Tenn.

Development of the PCUT plant for processing fuels base based on Th and U and their compounds is reviewed. The facility construction status is discussed along with data on larger capacity systems, and research progress. (J.R.D.)

ENGINEERING

General

39007 (AD-636914) RESISTANCE OF TUBULAR STRUCTURES TO DYNAMIC LOADING. Takahashi, S. K.; Gates, W. E.; Benuska, K. L. (Naval Civil Engineering Lab., Port Hueneme, Calif.). July 1966. 208p. (R-463). CFSTI $6.00 cy, $1.25 mn.

Static and dynamic experimental investigations were conducted to validate the NFEC computer program used to predict the behavior of microwave towers subjected to blast loading. Five small-scale towers representative of the prototype were made of composite sheet steel and microconcrete. The inside and outside diameters were 10.7 and 12.4 inches, respectively, and the height was about 39 inches. The following tests were conducted: static and dynamic tests on steel and concrete specimens; static tests on a simply supported tubular beam and on a cantilever model; and dynamic tests on three model towers — free-vibration tests, base-acceleration shock-pulse tests on a vibration machine, and air-blast tests in a 6-foot shock tube. The failure mode for the statically loaded beam and cantilever tower was of the same type as for the dynamically loaded cantilever tower: a semicircular bulge occurred in the inside and outside steel cylinders at the location of maximum moment in the compression zone. Models tested in the shock tube failed at peak overpressures of 44.4 psi. The model tests showed the NFEC computer program can predict the behavior of small cantilever towers under different types of dynamic loading, thus increasing the level of confidence in the program's prediction of strength for the prototype tower. (auth)

• **39008** (SWRI-1228-8-24) FUNDAMENTAL INVESTIGATION OF LIQUID-METAL LUBRICATED JOURNAL BEARINGS. Quarterly Technical Report No. 7, April 1–July 1, 1966. Report No. RS-487. Burton, R. A.; Hsu, Y. C. (Southwest Research Inst., San Antonio, Tex. Dept. of Aerospace Propulsion Research). July 1, 1966. Contract AT(11-1)-1228. 40p. Dep. mn. CFSTI $2.00 cy, $0.50 mn.

Numerical techniques, developed in this program for analysis of finite bearings, are shown to apply to both laminar and turbulent films. Comparisons with exact solutions for tilted pads in laminar flows confirm the accuracy of the approach. Data on leading-edge pressure for tilted pads in the large-scale turbulence apparatus are summarized, and shown to yield to correlation in terms of a leading-edge stagnation pressure. When this relationship is applied in tilted pad performance calculations, negative leading-edge pressure is predicted for small tilt angles, and the accompanying center of pressure movement is such as to be associated with instability in pivoted pad applications. (auth)

•**39009** (UCRL-14944) SIGNIFICANCE OF THERMAL EFFECTS IN MANUFACTURING AND METROLOGY. McClure, Eldon Ray (Lawrence Radiation Lab., Univ. of California, Livermore). June 24, 1966. Contract W-7405-eng-48. 17p. Dep. mn. CFSTI $1.00 cy, $0.50 mn.

A survey shows that errors induced in machining and gaging by thermal influences are having a technological and economical impact on the American machine tool industry. The user is often unaware of the actual extent of his own problems since he does not have convenient checking procedures. Success in the attainment of precision machining is at present heavily dependent on the skill of the operator. Increased use of numerically controlled machine tools will force a more methodical effort to overcome thermal problems. (auth)

39010 MAGNETOHYDRODYNAMIC INSTABILITIES IN AN ELECTRICAL EXPLOSION. Abramova, K. B.; Valitskii, V. P.; Vandakurov, Yu. V.; Zlatin, N. A.; Peregud, B. P. (Ioffe Inst. of Physics and Tech., Leningrad). Dokl. Akad. Nauk SSSR, 167: 778-81(Apr. 1, 1966). (In Russian).

The disintegration mechanism of an electrically exploded conductor was investigated experimentally by the method of pulse x-raying. The arrangement made it possible to obtain four exposures of 0.1 to 0.2 μsec during each experiment at selected instants from the beginning of current flow through the wire. Copper, tungsten, molybdenum, and lead wires and a thread of liquid lead were investigated. The data from the experiments show that two types of instabilities develop in the conductor which deform it and lead to its breakup into numerous parts. During the prethreshold period, a helical instability was observed, which was followed by a constrictive instability accompanying the actual explosion. (M.O.W.)

39011 STUDY OF THE MAGNETIC FIELD DISTRIBUTION IN THE USEFUL REGION OF A MULTIPOLAR MAGNETIC LENS. Audoin, Claude (Faculte des Sciences, Orsay, France). Rev. Phys. Appl., 1: No. 1, 2-10(Mar. 1966). (In French).

Based on the hypothesis that the poles are equipotential, expressions leading to the determination of the magnetic-flux density in the useful region of the multipolar magnetic lens iron-gap was established as well as the magnetic flux across the poles. These calculations concern the case where the poles show a cross section, whose profile consists of an arc of a circle tangential to the sides of an angle whose apex is on the axis of the lens. Numerical results are given for quadripolar, hexapolar and octopolar lenses. (auth)

39012 METHODS AND DEVICES FOR DETERMINING THE MEAN RADIUS OF PORES IN MICROPOROUS BARRIERS. Gremion, Robert (to Commissariat a l'Energie Atomique). U. S. Patent 3,256,732. June 21, 1966. Filed Nov. 13, 1962.

In a method for determining the mean radius of pores in a microporous barrier, a gas is delivered under constant conditions through a sound nozzle into one of the compartments of a confined space divided into two compartments by the barrier. The gas flows through the barrier into the other compartment which is closed. The prevailing pressures P_1 and P_2 are measured at two different but closely spaced instants of time to determine two different values of the half-sum $\bar{p}$ of these pressures. At two different instances, the value of the difference Δp between the pressure P_1 and P_2 is measured, and the value of the quantity $K = a/b$, which is equal to the mean radius of the pores, is deducted from the $\bar{p}$ and the Δp values. The K is a constant depending on the nature of the gas, the temperature, and the two constants a and b interrelated by the relation $1/\Delta p = w\bar{p} + f$. (B.L.M.)

39013 METHOD AND ARRANGEMENT FOR BURNING A FUEL CONTAINING HYDROGEN AT A VERY HIGH TEMPERATURE. Bernstein, Gustave (to Activatom). U. S. Patent 3,254,485. June 7, 1966. Priority date Nov. 6, 1962, Switzerland.

A method for burning a fuel containing hydrogen at very high temperatures consists of mixing the hydrogen with either deuterium or deuterium hydride, subjecting the mixture to thermal activation at a temperature ranging from 3000 to above 4000°C, and subjecting the activated mixture to the action of a combustion-supporting agent fed in countercurrent relation to the mixture. The thermal activation may be achieved by either heat produced by the combustion of fluorine burning with the combustive mixture or by an arc carrying a high density current. (B.L.M.)

Applications of Nuclear Explosions

39014 (TID-23184) APPLICATION OF NUCLEAR EXPLOSIVES TO CREATE UNDERGROUND GAS STORAGE RESERVOIRS. Progress Report. Atkinson, C. H.; Ward, Don C. (Bureau of Mines, Bartlesville, Okla. Bartlesville Petroleum Research Center). Jan. 1966. 18p. Dep. mn. CFSTI $1.00 cy, $0.50 mn.

The use of nuclear explosives to create underground gas storage reservoirs in impermeable rock appears technically feasible. Economic feasibility depends on the need for storage where there are no depleted oil and gas reservoirs, aquifers that can be located and developed relatively inexpensively, or salt deposits suitable for solution cavities. Storage cavities created with nuclear explosives offer a potential saving over mined cavities and liquifying natural gas storage. Areas in the U. S. meeting the above criteria for economic feasibility appear to be plentiful. If required, decontamination of nuclear storage cavities appears practicable using commercially available gas processing equipment. (R.C.K.)

39015 (UCRL-14877) ECONOMICS OF NUCLEAR EXPLOSIVES IN DEVELOPING UNDERGROUND GAS STORAGE. Witherspoon, Paul A. (Lawrence Radiation Lab., Univ. of California, Livermore). July 29, 1966. Contract W-7405-eng-48. 30p. Dep. mn. CFSTI $2.00 cy, $0.50 mn.

In an appropriate geologic setting, nuclear explosives can create underground chimneys with a wide range in storage capacity. Under optimum conditions, the gas capacity is of the order of 10,000 MCF per kt of yield. This assumes a maximum pressure equal to hydrostatic, but higher pressures should also be possible. A nuclear chimney has the distinct advantage that one can produce gas over a very wide range of flow rates with essentially the same equipment. Flow rates of 10,000 to 500,000 MCFD have been investigated, and optimum investments costs using a 50-kt explosive range from $2.00 to $4.00 per MCF of working gas. At a given flow rate, costs are essentially inversely proportional to the yield of the explosive. Optimum depths for nuclear explosives will probably range from 2000 to 4000 ft. (auth)

Facilities and Equipment

Refer also to abstract 38835.

39016 (COO-818-94) DEEP LAB CONFERENCE, JOHANNESBURG, SOUTH AFRICA, OCTOBER 12, 1965. Reines, Frederick (Case Inst. of Tech., Cleveland, Ohio). Oct. 1965. Contract AT(11-1)-818. 41p. (CONF-651078). Dep. mn. CFSTI $2.00 cy, $0.50 mn.

The usefulness to neutrino and cosmic ray research of a very deep underground laboratory housed in a spherical cavity 100 feet in diameter and 15,000 feet below the surface is described. It appears that the two major problems in providing such a location, i.e., temperature and mechanical strength, can be solved within existing technology. Various locations in the United States and South Africa which seem most suitable for such a laboratory are mentioned and the merits of locating below an existing mine, e.g., Anglo-American's Western Deep Levels west of Johannesburg, are discussed. The estimated cost of the laboratory ranged from 4 to 40 million dollars and the time for construction ranged from under two to eight years, depending on the location. (auth)

39017 (DP-1053) NONDESTRUCTIVE TEST OF CARBON BEDS FOR REACTOR CONFINEMENT APPLICATIONS. Progress Report, October 1964-January 1966. Muhlbaier, David R. (Du Pont de Nemours (E. I.) and Co., Aiken, S. C. Savannah River Lab.). June 1966. Contract AT(07-2)-1. 30p. Dep. mn. CFSTI $2.00 cy, $0.50 mn.

A nondestructive in-place test for detecting leaks in a bank of installed carbon beds with Freon-112 tracer was developed by the Savannah River Laboratory and demonstrated in the reactor confinement facilities at the Savannah River Plant. Leakage flow (flow that bypasses the carbon) of 0.01% of the total air flow through the beds is detected readily. Installed carbon beds with about 2 years exposure to exhaust air flow in the confinement system were evaluated successfully with the test. Standardization of the test is in progress for general application to in-place testing of carbon beds. (auth)

39018 (DP-MS-66-46) IN-PLACE NONDESTRUCTIVE LEAK TEST FOR IODINE ADSORBERS. Muhlbaier, D. R. (Du Pont de Nemours (E. I.) and Co., Aiken, S. C. Savannah River Lab.). July 13, 1966. Contract AT(07-2)-1. 24p. (CONF-660904-4). Dep. mn. CFSTI $1.00 cy, $0.50 mn.

For Presentation at 9th Air Cleaning Conference, Boston.

A nondestructive in-place test for detecting leaks in a bank of installed carbon beds with Freon-112 tracer was developed by the Savannah River Laboratory and demonstrated in the reactor confinement facilities of the Savannah River Plant. Leakage flow (flow that bypasses the carbon) of 0.01% of the total air flow through the beds is detected readily. Installed carbon beds with about 2 years exposure to exhaust air flow in the confinement system were evaluated successfully with the test. An equation was also developed that correlates the conditions for F-112 testing of carbon beds of different design. (auth)

39019 (GEAP-5149) RADIAL VANE STEAM SEPARATOR DEVELOPMENT. Seventh Quarterly Report, January-March 1966. Moen, R. H. (General Electric Co., San Jose, Calif. Atomic Power Equipment Dept.). Apr. 1966. Contract AT(04-3)-189. 98p. (EURAEC-1656). Dep. mn. CFSTI $3.00 cy, $0.75 mn.

Work Performed under United States-Euratom Joint Research and Development Program.

Two test programs to determine limiting nozzle-and-vane pair steam-water flows and to measure carryunder distribution in the wall flow in air-water tests were started. The results indicate that nozzle-and-vane pair capacity exceeds the needs of boiling water reactors, and that volumetric air carryunder is remarkably low. These findings indicate the successful application of the radial vane steam separator to boiling water reactors in general, and to the KRB reactor in particular. Further testing of the FCVR-4 in air-water was carried out to determine the effect of wall cylinder diameter and lower vortex water level on performance. Tests showed continued good performance of the model separator. Tests to determine angle of flow of the vane jet were extended, and air-water slip velocities were determined. Results of all the tests were reviewed, and the conclusion was reached that an in-reactor test should be proposed. A preliminary, rough design of a radial vane steam separator for the KRB reactor has been prepared. A study was made of the feasibility of using a number of small radial vane steam separators rather than one large one. This study indicated that only for large reactors (about 24-foot vessel diameter) would this be feasible. For reactors of this size, total flow could be increased by about one third using seven smaller separators. (F.L.S.)

39020 (K-1632(Pt.2)) A GRAVIMETRIC GAS FLOW STANDARD. PART II. PERFORMANCE AND EVALUATION. Collins, W. T.; Selby, T. W. (Oak Ridge Gaseous Diffusion Plant, Tenn.). Apr. 15, 1966. Contract W-7405-eng-26. 78p. (CONF-660902-1). Dep. mn. CFSTI $3.00 cy, $0.75 mn.

For Presentation at American Society of Mechanical Engineers Symposium, Pittsburgh, Pa.

Performance and evaluation of the Gravimetric Gas Flow Standard are reported. Precision estimates based on the standard deviation of linear fits to flow versus pressure relationships for critically operated flow elements were ±0.035% over the range of 0.05 to 1725 grams of dry air per minute. The accuracy of the GGFS was estimated from a rigorous analysis of all known sources of uncertainty. In terms of the standard deviation the uncertainty was calcu-

lated to be ±0.15% for the flow rate range of 0.06 to 0.3 grams of dry air per minute, and ±0.060 to ±0.065% for the flow rates from 0.3 to 1650 grams per minute. The principal sources of uncertainty are discussed and methods proposed for reducing their effect. It was concluded that the gravimetric method has a potential precision significantly less than ±0.10% standard deviation; and that the concept could be extended for calibrating gas flow rates of several thousand standard cubic feet per minute. (auth)

39021 (K-1665) STUDY OF THE PERIPHERAL COMPRESSOR. Cates, Phillip Stephen (Oak Ridge Gaseous Diffusion Plant, Tenn.). Aug. 26, 1966. Contract W-7405-eng-26. 163p. Dep. mn. CFSTI $5.00 cy, $1.00 mn.

The study had three objectives: (1) determine the "state of the art" by conducting a thorough survey of the available literature on peripheral pumps and compressors; (2) analyze the published theories for incompressible flow and propose a hypothesis for performance in compressible flow; and (3) obtain experimental data on gases for correlation with respect to the proposed hypothesis. The theories for incompressible flow operation were summarized and studied with regard to their limitations for application to compressible flow operation. Fundamental laws of continuity, thermodynamics, and motion for compressible flow were applied to control volumes in the peripheral compressor in the form of integral vector relations. From these equations, from experience in compressible flow problems, and from published literature on centrifugal compressor studies, qualitative predictions for peripheral compressor performance at high impeller Mach numbers were made. Functional relationships of dimensionless parameters were derived for correlation of experimental data measured in compressible flow. Data were obtained on an experimental compressor at speeds from 5000 to 14,000 rpm in gases with molecular weights of 4 to 400. In addition to the effects of Mach number, the influence of channel, impeller, and nozzle geometries and impeller-to-casing clearances were investigated. Generally, the experimental data confirmed the qualitative predictions for compressible flow operation. The peripheral compressor operated stably at all speeds and flows but exhibited some limitations at high Mach number operation. Methods to improve performance, particularly at high impeller Mach numbers, were developed, and significant advancement of design information was achieved. (auth)

39022 (NAA-SR-11943) AN ANALOG COMPUTER STUDY OF THE DYNAMICS OF THE MRP COMBINED ROTATING UNIT SHAFT-BEARING SYSTEM. Bick, J. H.; Presson, A. G. (Atomics International, Canoga Park, Calif.). July 15, 1966. Contract AT(11-1)-Gen-8. 76p. Dep. mn. CFSTI $3.00 cy, $0.75 mn.

A mathematical model formulated for the Combined Rotating Unit shaft-bearing system is discussed. The model includes the effects of shaft imbalance, magnetic rotational load, unidirectional load, and spin speed on the shaft dynamics. The bearing forces include hydrodynamic, hydrostatic, and squeeze film forces. It is possible to vary independently all bearing parameters as well as supply pressure. A short parameter survey of the Combined Rotating Unit operating conditions and of the stability envelope was completed, based on the mathematical model. The results are most encouraging as regards their correlation with experimental data. The theory and assumptions used in the derivations are given. Recommendations are made for improvements and suggested future investigations. (auth)

39023 (NAA-SR-11952) SNAP-10A EXPANSION COMPENSATOR. Final Report. Stone, L. R.; Whitaker, W. D. (Atomics International, Canoga Park, Calif.). July 15, 1966. Contract AT(11-1)-Gen-8. 81p. Dep. mn. CFSTI $3.00 cy, $0.75 mn.

The SNAP 10A Space Nuclear Power Unit was successfully flight tested utilizing expansion compensator units (ECUs) to absorb the NaK coolant thermal expansion and to pressurize the coolant system with a void-free device. An expansion compensator design utilizing a welded bellows assembly was extensively tested to ensure conformance with the SNAP 10A operational and reliability requirements. A unique feature of the ECU design was a secondary containment housing which would have permitted continued system operation at design conditions in the event of a bellows failure. The bellows assembly was fabricated from AM-350 (SCT-850) precipitation hardened steel foil. Component development and qualification tests were successfully performed. Expansion compensators were also installed on two SNAP 10A ground test systems which met all test objectives. A total of 71,200 hr at elevated temperatures was accumulated during the development and qualification testing of the ECUs. (auth)

39024 (ORNL-TM-1268) ORNL FACILITIES CAPABLE OF CONTRIBUTING TO PLUTONIUM FUEL CYCLE DEVELOPMENT. Ullmann, J. W. (Oak Ridge National Lab., Tenn.). Nov. 1965. Contract W-7405-eng-26. 77p. Dep. mn. CFSTI $3.00 cy, $0.75 mn.

A compilation was made of brief descriptions of ORNL facilities that could be used to support Pu fuel cycle development. The capability and experience of each facility is summarized with emphasis placed on handling of Pu and other high alpha materials. (auth)

39025 (ORO-2980-12) AN ON-LINE NUCLEAR ANALYSIS FACILITY. Interim Technical Report No. 3. Martin, Troy C.; Blake, Kenneth R.; Morgan, Ira Lon; Parker, C. Varren Jr.; Sieberg, Robert (Texas Nuclear Corp., Austin). June 15, 1966. Contract AT(40-1)-2980. 59p. Dep. mn. CFSTI $3.00 cy, $0.75 mn.

The description and operation of a nuclear analysis system for bulk materials is given. The facility includes a bulk material handling system and an automated neutron generator housed in a dust-ignition proof area, and a data analysis system with background subtraction and spectral stripping capabilities. A description of a simple liquid loop system is also presented along with the results obtained using this system. Preliminary results of on-line measurements of prompt and delayed gamma rays of a particular coal and bauxite are shown. (auth)

39026 (UCRL-14660(Rev.1)) HIGH-TEMPERATURE TESTING AND EVALUATION OF GRAPHITE HELICAL-SCREW EXPANDERS AND COMPRESSORS. Wells, W. M.; Hanner, D. W.; McElroy, J. L.; Robinson, E. (Lawrence Radiation Lab., Univ. of California, Livermore). July 6, 1966. Contract W-7405-eng-48. 10p. (CONF-660916-1). Dep. mn. CFSTI $1.00 cy, $0.50 mn.

From 1st Nonconventional Energy Conversion Applications Conference, Los Angeles, Calif.

A graphite expander, utilizing intermeshing helical rotors and following concepts of Lysholm and the Svenska Rotor Maskiner firm, is proposed for potential use with inert gas Brayton cycles. Two demonstration assemblies were tested. Each assembly consisted of a graphite expander and an identical compressor. Each assembly was installed in an argon atmosphere furnace where the motor-driven compressor provided pressurized argon to drive the expander. The graphite-on-graphite sliding bearings used were adequate for demonstration purposes but probably not for application. Work is under way on graphite roller and gas bearings. In the first assembly the compressor failed catastrophically due to rotor dragging. This defect was corrected in the second assembly which ran for 274 hr at furnace temperatures between 2350 and 2730°F before voluntary shutdown. Expander inlet temperatures are estimated to have exceeded 2900°F. Speeds to 14,100 rpm in the compressor and efficiencies to 37% in the expander were achieved. Shaft power to the compressor exceeded 10 hp and from the expander approached 1 hp. Pressure ratios in excess of 1.5 were achieved. For space application, expander specific weights below 1 lb/electrical kw appear plausible. (auth)

39027 (Y-DA-1287) POWER REQUIREMENTS FOR SINGLE-POINT TOOLS. Blanks, J. R. (Union Carbide Corp., Oak Ridge, Tenn. Y-12 Plant). Aug. 4, 1966. Contract W-7405-eng-26. 12p. Dep. mn. CFSTI $1.00 cy, $0.50 mn.

A knowledge of the power requirements and the forces acting on a tool is desirable in the design or selection of machine tools. A three-component lathe dynamometer was used to determine the forces acting on a single-point cutting tool while maching cast depleted uranium. Graphs and equations have been developed that show the relation between the tool forces and power required at the tool point and the feed rate and depth of cut. The resultant force varies from approximately 10 pounds for very light cuts to more than 1200 pounds for heavy cuts. (auth)

39028 TECHNOLOGY FOR LARGE RANKINE CYCLE SPACE POWER SYSTEMS. Zipkin, Morris A. (General Electric Co., Cincinnati). J. Spacecraft Rockets, 3: 1106-12(July 1966).

Some significant results have been obtained from technology programs requisite to the development of large Rankine cycle space power systems. It now appears that materials of sufficient nigh-temperature strength, and compatible with alkali metals, will be available for space power systems structures within a normal development time span. Also, the feasibility of operating a turbine on high-temperature potassium vapor has been effectively demonstrated; extensive experimental results in alkali metal heat transfer now permit the design of compact, lightweight boilers and condensers with specific weights of less than 1 lb/kw for the boiler and ½ lb/kw for the condenser; electromagnetic pumps are emerging as the preferred choice for flight-weight alkali metal systems, and such pumps can be demonstrated competitive, in specific weight, with canned motor pumps for the boiler feed application; and a vapor chamber radiator concept currently under development promises important weight and reliability advances in radiators for Rankine cycle power systems. (auth)

39029 INSTRUMENT FOR VARYING ANGLE OF INCIDENCE BETWEEN ION BEAMS AND A SPECTROMETER. Langley, Robert A. (Cambridge Research Labs., Bedford, Mass.). J. Spacecraft Rockets, 3: 1297-9(Aug. 1966).

An instrument is described for continuously varying the angle of incidence between an ion beam and the axis of an r-f quadrupole mass spectrometer from 0–90°. The shape and size of the spectrometer curve can be changed by varying almost any of the parameters associated with the r-f quadrupole mass spectrometer or the plasma source. For almost all conditions observed, the spectrometer response decreased only slightly in going from 0–10°, but decreased by a factor of almost 25 in going from 10–30°; whereas in going from 30–90°, the spectrometer response remained almost constant. (R.C.K.)

39030 INTERMEDIATE SPEED ZONAL CENTRIFUGES, TYPE B ROTORS (Engineering Materials). (Oak Ridge Gaseous Diffusion Plant, Tenn. Oak Ridge National Lab., Tenn.). (CAPE–1415).

9 drawings.

The centrifuge is designed to operate at 40,000 rpm when filled with 66% sucrose. It can remove fragile particles from culture fluids and may be used with pathogenic materials. (For details see TID-4100) (F.S.)

39031 EXTENDED RANGE WHITE-LIGHT INTERFEROMETER (Engineering Materials). (Union Carbide Corp., Oak Ridge, Tenn. Y-12 Plant). (CAPE–1451).

3 drawings.

This device combines white-light interferometry with an accurate positioner in a measuring system for optically reflective surfaces. More precise measurements can be made by using two systems and calculating the differences. (For details see TID-4100) (F.S.)

39032 SINGLE TRANSDUCER DIFFERENTIAL MEASURING DEVICE (Engineering Materials). (Union Carbide Corp., Oak Ridge, Tenn. Y-12 Plant). (CAPE–1450).

1 drawing.

The device allows diameter measurements on parts in machine tools without errors from uncontrolled gaging and operator bias. The device is mounted so that it is sensitive to changes in diameter but insensitive to deflections of equal magnitude. (For details see TID-4100) (F.S.)

39033 LOW PRESSURE CONDUCTIVITY FURNACE (Engineering Materials). (Los Alamos Scientific Lab., Univ. of California, N. Mex.). (CAPE–1431).

9 drawings.

The design allows necessary pre-experimental preparations to be completed in a convenient manner before the furnace is raised to the desired temperature. The furnace operates between 800 and 2700°C at or below atmospheric pressure. (For details see TID-4100 Suppl. 35) (F.S.)

39034 HIGH TEMPERATURE FURNACE (Engineering Materials). (Los Alamos Scientific Lab., Univ. of California, N. Mex.). (CAPE–1430).

8 drawings.

A furnace is described which operates at temperatures approaching 3000°C. It is constructed so that temperatures may be read visually. (For details see TID-4100 Suppl. 35) (F.S.)

39035 MAGNETIC GAS PUMP (Engineering Materials). (Goodyear Atomic Corp., Piketon, Ohio). (CAPE–1445).

9 drawings.

This pump, containing no seals, glands, or packings, circulates gases such as UF_6 and HF in a laboratory system. Its capacity is ~13.5 l/min at 1 atm absolute. The pump operates in a vertical position with a 6-in. stroke. (For details see TID-4100) (F.S.)

39036 BAG PASSOUT SYSTEM (Engineering Materials). (Lawrence Radiation Lab., Univ. of California, Berkeley). (CAPE–1413).

65 drawings.

A system used in passing out sealed plastic sleeves or bags from a multicurie-level processing enclosure is described. A welder-cutter is used for sealing the bags. (For details see TID-4100 Suppl. 35) (F.S.)

39037 ZONAL ROTORS, TYPES B XIV AND B XV (Engineering Materials). (Oak Ridge National Lab., Tenn.). (CAPE–1426).

15 drawings.

Two simplified zonal centrifuge rotors are described. Removable seals permit loading and unloading of gradient and samples at low speeds. The rotors operate at 22,000 to 36,000 rpm. (For details see TID-4100 Suppl. 35). (F.S.)

39038 ELECTRON PROBE ANALYZER (Engineering Materials). (Lawrence Radiation Lab., Univ. of California, Livermore). (CAPE–1447).

88 drawings.

Shielding and modifications of an electron microscope permit the analysis of radioactive materials with gamma intensities as high as 100 R/hr. Interlocking lead blocks provide biological shielding. Remote sample loading and transfer equipment, laboratory layout, and the electrical and piping schematics are also described. (For details see TID-4100 Suppl. 36). (F.S.)

39039 ION SOURCE HAVING PLASMA CONTROL MEANS. Wittkower, Andrew B. (to High Voltage Engineering Corp.). U. S. Patent 3,265,918. Aug. 9, 1966. Filed June 18, 1962.

An ion source which delivers directed high current ion beams with a current density >500 mamp/cm^2 and demonstrates improved focusing capabilities is described. A source aperture electrode with 2 aperture plates provide optimum beam divergence and intensity control. (F.S.)

39040 IMPROVEMENTS IN OR RELATING TO CONTAINERS FOR RADIOACTIVE MEMBERS. Power, Derek John; Ford, John Brian Malpas; Pearson, John Edwin James (to Tech Del Ltd.). British Patent 1,035,057. July 6, 1966. Filed Oct. 25, 1963.

A container for radioactive members consists of two shielding members, one inside the other, and a cap securable to the outer container for closing an opening in the first. The inner shield member can be rotated within the outer from a first position in which the entrance to a hole in the surface of the second shield member is masked

by the first shield member to a position in which the hole is exposed, and vice versa. The cap closes the entrance when the second shield member is disposed in the second position. First locking means are arranged to lock the second shield member in the first position when the cap is off the container. When the cap is on the container, it is operable to release the first locking means to permit rotation of the second shield member from the first position to the second position. A second locking means is provided to lock the cap on the container whenever the cap is operated to free the second shield member for rotation. (B.L.M.)

39041 APPARATUS WITH VERTICAL AND LATERAL MOVABLE MEANS FOR HANDLING GROUPS OF RADIOACTIVE SAMPLES. Frank, Edmund; Polic, Edward F. (to Packard Instrument Co., Inc.). U. S. Patent 3,257,009. June 21, 1966. Filed Apr. 15, 1963.

A transfer system is provided that is suitable for use with a radioactivity level measuring apparatus for delivering and removing discrete groups, each containing a number of samples, to and from a sample indexing mechanism. The device also permits storage of a number of groups of samples in spaced stacked relation so that each group can be readily moved from its storage point to a point of use upon demand. (B.L.M.)

39042 RADIOACTIVITY LEVEL DETECTING APPARATUS FOR SAMPLES CARRIED BY PORTABLE TRAYS WITH TRANSFER AND INDEXING MEANS FOR THE TRAYS. Packard, L. E.; Munn, Alfred A.; Smith, Roy E.; Polic, Edward F. (to Packard Instrument Co., Inc.). U. S. Patent 3,257,561. June 21, 1966. Filed Apr. 15, 1963.

An apparatus and method are described for an entirely automatic operation to handle trays of samples, count and record the radioactivity of the samples in a certain order or in any order desired. A certain sequential order of sample counting can be interrupted and a sample interjected with the sequential order then being resumed. The samples to be counted are contained in a sample tray of specified design, and handling and orienting mechanisms for the specific sample trays are provided. (B.L.M.)

39043 MAGNETOHYDRODYNAMIC POWER PLANT. Kantrowitz, Arthur R.; Brogan, Thomas R. (to Avco Corp.). U. S. Patent 3,264,501. Aug. 2, 1966. Filed Feb. 15, 1960.

A magnetohydrodynamic power plant demonstrates high operating efficiency and has high peak surge capability for meeting power requirement during periods of high demand. The power plant comprises several interdependent components for producing oxygen as a combustion supporting medium in which pulverized coal is burned to produce high temperature plasma to generate power. Part of the power is used to separate oxygen from ambient air. (F.S.)

39044 RADIOACTIVE SAMPLE CHANGING AND MEASURING APPARATUS. Sinila, Alexander; Soderquist, Charles E. Jr.; Meier, Walter (to Nuclear Data, Inc.). U. S. Patent 3,265,897. Aug. 9, 1966. Filed Nov. 5, 1962.

The apparatus automatically moves radioactive samples in and out of a magazine for counting by a gas flow detector. A paper tape record is provided by a recording system. The equipment is used in biological, medical, and radiochemistry laboratories. (F.S.)

Heat Transfer and Fluid Flow

See also PHYSICS – Fluid Physics and Thermodynamics

39045 (AEEW-M-650) THE MEASUREMENT OF RADIAL VOIDAGE DISTRIBUTION IN TWO-PHASE FLOW BY ISOKINETIC SAMPLING. Shires, G. L.; Riley, P. J. (Atomic Energy Establishment, Winfrith (England)). 1966. 52p. Dep. BIS $1.40. HMSO 7s. 0d.

In the study of two-phase flow there is a need for an instrument which will measure the detailed distribution of the phases and their local velocities. A probe is described through which a two-phase sample is withdrawn at such a rate that the pressure just inside the probe orifice is equal to the local static pressure in the stream. Theoretically, when the density of the gas is small relative to that of the liquid, the superficial velocity of the liquid on entering the probe is equal to the local value in the stream, i.e., the probe samples isokinetically in terms of superficial water velocity, and the voidage of the sample is equal to the local voidage in the stream. Both characteristics were confirmed experimentally in air/water flowing upwards for a 1-inch diameter tube at atmospheric pressure over a range of mean voidage from 0.1 to 0.8. Although theoretically it is possible to determine voidage from impact pressure, this alternative method was found to be unsatisfactory because of accumulation of errors and probe interference. (auth)

39046 (AEEW-R-477) BURNOUT IN A CHANNEL WITH NON-UNIFORM CIRCUMFERENTIAL HEAT FLUX. Lee, D. H. (Atomic Energy Establishment, Winfrith (England)). Mar. 1966. 24p. Dep. BIS $0.80. HMSO 4s. 0d.

Burnout experiments are reported for uniform flux and circumferential flux tilt (maximum/average flux about 1.25) with tubes and annuli, all the experiments having uniform axial heating. These show similar results, the burnout power with flux tilt being within 10% of that with uniform flux. For the same mean exit steam quality, the local maximum flux is higher than the predicted burnout value and generally a better prediction is obtained using the average flux. (auth)

39047 (AERE-M-1739) PRESSURE-DROP CHARACTERISTICS FOR THE FLOW OF SUBCOOLED WATER AT ATMOSPHERIC PRESSURE IN NARROW HEATED CHANNELS. PART I. Forgan, R.; Whittle, R. H. (Atomic Energy Research Establishment, Harwell (England)). May 1966. 83p. Dep. BIS $2.60. HMSO 13s. 0d.

Measurements were made of the pressure-drop flow characteristics for subcooled water in narrow heated channels, to provide data on subcooled-boiling pressure drop and in particular to locate the minimum in the characteristic curves. The experiments were done on a single channel 24 in. long × 1.0 in. × 0.127 in. Coolant velocities ranged from 6 to 24 fps and heat fluxes from 82 to 250 watts/cm^2. For this limited range of parameters, it was found that the minimum in the pressure-drop/flow curves always occurred when the temperature rise of the coolant in the channel was 0.8 (saturation temperature at outlet – inlet temperature). (auth)

39048 (GEAP-5115) IMPROVED HEAT TRANSFER PERFORMANCE WITH BOUNDARY LAYER TURBULENCE PROMOTERS. Sutherland, Wm. A. (General Electric Co., San Jose, Calif. Advanced Products Operation). June 1966. Contract AT(04-3)-189. 25p. Dep. mn. CFSTI $1.00 cy, $0.50 mn.

A substantial improvement in forced-convection heat transfer conductance is required for the development of advanced steam-cooled and gas-cooled power reactor systems. Boundary layer turbulence promoters on the heated surfaces are of great interest for these systems because of the large increase in the heat transfer performance which can be attained. The performance of boundary layer turbulence promoters in arrays of parallel rods is established. Discrete two-dimensional roughness elements, in the form of small fins transverse to the flow, are investigated experimentally to establish the effect of promoter height and promoter spacing. A general correlation is presented which then permits optimization of heat transfer performance. (auth)

39049 (UCRL-14754) TRUMP: A COMPUTER PROGRAM FOR TRANSIENT AND STEADY-STATE TEMPERATURE DISTRIBUTIONS IN MULTIDIMENSIONAL SYSTEMS. Edwards, Arthur L. (Lawrence Radiation Lab., Univ. of California, Livermore). Feb. 24, 1966. Contract W-7405-eng-48. 151p. Dep. mn. CFSTI $5.00 cy, $1.00 mn.

The TRUMP computer program was developed to solve

problems involving transient and steady state temperature distributions in multidimensional systems with arbitrary geometric configurations, initial conditions, boundary conditions, and physical properties. The mathematical method uses a unique combination of forward and backward difference equations to achieve fast, efficient, and accurate solutions. The program is written in separate versions for the IBM-7094, CDC-3600, and CDC-6600. Problems include heat transfer by conduction, free and forced convection, surface radiation, and mass flow. Heat may be produced or absorbed by internal heat sources and sinks, phase changes, and chemical reaction. The properties controlling these effects may be tabulated functions of time or temperature. Input data are organized to be as simple and clear as possible, providing maximum compactness, flexibility, and ease of modification. Optional forms of output include temperature distributions, complete heat balance information, values of variable properties, and a breakdown of the various modes of heat transfer and production at specified time intervals. Graphical output includes plots of temperature vs position at specified time intervals, temperature vs time at specified positions, and position vs time at specified temperatures. Accuracy is determined by the degree to which the system is subdivided into nodes, or volume elements, and by a specified maximum allowable temperature change per time increment. Criteria for ending a problem include exceeding specified time and temperature limits, accomplishment of steady state, and exceeding specified limits on the number of time increments and machine time. (auth)

39050 (UCRL–16535) CONVECTIVE TRANSFER PROCESSES IN LAMINAR GAS-LIQUID CHANNEL FLOW. Byers, Charles Harry; King, C. Judson (Lawrence Radiation Lab., Univ. of California, Berkeley). May 20, 1966. Contract W-7405-eng-48. 267p. Dep. mn. CFSTI $6.00 cy, $1.25 mn.

Thesis. Submitted by Charles Harry Byers.

Interphase mass transfer was studied experimentally and theoretically for cases where resistance to mass transfer is confined to the gas phase and where control is distributed between phases. A horizontal, rectangular channel of high aspect ratio was built. The gas and liquid phases, which move in stratified laminar flow, are contacted in an 18 in. long test section. The exit streams are analyzed in a gas-liquid chromatograph. A numerical solution was performed of the laminar transport equation for a parabolic velocity profile with a cocurrently moving boundary. Experiments in which pure ethanol was evaporated into two gases, CO_2 and oxygen, showed agreement with this theory within the estimated experimental error of 10%. It may be concluded from this study that cocurrent motion of the interface increases mass transfer. Experiments were carried out with the same fluids in countercurrent flow. Mass transfer is hindered by a flow reversal in the gas phase. A phenomenological model developed for this case correlated the data to within the experimental error of the method. Numerical solutions were performed of two cases of interphase mass transfer. The first is for parabolic velocity profiles in both phases, and the second assumes a parabolic profile in the gas and a constant velocity in the liquid. Experiments were carried out in which ether was evaporated from dilute ethanol solutions into two gases, CO_2 and helium, in cocurrent flow. The experimental results agreed with the first interphase mass transfer solution to within 15% in all cases. Equations for a more simplified model in which the liquid has a constant velocity and the gas velocity varies linearly with distance from the interface were solved analytically. Results of the appropriate interphase experiments agree with this theory. Interphase countercurrent experimental results agree substantially with a model that postulates penetration for the liquid phase and with the aforementioned countercurrent model for the gas phase. A series of cocurrent interphase experiments was made, using water as the solvent. Experimental results were lower than the predicted values by at least a factor of two. The apparent cause of the difficulty was accumulation of surfactants at the interface. Experimental mass-transfer coefficients indicate that the interfacial velocity was about 10 to 20% of the predicted velocity. This was confirmed by visual observation. (auth)

39051 EXPERIMENTAL METHODS FOR THE DIRECT INVESTIGATION OF FLOW PHENOMENA IN PILES OF SPHERICAL BODIES. Bedenig, D.; von der Decken, C. B.; Huendorf, B.; Rausch, W. (Brown Boveri/Krupp Reaktorbau GmbH, Juelich, Ger.). Tech. Mitt. Krupp. Forschungsber., 24: 147-57(July 1966). (In German).

A review of possible methods for directly investigating flow phenomena in piles of spherical bodies is given. The use of the ^{60}Co method is explained. A description and the characteristics of the glass-ball model are included. (F.S.)

39052 BOILING OF LIQUIDS. Nesis, E. I. Usp. Fiz. Nauk, 87: 615-53(Dec. 1965). (In Russian).

Recent research done on the physics of boiling and liquid-vapor phase transitions is summarized. The topics dealt with are the heat exchange mechanisms that operate during boiling and the different types of boiling (nucleate boiling, film boiling, and the intermediate state), including the mechanism of bubble formation and the critical nucleus size. The growth of the bubbles under different boiling conditions is described. Experimental methods for the study of boiling are discussed, including the photographic and acoustic methods. The nature of the sound accompanying the bubbling in heated and boiling liquids is analyzed. The thermodynamics of boiling is discussed and a theory of heat transfer as applied to boiling is developed. This discussion of the kinetics of the boiling process includes a detailed description of the physical process, derivation of a kinetic equation of boiling, and a detailed analysis of the phenomena accompanying boiling in real liquids. The article concludes with a section dealing with the boiling of mixtures and solutions. Orig. art. has: 14 figures and 17 formulas. (ATD)

Materials Testing

Refer also to abstract 39286.

Protective Structures

39053 STRUCTURE FOR ATOMIC BLAST RESISTANCE. Krantz, Frank M. (to U. S. Navy). U. S. Patent 3,266,203. Aug. 16, 1966. Filed May 3, 1963.

A metallic structure designed to withstand high impact loads of blast such as an atomic explosion is described. The structure is fabricated of rectangular panels riveted to column-ribs. The center section of the column-rib is rectangular in cross section while the side sections are triangular in cross section. Panels and column-ribs are connected to form a polygonal enclosure. The enclosure is secured to a floor or deck and covered with a hemispherical top. (F.S.)

39054 PROTECTIVE STRUCTURES FOR CIVILIAN POPULATIONS. Proceedings of the Symposium Held at Washington, D. C., April 19-23, 1965 by the Subcommittee on Civil Defense, National Academy of Sciences–National Research Council. Washington, D. C., National Academy of Sciences–National Research Council, 1965. 367p. (CONF-650415).

Separate abstracts were prepared for 35 of the 37 papers included. One paper was previously abstracted in NSA (19: 34397). The other paper outlined Canadian views on fire-safe shelter design. (G.O.Y.)

For abstracts of individual papers see: 39055–39089.

39055 BLAST AND OTHER THREATS. Brode, Harold (RAND Corp., Santa Monica, Calif.). pp 3-20 of Protective Structures for Civilian Populations. Washington, D. C., National Academy of Sciences–National Research Council, 1965.

A detailed survey of the effects of nuclear weapons in the case of a nuclear attack is presented. Fireball formation, cratering, shock waves, blasts, and consequent fallout are considered along with other related problems such as debris cleanup. (G.O.Y.)

39056 INTENSITY AND DISTRIBUTION OF INITIAL AND RESIDUAL RADIATION. Knapp, Harold (Institute for Defense Analyses, Arlington, Va.). pp 21-30 of Pro-

tective Structures for Civilian Populations. Washington, D. C., National Academy of Sciences–National Research Council, 1965.

A survey of contamination distribution of initial and residual radiation from nuclear weapon explosions is presented. (G.O.Y.)

39057 POSSIBILITIES OF OCCURRENCE OF AREA CONFLAGRATIONS AND FIRESTORMS WITH RESPECT TO FUEL DENSITY. Leutz, Hermann (Federal Ministry for Housing, Urbanization and Land Planning, Bad Godesberg, Ger.). pp 31-7 of Protective Structures for Civilian Populations. Washington, D. C., National Academy of Sciences–National Research Council, 1965.

A survey of the various types, causes, and effects of fires is presented. Some considerations for civilian protection in case of nuclear-weapon caused fires are considered. (G.O.Y.)

39058 TENTATIVE BIOLOGICAL CRITERIA FOR ESTIMATING BLAST HAZARDS. White, Clayton S. (Lovelace Foundation, Albuquerque, N. Mex.). pp 41-54 of Protective Structures for Civilian Populations. Washington, D. C., National Academy of Sciences–National Research Council, 1965.

Blast-induced hazards related to protective structures construction were investigated with animals exposed in above- and below-ground structures subjected to nuclear blast during the field operations carried out at Nevada Test Site in 1953, 1955, and 1957. A summary of these results is presented. Some biological criteria are derived. (G.O.Y.)

39059 FIRE AND NOXIOUS GASES: EFFECT ON INTERNAL ENVIRONMENTS OF PROTECTIVE SHELTERS. Johnson, J. Enoch; Ramskill, Eugene A. (Naval Research Lab., Washington, D. C.). pp 58-64 of Protective Structures for Civilian Populations. Washington, D. C., National Academy of Sciences–National Research Council, 1965.

Data are presented which show conclusively that a fire inside a protective shelter must be considered a serious menace because of the possible lethal effects on humans. The danger factor in a shelter fire is not the depletion of O_2, the evolution of CO_2 or of CO, or the output of noxious vapors and aerosols. The danger factor is the calories of heat released during combustion of as little as one pound of fuel. (G.O.Y.)

39060 GAMMA-RAY STREAMING THROUGH DUCTS. Huddleston, Charles M. (Naval Civil Engineering Lab., Port Hueneme, Calif.). pp 65-84 of Protective Structures for Civilian Populations. Washington, D. C., National Academy of Sciences–National Research Council, 1965.

A review is presented of various papers on experimental determinations of the attenuation of gamma-ray dose within concrete ducts as a function of distance from the radioactive source; on albedo — an important concept in gamma-ray scattering; and on some theoretical approaches to the duct-streaming problem. 32 references. (G.O.Y.)

39061 PROBLEMS OF SHIELDING AGAINST INITIAL RADIATIONS. Spencer, Lewis V. (National Bureau of Standards, Washington, D. C. Ottawa Univ., Kan.). pp 89-94 of Protective Structures for Civilian Populations. Washington, D. C., National Academy of Sciences–National Research Council, 1965.

Some problems of shielding against initial radiations are treated as a whole in order to point out the essential elements in this field within the context of the total shielding effort. (G.O.Y.)

39062 SHIELDING EXPERIMENTS. Chilton, A. B. (Univ. of Illinois, Urbana). pp 95-106 of Protective Structures for Civilian Populations. Washington, D. C., National Academy of Sciences–National Research Council, 1965.

Some shielding experiments, which are designed to check possible calculational errors in current design of shelters, are discussed. (G.O.Y.)

39063 PASSING PARADE OF SHIELDING-ANALYSIS METHODS: A REVIEW OF THE STATE OF THE ART. Farrell, Kenneth G. (Emergency Measures Organization, Ottawa). pp 107-20 of Protective Structures for Civilian Populations. Washington, D. C., National Academy of Sciences–National Research Council, 1965.

The status of shielding analysis methods is reviewed. Various methods and techniques are outlined, and their advantages and disadvantages are discussed. (G.O.Y.)

39064 ICHIBAN: DOSIMETRY PROGRAM FOR NUCLEAR BOMB SURVIVORS OF HIROSHIMA AND NAGASAKI. Auxier, John (Oak Ridge National Lab., Tenn.). pp 121-6 of Protective Structures for Civilian Populations. Washington, D. C., National Academy of Sciences–National Research Council, 1965.

The results of a series of projects on the dosimetry for nuclear bomb survivors at Hiroshima and Nagasaki are discussed. It is shown that shielding factors for Japanese dwellings can now be computed with simple formulas. The spatial and angular distributions of the dose are well defined, and the spectral distributions are crudely known. The normalization of the air-dose curves to the Hiroshima and Nagasaki weapons must yet be accomplished. (G.O.Y.)

39065 FIRE-SAFE SHELTER DESIGN. Degenkolb, John G. pp 129-33 of Protective Structures for Civilian Populations. Washington, D. C., National Academy of Sciences–National Research Council, 1965.

The need for fire-proof shelters is emphasized and criteria for making shelters fire-safe are given. (G.O.Y.)

39066 FIREPROOF SHELTERS WITH SECURED VENTILATING SYSTEMS. Leutz, Hermann (Federal Ministry for Housing, Urbanization, and Land Planning, Bad Godesberg, Ger.). pp 134-8 of Protective Structures for Civilian Populations. Washington, D. C., National Academy of Sciences–National Research Council, 1965.

It is shown that in fireproof shelters, provision must be made for the prevention of dangerous heating from outside fires which can lead to a situation similar to that in an oven. Ventilating systems are discussed and some specifications for preventing external and internal dangers are given. It is concluded that even in firestorm areas, survival appears possible in shelters with secured ventilation systems built according to German specifications. (G.O.Y.)

39067 FIRE-SAFE SHELTER DESIGN: SWEDISH VIEWS. Smitt, Goesta (Kungliga Civilforsvarsstyrelsen, Stockholm). pp 139-45 of Protective Structures for Civilian Populations. Washington, D. C., National Academy of Sciences–National Research Council, 1965.

The fire-safety features of the Swedish shelter designs are discussed. (G.O.Y.)

39068 FOOTINGS FOR PROTECTIVE STRUCTURES. Whitman, Robert V.; Luscher, Ulrich (Massachusetts Inst. of Tech., Cambridge). pp 151-8 of Protective Structures for Civilian Populations. Washington, D. C., National Academy of Sciences–National Research Council, 1965.

The design of footings or spread foundations for buried structures is discussed along with the evaluation of the effects of footing design and footing motion on the response of the structure as a whole. Data on the design of impulsively loaded footings and on the effect of footing response on the structure are synthesized. Some areas of uncertainty are indicated and areas of needed further research are identified. (G.O.Y.)

39069 ENGINEERING APPROACH TO PROTECTIVE STRUCTURES. FitzSimons, Neal (Office of Civil Defense, Washington, D. C.). pp 159-65 of Protective Structures for Civilian Populations. Washington, D. C., National Academy of Sciences–National Research Council, 1965.

Many diverse elements of a protective-structure project are discussed; their influences on the design of the structure and ways of obtaining some degree of optimization are also treated. Separate sections on physiological and psychological responses to shelter situations are also included. (G.O.Y.)

39070 STATE OF THE ART IN DYNAMIC ANALYSIS AND TECHNIQUES FOR THE DESIGN OF UNDERGROUND PROTECTIVE CONSTRUCTION. Newmark, Nathan M.

(Univ. of Illinois, Urbana). pp 166-79 of Protective Structures for Civilian Populations. Washington, D. C., National Academy of Sciences–National Research Council, 1965.

The soil structure interaction in underground protective structure construction is analyzed. The necessary design features against shock and vibrations are studied also. (G.O.Y.)

39071 MODEL ANALYSIS. Davies, I. Ll. (Suffield Experimental Station, Ralston, Alberta). pp 180-90 of Protective Structures for Civilian Populations. Washington, D. C., National Academy of Sciences–National Research Council, 1965.

The use of models for protective structures in nuclear weapons tests is discussed. Data are given for model and prototype structures in several dynamic tests. (G.O.Y.)

39072 BEHAVIOR OF SHOCK WAVES IN DUCTS AND WHEN ENTERING ENTRANCE STRUCTURES. Schardin, H. (Deutsch-Frauzoesische Forschungs-Institut, Hansjakohss, Ger.); Reichenbach, H. pp 193-206 of Protective Structures for Civilian Populations. Washington, D. C., National Academy of Sciences–National Research Council, 1965.

A detailed analysis of shock-wave propagation in ducts and entrance structures for shelters and protective constructions is presented. The analysis is performed in experimental models using shadow pictures of the shock events. (G.O.Y.)

39073 BLAST-CLOSURE SYSTEMS. Cohen, Edward; Weissman, Samuel (Amman and Whitney, New York). pp 207-25 of Protective Structures for Civilian Populations. Washington, D. C., National Academy of Sciences–National Research Council, 1965.

The design and construction of several types of blast doors and blast valves (structural elements that protect access or ventilation openings of a blast shelter) are discussed. (29 references) (G.O.Y.)

39074 VENTILATION AND AIR COOLING IN PROTECTIVE STRUCTURES. Drucker, Eugene E. (Syracuse Univ., N. Y.). pp 226-36 of Protective Structures for Civilian Populations. Washington, D. C., National Academy of Sciences–National Research Council, 1965.

The ventilation and air cooling in six types of community shelters were investigated by using a generalized FORTRAN program. The effects that changing various parameters had on shelter temperatures were investigated. It was shown that the variation in heat-transfer area, as well as changes of heat-transfer coefficients, had only a minor effect. The effects of inlet humidity and of solar radiation were shown to be very significant. The behavior of shelters with varying average inlet-air temperature, ventilation rate, and number of occupants was briefly examined. (G.O.Y.)

39075 PREFABRICATED BLAST-RESISTANT SHELTER. Basler, E. (Ingenieurbureau Basler und Hofmann, Zurich). pp 237-44 of Protective Structures for Civilian Populations. Washington, D. C., National Academy of Sciences–National Research Council, 1965.

Some design aspects of a prefabricated, post-tensioned, blast-resistant shelter are discussed. The shelter consists basically of two units, a barrel-shaped concrete structure and a rectangular concrete separation. A wide range of protective need and volumes can be met by varying the assembly combinations. A very positive interaction between the ground and soil was achieved. A design chart to investigate the influence of many parameters affecting the carrying capacity is given. The behavior of a long prismatic structure buried under an air-induced state of soil deformation is briefly considered, and a method for evaluating the amount of prestressing forces is described. (G.O.Y.)

39076 ACTIVITIES IN THE FIELD OF PROTECTIVE RECOMMENDATIONS, MEASURES, AND CONSTRUCTION IN THE NETHERLANDS. Ruyters, P. J. M. (Ministry of the Interior, The Hague). pp 247-62 of Protective Structures for Civilian Populations. Washington, D. C., National Academy of Sciences–National Research Council, 1965.

A survey of the protective recommendations, norms, and construction methods used in the Netherlands is presented. Town-planning recommendations, additional structural measures for new buildings, and shelter designs are considered. The Rotterdam underground is considered in detail. (G.O.Y.)

39077 SWEDISH 200-PSI BLAST-RESISTANT SEVEN-MAN SHELTER. Granstroem, Sune (Kungl Fortifikations-Forvaltningen, Stockholm). pp 263-8 of Protective Structures for Civilian Populations. Washington, D. C., National Academy of Sciences–National Research Council, 1965.

The Swedish shelter project is described. The structural design, production, transportation and burying operations are discussed. The air supply, the heating, and the shock-tube testing of the shelters is also considered. Both the production methods and the costs of the seven-man shelters have met the theoretical expectations. (G.O.Y.)

39078 USE OF UNDERGROUND PARKING LOTS AND GARAGES FOR THE PROTECTION OF CIVILIAN POPULATIONS. Walter, Hans (Ingenieurberatung, Essen). pp 269-74 of Protective Structures for Civilian Populations. Washington, D. C., National Academy of Sciences–National Research Council, 1965.

The results of studies done for and by the Planning Academy of Underground Traffic Facilities are summarized. The requirements of a multi-purpose structure are outlined, and the various costs are evaluated. (G.O.Y.)

39079 PUBLIC SHELTERS IN DENMARK. Rich, H. W. (Danish Defence Research Board, Copenhagen). pp 275-80 of Protective Structures for Civilian Populations. Washington, D. C., National Academy of Sciences–National Research Council, 1965.

Some technical problems concerning public shelters are discussed along with the problems of converting 4,400 small and primitive shelters into protective structures for a nuclear attack. (G.O.Y.)

39080 CANADIAN USE OF REINFORCED PLASTICS IN BLAST SHELTERS. White, S. N. (Emergency Measures Organization, Ottawa). pp 281-5 of Protective Structures for Civilian Populations. Washington, D. C., National Academy of Sciences–National Research Council, 1965.

The status of fiberglass shelter design in Canada is discussed. The use of plastic blast doors and anti-blast valves is also discussed. (G.O.Y.)

39081 TECHNICAL ASPECTS OF THE AUSTRIAN SHELTER PROGRAM. Panzhauser, E. (Technische Hochschule, Vienna). pp 286-91 of Protective Structures for Civilian Populations. Washington, D. C., National Academy of Sciences–National Research Council, 1965.

The results of various studies that led to the formulation and the legal codification of the technical requirements for the Austrian shelter program are summarized. (G.O.Y.)

39082 EXAMPLES OF SWISS PROTECTIVE STRUCTURES. Schlindler, G. (Architecture und Engineer Bureau, Zurich). pp 292-7 of Protective Structures for Civilian Populations. Washington, D. C., National Academy of Sciences–National Research Council, 1965.

It is shown that the emphasis of the Swiss Civil Defense shelter program is on basement protective structures. Shelters built as multistory shafts, and combination shelters with parking garage or tunnel, are briefly discussed. (G.O.Y.)

39083 PROTECTION AGAINST FALLOUT RADIATION AFFORDED BY CORE SHELTERS IN A TYPICAL BRITISH HOUSE. Jones, Daniel T. (Horseferry House, London). pp 298-303 of Protective Structures for Civilian Populations. Washington, D. C., National Academy of Sciences–National Research Council, 1965.

The results of experiments to evaluate the protection against fallout afforded by core shelters in a typical semi-detached British house are presented. The results show that the protective factor ranges from 2 to 28, depending on the position of the house. The experiments give the level of protection in various types of cores and show that

tective Structures for Civilian Populations. Washington, D. C., National Academy of Sciences–National Research Council, 1965.

A survey of contamination distribution of initial and residual radiation from nuclear weapon explosions is presented. (G.O.Y.)

39057 POSSIBILITIES OF OCCURRENCE OF AREA CONFLAGRATIONS AND FIRESTORMS WITH RESPECT TO FUEL DENSITY. Leutz, Hermann (Federal Ministry for Housing, Urbanization and Land Planning, Bad Godesberg, Ger.). pp 31-7 of Protective Structures for Civilian Populations. Washington, D. C., National Academy of Sciences–National Research Council, 1965.

A survey of the various types, causes, and effects of fires is presented. Some considerations for civilian protection in case of nuclear-weapon caused fires are considered. (G.O.Y.)

39058 TENTATIVE BIOLOGICAL CRITERIA FOR ESTIMATING BLAST HAZARDS. White, Clayton S. (Lovelace Foundation, Albuquerque, N. Mex.). pp 41-54 of Protective Structures for Civilian Populations. Washington, D. C., National Academy of Sciences–National Research Council, 1965.

Blast-induced hazards related to protective structures construction were investigated with animals exposed in above- and below-ground structures subjected to nuclear blast during the field operations carried out at Nevada Test Site in 1953, 1955, and 1957. A summary of these results is presented. Some biological criteria are derived. (G.O.Y.)

39059 FIRE AND NOXIOUS GASES: EFFECT ON INTERNAL ENVIRONMENTS OF PROTECTIVE SHELTERS. Johnson, J. Enoch; Ramskill, Eugene A. (Naval Research Lab., Washington, D. C.). pp 58-64 of Protective Structures for Civilian Populations. Washington, D. C., National Academy of Sciences–National Research Council, 1965.

Data are presented which show conclusively that a fire inside a protective shelter must be considered a serious menace because of the possible lethal effects on humans. The danger factor in a shelter fire is not the depletion of O_2, the evolution of CO_2 or of CO, or the output of noxious vapors and aerosols. The danger factor is the calories of heat released during combustion of as little as one pound of fuel. (G.O.Y.)

39060 GAMMA-RAY STREAMING THROUGH DUCTS. Huddleston, Charles M. (Naval Civil Engineering Lab., Port Hueneme, Calif.). pp 65-84 of Protective Structures for Civilian Populations. Washington, D. C., National Academy of Sciences–National Research Council, 1965.

A review is presented of various papers on experimental determinations of the attenuation of gamma-ray dose within concrete ducts as a function of distance from the radioactive source; on albedo—an important concept in gamma-ray scattering; and on some theoretical approaches to the duct-streaming problem. 32 references. (G.O.Y.)

39061 PROBLEMS OF SHIELDING AGAINST INITIAL RADIATIONS. Spencer, Lewis V. (National Bureau of Standards, Washington, D. C. Ottawa Univ., Kan.). pp 89-94 of Protective Structures for Civilian Populations. Washington, D. C., National Academy of Sciences–National Research Council, 1965.

Some problems of shielding against initial radiations are treated as a whole in order to point out the essential elements in this field within the context of the total shielding effort. (G.O.Y.)

39062 SHIELDING EXPERIMENTS. Chilton, A. B. (Univ. of Illinois, Urbana). pp 95-106 of Protective Structures for Civilian Populations. Washington, D. C., National Academy of Sciences–National Research Council, 1965.

Some shielding experiments, which are designed to check possible calculational errors in current design of shelters, are discussed. (G.O.Y.)

39063 PASSING PARADE OF SHIELDING-ANALYSIS METHODS: A REVIEW OF THE STATE OF THE ART. Farrell, Kenneth G. (Emergency Measures Organization, Ottawa). pp 107-20 of Protective Structures for Civilian Populations. Washington, D. C., National Academy of Sciences–National Research Council, 1965.

The status of shielding analysis methods is reviewed. Various methods and techniques are outlined, and their advantages and disadvantages are discussed. (G.O.Y.)

39064 ICHIBAN: DOSIMETRY PROGRAM FOR NUCLEAR BOMB SURVIVORS OF HIROSHIMA AND NAGASAKI. Auxier, John (Oak Ridge National Lab., Tenn.). pp 121-6 of Protective Structures for Civilian Populations. Washington, D. C., National Academy of Sciences–National Research Council, 1965.

The results of a series of projects on the dosimetry for nuclear bomb survivors at Hiroshima and Nagasaki are discussed. It is shown that shielding factors for Japanese dwellings can now be computed with simple formulas. The spatial and angular distributions of the dose are well defined, and the spectral distributions are crudely known. The normalization of the air-dose curves to the Hiroshima and Nagasaki weapons must yet be accomplished. (G.O.Y.)

39065 FIRE-SAFE SHELTER DESIGN. Degenkolb, John G. pp 129-33 of Protective Structures for Civilian Populations. Washington, D. C., National Academy of Sciences–National Research Council, 1965.

The need for fire-proof shelters is emphasized and criteria for making shelters fire-safe are given. (G.O.Y.)

39066 FIREPROOF SHELTERS WITH SECURED VENTILATING SYSTEMS. Leutz, Hermann (Federal Ministry for Housing, Urbanization, and Land Planning, Bad Godesberg, Ger.). pp 134-8 of Protective Structures for Civilian Populations. Washington, D. C., National Academy of Sciences–National Research Council, 1965.

It is shown that in fireproof shelters, provision must be made for the prevention of dangerous heating from outside fires which can lead to a situation similar to that in an oven. Ventilating systems are discussed and some specifications for preventing external and internal dangers are given. It is concluded that even in firestorm areas, survival appears possible in shelters with secured ventilation systems built according to German specifications. (G.O.Y.)

39067 FIRE-SAFE SHELTER DESIGN: SWEDISH VIEWS. Smitt, Goesta (Kungliga Civilforsvarsstyrelsen, Stockholm). pp 139-45 of Protective Structures for Civilian Populations. Washington, D. C., National Academy of Sciences–National Research Council, 1965.

The fire-safety features of the Swedish shelter designs are discussed. (G.O.Y.)

39068 FOOTINGS FOR PROTECTIVE STRUCTURES. Whitman, Robert V.; Luscher, Ulrich (Massachusetts Inst. of Tech., Cambridge). pp 151-8 of Protective Structures for Civilian Populations. Washington, D. C., National Academy of Sciences–National Research Council, 1965.

The design of footings or spread foundations for buried structures is discussed along with the evaluation of the effects of footing design and footing motion on the response of the structure as a whole. Data on the design of impulsively loaded footings and on the effect of footing response on the structure are synthesized. Some areas of uncertainty are indicated and areas of needed further research are identified. (G.O.Y.)

39069 ENGINEERING APPROACH TO PROTECTIVE STRUCTURES. FitzSimons, Neal (Office of Civil Defense, Washington, D. C.). pp 159-65 of Protective Structures for Civilian Populations. Washington, D. C., National Academy of Sciences–National Research Council, 1965.

Many diverse elements of a protective-structure project are discussed; their influences on the design of the structure and ways of obtaining some degree of optimization are also treated. Separate sections on physiological and psychological responses to shelter situations are also included. (G.O.Y.)

39070 STATE OF THE ART IN DYNAMIC ANALYSIS AND TECHNIQUES FOR THE DESIGN OF UNDERGROUND PROTECTIVE CONSTRUCTION. Newmark, Nathan M.

(Univ. of Illinois, Urbana). pp 166-79 of Protective Structures for Civilian Populations. Washington, D. C., National Academy of Sciences–National Research Council, 1965.

The soil structure interaction in underground protective structure construction is analyzed. The necessary design features against shock and vibrations are studied also. (G.O.Y.)

39071 MODEL ANALYSIS. Davies, I. Ll. (Suffield Experimental Station, Ralston, Alberta). pp 180-90 of Protective Structures for Civilian Populations. Washington, D. C., National Academy of Sciences–National Research Council, 1965.

The use of models for protective structures in nuclear weapons tests is discussed. Data are given for model and prototype structures in several dynamic tests. (G.O.Y.)

39072 BEHAVIOR OF SHOCK WAVES IN DUCTS AND WHEN ENTERING ENTRANCE STRUCTURES. Schardin, H. (Deutsch-Frauzoesische Forschungs-Institut, Hansjakohss, Ger.); Reichenbach, H. pp 193-206 of Protective Structures for Civilian Populations. Washington, D. C., National Academy of Sciences–National Research Council, 1965.

A detailed analysis of shock-wave propagation in ducts and entrance structures for shelters and protective constructions is presented. The analysis is performed in experimental models using shadow pictures of the shock events. (G.O.Y.)

39073 BLAST-CLOSURE SYSTEMS. Cohen, Edward; Weissman, Samuel (Amman and Whitney, New York). pp 207-25 of Protective Structures for Civilian Populations. Washington, D. C., National Academy of Sciences–National Research Council, 1965.

The design and construction of several types of blast doors and blast valves (structural elements that protect access or ventilation openings of a blast shelter) are discussed. (29 references) (G.O.Y.)

39074 VENTILATION AND AIR COOLING IN PROTECTIVE STRUCTURES. Drucker, Eugene E. (Syracuse Univ., N. Y.). pp 226-36 of Protective Structures for Civilian Populations. Washington, D. C., National Academy of Sciences–National Research Council, 1965.

The ventilation and air cooling in six types of community shelters were investigated by using a generalized FORTRAN program. The effects that changing various parameters had on shelter temperatures were investigated. It was shown that the variation in heat-transfer area, as well as changes of heat-transfer coefficients, had only a minor effect. The effects of inlet humidity and of solar radiation were shown to be very significant. The behavior of shelters with varying average inlet-air temperature, ventilation rate, and number of occupants was briefly examined. (G.O.Y.)

39075 PREFABRICATED BLAST-RESISTANT SHELTER. Basler, E. (Ingenieurbureau Basler und Hofmann, Zurich). pp 237-44 of Protective Structures for Civilian Populations. Washington, D. C., National Academy of Sciences–National Research Council, 1965.

Some design aspects of a prefabricated, post-tensioned, blast-resistant shelter are discussed. The shelter consists basically of two units, a barrel-shaped concrete structure and a rectangular concrete separation. A wide range of protective need and volumes can be met by varying the assembly combinations. A very positive interaction between the ground and soil was achieved. A design chart to investigate the influence of many parameters affecting the carrying capacity is given. The behavior of a long prismatic structure buried under an air-induced state of soil deformation is briefly considered, and a method for evaluating the amount of prestressing forces is described. (G.O.Y.)

39076 ACTIVITIES IN THE FIELD OF PROTECTIVE RECOMMENDATIONS, MEASURES, AND CONSTRUCTION IN THE NETHERLANDS. Ruyters, P. J. M. (Ministry of the Interior, The Hague). pp 247-62 of Protective Structures for Civilian Populations. Washington, D. C., National Academy of Sciences–National Research Council, 1965.

A survey of the protective recommendations, norms, and construction methods used in the Netherlands is presented. Town-planning recommendations, additional structural measures for new buildings, and shelter designs are considered. The Rotterdam underground is considered in detail. (G.O.Y.)

39077 SWEDISH 200-PSI BLAST-RESISTANT SEVEN-MAN SHELTER. Granstroem, Sune (Kungl Fortifikations-Forvaltningen, Stockholm). pp 263-8 of Protective Structures for Civilian Populations. Washington, D. C., National Academy of Sciences–National Research Council, 1965.

The Swedish shelter project is described. The structural design, production, transportation and burying operations are discussed. The air supply, the heating, and the shock-tube testing of the shelters is also considered. Both the production methods and the costs of the seven-man shelters have met the theoretical expectations. (G.O.Y.)

39078 USE OF UNDERGROUND PARKING LOTS AND GARAGES FOR THE PROTECTION OF CIVILIAN POPULATIONS. Walter, Hans (Ingenieurberatung, Essen). pp 269-74 of Protective Structures for Civilian Populations. Washington, D. C., National Academy of Sciences–National Research Council, 1965.

The results of studies done for and by the Planning Academy of Underground Traffic Facilities are summarized. The requirements of a multi-purpose structure are outlined, and the various costs are evaluated. (G.O.Y.)

39079 PUBLIC SHELTERS IN DENMARK. Rich, H. W. (Danish Defence Research Board, Copenhagen). pp 275-80 of Protective Structures for Civilian Populations. Washington, D. C., National Academy of Sciences–National Research Council, 1965.

Some technical problems concerning public shelters are discussed along with the problems of converting 4,400 small and primitive shelters into protective structures for a nuclear attack. (G.O.Y.)

39080 CANADIAN USE OF REINFORCED PLASTICS IN BLAST SHELTERS. White, S. N. (Emergency Measures Organization, Ottawa). pp 281-5 of Protective Structures for Civilian Populations. Washington, D. C., National Academy of Sciences–National Research Council, 1965.

The status of fiberglass shelter design in Canada is discussed. The use of plastic blast doors and anti-blast valves is also discussed. (G.O.Y.)

39081 TECHNICAL ASPECTS OF THE AUSTRIAN SHELTER PROGRAM. Panzhauser, E. (Technische Hochschule, Vienna). pp 286-91 of Protective Structures for Civilian Populations. Washington, D. C., National Academy of Sciences–National Research Council, 1965.

The results of various studies that led to the formulation and the legal codification of the technical requirements for the Austrian shelter program are summarized. (G.O.Y.)

39082 EXAMPLES OF SWISS PROTECTIVE STRUCTURES. Schlindler, G. (Architecture und Engineer Bureau, Zurich). pp 292-7 of Protective Structures for Civilian Populations. Washington, D. C., National Academy of Sciences–National Research Council, 1965.

It is shown that the emphasis of the Swiss Civil Defense shelter program is on basement protective structures. Shelters built as multistory shafts, and combination shelters with parking garage or tunnel, are briefly discussed. (G.O.Y.)

39083 PROTECTION AGAINST FALLOUT RADIATION AFFORDED BY CORE SHELTERS IN A TYPICAL BRITISH HOUSE. Jones, Daniel T. (Horseferry House, London). pp 298-303 of Protective Structures for Civilian Populations. Washington, D. C., National Academy of Sciences–National Research Council, 1965.

The results of experiments to evaluate the protection against fallout afforded by core shelters in a typical semi-detached British house are presented. The results show that the protective factor ranges from 2 to 28, depending on the position of the house. The experiments give the level of protection in various types of cores and show that

some of the cores provide considerably greater protection than the house alone. Core shelters of the kind described can double, triple, or quadruple the standard protective factor. The experimental protective factors agree in general with the theoretical values. (G.O.Y.)

39084 PUBLIC SHELTERS IN NORWAY: PROTECTION AGAINST GROUND SHOCK. Jenssen, Arnfinn (Forsvarets Bygningstjeneste, Oslo). pp 304-6 of Protective Structures for Civilian Populations. Washington, D. C., National Academy of Sciences–National Research Council, 1965.

Some methods for protecting public shelters in rock chambers, concrete bunkers, and basements against ground shock are described. (G.O.Y.)

39085 COOPERATIVE GROUP SHELTER NEAR LIVERMORE, CALIFORNIA. Hudgins, Arthur J. (Univ. of California, Livermore). pp 307-15 of Protective Structures for Civilian Populations. Washington, D. C., National Academy of Sciences–National Research Council, 1965.

The design and construction of a shelter, designed and built by private civilians to house their families in case of a nuclear attack, is described. The supplies and equipment in the shelter, which is owned and operated by Survival Associates, Inc., are discussed. The cost per family, results of occupancy tests, operational considerations, as well as future improvements are also considered. (G.O.Y.)

39086 ACTUAL VERSUS HYPOTHETICAL FALLOUT-SHELTER CASE STUDIES. Roembke, James (Office of Civil Defense, Washington, D. C.). pp 316-21 of Protective Structures for Civilian Populations. Washington, D. C., National Academy of Sciences–National Research Council, 1965.

A brief survey of case studies for buildings that incorporate in their design the plans for fallout shelter protection is presented. The architectural and engineering planning to provide some measure of shielding is emphasized. (G.O.Y.)

39087 TARGETING ASSUMPTIONS FOR ATTACKS AGAINST POPULATIONS. Knapp, Harold A. (Institute for Defense Analyses, Arlington, Va.). pp 322-32 of Protective Structures for Civilian Populations. Washington, D. C., National Academy of Sciences–National Research Council, 1965.

An analysis of the population of the United States is made with a view to determine the probability that specific shelter locations will be subjected to various combinations and levels of nuclear weapons effects. (G.O.Y.)

39088 METROPOLITAN-AREA BLAST-SHELTER SYSTEM. Narver, David L. Jr. (Holmes and Narver, Inc., Los Angeles). pp 333-7 of Protective Structures for Civilian Populations. Washington, D. C., National Academy of Sciences–National Research Council, 1965.

The results of a preliminary study for a tunnel system that will afford shelter for metropolitan area populations in the 100 psi contour are summarized. The tunnel grid system met all the initial test criteria. (G.O.Y.)

39089 RISK-ORIENTED SOLUTION FOR A TARGET COMMUNITY. Harrenstien, Howard P. (Univ. of Arizona, Tucson). pp 338-48 of Protective Structures for Civilian Populations. Washington, D. C., National Academy of Sciences–National Research Council, 1965.

A set of procedures for evaluating local hazards for cities closely associated with military targets is developed. These procedures are applied to Tucson, Arizona, and its environs. The results of targeting analyses, of survey, of loading, and of the designing and testing of the most feasible shelter system are discussed. (G.O.Y.)

Space Propulsion

See also ISOTOPE TECHNOLOGY — Power Application
REACTOR TECHNOLOGY — Propulsion and Space

39090 PRELIMINARY DESIGN CONSIDERATIONS OF A HIGH-PERFORMANCE HALL-CURRENT ACCELERATOR. Pinsley, Edward A. (United Aircraft Corp., East Hartford, Conn.). J. Spacecraft Rockets, 3: 1073-9(July 1966).

Recent experiments with a low density annular accelerator have shown that the Hall-current acceleration process involving a radial magnetic field and an axial electric field can be employed with cesium as a propellant to produce thrust densities, high efficiencies, and specific impulses between 1500 and 5000 sec. The relatively simple geometry of this accelerator and its low density feature (which decouples gross ion and electron motions) permit extrapolation of the results of the model experiments to performance regimes required by large prototype configurations. It is shown that the reduction in over-all thruster efficiency caused by ion swirl and by the leakage of electrons across the magnetic field can be minimized by the proper selection of the ratio of ion cyclotron radius to accelerator length. Constraints on thruster design imposed by fluctuations caused by the onset of a two-stream instability and by magnet and cathode requirements are discussed. Design parameters for a large, prototype, cesium Hall-current thruster are presented. (auth)

39091 SURFACE TENSION STORAGE AND FEED SYSTEMS FOR ION ENGINES. Forrester, A. Theodore; Barcatta, F. A. (Electro-Optical Systems Inc., Pasadena, Calif.). Contracts AF 33(657)-8157,-10980; AF 33(615)-1530; NAS3-5250. J. Spacecraft Rockets, 3: 1080-5(July 1966).

A type of zero-g vapor feed system involving no moving parts has been developed. Surface tension forces retain the liquid and pump it to a heated surface where vaporization occurs. An analysis has been carried out for both wetting and nonwetting liquids. Some zero-g experiments with wetting fluids have been conducted. These experiments used configurations similar to those used in actual propellant systems and provided verification of the surface energy concepts. Extensive laboratory testing of the feed system has also been conducted. One was used in an ion engine life test, which continued for 2160 hr with a propellant use efficiency of 99.33%. The feed system is lightweight, easily fabricated, has no moving parts, has excellent response, and is easily and accurately controlled. (auth)

39092 PERFORMANCE OF ION ENGINES AND SYSTEMS FOR SATELLITE CONTROL. Anderson, J. R. (Hughes Aircraft Co., Malibu, Calif.). Contracts NAS 3-2510,-4117. J. Spacecraft Rockets, 3: 1086-92(July 1966).

Recent achievements in the development of linear-strip, cesium-contact ion rockets of the 0.5-mlb class designed for a satellite attitude-control system with long life, high thermal efficiency, and low mass are described. A steady-state performance test of 2000-hr duration has been conducted satisfactorily. Since attitude control requires pulse operation, four thrusters were temperature-cycled from 40,500 to 85,000 times each; no deterioration of ionizer heater characteristics occurred. A novel feature of this linear-strip thruster is the use of a very low mass ionizer that can be heated from less than 100° to 1100°C within 15 sec with a warmup energy of only 0.5 w-hr. A laboratory demonstration system has been built which provides two-axis attitude-control and station-keeping functions. Included in this system are the necessary power conditioning, controls, propellant feed system, and six ion engines in early configurations. The testing consisted of prolonged operation in vacuum to determine general system behavior and to demonstrate feasibility. (auth)

39093 CESIUM ELECTRON BOMBARDMENT ION ENGINES. Sohl, G.; Reid, G. C.; Speiser, R. C. (Electro-Optical Systems Inc., Pasadena, Calif.). J. Spacecraft Rockets, 3: 1093-8(July 1966).

Both electromagnet and permanent magnet versions of the electron-bombardment cesium ion engine have been developed. The two types of engines are similar in performance. Mass utilization efficiencies over 90% are obtained at discharge energy expenditures of 350 to 400 ev/ion. Over-all engine efficiencies range from 55% at 3000-sec specific impulse (I_{sp}) to efficiencies of 87% at 9000 sec. In three consecutive tests, an engine system was operated for a total thrusting time of 2610 hr at the nominal design point of

7000-sec Isp, 10-mlb thrust, and 182 kw/lb. Each of the three runs was terminated by exhaustion of the cesium supply. In each case, over 99% of the initial cesium load in the zero-g feed system was extracted. As a result of these tests, lifetimes in excess of 10,000 hr can be extrapolated for electron-bombardment cesium ion engines. (auth)

39094 LIQUID-PROTECTED ELECTRODES. Moore, David (Electro-Optical Systems Inc., Pasadena, Calif.). J. Spacecraft Rockets, 3: 1269-73(Aug. 1966).

Ion propulsion engine lifetimes are limited by ion erosion of the accelerating electrode. Protecting an electrode from such erosion by a replenishable liquid film spread by surface forces could extend accelerator electrode lifetimes by several orders of magnitude. Experiments have led to the development of a liquid metal alloy that will give a protected tungsten substrate a lifetime over 15 times that of an identical unprotected tungsten substrate. Test conditions were extremely severe. The substrates were exposed to high-intensity (over 1 ma/cm^2) beams of 4-kv cesium ions, while the test liquid had to wick up the substrate to over an inch above the free liquid surface. Higher relative lifetimes are expected at lower beam intensities. Preliminary tests on a similar alloy also show it to be extremely effective in preventing electron emission from ion engine accelerating electrodes; the electron emission currents from a liquid-protected accelerator were less than 10% of those of the same accelerator without the liquid. (auth)

39095 ION PROPULSION DEVICE. Sunderland, Robert J.; Radbill, John R. (to Aerojet-General Corp.). U. S. Patent 3,263,415. Aug. 2, 1966. Filed Mar. 6, 1961.

An ion propulsion engine which produces a high density ion beam in a cavity fabricated of material with a high work function is described. Ions are guided out of the cavity by an electric field provided by an extraction electrode and accelerated by the extracting grid. A grounded decelerating electrode controls the ion velocity and specific impulse. Thrust is provided by the momentum of the ion beam. To produce negative ions, cavity walls must be fabricated of a material having a work function lower than the electron affinity of the material to be ionized. (F.S.)

Vacuum Engineering

39096 (AECD-EP-11) A DUAL-PURPOSE UNIT FOR HIGH VACUUM PUMPING SYSTEM AND LEAK DETECTION IN VACUUM CHAMBERS. Dutt, J. C.; Rahman, M.; Sabir, A.; Roberts, M. (Atomic Energy Centre, Dacca (Pakistan)). Mar. 1966. 25p. Dep. mn.

An apparatus using conventional mechanical and vapor-stream pumps was built which can be used as an exhaust system as well as a leak detector. Constructional principles and working instructions are given separately for the pumping and leak detection applications. The apparatus enables the evacuation of large chambers to a pressure of 10^{-6} torr; lower pressures (down to 10^{-7} torr) may be attained if the rotary pump is matched with the diffusion pump. (D.L.C.)

39097 (ORNL-3989, pp 128-33) VACUUM STUDIES. Strehlow, R. A.; Richardson, D. M. (Oak Ridge National Lab., Tenn.).

Organic peaks in a test vacuum system were found to be local to the ion source of the mass spectrometer and could be markedly decreased in magnitude by operating the spectrometer at an elevated temperature (about 125 to 150°C) continuously. The discrepancy between a normally enveloped gage and a nude gage was found to be more strongly influenced by the off-gassing from the surfaces near the gage or its tubulation than by any other factor. Improvements were made in the response time of the mass spectrometer used in the vacuum studies, which allowed mass analysis to be made of pressure pips of a variety of types. The pips which have been observed appear to originate with gasketed seals and may be air or off-gassing products. Both elastomer and metal gaskets in the presence or absence of oil were observed to yield the periodic pressure bursts. (auth)

39098 (WERL-2823-21) ULTRAHIGH VACUUM TECHNIQUES. Semi-Annual Report, December 1, 1965–May 31, 1966. Frauenfelder, R.; Lange, W. J.; Singleton, J. H. (Westinghouse Research Labs., Pittsburgh, Pa.). Contract AT(30-1)-2823. 47p. Dep. mn. CFSTI $3.00 cy, $0.50 mn.

Two studies are currently being pursued with primary effort on hydrogen permeation through tungsten and secondary effort on the replacement of one adsorbed gas by a second from the gas phase. Significant results have been obtained on the H_2-W problem including some supporting work on the N_2-W and H_2-Mo systems. (auth)

GEOLOGY, METEOROLOGY, AND MINERALOGY

General

Refer also to abstracts 38857, 38918, and 40440.

39099 (BNWL–235-3, pp 1-23) GEOLOGY AND HYDROLOGY. (Battelle-Northwest, Richland, Wash. Pacific Northwest Lab.).

Studies were conducted and results reported on: stratigraphy of the uppermost part of the basalt sequence and its implications; variations in the earth's gravity field at Hanford; vertical infiltration as influenced by errors in measuring capillary pressure; horizontal infiltration of liquids into porous media; computer program STREAM, for determination of ground water flow paths and travel times; solution capabilities by finite differences method to a large class of steady-state flow problems; use of new ground water potential distribution in heterogeneous porous media; and the simultaneous flow of two emmiscible fluid phases in heterogeneous porous media. (R.C.K.)

39100 MINERAL TABLES (HAND SPECIMEN PROPERTIES OF 1500 MINERALS). Dietrich, R. V. Bull. Va. Polytech. Inst., Eng. Exp. Sta. Ser., No. 160, 1-221 (1966).

The hand specimen properties of 1500 minerals, including hardness, mineral names, crystal systems, specific gravity, and chemical class, are given. There are two divisions based on luster: metallic and nonmetallic. Within each of these divisions there is a sub-table for each color. Another table consists of minerals arranged according to chemical composition. (D.H.M.)

39101 URANIUM RESOURCES. Cloos, H. (Bundesanstalt fuer Bodenforschung, Hanover). pp 9-43 of 2nd FORATOM Congress 1965. Bonn, Deutsches Atomforum e. V., 1965.

A review of U resources is presented. Information is included on long-term requirements for natural U, reserves and supplies, price trends for natural U, and processing capacities for U ores. (J.R.D.)

39102 SEARCH FOR ISOTOPIC ANOMALIES IN SILVER AND LITHIUM FROM METEORITES. Dews, Jon Robert. Berkeley, Calif., Univ. of California, 1965. 85p. Thesis.

Trace quantities of silver present in the iron meteorite Canyon Diablo were isolated by chemical procedures with an average yield of 80 percent. The isotopic composition of five samples of silver from the meteorite was measured on a 12-inch radius-of-curvature, double-focusing, fast-sweep mass spectrometer. The isotopic composition of 18 samples of terrestrial silver was measured for comparison. The meteoritic and terrestrial ratios of $^{107}Ag/^{109}Ag$ were found to be identical within one percent. The silver content of Canyon Diablo is 58 parts per billion from isotope dilution analyses of aliquots of the meteorite samples. Trace quantities of lithium present in the chondrules from Bruderheim and Bjurbole meteorites were isolated by chemical procedures with a yield greater than 90 percent. The isotopic composition of lithium in two samples of Bruderheim chondrules and one sample of Bjurbole chondrules was measured on a 9-inch radius-of-curvature, single-focusing mass spectrometer. An integration procedure was used to solve the problem of mass fractionation during the mass analysis. The isotopic composition of lithium from two samples of "whole rock" Bruderheim and one sample of the granite G-1 was also measured for comparison. The $^7Li/^6Li$ ratios were found to be identical within 4 percent (at the 95 percent confidence level). The lithium content of all the samples was determined by isotope dilution analyses of aliquots of each sample. The contents found were 0.404 ppM for "whole rock" Bruderheim, 0.267 ppM for Bruderheim chondrules, 0.089 ppM for a large lath chondrule from Bruderheim, 0.134 ppM for Bjurbole chondrules, and 20.8 ppM for G-1. (Dissertation Abstr.)

Meteorology

See also Site Survey and Selection

39103 (BNWL–235-3, pp 51-69) PARTICLES AND GASES. (Battelle-Northwest, Richland, Wash. Pacific Northwest Lab.).

Results are reported for studies on: use and performance of a spinning-disk aerosol generator; subisokinetic sampling of particles in an air stream; errors in sampling with nozzles designed to achieve isokinetic flow; particle deposition and re-entrainment in long vertical conduits; an ^{131}I generator for field release use; and release of noble gases from aqueous solution. (W.E.B.)

39104 METHODS FOR THE MEASUREMENTS OF ATMOSPHERIC RADIOACTIVITY. Teodorescu, G. Metrol. Apl. (Bucharest), 12: 29-37(Jan. 1965). (In Rumanian).

Radon and thoron represent the chief natural sources of radioactivity in the atmosphere; the short half life actinon plays a negligible role. Concentration of radioactive substances, such as ^7Be, ^{14}C, and ^3H, created by the bombardment of nitrogen, hydrogen and oxygen of the air by neutrons from cosmic radiation, is relatively low. The radioactivity is due to the decay products of the two gases, fixed on particles with a diameter of less than 0.04μ. In the absence of strong currents or precipitations, these aerosols may stay in the atmosphere for 10 days. Their concentration varies with the distribution of uranium, radium, and thorium in the soil. The activity above the levels of 10^{-9} C/liter is measured by means of G-M counters; for lower activity levels, the radioactive gas must be concentrated before measurement. Direct methods currently in use rely on ionization chambers, proportional counters or special scintillators. Indirect methods require the collection of the aerosols by means of thermal or electrostatic precipitation. Continuous measurement may be accomplished by moving a paper strip below a counter. In spite of atmospheric nuclear explosions, the natural activity can still be measured. The radiochemical and radiometric methods used for the identification of individual isotopes are reviewed together with problems related to paper chromatography and γ spectroscopy. (TTT)

39105 CORRELATION OF WIND TUNNEL AND FIELD MEASUREMENTS OF GAS DIFFUSION USING ^{85}Kr AS A TRACER. Martin, James Edward. Ann Arbor, Mich., Univ. of Michigan, 1965. 150p.
Thesis.

Atmospheric diffusion at a reactor site was investigated by reproducing in a wind tunnel the influences of buildings and terrain and measuring the dispersion of plumes. A full-scale field test with a radioactive tracer, krypton-85, confirmed the results obtained with a model-scale wind tunnel test. The work was done for The Ford Nuclear Reactor site of the University of Michigan. The wind-tunnel data correlated well with average field concentrations within 250 ft of the source where winds above 8–10 mph produced high concentrations at ground level. At wind speeds below about 8 mph and for conditions that allowed the plume to escape the influence of the reactor building, the peak field concentrations correlated well with the wind tunnel data. The relation between peak and average concentrations for downwind distances greater than 250 ft was found to be a function of the horizontal component of gustiness. Within the above limitations, the wind-tunnel data correlated with the field data for all atmospheric stability conditions. The wind-tunnel measurements agreed much more closely with the field measurements than did the concentrations calculated

by the Sutton equation. Methods of using ^{85}Kr as a tracer for studying atmospheric diffusion are described. These methods allow the measurement of both average and peak concentrations using portable Geiger counters connected to inexpensive, portable tape recorders. Procedures for using ^{85}Kr to measure concentrations in a double-return wind tunnel are also described. (Dissertation Abstr.)

Natural Radioactivity and Fallout

See also HEALTH AND SAFETY

Refer also to abstract 39991.

39106 (BMwF-FBK-65-05) KONZENTRATIONEN RADIOAKTIVER SUBSTANZEN IM NIEDERSCHLAG. (Concentration of Radioactive Substances in Precipitation). Kegelmann, G. (Heidelberg Univ. (West Germany). Zweites Physikalisches Institut). Dec. 1965. 67p. Dep. mn.

Discontinous and continous measurements of fission products and of ^{214}Pb and ^{214}Bi in precipitation are reported. The dependence on precipitation intensity of the specific radioactivity of precipitations was considered. It can be approximated by a hyperbolic relation valid for the integral and the differential behavior as well. A marked dependence on meteorological parameters was found, such as type of precipitation, kind of clouds, ceiling height, and also on physico-chemical parameters, e.g., solubility. The dependence on intensity was stronger with fission products than with ^{214}Pb and ^{214}Bi. A model for the attachment of activity to precipitation elements is suggested. It can explain the observations reasonably. (auth)

39107 (UCRL-14700) WASHOUT OF PARTICULATE MATTER IN LONG-TERM CLOUDS PRODUCED BY NUCLEAR EXPLOSIONS. Petersen, Allen H. (Lawrence Radiation Lab., Univ. of California, Livermore). Mar. 14, 1966. Contract W-7405-eng-48. 24p. Dep. mn. CFSTI $2.00 cy, $0.50 mn.

The theory of rain-scavenging of airborne particulate matter is extended to the more general case of moving, polydisperse populations. Values for a multidimensional washout coefficient as a function of particle radius and rain intensity are given. By using expressions for the concentration within an instantaneous point source cloud with a spectrum of particle sizes, formulas are derived which give the rate of deposition and integrated deposition of radioactivity or particles from a long-term nuclear device cloud at any point downwind. Two important meteorological situations which may occur during washout are analyzed separately. The general expressions show that in a long-term nuclear device cloud, both the rate of deposition and integrated deposition are functions of the following independent variables: radius of the device cloud in the direction of the wind speed; wind speed, or speed of the cloud relative to the rain-producing layer; shape of the cloud's concentration; distance downwind; and rain intensity. By employing recent empirical data for the distribution of radioactivity with particle size within the cloud from the Sedan event, the equations are used to calculate the maximum integrated deposition of radioactivity which might be scavenged from long-term clouds produced by a nuclear device used for excavation. The maximum percentage of the cloud's radioactivity deposited within the first meter is presented nomographically with various wind speeds in miles per hour and rain intensities in millimeters per hour. (33 references.) (auth)

39108 OBSERVATION OF FALLOUT AROUND THE LABORATORY. Mamuro, Tetsuo; Fujita, Akira; Matsunami, Tadao; Yoshikawa, Kazuko. Ann. Rep. Radiat. Center Osaka Prefect., 6: 1-4(1965).

The results are reported of observation during 1965 in Japan on rain-out, concentration of fallout activity in the atmosphere, and fallout collected in a basin. Fresh nuclear debris from the venting underground nuclear explosion carried out by the USSR on 15 January were detected in air-borne dust on 19 January and in rain water on 29 January. It was found that particulate component was much impoverished in the debris and that the debris activity was mainly due to ^{89}Sr and $^{140}Ba + {}^{140}La$. Fresh nuclear debris from the second Chinese nuclear explosion carried out on 14 May were detected in rain water on 20 May; some highly radioactive fallout particles were found and collected, which were 4 to 7 μ in diameter and had FP specific activities about a factor 100 higher than those of the highly radioactive particles originating from the first Chinese explosion carried out on 16 October 1964. (auth)

39109 ALPHA ACTIVITY OF HIGHLY RADIOACTIVE FALLOUT PARTICLES. Mamuro, Tetsuo; Matsunami, Tadao. Ann. Rep. Radiat. Center Osaka Prefect., 6: 5-13 (1965).

Alpha activity of three kinds of highly radioactive fallout particles collected in Japan, namely, those which originated from a Soviet large scale air burst carried out in autumn 1962, the first Chinese explosion (a small scale surface burst in 1964) and the second Chinese explosion (a small scale air burst in 1965), was investigated using an alpha spectrometer. Alpha activity of these particles was found to be mainly due to ^{239}Pu and ^{240}Pu. The experimental results are discussed in connection with the differences in burst conditions among the three explosions from which the three kinds of particles originated. The ratio of α activity to total activity ($\alpha/\alpha + \beta$) was found to be considerably smaller in the particles than in the rain water samples which were collected in the periods just before and after the days when the particles were found and collected. The Pu concentration in the mean rain water samples collected in the period from 1962 to 1965 was found to be about 1×10^{-3} dps/l. (auth)

39110 X-RAY MICROANALYSIS OF HIGHLY RADIOACTIVE FALLOUT PARTICLES ORIGINATING FROM THE FIRST CHINESE NUCLEAR EXPLOSION. Mamuro, Tetsuo; Fujita, Akira; Matsunami, Tadao; Shirai, Shogo; Murakami, Masahiro. Ann. Rep. Radiat. Center Osaka Prefect., 6: 14-22(1965).

X-ray microanalysis was carried out on the highly radioactive fallout particles collected in Japan and originating from the first Chinese nuclear test explosion Oct. 16, 1964. Seven metallic elements, Fe, Ca, Si, Al, K, Mn, and Ti were confirmed to be present in the particles. It was found that the four elements, Fe, Ca, Si, and Al were the main constituent metallic elements and that the darkness of particle color increased with Fe composition. X-ray scanning images suggested that in some particles these elements were distributed rather heterogeneously. The result of x-ray microanalysis is somewhat different from that obtained formerly on the Soviet highly radioactive particles collected in autumn 1962 and this is considered to be ascribed to the difference in burst conditions. (auth)

39111 EFFECT OF RADIOACTIVE FALLOUT UPON THE ELECTRIC CONDUCTIVITY OF THE LOWER ATMOSPHERE. Fujita, Akira. Ann. Rep. Radiat. Center Osaka Prefect., 6: 23-8(1965).

The effect of radioactive fallout upon the electrical conductivity of the lower atmosphere was studied. The records of atmospheric conductivity which were made at the Geophysical Institute of Kyoto University in the period from 1961 to 1963 were compared with the observation of fallout made in the same period at the Radiation Center of Osaka Prefecture. The radioactive fallout, which originated from the large scale nuclear test explosion of 50 Mt class carried out by the USSR at Novaya Zyemlya on October 30, 1961, caused a temporary increase in atmospheric conductivity up to a value twice as high as the normal one. The increase in conductivity was considered to have been caused mainly by radiations from the dry fallout accumulated on the ground surface, which was estimated to have exceeded 250 mμC/m^2 at that time. On the other hand radiations from the air-borne nuclear debris, the concentration of which reached as high as 120 $\mu\mu$C/m^3 at that time, were considered to have contributed little to the increase in conductivity. (auth)

39112 FALLOUT IN SOIL PARTICLES. Fujita, Akira. Ann. Rep. Radiat. Center Osaka Prefect., 6: 29-32(1965).

Fallout accumulation was studied in soil samples which were collected from the middle and the lowest courses of the Yamato River, and from bare ground at Osaka, Japan. It was found that the concentration of accumulated fallout in soil (cpm/g) is roughly inversely proportional to the soil particle size. (auth)

39113 WASHOUT OF RADIOACTIVE AEROSOLS FROM ATMOSPHERIC FALLOUT IN THE LAYER BELOW CLOUDS. Chalov, P. I.; Tsevelov, M. A. (Inst. of Physics and Mathematics, Academy of Sciences, Kirgiz, USSR). Fiz. Atmos. Okeana, 2: No. 2, 205-7(1966). (In Russian).

The amount of β radioactivity precipitated by rain per unit area of sample at various altitudes above sea level was measured. For various periods during 1963, data are presented for duration of sampling, lower limit of cloud level, type of cloud, amount of activity per unit area at 2070 m, 2477 m, and 2689 m, and the difference between values at 2070 and 2689 m, respectively: 2 June, 20, 3700, Cu, Sc, 1.74, 1.40, 1.00, 0.74; 3 June, 18, 3500, Cu, 1.04, 1.10, 1.00, 0.04; 4 June, 26, 3600, Sc, 8.90, 5.80, 1.00, 7.90, 8 June, 21.5, 3400, Cu, Nb, 2.27, 1.88, 1.00, 1.27; 9 June, 20.7, 3800, Sc, Cu, 3.00, 1.89, 1.00, 2.00; 12 June, 6.6, 3700, Nb, 1.15, 1.19, 1.00, 0.15; 15 June, 23, 3500, Cu, 1.06, 0.70, 1.00, 0.05. Some sort of correlation exists between the difference between levels and the type of cloud. Average values observed at the same three altitudes over 10-day periods were 1.27, 1.08, 1.00; 2.09, 1.36, 1.00; 1.15, 1.05, 1.00, for total fallout. Reasons for the correlation are discussed. (BBB)

39114 VARIATION OF THE CONCENTRATION OF NATURAL RADIOACTIVE GAS AND OF THE EQUILIBRIUM BETWEEN THIS GAS AND ITS DAUGHTER PRODUCTS IN THE AIR AT GROUND LEVEL. Fontan, Jacques; Birot, Andre; Blanc, Daniel (Faculte des Sciences, Toulouse). Geofis. Meteorol. (Genoa), 13: 80-7(1964). (In French).

Continuous measurements were made of the concentrations of radon and thoron and their daughter products in the lower atmosphere at Toulouse, and the effects of atmospheric conditions, especially air convection and turbulence, on the concentrations were examined. Stagnation of air was accompanied generally by an increase in radon, radon products, and thoron products in the atmosphere. Winds tended to lower the concentrations at ground level. Increased turbulence tended to favor an equilibrium between radon and its descendants (RaB + RaC), whereas convective movements created or increased disequilibrium. The presence of soil rich in uranium or thorium, or bodies of water, affected the levels. Relative humidity, as other meteorological factors, varied in the same way as the air concentration of radon. The presence of aerosols influenced the radioactivity levels; a fine rain, for example, tended to extract radioactivity from the air. The concentration of radon at ground level in Toulouse varied from 10^{-14} to 2×10^{-12} C/l. The extreme variation between daily maxima and minima reached a factor of 10. The concentration of thoron was between 0.4 and 2×10^{-12} C/l, and its daily variations were small. (BBB)

39115 PHYSICAL AND RADIOCHEMICAL PROPERTIES OF FALLOUT PARTICLES. Crocker, G. R.; O'Connor, J. D.; Freiling, E. C. (Naval Radiological Defense Lab., San Francisco). Health Phys., 12: 1099-1104(Aug. 1966).

A survey was made of the very large body of literature now existing on the characteristics of fallout particles. An attempt is made to summarize in concise form the ranges of physical and radiochemical properties of particles which have been observed to result from devices detonated under various conditions. The results of studies of the leaching action of various solvents on fallout particles are also summarized. (auth)

39116 TRANSURANIC ELEMENTS IN NATURE. Druin, V. A. pp 30-3 of Perspektivy Sinteza Transuranovykh Elementov. Moscow, Izdatel'stvo Znanie, 1965. (In Russian).

The possibility of finding traces of transuranium elements on Earth is examined. In view of the estimated age of five billion years of the Earth, only isotopes with half lives of at least 100 million years may be expected to be still found. Systematic searches reveal trace amounts of ^{239}Pu and ^{237}Np in uranium minerals, but their half-lives of 24,000 and 2 million years indicate that they could not have been present in the crust at the time of the formation of the Earth, but were probably formed by the interaction of neutrons with the uranium nuclei. Analysis of the A spectrum of New Hampshire thorite revealed the characteristics of the thorium family with small amounts of admixtures of lines originating from decaying members of the uranium family. The spectrum may be explained by ascribing certain lines to ^{247}Cm and ^{244}Pu; Soviet scientists reported similar findings. Other explanations of the very high ^{235}U/^{238}U ratio in these minerals are less plausible. (TTT)

39117 MOVEMENT OF ^{90}Sr IN GEORGIAN SOILS. Kvaratskhelia, N. T.; Glonti, G. L. Soviet Soil Sci. (Eng. Transl.), No. 10, 1187-93(May 1966).

The movement of strontium under various geomorphological and soil conditions was studied. Core samples were obtained from profiles taken in typical field plots covered with natural meadow vegetation. A core measuring 20 × 20 cm was cut from each genetic horizon to its entire depth. The ^{90}Sr content was determined, in hydrochloric acid extracts, from the daughter element ^{90}Y. The adsorption properties and water permeability of the soil and rock exerted an influence on the depth to which radioactive fallout reached within the soil zones. The dynamics of radiostrontium penetration indicates that: (1) it gradually accumulates in the soil profile and (2) gradually moves into the deeper levels. Topographic features were found to play a major part in the redistribution of radioactive fallout within a soil group. The ^{90}Sr accumulated largely in the low-lying elements of the relief (hollows and depressions) and in drainless plains; comparatively less so, on gentle slopes and plateau-like elevations; least of all, on rolling and steep slopes. Thus, radioactive fallout is distributed unevenly along slopes. Despite the brief contact of the atmospheric precipitation with the soil on a slope, ^{90}Sr nevertheless accumulates with time owing to its adsorption on the clay particles of the soil. (BBB)

39118 SUMMARY OF THE MEASUREMENTS MADE IN 1963 IN THE NETHERLANDS IN THE BIOSPHERE FOR DETERMINATION OF THE GENERAL RADIOACTIVE CONTAMINATION. Verslag. Mededel. Betreffende Volksgezondheid, No. 11, 1635-97(Nov. 1965). (In Dutch).

The results of measurements of the radioactivity of the atmosphere, soil, drinking water, and food materials in the Netherlands in 1963 are reported. The radiation dose received as a result of the deposition of radioactive fission products and contamination of the individual components of the biological media were the areas discussed. The results are tabulated. (J.S.R.)

39119 REPORT ON STUDIES ON THE β ACTIVITY OF THE LOWER ATMOSPHERE. Trippler, Klaus (Technische Hochschule, Brunswick). Z. Geophys., 32: 102-12 (1966). (In German).

Instrumentation, technics, and results are described for continuous measurements of the concentrations of RaB (^{214}Pb), RaC(^{214}Bi), and ThB(^{212}Pb) of the air in Braunschweig. Figures of the activity-wind interactions of RaB and ThB are given on the basis of the land-sea contributions as well as by consideration of the great areas of granite with increased release of radioactive gases from the soil in Czechoslovakia. The concentration of ^{222}Rn in the soil of the Harz mountains above granite masses is three times larger than in the environment but there is no higher β activity in the air at these sites than in soil. The daily variations of the natural activity in the air can be described by a simple quasi-stationary model in terms of

the theory of turbulence. In this model the diffusion coefficient is constant above a certain altitude. A coefficient of accumulation (α) of $1 \leq \alpha \leq 10$ cm/sec is the boundary condition at the soil surface if the measured ratio of C_{RaB}/C_{RaC} is taken into consideration. During great air turbulence in the daytime this ratio is about 1; in the quiet nocturnal atmosphere it is ~1.5. The value of α is usually ~2 cm/sec. (BBB)

39120 NATURAL VARIATION IN THE RATIO $^{234}U/^{238}U$ AND AN INVESTIGATION OF THE POTENTIAL OF ^{234}U FOR PLEISTOCENE CHRONOLOGY. Thurber, David Lawrence. [New York], Columbia Univ., 1964. 172p.
Thesis.

The study reported confirmed that ^{234}U is in excess over its predicted equilibrium value in all of the natural waters studied and in calcium carbonate deposited from these waters. The ratio $^{234}U/^{238}U$ varies over considerable range in continental waters. The ^{234}U concentration, usually between 10 percent and 100 percent in excess of the equilibrium value, is at least partly controlled by the terrain being weathered. The $A^{234}U/A^{238}U$ in sea water is apparently constant at 1.15. There appears to be enough variation in the $^{234}U/^{238}U$ ratio in continental deposits to make the prediction of the initial ratio in shells difficult if not impossible. This would make the dating of terrestrial carbonate deposits by the decay of ^{234}U highly tentative. The $A^{234}U/A^{238}U$ in coral samples from Eniwetok drill cores decreases in a systematic manner with depth, and ages of the material are in agreement with that calculated from the $^{230}Th/^{234}U$ ratio. This suggests the possibility that $^{234}U/^{238}U$ dating may be used in marine systems. The reason for the excess ^{234}U in natural waters is not known in detail, but is expected to be, in part, caused by weathering and removal of ^{234}U preferentially to ^{238}U owing to the radioactive history of the ^{234}U. (Dissertation Abstr.)

39121 TRANSPORT OF RADIONUCLIDES IN SURFACE AND ESTUARINE WATERS. Klingeman, Peter Clayton. Berkeley, Calif., Univ. of California, 1965. 424p.
Thesis.

The transport of fission radionuclides in the waters and sediments of river-estuary systems, the changing distributions of these radionuclides in estuarine waters, and the factors effecting these changes were studied. Particular emphasis was given to zirconium–niobium-95 and other fission products of recent fallout origin. The formation, atmospheric transport, and watershed deposition of fallout radionuclides were reviewed. The role of clay minerals in radionuclide transport was then considered, as were the sorption characteristics of $^{95}Zr-^{95}Nb$. General characteristics of sediment transport in rivers and estuaries were also reviewed. Field and laboratory data demonstrated that the bulk of fallout debris was associated with suspended river particulates and permitted formulation of a model for the transport of fission radionuclides through rivers with storm runoff. A change from river to estuarine environment was shown to have little effect upon the sorption relation for fission radionuclides, due to the relatively irreversible sorption of the predominating $^{95}Zr-^{95}Nb$. Laboratory experiments demonstrated the integrity of $^{95}Zr-^{95}Nb$ as a tracer of clay-silt suspensions in river-estuary systems. Many fundamental relations determining the deposition, resuspension, and redistribution of flocculent radionuclide-sorbed sediments within estuaries were observed during extensive field studies of San Pablo Bay, a major component of the San Francisco Bay System. Important differences exist between short-term and long-term estuarine distributions of sediment from storm runoff. Certain portions of the estuary were particularly susceptible to the accumulation of radionuclide-sorbed sediments. (Dissertation Abstr.)

39122 TELLURIUM ISOTOPE FRACTIONATION STUDY. Smithers, R. M.; Krouse, H. R. (Univ. of Alberta, Edmonton). 12p. (CONF-650664-8). ORAU. Gmelin, AED-CONF-65-288-10.
From Canadian Association of Physicists Congress, Vancouver, B. C.

Theoretical calculations have been made which suggest that the $^{122}Te/^{130}Te$ ratio may be altered by over 2% in laboratory reactions and natural processes. A preliminary study has realized variations of as high as 0.7% in the $^{122}Te/^{130}Te$ ratio in chemical and microbiological reduction studies in the laboratory. One natural sample has been found to be 0.4% enriched in the lighter isotope in comparison with others which have a fairly constant ratio. The results are compared to similar results found for selenium and sulfur isotopes. (auth)

39123 $^{18}O/^{16}O$ RATIOS IN SNOW AND ICE OF THE HUBBARD AND KASKAWULSH GLACIERS. Macpherson, D. S.; Krouse, H. R. (Univ. of Alberta, Edmonton). 42p. (CONF-651108-3). ORAU. Gmelin, AED-CONF-65-347-8.
From Symposium on Isotope Techniques, Urbana, Ill.

One hundred samples collected from the Hubbard and Kaskawulsh Glaciers in the St. Elias Mountains during the summer of 1963 were analyzed for $^{18}O/^{16}O$ content. The δ_{18} values ranged from −18 to −29 with an average of about −23. Pits studied before extensive melting, showed definite trends in δ_{18}, with the more negative values corresponding to winter precipitation. Pits studied later in the season had the seasonal trend masked by the action of downward percolating melt waters. The average of all pits and boreholes studied above the firn line gave no indication of an altitude variation of δ_{18} larger than the sampling error. A longitudinal profile below the firn line showed much scatter in the δ-value but the average trend was a decrease in δ_{18} in going down glacier from the firn line to the terminus. A transverse profile below the firn line, which sampled three main ice streams, gave remarkably consistent values of δ near the margins, while the stream centers had decidedly more positive or negative δ-values. These results are considered in terms of accepted modes of glacier flow. Precipitation studies exhibited much scatter and did not show the expected altitude variation of δ. (auth)

Techniques and Equipment

39124 (AD–632957) RED HOT. Long Range Seismic Measurements of VELA UNIFORM Project. Seismic Data Laboratory Report No. 145. (UED Earth Sciences Div., Teledyne Systems Co., Pasadena, Calif.). Mar. 5, 1966. 47p. CFSTI $2.00 cy, $0.50 mn.

An analysis of seismological data from an underground nuclear explosion, Red Hot, is presented as a continuing study to provide information to aid in distinguishing between earthquakes and explosions. A table of travel times and amplitudes of P, Pg, Lg, and surface waves are included along with other unidentified phases. (auth)

39125 FURTHER AGE MEASUREMENTS ON RADIOACTIVE MINERALS FROM SWEDEN. Welin, Eric; Blomqvist, Goeran (Aktiebolaget Atomenergi, Stockholm). Geol. Foren. Stockholm Forh., 88: 3-18(Mar. 31, 1966).

Values are given for total U, Th, and Pb and ratios of $^{206}Pb/^{238}U$, $^{207}Pb/^{235}U$, $^{207}Pb/^{206}Pb$, and $^{208}Pb/^{232}Th$ for radioactive minerals in the Precambrian bedrock of Sweden. The main objective of the investigations was to correlate the formation of the uranium ores with a geochronologically well-founded geologic evolution of Sweden. Uraninite and monazite from northern Sweden were found to have an age of 1775–1845 Myr, but a more precise result could not be obtained. The pegmatites in the Oestersund-Sundsvall area and the pegmatites and aplites in southeastern Sweden are 1380 and 1745 Myr old, respectively. A pegmatite associated with the Karlshamn granite and a granite on Romeleasen each have ages of 1455 Myr. Some previously determined K/Ar ages are discussed, and it is concluded that the uplift of the gneiss block in southwestern Sweden occurred during or after a period of igneous activity in western Sweden 935-1000 Myr ago. The age data also indicate a contemporaneity between the deposition of the Dal formation in western Sweden and the Jotnian sandstones, the former being of marine lithology, the latter representing a terrestrial facies. (BBB)

39126 Rb/Sr WHOLE ROCK AGE DATA ON SOME SWEDISH PRECAMBRIAN ROCKS. Welin, Eric; Blomqvist,

Goeran; Parwel, Alexander (Aktiebolaget Atomenergi, Stockholm). Geol. Foren. Stockholm Forh., 88: 19-28 (Mar. 31, 1966).

The ratios $^{87}Sr/^{86}Sr$ and $^{87}Rb/^{87}Sr$ were determined by the whole-rock method as a part of a program concerning the genetic aspects of the formation of uranium ores in Central and Southeastern Sweden, and the results were correlated with previously reported age data obtained by U/Pb measurements. The results of isotope dilution analyses and isotope ratio measurements are tabulated. The ratios of $^{87}Sr/^{86}Sr$ and $^{87}Rb/^{86}Sr$ of each sample were plotted. The age calculation was made by measuring the slope of the line and the intercept with the $^{87}Sr/^{86}Sr$ axis. With a decay constant of 1.39×10^{-11} yr^{-1}, the results were consistent with U/Pb ages. The calculated age of the Växjö granites (1740 Myr) in the Strålnäs area is in very good agreement with the U/Pb age of 1745 Myr on minerals genetically associated with Småland granites in the Västervik area. These data show that the Småland granites (and hence also the Värmland granites) are older than previously believed on the basis of K/Ar measurements, and they have accordingly been intruded only 60–70 Myr after the late-kinematic Svecofennian granites. (BBB)

39127 DEUTERIUM-ISOTOPE GEOCHEMISTRY OF GROUND AND SURFACE WATERS. Eichler, Roland (Univ., Bonn). Geol. Rundsch., 55: 144-59(1966). (In German).

Recent studies have shown differences in the HDO/H_2O ratios of natural waters, attributed largely to the difference in vaporization and condensation propensities of the isotopes, mainly from the lower vapor pressure of HDO. Various geophysical and geohydrological processes influence the mixing of waters with different isotope contents. Rain and spring water of several regions of central Europe as well as water from lysimeters and soil profiles were compared with respect to their hydrogen isotope content. Regional differences could be seen. Systematic variations in the deuterium content of rain, soil, and in part of lysimeter water were found to exist, but they do not exist in natural spring water. The applicability of deuterium investigations to the determination of percolation velocity and evaporation is suggested. In central Europe the mean deuterium content of spring water was found to decrease ~0.2% with each 100-m increase in altitude. (BBB)

39128 ESKDALEMUIR SEISMOLOGICAL STATION. Truscott, J. R. (Atomic Weapons Research Establishment, Aldermaston, Eng.). Geophys. J. Roy. Astron. Soc., 9: 59-68(Oct. 1964).

A description is given of the site, the layout of the array of seismometers, the electronic recording equipment and facilities, and some of the results obtained. Also described are the methods used to determine the crustal structure at the site, typical seismological background noise recorded during initial operation, and the capabilities of the array. The seismometer array consists of two straight lines of specially constructed instrument pits which intersect at right angles. The lines contain ten pits spaced 980 yd apart. The system used for the array enables one or two short-period seismometers to be operated in each pit over one six-core cable. Since a prime objective of the station is the recording of relatively small teleseismic events, background noise levels must be low even when using the added sophistication of separately recorded seismometers in array configuration. The noise background under typical conditions shows a peak particle velocity varying from 3.5×10^{-6} to 2×10^{-5} cm/sec in the band $\frac{1}{3}$ to 3 cps. (BBB)

39129 FRACTIONATION OF $^{18}O/^{16}O$ BETWEEN COEXISTING CALCITE AND DOLOMITE. Friedman, Irving (Geological Survey, Denver); Hall, Wayne E. J. Geol., 71: 238-43(Mar. 1963).

Although the fractionation of $^{18}O/^{16}O$ between coexisting calcite and dolomite has not been unequivocally established, it appears that a relatively large fractionation exists and that the difference in $\delta^{18}O$ values ($\Delta_{dolomite-calcite}$) in coexisting pairs is temperature dependent. Earlier studies of the Leadville limestone of Mississippian age, in the Gilman mine area, Colorado, indicated that there is no fractionation of $^{18}O/^{16}O$ between coexisting dolomite and quartz. Determinations were made of $\delta^{18}O$ and $\delta^{13}C$ of coexisting limestone and dolomite samples from several localities in the upper Mississippi Valley zinc–lead district. The fractionation of $^{18}O/^{16}O$ found in samples from various locations was discussed. (TSS)

39130 INSTRUMENTS AND METHODS: SNOW DENSITY PROFILING BY NUCLEAR MEANS. Leighty, Robert D. (Army Cold Regions Research and Engineering Lab., Hanover, N. H.). J. Glaciol., 6: 171-6(Feb. 1966).

A field investigation was conducted in Greenland to determine the feasibility of using a nuclear technique to determine snow and ice density profiles. A standard nuclear soil-moisture probe was used with two modes of pulse processing and recording. The probe had a 4.5-mC Ra–Be source and one BF_3 detector. The results of the correlation between scaler count ratio and the snow sample density are shown. Count ratio (which varies from 0 to 1.0 for any neutron probe) is the ratio of scaler count rate in snow to scaler count rate in water. The data are shown for snow sample densities from 0.32 to about 0.70 and ice densities of 0.87 to 0.91 g/cm^3. The maximum range in density for any given count ratio was from 0.40 to 0.70, a difference of 0.30 g/cm^3. This variation is unacceptable for profiling snow stratigraphy; however, some variation may be related to the inexperience of the snow samplers and to the difference between the effective sample volume in the nuclear method compared with that in the standard gravimetric method. While the nuclear method was found to be feasible, deficiencies related to poor resolution render the probe unusable for detailed profiling of snow stratigraphy in its present form. Expected progress in nucleonics should enable improved resolution and accuracy to be achieved. (BBB)

39131 USE OF NEUTRON METERS IN SOIL MOISTURE MEASUREMENT. J. Hydral. Div., Amer. Soc. Civil Eng., 92: 72-5(May 1966).

Some problems encountered in the use of neutrons to measure soil water content are discussed. Important causes of error, apart from electronic malfunctions and possible instability, include inaccurate calibration and the adsorption of neutrons by small quantities of neutron-absorbing elements in the soils. Errors or variations in the evaluations of soil-moisture volumes arising from the presence of neutron-absorbing elements can be reduced by a thin (0.015-in.) sheet of cadmium around the detector. Elements normally found in soils are not expected to complicate calibration of neutron moisture probes, but may have an effect on calibration of back-scattering type density gages. The use of lightweight portable calibration standards of polyethylene or similar highly hydrogenous plastic material for moisture probes provide convenient secondary standards for field reference and check, and allow direct comparison of the operating relation of and the results obtained with different meters. Demonstrations of changes in the shape, characteristics, and general volumes represented by soil-moisture profiles normally require only a reasonable degree of accuracy, but determinations of total volumes, small changes in water content (as in evapotranspiration or drainage studies) and the influences of soil types may require a higher degree of accuracy. (BBB)

39132 ORIGIN OF TRITIUM IN HYDROTHERMAL SOLUTIONS. Wilson, Stuart H. (Dept. of Scientific and Industrial Research, Private Bag, N. Z.). Nature, 211: 272-3(July 16, 1966).

The difficulty of deciding whether the tritium content of a natural water is a function only of the age of the water, or whether it arises from admixture of old water with new tritium, is particularly marked in the case of hydrothermal water. A hypothesis discussing the origin of tritium in these waters is described. (M.O.W.)

39133 URANIUM-234/URANIUM-238 RATIOS IN SEA WATER. Koide, Minoru; Goldberg, Edward D. (Univ. of California, La Jolla, San Diego). Progr. Oceanogr., 3: 173-7(1965). (UCSD-34P84-2).

The importance of radioactive disequilibrium within the natural uranium-238 series in various natural systems has steadily gained importance especially in geochronological and geochemical studies. Russian workers have shown that the parent member, U-238, and the daughter, U-234, in groundwaters do not exist in radioactive equilibrium concentrations. It has been postulated that while U-238 exists in crustal rocks primarily in the +4 state, as a result of the radioactive decays producing the daughter U-234, electrons are lost from the nucleus such that a part of the U-234 ends up in the +6 state. The latter form is preferentially brought into solution by weathering waters due to the formation of the strong complexes formed between uranyl and carbonate ions. Thus, the activity ratio A(U-234)/A(U-238) often exceeds one in surface waters. Experimentally determined values of the activity ratio in surface and deep sea waters from the Atlantic and Pacific Oceans and the Mediterranean Sea are uniform with a value of 1.14 ± 0.014. The error arises from the counting statistics in the radioactive assay of the alpha particles emitted by these two isotopes of uranium. This constancy in the ratio is consistent with the long residence time of uranium and relative lack of reactivity in sea waters. (auth)

39134 RECORDING AND ANALYSIS OF SEISMIC WAVES USING LINEAR CROSS ARRAYS. Whiteway, F. E. (Atomic Weapons Research Establishment, Aldermaston, Eng.). Radio Electron. Eng., 29: 33-46(Jan. 1965).

The instrumentation and technics being developed by the U.K. Atomic Energy Authority to detect underground nuclear explosions are described. Experimental work in the United Kingdom has so far concentrated on the use of linear cross arrays, spaced over a distance comparable to the longest wavelengths of the signal. Each seismometer is recorded on a separate track of magnetic tape. On playback, delays are inserted which phase the array for a range of azimuth and/or velocity. The phased outputs are processed by summation and correlation methods, resulting in discrimination against seismic noise and unwanted signal components. In this way, the onset of signal components may often be determined when obscured in a single seismometer output by previous arrivals or noise. It is also possible to determine the azimuth and velocity of many of the signal components of interest, thus aiding their identification. A signal/noise ratio improvement is also obtained for the first arrival, improving the accuracy of locating the hypocenters using triangulation methods from several stations. Linear cross arrays have been operated during recent years by the U.K. Atomic Energy Authority and many events analyzed, an example of which is shown. The theoretical performances of symmetrical cross and L-shaped arrays are given in the form of directivity patterns, and their method of use described. Correlation methods are shown to be necessary for obtaining a good azimuth or velocity response, and their advantages and limitations are considered. (BBB)

39135 AGE DETERMINATION OF TEKTITES AND OTHER NATURAL GLASSES BY MEANS OF TRACKS OF THE SPONTANEOUS FISSION OF ^{238}U (FISSION-TRACK METHOD). Wagner, Guenther A. (Max-Planck-Institut fuer Kernphysik, Heidelberg). Z. Naturforsch., 21a: 733-45(June 1966). (In German).

The fission-track age-determination method is described. A rapid and simple technique for dating natural glass is verified by experiment. Tektites and crater-glasses are dated by this method. The fission-track ages of samples of the same origin were found to be within 10%. Most of the measured ages are in good agreement with the known K–Ar ages. Explanations for the remaining discrepances are given. The absolute ages of the natural glasses are compared with their stratigraphic ages. The classification of the tektites into four groups, according to their K–Ar ages, is corroborated by the fission-track ages. The genetic relationship between the Nördlinger Ries and the moldavites from Czechoslovakia is confirmed. (auth)

39136 CHLORINE LOGGING APPARATUS WITH TEMPERATURE COMPENSATION CIRCUIT. Reed, Dale H.; McCallum, Robert E.; Pritchett, William C. (to Atlantic Refining Co.). U. S. Patent 3,258,593. June 28, 1966. Filed July 12, 1962.

A chlorine logging apparatus is provided with a gain stabilizing system for reducing the effects of temperature on the apparatus. In addition to the automatic electronic temperature compensating system, automatic adjustment of voltages is provided to compensate gain during a large initial temperature change in transfer of recorder from ground to borehole and for later occurring temperature changes down borehole. Both the photomultiplier and pulse-height analyzer circuit connected to the photomultiplier are modified to include temperature compensating equipment. (B.L.M.)

39137 METHOD AND APPARATUS FOR IDENTIFYING THE ELEMENTS IN THE FORMATIONS PENETRATED BY A DRILL HOLE. Youmans, Arthur H. (to Dresser Industries, Inc.). U. S. Patent 3,257,557. June, 21, 1966. Filed Sept. 20, 1960.

A neutron-gamma well logging apparatus for the identification of elements in the earths formations surrounding a borehole employs a gamma-free neutron source which accelerates deuterium ions onto tritium atoms to produce neutrons having an energy of about 14 Mev. The source generates the neutrons at spaced locations along the borehole, and the prompt gamma radiation resulting from the inelastic scattering of the neutrons is within a restricted energy level detected. The detector transmits a signal to recorders and analyzers at the surface where a record is made of the detected energy that is directly related to the element detected at a given location. (B.L.M.)

39138 EPITHERMAL NEUTRON WELL LOGGING. Hall, Hugh E. Jr. (to Texaco Inc.). U. S. Patent 3,264,477. Aug. 2, 1966. Filed Mar. 30, 1962.

A well logger consisting of a neutron source to irradiate earth formations and a neutron detector to defect epithermal neutrons is used in making an epithermal neutron log of earth formations surrounding a well bore. Epithermal neutrons are detected after removal of thermal neutrons by a shield which passes epithermal neutrons into hydrogeneous material where they are slowed to thermal energies and then detected by either a scintillation or proportional counter. (F.S.)

39139 HIGH RESOLUTION APPARATUS USING A GAMMA RAY SOURCE AND DETECTOR FOR INVESTIGATING EARTH FORMATIONS. Johnson, Frank Fawcett; Tittman, Jay (to Schlumberger Well Surveying Corp.). U. S. Patent 3,263,083. July 26, 1966. Filed Oct. 20, 1958.

Logging apparatus, including a gamma source and scintillation detector, is used to determine the density of earth formations. The ^{137}Cs gamma source must have an energy of at least 250 kev but not more than 800 kev. The scintillation radiation detector counter consists of a NaI crystal, photomultiplier tube, power supply amplifiers, pulse shaper, and a scaler. (F.S.)

39140 TEMPERATURE STABILIZED RADIOACTIVITY WELL LOGGING UNIT. Rabson, Thomas A.; Rabson, William R. (to PGAC Development Co.). U. S. Patent 3,265,893. Aug. 9, 1966. Filed June 13, 1963.

A new improved well logging unit of the scintillation crystal, photomultiplier type has a self-contained system for temperature regulation which can be used without opening the unit. The system includes a heat sink for temperature stabilization, a liquid path for heat conductivity, and a thermoelectric cooling device. (F.S.)

39141 DESIGN OF A NEUTRON SCATTERING WATER CONTENT GAGE FOR SOILS. Preiss, Kenneth (Univ. of Illinois, Urbana). 17p. (CONF-651108-4). ORAU. Gmelin, AED-CONF-65-347-5.

From Symposium on Isotope Techniques, Urbana, Ill.

The neutron scattering method of measuring the water content in soil is discussed. A method for reducing the effects of chemical composition of the soil and a design of a gage to minimize the error due to the randomness of nuclear decay is presented. (D.H.M.)

39142 DEVELOPMENT OF ISOTOPE METHODS APPLIED TO GROUNDWATER HYDROLOGY. Nir, A. (Weizmann Inst. of Science, Rehovoth, Israel). 19p. (CONF-651108–5). ORAU. Gmelin, AED-CONF-65-347-10.

From Symposium on Isotope Techniques, Urbana, Ill.

Critical evaluation of methods of isotope data interpretation in groundwater analysis is presented, and indications are that the assumptions made and the results obtained are not compatible with the problems and approaches of practicing hydrologists. Modifications of this approach may enable comparison of isotope survey results with those obtained by other conventional methods. More basic contribution of isotope methods to hydrology seems feasible in view of the analysis and the state of experimental techniques. (D.H.M.)

Thorium and Uranium Minerals

39143 APPLICATION OF ALPHA SPECTROMETRY TO THE SOLUTION OF GEOCHEMICAL QUESTIONS. Zeitler, G. (Staatliches Forschungsinstitut fuer Geochemie, Bamberg, Ger.). Mitteilungsbl. Strahlungsmessgeraete, 7: No. 15, 9-12(Apr. 1966). (In German).

The analytical methods used in the case of small thorium concentrations in uranium minerals, small uranium concentrations in thorium minerals, and for determination of the radioactive equilibrium of uranium isotopes in nature are summarized. The methods used in the preparation of sources for alpha spectrometry are indicated. (J.S.R.)

39144 ISOTOPIC DISTRIBUTION OF URANIUM AND THORIUM IN SOILS WEATHERED FROM GRANITE AND ALLUVIUM. Hansen, Richard Otto. Berkeley, Calif., Univ. of California, 1965. 135p.

Thesis.

Chemical techniques and physical instrumentation were developed to measure quantitatively the radioactivities of U-234, U-238, Th-230, and Th-232 in air-dry powdered samples of soils and rocks. These alpha emmitters were measured by alpha-particles spectrometry with ionization chambers and associated electronics constructed for these experiments. In residual soils of the Sierra Nevada, both uranium and thorium were concentrated to a greater degree than in the underlying rocks. Both uranium and thorium were most highly concentrated in clay fractions. Thorium-230 had redistribution patterns different from those of U-238, U-234, or Th-232 and often somewhat between those of isotopes of uranium and those of Th-232, showing the effects of Th-230 having existed as U-234 a significant fraction of the soil-forming period of time. Uranium-234 and U-238 usually had similar radioactivities. Curie radioactivity levels of individual nuclides ranged from 0.23×10^{-12} curies/gram for a fresh rock sample to 3.2×10^{-12} curies/gram for a clay formed from the rock in the case of U-238 and U-234. In the residual upland soils studied, uranium was preferentially retained whereas in the alluvial soils thorium was preferentially retained. Lime concretions from Ducor type soils showed enrichment of uranium in excess of thorium. Ages of 40,000 to over 180,000 years were calculated by means of two equations, one based upon the rapid initial accumulation of uranium and the other based upon a constant rate of accumulation of uranium. For an estimate of age for a primary soil (Ahwahnee sandy loam) with a developed "B" horizon, an equation was developed analogous to a branched decay where one branch represented leaching loss and another radioactive decay. An age of 32,000 years was calculated for the topsoil. (TCO)

39145 WORLD'S URANIUM RESOURCES. Lowell, A. F. (Rio Tinto-Zinc Corp. Ltd., London). 11p. (CONF-660220-2). ORAU. Gmelin, AED-CONF-66-022-1.

From American Nuclear Society, Canadian Nuclear Association Nuclear Energy Resources Meeting, Toronto.

Known information on the extent of uranium reserves outside the communist bloc is summarized and related to economic factors such as supply and demand and to commercial factors of interest to utilities and the nuclear fuel industry. Future developments in the uranium market are predicted. (F.S.)

HEALTH AND SAFETY

See also BIOLOGY AND MEDICINE — Radiation Hazards and Protection
GEOLOGY, METEOROLOGY, AND MINERALOGY — Natural Radioactivity and Fallout

Refer also to abstracts 38857, 39246, 39329, 40479, and 40482.

39146 (AD–636947) INDUSTRIAL RECOVERY TECHNIQUES. Brown, Stephen L. (Stanford Research Inst., Menlo Park, Calif.). Apr. 1966. Contract OCD-PS-64-201. 90p. CFSTI $3.00 cy, $0.75 mn.

Presented are some generalized concepts concerning industrial models, industrial vulnerability to nuclear weapons effects, industrial recovery requirements, and industrial recovery procedures. Mathematical expressions relating manufacturing outputs to inputs of materials, of facilities, and of people are presented and used to develop measures of damage and guidelines for allocating recovery resources. More qualitative descriptions of industrial operational organization, damage assessment methods, methods for determining recovery requirements, and specific recovery procedures are also formulated. Recommendations are submitted concerning (1) operational countermeasures for industry and for civil defense organizations and (2) desirable further research efforts in industrial civil defense. (auth)

39147 (CONF-660401-6) THE URECHIS PROGRAM: RAPID SURVEY OF FALLOUT CESIUM IN THE OCEAN. Folsom, T. R.; Sreekumaran, C. (Scripps Institution of Oceanography, La Jolla, Calif.). Apr. 15, 1966. Contract AT(11-1)-34. 15p. Dep. mn. CFSTI $1.00 cy, $0.50 mn.

From American Meteorological Society, American Geophysical Union, Annual Joint Meeting, Washington, D. C.

A new method for collecting large samples rapidly and at any depth for distribution studies is presented. Ocean water is forced through thin beds of granular potassium cobalt ferrocyanide (KCFC), a highly selective cesium absorbent, as they are towed behind a ship. It is possible to collect on about 50 grams of granular KCFC all the cesium that is present in about 100 liters of sea water in about one hour. The distribution of natural cesium in the ocean is used as an efficiency control. (J.G.B.)

39148 (GA–6511) GADOSE AND DOSET: PROGRAMS TO CALCULATE ENVIRONMENTAL CONSEQUENCES OF RADIOACTIVITY RELEASE. Lee, E.; Mack, R. J.; Sedgley, D. B. (General Dynamics Corp., San Diego, Calif. General Atomic Div.). Apr. 25, 1966. Contract AT(04-3)-633. 62p. Dep. mn. CFSTI $3.00 cy, $0.75 mn.

This report describes the digital computer program GADOSE, the calculational techniques used, and a sample calculation. The program was written specifically for the High-Temperature Gas-cooled Reactor (HTGR) type of plant, but no specific accident results are given. GADOSE is a FORTRAN program which calculates the radioactivity in various reactor plant locations and the doses to the public resulting from instantaneous accidental release of activity into any of the plant spaces. The calculations can be performed for any combination of isotopes and include consideration of decay, buildup, filtration, atmospheric dilution, fallout, and rainout. The companion program DOSET is also available to include the effects of a time dependent accidental fission product release into the various plant spaces. A typical calculation of the activities and doses at five times and five distances from the plant with 134 isotopes requires approximately 4 centihours of IBM 7044 machine time for the basic GADOSE program. (auth)

39149 (NVO–28) SAFETY INVOLVING DETONATION OF NUCLEAR DEVICES. (Reynolds Electrical and Engineering Co., Inc., Mercury, Nev. Management Engineering Dept.). May 1966. Contract AT(29-2)-162. 141p. Dep. mn. CFSTI $4.00 cy, $1.00 mn.

Long-range safety studies necessary to improve prediction capabilities and maintain pace with an active testing program are described. The day-to-day detonation safety activities necessary to support the testing program are described to the extent required to give an overall, though limited, version of event-related safety actions and procedures. The activities of the AEC laboratories designing and testing the nuclear devices are not described. (F.L.S.)

39150 (NYO–2753-4) ^{90}Sr LEVELS IN THE DIETS AND BONES OF CHILDREN. Progress Report, 1966. (Comision Nacional de Energia Atomica, Buenos Aires (Argentina)). Contract AT(30-1)-2753. 30p. Dep. mn. CFSTI $2.00 cy, $0.50 mn.

Measurements of natural Sr and ^{90}Sr content in foods, together with dietary information, were used to estimate the uptake of ^{90}Sr in children of different age groups residing in the vicinity of Buenos Aires, Argentina. The content of ^{90}Sr was also measured in bone samples from children of different age group collected in 1965. Dietary levels of ^{90}Sr in 1965 were lower than those of 1964 for all age groups. Analysis of the data indicates that the turnover rate of ^{90}Sr changes with age. Very young infants have a fast turnover rate of about 7%/mo but only 1.5/mo in the second year of life, and the adult rate of 3.5%/yr is reached during the third year of life. Strontium to Ca discrimination factors for the different age groups were also calculated from the data. The results indicate that Sr is discriminated against less in very young infants than in older children with a discrimination factor of about 0.7 in the first month after birth and 0.3 for the second year of life. Skeletal turnover rates and Sr and Ca discrimination factors appeared to be interrelated and both reached adult values during the third year of life with a faster turnover rate and correspondingly less discrimination occurring during adolescence. (C.H.)

39151 PROBLEM OF RADIOACTIVE CONTAMINATION OF THE SKIN. Schulte, John H. (Dept. of the Navy, Washington, D. C.). Arch. Environ. Health, 13: 96-101(July 1966).

Because of the rapid increase in utilization of radioactive materials, physicians in industry can anticipate seeing workers who have been contaminated with these substances. This report briefly reviews the physical and chemical characteristics of radioisotopes which are pertinent to such an eventuality and also describes the anatomy and defense mechanisms of the skin which are germane to the problem. The report concludes with a sequentially arranged list of procedures recommended by the author for the decontamination of the skin. An evaluation of decontamination solutions for use on skin is included. (C.H.)

39152 ^{137}Cs AND ^{90}Sr LEVELS IN DIET AND URINE OF AN ITALIAN CHILDREN'S COMMUNITY. Cigna, Arrigo A. (CNEN, Rome); Ferro-Luzzi, Anna; Mariani, Aldo; Spadoni, Maria Antonietta; Tomassi, Gianni. Health Phys., 12: 1105-8(Aug. 1966).

The variations of the ^{90}Sr and ^{137}Cs concentrations in the diet and in the urine of a group of thirty healthy children throughout the year were investigated. This set of experimental measurements allowed us to establish a correlation between the Cs contamination in diets and in the corresponding urines. The ratio between the contamination, in CU and SU, of the diets and of the urines, was found to be <1. (auth)

39153 HEALTH HAZARDS ASSOCIATED WITH THE FABRICATION OF PLUTONIUM–ALUMINUM FUEL ELE-

MENTS. Vernon, P. B. (E. I. du Pont de Nemours and Co., Aiken, S. C.). Contract AT(07-2)-1. Health Phys., 12: 1109-13(Aug. 1966).

A test program was conducted to assess contamination hazards and determine containment needs prior to design of Pu–Al fuel fabrication facilities. The tests, containment features developed, and operating experience are described. Hazards evaluation tests were conducted during melting, casting, machining, and decontaminating samples of 20 wt. per cent Pu–Al alloy in a glove box cabinet. Surface and airborne contamination released during the various test phases were determined; the results were used in defining contamination control requirements for billet preparation and tube extrusion facilities. Design features included (1) complete glove box containment of alloying and billet machining operations, (2) hooded billet outgassing furnaces with filtered exhaust and (3) a closed, vented box for receiving extruded fuel tubes which is connected to an alpha constant air monitor for detecting cladding failures. Operating experience has closely paralleled the results of the predesign contamination hazards tests. Radiation exposure problems have been controlled and direct handling of production components is possible. (auth)

39154 ^{137}Cs CONTENT OF MAN IN INDIA. Chhabra, A. S.; Sharma, R. C.; Katoch, D. S. (Atomic Energy Establishment, Trombay, India). Health Phys., 12: 1143-5 (Aug. 1966).

Whole-body counting techniques were used for the determination of ^{137}Cs in man in India from 1962 through 1965. The average ^{137}Cs content of healthy males per unit mass of K varied from 13.6 pc/gK for 1962 to about 32.5 pc/gK for the year 1965. (C.H.)

39155 SOME HEALTH PHYSICS IMPLICATIONS IN THE CHOICE OF RADIOACTIVE TRACERS FOR HYDROLOGICAL INVESTIGATIONS. Halevy, E. (Weizmann Inst. of Science, Rehovoth, Israel). Health Phys., 12: 1145-8(Aug. 1966).

A typical experiment in ground water investigations consists of the injection of a volume of marked water into an aquifer and subsequent pumping of the water out of the aquifer and constant monitoring of the activity of the water. The relation between the activity of the pumped water and the injected volume is used for computations of some characteristics of the aquifer. The selection of a tracer for ground water research is important from both hydrological and public health aspects. The relative merits and hazards of ^{58}Co, ^{60}Co, ^{51}Cr, and ^{46}Sc when used for this purpose are discussed. (C.H.)

39156 TECHNICAL PROBLEMS AND LEGAL PROBLEMS POSED IN BELGIUM FOR THE PHARMACEUTICAL CONTROL OF RADIOELEMENTS FOR MEDICAL USAGE. Fallais, C.; Constant, R. (CEN, Mol, Belg.). J. Pharm. Belg., Nos. 3-4, 137-45(Mar.-Apr. 1965). (In French). (BLG-357).

A study was made of the technical difficulties and legal problems to be faced by the pharmaceutical control of radioisotope production for medical uses. Some technical difficulties include contamination and irradiation. In the case of most regular productions, the sample taken for the control usually allows complete examination of the various properties of the whole lot. In the case of special productions or importation of radioelements for single delivery, the nature of the isotope and the level of radioactivity must be defined individually. Stipulations of the royal decree of February 28, 1963 concerning the pharmaceutical control of radioelements for medical use in Belguim are reviewed. (C.H.)

39157 RADIOACTIVITY AND DAIRY PRODUCTS. Garner, R. J. (United Kingdom Atomic Energy Authority, Harwell, Eng.). J. Soc. Dairy Technol., 18: 201-10(1965).

Sources of environmental contamination by artificially produced radiation and factors determining the importance of individual radionuclides for the exposure of human populations are reviewed. The importance of milk as a source of radioactivity in the diet is discussed in detail with emphasis on the transfer of ^{131}I from fresh fission products and ^{137}Cs and ^{90}Sr from stratospheric fallout to the diet of children through the consumption of fresh milk. Methods of reducing the content of ^{131}I, ^{137}Cs, and ^{90}Sr in milk are discussed and the effect of eliminating fresh milk from the diet are considered. It is concluded that since milk is the primary source of calcium for young children, and since milk contains less ^{90}Sr per gram of calcium than most other foods, the substitution of almost any other food as a source of calcium would increase the intake of ^{90}Sr by man. The transfer of environmental contaminants to man through milk can be reduced by prevention of the entry of nuclides into milk by various agricultural practices and the removal of nuclides from milk by suitable processing. (C.H.)

39158 RADIATION DOSIMETRY ABOARD MANNED SPACE VEHICLES. Baily, Norman A. (Hughes Research Labs., Malibu, Calif.); Sondhaus, Charles A. J. Spacecraft Rockets, 3: 1245-51(Aug. 1966).

Measurements necessary to characterize radiation exposure in space besides total dose are dose rate, distribution of dose in tissue, and local density of energy deposition, the latter generally characterized by the quality linear energy transfer (LET). In routine low-level exposures to known qualities of radiation on earth, measurement of total dose alone usually suffices to define an exposure; moreover, the known relation of dose in tissue for most radiations permits the measurement to be made in air or at the surface of the body and the tissue dose to be inferred from this. In contrast, the highly variable, high-energy particulate radiation of solar or cosmic origin entering the small metal-enclosed volume of air containing the astronaut can be expected to produce a buildup of secondaries, which depend on the local geometry. Hence, either direct tissue dose and LET measurement or a means of relating instrumental data to these is necessary in each case of space radiation exposure. Dose information required for this purpose can be acquired by relatively unsophisticated and highly reliable tissue equivalent instrumentation. Such instrumentation should give reliable values of the absorbed dose and some coarse breakdown of the LET spectra of the incident radiation in at least a sufficient number of ranges to allow weighting for changes of radiobiological effectiveness of the various LET groups. (auth)

39159 DOSAGE LOADS IN MEDICAL STAFF DEALING WITH COLLOIDAL ^{198}Au. Korenkov, I. P.; Slutskina, S. I.; Kozlov, V. F.; Bordyukova, M. A. (Moscow State Sanitation Station). Med. Radiol., 11: No. 3, 65-9(Mar. 1966). (In Russian).

Dosage loads in members of the medical staff using ^{198}Au are listed. Investigations proved that in some instances the contribution of beta-fluxes to the cumulative radiation dose of various critical organs reached quite an appreciable level. Therefore, when practicing individual dosimetry in medical establishments, it is necessary that gamma and beta radiation doses be measured with dosimeters placed on the outer surface of protective garments and with due account of specific work conditions. (auth)

39160 CHOICE OF A DOMINANT RADIATION IN CALCULATING THE PROTECTION AGAINST ELECTRON ACCELERATORS. Korenkov, I. P. (City Sanitation Center, Moscow). Med. Radiol., 11: No. 4, 47-50(Apr. 1966). (In Russian).

Indications are presented as to the choice of a dominant radiation in estimating protection against electron accelerators with the maximum energy of accelerated electrons of up to 30 Mev. (auth)

39161 DECONTAMINATION OF CERTAIN FABRICS INTENDED FOR USE IN PRODUCTION OF PROTECTIVE CLOTHING CONTAMINATED BY RADIOACTIVE ISOTOPES ^{90}Sr AND ^{137}Cs. Smal, Z. Prace Cent. Inst. Ochrony Pracy, 16: 179-93(1966). (In Polish).

Decontamination tests were made on fabrics used in protective clothing (impregnated and non-impregnated) that had been contaminated with ^{90}Sr and ^{137}Cs. Decontaminants used were detergents, citric acid of various concentrations, and

tap water of 20 and 50°C. The degree of decontamination depended on the kind of isotope, on the finish of the textile surface (impregnated or non-impregnated), and on both the kind and the concentration of the decontaminating agent. Also examined was the effect of repeated contamination and decontamination upon the degree of decontamination attained. (auth)

39162 A CLASSIFICATION OF CANADIAN HOSPITALS BASED ON FALLOUT EXPOSURE PROBABILITIES. Waters, W. R. Precis No. 2.03. Ottawa, Canadian Dept. of National Health and Welfare, 1962. 27p.

This survey is based on a computer study conducted by the Canadian Army Operational Research Establishment of the 96-hr dose of γ radiation which would be delivered at a number of points across Canada as a result of a heavy attack on North America. As designed, the computer program provides a figure of probability of any selected dose, at any particular point, not being exceeded. In designing the program, the Establishment included points where hospitals of interest to Emergency Health Services were located. It was not possible to include all hospitals but the major portion of those on the Emergency Health Services list was used. From the resulting data, hospital locations have been classified according to the probability of their being exposed to less than a 600-R dose integrated over 96-hr after the nuclear event. The 600-R point was selected since it was considered that most hospitals would have a limited area available where the protection factor was around 25 and there would be a larger area where the factor would be about 5 to 10; thus, the hospital would be able to function within its own confines throughout the period. The classification scale chosen was: Class A, 100% to 85% probability of dose not exceeding 600 R; Class B, 84% to 75%; Class C, 74% to 65%; Class D, 64% to 55%; and Class E, less than 55%. Thus, hospitals in class "A" or "B" localities would be preferred establishments. Those in class "C" locations would be less relied on; while those in classes "D" and "E" would be avoided. An examination of the integrated dose at the 90% probability level for the points of interest permit an estimation as to whether or not the intensity at any point will be greatly in excess of 10 R/hr at H + 24 or H + 48 hr. Thus an idea is obtained as to whether or not there would be access to the installation from the outside at these times. This report is regarded as a planning guide and not as an operational instruction; it should, however, be of use to persons faced with making decisions in relation to radiological conditions concerning which little may be known in advance of the event. (BBB)

39163 ASSAY OF ^{90}Sr IN HUMAN BONE IN THE UNITED KINGDOM. Results for 1965, Part I, with some Further Results for 1963 and 1964. Medical Research Council Monitoring Report Series No. 12. London, Her Majesty's Stationery Office, 1966. 20p. 2s. 3d.

Data are presented on the ^{90}Sr content in samples of human bone obtained from residents of Great Britain who died in the first half of 1965. Data from measurements made in 1963 and 1964 are included for comparison. (C.H.)

39164 WOODEN OVERCOAT (Engineering Materials). (Sandia Corp., Albuquerque, N. Mex.). (CAPE-1409). 1 drawing.

The Douglas fir plywood shell is used to enclose a steel-lead-steel type ICC-55 container. The shell will withstand a 30-ft drop test and fire exposure at 1800°F for one hour. (For details see TID-4100 Suppl. 35) (F.S.)

39165 PROBLEM OF INDUCED RADIOACTIVITY IN FOOD PRODUCTS. Tukhsheerer, T. Vienna, International Atomic Energy Agency, 1966, Preprint SM-73/53, 6p. (In Russian). (CONF-660609-9). ORAU.

From International Symposium on Food Irradiation, Karlsruhe, Ger.

Radioactivity induced by irradiation of foods is caused by the interaction of high-energy radiation with nuclei of food elements. The induced activity is a function of the applied energy, dose, sample thickness, and chemical composition of the food. A prime condition for predicting the radioactivity induced by irradiation is therefore the knowledge of the chemical composition of the sample. Suitable experimental methods of food analysis are described. Electron and gamma rays are equivalent in the production of induced radioactivity. In the energy range of 0.05 to 10 Mev induced radioactivity is due to stimulation of isomers in (γ,γ') reactions. In this range the ^{107}Ag $(\gamma,\gamma')^{107m}Ag$ reaction is responsible for the greatest part of the induced activity. Using a new simplified method of calculation the expected induced radioactivity is estimated, and it was concluded that the activity of these isomers presents no health hazards. By the same method the induced radioactivity in the energy range above 10 Mev–where besides (γ,γ')-reactions the possibility of (γ,n)-reactions exists–is calculated for the principal foodstuffs. Methods for experimental verification of calculated activities are discussed. The magnitude of induced radioactivity due to single elements is compared with the total maximal permissible concentration (MPC) of nuclides in foods (10^{-7} $\mu C/g$ food). Factors that determine the maximum permissible radiation energy and dose are discussed. (auth)

39166 MATERIALY TRETEI NAUCHNO-PRAKTICHESKOI KONFERENTSII PO RADIATSIONNOI GIGIENE, 16-20 APRELYA 1963 G. (Reports of the Third Scientific and Working Conference on Radiation Protection, April 16-20, 1963). Nevstrueva, M.A. (ed.) Leningrad, Leningrad Scientific Research Inst. on Radiation Protection, 1963. 87p. (CONF-630405).

Ninety-six papers are included on radiation protection and sanitation control for personnel handling radioactive materials in laboratories, industry, and in the field; permissible and absorbed doses; effects of single and chronic exposures to ionizing radiation; effects of combined electromagnetic waves and x radiation; rules and regulations for the operation of high-energy radiation installations; effects, metabolism, and excretion of radioisotopes; dosimetry and monitoring methods; and radioactive contamination in air, water, milk, and soil. (R.V.J.)

INSTRUMENTATION

General

Refer also to abstracts 38545, 38546, 39291, 39292, and 39335.

39167 (AD-636927) DESIGN AND CONSTRUCTION OF A MODIFIED LOZIER TUBE FOR IONIZATION STUDIES NOT INVOLVING MASS ANALYSIS. Ryan, K. R.; Miller, C. D. (Aerospace Research Labs., Wright-Patterson AFB, Ohio). Apr. 1966. 24p. (ARL-66-0072). CFSTI $1.00 cy, $0.50 mn.

The design parameters, construction, and some potential applications of an electron impact device which does not provide for mass analysis are discussed. Such a device was described by Lozier in 1930 but has not been used extensively since the use of mass spectrometers to study the ionization of molecules has become more general. Mass analysis obviously provides essential information on ionization processes, but the ion source used in mass spectrometry introduce some generally unknown degree of mass and energy discrimination. The Lozier tube therefore offers some promise as a device to supplement mass spectrometric studies of ionization processes. (auth)

39168 (AED-C-06-14) BIBLIOGRAPHIEN ZUR KERNFORSCHUNG UND KERNTECHNIK. SEKTION 06: MESSINSTRUMENTE UND MESSVERFAHREN IN DER KERNPHYSIK. (Bibliographies in Nuclear Science and Technology. Section 06: Instruments and Measureing Techniques in Nuclear Physics). Debertin, K. (comp.) (Zentralstelle fuer Atomkernenergie-Dokumentation, Gmelin-Institut fuer Anorganische Chemie und Grenzbebiete, Frankfurt am Main (West Germany)). May 1966. 196p. Dep. mn.

Bibliographies are presented on instruments and techniques in nuclear physics. Also included are report number, patent, author, and subject indexes. (B.G.D.)

39169 (ISS-66/17) APPARATO AUTOMATICO PER LA MISURA DI DEBOLI CORRENTI E, IN PARTICOLARE, PER LA TARATURA DI PREPARATI DI RADIO. (Automatic Apparatus for the Measurement of Weak Currents, Particularly Suited for the Calibration of Radium Medical Appliances). Corti, F.; Felici, C.; Vallone, A. (Istituto Superiore di Sanita, Rome (Italy). Laboratori di Fisica). Apr. 22, 1966. 25p. Dep. mn.

An automatic apparatus was built for the measurement of weak currents. It consists of two tunnel diode trigger circuits, in parallel, biased to different voltage and kept at constantly controlled temperature. The experimental results are displayed on a teletype, with the optimal punching of telex international code 5-channel paper tape. It is thus possible after tape-to-card conversion directly to feed the results to the electronic computer. (auth)

39170 (RISO-M-423) BERETNING OM ARBEJDET I ELEKTRONIKAFDELINGEN I TIDEN 1 JANUAR TIL 31 MARTS 1966. (Progress Report on Electronics for the Period January 1-March 30, 1966). (Danish Atomic Energy Commission, Risoe. Research Establishment). June 1966. 32p. Dep. mn.

A progress report is presented on instrumentation. Topics discussed are data handling techniques, industrial instrumentation, reliability studies, reactor dynamics, analog techniques, and isotope techniques. (B.G.D.)

39171 RADIOMETRIC EQUIPMENT ON THE COSMOS 41 SATELLITE. Savenko, I. A.; Tel'tsov, M. V.; Maduev, V. L.; Savun, O. I.; Yurovskiy, A. V. (Moscow State Univ.). Geomagn. Aeronomy (USSR) (Engl. Transl.), 5: 889-92 (1965).

Translated from Geomagn. Aeronomiya, 5: 1129-31 (1965).

The RE-2 radiometric equipment installed on Cosmos 41 satellite is described. The basic electric circuit of the radiometer is shown. Also, the circuit of a USK control mechanism is included and the ferrite-transistor scaling system is illustrated. Data indicate that the equipment installed on Cosmos 41 functioned normally for a long period of time. (J.H.M.)

39172 APPARATUS FOR THE PRECISE METERING OF RADIOACTIVE GASES OR SOLUTIONS. Benson, R. H.; Maute, R. L. (Monsanto Co., Texas City, Tex.). Int. J. Appl. Radiat. Isotop., 17: 427-30(July 1966).

A portable apparatus is described for the precise metering of radioactive materials into gas or liquid streams at constant rates. The apparatus uses a very long metal capillary as the metering section. It has a wide range of metering and permits measurements on large as well as small flows of gases or solutions into streams having pressure from zero to 450 psig. Applications to the metering of radioactive gases or liquids into streams are described. Block diagrams of the equipment are included. (C.H.)

39173 PARAMETERS OF RADIOISOTOPE RELAY INSTRUMENTS. Mlckovsky, Miloslav. Jad. Energ., 12: 261-3(1966). (In Czech).

Radioisotope relays used in industry need unified definitions of radiometric parameters. The terms relay operation threshold, relay release threshold, time of relay operation and release, hysteresis and statistic reliability are explained. With the aid of these terms and on the basis of measured results, conditions are indicated for the reliable operation of radioisotope relays. The parameters of MNA 301 radioisotope relay produced in Tesla-Liberec Works are given as an example of radiometric characteristics. (auth)

39174 CHARACTERISTICS OF A THERMAL NEUTRON TELEVISION IMAGING SYSTEM. Berger, Harold (Argonne National Lab., Ill.). Mater. Eval., 24: 475-81 (Sept. 1966).

A thermal neutron sensitive image-intensifier tube, capable of presenting a demagnified, bright visible image of a thermal neutron beam, is the major component of a neutron sensitive television system. The television system is capable of following object movements as fast as 5 m/min without objectionable blurring, resolves hole images as small as 0.5 mm, and displays a contrast sensitivity of 4 percent in a narrow thickness range for steel and uranium objects. The sensitivity and relative neutron-gamma response of the intensifier are sufficiently good so that gamma radiation levels as high as 4000 R/hr at the tube face cause little difficulty when the system is used at the described reactor facility. The possibility of using the detection system with non-reactor neutron sources is discussed, and the resolution and contrast sensitivity capabilities of the system are analyzed. Application areas are indicated. (auth)

39175 SURVEY OF DEVICES TO MEASURE FUEL ELEMENT COOLANT CHANNELS. De Meester, P.; Deknock, R.; Verstappen, G. (SCK/CEN, Mol, Belg.). Mater. Eval., 24: 482-6(Sept. 1966).

Several gages for the measurement of a 3-mm gap over a length of 1 m have been developed at SCK/CEN. A survey of these devices and measurements is given, as well as a brief comparison of the different systems. Gages based on capacitance or on ultrasonics—the latter ones especially for post-irradiation measurements of coolant channels—are considered to be the best. (auth)

39176 REVIEW OF MULTICHANNEL AND MULTIPARAMETER ANALYZER SYSTEMS. Guillon, H. (CEA, Saclay, France). Nucl. Instrum. Methods, 43: 240-7 (Aug. 1, 1966).

During the recent years, pulse height analyzers were improved to a high degree, as well for performances as for refinements. No major difficulties arise for the multiparametric analyzers realization if modest capabilities

are requested. Nevertheless development of more universal instruments raises important problems for compactness and for memory capacity. (auth)

39177 STABILIZED POWER SUPPLY OF THE TYPE ZNN 4. **Girulski, Ryszard (Instytut Badan Jadrowych, Warsaw). Nukleonika, 11: 63-5(1966). (In Polish).**

The power supply was designed for uses where a highly stable voltage is required for a large range of current drain. The circuit was designed for gain stable nanosecond pulse amplifiers. It provides voltages of +250, –150, +450, and 6.3 with respective output current ranges of 0–500, 0–50, 0–50 mamp and for the 6.3 v, 2 × 15 amp and a regulated 1amp. For a ±10% change of supply voltage (line voltage) or for a 0-maximum current range, the voltage stability is 6×10^{-4} for the +250 v supply and 2×10^{-3} for –150 v. The 8-hour stability is 1% for these supplies. Peak-to-peak ripple voltage is 10 mv, 26 mv, and 1 v for +250, –150, and +450 v supplies. (TTT)

39178 REGISTRATION OF THE STATE OF DECATRON COUNTING SYSTEMS BY MEANS OF TELEPRINTER CODE. **Czech, Zbigniew; Turala, Michal; Turek, Leszek (Instytut Badan Jadrowych, Krakow). Nukleonika, 11: 73-8(1966). (In Polish).**

A transistorized electronic system is described which can rapidly sense the state of a 10-decade scaler, codify the information, and provide output which can be used to operate a typewriter and/or punched paper tape type of data storage device. The state of the counter is sensed by means of a gating arrangement in which the various digits of the scaler are made to set the state of bistable circuit elements. A diode matrix system is used to codify these data, after which they are transmitted to the teleprinter and paper tape puncher. The paper tape output is obtained in a form suitable for input to a computer which is used to process the data. (TTT)

39179 A CHAMBER FOR MEASURING PHOTOCONDUCTIVITY OF HIGH-OHMIC MATERIALS UNDER STRONG IRRADIATION. **Tsukerman, V. G. (Inst. of Inorganic Chemistry, Academy of Sciences, Novosibirsk SSR). Prib. Tekh. Eksp., No. 6, 192-3(Nov.-Dec. 1965). (In Russian).**

The current induced in semiconductors by radiation is usually between 10^{-9} and 10^{-17} amp; its measurement requires special instrumentation with electrostatic input and protection against parasitic currents generated by the ionization of the air. Current measuring devices provided with a shield still record the parasitic currents. A study of the dependence of the ionization current on the intensity of x radiation revealed that the current is strongly dependent on the voltage applied on the electrodes. A new chamber was designed for measuring photocurrents and emf in the x-ray portion of the spectrum, eliminating completely the parasitic currents. The specimen placed in a teflon container within the chamber may be exposed to x radiation through a beryllium window. The measuring electrode is placed within a shielding cylinder placed on a teflon support, insulating it from the ground. The instrument was used for measuring the conductivity induced by x radiation in semiconducting films possessing high specific resistivity, and may be used to determine the conductivity induced in semiconductors and insulators by hard radiation. (TTT)

39180 IMPROVED ELECTRON BOMBARDMENT EVAPORATOR. **Semicond. Prod. Solid State Technol., 9: 37-8(Feb. 1966).**

An inexpensive focused-beam electron-bombardment evaporator developed at the National Bureau of Standards is described. This instrument possesses most of the desirable features of existing evaporators, and provides a simplified focusing cylinder which decreases the cost and increases the flexibility and the usefulness of the device. In this device an electrically isolated cylindrical shield is used to deflect and focus the electron beam so that interference by gas discharge is avoided and a more efficient and stable bombardment process is achieved. Despite its desirable features, the use of the electron bombardment technique has presented problems. Electron beam focusing is usually required, and the principal drawback until now has been the high cost of good focusing systems. The difficulty is that the focusing geometry necessitates close anode-to-cathode distances, causing the vapor density above the anode to be very high during evaporation. This high density allows vapor molecules to reach the cathode despite shielding attempts, which leads to gas discharge and its annoying problems. The most common way of solving this problem has been to increase the cathode-to-anode distances, but until now this solution has involved a sharp bending of the electron beam, resulting in the employment of costly electron gun modules. In the new system, bending of the beam is avoided by placing an electrically isolated cylindrical shield between the electron source and the material to be evaporated. The use of the shield allows large anode-to-cathode distances which act to suppress ionic gas conduction during operation. As electrons strike the cylindrical shield it assumes a negative charge. When this occurs a charge effect takes place which acts to repel electrons from the cylinder walls and thus tends to collimate, or to focus, the beam. In this way the unit achieves many of the advantages of evaporators using much more complex focusing arrangements. The evaporator is especially useful in situations where contamination is to be avoided. The economy and simplicity of design allow for dismantling to facilitate cleaning. (BBB)

39181 ANALYSIS OF DIGITAL ANGER CAMERA WITH THREE-DIMENSIONAL RESOLUTION FOR POSITRON EMITTERS. **Kenny, Peter J. (Sloan-Kettering Inst. for Cancer Research, New York); Lundy, Arvid; Laughlin, John S. Contract AT(30-1)-910. Trans. N. Y. Acad. Sci., 28: 628-34(Mar. 1966).**

An imaging system for the measurement of radioisotope distributions that provides spatial resolution in three dimensions for positron emitters is described. Annihilation gamma rays are detected in coincidence by scintillation detectors. The results of an investigation of the efficiency and resolution of the system are presented. (D.C.W.)

39182 FILM PROJECTOR, MURA "A" (Engineering Materials). (Argonne National Lab., Ill.). (CAPE-1439).

137 drawings.

The overhead projector is specifically designed for projecting bubble chamber film and consists of a four-view film platen, illumination system, projection lenses, and a film transport. The system is mounted on a steel "A" frame which can accommodate a viewing table, and/or an image-plane digitizer. (For details see TID-4100). (F.S.)

39183 TRANSISTORIZED 100-CHANNEL ANALYZER (Engineering Materials). (Los Alamos Scientific Lab., Univ. of California, N. Mex.). (CAPE–1427).

11 drawings.

The transistorized instrument consists of a monitor, memory, analyzer, printer relay, and power supplies. (For details see TID-4100 Suppl 35). (F.S.)

39184 SINGLE CHANNEL ANALYZER (Engineering Materials). (Health and Safety Lab., New York Operations Office (AEC), N. Y.). (CAPE–1424).

19 drawings.

The signal to be analyzed is routed, after amplification, to one of two independently biased and controlled discriminators. Coincidence or anticoincidence time conditions can be imposed to control the main output. One of the channels may be used independently as an integral discriminator to control coincidence routing in a multichannel analyzer. (For details see TID-4100 Suppl. 35). (F.S.)

39185 RIVER WATER SAMPLER /Q-2737/(Engineering Materials). (Oak Ridge National Lab., Tenn.). (CAPE–1389).

6 drawings.

The sampler obtains samples in proportion to the flow rate. The sampling rate is accurate to ±4%. (For details see TID-4100 Suppl. 35). (F.S.)

39186 OPERATIONAL D-C CURRENT LINEAR AMPLIFIER /Q-2773/(Engineering Materials). (Oak Ridge National Lab., Tenn.). (CAPE–1394).

1 drawing.

The transistorized amplifiers perform with a constant Q and gain at each harmonic, and discriminate against noise which lies outside the filter passbands. Three such amplifiers are used in a filter used to select the Fourier components of a periodic signal. (For details see TID-4100). (F.S.)

39187 T. C. VACUUM GAGES /Q-2173A AND Q-2254A/(Engineering Materials). (Oak Ridge National Lab., Tenn.). (CAPE-1446).

14 drawings.

Power supplies and packaging for thermocouple vacuum gages, a Hastings Model V T-6 and a Hastings Vacuum Controller CVT-6, are described. (For details see TID-4100). (F.S.)

39188 NUCLEAR PULSE AMPLIFIER (Engineering Materials). (Lawrence Radiation Lab., Univ. of California, Livermore). (CAPE-1423).

27 drawings.

Characteristics of the solid-state 6-loop amplifier include temperature stability, fast recovery, high count rate capabilities, common mode rejection, and a choice of pulse shaping. The amplifier demonstrates stability to within 50 ppM/°C at gains up to 1024, and it exhibits ±0.01% linearity up to 10v output. (For details see TID-4100 Suppl. 35). (F.S.)

39189 MASS DETERMINATION OF A FLUENT MATERIAL BY RADIOACTIVE MEASURING MEANS. Brunton, Donald C.; McMullen, James M. (to Industrial Nucleonics Corp.). U. S. Patent 3,263,077. July 26, 1966. Filed Aug. 30, 1961.

A penetrative radiation gauging system is adapted to measure and continuously indicate the mass of aircraft fuels. A beta source and a target form an x ray generator which produces penetrating rays detected by an ionization chamber. (F.S.)

39190 MISSILE SCORING SYSTEMS UTILIZING NUCLEAR RADIATION. Cohen, Martin J.; Carroll, David I.; Gibson, Henry C. Jr.; Grice, Karl R. Jr.; Wernlund, Roger F. (to Franklin GNO Corp.). U. S. Patent 3,265,894. Aug. 9, 1966. Filed Mar. 1, 1963.

Missiles or projectiles are labeled with a source of radiation to determine scaler miss-distance or firing error. Gamma radiation is normally used but alpha or beta particles may be used at higher altitudes or in outer space. Radiation can be associated with the missile as an ingredient in the shell material, nuclear reactor activation of the shell material, plating, painting, or by inserting an active source in the munition. The system consists of the source, detector, and telemetering equipment. (F.S.)

39191 COMPENSATED NUCLEAR RADIATION FLUID ANALYZER. Zwetzig, Gerald B.; Scherb, Maurice V. (to North American Aviation, Inc.). U. S. Patent 3,267,282. Aug. 16, 1966. Filed May 22, 1962.

This device measures the concentration of at least one element of high atomic number in a fluid of relatively low atomic number. The device consists of two radiation sources and two radiation detectors. Concentrations are determined by successively exposing the fluid stream to sources having different characteristics of attenuation and automatically calculating the concentration from the different attenuations. The device is particularly suited to the determination of sulfur in a stream of crude or refined petroleum or the determination of the concentrations of additives in gasoline. (F.S.)

Radiation Detection

Refer also to abstracts 38558, 38777, 39139, 39140, 39502, 39767, 40315, and 40333.

39192 (AD-636206) A FIELD DETECTOR STATION FOR THE DASA FALLOUT AND TRANSIT DOSE RATE MEASUREMENT SYSTEM. Paynter, D. A. (Edgerton, Germeshausen and Grier, Inc., Santa Barbara, Calif.). Aug. 1966. Contract DA-49-146-XZ-292. 33p. (NDL-TR-71(Suppl.); DASA-1688(Suppl.)). CFSTI $2.00 cy, $0.50 mn.

A solid-state version of the detector station electronics used in the DASA Fallout and Transit Dose Rate Measurement System is described. The performance of the solid-state version equals or exceeds that of the experimental vacuum tube model it replaces, and it reflects both cost and electric economies. A by-product of the design is the availability of a frequency modulated a-c output signal that can be readily transmitted, recorded, and digitized without intermediate signal processors as would be required with d-c data signals. The system's resulting economies are outlined. (auth)

39193 (AD-636736) COMPUTER-COUPLED QUALITY CONTROL PROCEDURE FOR GAMMA-RAY SCINTILLATION SPECTROMETRY. Covell, D. F. (Naval Radiological Defense Lab., San Francisco, Calif.). Apr. 25, 1966. 17p. (USNRDL-TR-1034). CFSTI $1.00 cy, $0.50 mn.

Long-term stabilization of instrumental performance is necessary for gamma-ray scintillation spectrometry whether used for nuclear spectroscopy studies or for radionuclide identification and estimation. This requirement is especially important if high-precision measurements are to be made on a routine basis. It is proposed to achieve sufficient stabilization through statistical quality control, a technique used to maintain the quality of output of a process or system. A quality control procedure was devised which consists of periodic measurement of a current standard spectrum and comparison of it, on a channel-by-channel basis on a computer, with a reference standard spectrum. Significant differences between the two spectra are interpreted as machine deviations that require correction. As part of the procedure, values obtained from this measurement are charted so that current and past performance can be compared easily. This makes possible a prompt awareness of unusual changes in performance. Application of the technique has resulted in improved stability, improved reliability, and reduced maintenance. Approximately 20 minutes of technician time are required per day to apply this procedure to a single instrument. Less time per instrument is required when several instruments are simultaneously controlled. (auth)

39194 (AD-638137) BROAD RANGE MAGNETIC NEUTRON SPECTROMETER. Cialella, C. M. (Ballistic Research Labs., Aberdeen Proving Ground, Md.). May 1966. 39p. (BRL-MR-1753). CFSTI $2.00 cy, $0.50 mn.

A broad range, low deflection, magnetic neutron spectrometer was designed and constructed to measure the neutron spectra from pulsed and steady state sources. The instrument will cover an energy range of 0.5 to 17 Mev with a single magnetic field setting and is designed to provide energy resolution of approximately 10 percent. A collimated beam of neutrons is allowed to impinge on a thin polyethylene radiator producing recoil protons. A small forward cone of these protons corresponding to the full energies of the incident neutrons, enters the magnetic field. The protons are analyzed and focused at a point outside the magnetic field. The focal line is straight and forms an angle of 10 degrees with the pole-piece edge. With 6 Mev neutrons, a 0.001 inch radiator, and 0.5 inch slit width, the energy resolution is 7.7 percent and the efficiency is 6.3×10^{-8} counts per incident neutron. (auth)

39195 (AE-235) OPTIMAL LINEAR FILTERS FOR PULSE HEIGHT MEASUREMENTS IN THE PRESENCE OF NOISE. Nygaard, K. (Aktiebolaget Atomenergi, Stockholm (Sweden)). July 1966. 18p. Dep. mn.

For measurements of nuclear pulse height spectra a linear filter is used between the pulse amplifier and the pulse height recorder so as to improve the signal/noise ratio. The problem of finding the optimal filter is investigated with emphasis on technical realizability. The maximum available signal/noise ratio is theoretically calculated on the basis of all the information which can be found in the output of the pulse amplifier, and on an

assumed a priori knowledge of the pulse time of arrival. It is then shown that the maximum available signal/noise ratio can be obtained with practical measurements without any a priori knowledge of pulse time of arrival, and a general description of the optimal linear filter is given. The solution is unique, technically realizable, and based solely on data (noise power spectrum and pulse shape) which can be measured at the output terminals of the pulse amplifier used. (auth)

39196 (AE–236) DETEC: A SUBPROGRAM FOR SIMULATION OF THE FAST-NEUTRON DETECTION PROCESS IN A HYDRO-CARBONOUS PLASTIC SCINTILLATOR. Gustafsson, B.; Aspelund, O. (Aktiebolaget Atomenergi, Stockholm (Sweden)). July 1966. 26p. Dep. mn.

A description is given of the subprogram DETEC, which for energies below 5 Mev simulates the detection process of a fast neutron within a large cylindrical plastic scintillator. DETEC was coded in FORTRAN IV, and consists of a subroutine and a BLOCK-DATA subprogram. The latter is in its present form adapted to the dimensions 5 cm ø × 8 cm of the scintillating materials NE102 and NE102A. The character of DETEC as a subprogram is manifest through the requirement of a main routine for generation of the following input parameters: fast-neutron position, direction, energy, entrance time, input weight; and discriminator threshold. When these are provided, the virtues of DETEC are recording of the detected weight and the time elapsed prior to the detection event. The merits of DETEC are finally demonstrated in two typical applications. (auth)

39197 (AECL-2565) USE OF Ge(Li) DETECTORS IN γ-γ COINCIDENCE EXPERIMENTS. Ewan, G. T.; Graham, R. L.; Mackenzie, I. K. (Atomic Energy of Canada Ltd., Chalk River (Ontario). Chalk River Nuclear Labs.). Mar. 1966. 11p. (CRGP-1237). Dep. mn. AECL $0.50.

Large volume Ge(Li) detectors were used in a γ-γ coincidence arrangement employing two Ge(Li) detectors. The results of studies of the timing properties of planar and coaxial diodes and the time resolution curves that can be obtained are reported. For two cylindrical coaxial diodes the full-width at half-maximum of the time resolution curve was 14 nsec for 511-kev γ rays. The application of the detectors in γ-γ coincidence experiments is described. The coincidence counting rates are limited by the total singles counting rates that can be tolerated without excessive loss of energy resolution. Results are shown illustrating the application of a Ge(Li)–Ge(Li) coincidence arrangement to a complex γ-ray spectrum and the ability of this technique to reveal new information on γ-γ cascades. (auth)

39198 (BNWL–250) ADVANCED ALPHA-BETA-GAMMA HAND AND SHOE CONTAMINATION MONITOR. Sheen, E. M.; Ratcliffe, C. A.; Zuerner, L. V. (Battelle-Northwest, Richland, Wash. Pacific Northwest Lab.). Aug. 1966. Contract AT(45-1)-1830. 25p. Dep. mn. CFSTI $1.00 cy, $0.50 mn.

A combination alpha-beta-gamma hand and shoe contamination monitor was developed which incorporates low-noise multiplier phototubes, special light pipes, probe-contained preamplifiers to provide a satisfactory signal-to-noise ratio, and all solid state circuitry with no relays. The main chassis contains power supplies, indicating registers, all circuitry except that used in the probes, and adjustment controls that are incorporated in a printed circuit card file. Solid state circuits were developed and fabricated on printed circuit cards that were size-compatible with available, commercial card files. These circuits, combined with commercially available logic units, provided an instrument that reduced both capital and maintenance costs. The basic design is that of a combination alpha-beta-gamma contamination monitor; however, the general design features are directly applicable to the manufacture of single-purpose instruments, as for beta-gamma only or for alpha-only monitors. (auth)

39199 (COO–1105-117) THE EFFECT OF THE QUALITY OF RADIATION ON THE THERMOLUMINESCENCE OF LiF(TLD-100). Wagner, J.; Cameron, J. R. (Wisconsin Univ., Madison. Dept. of Physics). July 15, 1966. Contract AT(11-1)-1105. 8p. Dep. mn. CFSTI $1.00 cy, $0.50 mn.

The effect of the quality of radiation on the thermoluminescence (TL) of LiF (TLD-100) in a supralinear region of the thermoluminescence vs energy response curve is reported. This energy dependence appears to correlate inversely with the linear ion density produced in the material for the radiation used. In order to test this hypothesis, the number of ion pairs formed per micron was evaluated for several radiation qualities. TL response curves were determined for five photon energies from 25 to 662 kev and for $^{90}Sr-^{90}Y$ beta rays. (B.G.D.)

39200 (COO–1105-118) EFFECTS OF IRRADIATION TEMPERATURE IN LiF(TLD-100). DeWerd, L. A.; Cameron, J. R. (Wisconsin Univ., Madison. Dept. of Physics). July 15, 1966. Contract AT(11-1)-1105. 10p. Dep. mn. CFSTI $1.00 cy, $0.50 mn.

Experimental results are presented on the effects of irradiation annealing on the thermoluminescence on LiF (TLD-100) at 290 and −54°C. The results are compared to previous results reported for room temperature irradiations. (B.G.D.)

39201 (EUR–2999.e) PHASE LOCKED FREQUENCY MULTIPLIER FOR A SPEED- AND PHASE SYNCHRONIZATION SYSTEM BETWEEN A D.C.- AND A SYNCHRONOUS MOTOR. May, F. (European Atomic Energy Community, Ispra (Italy). Joint Nuclear Research Center). July 1966. 16p. Dep. mn.

A phase locked frequency multiplier is described, which is designed for the purpose of a speed synchronization and phase control system a d-c and a synchronous motor. The speed of the motors is normally set to 6000 rpm. Two reference pulses per revolution delivered by the pick-up system of the d-c motor are multiplied by a factor of six. (12 pulses per revolution are needed to trigger the driving unit of the synchronous motor.) (auth)

39202 (IFA-PN–17) RELATIONS ENTRE LA CINETIQUE DE DEVELOPPEMENT LA SENSIBILITE DE L'EMULSION ET L'ECLAIREMENT. (Relations Between the Kinetics of Development of Emulsion Sensitivity and Illumination). Nicolae, M. (Institutul de Fizica Atomica, R. P. R., Bucharest (Romania)). 1966. 13p. Dep. mn.

It was established that there exists an exponential relation between the development speed and the redox potential of the developer in the case of feroxalate developers for emulsions of different sensitivities and different exposures (light, α particles, and electrons). The exponential constant varies with the sensitivity of the emulsion and the nature of the incident radiation. This can be explained by the influence of the degrees of dispersion of the latent image centers. It was also established that the relation existing between the activity of the developer and the activation energy of the developer depends on the exposure level. For a given redox potential, the activation energy increases as the exposure decreases. (tr-auth)

39203 (INP–476/PL) LARGE PERMANENT MAGNET SEMICIRCULAR BETA RAY SPECTROGRAPH. Kormicki, Jan; Niewodniczanski, Henryk; Stachura, Zbigniew (Institute of Nuclear Physics, Krakow (Poland)). May 1966. 41p. Dep.

A large permanent magnet semicircular beta-ray spectrograph with maximum radius of the electron path ρ = 420 mm is described. The dimensions of the pole pieces are 1000 × 630 mm^2. The gap height is 60 mm. Detection of electrons occurs on photographic plate or by using G-M counters. Energy resolution is about 0.04 per cent. A brief description of the applied method is given. Examples of the use of the spectrograph are presented. (auth)

39204 (INR–694/III/PL) INFLUENCE OF THE CHANNEL WIDTH OF THE MULTICHANNEL ANALYZER ON THE SPECTROMETER RESOLUTION. Kalisz, Jozef

(Institute of Nuclear Research, Warsaw (Poland)). Mar. 1966. 6p. Dep.

A method allowing evaluation of the influence of the analyzer channel width on the spectrometer resolution is described. The method is based on the assumption of Gaussian amplitude distribution at the analyzer input. (auth)

39205 (INR-703/III/PL) DETERMINATION OF COINCIDENCE-CIRCUIT STATISTICAL PARAMETERS BY MEANS OF THE POINT METHOD. Kalisz, J. (Institute of Nuclear Research, Warsaw (Poland)). Apr. 1966. 12p. Dep.

A mathematical method allowing determination of the resolving time, jitter breadth and efficiency of the two-fold coincidence circuit is described. The method may be used at the assumption of Gaussian jitter distributions and is an alternative to the earlier published G-parameter method. Exact graphs and an example illustrating the method are given. (auth)

39206 (INSJ-99) SINGLE RACE (REACTION CONVERSION ELECTRON) SPECTROMETER. Sakai, M.; Yamazaki, T.; Ejiri, H.; Ishihara, M. (Institute for Nuclear Study, Tokyo Univ. (Japan)). July 1, 1966. 18p. Dep. mn.

The design and performance of a beta spectrometer, which is especially suited for the measurement of conversion electrons from nuclear reactions, are reported. (auth)

39207 (ISS-66/18) MISURA DELLA QUANTITA DI MOTO DI ELETTRONI, CON CAMERE A SCINTILLA POSTE IN CAMPO MAGNETICO. (Measurement of Electrons Momentum by Spark Chambers in Magnetic Field). Farchi, G. (Istituto Superiore di Sanita, Rome (Italy). Laboratori di Fisica). Apr. 27, 1966. 23p. Dep. mn.

The calculation of the precision that is possible to attain in the measurement of the momentum of electrons deflected by a magnetic field and detected in the field by 3 or 4 one gap spark chambers. The momentum error is calculated starting from the measurement errors in each chamber. (auth)

39208 (JINR-P-2705) PRIMENENIE SLYUDY I KVARTSEVOGO STEKLA DLYA REGISTRATSII DELENIYA YADER PRI POVYSHENNYKH TEMPERATURAKH. (Use of Mica and Quartz Glass for Nuclear Fission Detection at High Temperature). Kapustsik, A.; Perelygin, V. P.; Sviderskii, V. I.; Tret'yakova, S. P. (Joint Inst. for Nuclear Research, Dubna (USSR). Lab. of Nuclear Reactions). 1966. 8p. Dep. mn.

The use of mica and quartz glass is described for the detection of rare acts of nuclear fission at 350-400°C. The efficiencies of detection of fission fragments are measured depending on the air layer thickness between the sample and the detectors. (auth)

39209 (JINR-P-2728) TREBOVANIYA PRED'YAVLYAEMYE K OPTICHESKIM GOLOVKAM STEREOFOTOAPPARATOV, PRIMENYAEMYKH NA PUZYR'KOVYKH KAMERAKH. (Requirements on the Optical Units of Stereoscopic Cameras Used in Bubble Chambers). Andreev, E. M.; Libman, G.; Selivanov, G. I. (Joint Inst. for Nuclear Research, Dubna (USSR). Lab. of Nuclear Problems). 1966. 12p. Dep. mn.

To facilitate the adjustment of stereoscopic cameras used in bubble chambers it is advisable to manufacture the optical part of these cameras as separate units. Some requirements are imposed on the accuracy of manufacturing of these units. Estimates are given by the example of the optical unit of the stereoscopic camera for an 8-liter liquid hydrogen bubble chamber. The chosen construction allows to provide easily required accuracy of manufacturing of the stereoscopic camera optical unit and guarantees the reliability of the operation of the system. (auth)

39210 (JINR-P-2745) ISKROVYE I STRIMERNYE KAMERY I METODY VYVODA DANNYKH S NIKH. (Spark and Streamer Chambers and Methods of Data Derivation From These Chambers). Pisarev, A. F. (Joint Inst. for Nuclear Research, Dubna (USSR). Lab. of Nuclear Problems). 1966. 18p. Dep. mn.

Methods of track particle detection by means of spark chambers are reviewed. The history of creation and development of spark and streamer chambers, their characteristics and ranges of application are considered. Modern methods of filmless extraction of information by using vidicons, light and sonic transducer, electrophotographic layers, wire and other systems are analyzed. (auth)

39211 (JINR-P-2842) IDENTIFIKATSIYA ZARYAZHENNYKH CHASTITS PO IONIZATSII I δ-ELEKTRONAM V PROPANOVOI PUZYR'KOVOI KAMERE. (Identification of Charged Particles by Ionization and δ-Electrons in a Propane Bubble Chamber). Bem, Ya.; Grishin, V. G.; Kriventsova, A. G.; Mumimov, M. M.; Trka, Z. (Joint Inst. for Nuclear Research, Dubna (USSR). Lab. of High Energy). 1966. 13p. Dep. mn.

The results of ionization measurements of positive particles in a 24-liter propane chamber are given. It is found that for the particles with $pc \leq 1$ Bev, by this method it is possible to distinguish between protons and π^+ mesons. A computer program is worked out and the method of the identification of the particles with $pc \geq 1$ Bev by δ electrons is tested. The ranges of electrons and positrons with $E \leq 8$ Mev in propane are calculated. (auth)

39212 (NYO-3421-7) PHOTOMULTIPLIER INVESTIGATION. Sixth Quarterly Report, February 15, 1966-May 14, 1966. Smith, H. M. Jr. (David Sarnoff Research Center, Princeton, N. J.). June 3, 1966. Contract AT (30-1)-3421. 22p. Dep. mn. CFSTI $1.00 cy, $0.50 mn.

Two problems often encountered by users of photomultiplier tubes today are those of dark pulses and gain shift with count rate or short term stability. Recent investigations of these problems are presented. Studies of afterpulses and their relation to dark pulses have indicated a definite correlation in that ions cause both afterpulses and dark pulses. The source of ions for dark pulses is still somewhat uncertain. High temperature baking of the walls has resulted in some interesting effects on dark pulses. Both types A and B can be reduced significantly by baking while pumping. (auth)

39213 (ORNL-TM-1578) ELECTRICAL SAFETY OF HEALTH PHYSICS INSTRUMENTS IN USE AT ORNL. Wintenberg, R. E. (Oak Ridge National Lab., Tenn.). July 29, 1966. Contract W-7405-eng-26. 6p. Dep. mn. CFSTI $1.00 cy, $0.50 mn.

Radiation monitoring instruments used by the Health Physics Division were investigated to determine their potential shock hazard. Commonly used, line operated instruments with the high-voltage connectors were tested by measuring the transient and steady-state voltages when the voltage source was connected to 50-ohm load. High-voltage characteristics of portable instruments and of instruments not in widespread use were calculated using worst case values. Instruments with connectors having exposed voltages of over 50 v were noted. In general, instruments used for measuring or monitoring radioactivity had less than 0.01 joule of stored energy and 1.0 ma of steady-state current, whereas the high-voltage power supplies had as high as 3.6 joules of stored energy and 180 ma of steady state current. No instrument in common use had more than 2000 v on a connector. (auth)

39214 (NP-tr-1394) THE APPLICATION OF A BORON COUNTER WITH CH_2 MODERATOR IN NEUTRON DOSIMETRY. Zolin, L. S. (Joint Inst. for Nuclear Research, Dubna (USSR). Lab. of High Energy). Translated by A. T. Sanders and Revised by N. Mouravieff (European Organization for Nuclear Research, Geneva, Switzerland), from report JINR-P-2252. 15p. Dep. mn. CFSTI $1.00 cy, $0.50 mn. JCL $1.60 fs, $0.80 mf.

A description of the construction and characteristics of a boron counter with CH_2 moderator for neutron dosimetry are presented. (B.G.D.)

39215 TIME DELAYS IN ARGON–PROPANE PROPORTIONAL AND GEIGER COUNTERS. Rainbow, M. T.; Fenton, A. G.; Fenton, K. B. (Univ. of Tasmania, Australia). Austral. J. Phys., 19: 583-6(Aug. 1966).

As part of an investigation of the properties of argon-propane mixtures for use in counters, the time intervals between the release of electrons from the cathode and the subsequent appearance of a pulse in a counter operated in the proportional and Geiger regions were measured. The method used consisted of allowing the uv light from a short duration spark (10 nsec) to release photoelectrons from the cathode of the counter. An oscilloscope method was used to measure the time delays between the sparks and the counter pulses. (W.D.M.)

39216 STUDY OF THE ELECTRON EFFICIENCY OF A FAST FILM EMULSIFIED ON TWO FACES WITH THE PURPOSE OF PERMITTING THE MEASUREMENT OF CONVERSION RATIOS BY THE PHOTOGRAPHIC METHOD. Gautier, Francoise (Centre National de la Recherche Scientifique, Orsay, France). Compt. Rend., Ser. B, 262: 1628-31(June 20, 1966). (In French).

By use of two semicircular magnetic spectrometers, the blackening densities obtained for different numbers of electrons with energies between 24 and 500 kev were measured. The shape of the curves obtained, which differ sharply between 100 and 250 kev from the usual blackening curves, is explained by the bi-layer character of the film studied. (tr-auth)

39217 SIMULTANEOUS SCINTILLATION SPECTROMETRY OF α AND β RAYS BY MEANS OF CESIUM IODIDE. Koenig, K.-H.; Hoyer, F. (Univ., Frankfurt am Main). Dechema Monogr., 54: 267-88(1965). (In German).

Optically transparent single crystals of cesium iodide, which absorb α and β rays completely even in thin layers, are suitable for scintillation spectrometry. In a new scintillation spectrometer the α and β rays interact in a light-tight measuring chamber at high geometry with the scintillator. The scintillations are transferred by light pipes to a photomultiplier connected to electronic pulse-height analyzers. The nonhygroscopic cesium iodide can be mounted without mechanical protection so that the radiation undergoes no energy loss from sample to scintillator. The instrument makes the simultaneous spectrometry of α and β radiation possible with separate well-resolved characteristic spectra. The continuous energy distribution of the β spectra (in contrast to the α radiation) shows a strong displacement of the frequency maximum towards small energies because of the dispersion of the β particles in the scintillator. In the falling part of the distribution curves at high energies the overlapping of several spectra can be recognized immediately. Therefore, even in mixtures of radioisotopes or with isotopes having several β groups, the maximum energies of the individual components can be determined with great accuracy by direct extrapolation of the experimental spectra. The nuclides can be identified with certainty. The combination of α and β spectrometry to the simultaneous spectrometry of both types of radiation is a valuable procedure for the rapid solution of radiochemical problems. (auth)

39218 PREPARATION OF REPRESENTATIVE MIXED SAMPLES OF TAP WATER WITH A SIMPLE CONTINUOUS SAMPLING DEVICE. Aurand, K.; Behrens, H. Gesundh.-Ing., 8: 1-2(1965). (In German).

A simple device for the continuous sampling of tap water was described. The device makes it possible to obtain average samples at selected time intervals, from which the amount of radioactive material present in the water and delivered to the population can be determined. Such investigations render possible a consistent monitoring of the water for radioactive materials for the protection of the population. (L.B.S.)

39219 LiF THERMOLUMINESCENT RESPONSE TO FAST NEUTRONS. Kastner, Jacob; Oltman, B. G.; Tedeschi, Pete (Argonne National Lab., Ill.). Health Phys., 12: 1125-8(Aug. 1966).

The relative thermoluminescent response of ^{6}LiF, per unit neutron fluence, has been determined for neutrons of varying energies ranging from thermal to more than 1 Mev. A marked increase in light output about 0.25 Mev is attributed to the $^6Li(n,\alpha)^3H$ reaction. (auth)

39220 MODIFICATION OF THE EBERLINE PAC-3G AND FM-3G SURVEY METERS TO DETECT LOW-ENERGY BETA ACTIVITY. Ello, J. G. (Argonne National Lab., Ill.). Health Phys., 12: 1139-41(Aug. 1966).

Procedures are described for the modification of Eberline PAC-3G and FM-3G survey meters so that either α activity or low-energy β activity can be detected by flicking a panel mounted switch. (C.H.)

39221 APPLICATION OF SOLID-STATE NUCLEAR TRACK DETECTORS TO THE HURST THRESHOLD DETECTOR SYSTEM. Kerr, G. D.; Strickler, T. D. (Oak Ridge National Lab., Tenn.). Health Phys., 12: 1141-2 (Aug. 1966). (ORNL-P-1850).

The application of solid-state nuclear track detectors to the Hurst threshold detector system improved the performance of the detectors and extended the energy range. (C.H.)

39222 DETERMINATION OF FAST NEUTRON FLUX DENSITIES BY THE ACTIVATION OF PHOSPHORUS COMPOUNDS. Mijnheer, B. J.; Aten, A. H. W. Jr. (Instituut voor Kernphysisch, Amsterdam). Health Phys., 12: 1142-3(Aug. 1966).

A method is described for the determination of fast neutron flux densities by the activation of P compounds using the $^{32}S(n,p)^{32}P$ reaction. (C.H.)

39223 ABSOLUTE NEUTRON FLUX DETERMINATION WITH THICK $(CH_2)_n$ RADIATORS. Huber, P.; Sick, I.; Stambach, Th. (Univ., Basel). Helv. Phys. Acta, 39: 208(1966). (In German).

The advantages of a thick radiator for the absolute flux determination of fast monochromatic neutrons are summarized. These include simple structure, high efficiency, slight effect of the angular distribution of the n-p scattering, applicability over a wide energy range, and good accuracy. (J.S.R.)

39224 PROTOTYPE THERMOLUMINESCENT DOSIMETRY SYSTEM FOR PERSONNEL MONITORING. Palmer, R. C.; Rutland, D.; Lagerquist, R.; Blase, E. F. (Edgerton, Germeshausen and Grier, Inc., Santa Barbara, Calif.). Contract NObsr-85506. Int. J. Appl. Radiat. Isotop., 17: 399-411(July 1966).

A prototype thermoluminescent system is described, wherein the thermoluminescent properties of CaF_2:Mn are used to monitor the γ radiation dose range of 2 mrad to 10^4 rad. Design specifications for the system are presented, together with performance data. The system showed characteristics of accuracy, reproducibility, and re-usability far superior to those of conventional personnel dosimetry systems. (auth)

39225 PROTOTYPE LiF RADIATION DOSIMETER FOR PERSONNEL MONITORING. Palmer, R. C. (Edgerton, Germeshausen and Grier, Inc., Santa Barbara, Calif.). Int. J. Appl. Radiat. Isotop., 17: 413-16(July 1966).

A LiF radiation dosimeter with a linear range from 1 mrad to 400 rad and which can be used up to at least 4000 rad γ radiation is described. The dosimeter is of vacuum tube construction. The dosimeter's characteristics are given, together with information on an energy-compensation shield. The dosimeter can be re-used without change in sensitivity. (auth)

39226 DIGITAL COMPUTER PROGRAM FOR CALCULATION OF EXTENT OF EXCHANGE FROM LIQUID SCINTILLATION COUNTING DATA. Schear, W. (E. I. du Pont de Nemours and Co., Inc., Wilmington, Del.). Int. J. Appl. Radiat. Isotop., 17: 430-1(July 1966).

A digital computer program was written in Fortran IV for the calculation of the extent of the exchange of labile atoms during radiometric analysis. The exchange may be the result of incorporation of a radioactive label or the result of the loss of a radioactive molecule into an inactive medium. The computer program accepts scintillation data

for quenched standards and subsequently for an unlimited number of exchanged samples and computes for each, by the method of least squares, the best straight-line relationship for concentration versus the logarithm of activity, or counting efficiency in the case of quenching data. The program then compares the activity of each exchanged sample with the initial one, corrects for quenching, and extrapolates the activity difference (counts/min) to 100% counting efficiency (dis./min). (C.H.)

39227 DOSIMETRY FOR FAST-NEUTRON IRRADIATIONS OF CULTURED CELLS AND INTACT ANIMALS. 1. CHARACTERISTICS OF TISSUE-EQUIVALENT IONIZATION CHAMBERS. Broerse, J. J. (TNO, Rijswijk, Netherlands); Van Ammers, H. Int. J. Radiat. Biol., 10: 417-27(1966).

For an accurate determination of the absorbed dose in fast-neutron irradiations of living organisms, tissue-equivalent ionization chambers were used. Three different gas mixtures have been suggested for use as filling gases for these chambers. To test the equivalence of these gases, two series of experiments were performed with mono-energetic neutrons produced by the D–D and the D–T reactions. The relative contributions of ionizing particles, produced in either the wall or the gas, to the current measured in the ionization chamber were investigated. With the different gas fillings the response of the chambers was studied for various neutron energies. The relative contribution of particles from the wall of the chamber was found to increase considerably with increasing neutron energy. Consequently, identical dose-rates (for equal neutron flux densities) were measured in 15 Mev neutron irradiations when the ionization chamber was flushed with different tissue-equivalent gas mixtures. For 3 Mev neutron irradiations a relatively lower measured dose rate was found for one of the tissue-equivalent gas mixtures. (auth)

39228 DOSIMETRY FOR FAST-NEUTRON IRRADIATIONS OF CULTURED CELLS AND INTACT ANIMALS. 2. COMPARISON BETWEEN ACTIVATION AND IONIZATION METHODS. Broerse, J. J. (TNO, Rijswijk, Netherlands). Int. J. Radiat. Biol., 10: 429-34(1966).

In addition to the use of tissue-equivalent ionization chambers for fast neutron dosimetry in cultured animal cells, sulfur activation detectors were employed for special dosimetry purposes. A comparison of the two dosimetry methods was carried out for neutrons produced by the D–D and the D–T reactions using the $^{32}S(n,p)^{32}P$ reaction. For 15 Mev neutron irradiations a good agreement between both methods was obtained. However, for 3 Mev neutron irradiations, it was found that the dose calculated on the basis of the sulfur activation had to be multiplied by a factor 1.65 to obtain the correct value corresponding to the tissue-equivalent ionization chamber. The large resonances in the cross-section curve for the (n,p) reaction in sulfur for the neutron energy region between 2.5 and 4 Mev may be responsible for the discrepancy in the doses measured with these independent methods. (auth)

39229 INSTRUMENTS FOR THE OBSERVATION OF GALACTIC X RAYS. Matsuoka, Masaru (Univ. of Nagoya, Japan). Jap. J. Appl. Phys., 5: 671-88(Aug. 1966).

Three types of rocket-borne x-ray instruments were constructed; they consisted of a scintillation counter, four proportional counters, and twenty-three G-M counters. The scintillation counter was used to observe isotropic x-rays in the energy ranges of 5 to 10, 10 to 15, 15 to 20, and ≥20 kev, and the proportional counters to observe the intensities of x rays from several sources in the energy ranges of 2 to 4, 4 to 8, and 8 to 16 kev. The G-M counters were prepared to observe the intensities of x rays from several sources in the wavelength ranges of 2 to 4, 4 to 8, and 7 to 11 Å. Their properties were tested by radioactive sources and were found to be suitable for analyzing the energy spectrum of galactic x rays while rejecting charged particles. Two of the counter systems were used for the observations of x rays. The method of data analysis as well as some of the raw data is described. (auth)

39230 SEMICONDUCTOR DETECTORS FOR NUCLEAR SPECTROMETRY. I. Goulding, F. S. (Univ. of California, Berkeley). Nucl. Instrum. Methods, 43: 1-54 (Aug. 1, 1966).

Background information is presented on the development of detectors. Topics discussed are semi-conductor materials and the theory of junctions necessary for an understanding of detectors, the methods of making detectors by diffusion and also by lithium drifting are detailed and the relative merits of different types of detectors are discussed, the problems associated with obtaining good energy resolution in detector systems dealing primarily with electrical noise and statistical fluctuations of the charge produced in the detector, semitheoretical treatment of the detector pulse shape considerations, and the subject of radiation damage. (B.G.D.)

39231 SEMICONDUCTOR DETECTORS FOR NUCLEAR SPECTROMETRY. II. Mayer, J. W. (Hughes Research Lab., Malibu, Calif.). Nucl. Instrum. Methods, 43: 55-64 (Aug. 1, 1966).

A general description is presented of the "position" detector and the avalanche detector including their uses and limitations. Several diverse factors concerned with detector performances are discussed, such as charge collection, energy resolution and Fano factor, energy required to form a hole-electron pair, fission fragment pulse height defect, etc. The considerations leading to the choice of materials for use in gamma-ray spectroscopy are discussed. Experimental results with CdTe are presented. A compendium of fabrication techniques is discussed with primary emphasis on diagnostic techniques, suitable to determine failure modes. (auth)

39232 IMPACT OF SEMICONDUCTOR DETECTORS ON GAMMA-RAY AND ELECTRON SPECTROSCOPY. Hollander, J. M. (Univ. of California, Berkeley). Nucl. Instrum. Methods, 43: 65-109(Aug. 1, 1966).

A discussion is given of the basic operating characteristics and some applications of lithium-drifted silicon and germanium detectors for conversion-electron and gamma-ray spectroscopy. The following properties of Ge(Li) detector systems are reviewed: photopeak resolution; energy linearity and calibration; photopeak detection efficiency; and Compton scattering and pair production. In discussion of the relevance of these properties to the practical use of Ge(Li) and Si(Li) detector systems an attempt is made to place their advantages and disadvantages in perspective with respect to the properties of other important gamma-ray and electron spectrometer systems. Some measurements with Ge(Li) systems are discussed briefly, in the areas: decay scheme studies with radioactive isotopes; in-beam spectroscopy; low-temperature nuclear orientation; and applied gamma-ray spectroscopy (activation analysis). The advantages of simultaneous use of Si(Li) and Ge(Li) detectors for electron-gamma spectroscopy is stressed and applications for measurements of internal conversion coefficients and electron-gamma angular are reviewed. (auth)

39233 RECENT DEVELOPMENTS IN SCINTILLATION DETECTORS. Aliaga-Kelly, D.; Nicholl, D. R. (Nuclear Enterprises, Ltd., Eng.). Nucl. Instrum. Methods, 43: 110-15(Aug. 1, 1966).

A survey is given of developments in NaI(Tl), CsI and CsI(Tl), CaI_2 and CaI_2(Eu) with their limitations, CaF_2(Eu), ^{6}LiI(Eu), and a wide variety of organic scintillators. The light output of liquid scintillators has been greatly increased. The use of relatively cheap commercial solvents for large liquid scintillators has increased light output and decreased the fire hazard compared with xylene and toluene. Problems in dissolving biological samples in liquid scintillators are discussed and techniques for reduction of chemiluminescence described. Large and small plastic scintillators, and the use of both plastic and glass scintillators for pulse shape discrimination are discussed. (auth)

39234 A SCHEME FOR HIGH LUMINOSITY, HIGH RESOLUTION INTERNAL AND EXTERNAL CONVERSION MEASUREMENTS. Bergkvist, K.-E. (Research Inst.

for Physics, Stockholm). Nucl. Instrum. Methods, 43: 170-81(Aug. 1, 1966).

In charged-particle spectrometers relying upon the dispersive power of some kind of imaging system one generally has to compromise between the desire of high resolution and the desire of high intensity at the detector. Starting from a source of given absolute and specific strength, and a given level of resolution, any factor of improvement in resolution can in principle be realized if the accompanying decrease in intensity is accepted. An investigation was made in order to realize the sufficient experimental conditions for proceeding about an order of magnitude in resolution in the well-known double focusing $\pi\sqrt{2}$ β-spectrometer without this normally occurring reduction of intensity. In the present case this has been achieved by adding of the magnetic $\pi\sqrt{2}$ spectrometer two electrostatic devices. One of these, the corrector, reduces the point source aberrations while keeping the aperture solid angle constant and the other device, a special source arrangement, allows a large source to be used in conjunction with high resolution. This latter possibility is realized by using a nonequipotential source surface. By the combined action of the corrector and the new source arrangement an increase in luminosity by a factor of 120 over that of the normal double focusing spectrometer has been experimentally achieved with even larger improvement within reach. In the case of external conversion measurements the above methods are also applicable but, however, are not always sufficient to meet the basic aim of fully retaining the intensity when improving the resolution. However, the large source area permitted by the above methods allows a special method to be used for the reduction of the Compton electron background often disturbing external conversion measurements. The reduction of the Compton background relies upon a geometrical separation of the image of the converter (i.e., the photo electron source) and the image of the γ-ray source with absorber (the main contributor to the Compton background). The possible background reduction factor increases with resolution and the method is hence especially suited to the present high-luminosity, high-resolution methods. (auth)

39235 IMPROVED BETA-SPECTROMETERS. Lee-Whiting, G. E. (Atomic Energy of Canada Ltd., Chalk River, Ont.). Nucl. Instrum. Methods, 43: 182-93(Aug. 1, 1966).

An attempt is made to estimate the transmission attainable with the best possible $\pi\sqrt{2}$ spectrometer. Then various routes along which a spectrometer of greater luminosity might be evolved from the $\pi\sqrt{2}$ concept are explored. The possibilty of replacing the circular central orbit of the $\pi\sqrt{2}$ spectrometer by a more general curve is examined. Necessary and sufficient conditions for a first-order two-directional focus are given for one class of more general central orbits; formulas for second-order radial aberration and for radial magnification are given. A start is made in applying the theorems to the design of spectrometers and spectrographs. (auth)

39236 PROPOSED ELECTROSTATIC CORRECTION OF THE CHALK RIVER $\pi\sqrt{2}$ BETA SPECTROMETER. Lee-Whiting, G. E. (Atomic Energy of Canada Ltd., Chalk River, Ont.). Nucl. Instrum. Methods, 43: 194-8(Aug. 1, 1966).

Calculations of the shape of a Bergkvist-type electrostatic corrector wer carried out for the Chalk River $\pi\sqrt{2}$ beta spectrometer. If the corrector is assumed to be equivalent to a surface of discontinuity of the electrostatic potential, then the radial aberration can be completely removed over the whole width of the aperture, for electrons emitted in the horizontal plane of symmetry. This aberration is small for skew orbits lying near the plane of symmetry, but it cannot be removed over the whole aperture with a cylindrical corrector. The approximation involved in replacing the system of grids by a discontinuity in the electrostatic potential was studied theoretically; it appears to be satisfactory, provided that the potential discontinuity is equated to an unknown fraction of the grid voltage. (auth)

39237 COMPUTER TECHNIQUES FOR THE ANALYSIS OF GAMMA-RAY SPECTRA OBTAINED WITH NaI AND LITHIUM-ION DRIFTED GERMANIUM DETECTORS. Heath, R. L. (National Reactor Testing Station, Idaho Falls, Idaho). Nucl. Instrum. Methods, 43: 209-29(Aug. 1, 1966).

Methods for the analysis of complex gamma-ray spectra obtained with NaI and lithium-ion drifted germanium detectors are examined in some detail. Computer programs are described that have been developed for the calculation of pulse-height distributions representing the response of detectors to monoenergetic photons. This method is based upon an interpolation between experimental spectra. Problems incidental to the analysis of gamma-ray spectra are discussed. Computer programs developed for the analysis of complex spectra are described—including linear and non-linear least squares programs for peak fitting and spectrum analysis, gain normalization and the calculation of sum spectra. (auth)

39238 REVIEW OF BASIC INSTRUMENTS AND TRENDS. Guillon, H. (CEA, Saclay, France). Nucl. Instrum. Methods, 43: 230-9(Aug. 1, 1966).

The present state of the basic instrumentation techniques is investigated. Excluding preamplifiers, the following items are reviewed: amplifiers, single-channel analyzers, coincidence circuits, linear gates, counting systems, ratemeters and test instruments. Particular emphasis is stressed on analog data processing owing to its more spectacular progress. (auth)

39239 REVIEW OF THEORIES AND EXPERIMENTS OF RESOLVING TIME WITH SCINTILLATION COUNTERS. Gatti, E. (CISE, Milan); Svelto, V. Nucl. Instrum. Methods, 43: 248-68(Aug. 1, 1966).

A critical survey of available theoretical results on time resolution with scintillation counters was made. Moreover typical experimental results obtained in timing with slow and fast scintillators are reported from the literature. (auth)

39240 INSTRUMENTATION FOR NUCLEAR-STRUCTURE ANALYSIS. Kane, John V. Phys. Today, 19: No. 7, 59-63; 65-7(July 1966).

The use of computer techniques in nuclear structure analysis is discussed. Topics considered include time-sharing computers, real-time time-sharing computers, and general purpose interfaces which permit the control of apparatus automatically and changes in experiments in response to data available. (B.G.D.)

39241 INSTRUMENTATION FOR HIGH-ENERGY RESEARCH. Tautfest, George W. (Purdue Univ., Lafayette, Ind.). Phys. Today, 19: No. 7, 69-71; 74-7(July 1966).

Developments in instrumentation for automated measuring of particle events are reviewed. Data storage and processing methods are discussed for bubble chambers, multiplate spark chambers, and wide-gap spark chambers. (L.B.S.)

39242 INSTRUMENTATION FOR FISSION STUDIES. Britt, Harold C.; Stein, William E. (Los Alamos Scientific Lab., N. Mex.). Phys. Today, 19: No. 7, 79-84(July 1966). (LA-DC-7854).

Multiparameter experiments for similtaneously measuring the velocities of fission fragments and particles emitted by the de-exciting fragments are described. The development of semiconductor detectors for high-resolution measurements are discussed. (L.B.S.)

39243 INSTRUMENTATION FOR GAMMA-RAY SPECTROSCOPY. Kennett, Terence J. (McMaster Univ., Hamilton, Ont.). Phys. Today, 19: No. 7, 86-9 (July 1966).

The development of semiconductor detector and computer technology along with analog-to-digital converters for collection storage, and analysis of gamma spectra are reviewed. The demands placed on existing data acquisition systems for spectrometers using Ge(Li) detectors are pointed out. A brief discussion of experimental results on neutron-capture gamma studies is given for illustration.

The new acquisition system designed and constructed for McMaster University is described. (L.B.S.)

39244 THE PLATEAU OF A GM COUNTER AT HIGHER INTENSITIES. Lindeman, H.; Mornel, E. (Israel Inst. of Tech., Haifa). Physica, 32: 1148-50(June 1966).

It is shown that the effective discriminating voltage of the counting apparatus has a considerable influence on the plateau curve of a G.M. counter at higher intensities. (auth)

39245 RECORDING OF PARTICLE PATHS IN A STREAMER HIGH-PRESSURE CHAMBER FILLED WITH HELIUM. Kulyukin, M. M.; Pontekorvo, D. B.; Falomkin, I. V.; Shcherbakov, Yu. A. (Joint Inst. for Nuclear Research, Dubna, USSR). Prib. Tekh. Eksp., No. 6, 70-1 (Nov.-Dec. 1965). (In Russian).

Streamer chambers were operated previously with neon gas kept under a pressure of $\ll 1$ atm; particle tracks were observed visually in chambers filled with helium, argon, xenon and their mixtures. It was considered desirable to increase the density of the medium in which the particles are stopped or are interacting. Streamer chambers, made of glass and epoxy glue, were filled with helium at much higher pressures; that gas was chosen because its simple structure facilitates interpretation of the results. The chambers were evacuated to 10^{-1} torr before filling. Stereo and motion pictures were taken to record the particle tracks, discharging 200 and 320-kv pulse generators through 200 and 385-picofarad condensers. Tracks of relativistic particles were obtained at pressures of 1, 4.5 and 6 atm at a pulse duration of 150 nanoseconds. The average number of streamers at 1 atm was 2.7 cm^{-1}, decreasing somewhat at higher pressures without changes in the brightness. An electric field gradient of 15 kv/cm was found suitable to obtain excellent tracks. The memory storage period was estimated at 100 μseconds. (TTT)

39246 MEASUREMENT OF SMALL DOSES IN RADIATION PROTECTION SUPERVISION. Schmidt, Theodor (Univ., Erlangen-Nuernberg, Ger.). Radiologe, 4: 355-9(Nov. 1964). (In German).

The author discusses the dose ranges of interest in protection of personnel from irradiation. These amount to doses as low as 20 μR/hr. The properties of measurement equipment necessary for measurement of doses as small as this depend on the energy of the radiation, direction of irradiation, size of the radiation beam to be measured, saturation properties of the measurement equipment, the inertial response of the meter to rapid changes in radiation intensity, and accuracy of the response to radiation. The equipment should be lightweight, portable, and easily carried by hand. It should be sturdy and insensitive to physical shocks, and relatively inexpensive. The pocket dosimeter with full scale of 200 mR permit values of ~5 mR to be read. Chambers of this type containing argon under pressure permit doses from 20 μR to 1 mR to be detected. Counting tubes have the advantage of high sensitivity, and can measure dose rates in the range of 10 μR/hr. Scintillation counters also have a high sensitivity, but the accessory electronic equipment required for them and the expense entailed make them impractical for use in radiation protection. Film dosimeters are very energy sensitive, but this can be partially corrected by filters so that they are valuable for radiation intensities up to 120 kv. Dose rates as low as 50 μR/hr can be measured. Solid state dosimeters depend on photoluminescent properties of glass of various compositions, such as LiF or CaF. Effective measurement range is from 10 mR to 10,000 R for ^{60}Co radiation. (BBB)

39247 DETERMINATION OF CONSTANTS FOR THE GEOMETRIC RECONSTRUCTION OF TRACKS ON np FILMS FROM THE NEUTRON-IRRADIATED 24-1 BUBBLE CHAMBER OF THE JOINT INSTITUTE FOR NUCLEAR RESEARCH. Hangea, N.; Ghiordanescu, N.; Pascu, L.; Teleman, M.; Tipa, I. (Pedagogic Inst., Bucharest). Stud. Cercet. Fiz., 18: 399-405(1966). (In Rumanian).

In order to be able to determine the x, y, z coordinates of a point from a bubble chamber, pictures must be taken by at least two cameras, measuring in the plane of the film under the microscope the coordinates of the same point with respect to a reference point. The cameras used in the experiments had parallel optical axes which were perpendicular to the plane of the film. The individual bubbles were identified by scanning. In order to determine the constants needed for the calculations, the contraction of the film was determined by comparing it with a reference film. The geometric reconstruction formulas used were symmetrical with respect to the y coordinate. In order to ensure that the constants obtained for one film are applicable to other films, the mean z coordinates of surface and background points were determined on two additional films, and the mean square deviation of the coordinates was calculated on the basis of measurements carried out ten times for each point. (TTT)

39248 EXPERIMENTAL DETERMINATION OF THE QUANTOMETER CONSTANT AT THE ENERGY 650 Mev. Aleksandrov, Yu. M.; Grushin, V. F.; Leikin, E. M.; Kruglov, S. P.; Lopatin, I. V.; Mus, K. F. (Ioffe Inst. of Physics and Tech., Leningrad). Yadern. Fiz., 3: 1076-8(June 1966). (In Russian).

The constants of several quantometers were determined experimentally by comparing their readings with the data of the calorimetric method. It is shown that the quantometer constant does not change more than 2.5% in the region 80–650 Mev. Its value agrees with the calculated one within 3%. (auth)

39249 DETECTOR OF RADIOACTIVITY. Soole, Bernard Walter; Jager, Frederick William (to National Research Development Corp.). British Patent 1,035,480. July 6, 1966. Filed Sept. 17, 1963.

A radiation detector includes a pair of hermetically sealed ion chambers to receive the same incident radiation. Both chambers are permeable to gamma and x radiation, but only one is permeable to beta radiation. Each chamber contains parallel plate electrodes connected to an electrometer circuit through a switch to permit either the ionization effects in both chambers to be applied to the electrometer in opposition for balancing out the results of the ambient gamma or x radiation, to allow determination of the beta dose rate, or the ionization effects in both chambers may be made additive to measure the gamma and x radiation. When both gamma and x radiation is being measured, a cover is used to exclude beta particles from the ion chamber normally permeable to beta particles. Means are also provided for calibration of the instrument by an external fixed current injected into the electrometer grid circuit. (B.L.M.)

39250 SELECTIVE MOESSBAUER DETECTOR AND USE THEREOF. Cook, Charles F.; Collins, Russell L.; Fink, Richard W. (to Phillips Petroleum Co.). U. S. Patent 3,257,558. June 21, 1966. Filed Oct. 5, 1962.

A Mössbauer spectrometer comprises a source of Mössbauer gamma rays and means for subjecting a sample of the material to be investigated to radiation from the source. The detector is positioned with respect to the sample so as to be subjected to the radiation from the source which is transmitted by the sample. Means are provided for causing relative motion between two of the three components, the source, the sample, and the detector. The detector comprises a housing enclosing an anode, a cathode, and an electron multiplier. The cathode is a single layer formed of a Mössbauer nucleus having a Mössbauer excitation level corresponding to the Mössbauer gamma rays emitted from the source. Means are provided for correlating each of the outputs of the detector with the corresponding degree of relative motion produced by varying the components. (B.L.M.)

39251 RADIATION DOSIMETER FOR MEASURING EXPOSURE TO HIGH AND LOW ENERGY RADIATION. Cowper, George; Simpson, Stuart Douglas (to Atomic Energy of Canada Ltd.). U. S. Patent 3,263,080. July 26, 1966. Filed Aug. 9, 1963.

The response of radiation sensitive film is improved by the use of a filter in a personal film dosimeter. The filter

is formed of lead 0.76 mm thick with 0.80 mm diameter holes spaced about 1.6 mm between centers. (F.S.)

39252 FLUX MAPPING SYSTEM FOR MEASURING RADIATION. Wiesemann, Robert A.; Ehrenpreis, Stanley N. (to Westinghouse Electric Corp.). U. S. Patent 3,263,081. July 26, 1966. Filed Apr. 18, 1962.

The flux measuring and mapping system utilizes a column of balls or suitably shaped pellets or particles fabricated of flux sensitive materials. Conduits are provided for inserting and withdrawing the measuring and mapping materials, and a way is provided for measuring the materials' activation. (F.S.)

39253 AIR SAMPLE CARD (Engineering Materials). (Union Carbide Corp., Oak Ridge, Tenn. Y-12 Plant). (CAPE–1410).

1 drawing.

The sampling device holds an IBM aperture card with a filter paper insert and is used in monitoring air for radioactive particulates. The sample and data are combined in a single unit, permitting machine identification of samples at all times. (For details see TID-4100). (F.S.)

39254 MINIATURE MODULAR ALPHA COUNTER (Engineering Materials). (Rocky Flats Div., Dow Chemical Co., Golden, Colo.). (CAPE–1419).

10 drawings.

The counter, mounted on a glove box, is used to monitor hands for α contamination during glove changes. The probe, which may be used with other α survey meters, is less microphonic than others. (For details see TID-4100). (F.S.)

39255 UNIVERSAL SPECTROMETER–3 CRYSTAL (Engineering Materials). (Brookhaven National Lab., Upton, N. Y.). (CAPE–1435).

331 drawings.

The general purpose spectrometer may be used in neutron diffraction studies using single crystals powders, and polarized beams. The spectrometer can be converted into 3-crystal machine for inelastic scattering studies. (For details see TID-4100). (F.S.)

39256 PARALLEL PLATE FISSION CHAMBER, 5 IN. DIA, 30 PLATES ^{238}U /Q-2577/(Engineering Materials). (Oak Ridge National Lab., Tenn.). (CAPE–1398).

2 drawings.

A parallel-plate fission chamber used in determining the capture-to-fission ratio for ^{238}U is presented. (For details see TID-4100 Suppl. 35). (F.S.)

39257 LARGE AREA ALPHA SCINTILLATION DETECTOR /Q-2741/(Engineering Materials). (Oak Ridge National Lab., Tenn.). (CAPE–1391).

4 drawings.

The α scintillation detector has a phosphor area of 72 in.^{2} and is used in monitoring objects having large areas, such as hands and shoes. (For details see TID-4100 Suppl. 35). (F.S.)

39258 AUTOMATIC FILM-BADGE READER /Q-2593/ (Engineering Materials). (Oak Ridge National Lab., Tenn.). (CAPE–1377).

12 drawings.

The reader provides direct measurement of exposure from each of 4 absorber areas on the ORNL β-γ film dosimeter and automatically records the information by punching IBM cards. About 3.5 sec are required to transfer the 4 exposure readings to the IBM cards. (For details see TID-4100). (F.S.)

39259 LOW ENERGY BETA AIR MONITOR /Q-2594/ (Engineering Materials). (Oak Ridge National Lab., Tenn.). (CAPE–1368).

5 drawings.

The instrument, a modification of the Constant Air Monitor, has an end window which allows low-energy particles to enter the G-M tube. The shield is also modified, as is the filter tape drive. (For details see TID-4100). (F.S.)

39260 TUDOR GAMMA RAY SHIELD /Q-2767/(Engineering Materials). (Oak Ridge National Lab., Tenn.). (CAPE–1408).

4 drawings.

This upright 2-door lead shield, used with a γ spectrometer, accommodates 4π operation or single-detector operation. A Cd–Cu liner attenuates lead x rays as well as the γ rays frequently present in shielding leads. (For details see TID-4100). (F.S.)

39261 NEUTRON CHOPPERS (Engineering Materials). (Brookhaven National Lab., Upton, N. Y.). (CAPE–1436).

398 drawings.

Two neutron spectrometers are presented. The slow chopper is used to study inelastic scattering of an enhanced cold neutron beam, and the fast chopper is used to study neutron transmission data. (For details see TID-4100). (F.S.)

39262 FILTER TAPE DRIVE AND BETA-GAMMA SHIELD /Q-2778/(Engineering Materials). (Oak Ridge National Lab., Tenn.). (CAPE–1370).

9 drawings.

The filter tape drive and β-γ shield is a special "deck" used with a constant air monitor in places where a high radiation level is present. (For details see TID-4100). (F.S.)

39263 FISSION CHAMBERS, MODELS 3 AND 4 /Q-2722 AND 2723/(Engineering Materials). (Oak Ridge National Lab., Tenn.). (CAPE–1375).

7 drawings.

The two parallel-plate fission chambers are used to determine the capture-to-fission ratios for ^{235}U, ^{233}U, and ^{239}Pu. (For details see TID-4100 Suppl. 35). (F.S.)

39264 IODINE MONITOR /Q-2725/Engineering Materials). (Oak Ridge National Lab., Tenn.). (CAPE–1380).

2 drawings.

The monitor is used for the continuous surveillance of radioactive gases for iodine. (For details see TID-4100 Suppl. 35). (F.S.)

39265 WHOLE BODY SCANNER, MARK 2 (Engineering Materials). (Lawrence Radiation Lab., Univ. of California, Berkeley). (CAPE–1412).

66 drawings.

The scanner permits a head-to-toe scan in 6 min. The device consists of 64 NaI scintillation counters arranged in 4 rows. An x-ray transmission image and a γ-ray emission image of the isotope distribution are recorded on photographic film. (For details see TID-4100 Suppl. 35). (F.S.)

39266 SOURCE LIFTING DEVICE (Engineering Materials). (Oak Ridge Gaseous Diffusion Plant, Tenn.). (CAPE–1449).

12 drawings.

In a mobile γ dose calibration unit the ^{60}Co is raised and lowered by an enclosed recycled air stream which permits rapid and precise positioning. When not in use, the source is stored in a lead safe beneath a mobile table. A wide range of dose rates can be obtained by varying either or both the distance from the source and the exposure time. (For details see TID-4100). (F.S.)

39267 PLUTONIUM WOUND MONITOR (Engineering Materials). (Argonne National Lab., Ill.). (CAPE–1416).

36 drawings.

The instrument will detect 5×10^{-4} μC of ^{239}Pu as a distributed source with a count rate equal to that for the background. Resolution for 14.4-kev γ is ~30%. (For details see TID-4100 Suppl. 35). (F.S.)

39268 DETECTOR SYSTEM FOR OGO-E SATELLITE EXPERIMENT (Engineering Materials). (Lawrence Radiation Lab., Univ. of California, Livermore). (CAPE–1428).

14 drawings.

The detector system is used on a NASA satellite to study electron and proton phenomena. (For details see TID-4100 Suppl 35). (F.S.)

39269 ALPHA CONSTANT AIR MONITOR (Engineering Materials). (North American Aviation, Inc., Downey, Calif.). (CAPE–1429).

5 drawings.

The monitor is used to detect low concentration of alpha and beta particles in air. Over-all performance is good; collection efficiencies are comparable to those of standard air-sampling equipment; and detection efficiencies are comparable to those obtained with standard counting equipment. (For details see TID-4100 Suppl. 35). (F.S.)

39270 SPARK CHAMBER PULSER (Engineering Materials). (Lawrence Radiation Lab., Univ. of California, Berkeley). (CAPE-1458).

11 drawings.

The small low-inductance spark chamber pulser has a capacity of 16,000 pF and a series inductance of 8 nH. It will drive a 5500 pF load with a rise time of 14 nsec. An avalanche transistorized Marx circuit drives the pulser. (For details see TID-4100, Suppl. 36). (F.S.)

39271 MONTE-CARLO CALCULATION OF INTRINSIC DOUBLE-ESCAPE PEAK EFFICIENCY OF CYLINDRICAL LITHIUM-DRIFT GERMANIUM GAMMA RAY DETECTORS. de Castro Faria, N. V.; Levesque, R. J. A. (Univ., Montreal). 9p. (CONF-660304-8). ORAU. Gmelin, AED-CONF-66-020-2.

From Tenth Scintillation and Semiconductor Counter Symposium, Washington, D. C.

Calculations were made of the intrinsic double-escape peak efficiency of cylindrical Li-Ge detectors for parallel beam of gamma rays ranging in energy from 1.5 to 10 Mev, using a computer code based on the Monte Carlo method. The detectors considered are 18 mm. in diameter with 2, 3.5, 4, 5, 8 and 10 mm. depletion depth. Comparison is made with the experimental results of Ewan and Tavendale for a 18 × 3.5 mm. detector. (auth)

39272 RADON FILM BADGE. Geiger, Eric L. (Eberline Instrument Corp., Santa Fe, N. Mex.). 23p. (CONF-660621-14). ORAU. Gmelin, AED-CONF-66-103-9.

From 11th Annual Meeting Health Physics Society, Houston, Tex.

A film badge was developed specifically for radon gas. The sensitivity is adequate to detect $(MPC)_a$ for ^{222}Rn (40-hour exposure) with 99+% confidence. The badge may be used to leak test radium sources, monitor areas for radon gas and other applications. (auth)

Radiation Effects

39273 (AD-635198) RADIATION EFFECTS ON INSULATED GATE FIELD EFFECT (MOS) INTEGRATED CIRCUITS. Third Quarterly Report, January 1-March 31, 1966. Long, D. M.; Flescher, H. L. (Martin Co., Baltimore, Md.). July 1966. Contract DA-28-043-AMC-01520(E). 20p. (ECOM-01520-3; MND-3264-3). CFSTI $1.00 cy, $0.50 mn.

A report is given which covers a radiation effects study on insulated gate field effect MOS integrated circuits. The activity was concentrated on pulsed radiation testing, and on the preparation for neutron tests. The data reported are for the transient current response of the gate or drain lead of a dummy MOS device packaged in a TO-5 can and an empty TO-5 socket, as a function of bias, and for the transient response of the gate or drain lead of six n-channel depletion and eight p-channel enhancement MOS transistors. The peak transient drain current for the p-channel units was measured to range from -460 to +620 microamperes and from 110 to 700 microamperes for the n-channel units. The data were taken at 1.6×10^7 r/sec with the magnitude and duration of the response being a function of gate resistance (R_g) and gate voltage (V_G). Measurements of the response of specially fabricated dummy MOS devices have demonstrated that the devices tested have a larger response (300 microamperes) when leads are positively biased than when the leads are negatively biased (-78 microamperes). The data also show that the current response is nonlinear with voltage and that interaction between leads can occur. This interaction is a function of the relative magnitude and polarity of the bias on adjacent leads. (auth)

39274 (N-66-18175) RADIATION-RESISTANT DEVICE PHENOMENA. Follmer, William C.; Spratt, James P. (Philco Corp., Blue Bell, Pa.). Mar. 1966. Contract NASw-997. 29p. (NASA-CR-389). CFSTI $2.00 cy, $0.50 mn.

The energetic electron mean-free-path experiment was carefully evaluated. Because of the extreme experimental difficulties encountered, and also because of the limited usefulness of the results in the light of the theoretical predictions regarding the input-to-output current transport efficiencies of a hot-carrier device, this experiment was terminated. The properties of reactively evaporated aluminum-oxide films were studied as a function of the oxygen pressure, deposition rate, and thickness of the film. It was determined experimentally that an oxide protective layer practically eliminates the sensitivity of the devices to atmospheric exposure. Insulating and semi-insulating films were prepared. The semi-insulating films show a small photosensitivity. (auth)

ISOTOPE TECHNOLOGY

General

39275 (DP–1066(Vol.1)) LARGE SCALE PRODUCTION AND APPLICATIONS OF RADIOISOTOPES. Proceedings of the American Nuclear Society National Topical Meeting, March 21-23, 1966, Augusta, Georgia. (Du Pont de Nemours (E. I.) and Co., Aiken, S. C. Savannah River Lab.). May 1966. Contract AT(07-1)-1. 333p. (CONF-660305-(Vol.1)). Dep. mn. CFSTI $7.00 cy, $1.50 mn.

Twenty-four papers are included; separate abstracts have been prepared for 16. For abstracts of remaining papers see CONF-660305 in the Report Number Index. (F.S.)

For abstracts of individual papers see: 38744, 39276, 39277, 39281–39286, 39304–39307, and 39314–39316.

39276 (DP–1066(Vol.1), pp III.45-50) PRODUCTION AND UTILIZATION OF RADIOISOTOPES IN CONTINENTAL EUROPE. Fisher, C. (Commissariat a l'Energie Atomique, Saclay (France). Centre d'Etudes Nucleaires).

European production of ^{60}Co in power reactors, separation of fission products, isotopic power generation, radiation processing, and operation of a mobile ^{137}Cs irradiator are summarized. (F.S.)

39277 (DP–1066(Vol.1), pp III.63-9) PRODUCTION AND APPLICATION OF ^{227}Ac FOR DIRECT CONVERSION SOURCES. De Troyer, A. (Union Miniere du Haut-Katanga, Brussels (Belgium)); Dejonghe, P. (Centre d'Etude de l'Energie Nucleaire, Brussels (Belgium)).

The Belgian program for large-scale production of radioisotopes for direct conversion purposes is concerned with producing ^{227}Ac by irradiating ^{226}Ra in the BR-2 reactor. (F.S.)

39278 (DP–1066(Vol.2)) LARGE SCALE PRODUCTION AND APPLICATIONS OF RADIOISOTOPES. Proceedings of the American Nuclear Society National Topical Meeting, March 21-23, 1966, Augusta, Georgia. (Du Pont de Nemours (E. I.) and Co., Aiken, S. C. Savannah River Lab.). May 1966. Contract AT(07-1)-1. 290p. (CONF-660305-(Vol.2)). Dep. mn. CFSTI $7.00 cy, $1.25 mn.

Twenty-three papers are included; separate abstracts have been prepared for 6. For abstracts of remaining papers see CONF-660305 in the Report Number Index. (F.S.)

For abstracts of individual papers see: 38996, 39308, 39309, and 39317–39319.

39279 PREPARATION OF RADIOISOTOPES, RADIATION SOURCES, AND LABELED COMPOUNDS IN CZECHOSLOVAK SSR. Chorvat, Karol (Inst. of Investigation, Preparation, and Utilization of Radioisotopes, Prague). Jad. Energ., 12: 225-7(June 1966). (In Czech).

The status of the preparation of radioisotopes, labeled compounds, sealed sources, luminous paints, and standards at the Institute for the Investigation, Production, and Utilization of Radioisotopes is described. For evaluation of the evolution of the use of radioactive substances in the Czechoslovakian radioisotope industry data are reported on the activities, price, number of deliveries, selections, and number of users of radioisotopes. Some information on the production and utilization of radioisotopes in foreign countries is included for comparison. (tr-auth)

39280 DETERMINATION OF TOTAL POTASSIUM IN SOILS USING THE GAMMA EMISSION OF ^{40}K. Redies, M.; Vimpany, I. (New South Wales Dept. of Agriculture, Australia). Nature, 210: 1078-9(June 4, 1966).

A large volume scintillation detector was used to measure the γ activity of ^{40}K in soils. The data were used to calculate the total K content in soil samples. Results agreed well with the results of chemical analysis. (C.H.)

Industrial Applications

Refer also to abstract 39155.

39281 (DP–1066(Vol.1), pp 13-18) ATOMIC ENERGY COMMISSION'S ROLE IN THE PROCESS RADIATION INDUSTRY. Fowler, E. E. (Division of Isotopes Development (AEC), Washington, D. C.).

Process radiation is defined and present uses are explained. The three missions of the Division of Isotope Development's Process Radiation Development Program are: to broaden the technology base in the area of radiation chemistry, to develop engineering process data, and to foster AEC/industry cooperative demonstration projects. (F.S.)

39282 (DP–1066(Vol.1), pp III.3-32) THE CANADIAN PROGRAM ON LARGE SCALE PRODUCTION AND APPLICATION OF RADIOISOTOPES. Errington, R. F. (Atomic Energy of Canada Ltd., Ottawa (Ontario)).

The principal Canadian programs falling within the context of large-scale production and applications of radioisotopes are therapy, food preservation, and industrial uses such as sterilization. Although other radioisotopes are significant, ^{60}Co is most prominent. The ^{60}Co is produced in the NRX and NRU reactors. (F.S.)

39283 (DP–1066(Vol.1), pp III.33-44) THE LARGE SCALE PRODUCTION AND UTILIZATION OF RADIOISOTOPES IN THE UNITED KINGDOM. Sheard, H. (Radiochemical Centre, Amersham (England)).

Large-scale production and utilization of radioisotopes in the United Kingdom has been confined to ^{60}Co. The use of radioisotopic heat sources for electric power generation is receiving more attention through studies of ^{242}Cm, ^{244}Cm, and ^{238}Pu. (F.S.)

39284 (DP–1066(Vol.1), pp IV.3-25) FOOD PRESERVATION. Josephson, E. S. (Army Natick Labs., Mass.); Shea, K. G. (Division of Isotopes Development (AEC), Washington, D. C.).

The technical feasibility of the radiation preservation of foods has been demonstrated for a wide variety of products. Large-scale uses of ^{60}Co and ^{137}Cs, as well as machine sources of ionizing energy, will be required in the future as this new process takes its place among other methods of food preservation. (F.S.)

39285 (DP–1066(Vol.1), pp IV.33-42) LARGE SCALE APPLICATION OF RADIOISOTOPES TO STERILIZATION. Artandi, C. (Ethicon, Inc., Somerville, N. J.).

A review of the criteria for the selection of the radiation source, radiation plant design, and the products that may be sterilized is presented. Selected bibliographies on radiation sterilization, effects of radiation on microorganisms, and sterilization of medical supplies are included. (F.S.)

39286 (DP–1066(Vol.1), pp IV.43-5) RADIOGRAPHY. Coleman, E. W. (Picker X-Ray Corp., Cleveland, Ohio).

Industrial applications of radiography are summarized. The principal isotopes in use are ^{60}Co and ^{192}Ir, upon which modern industrial radiography with isotopes was founded. The program for a library of standard radiographs for steel castings covering the range from 2 in. to 12 in. of steel is discussed. (F.S.)

39287 (KLX–1876) ENGINEERING AND EVALUATION STUDY FOR THE MANFACTURE OF WOOD-PLASTIC COMPOSITES. Frankfort, J. H.; Black, K. M. (Vitro Engineering Co., New York). June 3, 1966. Contract AT (30-1)-3493. 206p. Dep. mn. CFSTI $2.25 cy, $1.25 mn.

Sufficient research and development data have been generated to provide most of the information necessary for the

design of a pilot facility for methyl methacrylate–wood composites. The pilot plant would provide capabilities for further development efforts on other monomer systems such as ethyl acrylate–acrylonitrile, styrene–acrylonitrile, and possibly vinyl chloride. The pilot plant would demonstrate all of the basic design elements of a full size production facility. Economics evaluations of product costs have been considered in detail. The market potential for specialty flooring and furniture applications appears excellent. Specialty applications for radioinduced wood–plastic composites, such as sporting goods, institutional furniture, boat fittings, knife handles, salad bowls, etc., also show good marketing promise. (J.G.B.)

39288 (ORO–636) RADIATION PASTEURIZATION OF SHRIMP AND OYSTERS. Final Summary Report, January–December 1965. Novak, Arthur F.; Liuzzo, Joseph A. (Louisiana State Univ., Baton Rouge. Dept. of Food Science and Technology). Jan. 15, 1966. Contract AT(40-1)-2951. 28p. Dep. mn. CFSTI $2.00 cy, $0.50 mn.

Progress is reported on studies on the effects of γ radiation processing on the wholesomeness of shrimp and oysters from the Gulf of Mexico. Shrimp treated with N_2 in a brine immersion proved superior in keeping qualities than shrimp stored in crushed ice or stored in an N/N_2 atmosphere after dipping in brine. Results of studies of insecticidal residues in Gulf shrimp and oysters were negative. Results are reported from organoleptic comparisons and field tests of raw and fried x irradiated and non-irradiated oysters. Results indicated a preference for the irradiated product in both the raw and fried states. Studies of the effects of γ radiation on the vitamin content of oysters showed a decrease in thiamine, niacin, pyridoxine, biotin, and vitamin B_{12} after radiation treatment and an increase in riboflavin, pantothenic acid, and folic acid. Results are included from metabolic studies of radioresistant bacteria found in oysters and the effects of γ radiation on proteolytic mechanisms in these bacteria. Results of the study showed that many oysters taken from the Gulf at present do not meet the standards for total and coliform bacteria unless they are subjected to γ radiation. Radiation processing not only increases the storage life of oysters but converts an unacceptable product into an acceptable one. (C.H.)

39289 (UCD–34P73-9) RECENT RESEARCH ON THE IRRADIATION OF FRUITS AND VEGETABLES. Sommer, N. F.; Maxie, E. C. (California Univ., Davis. Dept. of Pomology). [1966]. Contract AT(11-1)-34. 23p. (CONF-660610–1). Dep. mn. CFSTI $1.00 cy, $0.50 mn.

From 3rd International Congress of Radiation Research, Karlsruhe, Ger.

Results of recent research on the radiation processing of fruits and vegetables are reviewed. Emphasis is placed on the use of radiation as a fungicidal treatment, the physiological response of fruits and vegetables to γ radiation, and the development of combined radiation-heat treatments for fruits and vegetables. It is concluded that bananas, cherries, figs, mangos, oranges, papayas, prunes, strawberries, tomatoes, potatoes, onions, and garlic are the most likely candidates for radiation processing. Data on radiation dose, physiological state when irradiated, desired effect, and expected extension of shelf life after radiation processing are summarized. (25 references.) (C.H.)

39290 INDUSTRIAL APPLICATION OF TRACER ISOTOPES IN POLAND. Akerman, K. (Inst. of Nuclear Research, Warsaw). Atomwirtschaft, 11: 365-9(July 1966). (In German).

A review is given of the industrial uses of tracer isotopes in Poland. Applications fall into two groups: the first is studies on the behavior of trace admixtures in various technological processes and the second is on studies on process techniques especially following material flows. Examples of each of these uses are given. New labeled compounds for the petroleum industry are also indicated. (J.S.R.)

39291 MEASUREMENT METHODS WITH RADIOISOTOPES FOR INDUSTRY AND GEOPHYSICS. Wiesner, L. (Hanover-Kirchrode). Atomwirtschaft, 11: 370-2 (July 1966). (In German).

A brief review is given of new radioisotopic measurement methods to be used in industry and geophysics. The techniques described include x-ray fluorescence analysis, the use of sealed sources for analysis, radiometric methods for the determination of density, thickness, and moisture, and nuclear methods in geophysics. (J.S.R.)

39292 GAGING AND CONTROLLING OF BASIS WEIGHT AND THICKNESS USING RADIONUCLIDES. Kosmowski, A. (Frieseke and Hoepener, G.m.b.H., Erlangen, Ger.). Instrum. Pract., 20: 512-16(June 1966).

A survey was made of radioisotope gages used in West German industry for measuring weight and thickness. The paper industry uses 21.4% of the gages in operation. A table shows the annual net savings achieved in the paper industry through the use of radiation equipment, and examples illustrate the commercial success achieved in individual cases. The basic features of the measuring equipment are shown. The central unit contains the main amplifier, the recorder, and the outside tolerance indicator. The radioactive source is arranged to subject the material to be tested to either direct or back-scatter radiations. In the most frequently used method the material is located between the source and the detector. In cases where the material to be measured passes over a glazing or cooling cylinder the back-scatter process is especially advantageous. Differential measurement is suitable for gaging and controlling coatings with minute variations in concentration factors, such as impregnated and coated paper, abrasive paper, artificial leather, or impregnated and treated textiles. Moisture gaging and controlling equipment serves for the continuous measurement and control of moisture in sheet-like material such as paper and textiles. New equipment has been developed for the measurement of very thin foils with high accuracy. Krypton-85 (100 mC) is used as a source. The source is totally enclosed and has an automatic shutter. Foils of 2.5 to 800 μ can be measured with high accuracy, and the actual thickness of the foil can be read directly. (BBB)

39293 GAMMA RADIATION AS A QUARANTINE TREATMENT FOR HAWAIIAN FRUIT FLIES. Balock, J. W.; Burditt, A. K. Jr.; Seo, Stanley T.; Akamine, Ernest K. (Dept. of Agriculture, Honolulu). J. Econ. Entomol., 59: 202-4(Feb. 1966).

Results of tests are reported that were conducted in Hawaii from 1957–62 with fruit fly-infested fruits and vegetables to explore the use of γ radiation as a quarantine treatment. Radiation from a cobalt-60 source was applied to egg and larval infestations of the oriental fruit fly, Dacus dorsalis; melon fly, D. cucurbitae; and Mediterranean fruit fly, Ceratitis capitata. A dose of 10 kR generally prevented immature stages of fruit flies from developing to adults. Doses over 100 kR failed to prevent pupation. Radiation dosages required to prevent pupal or adult development at 99.0 and 99.9968% levels are shown. $LD_{99.9968}$ was selected since this level represents the mortality at probit 9, the security probit recommended in quarantine treatments for fruit flies. Several fruits and vegetables were treated to determine their response to radiation dosages ranging from 10,000 to 200,000 R. Fruits and vegetables exhibited a wide range of tolerance to γ radiation. Avocados in general were extremely sensitive. Of Hawaiian-grown varieties, none tolerated a dosage of 25,000 R without some injury, such as discoloration of skin or flesh, obnoxious aroma, or loss of palatability. However, California-grown varieties showed no evidence of external or internal damage or impairment of flavor at a dose of 25,000 R, but some varieties developed bluish streaks in the flesh, a mealiness, and an unsavory taste. Bananas treated in the mature-green stage ripened and showed no impairment in flavor after exposure to 50,000 R but developed a slight russeting of the skin. Pirie mangoes were not adversely affected at doses up to 100,000 R. A dose of 200,000 R caused skinscald but did not affect palatability. Haden mangoes treated in the mature-green stage tolerated a max of only 15,000 R without injury, but fully colored mangoes tolerated 100,000 R.

Tomatoes tolerated doses of 25,000 to 100,000 R. Solo papayas showed no deleterious effects from dosages up to 100,000 R. Cucumbers tolerated dosages up to 50 kR without damage. A dose of 100 kR caused a slight loss in crispness and flavor. (BBB)

39294 RADIOACTIVE KRYPTONATES IN SCIENCE AND TECHNOLOGY. Tolgyessy, Juraj; Jesenak, Viktor (Slovak Technical Inst., Bratislava). Jad. Energ., 12: 213-20(June 1966). (In Czech).

The potential significance and future of radioactive kryptonates are emphasized. The characteristics of radioactive kryptonates, methods of their production (bombardment with ^{85}K ions and diffusion of ^{85}K in solids) are given. Their properties and technical and engineering safety during work with them are described. The separate areas for the utilization of radioactive kryptonates are described in detail: detection and determination of nonradioactive substances, studies of kinetics and mechanisms of chemical reactions, measurement of the temperature of surfaces, measurement of thicknesses, elimination of static electricity, bremsstrahlung sources, and light sources. (tr-auth)

39295 NUCLEAR INDUSTRY IN FRANCE. INDUSTRIAL APPLICATIONS OF RADIOISOTOPES: EQUIPMENT. Paris, Commissariat a l'Energie Atomique. 30p.

Research on the industrial uses of radioisotopes in France is discussed. Progress in the use of radioisotopes in radiography; density and thickness gages; and level gaging and activation analysis is reviewed. Industrial equipment utilizing radioisotopes is also described. (R.C.K.)

39296 IMPROVEMENTS IN OR RELATING TO THE ILLUMINATION OF TIMEPIECES. Ault, John Douglas (to Saunders Roe and Nuclear Enterprises Ltd.). British Patent 1,035,116. July 6, 1966. Filed Apr. 9, 1964.

A method of illuminating a timepiece consists of incorporating one or more self-luminous light sources of the type in which a phosphor is excited to luminescence by a gaseous radionuclide into the structure of the timepiece. (B.L.M.)

39297 HISTORICAL DEVELOPMENT OF THE IRRADIATION OF FOODSTUFFS. Goldblith, Samuel A. (Massachusetts Inst. of Tech., Cambridge). Vienna, International Atomic Energy Agency, 1966, Preprint SM-73/54, 16p. (CONF-660609-10). ORAU.

From International Symposium on Food Irradiation, Karlsruhe, Ger.

The historical development of the field of radiation preservation of food is discussed on the basis of a sequence of ideas. The debt owed by the new world to the old in terms of the origin and discovery of radiation, isotopes, and x rays and the development of these into potentially useful processes is described. In addition reference is made to the debt that discovery owes to knowledge in this field, and with it the potential impact of these new developments on improving man's estate in the future. The important milestones from a cosmopolitan-international viewpoint are described and their impact on the field discussed. (auth)

39298 THE USE OF ^{241}Am ALPHAS TO MEASURE PROPERTIES OF THIN FILMS. Halliday, F. O.; Passell, T. O.; Bailey, L. E. (Stanford Research Inst., Menlo Park, Calif.). 23p. (CONF-660611-5). ORAU. Gmelin, AED-CONF-66-172-3.

From Fifth National Meeting, Society for Applied Spectroscopy, Chicago.

A reasonably intense alpha source, such as ^{241}Am, a small angle geometry, and a multichannel analyzer can be used with good reliability to determine the uniformity of thin films. Thickness can be measured by x-ray absorption. A pack rolling process of foil manufacturing, producing a larger and larger foil of smaller and smaller cross section, is recommended. (F.S.)

39299 IRRADIATION FLAVOR AND THE VOLATILE COMPONENTS OF BEEF. Wick, E. L.; Murray, E.; Mizutani, J.; Koshika, M. (Massachusetts Inst. of Tech., Cambridge). 42p. (CONF-650902-35). ORAU. Gmelin, AED-CONF-235-81.

From American Chemical Society, 150th National Meeting, Atlantic City.

Knowledge of the volatile components of irradiated and nonirradiated beef is reviewed. Concurrent and nonconcurrent irradiation procedures cause production of the same compounds but in different relative quantities. Storage of irradiated beef causes a decrease in irradiation flavor and in the quantity of volatile constituents. Evidence is presented that methional, n-nonanal, and phenylacetaldehyde are of primary importance in beef irradiation off-flavor produced under the conditions described. (auth)

39300 ANALYSIS OF THE VOLATILE CONSTITUENTS OF IRRADIATED APPLE JUICE. Dubois, P.; Zenz, H.; Stehlik, G.; Kaindl, K. (European Nuclear Energy Agency, Seibersdorf, Austria). Vienna, International Atomic Energy Agency, 1966, Preprint SM-73/2, 10p. (In French). (CONF-660609-28). ORAU.

From International Symposium on Food Irradiation, Karlsruhe, Ger.

The volatile substances present in irradiated fruit juices were analyzed by gas chromatography, with direct injection of the emitted vapors at ambient temperature and at 60°C (Weurman's Head Space Technique). The volatile constituents were identified by comparing the amounts retained in the column with those for pure substances and by removing certain constituents from the vapor with the help of chemical reagents. In order to simplify the analyses, the first tests were carried out on concentrated apple juice from which the volatile substances had been removed before irradiation. Irradiation gave rise to five aldehydes in the normal apple juice (acetaldehyde, isobutyraldehyde, butyraldehyde, isovaldehyde, and capronaldehyde), but only three in the concentrated juice (acetaldehyde, isobutyraldehyde, and isovaleraldehyde). In addition, 2-butanone appeared in the concentrated juice; however, the peak corresponding to it on the chromatogram was completely masked by the ethanol peak in the case of non-concentrated juice. Furan was also detected. A volatile disulfide, probably responsible for the characteristic odor of the irradiated juice, was found by chemical methods in grape juice irradiated at 100 krad. (P.C.H.)

39301 CHEMICAL CHANGES INDUCED BY IRRADIATION IN MEATS AND MEAT COMPONENTS. Merritt, Charles Jr. (Army Natick Labs., Mass.). Vienna, International Atomic Energy Agency, 1966, Preprint SM-73/57, 22p. (CONF-660609-7). ORAU.

From International Symposium on Food Irradiation, Karlsruhe, Ger.

The analysis of volatile compounds in irradiated meats and meat components was accomplished by programmed cryogenic temperature gas chromatography for separation of the complex mixtures obtained and rapid scanning mass spectrometry for identification of the individually separated components. Comprehensive analyses of the volatiles from irradiated ground beef, pork, mutton, lamb, and veal, as well as the volatile irradiation degradation products of several amino acids and proteins, animal fats, methyl esters of fatty acids, and triglycerides were made. The results of the analysis of irradiated component meat substances are compared with those obtained from the irradiation of meat itself and of separate meat fractions, thus establishing the contribution of each fraction to the total. Mechanisms are postulated for the formation of volatile components from each fraction and for interactions among intermediates from different fractions. The significance of chemical changes on the future applications of radiation preservation and the direction of future research is also discussed. (auth)

39302 REVIEW OF THE U. S. ARMY WHOLESOMENESS OF IRRADIATED FOOD PROGRAM 1955–1966. Raica, Nicholas Jr. (Fitzsimons General Hospital, Denver); Howie, Donald L. Vienna, International Atomic

Energy Agency, 1966, Preprint SM-73/5, 16p. (CONF-660609–26). ORAU.

From International Symposium on Food Irradiation, Karlsruhe, Ger.

The wholesomeness (toxicological, nutritional, and, in part, microbiological safety) of irradiated foods is reviewed. Long-term feeding studies were completed, and it was demonstrated that irradiated foods are as wholesome and, in general, as acceptable as conventionally processed foods. Studies were made on 21 irradiated foods (meat, fish, fruits, and vegetables) fed to over 15,000 mice, 5000 parent generation rats, 250 dogs, and 37 monkeys. In general, the test foods were irradiated to 2.8 and 5.6 Mrads with spent fuel rod, ^{60}Co or 10 Mev electron sources, and were stored for a minimum of 3 months at room temperature before they were fed. Control, non-irradiated foods were stored frozen until fed. Diets containing 35% (dry weight) of the test food were fed to two different species for 2 years. Growth, reproduction, lactation, hematology, longevity, histopathology, and carcinogenicity were studied. To study carcinogenicity more specifically, mice were fed 100% irradiated diets for 2 years. Other studies included induced radioactivity, nutrient stability and adequacy, tissue enzyme levels, digestibility, vitamin K nutrition, and chemical changes. Human subjects were fed fifty-four different irradiated (9.3 krads-3.7 Mrads) foods in diets that contained 32–100% irradiated calories for 2-week periods. (P.C.H.)

39303 EXPERIENCES WITH MACHINE SOURCES IN FOOD IRRADIATION. Gruenewald, T. (Federal Research Center for Food Preservation, Karlsruhe, Ger.). Vienna, International Atomic Energy Agency, 1966, Preprint SM-73/16, 14p. (CONF-660609–23). ORAU.

From International Symposium on Food Irradiation, Karlsruhe, Ger.

A comparison was made between machine sources such as x-ray and electron generators and radioactive sources for food sterilization studies. Such properties as power, capacity, efficiency, and dose distribution are discussed. (P.C.H.)

Power Application

See also ENGINEERING — Space Propulsion

Refer also to abstract 40289.

39304 (DP–1066(Vol.1), pp 19-28) LONG RANGE SPECULATIONS ON ISOTOPIC POWER. Spinrad, B. I. (Argonne National Lab., Ill.).

A brief history of power produced using radioisotopes is related. The characteristics, applications, cost, and future of radioisotopic power sources are discussed. (F.S.)

39305 (DP–1066(Vol.1), pp V.3-16) U. S. ATOMIC ENERGY COMMISSION ISOTOPIC POWER APPLICATIONS Carpenter, R. T. (Division of Space Nuclear Systems (AEC), Washington, D. C.).

Highlights of the AEC work on isotopic power systems are presented. SNAP space, terrestrial, and marine systems, radioisotope thrusters for propulsion and altitude control, and devices for thermal applications are discussed. (F.S.)

39306 (DP–1066(Vol.1), pp V.17-25) PROJECTED LARGE SCALE USE OF RADIOISOTOPES BY NASA. English, R. E. (National Aeronautics and Space Administration, Cleveland, Ohio. Lewis Research Center).

Projected requirements of isotopes for use in the space program are presented. Problems of reentry, helium containment, passive heat rejection, heat sinks, type of mission, weights, and shielding for ^{238}Pu, ^{90}Sr, ^{244}Cm, ^{60}Co, ^{147}Pm, and ^{210}Po isotopic heat sources are discussed. Isotopic heat sources are compared with solar cell systems. (F.S.)

39307 (DP–1066(Vol.1), pp V.35-40) SAFETY OF ISOTOPIC POWER SOURCES FOR TERRESTRIAL APPLICATIONS. Aikens, A. Jr. (Division of Materials and Licensing (AEC), Washington, D. C.).

Radiological safety of the SNAP 7A-7F systems is discussed. The design of isotopic power sources utilizing ^{238}Pu, ^{90}Sr, ^{144}Ce, ^{60}Co, ^{137}Cs, and ^{144}Pm is evaluated. (F.S.)

39308 (DP–1066(Vol.2), pp III.3-16) APPLICATION OF A RADIOISOTOPE HEAT SOURCE INTERIOR TO A TUBULAR THERMOELECTRIC GENERATOR. Boman, L. H. (Westinghouse Electric Corp., Pittsburgh, Pa. Astronuclear Lab.).

A cylindrical isotopic heat source of ^{144}Ce, ^{210}Po, ^{242}Cm, or ^{244}Cm, surrounded by a tubular thermoelectric generator with provision for cooling, forms a simple, lightweight, rugged, compact power-generating system. Application for such a system, using lead telluride as the thermoelectric material, is limited to isotope capsules with power densities higher than 10 W/cc. (auth)

39309 (DP–1066(Vol.2), pp III.39-48) RADIOISOTOPE POWERED GENERATOR DEVELOPMENT IN THE UNITED KINGDOM. Hare, G. E. (Atomic Energy Research Establishment, Harwell (England)).

Small power sources RIPPLE I and II (Radio Isotope Powered Prolonged Life Equipment) are described. Strontium-90 titanate is used as the heat source. Power outputs to 100 W are planned. (F.S.)

39310 (GA–5781) TEST EVALUATION OF SNAP-15A GENERATOR. Campana, R. J.; Baker, F.; Leedy, R. (General Dynamics Corp., San Diego, Calif. General Atomic Div.). Nov. 30, 1964. Contract AT(04-3)-167. 140p. Dep. mn. CFSTI $4.00 cy, $1.00 mn.

Test results are reported of the performance, life, and reliability of the SNAP-15A generator, a metal-thermocouple generator fueled with ^{238}Pu. The generator, producing 1 Mw(e) at ~5 v when connected to a 22.5-kohm load, was designed to be highly reliable in continuous operation for 5 years without maintenance, even when exposed to extreme environmental conditions. (D.L.C.)

39311 (MND–SR–2586) FINAL SAFETY ANALYSIS FIVE-WATT RADIOSTRONTIUM-FUELED GENERATOR FOR UNATTENDED METEOROLOGICAL STATION. (Martin Co., Baltimore, Md. Nuclear Div.). [1960]. Contract AT(30-1)-2519. 46p. Dep. mn. CFSTI $2.00 cy, $0.50 mn.

A prototype generator fueled with 17,500 C of ^{90}Sr producing 108 thermal watts of decay energy, is used to fulfill the five-watt electrical power requirements of an unattended automatic meteorological station in the Arctic region. The safety criteria considered in the design of the generator are: absolute containment of the radiostrontium fuel; selection of an insoluble form of this fuel; and biological shielding to attenuate the ionizing radiations to permissible levels. Detailed analysis has shown that the generator integrity will be maintained under the following conditions: external hydrostatic pressures to and including 5000 psi; impact velocities up to 700 fps; heat up to 1.7×10^5 Btu; and 7000 years of corrosive action in the ocean. If the fuel capsule should become ruptured in water shortly after being fueled, the strontium concentration at 10 meters from the source will be 8.8×10^{-6} μC/cc; this activity will result in a dose rate of less than 1 μrem/hr. Readings taken after the generator was assembled showed that the dose rate was 50 mr/hr at the generator surface and 4 mr/hr at one meter from the centerline of the generator. It was concluded that the integrity of the system is maintained under conceivable accident conditions and that the safety criteria have been met. (auth)

39312 (SC–CR–66–2044) STUDY OF THE CHEMICAL INTEGRITY OF RADIOISOTOPE CONTAINMENT MATERIALS IN LAUNCH ABORT ENVIRONMENTS. Blumenthal, J. L.; Kuenzly, J. D.; Santy, M. J. (TRW Systems, Redondo Beach, Calif.). Apr. 1966. Contracts AT(19-1)-789; 48-2534. 240p. Dep. mn. CFSTI $6.00 cy, $1.25 mn.

For Sandia Corp., Albuquerque, N. Mex.

The materials investigated include cobalt-based "super-

alloys," nickel-based "superalloys," stainless steels, and coated and uncoated refractory metals. (auth)

39313 OCEANOGRAPHIC APPLICATIONS OF NUCLEAR ENERGY. Swartout, John A. (Atomic Energy Commission, Washington, D. C.). S. Afr. Mining Eng. J., 77: 969-72(Apr. 29, 1966).

Some characteristics of nuclear power that make it particularly suitable for use in the ocean are surveyed. These include lack of need for oxygen, capability of producing from milliwatts to megawatts of electrical power, ability to operate unattended for extended periods, and availability as a compact, self-contained unit. Development of power devices for sea use began with the SNAP-7A radioisotopic generator. A second generation of units having higher power outputs and/or more favorable economics is being developed, and such units, the SNAP's-21 and -23, will soon be entering the testing phase of development. SNAP-21 is designed for undersea applications and SNAP-23 for on-the-sea applications. SNAP-21 will be capable of operating under pressures to 10,000 psi with absolute containment of the fuel for a minimum of 300 yr. In the SNAP-23 program a 60-w unit is presently being developed. Units in the 100-w range are planned. These oceanographic isotopic units are direct conversion thermoelectric devices using lead telluride as the thermoelectric material and using a β emitter as fuel. A program for the development of nuclear reactor power for oceanographic use is also being carried out. Safety as a phase of development of oceanographic nuclear power units is also discussed. Extensive safety testing and analyses have been conducted in connection with the development of both isotopic and reactor units. (BBB)

Separation and Production

See also CHEMISTRY — Separation Processes and Procedures

Refer also to abstracts 39012 and 40364.

39314 (DP-1066(Vol.1), pp 29-39) PLUTONIUM AND OTHER RADIOISOTOPE SOURCES: DISCOVERY TO DEMAND. Tape, G. F. (Atomic Energy Commission, Washington, D. C.).

The discovery, demand for, and production of radioisotopes are discussed. Production of radioisotopes in reactors is summarized. Since it is possible to produce ^{90}Sr, ^{137}Cs, ^{144}Ce, and ^{147}Pr in tens of megacurie quantities, suitable uses of the isotopes must be found. (F.S.)

39315 (DP-1066(Vol.1), pp I.29-52) PRODUCTION OF RADIOISOTOPES IN POWER REACTORS. Rupp, A. F. (Oak Ridge National Lab., Tenn.).

The production of radioisotopes in power reactors is summarized. It appears that the projected demand for isotopic power fuels may exceed anticipated production; the commercial nuclear industry can contribute substantially to the supply of radioisotopes; careful recycling of power reactor fuels will be necessary; commercial chemical processing and target fabrication of ^{237}Np and actinides will be needed; and multiproduct, converter reactors should be envisioned for the future. (F.S.)

39316 (DP-1066(Vol.1), pp II.3-14) LARGE SCALE PROCESSING AND SOURCE PREPARATION OF NEUTRON-PRODUCED ISOTOPES. Lamb, E. (Oak Ridge National Lab., Tenn.).

Large-scale processing of radioisotopes for commercial and isotopic power applications is summarized. "Large-scale" is defined as being in excess of 10,000 C/year. The discussion is limited to radioisotopes produced by the (n,γ) reaction. In the future, production will increase by factors of tens or hundreds and refinements of the four basic process operations to permit practical and economic production of neutron-produced isotopes on a large scale will need to be made. (F.S.)

39317 (DP-1066(Vol.2), pp I.67-77) ^{60}Co PRODUCTION IN GRAPHITE GAS COOLED REACTORS. Henry, R.; Meyer-Heine, A. (Commissariat a l'Energie Atomique, Saclay (France). Centre d'Etudes Nucleaires).

The use of cobalt as a neutron absorber in gas-cooled reactors is considered from the neutronic and technological point of view. For economic reasons, the use of depleted uranium is considered to be more attractive than cobalt. Utilization of cobalt elements may be considered as a consequence of the refueling scheme. The calculation of the antireactivity of a cobalt absorber is shown. Production of ^{60}Co is evaluated with different fuel cycles. Mechanical and technological problems are summarized. (F.S.)

39318 (DP-1066(Vol.2), pp I.93-101) PRODUCTION OF ^{60}Co IN THE BR2 REACTOR, BELGIUM. Hebel, W. (European Atomic Energy Community).

A brief description of the BR2 is presented. The production of ^{60}Co in the BR2 is also described. Cobalt-60 with specific activities of above 50 c/g is produced in peripheral core positions in a year. (F.S.)

39319 (DP-1066(Vol.2), pp II.33-44) ELAN: INSTALLATION FOR THE RECOVERY AND PACKAGING OF ^{137}Cs IN FRANCE. Raggenbrass, A.; Courouble, J. M.; Lefevre, J.; Fradin, J.; Perebaskine, C. (Commissariat a l'Energie Atomique, Saclay (France). Centre d'Etudes Nucleaires).

ELAN is a program for the recovery and packaging of ^{137}Cs from fission product wastes. Cesium is recovered by ion exchange using zirconyl phosphate and ammonium phosphotungstate. Processes are described and diagrams of the laboratories are included. (F.S.)

39320 (MLM-1311) MOUND LABORATORY PROGRESS REPORT FOR NOVEMBER 1965. Eichelberger, J. F.; Grove, G. R.; Jones, L. V. (Mound Lab., Miamisburg, Ohio). Nov. 22, 1965, Contract AT(33-1)-Gen-53. 24p. Dep. mn. CFSTI $2.00 cy, $0.50 mn.

Developments are reported for studies on: half life determination of polonium-210 by decaying pairs; hydrolysis of plutonyl ions; carbon isotope separation by chemical exchange; neon isotope separation; xenon isotope separation by thermal diffusion; transport coefficients and properties in thermal diffusion studies on neon and helium isotopes; and vapor pressure thermometry measurements on helium. (P.C.H.)

39321 (MLM-1312) MOUND LABORATORY PROGRESS REPORT FOR DECEMBER 1965. Eichelberger, J. F.; Grove, G. R.; Jones, L. V. (Mound Lab., Miamisburg, Ohio). Dec. 20, 1965. Contract AT(33-1)-Gen-53. 30p. Dep. mn. CFSTI $2.00 cy, $0.50 mn.

Developments are reported for studies on: alpha-beta branching ratio of actinium-227; carbon isotope separation by chemical exchange; neon, argon, krypton, and xenon isotope separations by thermal diffusion, krypton-xenon separation by chromatography; and molecular beam scattering, collision integrals, transport coefficients, transport properties, and cascade theory in thermal diffusion. (P.C.H.)

39322 SEPARATION OF NEON ISOTOPES IN A FILM FRACTIONATING COLUMN. Grigor'ev, V. N.; Breslavets, K. G. At. Energ. (USSR), 20: 494-7(June 1966). (In Russian).

The separation of neon isotopes by fractionation in film columns at vapor velocities of 0.3, 0.4, and 0.5 cm/sec and different separation values was investigated. It was shown that the separating capacity of the column does not depend on the number of parallel operating tubes. The dependence of the number of theoretical plates on the separation is described by the Kuhn formula. In regimes without separation the number of theoretical plates is 2 to 2.5 times less than the calculated value. Gaseous neon with concentrations of ^{22}Ne of 84.5% was obtained. (tr-auth)

39323 ISOTOPE SEPARATION BY THERMAL DIFFUSION COLUMNS. Saxena, V. K.; Saxena, S. C. (Univ. of Rajasthan, Jaipur, India). Indian J. Technol., 4: 227-30(Aug. 1966).

The performance of a hot-wire type thermal diffusion

column, using neon of natural abundance as the test gas, was investigated with a view to obtaining data on optimum operating conditions and for setting up a pilot cascade thermal diffusion plant for the separation of isotopes. A glass tube, about 3.5 m long and 8 mm ID, and 0.7 mm dia nichrome wire stretched axially in the glass tube serve as the cold and hot walls respectively. The observed separation as a function of pressure for a fixed value of T_2/T_1 ratio (T_1 and T_2 being cold and hot wall temperatures respectively) using d-c power supply for heating the wire was compared with that predicted by theory on the basis of inverse power and Lennard-Jones (12-6) potentials; the two are found to be in reasonably good agreement. The performance of the column was checked by replacing the nichrome wire by a thinner (0.5 mm dia) platinum wire as the hot wall material and found to be equally satisfactory. As the use of a-c power supply for heating the wire resulted in an appreciable reduction in the separation achieved by the column, d-c power supply was preferable. (auth)

39324 PREPARATION OF CARRIER-FREE ^{59}Fe BY KOREAN TRIGA MARK II REACTOR. **Park, Keung Shik (Atomic Energy Research Inst., Seoul). J. Korean Chem. Soc., 9: No. 2, 96-100(1965).**

The possibility of carrier-free ^{59}Fe preparation by the Korean TRIGA Mark II reactor was investigated. The average cross section for the $^{59}Co(n,p)^{59}Fe$ reaction, separation using an anion exchange resin, and radiochemical purity were determined. The radiochemical purity of ^{59}Fe separated was checked by the method of γ spectrometry with a 256-multichannel pulse-height analyzer and half life determination. This method permits ^{59}Fe preparation with radiochemical purity of >99.9%. (auth)

39325 SEPARATION OF ^{10}B BY LOW-TEMPERATURE DISTILLATION OF BORON FLUORIDE–METHYL FLUORIDE COMPLEX. **Nakane, Ryohei; Isomura, Shohei (Inst. of Physical and Chemical Research, Tokyo). J. Nucl. Sci. Technol. (Tokyo), 3: 267-74(July 1966).**

A method for low-temperature distillation of boron fluoride–methyl fluoride complex in a packed column was studied. The minimum volume of the column for producing highly enriched ^{10}B was found to be smaller than required for the low-temperature distillation of boron fluoride. (auth)

39326 TEMPERATURE ASSIGNMENT TO THERMAL DIFFUSION FACTOR. **Laranjeira, M. F.; Moutinho, A.; Vasconcelos, M. H. (Comissao de Estudos de Energia Nuclear, Lisbon). Port. Phys., 4: 115-30(1965).**

A new formula to approach the temperature dependence of the isotopic thermal diffusion factor is proposed. It can be successfully applied to theoretical data of Lennard-Jones (12-6) and Exponential Six models, as well as to the available observations with isotopes of Ne, Ar, Kr, and Xe. This enables a reasonable comparison to be made between theory and experiments, showing that the above models are not satisfactory to explain, simultaneously, thermal diffusion and viscosity data of the referred noble gases. The assignment of a mean temperature associated with the experimental thermal diffusion factor is discussed, from the point of view of the formula proposed. (auth)

MATHEMATICS AND COMPUTERS

Refer also to abstracts 38549, 39107, 39148, 39226, 39240, 39998, and 40447.

39327 **(LA–3362)** TECNICAS ITERATIVAS DE GAUSS DE LOS MINIMOS CUADRADOS PARA COMPUTADORES MODERNOS. **(Gaussian Iterative Least Squares Techniques for Modern Computers).** **Chezem, C. G.; Moore, R. H.** **(Los Alamos Scientific Lab., Univ. of California, N. Mex.).** **Jan. 1962.** **Contract W-7405-eng-36.** 70p. Dep. mn. CFSTI $3.00 cy, $0.75 mn.

In Spanish and English.

The general problem of estimating the parameters of a function to be fitted to a set of experimental data points (curve fitting) by the method of least squares is reviewed. An iterative method of fitting functions in which the parameters appear non-linearly, first presented by Gauss in the early 1800's, is discussed in modern language compatible with any high-speed digital computing machine. Suggestions are offered to experimenters and computer programmers based on extensive Los Alamos experience, concerning the formulation and operation of such iterative routines, interpretation of the precision indicators of the fit, convergence criteria and the prevention of non-convergent oscillations. Some applications of the venerable Gauss method taken from the fields of nuclear science and chemistry are discussed. An appendix points the way toward the rigorous defense of the weighted least squares techniques independent of assumptions concerning the distribution functions of the observations. (auth)

METALS, CERAMICS, AND OTHER MATERIALS

General

Refer also to abstract 40440.

39328 (AD-624997) HIGH-PURITY METALS. Annotated Bibliography. Zurichenko, Alex (Aerospace Technology Div., Library of Congress, Washington, D. C.). Dec. 8, 1965. 30p. (N-66-14700; ATD-65-109). CFSTI $2.00 cy, $0.50 mn.

An annotated bibliography of Soviet and Soviet-bloc materials dealing with high-purity metals is presented. All of the articles included are cataloged at the Library of Congress Aerospace Technology Division, from which information about availability of translations can be obtained. (M.W.R.)

39329 (AECL-2432) A NOTE ON THE FAST FRACTURE OF A PRESSURE VESSEL. Hake, G. (Atomic Energy of Canada Ltd., Chalk River (Ontario)). May 1966. 10p. Dep. mn. AECL $0.50.

An indication of the size of opening that results when a pressure vessel or pressure piping, which contains a through-defect shorter than the critical length, is initially brought to operating conditions is given. This information is relevant to the analysis of the loss of the coolant accident. (auth)

39330 (BNL-962) HIGH-TEMPERATURE LIQUID-METAL TECHNOLOGY REVIEW. A Bimonthly Technical Progress Review. Volume 3, Number 5, October 1965. (Brookhaven National Lab., Upton, N. Y.). Dec. 1965. Contract AT(30-2)-Gen-16. 41p. Dep. mn. CFSTI $2.00 cy, $0.50 mn.

Seventeen reviews are presented on the following programs and topics: alkali metals evaluation, SNAP-50/SPUR, initiation of nucleate boiling, reactor development at Argonne, materials examination of model sodium-heated steam generator, alkali metals boiling and condensing, cavitation damage, thermophysical and transport properties, effect of high-temperature sodium in steels, measurement of impurities in sodium, SNAP-8 corrosion, liquid-metal-lubricated journal bearings, and boiling heat transfer. (D.L.C.)

39331 (UCRL-Trans-10044) REACTIONS OF OXIDES AND CARBIDES WITH METALS. Avgustinik, A. I. Translated for Univ. of California Lawrence Radiation Lab., Livermore, from Zh. Vses. Khim. Obshchestva im. D. I. Mendeleeva, 10: 512-18(1965). 30p. Dep. mn. CFSTI $2.00 cy, $0.50 mn. JCL $2.60 fs, $1.10 mf.

A review of literature data and information is presented on high-temperature reactions between metals and borides, carbides, oxides, and nitrides. The information is concerned mostly with chemical reactions between ceramic refractory materials and transition metals. It is noted that the high-temperature reactions are predominantly chemical. (J.R.D.)

39332 FUEL ELEMENTS. Boettcher, A. (Kernforschungsanlage, Juelich, Ger.). pp 45-81 of 2nd FORATOM Congress 1965. Bonn, Deutsches Atomforum e. V., 1965.

Reactor fuel technology is discussed. Information is included on American plans on private ownership and toll enrichment, capacities of fuel fabrication plants, reprocessing plants, and fuel cycle considerations. (J.R.D.)

39333 PRODUCTION OF ALUMINUM-URANIUM ALLOY NUCLEAR FUEL BY DIRECT REDUCTION. Seki, Yoshitatsu; Mitamura, Noritsugu (Mitsubishi Atomic Power Industries, Inc., Omiya, Japan). Genshiryoku Kogyo, 11: No. 9, 37-40(Sept. 1965). (In Japanese).

A study was made of Al-U production by the direct reduction of UF_4 with Al. The main reaction is $UF_4(s) + xAl(l) = UAl_{x-3}(l) + \frac{4}{3}AlF_3(s)$. This reaction readily goes to the right at 900 to 1200°C, and UF_4 is reduced to form Al-U alloy. AlF_3 formed becomes AlF by the reaction, $AlF_3(s) + 2Al(1\text{ in }1\text{ Al-U alloy}) = AlF(g)$; the equilibrium constant for this reaction is $\log K_2 = -22.157 - 33.810/T$. Thus, by the direct reduction under atmospheric pressure, followed by the redissolution at a reduced pressure of 900 to 1200°C, F is evaporated as AlF. The overall yield for the direct reduction is 90%, compared with 85% for the U addition method. The C content in the alloy is 30 to 70 ppM; F is approx. 30 ppM. The physical properties of direct-reduction Al-U alloys are as good as those obtained using the U addition method. The process for fabricating fuel plates is the same in both the methods. (auth)

39334 NEUTRON RADIOGRAPHY OF PYROTECHNIC CARTRIDGES. Rhoten, Merle L.; Carey, Walter E. (Ohio State Univ., Columbus). Mater. Eval., 24: 422-4; 430(Aug. 1966).

Neutron radiographic techniques used to answer the nondestructive testing problems of pyrotechnic cartridge inspection are described. The techniques and results are given, as well as the results of possible deterioration of the encased explosive powder. The information is presented to alert quality control personnel to the possible use of neutron radiographic techniques as an inspection tool. (auth)

39335 ENRICHMENT TESTER FOR 0.15 TO 3.0 WEIGHT PERCENT ^{235}U URANIUM FUEL. Jackson, C. N. Jr. (Battelle-Northwest, Richland, Wash.). Contract AT(45-1)-1830. Mater. Eval., 24: 431-5(Aug. 1966).

A combination single channel analyzer and gamma scintillation system was developed to measure enrichment of ^{235}U in metallic U. The technique uses a unique characteristic of the gamma decay of ^{235}U and ^{238}U to obtain a net activity proportional to the concentration of ^{235}U. This technique is independent of daughter equilibrium buildup products in U that is older than 60 days from the date of the last chemical separation. The tester is routinely used at Hanford to perform a rapid, nondestructive identification of reactor fuels with 0.72, 0.95, 1.25, 1.6, and 1.95 wt % enrichments. The capability of the tester was demonstrated for a range from 0.15 to 3.0 wt % enrichment. It has an approximate accuracy of a 0.1 % in equivalent enrichment level using a two-min counting period. Laboratory investigations of specimen geometry, cladding thickness, and other factors were conducted to obtain design data for developing the tester. The use, calibration, and performance of the tester for routine enrichment measurement are described. (auth)

39336 THE QUESTION OF THE LOCALIZATION OF INTERFACE REACTIONS IN METAL-AQUEOUS SOLUTION SYSTEMS. I. THE MEASUREMENT OF β/γ RATIOS IN RADIOACTIVE LABELING. Herold, C. (Zentralinstitut fuer Kernforschung, Deutsche Akademie der Wissenschaften, Rossendorf, Ger.). Z. Phys. Chem. (Leipzig), 232: 1-10(1966). (In German).

The measurement of β/γ ratios under solid geometry yields data on the localization of the labeling material in the depths of the carrier. By knowing the activity distribution determination of the layer thickness in which the active substances are contained is possible by comparison with the β/γ ratio of standards in which the emitter is fixed on the surface. The use of a 2-π counter as β detector permits the determination of layer thicknesses up to 0.225 mg/cm^{-2} in homogeneous distribution of ^{82}Br. (tr-auth)

39337 THE QUESTION OF THE LOCALIZATION OF BOUNDARY REACTIONS IN METAL-AQUEOUS SOLUTION SYSTEMS. II. THE PENETRATION OF ABSORBED ANIONS IN METALLIC ADSORBENTS. Herold, C.; Schwabe, K. (Zentralinstitut fuer Kernforschung, Deutsche Akademie der Wissenschaften, Rossendorf, Ger.). Z. Phys. Chem. (Leipzig), 232: 11-26(1966). (In German).

Investigations on the adsorption of $^{82}Br'$ on Ni sheets in

which the ratio of β/γ intensity was determined by comparison with standards gave no change of this ratio with time and with modification of the rinsing volume. Therefore it was concluded that the Br′ cannot penetrate the interior of the metal. The lower constant value of the β/γ ratios Ni sheets rubbed with emery in contrast with that of the standards can be explained by attenuation of the β radiation originating from the Br′ adsorbed in indentations of the Ni surface. (tr-auth)

39338 MATERIALS SCIENCE RESEARCH. VOLUME 3. THE ROLE OF GRAIN BOUNDARIES AND SURFACES IN CERAMICS. Proceedings of the Conference held November 16–18, 1964 at North Carolina State University at Raleigh. Kriegel, W. Wurth; Palmour III, Hayne (eds.). University Conferences on Ceramic Science. New York, Plenum Press, 1966. 643p. $22.50. (CONF-641116).

Information is presented concerning ceramics. Conference paper summaries are presented on kinetic processes at interfaces, electromagnetic wave behavior near interfaces, grain boundary contributions to deformation, grain boundary contributions to strength and thermomechanical behavior and surface and environmental contributions to mechanical behavior. The conference proceedings are published in 31 chapters. (J.R.D.)

39339 OPTICAL PROPERTIES AND ELECTRONIC STRUCTURE OF METALS AND ALLOYS. Proceedings of the International Colloquium, Held at Paris, 13–16 September 1965. Abeles, F. (ed.). New York, John Wiley and Sons, Inc., 1966. 652p. $18.50. (CONF-650929).

Information presented at the colloquium is published in a book divided into five sections. The sections contain information concerning simple metals; simple, d-band, and transition metals; rare earth metals; liquid metals; optical plasma effects; superconductors; magneto optical effects; and non-periodic systems. (J.R.D.)

39340 VIBRATORY GRINDING AND POLISHING EQUIPMENT (Engineering Materials). (Argonne National Lab., Ill.). (CAPE-1443).

28 drawings.

The equipment reduces the metallographic grinding operation to essentially one step by restricting horizontal and vertical components of vibration to specific requirements and by guiding the specimen in a controlled and predetermined manner. Specimens produced have minimum disturbed metal with little embedded abrasive. The polisher achieves a scratch free finish. (For details see TID-4100). (F.S.)

39341 RARE EARTH ACTINIDE METAL SOLS. Fitch, Frederick T.; Smith, Jean G. (to W. R. Grace and Co.). U. S. Patent 3,264,224. Aug. 2, 1966. Filed Dec. 2, 1963.

An invention is described relating to stable sols of particles composed of actinide and rare earth oxides as an intimate mixture or as solid solution oxide phases and the method of preparing these sols. In one particular embodiment, the invention relates to the method of preparing stable $Y_2O_3-UO_2$ sols and to the sols as compositions-of-matter. In the preparation of high-temperature ceramic nuclear elements, a sol with particles composed of a binary rare earth-actinide oxide mixture offers advantages as a fuel source due to the fine particulate actinide oxide dispersion. Other improvements result from the physical properties of the ceramic material prepared using colloidal materials. The rare earth-actinide oxide compositions may be used to stabilize certain of the actinide oxide fuels. The sols of the invention are incorporated in the fuel elements by adding the sols to the other components to form a paste which is subsequently fired. As stated previously, one of the components of the sols is the rare earths including the elements Y, La, Ce, Pr, Nd, Pm, Sm, Eu, Gd, Tb, Dy, Ho, Er, Tm, Yb, and Lu. Actinide metals include U, Pu, and the elements above Pu. (J.R.D.)

39342 IMPROVEMENTS IN OR RELATING TO THE PRODUCTION OF URANIUM METAL. Duxbury, Donald (to United Kingdom Atomic Energy Authority). British Patent 1,033,223. June 22, 1966. Filed Mar. 6, 1964.

A method is described for the production of U metal suitable for extrusion into rod-like fuel elements by the reduction in a reaction vessel of UF_4 using a metallic reducing agent such as Ca or Mg. A quantity of a reducible compound of Fe and Al or of the pure metals is included with the reactants in the reaction vessel. The quantity included is that which is needed to provide the refined grain structure and other satisfactory metallurgical properties. The preferred reducible compounds of Fe and Al are the hydrated trifluorides of each of the metals. (B.L.M.)

39343 IMPROVEMENTS IN OR RELATING TO HEAT TREATMENT OF REFRACTORY MATERIALS. Murray, Peter (to United Kingdom Atomic Energy Authority). British Patent 1,033,391. June 22, 1966. Filed July 11, 1961.

In a method for heat treating refractory materials, the refractory material in particulate form is flowed through a an induction-coupled plasma that has been set up in a moving stream of gas and then is cooled while the particles are substantially separated by the flowing gas. Using feed material in the size range of 100 to 150 μ, a spherical product in the size range of 80 to 140 μ is obtained, while a product of colloidal fineness is obtained if the feed material is smaller than 20 μ (B.L.M.)

Corrosion

Refer also to abstract 39356.

39344 (EUR–2997.e) STATISTICAL TECHNIQUES AND ANALYSIS IN CORROSION MEASUREMENTS OF Zr ALLOYS IN TERPHENYLS. Imarisio, G. C.; Cocchi, M. (European Atomic Energy Community, Ispra (Italy). Joint Nuclear Research Center). 1966. 18p. Dep. mn.

The theoretical criteria and the experimental procedures adopted to investigate the agents that cause corrosion of Zr–alloys in terphenyls are described. (auth)

39345 (GEAP–4831) SODIUM MASS TRANSFER. XV. BEHAVIOR OF SELECTED STEELS EXPOSED IN FLOWING SODIUM TEST LOOPS. Rowland, M. C.; Plumlee, D. E.; Young, R. S. (General Electric Co., San Jose, Calif. Atomic Power Equipment Dept.). Mar. 1965. Contract AT(04-3)-189. 105p. Dep. mn. CFSTI $4.00 cy, $0.75 mn.

The results of a series of test runs on materials behavior in high-temperature flowing Na loops are presented. Approximately 2500 test samples of 316 stainless steel, 2¼% Cr–1% Mo steel, and 5% Cr–½% Mo–½% Ti steel were examined after exposure to 12 and 50 ppm O_2, 1100 and 1200°F maximum temperature, and 500 and 250°F ΔT. Corrosion and mass transfer results from a statistical analysis of weight change data, composition and structural changes, carbon activity, and long-term exposure effects are discussed in detail. (H.D.R.)

39346 (LA–3488) LEACHING OF URANIUM BY HYDROGEN CHLORIDE FROM PYROLYTIC-CARBON-COATED URANIUM DICARBIDE BEADS. Smith, Maynard E.; Cappis, John H.; Waterbury, Glenn R. (Los Alamos Scientific Lab., Univ. of California, N. Mex.). Feb. 1, 1966. Contract W-7405-eng-36. 32p. Dep. mn. CFSTI $2.00 cy, $0.50 mn.

The corrosive action of HCl on pyrolytic-C-coated UC_2 beads was investigated over the range 1600 to 2100°C. It was necessary to develop an apparatus that could withstand the high temperature and the corrosive HCl–He mixture. A measured volume of the gas mixture was passed through each sample at temperatures ranging from 1600 to 2100°C. The UCl_4 vapor produced in the process was condensed, and the U determined spectrophotometrically. In the range from 1800 to 2100°C the relative standard deviations for median values of the amount of U leached varied from 4 to 21% for six or more determinations at any given temperature level for a single sample. The amount of U leached was greatly dependent on the temperature, which must be controlled rigorously. It was concluded that the rate-determining step in the leaching process was the diffusion of the U from the core of the bead through the pyrolytic C coating. (auth)

39347 (NP-16239) EFFECT OF HEAT TREATMENT ON THE CORROSION BEHAVIOR OF TWO ZIRCONIUM-COPPER-MOLYBDENUM ALLOYS. Dixon, C. F.; Skelly, H. M. (Department of Mines and Technical Surveys (Canada). Mines Branch). Mar. 1966. 14p. (R-183). Dept. of Mines and Technical Surveys, Ottawa, $0.50.

The effect of heat treatment on the corrosion properties of Zr-1.0% Cu-1.5% Mo and Zr-0.5% Cu-0.5% Mo alloys was investigated. The heat treatment found to give optimum corrosion resistance in steam was, for the Zr-1.0% Cu-1.5% Mo alloy, 1000°C for one hr, water quench, followed by aging at 500°C for 32 hr; and, for the Zr-0.5% Cu-0.5% Mo alloy, 1000°C for one hr, water quench, then aging at 500°C for 24 hr. Over-aging of the alloys resulted in growth of the intermetallic-phase particles, which then caused cracking of the corrosion film. Preparation of Zr-3.0% Cu-4.5% Mo alloy, which contained a larger percentage of the intermetallic phase, made it possible to identify, by x-ray diffraction, that phase as being a cubic structure with a unit cell of 4.999 Å. (auth)

39348 RETARDATION OF THE OXIDATION RATES OF NIOBIUM, TANTALUM, AND TUNGSTEN BY FLUORIDE COATING. Bhat, T. R.; Khan, I. A. (Atomic Energy Establishment, Trombay, India). J. Less-Common Metals, 11: 290-2(1966).

Results of thermogravimetric studies are presented concerning the effects of fluoride on oxidation of Nb, Ta, and W powders and strips. The powder specimens were mixed with 5% KHF_2 (negative catalyst) and the sheet specimens were coated by dipping in saturated solutions of KHF_2. Results show that Nb is not well protected by the coating while oxidation is well suppressed in the case of Ta and W by the fluoride coat. (J.R.D.)

39349 KORROZIONNAYA STOIKOST REAKTORNYKH MATERIALOV. (Corrosion Resistance of Reactor Materials). Gromova, A. I.; Kuznetsova, V. N.; Morozova, I. K.; Pavlova, F. S.; Parfenov, B. G.; Rodchenkov, B. S.; Sabinin, A. A.; Smirnov, V. V.; Shuvalov, V. A. Moscow, Atomizdat, 1966. 508p.

Tabulations of reactor materials compositions are included along with data on property-temperature relations, reactions of reactor materials with corrosive materials, and performance of coatings on high-temperature metals and alloys. (J.R.D.)

39350 ANTI-CORROSION TREATMENT OF NUCLEAR REACTOR FUEL ROD ENVELOPES. Berghaus, Bernhard (to Elektrophysikalische Anstalt Bernhard Berghaus). Canadian Patent 735,586. May 31, 1966. Priority date Nov. 6, 1961, Switzerland.

Corrosion resistant fuel rods are obtained by coating them in the solid state with Si, Cr, or Ni in an ionized gas atmosphere by cathode disintegration. By changing the method, the temperature may be adjusted to deposit the protective coating from the liquid or gaseous state. The coating is no more than 0.05 mm thick and extremely uniform so few neutrons are absorbed when the fuel or other component so treated is placed in a reactor. Such a corrosion resistant coating enables a reactor to be operated at a higher temperature with increased efficiency. (F.S.A.)

39351 METHOD OF PICKLING AND CHEMICALLY MILLING ZIRCONIUM AND ZIRCONIUM ALLOYS. McGrew, John W.; Jakobson, Kurt (to Martin Marietta Corp.). U. S. Patent 3,264,219. Aug. 2, 1966. Filed Feb. 14, 1963.

A method for the surface treatment of Zr and Zr-alloys to remove metal and scale is described. A 1 to 6% solution of alkali metal fluoride in 5 to 25% sulfonic acid is used for controlled etching, chemical milling, and pickling. (J R.D.)

Fabrication

Refer also to abstracts 38799, 39027, 39031, and 39032.

39352 (BM-RI-6817) HIGH-ENERGY-RATE EXTRUSION OF LOW-DENSITY TUNGSTEN POWDER BILLETS. Croeni, Jack G.; Howe, John S. Jr.; Kato, H. (Bureau of Mines, Albany, Oreg. Albany Metallurgy Research Center), Jan. 1966. 12p. Bureau of Mines Free.

A method is described for extrusion of low-density W powder billets into rods and sheet bar with high-energy-rate forming equipment. Billets were compacted and sintered in an atmosphere of H_2 to obtain a density of approximately 60%. Extrusion was conducted at reduction ratios of 6.25 to 1 and 9 to 1 at 1,800°C to produce high-density, sound material. Yield strengths obtained were higher than those of material produced by conventional powder-metallurgy techniques, but ductility was lower at high temperatures. (auth)

39353 (BMWF-FBK-66-07) THEORETISCHE UNTERSUCHUNGEN UEBER DIE CHEMISCHEN REAKTIONEN KARBIDISCHER UND OXIDISCHER WERKSTOFFE, DIE FUER DIE KATHODEN NUKLEARER, THERMIONISCHER KONVERTER IN BETRACHT KOMMEN. (Theoretical Evaluations on Chemical Reactions of Carbides and Oxides Suitable for the Construction of Nuclear-Fueled Thermionic Emitters). Poeschel, E.; Rochow, H. (Battelle Institute e. V., Frankfurt am Main (West Germany)). Apr. 1966. 70p. Dep. mn.

Combinations of suitable materials to prepare coated-particle filled emitters for thermionic converters are discussed. In the case of coated particles with a PyC outer layer and UC_x-containing kernels, the connecting matrix may be composed of NbC, TaC, or ZrC if Re is used as electron-emitting material. In the case of W emitters, the only suitable matrix material is ZrC. Coated particles with UO_2 kernels and outer layers of Mo or W are advantageously embedded into BeO. This is applicable to both W and Re as emitter material. (auth)

39354 (BMWF-FBK-66-09) LITERATURBERICHT UEBER DIE HERSTELLUNG VON SCHICHTEN AUS MOLYBDAEN, WOLFRAM UND RHENIUM DURCH THERMISCHE ZERSETZUNG IHRER CARBONYLE ODER DURCH REDUKTION VON FLUECHTIGEN HALOGENIDEN. (Literature Search on the Deposition of Layers of Molybdenum, Tungsten, and Rhenium by Thermal Decomposition of their Carbonyls or Reduction of their Gaseous Halides). Kadner, M. (Battelle Institut e. V., Frankfurt am Main (West Germany)). Apr. 1966. 22p. Dep. mn.

Pure coatings of Mo, W, or Re can be deposited from the vapors of fluorides (W, Re) or chlorides (Mo, W, Re) by reduction with H_2. Details, conditions, and results are discussed. (auth)

39355 (EUR-2988.f) OBTENTION D'UN GRAPHITE IMPERMEABLE PAR IMPREGNATION DE METAUX FONDUS. (Obtaining an Impermeable Graphite by Impregnation with Molten Metals). Burg, H.; Lanza, F.; Marengo, G. (European Atomic Energy Community, Ispra (Italy). Joint Nuclear Research Center). Apr. 28, 1966. 30p. Dep. mn.

A procedure for impregnating graphite with liquid metals such as Bi, Pb, Sn, Mg, Al-Si, and Hg was studied. Liquid metals have to be forced into the pores by means of applied pressure. Optimum impregnating conditions of temperature and pressure were obtained. The impregnation value giving rise to an impervious material was determined. The comparison of the impregnation values with data obtained by means of an Hg porosimeter offers the possibility of determining the minimum pore radius filled by the fused metals. (auth)

39356 (GEAP-5134) SPECIFIC ZIRCONIUM ALLOY DESIGN PROGRAM. Quarterly Progress Report No. 12. Klepfer, H. H.; Blood, R. E. (General Electric Co., San Jose, Calif. Vallecitos Atomic Lab.). Apr. 1966. Contract AT(04-3)-189. 15p. (EURAEC-1654). Dep. mn. CFSTI $1.00 cy, $0.50 mn.

Work Performed under United States-Euratom Joint Research and Development Program.

A Zr + 2.0 at. % Cr + 0.16 at. % Fe alloy is being evaluated as nuclear fuel cladding. Alloy-clad fuel rods are to be irradiated to a target exposure of 15,000 Mwd/t. A process is proposed for producing high-performance uniform intermetallics under vendor conditions. A slab of the ingot to be

used for a second batch of tubing was fabricated by three alternate schedules including that proposed to ensure fine uniform intermetallics. Cooling rates, reductions in area, and process times were controlled to simulate vendor conditions. Metallographic, tensile, and corrosion test data on the resultant material prompted minor refinements in the reference process for tubing fabrication. The new reference process is being confirmed in the laboratory on quenched vendor forging material. Vendor fabrication of tubing was authorized. The laboratory confirmation tests are leading the tubing process; each tubing step is being reviewed before fabrication. (J.R.D.)

39357 (MAB–212A-M) SUMMARY REPORT OF THE REFRACTORY METALS SHEET ROLLING PANEL. (Materials Advisory Board, National Academy of Sciences–National Research Council, Washington, D. C.). June 1966. 19p. CFSTI $1.00 cy, $0.50 mn.

The method of operation, accomplishments, and recommendations of the Panel are outlined (summarizing the contents of MAB-212-M, "Final Report of the Refractory Metals Sheet Rolling Panel"). (auth)

39358 (ORNL–3983) DEVELOPMENT OF A FORMING METHOD FOR CURVED ATR FUEL PLATES. Erwin, J. H.; Peterson, Sigfred; Leitten, C. F. Jr. (Oak Ridge National Lab., Tenn.). Aug. 1966. Contract W-7405-eng-26. 38p. Dep. mn. CFSTI $2.00 cy, $0.50 mn.

The design and operating conditions of the Advanced Test Reactor fuel elements dictate rigid control and reproducibility of the fuel-plate forming practice. Unlike those in conventional test reactor fuel elements, the width and radius of curvature of each of the 19 fuel plates that make up an individual ATR assembly are all different. These radius and curvature requirements were successfully met by using a process consisting of underforming the plate, measuring the degree of springback the plate had encountered, and finally on the basis of this observed springback selecting the desired die for reforming the plate to the required radius. When the plates had been cold reduced 7.4%, the springback and forming reproducibility depended on subtle variations in fabrication history. Better reproducibility of forming followed a process that included 20% cold reduction. Use of more than two forming steps did not improve accuracy and reproducibility of forming. (J.R.D.)

39359 (RISO–113) DISPERSION-STRENGTHENED ALUMINIUM PRODUCTS. Hansen, Niels (Danish Atomic Energy Commission, Risoe, Research Establishment). May 1966. 26p. (CONF-660915–1). Dep. mn.

For Presentation at 2nd International Powder Metallurgy Conference, Stary Smokovec-Vysoke Tatry, Czechoslovakia.

Dispersion-strengthened Al products consist of Al and a dispersed phase, normally Al_2O_3, and only this combination of materials is considered here. These products can be manufactured from Al powder either covered with the natural layer of Al_2O_3, high-temperature oxidized, or blended with $Al-Al_2O_3$ powder. The structure of the products is to a great extent determined by the extrusion step, and the structural changes during this process, which are followed by transmission electron microscopy, are related to the changes in mechanical properties. The microstructure of the extruded $Al-Al_2O_3$ products consists of an oxide phase finely dispersed in Al, containing a substructure of small grains. The formation and characteristics of these grains are discussed. (J.R.D.)

39360 (TRG-Report–1255) METHOD FOR GAS-HYDRIDING ZIRCONIUM ALLOYS AT 400 DEG C. Winton, J. (Reactor Group, United Kingdom Atomic Energy Authority, Culcheth (England)). May 20, 1966. 9p. Dep. BIS $0.30. HMSO 1s. 9d.

As part of an investigation into the diffusion of H_2 through the walls of Zr alloy tubes, an experimental method was developed for gas hydriding. It involves the addition of a low partial pressure of CCl_4 to the furnace atmosphere to disrupt the impermeable oxide skin. (auth)

39361 (WAPD–305) THEORY AND MECHANISM OF ZIRCALOY PRESSURE BONDING. Weber, J.; Frankhouser, W. L. (Bettis Atomic Power Lab., Pittsburgh, Pa.). July 1966. Contract AT(11-1)-Gen-14. 52p. Dep. mn. CFSTI $3.00 cy, $0.50 mn.

The pressure bonding operation was used to bond Zircaloy cladding components in PWR Core 2 fuel plates containing ceramic wafers. During the development of this process there were many bonding experiments which were never described in the literature. Several of these experiments offer considerable insight into the metallurgical mechanism involved in bonding Zircaloy. They are discussed to prove that bonding is achieved primarily by nucleation and growth across the bondline. Optimum conditions required to obtain excellent metallurgical bonds include removal of surface material, a high degree of surface cleanliness, intimate surface contact, and thermal transformation in the solid-solid region. Surface roughness itself is not a necessary condition, but generally is considered to be an aid in bonding. Optimum operational cycling in the bonding facility requires a simultaneous application of temperature and pressure. (auth)

39362 (WAPD-TM–577) FABRICATION OF FUEL PELLETS FROM POT-PROCESS DENITRATED ThO_2 POWDER. Johnson, R. G. R. (Bettis Atomic Power Lab., Pittsburgh, Pa.). July 1966. Contract AT(11-1)-Gen-14. 48p. Dep. mn. CFSTI $3.00 cy, $0.50 mn.

Pellets produced directly from denitrated ThO_2 powder were unsuitable because of their inability to be sintered to densities greater than 90% theoretical density, which was attributed to the coarseness of the as-received ThO_2 powder. Majac milling and micronizing were used to reduce the particle size of the powder to less than one micron, which permitted the fabrication of pellets having sintered densities in excess of 95% theoretical density. The low and high density pellets produced from the comminuted powder, although acceptable, were sensitive to thermal shock. This made it necessary to reduce the heating rate to alleviate pellet cracking. A reduced heating rate was also used during the removal of the porosity-producing additive (sucrose) in low density pellet fabrication to prevent pellet shattering from internal pressure buildup. Dense, crack-free, high integrity pellets were ultimately produced which were, with the exception of open porosity, chemically and physically similar to ThO_2 pellets made from oxalate-derived powders. (auth)

39363 MASS SPECTROMETRIC ANALYSIS OF THE BEHAVIOR OF IMPURITIES AND ADMIXTURES DURING A HIGH-TEMPERATURE SINTERING OF TUNGSTEN. Meerson, G. A.; Kormilitsyn, D. V.; Abeleva, L. G.; Amosov, V. M.; Liskovich, V. A. (Moscow Inst. of Steel and Alloys). Izv. Akad. Nauk SSSR, Neorg. Mater., 2: 592-7(Apr. 1966). (In Russian).

The behavior of impurities and admixtures during high-temperature (1200°C) sintering of tungsten in hydrogen and vacuum was studied using a mass spectrometer with a spark ion source, which enabled the behavior of various impurities and admixtures of various temperatures of sintering to be determined. (R.V.J.)

39364 MICROSCOPICAL STUDY OF THE STRUCTURE OF SPHERICAL THORIA SOL-GEL BEADS. Willmarth, T. E. (Oak Ridge National Lab., Tenn.). Microscope, 14: 425-8(May-June 1965).

A study was made of the microstructure of one of the beads produced during the evaluation of various non-ionic surfactants used in the development of ThO_2 sol-gel beads for reactor fuel rods. Examination under polarized light of metallographically polished and H_2SO_4 etched cross sections of the beads gave evidence of a color difference between a band at the circumference and the central body of the individual spheres. Electron microscopy of the polished and etched cross sections by means of Faxfilm-carbon Pd–Pt shadow cast replicas confirmed the presence of a shell without observable structure, surrounding a homogenous core of tightly bounded particles of limited size range. It was concluded that certain non-ionic surfactants can cause the surface structure of ThO_2 beads to be very different from that of the type of beads taken as standards. (D.H.M.)

39365 HIGH REMELT TEMPERATURE BRAZING OF COLUMBIUM HONEYCOMB STRUCTURES. Freedman, A. H.; Mikus, E. B. (Northrop Norair, Hawthorne, Calif.). Weld. J. (N. Y.), 45: 258s-65s(June 1966).

High remelt temperature brazing techniques were applied in the fabrication of Nb alloy honeycomb structures for service to 3000°F. A Ti–^{33}Cr alloy employed for diffusion sink brazing required a brazing temperature of 2650–2700°F foliowed by a diffusion treatment of 16 hr at 2400°F. A Ti–30V–4Be reactive braze alloy required a brazing temperature of 2350-2400°F followed by a diffusion treatment of 4 hr at 2050°F plus 16 hr at 2400°F. These processing temperatures were 600-900°F below those required for conventional brazing approaches. Remelt temperatures above 3300°F and excellent strength in the 2500-300°F range were obtained. Comparison of as-brazed and diffusion treated Ti–33Cr specimens showed that diffusion treatment raised remelt temperatures from approximately 2900 to 3500°F, essentially doubled lap-shear strength at 2500°F, and provided excellent strength at 3000°F. The techniques offered attractive advantages for fabrication of honeycomb structures. These advantages included low processing temperatures, minimal erosion of honeycomb core by the braze alloys, high joint strength, and high joint service temperature capabilities. (auth)

39366 WELDABILITY EVALUATION OF ADVANCED REFRACTORY ALLOYS. Donnelly, R. G.; Slaughter, G. M. (Oak Ridge National Lab., Tenn.). Weld. J. (N. Y.), 45: 250s-7s(June 1966). (ORNL-P-2057).

The results of a program to evaluate the general weldability of the five advanced refractory-metal alloys, D-43, B-66, FS-85, C-129Y, and T-111 are discussed. Sheet material in gages ranging from 0.030 to 0.060 in. was of primary interest, but a limited investigation for comparative purposes was also conducted on ½ in. thick plate. Gas tungsten-arc welds were made in a controlled-atmosphere chamber which had been evacuated to 5×10^{-5} torr and backfilled with high-purity argon. Electron beam welds were made in vacuum of about 5×10^{-6} torr. The results reported include 4T bend-transition-temperature curves for each type of weld in each material, minimum bend radii at room temperature, and comparisons of the bend behavior of welded and unwelded materials. The lowest transition temperature of welds in the three Nb alloys was obtained in the C-129Y material. Specimens of this alloy were still ductile at –100°F. The Ta alloy, T-111, was still ductile at –320°F. The type of welding process was found to exert a significant influence on properties. The susceptibility of welds in each alloy to high-temperature aging reactions was investigated. Specimens were aged in vacuum at 1500, 1800 and 2200°F for times up to 100 hr. An embrittling aging reaction occurs in welds in all of the Nb base alloys investigated. No aging reaction was detected for the T-111 welds. Transverse tensile specimens from the ½ in. plate welds exhibited significantly lower ductility (5-13% elongation) than is reported for wrought material in the 1800 to 2400°F range. Failures in the Nb alloy welded specimens occurred in the base metal, whereas failures in the T-111 specimens were in the weld metal. (auth)

39367 FABRICATION AND CHARACTERIZATION OF METAL CARBIDE-GRAPHITE COMPOSITES. Harada, Y.; Rubin, G. A. (IIT Research Inst., Chicago, Ill.). 22p. (CONF-660505-9). ORAU. Gmelin, AED-CONF-66-103-13.

From American Ceramic Society Meeting, Washington, D. C.

Refractory metal carbide-graphite composites were prepared by hot pressing and the effects of composition and processing on phase equilibration and physical properties such as flexural strength, hardness, thermal shock resistance, thermal expansion, and electrical resistivity were studied. The systems investigated include TiC–C, ZrC–C, HfC–C, VC–C, NbC–C, TaC–C, MoC–C and WC–C. It was found that the strength of all the composite materials investigated increased with increasing carbide content reaching a peak for the metal-carbide-graphite eutectic composition. An essentially linear relationship between electrical resistivity and flexural strength was found to be useful to calculate the strength level of the material and to understand the strengthening mechanism with increasing carbide content. (auth)

39368 IMPROVEMENTS IN OR RELATING TO PROCESSES FOR THE PRODUCTION OF PELLETS FROM PARTICULATE MATERIAL. Horsley, Geoffrey Winton (to United Kingdom Atomic Energy Authority). British Patent 1,033,201. June 22, 1966. Filed Apr. 25, 1963.

A method for the production of sintered pellets from particulate material consisting largely of the carbides, such as nuclear fuel metal carbides, comprises the steps of grinding the particulate material, selecting a specific size or range of sizes of particulate material, adding to the selected particulate material a proportion of a liquid paraffin having a specific density of 0.83 – 0.87 at 20°C, forming the mixture into pellets, and heating the pellets to sinter them. (B.L.M.)

39369 IMPROVEMENTS IN OR RELATING TO THE PRODUCTION OF CARBON TUBES. Losty, Howard Harold Walter (to General Electric Co. Ltd.). British Patent 1,033,207. June 22, 1966. Filed Sept. 25, 1963.

A process is described for the production of a carbon tube of low permeability to gases by subjecting a liquid polymerizable monomeric cyclic carbon-containing compound, preferably furfuryl alcohol, to a polymerization process. When the resulting polymer is still capable of plastic deformation, the polymer is formed into a tube; a rigid mandrel is inserted within the tube; and the assembly of tube and mandrel are heated at a sufficiently high temperature and for a sufficient length of time to cause the polymer to decompose completely into C and volatile matter and to drive off the volatile matter. The mandrel is smaller than the tube, but it is of such size that the tube will engage with the mandrel when the shrinkage of the tube occurs as a result of the carbonization. The mandrel is formed of a material having a coefficient of thermal expansion which is higher than that of the tube at the temperature at which engagement between the tube and the mandrel takes place. After the final carbonization, the assembly is cooled, and the mandrel is withdrawn. (B.L.M.)

39370 IMPROVEMENTS IN OR RELATING TO COATING WITH BERYLLIA. Lloyd, James Elgie; Martin, Frederick Samuel (to United Kingdom Atomic Energy Authority). British Patent 1,034,654. June 29, 1966. Filed Apr. 19, 1962.

A fluidized bed process is described for coating a body with beryllia. The process is applicable to the coating of particles of UO_2, which are then dispersed in a matrix of beryllia and suitably shaped to form a fission product retaining fuel element for a nuclear reactor. The body to be coated is exposed to an atmosphere of vapor produced by heating $Be_4O(NO_3)_6$ to above the temperature at which it decomposes to beryllia (350–1400°C). Alternatively, the body to be coated may be heated to the required temperature and the vapor absorbed on the body where it decomposes to the ceramic coating. Successive coatings may be deposited in either of these manners. (B.L.M.)

39371 AUTO-CANNING OF RADIATION SOURCES. Lahr, Thomas N. (to Minnesota Mining and Manufacturing Co.). U. S. Patent 3,253,152. May 24, 1966. Filed Apr. 20, 1962.

A method for encapsulating a radioactive source consists of mixing radioactive ceramic particles with either powdered Al or Zn having a particle size not larger than 100 μ, placing the mixture in a preformed shell of either monel or stainless steel, capping the shell with a plug of the same material, pressing the plug so as to compress the mixture to at least 90% of its theoretical density, heating the plugged shell to melt the entire mass of metal powder, and cooling the plugged shell. (B.L.M.)

39372 Nb–Zr SUPERCONDUCTOR AND PROCESS OF MAKING THE SAME. Treuting, Robert G.; Wernick,

Jack H. (to Bell Telephone Labs., Inc.). U. S. Patent 3,253,191. May 24, 1966. Filed Oct. 11, 1961.

A method of making a superconducting element comprises heat treating an alloy of the Nb–Zr system consisting of from 10 at.% Nb–90 at.% Zr to 90 at.% Nb–10 at.% Zr to result in an increase in the amount of at least one solid phase and cooling the alloy after heat treatment to substantially retain the phase distribution developed during heating. The resulting alloy is formed into a coil. (B.L.M.)

39373 PREPARATION OF DENSE URANIUM OXIDE. Brearton, Denis Stanislas (to Atomic Energy of Canada Ltd.). U. S. Patent 3,258,317. June 28, 1966. Filed Apr. 25, 1963.

A method of producing a dense UO_2 body of near stoichiometry comprises compacting an UO_2 powder having a surface area per unit weight of from 1 to 18 m^2/g, heating the compacted body in a steam-containing atmosphere to sintering temperatures, sintering the compacted body in a steam atmosphere below about 1450°C, and subjecting the sintered body while above about 1000°C to a hydrocarbonaceous reducing gas containing H_2 in amounts from about 3 to 25 vol % until the O/U ratio is reduced below about 2.025. (B.L.M.)

39374 BERYLLIUM ALLOY AND PROCESS. Bonfield, William; Sartell, Jack A. (to Honeywell Inc.). U. S. Patent 3,264,147. Aug. 2, 1966. Filed Oct. 16, 1963.

An invention relating to alloys composed predominately of Be is described. It has to do with a Be alloy containing relatively small amounts of Ag and a precipitation hardening process for preparing it for use in precision instruments, such as gyroscopes and accelerometers. The materials used in such devices must perform under load in a predictable manner and must return to the original zero-point on removal of the stress. In other words, deformation must be both isotropic and elastic in nature. It is an object of this invention to provide Be alloys possessing high microscopic yield stress (MYS). Another object is to provide a process for preparing Be–Ag alloys possessing high MYS. A further object is to provide a precipitation hardened Be–Ag alloy. Another object is to provide a precipitation hardening process for Be in which Ag is the precipitation hardener. Alloys of Be containing 1 to 8% Ag exhibiting the advantages of the invention were prepared by powder metallurgy techniques. Owing to the fact that the Be must exhibit isotropic properties and an essentially void free structure, only powder techniques were found successful in the preparation of this material. (J.R.D.)

39375 ZIRCONIA BASED FOAM INSULATING MATERIAL AND METHOD. Wiegert, Robert E.; Byrne, Thomas J. (to Aeronca Mfg. Corp.). U. S. Patent 3,261,696. July 19, 1966. Filed Oct. 27, 1964.

An invention relating to foamed or cellular insulating materials principally constituted by a composite of ZrO_2, $Zr_3(PO_4)_4$, Al_2O_3, and $AlPO_4$ is described. A principal objective of this invention was to provide a foamed insulating material especially adapted for use as a heat shield at 2500 to 3300°F range, and which is characterized by relatively low density, low thermal conductivity, excellent thermal shock resistance, and high strength throughout the 2500 to 3300°F range in use. ZrO_2, Al_2O_3, and powdered Al metal are mixed in specified proportions. This mixture is reacted under controlled conditions with orthophosphoric acid (H_3PO_4), and water, and is cast in a mold or form in which it sets, producing a self-supporting cellular body which is then hardened or cured at temperatures in the approximate range of 150 to 800°F. The product of this invention is especially adapted for use as a load-bearing low density highly insulative material. As such, it may be used in the manufacture of nuclear reactor coolant lines to reinforce thin corrosion resistant metal alloy tubing therein, and in the production of space vehicle shields. (J.R.D.)

39376 IMPROVEMENTS IN OR RELATING TO THE PRODUCTION OF SPHEROIDS. Kennedy, Peter (to United Kingdom Atomic Energy Authority). British Patent 1,033,143. June 15, 1966. Filed July 3, 1962.

A method for producing spheroids of fissile or fertile material or a mixture of the two suitable for use as nuclear fuels comprises the steps of placing granules of the material in a container having a smooth or very finely abrasive surface; applying a gyratory vibration to the container so as to cause the granules to be moved over the surface of the container to form spheroids; and after formation of the spheroids, causing enlargement of the spheroids to the desired size by the addition of further quantities of the material. The material that is added to increase the size of the spheroids that have already formed must consist of particles smaller than the granules employed for the initial generation of the spheroids and must be added at a lower rate than the initial addition to ensure that the added material contributes to the enlargement of the spheroids rather than the formation of fresh ones. (B.L.M.)

39377 NUCLEAR REACTOR FUEL ELEMENTS. Halliwell, James (to United Kingdom Atomic Energy Authority). British Patent 1,033,246. June 22, 1966. Filed Mar. 19, 1964.

A process is described for effecting an argon-arc edge sealing weld between the edges of a fuel element sheath and an end cap. The adjoining edges of the sheath and end cap are prepared to offer a Y-shaped groove partly in the internal edge of the sheath and partly in the adjoining edge of the end cap. The Y-shaped groove comprises a V-shaped groove connecting at its bottom with an annular shaped groove. (B.L.M.)

Properties and Structure

See also CHEMISTRY — Inorganic and Physical Chemistry
PHYSICS — Solid State Physics

Refer also to abstracts 38856, 39006, 39367, 39446, 39456, 39590, 39638, 39698, 39708, 39723, and 39724.

39378 (AD–635596) PETCH ANALYSIS OF HYDROGENATED TANTALUM SHEET. Gazza, George E. (Army Materials Research Agency, Watertown, Mass. Materials Engineering Div.). May 1966. 12p. (AMRA-TR–66-10). CFSTI $1.00 cy, $0.50 mn.

The anomalous behavior in ductility exhibited by Ta at low temperature, with H as an impurity was investigated utilizing a Petch-type analysis. The change in lattice friction stress and dislocation locking stress parameters were determined at room temperature to –196°C. The results of the investigation show the locking stress remained essentially unchanged by small H additions while the lattice friction stress increased significantly at temperatures below –78°C. (auth)

39379 (AECL–2453) TERMINAL SOLID SOLUBILITY OF HYDROGEN IN ZIRCALOY-2. Daniel, A. R. (Atomic Energy of Canada Ltd., Chalk River (Ontario)). June 6, 1965. 10p. (DF–65-CAP-31). Dep. mn. AECL $0.50.

A terminal solubility curve was developed so that the H_2 concentration of test pieces could be controlled by homogenization after electrolytic hydriding. The experimental procedure and the results obtained are given. (auth)

39380 (AECL-2570) ELECTRON PROBE MICROANALYSIS OF ALUMINUM-CLAD ZIRCALOY-2 SPECIMENS AFTER HEAT TREATMENTS AT 400 DEG C AND 500 DEG C. Williams, C. D.; Baird, J. (Atomic Energy of Canada Ltd., Chalk River (Ontario)). May 1966. 26p. Dep. mn. AECL $0.50.

A study of kinetics of oxide dissolution and interphase formation in Al-ZrO_2-Zircaloy-2 systems is discussed in which electron probe microanalysis and optical metallography was carried out The specimens used were sections of Zircaloy-2 tube, oxidized and clad internally with Al by a hot die sizing technique. The specimens had been subjected to a range of aging and cycling treatment at 400 and 500°C. Examination of these specimens showed that no significant reaction occurred at 400, but oxide dissolution and

intermetallic formation occurred during treatments at 500°C. The rate of extension of the interdiffusion layer was similar to that predicted from other experiments. Specimens subjected to thermal cycling treatments to 400 and 500°C showed no evidence of interdiffusion effects. (auth)

39381 (AECL-2585) ON THE EFFECT OF TiO_2 ADDITIONS ON DEFECT STRUCTURE, SINTERING, AND GAS RELEASE OF UO_2. Matzke, Hj. (Atomic Energy of Canada Ltd., Chalk River (Ontario)). May 1966. 34p. Dep. mn. AECL $1.00.

Small additions of TiO_2 are known to increase the density of sintered UO_2. It is shown that this effect coincides with an increase in the diffusion rate of the slower moving U ion. Quantitative metallography and measurement of the gas release following high-dose ion-bombardment show that small amounts of Ti are soluble in UO_2. Possible mechanisms by which TiO_2 affects the disorder of UO_2 are discussed. Reduction of TiO_2 and interstitial solution of the small Ti ions are favored. Similar experiments are reported for ThO_2 + TiO_2. A model for the disorder in UO_2 is given and the gas release data are discussed. (auth)

39382 (AEEW-R-473) AN ANALYSIS OF URANIUM METAL-GRAPHITE SYSTEMS USING THE MULTI-GROUP CODE "WIMS". Barclay, F. R. (Atomic Energy Establishment, Winfrith (England)). June 2, 1966. 26p. Dep. BIS $0.80. HMSO 4s. 0d.

A wide range of U metal-graphite lattice experiments were studied using the WIMS code which has, in its turn, been compared with more exact calculational models in the fast and resonance energy regions. No significant errors in the calculational model were observed. Comparison with experiment shows a systematic error with pitch which is ascribed to an error of some 15% in the best available ^{238}U resonance data. Within this, different sizes and enrichments of fuel rods, and different air channel sizes (streaming) are well predicted. (auth)

39383 (BMWF-FBK-66-08) HOCHTEMPERATURTESTS AN MIT WOLFRAM UMHUELLTEN UO_2-Mo-CERMETS FUER THERMIONISCHE REAKTORBRENNELEMENTE. (High-Temperature Tests on Tungsten-Coated UO_2-Mo-Cermets for Thermionic Nuclear Fuel Elements). Schuster, K. (Battelle Institute e. V., Frankfurt am Main (West Germany)). Apr. 1966. 34p. Dep. mn.

Cermets composed of UO_2 and Mo and coated with W were evaluated for their properties at high temperatures. Heating for long periods at temperatures up to 1800°C caused some of the cermets to swell. Mo and W diffused in a short time after the start of the test. The structure of the W coating changed, and quantities of UO_2 gradually escaped. (J.R.D.)

39384 (BNWL-263) STRUCTURAL ANALYSIS OF A HEXAGONAL TUBE OR RING UNDER INTERNAL PRESSURE. Flowers, C. D. (Battelle-Northwest, Richland, Wash. Pacific Northwest Lab.). June 1966. Contract AT (45-1)-1830. 51p. Dep. mn. CFSTI $3.00 cy, $0.50 mn.

The maximum stress in hexagonal reactor tubes occurs at the inside surface of the corner where the fibers are in tension consisting primarily of the bending stresses caused by the rigidity of the corner. This corner rigidity induces bending of the walls, thus giving maximum deflection at the middle of the flat side. An elastic stress and deflection analysis was made for a hexagonal tube or a hexagonal ring submitted to a constant internal pressure load. The analysis assumes a homogeneous and isotropic medium, and uses linear small deflection theory. A hyperbolic stress distribution was assumed for analyzing the corners of the tube or ring. All results are presented in equation form. Also, for the hexagonal tube, there are plots of maximum corner primary membrane plus bending stress, and maximum wall deflection across the flats. These graphs are dimensionless, and are applicable to a useful range of hexagonal tube sizes. (auth)

39385 (CEA-R-2852) INFLUENCE DE L'OXYGENE, DE L'AZOTE ET DU CARBONE SUR LE PARAMETRE RETICULAIRE DU MONOCARBURE D'URANIUM. (Influence of Oxygen, Nitrogen, and Carbon on the Lattice Parameter of Uranium Monocarbide). Magnier, Pierre (Commissariat a l'Energie Atomique, Saclay (France). Centre d'Etudes Nucleaires). Apr. 1966. 58p. Dep. mn.

Thesis. Submitted to Paris Univ. (France). Faculte des Sciences.

Results of studies on the effects of O and N on the lattice parameter of U(C,O,N) solid solutions around UC composition are discussed. The data lead to a determination of the solubility of O in UC: $U(C_{1-x}O_x)$ solid solutions exist if x is smaller than 0.37. The effects of C on the lattice parameter of U-UC solid solutions around UC was also investigated. Results of the study are used as a basis for determining the solubility of U in UC at the different temperatures and their effects on the U-C diagram are analyzed. (auth)

39386 (CEA-R-2905) ETUDE AU MOYEN DE LA RESISTIVITE ELECTRIQUE DES DEFAUTS PONCTUELS DANS LE FER PUR. (Study of Point Defects in Pure Iron by Means of Electric Resistivity). Minier-Cassayre, Colette (Commissariat a l'Energie Atomique, Grenoble (France). Centre d'Etudes Nucleaires). [1965]. 74p. Dep. mn.

Thesis. Submitted to Grenoble Univ., France.

The production, observation, and the annealing of point defects in metals are reviewed and the present state of research is discussed. The techniques employed to produce point defects at low temperatures such as irradiation, quenching, and cold-work, are also discussed, and results of studies of their migration and annealing are reported. The experimental results obtained for pure Fe and for Fe containing impurities are presented. A model is suggested which explains the different stages of annealing observed, and their properties. The energies of interaction between point defects are compared with the values deduced from the theory of elasticity. (auth)

39387 (CEA-R-2947) CONTRIBUTION A L'ETUDE, PAR ADSORPTION GAZEUSE, DE LA TEXTURE DES SOLIDES DIVISES. APPLICATION A L'ALUMINE, A LA GLUCINE ET A DIFFERENTS GELS ET OXYDES. (Texture Study of Divided Solids by Gas Adsorption. Application to Beryllia, Alumina and to Gels and Oxides). Rouquerol, Francoise (Commissariat a l'Energie Atomique, Saclay (France). Centre d'Etudes Nucleaires). 1966. 91p. Dep. mn.

Thesis. Submitted to Univ., Paris.

Surface areas of porous materials were measured in an adsorption apparatus with an accuracy of 1/1000. It appears convenient to substitute Ar for N_2. Calculation methods of the pore size distribution are analyzed and discussed. The experimental data shows that the thickness of the multimolecular layer must be estimated from the number of layers given by Shull using a layer thickness of 3.6 Å. A new method of analysis of the desorption curve is also given. It is also shown that a certain number of lamellar, nonporous, systems, such as $Be(OH)_2$ present a hysteresis branch on the adsorption isotherm of type I or II. It is concluded that this hysteresis can be ascribed to the lack of rigidity of the solid. Samples of microporous texture (r < 20 Å) of the BeO-type are an example of porous materials which do not exhibit a hysteresis phenomenon. The evolution of the texture during their progressive dehydration (thermal treatment from 150 to 1100°C) of samples of BeO and Al_2O_3, is described. (auth)

39388 (CEA-R-2956) TRANSFORMATION ISOTHERME $\beta \rightarrow \alpha$ DANS L'URANIUM PUR ET FAIBLEMENT ALLIE. ($\beta \rightarrow \alpha$ Isothermal Transformation in Pure and Weakly Alloyed Uranium). Aubert, Henri; Lelong, Claude (Commissariat a l'Energie Atomique, Saclay (France). Centre d'Etudes Nucleaires). Mar. 1966. 53p. Dep. mn.

The TTT diagrams describing the $\beta \rightarrow \alpha$ isothermal transformation were made by isothermal dilatometry for pure U and 21 alloys containing Cr, Si, Mo, Fe, Al, and Zr. The thermal cycle preceding the isothermal step

influences the decomposition kinetics at temperature corresponding to the eutectoid and martensitic mechanisms, but not in the range where the bainitic transformation occurs. The stability of the β phase decreases with the Cr, Mo, and Si concentration; it is affected differently for each of the three transformation mechanisms. The ternary additions, even at very low concentration have a considerable effect on the stability. When the concentration decreases the martensitic mechanism is active at progressively higher temperature, diminishing to the point of disappearance the temperature range where the transformation is considered as being of the bainitic mode. (auth)

39389 (CEA-R-2973) RELATIONS D'ORIENTATION ENTRE PHASES DANS LES TRANSFORMATIONS $\gamma \rightarrow \alpha$ DES ALLIAGES URANIUM-MOLYBDENE. (Orientational Relationships Between Phases in the $\gamma \rightarrow \alpha$ Transformations for Uranium–Molybdenum Alloys). Brun, Gilbert (Commissariat a l'Energie Atomique, Saclay (France). Centre d'Etudes Nucleaires). Apr. 1966. 77p. Dep. mn.

Thesis. Submitted to Univ., Paris.

A crystallographic study was made of the γ to $\alpha + \gamma$ transformation in an alloy containing 3% by wt Mo using electronic micro-diffraction. The orientational relationships governing the germination of the α phase in the γ phase were found to be: $(111)\gamma \parallel (100)\alpha$, $(11\bar{2})\gamma \parallel (010)\alpha$, and $(1\bar{1}0)\gamma \parallel (001)\alpha$. By choosing a monoclinic lattice containing the same number of atoms as the orthorhombic lattice for defining the γ mother phase, the change in structure was explained by adding a homogeneous $(11\bar{2})\gamma\ [111]\gamma$ shearing deformation to a heterogeneous deformation brought about by slipping of the atoms which are not situated at the nodes of this lattice. The identity of the orientation relationships γ/α and γ/α^{11}b and the loss of coherence γ/α as a function of temperature or of time lead to the conclusion that, in the range studied, the γ-to-α transformation begins with a martensitic process and continues by germination and growth. (auth)

39390 (CEA-R-3003) ETUDE DU RISQUE D'OXYDATION LORS DU FRITTAGE DU BIOXYDE D'URANIUM ET CARACTERISATION DE L'OXYGENE EXCEDENTAIRE. (Study of the Oxidation Risks During the Sintering of Uranium Dioxide, and Characterization of the Excess Oxygen). Conte, Madeleine; Brandela, Maxime (Commissariat a l'Energie Atomique, Grenoble (France). Centre d'Etudes Nucleaires). May 1966. 38p. Dep. mn.

During sintering in reducing atmospheres, UO_2 pellets can be oxidized by gaseous impurities. The effects of temperature cycles, the partial pressure of O_2 and the flow rate of the gas over the pellets were investigated. In these atmospheres, the O_2 partial pressure during sintering is low at high temperatures, as a consequence of the dissociation rate of the combined water, but below 1000°C, it can be high enough to result in a noticeable oxidation of the surface of the pellets during cooling. The crystalline phases which can occur have been identified and two methods of detection have been proposed; a micrographic examination after chemical etching and radiocrystallography. (auth)

39391 (CONF-660629-1) CREEP OF AXISYMMETRIC SHELLS. Diamant, E. S.; Greenbaum, G. A.; Rubin, C. P. (TRW Systems, Redondo Beach, Calif.). [1965]. Contract AT(04-3)-517. 23p. Dep. mn. CFSTI $1.00 cy, $0.50 mn.

From 5th National Congress of Applied Mechanics Meeting, Minneapolis.

Results of an analytical procedure developed to investigate the effects of creep in axisymmetric pressurized shells with head closures are presented. The analysis makes possible the evaluation of the effects of changes in the closure geometry on the creep of the shell. The effects of variable wall thickness, pressure history, and variations in assumed creep laws are also considered. The spectrum of shell creep problems which can be investigated is illustrated by presenting the results of computer calculations for thin-shell pressure vessels with various geometry and load specifications. (auth)

39392 (CU-2660-29) THE VISCOSITY OF THE ALKALI METAL VAPORS. I. CESIUM UP TO 5 BARS AND 1000 DEG C. Lee, D. I.; Bonilla, C. F. (Columbia Univ., New York. Dept. of Chemical Engineering). July 15, 1966. Contract AT(30-1)-2660. 35p. (CONF-660712-2). Dep. mn. CFSTI $2.00 cy, $0.50 mn.

From International Conference on the Alkali Metals, Nottingham, England.

The viscosity of superheated Cs vapor was measured up to 1000°C at 0.4 to 5 bars by a steady flow high-temperature coiled capillary viscometer. The interaction potentials between the species present in the Cs vapor were calculated as mixtures of monomer and dimer. From these potentials the transport properties were further extended as a function of temperature, pressure, and composition. (auth)

39393 (GEAP-4878) THE SOLID-LIQUID PHASE DIAGRAM FOR THE UO_2–PuO_2 SYSTEM. Lyon, W. L.; Baily, W. E. (General Electric Co., Pleasanton, Calif. Vallecitos Atomic Lab.). Dec. 1965. Contract AT(04-3)-189. 17p. Dep. mn. CFSTI $1.00 cy. $0.50 mn.

The liquidus and solidus were experimentally determined for the UO_2-PuO_2 system by a thermal arrest method. The phase diagram is typical of a binary pair with complete solid solution and without maximum or minimum. A melting point of 2840 ± 20°C was observed for UO_2, and a melting point of 2390 ± 20°C was observed for PuO_2. Calculated theoretical liquidus and solidus curves exhibit good agreement with the experimental values found. (auth)

39394 (GEMP-415) DEFCOT: PLANE-STRAIN PLASTIC-VISCOELASTIC DEFORMATION OF A COMPOSITE TUBE. Yalch, J. P. (General Electric Co., Cincinnati, Ohio. Nuclear Materials and Propulsion Operation). June 1966. Contract AT(40-1)-2847. 54p. Dep. mn. CFSTI $3.00 cy, $0.50 mn.

Supersedes GEMP-288.

A method and an associated computer program are described for calculating during successive time intervals the plastic stress/strain distributions in long hollow circular composite cylinders having a variable axisymmetric temperature distribution, subjected to axial load and internal and external pressures. The analysis and computer program reported in GEMP-288 was modified and corrected so that: the cylinder may be composed of more than two concentric cylinders, and the innermost cylinder may be solid; external pressures may be added to the input; the axial load function input is more convenient; equations were modified; the program was converted to the Fortran IV language for the GE 625/635 machines; and inputs were simplified and outputs were expanded. (J.R.D.)

39395 (IAE-1028) K TEORII ELEKTROPROVODNOSTI METALLOV S NEMAGNITNYMI PRIMESYAMI. (A Theory of Electrical Conductance of Metals with Nonmagnetic Impurities). Kagan, Yu.; Zhernov, A. P. (Institut Atomnoi Energii, Gosudarstvennyi Komitet po Ispol'zovaniyu Atomnoi Energii SSSR, Moscow). 1965. 32p. Dep. mn.

A theory of electrical conductivity of metals with impurities was developed which takes into account the deformation of the phonon spectrum caused by incorporation of the impurities and changes in the scattering of electrons on individual atoms. The admixture contribution to the resistivity is given for the entire temperature range. At low temperatures and low impurities concentrations, the electron scattering is governed by a T^2 relation, the interference of scattering on impurities and on the perturbed phonon spectrum changes the relation to T^4, while scattering on the deformed phonon spectrum changes it to $\sim T^5$. At increasing temperatures there appear anomalies which in the case of heavy admixtures lead to quasi-local levels. At high temperatures the impurity contribution changes linearly with temperature with a slope of arbitrary sign. The results obtained are used to explain the majority of known experimental results in the high and intermediate temperature range. Accurate measurements of impurity resistance at low temperatures are needed for verification of the conclusions. (JPRS)

39396 (IS-T-60) THE COMBINED EFFECT OF MEAN STRESS AND STRESS CONCENTRATIONS ON THE FATIGUE PROPERTIES OF 2011-T3 ALUMINUM ALLOY. Pettit, Donald Ethan (Ames Lab., Iowa State Univ. of Science and Tech.). Nov. 1965. Contract W-7405-eng-82. 106p. Dep. mn. CFSTI $4.00 cy, $0.75 mn.

Thesis.

The predictions of equations widely used to describe fatigue failure were compared with the results of axial fatigue tests on 2011-T3 Al alloy rod tested in the notched and unnotched condition. Best prediction of the shape of the curve relating allowable alternating stress to mean stress was found by using equations proposed by Gunn: (1) Where maximum stress at a notch is less than the yield stress: $(K_t\sigma_a/\sigma_e) + (K_tS_m/S_u)^n = 1$. (2) Where maximum stress at a notch is greater than the yield stress: $(K_t\sigma_a/\sigma_e) + (S_y - K_t\sigma_a/S_u)^n = 1$. K_t = stress concentration factor at notch, σ_a = applied alternating stress, σ_e = endurance limit, S_y = yield stress, S_u = ultimate stress, S_m = ultimate stress, and n = experimentally determined exponent. The best quantitative agreement of the above equations and experiment was found when K_t was replaced by K_f, the fatigue notch factor. K_f is not a constant as often supposed, but is a function of fatigue life. The functional relation between K_f and N, the number of stress cycles, was determined experimentally. (J.R.D.)

39397 (NASA-TM-X-1252) EFFECT OF ORIENTATION ON DUCTILE-TO-BRITTLE TRANSITION OF TUNGSTEN SINGLE CRYSTALS. Garlick, Ralph G. (National Aeronautics and Space Administration, Cleveland, Ohio. Lewis Research Center). July 1966. 7p. CFSTI $1.00 cy, $0.50 mn.

An investigation was conducted of the ductile-brittle transition behavior of zone-refined W single crystals as a function of orientation. Tensile-axis orientations ⟨100⟩, ⟨110⟩, and ⟨111⟩ were studied. The transition behavior was determined to be orientation dependent. Crystals of the ⟨110⟩ orientation exhibited a sharp ductile-brittle transition based on reduction-in-area measurements and showed the lowest transition temperature, 205°K. Crystals of the ⟨100⟩ tensile axis exhibited a much more gradual transition with temperature from ductile to brittle behavior, with a transition temperature of about 380°K, based on a 50% reduction in area. The transition temperature of the ⟨111⟩ crystals was intermediate between those of the other orientations. Specimens of all orientations exhibited measurable plastic deformation at temperatures far below their respective ductile-brittle transition temperatures. Orientation also significantly affected the tensile flow characteristics of the crystals. The ⟨110⟩ oriented specimens exhibited a high yield strength and a yield-point drop, and necking almost immediately followed yielding. In contrast, ⟨100⟩ and ⟨111⟩ crystals exhibited no yield-point drop and, for crystals tested above the transition temperature, showed considerable uniform elongation before necking. These orientations also exhibited conventional work-hardening behavior. (auth)

39398 (NASA-TN-D-3527) METALLOGRAPHIC STUDY OF DISPERSION-STRENGTHENED ALLOYS AFTER FAILURE IN STRESS RUPTURE. Hoffman, Charles A.; Weeton, John W. (National Aeronautics and Space Administration, Cleveland, Ohio. Lewis Research Center). Aug. 1966. 35p. CFSTI $2.00 cy, $0.50 mn.

A metallographic study was conducted on stress-rupture failed specimens of dispersion-strengthened materials to determine the microstructural factors affecting their stress-rupture strengths. It was concluded that; in general, the dispersion strengthened materials that exhibited best overall retention of stress-rupture strength had the most stable microstructures, those products which contained appreciable amounts of excess particles had good strength and stability at lower temperatures, but at higher temperatures their strengths decreased at a more rapid relative rate, and their microstructures exhibited increased porosity, there was no unique fracture mode that could be associated with those materials that retained a relatively greater portion of their stress-rupture strength at high temperatures, the best overall retention of stress-rupture strength with increased use temperature was associated with materials having uniformly distributed dispersoid particles with fine characterizing dimensions (<0.050 μ), and large particles, such as the $FeAl_3$ inclusions in an Al + 5 vol % Al_2O_3 alloy, may be deleterious. (auth)

39399 (NASA-TN-D-3528) COLD REDUCTION AS A MEANS OF REDUCING EMBRITTLEMENT OF A COBALT-BASE ALLOY (L-605). Sandrock, Gary D.; Leonard, L. (National Aeronautics and Space Administration, Cleveland, Ohio. Lewis Research Center). Aug. 1966. 27p. CFSTI $2.00 cy, $0.50 mn.

The effect of prior cold reduction (up to 40%) by rolling on the room-temperature tensile ductility of L-605 (HS-25) after aging at 1600°F for times up to 1000 hr was determined. Prior cold work was found to lessen the embrittling effect of 1600°F exposure and cause increased room-temperature tensile strength and hardness, which were largely maintained even after long (1000 hr) aging times. The nature of the precipitation was changed from that of a preferential intergranular type, as observed in unworked L-605 after aging, to a much more homogeneous type within the grains. This effect was believed to be the primary reason for improved post-aging ductility. X-ray-diffraction studies confirmed the previously reported precipitation of Co_2W and an M_6C type carbide, but showed that prior cold work tended to alter the carbide reaction. (auth)

39400 (NASA-TN-D-3531) EFFECT OF ALLOYING ON GRAIN REFINEMENT OF ELECTRON-BEAM-MELTED TUNGSTEN. Witzke, Walter R. (National Aeronautics and Space Administration, Cleveland, Ohio. Lewis Research Center). July 1966. 18p. CFSTI $1.00 cy, $0.50 mn.

Ingot structures resulting from electron-beam melting of W consist mainly of columnar grains extending the length of the ingot. In order to examine the grain refining capabilities of various elemental and refractory compound additions, small ingots of W containing these additions were prepared by electron-beam melting. Measurements on transverse ingot sections from each melt indicated that all the additions decreased the average grain dia of the columnar grains typical of electron-beam melted W and that grain refining effectiveness varied with the concentration of the solutes. Losses of the additions during melting were in excess of 90% in many cases. The most potent grain refiner was B. A nominal addition of 0.5 wt. % decreased the average grain dia of the columnar grains from 0.48 to 0.008 cm. The effectiveness of the elemental additions decreased in the following order: B, Y, C, Hf, Zr, Mo, Nb, Re, and Ta. The losses of these elements during melting also decreased in approximately the same order. The elemental additions were generally more effective grain refiners than the refractory compounds. The elements with the smallest distribution coefficients were the most effective grain refiners. (auth)

39401 (ORNL-3963) EXAMINATION OF HYDROUS-URANIUM DIOXIDE PRECIPITATES AND SOLS BY ELECTRON MICROSCOPY, ELECTRON DIFFRACTION, AND SPECTROPHOTOMETRY. Hardy, C. J. (Oak Ridge National Lab., Tenn.). Aug. 1966. Contract W-7405-eng-26. 22p. Dep. mn. CFSTI $2.00 cy, $0.50 mn.

Electron micrographs and selected-area electron diffraction patterns were obtained for hydrous UO_2 precipitated from uranous nitrate and uranous nitrate-formate solutions and aged for periods of a few minutes to a few days at 25°C, and heated for several hours at 60°to form sols. Thus the particles of UO_2 can be characterized as they are converted from a precipitate into a sol, which in turn is converted into UO_2 microspheres for use in fuel elements. Studies showed that the initial precipitates (hydrous UO_2) consisted of irregularly shaped aggregates of particles about 15 to 25 Å in diameter. The initially diffuse lines in the electron diffraction patterns became sharper with increased aging at 25°C. Sols prepared by heating the filtered and washed precipitates at 60°C consisted of cubic crystals with sides 10 to 20 Å long. The presence

of 0.4 mole of formate per mole of U in the sols gave more uniform dispersion on the electron microscope grids, but did not appreciably affect the size or the lattice spacing of the primary crystallites. The turbidities or apparent absorption spectra of the diluted sols were measured from 8000 to 3000 Å. The optical density varied inversely with the 1.2 to 1.4th power of the wavelength from 8000 to 4000 Å and with the fourth power of the wavelength at less than 4000 Å. The maximum diameter of the scattering particles, calculated from the turbidity at 4000 Å, was about 800 Å, which agrees with the size of aggregates observed on the electron micrographs. A model is proposed for the physical and chemical constitution of the formate-containing sol particles in which formate ions bridge pairs of U atoms on the surface of primary cubic crystallites of 10.9 Å edge length; these crystallites are then considered to form aggregates up to 800 Å in diameter. (auth)

39402 (ORNL–3979) METHODS OF REDUCTION OF TEXTURE DATA TO INVERSE POLE FIGURES. Williams, R. O. (Oak Ridge National Lab., Tenn.). Aug. 1966. Contract W-7405-eng-26. 26p. Dep. mn. CFSTI $2.00 cy, $0.50 mn.

Several methods have been devised to facilitate the inversion of texture data to inverse pole figures, which give the distribution of a physical direction over the crystallographic triangle. Graphical integration is replaced by summing the distribution over a set of points. The coordinates of these sets are given for seven planes in the cubic system. A graphical method is presented which gives an improved starting distribution and will give an adequate inversion for simple textures. (auth)

39403 (ORNL-TM–1450) APPROPRIATE VALUES FOR THE THERMAL CONDUCTIVITY OF UO_2 FOR USE IN THE DESIGN OF THE BONUS SUPERHEATERS. Sanders, J. P. (Oak Ridge National Lab., Tenn.). Apr. 22, 1966. Contract W-7405-eng-26. 8p. Dep. mn. CFSTI $1.00 cy, $0.50 mn.

A survey of the current literature was made to determine the most appropriate values for the thermal conductivity of UO_2 to use in the reevaluation of the design of the BONUS superheater elements. Two types of thermal conductivities are encountered in the literature; these are effective thermal conductivities, which include the resistance of a gas gap between the fuel and cladding, and absolute thermal conductivities, which are based on measurements made in continuous blocks of UO_2. Effective and absolute values were found to differ both in magnitude and temperature difference. The values were also found to be dependent upon irradiation and thermal-cycling history. The best values for the absolute thermal conductivity as a function of temperature are reported. It is also recommended that, in the range of temperature encountered in the BONUS superheater assemblies, an appropriate average effective thermal conductivity in the range of 1.0 to 1.2 Btu/hr · ft · °F be used. (auth)

39404 (SWRI–1228-4-20) LOW-CYCLE FATIGUE STRENGTHS OF DISSIMILAR WELDMENTS. Topical Report No. 3. McDonald, J.; Watson, P. D. (Southwest Research Inst., San Antonio, Tex.). May 23, 1966. Contract AT(11-1)-1228. 65p. Dep. mn. CFSTI $3.00 cy, $0.75 mn.

Investigations were made to determine the low cycle fatigue strength of weldments that simulate the A105 Grade II–to–Type 304 stainless steel dissimilar welds now in service on the Elk River Reactor. The weldments simulated were 8 and 10-in nozzle-to-external piping welds, 16-in nozzle-to-cap welds (as welded), and 16-in nozzle-to-cap welds (stress relieved). Low cycle fatigue curves were developed for all three types at both ambient and elevated temperatures (600°F). In addition, the effects of superimposed fatigue-thermal cycling (simulating reactor startup and shutdown) were determined. The fatigue curves developed in this phase of the program will be used as standards for the post-irradiation tests to be performed on the dissimilar weld surveillance specimens. (auth)

39405 (UCRL–16844) STRENGTH IN A TWO-PHASE MODEL SYSTEM WITH FIBER REINFORCEMENT. Einmahl, Gerd (Lawrence Radiation Lab., Univ. of California, Berkeley). May 2, 1966. Contract W-7405-eng-48. 40p. Dep. mn. CFSTI $2.00 cy, $0.50 mn.

Thesis.

Model systems consisting of a glass matrix reinforced by randomly oriented W or Ni fibers with an aspect ratio of 50 were fabricated by vacuum hot-pressing and tested by bending. The systems were distinguished by interfacial bonding and different thermal expansion coefficients of the matrix and the dispersed phase. In systems that could be densely fabricated the strength was found to increase linearly with increasing volume fraction of fibers. Reversing the sign of the thermal expansion coefficient of the matrix relative to that of the inclusions had little effect on the strength. A greater strengthening effect was achieved in the W-glass systems where an interfacial bond existed as opposed to the Ni-glass series. The strengthening effect of the Ni fibers is explained by gripping of the fiber ends by the glass due to irregularities in shape from the cutting operation used to obtain short fibers. (auth)

39406 (WAPD-T–1864) FATIGUE PROPERTIES OF IRRADIATED PRESSURE VESSEL STEELS. Gibbons, W. G.; Mikoleit, A. E.; O'Donnell, W. J. (Bettis Atomic Power Lab., Pittsburgh, Pa.). June 1966. Contract NObs-90029. 46p. (CONF-660627–2). Dep. mn. CFSTI $1.00 cy, $0.50 mn.

From American Society for Testing and Materials, 69th Annual Meeting, Atlantic City.

The effects of neutron irradiation on the unnotched strain-cycled fatigue properties of pressure vessel steels were evaluated. Two heats of A302 low alloy steel and one heat of A212B C–Si steel were investigated. Results from room temperature tests on non-irradiated material were compared with those from material irradiated up to 6×10^{19} nvt > 1 Mev (1.6×10^{23} Dt). The fatigue notch sensitivities of these materials were also investigated using V-notch specimens with two and ten mil root radii respectively. Results were compared with theoretical predictions based on the δ theory of fatigue notch sensitivity. (auth)

39407 (ANL-Trans–344) NEUTRON DIFFRACTION STUDY OF ORDERED Ni–Mn ALLOYS. Sidorov, S. K.; Doroshenko, A. V. Translated by Elmar K. Wilip (Argonne National Lab., Ill.), from Fiz. Metal. Metalloved., 20: 850-9(1965). 16p. Dep. mn. CFSTI $1.00 cy, $0.50 mn. JCL $1.60 fs, $0.80 mf.

It was shown that the observed concentration dependence of the mean magnetic moment per atom of ordered Ni–Mn alloys can be explained starting from the concept of a paired mutual interaction of the atoms of the components. This permitted a formulation of conclusions concerning the dependence of the degree of the long-range order and of the correlation in Ni–Mn alloys for a prolonged period of time on the Mn content. A gradual transition from the ferromagnetic to the antiferromagnetic state appears to take place with the increase of the Mn-content in the alloy from 25 to 50 at. % via a system of noncollinear magnetic structures. (J.R.D.)

39408 (NSJ-tr–46) STATISTICAL ANALYSIS OF MECHANICAL STRENGTH OF GRAPHITE. Sato, Sennosuke Translated for Japan Atomic Energy Research Inst., Tokyo, from Tanso, No. 38, 20-9(1964). 18p. Dep. mn. JCL $1.60 fs, $0.80 mf. JAERI.

The mechanical strength of graphite is explained by applying the fracture probability theory, based on the Griffith-Weibulls brittle fracture theory for brittle materials. The theoretical bases is given statistically for the applicability of data on the bending strength to specified cross-sectional shapes, dimensions and loading modes, and to other shapes, dimensions, and loading modes. These results are compared with the experimental results. (J.R.D.)

39409 THE CRYSTAL STRUCTURE OF $CeFe_7$, $PrFe_7$, $NdFe_7$, AND $SmFe_7$. Ray, A. E. (Univ. of Dayton, Ohio).

Contract AF 33(657)-8553. Acta Crystallogr., 21: 426-30(Sept. 10, 1966).

The isostructural phases $CeFe_7$, $PrFe_7$, $NdFe_7$, and $SmFe_7$ are rhombohedral; the probable space group is R3m. The lattice constants for the triply primitive hexagonal unit cells are:

	a	c	c/a
$CeFe_7$	8.488 ± 0.003 Å	12.402 ± 0.007 Å	1.461
$PrFe_7$	8.582 ± 0.003	12.462 ± 0.007	1.452
$NdFe_7$	8.578 ± 0.003	12.462 ± 0.007	1.453
$SmFe_{17}$	8.554 ± 0.003	12.441 ± 0.007	1.454

The hexagonal unit cells contain seven rare earth and forty-nine Fe atoms. The atomic arrangements are intermediate between those of the $D2_d$-$CaCu_5$ and Th_2Zn_{17} structural types. A statistical occupancy of one set of positions was proposed to account for the observed rhombohedral symmetry. (auth)

39410 MULTIPROCESS CREEP IN URANIUM DEDUCED FROM LITERATURE DATA. Holmes, J. J. (Atomics International, Canoga Park, Calif.). Contract AT(11-1)-GEN-8. Amer. Soc. Metals, Trans. Quart., 59: 557-67(1966).

Steady-state creep data for α-U are analyzed, to determine the boundaries of controlling processes and to establish the existence of unreported mechanisms. Four different processes were found to be controlling at 250 to 660°C. Irradiation-induced cavitation swelling correlates well with a creep process, probably involving nonconservative dislocation motion and boundary migration. (auth)

39411 NIOBIUM OXIDE–TITANIUM DIOXIDE SYSTEM. Burdese, Aurelio; Borlera, Maria Lucco. Atti Accad. Sci. Torino: I. Cl. Sci. Fis., Mat. Natur., 100: 567-74 (1965-66). (In Italian).

The constitution diagram of Nb_2O_5–TiO_2 was examined. In the zone rich in Nb_2O_5 there are 3 niobates analogous to the Magneli phases ($NbO_{2.48}$, $NbO_{2.46}$, and $NbO_{2.40}$). The first two can be indicated with good approximation with the formulas $TiO_2 \cdot 12Nb_2O_5$ and $TiO_2 \cdot 6Nb_2O_5$. They melt incongruently at 1485 and 1475°C; the third has a region of existence extending from 28 to 34 mol% Nb_2O_5. In correspondence with the composition $TiO_2 \cdot 2.5Nb_2O_5$ there is a congruent melting point at 1490°C. This phase forms 2 eutectics, both melting at 1470°C with $TiO_2 \cdot 6Nb_2O_5$ and $TiO_2 \cdot Nb_2O_5$. This last niobate with a congruent melting point of 1500°C has a wide area of composition and gives origin to a eutectic at 1480°C with a solid solution of a rutile type. (tr-auth)

39412 PREPARATION, COMPOSITION, AND STABILITY OF β-PHASE TUNGSTEN. Dufour, Louis-Claude (CNRS, Dijon, France). Bull. Soc. Chim. France, No. 6, 2107-8(June 1966). (In French).

A kinetic study was made of the reduction by dry H_2 of WO_3 from 400 to 800°C. The results showed that under the best experimental conditions reduction procedes by the passage of WO_3 into $WO_{2.90}$, which is reduced to β–W. The β–W is transformed irreducibly into α-tungsten at 600°C. The compound obtained below 600°C, called β–W, has a grey-black color and always contains a very low fraction of O_2. The specific surface of β–W increases linearly as an inverse function of the reduction temperature. The β–W fixes O_2 very easily, but after tempering at the temperature of liquid N_2 it is no longer pyrophoric. The β–W obtained after tempering under N_2 can be conserved for a long time without alteration of its x-ray diffraction spectrum. (J.S.R.)

39413 ISOTHERM SECTION AT ROOM TEMPERATURE OF THE URANIUM–CARBON–SILICON DIAGRAM. Guinet, Philippe; Vaugoyeau, Henri (CEN, Grenoble, France). Compt. Rend., Ser. C, 262: 1856-9(June 27, 1966). (In French).

The cross section at room temperature of the uranium–carbon–silicon diagram was determined by metallography and x-ray diffraction, using arc-melted samples. Two ternary compounds, with the formulas $U_3C_3Si_2$ and $U_{20}C_3Si_{16}$, were detected. The compound U_3Si_2 forms with carbon solid solutions of the interstitial type containing up to 4 at. % C. The Si concentration of these solutions is slightly variable, and the amplitude of these variations is of the order of 0.9 at. % Si. (tr-auth)

39414 TERNARY COMPOUNDS WITH A $ThMn_{12}$ SUPERSTRUCTURE IN THE SYSTEMS YTTRIUM–TRANSITION METAL–ALUMINIUM. Zarechnyuk, O. S. (Lvov State Univ.). Dopov. Akad. Nauk Ukr. RSR, No. 6, 767-9 (1966). (In Russian).

X-ray-diffraction analysis was used to establish the existence of ternary compounds with a $ThMn_{12}$ superstructure (ψ-phases) in the systems Y–T–Al (T = Cr, Mn, Fe, Cu) with composition YT_4Al_8 (space group I4/mmm–D_{4h}^{17}; 2 Y in 2 (a), 8 T in 8 (f), 16 Al in 8 (i) with x = 0.364 and 8 (j) with x = 0.275). Data on lattice constants are included. (auth)

39415 CRYSTAL STRUCTURE OF $EuNi_5$, $TmNi_5$, and $LuNi_5$ COMPOUNDS. Kripyakevich, P. I.; Gladyshevskii, E. I. (Lvov State Univ.). Dopov. Akad. Nauk Ukr. RSR, No. 6, 769-71(1966). (In Russian).

By means of x-ray-diffraction analysis, new compounds $EuNi_5$, $TmNi_5$ and $LuNi_5$ having structures of the $CaCu_5$ type were found. Data on lattice constants are included. (auth)

39416 CRYSTAL STRUCTURE OF COMPOUNDS $Zr_2Ni_{21}B_6$ AND $Zr_6Co_{21}B_6$. Kuz'ma, Yu. B.; Lakh, V. I.; Voroshilov, Yu. V.; Stadnik, B. I. (Lvov State Univ.). Dopov. Akad. Nauk Ukr. RSR, No. 6, 772-4(1966). (In Russian).

X-ray-diffraction analysis revealed the existence of compounds $Zr_2Ni_{21}B_6$ and $Zr_2Co_{21}B_6$ with a structure of the $W_2Cr_{21}C_6$ type (for $Zr_2Ni_{21}B_6$ α = 10.628 ± 0.005 Å, for $Zr_2Co_{21}B_6$–α = 10.597 ± 0.0055 Å). In the system Zr–Co–B a compound with the approximate composition $ZrCo_3B$ was also found. (auth)

39417 NEW RARE EARTH COMPOUNDS WITH ZINC AND THEIR CRYSTAL STRUCTURE. Kuzma, Yu. B.; Kripyakevich, P. I.; Ugrin, N. S. (Lvov State Univ.). Izv. Akad. Nauk SSSR, Neorg. Mater., 2: 630-5(Apr. 1966). (In Russian).

Crystal structures of rare earth compounds with zinc, Gd_6Zn_{23}, Dy_6Zn_{23}, Tm_6Zn_{23}, and Lu_6Zn_{23} (of the Th_6Mn_3 type); Pr_2Zn_{17}, Nd_2Zn_{17}, Er_2Zn_{17}, Yb_2Zn_{17}, and Lu_2Zn_{17} (of Th_2Ni_{17} type); $SmZn_{12}$, $GdZn_{12}$, $HoZn_{12}$, $TmZn_{12}$, and $LuZn_{12}$ (of $ThMn_{12}$ type); and $LaZn_{13}$, $EuZn_{13}$, and $YbZn_{13}$ (of the $NaZn_{13}$ type), are described. (R.V.J.)

39418 COMPARISON OF MEASURED AND PREDICTED BULK MODULI OF TANTALUM AND TUNGSTEN AT HIGH TEMPERATURES. Soga, Naohiro (Bell Telephone Labs., Inc., Murray Hill, N. J.). J. Appl. Phys., 37: 3416-20(Aug. 1966).

The elastic constants of Ta were determined from room temperature to 500°C by means of a dynamic resonance method to obtain the adiabatic bulk modulus at elevated temperature. The adiabatic bulk modulus (B_s) of Ta were found to be 1897 kbar at room temperature and it decreases almost linearly with a slope (dB_s/dT) of –0.11 kbar/°C as temperature rises. The calculation of the Grüneisen constant γ and a parameter δ, defined as $-(dB_s/dT)/\alpha B_s$, from the present data showed that both parameters were almost independent of the temperature (1.57 for γ and 3.1 for δ). The constancy of γ and δ at high temperatures was also tested for tungsten by using the recent data of Lowrie and Gonas (J. Appl. Phys. 36: 2189(1965)). The results indicate that both γ and δ are virtually constant at high temperature. The applicability of the following equation to estimate the bulk-modulus-temperature relationship for the refractory metals Ta and W was also tested: $B_T^T = B_S^{25} - (\delta\gamma/V)(H^T - H^{25})$, where H is the enthalpy and the superscripts indicate values at 25° and T°C. (auth)

39419 CORRELATION OF THE FATIGUE PROPERTIES OF MAGNOX AL80 IN TERMS OF THE PLASTIC STRAIN RANGE. Raraty, L. E. (United Kingdom Atomic

Energy Authority, Reactor Group, Springfields Works, Salwick, Eng.); Suhr, R. W. J. Inst. Metals, 94: 292-300 (Aug. 1966).

A method is described for estimating the plastic strain range, ϵ_p, in fatigue of the Mg−0.8% Al alloy AL80, during experiments in which only the stress range or the total strain range was measured. The plastic range is shown to be a useful parameter in correlating the results of experiments at 350 to 500°C and frequencies between 1 c/h and 3×10^7 c/h. For endurances, N, > 10^4 cycles the fatigue law is found to be $N^{\frac{1}{2}}\epsilon_p = 0.02$ and is independent of the temperature at 350 to 500°C and of frequency up to 3×10^5 c/h. At larger amplitudes the endurance is higher than predicted by this law and tends to the value expected from the Coffin-Manson high-strain fatigue law $N^{\frac{1}{2}}\epsilon_p \simeq 0.5$. Fatiguing in air or in Ar is more damaging than fatiguing in Co_2. The difference first becomes apparent in tests lasting >100 hr and becomes progressively greater for test of longer duration. (auth)

39420 SNOEK PEAKS AND THEIR STABILITY IN ANNEALED AND DEFORMED TANTALUM. Szkopiak, Z. C.; Eliasz, W. (Battersea Coll. of Technology, London). J. Less-Common Metals, 11: 273-85(1966).

The internal friction behavior of electron-beam refined Ta, containing O, N, and C was investigated during constant rate heating and cooling cycles at 20 to 400°C. The height of the Snoek peaks remained unchanged in specimens which had been slowly cooled prior to testing and only slight change in peak height occurred as the result of vacuum quenching. However, the height of the O peak decreased and that of the N−C peak increased appreciably on heating prestrained specimens; on cooling the reverse occurred. An exchange mechanism between O atoms at dislocations and N and/or C atoms in free solution is proposed to account for these variations. Isothermal measurements at the Snoek peak temperatures showed that the peak heights decrease with time, after straining, at a rate which obeys the $t^{\frac{1}{2}}$ law proposed by Cottrell and Bilby. The data obtained from these investigations were used to calculate dislocation densities in 6% pre-strained Ta−O solid solutions and dislocation atmosphere densities in the fully-strain-aged condition at 150°C. (auth)

39421 THE EFFECT OF COLD WORK (FILING) ON THE X-RAY DIFFRACTION PATTERNS OF SOME RARE-EARTH METALS. Harris, I. R.; Raynor, G. V. (Univ. of Birmingham, Eng.). J. Less-Common Metals, 11: 286-8(1966).

The effects of cold work on x-ray-diffraction patterns in Ce, Pr, Nd, Pm, Sm, and Eu are discussed. Diffraction pattern illustrations are included for Pr and Sm. (J.R.D.)

39422 ANTIFERROMAGNETISM OF URANIUM MONOPHOSPHIDE. Sidhu, S. S.; Vogelsang, W.; Anderson, K. D. (Argonne National Lab., Ill.). J. Phys. Chem. Solids, 27: 1197-1200(Aug. 1966).

UP crystallizes in a NaCl-type structure with $\alpha_0 = 5.590 \pm 0.004$ Å. It is paramagnetic at room temperature and antiferromagnetic at liquid N_2 temperature. The chemical and magnetic unit cells are of the same size. The magnetic moment directions and the positions of the 4 U atoms in the magnetic cell are, +: 0 0 0; ½ ½ 0 and −: ½ 0 ½; 0 ½ ½. They are aligned ferromagnetically in each layer but oppositely aligned in alternating layers perpendicular to (001) plane. The symmetry of the chemical cell is cubic but of the magnetic cell tetragonal. The atomic magnetic moment at liquid N_2 temperature is 1.72 ± 0.02 Bohr magnetons. A magnetic form-factor curve for the U atoms is given. (auth)

39423 PHASE DIAGRAM AND COMPRESSIBILITY OF NEPTUNIUM. Stephens, D. R. (Univ. of California, Livermore). Contract W-7405-eng-48. J. Phys. Chem. Solids, 27: 1201-4(Aug. 1966). (UCRL-14579(Rev.1)).

The compressibility and pressure-temperature phase diagram of Np were measured to 35 kb. The compressibility was similar to that of neighboring actinides such as U and Pu. The phase diagram showed 1 triple-point, tetragonal-bcc-liquid, at 725°C and 32 kb. (auth)

39424 MAGNETIC STUDY OF THE INTERMETALLIC COMPOUND $NdCo_5$. Bartholin, H. (CNRS, Grenoble, France); van Laar, B.; Lemaire, R.; Schweizer, J. J. Phys. Chem. Solids, 27: 1287-93(Aug. 1966). (In French).

Magnetic studies on the alloy $NdCo_5$ show an anomaly in the constant field magnetization curve near room temperature. An x-ray diffraction study on powder samples, oriented and glued in a magnetic field at different temperatures indicates a rotation of the magnetization axis between 230° and 290°K. From a neutron diffraction study at several temperatures one can deduce a ferromagnetic arrangement at all temperatures and a regular decrease of the magnetic moments with increasing temperature. Measurements of the magnetic anisotropy coefficients K_1 and K_2 were carried out upon a powder oriented and glued in a magnetic field. The thermal variation of these coefficients allows the magnetization curve anomaly to be explained. (auth)

39425 PECULIARITIES OF SHOCK COMPRESSION OF LANTHANIDES. Al'tshuler, L. V.; Bakanova, A. A.; Dudoladov, I. P. JETP Lett. (USSR) (Engl. Transl.), 3: 315-17(June 15, 1966).

Translated from Zh. Eksp. Teor. Fiz., Pis'ma Redaktsiyu, 3: 483-7(June 15, 1966).

The first results of an investigation of the dynamic compressibility of five lanthanides, La, Ce, Sm, Dy, and Er, up to 3.5 M bar pressure, are reported. The shock-compression parameters were obtained by the reflection method, where shock waves of fixed intensity were produced in screens covering the samples. The directly measured quantities were the velocities of the shock waves in the metals, which were used to determine, with the aid of conservation laws and the conditions on the screen-sample boundary, the mass velocities, the shock-compression pressures, and the degrees of compression. (L.B.S.)

39426 STUDY ON THE TERNARY ALLOYS OF IRON AND BORON. Hasegawa, Masayoshi; Okamoto, Masafumi (Waseda Univ., Tokyo). Nippon Kinzoku Gakkaishi, 30: 533-40(1966). (In Japanese).

In order to find the properties of the ternary alloys of Fe and B containing Si, Ti, V, Cr, Mn, Ni, Zr, Nb, Mo and W free from carbon, investigations have been made on the peritectoid reaction, microstructure, hardness, tempering properties, hardenability, and mechanical properties. The B contents in the specimens were 0.02% and 0.20%, and the alloying elements were added in consideration of the stoichiometric metal/B ratio. Zr, Ti, Mo, and Nb raised the peritectoid reaction temperature of Fe−B alloy, but Cr, Ni, and Mn lowered it. In the Fe−B ternary alloys solution-quenched, the acicular structure consisting of body-centered cubic appeared, and the formation of this structure was closely related to the cooling rate and the alloying element. Si, Ni, Mn and Cr had a weak tendency to form alloy boride (special boride) and mainly formed iron boride, but Ti, Zr, Nb, Mo and W had a strong tendency to form alloy boride. W, Nb, Mo, Ti and Zr forming the fine-distributed alloy boride markedly increased the hardness of the Fe−B alloy annealed and solution-quenched. In the tempering of Fe−B ternary alloys after water-quenched from 1100°C, a secondary hardening associated with the precipitation of iron boride or alloy boride was found. In the specimens alloyed with Ni, Si and Cr, the peak hardness was developed at 100 to 200°C, but at 450 to 600°C in cases of Nb, Mo and W. W, Nb, Mn and Mo markedly increased the tensile strength of Fe−B alloys air-cooled and water-quenched at room temperature, but deteriorated their ductility and toughness. (auth)

39427 A STUDY ON THE Co PHASE COMPOSITION CONTAINED IN WC–Co BASE CEMENTED CARBIDES. Miyoshi; Akiyoshi; Hino, Koichi; Hara, Akio; Kurata, Sueno (Sumitomo Electric Industry, Ltd., Itami, Japan). Nippon Kinzoku Gakkaishi, 30: 603-6(1966). (In Japanese).

The Co phase contained in cemented carbides is not pure Co but a Co solid solution which sometimes contains more than 10% metallic elements. With a decrease in C content, the amount of dissolved elements increases. In the case of the WC−Co cemented carbide, the dissolved element is only W and the amount can be obtained by measuring the lattice parameter of the Co phase. However, it is impossible for

the cemented carbide to contain TiC, TaC or NbC. The quantitative analytical method and the results for various cemented carbides are described. When the crushed particles are heated in a HCl aqueous solution, only the Co phase is leached. The leached solution was chemically analyzed to measure W and Ti contents. The W content obtained by this method coincides with the one by measuring the lattice parameter of the Co phase. It is concluded that Ti, Ta and Nb rarely dissolve into the Co phase in the composition range where the WC phase exists in the microstructure of the cemented carbide. (auth)

39428 THE HYDROGEN–PALLADIUM SYSTEM. THE ROLE OF X-RAY AND NEUTRON DIFFRACTION STUDIES. Maeland, A.; Flanagan, T. B. (Univ. of Vermont, Burlington). Platinum Metals Rev., 10: 20-3(1966). (NYO–3000-11).

The use of diffraction techniques in investigations of H-Pd systems is discussed. Cold neutron incoherent scattering data are presented to show that H motions in the H-Pd lattice can be treated by the Einstein model. Discussions of x-ray reflection line broadening as H is absorbed by Pd are included, along with information used in support of theories concerning hysteresis mechanisms in the system. (J.R.D.)

39429 WETTABILITY OF REFRACTORY CARBIDE, BORIDE, AND NITRIDE BY MOLTEN METAL. Yasinskaya, G. A. Porosh. Met., Akad. Nauk Ukr. SSR, No. 7, 53-6(July 1966). (In Russian).

The investigations showed that wettability of the refractory compounds by metals is directly connected with the character of their chemical interaction, as well as with the direction of the primary migration (transfer) of elements from the melt to the refractory backing and vice versa. The wettability of the backing by the melt can be regulated by introduction of additions to one of the contacting materials, intensifying or weakening the migration of chemically interacting atoms in the necessary direction. (auth)

39430 YOUNG'S MODULUS OF CARBIDES OF SOME TRANSITION METALS. Frantsevich, I. N.; Lyashchenko, A. B. Porosh. Met., Akad. Nauk Ukr. SSR, No. 7, 73-5 (July 1966). (In Russian).

Values of Young's modulus are presented for carbides of Ti, V, Cr, Zr, Nb, Mo, and W obtained on samples with a composition similar to the stoichiometric. The values of Young's modulus are determined for the compact state. It was found that Young's modulus of carbides depends on the quantity of s + d-electrons in the metal atom in the Ti, V, Cr and Zr, Nb, Mo series. It is assumed that a similar dependence will take place in the W, Ta, Hf series and this permits estimating the value of Young's modulus of Ta and Hf carbides. (auth)

39431 PREPARATION OF THE CARBIDES (Ti, W, Cr) C AND A STUDY OF THEIR PROPERTIES. Chaporova, I. N.; Rybalchenko, R. V.; Vrzheshch, E. Y. Porosh. Met., Akad. Nauk Ukr. SSR, No. 7, 76-83(July 1966). (In Russian).

The effects of Cr_3C_2 additions of 0 to 20% by wt on physical and mechanical properties of the carbide (Ti, W, Cr) C with a constant ratio of TiC–WC = 35 to 65% by wt were studied. It is shown that addition of Cr_3C_2 increases scaling resistance, electric resistance, and leaves the hardness, modulus of elasticity, and other properties practically unchanged. (auth)

39432 DISLOCATION ETCHING OF DEFORMED MOLYBDENUM. Pink, Erwin (Metallwerk Plansee AG, Reutte, Tyrol, Austria). Prakt. Metallog., 3: 248-52(Aug. 1966). (In German).

Owing to the possibility of simultaneous microscopic observation, electrolytic etching can be carried out with good reproducibility using the model ELYPOVIST. Early stages in dislocation etching can easily be obtained. Thus Mo of low and medium degrees of deformation exhibits dislocations arranged in slip bands. Substructures obtained in cold-worked as well as in annealed materials resemble those observed by means of transmission electron microscopy. Etch-pit density seems to be in agreement with dislocation density. (auth)

39433 MAGNETIC PROPERTIES OF SOME RARE-EARTH ALUMINIUM COMPOUNDS. Buschow, K. H. J.; Fast, J. F. (Philips Research Labs., Eindhoven, Netherlands). Z. Phys. Chem. (Frankfurt), 50: 1-10(July 1966).

Rare earth aluminum compounds were prepared by arc-melting followed by an annealing treatment, and magnetization and susceptibility measurements were determined by a Faraday method using a null coil pendulum magnetometer. The magnetic measurements were carried out for various field strengths up to 18,000 Oe. Except $SmAl_3$ all compounds showed good agreement with the Curie-Weiss law in the high temperature region (200 to 600°K). At low temperatures deviations from the Curie-Weiss law were observed in all cases. Results for individual compounds are discussed. (P.C.H.)

39434 STRUCTURE OF THE Zr–C–Nb SYSTEM. Ordan'yan, S. S.; Avgustinik, A. I.; Vigdergauz, V. Sh. Zh. Prikl. Khim., 39: 312-17(Feb. 1966). (In Russian).

Isothermal phase diagrams for Zr–C–Nb alloys at 2273°K were constructed. The systems revealed no ternary compounds. Three one-phase fields of (Nb, Zr), $Zr_xNb_yC_z$ and (Nb, Zr)$_2$C; three two-phase fields (Nb, Zr) + $Zr_xNb_yC_z$, (Nb, Zr) + (Nb, Zr)$_2$C, and (Nb, Zr)$_2$C + $Zr_xNb_yC_z$; and a triple-phase field (Nb, Zr) + (Nb, Zr)$_2$C + $Zr_xNb_yC_z$ were observed. The melting point and Nb solubility in ZrC were determined and a polythermal phase diagram of ZrC–Nb was constructed. (R.V.J.)

39435 RARE EARTH METAL AND YTTRIUM DISTRIBUTION DURING ZINC CRYSTALLIZATION IN LEAD MELT. Bayanov, A. P.; Gurskaya, S. F.; Serebrennikov, V. V. (Tomsk State Univ., USSR). Zh. Prikl. Khim., 39: 447-51(Feb. 1966). (In Russian).

Data are presented to show that Zn crystallizing in Pb–lanthanide melts transforms into solid-phase or Zn froth. It was also observed that during crystallization of the Zn froth, the lanthanides (up to Sm) were concentrated in melted Pb while Y elements (63 to 71) were concentrated in the Zn froth. (R.J.V.)

39436 IMPACT AND HARDNESS PROPERTIES OF IRRADIATED BERYLLIUM. Hesse, John Lamborn. University Park, N. Mex., Nex Mexico State Univ., 1966. 140p. Thesis.

A machine was designed and constructed capable of delivering repeated longitudinal compressive impact blows to Be specimens between one and one-quarter and one and one-half inches in length, with either round or square cross sections. The velocity of the impacting mass was measured by a system of photoelectric cells, and the permanent deformation of the unirradiated Be was measured by strain gages following impact. Irradiated samples were tested to failure, and total input energy to failure was measured. Ten cylindrical unirradiated Be specimens were tested for a limited number of cycles, and curves of permanent deformation versus energy input were obtained. Data obtained at room temperature, at 200°F, and 350°F were extrapolated to failure using a longitudinal strain criterion furnished by the fabricator. Fourteen samples of irradiated Be obtained from a Materials Testing Reactor fractured lattice piece were tested under repeated compressive impacts of 64.57 foot pounds per blow. These samples had been irradiated to exposures in the range 1.75×10^{21} to 3.86×10^{21} nvt. Data were obtained on total energy input to failure in this test mode. Forty-five similar specimens in the exposure range 1.75×10^{21} to 4.80×10^{21} nvt were tested for Rockwell hardness, and twenty-two in the exposure range 1.75×10^{21} to 4.38×10^{21} nvt were subjected to Izod tests using equipment on hand at the National Reactor Testing Station. An additional seven unirradiated samples of original MTR Be were tested for both Rockwell hardness and Izod impact strength. Data obtained are presented as a function of time-integrated fast neutron exposure. Relationships were developed between compressive impact data, Izod data, and Rockwell hardness data. These equations relate exposure to the variables above, and extrapolation of the trends shown to a point of minimum residual impact resistance permitted establishment of a critical impact exposure range for Be of 3.8×10^{21} to 8.5×10^{21} nvt. (Dissertation Abstr.)

39437 HIGH-TEMPERATURE THERMAL ANALYSIS OF CERAMIC SYSTEMS. Grossman, Leonard N. 23p. (CONF-660505-8). ORAU. Gmelin, AED-CONF-66-103-9.

From American Ceramic Society Meeting, Washington, D. C.

Apparatus and experimental procedures for determining phase boundaries by high-temperature thermal analysis are described. Examples of the application of thermal analysis between 700 and 3000°C are taken from the following systems: UO_2–Eu_2O_3, Gd_2O_3–Al_2O_3, Y_2O_3–W, and Al_2O_3–W. The UO_2–Eu_2O_3 system is eutectic with extensive fluorite solid solution. The system Gd_2O_3–Al_2O_3 is simple eutectic. Y_2O_3 and Al_2O_3 apparently form simple eutectics with W; a high-temperature phase change in Y_2O_3 was identified. A measurement of the heat of fusion of UO_2 as determined by thermal analysis is also described. (auth)

39438 DYNAMIC MODULUS OF STABILIZED ZIRCONIA. Buckley, John D.; Braski, David N. (Langley Research Center, Hampton, Va.). 17p. (CONF-660505-1). ORAU. Gmelin, AED-CONF-66-103-7.

From American Ceramic Society Meeting, Washington, D. C.

Dynamic modulus measurements were made on ZrO_2 stabilized with various amounts of CaO and Y_2O_3. The results showed that the dynamic modulus of highly stabilized ZrO_2 decreases with decreasing amounts of stabilizer, decreasing density, and increasing temperature. An increase in dynamic modulus was noted in the vicinity of 1200°F for ZrO_2 which was partially stabilized with either CaO or Y_2O_3. Elevated temperature x-ray-diffraction patterns for both partially stabilized materials indicated that the beginning of polymorphic transformation also occurred near 1200°F. (auth)

39439 DECORATION OF INDIVIDUAL LATTICE VACANCIES IN GRAPHITE. Hennig, Gerhart R. (Argonne National Lab., Ill.). 6p. (CONF-650452-1). ORAU.

From 2nd Conference on Industrial Carbon and Graphite, London.

Quantitative procedures were developed for determining the concentration of vacancies, of vacancy clusters, and of substitutional B in graphite at concentrations of 10^{-5} to 10^{-10} defects per C atom. The method consists of controlled cleavage to expose the desired position in the crystal as a surface layer, etching of this surface to convert the defects into surface depressions whose depth equals the number of lattice sites occupied by each defect, and decoration with Au to render these depressions visible by electron optics. Specific differences in reactivity between the three types of defects listed permit discriminatory etching. The method facilitates high-precision measurements of rates and anisotropies of chemical surface reactions. The method was used to measure the mobilities of vacancies and B impurities parallel and perpendicular to the layer planes and to establish a lower limit of 6 ev for the formation energy of vacancies. The kinetics of formation and annealing of vacancies by irradiation of graphite were investigated. (auth)

39440 STRUCTURAL, HIGH STRENGTH URANIUM ALLOYS. Greenspan, Jacob; Rizzitano, Fortunato J. (to U. S. Army). U. S. Patent 3,266,890. Aug. 16, 1966. Filed Mar. 23, 1964.

An invention is described concerning U-base alloys containing Mo, Nb, Ti, and Zr for use as high-strength structural materials. These alloys exhibit high strength and maximum hardness, ductility, and impact resistance depending on processing and percentage composition. (J.R.D.)

39441 PRODUCTION OF AGE HARDENABLE TANTALUM-BASED ALLOYS. Foley, Dennis D. (to American Radiator and Standard Sanitary Corp.). U. S. Patent 3,265,540. Aug. 9, 1966. Filed Nov. 19, 1963.

An invention is described for preparation of dispersion hardened Ta-based alloys by dispering W-coated MoC or WC particles in Ta alloyed with small quantities of Zr or Hf at high temperature. The elevated temperature is maintained until the carbide coatings are diffused in the alloy. (J.R.D.)

39442 SOLS OF ZIRCONIA AND HAFNIA WITH ACTINIDE OXIDES. Fitch, Frederick T.; Smith, Jean G. (to W. R. Grace and Co.). U. S. Patent 3,265,626. Aug. 9, 1966. Filed Dec. 20, 1963.

An invention is described concerning preparation stable sols composed of actinide oxides and ZrO_2 or HfO_2 in mixtures or as solid solution oxide phases. The particles in these sols and solid solutions range from about 10 to 120 μ in diameter. (J.R.D.)

39443 IMPROVEMENTS IN OR RELATING TO MAGNESIUM BASE ALLOYS. Fisher, Philip Andrew; Demaine, Peter Darien (to Magnesium Elektron Ltd.). British Patent 1,034,227. June 29, 1966. Filed June 4, 1964.

A Mg-base alloy is patented that combines improved creep strength with fine grain size to yield an alloy that is suitable for canning U for use as reactor fuel. The alloy consists of 0.05 to 0.3 wt % Al, 1.0 to 1.7 wt % Si, up to 0.1 wt % Be, up to 0.4 wt % Ca, up to 0.25 wt % Mn, and up to 0.1 wt % Zn, the balance being Mg. (B.L.M.)

39444 IMPROVEMENTS RELATING TO LOW ALLOY STEELS. Cowan, Arthur; Nichols, Roy Woodward (to United Kingdom Atomic Energy Authority). British Patent 1,034,424. June 29, 1966. Filed May 11, 1962.

A low alloy steel is patented that is applicable in the form of normalized plates of a thickness of 3 in. or more to the fabrication by welding of massive pressure vessels. The alloy contains, in proportions by weight, less than 0.15% C, from 1.0 to 1.2% of Mn, from 1.4 to 1.7% Ni, from 0.25 to 0.35% Mo, from 0.08 to 0.13% V, from 0.40 to 0.55% Cr, and an addition of Nb up to 0.25%, the balance being constituents which are usual in mild steel. (B.L.M.)

39445 COLUMBIUM–HAFNIUM BASE ALLOYS WITH YTTRIUM ADDITION. Worcester, Samuel A.; Torgerson, Ronald T.; Baginski, Willi A. U. S. Patent 3,266,892. Aug. 16, 1966. Filed Jan. 4, 1965.

An invention relating to Nb-Hf base alloys, of the solid solution type is described which, by the addition of Y and/or W, exhibits improved characteristics rendering the alloys especially useful for high temperature service. (J.R.D.)

Radiation Effects

See also CHEMISTRY — Radiation Chemistry

Refer also to abstracts 38974, 39381, 39403, 40298, 40302, 40303, 40306, 40334, 40337, and 40341.

39446 (AECL-2564) THE EFFECT OF DENSITY AND GRAIN SIZE ON THE THERMAL CONDUCTIVITY OF UO_2 DURING IRRADIATION. Aragones, M.; Guerrero, H. (Atomic Energy of Canada Ltd., Chalk River (Ontario)). Apr. 1966. 45p. Dep. mn. AECL $1.50.

Specimens of UO_2 were irradiated in the NRX facility for three minutes. From the extent of melting in the UO_2 fuel, values of $\Lambda(\theta_s,\theta_m)_p$, where θ_s = temperature at pellet surface, and θ_m = temperature at limit of melting, were calculated. The differences due to variations in density from 10.5 to 10.8 g/cm^3 were given by the expression: $\Lambda(\theta_s, \theta_m)_p = \Lambda(\theta_s, \theta_m)_0 [1 - (2.8 \pm 1.0)_p]$. Increasing the grain size from 10 μm to 100 μm did not appreciably alter the value of $\Lambda(\theta_s, \theta_m)_p$ in UO_2 with a density of 10.8 g/cm^3. (auth)

39447 (AECL-2581) SHORT DURATION IRRADIATION BEHAVIOR OF UO_2 DOPED WITH 1/4 mol PERCENT NB_2O_5 OR 1/4 mol PERCENT Y_2O_3. Bain, A. S. (Atomic Energy of Canada Ltd., Chalk River (Ontario)). May 1966. 18p. Dep. mn. AECL $0.50.

Twelve specimens were prepared for short duration irradiations in the NRX reactor. The irradiation was to test UO_2 and to compare its performance with UO_2 doped with 1/4 mole % Nb_2O_5 or 1/4 mole % Y_2O_3. The irradiation behavior of the CICAF pure UO_2 was similar to that of AECL UO_2. The addition of 1/4 mole % Nb_2O_5 or Y_2O_3 did not improve the irradiation performance. (auth)

39448 (AERE-X-PR-2596-9) LOW-TEMPERATURE PROPERTIES OF TRANSURANIC AND OTHER HEAVY METALS: A STUDY OF THE EFFECTS OF SELF-IRRADIATION DAMAGE ON THE ELECTRICAL RESISTIVITY OF ALPHA AND DELTA STABILISED PLUTONIUM, URANIUM, AND NEPTUNIUM. Wigley, D. A. (Atomic Energy Research Establishment, Harwell (England)). Feb. 1964. 170p. Dep. mn.

Thesis. Submitted to Oxford Univ. (England).

The metals, Np and Pu, are strong alpha emitters and have to be handled under special conditions. The relative merits of the use of glove boxes and sealed capsules for cryogenic experiments with these elements are discussed. At room temperature radioinduced self heating has little effect on the physical properties of these metals, but at low temperatures it is possible for the defects produced in the lattice to remain in equilibrium with their surroundings. The resistivities of α and Δ stabilized Pu, Np, and ^{233}U are found to increase when these metals are held at low temperatures for long periods of time. The storage and annealing of defects in α and Δ stabilized Pu were studied in considerable detail. The resistivity of α Pu has an anomalous temperature dependence. As the temperature falls from room temperature the resistivity first rises slowly to a maximum at ~105°K, then drops sharply as the temperature is further lowered to zero. The resistivity of Δ stabilized Pu also increases when held at low temperatures for long periods of time. The additional resistivity produced in α Pu is found to anneal in two distinct stages. The first stage is centered about 80°K and the second at about 160°K. None of the theories proposed to explain the low temperature properties of Pu have gained universal acceptance. (J.R.D.)

39449 (BNWL-SA-272) IRRADIATION BREWING OF UO_2. Horn, G. R.; Bates, J. L.; de Halas, D. R. (Battelle-Northwest, Richland, Wash. Pacific Northwest Lab.). Aug. 3, 1965. Contract AT(45-1)-1830. 25p. Dep. mn. CFSTI $1.00 cy, $0.50 mn.

Changes within the fuel during irradiation and factors introduced during fabrication may grossly affect the release of gases from UO_2 during irradiation. Genrally complex, these changes and their relationship to fission gas release are not always clearly understood. The irradiation process is akin to brewing, not only in the amount of agitation that may exist, but in that it is not necessary to precisely understand the basic mechanisms involved in order to produce useful results. Fission gas release can be related graphically to the total fuel volume above 2000°C. The points for high-rated fuel elements in such curves lie essentially on the line, x = y. This implies that, for all practical purposes, 100% of the gases are released from fuel above 2000°C and 0% of the gases are released from fuel below 2000°C. Without having any knowledge of the release mechanisms involved, this relationship is simple to apply and provides a reasonably accurate description of fission gas release rates. In low-rated fuel elements, it is important to have some knowledge of gas release mechanisms in order to prevent gross over-design. Irradiation brewing has only a small effect on internal pressures; microscopic release mechanisms (both for fission gases and gases introduced during fabrication) effectively control eventual internal pressures. (J.R.D.)

39450 (CEA-R-2963) ETUDE AU MICROSCOPE ELECTRONIQUE DE L'OXYDE DE BERYLLIUM IRRADIE. (Electron Microscope Study of Irradiated Beryllium Oxide). Bisson, Auguste-Andre (Commissariat a l'Energie Atomique, Saclay (France). Centre d'Etudes Nucleaires). June 9, 1965. 62p. Dep. mn.

Thesis. Submitted to Paris Univ. (France). Faculte des Sciences.

BeO was studied by fractography, before and after irradiation, using sintered samples. The fractures were examined microscopically. It is possible to mark the difference between the pores left by sintering and the bubbles of gases produced by former thermal treatments. After irradiation, the grain boundaries are weakened. By annealing, it is possible to observe evolved gases produced by the reactions (n, 2n) and (n, α); and also those gathered on the grain boundaries. The irradiated Be was studied by transmission using small chips of the crushed material. Clusters of point defects produced by neutrons are thus detected in crystals irradiated at the following doses: 6×10^{19}, 9×10^{19} and 2×10^{20} n_f cm^{-2} at a temperature below 100°C. For the irradiation at 6×10^{19} n_f cm^{-2}, the defects are merely visible, but at 2×10^{20} n_f cm^{-2} the crystals are crowded with clusters and the Kikuchi lines have disappeared from the microdiffraction diagrams. The evolution of the clusters into dislocation loops is studied by a series of annealings. The activation energy (0.37 ev) calculated from the annealing curves suggests that it must be interstitials that condense into dislocation loops. Samples irradiated at high temperatures (650, 900 and 1,100°C) were also studied. In those specimens the size of the loops is not the same as the equilibrium size obtained after out-of-pile annealing at the same temperature. The former loops were more specifically studied and their Burgers vector was determined by microdiffraction. (auth)

39451 (EUR-2968.e) CONTRIBUTION TO THE ENHANCED DIFFUSION OF ^{63}Ni IN ALPHA-IRRADIATED PURE COPPER. Schuele, W. (European Atomic Energy Community, Ispra (Italy). Joint Nuclear Research Center). Nov. 15, 1965. 6p. Dep. mn.

A theoretical model is applied to experimental results of ^{63}Ni diffusion in pure Cu found by H. P. Bonzel. With this model the sink concentration and the concentration of the point defects during alpha-irradiation is estimated. It is shown that the ^{63}Ni atoms diffuse by an interstitial diffusion mechanism during the irradiation. (auth)

39452 (EUR-2981.f) STRUCTURE FINE DU FLUX THERMIQUE ET EFFET DE BOUT DANS DES ELEMENTS COMBUSTIBLES TUBULAIRES D'URANIUM METALLIQUE REFROIDIS PAR UN PRODUIT ORGANIQUE. (Fine Structure of the Thermal Flux and End-Effect in Tubular Composite Uranium Fuel Elements Cooled by an Organic Compound). Boeuf, A.; Tassan, S. (European Atomic Energy Community, Ispra (Italy). Joint Nuclear Research Center). June 1966. 20p. Dep. mn.

The measurements of the fine structure of the thermal flux in a composite fuel element consisting of two concentric annuli of natural U, cooled by an organic compound and moderated by heavy water, and of the flux peaking at the junction of two elements of this type are described. The measurements were performed by the activation technique, using Dy detectors. (auth)

39453 (EUR-3054.e) IRRADIATION DAMAGE IN BERYLLIUM OXIDE. Buerkholz, A. (Centre d'Etude de l'Energie Nucleaire, Mol (Belgium)). July 1966. 26p. Dep. mn.

A survey was made of the most important of the available publications on irradiation damage in BeO. The references of the articles are included. The principal radiation effect is growth and fracturing of the BeO specimens. The higher the irradiation temperature the higher the dose required to start damage. Equally important is the fabrication history of the material, small grain size being favorable for radiation resistance. It is not yet possible to find experimentally an influence of the dose rate on radiation damage. Provided that the right irradiation conditions are chosen, BeO should nevertheless withstand much higher doses than formerly expected. (auth)

39454 (EUR-3055.e) IRRADIATION DAMAGE IN BERYLLIUM. Buerkholz, A. (Centre d'Etude de l'Energie Nucleaire, Mol (Belgium)). July 1966. 26p. Dep. mn.

A survey was made of the most important of the available publications on irradiation damage in Be. The references of the articles are given in the bibliography. An irradiation effect characteristic of Be is the production of He-atoms by fast neutrons. Principal irradiation damage is the severe embrittlement of the material after exposure to high doses. At temperatures above 600°C, bubble formation at grain boundaries leads to extensive swelling of Be. (auth)

39455 (EUR-3056.e) IRRADIATION DAMAGE IN GRAPHITE. Buerkholz, A. (Centre d'Etude de l'Energie Nucleaire, Mol (Belgium)). July 1966. 30p. Dep. mn.

Reports dealing with the radiation effects on graphite were surveyed to determine the behavior of graphite under irradiation. The review covers the main radiation effects and makes available survey-type information on this subject. Owing to the complicated structures of the graphite materials, past reviews on radiation damage on graphite have been compilations of experimental data. Recent investigations, especially those of British workers, allow a deeper insight into the nature of the radiation effects. (auth)

39456 (GEAP–5100–1) UO_2 POWDER AND PELLET THERMAL CONDUCTIVITY DURING IRRADIATION. Lyons, M. F.; Coplin, D. H.; Hausner, H.; Weidenbaum, B.; Pashos, T. J. (General Electric Co., Pleasanton, Calif. Nuclear Technology Dept.). Mar. 1966. Contract AT (04-3)-189. 76p. (EURAEC–1626). Dep. mn. CFSTI $3.00 cy, $0.75 mn.

Work Performed under United States–Euratom Joint Research and Development Program.

The integrity of data on thermal conductivity of both sintered pellet and comparted powder UO_2 under irradiation was improved in the past year. The thermal conductivity of 95% dense, sintered pellet UO_2, expressed as an integral value from 0°C to melting, is 90 w/cm($\int_0^{Tm}$kdT). A similar analysis based on post-irradiation microstructures was performed for compacted powder fuel rods irradiated with gross central melting. The effective bulk density of the UO_2 in these rods ranged from 83%, obtained by straight vibratory compaction, to 90.5% density obtained by a combination of vibratory compaction and swaging. These indirect results indicate an approximate powder conductivity integral value from the fuel surface temperature to melting ($\int_{Ts}^{Tm}$kdT) of 49 w/cm. This value is 20% less than the directly comparable value of 60 w/cm for sintered pellets and indicates a basically lower thermal conductivity for powder fuel, probably at the unsintered periphery near the fuel surface. The first direct measurement of powder-conductivity in-pile to a center temperature of 2500°C indicates an even lower integral value ($\int_{Ts}^{Tm}$kdT) of 36 w/cm, or 46% less than the truly comparable value of 67 w/cm for low surface temperature, sintered pellets. This direct measurement covered only the inital 50 hr of high-temperature operation, and there is some indication that the powder conductivity may improve with further sintering and densification. The confidence in the indirect results from post-irradiation microstructures was also further enhanced by an out-of-pile experiment that verifies the microstructure characteristic used previously to identify the UO_2 molten boundary. This experiment employed relatively massive W markers sinking through a half-molten column of UO_2 operating in an axial temperature gradient. The post-heating location of the W markers corresponded precisely to the initial termination of porosity in the microstructure, moving up the temperature gradient. (J.R.D.)

39457 (GEAP–5100–9) MECHANICAL PROPERTY CHANGES IN ZIRCALOY-2, INCONEL AND INCOLOY FOR NEUTRON EXPOSURES TO 2.5×10^{21} nvt (ABOVE 1 Mev). Coplin, D. H.; Lyons, M. F.; Pashos, T. J.; Weidenbaum, B. (General Electric Co., Pleasanton, Calif. Vallecitos Atomic Lab.). June 1966. Contract AT(04-3)-189. 40p. (EURAEC–1681). Dep. mn. CFSTI $2.00 cy, $0.50 mn.

Work Performed under United States–Euratom Joint Research and Development Program.

Tensile coupons of Zircaloy-2, Incoloy-800, and Inconel-600 were irradiated at 180°C to a maximum integrated fast neutron flux of 2.5×10^{21} nvt (E >1 Mev). These samples were then tensile tested at 24°C, 316°C, and 593°C. The results of the tensile tests in terms of yield strength, ultimate strength, and uniform and total elongation are presented as a function of exposure. Empirical equations are derived to describe the changes in yield strength with exposure. (auth)

39458 (NP–16225) CHARGED PARTICLE RADIATION DAMAGE IN SEMICONDUCTORS, XII. EFFECTS OF HIGH ENERGY ELECTRONS IN SILICON AND SILICON SOLAR CELLS. Final Technical Report. Carter, J. R.; Downing, R. G.; Flicker, H. (TRW Space Technology Labs., Thompson Ramo Wooldridge Inc., Redondo Beach, Calif.). May 25, 1966. Contract NAS5-3805. 67p.

A broad experimental program was conducted to study the effects of electron bombardment in Si and Si solar cells. Using Hall effects measurements, it was found that the defect introduction rate of the $E_v + 0.3$ ev level is independent of dopant material in crucible grown p-type Si. Annealing experiments indicate that the 0.3 ev level begins to anneal rapidly around 500°C with complete annealing at 500 to 600°C in low dislocation material. In high dislocation material the annealing occurs in two stages at 350 to 400°C and 550 to 600°C. Complete annealing of n/p solar cells is also observed to occur in the 400°C range. In addition, a series of experiments were performed on the dependence of solar cell degradation under electron bombardment on irradiation temperature. It is observed that both p/n and n/p solar cells exhibit recombination center introduction rates which are independent of temperature over a range of 77 to 373°K for p/n solar cells and over a range of 198 to 373°K for n/p solar cells. At 77°K n/p solar cells exhibit an apparent factor of 5 increase in degradation rate. The recombination center responsible for this effect can be produced and observed only at 77°K and is not stable at higher temperatures. (auth)

39459 (TRG-Report–1278) THE MECHANISM OF FAILURE IN UO_2/STAINLESS STEEL CERMETS. Gittus, J. H. (Reactor Group, United Kingdom Atomic Energy Authority, Springfields (England)). July 12, 1966. 8p. Dep. mn.

Reprint of TRG-Memo–1249, issued Sept. 1962.

A model is proposed for explanation of the irradiation-induced failure of UO_2-stainless steel cermets in terms of the growth of fission-gas bubbles in the damage halos surrounding the fissile particles. A numerical elaboration of the failure model leads to the criterion: $(B\theta)^{\frac{1}{3}}$ t exp $(-Q/\theta) > kV_{lim}$ where B is burn-up, θ is the absolute temperature, t is the time, Q is half the activation energy for bubble nucleation, V_{lim} is a limiting value of the total volume of gas in bubbles, and k is a constant. The model can be used to discriminate between failures and non-failures. (auth)

39460 (WAPD-TM–514(Add.1)) CYGRO-1 STRESS ANALYSIS OF THE GROWTH OF CONCENTRIC CYLINDERS. Friedrich, C. M. (Bettis Atomic Power Lab., Pittsburgh, Pa.). July 1966. Contract AT(11-1)-Gen-14. 18p. Dep. mn. CFSTI $1.00 cy, $0.50 mn.

The digital computer program CYGRO-1 determines stresses and strains in two concentric cylinders undergoing thermal strains and irradiation growth where elastic, plastic, and creep properties are given as functions of temperature, fissioning rate, and integrated flux. In addition to the analysis presented in WAPD-TM-514, the computer program includes fuel sintering and hot-pressing and has provision for including an incompressible center plug. (auth)

39461 (WCAP–6074) ENGINEERING AND METALLURGICAL EVALUATION OF AN IRRADIATED YANKEE CORE I CONTROL ROD. Smalley, W. R.; Paxson, E. (Westinghouse Electric Corp., Pittsburgh, Pa. Atomic Power Div.). July 1966. Contract AT(30-1)-3017. 58p. Dep. mn. CFSTI $3.00 cy, $0.50 mn.

Ni-plated Ag–In–Cd control rods from Yankee Core I were examined to determine the effects of reactor exposure on their irradiation stability. The samples were evaluated for changes in surface condition, dimensions, microstructure, and tensile properties. Visual and metallographic examination revealed that large areas of the control rods absorbers were devoid of Ni plate and that the remaining plating had been attacked by the reactor coolant. The metallographic evaluation further indicated that the Ni plate and associated diffusion layer were not effective in preventing internal oxidation of the base metal. The Ag–In–Cd alloy itself displayed good dimensional and irradiation stability during reactor operation. The microstructure of the alloy was essentially unchanged, with no evidence of new phases or significant precipitation. Similarly, the hardness

and tensile properties of irradiated absorber samples showed no appreciable changes as a result of exposure in Yankee Core I. (auth)

39462 THE INFLUENCE OF NEUTRON IRRADIATION TWINNING IN A NIOBIUM–VANDIUM ALLOY (40 PERCENT V). McCoy, H. E.; Hobson, D. O. (Oak Ridge National Lab., Tenn.). Amer. Soc. Metals, Trans. Quart., 59: 568-70(1966). (ORNL-P-2197).

Results of an investigation are reported in which coupons of Nb–40 wt % V alloy were annealed at 1350°C and neutron-irradiated to various doses. Twinning was determined by loading the specimen with a Rockwell hardness machine submerged in a controlled-temperature bath. Twinning is detected audibly as the load is applied. Data are presented concerning neutron dose effects on the twinning transition temperature of the alloy. (J.R.D.)

39463 RADIATION DAMAGE IN GRAPHITE. Simmons, J. H. W. (Atomic Energy Research Establishment, Harwell, Eng.). Int. Ser. Monogr. Nucl. Energy, 102: 1-242(1965).

A general account of studies on the changes in the physical properties of graphite by irradiation is given. The theory of irradiation damage processes is discussed and defect structures in irradiated graphite are examined. Radiation effects on electrical and magnetic properties, thermal and structural properties, dimensional changes, and mechanical properties are treated in separate chapters. Stored energy measurements and annealing effects in reactor graphite are discussed. (H.D.R.)

39464 SINGULARITIES IN RADIATION-THERMAL TREATMENT OF WHITE CAST IRON. Shalashov, V. A. Metalloved. Term. Obrabotka Metal., No. 7, 65-7(July 1966). (In Russian).

Alloys containing metastable phases, subjected simultaneously to radiation and heat treatment, were found to undergo phase transformation even under conditions which otherwise slow down the process. In order to clarify the mechanism involved, the transformation occurring in white cast iron exposed to an electron beam were examined. The 3-mm thick specimens were irradiated by a 2.4-Mev electron beam at 540 to 580°C. Because of graphitization, the back surface of the specimens was decarbonized. The following layers could be distinguished in the exposed specimens: the surface layer, containing perlite, fine graphite, traces of ferrite and residues of ledeburite cementite; the transformed layer, consisting of completely sorbitized perlite, fine graphite and traces of ferrite, together with a transition layer containing large amounts of free cementite. The depth at which the transformations were observed agreed with the calculated depth of penetration of the electrons, confirming the anticipated radiative-thermal character of the interaction of the electron beam and the decomposition of the cementite. (TTT)

39465 DIMENSIONAL CHANGES IN PYROLYTIC GRAPHITE UNDER FAST-NEUTRON IRRADIATION. Kelly, B. T.; Martin, W. H.; Nettley, P. T. (United Kingdom Atomic Energy Authority, Culcheth, Eng.). Phil. Trans. Roy. Soc. London, Ser. A, 260: 37-41(June 16, 1966).

Strains and changes in thermal expansion coefficients of three grades of pyrolytic graphite were studied after fast-neutron bombardment at 150 to 650°C. The three grades, designated α, β, and γ corresponded to a poorly graphitized soft C, a well-crystallized reactor graphite, and the best monocrystals available, respectively. The dimensional changes observed perpendicular to the plate (c axis direction) and parallel to the plate (a axis direction) after irradiation are shown. The effect of irradiation on the principal thermal expansion coefficients, α_c and α_a, of the β material is presented, and the dimensional change and thermal expansion behavior of the α, β, and γ materials at 170°C are shown. (BBB)

39466 DIMENSIONAL CHANGES IN POLYCRYSTALLINE GRAPHITES UNDER FAST-NEUTRON IRRADIATION. Kelly, B. T.; Martin, W. H.; Nettley, P. T. (United Kingdom Atomic Energy Authority, Culcheth, Eng.). Phil. Trans. Roy. Soc. London, Ser. A, 260: 51-71(June 16, 1966).

Changes in dimensions and linear thermal expansion coefficients of five polycrystalline graphites irradiated at 170 and 200°C are presented. The results are compared with the changes in these parameters which were observed in very highly oriented pyrolytic polycrystalline graphite. The relation between dimensional changes occurring in polycrystalline aggregates and those in a monocrystal is discussed in terms of structural parameters A_∞. The variation of these parameters with crystal strain is derived for the different graphites which have been investigated. (BBB)

39467 SPONTANEOUS DISCHARGE FROM ELECTRON-IRRADIATED POLYETHYLENE TEREPHTHALATE FILMS. Monteith, Larry King. Durham, N. C., Duke Univ., 1965. 83p.

Thesis.

Electron irradiation of capacitor-type structures consisting of polyethylene terephthalate films with thin Al electrodes results in a trapped charge distribution in the dielectric region. The decay of the trapped irradiation electrons was detected and shown to be consistent with a no-retrapping release model based upon a density of traps that is uniform with respect to energy measured from the conduction band. A minimum value of 1.7×10^{16} per cm^3 per ev was determined for the trap density. A saturation effect for irradiation electron trapping was also noted. Based upon the model used to describe the observations a value of 4.25×10^{15} electrons/cm^3 resulting in a maximum value of built-in electric field of 4×10^5 v/cm was inferred. This is approximately an order of magnitude below quoted values for the field strength of the material. The trapped charge that results in the built-in field decays to ½ the initial value after ceasing the irradiation in approximately 48 seconds. Reproducible results without any evidence of residual charging can be obtained if the decay of trapped charge is observed for at least 10^3 sec after each irradiation. Irradiation of the capacitor-type structure using a beta source, ^{147}Pm, resulted in spontaneous discharge. The average value of the discharge pulse height was 30 mv while the maximum value was 400 mv. The pulse is an exponential decay from its maximum amplitude as predicted by theoretical considerations. Within the sensitivity of the experiment the rise time of the pulse occurs in zero time. However, it is shown that a finite rise time should exist. Finally the origin of the breakdown is investigated. All observations lead to the conclusion that breakdown initiated by the electrical field resulting from the trapping of irradiation electrons occurs at defects in the polyethylene terephthalate film and does not liberate all the trapped charge. (Dissertation Abstr.)

39468 RADIATION-INDUCED INSTABILITY IN REFRACTIVE PROPERTIES OF SOME OPTICAL GLASSES. Malitson, Irving H. (National Bureau of Standards, Washington, D. C.); Dodge, Marilyn J.; Gonshery, Marvin E. 17p. (CONF-651074–1). ORAU.

From Optical Society of America, Fall Meeting, Philadelphia.

Results of initial studies on the effects of ^{60}Co γ radiation on the refractive index of some commonly used optical glasses are presented. All glasses were exposed to either 10^6 or 10^8 rads of γ radiation. The refractive index was measured within ½ hr after exposure and at various intervals thereafter. Results indicate that the refractive index of glasses can change in the fourth decimal place as a result of exposure to 10^6 rad. The largest changes occur at wavelengths close to or into the radiation-induced absorption bands. The values change erratically as a function of time after irradiation, but the magnitude of the effect, in general, diminishes as the induced absorption decays with time. The use of Ce in glass, although effective in preventing irradiation-induced absorption in the visible region, does not prevent measurable changes in refractive index. (A.G.W.)

PHYSICS

General

39469 (LA-3453) CONTRIBUTIONS TO THE FEASIBILITY STUDY OF AN EARLY LUNAR FLARE. Jeffries, R. A.; Wackerle, Jerry (Los Alamos Scientific Lab., Univ. of California, N. Mex.). Jan. 14, 1966. Contract W-7405-eng-36. 81p. Dep. mn. CFSTI $3.00 cy, $0.75 mn.

A limited investigation of certain aspects of the feasibility of the ELF concept, a proposal for obtaining chemical and physical information about the lunar surface, is described. This information will be gathered by the earth-based observation of the impact of a highly reactive chemical flare upon the moon. Results are given of shock-wave compression measurements of the liquid chlorine trifluoride–aluminum mixture currently favored as the flare material. Also reported are experiments which demonstrated that modest amounts of this mixture do not sustain high-order detonation under strong shock loading. Finally, experiments are described which were designed to simulate, in reduced scale, the anticipated impact event. While some observations of the latter experiments did, on cursory study, appear detrimental to the feasibility of the ELF proposal, on more careful examination these results were invariably caused by experimental limitations and were not due to any inherent weaknesses in the concept. Suggestions are made for future investigations leading to a more thorough understanding of an impact event. (auth)

39470 (ORNL-3924) PHYSICS DIVISION ANNUAL PROGRESS REPORT FOR PERIOD ENDING DECEMBER 31, 1965. (Oak Ridge National Lab., Tenn.). May 1966. Contract W-7405-eng-26. 179p. Dep. mn. CFSTI $5.00 cy, $1.00 mn.

A report is presented on research in progress by the physics division of ORNL. Preliminary results are presented on research in high energy physics, instrumentation, nuclear reactions, neutron scattering, fission, solid state physics, superconductivity, mathematics, and biomedicine. A brief description of the 3.0-Mv, 5.5-Mv, and Tandem Van de Graaff facilities, including a cross reference to reports and papers resulting from research done on each is included. Abstracts of papers which have been published since the last annual report are also presented. (B.G.D.)

39471 INVERSE PROBLEM OF PARTICLE MOTION AND ITS APPLICATION. Naidu, P. S. (Univ. of British Columbia, Vancouver); Westphal, K. O. Appl. Sci. Res., Sect. B, 12: 435-50(1965-1966).

The theory of the inverse problem of charged particle motion is presented. A potential distribution required to guide a group of particles along a set of prescribed paraxial paths was found. An application of the theory of the inverse problem to the design of an efficient ion source for the mass spectrometer is discussed. The potential distribution required to guide the ions along a set of exponentially converging and damped oscillatory paths was found. An interesting situation is encountered, where a particle is turned back at certain points called mirror points. The particles which do not satisfy the initial condition of uniform energy and direction may deviate considerably from their projected paths, leading to an unstable situation. A method for finding the perturbation function was developed. It was found that the system with exponentially converging paths is unstable, while the second system with damped oscillatory paths is stable. (auth)

39472 RECENT DEVELOPMENTS IN ELECTROSTATICS. Bright, A. W. Electron. Power, 12: 291-6 (Aug. 1966).

Advances in electrostatic technology, which were made without recourse to the underlying theory, are reviewed. Work on space-vehicle propulsion has again focused attention on the fundamental processes. Progress in particle adhesion, powder deposition, electrostatic propulsion, and electrodialysis is discussed. The search for a high-permittivity insulating medium and the use of such a medium in liquid-insulated generators are outlined. (M.H.R.)

39473 MEASUREMENT OF SYNCHROTRON RADIATION IN THE X-RAY REGION. Bathow, G. (DESY, Hamburg); Freytag, E.; Haensel, R. J. Appl. Phys., 37: 3449-54(Aug. 1966).

Synchrotron radiation was investigated by means of scintillation counters at electron energies between 4.0 and 6.3 Bev. Measurements were performed of the integrated radiation, the spectral distribution, the polarization, and the angular dependence of them at photon energies between 15 and 300 kev. The results agree with theoretical calculations. (auth)

39474 ONE-DIMENSIONAL IMPENETRABLE BOSONS IN THERMAL EQUILIBRIUM. Lenard, A. (Inst. for Advanced Study, Princeton, N. J.). J. Math. Phys. (N. Y.), 7: 1268-72(July 1966).

The simple relation between the wavefunctions of a system of impenetrable one-dimensional bosons and impenetrable one-dimensional fermions is exploited to derive an expansion of the boson reduced density matrices in terms of the fermion reduced density matrices and vice versa This expansion is independent of the statistical ensemble used, and of the interparticle potential (subject to the impenetrability condition). The special case of zero impenetrability radius with no other forces is treated in detail, using the grand canonical ensemble. This leads to a natural generalization of a formula previously found for zero temperature only, for the one-particle reduced density matrix. (auth)

39475 POSTULATE OF THE RELAXATION OF NONSTATIONARY PROCESSES CAUSED BY THE FINITE TRANSPORT VELOCITY OF INTERACTION IN THE MATTER. Kranys, M. (Inst. of Plasma Physics, Czechoslovak Academy of Sciences, Prague). Phys. Lett., 22: 285-6(Aug. 15, 1966).

A more accurate approximation of the phenomenological equations of continuum theory is proposed. This approximation removes the paradox of infinite transport velocity of interaction in the matter. (auth)

Accelerators

Refer also to abstracts 39584, 40101, and 40455.

39476 (AD-636185) PROCEDURE FOR MINIMIZING PERSONNEL HAZARDS WHILE CHANGING TRITIUM TARGETS IN ACCELERATORS. Aberle, J. A.; Macdonald, A. R.; Porter, S. W. Jr. (Armed Forces Radiobiology Research Inst., Bethesda, Md.). May 1966. 19p. (AFRRI-TN-66-5). CFSTI $1.00 cy, $0.50 mn.

A detailed procedure for minimizing personnel hazards while changing tritium targets in accelerators is given. The step-by-step process utilizes an airtight stainless steel glove box. The use of a plastic containment area is also described. (auth)

39477 (BMWF-FBK-66-15, pp 1-15) BESCHREIBUNG DER EIGENSCHAFTEN DES BROAD RANGE ANALYSER MAGNETEN (AM) VOM INSTITUTE FOR NUCLEAR STUDY, UNIVERSITY OF TOKYO. (Description of the Characteristics of the Broad Range Magnetic Analyzer (MA) of the Institute for Nuclear Study, University of Tokyo). (Hamburg Univ. (West Germany). I. Institut fuer Experimentalphysik).

Construction and characteristics of a particle analyzer at the cyclotron of the INS, Tokyo, are described. The

analyzer can be applied up to 57 Mev of proton energy, having an impulse resolution of 0.05%. (auth)

39478 (BNL–10376) MEASUREMENTS ON THE MULTISTEM DRIFT TUBE STRUCTURE FOR PROTON ACCELERATORS. Giordano, S. (Brookhaven National Lab., Upton, N. Y.). June 22, 1966. Contract AT(30-2)-Gen-16. 17p. Dep. mn. CFSTI $1.00 cy, $0.50 mn.

The operating characteristics of a multistem drift tube structure for accelerating protons below an energy of 200 Mev are described. (B.G.D.)

39479 (BNL–10495) DIGITAL CALCULATIONS OF MAGNETIC FIELDS OWING TO CURRENTS IN Nb_3Sn RIBBON IN SUPERCONDUCTING QUADRUPOLE LENS. Kruger, P. Gerald; Snyder, J. N.; Sampson, W. B. (Brookhaven National Lab., Upton, N. Y.). July 26, 1966. Contract AT(30-2)-Gen-16. 12p. Dep. mn. CFSTI $1.00 cy, $0.50 mn.

Digital calculations were made of the magnetic field components due to currents in Nb_3 Sn ribbons in superconducting quadrupole lenses. The magnetic field was calculated for radial distance and along distance of the quadrupole axis. (B.G.D.)

39480 (BNL–10508) A 200 Bev ACCELERATOR EMPLOYING A SEPARATED FUNCTION MAGNET LATTICE. Danby, G. T.; Allinger, J. E.; Jackson, J. W. (Brookhaven National Lab., Upton, N. Y.). Aug. 5, 1966. Contract AT(30-2)-Gen-16. 74p. Dep. mn. CFSTI $3.00 cy, $0.75 mn.

It is shown that a separated function 200-Bev proton synchrotron is inherently a better and more flexible machine than the conventional combined function design. Additional advantages are discussed. A cost estimate is also presented. (auth)

39481 (CEAL–1031) SEMI-ANNUAL REPORT FOR THE PERIOD, JULY 1, 1965–DECEMBER 31, 1965. (Cambridge Accelerator, Mass.). July 13, 1966. Contract AT (30-1)-2076. 7p. Dep. mn. CFSTI $1.00 cy, $0.50 mn.

A report is presented on the activities of the Cambridge 6-Bev Synchrotron group during latter part of 1965. Topics discussed are policies of the laboratory, explosion and fire of July 5, 1965, experiments, new 100 Mev linac, project BYPASS, and safety. (B.G.D.)

39482 (CERN–66-20) INTRODUCTION A L'ETUDE DES ACCELERATEURS LINEAIRES. (An Introduction to the Study of Linear Accelerators). Lapostolle, P. (Institut National des Sciences et Techniques Nucleaires, Saclay (France)). June 7, 1966. 75p. Dep. mn.

An introduction to the study of linear accelerators is presented, rather than an extensive report making a completely up-to-date review of all linear accelerator problems. It endeavors to collect together the basis of theory and the relevant technical ideas, which are usually dispersed among many reports, though it has no pretensions to being complete. Emphasis is placed on proton linacs, though electrons and heavy ions are also included. The presentation is dictated by pedagogical concern, but a table of contents will guide the reader in finding the appropriate chapters. (auth)

39483 (CERN–66-21) LECTURES ON BEAM OPTICS. Lectures given in the Academic Training Programme of CERN in 1965. de Raad, B.; Minten, A.; Keil, E. (European Organization for Nuclear Research, Geneva (Switzerland)). June 23, 1966. 84p. Dep. mn.

Separate abstracts were prepared for the three lectures on beam optics presented. (B.G.D.)

For abstracts of individual sections see: 39484–39486.

39484 (CERN–66-21, pp 1-30) INTRODUCTION TO BEAM OPTICS. de Raad, B. (European Organization for Nuclear Research, Geneva (Switzerland)).

Equations and some general considerations which were useful in designing beams for the CERN Proton Synchrotron are presented. Topics included are equations of motion in a quadrupole field, thick lens equations for a quadrupole, doublets and triplets, matrix formulation, chromatic aberrations, phase-space representation and Liouville's theorem, matching and representation of phase-space ellipses by complex numbers, and bending magnets. (B.G.D.)

39485 (CERN–66-21, pp 31-42) LOW-ENERGY SEPARATED BEAMS. Minten, A. (European Organization for Nuclear Research, Geneva (Switzerland)).

A discussion is presented on the separation of particle beams in momentum and mass for physics experiments, especially bubble chamber experiments. (B.G.D.)

39486 (CERN–66-21, pp 43-54) RADIO-FREQUENCY SEPARATED BEAMS. Keil, E. (European Organization for Nuclear Research, Geneva (Switzerland)).

A discussion is presented on r-f separated beams for accelerators. Topics discussed are principles of r-f separators, formulas, optical systems, background considerations and collimator arrangement, operation of a r-f separated beam, and comparison with electrostatic separators. (B.G.D.)

39487 (EGG–1183-2009) LINAC ADAPTATION FOR WEAPONS SIMULATION. AEC R and D Quarterly Progress Report. Report No. S-268-R. George, W.; Norris, N.; Hanst, K. (Edgerton, Germeshausen and Grier, Inc., Santa Barbara, Calif.). Jan. 1965. Contract AT(29-1)-1183. 27p. Dep. mn. CFSTI $2.00 cy, $0.50 mn.

A progress report is presented on the linear accelerator adaptation program directed toward the obtaining of the shortest possible beam pulse, ultimately a single r-f bunch, and the investigation of electron beam characteristics during the transient mode as imposed by the fundamental process of electron acceleration in traveling wave structures. (auth)

39488 (EGG–1183-2027) LINAC ADAPTATION FOR WEAPONS SIMULATION. AEC R and D Quarterly Progress Report. Report No. S-277-R. Norris, N.; Hanst, K.; Johnson, E. (Edgerton, Germeshausen and Grier, Inc., Santa Barbara, Calif.). Apr. 1965. Contract AT(29-1)-1183. 24p. Dep. mn. CFSTI $1.00 cy, $0.50 mn.

A status report is presented on the linear accelerator (Linac) adaptation program which is directed toward obtaining the shortest possible beam pulse (ultimately a single r-f bunch), and the investigation of electron beam characteristics during the transient mode as imposed by the fundamental process of electron acceleration in traveling wave structures. (auth)

39489 (EGG-1183-2050) LINAC ADAPTATION FOR WEAPONS SIMULATION SUBHARMONIC BUNCHER PROGRAM. AEC R and D Quarterly Report. Report No. S-300-R. Norris, N.; Hanst, K. (Edgerton, Germeshausen and Grier, Inc., Santa Barbara, Calif.). Oct. 1965. Contract AT(29-1)-1183. 9p. Dep. mn. CFSTI $1.00 cy, $0.50 mn.

A progress report is presented on the design and construction of an injector system for the linear accelerator incorporating subharmonic bunching to enhance the output beam intensity in the single r-f pulse mode of operation. (B.G.D.)

39490 (EGG–1183-2051) LINAC ADAPTATION FOR WEAPONS SIMULATION HIGH CURRENT GUN PROGRAM. AEC R and D Quarterly Report. Report No. S-301-R. Norris, N.; Hanst, K. (Edgerton, Germeshausen and Grier, Inc., Santa Barbara, Calif.). Oct. 1965. Contract AT(29-1)-1183. 12p. Dep. mn. CFSTI $1.00 cy, $0.50 mn.

A progress report is presented on the high current gun program which is designed to obtain a high current electron gun and focusing system to be used on the EG & G Linac, which will increase the current in a single r-f pulse. The gun is compatible with the subharmonic pre-buncher system. (B.G.D.)

39491 (JINR–P-2732-1) PROGRAMMIROVANIE AMPLITUDY USKORYAYUSHCHEGO NAPRYAZHENIYA NA MODELI VYSOKOCHASTOTNOI SISTEMY KOL'TSEVOGO PROTONNOGO FAZOTRONA. (Programming the Acceler-

ating Voltage Amplitude of a Model of the Circular Proton Phasotron R. F. System). Glazov, A. A.; Skhvabe, E. (Joint Inst. for Nuclear Research, Dubna (USSR). Lab. of Nuclear Problems). 1966. 38p. Dep. mn.

The results of programming the accelerating voltage amplitude of the model of the circular proton phasotron r-f system are reported. By using the self-anode modulation circuit of the powerful oscillator the programming of the accelerating voltage amplitude is carried out by means of a low-powered and simple modulator. The conditions of modulation linearity considered theoretically were proved experimentally. (auth)

39492 (JINR-P-2811) NAKOPLENIE CHASTITS V SINKHROTSIKLOTRONE NA 680 Mev. (Accumulation of Particles in a 680-Mev Synchrocyclotron). Danilov, V. I.; Enchevich, I. B.; Kulyukin, M. M.; Polferov, E. A.; Tomilina, T. N. (Joint Inst. for Nuclear Research, Dubna (USSR). Lab. of Nuclear Problems). 1966. 15p. Dep. mn.

A method of beam extraction from a synchrocyclotron based on the radial oscillation excitation by an alternating field during final acceleration radii is described. The accumulation of particles was achieved by switching of accelerator current at a certain alternating magnetic field radius point. The number of accumulated particles increased linearly to 13 accumulation cycles and reached the saturation at 30 cycles. In the latter case the intensity of the accumulated beam was 12 fold higher than the intensity of single pulse and comprised 2×10^{12} r/imp. Such a method of accumulation exceeds the experimental physical efficiency of the accelerator and enlarges the scope of synchrocyclotron operation as an injector for high energy accelerators. (tr-auth)

39493 (LA-DC-7776) HARD TUBE MODULATORS FOR THE LOS ALAMOS MESON FACILITY. Freyman, Robert W. (Los Alamos Scientific Lab., Univ. of California, N. Mex.). [1965]. Contract W-7405-eng-26. 9p. (CONF-660528-5). Dep. mn. CFSTI $1.00 cy, $0.50 mn.

From 9th Modulator Symposium, Fort Monmouth, N. J.

The super power r-f program for the Los Alamos Meson Facility requires modulators at 25 kv (250 amperes) and 45 kv (100 amperes). The modulators are capable of regulating during the pulse, operating into a variable impedance load, and maintaining control at all levels of current and voltage. Both modulators are designed around the Machlett ML-8618 magnetically beamed switch tube. The floating deck driver uses a single 5CX1500A driver tube. To cross the high voltage interface to the driver deck three approaches were used; an amplitude modulated r-f pulse, lightpipe, and pulse transformer. The modulators were conservatively designed for 1 millisecond pulses at 6% duty factor with 5% capacitor voltage slump. During the pulse the modulator must vary the power output of the r-f amplifier by as much as 30%. The r-f amplifiers may be operated either cathode or anode at d-c ground. (auth)

39494 (LNF-66/15) STUDIO DELLE PROPRIETA' OTTICHE DI UN MAGNETE A FOCHEGGIAMENTO FORTE (TIPO SACERDOTI-TAU). (Study of the Optical Properties of a Strong-Focusing Magnet (Sacerdoti-Tau Type)). Note No. 314. Borgia, B.; Joos, P.; Grilli, M. (Laboratori Nazionali di Frascati, Comitato Nazionale per l'Energia Nucleare (Italy)). Mar. 21, 1966. 41p. Dep. mn.

Magnetic and optical measurements were made of a strong-focusing magnet of the Sacerdoti-Tau type. The principal parameters of the magnet are tabulated. The B field was measured at various points along the principal trajectory and along the radial directions for various excitation currents of the magnet. The field index and the disperse field at the boundary were determined. The optical measurements were made with the wire method and the α method. The magnet constant, dispersion, resolving power, and focal distance were calculated from the measurement results. (J.S.R.)

39495 (LNF-66/22) STIMA DEI FONDI DI MACCHINA INTORNO AD ADONE. (Evaluation of the Apparatus Background Around the Adone). Note No. 319. Bernardini, M.; Tazzari, S. (Laboratori Nazionali di Frascati, Comitato Nazionale per l'Energia Nucleare (Italy)). Apr. 15, 1966. 10p. Dep. mn.

The existing background can be divided into the background from showers generated by electrons lost by mean-life effect and background from the interactions of circulating electrons with the residual gas. The approximations made in the calculation of both background sources are given, and the calculations were reported. (J.S.R.)

39496 (RHEL-R-117) THE PLUNGING MAGNET SYSTEM FOR THE NIMROD EXTRACTED PROTON BEAM. Major, J. H.; Swain, J. H. (Rutherford High Energy Lab., Science Research Council, Chilton (England)). Mar. 1966. 37p. Dep. mn. BIS $2.60. HMSO 13s.

A servo-controlled hydraulic mechanism for repetitively plunging the one-ton extraction magnet for the NIMROD extracted proton beam is described. (auth)

39497 (SLAC-65) TWO-MILE ACCELERATOR PROJECT. Quarterly Status Report, January 1-March 31, 1966. (Stanford Linear Accelerator Center, Stanford Univ., Calif.). June 1966. Contracts AT(04-3)-400; AT(04-3)-515. 88p. Dep. mn. CFSTI $3.00 cy, $0.75 mn.

The status of the Stanford Linear Accelerator and associated facilities is summarized, together with support activities. (B.G.D.)

39498 (UCRL-16809) BEVATRON OPERATION AND DEVELOPMENT. 49. JANUARY-MARCH 1966. Crebbin, Kenneth C.; Lothrop, Fred H. G.; Frias, Robert (Lawrence Radiation Lab., Univ. of California, Berkeley). May 24, 1966. Contract W-7405-eng-48. 20p. Dep. mn. CFSTI $1.00 cy, $0.50 mn.

The beam was on for experimenters 87.1% of the scheduled operating time. During the second half of 1965 a beam loss at 40 to 50 msec after injection had sporadically appeared and disappeared, causing a number of hours of lost operating time. It was determined this quarter that the new values of pole-face-winding currents set in July 1965 were in part responsible for this loss. By changing to a previous set of operating values, we were able to eliminate this sporadic loss, and have had no further outages due to early beam-loss problems. Damage was discovered in the epoxy coil potting on the septum of the first magnet in the external proton beam extraction system. It was not clear whether it was a radiation, thermal, or potting problem. A noise pickup problem that existed for some months was eliminated in the Bevatron beam induction-electrode system by the installation of a new cathode-follower circuit. This permitted use of the radius feedback system (Autotrack) to control the radial position of the beam during acceleration. The Autotrack system is necessary for beam tracking through a new mode of magnet pulsing known as mezzanine. Final tests of this mode of pulsing were made and mezzanine is about to become an operating mode at the Bevatron. (auth)

39499 (UCRL-16959) MAGNETOSTATIC COMPUTER PROGRAM TRIM OPERATIONS MANUAL. Colonias, John S. (Lawrence Radiation Lab., Univ. of California, Berkeley). Dec. 28, 1965. Contract W-7405-eng-48. 43p. Dep. mn. CFSTI $2.00 cy, $0.50 mn.

The capabilities and limitations of the magnetostatic computer program TRIM is described, with particular emphasis on the usage of this program, preparation of input data, and general utilization. The program is a general two-dimensional magnetostatic code capable of solving mathematical models of two-dimensional magnets. (auth)

39500 FORMATION OF HYDROGEN NEGATIVE IONS IN MERCURY VAPOR. Masuda, Seizo; Terasawa, Michitaka; Kumagai, Michikazu (Central Research Lab., Tokyo. Shibaura Electric Co., Kawasaki, Japan). Jap. J. Appl. Phys., 5: 719-24(Aug. 1966).

A negative ion source utilizing mercury vapor as a charge-exchange target was developed for a tandem electrostatic accelerator. Collision processes for hydrogen

ions passing through matter are discussed for negative ion production. It was found that a mercury vapor target gave larger hydrogen negative ion yields than a hydrogen gas target, and a maximum of 3.3% of the incident proton beam was converted to negative ions at an energy of 15 kev. (auth)

39501 TRAVELING-WAVE NATURE OF CHERENKOV INTERACTION. Stekert, James Joseph. Philadelphia, Univ. of Pennsylvania, 1965. 125p.

Thesis.

The traveling wave nature of Cherenkov interaction is examined by analyzing the dispersion properties of three circularly symmetric cylindrical systems. The primary system is composed of a circular waveguide, partially loaded with a uniform, isotropic dielectric, in which a density-modulated electron beam flows through a central passage. A dispersion equation is derived and analyzed for real and complex roots, which are interpreted in terms of mode coupling and wave kinematics in the dispersion plane. A discussion of wave kinematics and the dispersion properties of the beam and waveguide subsystems is included. A parallel investigation is afforded a simpler, completely homogeneous beam and waveguide system. Computer solutions for both the homogeneous and inhomogeneous systems are presented. The connection between the interaction in the inhomogeneous waveguide and the more familiar Cherenkov radiation into an unbounded dielectric is established by mathematically allowing the outer boundaries of the waveguide to recede, thereby establishing a new dispersion equation. The process of achieving the unbounded limit is discussed, and an appropriate description of the dispersion properties of the unbounded dielectric is evolved and identified with well-known Cherenkov characteristics. All systems studied are found to exhibit the Cherenkov threshold condition for interaction, as well as a slight dispersion about the characteristic Cherenkov propagation angle. Below threshold, each system is found to exhibit the characteristics of a beam in a drift space. It is concluded that the bounded and unbounded systems exhibit qualitatively identical traveling wave interactions. It is felt that the Cherenkov traveling wave interaction does not fundamentally differ from the more familiar forms of traveling wave interaction, other than in the specific properties of the dielectric as a slowing circuit. (TCO)

39502 VELOCITY SPECTROMETER, MARK 6 (Engineering Materials). (Lawrence Radiation Lab., Univ. of California, Berkeley). (CAPE–1414).

202 drawings.

This parallel-plate velocity spectrometer is used to study deflected beams from the Bevatron. Particles to be studied are selected by adjustment of the crossed electric and magnetic fields. (For details see TID-4100) (F.S.)

39503 MAGNETIC CENTER DETECTOR (Engineering Materials). (Stanford Linear Accelerator Center, Stanford Univ., Calif.). (CAPE–1420).

12 drawings.

The detector is used to determine the magnetic center of quadrupole magnets. The magnetic center line coincides with the center line of a charged particle beam. The drift tube of the Stanford Linear Accelerator is also described. (For details See TID-4100 Suppl. 35). (F.S.)

39504 ^{3}He PURIFICATION TRAP (Engineering Materials). (Los Alamos Scientific Lab., Univ. of California, N. Mex.). (CAPE–1434).

1 drawing.

The liquid nitrogen-cooled charcoal trap is used to continuously recover and purify He gas in the ion source of a variable-energy cyclotron. The system is completely interlocked to ensure safety. With a flow rate of 6 cc/min, ^{3}He loss in 200 hrs is less than 3 cc/hr. (For details see TID-4100). (F.S.)

39505 ION SOURCE FOR 42 IN. CYCLOTRON (Engineering Materials). (Los Alamos Scientific Lab., Univ. of California, N. Mex.). (CAPE–1433).

10 drawings.

The ion source for the 42-in. cyclotron consists of the source, cone, and the filament holder. Alternate cone designs are provided for protons or deuterons and for α particles. (For details see TID-4100) (F.S.)

39506 STANFORD 20 Bev ACCELERATOR EQUIPMENT (Engineering Materials). (Stanford Linear Accelerator Center, Stanford Univ., Calif.). (CAPE–1401).

67 drawings.

The thermionic diode housing and the beam position monitor are described. The diode is part of an automatic system used in phasing klystron power with the electric beam induced power. (For details see TID-4100) (F.S.)

39507 ORIC BIOLOGICAL EXPERIMENT EQUIPMENT /Q-2701/(Engineering Materials). (Oak Ridge National Lab., Tenn.). (CAPE–1407).

2 drawings.

A current integrator, controller, and decade scaler used to accurately measure and control the total exposure of a biological specimen to the beam from the ORNL Relativistic Cyclotron are described. (For details see TID-4100) (F.S.)

39508 STEPPED MAGNET (Engineering Materials). (Lawrence Radiation Lab., Univ. of California, Berkeley). (CAPE–1453).

3 drawings.

This 20-channel pulsed magnet sweeps the Bevatron particle beam across the 72-in. hydrogen bubble chamber in steps avoiding superimposed tracks. Each magnet has a short rise time and a long fall time. The scan is symmetrical with respect to the centerline of the beam. (For details see TID-4100). (F.S.)

39509 ELECTRIC DISCHARGE DEVICE FOR PRODUCING INTERACTIONS BETWEEN NUCLEI. Farnsworth, Philo T. (to International Telephone and Telegraph Corp.). U. S. Patent 3,258,402. June 28, 1966. Filed Jan. 11, 1962.

An electric discharge device for producing interactions between nuclei comprises means for forming space current, means for converging the space current toward a reference point in free space to produce a localized virtual cathode adjacent to that point, and means for propelling projectile particles through the virtual cathode at nuclear-reacting velocities so that the particles collide to produce nuclear reactions. The device, in one of its embodiments, is of spherical geometry in which a cathode concentrically surrounds an electron-permeable anode having an inner, concentric cavity or space. The anode and cathode are designed and assembled so as to form an electron-optical system in which the anodic space is maintained completely filled with the electrical discharge without the electrons reaching the anode structure itself. Transversing electrons follow radial paths through the space and are kept from being intercepted by the anode. The electron optics direct the electrons through the permeable portion of the anode toward the outer structural cathode. Electron temperature is maintained at a minimum value resulting in the development of a high-order-magnitude electron circulatory current which serves in producing the necessary potential gradient in the anodic space. An ion gun attached to the cathode generates and injects ions directly into the anodic space. The reactant products produced at the center by the ion or particle collisions vary depending upon operating parameters and the gases used. (B.L.M.)

39510 INTERNATIONAL CONFERENCE ON ISOCHRONOUS CYCLOTRONS, GATLINBURG, TENNESSEE, MAY 2–5, 1966. Shea, R. F. (ed.). IEEE (Inst. Elec. Electron. Eng.), Trans. Nucl. Sci., NS-13: No. 4, 1-531 (Aug. 1966). (CONF-660510).

Fifty-eight papers are included; separate abstracts were prepared for 45 papers and also the appendix. Thirteen papers were previously abstracted for NSA; see papers under CONF-660510 in the report number index. (L.B.S.)

For abstracts of individual papers see: 39511–39554, 39584, and 40101.

39511 PROBLEMS AND PERFORMANCE IN THE CYCLOTRON CENTRAL REGION. Blosser, H. G. (Michigan State Univ., East Lansing). IEEE (Inst. Elec. Electron. Eng.), Trans. Nucl. Sci., NS-13: No. 4, 1-14(Aug. 1966).

A good central region yields a compact, dense, well-centered beam in a phase interval which will optimize the following acceleration and extraction processes. A review is given of the role of various central region features in attaining desired beam properties. Results of careful calculations are shown to closely agree with observed beam properties. (auth)

39512 CENTRAL REGION STUDIES FOR INCORPORATING AN AXIAL ION SOURCE IN THE DAVIS 76-INCH CYCLOTRON. Kibbe, L. J.; Jungerman, J. A.; Peek, N. F. (Univ. of California, Davis). IEEE (Inst. Elec. Electron. Eng.), Trans. Nucl. Sci., NS-13: No. 4, 24-6(Aug. 1966).

Model studies were previously made on the 0.275 scale model magnet to determine if a satisfactory magnetic field could be achieved in the central region using an axial ion source originally designed for the 88-inch Berkeley cyclotron. Full scale radial profiles of the iron field resulting from the original model design compared with the profiles of the final design and the ORIC iron are presented. It is believed that the installation of the axial ion source will contribute reproducible operation as well as making possible future axial injection through an 8 inch axial hole in the top of the magnet. (L.B.S.)

39513 CENTRAL REGION OF 240 CM VARIABLE ENERGY CYCLOTRON. Litunovskii, R.; Nikolaev, V. (Scientific Research Inst. for Electrophysical Apparatus, Leningrad). IEEE (Inst. Elec. Electron. Eng.), Trans. Nucl. Sci., NS-13: No. 4, 27-9(Aug. 1966).

A description of the central optics for the 2.4 m isochronous cyclotron is given. The original orbits property studies were undertaken in order to obtain a compact ion beam at long time duration of the current pulse. In addition, the control flexibility requirement for the position of all central optics elements is taken into account, which is important for variable energy cyclotrons. (L.B.S.)

39514 NON-INTERCEPTING ION PHASE MEASURING EQUIPMENT OF THE ISOCHRONOUS CYCLOTRONS AT KARLSRUHE AND JUELICH. Feldmann, Hans-Helmut (AEG-Forschungsinstitut, Frankfurt am Main). IEEE (Inst. Elec. Electron. Eng.), Trans. Nucl. Sci., NS-13: No. 4, 30-5(Aug. 1966).

A non-intercepting ion phase measuring equipment is in use at the Karlsruhe cyclotron. Five phase signals, steadily and simultaneously displayed are presenting a good survey of phase width and phase distribution versus radius. High noise immunity is obtained by the use of differential electrostatic pickup probes. Concerning the Jülich cyclotron a similar device with twelve double electrostatic probes is in construction. (auth)

39515 MEASUREMENTS OF BEAM BEHAVIOR IN THE KARLSRUHE CYCLOTRON. Dietrich, Helmut (AEG-Forschungsinstitut, Frankfurt am Main). IEEE (Inst. Elec. Electron. Eng.), Trans. Nucl. Sci., NS-13: No. 4, 36-40(Aug. 1966).

From the measurements made during the first operation period of the Karlsruhe cyclotron those of radial beam density, phase width, and axial beam distribution are mentioned. Because of the satisfactory separation of the single orbits in a large radial range it has been easy to obtain information on the energy gain per turn, the amplitudes of the coherent radial oscillation and the radial dependence of the radial and axial betatron frequencies. (auth)

39516 BEAM PROPERTIES OF PHILIPS' A.V.F. CYCLOTRONS. van Kranenburg, A. A. (Philips' Research Labs., Eindhoven, Netherlands); Hagedoorn, H. L.; Kramer, P.; Wierts, D. IEEE (Inst. Elec. Electron. Eng.), Trans. Nucl. Sci., NS-13: No. 4, 41-7(Aug. 1966).

Some parameters determining the beam-quality and energy resolution, are discussed. Experiments were performed, and results are given. (auth)

39517 SINGLE TURN EXTRACTION. Gordon, M. M. (Michigan State Univ., East Lansing). IEEE (Inst. Elec. Electron. Eng.), Trans. Nucl. Sci., NS-13: No. 4, 48-57 (Aug. 1966).

Certain aspects of the resonance-extraction method which have not been treated before, or else only incompletely, are discussed, and an attempt made to clarify certain features of this process. It is demonstrated that an ideal central ray exists for accelerated orbits such that a beam centered on this ray will exhibit only insignificant coherent oscillations over most of the acceleration range. A semi-quantitative analysis of the orbit displacement produced by a resonance-extraction mechanism and the influence of the field bump parameters is provided. The section on voltage and field errors analyzes the effect of such errors and discusses the tolerances required for reliable performance. The succeeding section demonstrates that for an internal beam of 0.1 inch radial width the resonance extraction system does indeed produce clean turn separation, and discusses the factors which have brought the axial instability of the coupling resonance under control. The last section describes the procedure for optimizing the frequency so that for single-turn extraction the energy spread of the beam is minimized; this section also provides a comparison between single and multiple turn extraction with regard to energy spread and phase width in the extracted beam. (L.B.S.)

39518 EXTRACTION STUDIES IN AN AVF CYCLOTRON. Hagedoorn, H. L.; Kramer, P. (Philips' Gloeilampenfabrieken, Eindhoven, Netherlands). IEEE (Inst. Elec. Electron. Eng.), Trans. Nucl. Sci., NS-13: No. 4, 64-73(Aug. 1966).

For the extraction of the beam in an AVF cyclotron a regenerative system or an electrostatic channel can be used. Some factors of importance for the beam are discussed. Extraction with an electrostatic channel can give very high external beam quality and extraction efficiency. For such a system it is of importance whether the beam is extracted before or after the $\nu_R = 1$ resonance. The beam can even pass the $\nu_R = 2\nu_z$ resonance without blowing up vertically if attention is being paid to the radial oscillation amplitude and some machine parameters. The general orbit theory can be used for an analytical study of a regenerative system in an AVF cyclotron. (auth)

39519 VARIABLE ENERGY EXTRACTION FROM NEGATIVE ION CYCLOTRONS. Paul, Arthur C.; Wright, Byron T. (Univ. of California, Los Angeles). IEEE (Inst. Elec. Electron. Eng.), Trans. Nucl. Sci., NS-13: No. 4, 74-83(Aug. 1966).

Negative hydrogen ions are accelerated at a fixed magnetic field. The energy of an extracted beam is determined by the radius of a stripping foil and its azimuth and radius determine the exit point of the beam from the cyclotron. The exit points can be adjusted so that an auxiliary magnet causes the various extracted beams to enter a common beam transport system. Since February, 1966, external beams whose energy is variable from 25 to 50 Mev have been produced by the above means at UCLA and the University of Manitoba. A report is given on the UCLA system and its performance, special features of the Manitoba system are presented. (auth)

39520 STUDY OF THE MODIFIED RESONANCE EXTRACTION METHOD FROM A RELATIVISTIC CYCLOTRON. Dmitrievskii, V. P.; Kolga, V. V.; Polumordvinova, N. I.; Rybalko, V. S.; Sarkisyan, L. A.; Vorozhtsov, S. B.; Zamolodchikov, B. I.; Zaplatin, N. L. (Joint Inst. for Nuclear Research, Dubna, USSR). IEEE (Inst. Elec. Electron. Eng.), Trans. Nucl. Sci., NS-13: No. 4, 84-7 (Aug. 1966).

The problems involved in the extraction of accelerated particles from relativistic cyclotrons and conditions under which the resonance-extraction method can be effectively used are briefly discussed. A description is given of the

further development of a modified resonance method related to the 700-Mev relativistic cyclotron. (L.B.S.)

39521 OPERATING CHARACTERISTICS OF THE ORIC BEAM EXTRACTION SYSTEM. Hudson, E. D.; Lord, R. S.; White, W. H. Jr. (Oak Ridge National Lab., Tenn.). IEEE (Inst. Elec. Electron. Eng.), Trans. Nucl. Sci., NS-13: No. 4, 101-5(Aug. 1966).

Several modifications of the ORIC extraction system have been performed; a diagram is shown of the system including both electrostatic and electromagnetic elements. The operating characteristics and results of measurements of external beam characteristics and phase width are briefly discussed. (L.B.S.)

39522 SOME STUDIES ON REGENERATIVE BEAM EXTRACTION IN SYNCHROCYCLOTRONS. Kullander, S.; Lindbaeck, S.; Svanheden, A. (Uppsala Univ.). IEEE (Inst. Elec. Electron. Eng.), Trans. Nucl. Sci., NS-13: No. 4, 106-13(Aug. 1966).

It is shown that the extraction efficiency in a synchrocyclotron can be increased considerably by selecting proper values for the internal circulating beam parameters. A good energy homogeneity and a high microscopic duty cycle can be achieved simultaneously. A calculation for some relevant radial amplitudes and energy gains/turn gives the energy diagram. From this it can be found that, if the internal beam is composed of 0.4–0.6 cm incoherent radial amplitudes and if the useful acceleration voltages are 7.2–10.6 kv, the gross extraction efficiency is 40% for an energy spread of 300 kev. The duty cycle will be about 20%. These results are valid if the vertical amplitudes are small so that the median plane motion program is correct. (auth)

39523 SUPERCONDUCTING PLATES AS MAGNETIC SHIELDS. Benaroya, R.; Khoe, T.; Ramler, W. J. (Argonne National Lab., Ill.). IEEE (Inst. Elec. Electron. Eng.), Trans. Nucl. Sci., NS-13: No. 4, 114-18(Aug. 1966).

The effectiveness of magnetic shielding between superconducting niobium tin plates was studied. Shielding factors, field profiles, and gradients were established for transverse magnetic fields up to 19.5 kG. In addition, it was found that starting with a "frozen-in" field of –19.5 kG between the plates, it is possible to return the magnetic field to +19.5 kG suitable for particle acceleration, leaving –13.3 kG between the plates to establish reverse orbit curvature. The details of these studies are discussed for possible application to future accelerator extraction systems. (auth)

39524 CALCULATING THE DISTURBED MOTION OF PARTICLES IN CYCLIC ACCELERATORS. Wideroee, R. IEEE (Inst. Elec. Electron. Eng.), Trans. Nucl. Sci., NS-13: No. 4, 119-26(Aug. 1966).

A few examples demonstrate an elementary method of calculating the closed orbit in a cyclic accelerator when perturbative forces are present. The free oscillations can be found in a similar way, the criterion for stability being the same as for the strong focusing synchrotron. A steadily increasing extraction force will, however, destroy the condition necessary for resonance. (auth)

39525 POLARIZED ION SOURCES FOR CYCLOTRONS. Craddock, M. K. (Univ. of British Columbia, Vancouver). IEEE (Inst. Elec. Electron. Eng.), Trans. Nucl. Sci., NS-13: No. 4, 127-41(Aug. 1966).

Since their advent six years ago polarized ion sources have been successfully installed in 15 accelerators of various types around the world, including FF, FM, and isochronous cyclotrons. The advantages of sources over nuclear reactions for providing polarized particles are (1) greater intensity, (2) control of polarization mode and direction, and (3) freedom from background radiation from the primary target. Currently operating polarized ion sources can produce several tenth-microamperes of up to 80% polarized protons or 100% polarized deuterons and negative ion currents a thousand times smaller. Basic principles and recent developments in polarized ion source design and technology are reviewed, with particular reference to the problems peculiar to cyclotrons. Some of the major contributions to polarized ion source development have been made at cyclotrons laboratories, first at CERN and later at Saclay, where the powerful adiabatic passage process for inducing hyperfine transitions has been extensively developed. More recently, the achievement of axial injection at Birmingham and the successful acceleration of polarized particles in the isochronous cyclotrons there and at Saclay indicate that polarized ion sources installed on this latest range of cyclotrons could provide the most powerful tool yet for examing nuclear polarization phenomena in the intermediate energy region. (auth)

39526 ION INJECTION FROM EXTERNAL SOURCES. Powell, W. B. (Univ. of Birmingham, Eng.). IEEE (Inst. Elec. Electron. Eng.), Trans. Nucl. Sci., NS-13: No. 4, 147-59(Aug. 1966).

Low- and medium-energy cyclotrons are discussed. Some reasons for using external injection are given. At the present time injection is either in the median plane or axial. Among the possibilities for injection in the median plane are cycloidal motion along a sector edge, linear motion by electrostatic compensation, and high energy injection with trapping into cyclotron orbits by change of charge. In the axial direction all methods have much in common—focusing down a hole in the magnet pole and inflection into a cyclotron orbit. As an example of the problems and possibilities with external injection the axial method is discussed in more detail. Topics include basic principles, beam quality, variable energy arrangements, bunching and the choice of injection energy. (auth)

39527 POLARIZED PROTONS AND DEUTERONS SOURCE FOR AXIAL INJECTION INTO THE GRENOBLE ISOCHRONOUS CYCLOTRON. Ripouteau, F. A.; Tripier, R. V. (Univ., Grenoble, France). IEEE (Inst. Elec. Electron. Eng.), Trans. Nucl. Sci., NS-13: No. 4, 160-2 (Aug. 1966).

A 50-kv polarized proton and deuteron source is under construction for axial injection into the Grenoble isochronous cyclotron. Brief descriptions and diagrams are given of the Keller dissociator, Stern-Gerlach magnet, Abragam r-f system, and the new axial ionizer used. (L.B.S.)

39528 PHASE SPACE DENSITY STUDIES ON CYCLOTRON ION SOURCES. Mallory, M. L.; Blosser, H. G. (Michigan State Univ., East Lansing). IEEE (Inst. Elec. Electron. Eng.), Trans. Nucl. Sci., NS-13: No. 4, 163-70 (Aug. 1966).

Using the MSU source testing facility, the phase space density of a cyclotron-type ion source was computed from axial and radial emittance-area measurements at a variety of arc conditions and for a number of source geometries. Geometrical variations have thus far been principally concerned with explorations of the focusing effects of various source face shapes. Both axial and radial emittance areas from a normal flat source are found to have a considerable admixture of coherent motion which results in inefficient use of aperture and also, in combination with non-linear fields, can lead to an effective dilution of the phase space density. Moderate recessing of the source contributes a focusing force in both r and z and makes the phase space volume much more compact. The effects of plasma boundary and space charge are evidenced in the axial measurements. The axial plasma boundary is found to be concave. with the results that ions emitted from the top and bottom of the ion source slit are focused toward the median plane. Space charge effects are clearly discernible; the axial width of the beam linearly increases as a function of total beam current. In the radial emittance area measurements, an asymmetry of the radial position of maximum current which varied as arc current was found and traced to a shifting plasma boundary, which was the result of a strain displacement of the ion source filament. (auth)

39529 SPACE CHARGE EFFECTS AND CURRENT LIMITATIONS IN CYCLOTRONS. Reiser, Martin (Univ. of Maryland, College Park). IEEE (Inst. Elec. Electron. Eng.), Trans. Nucl. Sci., NS-13: No. 4, 171-8(Aug. 1966).

The effects of the electric fields generated by the ion

beam in a cyclotron are investigated theoretically on the assumption that the beam consists of well defined bursts of ions moving on separated orbits. The theoretical analysis is carried out in two steps by first calculating the field acting on an ion at the surface of an individual burst due to the charge contained in the burst itself and then adding the contributions of charges on neighboring orbits. The electric field is found to be a function of the burst's radial position, inversely proportional to the velocity (or radius) on the first turns and then rapidly leveling off at intermediate radii. The influence of various parameters (dimensions of the bursts, energy gain per turn, etc.), the changes in the betatron frequencies and current limitations due to the space charge forces are discussed and illustrated in a numerical example. (auth)

39530 NEW INJECTION METHOD FOR CYCLOTRONS. Beurtey, R.; Maillard, R.; Thirion, J. (CEN de Saclay, Gif-sur-Yvette, France). IEEE (Inst. Elec. Electron. Eng.), Trans. Nucl. Sci., NS-13: No. 4, 179-81(Aug. 1966).

The conditions necessary for injecting a charged-particle beam up to the center of a cyclotron in the median plane are considered. Three different systems were investigated, and the results are briefly discussed. (L.B.S.)

39531 HEAVY ION INJECTION FOR STRIPPING IN THE CENTRAL REGION OF THE CEVIL. Bieth, C.; Cabrespine, A.; Goldstein, Ch. (Nuclear Physics Inst., Orsay, France). IEEE (Inst. Elec. Electron. Eng.), Trans. Nucl. Sci., NS-13: No. 4, 182-90(Aug. 1966).

A plan to inject a heavy-ion beam, previously accelerated, into the median plane of the Orsay CEVIL is discussed. The heavily charged ions, obtained after the stripping operation in the central region of the cyclotron, can achieve an energy proportional to the square of the charge number. The choice of injection energy represents, in fact, a compromise between price and performance. The e/m ratio, chosen to be ±0.1, will give the possibility of accelelerating heavy ions up to bromine, and krypton. The injector will be a linear accelerator, either pulsed or continuous. The distance between the linear accelerator and the cyclotron will allow the debunching of beam packets, at the r-f frequency (25 Mc/s). The drift tube circuit is similar to the Manchester one. The problem of the focusing system is considered in order to obtain an accelerated beam of more than 100 μA. The chosen solution was strong focusing grids, obtained by means of two parallel tungsten strips placed at the beginning of each drift tube, each pair being at 90° to the preceeding one. The theoretical studies of this apparatus are well advanced at present; the industrial production of the main elements is under way. The whole equipment should be completely finished in July 1967. (auth)

39532 STUDY OF AXIAL INJECTION FOR THE GRENOBLE CYCLOTRON. Belmont, J. L.; Pabot, J. L. (Faculte des Sciences, Grenoble, France). IEEE (Inst. Elec. Electron. Eng.), Trans. Nucl. Sci., NS-13: No. 4, 191-3(Aug. 1966).

The possibility of injection of ions into a cyclotron through a hole drilled in the axis of the yoke was investigated. A deflection system that satisfies the conditions for the Grenoble cyclotron is discussed. An electron model using a vertical 1035-ev electron beam and a 42.5 gauss constant magnetic field was built in order to check the functioning of the deflection system. The system simulates proton injection at 62.5 kev with a magnetic field of 141,500 gauss. The injection principle was shown to operate with electrons. (L.B.S.)

39533 PROGRESS REPORT ON THE 500 Mev ISOCHRONOUS CYCLOTRON MESON FACTORY OF ETH ZURICH. Blaser, J. P.; Willax, H. A. (Eidgenoessische Technische Hochschule, Zurich). IEEE (Inst. Elec. Electron. Eng.), Trans. Nucl. Sci., NS-13: No. 4, 194-214 (Aug. 1966).

The goal is a continuous external proton beam of the order of 100 μA, the usable current depending mainly on extraction rate because of activation. The energy of 500 Mev is best suited to produce high fluxes of low energy or stopped mesons. The main fields of the research planned are: properties and interactions of mesons and nucleons, nuclear structure physics and medical and biological applications. The use of internal targets in field free regions as well as external targets should provide a great variety of beams for simultaneous experiments. The two-stage accelerator has a 70 Mev sector focussed cyclotron for injection into an isochronous ring accelerator consisting of eight spiral sector magnets. Four cavities operating at 50 MHz should provide at least 1 Mev energy gain per turn. In the course of present development the main fields of work are orbit dynamics and measurement on 1 : 5 scale magnets and design of a 1 : 1 model magnet sector. ν_z is to be kept around 0.95 throughout acceleration and $\nu_r = 1.5$ may be used for resonance extraction. Experiments to reach high gap voltage on a full scale cavity in vacuum are in progress (200–300 kv obtained at present). Remaining problems are some aspects of mechanical structure, in particular the vacuum chamber and schemes for quantitative extraction and secondary beam production from external targets at very high radioactivity levels. Funds of 21 million dollars have been approved for construction of accelerator and buildings. A building time of 5 to 6 years is expected if development can continue in favorable conditions. (auth)

39534 DEVELOPMENT AND PROSPECTS FOR THE APPLICATION OF MESON FACTORIES. Dmitrievskii, V. P.; Dzhelepov, V. P.; Kolga, V. V.; Zamolodchikov, B. I. (Joint Inst. for Nuclear Research, Dubna, USSR). IEEE (Inst. Elec. Electron. Eng.), Trans. Nucl. Sci., NS-13: No. 4, 215-19(Aug. 1966).

The development and construction of accelerator designs for meson factories are surveyed. The proposed utilization of the meson factory for experimental investigations of fundamental particle physics and the atomic nucleus and also for outlining new ways for developing the branch of science in the pre-Bev region is treated. The development of theory, central optics in relativistic cyclotrons, and the development of the cyclotron accelerator method are discussed. (L.B.S.)

39535 PROPOSAL FOR A SECTOR-FOCUSING SYNCHROCYCLOTRON. Kullander, S.; Holm, S.; Johansson, B.; Tidriks, A. (Uppsala Univ.). IEEE (Inst. Elec. Electron. Eng.), Trans. Nucl. Sci., NS-13: No. 4, 227-34(Aug. 1966).

A modification is proposed for the Uppsala 185-Mev synchrocyclotron to obtain a high intensity beam of different particles. By introducing sectors, a radially increasing magnetic field can be used. The reduced bandwidth makes it possible to replace the present rotating condenser by an electronically tuned broadband system. Protons will be accelerated with decreasing and heavier particles with increasing frequencies. No correction coils are required. Expected external currents are of the order of 10 μamp. (auth)

39536 NEVIS SYNCHROCYCLOTRON CONVERSION PROJECT. Cohen, R. (Columbia Univ., New York). IEEE (Inst. Elec. Electron. Eng.), Trans. Nucl. Sci., NS-13: No. 4, 240-3(Aug. 1966).

Studies directed towards improving the beam quality and intensity of the NEVIS synchrocyclotron by conversion to a partially isochronous cyclotron are discussed. (L.B.S.)

39537 POSSIBLE IMPROVEMENTS TO THE CARNEGIE INSTITUTE OF TECHNOLOGY SYNCHROCYCLOTRON. Foss, M. H. (Carnegie Inst. of Tech., Saxonburg, Pa.). IEEE (Inst. Elec. Electron. Eng.), Trans. Nucl. Sci., NS-13: No. 4, 244-6(Aug. 1966).

Some modifications proposed for increasing the beam energy and intensity of the 450-Mev synchrocyclotron are presented. Two computer programs are described for calculating the orbit of an ion in a magnetic field and for calculating the magnetic potential on the points of a mesh. (L.B.S.)

39538 STRONG FOCUSSING RING, AS BEAM STRETCHER FOR SYNCHROCYCLOTRONS. Brianti,

G.; Skarek, P. (CERN, Geneva). IEEE (Inst. Elec. Electron. Eng.), Trans. Nucl. Sci., NS-13: No. 4, 247-54 (Aug. 1966).

The possibility of injecting the synchrocyclotron extracted proton beam into a strong focusing ring called CYBEST, is investigated. It is seen that pion beams produced in internal targets of such a device show some advantages with respect to present synchrocyclotron beams. More detailed studies are needed however for final judgement. CYBEST is realizable if a sufficiently fast extraction from the synchrocyclotron could be obtained. The magnetic structure is simple but occupies a large area and the required aperture is also relatively large. (auth)

39539 DESIGN OF AVF CYCLOTRONS ABOVE 100 Mev. Avery, Robert T.; Brobeck, William M.; Meads, Philip F. Jr. (William M. Brobeck and Associates, Berkeley, Calif.). IEEE (Inst. Elec. Electron. Eng.), Trans. Nucl. Sci., NS-13: No. 4, 255-61(Aug. 1966).

Certain problems associated with cyclotrons in the energy range above 200 Mev are discussed and possible solutions suggested. These concern: producing the flutter and profile changes required for the acceleration of a wide range of particles and energies, the proportion between rf wave length and the exit radius, phase acceptance, phase slip at extraction, extraction electrical field, turn separation and tolerances on the power supplies. Computer applications in this energy range are also discussed. (auth)

39540 H^- MESON FACILITY. Vogt, Erich W. (Univ. of British Columbia, Vancouver); Richardson, J. Reginald. IEEE (Inst. Elec. Electron. Eng.), Trans. Nucl. Sci., NS-13: No. 4, 262-76(Aug. 1966).

With the continuing evolution of the various types of meson factories the relative merits of the H^- spiral ridge cyclotron appear to be improving. The development and design of such an accelerator has been led by UCLA. Recently three universities in British Columbia have combined personnel for a design study intended to lead to an H^- meson facility (called TRIUMF—Tri University Meson Facility). Among the various meson factories the H^- facility is the only one which combines the following advantages: (1) large duty factor; (2) variable energy; (3) ease of beam extraction; (4) use of simultaneous beams; (5) high beam quality. Until recently it faced two problems: (a) uncertainty about field dissociation of negative ions; (b) lack of polarized ion sources. Recent UCLA measurements of field dissociation and the advent of polarized H^- ion sources and axial injection into cyclotrons remove these problems. The field dissociation measurements agree with Hiskes' calculations and enable the use of higher fields than previously proposed for H^- facilities. The TRIUMF project concerns a machine whose beam characteristics (maximum energy 500 Mev; maximum beam radius 271 inches; beam current 20–100 μA) were selected for optimum use in nuclear structure experiments, for low cost, and for operating simplicity. (auth)

39541 SEPARATED-ORBIT CYCLOTRON. Martin, J. A. (Oak Ridge National Lab., Tenn.). IEEE (Inst. Elec. Electron. Eng.), Trans. Nucl. Sci., NS-13: No. 4, 288-99(Aug. 1966).

The developments in SOC design during the past three years are discussed. A brief review is given of the separated-orbit cyclotron programs at Rutherford High Energy Laboratory (RHEL), Chalk River Nuclear Laboratories (CRNL) of Atomic Energy of Canada Limited, and the Oak Ridge National Laboratory (ORNL). (auth)

39542 RESEARCH POSSIBILITIES WITH AN INTENSE NEUTRON GENERATOR. Bartholomew, G. A. (Atomic Energy of Canada Ltd., Chalk River, Ont.). IEEE (Inst. Elec. Electron. Eng.), Trans. Nucl. Sci., NS-13: No. 4, 300-8(Aug. 1966).

The development of an intense neutron generator (ING) facility using a high-current intermediate-energy proton accelerator is discussed. A description is given of the presently conceived layout of the ING facility, and research capabilities are summarized in terms of neutron beam characteristics. (L.B.S.)

39543 SUPER-SOC. Russell, F. M. (Rutherford High Energy Lab., Chilton, Eng.). IEEE (Inst. Elec. Electron. Eng.), Trans. Nucl. Sci., NS-13: No. 4, 309-12 (Aug. 1966).

A new concept in cyclic particle accelerators is described in which time harmonic accelerating fields are produced without recourse to conventional power amplifiers. Instead, the accelerating fields are produced by extracting energy from a bunched beam of particles. In essence the new machine consists of two intimately connected separated-orbit cyclotrons, one of which is operated in the decelerating mode. The decelerating particles obtain their energy initially from a d-c high voltage supply. (auth)

39544 RESEARCH WITH AVF CYCLOTRONS IN EUROPE. Schopper, H. (Technische Hochschule, Karlsruhe, Ger. Kernforschungszentrums, Karlsruhe, Ger.). IEEE (Inst. Elec. Electron. Eng.), Trans. Nucl. Sci., NS-13: No. 4, 318-25(Aug. 1966).

A survey is presented of typical experiments performed with AVF cyclotrons in Europe. Four types discussed include high-energy resolution experiments, optical model studies, time-of-flight experiments, and polarization experiments. (L.B.S.)

39545 ION OPTICAL STUDIES OF EXTRACTION TRANSPORT AND ANALYSIS SYSTEMS FOR 240 CM CYCLOTRON. Barkovskii, V. N.; Basargin, Yu. G.; Litunovskii, R. N.; Minyaev, O. A.; Popov, A. V.; Stepanov, A. V. (Scientific Research Inst. for Electrophysical Apparatus, Leningrad). IEEE (Inst. Elec. Electron. Eng.), Trans. Nucl. Sci., NS-13: No. 4, 344-8(Aug. 1966).

High demands on beam quality of modern cyclotrons led to studies on the problems of extraction and transport of particles. In the 240 cm cyclotron design six experimental rooms with total area of about 1000 m^2 are provided. Some results of electronic computer calculations of the extraction and transport systems' parameters are given. A brief description of secondary particle analyzers is also given. (auth)

39546 NOVEL DEFLECTION-BUNCHING SYSTEM AT THE KARLSRUHE ISOCHRONOUS CYCLOTRON USED WITH A NEUTRON TIME-OF-FLIGHT-SPECTROMETER. Cierjacks, S.; Duelli, B.; Kropp, L.; Loesel, M.; Schweickert, H.; Unseld, H. (Kernforschungszentrum, Karlsruhe, Ger.). IEEE (Inst. Elec. Electron. Eng.), Trans. Nucl. Sci., NS-13: No. 4, 353-9(Aug. 1966).

A system consisting of two coupled electrostatic deflectors and the associated electronics is described. The principle of the system is illustrated. One deflector, which is located near the center of the machine, is used for a two-fold purpose (a) to eliminate two out of three microstructure pulses by deflection to a beam stop and (b) to form ion bunches of 4.5 μsec duration each consisting of fifty microstructure pulses. A second pair of deflector plates is located at a mean radius of 39 inches and serves to simultaneously deflect the set of microstructure pulses to a target positioned above the median plane of the cyclotron. At the time of deflection, the bunch is distributed over 4 inches in radius. Using this method neutron pulses of 1 ± 0.3 nsec duration with a repetition rate of 20 kc/sec can be produced. A neutron time-of-flight spectrometer has been put in operation using this "deflection-bunching" system. (auth)

39547 MACHINE DEVELOPMENT AT THE BERKELEY 88-INCH CYCLOTRON. Burger, R.; Clark, D. J.; Close, E.; Kim, H. (Univ. of California, Berkeley). IEEE (Inst. Elec. Electron. Eng.), Trans. Nucl. Sci., NS-13: No. 4, 364-70(Aug. 1966).

Machine development at the 88-inch cyclotron is described. Topics include instrumentation, deflector development, a radioactivity survey of the dee tank, and computer calculations on the gap-crossing resonance. Studies were made of external beam energy spread and pulse shape. Axial injection progress is describe

ommendations are made for design improvements on the 88-inch cyclotron. (auth)

39548 SURVEY OF ISOCHRONOUS CYCLOTRON TECHNOLOGY. Grunder, H. A. (Univ., Basel). IEEE (Inst. Elec. Electron. Eng.), Trans. Nucl. Sci., NS-13: No. 4, 371-9(Aug. 1966).

A survey is presented of isochronous cyclotron technology for existing and proposed machines operating from 8 to 130 Mev. Some of the topics discussed include: experimenters specification, operation, construction and startup, magnetic guide field, auxiliary coils, polarized particles, r-f systems, vacuum, extraction, septums, and cyclotron development. (L.B.S.)

39549 EXPERIMENTS ON ION ACCELERATION AT 685-mm SECTOR CYCLOTRON. Barkovskii, V.; Vasilev, V.; Litunovskii, R.; Minaev, O.; Nikolaev, V.; Stepanov, A.; Fodorov, A. (Scientific Research Inst. for Electrophysical Apparatus, Leningrad). IEEE (Inst. Elec. Electron. Eng.), Trans. Nucl. Sci., NS-13: No. 4, 380-2(Aug. 1966).

A brief review is given of the design, magnetic field characteristics, and ion-acceleration experiments for the 685-mm sector cyclotron. (L.B.S.)

39550 ACCELERATION OF H^- IONS AND EXTRACTED BEAM MEASUREMENTS IN THE MILAN CYCLOTRON. Acerbi, E.; Castiglioni, M.; Dutto, G.; Resmini, F.; Strini, G.; Succi, C.; Tagliaferri, G. (Univ., Milan. Istituto Nazionale di Fisica Nucleare, Milan). IEEE (Inst. Elec. Electron. Eng.), Trans. Nucl. Sci., NS-13: No. 4, 383-6 (Aug. 1966).

The characteristics of the proton beam extracted from the Milan AVF cyclotron by H^- ion stripping were studied. Quality and phase measurements were made in an external beam which was obtained without any geometrical definition of the internal H^- beam path. (auth)

39551 OPERATION OF THE ORSAY CEVIL AND ITS EXTRACTION SYSTEMS. Bourgarel, M. P.; Bieth, C.; Cabrespine, A.; Debray, P.; Martin, E. (Nuclear Physics Inst., Orsay, France). IEEE (Inst. Elec. Electron. Eng.), Trans. Nucl. Sci., NS-13: No. 4, 387-93(Aug. 1966).

It is possible to obtain an isochronous magnetic field over a wide range of average induction for a given ion by changing the structure of the electromagnet. This new structure allows great reduction of correcting adjustments. Encouraging results were obtained at Orsay by the use of shims with variable permeability and damping gaps. Only two correction coils were necessary to make the average field isochronous to within 30 gauss, for all the ions. The internal beam tests confirmed the good quality of the magnetic field and verified the theoretical calculations; the intensity of the multicharged ion beam was generally greater than the initial evaluation. Two extractors are at present set up: an electrostatic deflector and a stripping extractor. This latter device preserves the optical qualities of the beam. Furthermore, one or more simultaneous beams can be obtained with an excellent efficiency, and with various energies, depending on the radius. (auth)

39552 CONTROL OF THE MICHIGAN STATE UNIVERSITY CYCLOTRON. Berg, R. E.; Blosser, H. G.; Gordon, M. M. (Michigan State Univ., East Lansing). IEEE (Inst. Elec. Electron. Eng.), Trans. Nucl. Sci., NS-13: No. 4, 394-400(Aug. 1966).

To operate the MSU cyclotron, controls are set to precomputed values prepared by a computer program known as SETOP; to obtain a complete set of operating instructions the experimenter need only specify the particle of interest and a field identification number roughly proportional to energy. The program uses this information along with measured field data and a pre-computed set of ideal fields to determine the desired "operating point" in a straightforward series of calculations: (1) the fields at the desired excitation are synthesized by interpolation in the measured field data, (2) an average field is obtained using a modified least squares fit of the desired average field by the trim coils, and (3) the r-f frequency is determined so as to minimize the energy spread of the beam in a single turn at the extraction energy. The procedure used in SETOP to determine such operating points, and the principal features of these computations are described. A typical SETOP sheet is presented along with instructions for its use. Results of beam measurements are in excellent agreement with computed beam behavior. (auth)

39553 CONVERSION OF KAZAKHSTAN CYCLOTRON TO A VARIABLE ENERGY ISOCHRONOUS CYCLOTRON. Nemenov, L. M.; Arzumanov, A. A.; Bersenev, P. A. (Inst. of Nuclear Physics, Alma-Ata, USSR). IEEE (Inst. Elec. Electron. Eng.), Trans. Nucl. Sci., NS-13: No. 4, 411-16(Aug. 1966).

The main design features of the 150-cm Kazakhstan cyclotron are described, and the proposals for converting to a variable energy sector cyclotron are discussed. Results of measurements made on a 1:3 model magnet are presented. (L.B.S.)

39554 APPENDIX: ISOCHRONOUS CYCLOTRONS, STATUS AND PROGRESS SUMMARIES. IEEE (Inst. Elec. Electron. Eng.), Trans. Nucl. Sci., NS-13: No. 4, 417-19(Aug. 1966).

The specifications of isochronous cyclotrons proposed, under construction, or in operation in various countries are tabulated. Status and progress summaries are presented on each cyclotron. (L.B.S.)

Astrophysics and Cosmology

Refer also to abstracts 39963 and 40144.

39555 GRAVITATIONAL COLLAPSE AND SCALAR INTERACTION IN SUPERDENSE MATTER. Pacini, Franco (Institut d'Astrophysique, Paris). Ann. Astrophys., 29: 193-5(May-June 1966).

The problem of the gravitational collapse is considered for a uniform, spherically symmetrical assembly of particles by assuming that the particles interact via a short-range attractive scalar field. When the particle density exceeds a critical value, states of negative density arise. As consequence, the collapse of the configuration becomes impossible and the mechanical behavior of the body is identical to that investigated by Hoyle and Narlikar in the framework of the steady-state cosmology. (auth)

39556 EVAPORATIVE AND HYDRODYNAMICAL ATMOSPHERIC MODELS. Lemaire, J. (Institut d'Astrophysique, Cointe-Sclessin, Belg.). Ann. Astrophys., 29: 197-203(May-June 1966).

A comparison between Chamberlain's evaporative model and his "solar breeze" model, and Opik and Singer's evaporative model and Parker's "solar wind" model ($\alpha = 3/2$), shows that, in both cases, the asymptotic behavior at great radial distances ($r \to \infty$) of the density (ρ), mean velocity (W), and non-radial pressure components ($T_{\theta\theta}$ or $T_{\varphi\varphi}$) are the same for the evaporative and hydrodynamical models. In both evaporative models the radial component (T_{rr}) of the pressure tensor is greater than the other ($T_{\theta\theta}$ or $T_{\varphi\varphi}$). This anisotropy is growing with increasing radial distances. Therefore the assumed isotropic pressure of the ordinary hydrodynamical models is probably too low. (auth)

39557 MORPHOLOGICAL STUDY OF THE MAGNETIC STRUCTURE IN THE ACTIVE REGIONS WITH RELATION TO CHROMOSPHERIC PHENOMENA AND SOLAR FLARES. I. MAGNETIC AND FLARE CLASSIFICATION. Martres, M.-J.; Michard, R.; Soru-Iscovici, I. (Observatoire de Meudon, France). Ann. Astrophys., 29: 245-8(May-June 1966). (In French).

On the basis of 194 "qualitative" maps of longitudinal magnetic field in 57 solar active regions observed in Meudon (October 1962-December 1963) a scheme of magnetic classification is suggested. This scheme takes also into account the fields outside sunspots, of intensity higher than about 50 gauss. The production of flares by an active region is closely related to its class in the new system. (auth)

39558 MORPHOLOGICAL STUDY OF THE MAGNETIC STRUCTURE IN THE ACTIVE REGIONS WITH RELATION TO CHROMOSPHERIC PHENOMENA AND SOLAR FLARES. II. LOCALIZATION OF BRIGHT PLAGES, FILAMENT AND FLARES. Martres, M.-J.; Michard, R.; Soru-Iscovici, I. (Observatoire de Meudon, France). Ann. Astrophys., 29: 249-53(May-June 1966). (In French).

Morphological relations between magnetic fields, bright plages in K and H_α, filament and flares are described. Various results already known are confirmed or precised. In addition, it is shown that, when a flare is made up of two or more bright points (the most general case) these are distributed along both sides of a line of change of magnetic polarities. (auth)

39559 SECULAR VARIATIONS IN THE MAGNETIC FIELD STRENGTH OF SUNSPOT GROUPS. Ringnes, Truls S. Astrophys. Norv., 10: 27-68(Mar. 1965).

The relation between area and magnetic field strength of sunspot groups, the magnetic life history of long-lived spots, and frequency distribution of observed maximum field strength of sunspot groups have been studied over the period 1917–1958. The secular variations which are detected are discussed and compared with the secular variations established previously in the number of sunspot groups, their areas, area distribution, etc. A brief account is given of the eighty-year cycle of sunspots. (auth)

39560 GRAVITATION AND THE ABUNDANCE OF HYDROGEN. Gehlot, G. L.; Durgapal, M. C. (Univ. of Jodhpur, India). Austral. J. Phys., 19: 531-4(Aug. 1966).

The effect of gravitation on the physical constants was used in an investigation of the formation of elements in the Universe. It is shown that there should be an abundance of hydrogen. (auth)

39561 VARIABILITY OF FLUXES OF THE MAGNETIC FIELDS OF SUNSPOTS AND FACULAE. Zhulin, I. A.; Mogilevskiy, E. I. (Inst. of Terrestrial Magnetism, Ionosphere and Radio Wave Propagation, Academy of Sciences, USSR). Geomagn. Aeronomy (USSR) (Engl. Transl.), 5: 856-8(1965).

Translated from Geomagn. Aeronomiya, 5: 1092-4(1965).

An attempt is made to determine the independence of the variability of the magnetic fields of sunspots and neighboring faculae. Some of the data are included on local magnetic fields on the sun obtained from systematic observations at Mount Wilson during the IGY. (J.H.M.)

39562 THERMAL INSTABILITIES IN THE SOLAR CHROMOSPHERE. Hunter, James H. Jr. (Yale Univ., New Haven). Icarus, 5: 321-8(July 1966).

The thermal stability of small amplitude disturbances in the solar chromosphere is examined. It is shown that linear waves can be amplified by thermal instability, and that, under chromospheric conditions, the growth rates for the wave amplitudes can be of the same order as the observed rise times for solar flares. In addition, the velocities of linear wave propagation are shown to be of the same order of magnitude as the observed rates of flare expansion. It is suggested that the optical flare event be identified with the formation of shock waves in the chromosphere, which develop as a result of the thermal overstability of small amplitude waves. Finally, reasons are given for believing that thermal instabilities would occur near active solar regions. (auth)

39563 DIFFERENT CLASSES OF SOLAR AND SOLAR TERRESTRIAL EVENTS IN RELATION TO THE PHASE OF THE SOLAR CYCLE. Basu, D.; Das Gupta, M. K. (Univ. of Calcutta). Indian J. Phys., 40: 117-25 (Mar. 1966).

The frequency of occurrence of solar and solar-terrestrial events in relation to the phase of the solar cycle was studied for the period 1956–63. The events include sunspot, Ca-plage, solar flare, solar radio burst at meter wavelengths, geomagnetic storm, and short wave fadeout. Each event was classified into four different groups—viz., small, moderate, large, and outstanding—depending on its degree of activity. It was found that solar and solar-terrestrial phenomena show maximum correlation with sunspot cycle when considered as a whole (without classification) as also for small, moderate and large magnitudes of their activities. Outstanding events of all types tend to occur during the ascending phases of the solar cycle, avoiding the peak phase. (auth)

39564 SOLAR COSMIC-RAY MULTIPLY CHARGED NUCLEI AND THE JULY 18, 1961, SOLAR EVENT. Biswas, S. (Tata Inst. of Fundamental Research, Bombay. Goddard Space Flight Center, Greenbelt, Md.). J. Geophys. Res., 71: 4071-7(Sept. 1, 1966).

Energetic helium and heavy nuclei ($Z \geq 3$) were detected in the July 18, 1961, solar particle event. This result brings to four the number of solar cosmic-ray bursts in which heavy nuclei were seen. The particles were detected in nuclear emulsions flown on a balloon launched from Fort Churchill shortly after the associated flare appeared on the sun. The average flux of medium nuclei ($6 \leq Z \leq 9$) during the early part of the solar event was 12.0 ± 1.8 particles m^{-2} $ster^{-1}$ sec^{-1} in the energy interval from 120 to 204-Mev/nucleon, or about 40 times the normal galactic cosmic-ray medium nuclei flux at that particular time in the solar cycle. The helium-to-medium nuclei ratio in the same energy interval was 79 ± 16. These values are consistent with those anticipated on the basis of the relative abundance of hydrogen, helium, and medium nuclei in other events. Some large nuclei ($Z \geq 10$) were detected, but light nuclei were so rare that only an upper limit to their abundance could be set ($L/M \leq .07$). The unbiased acceleration of multiply charged nuclei in every major solar event now seems more certain, and, therefore, it seems to be worth considering this feature in any theory of solar particle acceleration. (auth)

39565 SEARCH FOR THE QUIET-TIME SOLAR GAMMA RAYS FROM BALLOON ALTITUDES. Frost, K. J. (Goddard Space Flight Center, Greenbelt, Md.); Rothe, E. D.; Peterson, Laurence E. J. Geophys. Res., 71: 4079-89(Sept. 1, 1966).

A balloon observation at 3.5 g cm^{-2} over Minneapolis on June 10, 1962, has resulted in upper limits from the quiet sun of less than 0.05 count cm^{-2} sec^{-1} over the range to 800 kev. This limit is considerably below those previously available. The detector consisted of a 3.4-cm diameter by 5.4-cm NaI crystal surrounded, except for a 1-ster forward aperture, by a 14.6-cm diameter and 20 cm long CsI collimating shield connected in active anticoincidence. The detector was servo-controlled to observe the sun, 180° in azimuth from the sun, as well as vertical, horizontal, and downward. The differences between the rates pointing to and away from the sun give upper limits for the solar flux at a 95% confidence level of 0.058, 0.048, 0.050, and 0.043 count cm^{-2} sec^{-1} Mev^{-1} over the 163–325, 325–488, 488–651, and 651–774 kev range, respectively. Since the Crab nebula was in the detector aperture during the flight, these upper limits also apply to that object. Correction for the counter efficiency will give upper limits for the true flux somewhat higher than the above numbers, depending on the shape of the photon spectrum. Observation of the diffuse background γ-ray spectrum over this range due to cosmic-ray interactions in the atmosphere gave a result of 0.72 count cm^{-2} sec^{-1} $ster^{-1}$ Mev^{-1} around 300 kev, in general agreement with Peterson's previous results. The atmospheric line at 0.5 Mev due to positron annihilation was resolved. A γ-ray line at 660 kev was also detected and was determined to be due to ^{137}Cs from fallout debris. The implied activity is $8 \pm 2 \times 10^{-3}$ disintegrations per g sec, averaged from 70,000 to 128,000 feet. Additional information pertinent to the application of this detector system to γ-ray astronomy was obtained. (auth)

39566 HYDROGEN-BURNING MODELS FOR STARS IN THE HORIZONTAL BRANCH OF GLOBULAR CLUSTERS. Peterson, Jorgen Otzen (Copenhagen Univ. Observatory). Kongel. Dan. Vidensk. Selsk., Mat.-Fys. Medd., 34: No. 16, 35p(1966).

The structure of stars in the horizontal branch of

globular clusters is discussed, and hydrogen-burning models, assumed to be mixed by the helium flash, are studied in detail to investigate whether such model sequences can provide an accurate description of the observed properties of horizontal branch stars. It is shown that homogeneous models with reasonable masses and chemical compositions correspond satisfactorily to the hottest stars of the observed horizontal branches, but in the later, fast stages their evolutionary tracks fall more than one magnitude above the horizontal branch region. Models containing an outer zone of the original chemical composition are shown to be placed along the horizontal branch, the position being determined by the mass fraction of the outer zone. Also their evolutionary tracks will, in general, fall above the branch when the fast evolution after the hydrogen burning in the central region starts. Hence, according to this interpretation the horizontal branch is not an evolutionary sequence, but rather a main-sequence-like phenomenon. From a comparison of the model sequences with observed color magnitude diagrams for M5 and M15, it is concluded that such sequences can explain several features of the observed diagrams satisfactorily. It is emphasized that the time scale for the evolution agrees reasonably well with the empirical value determined for M3. These results may be understood if the helium flash gives rise to mixing of the stars, and this mixing is more violent for stars poor in metal than for stars rich in metal. Some other predictions based on this picture of the evolution of horizontal branch stars are provided. (BBB)

39567 EXPULSION OF MAGNETIC FLUX BY EDDIES. Weiss, N. O. (United Kingdom Atomic Energy Authority, Abingdon, Eng.). Proc. Roy. Soc. (London), Ser. A, 293: 310-28(Aug. 9, 1966).

A convective eddy imposed on an initially uniform magnetic field in a highly conducting fluid distorts the lines of force and amplifies the field. Flux is concentrated outside the eddy; within it, the field grows and its scale of variation decreases until resistive effects become important. Closed lines of force are then formed by reconnection. The central field decays and a steady state is reached. Within a period, small compared with the characteristic time for resistive decay, magnetic flux is almost entirely expelled from regions of rapid motion and concentrated at the edges of convection cells. This process is demonstrated from numerical experiments. The results are applied to the sun, where the concentrated fields are strong enough to inhibit convection locally. (auth)

39568 PROBLEMS OF STAR FORMATION. II. Mestel, L. Quart. J. Roy. Astron. Soc., 6: 265-98(Dec. 1965).

Gravitational instability in a non-rotating medium permeated by a strong large-scale magnetic field of simple structure is studied. Strict freezing of the field into the gas is assumed as a plausible working hypothesis. Conditions for gravitational binding, gravitational collapse of a magnetic cloud, and fragmentation of a magnetic cloud are considered. Star formation in rotating magnetic clouds is studied in detail. (W.D.M.)

39569 EVIDENCE FOR HYDROMAGNETIC WAVES IN THE INTERPLANETARY PLASMA. Coleman, Paul J. Jr. (Univ. of California, Los Angeles). 20p. (CONF-660411-16). ORAU. Gmelin, AED-CONF-66-060-65.

From American Physical Society Meeting, Washington, D. C.

Measurements were made on board the spacecraft, Mariner 2, with a fluxgate magnetometer, ion spectrometer, and plasma probe of the electrostatic analyzer type which present evidence for the possible propagation of hydromagnetic waves in the interplanetary plasma. These measurements are described. (M.O.W.)

39570 INTRODUCTION TO RADIATIVE TRANSFER PROBLEMS IN STELLAR ATMOSPHERES. Hummer, D. G. (London Univ.). 48p. (CONF-660217-6). ORAU. Gmelin, AED-CONF-66-013-13.

From Symposium on Interdisciplinary Aspects of Radiative Energy Transfer, Philadelphia.

Attention is limited to the interstellar radiation field in resonance lines. From the considerable body of numerical solutions now available, it is possible to discern some rather general features of these problems, which can be conveniently discussed in terms of processes coupling the radiation field to the electron gas. Solutions are presented for the combined transfer and statistical equilibrium equations for an atmosphere with optical properties depending on depth. Mathematically, the problem is the numerical solution of a set of coupled linear differential equations with non-constant coefficient, with two-point boundary conditions. Some recent work on this problem is discussed, in which the linear equations are converted into a set of coupled non-linear equations with a one-point boundary condition by means of a transformation due to Rybicki and Usher. (M.O.W.)

39571 COSMIC RAY MODULATIONS IN THE SOLAR SYSTEM AND IN INTERSTELLAR SPACE. Silberberg, Rein (Naval Research Lab., Washington, D. C.). 42p. (CONF-660411-29). ORAU. Gmelin, AED-CONF-66-060-63.

From American Physical Society Meeting, Washington, D. C.

The local interstellar spectra of cosmic ray protons and helium are investigated, assuming their local interstellar spectra are similar in shape between values of energy of 1 and 10 Bev/nucleon. Using these results, such parameters of the interplanetary medium as the number of scattering centers along the cosmic ray path and the radial extent of the cosmic ray convection and diffusion region are evaluated, and are found to agree with those proposed by Parker. The scale factors of the scattering centers are found to be distributed between 6×10^{10} cm and 10^{12} cm, or more, provided that the magnetic field strengths of the scattering centers do not vary beyond the earth's orbit with the radial distance from the sun. (M.O.W.)

39572 ELECTRON AND THE ION TEMPERATURE IN THE SOLAR CORONA. Sen, Hari K.; Kushwake, Ram S. (Air Force Cambridge Research Labs., Bedford, Mass.). 9p. (CONF-660401-5). ORAU. Gmelin, AED-CONF-66-061-14.

From American Meteorological Society, American Geophysical Union, Annual Joint Meeting, Washington, D. C.

Some hitherto unexplained discrepancies have been noted by astronomers between various estimates of the coronal temperature. The temperature derived from the degree of ionization or radio observations corresponds to the electron temperature and is the lowest. The scale height temperature is higher by a factor of two. The temperature obtained from line widths, which corresponds to the ion temperature, is still higher (about three times the electron temperature). It is shown that the Alfvén shock waves in the corona have the right order of frequency to allow the electrons and the ions to thermalize separately, but do not allow enough time to establish thermal equilibrium between the electron and the ion. The ion temperature, therefore, stays higher than that of the electrons. These shock waves can reasonably have the required Mach number to maintain the observed temperature difference. The scale height temperature follows from taking the average of the electron and the ion hydrostatic pressures. (auth)

39573 INTERACTION BETWEEN THE SOLAR WIND AND SUN'S GENERAL MAGNETIC FIELD. Yen, K. T. (General Electric Co., Philadelphia). New York, American Inst. of Aeronautics and Astronautics, 1966, Preprint No. 66-509, 26p., $1.50. (CONF-660632-7). ORAU.

From American Inst. of Aeronautics and Astronautics, 4th Aerospace Sciences Meeting, Los Angeles, Calif.

An analytical study of the interaction between a radial plasma flow assumed to start uniformly from the sun's surface and sun's general magnetic field assumed to be a dipole is presented. Coupled hydrodynamic and hydromagnetic equations are used to solve for interaction with the property of axial symmetry about the dipole axis. The

sun's rotation is not considered. A perturbation analysis is carried out to show how the dipole magnetic field is drawn out by the flow, and how the flow is distorted by the magnetic field and becomes non-uniform. Both incompressible and compressible radial flows were analyzed. Solutions for the interplanetary magnetic field will be presented and compared with Parker's curl-free solution. One effect of compressibility is that the dipole magnetic field will be drawn out more effectively into the interplanetary space. (auth)

39574 INVESTIGATION OF PROBLEMS IN PRE-MAIN-SEQUENCE STELLAR EVOLUTION. Bodenheimer, Peter Herman. Berkeley, Calif., Univ. of California, 1965. 97p. Thesis.

The available observational material relating to pre-main-sequence evolution is reviewed and compared with the predictions of theory. New calculations are presented, which focus upon two aspects of the problem: first, the influence of different assumed starting models on subsequent evolutionary tracks, and second, the depletion of the rare light nuclei ^{2}D, ^{6}Li, and ^{9}Be and comparison of theory with observed abundances of these species in stellar atmospheres. Some additional calculations indicate the extent to which uncertainties in theoretical model stellar atmosphere calculations could influence the results of these two primary investigations. Several main conclusions can be reached from the results of the calculations. First, the possible effects of variations in initial conditions during fully and partially convective evolutionary phases do not cause significant deviations from previously calculated evolutionary tracks of the Hayashi type. Second, the calculations of the depletion of lithium show that the presence of deep convection during pre-main-sequence evolution can explain the general behavior of observed abundances of lithium as a function of spectral type on the main sequence. Third, the calculations of the depletion of ^{6}Li are not completely consistent with the existing observations of the presence of this isotope in main-sequence stars. Fourth, the theoretical calculations on the depletion of deuterium predict that this isotope, if initially present in stars, should be detectable in main-sequence stars with masses above $3M_{\odot}$. No observations exist which can confirm this result. Fifth, the calculations predict that the element beryllium, if present or produced at the time of formation of stars, should be observable on the main sequence down to about spectral type K5. Finally, within the framework of the present theory, the results do not appear to indicate major inconsistencies with pre-main-sequence evolutionary tracks of the type first calculated by Hayashi, despite some observational evidence to the contrary. (TCO)

39575 IRREGULARITIES IN THE INTERPLANETARY MAGNETIC FIELD. Coleman, Paul Jerome Jr. Los Angeles, Univ. of California, 1966. 334p. Thesis.

A description of variations in the quiet interplanetary magnetic field is developed and certain effects of these variations upon the propagation of solar cosmic rays are established. The observations of the magnetic field were obtained with the magnetometer on board the spacecraft Mariner 2 in transit to the vicinity of Venus in late 1962. Data obtained over 27-day periods are first re-examined. It is shown that orientation of the vector component in the solar equatorial plane was typically that indicated by the spiral-field model of Parker (1958) and that the polarity of this component reversed periodically. The polarity reversals were found to be in phase with the sun's rotation. The magnitude of this component was found to average 4.0γ. It is also shown that the vector component normal to the solar equatorial plane is typically directed from north to south with an average magnitude of 1.5γ. Variations about these typical values during 27-day intervals are examined. It is shown that amplitude distributions for the vector components are well represented by Gaussian distribution functions. The half-widths of the distribution functions are estimated. Variations with periods shorter than one day are examined. The power spectra of each of the vector components and of the field magnitude are estimated. Cross spectra of the variables describing the field and the velocity of the solar plasma are estimated. Evidence is given for the existence of at least two distinct modes in the field variations. A model for the quiet interplanetary field is developed using the power spectra of the vector field to establish the time dependence and the concept of a perfectly conducting, radially expanding interplanetary plasma to establish the spatial dependence. The propagation of solar-flare protons in the model field is examined. This examination indicates that most of the observed properties of typical directional spectral intensities of solar-flare protons may be accounted for by this single model for the interplanetary field. (TCO)

Atomic Physics

Refer also to abstracts 39500, 39773, 39817, and 39818.

39576 (AD-636533) THEORY OF ELECTRON COLLISION EXPERIMENTS AT INTERMEDIATE AND HIGH GAS DENSITIES. Technical Report No. 32. Chantry, P. J.; Phelps, A. V.; Schulz, G. J. (Westinghouse Research Labs., Pittsburgh, Pa.). Apr. 29, 1966. Contract NONR-2584(00). 76p. CFSTI $3.00 cy, $0.75 mn.

By means of a two stream approximation an analytical solution was obtained to the equation of transfer governing the steady-state concentration of monoenergetic electrons within a slab of gas bounded by two infinite planes, one of which emits a constant current density normal to its surface. The theory places no restriction on the gas pressure and includes the effects of inelastic collisions and partial reflection of scattered electrons at one or both boundaries. The results were applied to electron beam experiments at intermediate and high pressures where the mean free path of electrons is comparable to or less than the length of the collision chamber. Analytical expressions were obtained for the electron current transmitted through the gas and for the normalized ion currents to be expected in the case of total ion collection and in the case of sampling through a slit. The effect of elastic and inelastic collisions may be represented by an "equivalent length factor" which modifies the equations normally applicable under low-pressure conditions. The results of the present theory are compared with previous theories with particular reference to their use in interpreting experiments of the Maier-Leibnitz type, designed to measure absolute values of inelastic collision cross sections. (auth)

39577 (JINR-P-2791) KORRELYATSIYA VREMEN ISPUSKANIYA I POGLOSHCHENIYA OBMENNOGO FOTONA. (Time Correlation of the Emission and Absorption of the Exchange Photon). Zon, B. A.; Shirokov, M. I. (Joint Inst. for Nuclear Research, Dubna (USSR). Lab. of Theoretical Physics). 1966. 15p. Dep. mn.

Time correlation for the quantum electrodynamics effect is calculated, using a somewhat generalized version of the Goldberger and Watson apparatus. There are two atoms, separated by a large distance R. Initially only atom A is excited. A calculation was made for the probability of excitation of the second atom B at a moment t, provided the moment of photon emission by atom A is known. Such an effect can be considered as quantal experiment for measurement the photon velocity. The obtained results in a qualitative respect could be anticipated. But in specific conditions (very soft photon) the calculation gives appreciable probability that the photon velocity exceeds C. (auth)

39578 (JINR-P-2807) ISSLEDOVANIE STRUKTURY K-SERII ARGONA PRI ATOMNOM ZAKHVATE OTRITSATEL'NYKH MYUONOV V CHISTOM GAZE I V SMESI S VODORODOM. (Investigation of the Structure of Argon K-Series During an Atomic Capture of Negative Muons in Pure Gas and in a Mixture With Hydrogen). Budyashov, Yu. G.; Ermolov, P. F.; Zinov, V. G.; Konin, A. D.; Mukhin, A. I. (Joint Inst. for Nuclear Research, Dubna (USSR). Lab. of Nuclear Problems). 1966. 7p. Dep. mn.

The experiments showed that during the argon intercep-

tion of the negative muon in (p-μ) nucleus, the intensity of the hard lines in argon k-series is sharply increased in comparison to the case of direct muon capture by argon. (M.O.W.)

39579 (JINR-P-2838) IZMERENIE VREMENI KASKADNOGO PEREKHODA π^--MEZONA V GAZOOBRAZNOM GELII-3. (Measurement of the Cascade Time of Negative Pions in Gaseous ^{3}He). Zaimidoroga, O. A.; Sulyaev, R. M.; Tsuko-Sitnikov, V. M. (Joint Inst. for Nuclear Research, Dubna (USSR). Lab. of Nuclear Problems). 1966. 7p. Dep. mn.

The cascade time of negative pions in gaseous helium-3 was measured by using a diffusion chamber in a magnetic field. It was found to be $(1.4 + 0.7)\ 10^{-10}$ sec. The measured time coincides with that of analogous measurement in liquid helium. This means that the cascade time of pions in helium does not depend on the medium density. (auth)

39580 (ORNL-3989, pp 78-88) ATOMIC AND MOLECULAR CROSS SECTIONS. Barnett, C. F.; Krause, M. O.; Langley, R. A.; Ray, J. A. (Oak Ridge National Lab., Tenn.).

Progress is reported on the following projects: measurements of kinetic energy of H^+ and H following dissociation of H_2 by electrons; high-energy charge-exchange cross sections; charge states of atoms following inner-shell ionization; absolute vacuum measurements; and the Atomic and Molecular Processes Information Center. (M.O.W.)

39581 (ORNL-3989, pp 134) SPUTTERING OF COPPER, MOLYBDENUM, 304 STAINLESS STEEL, AND TUNGSTEN BY DEUTERIUM IONS. Yonts, O. C.; Wood, J. P.; Huff, H. L. (Oak Ridge National Lab., Tenn.).

Copper was sputtered with D^+ and D_2^+ ions to check new equipment which will enable one to attain 80 to 100 kev energy. Results of sputtering measurements for this report period are given. (auth)

39582 (AERE-Trans-1053) ELECTRON EXCHANGE IN ELECTRON-ATOM COLLISIONS. Peterkop, R. K. Translated by J. B. Sykes (U.K.A.E.A. Atomic Energy Research Establishment, Harwell, Eng.), from pp 105-38 of Elektronno-Atomnye Stolknoveniya, Izdatel'stvo Zinatne, Riga, 1965. 32p. Dep. BIS $0.90. HMSO 4s. 6d.

Included is a discussion on the treatment of exchange and the part played by exchange effects in electron-atom collisions. The case is considered where the Hamiltonian of the multi-electron system is independent of the spins. Then the calculations reduce to the evaluation of the coordinate wave functions. Problems relating to the allowance for exchange in collision theory for systems of two or three electrons are discussed. A survey is presented of exchange effects in collisons of electrons with atoms of H, He, and the alkali metals. (M.O.W.)

39583 EXCITATION OF HYDROGEN BY PROTONS. McCarroll, Ronald; Salin, Antoine (Observatoire de Paris). Ann. Phys. (Paris), 1: 283-7(May-June 1966). (In French).

A new method, which takes account of the electron-ion attraction is proposed for calculating cross-sections for the excitation of neutral atoms by positive ions. At high energies the new approximation converges to the Born approximation and in general the cross-sections are smaller than the corresponding Born cross-sections. The maximum is displaced to higher energies as compared with the Born maximum. Calculations are carried out for the excitation of the 2s and 2p state of atomic hydrogen by proton impact. It would appear from the scanty evidence available that our results should be reliable for proton energies above 20 kev. (auth)

39584 POLARIZED NEGATIVE IONS PRODUCED BY CHARGE EXCHANGE PROCESS. Drake, C. W. Jr.; Krotkov, R. V. (Yale Univ., New Haven). IEEE (Inst. Elec. Electron. Eng.), Trans. Nucl. Sci., NS-13: No. 4, 142-6(Aug. 1966).

A measure of the deuteron tensor polarization of a beam of negative ions produced by charge-exchange methods is described. The polarization is produced by making use of the properties of the metastable n = 2 state in hydrogen or deuterium. (L.B.S.)

39585 CESIUM ION SPUTTERING OF ALUMINUM. Andrews, A. E.; Hasseltine, E. H.; Olson, N. Thomas; Smith, Harold P. Jr. (Univ. of California, Berkeley). J. Appl. Phys., 37: 3344-7(Aug. 1966).

A neutron activation technique was developed to investigate cesium–aluminum sputtering in measured, rarefied atmospheres of oxygen. The sputtering yield was measured as a function of cesium ion energy and as a function of the ratio of oxygen molecular flux arriving at the target surface to sputtered aluminum flux leaving the surface. In all measurements the ion beam was normal to the monocrystalline aluminum target surface and to the (110) crystallographic plane. The yield increased monotonically from 0.74 (atoms/ion) at 1 kev to 2.4 at 10 kev and was unaffected by flux ratios less than 0.2. The yield decreased for higher values of the flux ratio and eventually reached a saturation value where it is conjectured that a surface film of Al_2O_3 is maintained. (auth)

39586 SINGULARITIES IN THE COHERENT DIFFUSE SCATTERING OF X RAYS. Ishibachi, T.; Rudee, M. L. (Rice Univ., Houston, Tex.). J. Appl. Phys., 37: 3359-61(Aug. 1966).

It is demonstrated that there is an error in von Laue's treatment of diffuse scattering of x rays from random alloys and that a correct formulation predicts that the diffuse intensity must vanish at reciprocal lattice points. Thus there is no reason to reconstruct the Cowley theory, as has been recently suggested. The physical origin of this effect and some of its consequences are discussed. (auth)

39587 GROWTH OF SPUTTERED VS EVAPORATED METAL FILMS. Chopra, K. L. (Kennecott Copper Corp., Lexington, Mass.). J. Appl. Phys., 37: 3405-10(Aug. 1966).

The early growth stages of sputtered (S) vs evaporated (E) Ag/mica and Ag/NaCl films have been studied by transmission electron microscopy and electron diffraction. The observed maximum density of the islands at thicknesses less than 20 Å is slightly higher for S films, although the order of magnitude is the same ($\sim 10^{11}/cm^2$) for both the S and E films. Electrostatic charges carried by the S atoms and the point defects caused by the penetration of the energetic S atoms could account for the observed higher S-island density. As the film thickness increases, the S-island density at 25°C decreases rapidly to reach a constant value before the film becomes continuous. The corresponding E-island density decreases slowly. The higher mobility, as indicated by the rate of change of the island density, and the observed epitaxial growth of the S films at a temperature considerably lower than that obtained for E films, are attributed to the higher kinetic energy of the S atoms. The E-island density decreases rapidly as the substrate temperature is increased. The decrease in S-island density is, however, accompanied by an increase in the surface area of the islands and formation of bridges between the islands, thereby resulting in coalescence at a smaller nominal thickness than is observed in E films. These observations are explained on the basis of the effects of higher electrostatic charges and kinetic energy of the S atoms. The activation energies for the diffusion processes, calculated from the temperature dependence of the separation between the islands, are 0.1 and 0.15 ev for S and E films, respectively, at substrate temperature below 250°C. Above 250°C, the activation energies increase rapidly to 0.5 and 0.9 ev, respectively. (auth)

39588 ANALYTICAL EXPRESSION FOR THE MASS-SCATTERING CROSS SECTION OF CARBON. Sarkar, N. H. (Saha Inst. of Nuclear Physics, Calcutta). J. Appl. Phys., 37: 3639(Aug. 1966).

The total mass-scattering cross section S_t for carbon, computed from the theory of Sarkar in the voltage (ϕ)

range 40 to 100 kv and for scattering angles (Θ) from 1×10^{-3} to 2×10^{-2} rad, was found to vary linearly with $\log \Theta$ and may be represented as $S_t = -(m \log \Theta + c) \times 10^4$ cm^2/g, where m and c are constants that depend only on ϕ. (W.D.M.)

39589 SPUTTERING-YIELDS CROSSOVER IN SINGLE-CRYSTAL COPPER. Wolsky, S. P.; Zdanuk, E. J. (Laboratory for Physical Science, Burlington, Mass.). J. Appl. Phys., 37: 3641-2(Aug. 1966).

A recent publication by Snouse and Haughney (J. Appl. Phys. 37: 700 (1966)) (S-H) reported yield data for the (111), (100), and (110) copper planes over an energy range of 0.1 to 200 kev. It is pointed out that the S-H experiments are in agreement with previous measurements, E. J. Zdanuk and S. P. Wolsky (J. Appl. Phys. 36: 1683 (1965)), in that they also clearly indicate a crossover of the (111) and (100) yield curves in the low-energy range. The two sets of measurements are discussed and it is concluded that the transparency model which explains the dependence of the yield on crystallographic orientation in the high-energy regions is not adequate in the low-energy region. (W.D.M.)

39590 REFLECTION AND THERMAL ACCOMMODATION OF HELIUM BEAMS ON PLATINUM. Moore, George E.; Datz, Sheldon; Taylor, Ellison H. (Oak Ridge National Lab., Tenn.). Contract W-7405-eng-26. J. Catalysis, 5: 218-23(Apr. 1966). (ORNL-P-1387).

Molecular beam techniques were used to investigate gas-surface interactions, which are preliminary processes in gaseous heterogeneous catalysis. These first investigations studied the nature of the reflection of He beams from Pt surfaces and their concomitant thermal accommodation (α'). At least three different conditions for the Pt surface, as judged by the nature of the reflection of a beam of He atoms, were observed. Surfaces achieved by an oxygen treatment of the incandescent Pt target gave intense specular reflection of He atoms and $\alpha' < 0.1$, and were, therefore, believed to be clean. (auth)

39591 LOW-ENERGY LARGE-ANGLE ELECTRON SCATTERING SPECTRUM OF HELIUM. Doering, John P. (Johns Hopkins Univ., Baltimore). J. Chem. Phys., 45: 1065-6(Aug. 1, 1966).

Experiments were undertaken to clarify the qualitative aspects of the helium scattering spectrum at large angles and low energies where the Born approximation would not be expected to apply. Electrons were produced by a thoria-coated iridium filament and accelerated into the collision chamber which contained He at a typical pressure of 10 μ. The unscattered beam was collected by a Faraday cup biased at +22.5 v. Electrons scattered through 90° left the chamber, were retarded to 3 ev before entering the 127° electrostatic analyzer, and were collected at a shielded plate and detected with an electrometer. In no case was the forbidden transition to the $2\ ^3S$ state observed. It was concluded that the transition to this state must be at least a factor of 5 less intense than the transition to the $2\ ^1P$ state. (W.D.M.)

39592 CHARGE-EXCHANGE CROSS SECTIONS FOR ARGON IONS IN H_2 AND D_2 BELOW 1 kev. Amme, Robert C.; McIlwain, John F. (Univ. of Denver). J. Chem. Phys., 45: 1224-7(Aug. 15, 1966).

Charge-exchange cross sections for Ar^+ ions incident on hydrogen and deuterium were measured over the energy range of 30 to approximately 1000 ev. The argon-ion beam was formed by electron bombardment and electrostatic acceleration. Ionizing electron energy was nominally 18 ev, although the results appeared to be insensitive to this parameter. The measured cross sections for $Ar^+ + H_2 \rightarrow Ar + H_2^+$ as a function of ion energy are compared with the results of other investigators, which are in rather poor agreement. The measurements confirm that the cross section exhibits a maximum at approximately 180-ev incident-ion energy. Theoretical calculations by Gurnee and Magee and by Karmohapatro are discussed for this reaction. The cross section for $Ar^+ + D_2 \rightarrow Ar + D_2^+$ was found to exhibit a maximum, but at approximately 85 ev, which is nearly the same center-of-mass energy as for the H_2 target. The possible influence of ion–molecule reactions on the charge-transfer cross sections is discussed. (auth)

39593 COLLISIONAL EXCITATION OF ATOMIC SPECTRA IN ACCELERATED BEAMS OF LIGHT ELEMENTS. Bashkin, S. (Univ. of Arizona, Tucson); Fink, D.; Malmberg, P. R.; Meinel, A. B.; Tilford, S. G. J. Opt. Soc. Amer., 56: 1064-75(Aug. 1966).

The light emitted by high-speed particles produced by a Van de Graaff accelerator and excited by passage through a thin foil of carbon was studied in the wavelength range 2700–6600 Å. Lines from deuterium, helium, nitrogen, and oxygen are presented including some that were not previously reported. Qualitative observations are presented on the mean lives of the excited states and on the dependence of spectral line intensity upon particle energy. (auth)

39594 PRODUCTION OF ELECTRON-POSITRON PAIRS BY HIGH-ENERGY GAMMA QUANTA. Bem, J.; Grishin, V. G.; Kistenev, E. P. (Joint Inst. for Nuclear Research, Dubna, USSR). JETP Lett. (USSR) (Engl. Transl.), 4: 24-6(July 1, 1966).

Translated from Zh. Eksp. Teor. Fiz., Pis'ma Redaktsiyu, 4: 36-9(July 1, 1966).

An investigation was made on the production of e^+e^- pairs by γ quanta with energy E = 10 to 5000 Mev with the aid of the 23-liter propane bubble chamber of the JINR high-energy laboratory. The histograms of the distributions of the events with respect to V (V = ratio of positron to γ-quantum energies) are given. (M.O.W.)

39595 WHY NUCLEAR SPECTROSCOPISTS SHOULD KNOW ABOUT THE RECENT DEVELOPMENT IN THE FIELD OF ATOMIC STOPPING. Bergstroem, I.; Domeij, B. (Royal Inst. of Tech. and Research Inst. of Physics, Stockholm). Nucl. Instrum. Methods, 43: 146-69(Aug. 1, 1966).

A review is given of the new theoretical and experimental trends in the field of atomic stopping, which have occurred since about 1960. Some new approaches in the experimental techniques are described. The theory of Lindhard, Sharff, and Schiott for stopping of atoms in random substances is presented in some detail and compared with available experimental data. Some discrepancies between theory and experiment are discussed. The discovery of the strong lattice effects on range distributions of heavy particles in single crystals is described and the theoretical and experimental data surveyed. The theory of the so called string effect is presented and the experimental evidence for its existence is described. Finally a qualitative analysis is made of possible errors which might arise in nuclear experiments due to the recently discovered phenomena in the field of atomic stopping. (auth)

39596 COMMENTS ON BROWNIAN MOTION THEORY. Resibois, P.; Dagonnier, R. (Univ. Libre, Brussels). Phys. Lett., 22: 252-4(Aug. 15, 1966).

The validity of the Fokker-Planck equation for a Brownian particle is considered. (auth)

39597 LIFETIMES OF THE EXCITED STATES $(6s6p)^1P_1$ AND $(6s6p)^3P_1$ OF YTTERBIUM. Baumann, M.; Wandel, G. (Univ., Tuebingen, Ger.). Phys. Lett., 22: 283-5(Aug. 15, 1966).

The lifetimes $\tau(6^1P_1) = (5.50 \pm 0.25) \times 10^{-9}$ sec and $\tau(6^3P_1) = (8.27 \pm 0.4) \times 10^{-7}$ sec were determined by zero field level crossing technique. From these values the intermediate coupling coefficients $\alpha = 0.991$ and $\beta = -0.133$ were derived. (auth)

39598 ENHANCEMENT FACTOR FOR THE ELECTRIC DIPOLE MOMENT OF THE VALENCE ELECTRON IN AN ALKALI ATOM. Sandars, P. G. H. (Oxford Univ.). Phys. Lett., 22: 290-1(Aug. 15, 1966).

The atomic electric dipole moment caused by a moment on the electron is calculated for the alkalis in their ground states. The ratio of the atomic to electronic moments is found to range from 4×10^{-3} for lithium to 10^3 for francium. (auth)

39599 VELOCITY DEPENDENCE OF ATOM-ATOM TOTAL SCATTERING CROSS SECTIONS IN THE 7-500 ev ENERGY RANGE. Neumann, W.; Pauly, H. (Univ., Bonn). Phys. Lett., 22: 291-2(Aug. 15, 1966).

Total scattering cross sections for fast alkali metal atomic beams scattered by a thermal Hg beam were measured for energies of 7–500 ev. Glory-oscillations and the transition to the high energy behavior were observed. (auth)

39600 FOCUSONS IN POTASSIUM CHLORIDE. Kelly, J. C.; Petersen, M. C. E. (Univ. of New South Wales, Kensington, Australia). Phys. Lett., 22: 295-6(Aug. 15, 1966).

The first experimental confirmation of the existence of focusons in alkali halides is reported. Energetic argon ion bombardment of KCl (100) surfaces produced preferential positive ion ejection along ⟨111⟩ and ⟨112⟩ directions. The results are interpreted in terms of an energy dependent hard sphere model. (auth)

39601 EFFECT OF π AND Σ MOLECULAR STATES IN Ne^+-Ne SCATTERING. Jones, P. R.; Batra, T. L.; Ranga, H. A. (Univ. of Massachusetts, Amherst). Phys. Rev. Lett., 17: 281-3(Aug. 8, 1966).

The neutral fraction P_0 of the scattered particle current is shown versus scattering angle, θ, for single collisions of Ne^+ ions on neutral Ne atoms at an incident-ion energy of 800 ev. This collision is described by a mixture of Σ_g, Σ_u, π_g, and π_u molecular states. (M.O.W.)

39602 DETERMINATION OF INTERATOMIC POTENTIALS AND STOPPING POWERS FROM CHANNELED-ION ENERGY-LOSS SPECTRA. Lutz, H. O.; Datz, S.; Moak, C. D.; Noggle, T. S. (Oak Ridge National Lab., Tenn.). Phys. Rev. Lett., 17: 285-7(Aug. 8, 1966). (ORNL-P-2277).

Structure was observed in the energy-loss spectrum of 60-Mev ^{127}I ions and 3-Mev α particles channeled in gold single crystals. The explanation of this structure was found to lie in the nature of transverse oscillations of the particles in the channels. The energy losses associated with given wavelengths and amplitudes allow a mapping of the stopping power in the channel and should permit the direct determination of interatomic potentials. (auth)

39603 NEW RESULTS ON THE QUESTION OF AUGER AFTEREFFECTS. Mullen, James G.; Ok, Hang Nam (Purdue Univ., Lafayette, Ind.). Phys. Rev. Lett., 17: 287-90(Aug. 8, 1966).

Previous studies have indicated that in some materials the time required to reach electronic equilibrium, following the emission of an Auger electron, can be of the order of or greater than 10^{-7} sec. The results of studies to investigate the Auger aftereffects of CoO_x for x = 0 to 1.5 are described. The Moessbauer spectra for Co, CoO(I), CoO(II), and Co_3O_4 are given. The results indicate no evidence of Auger aftereffects. (M.O.W.)

39604 STRUCTURE OF THE SPECTRUM OF NEUTRAL TERBIUM, Tb I. Klinkenberg, P. F. A. (Univ., Amsterdam). Physica, 32: 1113-47(June 1966).

Analysis of the optical spectrum of the Tb atom by means of wavenumbers and intensities, data on self reversal and Zeeman effect resulted in the detection of 19 low levels of the even configuration $4f^85d6s^2$ in Tb I and hundred of odd levels with J-values from $\frac{1}{2}$ to $\frac{15}{2}$, and the classification of nearly 2000 observed spectral lines. Material is presented concerning the 12 even levels completing the $4f^85d6s^2$ ^8G and ^8D terms (except $^8G_{\frac{1}{2}}$) and 296 odd levels. The number of observed lines explained by these levels is 1366, of which 24 are doubly classified. A discussion of the term structure is given in connection with the vector model, the coupling scheme, the structure of other rare earth spectra and the results of other investigations. (auth)

39605 ION DENSITY IN ELECTRON BEAMS. II. ADEQUACY OF A TREATMENT BASED ON AVERAGES. Callebaut, D. K. (Interuniversitair Instituut voor Kernwetenschappen, Ghent). Physica, 32: 1151-8(June 1966).

The charge trapped in electron or ion beams at pressures below breakdown may be determined from an integro-differential equation which was studied in paper I (Physica 31: 1177(1965)). New cases are treated and compared quantitatively with one another to illustrate to what extent the effective potential depends on the shape of u_p (ion production) and u_e (beam). It turns out that the treatment with the averages of u_p and u_e is a quite reliable approximation, except in the rather unusual case where u_p shows a deep minimum. (auth)

39606 TRANSITION PROBABILITIES FOR ELECTRON CAPTURE. Coleman, J. P. (Univ. of Durham, Eng.); McDowell, M. R. C.; Van Den Bos, J.; De Heer, F. J. Physica, 32: 1164-9(June 1966).

A comparison is made in an impact parameter formulation, between the impulse approximation and the Brinkman-Kramers approximation for the electron capture processes $H^+ + H(1s) \rightarrow H(nl) + H^+$, where nl = 1s, 2s, 2p. The transition probabilities given by the former approximation are always smaller than those of the latter. It is pointed out that in the impulse approximation (within its range of validity) the probability of capture into the 2p state is less than that for capture into the 2s state for all values of the impact parameter, while in the Brinkman-Kramers approximation this only holds for small impact parameters. Nevertheless both methods yield approximately the same ratio for the total 2s and 2p cross sections. (auth)

39607 CLASSICAL IMPULSE APPROXIMATIONS. McDowell, M. R. C. (Univ. of Durham, England). Proc. Phys. Soc. (London), 89: 23-6(Sept. 1966).

The classical impulse approximation to the electron and proton impact ionization cross sections is expressed as $u^2Q(y) = g(y)_{m_2}$, where $g(y)_{m_2}$ is a unique function of $y = E_i/u$ (E_i being the impact energy and u the ionization potential) for a given incident particle of mass m_2. Results are presented for H and Li, and are compared with the Thomson and the Born approximations. (auth)

39608 REMEASUREMENT OF THE TOTAL CROSS SECTION FOR EXCITATION OF THE HYDROGEN 2 $^2S_{\frac{1}{2}}$ STATE BY ELECTRON IMPACT. Hils, D.; Kleinpoppen, H.; Koschmieder, H. (Univ., Tuebingen, Germany). Proc. Phys. Soc. (London), 89: 35-40(Sept. 1966).

The cross section for excitation of the 2 $^2S_{\frac{1}{2}}$ state of atomic hydrogen by electron impact has been remeasured in the energy range from the threshold 10.2 ev to 500 ev. The shape of the $\sigma(1s,2s)$ cross section curve observed agrees with the earlier measurements. The absolute values of the $\sigma(1s,2s)$ cross section disagrees with those of Lichten and Schultz by about a factor of 3. The maximum of the cross section and its total error is $\sigma_{max}(1s,2s) = (0.11 \pm (0.025)\pi\alpha_0^2$; this is somewhat smaller than that of Stebbings et al., which is $(0.16 \pm 0.1)\pi\alpha_0^2$. Comparison was made with theoretical results. (auth)

39609 COLLISION-INDUCED DE-ACTIVATION OF METASTABLE HELIUM. Allison, D. C. (Royal Coll. of Advanced Technology, Salford, England); Browne, J. C.; Dalgarno, A. Proc. Phys. Soc. (London), 89: 41-4(Sept. 1966).

The cross section for the thermal collision-induced radiative de-activation process $He(1\,^1S) + He(2\,^1S) \rightarrow He(1\,^1S) + He(1\,^1S) + h\nu$ is calculated to be 2×10^{-20} cm^2, in harmony with the value derived experimentally by Phelps. (auth)

39610 EXCITATION OF ATOMIC HYDROGEN BY ELECTRON IMPACT. Morrison, D. J. T.; Rudge, M. R. H. (Queen's Univ., Belfast). Proc. Phys. Soc. (London), 89: 45-53(Sept. 1966).

Calculations are described for the processes $e + H(1s) \rightarrow e + H(n,l)$, where the n,l values are 2s, 2p, 3s, 3p, and 3d, the approximation used being a modification of earlier work by Rudge who considered the cases of elastic scattering and excitation of the 2s state. By interpolating between our calculations for these values of n,l and partial wave values for the ionization cross section an estimate is made of the excitation cross section to more highly excited states. Using these data, the contribution to the measurements of the 1s–

2s and 1s–2p cross sections due to cascade is estimated and our results compared for these cases with experimental measurements. Satisfactory agreement is obtained. A comparison is also made with the classical theory of Gryzinski. It is observed that the classical theory does not yield close agreement with this theory or experiment and that, over certain ranges of energy, it can be in error by several orders of magnitude. (auth)

39611 STOPPING POWERS AND STRAGGLING IN THE RARE GASES. Bell, R. J. (National Physical Lab., Teddington, England); Dalgarno, A. Proc. Phys. Soc. (London), 89: 55-7(Sept. 1966).

The penetration of matter by fast charged particles can be characterized by the mean excitation energies I appropriate to stopping and I_1 appropriate to straggling. A semi-empirical procedure is used to obtain I and I_1 for helium, xenon, and radon; the results are in satisfactory agreement with available experimental data. (auth)

39612 CLASSICAL ELECTRON IONIZATION CROSS SECTIONS. Kingston, A. E. (Queen's Univ., Belfast). Proc. Phys. Soc. (London), 89: 177-8(Sept. 1966).

The cross section for electron ionization of the first five excited states of hydrogen are calculated using Gryzinski's classical theory. These cross sections are compared with cross sections calculated using the first Born approximation. The classical cross sections are in good agreement with the quantal cross sections except at very large impact energies where the classical cross sections do not have the correct fall-off. If the correct fall-off is added to the classical cross sections, these cross sections differ only slightly from the Born cross sections at high impact energies. (auth)

39613 NEW FORBIDDEN LINES IN THE L SPECTRUM OF LUTETIUM. Deodhar, G. B.; Singh, R. B.; Varma, P. P. (Univ. of Allahabad, India). Proc. Phys. Soc. (London), 89: 183-4(Sept. 1966).

Using a curved crystal x-ray spectrograph of the transmission type two new forbidden lines $L_I M_I \lambda$ 1476.64 x.u. and $L_{III} N_{III} \lambda$ 1393.06 x.u. were found for lutetium. (auth)

39614 GROUND STATE OF H_2^-. Somerville, W. B. (London Univ.). Proc. Phys. Soc. (London), 89: 185-7 (Sept. 1966).

Variational calculations by Taylor and Harris for the ground state of H_2^- have been interpreted as showing that the state is not stable. It is pointed out that this conclusion is false since the adiabatic approximation is not valid when one electron is at a large distance from the rest of the system. A five-particle non-adiabatic calculation is required. (auth)

39615 DETERMINATION OF THE LOCAL FIELD PARAMETERS IN MOESSBAUER HYPERFINE SPECTRA. Karyagin, S. V. (Inst. of Chemical Physics, Moscow). Soviet Phys.-Solid State (Engl. Transl.), 8: 391-6(Aug. 1966).

Translated from Fiz. Tverd. Tela, 8: 493-9(Feb. 1966).

It is shown that for a $\frac{1}{2} \rightarrow \frac{3}{2}$ transition it is possible to determine approximately the parameters e^2Qq, η, ϑ, and φ, to determine precisely $g_n\beta H$, $g\ \beta H$, $\epsilon \equiv (1/2)|e^2Qq|\sqrt{1 + (1/3)\ \eta^2}$, and to calculate the relative intensities in the spectrum, from the frequencies (relative velocities) of the hyperfine structure (hfs) components. Certain methods are also pointed out for determining the energies of the hfs sublevels and the chemical shift δ. The corresponding formulas are given. A number of the formulas and conclusions of a more general nature can be applied to any transition. The work is of interest for experiments which study the hfs arising in Mössbauer spectra where quadrupole and magnetic interactions are present simultaneously. (auth)

39616 DEPOLARIZATION OF μ-MESONS IN THE CREATION OF μ-MESICATOMS OF NUCLEI WITH SPIN I = 1. Bukhovostov, A. P. (Ioffe Inst. of Physics and Tech., Leningrad). Yadern. Fiz., 4: 83-7(July 1966). (In Russian).

The depolarization of μ-mesons in cascade transitions is calculated for nuclei with spin one. The hyperfine splitting is assumed to be large in comparison with the level width. The result almost coincides with that obtained neglecting the hyperfine splitting of the excited levels. The case of nuclei with arbitrary spins is discussed. (auth)

39617 AN APPROXIMATION TO THE HARTREE-FOCK SCHEME FOR OBTAINING ELECTRONIC WAVE-FUNCTIONS, USEFUL FOR CRYSTAL CALCULATIONS. Shankland, Donn G. 5p. (CONF-660411-49). ORAU. Gmelin, AED-CONF-66-060-101.

From American Physical Society Meeting, Washington, D. C.

A technique is considered for obtaining Hartree-Fock wavefunctions for electrons in a crystal lattice. The procedure is important because it provides a straightforward way to take exchange effects exactly into account, without assuming the usual $p^{\frac{1}{3}}$ exchange potential approximation, and because it can be formally extended to compute correlation effects through a Brueckner calculation. The general theoretical derivation of the procedure is outlined, and its use is shown by applying it to beryllium. (W.D.M.)

39618 "MULTIPLE-SCATTERING" MODEL FOR POLYATOMIC MOLECULES. Johnson, Keith H. (Univ. of Florida, Gainesville). 36p. (CONF-660411-43). ORAU. Gmelin, AED-CONF-66-060-117.

From American Physical Society, 1966 Spring Meeting, Washington, D. C.

The multiple-scattering technique of determining energy bands in solids is modified for the problem of calculating bound one-electron eigenstates of polyatomic molecules. The computational simplicity and applicability of this method to molecules of arbitrary complexity are dependent on the adoption of a model Hartree-Fock Hamiltonian based on the Slater approximation to the exchange potential and on the assumption of truncated spherically averaged potentials. The composite wave functions are expanded in rapidly convergent partial-wave series around each atomic site. For molecules of moderate size, the calculations can easily be carried to self consistency within the spherical approximation, and first-order perturbation theory can be applied to correct for the non-spherical components of the potential. Emphasis is placed on the advantages of this technique as a first step in calculating the theoretical electronic spectra of complex polyatomic systems. (auth)

39619 EXTRACTION OF A HELIUM ION BEAM FROM AN OPTICALLY POLARIZED HELIUM SOURCE GAS. Stockwell, Norman David (Rice Univ., Houston, Tex.). 86p. (CONF-650220-7). ORAU.

From American Physical Society, Southwest Meeting, Norman, Okla.

Optical pumping techniques can be used to produce nuclear polarization in ^{3}He gas excited by a weak electric discharge. By optically polarizing ^{3}He to a polarization P_0 and extracting ions from the gas, the resulting ion beam is expected to retain a polarization between P_0 and $P_0/2$ depending on the experimental conditions. Such a polarized beam would have great utility in nuclear physics. An ion source using this principle has been built by straightforward modifications of normal rf ion-source geometry to provide the higher pressure and lower flow rate needed for the optical pumping. The dependences of ion current upon source gas pressure and cleanliness, electrical discharge intensity, the axial magnetic field, and the extraction voltage are measured. ^{4}He rather than ^{3}He has been used to date and ion-beam polarization cannot be measured with the present apparatus. However, under discharge and flow conditions which appear suitable for ^{3}He polarization, beam current of 1 μA are attained. Methods for measuring beam polarization are proposed. Some future experiments in atomic physics are considered. (auth)

39620 THEORY OF SLOW ATOMIC COLLISIONS. II. EXTENSION TO A GENERAL DIATOMIC SYSTEM. Boorstein, Seth A.; Thorson, Walter R. (Massachusetts Inst. of Tech., Cambridge). 33p. (CONF-650833-3). ORAU. Gmelin, AED-CONF-65-315-50.

From Fourth International Conference on the Physics of Electronic and Atomic Collisions, Quebec.

In an earlier paper a completely quantum-mechanical theory of slow atomic collisions was presented for the H_2^+ system. The formal extension of that theory is given for collision of atoms having more than one electron. The electron translation is again explicitly accounted for, and the more complex angular momentum coupling is treated in such a way as to preserve the adiabatic nature of the theory. (auth)

39621 COMPARISON OF APPROXIMATE POLARIZATION POTENTIALS. LaBahn, R. W.; Callaway, Joseph. 18p. (CONF-660411-21). ORAU. Gmelin, AED-CONF-66-060-69.

From American Physical Society Meeting, Washington, D. C.

The polarization of an atom by an external charge gives rise to an effective polarization potential which is of great importance in scattering of low energy electrons by atoms. Several approximate representations of this potential were earlier proposed. In order to compare these approximations in scattering theory, the phase shifts and cross sections for electron-helium scattering were calculated using several different dipole polarization potentials. (M.O.W.)

39622 SCATTERING OF ELECTRONS BY IODINE MONOCHLORIDE. Fetzer, Homer Donald. [Austin], Tex., Univ. of Texas, 1965. 82p.

Thesis.

The scattering of electrons from iodine monochloride was investigated by a counting system developed for this experiment. Electrons with an energy of forty-five kilovolts impinged upon an ICl vapor stream and the scattered electrons were detected with a solid-state detector. The detector was moved through an arc about the scattering center. The intensity of scattering as a function of detector position was analyzed in order to test the amplitudes and phases of atomic scattering factors obtained from partial wave scattering theory. Excellent agreement was obtained between theory and experiment. (Dissertation Abstr.)

Cosmic Radiation

See also Elementary Particles and Radiations
Nuclear Properties and Reactions

Refer also to abstracts 38735, 39825, and 39831.

39623 (AECL-2598) COSMIC RAY NM-64 NEUTRON MONITOR DATA-III, JANUARY-APRIL 1966. Monthly Graphs, January 1964-April 1966. Steljes, J. F. (Atomic Energy of Canada Ltd., Chalk River (Ontario)). June 1966. 92p. (CRGP-1239). Dep. mn. AECL $2.00.

Uncorrected and barometer-corrected results from the cosmic ray stations in Canada using equipment maintained by AECL are given in tabular form for the period from January to April 1966. Normalized graphs are given for the period January 1964 to April 1966. (auth)

39624 (D-1-82-0529) EXPERIMENTAL EVALUATION OF VARIOUS RIGIDITY MODELS. Kenney, J. F.; Gauger, J.; Shea, M. A.; Smart, D. F. (Boeing Scientific Research Labs., Seattle, Wash. Geo-Astrophysics Lab.). May 1966. 24p.

Atmospheric cosmic-ray fluxes which have recently been measured over large portions of the globe are discussed. The measured fluxes were plotted as a function of the vertical cutoff rigidity for several different models. The rigorous trajectory calculations of Shea et al. give good agreement with the counting rates. The Makino model also orders these data equally well, and therefore must be within a few percent of the value determined by rigorous orbit calculations taken over the portions of the globe covered in the survey. The other models are demonstrably worse, and a discussion of where these models are inadequate is given. Particular attention is paid to the use of the L parameter as a substitute for rigorous integration procedures. It is shown both experimentally and theoretically that the L parameter is not a good demographic parameter for galactic cosmic radiation at the lower latitudes, but should be sufficiently accurate at higher latitudes for most purposes. (auth)

39625 FORMAL DERIVATION FOR ELECTRON PRODUCTION IN THE IONOSPHERE UNDER THE EFFECTS OF COSMIC RADIATION. Velinov, P. (Bulgarian Academy of Sciences, Sofia). Compt. Rend. Acad. Bulg. Sci., 19: 109-12(1966). (In German).

Formulas were derived describing the electron production induced by cosmic radiation in the ionosphere were derived as a function of height. A model profile of the cosmic radiation was calculated. (J.S.R.)

39626 SIDEREAL VARIATION OF THE COSMIC MUON COMPONENT AT 440-m DEPTH. Mabboux, Claude; Mosrin, Pierre; Scherer, Maurice (Univ., Caen, France). Compt. Rend., Ser. B, 262: 1632-5(June 20, 1966). (In French).

A study of the time distribution of muons underground at 1300 m.w.e. showed an apparent galactic component of the cosmic radiation. The amplitude of this variation as well as its period and phase were determined. (tr-auth)

39627 RADIATION MEASUREMENTS IN SPACE. Wujek, Joseph H. Jr. Electron. World, 76: 19-21; 72-3(Aug. 1966).

Some experiments and instrumentation used in space exploration radiation measurements are reviewed. Typical radiation-measuring devices are illustrated and shown in block diagrams. The transducer used for radiation detection converts the event of a particle striking the device into an electrical signal. Some means of signal amplification is usually required. If the signal is of the digital variety, i.e., a series of discrete pulses, these pulses are counted and stored in a chain of flip-flops or magnetic-core memories. If the signal is an analog function, the pulses can be amplified and fed into the telemetry system directly. Some detectors put out a signal which is both analog and digital. The presence of a digital pulse indicates that a particle is striking the detector, while the amplitude of this pulse is proportional to the energy of the particle. The various types of detectors are described and their characteristics compared. In addition to the principal types of standard detectors described, other radiation-detection devices are considered which have been used or are in development. One of these is the cadmium sulfide cells, the resistivity of which changes with the rate at which energy is received by the detector. The CdS detector is quite sensitive and is normally shielded to prevent saturation. Photographic film and spark chambers may be used to record the path of charged particles. Many amplifiers used in radiation measurements are of conventional broadband design; the charge amplifier is examined. The problems of calibration and noise are also dealt with. (BBB)

39628 SOLAR-DIURNAL AND SEMIDIURNAL VARIATIONS OF COSMIC RAYS AND THEIR SPECTRA AS A FUNCTION OF SOLAR ACTIVITY. Dorman, L. I.; Kolomeets, E. V.; Sergeeva, G. A. (Kirov Kazakh State Univ., USSR). Geomagn. Aeronomy (USSR) (Engl. Transl.), 5: 790-3(1965).

Translated from Geomagn. Aeronomiya, 5: 1003-8(1965).

Solar-diurnal and semidiurnal variations of the cosmic-ray neutron component are analyzed on the basis of data from the global network of stations for 1959-1962. The spectra and changes in amplitude and phase variations with time are found. The phase of diurnal variation changes relatively little with time, while the phase of the semidiurnal variation changes strongly, although no correlation with solar activity is found. The amplitude of diurnal variation decreases somewhat from the solar activity maximum to the minimum at low and middle latitudes and tends to increase toward high latitudes. The amplitude of the semidiurnal variation also decreases somewhat with decreasing

solar activity. The variation spectrum has a power-law form and remains practically unchanged as solar activity decreases. (auth)

39629 COMPLEX AMPLITUDE-PHASE MODULATION OF PERIODIC COSMIC-RAY VARIATIONS. Dorman, L. I.; Mazaryuk, E. A. (Inst. of Terrestrial Magnetism, Ionosphere and Radio Wave Propagation, Academy of Sciences, USSR). Geomagn. Aeronomy (USSR) (Engl. Transl.), 5: 862-5(1965).

Translated from Geomagn. Aeronomiya, 5: 1099-1102 (1965).

The simultaneous amplitude-phase modulation of periodic cosmic-ray variations with a period substantially exceeding the fundamental period was examined (Geomag. i Aeronomiya, 5: 40 (1965)). An attempt was made, using experimental data on the solar-diurnal variation from crossed telescopes and neutron monitors, to investigate arising side frequencies to determine the modulation parameters, and to find the true stellar-diurnal wave (Izv. Akad. Nauk (SSSR) Ser. Fiz., 29 (1965)). Calculations are given to determine when modulations of the periodic variations occur simultaneously with several periods. This modulation is associated primarily with the rotation of the earth about the sun and with the rotation of the sun about its own axis. (J.H.M.)

39630 GALACTIC COSMIC-RAY ELECTRONS. Ramaty, R.; Lingenfelter, R. E. (Univ. of California, Los Angeles). J. Geophys. Res., 71: 3687-3703(Aug. 1, 1966).

The production and equilibrium spectra of secondary electrons (negatrons and positrons) resulting from cosmic-ray interactions in the galaxy are calculated. These electrons arise from the decay of secondary pions and neutrons produced by nuclear interactions of cosmic-ray protons and alpha particles with the interstellar gas. The equilibrium flux is determined by escape of electrons from the galaxy and by ionization, inverse Compton, and synchrotron energy losses. A comparison of the calculated secondary electron equilibrium spectrum with the measured electron intensity, positron-negatron ratio, and nonthermal radio emission from the galactic halo suggests that an additional primary electron source of roughly the same magnitude is required. (auth)

39631 POSSIBLE PRESENCE OF RELIC QUARKS IN COSMIC RAYS. Feinberg, E. L. (Lebedev Inst. of Physics, Moscow). JETP Lett. (USSR) (Engl. Transl.), 3: 324-6(June 15, 1966).

Translated from Zh. Eksp. Teor. Fiz., Pis'ma Redaktsiyu, 3: 497-501(June 15, 1966).

Several possible mechanisms of cosmic-ray generation of quarks are considered. It is concluded that the primary flux of cosmic rays can be expected to contain quarks, especially in the low-energy region, $Eq/mgc^2 \lesssim 10$. The ratio ξ of their flux to the proton flux can be smaller than the average relative concentration of cold quarks by several orders of magnitude, $\xi \sim 10^{-15}\ m_N$ 1 mg, but can also reach $\xi \sim Q \sim 10^{-11}$, for example, if the cosmic-ray acceleration is by the statistical noninjective mechanism. (L.B.S.)

39632 SEARCH FOR DISCRETE SOURCES OF HIGH-ENERGY COSMIC GAMMA RAYS. Oegelman, Hakki Boran. Ithaca, N. Y., Cornell Univ., 1966. 82p.

Thesis.

An attempt to detect discrete sources of cosmic gamma rays above 1 Bev with a balloon-borne instrument is reported. The apparatus consisted of a pair of sonic spark chambers, 850 cm^2 in area and separated by 22.5 cm, which recorded the direction of the pair formed after conversion of the photon in the one radiation length of lead above the upper chamber. An energy detector consisting of alternate layers of lead and scintillation in coincidence with a counter placed under the lead converter and an anticoincidence scintillator umbrella over the whole system selected the gamma-ray events above 1 Bev and also defined the cone of acceptance. The aspect of the apparatus with respect to earth was measured by a down-pointing camera. In the final analysis, the sidereal direction of the gamma ray was determined with a maximum likely error of 3°. After the screening of the data recorded at a float altitude of 105,000 feet, 845 events were chosen as fit for analysis. These were distributed between 20^h and 4^h in right ascension, −20° and 80° in declination. From this distribution it was concluded that within this region, there are no discrete sources of high-energy gamma rays with intensities greater than 10^{-4} photons/cm^2 sec. In particular, upper limits to the gamma-ray flux from some of the likely sources are given. (Dissertation Abstr.)

Direct Energy Conversion

Refer also to abstracts 39938, 40307, 40364, and 40451.

39633 (CEA-R-2788) CONVERTISSEURS A RADIO-ISOTOPES. (Radioisotope Converters). Alleau, Thierry; Devin, Bernard; Vandevyver, Michel (Commissariat a l'Energie Atomique, Saclay (France). Centre d'Etudes Nucleaires). June 1966. 14p. Dep. mn.

Due to the surface power density required for thermoelectric and thermoionic converters, available radioactive sources are surveyed and listed. Curves of specific minimum diameter versus thermal flux density are given. ^{210}Po and ^{242}Cm appear to be suitable for direct thermionic while alpha emitters such as ^{238}Pu and ^{244}Cm are still suitable for thermoelectric conversion. This mode will also work with beta emitters ^{170}Tm, ^{90}Sr, ^{144}Ce, and ^{137}Cs. Some thermoelectric radioisotope heated converters are suggested. (auth)

39634 (JPL-32-946) COMPARISON OF LIQUID-METAL MAGNETOHYDRODYNAMIC POWER CONVERSION CYCLES. Weinberg, E.; Hays, L. G. (Jet Propulsion Lab., Calif. Inst. of Tech., Pasadena). Aug. 15, 1966. 27p.

Various two-phase liquid-metal magnetohydrodynamic (MHD) power conversion cycles employing either a separator or jet condenser were compared on the basis of cycle efficiency, prime radiator area, and specific weight. The cycles were investigated first from the standpoint of coalescence on a wall (of the separator or jet condenser) with attendant friction and deflection energy losses and, second, from the standpoint of liquid coalescence with no friction or deflection energy losses. The results of this study for the first condition showed that (1) the two-component cycles, both separator and condenser (employing lithium and cesium), had efficiencies of 6 to 7%, while the single-component (one chemical species — cesium or potassium) had maximum efficiencies of only 3 to 4%, and (2) the two-component separator cycle (cesium–lithium) had a slightly higher efficiency and smaller radiator area than the two-component condenser cycles (cesium–lithium), if 100% liquid impingement was assumed on the condenser and separator walls. For the second condition — operation without separator and condenser friction or deflection — it was shown that (1) the two-component cycles required about half as much radiator area as the single-conponent cycles, for a given efficiency, and (2) the efficiency of the two-component condenser cycles (cesium–lithium) increased indefinitely with decreasing rejection temperature, while the efficiency of the two-component separator cycle (cesium–lithium) was limited to 13%. It thus appears that the most promising cycle for space applications is the two component (cesium–lithium) separator cycle, if 100% liquid impingement occurs on the walls of the jet condenser and on the separator. The two-component (cesium–lithium) condenser cycles appear promising for ultimate high efficiency, should it be possible to eliminate condenser friction. (auth)

39635 (UCRL-16699) THERMIONIC EMISSION FROM PLANAR MONOCRYSTALLINE TUNGSTEN. Schreiner, Sheldon Ira (Lawrence Radiation Lab., Univ. of California, Berkeley). June 1966. Contract W-7405-eng-48. 54p. Dep. mn. CFSTI $3.00 cy, $0.50 mn.

Thesis.

A thermionic diode and a vacuum system to test it were constructed to investigate the bare work function of (110) and (111) planar monocrystalline tungsten. The collector was (100) monocrystalline copper held at constant temperature. The work function for (110) tungsten was found to be 5.22 ± 0.01 V over the temperature range 2163 to 1697°K. For (111) tungsten the work function was found to be 4.74 ± 0.15 V over the range 2237 to 2013°K. At lower temperatures effects attributed to adsorption on the (111) surface were observed. The (100) copper work function was found to be 4.07 and 4.43 V for the two runs made but neither value is representative of a truly bare (clean) surface. The system pressure throughout the runs varied from 5×10^{-10} to 8×10^{-9} torr. (auth)

39636 EXPERIMENTAL STUDY ON THE SEEDED COMBUSTION GAS OF MHD GENERATION. Ito, Toshio (Mitsubishi Electric Mfg. Co., Ltd., Japan); Tominaga, Moriyuki. Mitsubishi Heavy Ind. Tech. Rev., 3: 205-12 (May 1966). (In Japanese).

The results of an experimental study on the physical properties of combustion gases as MHD working fluid are discussed. In this experiment, seeded combustion gas was generated by an acetylene–oxygen burner at seeded mass flow rate of 20 to 100 g/sec. In the combustion chamber, potassium as seed material and nitrogen were mixed by high-temperature flame to flow through a duct for measurement, in which fluid with a high velocity of 300 to 500 m/sec was generated. Temperature was carefully measured by Na–D line reversal method. The electrical conductivity of gas was measured by impressing d-c voltage from batteries to the electrodes. The functional relations between the electric conductivity and the temperature showed a fairly good agreement with the theoretical values which were calculated by the method proposed by Frost. The interesting fact was that the current could flow even in the case of cold copper electrodes with an electrode drop of only 65 to 80 volts. This phenomenon referring to the optical observation of electrode surface was examined. In parallel with the above measurements, the rates of heat transfer were measured at the wall of combustion chamber and at the surface of the electrodes. It was found that heat transfer rate at the combustion chamber showed a fairly good agreement with the calculated values in which only radiation loss was taken into account. On the other hand, heat transfer rate at the electrode surface was shown to be higher than the values estimated from the convective heat transfer in the turbulent flow. (auth)

39637 THERMIONIC CONVERTERS. Thomas, Donald E. (to Westinghouse Electric Corp.). U. S. Patent 3,265,910. Aug. 9, 1966. Filed Oct. 18, 1962.

A thermionic converter is described in which a gas is introduced into the space between the anode and the cathode of the converter to form a volatile compound of the cathode material that is unstable at the cathode temperature; thus depositing material on the cathode surface. Cesium vapor is ordinarily introduced in the space between the cathode and the anode to reduce the space charge and to lower the work function of the cathode to enhance electron emission from the cathode. In the thermionic converter described, the space between the anode and the cathode is filled with a halogen gas. The halogen gas serves the dual purpose of reducing the space charge while also protecting the cathode from evaporation. (F.S.)

39638 CERAMIC STRUCTURES FOR DIRECT ENERGY CONVERSION DEVICES. Tubman, Philip E. (Consolidated Controls Corp., Bethel, Conn.). 17p. (CONF-660505–10). ORAU. Gmelin, AED-CONF-66-103-12.

From American Ceramic Society Meeting, Washington, D. C.

The hostile environment capability of ceramic materials is challenged by the effort to convert heat directly into electric power. In concert with the genesis of the "Cesium Vapor Thermionic Diode" and on an equal level to it, was the development of its several associated ceramic structures. Among the ceramic components of a diode system are: a metal-ceramic heating plate, a potted heater, a plasma sprayed ceramic heater structure, a ceramic-to-metal lead through, exact spacing ceramic to metal seals, fossil fuel heat source parts, flame containment shells, insulators both heat and electrical, and ceramic-based cathode and collector structures. Several of these structures are discussed from a ceramic technologist's point of view. (auth)

39639 SHOCK-WAVE MHD GENERATOR USING A NUCLEAR REACTOR AS AN ENERGY SOURCE. Brocher, E.; Chevalley, J. L. (Battelle Memorial Inst., Geneva, Switzerland). 9p. (CONF-660326–5). ORAU. Gmelin, AED-CONF-66-047-8.

From 7th Symposium on Engineering Aspects of Magnetohydrodynamics, Princeton, N. J.

The use of shock-waves of moderate intensity is an efficient way of superheating a gas, preheated by a nuclear reactor for example, up to temperatures of interest for MHD power generation. A scheme is proposed to pulsate the preheated gas with shock-waves so as to directly produce a-c power with the MHD generator. A thermodynamical cycle comprising, among other components, an advanced type of high temperature gas-cooled reactor ($T \sim 1500$°K), a pressure exchanger, and a shock-wave MHD generator is analyzed. It is shown that the cycle efficiency is about 52%, and that the dimensions of the shock-wave MHD generator are very reasonable for a practical design. (auth)

39640 ELECTRICAL CHARACTERISTICS OF THE LINEAR HALL AND FARADAY GENERATORS AT SMALL HALL PARAMETERS. Zauderer, B. (General Electric Co., Philadelphia). 37p. (CONF-660326–4). ORAU.

From 7th Symposium on Engineering Aspects of Magnetohydrodynamics, Princeton, N. J.

Experiments were performed to determine the electrical characteristics of the linear, segmented-electrode, Hall, and Faraday MHD generators. The generator working fluid was shock-heated xenon at 7000°K gas temperature, one atmosphere pressure, equilibrium conductivity of 850 mhos/m, and a Hall parameter which ranged in value from 0.7 to 2.5. The study was performed with and without magnetically induced ionization effects in the generator. If the electrode voltage losses were included in the data analyses, the Faraday generator load characteristics were in agreement with the theory of Hurwitz, Kilb, and Sutton. If the voltage losses at the Hall current electrodes were included in the data analyses, the Hall generator load characteristics obtained under equilibrium plasma conditions were in agreement with the theory of Dzung. In the presence of magnetically induced ionization, the open circuit Hall voltage and the Hall load characteristics were on the average 30% and 10%, respectively, below the theoretically predicted values. The Hall output reduction is attributed to plasma nonuniformities caused by gas dynamic forces, Lorentz forces and nonuniform extra-thermal ionization effects. (auth)

39641 MODELS FOR ELECTRON EMISSION FROM METALS WITH ADSORBED MONOLAYERS. Kaplit, M.; Schrenk, G. L. (Univ. of Pennsylvania, Philadelphia). 11p. (CONF-660324–4). ORAU. Gmelin, AED-CONF-66-036-8.

From 26th Annual Conference on Physical Electronics, Cambridge, Mass.

The ability of a semi-classical model to describe a metal-gas interface was investigated theoretically. Using the Thomas-Fermi-Dirac theory, both the microscopic charge distribution and the total electronic energy of the interface were evaluated in such a way that one can distinguish between the classical and quantum mechanical contributions. It was shown that the quantum mechanical corrections are a significant part of the total energy and may not be neglected. It is concluded that a semi-classical model, using only the concepts of classical atomic physics, is not an adequate representation of the electronic properties of alkali–refractory metal or alkaline earth–refractory metal interfaces. Detailed results for both cesium and barium adsorption on (100) and (110) faces of tungsten are presented. (auth)

39642 EFFECT OF SURFACE MICROPATCHES ON THE AVERAGE THERMIONIC CONSTANTS OF METALLIC EMITTERS. Coomes, E. A.; Boeck, W. L. (Univ. of Notre Dame, Ind.). 5p. (CONF-651049-21). ORAU. Gmelin, AED-CONF-65-324-23.

From IEEE Thermionic Conversion Specialist Conference, San Diego, Calif.

Measurements of "monocrystallographic" Richardson constants for recrystallized W and Mo filaments with a resolution of about 20,000 angstroms gave evidence of micropatches; similar evidence appeared for thorium adsorbed on these single crystals. A computer analysis based on the assumption that a micropatch is that fundamental area on an emitter over which the Richardson equation in the form derived from statistical mechanics rigorously applies, was completed. Some conclusions of interest in experimental thermionics are the following: (a) a functional relation will exist between A_R and ϕ_R, if these averages are strongly influenced by micropatches; (b) $A_R > 120$ cannot be obtained without a micropatch temperature coefficient; (c) the micropatch distribution which gives the observed functional relation between A_R and ϕ_R seems to be an area-weighted Gaussian. In fact, the best fit given by the computer follows from a distribution quite similar to that found experimentally by Haas for uranium carbide. (auth)

39643 LARGE EXPERIMENTAL SUPERCONDUCTING MAGNET FOR MHD POWER GENERATION. Stekly, Z. J. J.; Hatch, A. M.; Zar, J. L.; Latham, W. N.; Borchert, C.; El Bindari, A.; Bernert, R. E.; de Winter, T. A. (Avco-Everett Research Lab., Everett, Mass.). 24p. (CONF-660628-7). ORAU. Gmelin, AED-CONF-66-173-11.

As a part of an overall program to develop MHD for central station electric power generation, a large model superconducting magnet was built and tested. It was demonstrated that a superconducting magnet of the size and type under consideration would operate in a reliable manner and would have performance reasonably close to design predictions. The specifications established at the start of the project were to provide a magnetic field to approximately 40 kilogauss perpendicular to the axis in a 30.5-cm diameter cylindrical hole for a length of 1.22 m. A preliminary test was made on one layer of winding, representing about one-tenth of the full winding. Fully stable operation was demonstrated on this test. When the complete ten-layer magnet winding was completed it was subjected to a series of tests to determine its performance and operating characteristics. (M.O.W.)

39644 ENGINEERING DEVELOPMENTS IN ENERGY CONVERSION. Presented at International Conference on Energetics, University of Rochester, August 18–20, 1965. New York, American Society of Mechanical Engineers, 1965. 331p. (CONF-650826).

Separate abstracts were prepared for 8 of the 22 included papers. Ten of the remaining were not in the scope of NSA, and hence, omitted. For abstracts of the remaining 4 papers see CONF 650826 in the report number index. (M.O.W.)

For abstracts of individual papers see: 39645–39652.

39645 EVALUATION OF THE PERFORMANCE CHARACTERISTICS FOR A FARADAY GENERATOR. Schultz-Grunow, F.; Denzel, D. L. (Technische Hochschule, Aachen). pp 1-14 of Engineering Developments in Energy Conversion. New York, American Society of Mechanical Engineers, 1965.

A complete quantitative description of open circuit voltage, inner resistance and Hall voltage is presented for a Faraday generator. Tensorial conductivity and one arbitrary velocity profile are considered. Use is made of conformal mapping for a single pair of electrodes. This implies that the usual assumption of homogenous current distribution along the center line is unnecessary. The extension of the procedure to an infinite number of electrodes is achieved by determining the current dividing line by the condition of equal electric potential differences between similar points on the current dividing lines. This is done by iteration. With this also the limit for the current leakage between adjacent electrodes is determined. The mapping of the field lines shows a considerable concentration of the current at one edge of each electrode with a high potential drop along the insulator. With this the essential quantities for the performance of a Faraday generator are determined. (auth)

39646 CURRENT-VOLTAGE MEASUREMENTS IN A SUPERSONIC MHD GENERATOR WITH AN ARC HEATED ARGON PLASMA. Mantenieks, M. A.; Nichols, L. D. (Lewis Research Center, Cleveland). pp 33-48 of Engineering Developments in Energy Conversion. New York, American Society of Mechanical Engineers, 1965.

The electrical characteristics of a supersonic magnetohydrodynamic generator with an arc-heated argon plasma are presented. The argon at about one-half atmosphere and heated to a total temperature of 9500 K is expanded to Mach 3.5. The resulting nonequilibrium plasma in the generator section has electron temperatures between 6300 and 6600 K at pressures of about 6 to 8 millimeters of mercury. A magnetic field of up to 0.58 Tesla was used for the generator. The electrodes were immersed in the stream to obtain thermal emission and to penetrate the relatively cold boundary layer at the walls. Current-voltage characteristics indicate two modes of discharge in the generator. In the first mode, the performance seemed to depend strongly on the surface characteristics of the electrodes and on the plasma boundary layers. In this mode, Hall effects and ion slip appear to play an important part in the plasma resistance at the electrode surfaces. In the second mode, performance is determined more by bulk plasma properties independent of the magnetic field and the electrode surface effect. (auth)

39647 CALCULATION OF IDEALIZED MHD GENERATOR PERFORMANCE WITH NON-EQUILIBRIUM ELECTRON HEATING. Oliver, D. A.; Eustis, R. H. (Stanford Univ., Calif.). pp 49-57 of Engineering Developments in Energy Conversion. New York, American Society of Mechanical Engineers, 1965.

The theoretical performance of a K-seeded Ar, infinitely segmented MHD generator was calculated using energy dependent electron collision cross sections. A new upper bound on performance for nonequilibrium operation was presented which is significantly lower than reported by Hurwitz et al., but is still far superior to equilibrium performance. (M.O.W.)

39648 PROSPECT FOR ELECTROGASDYNAMIC POWER. Gourdine, M. C.; Malcolm, D. H. (Gourdine Systems, Inc., Livingston, N. J.). pp 58-75 of Engineering Developments in Energy Conversion. New York, American Society of Mechanical Engineers, 1965.

It is estimated that a 1-kilowatt closed-cycle EGD generator can be built operating with an output voltage of several million volts and the energy cost would be around $0.10 per kilowatt hour. Comparing this with the cost of high-voltage electricity from Van de Graaff generators or other high voltage machines, there is a factor of 10 reduction in price. This can conceivably be achieved in the near future. When this happens, high voltage applications will multiply rapidly For example, the irradiation of food for preservation will become economically feasible. New chemical processes with x-ray radiation can be developed; high energy electron beam welding will be practicable. These and other applications will deserve a new look from industry. Military applications, as yet unforeseen, will come forth as engineers are presented with these new, convenient, and relatively cheap sources of high voltage electricity. (M.O.W.)

39649 EXPERIMENTAL INVESTIGATION OF THE PERFORMANCE CHARACTERISTICS OF AN ELECTROGASDYNAMIC POWER GENERATOR. Shiue, James C.; Kahn, Bernard; Brandmaier, Harold E. (Curtiss-Wright Corp., Wood-Ridge, N. J.). pp 76-94 of Engineering Developments in Energy Conversion. New York, American Society of Mechanical Engineers, 1965.

An experimental program involving the generation of high-voltage electricity by transporting unipolar charged particles in a high velocity gas flow is presented. A number of experiments involving the significant parameters which affect the characteristics of the generation process are described and the results are given. These are compared with theoretical estimates based on a one-dimensional analysis. The electrogasdynamic generator under investigation appears to have applications in improved high-voltage, low-current power sources. (auth)

39650 ANALYTIC SOLUTION FOR A TWO DIMENSIONAL, AXISYMMETRIC EGD CONVERSION CHANNEL. Wang, Kenneth (Curtiss-Wright Corp., Wood-Ridge, N. J.). pp 95-109 of Engineering Developments in Energy Conversion. New York, American Society of Mechanical Engineers, 1965.

Electric power generation using monopolar charged particles in fluid flow is investigated. Analytic solutions for the charge distribution and electric field are derived based on a two-dimensional, axisymmetric EGD channel. In obtaining the solution, fluid flow is simplified as one dimensional. It is shown that both charge distribution and radial electric field increase sharply near the dielectric wall of channel and form a "charge layer effect." Furthermore, the potential and the field in the axial direction deviate little from their values at the wall. Therefore, for practical computations, approximate relations derived for charge density, potential and electric field in the radial direction in combination with boundary conditions, can be used. Adapting a criterion for spark breakdown as that of the total electric field, the voltage-current limitations of EGD power generation are determined. Numerical examples are presented to show the potentials of EGD device operating under normal conditions. By examining the governing parameters the possible improvements obtainable by varying different operating conditions are analyzed. It is seen that for EGD power generation to be practical pressurization of the conversion channel offers the best approach. (auth)

39651 SURVEY OF THEORY AND LABORATORY PERFORMANCE OF CESIUM THERMIONIC CONVERTERS. Houston, John M. (General Electric Research Lab., Schenectady, N. Y.). pp 216-37 of Engineering Developments in Energy Conversion. New York, American Society of Mechanical Engineers, 1965.

A theoretical discussion of cesium thermionic converters is presented. The power output, efficiency, and lifetime measurements using electrically heated laboratory-type cesium thermionic converters are described. (M.O.W.)

39652 GAMMA-ELECTRIC CELL THEORY AND EXPERIMENT. Miley, G. H.; Sampson, H. T. (Univ. of Illinois, Urbana). pp 238-51 of Engineering Developments in Energy Conversion. New York, American Society of Mechanical Engineers, 1965.

The Gamma-Electric Cell is a device which directly converts gamma-ray energy into electrical energy. Basic theory and preliminary experimental results from reactor and cobalt-60 irradiations are presented. (auth)

39653 SOME MECHANICAL ENGINEERING ASPECTS OF MHD POWER GENERATION. Vienna, International Atomic Energy Agency, 1966, Preprint No. SM-74/43, 21p. (CONF-660704-2). ORAU.

From Magnetohydrodynamic Electrical Power Generation, 2nd International Symposium, Salzburg.

The factors affecting the design of possible directly and indirectly fired air heaters are discussed and the features of some are described. One of these is a concept in which a circulating stream of molten material is used to transfer heat between hot combustion products and air. For an oil-fired unit the medium used would be potassium sulfate, the seed material itself. This would pick up impurities from the oil combustion products until an equilibrium concentration is reached. For a coal-fired unit the medium would be molten coal ash, although the separation of seed from coal ash would then require a separate operation. Experiments which are being carried out to provide design data for possible air heaters are described and cover the pumping and atomization of high temperature fluids; the testing of suitable refractory materials, aerodynamic model studies; the development of refractory seals. Seeding chemicals introduced to enhance gas conductivity pose special problems of corrosion and deposition in the air heater, and this has led to an extensive study of the physical chemistry of the seed. Some relevant aspects of this work are also recorded. These will include measurements of the partial vapor pressure of solid and liquid potassium sulfate in the temperature range 900 to 1700°K, a study of the liquid phases which occur in seed mixed with oil ash impurities or coal ash slag, and potassium sulfate vapor pressure in equilibrium with these mixed liquids up to 2200°K in a typical flue gas. For completeness the studies of residual fuel-oil and coal combustion systems are briefly described. (auth)

39654 LARGE EXPERIMENTAL COMBUSTION FIRED GENERATOR. Vienna, International Atomic Energy Agency, 1966, Preprint No. SM-74/44, 16p. (CONF-660704-3). ORAU.

From Magnetohydrodynamic Electrical Power Generation, 2nd International Symposium, Salzburg.

Design considerations and performance calculations are presented for an experimental constant velocity generator with a design input of 200 Mw. Two electrical modes are considered: the first using segmented Faraday connections with constant load factor, K, the second using diagonally cross-connected electrodes with the field direction E at a constant angle to the duct axis. A load condition for the latter is described and the power output and pressure drop of the two types compared. The cross-connected case is shown to give a higher output and a lower pressure drop than the constant-K segmented generator. The optimum output with variation of velocity and seed concentration is calculated for the cross-connected case with E at 45° to the axis. Calculation of power output as a function of length shows a very slow increase beyond 2 m due to the high pressure drop produced by the restriction of field angle. The available data on the effect of roughness on heat transfer and friction are considered and the influence on performance is calculated. A practical, quasi-constant velocity, experimental subsonic generator presently being erected is described. The first duct is made up of tube loops at 45° to the axis with constant electrode separation and an inlet to outlet area ratio of 3.5 : 1. The performance of this generator has been calculated for energy inputs between 80 Mw and 280 Mw and for a range of load factors. An efficiency of 8% is expected over a wide range of mass flows. The performance in the end regions is calculated using one-dimensional equations together with the magnetic field profile of the actual magnet. The effects of using a single load with this generation duct and the design of a duct specifically to use a single load connection are considered. (auth)

39655 ELECTRICAL MEASUREMENTS ON A MOVING ARGON PLASMA. Abbas, A. A. M.; Howatson, A. M. (Oxford Univ.). Vienna, International Atomic Energy Agency, 1966, Preprint No. SM-74/26, 16p. (CONF-660704-4). ORAU.

From Magnetohydrodynamic Electrical Power Generation, 2nd International Symposium, Salzburg.

Experimental current-voltage characteristic curves were obtained for a moving argon plasma at two stations in an electrically driven 5-cm shock tube. The standard energy was 1 kJ and the base pressure 10 torr, giving a shock of about Mach 4. The measurements were made on the highly ionized driver gas which followed the shock at speeds between 800 and 1100 m/sec. (W.D.M.)

39656 ANALOGY BETWEEN A HIGH-DENSITY PLASMA AND METAL–AMMONIA SOLUTIONS. Alekseev, V. A.; Velikhov, E. P.; Lopantseva, G. B. (Kurchatov Inst. of Atomic Energy, Moscow). Vienna, International Atomic Energy Agency, 1966, Preprint No. SM-74/102, 6p. (In Russian). (CONF-660704-5). ORAU.

From Magnetohydrodynamic Electrical Power Generation, 2nd International Symposium, Salzburg.

Bethe has proposed as the working fluid of an MHD generator a dense plasma in which quantum phenomena associated with the overlapping wave functions of the electrons of neighboring atoms play an important part. Virtually no theoretical or experimental investigations have been carried out on such a plasma. Information about the plasma properties to be expected is derived by comparing the plasma with metal–ammonia solutions and strongly alloyed semiconductors, which have been the subject of more extensive study. (auth)

39657 INSULATORS AND CONDUCTORS FOR MHD FLOW. Anthony, A. M.; Foex, M. (Centre National de la Recherche Scientifique, Paris). Vienna, International Atomic Energy Agency, 1966, Preprint No. SM-74/67, 20p. (In French). (CONF-660704–6). ORAU.

From Magnetohydrodynamic Electrical Power Generation, 2nd International Symposium, Salzburg.

Results published at the 1964 Symposium showed that, whereas it is possible to find an insulator at 1900°K, above that temperature all the oxides considered (ZrO_3Ca, ZrO_3Sr, MgO), whatever their origin, become too conductive ($\sigma > 1$ ohm^{-1}m^{-1}) for use as an MHD duct wall. Conduction in the oxides is due principally to thermal agitation which causes defects in the crystal lattice, and it may therefore be considered that, the more perfect the lattice, the greater will be the energy required for the occurrence of defects—with the latter appearing only at high temperatures. For this reason pure compounds (ZrO_3Ca and ZrO_3Sr) were prepared in the solar furnace and the effect of stoichiometry on their electrical conductivity was studied. Maximum resistance was observed to be a function of variation in the ZrO_2/MO (M = Sr or Ca) ratio, but this was attenuated with temperature: for ZrO_3Sr, the maximum resistance decreased from 23 ohm.m at 1700°K to 1.3 ohm.m at 2000°K. Bearing in mind the fact that in an MHD duct the material will exhibit evolution even if highly stoichiometric, results confirm the preliminary trials: insulating walls cannot be expected to operate at temperatures of above 1800°K. (auth)

39658 RECOVERY OF RESIDUAL ENTHALPY OF GASES AT THE OUTLET OF AN MHD DUCT. Aptel, J. (S. A. Heurtey, Paris). Vienna, International Atomic Energy Agency, 1966, Preprint No. SM-74/117, 16p. (In French). (CONF-660704–7). ORAU.

From Magnetohydrodynamic Electrical Power Generation, 2nd International Symposium, Salzburg.

It may be expected that, in whatever form seeding material is injected into an MHD duct, the alkaline metal which it contains will reappear as a carbonate, and as a sulfate if the fuel contains sulfur, in the exhaust gases when their temperature falls below 1900°K. It appears in the liquid phase and solidifies at about 1200°K. Because of its dissociation at above approximately 1900°K and its extremely corrosive nature in the liquid phase, a method of recovery is employed in which a fluidized-bed heat exchanger first of all reduces the temperature of the exhaust gases from 2500 to 2000°K. The exhaust gases are then quenched in a diluting channel by the addition of cold air; this reduces their temperature to 1200°K and causes the carbonate and sulfate within the gas current to solidify into a powder. The recovery of enthalpy then proceeds in the conventional manner, the carbonate and sulfate, which can be re-utilized as seeding material, being recovered by means of a dust collector before the cold gases pass into the atmosphere. The thermodynamic balance resulting from this method is considered. The possibility of separating the sulfate from the carbonate and of re-utilizing only the latter as seeding material is mentioned, and the energy cost of this operation is estimated. The characteristics of a fluidized-bed heat exchanger coupled to a 500 Mw(th) generator are considered, and the technical and technological design problems are reviewed. Such an exchanger consists of a hot chamber (diameter 13 m), at the base of which the exhaust gases enter from the duct, and a cold chamber (diameter 7 m), at the bottom of which the air to be reheated enters; the hot chamber is mounted above the cold chamber. The heat-carrying granules pass by gravity in a dense phase from the hot to the cold chamber through a column in which the leakage of cold air towards the hot chamber is limited by friction losses. The granules return from the cold to the hot chamber in a fluid phase, the necessary cold air flow being of the order of 1% of the total flow. For design reasons the duct is arranged vertically, so that the length of the high-temperature channelling can be reduced to a minimum. The assumptions regarding the movement of the granules between the two chambers and the flow rate of the escaping gas corresponding to the differences in pressure between them are compared with the experimental results obtained with a model which is described. Results of tests on the resistance of the granules to thermal shock are given. The solutions to the technological problems involved in designing the diluting channel are outlined, in particular the use of porous refractory materials through which is blown part of the air required for dilution. (auth)

39659 EFFECT OF GASEOUS IMPURITIES ON THE CONDUCTIVITY OF AN ALKALI METAL PLASMA. Archambault, Y. (CSF-CEPEC, Orsay, France). Vienna, International Atomic Energy Agency, 1966, Preprint No. SM-74/199, 6p. (In French). (CONF-660704-8). ORAU.

From Magnetohydrodynamic Electrical Power Generation, 2nd International Symposium, Salzburg.

In order to determine the effect of polyatomic impurities on an alkaline plasma usable in closed-cycle magnetohydrodynamic conversion, the axial electric field and the electron temperature were measured in a positive column of gaseous cesium by means of probes. The cesium pressure was between 10^{-1} and 1 torr. The impurities introduced were nitrogen and hydrogen, at pressures varying between 10^{-4} and 1 torr. The following results were observed: For diatomic impurity pressures less than 10^{-2} torr, a rapid growth in the electric field was found to accompany an increase in the impurity pressure, with no marked change in the electron temperature. The electric field increased as the alkaline pressure and current density decreased. This increase is due to a drop in the electron density, which in turn is due to a decrease in the number of fast ionizing electrons, lost through inelastic collisions on the vibration levels of the impurity molecules. For impurity pressures above 10^{-2} torr, a rapid decrease in the electric field in the discharge was observed when the impurity pressure was increased at constant current. At the same time there is a visible striction of the positive column, which assumes a thread-like structure. The electron temperature also increases slightly. This phenomenon is explained as follows: in a region of low electron density ($<10^{12}$ cm^{-3}), the electron distribution tail is weak since the inelastic collisions on impurities absorb more fast electrons than the electron-electron collisions can supply. The plasma cannot therefore by sustained. For high electron densities ($>10^{15}$ cm^{-3}), however, the electron-electron collisions constitute a very efficient source of fast electrons and compensate for the losses due to collisions on impurities. In these circumstances the discharge can only exist at high density, and this would explain the striction and high conductivity of the discharge. (auth)

39660 MHD GENERATOR OPERATION AS AFFECTED BY ELECTRODE CURRENT SATURATION. Armstrong, J. F.; George, D. W.; Messerle, H. K. (Univ. of Sydney). Vienna, International Atomic Energy Agency, 1966, Preprint No. SM-74/27, 8p. (CONF-660704–9). ORAU.

From Magnetohydrodynamic Electrical Power Generation, 2nd International Symposium, Salzburg.

The effect of electrode-to-plasma conduction processes on the performance of an MHD generator was studied. An extended series of tests in a generator duct using argon seeded with potassium sulfate indicated that operating conditions could be severely modified by saturation effects. Once saturation conditions were exceeded it was found that non-equilibrium conditions at the cathode dominate the

overall current conduction through a generator duct. Current saturation at a cathode in an MHD generator is due to two primary effects. For a cold cathode with no thermionic emission the current is due to positive ions reaching the cathode and the free flow of ions is limited by the random ion current hitting the surface. If an attempt is made to raise the current beyond this value extra ions have to be attracted from the plasma. These extra ions undergo collisions before reaching the cathode and are thus impeded. The current increase is then limited by the ionic resistivity in the plasma leading to a saturation effect. If the cathode emits electrons, the saturation current is increased by the emission saturation current. As it happens, for low cathode surface temperatures, the emission current becomes negligible and the saturation effect is dominated by the random ion current. At high surface temperatures the thermionic emission effect takes over. The transition depends on bulk gas temperature, seed conditions, and cathode work function. For a work function of the order of 4.5 ev the transition is found to be near 1800°K under practical operating conditions when the bulk gas temperature exceeds that of the cathode surface. The random ion current is shown to be independent of cathode surface temperature and is thus determined by the bulk gas conditions. It increases with bulk gas temperature and seed ratio. The performance of a saturation-limited generator can only be improved then by changing the bulk gas conditions. In effect, increased surface temperatures only help in practical cases when the surface work functions are well below 4 ev. The results were obtained in a specially designed generator duct using an arc torch (40 kw) as heat source. The duct measured $1 \times \frac{1}{2}$ in. with alumina side walls and indirectly heated, full-width graphite electrodes. Electrode temperatures could be independently controlled from 900 to 2100°C and the gas temperature ranged from 2700 to 6000°C. (auth)

39661 CONFORMAL TRANSFORMATION INVESTIGATIONS ON MHD DUCTS OF FINITE LENGTH AND SEGMENTATION. Aufaure, M.; Croitoru, Z. (Electricite de France, Clamart). Vienna, International Atomic Energy Agency, 1966, Preprint No. SM-74/78, 12p. (In French). (CONF-660704-10). ORAU.

From Magnetohydrodynamic Electrical Power Generation, 2nd International Symposium, Salzburg.

Several methods of calculation using the Schwarz conformal transformation have been proposed for the electrical study of MHD generators with tensorial conductivity. Generally speaking, these methods have permitted the study of the end effects of generators with continuous or infinitely segmented electrodes, or the performances of generators of infinite length with regularly spaced segments. A rigorous method has recently been published, which can be used for the simultaneous study of the end effect and finite segmentation effects of any MHD duct. This method was used to make a general study of the performances of ducts of finite length with electrodes of finite segmentation. The laws governing the separation of lines of current between adjacent electrodes remote from and near to the ends of the duct are demonstrated. (auth)

39662 PLASMA PROPERTIES INDUCED IN AIR BY ALPHA RADIATION. August, Henry (North American Aviation, Inc., Los Angeles). Vienna, International Atomic Energy Agency, 1966, Preprint No. SM-74/119, 10p. (CONF-660704-11). ORAU.

From Magnetohydrodynamic Electrical Power Generation, 2nd International Symposium, Salzburg.

The plasma characteristics of partially dissociated and ionized air due to alpha emissions from a radioisotope surface material were investigated. Preliminary estimates of average electron energy, electron attachment coefficient, electron-ion recombination coefficient, distribution of equilibrium electron density, plasma frequency, electrical conductivity, and dielectric properties normal to a radioactive surface were made for alpha-radiated air. (W.D.M.)

39663 CONDITIONS FOR THE USE OF DUCTS OF DISK GEOMETRY IN MHD CONVERSION. Azalbert, Jean-Paul; Zettwoog, Pierre (CEN, Gif-sur-Yvette, France). Vienna, International Atomic Energy Agency, 1966, Preprint No. SM-74/141, 16p. (In French). (CONF-660704-12). ORAU.

From Magnetohydrodynamic Electrical Power Generation, 2nd International Symposium, Salzburg.

The conditions governing the use of ducts of disk geometry for the MHD conversion of the thermal energy contained in a cesium-seeded noble gas are examined. Hot source temperatures of between 1600 and 2000°K and helium or argon pressures of 1 to 50 bars were considered. The total temperature of the MHD out-going gas was fixed at 1250°K, beyond which value the gas could be taken over by more conventional units. For each pressure level, determinations were made of the thermal power beyond which the viscous entropy losses per unit length of wall were negligible in relation to the volume Joule losses corresponding to the normal operation of the duct. It was assumed that the magnetic fields are obtained from superconductor coils; 5-Teslas and 6-Teslas possibilities were studied. (W.D.M.)

39664 MINIMUM-VOLUME CONVERSION DUCT. Azalbert, Jean-Paul; Ricateau, Pierre (CEN, Gif-sur-Yvette, France). Vienna, International Atomic Energy Agency, 1966, Preprint No. SM-74/142, 12p. (In French). (CONF-660704-13). ORAU.

From Magnetohydrodynamic Electrical Power Generation, 2nd International Symposium, Salzburg.

In connection with an MHD conversion duct with known upstream and downstream stagnation conditions, the conditions which will make for the minimum volume, which is thought to correspond largely to the most economic conditions, are considered. On this basis, the problem of the optimum for the duct and the optima for the other components of the power plant are separated. The most general problem of the optimum specific power $\sigma U^2B^2K(1-K)$ for a segmented electrode Faraday duct in the absence of thermal losses and friction is discussed, without the usual arbitrary separation of the optimization of the factor $K(1-K)$ and that of the product σU^2; the magnetic field is assumed to be constant. The conversion equations are written in a simple form which makes it possible to utilize the calculus of variation. A system of two differential equations is obtained characterizing the evolution of the fluid. It is shown that the Mach number and the load factor are no longer independent. The integration of the differential system is performed numerically for a perfect gas in the case of thermodynamic equilibrium, the load factor at the inlet being varied for given initial conditions. It is ascertained that the evolution is different depending on whether the inlet load factor is more or less than 0.5. If a diagram is drawn showing the mean specific power efficiency—the scatter of points representing all the optimum ducts possible—it is found that this scatter has an envelope. Similarly, all the figurate points of the ducts with constant velocities and load factors are found in an envelope inside the first. The differential equations for the optimization of a real gas are given. (auth)

39665 IONIZATION AND TEMPERATURE MEASUREMENT IN MPD EXPERIMENTS. Balfour, D.; Watson, M. D. S. (International Research and Development Co. Ltd., Newcastle-upon-Tyne, Eng.). Vienna, International Atomic Energy Agency, 1966, Preprint No. SM-74/34, 12p. (CONF-660704-14). ORAU.

From Magnetohydrodynamic Electrical Power Generation, 2nd International Symposium, Salzburg.

During MPD experiments with the IRD loop and cesium vaporization tests with a small-scale version of the center core of the CNEN blow-down facility heater, experiments were performed at IRD in which the electron concentration and temperature of cesium-seeded helium were measured by microwave and reversal techniques. The Q band microwave interferometer (employing tantalum propagation horns

and sapphire windows) used for the electron concentration measurements is described. Phase-shift measurements at temperatures between 1400 and 1900°K and with cesium seeding fractions between 0.006 and 1.0 atomic per cent enabled the magnitude and temporal variation of the electron concentration to be studied. Fluctuations in the electron concentration are shown to result from the irregular injection of cesium into the helium flow however; the measured ionization level was in accord with thermal equilibrium ionization for magnetic fields less than one Tesla. To obtain accurate temperature measurement in the range 1400 to 2000°C line reversal methods were employed. The intensities of the 4593 Å cesium line and a calibrated tungsten strip filament lamp were compared. Since the cesium line was used for these measurements no additional impurities were introduced into the plasma. The optical arrangement employed a lens system and a narrow band interference filter in conjunction with a photomultiplier. An arrangement of rotating sectors enabled the absorption and emission of the gas to be monitored continuously: the reversal temperature was deduced from the resulting signals. The physical significance of this temperature is discussed. (auth)

39666 ELECTRIC ARC IN A FLOW OF IONIZED AND NON-IONIZED GAS. Baranov, V. Yu.; Vasileva, I. A.; Ulyanov, K. N. (Lenin All-Union Electrotechnical Inst., Moscow). Vienna, International Atomic Energy Agency, 1966, Preprint No. SM-74/238, 12p. (In Russian). (CONF-660704-15). ORAU.

From Magnetohydrodynamic Electrical Power Generation, 2nd International Symposium, Salzburg.

A d-c electric arc in a flow of spectroscopically pure argon and a mixture of argon with cesium was investigated for argon pressures of 20 to 200 torr, cesium pressures to 0.1 torr, arc currents of 0.01 to 5.0 A, and flow velocities to 10^4 cm/sec. The flow was produced in a closed glass loop (200 by 4 cm) by means of an electromagnetic accelerator consisting of a number of electric arcs in a transverse magnetic field. Measurements were made of the spatial distributions of the electron concentration and temperature, the gas temperature, and the strength of the electric field by probe and spectral methods. In addition, photographs and films were made. The experiments showed that the flow deflects the transverse arc, the degree of deflection depending on the velocity of the flow, the pressure, the composition of the mixture, and the arc current. (W.D.M.)

39667 EXPERIMENTAL EVALUATION OF MHD GENERATORS OPERATING AT HIGH HALL COEFFICIENTS. Bartlelemy, Robert R.; Stephan, Brian G.; Cooper, Robert F. (Air Force Aero Propulsion Lab., Wright-Patterson AFB, Ohio). Vienna, International Atomic Energy Agency, 1966, Preprint No. SM-74/166, 8p. (CONF-660704-16). ORAU.

From Magnetohydrodynamic Electrical Power Generation, 2nd International Symposium, Salzburg.

The operation of open-cycle MHD generators under a wide variety of gas conditions has been the subject of many papers in recent years. However, the experimental evaluation of such operation, particularly at large values of the Hall parameter and Mach number, has been scarce. A flexible combustion-driven MHD generator test facility is being constructed to allow investigations of various generator-operating parameters, generator configurations and designs, and component materials. A schematic of the open cycle test facility is shown. The plasma source is a combustion chamber in which toluene, or another suitable fuel, is burned with gaseous oxygen diluted with nitrogen. Potassium hydroxide seed is injected with the fuel to produce the necessary plasma conductivity. The gas stream is accelerated in a supersonic nozzle and then flows through the channel. The first generator channel to be tested is described and future experiments are discussed. (W.D.M.)

39668 OPTIMUM MAGNETS FOR MHD GENERATORS. Barthelemy, Robert R.; Oberly, Charles E. (Air Force Aero Propulsion Lab., Wright-Patterson AFB, Ohio). Vienna, International Atomic Energy Agency, 1966, Preprint No. SM-74/167, 16p. (CONF-660704-17). ORAU.

From Magnetohydrodynamic Electrical Power Generation, 2nd International Symposium, Salzburg.

The areas of applicability for permanent, conventionally cooled resistive, cryogenically cooled resistive, and superconductive magnets to open-cycle MHD power generation systems are defined. Combustion-driven MHD generators utilizing continuous-electrode Faraday, segmented-electrode Faraday, and Hall configurations were investigated. In all cases, typical values of gas scalar conductivity, gas velocity, and Hall coefficient were used. Operation of such generators was considered over the range of net power output from 100 kw to 1000 Mw for power durations of one millisecond to one year. Relationships were derived between the net power output of any MHD system and the field strength and geometry of its magnet. The analysis took into consideration the effect of magnet characteristics and generator design on the overall efficiency and various energy losses of the system. The relations were used to select the type, design, and characteristics of the magnet which optimizes the cost and weight of the generation system for each point on the net power spectrum. In carrying out the optimization process, magnets and refrigerant systems are assumed to be operated with power generated by the MHD process. The cost, weight, and power requirements of magnet cooling systems were calculated and included in the magnet design criteria. Other factors, such as relative MHD duct configurations, thermal insulation requirements, and magnet packing fraction are discussed in terms of their effect on the final design of a magnet for a fully optimized generator configuration. Selection of magnet types for stationary and mobile systems and for short and long duration systems was made. The results are presented for the three types of MHD generators. These results were plotted on power duration and net power output coordinates to show the economical operating regimes for the various magnets. Both a weight and cost optimum regime are shown for the entire generator operating regime. (W.D.M.)

39669 INJECTION OF LIQUID METALS IN MHD CONVERTERS. Basov, S. N.; Kirillov, P. L.; Subbotin, V. I.; Turchin, N. M. Vienna, International Atomic Energy Agency, 1966, Preprint No. SM-74/107, 18p. (In Russian). (CONF-660704-18). ORAU.

From Magnetohydrodynamic Electrical Power Generation, 2nd International Symposium, Salzburg.

The advantage of an injector over other methods of introducing liquid metals under pressure is that, after the energy of the vapor has been expended in accelerating the atomized liquid, the vapor need not be separated from the liquid since it condenses on it. The thermodynamic cycle of an injector is similar in configuration to the cycles of steam-turbine systems and they can have the same thermal efficiency. The internal efficiency of an injector depends mainly on the injection coefficient, which in turn depends on the ratio of heat of evaporation to thermal capacity. In the case of metals this ratio is such that it precludes an internal efficiency greater than 0.03. The internal efficiency can be increased by using two metals (two-component injector). Other methods for increasing efficiency include: arrangement of diffusion flow, injection of a cold liquid into the vapor flow, repeated addition of a liquid to the vapor before it leaves the nozzle, and arrangement of boiling in the nozzle followed by condensation of the vapor. In the system proposed by Elliot there are no losses due to collisions between the liquid and the vapor, and hence the efficiency of the system is higher. The main difficulty in the arrangement is the problem of separating the liquid from the vapor. Ways of improving the system by using a free jet for separating the liquid are considered. The losses and efficiency of vapor energy conversion by this method are estimated. The experimental arrangement is described and the measured velocities of the potassium in the nozzles are presented. The experimental results agree with the calculations. It was established in the experiments that it is possible to avoid both overheating of the liquid metal and delays in reaching the boiling point. (auth)

39670 EXPERIMENTAL STUDY OF THE ELECTRIC CONDUCTIVITY OF AN ARGON PLASMA WITH AN IONIZING ADDITIVE. Batenin, V. M.; Sheindlin, A. E.; Asinovskii, E. I. (Moscow State Univ.). Vienna, International Atomic Energy Agency, 1966, Preprint No. SM-74/226, 10p. (In Russian). (CONF-660704-19). ORAU.

From Magnetohydrodynamic Electrical Power Generation, 2nd International Symposium, Salzburg.

The electric conductivity of a weakly ionized argon plasma in a direct current arc was determined experimentally. The experimental rig, which consists of an arc heater giving an argon stream with a temperature of 1000 to 2000°K and a measuring section, is described. An experimental method is proposed for varying the ratio between the contaminated and neutral components of the plasma over a wide range by introducing an easily ionizable additive. Measurements were carried out at temperatures of 3000 to 5000°K for contaminated particle concentrations in the range 10^{13} to 10^{15} cm^{-3}. The experimental data were used to study the validity of different approximations of the Chapman-Cowling theory as applied to calculating the electric conductivity of a weakly ionized argon plasma. It is shown that the fourth approximation of the theory is unsatisfactory for calculating the electric conductivity of an argon plasma in the range of contaminated particle concentrations concerned. (auth)

39671 IONIZATION INSTABILITY AND TURBULENT CONDUCTIVITY OF NON-EQUILIBRIUM PLASMA. Belousov, V. N.; Eliseev, V. V.; Shipuk, I. Ya. (Kurchatov Inst. of Atomic Energy, Moscow). Vienna, International Atomic Energy Agency, 1966, Preprint No. SM-74/88, 16p. (In Russian). (CONF-660704-20). ORAU.

From Magnetohydrodynamic Electrical Power Generation, 2nd International Symposium, Salzburg.

A pulsed discharge in a transverse magnetic field in a discharge tube of rectangular geometry with segmented electrodes was investigated. The experiments were carried out on mixtures of argon with mercury and argon with cesium. The electron temperature, the electric fields, the electron density, and the topology of nonhomogeneities in the plasma were measured. Typical experimental conditions were a gas pressure of the order of 100 mm/Hg, a concentration of atoms in the admixture of 10^{14} to 10^{15} cm^{-3}, a current density of 1 to 10 A/cm^2, and magnetic-field strength B of 0 to 10^4 Oe. The maximum value of the ratio of the Larmor frequency of revolution of the electron to its frequency of collision attained in the experiment was of the order of 10. (W.D.M.)

39672 SOME RESULTS OF EXPERIMENTS WITH A 100-kw MHD GENERATOR MODEL. Berger, M. S.; Mikhin, V. V.; Kurbatovskii, Yu. N. Vienna, International Atomic Energy Agency, 1966, Preprint No. SM-74/212, 12p. (In Russian). (CONF-660704-21). ORAU.

From Magnetohydrodynamic Electrical Power Generation, 2nd International Symposium, Salzburg.

Experiments were carried out with a model of a linear conduction MHD generator at fairly high levels of specific power, current density, and electric field strength. To obtain results free of secondary effects, MHD interaction parameter values greater than unity were used. The MHD interaction was achieved in the fairly small model by raising the electric conductivity of the working fluid by heating it to 3500 to 4500°K in an electric arc preheater. The load characteristics under steady-state conditions were recorded for short runs of two seconds. Results obtained with an uncooled model with segmented electrodes and segmented load and using helium seeded with K_2CO_3 are given. (W.D.M.)

39673 EFFECT OF IONIZATION SATURATION AND DUCT SHAPE ON LOSSES NEAR WALLS. Bernard, Jean; Ricateau, Pierre; Zettwoog, Pierre (CEN, Gif-sur-Yvette, France). Vienna, International Atomic Energy Agency, 1966, Preprint No. SM-74/143, 14p. (In French). (CONF-660704-22). ORAU.

From Magnetohydrodynamic Electrical Power Generation, 2nd International Symposium, Salzburg.

In ducts where there is a large Hall effect the distribution of the current density is known to be very irregular near the walls which support the electrodes. These irregularities are due to the boundary conditions imposed on the surface of the electrode, which is equipotential, and also on the surface of the intermediate insulating layer, which does not allow a normal current component. These losses are a matter for concern in a open-cycle conversion duct since they give rise to the need for considerable electrode subdivision, which is liable to be expensive. They are disastrous in the case of closed-cycle gas systems when an electron heating effect is involved. A very elementary analysis shows that it is possible to make the current distribution almost completely regular along the electrodes, thanks to the low resistivity of the gas parallel to B, by simply inclining the wall in relation to the magnetic field. An equally simple analysis indicates that inclining the wall cuts out the inter-electrode "short-circuit" effect because the current component which is perpendicular to B and u is no longer zero along the insulator. This is equivalent to increasing the apparent resistivity parallel to u. It is almost impossible to establish the correct formulae because of the tridimensionality of the field but the very approximate formulae obtained indicate that an inclination of 45° is perfectly adequate. It seems reasonable to suppose, therefore, that by breaking down the walls of the electrode into elementary planes inclined in relation to B, the supplementary distortion losses caused by the Hall effect will disappear. In the specific case where the electron heating effect considerably aggravates the "short-circuit" effect, another type of remedy might be possible: the seeding concentration could be adjusted so as to achieve almost complete ionization of the atoms in the normal operation of the duct. The conductivity investigations reported at the Paris Symposium in 1964 have been pursued along these lines and a region of complete cesium inonization has been established in an argon gas. This region is indicated by a current zone in which the conductivity is more or less constant and whose upper limit is imposed by the beginning of the ionization of the argon. The theoretical interpretation, which takes account of the ionization of the two gases, provides very good confirmation of the measured results in this region. It is thus possible to calculate the seeding that has to be used in a duct to ensure that the conductivity appears constant in the apparatus as a whole, including the regions near the inter-electrode spacers. (auth)

39674 RELAXATION PHENOMENA IN MPD GENERATORS. Bertolini, E. (CNEN, Frascati, Italy); Toschi, R.; McNab, I. R. Vienna, International Atomic Energy Agency, 1966, Preprint No. SM-74/23, 14p. (CONF-660704-23). ORAU.

From Magnetohydrodynamic Electrical Power Generation, 2nd International Symposium, Salzburg.

From the basic equations for MPD quasi-one-dimensional flow, five differential equations (momentum and energy equations for the plasma and for the electron specie and continuity equation for the electrons) were derived and used to investigate, in linear MPD generators, relaxation lengths of electron temperature and density using a two-temperature fluid model. The variations along the channel, of other parameters (i.e., gas temperature, pressure and electrical conductivity, flow Mach number, power density, etc.), were also computed. The computations were performed for different inlet conditions of the gas, magnetic fields, channel dimensions, and configurations. It was found that, for the case of equilibrium flow through the nozzle, the electron density reached its asymptotic value in lengths which satisfactorily agreed with the experimental data on transient time for ionization. The transients of the electron temperature and density in the direction transverse to the flow were also analyzed to show their importance in particular cases. For values of the generator parameters typical of some experimental situations, the electron concentration may never reach a value consistent with the equilibrium of the magnetically induced ionization: this could be one of the possible explanations for the partial failure of small experiments in

observing magnetically induced ionization. When frozen flow through the nozzle occurs (the extreme of nonequilibrium flow through the nozzle), the relaxation length appeared to be shorter than in the previous case. The electron concentration at the duct inlet may also exceed the level appropriate to magnetically induced ionization: in this case the electron concentration falls to the nonequilibrium level at a rate governed by the recombination mechanism. The integration of the differential equation system was performed for lengths of the duct up to 50 cm. (auth)

39675 CNEN HELIUM–CESIUM BLOW-DOWN MPD FACILITY AND EXPERIMENTS WITH A PROTOTYPE DUCT. Bertolini, E. (CNEN, Frascati, Italy); Toschi, R.; Lindley, B. C.; Brown, R.; McNab, I. R. Vienna, International Atomic Energy Agency, 1966, Preprint No. SM-74/24, 20p. (CONF-660704–24). ORAU.

From Magnetohydrodynamic Electrical Power Generation, 2nd International Symposium, Salzburg.

The CNEN blow-down loop has been designed to study a helium–cesium MPD generator with particular regard to nonequilibrium ionization effects. A sufficiently wide range of the stagnation conditions can be obtained with the present arrangement of the loop (temperature up to 2000°K, pressure from slightly subatmospheric to 6 ata, gas mass flow from 50 gr/sec to 400 gr/sec, seed fraction from 0.1% to 2% atomic weight). The storage heater is an alumina pebble bed electrically heated with tungsten elements and thermally insulated with zirconia fiber; the thermal capacity at 2000°K is about 1000 MJ. Liquid cesium is injected into a limited section of the pebble bed to provide a mixture of the two gases uniform in density and temperature. The duct walls and transfer can be preheated up to 1700°K. A magnetic field of 4 Wb/m^2 is obtained with a pulsed cryogenic magnet with pulse duration of 6 sec. Two series of experiments were completed to assess the feasibility of the helium-cesium heating system and the generator duct. A third series of experiments concerning the behavior of the working channel as an MPD generator was performed with the IRD closed-loop facility using a scale constant cross-section duct. Over 60 hours of high-temperature operation with helium, and 63 individual cesium-seeded runs (duration 30 sec to 2 min) were performed. The results, over a range of temperatures from 1460 to 1740°K, magnetic field from 0.35–1.03 Wb/m^2, seed fraction from 0.009–0.178 at. % indicated the satisfactory operation of the channel. (W.D.M.)

39676 ELECTRICAL PARAMETERS OF A SYNCHRONOUS MHD GENERATOR WITH PULSATING ELECTRIC CONDUCTIVITY OF THE MEDIUM. Bezusy, L. G. (Inst. of Electrodynamics, Kiev). Vienna, International Atomic Energy Agency, 1966, Preprint No. SM-74/210, 10p. (In Russian). (CONF-660704–25). ORAU.

From Magnetohydrodynamic Electrical Power Generation, 2nd International Symposium, Salzburg.

Electrodynamic equations were solved for the flow of a fluid with periodically changing electric conductivity in a constant external magnetic field. The thickness of the insulation of the magnetic pole surfaces was assumed to be finite. From the results obtained it was possible to estimate the specific power, the synchronous inductive resistance, the output voltage, and other parameters of a synchronous MHD generator with pulsating electric conductivity. (auth)

39677 ENERGY EXCHANGE BETWEEN ELECTRON AND MOLECULAR GASES. Biberman, L. M.; Mnatsakanyan, A. Kh. (Moscow State Univ.). Vienna, International Atomic Energy Agency, 1966, Preprint No. SM-74/215, 6p. (In Russian). (CONF-660704–26). ORAU.

From Magnetohydrodynamic Electrical Power Generation, 2nd International Symposium, Salzburg.

The energy exchange between electrons and heavy particles is one of the main problems involved in investigating nonequilibrium plasma. The energy exchange between an electron gas and a molecular gas was considered and it was shown that the exchange mechanism depends essentially on the composition of the latter. For a gas consisting of molecules capable of forming an unstable negative ion (N_2, CO, etc.) this process was decisive. Calculations were made of the rate of energy exchange between an electron gas and nitrogen at different temperatures of the two gases, and it was shown that the rate of exchange, which was governed by this mechanism, exceeded by some orders of magnitude the corresponding value associated with other processes, which were generally taken into account. (auth)

39678 MHD GENERATOR USING AN EMULSION. Bidard, Rene; Sterlini, Jacques (Cie Electro-Mecanique, Paris). Vienna, International Atomic Energy Agency, 1966, Preprint No. SM-74/108, 14p. (In French). (CONF-660704–27). ORAU.

From Magnetohydrodynamic Electrical Power Generation, 2nd International Symposium, Salzburg.

An MHD generator is proposed in which the working fluid is an emulsion consisting of gas or steam in a liquid metal. The emulsion is subjected to a magnetic field and expanded in the MHD channel itself. Various solutions involving liquid metals have been proposed, but the transfer of energy from the gas to the liquid metal is usually inefficient. Moreover, there are considerable losses as the liquid metal enters and leaves the magnetic field. With the proposed solution, however, and provided the emulsion is sufficiently fine and homogeneous, the problem of energy transfer between the nonconducting, but elastic, gas or steam and the nonelastic, but conducting, liquid metal is solved in a highly satisfactory manner. Moreover, it is then possible to locate entirely within the magnetic field MHD loops in which the gas is introduced and extracted, but where the liquid metal circulates in a closed circuit. In this way MHD losses as the liquid metal enters and leaves the magnetic field are eliminated. With MHD loops of this type the working fluid can be made to flow in complete thermodynamic cycles; compression of the gas (at low temperature) may possibly also be achieved within an MHD system using an emulsion, so that the assembly will be completely closed and without moving parts. Various arrangements are described by means of which suitable thermodynamic cycles can be achieved, allowance being made for the limitations imposed by the nature of the working fluid (possible expansion ratios in the case of an emulsion) and for partial evaporation of the liquid metal. A number of loops are arranged in series at the gas outlet and operate at successively higher temperature levels obtained by adventitious recycling of the liquid metal. (auth)

39679 INVESTIGATION OF MAGNETICALLY INDUCED IONIZATION IN RARE GAS MIXTURES. Blackman, Vernon H.; Sunderland, Robert J.; Jones, Malcolm S. Jr. (MHD Research, Inc., Newport Beach, Calif.). Vienna, International Atomic Energy Agency, 1966, Preprint No. SM-74/165, 24p. (CONF-660704–28). ORAU.

From Magnetohydrodynamic Electrical Power Generation, 2nd International Symposium, Salzburg.

An investigation was carried out to determine whether an MHD generator could be operated in a nonequilibrium ionization mode without seeding the gas flow with a low ionization potential component such as cesium. Elimination of the seed material would simplify the working fluid circulation loop and ease the channel wall materials problem. The approach followed was to seek a gas combination which possessed a low breakdown potential and a low mean atomic weight to ensure a large streaming velocity, resulting in high values of induced E/p for moderate magnetic fields and pressures. A mixture of helium and argon appeared to offer the desired properties and calculations were made to compare the conductivity of a helium rich mixture with that of pure argon under the same operating conditions. The appearance consisted of an MHD channel with segmented electrodes coupled to a plasma jet heater. Experiments were performed to measure the plasma conductivity as a function of magnetic field and external load resistance. The results indicate that limited magnetically induced ionization was achieved. (auth)

39680 CLOSED MHD-LOOP ARGAS. Bohn, Th.; Foerster, S.; Kolb, G.; Holzapfel, C.; Noack, G. (Kern-

forschungsanlage, Juelich, Ger.). Vienna, International Atomic Energy Agency, 1966, Preprint No. SM-74/124, 16p. (CONF-660704-29). ORAU.

From Magnetohydrodynamic Electrical Power Generation, 2nd International Symposium, Salzburg.

The experimental plant ARGAS is described with regard to its technological and constructional particularities as well as to the intended research program and measuring devices. The cross-sectional area of the channel is 50 cm^2. The maximum operating data are: mass flow rate 4.2 kg/sec (argon), Mach number 0.85; stagnation temperature 1800°K; magnetic induction 2 Teslas. The static pressure in the channel may be varied between 0.5 and 8 bars. The purpose of the ARGAS-Loop, containing the same principal components as existing in later MHD power plants is to collect experiences for closed MHD energy conversion plants as well as to investigate plasma diagnostic measurements in the MHD channel. The main design data of the installation are explained and explanatory illustrations of the functional mode and construction of the plant parts are given. (auth)

39681 LAY-OUT DATA OF A HOMOGENEOUS CLOSED-CYCLE 300 Mw MHD GENERATOR. Bohn, Th.; Kolb, G.; Holzapfel, C. (Kernforschungsanlage, Juelich, Ger.). Vienna, International Atomic Energy Agency, 1966, Preprint No. SM-74/125, 10p. (CONF-660704-30). ORAU.

From Magnetohydrodynamic Electrical Power Generation, 2nd International Symposium, Salzburg.

The conductivity in a fine segmented Hall generator and a Faraday generator with semiconducting electrodes was calculated from the energy balance of the electrons under consideration of the radiative losses. In the calculation of the radiative losses the levels were assumed to be in the energy equilibrium with the electrons. The ionization was calculated from the Saha equation. The influence of big dimensions of the channel on the radiative losses is described. From the conductivity thus determined and with the aid of the linear fundamental equations of the generator, the energy conversion and the dimensions of the channel were determined. Heat and friction losses were taken into account. (auth)

39682 ANALYSIS OF ESSENTIAL CHARACTERISTICS FOR CLOSED MHD POWER STATIONS. Bohn, Th.; Foerster, S.; Noack, G. (Kernforschungsanlage, Juelich, Ger.). Vienna, International Atomic Energy Agency, 1966, Preprint No. SM-74/126, 12p. (CONF-660704-31). ORAU.

From Magnetohydrodynamic Electrical Power Generation, 2nd International Symposium, Salzburg.

In view of the rapid development of the gas-cooled high-temperature reactors, interest is growing towards the pure gas circulating systems, in which the energy conversion in the MHD converter is followed by energy conversion in a gas turbine furnishing directly the compressor drive power. With a view to low plant costs this station type requires increased consideration. Various working processes of power stations are compared in order to show clearly their typical particularities. The different types of power stations considered are combinations of conventional power converters equipped with MHD generators. For a comparison with each other the most important values are determined. Those values are the frictional and heat losses, the specific mass flow rates, the volume of the different plant parts, the compressor drive power, and the gas temperature at the reactor entrance. All these values are computed as a function of the initial gas temperature of the process. The results will be taken for an estimation of the plant costs. (W.D.M.)

39683 MEASUREMENT OF THE ELECTRICAL CONDUCTIVITY OF ^3He INDUCED BY NEUTRON IRRADIATION. Braun, J.; Nygaard, K. (Aktiebolaget Atomenergi, Studsvik, Sweden). Vienna, International Atomic Energy Agency, 1966, Preprint No. SM-74/33, 26p. (CONF-660704-32). ORAU.

From Magnetohydrodynamic Electrical Power Generation, 2nd International Symposium, Salzburg.

The conductivity of a ^3He plasma created by the inelastic reaction with thermal neutrons ($^3He + n_{th} \rightarrow {}^3H + p + 0.76$ Mev) was studied as a function of neutron flux, gas temperature, and gas density. Using reported values of the electron mobility the electron density was calculated from experimental conductivity values. Further, by accepting a reasonable value for the mean energy lost in creating one ion-pair, the recombination coefficient was estimated. The measurements covered temperatures between 300–1600°K and densities between 0.25–1 times the density at atmospheric pressure and 300°K. The neutron flux was varied between 10^{10}–10^{11} n $cm^{-2}s^{-1}$. As a sample of results achieved at 1600°K and the lowest density (corresponding to about atmospheric pressure) and the highest neutron flux the following values were obtained for the conductivity, the electron density, and the recombination coefficient respectively: $\sigma = 0.2\ S_m^{-1}$; $n_e = 6 \cdot 10^{11}\ cm^{-3}$; $\alpha = 2 \cdot 10^{-10}\ cm^3\ s^{-1}$. An extrapolation of data obtained showed that the concept of neutron induced conductivity should be attractive for MHD power generation. (auth)

39684 NON-EQUILIBRIUM CONDUCTIVITY IN AN ARGON–POTASSIUM PLASMA IN CROSSED ELECTRIC AND MAGNETIC FIELDS. Brederlow, G.; Feneberg, W.; Hodgson, R. (Institut fuer Plasmaphysik, Garching, Ger.). Vienna, International Atomic Energy Agency, 1966, Preprint No. SM-74/15, 12p. (CONF-660704-33). ORAU.

From Magnetohydrodynamic Electrical Power Generation, 2nd International Symposium, Salzburg.

The tensor conductivity was measured in an argon-potassium plasma under MHD generator conditions. Typical conditions in the streaming plasma were: pressure 1.2 atmosphere, gas temperature 2000°K, argon flow rate 16 gr/sec, gas mixture 0.2% K + 98.8% Ar magnetic field 0–17 kΓ. The measurement volume was 15 mm × 20 mm × 100 mm. The electric field strength and direction were measured with tungsten probes set in the measurement channel. The uniformity of the current density and its direction could be checked by the electric field uniformity. The homogeneity of the current density distribution could also be checked by measuring the intensity distribution of the light emitted from the plasma in the direction of the magnetic field. The tensor conductivity was calculated from the known electric field, current density vector, and the angle between them. The electron temperature was measured as a function of current density and magnetic field by the line reversal method. The conductivity of an argon-potassium mixture was calculated at electron temperatures between 2000 and 3500°K. The results of these calculations showed a drop in the scalar conductivity with an applied magnetic field in qualitative agreement with the experimental results. (auth)

39685 DEVELOPMENT OF THE FLOW OF A VISCOUS, ANISOTROPICALLY CONDUCTING FLUID IN THE DUCT OF AN MHD GENERATOR. Breev, V. V.; Gubarev, A. V. (Kurchatov Inst. of Atomic Energy, Moscow). Vienna, International Atomic Energy Agency, 1966, Preprint No. SM-74/103, 16p. (In Russian). (CONF-660704-34). ORAU.

From Magnetohydrodynamic Electrical Power Generation, 2nd International Symposium, Salzburg.

The flow of a viscous, anisotropically conducting fluid in the radial (or cylindrical) duct of a Hall-type MHD generator employing a nonequilibrium plasma as fuel possesses the following characteristics: 1. The velocities as the fluid enters the generator duct can have a uniform, a developed laminar (Poiseuille), or a turbulent profile depending on the shape of the acceleration nozzle. In any one of these cases the velocity profile in the first sections of the duct differs from the steady-state MHD profile, i.e., at least in the first sections of the duct the problem can be solved by considering the development of a viscous fluid flow for a given velocity profile at the entry to the duct. The problem was solved analytically

and on a computer. It was shown that the length of channel through which the flow passes before becoming stabilized depends essentially on the Hartmann and Hall numbers and on the initial velocity profile, and that there is a considerable difference between the distances traversed before stability of the profile of the longitudinal and transverse velocity components is achieved. 2. Due to the presence of a longitudinal current component the flow developes rotation in the generator duct. When the flow is stabilized (at high interaction parameter values) the transverse component is of the same order as the longitudinal component; in this situation the direction of the velocity vector is not constant through the depth of the viscous boundary layer. The boundary layer "depth" ascertained from the profile of the transverse velocity component may be considerably greater than that ascertained from the profile of the longitudinal component. Moreover, it is found that there is a velocity maximum near the insulating wall. 3. The "heating" field, which is everywhere greater than zero, varies through the depth of the viscous boundary layer. For this reason Joule heating of the electrons is found to vary through the depth of the boundary layer. Consequently, and also as a result of diffusion, radiation, and thermal conductivity of the electrons, the conductivity of the gas in the boundary layer is found to vary, which considerably alters the flow conditions in the boundary layer. (auth)

39686 AN a-c MHD GENERATOR WITH PULSATING FLOW IN A PRE-HEATED GAS. Brocher, E.; Chevalley, J. L. (Battelle Memorial Inst., Geneva). Vienna, International Atomic Energy Agency, 1966, Preprint No. SM-74/118, 13p. (CONF-660704-35). ORAU.

From Magnetohydrodynamic Electrical Power Generation, 2nd International Symposium, Salzburg.

The use of shock-waves of moderate intensity is an efficient way of superheating a gas, preheated by a nuclear reactor for example, up to temperatures of interest for MHD power generation. A scheme is proposed to pulsate the preheated gas with shock-waves so as to directly produce a-c power with an MHD generator. A thermodynamical cycle comprising, among other components, an advanced type of high-temperature gas-cooled reactor (T ~1500°K), a pressure exchanger, and a shock-wave MHD generator, is analyzed. The efficiency of the different components of the plant is estimated, and it is shown that the thermal-to-electric efficiency is about 52%. (auth)

39687 FURTHER DEVELOPMENT, OPERATION AND EXPERIMENTS WITH THE IRD CLOSED-CYCLE MPD LOOP. Brown, R. (International Research and Development Co. Ltd., Newcastle-upon-Tyne, Eng.); Lindley, B. C.; McNab, I. R. Vienna, International Atomic Energy Agency, 1966, Preprint No. SM-74/36, 28p. (CONF-660704-36). ORAU.

From Magnetohydrodynamic Electrical Power Generation, 2nd International Symposium, Salzburg.

The IRD closed-cycle MPD loop has been operated as a power generator since April 1964 and several hundred separate experiments have been carried out. In the closed-cycle loop continuously filtered and purified helium is heated electrically by a graphite electrical resistance heater capable of producing gas temperatures up to 2200°C. A metered flow of liquid cesium is vaporized and superheated with the helium. In the present system the mixture of helium and ionized cesium passes through a subsonic nozzle to the constant area MPD generator duct, followed by a diffuser, recuperative heat exchanger and final cooler. Cesium is removed in a series of traps and filters before helium re-enters the circulator. The magnetic field is provided by a water-cooled copper 22 kilogauss magnet with an axial field length of 22 in. Loop development has included investigation of transport and reaction mechanisms within the high-temperature regions resulting in formation and deposition of electrically conducting layers on the generator duct walls. The present loop has operated successfully and remained clean after frequent cycles and periods of high-temperature operation exceeding 50 hr. Generator duct wall heaters have been developed to give control of the wall temperature. High-temperature windows have allowed pyrometric temperature measurement of nozzle inlet stagnation temperature, visual, and spectroscopic viewing of the cesium vapor injection and helium-cesium plasma, and microwave and spectroscopic analysis of plasma parameters. Investigations have been carried out on problems of vaporizing and superheating cesium seed in the high-temperature helium flow, cesium seed recovery, filtration and purification. Improved helium purification and analysis plant incorporating a fully automatic chromatograph sampling valve provides impurity gas analysis to levels of less than 1 ppM. In the experimental program the variation of electrical conductivity over a wide range of important parameters has been investigated. Segmented Faraday and Hall mode operation have been investigated. In the majority of the experiments the measured open-circuit voltage is considerably less than anticipated; the reasons for this discrepancy are examined in detail. (W.D.M.)

39688 OPERATING EXPERIENCE OF AN OPEN CYCLE MHD TEST FACILITY. Brzozowski, W. S.; Celinski, Z. N.; Kozlowski, T. (Inst. of Nuclear Research, Swierk, Poland). Vienna, International Atomic Energy Agency, 1966, Preprint No. SM-74/53, 20p. (CONF-660704-37). ORAU.

From Magnetohydrodynamic Electrical Power Generation, 2nd International Symposium, Salzburg.

The test facility used for experiments on open-cycle power generation is described. Its main part consists of a combustion chamber burning kerosene as fuel at a rate of approximately 25 to 45 kg/h and alcohol solution of KOH as seeding source. The chamber is fed by air preheated to the temperature of 650 to 750°C. Oxygen enrichment is used to the maximum amount of 10%. A conventional magnet provides a magnetic field of 25,000 gauss intensity, over a volume of 50 cm × 12 cm × 6 cm, consuming approximately 80 kw. Air supplied to the combustion chamber is pre-heated in the recuperator. The design enables air to be pre-heated to the nominal temperature of 750°C with short-lived excursions to 900°C. Some experimental results are presented from the tests carried out in order to find out the electrode material and design most suitable for severe conditions prevailing inside the generator duct. Numerous materials were tested as possible duct electrodes. Cold electrodes made of copper or of copper plated with tantalum, niobium, and nickel, with internal water cooling, were tested as well as electrodes made of borides with gas cooling. Hot electrodes, without any cooling at all made of specially doped zirconia were thoroughly examined. Results of measured average heat flux to the walls versus combustion gases flow rate are presented. (W.D.M.)

39689 OPEN-CYCLE POWER GENERATION EXPERIMENT WITH HIGH PREHEAT TEMPERATURE OF AIR. Brzozowski, W. S.; Dul, J.; Fuksiewicz, E.; Kozlowski, T. (Inst. of Nuclear Research, Swierk, Poland). Vienna, International Atomic Energy Agency, 1966, Preprint No. SM-74/57, 16p. (CONF-660704-38). ORAU.

From Magnetohydrodynamic Electrical Power Generation, 2nd International Symposium, Salzburg.

An open-cycle MHD rig has been designed and is being constructed. The main purpose of the planned experiment is to gain practical experience with the operation of the high-temperature part of the cycle. It will consist of: a main combustion chamber of approximately 1.5 to 2 Mw thermal input, burning kerosene or light oil with potassium seeding; MHD generator of 0.5 m length; medium-temperature heat exchanger of the radiative type; low-temperature heat exchanger of the convective type; high-temperature heat exchanger of the pebble-bed type; auxiliary combustion chambers to heat the matrix composed of pebbles; air supply from compressor station or from the gas turbine. The circuit flow diagram is shown and general arrangements of the rig discussed. (auth)

39690 PRODUCTION AND INVESTIGATION OF MATERIALS FOR A MAGNETOHYDRODYNAMIC GENERATOR. Brzozowski, W. S.; Fiszdon, J.; Gauk, W.; Wang, R. (Inst. of Nuclear Research, Swierk, Poland). Vienna, International Atomic Energy Agency, 1966, Preprint No. SM-74/62, 16p. (In Russian). (CONF-660704-39). ORAU.

From Magnetohydrodynamic Electrical Power Generation, 2nd International Symposium, Salzburg.

In investigating materials for a magnetohydrodynamic generator a study was made of the production of ceramic and cermet laminated walls. Special equipment was used in experiments for determining the stability of the materials under the influence of thermal cycling and thermal flux, and a study was made of the stability of materials based principally on silicon. (auth)

39691 CHOICE OF OPTIMUM MACH NUMBER FOR A FLOW OF A NON-EQUILIBRIUM HELIUM–CESIUM PLASMA IN AN MHD GENERATOR DUCT. Burenkov, D. K.; Morozov, A. E.; Ovcharenko, V. A. (Moscow State Univ.). Vienna, International Atomic Energy Agency, 1966, Preprint No. SM-74/220, 12p. (In Russian). (CONF-660704-40). ORAU.

From Magnetohydrodynamic Electrical Power Generation, 2nd International Symposium, Salzburg.

The dependence of the local value of the specific output power of an MHD generator on the Mach number for a helium-cesium plasma was investigated. It is shown that the specific power optimum occurs at certain Mach numbers, and the effect of deceleration temperature and internal efficiency level on the optimum pressure is explained. It is also shown that as pressure increases and deceleration temperature decreases the optimum Mach number is lower and the specific output power of the generator falls sharply. (auth)

39692 EFFECT OF INHOMOGENEITY OF THE MAGNETIC FIELD ON THE FLOW OF CONDUCTING FLUID IN HALL-TYPE MHD GENERATORS. Burenkov, D. K. (Moscow State Univ.). Vienna, International Atomic Energy Agency, 1966, Preprint No. SM-74/227, 12p. (In Russian). (CONF-660704-41). ORAU.

From Magnetohydrodynamic Electrical Power Generation, 2nd International Symposium, Salzburg.

The effect of inhomogeneity of the magnetic field on flow distribution in the duct of a Hall-type MHD generator using a magnetic system whose density varies along the radius of the duct is discussed. Assuming an incompressible working fluid, the effect of inhomogeneity of the magnetic field on the characteristics of the MHD generator is discussed as a function of the ratio between internal and external duct radius and the Hall number. (auth)

39693 REDUCTION OF THE DIMENSIONS OF INDUCTION CONVERTERS BY SKIN-HEATING. Burkhardt, H.; Ruhs, N. (Technische Hochschule, Stuttgart). Vienna, International Atomic Energy Agency, 1966, Preprint No. SM-74/49, 16p. (CONF-660704-42). ORAU.

From Magnetohydrodynamic Electrical Power Generation, 2nd International Symposium, Salzburg.

So far calculations and experiments on induction converters have been reported under conditions where skin heating is not important. With the achievable electrical conductivities and velocities in combustion gases, there result small magnetic Reynolds numbers for technically feasible dimensions. At high magnetic field intensities however, skin heating leads to an increased electrical conductivity within a surface sheath and thus to an increased effective magnetic Reynolds number. The calculations performed included skin heating and, dynamical stability. A reduction of the size for induction converters by about two orders of magnitude was found. It seems to be possible that the large amounts of energy at high energy densities of explosives may be gained as electrical energy in apparatus of reasonable technical dimensions, for example in a theta-pinch configuration. In order to give a rough estimation of skin heating, at first a semi-infinite space of an incompressible homogenous plasma is considered, moving with a constant velocity into a constant magnetic field region. The direction of motion is perpendicular to the magnetic field lines and to the boundary layer of the plasma. For this model there results an exponential decrease of the magnetic field towards the interior of the plasma. It is shown that the heating is proportional to the electrical conductivity and the squares of magnetic field intensity and velocity, and that the heating is more restricted to the boundary than the magnetic field. (auth)

39694 INFLUENCE OF A CURVED DUCT ON EXPLOSIVE-DRIVEN MHD CONVERTERS. Burnham, Marvin W.; Marshall, Scott J.; Krill, Arthur M. (Falcon Research and Development Co., Denver). Vienna, International Atomic Energy Agency, 1966, Preprint No. SM-74/173, 10p. (CONF-660704-43). ORAU.

From Magnetohydrodynamic Electrical Power Generation, 2nd International Symposium, Salzburg.

The objective of the research was to maximize the energy conversion in a period of less than 20 microseconds. To minimize the influence of the inhomogeneity of the stream, and to exploit the influence of mechanical pressure on the conductivity, experiments were conducted using curved ducts. The curved ducts were observed to increase the generator energy output by a factor of almost 2 for time periods of less than 20 μsec. as compared with straight ducts. Furthermore, the generator internal impedance using a curved duct, was an average of 30% of the internal impedance of the comparable straight duct, with low impedance external loads. High-speed framing camera sequences are shown which give details of the properties of the conductive stream as well as the behavior of the stream within a curved duct device. Reversal of electrode polarity in the curved duct device was observed to lower the output, verifying that the curvature minimized the influence of the "electron sheath" formed at the anode and this contributed to lowering the generator's internal impedance. Output data as well as photographic sequences are shown. The implications of the results are discussed. (W.D.M.)

39695 CHEMICAL RECOVERY OF ENERGY IN A COMBINED MHD/STEAM POWER STATION. Carrasse, J. (Societe ALSTHOM, Paris). Vienna, International Atomic Energy Agency, 1966, Preprint No. SM-74/156, 20p. (In French). (CONF-660704-44). ORAU.

From Magnetohydrodynamic Electrical Power Generation, 2nd International Symposium, Salzburg.

The energetic and chemical aspects of the operation of a combined MHD/steam power station using the combustion gases from a fossil fuel in an open circuit with potassium seeding are described. A process for the recovery of energy by endothermal chemical conversion of the fuel is considered. The various processes intended to ensure the thermal operating conditions required, including re-heating of the air, oxygen enrichment etc., are described and their effects on the overall energy yield of the station and the present or future associated technological limitations are indicated. The principle and various feasible methods of application of a process at present under study and experimentation are explained. (W.D.M.)

39696 ELECTRICAL EQUIVALENT CIRCUITS OF THE d-c MHD GENERATORS. Celinski, Z. N. (Inst. of Nuclear Research, Swierk, Poland). Vienna, International Atomic Energy Agency, 1966, Preprint No. SM-74/55, 14p. (CONF-660704-45). ORAU.

From Magnetohydrodynamic Electrical Power Generation, 2nd International Symposium, Salzburg.

The equivalent circuits of the generators with segmented electrodes electrically connected in various ways were determined (generators with the electrodes connected in series, with Hall- and Faraday-connected electrodes). Constant gas dynamic parameters, constant generator cross section, constant magnetic field, uniformity of current density and electric field were assumed. Electrode effects, end effects, and "ion slip" were neglected. From the equivalent circuits the following electrical terminal values of

the generator such as voltage, current, internal resistance, electric power, brake power, ohmic losses, and electrical efficiency were determined. Terminal values are given as function of geometric dimensions of generator, Hall parameter, and connection system of electrodes. (auth)

39697 EFFECT OF FINITE-LENGTH ELECTRODES ON ELECTRICAL PARAMETERS IN d-c MHD GENERATOR WITH ELECTRODES CONNECTED IN SERIES. Celinski, Z. N. (Inst. of Nuclear Research, Swierk, Poland). Vienna, International Atomic Energy Agency, 1966, Preprint No. SM-74/56, 12p. (CONF-660704-46). ORAU.

From Magnetohydrodynamic Electrical Power Generation, 2nd International Symposium, Salzburg.

Distribution of electrical parameters in an MHD generator with electrodes connected in series was determined by numerical analysis for a wide range of electrode dimensions and for the values of Hall parameters usually met in practice. The method of determination of generator terminal values, based upon the results of the numerical calculations, was worked out. Deviations of the generator terminal values with finite-length electrodes from those in the ideal case of infinitely-segmented electrodes were determined. The correction factors λ were calculated and are presented in the form of curves as functions of geometric dimensions, electrode size, Hall parameter, and electrical connections. Constant gas dynamic parameters and constant generator cross-section were assumed. Optimal electrode size and connection (with regard to the maximum electrical power), was determined. As a result of the comparison of various systems of connections of electrodes the most advantageous system was found. Maximal possible electrical power, minimal possible number of separate load circuits, and the most advantageous parameters of electrical power: high voltage and low current was obtained. (auth)

39698 EXPERIMENTAL DETERMINATION OF THE THERMAL CONDUCTIVITY OF HEAT-RESISTING HIGH-ALUMINA CONCRETES AT TEMPERATURES BETWEEN 200 AND 1500 DEG C. Chekhovskii, V. Ya.; Kaulenas, A. A. (Moscow State Univ.). Vienna, International Atomic Energy Agency, 1966, Preprint No. SM-74/232, 4p. (In Russian). (CONF-660704-47). ORAU.

From Magnetohydrodynamic Electrical Power Generation, 2nd International Symposium, Salzburg.

High-alumina concretes have great potentialities as high-temperature material for electrical insulation in MHD generators. It is therefore important to know the thermophysical properties of such types of concrete, including their thermal conductivity. The thermal conductivity coefficient of high-alumina concrete was determined by means of a steady-state method employing the radial heat flow from an axially embedded heater. The results obtained from thermal conductivity measurements at temperatures between 200 and 1500°C are presented. The maximum relative error of a single measurement was estimated to be 6 to 12%. (auth)

39699 EXPERIMENTAL INVESTIGATION OF THE RADIATION OF AN Ar/K PLASMA. Chinnov, V. F. (Moscow State Univ.). Vienna, International Atomic Energy Agency, 1966, Preprint No. SM-74/216, 12p. (In Russian). (CONF-660704-48). ORAU.

From Magnetohydrodynamic Electrical Power Generation, 2nd International Symposium, Salzburg.

A description is presented of an experimental rig for investigating the radiation properties of alkali metal vapors and mixtures of inert gases with alkaline additives. Experimental data are given on determination of the basic parameters of a non-equilibrium Ar/K plasma in a d-c electrical discharge. Methods of determining the distribution of excited atoms by the coordinates of a cylindrosymmetrical nonisothermal plasma column, using single and double light probes, are explained. An investigation was made of the suppression of the resonance radiation of potassium in the arc column at the parameters concerned and with geometrical dimensions of the order of 15 to 20 mm. (auth)

39700 RELAXATION PHENOMENA IN RARE GASES SEEDED WITH ALKALI-METAL SUBSTANCES. Croitoru, Z.; Pytlinski, J. (Electricite de France, Clamart). Vienna, International Atomic Energy Agency, 1966, Preprint No. SM-74/76, 12p. (In French). (CONF-660704-49). ORAU.

From Magnetohydrodynamic Electrical Power Generation, 2nd International Symposium, Salzburg.

Insufficient stress has been placed on the important role which relaxation phenomena will play in MHD generators using ionization phenomena in a state of nonequilibrium. It is generally expected that a state of nonequilibrium will be attained by the Joule effect, but it is not certain that this is possible in short ducts. The desired state of nonequilibrium might be attained by applying an additional electric field at the input to the duct, the Joule effect merely serving to maintain this state. The problem is that of maintaining the ionization between the zone within the auxiliary field and the entry to the generator, as recombination phenomena might make this state difficult to maintain. The experimental assembly consisted of two h-f coils, one to ionize the gas by induction and the other to measure the conductivity as a function of time. It is shown that high electrical conductivity can be achieved even in cold gases which are practically nonconducting at equilibrium. Moreover, recombination durations of several milliseconds can be attained in very pure gases. The influence of argon pressures and cesium vapor on these phenomena is discussed. (auth)

39701 ELECTROGASDYNAMIC CENTRAL POWER STATIONS. Daman, E. L. (Foster Wheeler Corp., Livingston, N. J.); Gourdine, M. C. Vienna, International Atomic Energy Agency, 1966, Preprint No. SM-74/197, 12p. (CONF-660704-50). ORAU.

From Magnetohydrodynamic Electrical Power Generation, 2nd International Symposium, Salzburg.

The basic principles of EGD power generation with fossil fuels are given. Power density, efficiency, and electrical output characteristics based on experimental work are discussed. Optimum cycle arrangements using the EGD system for power generation are presented, together with studies showing relationship of major cycle arrangement variables on overall efficiency. Actual industrial size channel arrangement is shown and its performance given. (W.D.M.)

39702 EXPERIMENTAL AND THEORETICAL COMPARISON OF THE PERFORMANCE OF DIAGONAL WALL GENERATORS, FARADAY GENERATORS, AND HALL CURRENT GENERATORS. Dicks, J. B. Jr.; Wu, Yingchu Lin; Shanklin, R. V.; Zitzow, U. (Univ. of Tennessee, Tullahoma). Vienna, International Atomic Energy Agency, 1966, Preprint No. SM-74/169, 14p. (CONF-660704-51). ORAU.

From Magnetohydrodynamic Electrical Power Generation, 2nd International Symposium, Salzburg.

Results are reported of an experimental and theoretical effort to compare performance of diagonal wall generators. A computer program was composed to predict what the loading of the generator should be to accomplish operation at various points. The computer program was written in terms of the external loading of the generator rather than in terms of current densities and electric fields, as is usually the case. This was accomplished by expressing the external loading equations in a tensor form and by solving them simultaneously with generalized Ohm's law equations on the interior of the generator to eliminate current densities and electric fields from the equations. The program was general enough to predict the operation of all types of open cycle MHD generators compared in the experimental part of the investigation. In the experimental part of the program, combustion gas was formed from RP-1, oxygen, alcohol, and potassium hydroxide and was expanded through a nozzle to a range of supersonic velocities from Mach 1.3 to Mach 2. This flow was directed into one of three MHD channels used in the investigation. These channels were of heat-sink diagonal conducting wall construction and designed for runs between 15 seconds and 60 seconds. The

width of the electrodes and the cross sectional area was the same in each channel, and each channel contained 60 active electrode pairs. The length of the usable section of the magnetic field was 36 inches, the width 4 inches and the height was 5 inches. A 23,000 pound c-frame magnet produced a magnetic field of two webers in the gap for continuous operation. Higher fields than this was produced for a shorter duty cycle. Each conducting strip in the wall was split so that the wall current could be measured. A panel of 68 ammeters, 60 volt-meters, and 20 pyrometers recorded current, voltage and temperature of the channel once each second. Forty static pressures in the MHD channel and 5 stagnation pressures from a variety of interchangeable rakes in the diffuser were recorded also. All combustor parameters, fuel flows, water temperature changes, etc., were recorded. The computer program took the combustor data and the data on generator loading and predicted the fields, power, and gas dynamic conditions in the channel. The predictions were compared with the experimental results for a variety of generator load configurations. The load configuration was set up on a resistor matrix which contained 1000 separate resistors rated at a total of 400 kw power absorption. Movable bus bars allowed any desired series or parallel arrangement. (auth)

39703 GENERAL FORMULATION OF THE POSTULATE FOR MINIMUM VOLUME OF THE MHD GENERATOR DUCT WITH FIXED OUTER BOUNDARY VALUES. Denzel, P.; Buecken, R. (Technische Hochschule, Aachen). Vienna, International Atomic Energy Agency, 1966, Preprint No. SM-74/154, 12p. (CONF-660704-52). ORAU.

From Magnetohydrodynamic Electrical Power Generation, 2nd International Symposium, Salzburg.

The most important data to describe the influence of the MHD expansion group (consisting of nozzle, duct, and diffuser) on the characteristic parameters of the overall cycle, in particular on the overall efficiency, are the thermodynamic-state quantities at the entrance of the nozzle and at the exit of the diffuser — "the outer boundary values." With these data unchanged, variation of the shape of the expansion line does not affect the overall performance of the process. Therefore the question arises which expansion shape is best from the point of view of MHD generator, if the outer boundary values are fixed or, in general, as a function of the outer boundary values. As the generator duct is the most complicated and, especially with regard to the appertaining magnet, the most expensive element of the expansion group, minimizing of the duct volume is a reasonable criterion to be applied in the determination of the expansion shape. It is shown how this criterion leads to a simple differential relationship between the electrical conductivity of the working gas, the gas velocity, and the cross section of the channel. If this relationship is used to complete the system of differential equations governing the energy conversion process, the resulting expansion shape is optimal with respect to minimum duct volume. Usually a somewhat arbitrary condition is taken to determine the expansion shape, e.g. the gas velocity or Mach number is postulated to be constant. An example is calculated for the MHD expansion under consideration of the optimization criterion. (auth)

39704 EVALUATION OF RAYLEIGH-TAYLOR INSTABILITY AND TURBULENT DIFFUSION EFFECTS IN INHOMOGENEOUS FLOW CONVERSION. Devime, R. (Institut Francais du Petrole, Rueil-Malmaison, France); Karr, C.; Lecroart, H.; Malplat, J.; Marle, C.; Nguyen Duc, X.; Porte, R. Vienna, International Atomic Energy Agency, 1966, Preprint No. SM-74/80, 20p. (In French). (CONF-660704-53). ORAU.

From Magnetohydrodynamic Electrical Power Generation, 2nd International Symposium, Salzburg.

The production of a conversion duct based on inhomogeneous flow is handicapped by two phenomena which tend to re-establish the homogeneity of the system: Rayleigh-Taylor instability and turbulent diffusion. An attempt is made to evaluate these effects. Theoretical analyses of the two phenomena are given. Some experimental results covering three types of experiment are presented. For the study of Rayleigh-Taylor instability, recourse was had to a hydrodynamic model using two superimposed liquids, an electrolyte, and an insulator, of very similar densities; the first results relating to the characteristic growth time and modes of instability, as derived from observation, are presented and compared with theoretical estimates. For the study of thermal diffusion, measurements were carried out on an analogical model in which two gases (nitrogen and a mixture of nitrogen and carbon dioxide, at ambient temperature) represent respectively the medium- and the high-temperature sections of the conversion flow. For the overall investigation of the actual phenomenon, tests were carried out on an inhomogeneous flow using combustion gases circulating in a magnetic field, with the passage of current densities chosen in such a way as to respect the similitude with an industrial-scale flow and to represent correctly the effects tending to destroy inhomogeneity. The test duct, of section 4×10 cm^2, is traversed by a 200 kw gas flow circulating at a velocity of 100 m/sec in a magnetic field of 1.7 Tesla over an effective length of 0.9 m. The work known as the MHD-6 project, the experiments carried out, and the results obtained regarding the persistence of temperature inhomogeneity during conversion are described. (W.D.M.)

39705 EFFECT OF VARIOUS PARAMETERS ON THE EFFICIENCY OF THE MHD POWER STATIONS. Dinelli, G. (Ente Nazionale per Energia Elettrica, Rome); Masse, J. Vienna, International Atomic Energy Agency, 1966, Preprint No. SM-74/75, 26p. (In French). (CONF-660704-54). ORAU.

From Magnetohydrodynamic Electrical Power Generation, 2nd International Symposium, Salzburg.

The possibility of large-scale power production using an MHD generator and a conventional power station is considered. The main components defining the gas cycle are the fuel burner and combustion chamber, converging section, MHD duct, diffuser, heat exchanger and the steam power station. The other important components are: the electromagnet, compressor, switching unit, unit for the recovery of seeding material, and possibly a unit for the extraction of oxygen from the air. The main parameters influencing the overall output of the plant are: rate of oxygen enrichment, pre-heating temperature, magnetic field, wall losses, and gas velocity in the MHD duct. The fuel is No. 2 heavy fuel oil. The seed is introduced into the burner as K_2SO_4. In calculating the physical properties of the combustion gases, it is assumed that physico-chemical equilibrium has been attained. Electrical conductivity is calculated taking into account the large number of substances present in the combustion gases. Expansion in the MHD duct is calculated by a method making local allowance for the various expansion efficiencies, but is independent of the type of duct used. Allowance is also made for the efficiency of each of the various components constituting the power station. (auth)

39706 EXPERIMENTAL INVESTIGATION OF THE MAGNETOHYDRODYNAMIC FLOW OF A LIQUID METAL IN A RECTANGULAR DUCT WITH CONDUCTING WALLS. Dmitriev, K. I.; Mikhailov, Yu. M.; Presnyakov, V. S. (Kurchatov Inst. of Atomic Energy, Moscow). Vienna, International Atomic Energy Agency, 1966, Preprint No. SM-74/93, 12p. (In Russian). (CONF-660704-55). ORAU.

From Magnetohydrodynamic Electrical Power Generation, 2nd International Symposium, Salzburg.

Results are given of an experimental investigation of the laminar and turbulent magnetohydrodynamic flow of liquid sodium in a rectangular duct with conducting walls. The investigations were carried out on a specially devised sodium loop. Their purpose was to determine losses in the walls and magnetohydraulic losses under various conditions of movement of the metal (Hartmann numbers up to 10^3 to 10^4, Reynolds numbers up to 10^5 to 10^6, magnetic Reynolds numbers up to 1 to 2). The laminar movement regime was compared with the theoretical calculations of

Chang and Lundgren and of Hunt and Stewartson. The dependence of pressure difference at the ends of the duct Δp on the Hartmann number M and the Reynolds number Re was taken as the hydraulic characteristic of the duct. The relationship $\Delta p(M,Re)$ agreed within 8% with the theoretical relationship proposed by Chang and Lundgren. The differences in potential on the side walls as a function of M and Re were also measured. This relationship was compared with the theoretical calculations of Hunt, in order to differentiate between losses in the walls and magnetohydraulic losses in the metal. The relative magnitudes of the losses under different M and Re regimes are given. Similar relationships were measured in turbulent and transition regimes. (auth)

39707 PROBLEMS OF MHD CONVERSION: SOME EXPERIMENTAL RESULTS. Donskoi, K. V.; Chekmarev, I. B.; Shakhnov, I. I. (Inst. of Physics and Tech., Moscow). Vienna, International Atomic Energy Agency, 1966, Preprint No. SM-74/241, 20p. (In Russian). (CONF-660704-56). ORAU.

From Magnetohydrodynamic Electrical Power Generation, 2nd International Symposium, Salzburg.

Theoretical investigations of linear and turbulent MHD generators of the conduction type were carried out. Linear converters were considered in which the distances between the magnet poles and the electrodes varied as the length of the duct. The initial parameters for calculation were selected in accordance with the characteristics of the experimental device. The theoretical and experimental results were in qualitative agreement. The optimum operating conditions for linear generators were investigated. The optimum M number at the entry to the converter duct was established theoretically and experimentally for a plasma consisting of combustion products. By solving the problem of the most favorable generator it became possible to find a fairly simple analytical relationship between the parameters of the converter. The problem of a converter with coaxial geometry was considered under the following assumptions. The compressed, electrically conducting gas enters the duct through the porous surface of the external electrode and leaves through the internal electrode. The external uniform magnetic field is directed along the duct axis. A solution was obtained for the initial system, the nonlinear equation for the radial velocity component being integrated numerically. Analysis of the solution showed the need for taking into account the radial velocity component of the flow. A region was found in which the characteristic parameters of the problem varied and where the condition of plasma flow continuity was fulfilled. It was shown that such generators are very efficient. The variation in the electron temperature as a weakly ionized plasma flows through crossed magnetic and electric fields was studied. The problem was considered in the one-dimensional approximation. As a result of the simultaneous solution of the equations of motion and energy and the Saha equation for the electron gas, the dependence of electron temperature on the characteristic parameters was found. A fully developed flow regime and a transitional flow regime were investigated. It was shown that the electron temperature in the magnetohydrodynamic duct could be raised considerably by means of magnetic and electric fields. (auth)

39708 INVESTIGATION AND TESTS ON CERAMIC MATERIALS FOR MAGNETOAERODYNAMIC CONVERSION DUCT ELECTRODES. Dubois, Andre (Compagnie Generale d'Electricite, Marcoussis, France); Christen, Michel; Sadoune, Joseph; Le Thomas, M. Vienna, International Atomic Energy Agency, 1966, Preprint No. SM-74/150, 16p. (In French). (CONF-660704-57). ORAU.

From Magnetohydrodynamic Electrical Power Generation, 2nd International Symposium, Salzburg.

A number of zirconia-based ceramics containing additives made up of metallic oxides, and in particular alkaline earth oxides, were studied with a view to the production of hot electrodes for magnetoaerodynamic generators. Since the electrical conductivity of these materials is ionic, the lifetime of the electrodes has to be compatible with that of the generators envisaged. A series of laboratory electrodes of varying composition was produced and these were used to carry out a coherent program of electrical measurements and endurance tests. Research carried out on lanthanum derivatives of the (La_2O_3) (M_2O_3) type revealed that, when M was aluminium or chromium, these refractory and conducting substances could sometimes acquire electron conductivity properties, The influence of environmental characteristics (nature, oxygen content, temperature) on the mechanism and nature of the conduction is discussed. It is indicated how these products might be used in the production of ceramic electrodes for magnetoaerodynamic generators. (auth)

39709 MAGNETOAERODYNAMIC CONVERSION TEST RIG WITH SUB-ATMOSPHERIC OPERATING CONDITIONS. Dubois, Pierre; Dubois, Andre; Parizot, Daniel (Compagnie Generale d'Electricite, Marcoussis, France). Vienna, International Atomic Energy Agency, 1966, Preprint No. SM-74/145, 16p. (In French). (CONF-660704-58). ORAU.

From Magnetohydrodynamic Electrical Power Generation, 2nd International Symposium, Salzburg.

In a conversion duct operating under sub-atmospheric conditions, the stagnation pressure is less than the atmospheric pressure. Low pressure operation brings about an increase in the electrical conductivity of the plasma, a decrease in wall losses and a rise in the density of power generation. In addition, the increase in mobility of the electrons brings about an increase in the Hall factor. These peculiarities of sub-atmospheric generators make it possible to use test rigs of moderate thermal power to study the operation of a magnetoaerodynamic conversion duct and, in particular, a Hall-type generator. The characteristics of sub-atmospheric generators are enumerated and the 1 Mw(th) sub-atmospheric conversion test rig at the Research Center of the Compagnie Générale d'Electricité is described. The results obtained from thermodynamic and electrical measurements carried out on the ionized gas in the conversion duct are given and the experimental results are compared with theoretical calculations. (auth)

39710 RADIATION OF FLAMES USED IN MHD. Nguyen Duc, X. (Institut Francais du Petrole, Rueil-Malmaison, France). Vienna, International Atomic Energy Agency, 1966, Preprint No. SM-74/84, 14p. (In French). (CONF-660704-59). ORAU.

From Magnetohydrodynamic Electrical Power Generation, 2nd International Symposium, Salzburg.

The flames used in MHD conversion contain alkali metals such as potassium. Hitherto, no information was available on the thermal radiation of these flames. The radiated energy was measured using a total-radiation pyrometer, as a function of the temperature and optical thickness of the flames. The experimental results showed that the radiation flux is large. For a flame temperature of 2700°K and seeding with 0.8 mole % of potassium, the increase in the total emission factor was about 35% for an optical thickness of 1 m-atm. It dropped practically to zero for an optical thickness of 7 m-atm. (auth)

39711 SOLUTION OF THE BOLTZMANN AND RATE EQUATIONS FOR THE ELECTRON DISTRIBUTION FUNCTION AND STATE POPULATIONS IN NON-EQUILIBRIUM MHD PLASMAS. Dugan, J. V. Jr.; Lyman, F. A.; Albers, L. U. (Lewis Research Center, Cleveland). Vienna, International Atomic Energy Agency, 1966, Preprint No. SM-74/191, 16p. (CONF-660704-60). ORAU.

From Magnetohydrodynamic Electrical Power Generation, 2nd International Symposium, Salzburg.

Many calculations of the electrical conductivity of non-equilibrium MHD plasmas have been based on a simple two-temperature theory. This theory assumes that (a) the electron number density has the equilibrium (Saha) value corresponding to the electron temperature T_e, and (b) the free electron energy distribution f(u) is Maxwellian. The validity of assumption (a) has been studied by several au-

thors, who, however, used assumption (b) in their analyses. Assumption (b) has been less thoroughly studied. Because both excitation and ionization rates are sensitive to f(u), and bound states may be out of equilibrium due to radiative transitions, it is unrealistic to treat these two assumptions separately. Results are reported of simultaneous solution of the Boltzmann equation for the free electron energy distribution, f(u), and the steady-state rate equations for the bound states under MHD conditions. The problem was attacked in the following three stages. First, f(u) was calculated from a Boltzmann equation which included the electric field and elastic collision terms. The results showed that for typical MHD systems (e.g., Ar + K at 1 atm), electron-electron collisions drive f(u) to Maxwellian. Second, the solution of the rate equations for a Maxwellian f(u), using a five-level cesium atomic model, demonstrated the importance of radiative transitions in determining the bound-state populations and magnitudes of the inelastic collision terms. The model atom consisted of four discrete states (6S; 6P, P'; 5D, D'; 7S) and a lumped state, which was assigned various binding energies and degeneracies. Criteria for selecting the latter were based on the maximum stable orbit radius which would be likely for the plasmas of interest. Both the classical Bohr-Thomson and Gryzinski cross sections were used to calculate the rate coefficients and collision terms for excitation, de-excitation, ionization, and three-body capture. Some calculations were also performed using recent experimental data for the 6S → 6P, P' excitation. Known values of radiative probabilities were used for transitions between discrete states. Finally, a Boltzmann equation including all relevant elastic and inelastic collision terms, and the bound state rate equations were solved simultaneously by an iterative technique. Results are presented for plasmas of various thicknesses to line radiation. In the extreme case of a gas transparent to all such radiation, the departure of the state populations from equilibrium causes a large reduction in the free electron number density, especially at low values of T_e. Because excitation collisions are not balanced by superelastic collisions in this case, they cause f(u) to depart from Maxwellian at high energies. This effect is much less pronounced for plasmas which are optically thick to resonance radiation, and disappears altogether for a plasma optically thick to all radiation. For each of the cases of optical thickness considered, f(u) is shown for a range of values of electric field and gas density appropriate to MHD generators. The dependence of the electrical conductivity on the current density is compared with experimental results. (auth)

39712 INFLUENCE OF WALL CONDUCTANCE ON THE PERFORMANCE OF MHD GENERATORS WITH SEGMENTED ELECTRODES. Dzung, L. S. (Brown Boveri and Co. Ltd., Baden, Switzerland). Vienna, International Atomic Energy Agency, 1966, Preprint No. SM-74/4, 12p. (CONF-660704-61). ORAU.

From Magnetohydrodynamic Electrical Power Generation, 2nd International Symposium, Salzburg.

MHD generators with segmented electrodes and especially those utilizing non-equilibrium ionization have not been found to approach the performance superiority as predicted by the theory. Experiments with significant Hall effect have disclosed the inadequacy of segmented electrodes in establishing a Hall potential gradient in the flow direction. Several theories have been advanced to explain the inferior performance, but none of these theories seems to be satisfactory quantitatively. An attempt is made to provide an appropriate explanation. It is shown that the wall conductance of the insulating gaps between the electrode segments may be one principal cause for the poor performance of laboratory generators with equilibrium or non-equilibrium ionization. Previously the electrical potential and current streamline distributions of an MHD channel with electrode segments of finite width were established in a general way. Using these results, it is shown that the effect of the electrode gap conductance is a severe reduction of the maximum attainable axial Hall voltage and of the usable output power density. Estimation of the possible gap conductance indicates that the performance deterioration as calculated is in line qualitatively and quantitatively with the experimental results. It also reveals that in a large-scale generator the effect should not be serious, so that any pessimistic prediction about the combination of non-equilibrium ionization and segmented electrodes seems to be premature. The inadequacy of analyzing the performance of MHD generators by the assumption of infinitesimal segmentation, tacitly assumed in many previous publications, is discussed. (auth)

39713 MHD GENERATORS WITH ION SLIP AND FINITE ELECTRODE SEGMENTS. Dzung, L. S. (Brown Boveri and Co., Baden, Switzerland). Vienna, International Atomic Energy Agency, 1966, Preprint No. SM-74/6, 12p. (CONF-660704-62). ORAU.

From Magnetohydrodynamic Electrical Power Generation, 2nd International Symposium, Salzburg.

The performance characteristics of the Faraday-type and Hall-type MHD generators using very strong magnetic fields were investigated with inclusion of the effects of ion slip and of finite electrode segmentation. In a paper presented at the International MHD Symposium at Paris, 1964, Tsu analyzed the effects of a strong field on the performance characteristics due to ion slip. The electrode segmentation for generators of both types was tacitly assumed to be infinitesimally fine. At very high magnetic fields and hence high Hall effect, the influence of finite segmentation may be serious. Hence the quantitative correctness of Tsu's results cannot be taken for granted. An attempt is made to fill the gap by considering the influence of finite segmentation in addition to that of ion slip. The results confirm those by Tsu qualitatively, but quantitatively there is a considerable discrepancy. In case of Faraday-type generators, the output power density becomes saturated, but at a much higher field than that predicted by Tsu. Below saturation fields, the power density is less than that given by Tsu by almost an order of magnitude for the same magnetic field strength. In case of Hall-type generator, the output power density reaches a maximum and then declines to zero at extremely high field. The maximum power density is again shifted to much higher fields than predicted by Tsu. Also the power density below maximum is very much lower for the same magnetic induction. The efficiency of the Hall-type generator is also reduced by finite segmentations. It is found that reasonable efficiencies are feasible only within a limited range of magnetic inductions. (auth)

39714 INFLUENCE OF NON-EQUILIBRIUM EXCITATION ON THE ELECTRON DENSITY IN ONE-DIMENSIONAL MFD CHANNEL FLOW. Eichert, K.; Kaeppeler, H. J. (Technische Hochschule, Stuttgart). Vienna, International Atomic Energy Agency, 1966, Preprint No. SM-74/48, 12p. (CONF-660704-63). ORAU.

From Magnetohydrodynamic Electrical Power Generation, 2nd International Symposium, Salzburg.

In previous publications, a system of equations was derived from the gaskinetic description of a multi-component reacting plasma and employed for the calculation of one-dimensional subsonic flows. This system was extended to include nonequilibrium excitation. No thermal or chemical equilibrium between the various components of the plasma was assumed. The components of the plasma considered were a non-reacting working fluid, an alkali metal vapor as a seeding material, ions of this seeding substance, and electrons. Three levels for the excited states were introduced. The reactions considered were excitation and ionization by electron collisions, and photo-ionization, as well as the corresponding reverse processes. For the reaction velocities, analytical equations were introduced permitting insertion of any excitation or ionization cross sections of either experimental or theoretical origin. The degrees of excitation and ionization in the flow of a helium working fluid 1 percent cesium seeding through a channel against transverse magnetic fields of 15 and 40 kGauss at Mach numbers of 0.7 and 0.8, respectively, were calculated. The results of the calculations showed that for relatively small magnetic fields there was no rapid rise of the ionization to Saha-equilibrium as a

function of electron temperature. A comparison with the results of a calculation neglecting excitation showed that especially for relatively large magnetic fields nonequilibrium excitation had an essential influence on the electron density and its approach to equilibrium. Neglecting excitation, there resulted a nearly frozen behavior of the degree of ionization within channel lengths of technical interest for small magnetic fields. (auth)

39715 ATMOSPHERIC PRESSURE DISCHARGES IN INERT GASES SEEDED WITH ALKALI METAL VAPOR. Ellington, H. I.; Ralph, J. C. (Atomic Energy Research Establishment, Harwell, Eng.). Vienna, International Atomic Energy Agency, 1966, Preprint No. SM-74/10, 10p. (CONF-660704-64). ORAU.

From Magnetohydrodynamic Electrical Power Generation, 2nd International Symposium, Salzburg.

A series of experiments is described in which very slow moving seeded inert gases were heated in a furnace and were then subjected to electric fields applied between movable disc electrodes. Above a critical applied voltage which is a function of electrode spacing, temperature, and composition of the gas/vapor mixture, a transition to a low-voltage high-current discharge occurred. Provided the electrodes were hot enough and sufficient seed vapor was present the discharge was stable, diffused, and possessed high electrical conductivity. Experiments were carried out with argon, helium, and neon, seeded with potassium, cesium, or sodium. Measured electrode potential drops and positive column fields are given for gas temperatures from 550 to 950°C and seed pressures ranging from 10^{-2} to 40 torr with currents up to 20 amps. Conclusions drawn from the observations are presented. (auth)

39716 THEORETICAL AND EXPERIMENTAL INVESTIGATION OF LIQUID-METAL MHD POWER GENERATION. Elliott, D. G.; Cerini, D. J.; Hays, L. G.; Weinberg, E. (California Inst. of Tech., Pasadena). Vienna, International Atomic Energy Agency, 1966, Preprint No. SM-74/177, 36p. (CONF-660704-65). ORAU.

From Magnetohydrodynamic Electrical Power Generation, 2nd International Symposium, Salzburg.

Liquid-metal magnetohydrodynamic power generation for space was studied. Closed-loop circulation of liquid metal without moving mechanical parts, and generation of electric power from the circulating metal, were investigated analytically and experimentally, and the attainable cycle efficiencies were calculated. Liquid-metal circulation was achieved by accelerating the metal in a two-phase nozzle, coalescing the liquid into a stream, and returning the liquid to the nozzle through a diffuser. The experiments employed room-temperature sodium-potassium alloy (NaK) as the liquid metal and nitrogen as the driving gas. The NaK flow rate was 85 kg/sec. In the absence of a generator, the available fluid power was dissipated by incomplete pressure recovery in the diffuser and the net fluid power available for a generator was calculated to be 80 kw. Recent literature has pointed out the possibility of efficient a-c generators with liquid metal as the working fluid, and this type of generator was studied. Analysis indicated that efficiencies up to 70% are attainable in a travelling-wave induction generator at the available liquid-metal velocities of 100–200 m/sec, provided the generator has a length/gap ratio of no more than 20 for low friction loss, has an electrical length of no more than one or two wavelengths for low winding loss, and has end-effect compensation for cancelling finite-length effects in the power-generating region. The analysis leading to these conclusions is presented and the pertinent literature is reviewed. The type of end-effect correction studied was the "compensating-pole" technique in which an oscillating magnetic field is applied to the fluid entering and leaving the generator to make the flux linkages within the generator the same as those in a rotating or "infinite" generator. An experimental one-wavelength generator employing compensating poles was fabricated, and empty-channel magnetic field measurements were completed in preparation for tests with NaK. Two types of field measurements were made: d-c measurements to determine the field profile as a function of phase angle and a-c measurements to investigate the synchronization of the compensating poles with the travelling wave. The d-c results showed that the flux linkages in the power-generating region can be held close to those in a rotating machine, and the a-c results showed that the compensating poles can be accurately synchronized with the travelling wave through transformer coupling. The component efficiencies from the analyses and experiments were combined to predict the cycle efficiencies possible in space and ground-based applications. The calculations included the different liquid MHD cycles and working fluids that have been proposed in the literature, and these cycles are reviewed and compared. (auth)

39717 END EFFECTS ON THE LINEAR INDUCTION MHD GENERATOR CALCULATED BY TWO-SIDED LAPLACE-TRANSFORM. Engeln, F.; Paschka, W. (Deutsche Versuchanstalt fuer Luft- und Raumfahrt e.V., Stuttgart). Vienna, International Atomic Energy Agency, 1966, Preprint No. SM-74/71, 22p. (CONF-660704-66). ORAU.

From Magnetohydrodynamic Electrical Power Generation, 2nd International Symposium, Salzburg.

The two-dimensional induction MHD generator of finite length, using a polyphase winding system in order to obtain a travelling magnetic field, was treated as a boundary value problem by two-sided Laplace transform. For simplication incompressibility was assumed. The two-dimensional boundary value problem of the induction engine was solved for $-\infty \leq x \geq \infty$. x was parallel to the flow direction of the linear MHD generator. In the region $0 \leq x \leq L$ the magnetic travelling wave was sinusoidal with a cyclical frequency ω and a phase-velocity v_s. At x = 0 the conducting incompressible working fluid entered the field region and leaves it at the point x = L. Two mathematical methods were suitable to solve the boundary value problem, the Fourier-transform or the two-sided Laplace-transform. The latter offered the advantage of a complex analytical function in the image space. Moreover, it was possible to obtain the characteristics of the generator in the image space (e.g., field configuration, power flow function, etc.). That implied a large simplification of mathematical treatment. The solution in the original space was given by asymptotic expansion of the known image function. (auth)

39718 EXPERIMENTAL DETERMINATION OF THE CURRENT DISTRIBUTION IN A SIMULATED MHD GENERATOR. Fischer, F. W. (Institut fuer Plasmaphysik, Garching, Ger.). Vienna, International Atomic Energy Agency, 1966, Preprint No. SM-74/20, 10p. (CONF-660704-67). ORAU.

From Magnetohydrodynamic Electrical Power Generation, 2nd International Symposium, Salzburg.

An iterative solution was obtained for the equations describing the current distribution in MHD generators with segmented electrodes. The calculated data were compared with the results of experimental measurements. The measurements were performed in a potassium-seeded argon plasma at 2000°K (1.1 atm) and 130 m/sec flow velocity. The maximum intensity of the applied magnetic field was 10 kΓ. Since at these plasma parameters the current intensity produced by the induced $(\bar{v} \times \bar{B})$ EMF is too low, an additional electric field has been applied to each electrode pair in such a manner that E > (vB). The current density was determined from the intensity of the potassium resonance lines. The intensity of these lines is a measure of the electron temperature which in turn is a measure of the local current density. The light emission in the direction of the applied magnetic field was measured in the region between two electrode pairs at a sufficiently high spatial resolution. The measurements were repeated at various current and magnetic field strengths. The direction of the applied electrostatic field was either parallel or antiparallel to that of the induced $(\bar{v} \times \bar{B})$ EMF. The experimental data were qualitatively in good correspondence with the calculated values. However, the centrally symmetric current distribution assumed in the calculations was not found

in the experiments. Since this discrepancy was found to be independent of the current direction, it could be related to electrode effects (cathode drop etc.). At those electrodes where the current concentrates at the upstream electrode edge, the correspondence between the calculated and the measured data has always been satisfactory. At those electrodes where the current concentrates at the downstream electrode edge the discrepancy between the analytical and the experimental results was found to be independent of the polarity of the electrode. The potential distribution along the insulator wall between two electrodes on the same side of the duct was also measured by means of electrostatic probes. The measurements taken on the side where the current concentrates at the upstream electrode edges were qualitatively in good agreement with the calculated data. The deviation from the theoretical values detected at the opposite wall were consistent with the results of the optical measurements. No theoretical explanation was found for these deviations. They might have been due to the effect of the plasma motion upon the current distribution. (auth)

39719 OPTIMIZATION OF OPEN CYCLE MHD POWER PLANTS. Gebel, R. (Siemens-Schuckertwerke AG, Erlangen, Ger.). Vienna, International Atomic Energy Agency, 1966, Preprint No. SM-74/112, 20p. (CONF-660704-68). ORAU.

From Magnetohydrodynamic Electrical Power Generation, 2nd International Symposium, Salzburg.

The optimization of oil-fired MHD plants was considered. The efficiency of an MHD duct and of an MHD power plant (MHD generator combined with steam power plant) was calculated. The equations used for the MHD duct were one-dimensional and apply for a Faraday-type generator. The initial calculations were based on the use of infinitely segmented electrodes, followed by a determination of the effect of division into finite segments on the overall efficiency. Heat losses and wall friction were taken into account. The magnetic induction, the generator coefficient, and the Mach number were kept constant over the length of the duct. The efficiency assumed for the steam power plant was a function of the electrical output and represented an average value for modern power plants. Those parameters, for which a free choice is still possible and some of which depend on technical questions which are not yet fully settled, were initially given values resulting from approximate optimization or according to technical feasibility and then varied individually. The individual parameters were then assessed from economic aspects. It was found that combustion with oxygen as oxidizer did not give the necessary efficiencies to compensate for the high cost of the oxygen. It was suggested to aim for combustion with air pre-heated to as high a temperature as possible. Since the pressure rises with increasing duct length, only a small amount of the initial energy available could be converted economically into electrical energy. Economical duct lengths were less than 12 m. The efficiencies with conventional magnets were too low to assure economical operation. Superconducting magnets would be required for this purpose. The optimum plasma velocity was in the region of the velocity of sound. To avoid shock waves the velocity should be kept below Mach 1. The optimum value of the generator coefficient (voltage ratio) was approximately 0.7 to 0.8. The optimum amount of seed material was approximately 1% by weight of potassium in the plasma. For power plant ratings of approximately 500 Mw net, the heat losses and the wall friction no longer play a significant part, even with water-cooled electrodes. For MHD power plants with net ratings of 500 Mw, efficiencies of 49 to 52% (steam power plant 42%) may be expected with magnetic flux densities of 50 kG, provided that the capital costs of the magnet and the air pre-heater were not too high. (auth)

39720 EVALUATING THERMODYNAMIC PARAMETERS AND SELECTING FLOW SCHEMES FOR CLOSED CYCLE MHD POWER PLANTS. Gilli, P. V. (Waagner-Biro AG, Vienna). Vienna, International Atomic Energy Agency, 1966, Preprint No. SM-74/45, 16p. (CONF-660704-69). ORAU.

From Magnetohydrodynamic Electrical Power Generation, 2nd International Symposium, Salzburg.

Considering that high overall efficiency is essential for base-load MHD plants, thermodynamic parameters, and efficiencies of possible closed-cycle flow schemes were analyzed. Apart from the well-known temperature entropy (T-s) and enthalpy-entropy (h-s) plots, T-h- and 1/T-h-plots were used for semigraphical analysis and optimization, particularly of combined cycles. 1/T-h-plots showed entropy and "exergy" (available energy) as areas and indicate quantitatively where and how irreversibilities, i.e., exergy losses, occur. Conclusions are listed. (W.D.M.)

39721 BOUNDARY LAYERS IN TWO-TEMPERATURE PLASMA. Gogosov, V. V. (Moscow State Univ.). Vienna, International Atomic Energy Agency, 1966, Preprint No. SM-74/205, 12p. (In Russian). (CONF-660704-70). ORAU.

From Magnetohydrodynamic Electrical Power Generation, 2nd International Symposium, Salzburg.

Boundary-layer equations were derived for completely ionized two-temperature plasma. It was shown that in such a plasma there are two temperature boundary layers which must normally be considered when studying temperature behavior close to the wall. These were the electron-temperature boundary layer and the ion-temperature boundary layer. The equations for these layers are given. It was established that the electron-temperature boundary layer was much thicker than the ion-temperature layer. A means of approximate calculation of the boundary layers in two-temperature plasma is described, and cases are indicated in which the electron-temperature boundary layer is absent. It was shown that apart from these two layers there may also exist in two-temperature heat-conducting plasma a specific "screening" boundary layer close to the wall, in which any difference in electron and ion temperatures caused by external sources close to the wall amounts to a value determined, generally speaking, by the joint action of viscosity, Joule heat and thermal conductivity, in accordance with the equations given. The thickness of this layer was $\delta \sim \sqrt{\varkappa_i/\gamma}$, and over a wide range of variation in the determining parameters it was much less than that of the electron- and ion-temperature boundary layers ($\varkappa_i$ = ion thermal conductivity and γ = coefficient standing for the differences between electron and ion temperature in the energy equations). The behavior of electron and ion temperatures in this layer is discussed. It was established that in an external flow, when the viscosity and thermal conductivity of the medium can be disregarded, there may also be a thin "screening" layer, of thickness $\delta \approx L\gamma_0^{-1}$, $\gamma_0 = (\gamma L/nu)$; here there is a sharp change in the difference in electron and ion temperatures, caused by external sources in a certain section of the flow (e.g., at the entrance to the duct), to a figure determined by Joule heat in accordance with the equations for external flow. These layers are characteristic of two-temperature plasma, being absent in one-temperature plasma. Data are given from numerical calculations on the behavior of electron and ion temperatures when a two-temperature plasma moves through a duct with dielectric walls in a magnetic field. (auth)

39722 SPECTROSCOPIC INVESTIGATION OF ARGON-CESIUM PLASMA. Gridneva, S. M.; Kasabov, G. A. (Kurchatov Inst. of Atomic Energy, Moscow). Vienna, International Atomic Energy Agency, 1966, Preprint No. SM-74/89, 14p. (In Russian). (CONF-660704-71). ORAU.

From Magnetohydrodynamic Electrical Power Generation, 2nd International Symposium, Salzburg.

The spectral distribution of the absolute intensity of the cesium recombination continuum was measured. Processing of these data gave the relationships between the radiative recombination cross sections and the energy of the recombination electron which were in good agreement with the results of the calculations carried out by the formulae of Burgess and Seaton and with the experimental data reported by Agnew and Summers, but which differed considerably from the results found by Moler. The relationship between the population of the various excited cesium lev-

els and cesium pressure and electron concentration in the positive column of a discharge in a mixture of argon and cesium at an argon pressure of 80 mm/Hg was investigated. Local thermodynamic equilibrium was observed up to a cesium pressure of 2×10^{-3} mm/Hg and an electron concentration of 10^{13} cm^{-3}. With a further reduction in the electron concentration, quasi-Boltzmann relative distribution of the excited levels was established, with a temperature lower than electron temperature. The relative distribution of the uppermost excited levels with an ionization potential of less than 0.1 V was also, over a wide range of conditions, Boltzmannian with the temperature of the gas. This feature of the relative population of these levels was also observed in conditions of local thermodynamic equilibrium, at a cesium pressure of 0.5 mm/Hg and an electron concentration of 10^{14} cm^{-3}. (W.D.M.)

39723 ELECTROCHEMICAL CRITERIA FOR SELECTING MHD ELECTRODE MATERIALS RESEARCH ON AN ELECTRONICALLY-CONDUCTING ZIRCONIUM OXIDE. Guillou, Michel; Millet, Jacques (Electricite de France, Clamart, France). Vienna, International Atomic Energy Agency, 1966, Preprint No. SM-74/77, 26p. (In French). (CONF-660704-72). ORAU.

From Magnetohydrodynamic Electrical Power Generation, 2nd International Symposium, Salzburg.

Analysis of the operating conditions of MHD electrodes used in an open circuit has led to a suggestion to use hot or semi-hot electrodes, as the voltage drops between plasma and electrodes induced by cold electrodes are too high in relation to the open-circuit voltages of the generators. Due to their structure, the materials usually proposed for these electrodes are solid, mixed electron-ion conducting electrolytes. The electrochemical criteria for the operation of such materials in an MHD flow between two electron conductors—the plasma and the current collector—are demonstrated in the light of electrochemical concepts established for fused electrolytes and solid electrolytes for fuel cells. Test rigs, which permit measurements of the electrochemical parameters to be optimized in MHD systems, are described, and first experimental results obtained in following this line of research are given. (auth)

39724 MASS SPECTROMETRIC INVESTIGATION OF GASEOUS COMPOUNDS OF ALKALI METALS. Gusarov, A. V.; Gorokhov, L. N. (Moscow State Univ.). Vienna, International Atomic Energy Agency, 1966, Preprint No. SM-74/233, 8p. (In Russian). (CONF-660704-73). ORAU.

From Magnetohydrodynamic Electrical Power Generation, 2nd International Symposium, Salzburg.

No information has hitherto been available on the composition and thermodynamic properties of the vaporization products of many alkaline metal compounds of interest in MHD-generator operation, including oxides (except lithium oxide) and carbonates. A mass spectrometric examination was therefore made of the vaporization products of potassium and cesium oxides and carbonates. Together with metal atoms and oxygen molecules, molecules of oxides and peroxides were found in the vaporization products of potassium and cesium oxides. When potassium and cesium carbonates were vaporized, gaseous carbonate molecules were found in the vapor. The heats and free energies of formation of the gaseous oxides and carbonates of potassium and cesium were measured. (auth)

39725 HIGH TEMPERATURE REGENERATIVE AIR PREHEATER FOR MHD POWER PLANTS. Hals, F.; Keefe, L. (Avco-Everett Research Lab., Everett, Mass.). Vienna, International Atomic Energy Agency, 1966, Preprint No. SM-74/68, 16p. (CONF-660704-74). ORAU.

From Magnetohydrodynamic Electrical Power Generation, 2nd International Symposium, Salzburg.

In order to attain sufficiently high flame temperatures so that combustion products can be used as a working fluid in an MHD generator, the combustion air must either be enriched with oxygen or preheated to relatively high temperatures. Ideally the regenerative preheat of the combustion air should be as high as possible, as this would give the highest overall net efficiency with the best utilization of the fuel and plant equipment. The air preheat temperature is limited by the availability and cost of high-temperature materials, together with the feasibility of operating with seed impurities in the combustion products as well as of recovery of the seed added. The use of a high temperature heat exchanger system consisting of pebble beds with magnesium oxide as the pebble material is proposed. Experimental apparatus to study such a system is described, and experimental results are given. The system operates on the principle of successive heating and cooling of the bed matrix material by the hot combustion products and combustion air respectively. The conditions governing condensation and evaporation of seed are described. During the heating of the bed, seed will at first condense when the gas is cooled below the dew point temperature for seed in the gas, but the condensed seed will evaporate again when the pebble surface temperature is brought above the equilibrium temperature for the vapor pressure of seed in the gas. With proper operation the temperature of the bed matrix material can be varied during normal cycling of the bed, such that the bed cleans itself of seed. The seed is then transported through the bed with the gas and recovered in electrostatic precipitators at the end of the system. Previous experiments with a pilot electrostatic precipitator have demonstrated that very high collection efficiencies can be obtained. The chemistry of seed and compatibility of using magnesium oxide as pebble and bed refractory material with alkali-laden gas and condensed seed were investigated. The experiments simulated MHD generator operating conditions, and the experimental results indicated that the proposed heat exchanger system could be used in MHD power plants using natural gas as fuel. (auth)

39726 MAGNETOHYDRODYNAMIC LIQUID METAL POWER CONVERSION SYSTEMS. Hammitt, A. G. (TRW Systems, Redondo Beach, Calif.). Vienna, International Atomic Energy Agency, 1966, Preprint No. SM-74/193, 12p. (CONF-660704-75). ORAU.

From Magnetohydrodynamic Electrical Power Generation, 2nd International Symposium, Salzburg.

An investigation of various MHD liquid metal power conversion systems is presented. The investigation was accomplished using a general representation of thermodynamic properties termed a "perfect thermodynamic vapor" which allows an analytic description of the various cycles considered. Three cycles were considered in which the gas phase was separated from the liquid phase before condensation of the gas phase and return to the high pressure side of the cycle. These cycles were considered both when the liquid and gas were the same substance and when the liquid and gas were different substances: monofluid and bifluid cases. Two high-speed condenser arrangements were also considered in which the whole liquid vapor mixture was passed through the condenser and the kinetic energy of the mixture preserved during condensation. The "perfect thermodynamic concept" allowed, for the first time, an analytic analysis of these various cycles, a consistent comparison between them, and an easy identification of the effect of the vapor properties. (W.D.M.)

39727 DIRECT MEASUREMENTS OF FLOW VELOCITIES, SEEDING RATIOS AND ELECTRICAL CONDUCTIVITIES IN SEEDED ARGON PLASMAS. Hiramoto, Tatsumi; Matsunaga, Sakuro; Shirakata, Hirofumi; Yano, Syukuro (Japan Atomic Energy Research Inst., Tokyo). Vienna, International Atomic Energy Agency, 1966, Preprint No. SM-74/132, 16p. (CONF-660704-76). ORAU.

From Magnetohydrodynamic Electrical Power Generation, 2nd International Symposium, Salzburg.

The apparatus used for the measurements of plasma velocities, seeding ratio and electrical conductivity, are described. All the measurements were done with the JAERI MHD experimental facility, in which the plasma was produced with a plasma-jet having a maximum electrical input power of 240 kw and a maximum argon flow rate of about 100 g/s. The velocity of plasma was obtained by producing an electric discharge in the plasma

on the center axis of the flow and measuring the time the luminous cloud took to move for a measured distance by detecting the light signals with the two photomultipliers. The results indicated that the measured velocities agreed with the ones calculated from the mass flow equation, within the experimental error of 10% or less, when the temperatures indicated by a thermocouple were corrected for the radiations and the velocity distribution was assumed as the turbulent flow. The apparatus for recording of seeding ratio in MHD channels was designed and tested. The principle of the measurements is based on the resonance absorption of light by neutral seeding atoms in the plasma, through which the light emitted from a standard lamp passes. The experiments were done with a potassium-seeded argon gas in the temperature range of 1500 to 2500°K. The seeding ratios measured covered the range of 10^{-1} to 10^{-5}. The electrical conductivity of the plasma was examined from the quality factor of a high-frequency coil surrounding the plasma flow. Compared to the electrode method, this method gives the average conductivity over a volume, and can eliminate the uncertainties resulting from the boundary effect of a plasma sheath. The measurements were made for the plasma in which no electric field was applied, and also for the nonequilibrium plasma in which the axial current was produced by an external power supply. The rise of the electron temperature and of the electrical conductivity are described and comparisons with those measured by other methods are given. (auth)

39728 CLOSED-CYCLE NUCLEAR MHD STUDIES USING DUST SUSPENSIONS. Hooper, A. T.; Newby, D.; Russell, A. H. (Atomic Energy Establishment, Winfrith, Eng.). Vienna, International Atomic Energy Agency, 1966, Preprint No. SM-74/121, 16p. (CONF-660704-77). ORAU.

From Magnetohydrodynamic Electrical Power Generation, 2nd International Symposium, Salzburg.

Sodha and Bendor have proposed the use of a barium oxide–argon gas mixture as a working fluid in a reactor MHD cycle. An account is given of more detailed investigations using exact equations and fewer arbitrary assumptions than was necessary in Sodha and Bendor's survey. The use of heavy loading of dust was considered since this would lead to increased reactor heat transfer performance; in a duct, however, it was impractical because of the low value of γ which leads to a high-pressure ratio for a small-temperature ratio. The main difficulty in evaluating the overall cycle efficiency lies in ascribing a value to the pressure drop across the MHD duct. Sodha and Bendor used the constant Mach number concept of Swift-Hook and Wright. A more general expression, making no assumptions other than the usual ones of ignoring friction and heat losses to the walls, was derived incorporating the duct design variables into a single multiplier of the temperature ratio in the usual adiabatic expression. Calculations were made to determine the pressure drop across the MHD duct under various regimes of flow and profiles of all the dependent variables were also derived. The use of constant values of Mach number and load/resistance parameter lead to an optimum value for Mach number at about 0.85; this agrees with the Swift-Hook and Wright result. An envelope curve is presented from which the highest average duct power density for a given duct pressure ratio can be read off. This fixed the value of the load/resistance parameter. However, a significantly higher value of power density could be obtained if the load resistance parameter was allowed to vary along the duct. The electrical conductivity of the working fluid was calculated for a range of loadings, temperatures, and pressures using the full equations given by Sodha. Curves are presented showing that the conductivity temperature curve for low pressure lies below the curve for high pressure at the end of the temperature scale but rises above it at low temperature. This has beneficial effects on duct design over the range of pressure and pressure ratios of interest in reactor MHD cycles. Using the general expression already mentioned, overall performance curves are presented relating temperature ratios, cycle efficiency, and compressor power demand for various values of the temperature ratio multiplier. These curves can be generally applied for any working fluid, since the properties of the working fluid only enter into the selection of the appropriate multiplier value. The inlet and outlet gas temperatures in the steam boiler were taken as 1000°K, 375°K since these were suitable to give the steam conditions appropriate to modern power station and turbine practice. This choice limited the range of other parameters which could be used and implied that the compressor power demand will always exceed the turbine power output for practical cycles. (auth)

39729 SOME FLUID DYNAMIC EFFECTS IN LARGE-SCALE MHD GENERATORS. Hunt, J. C. R. (Univ. of Warwick, Coventry, Eng.). Vienna, International Atomic Energy Agency, 1966, Preprint No. SM-74/13, 12p. (CONF-660704-78). ORAU.

From Magnetohydrodynamic Electrical Power Generation, 2nd International Symposium, Salzburg.

At the present time a complete analysis of the fluid dynamics and electrodynamics of an MHD generator cannot be carried out. However, various aspects of the behavior of an MHD generator may be examined by the use of simplified models. A simplification is considered in which the electromagnetic forces are assumed to be much larger than the inertial forces. The ratio of these two forces is measured by the parameters, $S = \sigma B_0^2 x/\rho U$, where σ is the conductivity, B_0 the magnetic field, x the width of the duct, ρ the density and U the mean velocity. Thus $S \gg 1$. It is also assumed that the magnetic Reynolds number is very much less than one. In the largest experimental generators now being built $S \sim 2$. Thus, though the results of this model are not immediately applicable, they should indicate the effects of increasing the magnetic field strength and the size of MHD generators. When $S \gg 1$, the duct is divided into two regions: (i) A core region where electromagnetic forces are balanced by the pressure gradient and where inertial as well as viscous forces are negligible. (ii) Boundary layers on the walls where again inertial forces are negligible but where the viscous, electromagnetic and pressure forces are of the same order. It is shown how it is then possible to calculate the core flow in diverging ducts and in ducts with non-uniform magnetic fields, with the Hall effect and compressibility included, and obtain approximate answers for these otherwise very difficult problems. The simplifications in the analysis of the boundary layers which result from this approximation are demonstrated. (W.D.M.)

39730 NON-STEADY MODULATED MHD SYSTEMS. Ibberson, V. J. (London Univ.); Harris, D. Vienna, International Atomic Energy Agency, 1966, Preprint No. SM-74/73, 24p. (CONF-660704-79). ORAU.

From Magnetohydrodynamic Electrical Power Generation, 2nd International Symposium, Salzburg.

The "conventional" MHD open cycle may be improved by utilizing non-steady combustion. The resulting pressure modulation of the plasma stream can circumvent the σv^2 limitation of the classical generator by the possibility of increasing both conductivity (σ) and particle velocity (v) over that of the steady flow case. A high power density thus becomes available from a range of generators which includes the "acoustic" and the detonation wave types. The theoretical conductivity modulation obtained due to a travelling tangential wave in a vortex generator is considered and the resultant power density estimated taking into account the accompanying velocity modulation. The different wave types applicable to an MHD system are discussed with particular reference to the longitudinal and tangential modes. Experimental work is being carried out by Sheffield University on a 6 in. diameter pancake-shaped motor operating on a vortex flow, modulated by a travelling tangential combustion wave. A linear rocket-shaped generator using longitudinal oscillations is being investigated by Queen Mary College. This program and the results to date are discussed. (auth)

39731 MATERIAL LIMITATIONS IN THE MHD INDUCTION GENERATOR. Jackson, W. D.; Pierson,

E. S. (Massachusetts Inst. of Tech., Cambridge). Vienna, International Atomic Energy Agency, 1966, Preprint No. SM-74/161, 14p. (CONF-660704-80). ORAU.

From Magnetohydrodynamic Electrical Power Generation, 2nd International Symposium, Salzburg.

The basic problem in the development of the MHD induction generator is to achieve an acceptable performance in a power cycle when all generator loss mechanisms are taken into account. Cycle calculations have established that the total generator efficiency must exceed 60%, and should be at least 70% in large-scale applications. Important constraints are imposed by materials considerations. The effects of channel wall and field structure materials limitations are considered. The channel must be able to withstand liquid metals at temperatures of at least 1600°F and velocities of several hundred feet per second with negligible corrosion and erosion. The materials presently envisioned for the walls are refractory metals, such as niobium and its alloys, which are good electrical and thermal conductors. Thermal insulation is required between the hot liquid metal and the field structure to protect the magnetic core and windings from excessive temperatures. To minimize the insulation thickness and the refrigeration power required for space applications, the magnetic core should be operated at the highest temperature consistent with high permeability and low loss. Feasible operating temperatures for magnetic materials and the excitation winding are discussed, along with the cooling of the field structure. The theory of the MHD induction generator is extended to include both conducting channel walls and thermal insulation between the fluid and the field structure. Both an exact theory and an approximate theory which demonstrate the major points of interest are presented. Typical numbers are substituted into the resulting equations to show the effect of the conducting walls on machine performance. The wall thickness required to contain pressures of the order of several hundred pounds per square inch, calculated using pressure-vessel codes, shows that conventional construction methods are not feasible because the wall loss is greater than the generated power. The effect of the thermal insulation is shown to be small. Novel schemes of generator construction are discussed, and practical questions are presented for the consideration of materials engineers. (auth)

39732 STUDY OF CYCLE DIAGRAMS OF POWER PLANTS WITH MHD GENERATORS. Jedrzejowski, Zb.; Andrzejewski, St. (Technical Univ., Warsaw). Vienna, International Atomic Energy Agency, 1966, Preprint No. SM-74/54, 22p. (CONF-660704-81). ORAU.

From Magnetohydrodynamic Electrical Power Generation, 2nd International Symposium, Salzburg.

A combined 500-Mw MHD-steam power plant is discussed. As fuel, residual oil burnt in preheated air, without oxygen enrichment, was assumed. The MHD generator works as a topping unit followed by the steam plant. Overall efficiency of the combined plant is about 53%. Solutions to the most important difficulties are proposed, namely: regenerative air pre-heat, generator and combustor walls cooling heat utilization, exhaust gas temperature reduction, compressor intercooler heat utilization, and separation of MHD generator and steam cycle. The influence of the most important factors upon the overall efficiency is discussed: generator and combustor cooling intensity, exhaust gas temperature, heat exchanger system, steam cycle parameters. Constant air pressure (maximum) and pre-heat temperature, 4 kg/cm^2 and 1400°C, were assumed. Some methods of increasing of combined plant thermal efficiency through reduction of heat losses in cycle diagram elements are shown. (auth)

39733 MODEL MHD TYPE SUPERCONDUCTING MAGNET. Kantrowitz, Arthur; Stekly, Z. J. J. (Avco-Everett Research Lab., Everett, Mass.). Vienna, International Atomic Energy Agency, 1966, Preprint No. SM-74/256, 6p. (CONF-660704-82). ORAU.

From Magnetohydrodynamic Electrical Power Generation, 2nd International Symposium, Salzburg.

A superconducting magnet is a very desirable component in MHD generator systems where efficiency or light weight are important. While the operation of an MHD channel in an external magnetic field has been successfully accomplished, successful operation of large MHD type superconducting magnets has up to now not been demonstrated. A description is presented of a fully stable MHD type (i.e., "saddle shaped") superconducting magnet that was built to show that the state of the art of superconductivity had reached the stage where the performance of magnets could be predicted with standard engineering accuracy. The magnet produced a maximum field of 40 kilogauss in a 12 inch diameter bore. The field was uniform for 45 inches, and the overall length of the magnet system was 128 inches. The outside diameter of the windings was 34 inches. The windings themselves were held in place by a structure, the outside diameter of which was 54 inches. The total weight of the magnet was 16,000 lbs. (auth)

39734 PROBE MEASUREMENTS AT INTERMEDIATE AND HIGH PRESSURES. Kagan, Yu. M. (Leningrad State Univ.). Vienna, International Atomic Energy Agency, 1966, Preprint No. SM-74/211, 14p. (In Russian). (CONF-660704-83). ORAU.

From Magnetohydrodynamic Electrical Power Generation, 2nd International Symposium, Salzburg.

Application of the normal Langmuir probe method is limited to cases when $\lambda \gg a$, where λ is the free path of the particles, and a represents the probe dimensions. However, this inequality does not hold in many cases of practical importance. Methods of determining the plasma parameters in such cases are discussed. Consideration is given to the theory of the electron portion of the characteristic of a single probe in the diffusion approximation. This approximation is valid when $\lambda \sqrt{M/m} \leq a$, where m and M are the electronic and atomic masses. The dependence of the electron current to the probe on the probe potential is considered. The electron temperature, T_e, can be found by calculation from the double probe characteristic, or from the single probe characteristic for potentials close to that of a floating probe after single differentiation of the characteristic. If $| \leq a$ and $| \sqrt{M/m} > a$, then the diffusion method for electrons cannot be applied. In the case of a spherical probe an approximate solution of the kinetic equation leads to a dependence of the electron current to the probe on the probe potential, from which it follows that the T_e can be found by methods similar to those used in the previous case. The diffusion approach is always valid for the theory of the ion portion of the single probe characteristic when $\lambda \leq a$. An expression is obtained for the ion current to the spherical and cylindrical probes. Charged particle concentration can be found from the ion portion of the probe characteristics. The relationships discussed are verified for the case of a plasma at rest. They are also valid for a moving plasma if the velocity of plasma motion is small by comparison with the thermal velocities of the electrons or ions. (auth)

39735 QUASI-ONE-DIMENSIONAL MOVEMENT OF PLASMA IN HALL-TYPE MHD GENERATOR DUCTS. Kareev, Yu. A. (Kurchatov Inst. of Atomic Energy, Moscow). Vienna, International Atomic Energy Agency, 1966, Preprint No. SM-74/99, 16p. (In Russian). (CONF-660704-84). ORAU.

From Magnetohydrodynamic Electrical Power Generation, 2nd International Symposium, Salzburg.

The operation of an MHD duct with Hall currents is unambiguously defined by the load factor $\varphi = \Omega\tau(UB/E_x)$, where Ω is the cyclotron frequency of revolution of the electron in a magnetic field of strength B, τ is the time of free flight of the electrons between collisions with the components of the plasma, U is the rate of movement of the plasma in the MHD duct, and E_x is the voltage of the Hall electrical field in the duct. Generating conditions are achieved when $\varphi < -1$, slowing down conditions when $-1 < \varphi < 0$ and $\varphi > \Omega^2\tau^2$, and the accelerating conditions $0 < \varphi < \Omega^2\tau^2$. However, knowledge of the load factor φ alone does not allow determination of the nature of the change in the

thermodynamic and gas-dynamic parameters of the plasma on movement in MHD ducts of arbitrary geometry. Since the equations for movement of plasma in an MHD duct contain more variables than there are equations, a number of studies analyzing the movement of plasma in MHD ducts have made use of simplifying conditions. These studies have dealt with problems of movement in ducts of constant section, at constant speed, Mach number, temperature, etc.–i.e., with special cases of plasma movement. It is shown that if the index of the polytropic curve of the process is introduced, as $N = d\ln P/d\ln\rho$, where P and ρ are the pressure and density of the plasma, its value fully determines the change in thermodynamic parameters (P, ρ, T) of the plasma in any of the three operating conditions of the MHD duct. Joint definition of the polytropic curve index N and the load factor φ determines the change in gas-dynamic parameters (U,m) of the flow and of the section (W) of the MHD duct. The results are presented graphically on the plane (φ,n). Lines are drawn on it where the parameters P, ρT, U, M, W are constant, and the regions with a specific direction of change in these parameters are indicated. Criteria are found in which transition through the speed of sound, and also movement of the flow with a constant Mach number, are possible in ducts of constant cross-section. (auth)

39736 INVESTIGATION OF HIGH-MELTING METAL ELECTRODES FOR MHD GENERATORS WITH NON-EQUILIBRIUM CONDUCTIVITY. Karpukhin, V. T.; Muzychenko, A. D. (Kurchatov Inst. of Atomic Energy, Moscow). Vienna, International Atomic Energy Agency, 1966, Preprint No. SM-74/92, 8p. (In Russian). (CONF-660704-85). ORAU.

From Magnetohydrodynamic Electrical Power Generation, 2nd International Symposium, Salzburg.

The problem of choosing an electrode material for MHD generators with nonequilibrium conductivity is discussed. A number of works have shown the possibility of obtaining a conductivity of the order of 1 mho/cm with "heating" electric fields of 3 to 5 v/cm and technically acceptable pressure and temperature of the working gas. Thus, the electrode system must ensure a mean current density in such an MHD generator of the order of several A/cm^2. In conditions when the electrons of the plasma are magnetized, uneven distribution of the current over the electrode surface is to be expected. This means that the current density of the electron emission must be increased to 10 to 15 A/cm^2. In the temperature range 1300 to 2000°K the thermionic emission of pure high-melting metals in cesium vapors does not give this current density. An experimental investigation was made of emission by cathodes of niobium, molybdenum, tantalum, and tungsten in vapors of mercury and argon containing an admixture of cesium vapors at a pressure of 0.2 mm/Hg. The temperature of the cathode was maintained at about 1200°K. Depending on the material of the cathode, the current density obtained in a mixture of mercury and cesium was 3 to 8 A/cm^2, with even emission of electrons from the surface, and total cathode and anode potential drops of 10 to 13 v. At current densities of more than 10 A/cm^2, considerable excitation of mercury atoms occurred in the cathode region. Similar emission current densities were obtained in argon with cesium. (auth)

39737 ESTIMATION OF THE EFFICIENCY OF AN INHOMOGENEOUS-FLOW MHD GENERATOR. Karr, C. (Institut Francais de Petrole, Rueil-Malmaison, France); La Porte, M.; Porte, R. Vienna, International Atomic Energy Agency, 1966, Preprint No. SM-74/114, 28p. (In French). (CONF-660704-86). ORAU.

From Magnetohydrodynamic Electrical Power Generation, 2nd International Symposium, Salzburg.

The growing interest aroused by striated-flow MHD conversion processes and the development of ambitious experimental programs call for a realistic estimate of the energy characteristics of such generators. Results are reported of computer calculations for open-cycle, striated-flow MHD generators fed with combustion products (No. 2 heavy fuel-oil) by means of a conventional electromagnet. The same computer program was used, after modification, to estimate the characteristics of homogeneous-flow MHD generators for comparison with the striated-flow generators. Two types of striation were studied: (a) striation by preferential Joule heating before conversion (electric modulation); (b) striation by combustion in an oxidizer in which the oxygen concentration is modulated mechanically (modulation by combustion). The optimum results for conventional and for striated-flow converters are compared, and the influence of the various MHD conversion parameters on the efficiency of the integrated steam-turbine/MHD station is described. (W.D.M.)

39738 INVESTIGATION OF A MERCURY–CESIUM PLASMA WITH NON-EQUILIBRIUM CONDUCTIVITY. Kasabov, G. A.; Konakh, V. F. (Kurchatov Inst. of Atomic Energy, Moscow). Vienna, International Atomic Energy Agency, 1966, Preprint No. SM-74/90, 10p. (In Russian). (CONF-660704-87). ORAU.

From Magnetohydrodynamic Electrical Power Generation, 2nd International Symposium, Salzburg.

An experimental investigation of the physical parameters (electron concentration and temperature, gas temperature, voltage of the electrical field, and conductivity) of a mercury–cesium plasma is described. The investigations were made on both steady-state and pulsed discharges. The mercury pressure was determined with a glass diaphragm pressure gage and the cesium pressure by spectrometric methods. Data were obtained on the nonequilibrium conductivity of a mercury–cesium plasma under varying conditions, on the energy required to obtain and maintain it and on the amount of inelastic losses of electron energy. Data were also obtained on the mean transport cross section of the mercury atom at electron temperatures of 3000 to 6000°K; $\langle Q \rangle \approx 10^{-14}$ cm^2. It was shown that at mercury pressures of the order of 10 mm/Hg and electric fields of the order of 1 v/cm it was possible to obtain nonequilibrium conductivity of the order of 1 ohm^{-1} cm^{-1}. Inelastic losses in the plasma were disregarded; the energy necessary for the development of breakdown and ionization in this mixture was the same as in a mixture of an inert gas plus cesium, which testified to the insignificant part played by mercury–cesium molecules in the electron energy balance. (auth)

39739 ELECTROMAGNETIC PHENOMENA IN A DENSE PLASMA WITH NON-EQUILIBRIUM ELECTRIC CONDUCTIVITY IN A VARIABLE MAGNETIC FIELD. Kim, K. I. (Inst. of Electrodynamics, Kiev). Vienna, International Atomic Energy Agency, 1966, Preprint No. SM-74/202, 7p. (In Russian). (CONF-660704-88). ORAU.

From Magnetohydrodynamic Electrical Power Generation, 2nd International Symposium, Salzburg.

An investigation of the group properties of electrodynamics equations with electric conductivity of the type $\sigma = |\bar{j}|^{\gamma}$ (c = atom temperature function, $\bar{j}$ = current density in the plasma, and γ = a constant) serves as a basis for the statement of functionally independent invariant solutions of nonlinear electrodynamics in single-parameter subgroups. The problem discussed is that of the use of invariant solutions to analyze nonlinear electromagnetic phenomena in a dense plasma with nonequilibrium electric conductivity moving: in a cavity formed by parallel planes; in a cylindrical tube; and along a duct formed by coaxial cylinders. Nonhomogeneity of the external magnetic field was assumed in all cases. The features of the solutions obtained are analyzed for the special case when the external magnetic field has the form of a traveling wave. (auth)

39740 EXPERIMENTAL INVESTIGATION OF THE HALL EFFECT IN LOW-TEMPERATURE PLASMA IN A NON-HOMOGENEOUS MAGNETIC FIELD. Kim, K. I.; Chemeris, V. T.; Markovskii, N. V.; Aristov, A. I. (Inst. of Electrodynamics, Kiev). Vienna, International Atomic Energy Agency, 1966, Preprint No. SM-74/203, 16p. (In Russian). (CONF-660704-89). ORAU.

From Magnetohydrodynamic Electrical Power Generation, 2nd International Symposium, Salzburg.

Hall phenomena in low-temperature combustion-product

plasma with added potassium hydroxide, moving through a duct of rectangular cross section in an external magnetic field having the form of a wave stationary in space, are discussed. By measuring the potential distribution along the duct in the region where the induction of the external magnetic field passes through zero, it was shown that the Hall effect considerably distorts the symmetrical distribution of induced currents in plasma in a sign-changing magnetic field. The results of the experiments were analyzed on the basis of a theory which predicts the existence in the plasma of currents not only of the main frequency, but also of zero and short frequencies (the latter appear at higher values of the Hall parameter). The contour of the zero-frequency current was clearly apparent under the conditions of the experiments. It was experimentally demonstrated that the phenomena caused by the Hall effect are attenuated when the side walls of the duct were made of conducting material. Conditions were found which established a formal correspondence between the electromagnetic phenomena in a plasma moving in a traveling magnetic field and a plasma moving in a stationary-wave magnetic field. (auth)

39741 SOME PROBLEMS OF THE OPERATION OF MHD GENERATOR PLANTS. Kirillin, V. A.; Sheindlin, A. E. (Moscow State Univ.). Vienna, International Atomic Energy Agency, 1966, Preprint No. SM-74/221, 14p. (In Russian). (CONF-660704-90). ORAU.

From Magnetohydrodynamic Electrical Power Generation, 2nd International Symposium, Salzburg.

Various problems connected with the development of power plants using open- and closed-cycle MHD generators are discussed. Particular attention was paid to considerations of the efficiency of MHD-generator plants, high-temperature heat exchangers, systems for the introduction and extraction of the ionizing additive, the optimization of the operating conditions for MHD generators, some processes in MHD generator ducts, and the properties of low-temperature plasma. (auth)

39742 MEASURING THE ELECTRICAL CONDUCTIVITY OF A LIQUID–VAPOR POTASSIUM MIXTURE. Kirillov, P. L.; Subbotin, V. I.; Stakhanov, I. P.; Turchin, N. M. Vienna, International Atomic Energy Agency, 1966, Preprint No. SM-74/106, 12p. (In Russian). (CONF-660704-91). ORAU.

From Magnetohydrodynamic Electrical Power Generation, 2nd International Symposium, Salzburg.

Alkali metal MHD conversion cycles can be designed for operation in the liquid phase only and with liquid-vapor mixtures. In the latter case it is important to know the electrical conductivity as the mixture flows along the duct. Experiments were carried out with wet potassium vapor obtained in a closed-circulation loop. A round steel tube with internal diameter 6 mm was used as an MHD generator model. The average vapor temperature was 1100°K. The potential difference at the tube surface and the hydraulic resistance were measured with the electromagnet on and off. The vapor content, obtained from the thermal balance in the vapor generator, varied between 2 and 95%. It was found that, even for high vapor contents, both the potential difference and the hydraulic resistance component due to the magnetic field were appreciable. The dependence of the latter component on induction was not unique. On the basis of the measurements carried out the feasible upper values for electric conductivity of the wet vapor for a homogeneous two-phase flow were calculated. The view that the emission of electrons from the surface of the liquid droplets may be a cause of the electric conductivity was considered. Analysis of the influence of the liquid film in cases of striated flow showed that the observed effects (tension, increased hydraulic resistance) may be due to friction drag on the liquid at the surface of the tube. Since it is difficult to reconcile the fact that the dependence of hydraulic resistance on induction is not unique with the film concept, it is suggested that the wet vapor may be electrically conducting. (auth)

Elementary Particles and Radiations

See also Field Theory, Scattering Theory, and Symmetries

Refer also to abstracts 39598 and 40129.

39743 (CALT-68-92) SOME TOPICS OF RECENT INTEREST IN π AND η PHOTOPRODUCTION. Heusch, Clemens A. (California Inst. of Tech., Pasadena). [1966]. Contract AT(11-1)-68. 28p. Dep. mn. CFSTI $2.00 cy, $0.50 mn.

Some reasons for renewed theoretical interest in photoproduction processes in the lower energy region are considered. A review is presented on recent experiments on the photoproduction of neutral pseudoscalar mesons. (B.G.D.)

39744 (CERN-66-18) PION-PROTON ELASTIC SCATTERING. Focacci, M. N.; Giacomelli, G. (European Organization for Nuclear Research, Geneva (Switzerland). Bologna Univ. (Italy). Istituto di Fisica. Istituto Nazionale di Fisica Nucleare, Bologna (Italy)). Apr. 25, 1966. 129p. Dep. mn.

A review is presented on the present phenomenological situation of pion-proton elastic scattering, with an emphasis on high-energy data. Topics discussed are notation and general formulas, crossing symmetry, partial wave expansion, optical theorem, impact parameter expansion, connection between partial wave and impact parameter expansions, isospin analysis of the pion-nucleon system, phase-shift analysis, exchange amplitude, S-matrix, dispersion relations for the real part of the forward scattering amplitude, interference between Coulomb and nuclear scattering, Pomeranchuck theorems, implications of SU(6) symmetry for the total cross sections, optical models, Born approximation, statistical, model for large-angle scattering, Regge poles, elastic scattering as the shadow of inelastic processes, and analysis of experimental data. (B.G.D.)

39745 (CERN-66-22) CREATION OF PARTICLES AT COSMIC-RAY ENERGIES. Seminar for an Intersecting Storage Rings Study Group held at CERN, 10 March 1966. Peters, B. (Niels Bohr Institute, Copenhagen (Denmark)). June 24, 1966. 23p. Dep. mn.

The general features of nuclear collisions at very high energy are summarized, interpreted according to a simple phenomenological model, and used to predict secondary particle spectra for future accelerators. (auth)

39746 (CERN-66-24) LAYOUT OF THE NEW CERN NEUTRINO BEAM. Asner, A.; Iselin, Ch. (European Organization for Nuclear Research, Geneva (Switzerland)). July 4, 1966. 28p. Dep. mn.

A discussion is presented on the flexible layout of the CERN neutrino beam. Different possible versions with their parameters and corresponding neutrino and antineutrino fluxes are discussed. The parameter values giving an optimum spectra are described. (B.G.D.)

39747 (COO-881-75) EVIDENCE FOR A $\Sigma^-\eta$ ENHANCEMENT NEAR THRESHOLD. Cline, D.; Olsson, M. (Wisconsin Univ., Madison. Dept. of Physics). July 1966. Contract AT(11-1)-881. 17p. (CONF-660808-8). Dep. mn. CFSTI $1.00 cy, $0.50 mn.

From 13th International Conference on High Energy Physics, Berkeley, Calif.

Evidence from a deuterium bubble chamber experiment is presented for a large cross section for the process $K^-n \rightarrow \Sigma^-\eta$ in the center of mass energy region of 1746-1900 Mev. Using the Fermi momentum of the neutron in D_2 the cross section is shown to fall with increasing center of mass energy. The threshold enhancement appears to be similar to that observed in the $K^-p \rightarrow \Lambda\eta$ and $\pi^-p \rightarrow n\eta$ systems. The angular distribution is shown to be consistent with isotropy throughout this region. (auth)

39748 (COO-881-76) STUDY OF THE POLARIZATION OF THE NEUTRON FROM $\Sigma^+ \rightarrow \pi^+ + n$. Cline, D.; Robinson, J. (Wisconsin Univ., Madison. Dept. of Physics). July 1966. Contract AT(11-1)-881. 11p. (CONF-660808-6). Dep. mn. CFSTI $1.00 cy, $0.50 mn.

From 13th International Conference on High Energy Physics, Berkeley, Calif.

The orbital angular momentum of polarized Σ^+ decay is determined by measuring the polarization of the neutron using n-p scattering as an analyzer in a hydrogen bubble chamber. On the basis of 65 events preliminary results of the experiment favor a $P_{\frac{1}{2}}$ state for the π^+n system. (auth)

39749 (COO-881-77) REGGE RECURRENCE PARITY ASSIGNMENTS FOR THE S = 0 REGGE RECURRENCES. Barger, V.; Cline, D. (Wisconsin Univ., Madison. Dept. of Physics). July 1966. Contract AT(11-1)-881. 21p. (CONF-660808-7). Dep. mn. CFSTI $1.00 cy, $0.50 mn.

From 13th International Conference on High Energy Physics, Berkeley, Calif.

The S = 0 fermion resonances are classified as Regge recurrences on three straight line trajectories (namely, Δ_δ, N_α, N_γ) in a Chew-Frautschi plot. These Regge recurrence parity assignments are shown to be consistent with the structure observed in backward pion-nucleon scattering. (auth)

39750 (HEPL-236) RELATIVISTIC TWO-BODY KINEMATICS: A PROGRAM FOR THE BURROUGHS 220 COMPUTER. (Stanford Univ., Calif. High-Energy Physics Lab.). Apr. 18, 1961. Contract AT(04-3)-236. 151p. ORAU.

A program was written to calculate various quantities of interest in a two-body reaction involving particles of arbitrary masses and incident energy. It is assumed that one of the particles is initially at rest in the laboratory. All masses are arbitrary, within the limitation that the incident energy be sufficient to produce them. It is also possible to use this program for the n-body production reaction if only one particle in the final state is observed and the total energy in the center-of-mass frame of the other n-1 particles is specified as the mass of the other particles. (B.G.D.)

39751 (JINR-E-2738) THE MOMENTUM SPECTRA OF SECONDARY PARTICLES IN (π^-,N) INTERACTIONS AT 7 Gev. Legar, F.; Petrzhilka, V.; Suk, M. (Joint Inst. for Nuclear Research, Dubna (USSR). Lab. of Nuclear Problems). 1966 14p. Dep. mn.

The experimental momentum spectra of secondary π^--mesons and protons from the (π^-,N)-interactions at 7 Bev in the laboratory system are compared with the semi-empirical formula given by Aly, Kaplan and Shen. The parameters of this formula are found by the least squares method. It is shown also that this formula gives a satisfactory description of the experiment. The best description of the spectrum of the transverse momentum components is obtained by the linear exponential distribution when an average value of the transverse momentum component $\langle p_t \rangle$ is (0.299 ± 0.010) Bev/c. (auth)

39752 (JINR-E-2765) PLANNING OF n-p SCATTERING EXPERIMENTS ABOVE THE PION-PRODUCTION THRESHOLD. Janout, Z.; Fedorov, V. V.; Lehar, F. (Joint Inst. for Nuclear Research, Dubna (USSR). Lab. of Nuclear Problems). 1966. 26p. Dep. mn.

The planning of the optimal experiment was performed for the measurements of D, R, A, C_{nn}, A_{ss} in n-p-scattering at 400 and 630 Mev. From the obtained results follows that the measurement of the parameter D is most effective for discrimination of two phase-shifts sets at both energies. The measurements must be made on the angles 60 and 115° cms at 400 and 630 Mev, respectively. (auth)

39753 (JINR-E-2827) ON THE RATIO OF THE AXIAL AND VECTOR CONSTANTS IN DYNAMICAL QUARK MODEL. Bogolyubov, P. N. (Joint Inst. for Nuclear Research, Dubna (USSR). Lab. of Theoretical Physics). 1966. 4p. Dep. mn.

The quark magnetic moment in the potential well is calculated. On the basis of the experimental value of the proton magnetic moment, (g_A/g_V) is obtained to be 1.185. (auth)

39754 (JINR-E-2858) OBSERVATION OF THE $\Lambda\eta^0$ RESONANCE IN π^-p INTERACTIONS AT 4.0 Bev/c. Bannik, B. P.; Bubelev, E. G.; Chadraa, B. (and others) (Joint Inst. for Nuclear Research, Dubna (USSR). Lab. of High Energy). 1966. 16p. Dep. mn.

The radiative decays of resonances with Λ hyperons involved were studied in the JINR 24-liter propane bubble chamber exposed to 4.0 Bev/c negative pions. The $M_{\Lambda\gamma}$ effective mass distribution exhibits a peak which can be explained by the existence of the $\Lambda\eta^0$ resonance with mass of about 1680 Mev. The kinematic influence of the known hyperon resonances on the distribution is discussed. An attempt is being made to determine the $\Lambda\eta^0$ spin. (auth)

39755 (JINR-P-2736) ISSLEDOVANIE PROTSESSA VZAIMODEISTVIYA π^--MEZONOV S YADRAMI KSENONA PRI 5 I 9 Gev/c POSREDSTVOM IZUCHENIYA KHARAKTERISTIK OBRAZOVANNYKH V NEM π^0-MEZONOV. (Investigation of the Interaction of π^--Mesons With Xenon Nuclei at 5 and 9 Gev/c by Studying the Distributions of the Produced π^0-Mesons). Dashkevich, N.; Slovinskii, B.; Strugal'skii, Z. S. (Joint Inst. for Nuclear Research, Dubna (USSR). Lab. of High Energy). 1966. 16p. Dep. mn.

Energy, angular, and multiplicity distributions of γ quanta produced by 5 and 9 Bev/c meson (π^-) interactions with xenon nuclei are investigated. The analysis shows that the quasi-elementary interactions play a predominant role in the considered π^--Xe interactions with a small (≤4) number of charged secondary particles. (auth)

39756 (JINR-P-2742) FAZOVYI ANALIZ NUKLON-NUKLONNOGO RASSEYANIYA PRI ENERGII 14.5 Mev. (Phase-Shift Analysis of the Nucleon-Nucleon Scattering at 14.5 Mev.). Kazarinov, Yu M.; Legar, F.; Yanout, Z. (Joint Inst. for Nuclear Research, Dubna (USSR). Lab. of Nuclear Problems). 1966. 12p. Dep. mn.

The phase-shift analysis of the experimental data obtained at an energy near 14.5 Mev is performed. Three phase-shift sets with a positive phase-shift $^1S_0$ wave are obtained which give a satisfactory description of available experimental data. The results of the analysis show that the polarized beam and polarized target experiments are the most effective way to determine precisely the deviation from the pure S-state scattering. (auth)

39757 (JINR-P-2763) O RASPADE NEITRAL'NYKH PIONOV NA TRI FOTONA. (On the Decay of Neutral Pions into Three Photons). Tarasov, A. V. (Joint Inst. for Nuclear Research, Dubna (USSR). Lab. of Nuclear Problems). 1966. 8p. Dep. mn.

The process $\pi^0 \rightarrow 3\gamma$ is considered. The general form of the amplitude is determined. The probability ratio is shown to be $[\overline{W}(\pi^0 \rightarrow 3\gamma)/\overline{W}(\pi^0 \rightarrow 2\gamma)] \lesssim 10^{-9}$. (auth)

39758 (JINR-P-2773) NEUPRUGIE π^-p VZAIMODEISTVIYA PRI ENERGII 7.5 Gev. CHAST II. 4-LUCHEVYE SOBYTIYA S PROTONAMI. (Inelastic π^-p-Interactions at Energy 7.5 Gev. Part II. Four-Prong Events With Protons). Balya, E.; Balya, O.; Belyakov, V. A.; Kladnitskaya, E. N.; Kuznetsova, E. S.; Mikhul, A.; Sabeu, M. (Joint Inst. for Nuclear Research, Dubna (USSR). Lab. of High Energy). 1966. 32p. Dep. mn.

729 events of the reaction $\pi^-p \rightarrow p\pi^+\pi^-\pi^-m\pi^0 (m \geq 0)$ at 7.5 Bev were analyzed on the photographs of 24-liter JINR propane bubble chamber. The cross section 5.1 ± 0.3 mb of analyzed reactions is obtained. The angular and momentum distributions of p, π^+,π^--particles are investigated. Production of meson and baryon resonant states are studied. particularly $N^{*++}_{3,3}$, $N^{*0}_{3,3}$ and ρ^0-meson are observed. (auth)

39759 (JINR-P-2776) SPINOVAYA KORRELYATSIYA PRI UPRUGOM RASSEYANII POLYARIZOVANNYKH PROTONOV S ENERGIEI 605 Mev NA PROTONAKH. (Spin Correlation in Elastic Scattering of 605-Mev Polarized Protons on Protons). Golovin, B. M.; Zul'karneev, R. Ya.;

Kiselev, V. S.; Medved, S. V.; Nikanorov, V. I.; Pisarev, A. F.; Semashko, G. L. (Joint Inst. for Nuclear Research, Dubna (USSR). Lab. of Nuclear Problems). 1966. 8p. Dep. mn.

Spin correlation coefficients for elastic p-p scattering were measured at the angle of 90°cms. A polarized 605 Mev proton beam was used in the experiment. The measurements were made with spark chambers controlled by scintillation counters. The following coefficient values were found to be $C_{nn} = 0.56 \pm 0.18$; $C_{kp} = 0.27 \pm 0.18$; $C_{qkn} = 0.92 \pm 0.38$. (auth)

39760 (JINR-P-2802) IZMERENIE OTNOSHENIYA VREMEN ZHIZNI π^+-I π^--MEZONOV. (Measurements of Half-Life Ratio of π^+ and π^- Mesons). Komarov, V. I.; Petrukhin, V. I.; Savchenko, O. V. (Joint Inst. for Nuclear Research, Dubna (USSR). Lab. of Nuclear Problems). 1966. 12p. Dep. mn.

The lifetime ratio of π^+ and π^- mesons was measured in order to determine CPT invariance of the weak interaction responsible for pion decay. An isotropic discharge helium or neon chamber was used for recording 15 Mev pion decay. The results of the first series of photographs showed the magnitude $[t(\pi^+)/t(\pi^-)] = 0.98 \pm 0.08$. (tr-auth)

39761 (JINR–P–2809) NEUPRUGIE VZAIMODEISTVIYA PROTONOV S IMPUL'SOM 19,8 Gev/c S NEITRONAMI. (Inelastic Interactions of 19,8-Gev/c Protons With Neutrons). Bogachev, N. P.; Merekov, Yu. P. (Joint Inst. for Nuclear Research, Dubna (USSR). Lab. of Nuclear Problems). 1966. 4p. Dep. mn.

The nuclear emulsion method was used to determine energy and angular distributions of secondary particles (protons and charged π-mesons) produced by inelastic p-n interactions. The upper boundary of the coherent production of π mesons by 19.8-Bev/c protons in complex nuclear emulsions was evaluated. (tr-auth)

39762 (JINR-P-2849) POISKI "DOLGOZHIVUSHCHIKH" Λ^0-GIPERONOV. (The Search for "Long-Lived" Λ^0-Particles). Anikina, M.; Vardenga, G.; Zhuravleva, M.; Kotlyarevskii, D.; Lukstyn'sh, Yu.; Okonov, E.; Takhtamyshev, G.; Khorozov, S.; Chkhaidze, L. (Joint Inst. for Nuclear Research, Dubna (USSR). Lab. of High Energy). 1966. 6p. Dep. mn.

The search for long-lived Λ^0 particles was made under conditions similar to those of experiments in which $K_L^0 \rightarrow \pi^+\pi^-$ decay had been observed. The distance from the target to the cloud chamber was 200 mean decay lengths. The number of decays of long-lived Λ^0-hyperon (N_Λ) in our conditions was estimated to be $N_\Lambda^0 = 10$ if one supposes the character of nonexponentiality in K_S^0 and Λ^0 decays to be similar. The result of this experiment is: $N_\Lambda \leq 1$. The comparison of these two values demonstrates as being very unlikely the models which assume the $K^0 \rightarrow \pi^+\pi^-$ to be due to the nonexponentiality in unstable particles decays. (auth)

39763 (JINR-P-2850) EKSPERIMENTAL'NYE VOZMOZHNOSTI PROVERKI CP-INVARIANTNOSTI V RASPADAKH $K_S^0 \rightarrow 3\pi$ V KORRELYATSIONNYKH OPYTAKH S PARAMI $K^0\overline{K}^0$. (On Possibility of an Experimental Test of CP-Invariance in $K_S^0 \rightarrow 3\pi$ Decays in Correlation Experiments With $K^0\overline{K}^0$ Pairs). Lukstyn'sh, Yu.; Okonov, E. (Joint Inst. for Nuclear Research, Dubna (USSR). Lab. of High Energy). 1966. 6p. Dep. mn.

The correlation experiments with $K^0\overline{K}^0$ pairs are considered, which allow to observe and investigate in pure state $K_S^0 \rightarrow 3\pi$ decays forbidden by CP invariance. One can choose such conditions of the experiment, when the interference in $K_S^0 \rightarrow 3\pi$ and $K_L^0 \rightarrow 3\pi$ decays is strongly pronounced. The possibility of an experimental investigation of $K_S^0 \rightarrow K_L^0$ regeneration is marked. (auth)

39764 (NP–16232) SELECTED TOPICS IN WEAK INTERACTIONS. Matscience Report 46. Meyer, Ph. (Institute of Mathematical Science, Madras (India)). [1965]. 82p. Dep. mn. Inst. of Mathematical Sciences, Madras-20, India $1.00.

Various aspects of the theory of weak interactions are discussed. The 11 lectures include such topics as the conserved vector current hypothesis, partially conserved axial vector current theory and the Goldberger-Treiman relation, elastic and inelastic neutrino reactions, the intermediate vector boson, SU(3) symmetry for weak interactions, and the CERN neutrino experiment. (B.G.D.)

39765 (ORO–2504-91) BARYON-BARYON REACTIONS AND SU3 SYMMETRY. Technical Report No. 565. De Souza, Patrick D. (Maryland Univ., College Park. Dept. of Physics and Astronomy). May 1966. Contract AT(40-1)-2504. 88p. Dep. mn. CFSTI $3.00 cy, $0.75 mn.

Thesis.

SU(3) symmetry was used in order to obtain relations between the cross sections for baryon-baryon reactions in the $_1S^0$ and $_3S^1$ states. The modifications of these relations for higher angular momentum states are derived and it is shown that the possible existence of strong coupling of the $_3D^1$ state to the $_3S^1$ state does not invalidate the above derived relations. In order to investigate the effect of mass splitting on these results a potential model calculation is carried out in order to verify the predicted equality of $_1S^0$ n-p and $\Sigma^+ - p$ cross sections. The calculation indicates that this relationship is indeed satisfied and that further the $\Sigma^- - n$ system has a possible bound singlet state with a binding energy $\lesssim 1$ Mev. The multichannel $\Sigma^- - p$ reactions are investigated with an SU(3) invariant K matrix using the $\Lambda - p$ parameters of Burnstein and Alexander. A calculation of $\Sigma^- - p$ cross sections is carried out for center of mass energies <10 Mev. The results of this calculation are not in agreement with experiment. (auth)

39766 (ORO–3065-10) EVIDENCE CONCERNING C VIOLATION IN ETA DECAY. Fortney, L. R.; Chapman, J. W.; Dagan, S.; Fowler, E. C. (Duke Univ., Durham, N. C.). July 1966. Contract AT(40-1)-3065. 14p. (CONF-660808–5). Dep. mn. CFSTI $1.00 cy, $0.50 mn.

From 13th International Conference on High Energy Physics, Berkeley, Calif.

An experiment is described in which the symmetry between π^+ and π^- in the decay $\eta \rightarrow \pi^+\pi^-\pi^0$ was studied. (B.G.D.)

39767 (TID–23278) THREE-PION PRODUCTION BY 1.95 Bev/c POSITIVE PIONS ON PROTONS. Chapman, J. W.; Fortney, L. R.; Fowler, E. C. (Duke Univ., Durham, N. C.). [1965]. Contract AT(40-1)-3065. 20p. Dep. mn. CFSTI $1.00 cy, $0.50 mn.

An experiment is described in which three pion production is studied by 1.95 Bev/c π^+ interactions with protons, utilizing a sophisticated system for scanning and measuring bubble chamber film. (B.G.D.)

39768 (UCRL–11100(Rev.1)) AN ELEMENTARY GUIDE TO THE ELEMENTARY PARTICLES. Rosenfeld, Arthur H.; Tripp, Robert D. (Lawrence Radiation Lab., Univ. of California, Berkeley). Dec. 1965. Contract W-7405-eng-48. 24p. Dep. mn. CFSTI $2.00 cy, $0.50 mn.

A guide to the elementary particles is presented which summarizes the four basic forces of nature, atomic and nuclear states, seven quantum numbers, particles and resonances, occurrences and recurrences, supermultiplets, eightfold way, field quanta, new mesons, and new baryons. (B.G.D.)

39769 (UCRL-16655) PION-PION INTERACTIONS FROM π^-p COLLISIONS AT 3 AND 4 Bev/c. Noble, Carl M. Jr. (Lawrence Radiation Lab., Univ. of California, Berkeley). Mar. 3, 1966. Contract W-7405-eng-48. 70p. Dep. mn. CFSTI $3.00 cy, $0.75 mn.

Thesis.

The final state π-π interaction in the process $\pi^- + p \rightarrow \pi^+ + \pi^- + n$ was studied at incident momenta of 3 and 4 Bev/c by means of a magnetic spectrometer and spark chambers. A lead-sandwich counter system surrounding part of the hydrogen target rejected events of higher multiplicity to enhance detection of the $\pi^+\pi^-n$ final state. The

system, biased for low four-momentum transfer (Δ^2) acceptance, recorded 879 and 1248 $\Delta^2 < 9\mu^2$ events at 3 and 4 Bev/c, respectively. The energy of the ρ peak in the dipion mass spectrum depends on Δ^2, $\theta_{\pi\pi}$ (the π-π scattering angle), and ϕ_{TY} (the Treiman-Yang angle). This dependence indicates that processes other than one-pion exchange are important. The absorptive theory (which includes an I = 0, J = 0 particle, the ϵ^0) as proposed by Durand and Chiu qualitatively explains the ρ decay distribution (cos $\theta_{\pi\pi}$ vs ϕ_{TY}). Unfortunately the geometrical bias precludes quantitative comparison and the calculation of meaningful cross sections. In the ρ region, the forward-to-backward π-π scattering ratio is $\approx$0.5 for $\Delta^2 < 3\mu^2$ and decreases with increasing Δ^2. No direct evidence was seen for the $\omega \rightarrow 2\pi$ decay. (auth)

39770 (UCRL-16788) ANALYSIS OF STRANGE-PARTICLE RESONANT STATES FROM π^-p INTERACTIONS. Hardy, Lyndon Mauriece (Lawrence Radiation Lab., Univ. of California, Berkeley). July 11, 1966. Contract W-7405-eng-48. 103p. Dep. mn. CFSTI $4.00 cy, $0.75 mn.

Thesis.

An analysis is presented of π^-p interactions producing strange-particle final states with an incident laboratory momentum ranging from 1.6 to 4.2 Bev/c. These final states were found to be dominated by the production of well-established resonant states. No evidence was seen for the existence of new resonant phenomena. The reactions $\pi^-p \rightarrow Y^0K^{*0}$ and $\pi^-p \rightarrow Y^{0*}K^0$ proceed peripherally. Simple one-particle exchange does not describe the processes $\pi^-p \rightarrow \Sigma^0K^{*0}$ and $\pi^-p \rightarrow \Lambda K^{*0}$. The absorption model gives an adequate fit to the data for these reactions and indicates the dominance of K* exchange over K exchange. (auth)

39771 (UCRL-16923) STUDY OF THE REACTION $\eta \rightarrow \pi^+\pi^-\gamma$. Price, LeRoy Raymond (Lawrence Radiation Lab., Univ. of California, Berkeley). June 8, 1966. Contract W-7405-eng-48. 42p. Dep. mn. CFSTI $2.00 cy, $0.50 mn.

Thesis.

The results of an analysis of 33 decays of the type $\eta \rightarrow \pi^+\pi^-\gamma$ are presented. It is found that the rho-dominant model fits the data quite well. No conclusions can be drawn regarding the possible existence of a C-nonconserving interaction. (auth)

39772 (UCRL-17007) SIGN OF THE K_1^0-K_2^0 MASS DIFFERENCE. Meisner, Gerald Warren (Lawrence Radiation Lab., Univ. of California, Berkeley). July 22, 1966. Contract W-7405-eng-48. 51p. Dep. mn. CFSTI $3.00 cy, $0.50 mn.

Thesis.

An experiment was performed to measure the sign of $m_1 - m_2$ by following the time development of $K_{neutral}$-p elastic scatters. The K_2^0 was found to be heavier than K_1^0. The statistical confidence level depended on the unresolved Fermi-Yang-type (F-Y) ambiguity that exists at present in the KN (strangeness S = +1) phase shifts in isotopic-spin state I = 0. If the F solution (large positive $p_{\frac{1}{2}}$ phase shift) is correct, the Monte Carlo betting odds of 45 to 1 for $m_2 > m_1$ are obtained, assuming $|m_1 - m_2| = 0.57\tau_1^{-1}$. If instead the Y solution (large positive $p_{\frac{1}{2}}$ phase shift) is correct, the betting odds for $m_2 > m_1$ are 5 to 1. The F-Y ambiguity was not resolved. (auth)

39773 COMPTON EFFECT ON BOUND K ELECTRONS. Lambert, M.; Mueller, R.; Lang, J.; Boesch, R.; Woelfli, W. (Eidgenossische Technische Hochschule, Zurich). Helv. Phys. Acta, 39: 355-60(1966). (In German).

The differential cross section for (incoherent) scattering of γ rays by the bound K-electrons was calculated using the form factor approximation. Numerical values are given for Z = 13, 29, 50, 79, 92, E_γ = 164, 328, 662, 1332, 2620 kev, and $\theta_{\gamma'}$ = 30, 90, 180°. (auth)

39774 DIFFRACTION DISSOCIATION $\pi \rightarrow 3\pi$ IN THE FIELD OF HEAVY NUCLEI. Beter, E. V.; Gulyamov, U. G. (Inst. of Nuclear Physics, Academy of Sciences, Uzbek SSR). Izv. Akad. Nauk Uz. SSR, Ser. Fiz.-Mat. Nauk, No. 1, 86-8(Jan.-Feb. 1966). (In Russian).

Coherent reactions in which target nucleus participates as a whole represent one type of inelastic interaction of highly energetic particles; the energy transmitted is only a few Mev. Such a coherent reaction, $\pi^- + A \rightarrow \pi^- + \pi^+ + \pi^- + A'$, in which the diffraction type dissociation predominates, was examined. In addition, in most cases, a strong $\pi^+\pi^-$ interaction, and in the end state, a ρ^0 resonance is observed. It was attempted to estimate the cross section of the above reaction, involving the generation of ρ^0 mesons at the heavy nuclei. The calculations indicated that the ρ mesons carry away the largest portion of the primary energy; in most cases, pions with a relatively low (about 1 Bev) energy are observed. From the upper limit of the parallel pulse transmission it is possible to obtain the upper limit of the invariant mass of the $\rho\pi$ system, and the kinematic boundaries of ϵ. For the Br nucleus, $\epsilon_{min} = 0.532$; $\epsilon_{max} = 0.963$ at a primary π meson energy of E = 17.2 Bev. From this, the reaction cross section is estimated at about 1.1 mbarn. The method used represents a generalization of the Ademollo-Chiuderi model. (TTT)

39775 MOTION OF ELECTRONS SCATTERED FROM AN INFINITE SLAB. Taylor, C. D. (Sandia Corp., Albuquerque, N. Mex.). J. Math. Phys. (N. Y.), 7: 1332-4 (July 1966).

A nonlinear integral equation of the Volterra type is derived to describe the motion of the electrons egressing from an infinite slab—one formed by parallel planes of infinite area. This motion depends on the flux density of electrons egressing from the slab, and the distribution of the forward components of the electrons' velocities upon egressing from the slab, i.e., the velocity components along the normal to the slab. It is proved that the nonlinear integral equation can be solved by a method of successive approximations and that the solution is unique. The integral equation is solved for two special cases. The most important application of this work is in the study of electrons scattered by the high-density gamma flux from a nuclear explosion. Therefore, the treatment presented is made directly applicable to that study. (auth)

39776 ALLOWANCE FOR THE INFLUENCE OF $\pi\pi$ SCATTERING ANNIHILATION CHANNELS IN THE REACTION N(π,2π)N. Afonin, A. A. (Inst. of Nuclear Physics, Academy of Sciences, Kazakh SSR). JETP Lett. (USSR) (Engl. Transl.), 3: 326-8(June 15, 1966).

Translated from Zh. Eksp. Teor. Fiz., Pis'ma Redaktsiyu, 3: 501-4(June 15, 1966).

The model of $\pi\pi$ interaction via ρ-meson exchange is used to calculate the cross section for the $\pi^+\pi^- \rightarrow \pi^+\pi^-$ reaction, taking into account not only the direct channel but also annihilation channels. It is shown that the cross section does not reach the unitary limit for the P-wave at the ρ meson resonance point. (L.B.S.)

39777 HIGH-ENERGY LARGE-ANGLE SCATTERING BY A STRONGLY SINGULAR COMPLEX POTENTIAL. Kouris, C. B. (Nuclear Research Center Democritus, Athens). Nuovo Cimento (10), 44A: 598-612(Aug. 1, 1966).

The experimental data for high-energy proton-proton and pion-proton scattering at large angles are analyzed in terms of a complex, energy-dependent potential of the form $V(r) = e^{-i\Delta}gr^{-4}$ with $g = \eta^4k^2$. In general, for center-of-mass angles above 30° a good fit to the data is found. The ratio of the elastic to the total cross section for the above potential is also calculated and is compared with the experimental values at different energies. (auth)

39778 KAON-NUCLEON SCATTERING AND THRESHOLD K* PRODUCTION. de Bonte, W. J. (Massachusetts Inst. of Tech., Cambridge); Lomon, E. O. Nuovo Cimento (10), 44A: 647-58(Aug. 1, 1966).

Using the boundary-condition model, it is shown that the rise of the I = 0 S-state KN phase shift near P_L (kaon laboratory momentum) = 800 Mev/c can be attributed to the effect of the K*N threshold. Approximately 2.8 mb of K* production at 1140 Mev/c is predicted for that channel. If

the interchannel coupling is reduced for the I = 1 channel in the ratio given by isovector exchange, the experimental production cross section is obtained and the earlier fit to the I = 1 S-state phase shift altered negligibly. Elastic-boundary-condition fits are given for the P and D waves. The boundary radius, consistent with theory, is $0.45\mu^{-1}$ except for one D-state. The $0.7\mu^{-1}$ radius required in the latter case indicates a significant repulsive potential tail. (auth)

39779 SEARCH FOR A RESONANT π-π INTERACTION IN THE PROCESS $\pi^-p \rightarrow \pi^+\pi^-n$ NEAR THRESHOLD. Blair, I. M.; Torelli, G.; Zavattini, E. (CERN, Geneva). Nuovo Cimento (10), 44A: 671-97(Aug. 1, 1966).

The π-π interaction in the final state of the process $\pi^-p \rightarrow \pi^+\pi^-n$ was investigated at an incoming kinetic energy of 276 Mev. No resonant behavior was found in the invariant-mass range examined ((280 to 350) Mev). The π-π mass distribution is discussed and compared with other experimental and theoretical results. (auth)

39780 π^--p INTERACTIONS AT 775 Mev. Bertanza, L.; Bigi, A.; Carrara, R.; Casali, R. (Univ., Pisa, Italy. Istituto Nazionale de Fisica Nucleare, Pisa, Italy). Nuovo Cimento (10), 44A: 712-25(Aug. 1, 1966).

The interactions of 775 Mev (kinetic energy) π^- mesons in a hydrogen bubble chamber were studied. Total and partial cross sections were determined with the following results: σ (total) = (39.0 ± 1.6) mb, σ (elastic) = (14.8 ± 0.7) mb, σ (π^- + p → all neutrals) = (9.0 ± 0.5) mb, σ (π^- + p = π^- + π^+ + n) = (9.8 ± 0.5) mb, and σ (π^- + p = π^- + p + π^0) = (4.8 ± 0.3) mb. The elastic-scattering angular distribution was fitted with a Legendre polynomial series terminated at the fifth order. Various angular and effective-mass distributions of single-π production are presented and discussed in terms of the Olsson-Yodh and O.P.E. models. (auth)

39781 METHOD OF DETERMINING ELECTROMAGNETIC FORM FACTORS OF NUCLEONS BY COSMIC RAY EXPERIMENTS. Kastrup, H. A.; Mack, G. (Princeton Univ., N. J.). Phys. Lett., 22: 331-2(Aug. 15, 1966).

A possible method of determining form factors by measuring the momentum transfer of the nucleon and the multiplicity of emitted soft mesons is discussed. (auth)

39782 NEW EVIDENCE FOR THE SIGMA MESON. Lovelace, C.; Heinz, R. M.; Donnachie, A. (CERN, Geneva). Phys. Lett., 22: 332-5(Aug. 15, 1966).

Assuming only dispersion relations, backward πp elastic scattering experiments give an F ratio probability of 10^8 : 1 for the presence of a $\pi\pi S_0$ wave and require it to have a broad σ resonance. (auth)

39783 TWO-BARYON APPROXIMATION TO THE DECAY OF NEUTRAL PSEUDOSCALAR MESONS. Lautrup, B. (NORDITA, Copenhagen); Olesen, P. Phys. Lett., 22: 342-4(Aug. 15, 1966).

The decay widths of η and π^0 are calculated using two intermediate baryons and SU(3) coupling constants. Within reasonable limits one gets agreement with the latest experimental value for the π^0 decay width. The total η width is predicted to be 1.09 kev. (auth)

39784 SEARCH FOR THE KAPPA MESON. Goshaw, A. T.; Erwin, A. R.; Walker, W. D.; Weinberg, A. (Univ. of Wisconsin, Madison). Contract AT(11-1)-881. Phys. Lett., 22: 347-9(Aug. 15, 1966). (COO-881-72).

An experiment was completed in which the reaction $K^+ + p \rightarrow K^0 + \pi^+ + \pi^- + \pi^+ + p$ using 3.52 Bev/c K^+ mesons in the BNL 80'' chamber was observed. This type of reaction produced a high yield of κ's for an incoming K^+ of 3.0 Bev/c. No evidence is found of the κ at this energy. Some evidence of κ production is seen in the reaction $K^+ + p \rightarrow K^0 + \omega^0 + \pi^+ + p$. The conclusion is that the κ is not a resonant state. (auth)

39785 MEASUREMENT OF THE REAL PART OF π^-p ELASTIC SCATTERING AMPLITUDE IN THE COULOMB INTERFERENCE REGION AT 3.5 Gev/c. Nomofilov, A. A.; Sitnik, I. M.; Slepets, L. A.; Strunov, L. N.; Zolin, L. S. (Joint Inst. for Nuclear Research, Dubna, USSR). Phys. Lett., 22: 350-2(Aug. 15, 1966).

The π^-p elastic scattering differential cross section was measured for $1.22 \times 10^{-3} \leq -t \leq 4.22 \times 10^{-3}$ (Bev/c)^2 using recoil protons. The real part of the nuclear amplitude determined from the Coulomb and the nuclear scattering interference is in agreement with dispersion-relation calculations. (auth)

39786 ISOTOPIC SPIN OF THE η^* (960 Mev) MESON. Martin, H. J. Jr.; Crittenden, R. R.; Schroeder, L. S. (Indiana Univ., Bloomington). Phys. Lett., 22: 352-4 (Aug. 15, 1966).

A search for production of a negatively charged η^* (I = 1) in the reaction $K^-n \rightarrow \Lambda^0\eta^{*-}$ is reported. The results confirm the I = 0 assignment for the η^*. (auth)

39787 OBSERVATION OF $\omega^0 \rightarrow \pi^0 + \gamma$. Shibata, E.; Wahlig, M. (Massachusetts Inst. of Tech., Cambridge). Contract AT(30-1)-2098. Phys. Lett., 22: 354-7(Aug. 15, 1966). (MIT-2098-257).

In a spark chamber experiment measuring $\pi^- + p \rightarrow n + 3\gamma$ at 10 Bev/c, a peak which we interpret as $\omega^0 \rightarrow \pi^0 + \gamma$ decay is observed in the $\pi^0\gamma$ mass spectrum at 800 ± 30 Mev. (auth)

39788 OBSERVATION OF A (K$\pi\pi$) RESONANCE NEAR 1800 Mev. Bartsch, J. (Technische Hochschule, Aachen); Deutschmann, M.; Keppel, E.; (and others). Phys. Lett., 22: 357-60(Aug. 15, 1966).

Both in the reaction $K^-p \rightarrow pK^-\pi^+\pi^-$ and in the reaction $K^-p \rightarrow p\bar{K}^0\pi^-\pi^0$ induced by 10 Bev/c negative kaons on hydrogen, an enhancement is observed in the $(K\pi\pi)^-$ effective mass distribution, at mass M = 1789 ± 10 Mev and with full width at half height $\Gamma = 80^{+20}_{-40}$ Mev. Evidence is presented which is consistent with the interpretation of this enhancement as a resonant state of isospin I = ½, with possible decay modes into Kρ, K*π and Kω. It is proposed to name this resonance the L-meson. (auth)

39789 POLARIZATION IN PROTON-PROTON SCATTERINGS AT 735 Mev. McManigal, Paul G.; Eandi, Richard D.; Kaplan, Selig N.; Moyer, Burton J. (Univ. of California, Berkeley). Contract W-7405-eng-48. Phys. Rev., 148: 1280-1(Aug. 26, 1966). (UCRL-16720).

New measurements by Cheng of p-C polarization as a function of angle and incident proton energy allow an uncertainty in a previously reported measurement of p-p polarization to be reduced. On the basis of this new information, it is concluded that the p-p polarization at 735 Mev reaches a maximum of (60 ± 2)%. (auth)

39790 A_1 AND A_2 PRODUCTION IN THE REACTION $\pi^- + p \rightarrow \pi^- + \pi^- + \pi^+ + p$ AT 7.0 Bev/c. Cason, Neal M. (Univ. of Wisconsin, Madison). Phys. Rev., 148: 1282-9 (Aug. 26, 1966).

Two-hundred thirteen events of the type $\pi^- + p \rightarrow \pi^- + \pi^- + \pi^+ + p$ occurring in the Shutt 20-in. hydrogen bubble chamber at an incident-beam momentum of 7.0 Bev/c were analyzed. The event separation was performed utilizing kinematic fitting and ionization criteria. The contamination of the sample due to other final states is less than 10%. The cross section for this reaction was measured to be 1.7 ± 0.2 mb. The partial cross sections for the production of resonant final states were measured with the results: $\sigma(\pi^- + p \rightarrow \pi^- + \pi^- + N^{*++}) = 0.55 \pm 0.11$ mb; $\sigma(\pi^- + p \rightarrow \pi^- + \rho^0 + p) = 0.38 \pm 0.10$ mb; and $\sigma(\pi^- + p \rightarrow N^{*0} + \rho^0) = 0.035 \pm 0.013$ mb. The N^{*++} isobar mass and width were found to be 1216 ± 14 Mev and 114 ± 30 Mev, respectively. The ρ^0 parameters are $M^* = 773 \pm 12$ Mev and $\Gamma = 57^{+16}_{-15}$ Mev. ρ^0 production is peripheral and is dominated by final states with low $\pi^-\rho^0$ effective mass; limited statistics prevent us from resolving this enhancement into the A_1 and the A_2. Angular distributions in the $\pi^-\rho^0$ and the ρ^0 rest frames are presented as a function of the $\pi^-\rho^0$ mass. Conclusions drawn about the spin-parity of the A_1 and the A_2 from these distributions are highly model-dependent. The model used indicates that the most likely spin-parity assignments for the A_2 are, in order of liklihood, 2^-, 1^-, or 1^+. If the A_1 is

a resonance rather than a kinematic reflection, its most likely spin-parity assignments are 1^+ or 2^-. (auth)

39791 POLARIZATION PARAMETER IN p-p SCATTERING FROM 328 TO 736 Mev. Betz, F.; Arens, J.; Chamberlain, O.; Dost, H.; Grannis, P.; Hansroul, M.; Holloway, L.; Schultz, C.; Shapiro, G. (Univ. of California, Berkeley). Contract W-7405-eng-48. Phys. Rev., 148: 1289-96(Aug. 26, 1966). (UCRL-16749).

The polarization parameter in elastic proton-proton scattering was measured using an unpolarized proton beam and a polarized proton target. Measurements were taken at a laboratory kinetic energies of 328, 614, 679, and 736 Mev in the angular regions from 33 to 110 degrees center-of-mass. The results indicate that the maximum polarization at a given energy increases in the region from 328 to 679 Mev. At 328 Mev the results are in good agreement with those of a previous experiment at 315 Mev performed by the double-scattering technique. (auth)

39792 POLARIZATION PARAMETER IN p-p SCATTERING FROM 1.7 TO 6.1 Bev. Grannis, P.; Arens, J.; Betz, F.; Chamberlain, O.; Dieterle, B.; Schultz, C.; Shapiro, G.; Steiner, H.; Van Rossum, L.; Weldon, D. (Univ. of California, Berkeley). Contract W-7405-eng-48. Phys. Rev., 148: 1297-1302(Aug. 26, 1966). (UCRL-16750).

The polarization parameter in proton-proton scattering was measured at incident proton kinetic energies of 1.7, 2.85, 3.5, 4.0, 5.05, and 6.15 Bev and for four-momentum transfer squared between 0.1 and 1.0 $(Bev/c)^2$. The experiment was done with an unpolarized proton beam from the bevatron striking a polarized proton target. Both final-state protons were detected in coincidence and the asymmetry in counting rate for target protons polarized parallel and antiparallel to the scattering normal was measured. The maximum polarization was observed to decrease from 0.4 at 1.7 Bev to 0.2 at 6.1 Bev. The maximum of the polarization at all energies studied occurs at a four-momentum transfer squared of 0.3 to 0.4 $(Bev/c)^2$. (auth)

39793 π^-p INTERACTIONS AT 460 Mev. Poirier, C. P.; Tilger, C. A.; Alyea, E. D. Jr.; Martin, H. J. Jr.; Rhode, J. I.; Scandrett, J. H. (Indiana Univ., Bloomington). Phys. Rev., 148: 1311-14(Aug. 26, 1966).

A total of 1589 two-prong events were observed in an exposure of the Brookhaven National Laboratory 14-in. bubble chamber at the Cosmotron. The fit to the elastic angular distribution requires terms through $\cos^4\theta_{c.m.}$. The ratio of the inelastic cross sections $\sigma(\pi^-p \to \pi^-\pi^+n)/\sigma(\pi^-p \to \pi^-\pi^0p)$ is 3.75 ± 0.46. The $\pi^-p \to \pi^-\pi^+n$ reaction is dominated by formation of the π^-n isobar and an enhancement in the di-pion mass spectrum previously reported by Kirz. The $\pi^-p \to \pi^-\pi^0p$ reaction shows no structure in the effective-mass spectra. (auth)

39794 PARTICLE PRODUCTION BY 2.9-Bev PROTONS INCIDENT ON BERYLLIUM AND PLATINUM. Piroue, P. A.; Smith, A. J. S. (Princeton Univ., N. J.). Contract Nonr-1858(06). Phys. Rev., 148: 1315-26 (Aug. 26, 1966). (PPAD-589-E).

Differential cross sections as a function of momentum are presented for the production of π mesons, K mesons, protons, deuterons, tritons, and ^{3}He at various laboratory angles by 2.9-Bev protons striking Be and Pt targets. The Be data were taken at 13, 30, 60, and 93° relative to the direction of the Princeton-Pennsylvania Accelerator internal proton beam; the Pt data were taken at 13 and 93° only. The results are compared with the corresponding data in hydrogen in order to investigate the role of the complex nucleus in particle production at this energy. (auth)

39795 DEUTERON ELECTROMAGNETIC FORM FACTORS FOR $3\ F^{-2} < q^2 < 6\ F^{-2}$. Benaksas, D.; Drickey, D.; Frerejacque, D. (Ecole Normale Superieure, Orsay, France). Phys. Rev., 148: 1327-31(Aug. 26, 1966).

Two groups of measurements were made on the elastic scattering of electrons by deuterium; in each case the recoil deuteron was observed, instead of the scattered electron. In the first case the spectrometer was set at 45° so that magnetic scattering was unimportant (about 10%) and the electric form factors of the deuteron were deduced. In the second case deuterons were observed at 0°, allowing the magnetic form factor of the deuteron to be measured directly. Form factors of the neutron were deduced from these measurements for the transfer values $q^2 = 3$, 4, and 5 (F^{-2}). Preliminary results were given in a first paper. A description of the experimental setup is also included and relativistic and exchange-current corrections are discussed. (auth)

39796 K_{l3} FORM FACTORS AND THE PION CHARGE FORM FACTOR. Nieh, H. T. (Harvard Univ., Cambridge, Mass.). Phys. Rev., 148: 1344-7(Aug. 26, 1966).

Phenomenological Lagrangian models for K_{13} decays and the pion charge form factor are introduced by assuming single-particle dominance and the trilinear meson interactions derived by Schwinger from his composite model for mesons. The usual pole models in the dispersion approach assume that the structure of a "particle" is entirely due to emission and absorption of another particle or particles by a point-like source. The new models differ from these by allowing the "structure" of the source to be included. In other words, all q^2 dependences of the form factors are kept where they are. For small momentum transfers, the form factors can be effectively put into the standard form $(1 + q^2/m^2)^{-1}$, with m an effective-mass parameter. Assuming K* dominance, the effective-mass parameters in the K_{13} form factors $f_+(q^2)$ are predicted to be about 700 Mev. By assuming ρ^0 dominance, the effective-mass parameter for the pion charge form factor $f_\pi(q^2)$ is predicted to be about 600 Mev. (auth)

39797 THEORY OF W PRODUCTION IN NUCLEON-NUCLEON COLLISIONS. Chilton, Frank (Argonne National Lab., Ill.); Saperstein, A. M.; Shrauner, E. Phys. Rev., 148: 1380-4(Aug. 26, 1966).

The cross section for $N + N \to W + N + N$ is calculated in a double peripheral model. The effects of the principal corrections such as absorption, resonant final-state interactions, and the $\pi\pi$W form factor are considered. μ pair production, which is intrinsically related to W production through the conserved vector current, is examined as a means of testing this model and also as a source of background. (auth)

39798 CROSSING PROBLEM FOR THE BACKWARD CONE AND THE THRESHOLD. Sakmar, Ismail A. (Univ. of Miami, Coral Gables, Fla.). Phys. Rev., 148: 1408-11(Aug. 26, 1966).

Recent high-energy pion-nucleon experiments with large momentum transfer have made the backward scattering problem attractive for theoretical investigation. A study is made of the problem of crossing for particular regions of the physical s channel, namely, the backward cone and the threshold. Since the backward cone angle is a function of the energy, this is not a high-energy crossing problem alone, but the crossing region extends to a minimum energy given by $s = (M + 1)^2$ in pion mass units, for which case the cone extends from backward direction to forward direction. (auth)

39799 APPLICATION OF PARTIAL-WAVE ANALYTICITY TO NUCLEON-NUCLEON SCATTERING. Kantor, Paul B. (State Univ. of New York, Stony Brook). Phys. Rev., 148: 1411-18(Aug. 26, 1966).

In order to give a quantitative discussion of models for nucleon-nucleon scattering which are founded on analyticity and unitarity of the S matrix, the fact that each partial-wave amplitude has a nonvanishing imaginary part in the physical region must be dealt with unambigously. That goal is achieved by evaluating certain integrals over the physical region, using rigorous bounds when experimental data are unavailable. The resulting modified amplitudes have known experimental uncertainty, and can validly be compared directly with dynamical models which do not themselves satisfy the requirements of unitarity, such as the popular single-boson-exchange models. The modified amplitudes

are tabulated and various tests for models are discussed. (auth)

39800 CONSEQUENCES OF CHARGE INDEPENDENCE IN STRONG INTERACTIONS: A GRAPHICAL METHOD. Toernqvist, Nils A. (Univ. of Helsinki). Phys. Rev., 148: 1418-23(Aug. 26, 1966).

The hypothesis of charge independence is studied using a simple graphical method. This method is applicable in the common situation when a particle reaction can proceed through several charge channels but only through two isospin channels. The branching ratios of the charge channels are plotted in a two-dimensional diagram, which is possible because only two of these ratios are independent. The triangular inequalities are shown to be equivalent to a single inequality, and they determine in the diagram an elliptic boundary curve of a physical region. The plot is also useful for studying isospin properties of intermediate states in the reaction. The method is demonstrated with two examples, the reactions $K^+p \rightarrow KN\pi$ and $N \rightarrow \pi N$. (auth)

39801 REGGE-POLE MODEL AND TOTAL CROSS SECTIONS IN THE INTERMEDIATE LABORATORY MOMENTUM RANGE 2-6 Bev/c. Barger, V.; Olsson, M. (Univ. of Wisconsin, Madison). Contract AT(11-1)-881. Phys. Rev., 148: 1428-30(Aug. 26, 1966). (COO-881-65).

The total cross-section data on $\pi^{\pm}p$, $K^{\pm}p$, $K^{\pm}n$, pp, $\bar{p}p$, pn and $\bar{p}n$ for laboratory momenta in the range 2 to 6 Bev/c are shown to be roughly consistent with the extrapolation of an SU(3) Regge-pole model previously used to describe high-momentum (6-20 Bev/c) total cross-section data. This fact suggests that a large part of strong-interaction dynamics in the intermediate energy range may eventually be understandable in terms of SU(3) and Regge poles. (auth)

39802 MESON PRODUCTION FROM ELECTRON-POSITRON ANNIHILATION. Lo, Shui-yin (Univ. of Chicago). Contract AT(11-1)-264. Phys. Rev., 148: 1431-6(Aug. 26, 1966). (COO-264-305; EFINS-66-23).

The processes $e^+ + e^- \rightarrow P + P$, $P + V$, $V + V$, $P + \gamma$ (P = pseudoscalar meson, V = vector meson, γ = photon) are discussed in the context of a meson-pole model. M(12) symmetry with kineton corrections [i.e., $SU(6)_w$ symmetry] is used to determine all the coupling constants. The total cross sections of all these processes are given as functions of the total c.m. energy. (auth)

39803 APPLICATION OF π-N SCATTERING RESULTS TO Λ-K^0 PRODUCTION. Rush, J. E. (Univ. of the South, Sewannee, Tenn. Vanderbilt Univ., Nashville); Holladay, W. G. Phys. Rev., 148: 1444-51(Aug. 26, 1966).

The appearance of numerous phase-shift analyses of pion-nucleon scattering and the tentative identification of resonances in that process lead naturally to an application of these results to processes involving other decay channels. The three isospin-$\frac{1}{2}$ resonances of the π-N system on which there seems to be the widest agreement are chosen and their effect on the process $\pi^- + p \rightarrow \Lambda + K^0$ near 900 Mev is considered. The background term used is a K^* pole modified by an arbitrary constant factor of modulus unity. A comparison with available data is given for various resonance pairs and for the three resonances together. (auth)

39804 RANDOM-PHASE K-MATRIX APPROACH TO ABSORPTION IN PERIPHERAL INTERACTIONS. Trefil, J. S. (Stanford Univ., Calif.). Contract AT(04-3)-400. Phys. Rev., 148: 1452-67(Aug. 26, 1966). (SLAC-PUB-169).

Initial- and final-state corrections to single-particle exchange amplitudes are studied. Two multichannel K-matrix formalisms, which are expected to be valid for different energy regions, are developed by means of a random-phase approximation, and two similar absorption formulas are derived. Both reduce to the Gottfried-Jackson form for weak absorption, but give more absorption in the lower partial waves. The models are applied to the reactions $\pi^+p \rightarrow \pi^+p$ for scattering angles near 180°, and to the reaction $\pi^-p \rightarrow \pi^0n$ for small momentum transfer. It is found that the improved absorption models do not solve the problem found in earlier work of failing to fit the energy dependence of the cross sections. However, the increased absorption makes it possible to fit the data in the 4-10 Bev/c region by an arbitrary choice of absorption parameters. (auth)

39805 ABSORPTIVE MODEL FOR $\bar{K}N$ CHARGE-EXCHANGE REACTION. Dass, Guru Vachan; Tripathy, K. C. (Univ. of Delhi). Phys. Rev., 148: 1479-82(Aug. 26, 1966).

The absorptive peripheral model was applied to a study of the reaction $K^-p \rightarrow \bar{K}^0n$ assuming the exchange of a T = 1 scalar particle S (mass 750 Mev) to provide the underlying peripheral mechanism. The calculated angular distribution with S and (S + ρ) exchanges turns out to be in better agreement with the experimental results (for reasonable values of the coupling strength of S) than the pure ρ-exchange case. The effect of introducing a form factor was studied. Also, the energy dependence of the differential cross section at fixed momentum transfer was investigated. (auth)

39806 GENERAL ANALYSIS OF NUCLEON-NUCLEON SCATTERING: CRITICAL TESTS FOR REGGE-POLE THEORY. Leader, Elliot (Cambridge Univ., Eng.); Slansky, Richard C. Contract W-7405-Eng-48. Phys. Rev., 148: 1491-1501(Aug. 26, 1966). (UCRL-16597).

Using analyticity and crossing, the experimental quantities for the physical channel can be expressed in terms of the crossed-channel amplitudes. For N-N scattering, a new set of t-channel amplitudes $\{g_i\}$ are introduced for which the s-channel experimental quantities I_0, D, D_t, C_{NN}, C_{KP}, P, R, A, R′, and A′ are very simple in form. By use of these it is shown that the measurement of certain spin-dependent parameters in N-N scattering can provide critical tests of the validity of the Regge-pole model of high-energy scattering. In particular it is possible to test the factorization theorem, which is an immediate consequence of the simple-pole Regge theory. The relationship of the new amplitudes g_i to the Wolfenstein parameters is given. (auth)

39807 STUDY OF THE ρ AND B MESONS IN π-ω SCATTERING. Land, David J. (Brown Univ., Providence); Kang, Kyungsik; Franklin, Jerrold. Contract AT(30-1)-2262. Phys. Rev., 148: 1501-14(Aug. 26, 1966). (NYO-2262-112).

The reciprocal bootstrap idea is applied to the ρ and B mesons in π-ω scattering. The ρ appears as a 1^- bound state in the π-ω system, while arguments favoring a 2^- p-wave B meson are presented. The method of calculation follows a previously developed general theoretical framework that treats the interaction of pseudoscalar and vector-meson systems. Because of the divergence difficulties associated with higher spin particles and the eventual necessity for an additional parameter in the form of a cutoff, it is demanded only that the masses of the ρ and B mesons be self-consistent. Values of the $\pi\rho\omega$ and $\pi B\omega$ coupling constants required to give this self-consistency are compared with the corresponding output parameters characterizing these solutions. The results show that the ρ can be produced self-consistently at its experimental mass, although the B width and $\pi\rho\omega$ coupling constant required to do this are somewhat larger than what experiment indicates. On the other hand, a completely self-consistent B meson can be obtained in reasonable agreement with experiment only if the distant singularities associated with ρ exchange are neglected. Otherwise, ρ exchange is effectively repulsive in the 2^- amplitude because of the change in sign of the Born term, thus requiring a large B width to produce a resonance at the experimental mass of the B. (auth)

39808 GHOST IN SCALAR STATE. Patil, Sharashchandra H. (Inst. for Advanced Study, Princeton, N. J.). Phys. Rev., 148: 1515-17(Aug. 26, 1966).

An analysis is made of s-wave $\pi\pi$ scattering under the assumption of the existence of an SU(3)-symmetric scalar nonet satisfying the inverted equal-spacing rule. It is found that in the case of mixing this leads to a result that there is

a ghost at negative squared mass, which couples strongly to pseudoscalars. The various implications of this result are analyzed. Specifically, it is concluded that the $\pi\pi$ scattering length is negative and that the forward-backward symmetry in $\pi^+\pi^-$ production must change sign between 400 and 600 Mev. Scattering lengths in different isospin states are related by using a vector exchange model. (auth)

39809 SUM RULES FOR THE STRANGENESS-CHANGING AXIAL-VECTOR COUPLING CONSTANTS. Bose, Shubha (Univ. of Delhi); Bose, Subir. Phys. Rev., 148: 1518-19(Aug. 26, 1966).

Utilizing the techniques of Adler and Weisberger two sum rules for the renormalization of the strangeness-changing axial-vector coupling constants are obtained. G_A/G_V ratios for $\Xi^- \to \Lambda$ and $\Xi^0 \to \Sigma^+$ β decays are estimated. The former is then compared with an analysis of the same decay by Dalitz. (auth)

39810 RECIPROCITY RELATIONS IN PHOTOPION REACTIONS. Christ, N.; Lee, T. D. (Columbia Univ., New York). Contract AT(30-1)-1932. Phys. Rev., 148: 1520-7(Aug. 26, 1966). (NYO-1932-109).

The reciprocity relation in the photopion processes $\gamma + N \rightleftharpoons \pi + N'$ as a possible test of C_{st} and T_{st} invariances of the electromagnetic interaction is discussed, where N can be any nucleus or nucleon. The sensitivity of such a test is estimated for the special case N = n or p in the energy range near the $(3/2, 3/2)$ resonance. (auth)

39811 ANALYSIS OF PHOTOPRODUCTION OF VECTOR MESONS. Maor, U. (Harvard Univ., Cambridge, Mass.); Yock, P. C. M. Phys. Rev., 148: 1542-51(Aug. 26, 1966). (MIT-2098-253).

The photoproduction of neutral vector mesons, in the reactions $\gamma + p \to V + p$ and $\gamma + p \to V + N^{*+}(1238)$ at photon momenta of a few Bev/c, is discussed in terms of the one-particle-exchange and absorption models. Initial- and final-state interaction effects are included. The absorptive amplitudes are calculated by recourse to the unitarity equation. Difficulties arising in this calculation associated with Born amplitudes involving particles of high spin are discussed in detail. The analysis indicates that both the one-particle-exchange and absorptive mechanisms fail to account for the observed ρ photoproduction data. On the other hand, the presently available ω photoproduction data are found to be consistent with the one-pion-exchange model, corrected for absorption in the final state. (auth)

39812 SUM RULES FOR K-MESON DECAYS WITH CP NONCONSERVATION. Gupta, V. (Tata Inst. of Fundamental Research, Bombay). Phys. Rev., 148: 1556-7 (Aug. 26, 1966).

The well-known isospin relations for $K \to 2\pi$ and $K \to 3\pi$ decays with CP conservation are generalized to include the case of CP-nonconserving weak interaction, but keeping CPT invariance and $|\Delta I| \leq 3/2$. Specifically the amplitude relation $2(K^+ \to \pi^+\pi^0) = (K_1^0 \to \pi^+\pi^-) - 2(K_1^0 \to \pi^0\pi^0)$ is generalized and found to be in agreement with experiment. (auth)

39813 AMBIGUITY OF THE MESON-BARYON COUPLINGS IN A BOOTSTRAP STATIC MODEL OF SU(6) SYMMETRY. Belinfante, J. G.; Renninger, G. H. (Carnegie Inst. of Tech., Pittsburgh). Phys. Rev., 148: 1573-8(Aug. 26, 1966).

An attempt is made to clarify certain aspects of SU(6) theory which have an important bearing on the problem of formulating a bootstrap dynamical description of symmetry breaking. In particular, a certain ambiguity of the meson-baryon coupling is discussed, which exists even in the limit of exact SU(6) symmetry, and which is called assignment mixing. It is possible to recover certain special theories, such as the so-called W-spin theory, by a particular choice of the assignment mixing angles. Bootstrap equations in the exact SU(6) limit do not fix the angles unless one also considers mesonic bootstrap equations corresponding to Fermi-Yang-type theories. It is also shown that in the exact SU(6) limit, the normalization and vertex equations of the Cutkosky-Leon bootstrap method both yield the same equation, which relates the coupling constant f to the ratio of the meson mass m to the cutoff parameter k_A. Approximate solutions of the Bethe-Salpeter equation are obtained. (auth)

39814 DISPERSION RELATION FOR THE AXIAL-VECTOR VERTEX AND A SUM RULE FOR THE AXIAL-VECTOR COUPLING-CONSTANT RENORMALIZATION. Suura, H.; Simmons, L. M. Jr. (Univ. of Minnesota, Minneapolis). Contract AT(11-1)-1371. Phys. Rev., 148: 1579-?(Aug. 26, 1966). (COO-1371-29).

A dispersion relation for the nucleon axial-vector vertex, in which the subtraction term at infinite nucleon mass is given by the unrenormalized vertex, is derived from the axial current-field commutation relations. Using the hypothesis of partially conserved axial-vector current, a sum rule for the axial-vector coupling-constant renormalization g_A is obtained in terms of the π-N form factor. In the elastic-unitarity approximation, the sum rule involves the integral over the difference of the P_{11} and S_{11} phase shifts. Certain experimental phase shifts up to 1-Bev pion kinetic energy give $g_A \approx 1.1$. However, because of the lack of consistent experimental data beyond 500 Mev, and also because of the lack of reliable theory to estimate the important contribution from inelastic channels, it is only concluded that the sum rule is not inconsistent with the experimental data. (auth)

39815 CURRENT-COMMUTATOR CALCULATION OF K_{l4} FORM FACTORS. Weinberg, Steven (Univ. of California, Berkeley). Phys. Rev. Lett., 17: 336-40(Aug. 8, 1966).

Callan and Treiman attempted a calculation (Phys. Rev. Letters 16: 153(1966)) of the decay $K \to 2\pi + l + \nu$ (l = e or μ), and concluded that the final-state π-π interaction makes the K_{l4} form factors vary too rapidly to allow a meaningful confrontation of a partially conserved axial-vector current and the current commutation relations (PCAC and CCR) with present experimental data on K_{e4} decay. It is shown that in fact using the full strength of PCAC and CCR allows an unambiguous calculation for all K_{l4} form factors, with results in excellent agreement with experiment. (B.G.D.)

39816 THE IDENTICAL RELATIONS BETWEEN THE BILINEAR COVARIANTS OF DIRAC'S THEORY OF THE ELECTRON. Van Oosterhout, G. W. (Philips Research Labs., Eindhoven, Netherlands). Physica, 32: 1090-6 (June 1966).

A new proof is given of the identical relations between the bilinear covariants $\varphi^T e_m \psi$ of Dirac's theory of the electron. It depends on the observation that these covariants are the coefficients p_m in $4\psi\varphi^T = \sum_0^5 p_m e_m$ and the rather evident fact that $\psi\varphi^T$ is pseudo-idempotent. (auth)

39817 POSITRON SCATTERING BY HYDROGEN AND THE ADIABATIC POTENTIAL. Bransden, B. H.; Jundi, Z. (Univ. of Durham, England). Proc. Phys. Soc. (London), 89: 7-11(Sept. 1966).

The sensitivity of s- and p-wave positron–hydrogen-atom elastic phase shifts to the presence or absence of various multipole components of the adiabatic polarization potential is discussed. It is concluded that higher multipoles than the quadrupole component are unimportant and support is given to the view of Drachman that in s-wave scattering the monopole component of the adiabatic potential should be suppressed. (auth)

39818 ELECTRON EXCHANGE IN BINARY ENCOUNTER COLLISION THEORY. Vriens, L. (Univ., Utrecht). Proc. Phys. Soc. (London), 89: 13-21(Sept. 1966).

The cross-section formulae for transfer of energy and momentum between a pair of free colliding electrons in an arbitrary frame in nonrelativistic quantum mechanics were derived. These formulas are applied in the electron-atom binary encounter collision theory in order to obtain the quantum-mechanical differential and total cross-section formulas for electron–atom collisions. This work represents an advance over the work of Gryzinski in that it includes interference between direct and exchange terms. Moreover, in the application some influ-

ence of the nucleus is taken into account since use is made of the symmetrical collision model. The interference term in the application to the binary encounter theory of electron-atom collisions corrects an earlier form of this term. (auth)

39819 ANNIHILATION OF SLOW POSITRONS IN IONIC MEDIA. Goldanskii, V. I.; Prokopev, E. P. (Inst. of Chemical Physics, Moscow). Soviet Phys.-Solid State (Engl. Transl.), 8: 409-15(Aug. 1966).

Translated from Fiz. Tverd. Tela, 8: 515-24(Feb. 1966).

An examination is made of the ground states of thermalized positrons bound by negative ions in ionic media. Annihilation from these ground levels gives one component with $\tau_0 \sim 10^{-11}$ sec and another with a lifetime shorter than $\tau_1 \sim 2 \cdot 10^{-10}$ sec. (auth)

39820 SUPPRESSION OF LARGE TRANSFERS IN PERIPHERAL INTERACTIONS AS AN EFFECT OF THE NUCLEON DIFFUSENESS. Kuchin, I. A.; Toleubaeva, A. S.; Usik, P. A. (Inst. of Nuclear Physics, Academy of Sciences, Kazakh SSR). Yadern. Fiz., 4: 102-4(July 1966). (In Russian).

The peripheral model with a nucleon form-factor is used to describe inelastic pp scattering at 1 to 3 Bev. The results of two methods describing the scattering of a virtual meson on a nucleon are compared: a description in terms of a finite number of partial waves and one in terms of the elastic scattering cross-section. It is shown that the suppression of large transfers, ensuring the agreement between the one-meson exchange model and experiments, differs when different methods are used to describe virtual scattering. (auth)

39821 MEASUREMENT OF π^+-MESON LIFETIME. Dunaitsev, A. F.; Pikhtelev, R. N.; Prokoshkin, Yu. D.; Simonov, Yu. N. (Joint Inst. for Nuclear Research, Dubna, USSR). Yadern. Fiz., 4: 105-9(July 1966). (In Russian).

The mean lifetime of the meson (π^+) was measured by a method in which the influence of the background due to the accompanying $\mu^+ \rightarrow e^+$ decay is excluded. The measured lifetime is equal to 25.85 ± 0.35 nsec. (auth)

39822 PHOTOPRODUCTION OF π^0 MESONS ON ^{4}He NEAR TO THE THRESHOLD. Belousov, A. S.; Rusakov, S. V.; Tamm, E. I.; Tatarinskaya, L. S. (Lebedev Inst. of Physics, Moscow). Yadern. Fiz., 4: 110-17(July 1966). (In Russian).

The differential and total cross sections for the photoproduction of mesons (π^0) on ^{4}He in the energy region 159 to 209 Mev were determined using the measured cross sections for γ quanta production in the decay of mesons (π^0). The cross-sections are used to determine the photoproduction amplitude F_2^+ for mesons (π^0) on nucleons. The results are compared with the theory, which makes use of the impulse approximation and the amplitude F_2^+ are obtained with the help of dispersion relations, in order to calculate the cross sections for the photoproduction of mesons on nuclei. (auth)

39823 POSSIBILITY OF DETERMINING ELECTROMAGNETIC FORM FACTORS OF THE W MESON. Nhuong, Doan (Joint Inst. for Nuclear Research, Dubna, USSR). Yadern. Fiz., 4: 123-5(July 1966). (In Russian).

The electromagnetic vertex of the intermediate meson with spin 1 depends on three unknown form factors. It is pointed out that it is possible on the basis of annihilation experiments with polarized protons and antiprotons to determine the values of these form factors, i.e., the values of the anomalous magnetic and quadrupole electric moments of the meson (W). (auth)

39824 POSSIBLE EXPERIMENTS CHECKING THE ISOTOPIC STRUCTURE OF ELECTROMAGNETIC INTERACTIONS. Grishin, V. G.; Lyuboshits, V. L.; Ogievetskii, V. I.; Podgoretskii, M. I. (Joint Inst. for Nuclear Research, Dubna, USSR). Yadern. Fiz., 4: 126-9(July 1966). (In Russian).

Possible experiments checking the rule $\Delta T = 0.1$ in processes involving γ quanta are discussed. (auth)

39825 GENERATION OF DEUTERIUM NUCLEI IN COSMIC RAYS. Kuzhevskii, B. M. (Inst. of Research in Cosmophysics and Aeronomics, Academy of Sciences, Siberian SSR). Yadern. Fiz., 4: 130-1(July 1966). (In Russian).

The role of the reaction $p + p \rightarrow d + \pi^+$ in the production of deuterium nuclei in cosmic rays is discussed. The contribution of this reaction is of the same order as that of the fragmentation reaction in the deuteron energy region 150 to 700 Mev/nucleon. It is evident that the reaction $p + p \rightarrow d + \pi^+$ determines a lower limit of the flux of deuterium nuclei in the given energy region. It is shown that an anomalous increase of the deuteron flux in cosmic rays should be observed in the mentioned energy region. (auth)

39826 PION PRODUCTION IN np COLLISIONS AT 600 Mev. Kazarinov, Yu. M.; Simonov, Yu. N. (Joint Inst. for Nuclear Research, Dubna, USSR). Yadern. Fiz., 4: 139-47(July 1966). (In Russian).

Angular distributions of charged pions have been measured as well as the total production cross section of neutral pions generated in np collisions at 600 ± 10 Mev. It was found that $\sigma_\pi(\theta) = [(0.115 \pm 0.005) \mp (0.004 \pm 0.013) \cos\theta + (0.04 \pm 0.02) \cos^2\theta] \times (1.073 \pm 0.104) \cdot 10^{-27}$ cm^2/steradian in the c.m.s. of the colliding nucleons. The total cross sections of the reactions are $\sigma(np \rightarrow \pi^0) = (4.6 \pm 0.6) \cdot 10^{-27}$ cm^2, $\sigma(np \rightarrow \pi^+) = \sigma(np \rightarrow \pi^-) = (1.68 \pm 0.17) \cdot 10^{-27}$ cm^2. The obtained data do not contradict the hypothesis of charge independence of nuclear forces. The cross sections for pion production in collisions of two nucleons in states with the total isotopic spin T = 0 and T = 1 were found to be $(4.4 \pm 1.0) \cdot 10^{-27}$ cm^2 and $(10.85 \pm 0.42) \cdot 10^{-27}$ cm^2, respectively. (auth)

39827 ANALYSIS OF THE REACTION $\pi N \rightarrow \pi_1\pi_2 N'$ IN THE ENERGY REGION UP TO 1 Gev. Zhukov, V. A.; Nemenov, L. L.; Yuan, Jung-Fang (Joint Inst. for Nuclear Research, Dubna, USSR). Yadern. Fiz., 4: 148-55(July 1966). (In Russian).

The cross sections of the processes $\pi N \rightarrow N^*_{3/2} + \pi$ in the energy region 290 to 905 Mev were determined. (auth)

39828 INTERACTIONS OF 1- TO 30-Gev ELEMENTARY PARTICLES WITH ATOMIC NUCLEI. Artykov, I. Z.; Barashenkov, V. S.; Eliseev, S. M. (Joint Inst. for Nuclear Research, Dubna, USSR). Yadern. Fiz., 4: 156-60(July 1966). (In Russian).

Results of statistical calculations are given for the interactions between 6.2, 9, 17, and 25 Bev protons and photoemulsion nuclei. The calculations were performed on the basis of the cascade-evaporation model. Special emphasis is laid upon interactions with a group of heavy nuclei. The results of the calculations are in good agreement with the experimental data. (auth)

39829 INFLUENCE OF THE POLARIZATION OF THE MEDIUM ON THE DEVELOPMENT AND ENERGY CHARACTERISTICS OF ELECTRON-PHOTON SHOWERS. Bakhtadze, A. K.; Ivanenko, I. P. (Moscow State Univ.). Yadern. Fiz., 4: 161-8(July 1966). (In Russian).

A solution of the one-dimensional electromagnetic cascade theory is obtained, taking the polarization of the medium into account. The energy spectra and dependence of the number of particles in the shower on the depth are calculated. (auth)

39830 INELASTIC π^-p INTERACTIONS WITH SLOW-RECOIL PROTONS AT 17 Gev. Azimov, S. A.; Nikishin, B. K.; Rechitskii, I. V.; Chudakov, V. M. (Inst. of Nuclear Physics, Academy of Sciences, Uzbek SSR). Yadern. Fiz., 4: 169-77(July 1966). (In Russian).

Some π^-p interactions with free and quasifree photoemulsion protons, in which 4 and 6 secondary charged particles are emitted, were investigated. A method of analyzing the angular correlations and the distribution of residual effective masses is described, which can prove useful in investigating multipion resonances. Experimental data indicate the possible existence of a resonance with the mass 3.2 Bev. (auth)

39831 ANGULAR DISTRIBUTIONS OF MUONS IN GROUND AND UNDER WATER AND THEIR GENERATION MECHANISM. Ilina, N. P.; Sarycheva, L. I. (Moscow State Univ.). Yadern. Fiz., 4: 178-80(July 1966). (In Russian).

The possibility is discussed of determining the nature of particles, generating muons in cosmic radiation, from an analysis of the angular distributions of muons in ground and under water. (auth)

39832 FOUR-FERMION INTERACTION AND LEPTON MASSES. Ivanter, I. G.; Zaretskii, D. F. Yadern. Fiz., 4: 181-7(July 1966). (In Russian).

It is shown that a strong four-fermion interaction can be responsible for the observed lepton masses. A connection between the lepton and baryon masses is found. The results are in satisfactory agreement with experiments. Other lepton properties following from the octet classification are considered, in particular the non-renormalizability of the lepton magnetic momenta. (auth)

39833 CROSS SECTIONS FOR GENERATING $K\bar{K}$ PAIRS IN $\pi\pi$ COLLISIONS AT LOW ENERGIES. Isaev, P. S.; Matveev, V. A. (Joint Inst. for Nuclear Research, Dubna, USSR). Yadern. Fiz., 4: 198-204(July 1966). (In Russian).

The cross sections of the process $\pi\pi \rightarrow K\bar{K}$ in the states with T = 0 (s-wave) and T = 1 (p-wave) in the low energy region, are calculated using dispersion relations. A comparison is made with data obtained from experiments, using the Chew-Low extrapolation procedure. (auth)

39834 FORMATION OF CHARGED π MESONS IN COLLISIONS BETWEEN 600-Mev NEUTRONS AND PROTONS. Dzhelepov, V. P.; Kiselev, V. S.; Oganesyan, K. O.; Flyagin, V. B. (Joint Inst. of Nuclear Research, Dubna, USSR). Zh. Eksp. Teor. Fiz., 50: 1491-1504(June 1966). (In Russian).

The energy spectra of charged mesons produced in n–p encounters involving 600-Mev neutrons are measured in a broad angular range by means of a multichannel magnetic spectrometer. The spectra are characterized by the presence of a large number of low-energy mesons. The peak of the spectra is at an energy of ~0.6 from the largest possible value. The angular distributions of $\pi^{\pm}$ mesons in the c.m.s. is described by a formula. The total meson production cross section $\sigma_{np}(\pi^+) = \sigma(\pi_n p^-) = (1.3 + 0.2) \cdot 10^{-27}$ cm^2. An analysis of the results shows that despite the dominating role of resonance pion production, in phenomenological studies the contribution of nonresonance transitions should be taken into account. (auth)

39835 ELECTROMAGNETIC PROPERTIES OF BARYONS AND MESONS IN A NONRELATIVISTIC QUARK MODEL. Gerasimov, S. B. (Joint Inst. for Nuclear Research, Dubna, USSR). Zh. Eksp. Teor. Fiz., 50: 1559-64(June 1966). (In Russian).

The electromagnetic properties (magnetic moments, electromagnetic mass splitting, radiative decays, electromagnetic radii) of mesons and baryons are considered within the framework of a nonrelativistic quark model under the assumption that the medium strong interaction violating SU(3) symmetry modifies the "strange" quark mass and magnetic moment. An expression is obtained for the electric quadrupole moments of vector mesons, which are determined by relativistic effects. (auth)

39836 EMISSION OF TWO PHOTONS INTO A GIVEN ANGLE IN ELECTRON COLLISIONS. Baier, V. N.; Fadin, V. S.; Khoze, V. A. (Novosibirsk State Univ., USSR). Zh. Eksp. Teor. Fiz., 50: 1611-16(June 1966). (In Russian).

Emission of two photons of arbitrary energy into a given angle in electron collisions is considered. The cross section $d\sigma_{\omega_1\omega_2}$ is a polynomial in powers of ω_1, ω_2. The coefficients of this polynomial are calculated numerically for the case when the angular dimensions of the detectors θ_0 are of the order of $1/\gamma$. For $\theta_0 \gg 1/\gamma$ an analytic expression for the cross section was obtained. (auth)

39837 DECAY ASYMMETRIES AND PRODUCTION ANGULAR DISTRIBUTIONS OF Λ^0 HYPERONS FROM $\pi^- + p \rightarrow \Lambda^0 + K^0$. Uto, Hiroaki. Philadelphia, Univ. of Pennsylvania, 1965. 104p.

Thesis.

The decay asymmetries and production angular distributions of Λ^0 hyperons at various incident pion momenta were measured. The Λ^0 hyperons were produced in the reaction $\pi^- + p \rightarrow \Lambda^0 + K^0$ with 1020 Mev/c mean momentum pions incident on a liquid hydrogen target. The events were observed in two thin foil spark chambers. A sample of 2500 events with incident pion momenta between 900 and 1050 Mev/c was obtained. The prodution angular distributions $d\sigma/d\Omega$, decay asymmetries αP_Λ (θ_Λ^{CM}), and $\alpha\overline{P}_\Lambda$ were studied for each incident pion momentum, where θ_Λ^{CM} is the production angle of the Λ^0 hyperon in the center of mass of production. The distributions αP_Λ (θ_Λ^{CM}) had sine wave shapes and the maximum occurred around $\theta_\Lambda^{CM} = 90°$. The polarization was close to 100% at this angle. The distributions $\alpha P_\Lambda\, d\sigma/d\Omega$ were fitted to a polynomial of the form

$$\alpha P_\Lambda(\theta_\Lambda^{CM}) \frac{d\sigma}{d\Omega_\Lambda^{CM}} = 2 \sin\theta_\Lambda^{CM} \sum_{n=0}^{\infty} a_n \cos^n\theta_\Lambda^{CM}$$

The S-P-D fit was adequate except at the highest pion momentum where the F wave amplitude was needed. The possible presence of $F_{\frac{7}{2}}$ resonance was examined. The decay asymmetry parameter times polarization averaged over the angle θ_Λ^{CM}, $\alpha\overline{P}_\Lambda$, was 0.3 at the Λ^0K^0 threshold (P_π = 900 Mev/c) and increased linearly with the incident pion momentum and was 0.55 at the production maximum (P_π = 1050 Mev/c). Results were compared with previously published data for incident pion momentum less than 1500 Mev/c and general conclusions were obtained. (TSS)

39838 RESONANCE PRODUCTION IN K^-p INTERACTIONS AT 1.80 TO 1.95 Gev/c. Smith, Lewis Taylor. Los Angeles, Univ. of California, 1966. 209p.

Thesis.

Selected final states produced by the interaction of K^- mesons with protons at 1.80 and 1.95 Bev/c were studied. These interactions were photographed at the Lawrence Radiation Laboratory 72-inch liquid-hydrogen bubble chamber. The total K^- track lengths for the two momenta were equivalent to 1.25 ± 0.04 events/μb at 1.80 Bev/c and 1.18 ± 0.04 events/μb at 1.95 Bev/c. The reactions studied were those associated with the topology of a vee plus two prongs, with the addition of a sample of four prong events at 1.95 Bev/c. The experiment encompassed the following reactions: $K^- + p \rightarrow \Lambda + \pi^+ + \pi^-$ (1), $K^- + p \rightarrow \Lambda + \pi^+ + \pi^- + \pi^0$ (2), $K^- + p \rightarrow \Sigma^0 + \pi^+ + \pi^-$ (3), $K^- + p \rightarrow \overline{K}^0 + \pi^- + p$ (4), $K^- + p \rightarrow \overline{K}^0 + \pi^- + p + \pi^0$ (5), $K^- + p \rightarrow \overline{K}^0 + \pi^- + \pi^+ + n$ (6), and $K^- + p \rightarrow K^- + \pi^+ + \pi^- + p$ (7). The total cross sections for reactions (1) through (7) are 1.70 ± 0.10, $1.84^{+0.12}_{-0.18}$, 0.60 ± 0.05, 1.73 ± 0.11, 0.34 ± 0.04, 0.33 ± 0.04 and 0.43 ± 0.03 mb, respectively at 1.80 Bev/c. At 1.95 Bev/c they are 1.47 ± 0.09, $2.11^{+0.13}_{-0.18}$, 0.57 ± 0.05, 1.89 ± 0.12, 0.65 ± 0.06, 0.57 ± 0.05 and 0.58 ± 0.04 mb, respectively. Each of the reactions is characterized by the production of one or more intermediate resonant states. Maximum likelihood fits to the data were made in order to obtain best estimates of the values of the various resonant fractions. A detailed angular correlation analysis was made for various quasi two-body resonant states. These states were $K^{*-} + p$, Y_1^{*+} (1385) + π^-, $\Sigma^0 + \rho^0$, $\Lambda + \omega$, $K^* + N^*$ and Y_1^{*+} (1385) + ρ^-. For the K^{*-}, after averaging over production angles and beam momenta, $\langle\rho_{00}\rangle = 0.31 \pm 0.05$, $\langle\rho_{1,-1}\rangle = 0.06 \pm 0.05$, $\langle \mathrm{Re}\rho_{10}\rangle = -0.02 \pm 0.03$. On the peripheral model, these values predict strong contributions from both pseudoscalar and vector meson exchange. For the Y_1^{*+} (1385), $\langle t_0^{\frac{3}{2}}\rangle = -0.24 = 0.10$, $(\mathrm{Re}t_2^{\frac{3}{2}}) = 0.02 \pm 0.06$, $\langle \mathrm{Im}t_2^{\frac{3}{2}}\rangle \pm -0.16 \pm 0.06$. The latter values are in good agreement with the predictions of the Stodolsky-Sakurai model for isobar production, as modified by absorption effects. (TSS)

39839 PION-NUCLEON COLLISIONS AND PION PRODUCTION. Gleeson, Austin Michael. Philadelphia, Univ. of Pennsylvania, 1965. 185p.

Thesis.

A model is formulated, which, while still retaining all the

complications of spin and isospin, satisfies the unitarity conditions. This model is then utilized to study the effects of the inelastic channels on the elastic pion-nucleon channel and to examine the single-pion production channel. The proper physical amplitudes in the helicity representation are constructed. The requirements of unitarity are studied and a discontinuity equation is formulated. The one-pion exchange diagram and other Born terms are discussed. A pole model is then formulated, which includes the effects of these Born terms and the anomalous thresholds associated with production processes. The resulting nonlinear integral equations are solved by a multichannel N/D method. The effects of the inelastic channels on the elastic channel are discussed. This is done by examining the positions and widths of the pion-nucleon resonances. The $N_{\frac{3}{2}}(1236)$, $N^*_{\frac{1}{2}}$ (1518), and $N^*_{\frac{3}{2}}(1688)$ are found. The predicted positions are somewhat low in the $N^*_{\frac{3}{2}}$ but high in the other two cases. The half widths are high in all cases. The last two resonances are due to the presence of the inelastic channels. The inelastic cross sections predicted by the model are found to be in reasonable agreement with experiment. There are indications that the S-wave dipion resonance effects are overly strong in this model. The predicted angular distributions of the inelastic channel are also examined. (TSS)

39840 STUDY OF $\bar{K}N$ AND KN INTERACTIONS. Cho, Kyu Suk. Philadelphia, Univ. of Pennsylvania, 1965. 124p. Thesis.

$\bar{K}N$ and KN interactions are studied using the double dispersion representation together with the approximation scheme of Balazs. The unitarity condition requires the study of the πY system as well as the $\bar{K}N$ scattering; therefore, the partial wave amplitudes are discussed for the multichannel case. Analyticity and crossing relations are discussed for the individual amplitudes. The partial wave dispersion relation is applied to the I = 0 and I = 1 $s_{\frac{1}{2}}$ states for the $\bar{K}N$ scattering, and to the I = 0 and I = 1 $s_{\frac{1}{2}}$, $p_{\frac{1}{2}}$, and $p_{\frac{3}{2}}$ states for the KN scattering. These relations are solved by the N/D method representing the unphysical cut by a series of poles. The positions of the poles are not arbitrary parameters. The residues are determined by matching N/D amplitudes to the amplitudes calculated from the fixed energy dispersion relations at the suitably chosen matching point w_m. In the KN scattering the coupling constants $g_{Y_0^*KN}$ for $Y_0^*(1405)$, $g_{Y_1^*KN}$ for $Y_1^*(1385)$, $g_{\rho NN}g_{\rho KK}$, and of $g_{SNN}g_{SKK}$ are adjusted to reproduce the experimental scattering lengths. It is found that their values are compatible with those predicted by the SU(3) symmetry. It is also found that the contribution to the potential for the I = 0 state $Y_1^*(1385)$, $Y_0^*(1520)$, and the ρ-meson exchange is repulsive, while that from the S-meson exchange is attractive; for the I = 1 state the contribution from the ρ, S, and $Y_0^*(1520)$ exchange is attractive, while that from the hyperon is repulsive. The calculated phase shifts agree quite well with the experimental values. In the $\bar{K}N$ process both solutions of Humphrey and Ross do not support the resonance $Y_0^*(1405)$ below the $\bar{K}N$ threshold, while the requirement that $Y_0^*(1405)$ be the $s_{\frac{1}{2}}$ $\bar{K}N$ bound state gives the scattering lengths $a^{(0)} = -0.89$ F and $b^{(0)} = 0.14$ F. The assignment of $Y_0^*(1405)$ to the unitary singlet in the octet model is in agreement with this calculation. Finally, the vector meson exchange alone is not sufficient to reproduce the $Y_0^*(1405)$ resonance. (TSS)

39841 DEUTERON AND BOUND STATES OF THE NUCLEON-ANTINUCLEON SYSTEM. Berger, Edmond Louis. Princeton, N. J., Princeton Univ., 1965. 220p. Thesis.

An attempt is made to understand to what extent the pion can be treated as a bound nucleon-antinucleon system and to measure the effect of the binding force associated with deuteron exchange. The relativistic nucleon-antinucleon process is thoroughly analyzed. After invariant amplitudes having the Mandelstam analyticity are chosen, the partial wave with the quantum numbers of the pion is singled out, and its analytic structure is displayed through a partial wave dispersion relation. The structure of the partial wave is then simplified by various approximations to both the forces and the unitarity discontinuities. Unsubtracted N/D methods are employed to solve the resulting partial wave dispersion relations; a numerical matrix inversion technique is used to obtain N and D. It is shown that due to the large magnitude of its residue parameters, the deuteron pole term of the crossed nucleon-nucleon channel generates extremely strong attractive forces in the nucleon-antinucleon amplitude of interest, much stronger than those associated with any other single exchange. Indeed, assuming deuteron exchange and elastic unitarity, the binding force is so strong that a zero of the denominator function simply cannot be located in the physical region. With the intention being to compute the output pion-nucleon coupling constant, the appropriate partial wave is also investigated assuming elastic unitarity and various combinations of exchange forces from among those associated with pi, eta, rho, omega, phi, and deuteron exchange, adjusting input couplings so as to produce a pole at the proper pion location; the output coupling constant is consistently two orders of magnitude too large. Inelastic effects are subsequently included in an approximate way; no improvements result. Seriously questioned is the notion that the pion can be demonstrated to be a composite system without careful incorporation into the analysis of many contributory channels at once. (TSS)

39842 PION-NEUTRON INTERACTIONS AT 3.5 Bev/c. Galloway, Kenneth Franklin. Columbia, S. C., Univ. of South Carolina, 1966. 82p. Thesis

An experiment was done to determine some of the general features of negative pi meson–neutron interactions at 3.5 Bev/c using nuclear track emulsion. The emulsion plates were exposed to an external beam of pions at the Bevatron. Events were found by a beam following method and measured to determine the identity, momentum, and space angles of the charged secondary particles. A total of 537.90 meters of track was scanned by the beam following method. This resulted in a mean interaction length of 6.33 ± 0.56 meters for events identified as π^-–n interactions. The angular and momentum distributions were measured; the partial cross sections for elastic scattering, meson production, and strange particle production were determined using the total cross section for π^+-p interactions at this energy. A charged multiplicity of 1.75 ± 0.11 was obtained for the inelastic events. Calculations of relative probabilities were made using a statistical theory for multiple meson production. These calculations were made both with and without the inclusion of the $\frac{3}{2}-\frac{3}{2}$ nucleon isobar. The experimental data are not in good agreement with these statistical theory calculations. Predictions of the peripheral collisions model seem to be consistent with the data. (Dissertation Abstr.)

39843 INTEGRAL EQUATION FOR THE ANOMALOUS DEUTERON VERTEX AND A COMPARISON OF TWO NORMALIZATION CONDITIONS. Cawley, Robert Gerald. [Urbana], Ill., Univ. of Illinois, 1965. 140p. Thesis.

A set of coupled inhomogeneous integral equations is found for the imaginary parts of the four invariant amplitudes of the anomalous deuteron vertex. The equations are algebraically homogeneous, however, so the possibility of an eigenvalue condition exists if unsubtracted dispersion relations are postulated. The anomalous region is treated by means of a modification of the Nishijima continuation procedure. The equations are derived in a one-pion model to illustrate the method. A partial diagrammatic analysis of the deuteron vertex is performed below the normal threshold, $s_0 = (M + \mu)^2$. A proof is given that the propagator normalization of a scalar or a vector particle is equivalent to the normalization of its electromagnetic form factor. The basis for the proof is the Ward identity. This permits a direct comparison of the two normalization conditions and this is done in lowest approximation for two scalar deuteron models and for the vector case as well. The normalization of the deuteron vertex is computed from the triangle graph approximation to the deuteron electromagnetic form factor. This result is inserted into the expansion arising from the dispersion relation for the inverse deuteron propagator at infinity, and an approxima-

tion to the deuteron field operator renormalization constant Z is thereby found. The result in each of the scalar models is Z = 0. The vector case is more sensitive to the form factors which enter in, but in a model which is in spirit comparable to the scalar examples yields Z = 0. An independent argument for Z = 0 for a vector field is advanced when no zero-mass scalar particles are present. (Dissertation Abstr.)

39844 NUCLEON-NUCLEON POLARIZATION AT 700, 600, 500, AND 400 Mev. Cheng, David. Berkeley, Calif., Univ. of California, 1965. 105p.

Thesis.

The polarization parameters for the two-nucleon systems were measured at the 184-in. cyclotron at beam energies of 700, 600, 500, 400, and 310 Mev. They are measured for both the pp and pn systems by means of a polarized proton beam initially produced by scattering the external proton beam on a carbon target at ±6 deg, and then scattered in a liquid hydrogen target or a liquid deuterium target. The outgoing particles are detected by 19 proton counters and 8 neutron counters fixed in space. All possible coincidence pairs are recorded through an on-line computer. The asymmetry is measured by reversing the sign of the beam polarization by reversing the pC scattering angle. The angular range treated is between 30 and 150 deg in the center-of-mass system, and involves measurements at eight angular positions at each energy. In order to calibrate the beam polarization, the polarization parameter for pC is also measured at the above energies in the forward direction between 6 and 14 deg in the laboratory frame. The NN polarization parameters, $P(\theta)$, are almost independent of energy. In the pp system, $P(\theta)$ can be approximated by A sin θ^* cos θ^* where A varies between 0.85 at 310 Mev and 1.1 at 700 Mev. In the pn system P_{max} in the forward direction varies between 0.42 at 310 Mev and 0.34 at 700 Mev, and P_{min} in the backward direction varies between −0.25 at 310 Mev and −0.4 at 700 Mev. When fitting both the differential cross section, I_0, and polarization, P, with all the data available in this energy region, in terms of power series, the differential cross sections in both the pp and pn systems were found to vary with energy to a greater extent than the polarization parameters. From these fits, I_0 and P, for the isotopic spin singlet (I = 0) state of the 2-nucleon system, are also calculated. The energy variation is considerable in this state. The polarization is small, but it tends to increase and be negative at the high end of this energy range. (Dissertation Abstr.)

39845 STUDY OF THE N*(1920) RESONANCE. Gutay, Laszlo Janos. Tallahassee, Florida State Univ., 1964. 101p.

Thesis.

In the $\pi^+ + p$ elastic and inelastic cross section a prominent peak has been found at 1350 Mev incident pion kinetic energy. It is an experimental fact that if a resonance was found in the total cross section as a function of energy in pion-nucleon scattering, a similar resonance effect shows up in the final state of an inelastic scattering if the total energy of a final state of a nucleon and one or more pions is the same as a resonance. The 1350-Mev resonance in the $\pi + \pi + N$ and $\pi + \pi + \pi + N$ final states is studied. It has been proposed that if the N*(1920) decays into an N*(1238) and pion, it might be possible to relate the decay angular distribution and polarization of the N*(1238) to the spin and parity of the N*(1920). The experimentally found azimuthal angle distribution excludes a possible N*(1238) polarization, and at the same time indicates an N*(1238) production via ρ exchange. An application of cascade decay to determine the spin and parity of N*(1920) in $\pi^- + \pi^- + \pi^+ + p$ final state was attempted. Evidence for the correlation was found and suggested further extension of the theoretical and experimental study initiated in this work. The study of the $\pi + \pi + N$ final state shows a very strong ρ,N*(1238) and N*(1920) overlap. This overlap was studied and it gives a hint regarding the puzzling asymmetry found in ρ^0 decay. (Dissertation Abstr.)

39846 ANALYSIS OF 3587 τ^+ DECAYS. Huetter, Godfrey Thomas. Hoboken, N. J., Stevens Inst. of Tech., 1965. 47p.

Thesis.

An analysis of 3587 $\tau^+ \rightarrow \pi^- + \pi^+ + \pi^+$ decay events is presented. These events were found in an area scanning of an emulsion stack of 600 μ Ilford G5 emulsion pellicles exposed to a 300-Mev/c separated K^+ beam at the Bevatron of the Lawrence Radiation Laboratory. The pion energy spectra are compared to the predictions of linear matrix element theory, the pion pole model, and the s-wave resonance model, and to the existing spectra of the secondaries from η, $\tau^\pm$, τ', and K^0_2. (Dissertation Abstr.)

39847 MEASUREMENT OF THE N^{*-}-N^{*++} MASS DIFFERENCE. Kim, Sedong. Berkeley, Calif., Univ. of California, 1965. 65p.

Thesis.

A measurement of the mass and width difference between N^{*-} ($I_Z = -3/2$) and N^{*++} ($I_Z = +3/2$) is described, where N* is the pion-nucleon p-wave resonance of spin and isotopic spin 3/2 and mass approximately 1240 Mev. The resonances were produced in the inelastic reactions $nn \rightarrow pn\pi^-$ and $pp \rightarrow np\pi^+$, which are known to proceed almost entirely via N^{*-} and N^{*++} production, respectively, in the observed energy region of a few Bev. The masses and widths of N^{*-} and N^{*++} were obtained from their respective effective mass distributions. In fitting the data for the masses two different formulas were used: a) the OPE (one-pion-exchange) formula and b) the resonance formula with constant matrix element, which goes according to the phase space. Because the above inelastic reactions are known to be dominated by OPE, the values obtained with the OPE formula are taken to be the best estimate of the resonance parameters. This gives a mass difference of $\delta\omega_0 = N^{*-} - N^{*++} = 7.9 \pm 6.0$ Mev and a width difference of $\delta\Gamma_0 = 24.7 \pm 23.0$ Mev. This result agrees with the predictions based on the SU(3) and SU(6) symmetry schemes and various dynamical theories. (Dissertation Abstr.)

39848 INFLUENCE OF THE NN* CHANNEL ON ELASTIC NN SCATTERING. Shepard, Harvey Kenneth. Pasadena, Calif., California Inst. of Tech., 1966. 151p.

Thesis.

The problem of two channels, NN and NN*, coupled through unitarity, is studied to see whether sizable peaks can be produced in elastic nucleon-nucleon scattering due to the opening of a strongly coupled inelastic channel. One-pion-exchange (OPE) interactions are calculated to estimate the $NN^* \rightarrow NN^*$ and $NN \rightarrow NN^*$ amplitudes. The OPE production amplitudes are used as the sole dynamical input to drive the multichannel ND^{-1} equations in the determinantal approximation, and the effect on the $J = 2+$ ($^1D_2$) elastic NN scattering amplitude is studied as the width of the unstable N* and strength of coupling to the inelastic channel are varied. A cusp-type enhancement appears in the NN channel near the NN* threshold but for the known value of the N* width the cusp is so "wooly" that any resulting elastic peak is likely to be too broad and diminished in height to be experimentally prominent. A brief survey of current experimental knowledge of the real part of the $^1D_2$ NN phase shift near the NN* threshold is given, and the values are found to be much smaller than the nearly resonant phase shifts predicted by the coupled channel model. (Dissertation Abstr.)

39849 MEASUREMENT OF Λ^0 HYPERON AND K^0_1 MESON LIFETIMES AND SEARCH FOR COHERENT INTERFERENCE IN THE DECAY $K^0 \rightarrow \pi^+\pi^-$. Young, Kenneth Kong. Philadelphia, Univ. of Pennsylvania, 1965. 108p.

Thesis.

The time distribution of the charged decays of the K^0 meson and the lambda hyperon produced in the reaction $\pi^- + p \rightarrow K^0 + \Lambda^0$ was analyzed. The reaction was produced by a 1.03-Bev/c pion beam for the BNL cosmotron incident on a liquid hydrogen target. The events were observed in a thin foil spark chamber, which was counter

triggered. By use of the maximum likelihood method the lifetimes of the Λ^0 and the K_1^0 were estimated to be $(2.68^{+0.12}_{-0.11}) \times 10^{-10}$ sec and $(0.90^{+0.06}_{-0.05}) \times 10^{-10}$ sec respectively. A fit to the $K^0 \to \pi^+\pi^-$ time distribution was made assuming the distribution $P(t;\alpha,\Delta m,\varphi) = e^{-\lambda_1 t} + \alpha^2 e^{-\lambda_2 t} + 2\alpha e^{-[(\lambda_1+\lambda_2)/2]t}\cos(\Delta m t + \varphi)$. This distribution assumes interference between the long- and short-lived components of $K^0 \to \pi^+\pi^-$ where α = amplitude $(K_2^0 \to \pi^+\pi^-)$/ ampl. $(K_1^0 \to \pi^+\pi^-) = |\alpha|e^{i\varphi}$, $\Delta m = m_{K_2^0} - m_{K_1^0}$, and λ_1, λ_2 = decay rates of K_1^0 and K_2^0. The time, t, is measured from the production point. By use of a maximum likelihood function derived from the above a priori distribution, a three-parameter fit was made in α, Δm, and φ, to the data. The best fit gives $\alpha = (8.0 \pm 4.5) \times 10^{-3}$, $\Delta m = (1.20 \pm 0.35) \times 10^{10}$ sec^{-1}, and $\varphi = 180^{\circ}{}^{+75^{\circ}}_{-65^{\circ}}$. If the average value of Δm from previous measurements is used $\Delta m = 0.75 \times 10^{10}$ sec^{-1}, then $\alpha = (6 \pm 4) \times 10^{-3}$ and, $\varphi = (45 \pm 48)^{\circ}$. (Dissertation Abstr.)

Field Theory, Scattering Theory, and Symmetries

See also Elementary Particles and Radiations

39850 (IC-66/77) DEGENERATE REPRESENTATIONS OF THE SYMPLECTIC GROUPS. I. THE COMPACT GROUP Sp(n). Pajas, P.; Raczka, R. (International Centre for Theoretical Physics, Trieste (Italy)). June 1966. 48p. Dep. mn.

The theory of the degenerate representations of the rotation and unitary groups is extended to unitary symplectic groups, i.e., those which conserve symmetric and antisymmetric bilinear forms. (B.G.D.)

39851 (IC-66/96) A REFINED SOLUTION OF TWO-DIMENSIONAL MODEL THEORIES. Schwabl, F.; Thirring, W.; Wess, J. (International Centre for Theoretical Physics, Trieste (Italy)). Aug. 1966. 27p. Dep. mn.

In the formulation of the model, special care was given to the definition of the current as the product of field operators. It is shown that a product of field operators, where the space-time points coincide, can be defined as the limit of products with the points separated and that the limit exists in the Borchers topology. A consistent definition of the current can be given this way, and the model where a massive vector field is coupled to this current is solved through an ansatz. The interacting fields can be expressed in terms of free canonical quantities. To avoid infrared divergences, a finite volume is used. (auth)

39852 (INP-480/PL) EQUAL TIME COMMUTATORS AND SCALAR MESONS DECAYS. Kwiecinski, Jan (Institute of Nuclear Physics, Krakow (Poland)). May 1966. 8p. Dep.

The equal time current commutation relations are used to estimate the relevant coupling constants of scalar mesons under an additional assumption that the operators resulting from commutation relations between the axial charges and divergences of isospin axial vector currents are proportional to the respective scalar meson field operators. (auth)

39853 (JEN-157-DF/I-48) CAMPOS LIBRES DEL NEUTRINO Y DEL FOTON. (Free Fields for Neutrinos and Photons). Nunez-Lagos Rogla, Rafael (Junta de Energia Nuclear, Madrid (Spain). Division de Fisica). 1965. 148p. Dep. mn.

A relativistic quantum field theory is presented in a general and intrinsic way. The building blocks are the one particle states and the unitary representations of the Lorentz group. From these, different useful many-particle states and applications to relate them are defined. One particle operators are extended to the field spaces. Annihilation and creation operators are introduced in a natural way, their algebra being fixed by the microscopic causality. The theory is applied to the spin ½ case, and different realizations for the neutrino and antineutrino fields are obtained and analyzed. The spin 1 case follows as a consequence of the fusion method, and Maxwell equations and Lorentz and Gange conditions are easily deduced. There are no difficulties related to the metric and the local commutation rules. (auth)

39854 (JINR-E-2754) S-MATRIX, NON-COMPACT SYMMETRY GROUPS AND THEIR COLLINEAR SUBGROUPS. Nguyen Van Hieu (Joint Inst. for Nuclear Research, Dubna (USSR). Lab. of Theoretical Physics). 1966. 6p. Dep. mn.

The structure of the S-matrix in the symmetry with noncompact group as well as the connection with the $SU(6)_W$ symmetry are investigated. (auth)

39855 (JINR-E-2771) CALCULATION OF THE COEFFICIENTS OF THE MASS OPERATORS. Robaschik, D.; Uhlmann, A. (Joint Inst. for Nuclear Research, Dubna (USSR). Lab. of Theoretical Physics). 1966. 12p. Dep. mn.

For normed orthogonal systems of operators the coefficients for SU(3) and SU(6) mass formulas are calculated and relations between these coefficients are considered. (auth)

39856 (JINR-E-2826) CONSISTENT RELATIVIZATION OF SU(6) FOR TWO-PARTICLE REACTIONS. Ogievetskii, V. I.; Polubarinov, I. V. (Joint Inst. for Nuclear Research, Dubna (USSR). Lab. of Theoretical Physics). 1966. 6p. Dep. mn.

Group $SU_x(6)$ is found which is isomorphic to SU(6) and leaves free equations of motion invariant. Every particle in the reaction is transformed according to its own low. In spite of this a very simple rule is obtained on how to construct invariant amplitudes. (auth)

39857 (JINR-E-2876) ADLER-WEISBERGER RELATION AND DISPERSION SUM RULES IN THE THEORY OF STRONG INTERACTIONS. Bogolubov, N. N.; Matveev, V. A.; Tavkhelidze, A. N. (Joint Inst. for Nuclear Research, Dubna (USSR). Lab. of Theoretical Physics). 1966. 10p. Dep. mn.

Assuming the unsubtracted dispersion relation for the quantity related to the divergences of the local axial currents, the Adler-Weisberger sum rule was derived for the renormalization of the axial weak constant by the strong interactions under some additional assumptions. These assumptions are as follows: the additivity principle for the scattering amplitude of the massless pseudoscalar particle on the nucleon near the threshold in the quark model and the nonrenormalization of the proper quark axial weak constant. (auth)

39858 (JINR-P-2760) O SVOISTVAKH RAZLOZHENIYA PO PUCHKAM PRICHINNOI S-MATRITSY. (On Properties of the Cluster Expansions of the Causal S-Matrix). Khodzhaev, L. Sh. (Joint Inst. for Nuclear Research, Dubna (USSR). Lab. of Theoretical Physics). 1966. 14p. Dep. mn.

Space-like properties of the cluster expansions of the vacuum expectation values of radiational operators as well as the matrix elements of the S-matrix are investigated in the framework of the Bogoliubov's asymptotic causal matrix theory. (auth)

39859 (JINR-P-2761) PRIBLIZHENNOE VYCHISLENIE BLIZHAISHIKH POLYUSOV FUNKTSII S'_F I Δ'_F V SLUCHAE SIL'NOI $\bar{\psi}\psi\phi$ SVYAZI. (An Approximate Calculation of the Nearest Poles of the Functions S'_F and Δ'_F in Case of Strong $\bar{\psi}\psi\phi$ Coupling). Kyunel, A. (Joint Inst. for Nuclear Research, Dubna (USSR). Lab. of Theoretical Physics). 1966. 16p. Dep. mn.

Starting from the expressions for the Green functions derived in a functional formulation of quantum field theory one obtains series for the Green functions; of the scalar and spinor fields in the strong interaction of the Yukawa type. The expressions under the functional integral are expanded in a free Lagrangian. The necessary functional integrations are made in the lattice space. The ratio of the lowest mass of each field is given. (auth)

39860 (JINR-P-2790) O SUSHCHESTVOVANII NEKOTORYKH BARIONNYKH I MEZONNYKH UNITARNYKH MUL'TIPLETOV. **(Existence of Certain Baryon and Meson Unitary Multiplets). Enkovskii, L.; Kukhtin, V. V.; Nguyen Thi Hong (Joint Inst. for Nuclear Research, Dubna (USSR). Lab. of Theoretical Physics). 1966. 10p. Dep. mn.**

The existence of unitary octets, decuplets, and singlets of baryon resonances with spin and parity $5/2^+$, $7/2^+$, and $1/2^-$ respectively, and meson resonance nonet 1 was investigated. The ratio of the probability of decay of the following types: $5/2^+ \rightarrow 1/2^+ + 0$, $7/2^+ \rightarrow 1/2^+ + 0$, $1/2^- \rightarrow 1/2^+ + 0$, and $1^+ \rightarrow 0^- + \gamma$ was found. (tr-auth)

39861 (JINR-P-2821) SMESHIVANIE KONFIGURATSII V MODELI KVARKOV. **(Configuration Mixing in Quark Model). Matveev, V. A.; Struminskii, B. V.; Targamadze, V. G. (Joint Inst. for Nuclear Research, Dubna (USSR). Lab. of Theoretical Physics). 1966. 8p. Dep. mn.**

The magnetic moments and the axial constants are obtained in the assumption of the configuration mixing in the quark model. The obtained results are in good agreement with experiment. (auth)

39862 (NP-16242) INTRODUCTORY LECTURES ON SU_3 SYMMETRY. **Kajantie, Keijo (Helsinki Univ. (Finland). Research Inst. for Theoretical Physics). 1966. 66p. Dep. mn.**

Five lectures are presented on SU(3) symmetry. Topics discussed are SU(2) symmetry, irreducible tensors, representations of SU(3) lie algebra A_2, experimental consequences of SU(3) symmetry, and broken symmetry. (B.G.D.)

39863 COMPLEX ANGULAR MOMENTA AND THE GROUPS SU(1,1) AND SU(2). **Holman III, Wayne J.; Biedenharn, Lawrence C. Jr. (Duke Univ., Durham, N. C.). Ann. Phys. (N. Y.), 39: 1-42(Aug. 1966).**

The Wigner coefficients coupling any two discrete representations of the noncompact group SU(1, 1) are derived, and it is shown that they can be expressed as analytic continuations of one another and of the Wigner coefficients of SU(2) in the planes of complex angular momenta. It is further shown that these Wigner coefficients, in certain well-defined limits, approach the form of the representation functions: The Wigner coefficients coupling two discrete representations of SU (1, 1) approach the representation functions of SU(1, 1) while those of SU(2) approach the SU(2) functions. The Wigner coefficients coupling a positive and a negative discrete representation of SU(1, 1) are used to define states of the continuous series of its unitary representations. It is shown that a definition of the norm of these states exists under which the states of all the unitary representations of SU(1, 1)—positive and negative discrete and both the principal and exceptional series of the continuous representations—are mutually orthogonal in the same Hilbert space. (auth)

39864 NEW FORMS OF THE IRREDUCIBLE UNITARY REPRESENTATIONS OF THE POINCARE GROUP. [PART] I. **Guillot, J. C.; Petit, J. L. (Univ., Geneva). Helv. Phys. Acta, 39: 281-99(1966). (In French).**

Different forms of representations of the Poincaré group are studied and their interrelations established. Starting with the induced representations by Mackey, the isomorphisms to the forms defined on the space of functions on a homogeneous space are constructed explicitly. As a particular case the representations of Wigner are found, and the arbitrary parameters involved are specified. Different possible forms of representations defined on either the Poincaré group or the Lorentz group are then given. Finally the different conventions which are used for different physical situations are specified. (auth)

39865 NEW FORMS OF THE IRREDUCIBLE UNITARY REPRESENTATIONS OF THE POINCARE GROUP. [PART] II. **Guillot, J. C.; Petit, J. L. (Univ., Geneva). Helv. Phys. Acta, 39: 300-24(1966). (In French).**

A new form of representations of the Poincaré group is studied in detail by means of functions defined on the Lorentz group. Several parametrizations of this group which allow construction of representations of the Poincaré group and its Lie algebra for the cases $m \geq 0$ are considered. Some of these parametrizations define forms corresponding to the canonical and to the helicity formalisms. Two methods for calculating the infinitesimal operators are mainly used: the one is related directly to the mass hyperboloid and the other one is constructed by replacing the spin matrices by differential operators. (auth)

39866 UNITARITY OF THE S MATRIX FOR MULTICHANNEL SCATTERING. **Jauch, J. M.; Marchand, J.-P. (Univ., Geneva. CERN, Geneva). Helv. Phys. Acta, 39: 325-37(1966).**

The usual proofs for the unitarity of the S matrix are based on the assumption that the wave functions in different channels are orthogonal to each other. This is not the case in rearrangement collisions where the colliding particles and the collision products are composite fragments (overlapping channels). A correct proof for the usual unitarity property of the S matrix is given for the case of overlapping channels. The proof is greatly facilitated by a systematic use of the spectral representation for a complete system of commuting observables. Each channel defines as a consequence of the asymptotic condition a pair of wave operators. These are partial isometries with orthogonal ranges for different channels. This orthogonality property, which was proved earlier, is the essential property which implies unitarity for the S matrix in the usual sense. Unitarity is then shown to be a direct consequence of the asymptotic condition and nothing more. (auth)

39867 MAJORIZATION OF FEYNMAN GRAPHS. **Chow, Yutze (Univ. of Wisconsin, Milwaukee). J. Math. Phys. (N. Y.), 7: 1158-70(July 1966).**

The different methods of majorization of Feynman graphs are reviewed and their respective domains of application and relative merits are discussed. The initial steps of Wu's majorization method are discussed in a variational formalism. Effort is made to present the rather complex arguments involved in Nakanishi's "path method" in a systematic manner. (auth)

39868 POLES OF THE S MATRIX FOR LONG-RANGE POTENTIALS. **Ferreira, Erasmo M.; Teixeira, Antonio F. F. (Centro Brasileiro de Pesquisas Fisicas, Rio de Janeiro). J. Math. Phys. (N. Y.), 7: 1207-17(July 1966).**

The analytic properties in the complex k plane of the S matrix for scattering by a screened Coulomb potential are studied. Particular attention is given to the limit as the screening radius tends to infinity, so as to show, in an explicit example, the effect of the tail of the potential on the properties of the analytically extended S matrix. It is shown that the pole configuration obtained in this way is different from that obtained in the usual description of the analytic properties to the Coulomb S matrix. (auth)

39869 KINKS. **Finkelstein, David (Yeshiva Univ., New York). J. Math. Phys. (N. Y.), 7: 1218-25(July 1966).**

In sufficiently nonlinear field theories there are extended objects whose number is strictly conserved because of continuity of the underlying field as a function of space. These are called kinks. Kinks provide a covariant description of extended but indestructible particles. The properties the field theory must possess in order for kinks to exist, and the circumstances under which kinks can have spin $1/2$ are given. (auth)

39870 SOLUTION OF VERY SINGULAR N/D EQUATIONS: APPROACH TO NONRENORMALIZABLE FIELD THEORY. **Halpern, Martin B. (Harvard Univ., Cambridge, Mass.). J. Math. Phys. (N. Y.), 7: 1226-50(July 1966).**

Closed form solutions to unsubtracted and once-subtracted N/D equations, both nonrelativistic and relativistic, with pathological left-hand absorptive parts that increase at large ν like $\alpha(-\nu) \sim -\lambda\nu^m$, m not necessarily integral, are found. The solutions allow dispersive, unitary and regulator-free calculation in nonrenormalizable field theory. For example, N/D equations with exchange of a higher

spin particle (spin $^3/_2$ etc.) can be solved. In general, the technique allows the use of a large class of divergent graphs as input, that is, those whose left-hand absorptive parts are finite, although asymptotically ill-behaved. For example, in the W theory of leptonic weak interactions, one of the possible inputs is any number of ladder graphs cut so that all the bosons are on the mass shell. Many non-planar graphs can be included as well. In much the same way, in the Fermi theory, (multiple exchanges in) theories of higher spin in general, and theories with derivative coupling can be calculated. There are an infinite number of solutions to these singular integral equations, each of which is characterized by a branch point at $g^2 = 0$, and a branch point of oscillatory nature at infinite $|\nu|$. Out of these, the solution which sums the iterative expansion of the equations as most meaningful is selected. It is seen explicitly that the unitary requirement generates its own regulation in the form of rapid oscillations at large unphysical energies, thus eliminating the need for any regulator limiting process. The oscillations are associated with an infinite number of ghosts, but these stay very far from the physical region. In addition, the solutions violate unitarity in the cross channels, the program is expected to be useful at most in and near the physical region. As shorter range forces are systematically included, there is some indication that the program may converge rapidly for small physical energies. (auth)

39871 UNITARY IRREDUCIBLE REPRESENTATIONS OF SL(3,R). Rosen, Gerald (Southwest Research Inst., San Antonio). J. Math. Phys. (N. Y.), 7: 1284-94(July 1966).

It is shown that to each finite-dimensional single-valued irreducible representation of SL(3,R) there corresponds an infinite-dimensional representation which is unitary on any member of a certain one-parameter family of Hilbert spaces. An eigenfunction problem for the members of a three-parameter family of Hilbert subspaces on which such a unitary representation is irreducible. The relatively simple but especially important three-dimensional case is worked out completely. Unitary irreducible representations for the unimodular real linear groups SL(N, R) with $N > 3$ and their subgroups can be obtained by generalizing the formalism described here. (auth)

39872 CHAKRABARTI TRANSFORMATION. Sesma, J. (Univ. Central de Venezuela, Caracas). J. Math. Phys. (N. Y.), 7: 1300-2(July 1966).

An appropriate hamiltonian formulation for the extension of the Chakrabarti transformation [A. Chakrabarti, J. Math. Phys. 4: 1215 (1963)] to spin-0 and spin-1 particles is presented. The suggested formulation is derived from the Duffin-Kemmer one and was used previously to achieve a generalization of the Foldy-Wouthuysen transformation. (auth)

39873 NOTE ON THE QUANTUM THEORY OF ELECTRICAL CONDUCTIVITY. Tjon, J. A. (Univ. of California, San Diego, La Jolla). J. Math. Phys. (N. Y.), 7: 1335-6(July 1966).

A formal method is given for calculating the electric conductivity tensor in ascending powers of the interaction for a system of electrons interacting with a random distribution of scattering centers. (auth)

39874 REDUCED-AMPLITUDE EQUATIONS FOR TWO- AND THREE-PARTICLE SYSTEMS. [PART] I. Taha, M. O. (Cambridge Univ., Eng.). Nuovo Cimento (10), 44A: 561-71(Aug. 1, 1966).

Reduced-amplitude equations for two- and three-particle systems are stated and their significance discussed. A relativistic generalization of the Faddeev equations for three particle → three particle interactions is obtained as a special case. Equations for final-state interactions in two particle → three particle processes are given. (auth)

39875 RELATIVISTICALLY INVARIANT MODEL OF SU_6 SYMMETRY WHICH INVOLVES INFINITE REPRESENTATIONS OF THE INTERNAL SYMMETRY GROUP. Ruehl, W. (CERN, Geneva). Nuovo Cimento (10), 44A: 572-97(Aug. 1, 1966).

A relativistic SU_6 symmetry model based on the group $SL_{6,C}$ is studied. It uses infinite-dimensional, unitary representations of this group as they are known from the theory of Gel'fand and Neumark. The states for mesons and baryons and compute the integral kernel which allows coupling of meson and baryon representations to an invariant vertex are constructed. There are no troubles with the unitarity of the S-matrix in this model. (auth)

39876 OPERATORS FOR SYMMETRY TRANSFORMATIONS IN CANONICALLY QUANTIZED FIELD THEORIES. Boyer, T. H. (Harvard Univ., Cambridge, Mass.). Nuovo Cimento (10), 44A: 613-26(Aug. 1, 1966).

The construction of symmetry operators in quantum field theory is analyzed from the viewpoint of formal power series in the quantum fields and conjugate momenta. In the first part, the operator generators for a one-parameter continuous group of symmetries are derived in a manner allowing a somewhat wider application than does Noether's theorem. Discrete symmetries, and in particular with the limitations on the applicability of exponential expressions for operators for discrete symmetries are considered. It is emphasized that any symmetry operator expressible as the exponential of a time-independent anti-Hermitian operator which is a finite power series in the fields and conjugate momenta has an immediate natural extension to a continuous symmetry group. The operators proposed by Federbush and Grisaru for some "discrete" symmetries are investigated as to the continuous embedding symmetry groups of which the operators are elements. (auth)

39877 BROKEN RELATIVISTIC SUPERMULTIPLET SYMMETRIES AND THE WEAK CURRENTS. Papastamatiou, N. J.; Taylor, J. C. (Oxford Univ.). Nuovo Cimento (10), 44A: 627-46(Aug. 1, 1966).

Relativistic supermultiplet schemes based upon broken inhomogeneous group (IHG) and broken noncompact group (NCG) symmetries are reviewed. The influence of symmetry breaking on matrix elements, via the spectrum of intermediate states in unitarity, is more violent in NCG than in IHG theories. In the exact-symmetry limit, NCG theories predict zero magnetic moments, while IHG theories say nothing without the additional assumption of vector meson dominance. The space components of axial currents may be successfully connected with generators of NCG symmetries, but for one fact — the known time-component commutators are not then included in the theory. To do this requires a larger group, such as SL_{12}. Disadvantages of this group are overcome if all particles have zero mass in the exact-symmetry limit. The effective classification group is then an SU_6, and the usual SU_{6W} results remain. Although SL_{12} contains the chiral group $SU_3 \times SU_3$, the less satisfactory features of this group are removed by a re-allocation of particle states among its representations. For energies and momentum transfers large compared with the masses, a new group SU_{6C} is expected to hold for coplanar processes. As a consequence, the results of SU_{6W} for forward and backward scattering differential cross sections are predicted to hold for general scattering angles provided that $s, |t|, |u| \gg m^2$. (auth)

39878 MULTILINEAR INVARIANT FORMS BUILT OF AN ARBITRARY NUMBER OF UNITARY REPRESENTATIONS OF $SL_{n,C}$. Ruehl, W. (CERN, Geneva). Nuovo Cimento (10), 44A: 659-70(Aug. 1, 1966).

A method to construct multilinear invariant forms from a given set of unitary irreducible representations of the group $SL_{n,C}$ is studied. A global technique based on the theory of Gel'fand and Neumark is used. (auth)

39879 EQUAL-TIME COMMUTATORS AND PHOTOPRODUCTION SUM RULES. Mukunda, N. (Princeton Univ., N. J.); Radha, T. K. Nuovo Cimento (10), 44A: 726-32(Aug. 1, 1966).

Generalized sum rules derived from equal-time commutators for arbitrary values of momentum transfer square are given for photoproduction amplitudes. In particular, it is shown that, in the decuplet dominant model, the electric quadrupole transition part of the γNN^* vertex has to vanish,

which seems to be true experimentally. However, the sum rule for the anomalous magnetic moments of the nucleons obtained from charged photoproduction amplitudes does not seem to hold in this approximation. Possible reasons for this discrepancy are discussed. (auth)

39880 APPROXIMATE SOLUTION TO THE MULTICHANNEL N/D EQUATIONS. Smith, J. (Univ. of Copenhagen). Nuovo Cimento (10), 44A: 733-9(Aug. 1, 1966).

The approximate solution to the multichannel N/D equations proposed by Pagels is used to predict S-wave bound states in an attractive Yukawa potential. In the first-order Born approximation the results are reasonable, but large deviations occur when the second-order Born approximation is added to the potential. This raises a serious problem of how to take into account higher-order corrections to the potential. (auth)

39881 ALGEBRA OF SCALAR AND VECTOR VERTEX STRENGTHS IN REGGE RESIDUES. Cabibbo, N. (CERN, Geneva); Horwitz, L.; Ne'eman, Y. Phys. Lett., 22: 336-40(Aug. 15, 1966).

An algebra of strong scalar and vector currents coupled to Regge residues accounts for the composite model predictions in high-energy elastic scattering. Some new relations are given; $\sigma(K^+N) = \sigma(K^+P)$ is accounted for in a simple way. (auth)

39882 REMARK ABOUT THE GENERAL METHODS IN CURRENT ALGEBRA. Gourdin, M. (Faculte des Sciences, Orsay, France). Phys. Lett., 22: 340-1(Aug. 15, 1966).

Two methods used in the framework of the algebra of currents to obtain sum rules are compared in a particular case from which the Adler-Weisberger sum rule follows. (B.G.D.)

39883 ADLER-WEISBERGER SUM RULES FOR HIGHER SPIN PARTICLES. Gasiorowicz, S.; Geffen, D. A. (Univ. of Minnesota, Minneapolis). Contract AT(11-1)-3171. Phys. Lett., 22: 344-6(Aug. 15, 1966).

It is pointed out that, for particles of spin J or $J + \frac{1}{2}$ (J an integer), there are $J + 1$ independent Adler-Weisberger sum rules. The case of πp scattering is treated as an example to show that more useful information can be obtained by considering all of them. (auth)

39884 QUANTIZATION OF SPIN-2 FIELDS. Chang, Shau-Jin (Harvard Univ., Cambridge, Mass.). Phys. Rev., 148: 1259-63(Aug. 26, 1966).

A massive spin-2 field was quantized using Schwinger's action principle. Lorentz invariance and physical positive-definiteness requirements were verified. (auth)

39885 $SU(6)_w$-SYMMETRIC MESON BOOTSTRAP MODEL. Capps, Richard H. (Northwestern Univ., Evanston, Ill.). Phys. Rev., 148: 1332-40(Aug. 26, 1966).

A bootstrap model of the pseudoscalar-meson octet and singlet and the vector-meson octet and singlet is constructed. The mesons (M) are assumed to be MM bound states, produced by one-M-exchange forces. The input MMM interaction is assumed $SU(6)_w$-symmetric, and the forces in all P-wave MM states are examined. The forces are most attractive in 36 states of the quantum numbers of the mesons; identification of these states with the M leads to output MMM interactions consistent with those assumed originally. However, the $SU(6)_w$ symmetry requires that the total coupling of the singlet vector meson should be only $\frac{2}{3}$ that of the other mesons. The method of calculation involves continuing the interaction off the mass shell in an $SU(6)_w$-symmetric fashion, and comparing the P-wave amplitudes at threshold in Born approximation. The technique can also be used to predict heavier resonances that do not correspond to SU(6) representations. This fact is encouraging, since it appears that only the lighter observed hadrons form complete representations of SU(6). (auth)

39886 MESON MASS FORMULAS FOR THE 405 MULTIPLET OF SU(6). Resnikoff, M. (Univ. of Maryland, College Park); Silbar, R. R. Contract AFOSR-500-64. Phys. Rev., 148: 1341-4(Aug. 26, 1966).

Mass formulas for mesons in a 405-dimensional representation of SU(6) are derived. A table of the particles and their quantum numbers is given for the $SU(3) \otimes SU(2)_J$ and the $SU(4) \otimes SU(2)_S$ chains, along with the recoupling transformations which relate the chains. The results are in a form which may be applied to the newly discovered positive-parity mesons, in particular, the 2^+ nonet. Under the assumption that the 27-plet of 2^+ mesons is much higher up, a quadratic relation is found for the 2^+ nonet which is satisfied within experimental errors. (auth)

39887 DECOUPLING OF A MULTICHANNEL PROBLEM IN THE STATIC MODEL. Kumar, Arvind (Tata Inst. of Fundamental Research, Bombay). Phys. Rev., 148: 1347-51(Aug. 26, 1966).

A multichannel dynamical calculation for the meson-baryon scattering problem is made in the static model. It is shown that with degenerate isobars, the problem decouples into a set of single-channel problems. This helps the surprisingly exact coincidence of the results of the strong-coupling theory due to Cook, Goebel, and Sakita and to Singh with those of single-channel calculations by Abers, Balázs, and Hara to be understood. Decoupling is also shown to be obtained in the nondegenerate case under some additional restrictions. (auth)

39888 RELATIVISTIC U(6,6) THEORY. Salam, Abdus; Strathdee, J. (International Centre for Theoretical Physics, Trieste, Italy). Phys. Rev., 148: 1352-8(Aug. 26, 1966).

Infinite-dimensional unitary representations of the non-compact group U(6,6) are employed to classify elementary particles and, following ideas related to those of Fronsdal, are used to construct relativistic S-matrix elements. Like the previously treated relativistic theories where finite-dimensional representations of U(6,6) were used, a particular S-matrix element shows no symmetry higher than that of the appropriate hybrid subgroup. The over-all U(6,6) symmetry may give new relations between form factors for different processes but will not, in general, give anything beyond the results of the previous formulations for the scattering processes. The unitarity of the S matrix is compatible with the subgroup hierarchy, provided that an infinity of multiplets for elementary particles exists and provided that all such multiplets possess the same mass. The crucial point of our formulation is that if mass differences are introduced, these affect not the relativistic invariance but the unitarity of the S matrix. (auth)

39889 COMPOSITE PARTICLES IN SEPARABLE-POTENTIAL MODELS. Childress, J. D.; Urrechaga-Altuna, J. (Louisiana State Univ., Baton Rouge). Phys. Rev., 148: 1359-75(Aug. 26, 1966).

Composite particles (bound states) are investigated in three separable potential models—(1) a model with one kind of static heavy neutral scalar boson interacting with one kind of light neutral scalar boson, (2) a model with one kind of static heavy boson and two (or any number of) kinds of light bosons, (3) a model with two (or any number of) kinds of static heavy bosons and one kind of light boson. These models are solved exactly, the last one only in the case of equal interaction form factors. The S-matrix elements are calculated both directly and dispersion-theoretically. The allowed physical processes are found to be elastic scatterings only; composite particles can exist but can neither be created, nor destroyed, nor altered in any way within the framework of the models studied. The S-matrix elements are shown to be independent of whether the scattering target is a number of heavy bosons or any composite particle which could be formed by the same number (and kinds) of heavy bosons. The composite particle states are identified as those eigenstates of the hamiltonian for which the total number of heavy bosons is nonzero, the number of free heavy bosons is zero, and the total number of light bosons is greater than the number of free light bosons. The energy of such a state is less than the rest energy of its components, i.e., the state is a bound state. Particle operators for the composite particles are constructed but are observed to lack

satisfactory Lehmann-Symanzik-Zimmermann asymptotic limits. (auth)

39890 PECULIARITIES OF A FREE MASSLESS SPIN-3/2 FIELD THEORY. Bender, Carl M.; McCoy, Barry M. (Harvard Univ., Cambridge, Mass.). Phys. Rev., 148: 1375-80(Aug. 26, 1966).

The properties of a massless spin-3/2 system are investigated. It is found that the energy density does not commute with itself at spacelike separation, does not transform as a tensor, and is not gauge-invariant, although the theory is shown to be relativistically invariant. (auth)

39891 SPACE INVERSION, TIME REVERSAL, AND OTHER DISCRETE SYMMETRIES IN LOCAL FIELD THEORIES. Lee, T. D.; Wick, G. C. (Columbia Univ., New York). Contract AT(30-1)-1932. Phys. Rev., 148: 1385-1404(Aug. 26, 1966). (NYO-1932-108).

The general algebraic relations between space inversion, time reversal, and the internal symmetry group are analyzed within the framework of a Lorentz-invariant local field theory. The problem of unitary representations of the full Poincaré group including the space and time reflection operators has been studied by Wigner, and the representations are classified into 4 cases. It is shown that, with the added assumption of the local field theory, Wigner's cases 2, 3, and 4 either do not occur or can be reduced to his case 1. The concept of minimal group extension is introduced and the related mathematical analysis is given. The symmetry properties under space inversion, time reversal, and other discrete operators such as charge conjugation are analyzed separately for each of the three known interactions: strong, electromagnetic, and weak. (auth)

39892 CURRENT ALGEBRAS AND MATRIX ELEMENTS OF THE AXIAL-VECTOR CURRENT. Lipkin, H. J. (Weizmann Inst. of Science, Rehovoth, Israel); Rubinstein, H. R.; Meshkov, S. Contract NA-onr-7-66. Phys. Rev., 148: 1405-7(Aug. 26, 1966).

The matrix elements of the axial-vector current are calculated directly from the algebra of chiral U(3) × U(3) and from its chiral isospin U(2) × U(2) subgroup without writing down sum rules. G_A is evaluated for the $SU(6)_w$ 56, 70, and 20 representations for various values of L and W. (auth)

39893 NONLEPTONIC DECAYS OF HYPERONS IN BROKEN SU(3) X SU(3). Schechter, J. (Univ. of Chicago); Ueda, Y. Contract AT(11-1)-264. Phys. Rev., 148: 1424-7(Aug. 26, 1966). (COO-264-304; EFINS-66-12).

The hyperon nonleptonic decays are discussed in the broken chiral SU(3) × SU(3) symmetry scheme. A new sum involving both the S- and P-wave amplitudes is obtained, which is in rough agreement with experiment. Also by using this group, together with the generalized Sugawara-Suzuki method, octet dominance is proved for these decays. (auth)

39894 ASYMPTOTIC BEHAVIOR OF THE INELASTICITY PARAMETER. Kreps, R. E.; Nath, P. (Univ. of Pittsburgh). Phys. Rev., 148: 1436-9(Aug. 26, 1966).

The asymptotic behavior of the inelasticity parameter η is examined under the assumption that an infinite number of 2-particle channels open up as energy becomes infinite. Three specific models are investigated in detail, which can be handled analytically, and it is found that in general $\eta(\infty) = 1$ in these models. It is speculated that this may in fact be the general asymptotic behavior of η in the physical situations. It is also observed that a purely imaginary elastic-scattering amplitude can be realized even as $\eta \to 1$. (auth)

39895 FURTHER CONSEQUENCES OF SUGAWARA'S THEORY OF HYPERON NONLEPTONIC DECAYS. Babu, P. (Tata Inst. of Fundamental Research, Bombay). Phys. Rev., 148: 1440-3(Aug. 26, 1966).

The application by Sugawara of the chiral SU(3)⊗SU(3) of Gell-Mann for nonleptonic decays is discussed. It is shown that one can give a simple group-theoretic interpretation for this theory. It is also shown that his theory predicts the vanishing of parity-conserving decay amplitudes. This difficulty is eliminated by including an octet-type violation of SU(3). Further, in this procedure it is possible to treat the parity-conserving and parity-violating isospin amplitudes together. These isospin considerations suggest that the theory can be recast within the framework of chiral SU(2)⊗SU(2). The transformation properties of the Hamiltonian consistent with the isospin relations are obtained. (auth)

39896 APPLICATIONS OF THE CHIRAL U(6)⊗U(6) ALGEBRA OF CURRENT DENSITIES. Bjorken, J. D. (Stanford Linear Accelerator Center, Calif.). Phys. Rev., 148: 1467-78(Aug. 26, 1966). (SLAC-PUB-165).

Consequences of the local commutation relations of vector and axial currents proposed by Gell-Mann are explored: (1) A recipe for detecting and isolating Schwinger terms in the commutators, proportional to derivatives of the δ function, is discussed. (2) Under assumptions of smooth asymptotic behavior of form factors for forward scattering of the isovector current from a proton, it is shown that the U(3)⊗U(3) algebra for the time components of the currents implies the U(6)⊗U(6) algebra for space components, at least for spin-averaged diagonal single-particle states. (3) The derivation of the Adler-Weisberger formula for G_A/G_V is sharpened by giving arguments that, at fixed energy, the forward π-p Green's function satisfies an unsubtracted dispersion relation in the pion mass. (4) A lower bound for inelastic electron-nucleon scattering at high momentum transfer is derived on the basis of U(6)⊗U(6). (5) The contribution of very virtual photons to the hyperfine anomaly in hydrogen is shown to be related to an equal-time commutator of currents; this contribution is crudely estimated to be <4 parts per million (ppm). (6) The logarithmically divergent part of electromagnetic mass differences of hadrons is shown to be proportional to matrix elements of the equal-time commutator of the electromagnetic current with its time derivative. It is suggested that this "divergent" part be identified with the Coleman-Glashow "tadpoles"; this suggestion is discussed in the framework of a simple quark model. (7) The logarithmically divergent part of the electromagnetic correction to the process $\pi^- \to \pi^0 + e^- + \bar{\nu}$ is, on the basis of the U(6)⊗U(6) current algebra, shown to be nonvanishing, and is computed. (8) A speculative argument is presented that the rate $e^+ + e^- \to$ hadrons is comparable to the rate $e^+ + e^- \to \mu^+ + \mu^-$ in the limit of large energies. (auth)

39897 n-BODY SCATTERING AMPLITUDE: SEPARATION OF TOTAL ANGULAR MOMENTUM. Pestieau, J. (Univ., Louvain, Belg.). Phys. Rev., 148: 1483-90 (Aug. 26, 1966).

A complete set of states of the n-particle system is constructed in which the total angular momentum is diagonal. The angular part in the Faddeev-Weyers equation is separated. Two cases are dealt with in greater detail: the scattering of n-free particles, and the transition from a state of $(n-1)$ bound particles and one free to another state of the same structure. In the latter case the helicity of the initial-(final) bound state is explicitly displayed. (auth)

39898 CURRENT ALGEBRAS AND FORM FACTORS. Oehme, Reinhard (Univ. of Chicago). Contract AT(11-1)-264. Phys. Rev., 148: 1537-8(Aug. 26, 1966). (COO-264-306; EFINS-66-16).

The collinear U(3)⊗U(3) subalgebra of the chiral U(6)⊗U(6) algebra is considered. Assuming that the densities transform like the generators, the commutation relations are saturated by using the octet and the decuplet of baryons. The matrix elements of the commutators are taken with respect to states of opposite momentum parallel to the direction specified by the algebra. The resulting equations give rise to relations between vector and axial-vector form factors for all values of the momentum transfer. A discussion is given of the connection of these results with similar relations obtained from the spurion scheme of broken U(6,6) symmetry. (auth)

39899 PHASE OF THE SCATTERING AMPLITUDE FOR CHARGED BOSONS. Rolnick, William B. (Case Inst. of Tech., Cleveland). Phys. Rev., 148: 1539-41 (Aug. 26, 1966).

A calculation, to order α, of the phase of the scattering amplitude for charged bosons is shown to involve the double spectral function for the box graph. At small angles the result agrees with a (Bakamjian-Thomas) equivalent-potential calculation and reduces to the potential-scattering-theory result in the nonrelativistic limit; the infrared-divergent part agrees with that obtained for a Yukawa potential, as the shielding radius approaches infinity. (auth)

39900 EXISTENCE OF SPURIOUS SOLUTIONS TO MANY-BODY BETHE-SALPETER EQUATIONS. Federbush, Paul G. (Massachusetts Inst. of Tech., Cambridge). Contract AT(30-1)-2098. Phys. Rev., 148: 1551-2 (Aug. 26, 1966). (MIT-2098-235).

The many-body equations studied by Weinberg are applied to a particular system of three particles interacting with separable potentials. For certain values of the energy, it is found that the homogeneous equation has extraneous nonzero solutions. (auth)

39901 DISCUSSION OF A NOTE BY FEDERBUSH ON SPURIOUS SOLUTIONS OF THREE-PARTICLE EQUATIONS. Noble, Julian V. (Princeton Univ., N. J.). Contract AT(30-1)-937. Phys. Rev., 148: 1553-5(Aug. 26, 1966). (PUC-937-208).

Federbush's recent construction of spurious homogeneous solutions of Weinberg's connected three-particle scattering equation (in a special model) is extended and generalized. The extended result is that for the special case $m_3 = \infty$, $V_{12} = 0$, and V_{13} and V_{23} of unit rank, every complex energy W [with $\mathrm{Im}(\sqrt{W}) \neq 0$] is an eigenvalue of the homogeneous equation, and the corresponding eigenfunctions are square integrable. The Faddeev equations corresponding to this case are examined and found not to have this deficiency. It is believed that these spurious solutions of Weinberg's equation occur only in the special case noted above, and that the Weinberg equation is usable except in this case. (auth)

39902 INTERNAL SYMMETRIES IN A COUPLED-CHANNEL SOLUBLE MODEL WITH INELASTICITY. Cushing, James T. (Argonne National Lab., Ill.). Phys. Rev., 148: 1558-73(Aug. 26, 1966).

The conjecture that an internal symmetry group may be selected by a bootstrap mechanism is studied within the framework of a closed, exactly soluble model. In order to have two-body unitarity and crossing without necessarily identically zero amplitudes, two types of particles of different mass (each possessing internal quantum numbers corresponding to an unspecified internal symmetry group and each assigned to irreducible representations of this group) are allowed to scatter in a two-dimensional world. The symmetry group makes its appearance explicitly only through the crossing matrix, characterized by a parameter which is to be determined self-consistently. All two-body channels, both elastic and inelastic, are treated exactly. Unitary, crossing-symmetric, analytic scattering amplitudes corresponding to the various processes are constructed for continuous ranges of the parameter of the crossing matrix. Even with the additional constraint of a self-consistency requirement in the form of Levinson's theorem, an internal symmetry group is not selected by the bootstrap mechanism in this model. Also, a technique is developed for converting a coupled set of singular, linear Cauchy integral equations into an equivalent uncoupled Fredholm set. (auth)

39903 REPRESENTATION OF LOCAL CURRENT ALGEBRA AT INFINITE MOMENTUM. Dashen, Roger; Gell-Mann, Murray (California Inst. of Tech., Pasadena). Phys. Rev. Lett., 17: 340-3(Aug. 8, 1966). (CALT-68-72).

It is suggested that the algebra of SU(3) × SU(3) generated by the charge density operators be used to classify an infinite number of stable and resonant particle states according to approximate representation of commutation rules and prediction for complete form factors. (B.G.D.)

39904 THE SU(6) SYMMETRY AND CORRELATIONS BETWEEN THE CROSS SECTIONS OF MESON-BARYON PROCESSES AT LOW ENERGIES. Laperashvili, L. V. (Inst. of Physics, Academy of Sciences, Georgian SSR). Soobshch. Akad. Nauk Gruz. SSR, 42: 551-3(June 1966). (In Russian).

When using the nonrelativistic theory of the SU(6) symmetry for calculating the correlations between the cross sections of the meson–baryon processes, the results obtained by V. Barger and M. H. Rubin were found to be applicable only for the S-wave processes near the reaction threshold. This study was extended toward low energies, at which the symmetry is known to be disturbed, in an attempt to establish new correlations between the cross sections of the following types of processes: M(1) + B(2) = M(3) + B(4), whereby M and B represent mesons and baryons of the 35 and 56 SU(6) group concept. The correlation derived was expressed as $\tilde{\sigma} = Ep_{in}/p_{out}\,\sigma(Q)$, whereby $\sigma(Q)$ is the total cross section of the process, considered as a function of energy; E is the total energy in the center of mass system, while p_{in} and p_{out} represent the momentum of the initial and final particles in the center-of-mass system. (TTT)

39905 ANALYTICAL PROPERTIES AND ASYMPTOTIC BEHAVIOR OF MULTICHANNEL, QUASI-POTENTIAL SCATTERING AMPLITUDE. Khelashvili, A. A. (Tbilisi State Univ., Georgian SSR). Soobshch. Akad. Nauk Gruz. SSR, 42: 555-62(June 1966). (In Russian).

Logunov's quasi-potential approach to the problem of elementary particle scattering and of the bound-state spectrum of two homologous particle makes use of Schroedinger's quantum field theory equation for the two-particle system. The potentials are a complex function of the variables, representing the three-dimensional momentum of particles in the center-of-mass system. The analytical properties of the partial amplitudes of such potentials were examined, making use of Legendre polynomials. As a result of the study, an asymptotic correlation between the differential and total cross sections of the various channels was derived. (TTT)

39906 COMMUTATORS OF THE COVARIANT BILINEAR FORMS OF THE QUANTIFIED SPINORIAL FIELD. Hristev, P. Anatolie. Stud. Cercet. Mat., 17: 95-104 (1965). (In Rumanian).

The Dirac tensors are defined as bilinear forms of spinors. Since in the second quantization the spinors are changed into noncommutative operators that are particle-generators and annihilators, the Dirac tensors defined as natural products become noncommutative operators whose commutators play a major role in the quantum theory of electrons and photons. These commutators are calculated in the E_6 space. The work consists of five chapters. Chapter one deals with the problem of unifying the matrices and Dirac tensors; chapter two considers the spinor anticommutators. Chapter three gives the definition of the tensors $\varphi(+/ab)$ as normal product as well as a number of properties of Dirac tensors in "the q theory". In chapter four, the general expressions of commutators are obtained according to the considered rule of commutation. Chapter five gives the fundamental result of the work. The charge density $\rho = \varphi^{+}_{64}$ is commutable to all Dirac tensors, i.e., $[\rho, \varphi(+/ab)] = 0$, $[\rho, j^{\pm}_{0}] = 0$. (Rum. Sci. Abstr.)

39907 ASSIGNMENTS OF THE BARYON RESONANCES IN $\tilde{SU}(12)$ AND THEIR STRONG DECAYS. Ma, Chung-chi; Liu, Lian-sou; Chen, Ji (Peking Univ.). Wu Li Hsueh Pao, 22: 589-600(May 1966). (In Chinese).

The assignments of resonances $^3/_2^-$, $^1/_2^-$ and $^1/_2^+$ within the multiplets of $\tilde{SU}(12)$ and their strong decays are discussed. It is found that the $(^1/_2^+ + 0^-)$ decay modes of the $^3/_2^-$ particles belonging to the multiplets 16016 and 35100 are forbidden. By redefining the parity of the representations by changing the sign of the mass terms in the wave equations,

it is possible to assign the particles ($\frac{3}{2}^-$, 8) and ($\frac{1}{2}^-$, 1) in the representation 572. However, the decays of ($\frac{3}{2}^-$, 1) and $\frac{7}{2}^+$ particles through an effective vertex with SU(12) symmetry are still forbidden. The success and failure of SU(12) in the problem of classification and strong-decays of elementary particles are analyzed and discussed in detail. (auth)

39908 WEAK INTERACTIONS IN THE SU(6) SYMMETRY THEORY. Song, Xing-chang (Peking Univ.). Wu Li Hsueh Pao, 22: 601-6(May 1966). (In Chinese).

An intermediate boson scheme of weak interactions is proposed within the framework of the SU(6) symmetry theory. Under the assumptions that: the intermediate bosons belong to the IR (irreducible representation) 21; the weak currents belong to the adjoint representation IR 35; and (3) the s- and p-wave semiweak interactions are assigned to the (3*,1) part of the IR 21 and the (3*,3) part of the IR 15 respectively. An effective nonleptonic interaction is obtained which gives three sum rules for the s-wave (parity-violating) and one for the p-wave (parity-conserving) decay amplitudes of the hyperons. These relations seem to be well-satisfied by the experimental data. (auth)

39909 POLARIZATION TENSOR IN THE SCATTERING OF POLARIZED NUCLEONS ON A POLARIZED PROTON TARGET. Bilenkaya, S. I.; Winternitz, P.; Legar, F.; Yanout, Z. (Joint Inst. for Nuclear Research, Dubna, USSR). Yadern. Fiz., 4: 132-8(July 1966). (In Russian).

The components of the polarization tensor in the scattering of polarized nucleons on polarized nucleons are discussed and calculated using phase-shift analysis data for various energies in the region 23.1 to 630 Mev. (auth)

39910 MASS FORMULAE FOR PARTICLES WITH SPIN 1 AND 3/2 IN BROKEN SU(3) SYMMETRY. Vainshtein, A. I. Yadern. Fiz., 4: 188-91(July 1966). (In Russian).

A covariant approach, using equal-time commutation relations and dispersion relations is applied to show that mass formulas in the broken SU(3)-symmetry hold for squared masses, in the case of vector particles, and are linear in the masses for particles with spin $\frac{3}{2}$. (auth)

39911 ANALYTICAL PROPERTIES OF THE RELATIVISTIC MULTICHANNEL SCATTERING AMPLITUDE. Kolomiets, V. M.; Tsekhmistrenko, Yu. V. (Inst. of Physics, Academy of Sciences, Ukrainian SSR). Yadern. Fiz., 4: 192-7(July 1966). (In Russian).

The analytical properties of the amplitude for the nonrelativistic inelastic scattering of spinless particles on the physical energy plane are determined in the case of an infinite number of channels, using Fredholm techniques. (auth)

39912 QUANTUM FIELD THEORY WITH INDEFINITE METRIC IN HILBERT SPACE. Galanin, A. D. (Inst. of Theoretical and Experimental Physics, State Atomic Energy Commission, USSR). Yadern. Fiz., 4: 205-15(July 1966). (In Russian).

A system of equations in functional derivatives is constructed for the four-fermion interaction under the condition that the anticommutator in the cone vertex is a C-number, but without specifying its dependence on the coordinates. It is shown, with the help of a formal solution of these equations in the form of a continuous integral, that the cancellation of the δ function in the commutation relations, which is possible for an indefinite metric, must not imply the cancellation of all singularities of the anticommutator in the cone vertex, since this would become zero identically in the whole space. The generalization of the usual interpretation of a continuous integral from a mechanical system to a field implies restrictions on the commutation relations, and specifically forbids canonical quantization for the four-fermion interaction. A new generalized function, determined by integration rules with functions, which are singular solutions of the classical field equations, must be introduced to describe the anticommutator singularities at the cone vertex. The suggested scheme is not a Hamiltonian one, since it is not possible to construct a complete system of commuting operators on a space-like surface. (auth)

39913 ON A THEORY OF THE CLEBSCH-GORDAN COEFFICIENTS FOR THE SU_n GROUPS. Shelepin, L. A. (Lebedev Inst. of Physics, Moscow). Zh. Eksp. Teor. Fiz., 50: 1666-73(June 1966). (In Russian).

A theory of the Clebsch–Gordan coefficients for SU_n groups is developed, which is based on a generating invariant technique proposed. It is demonstrated that the coefficients of the Clebsch–Gordan coefficients of the SU_n groups and the corresponding Racah coefficients and also other transformation matrices reduce to a set of $n \times n$ symbols introduced previously. Expressions are presented for Wigner coefficient of the SU_3, SU_4 groups and the Racah coefficient of the SU_3 group. The method proposed also simplifies the SU_2 group Clebsch–Gordan coefficients. (auth)

39914 RELATIVISTIC THREE PARTICLE EQUATIONS. I. Taylor, John G. (Rutgers-The State Univ. of New Jersey, New Brunswick). 31p. (CONF-660107-61). ORAU. Gmelin, AED-CONF-66-003-141.

From American Physical Society 1966 Annual Meeting, New York.

Linear integral equations are given for three-particle scattering amplitudes in any Lorentz invariant local field theory; they are three particle analogs of the Bethe-Salpeter equation. The kernels of these equations are off-mass-shell relativistic generalizations of two- and three-particle potentials. The equations are transformed by the method of Faddeev so that the two-particle potential no longer appears, but only the two-particle scattering amplitude. Particular cases of these equations are presented. It is shown that two and three particle unitarity is satisfied provided the relativistic potentials are real in the relevant energy region. (auth)

39915 THE TWO USES OF NON-COMPACT GROUPS IN PARTICLE PHYSICS AND THEIR RELATIONS. Barut, A. O. (Univ. of Colorado, Boulder). 19p. (CONF-660540-4). ORAU. Gmelin, AED-CONF-66-113-5.

From Conference on Non-Compact Groups in Particle Physics, Milwaukee.

A series of hypotheses are formulated in a systematic discussion of the structure and the dynamical group of strongly interacting particles. The consequences of these hypotheses, the mass formula, the transformation property of the S-matrix and the minimal extensions of the dynamical group are deduced and compared with experiment. (auth)

39916 TENSOR OPERATORS AND MASS FORMULA IN THE MINIMAL EXTENSION OF U_3 BY CHARGE CONJUGATION. Barut, A. O.; Kleinert, H. (Univ. of Colorado, Boulder). 5p. (CONF-660540-5). ORAU. Gmelin, AED-CONF-66-113-4.

From Conference on Non-Compact Groups in Particle Physics, Milwaukee.

The transformation property of the mass (or mass square) M is specified in the extended group and the most general mass formula $M = M_0 + a(\alpha)\,[I(I+1) - Y^2/4 - K(\alpha)] + b_1(\alpha)NY + b_2(\alpha)Q_2Y$ is derived where $a(\alpha)$, $b_1(\alpha)$, $K(\alpha)$ are constants depending on a charge-even set α, and Q_2 is the second invariant operator of SU_3. (auth)

39917 PROBLEMY TEORII ELEMENTARNYKH CHASTITS. (Lectures on Problems in the Elementary Particle Theory). Chernov, A. G. (ed.). Novoye v Zhizni, Nauke, Tekhnike. Ser. 9, Fizika, Matematika, Astronomiya, 1964, No. 20. Besedy po Aktual'nym Problemam Nauki, No. 4. Moscow, Izdatel'stvo Znanie, 1964. 25p.

Separate abstracts were prepared for the 5 lectures presented. (B.G.D.)

For abstracts of individual papers see: 39918–39922.

39918 WHAT IS AN ELEMENTARY PARTICLE? Kuznetsov, B. G. pp 3-6 of Problemy Teorii Elementarnykh Chastits. Moscow, Izdatel'stvo Znanie, 1964. (In Russian).

Current theories of elementary particles are critically analyzed. It is found that the concept is far from being precise; it is not easy to differentiate nonelementary particles on the basis of the definitions used. The chief criteria used, charge and spin, are not fundamental but arbitrary. Heisenberg rejected the criterion of stability: the unstable deuteron is not considered an elementary particle but the equally unstable neutron is. The transmutational criteron of elementary character is applied for the very short time periods and distances, of the order of 10^{-24} sec and 10^{-13} cm, respectively; thus, particles moving for longer distances and existing for longer periods of time may be considered as a time aggregate of elementary particles with minimum lifetimes. (TTT)

39919 INTERACTIONS OF ELEMENTARY PARTICLES. Pomeranchuk, I. Ya. pp 6-11 of Problemy Teorii Elementarnykh Chastits. Moscow, Izdatel'stvo Znanie, 1964. (In Russian).

Elementary-particle interactions are divided into three groups: weak, electromagnetic, and strong. As an example, the passage of a fast-electron beam through matter at a velocity close to the speed of light is examined. Collision with nuclei results in elastic scattering or in the emission of soft electromagnetic radiation in the visible range or of hard, x-ray type quanta. Emission of two quanta per collision is 100 to 150 times less probable than elastic scattering. Weak interactions occur in processes involving decay of elementary particles. In such cases, parity is not conserved; all charges are identical, although the existence of fractional $\frac{1}{3}$ or $\frac{2}{3}$ type charges has been advanced. The strong interactions, involving protons and neutrons, correspond to nuclear energy. Collision of fast protons possessing a velocity close to the speed of light results in the emission of other particles, corresponding to quanta, such as mesons. The perturbation theory cannot be applied in this case. The causality principle and conservation of probability play an important part in the theory which should be more closely related to the theory of relativity. (TTT)

39920 PARTICLES, PREDICTED BY THEORY. Smorodinskii, Ya. A. pp 11-16 of Problemy Teorii Elementarnykh Chastits. Moscow, Izdatel'stvo Znanie, 1964. (In Russian).

Prediction of the existence of many elementary particles on the basis of the laws of physics; conservation of charge, mass, energy, pulse, spin, strangeness, and laws of symmetry, is discussed. (B.G.D.)

39921 CONSERVATION LAW IN ELEMENTARY PARTICLE PHYSICS. Shapiro, I. S. pp 16-19 of Problemy Teorii Elementarnykh Chastits. Moscow, Izdatel'stvo Znanie, 1964. (In Russian).

Elementary particles are classified as resonance-type particles, with lifetimes of few tens or hundreds of times longer than the time of interaction, and about 35 long-lived particles with lifetimes ranging from 10^{-16} sec to 17 minutes, including also the stable particles: photon, proton, antiproton, electron, positron, 2 neutrinos, and the corresponding antineutrinos. The macroscopic laws of conservation of energy, moment of rotation, and charge are valid for elementary particles. Many decay and other processes do not take place because they are forbidden by the conservation laws. Other, permissible processes, such as the decay of proton into positron and photon and of muon into electron and photon, are forbidden for other reasons. These additional laws include the conservation of baryon charge and of strangeness. Knowledge of these laws contribute greatly to the understanding of the elementary particle processes. (B.G.D.)

39922 FUNDAMENTAL PROBLEMS IN CONTEMPORARY PHYSICS THEORY. Tamm, I. E. pp 19-24 of Problemy Teorii Elementarnykh Chastits. Moscow, Izdatel'stvo Znanie, 1964. (In Russian).

A discussion is presented on the capabilities of quantum theory in contemporary theoretical physics. Newtonian mechanics and its use in classical physics are described. It is shown that the understanding of phenomena occurring in the very small space-time scale requires radically new physical concepts. It is suggested that the principle of indeterminacy, which limits our knowledge of the universe, may become the initiating point of this new theory. Determination of all the coordinates which define the position of a particle is also shown to be a matter of increasing importance. (B.G.D.)

39923 SOME APPROXIMATION METHODS FOR REGGE PARAMETERS IN POTENTIAL SCATTERING. Pearson, Charles James. Riverside, Calif., Univ. of California, 1965. 150p.

Thesis.

The S-matrix formalism in potential scattering is presented along with a discussion of Regge trajectories and their behavior in the case of Yukawa-like, exponential, and square-well potentials. The determinantal method of determining these trajectories is discussed and tested numerically in the case of the square-well potential. It is found that the first-order determinantal approximation gives qualitatively good results, in general, but the second-order in this approximation is less good, qualitatively, introducing undesirable branch points and unphysical bound states in the upper-half k-plane. A second approximation method is formulated in which the trajectories are obtained directly as the solutions of (in general a set of coupled) nonlinear singular integral equations derived from dispersion relations and using any one of three representations of the scattering amplitude in terms of Regge poles and the unitarity condition applied at $l = \alpha(s)$. The three representations discussed are those of Regge, of Khuri, and a modified Khuri representation given by Ahmadzadeh and by Kaus, Frautschi, and Zachariasen. Numerical tests of these approximation methods are made and discussed in the case of the simple Yukawa potential. The results, shown here and elsewhere, have the desirable property that as more physics is included through the representations listed above the approximation improves. Only the one-trajectory approximation is tested with all three representations. The two-trajectory approximation is tried in the Regge case only. (Dissertation Abstr.)

39924 DYNAMICAL CALCULATION OF THE REGGE-POLE PARAMETERS. Hankins, Denis. Riverside, Calif., Univ. of California, 1965. 89p.

Thesis.

A method for the self-consistent determination of the Regge pole parameters is formulated on the basis of analyticity, unitarity, and crossing symmetry postulates. In this approach, the parameters can be obtained without recourse to cutoff parameters prevalent in previous bootstrap calculations. The method, based on the use of dispersion relations for the Regge trajectories, is tested in the light of potential theory. Approximations are made when coupling the residue functions β to the pole-positions α through the unitarity condition applied at $l = \alpha$ and retaining only the first few pole terms. When the generalized potential is replaced by a nonrelativistic potential, the coupling equations can be compared to exact results. Various representations for the scattering amplitude are tested numerically and it is found that the "modified Khuri" representation for A(l,s) gives good results for $\alpha_1(s)$ in the one-trajectory approximation for Yukawa potentials strong enough to cause bound S-states. The results for $\beta_1(s)$ are less satisfactory The effect of coupling in the second trajectory is considered. (Dissertation Abstr.)

39925 VACUUM REGGE TRAJECTORY IN CONVENTIONAL FIELD THEORY. Dolen, Richard. Pasadena, Calif., California Inst. of Tech., 1966. 124p.

Thesis.

The effect of the scattering amplitude of the existence of a pole in the angular momentum plane near $J = 1$ in the channel with the quantum numbers of the vacuum is calculated. This is then compared with a fourth order calculation of the scattering of neutral vector mesons from a fermion pair field in the limit of large momentum transfer. The presence of the third double spectral function in the perturbation amplitude complicates the identification of pole

trajectory parameters, and the limitations of previous methods of treating this are discussed. A gauge invariant scheme for extracting the contribution of the vacuum trajectory is presented, which gives agreement with unitarity predictions, but further calculations must be done to determine the position and slope of the trajectory at s = 0. The residual portion of the amplitude is compared with the Gribov singularity. (Dissertation Abstr.)

39926 MANY-PARTICLE PROCESSES. Silverstein, Martin Louis. Princeton, N. J., Princeton Univ., 1965. 139p.

Thesis.

In the class of processes considered a single original particle moves according to a single-particle Markov process until a random terminal time when it is destroyed and replaced by n new particles, $0 \leq n \leq \infty$, its direct descendants. The number of direct descendants and their initial positions are random variables that depend on the terminal position of the original particle. Each direct descendant moves according to the same single-particle Markov process until its terminal time when it too is destroyed and replaced by second generation particles. The process continues in this manner. Conditioned on their initial positions, the direct descendants of a particle are independent of one another and of that particle. The trajectories of the single-particle Markov process are assumed to be right continuous and to have left-hand limits everywhere in a fixed, second countable, locally compact metric space K (the single particle phase space). The central result is the fundamental existence theorem. It is proved that a single-particle Markov process together with a family of creation probabilities determines a unique many-particle process such that the trajectories of individual particles are governed by the single-particle Markov process, and the conditional distribution for initial positions of direct descendants are governed by the creation probabilities. (TSS)

39927 I. POTENTIAL CALCULATIONS WITH THE N/D METHOD. II. A BOOTSTRAP OF THE RHO RESONANCE. Fung, Yun-Tong. Berkeley, Calif., Univ. of California, 1965. 82p.

Thesis.

In Part I, the determinantal and N/D methods are applied to non-relativistic scattering by a single Yukawa potential. S, p, and d wave phase shifts are calculated using the first order determinantal and the first and second order N/D approximations. The minimum potential strength required for a bound state is calculated using the first and second order approximations of both methods. The results are then compared with those obtained by numerically integrating the Schroedinger equation. It is found that for small couplings, both methods, in the first approximation, work well. Results with the second approximation show that the second determinantal approximation did not improve over the first. On the other hand, the second N/D approximation shows marked improvement over the first approximation. Part II consists of an attempt to bootstrap the rho trajectory using the mass shell approximation proposed by Jacobson. A Reggeized potential depending on three bootstrap parameters is used. Three self-consistent requirements, equality of input and output masses and widths and equality of the threshold values of the input and output trajectories are used to determine these parameters. Solutions that satisfy the mass and threshold bootstraps are found. The width bootstrap cannot be satisfied because the slope of the real part of the output trajectory is extremely small and cannot be computed with any accuracy. A sample output trajectory is computed. The difference between a "narrow width" potential (with a delta function) and a Breit-Wigner potential for a resonance is then investigated. It is found that in the mass shell approximation these potentials give entirely different results. (Dissertation Abstr.)

39928 BARYON ELECTROMAGNETIC MASS DIFFERENCES. Gilman, Frederick Joseph. Princeton, N. J., Princeton Univ., 1965. 146p.

Thesis.

The relation of the "S-matrix perturbation theory" of Dashen and Frautschi (Phys. Rev. 135: B1190(1964)) to other perturbation theories and perturbation calculations is explored. A simple D-matrix perturbation theory is developed and shown in potential theory to lead to expressions for the first and second order change in the energy of a bound state, which are equivalent to the usual quantum mechanical perturbation theory results. On writing an unsubtracted dispersion relation, this D-matrix perturbation theory is also shown to reproduce the expression of Dashen and Frautschi for the first order shift in energy of a bound state. After a review of the relativistic multichannel formulation of the method of Dashen and Frautschi for calculating mass shifts, the relation between calculations of the bubble diagram for the baryon electromagnetic self-energy and the method of Dashen and Frautschi for calculating the baryon electromagnetic mass shift is studied. Electromagnetic mass differences of particles in the baryon octet and decuplet are calculated. The Σ and Y_1^* are considered as $\pi\Lambda$ and $\pi\Sigma$ bound states forming a reciprocal bootstrap subsystem split off from the rest of the octet and decuplet by the breaking of SU(3) symmetry. It is shown that the self consistent terms arising from the reciprocal bootstrap of the Σ and Y_1^* lead to an enhancement by a factor of 3 or more of the Σ and Y_1^* electromagnetic mass differences transforming as $\Delta I = 1$ over those transforming as $\Delta I = 2$, in agreement with experiment. An evaluation of contributions from low mass intermediate states to the dispersion relation for the Σ and Y_1^* mass differences is then attempted. A still incomplete calculation gives $M^{\Sigma^+} - M^{\Sigma^-} \approx -10$ Mev, $M^{Y^+} - M^{Y^-} \approx -6$ Mev, $|M^{\Sigma^+} + M^{\Sigma^-} - 2M^{\Sigma^0}|$ and $|M^{Y^+} + M^{Y^-} - 2M^{Y^0}|$ 1 to 3 Mev. A similar calculation is then attempted for the Ξ and Ξ^* which are considered as $\pi\Xi$, $\bar{K}\Lambda$, and $\bar{K}\Sigma$ bound states (resonances). Here, however, it is found that there is no enhancement of the mass differences from a Ξ-Ξ^* reciprocal bootstrap. In an analysis of the contributions to the dispersion relation for the mass differences it is found that the change in external Σ masses gives a contribution of the right sign and magnitude to explain the observed Ξ^0-Ξ^- mass difference of -6.5 ± 1.0 Mev. (Dissertation Abstr.)

Fluid Physics and Thermodynamics

See also Plasma Physics and Thermonuclear Processes

Refer also to abstracts 39704, 39727, 39737, 40216, 40237, 40238, 40239, 40241, and 40403.

39929 FREE CONVECTION FLOW OF AN ELECTRICALLY CONDUCTING FLUID PAST A POROUS FLAT PLATE UNDER TRANSVERSE MAGNETIC FIELD. Gupta, K. C. (Hindu Coll., Delhi). Appl. Sci. Res., Sect. B, 12: 325-30(1965-1966).

An analysis is made of the laminar free convection of a viscous electrically conducting fluid from a hot infinite porous flat plate maintained at constant temperature under transverse magnetic field. Expressions were obtained for the velocity, magnetic field, skin friction at the plate, and the momentum thickness. The effect of the Grashof number and the Prandtl number on these quantities is discussed. (auth)

39930 COMBINED THERMAL CONVECTIVE MAGNETOHYDRODYNAMIC FLOW. Singer, Ralph M. (Argonne National Lab., Ill.). Appl. Sci. Res., Sect. B, 12: 375-404(1965-1966).

The role of combined natural and forced thermal convection in the flow of an electrically conducting fluid through a magnetic field is analyzed. The conditions under which the magnetic field renders the free convective contribution to the total thermal exchange negligible are discussed. Effects of wall electrical conductivity, magnetic field strength, internal energy generation, free convection, and thermal Prandtl number on the flow and heat transfer are presented and discussed. (auth)

39931 MAGNETOHYDRODYNAMIC FLOW IN A CURVED PIPE. Singh, S. N. (Indian Inst. of Tech., Bombay). Appl. Sci. Res., Sect. B, 12: 405-23(1965-1966).

The effect of a transverse magnetic field on the steady motion of a conducting, viscous, and incompressible liquid through a pipe of circular cross-section, coiled in a circle was studied. The solution was obtained by successive approximations in ascending powers of the Hartmann number; the first approximation corresponds to the non-magnetic case. It was assumed that the walls of the pipe are nonconducting and the radius of the cross-section is small in comparison with that of the circle in which the pipe is coiled. The stream-lines in the central plane and the projection of the stream-lines on a normal section are shown graphically and are compared with those of a non-conducting fluid. (auth)

39932 EXTENSION OF SOME THEOREMS OF MAGNETOFLUIDDYNAMICS TO THE CASE OF VISCOUS FLUIDS OF FINITE ELECTRIC CONDUCTIVITY. Vacca, Jacopa. Atti Accad. Sci. Torino: I. Cl. Sci. Fis., Mat. Natur., 100: 499-508(1965-66). (In Italian).

The Alfvén theorem and some relations regarding the vortex motion in magnetohydrodynamics, valid in the hypothesis of perfect fluids of high electric conductivity, are extended to the case of viscous fluids with finite electric conductivity. (tr-auth)

39933 CALCULATION OF THE BOUNDARY LAYER ON INSULATOR WALLS IN MAGNETOHYDRODYNAMIC GENERATOR CHANNEL WITH ACCOUNT FOR THE HALL CURRENT. Apollonskii, S. M. (Dzerzhinskii Naval Engineering Academy, Leningrad). Inzh.-Fiz. Zh., 10: 495-502(Apr. 1966). (In Russian).

Mathematical expressions are presented in the form of differential equations for the calculation of the distribution of magnetohydrodynamic flow parameters in a boundary layer. An example of the calculation method is presented. The predicted curves are shown. For a comparison, velocity and temperature curves in an ordinary thermal boundary layer at a plate are also given. The distribution of parameters in a magnetohydrodynamic boundary layer at an insulator wall depends considerably on the flow velocity in the main stream u_∞, the wall temperature Θ_w and the coefficient of electromagnetic load K. The calculation method presented may be used for consideration of both subsonic and supersonic plasma flows in generator and engine regimes. (auth)

39934 PROPAGATION OF A PLANE JET OF CONDUCTING LIQUID IN A MAGNETIC FIELD. Dzhaugashtin, K. E. Inzh.-Fiz. Zh., 10: 503-7(Apr. 1966). (In Russian).

A plane free jet of conducting liquid in a magnetic field with small values of the magnetic Reynolds number is studied and the dependence of conductance on temperature is taken into account. The jet is supposed to have a considerable excessive enthalpy. The equations are integrated on the continuous action computer of the type EMU-10. The dependence of the jet damping on the magnetic interaction parameter is shown and velocity and temperature profiles are determined. The effect of each parameter of the problem on the jet development is revealed. In a particular case the solution of equations is presented in quadratures. The solution is illustrated by figures. (auth)

39935 SOME PROBLEMS OF MAGNETOHYDRODYNAMIC BOUNDARY LAYER. Tsinober, A. B.; Shcherbinin, E. V. (Inst. of Physics, Academy of Sciences, Latv. SSR). Latv. PSR Zinat. Akad. Vestis, Fiz. Teh. Zinat. Ser., No. 2, 10-15(1966). (In Russian).

Two-dimensional jet flow of a conducting fluid in a coplanar magnetic field and a nonstationary flow past a body with the magnetic field perpendicular to the surface of the body are considered. (auth)

39936 MAGNETOHYDRODYNAMIC BOUNDARY LAYER OF ROTATIVE LIQUIDS OVER A STATIONARY BASE. Glazov, O. A. (Inst. of Power Engineering, Academy of Sciences, Latv. SSR). Latv. PSR Zinat. Akad. Vestis, Fiz. Teh. Zinat. Ser., No. 2, 16-21(1966). (In Russian).

Magnetohydrodynamic boundary layer of incompressible conducting rotative liquids over a dielectric disc with infinitely great radius was considered. The problem was solved by assuming the rotation velocity being proportional to the distance of the liquid flow from the center of the disc. The dependence of a full radial liquid flow in the boundary layer was obtained. (auth)

39937 EFFECT OF A TOOTHED INDUCTOR ON THE ELECTROMAGNETIC-FIELD DISTRIBUTION IN A CONDUCTING SLAB. Mikelson, Yu. Ya.; Mikelsons, J.; Sermons, G. Ya.; Sermons, G. (Latvian State Univ., USSR). Latv. PSR Zinat. Akad. Vestis, Fiz. Teh. Zinat. Ser., No. 1, 26-33(1966). (In Russian).

The solution is presented for the problem of a vector potential in a conducting slab. The slab was placed in the gap between two media of infinite magnetic permeability and zero conductivity under the assumption that one of the media had a smooth surface, the other a toothed one. A constant amplitude of current density in pitches occupied by current loops was given instead of a constant difference of magnetic potential between media surfaces. The current was supposed to be a harmonic function of time with the frequency ω. The expression of the vector potential was used for determining the field in a number of particular cases. (TSS)

39938 ANALYSIS OF THERMODYNAMIC PROPERTIES OF HIGH-TEMPERATURE GAS. Ito, Toshio; Murai, Yutaka (Mitsubishi Electric Mfg. Co., Ltd., Japan). Mitsubishi Denki Giho, 40: 716-22(Apr. 1966). (In Japanese).

In the analysis of the thermodynamic properties of a high-temperature gas, a generalized method was worked out by means of statistical machines on the assumption that all the chemical reactions taking place are in thermal equilibrium. The method was applied, as an example, to the numerical evaluation of the thermodynamic properties of heavy oil combustion products expected to be as a fuel for the commercial open cycle MHD generator. The results show that the combustion gas of heavy oil can be treated as an ideal gas in approximation in the temperature below around 2,000°K, but if the temperature exceeds 2,000°K, its thermodynamic properties widely deviate from those of the ideal gas. (auth)

39939 THE INFLUENCE OF A MAGNETIC FIELD ON SCHWARZSCHILD'S CRITERION FOR CONVECTIVE INSTABILITY IN AN IDEALLY CONDUCTING FLUID. Gough, D. O.; Tayler, R. J. Mon. Notic. Roy. Astron. Soc., 133: 85-98(1966).

The influence of a magnetic field on the onset of adiabatic thermal convection in a compressible ideally conducting fluid is studied. In the absence of a magnetic field, Schwarzschild's criterion for the onset of convection is a purely local criterion; a magnetic field connects fluid at different levels and a local criterion which is necessary and sufficient for stability against convection can no longer be obtained. However, it is shown that, for certain simple magnetic field configurations which do not introduce hydromagnetic instabilities, there are simple local criteria which are sufficient for the stability of the system. It is pointed out that, in a fluid of finite electric resistivity, a magnetic field cannot be expected to lead to complete stabilization of convective motions. In such a case, if the sufficient condition is satisfied, there should probably be a substantial reduction in the growth rate of the instability and in the energy carried by fully developed convection. One of the sufficient conditions for stability is applied to a sunspot model recently constructed by Chitre and it is found that it is satisfied throughout most of the model. Although the theory is not general enough to apply to this case, it is suggestive that a high degree of suppression of convection by a magnetic field should occur in such a spot. (auth)

39940 COMPARISON OF SATURATED-LIQUID VISCOSITIES OF LOW MOLECULAR SUBSTANCES ACCORD-

ING TO THE QUANTUM PRINCIPLE OF CORRESPONDING STATES. Rogers, John D.; Brickwedde, F. G. (Los Alamos Scientific Lab., N. Mex.). Physica, 32: 1001-18 (June 1966). (LA-DC-7546).

The quantum mechanical principle of corresponding states, in which the thermodynamic state variables are reduced by the molecular parameters of the Lennard-Jones two-body interaction potential and quantum deviations from calssical behavior are correlated, was used to investigate the saturated-liquid viscosity of ^3He, ^4He, H_2, D_2, T_2, Ne, N_2, and Ar. Values were obtained for: the critical-point viscosities of ^4He, normal H_2, equilibrium D_2, and T_2; the triple-point viscosities of n-H_2, p-H_2, D_2, T_2, Ne, N_2, Ar, Kr, and Xe; and the saturated viscosities for ^3He, ^4He, D_2, and T_2. (auth)

39941 WHAT'S NEW IN TWO-PHASE FLOW. Fauske, Hans K. Power Reactor Technol., 9: 35-46(Winter 1965-1966).

Presented is a summary of papers from the Symposium on Two-Phase Flow held at Exeter, England, June 21-23, 1965. The topics discussed include flow regimes, wave mechanics, void fractions and holdup, two-phase flow characteristics, nucleate and film boiling, entrainment, flooding, critical flow, and two-phase flow dynamics. (H.D.R.)

39942 PULSATING MAGNETOHYDRODYNAMIC FLOW IN AN ANNULAR CHANNEL. Rudraiah, N. (Univ. of Bangalore, India). Proc. Indian. Acad. Sci., Sect. A, 63: 293-304(May 1966).

Pulsating laminar flow of a viscous incompressible electrically conducting fluid in an annular channel between two infinitely long circular cylinders under a radial impressed magnetic field is considered. The solutions of magnetohydrodynamic equations have been obtained on the assumption that the space between two cylinders is small compared to their mean radius. The solutions were also obtained on the assumption of small magnetic Reynolds number with special consideration of those for low and high frequencies. (auth)

39943 STABILITY OF PARALLEL FLOWS WITH PARALLEL MAGNETIC FIELDS. Hunt, J. C. R. (Central Electricity Research Labs., Leatherhead, Eng.). Proc. Roy. Soc. (London), Ser. A, 293: 342-58(Aug. 9, 1966).

A physical discussion of the way in which a magnetic field affects the stability of a fluid in motion is presented. Particular emphasis is given to how the magnetic field affects the interaction of the disturbance with the mean motion. An analysis of the stability of plane parallel flows of fluids with finite viscosity and conductivity under the action of uniform parallel magnetic fields is given. It is shown that, in general, three-dimensional disturbances are the most unstable. Results obtained for two-dimensional disturbances can be used to calculate the most unstable three-dimensional disturbances and thence prove that a parallel magnetic field can never completely stabilize a parallel flow. (auth)

39944 BLAST WAVES IN MAGNETOGASDYNAMICS WITH FINITE ELECTRICAL CONDUCTIVITY. Secrest, Bruce G. (Univ. of Nebraska, Lincoln); Nariboli, Gundo A. Z. Angew. Math. Phys., 17: 391-7(May 25, 1966).

A blast wave of arbitrary shape in magnetogasdynamics with electrical conductivity as the only dissipative mechanism is considered. The results show the effect of the tangential component of the magnetic field on the growth of the discontinuities. Calculations are included on basic equations and shock relations, growth of the wave, and shock velocity. It is concluded that in a gaseous medium devoid of viscosity and heat conduction but with finite electrical conductivity, a shock wave is a possibility in the presence of a magnetic field. Though the variations of field variables do not depend on the magnetic field, the variations of their gradients do depend on its tangential component. (J.H.M.)

39945 MAGNETOHYDRODYNAMIC FLOW PAST A SEMI-INFINITE PLATE. Meksyn, David (Imperial Coll. of Science and Tech., London). Z. Angew. Math. Phys., 17: 397-403(May 25, 1966).

The flow of viscous electrically conducting fluid past a semi-infinite plate in the presence of an aligned magnetic field was considered [Aero/Space Sci. 29, No. 6, 662(1961)]. The flow depends on $\gamma = R_m/R$, the ratio of the magnetic to the viscous Reynolds numbers, and on $\beta = \mu H_0^2/4\pi\rho U_0^2$, the ratio of the density of the magnetic to the density of the kinetic energy of the main flow. The problem was solved for the case when γ changes from zero to infinity and $\beta < 1$. It appears that $\beta = 1$ is a critical point of the equations when $\gamma \geq 1$. The case when $\gamma \to \infty$ and $\beta \geq 1$ is considered in detail here. (auth)

39946 MODIFIED KINETIC MODEL FOR CALCULATION OF $G_s(r,t)$ IN DENSE FLUIDS. Gibbs, Alan G. (Battelle Memorial Inst., Richland, Wash.). 12p. (CONF-650932-8). CRAU. Gmelin, AED-CONF-65-292-8.

From Symposium on the Inelastic Scattering of Neutrons by Condensed Systems, Upton, N. Y.

An extension is given to preview work (Gibbs and Ferziger, Phys. Rev., 138: A701 (1965)) in which the classical counterpart of the Van Hove self-correlation function $G_s(r,t)$ is applied to the kinetics of dense gases and liquids. The previous ccalculations are compared with the results (Rahman, Phys. Rev. 136: A405 (1964)) of a digital simulation of liquid argon. The computer results show the effects of appreciable oscillatory contributions, whereas the $G_s(r,t)$ calculations considered only diffusive effects. An extension of the theory in which both diffusive and oscillatory features are present improves agreement with the computer results. (S.F.L.)

Geophysics

Refer also to abstracts 39565 and 39625.

39947 PHYSICAL COMPOSITION OF AURORA. Omholt, A. (Univ. of Oslo). Ann. Geophys., 22: 217-23(1966).

The aurora is considered as an atmospheric phenomenon, i.e. primary particles considered only as a source of excitation of the atmospheric gases, by means of which some properties of the atmosphere can be studied, as well as the disturbing influence such particle injection may have on the atmosphere itself. A brief description of the most important and interesting features of the auroral spectrum is given and then a description of the disturbances introduced by the aurora, such as production of metastable, excited atoms and molecules, dissociation, and heating. The use of the aurora for studying atmospheric parameters is also discussed. From the available data on the intensities in the auroral spectrum conclusions are drawn on the densities of metastable atoms and molecules, and on the rates of dissociation and ionization. It is not likely that the density of metastables or the rate of dissociation are able to influence the composition of the atmosphere significantly. Ionization is of great importance. Atmospheric heating due to Joule heating is not likely to be important. Heating due to the impact of energetic particles may be important at relatively great heights (>150 km). From auroral spectra, atmospheric temperatures may be derived. These are in agreement with the general information on temperature distribution and possible heating. The possibility of studying winds, diffusion, and electric fields by means of auroral emission is briefly discussed. (BBB)

39948 ION COMPOSITION MEASUREMENTS AND RELATED IONOSPHERIC PROCESSES IN THE D AND LOWER E REGIONS. Narcisi, R. S. (Air Force Cambridge Research Labs., Bedford, Mass.). Ann. Geophys., 22: 224-34(1966).

Observational results of positive ion composition of the lower ionosphere, between 60 and 120 km, are reviewed and limitations and errors in the measurements are discussed. The most comprehensive information on positive ion composition in the lower ionosphere was obtained

from direct in situ measurements made with ion mass spectrometers aboard rockets. The results of other workers for the altitude range 90 to 120 km are also discussed. An attempt is made to explain, at least qualitatively, the positive ion structure indicated by the measurements. In the region below 82 km, the problem is to find a source of the water vapor-like ions of H_3O^+ and $H_5O_2^+$. Possible mechanisms which can account for the presence of the water conglomerates in the D region are discussed. A process of simultaneous ionization and fragmentation of these water conglomerates is then suggested as one possible source of the water ions. About 82 km the problem is to explain the highly stratified layers of metallic ions at 95 and about 110 km. From an examination of the work on optical measurements in the twilight which yielded the metal atom profiles, likely processes for the formation of the lower metal ion layer at 95 km are discussed. Analogies are drawn from the results of rockets measurements of wind shears and a theoretical analysis is made of sporadic E from wind shear effects to offer an explanation for the metal ion layer at about 110 km. It is concluded that H_3O^+ and $H_5O_2^+$ are true constituents of the D region rather than the products of rocket contamination, but that it is not possible to account for their observed concentrations on the basis of presently known processes and available data. It is suggested that the highly stratified layers of metallic ions observed at 95 km results primarily from chemical, photochemical, and ionization processes while the layer at around 110 km may be generated by a wind shear effect. (BBB)

39949 NEGATIVE IONS IN THE LOWEST IONOSPHERE WITH SPECIAL REFERENCE TO EXPERIMENTAL EVIDENCE FROM UPPER ATMOSPHERE RESEARCH. **Hultqvist, Bengt (Kiruna Geophysical Observatory, Sweden). Ann. Geophys., 22: 235-46(1966).**

A review is presented of the following types of data obtained in the ionosphere, related to negative-ion problems: variation during sunrise and sunset of polar cap absorption, auroral absorption, VLF soundings, other radio transmission effects, rocket measurements of negative and positive ions, and rocket observations of the relation between electron density increase and flux of near uv light as function of height for several solar zenith angles during a sunrise period. Most measurements in the ionosphere related to its negative ion composition and density in the lowermost ionosphere are carried out by radio waves, the propagation of which is influenced by free electrons but not by negative or positive ions. The existence of the negative ions can then be observed directly when the density of free electrons is changed without ionizing uv radiation being present, which occurs when the equilibrium of attachment and detachment reactions is changed, for instance by the light flux changing at sunrise and sunset. Available measurements are related to the problem whether photodetachment is important for the electron density or not in the height interval 70–90 km, i.e. whether there is any appreciable increase in the free density due to detachment of electrons from the negative ions by photons at sunrise. According to the widely adopted O_2^- model for the electron chemistry in this altitude range, based on laboratory measurements of reaction constants, there should be more negative ions than free electrons per unit volume in the night up to 90 km, and a large increase of the electron density should therefore occur at sunrise. It is concluded, however, that the existing experimental information is not consistent, and that the O_2^- model for the electrons in the lowest ionosphere is not correct. (BBB)

39950 OBSERVATIONAL RESULTS ON ATMOSPHERIC IONS IN THE REGION OF THE OUTER IONOSPHERE. **Istomin, V. G. (Inst. of Applied Geophysics, Moscow). Ann. Geophys., 22: 255-65(1966).**

Measurements of the ionospheric ion composition using Explorer-VIII, Ariel and Cosmos-2, and from some other experiments conducted in 1960-1964, are compared. The analysis of results of radiofrequency mass-spectrometer measurements of the outer ionosphere ion composition from Electron-1 and Electron-2 satellites is also presented. Ions with mass numbers M = 1, 4, 14, and 16 amu identified with single charged ions of hydrogen H^+, helium He^+, nitrogen N^+, and oxygen O^+ were found in these measurements. Measurements were conducted at altitudes from 406 to 2750 km within 10°–61°N latitude. The molecular ions N_2^+, NO^+, and O_2^+ were not observed. This shows that relative concentration of these ions decreases at least by an order in comparison with years of max solar activity. Hydrogen ions H^+ were registered well throughout the whole height range. Mass peaks of H^+ ions became equal to peaks of O^+ at an altitude of about 900 km from the 10th to 19th February 1964, in the afternoon from 16 to 19 hours local time. Helium ions, He^+, are registered irregularly as weak mass peaks. It is concluded that concentration of He^+ ions at all altitudes is only a small part of the total ion concentration, thus there is probably no helium ion layer in the earth's atmosphere. Comparison of the data available indicates that the mass-spectrometric technique gives noncontradictory results, in agreement with themselves and with data from other measurements. Mass-spectrometric measurement methods for the ion composition seem to be to free from restrictions in interpretation resulting from an incomplete knowledge of the medium parameters where the measurements are made. (BBB)

39951 THE DETERMINATION OF ABSORPTION IN THE IONOSPHERE BY RECORDING THE FIELD STRENGTH OF A DISTANT TRANSMITTER (FUNDAMENTALS OF THE A3 METHOD AND RESULTS OF CONTINUOUS MEASUREMENTS SINCE 1956). **Schwentek, Heinrich (Max-Planck-Institut fuer Aeronomie, Lindau, Ger.). Ann. Geophys., 22: 276-88(1966).**

A survey is given on the use of the A3 method to measure absorption in the ionosphere by recording field strength of a distant transmitter. With this method data can be obtained which are comparable in accuracy with those obtained by pulse methods. Diurnal variation of absorption can be measured especially easy. It is shown how the change in absorption from night to day for a wave which is reflected in the same region may be computed from the day-time and night-time field strengths and the corresponding half-path lengths. Transmission distance and frequency must be chosen carefully. Distances of about 300 km and frequencies about 2.5 Mc are suitable. The first principle to be observed in choosing the transmitting and receiving aerials is that the combination must reject high-angle waves so that the effects of multiple reflections are small. In practice, it is most convenient to use a vertical monopole at the transmitter and a horizontal dipole at the receiver. Absorption values of the 24 most regular diurnal variations in the four different seasons of the years 1961 to 1963 are described and analyzed. The values were derived from the frequency distributions of field strength taken every 30 min. It was found that the absorption values follow the sun's zenith angle (χ) in a regular way. The values are a function of $\cos^n\chi$, where the exponent n is most frequently ~0.75, independently of the subsolar absorption. An exception occurred only in winter when the amount of both subsolar absorption and n frequently was higher (n up to 1). (BBB)

39952 A SURVEY OF A3: ABSORPTION MEASUREMENTS AT LOW AND MEDIUM FREQUENCIES. **Lauter, E. A. (Observatorium fuer Ionosphaerenforschung, Kuehlungsborn, Ger.). Ann. Geophys., 22: 289-99(1966).**

Absorption measurements on low and medium frequencies at steep ionospheric incidence are used to demonstrate diurnal, annual, and sunspot cycle changes in the plasma of the lower ionosphere. On frequencies between 100 and 1000 kc there exists also a marked absorption at negative sun heights ($90° < \chi < 100°$) produced in the lowest D region by photodetachment ionization in the presence of invading high-energy particles. When during daytime the total LE absorption is corrected for this nearly constant absorption in the CR-D layer, a $\cos^n\chi$ law describes the diurnal and annual variations with exponents between 0.9 and 1.5. The winter anomaly of high absorption markedly decreases from medium to low frequencies and also with height from 90 to 80 km. With decreasing frequency there is an anomaly

of high absorption also in the summer months, which is not yet well understood. Absorption increases considerably with sunspot number, but in the latitude of the observatory ($\Phi = 54°$) there is still a marked contribution of high-energy particle precipitation effects to the observed attenuation in this frequency range. Studies of special absorption events connected with strong magnetic storms indicate that there exists an excessive absorption produced by precipitating electrons from the outer radiation belt during high refilling periods of the belt after some storms. (BBB)

39953 MEASUREMENT OF THE IONOSPHERIC ABSORPTION OF EMISSIONS OF RADIO SOURCES AND ITS APPLICATION TO KNOWLEDGE OF THE IONOSPHERE. Simon, P. (Observatoire de Meudon, France). Ann. Geophys., 22: 300-9(1966). (In French).

The fact that cosmic radio waves are weaker in the daytime than at night indicates their partial absorption by the ionosphere. Measurement of the degree of absorption is imprecise because of inability of accurately measuring the absolute flux. Some other difficulties in the measurement of ionospheric absorption include the practical difficulties of the absorption measurement: determination of the cosmic radio noise absolute flux introduces a number of problems. The comparison of ordinary and extraordinary wave fluxes seems to supply the best results. Also there are interpretation difficulties: the ionospheric conditions change entirely from the base to the highest regions, which considerably limits the interpretation of the results. The method permits continuous measurements by a relatively simple apparatus, as it requires only reception. This permits multiple measurement points to be used and very precise analysis of geographic extension of abnormal absorption phenomena. (BBB)

39954 STUDY OF THE SCINTILLATION-RATE SPECTRUM OBSERVED IN THE AURORAL ZONE. Liszka, Ludwik (Kiruna Geophysical Observatory, Sweden). Arkiv Geophys., 4: No. 27, 529-35(1964).

The scintillation-rate spectrum of satellite signals at 54 Mc observed at Kiruna, Sweden (67.8°N, 20.3°E) is examined. Temporal variations in the scintillation-rate spectrum, in particular the occurrence of slow and fast scintillation, are shown. The data from satellite amplitude records show that the slow part of the scintillation-rate spectrum (slower than 1 cps) has different properties from the fast part. The two parts seem to have different geographical distribution. Within the region between latitudes 60°N and 68°N the slow scintillation increases gradually towards a max of the auroral zone. The fast scintillation also varies in a similar manner, but more slowly. The two parts of the scintillation-rate spectrum also have different diurnal variations. The slow scintillation has a max at midnight and the fast scintillation has two distinct maxima: one during the evening and one early in the morning. The dependence of scintillation on magnetic activity also changes during the day and may be, at the same time, different for various parts of the scintillation-rate spectrum. The diversity in the properties of the scintillation-rate spectrum may be explained in at least two different ways: (1) Slow and fast scintillation is produced by different mechanisms; (2) Irregularities responsible for both components are produced at various heights, possibly by particles of different energy. (BBB)

39955 MORPHOLOGY OF THE POLAR LIGHTS. Schroeder, Wilfried (Geophysikalische Station, Bremen-Roennebeck, Ger.). Beitr. Geophys., 74: 374-7(1965). (In German).

The form of polar displays by visual observation is discussed. The large and structured forms correlate well with geomagnetically disturbed days. A particular instability of the magnetic field is thus the cause of these displays. Weak displays, consisting frequently of G forms and often observed only for periods of a few minutes, occur in connection with very small disturbances. The appearance of auroral displays in middle latitudes is in general related to such weak disturbances; they occasionally consist of multiple forms, as, for example, on Oct. 20-21, 1957, and July 20-21, 1960. Data are tabulated for displays of particular intensity, observable in Germany, and their correlation with geomagnetic disturbance (12 cases). Data for weaker displays (10 cases) are separately correlated; all data are collected between 1957 and 1962. (BBB)

39956 GEOGRAPHICAL SPREAD OF THE POLAR LIGHTS. Schroeder, Wilfried (Geophysikalische Station, Bremen-Roennebeck, Ger.). Beitr. Geophys., 74: 378-82(1965). (In German).

The relation between great auroral displays in middle and low latitudes and geomagnetic activity is analyzed. Nine displays from 1957 to 1962, at least partially observable in tropical latitudes, are correlated with particularly conspicuous solar flares; in two cases, such a correlation cannot be made. Positions of ships observing the displays of 21 Jan. 1957, 8 July 1958, 4 Sept. 1958, 15 July 1959, and 28 Oct. 1961 are mapped; all displays were intense, and the morphology included all forms, even in middle latitudes. These are observed only during periods of max solar activity, and then not always. Several important displays occurred shortly after the sunspot max. of 1957-9; this is correlated with earlier similar observations. Data for displays are tabulated. (BBB)

39957 RADIATION BELTS. Shabanskii, V. P. (Moscow State Univ.). Geomagn. Aeronomy (USSR) (Engl. Transl.), 5: 765-89(1965).

Translated from Geomagn. Aeronomiya, 5: 969-1002 (1965).

Basic information on geomagnetically trapped radiation is examined (chiefly according to data as of April 1964), and ideas on the structure of the earth's magnetosphere are discussed. (auth)

39958 ROCKET DATA ON THE BEHAVIOR OF ELECTRON CONCENTRATION IN THE IONOSPHERE AT HEIGHTS OF 100-300 KM. I. Kazachevskaya, T. V.; Ivanov-Kholodnyi, G. S. Geomagn. Aeronomy (USSR) (Engl. Transl.), 5: 794-805(1965).

Translated from Geomagn. Aeronomiya, 5: 1009-24 (1965).

The results of rocket measurements of electron concentration in a quiet ionosphere are compared with solar and geomagnetic activity as a function of time of day, season, etc. An empirical model of the daytime ionosphere is constructed for winter and summer at high and low solar activity levels. The character of $n_e(h)$ profiles changes throughout the day. A power-law dependence of the n_e variation on atmospheric air mass is found for definite solar zenith angles; the rate of the n_e decrease at noon in winter is ~2 times higher than in summer for $z_\odot = 70$ to 90°. When the sun is in a low position a maximum forms at the horizon at heights of 110 to 130 km and a "trough" appears in the $n_e(h)$ profile above it. An explanation is given for the characteristics found in the behavior of n_e. (auth)

39959 HARMONIC ANALYSIS OF THE DIURNAL VARIATION OF CRITICAL F_2-LAYER FREQUENCIES. Singler, A. Geomagn. Aeronomy (USSR) (Engl. Transl.), 5: 806-12(1965).

Translated from Geomagn. Aeronomiya, 5: 1025-33 (1965).

The diurnal variation of critical F_2-layer frequencies is investigated with the view of determining its dependence on season and solar activity. The results show that the diurnal pattern changes continuously with the season and with the solar cycle and it can be represented with a good approximation by means of simple empirical interpolation formulas. (auth)

39960 SPACE AND TIME VARIATIONS OF LONG WAVE IONOSPHERIC ABSORPTION AT SMALL SOLAR HEIGHTS AND AT NIGHT. Lauter, E. A.; Hruskova, I.; Nestorov, G.; Sprenger, K. Geomagn. Aeronomy (USSR) (Engl. Transl.), 5: 813-21(1965).

Translated from Geomagn. Aeronomiya, 5: 1034-45 (1965).

The results are reported of long-period measurements by the A3 method in the long-wave range on paths 350 km

long in Central and Southern Europe. An idea is given of the frequency dependence of average night absorption in the extra long-, long-, and medium-wave ranges that has a maximum of about 17 db of f = 200–400 kc/s. The diurnal variation of ionospheric absorption in the long-wave range at low solar heights and at night shows that purely night conditions occur at solar zenith angles $\chi > 100°$, while at χ to –9° photodetachment takes place. The annual pattern of night absorption has the form of a double wave with maxima in winter and summer and minima soon after the equinoxes. The injection of high-energy particles into the lower ionosphere during and after magnetic storms results in a strong increase of absorption in the long-wave range, particularly at χ from +10 to –10°, as well as at night. The frequency of such cases at geomagnetic latitude 55° depends on the solar activity cycle, while below 50° the injection of high-energy particles is very rare. (auth)

39961 SOME VERTICAL DISTRIBUTION PATTERNS. Andrienko, D. A. (Kiev State Univ.). Geomagn. Aeronomy (USSR) (Engl. Transl), 5: 838-40(1965).

Translated from Geomagn. Aeronomiya, 5: 1068-70 (1965).

The height of the lower edge of auroras is examined as a function of auroral intensity and of the lunar hour angle. The auroral observations were made at Tixie Bay in 1962-1964, using wide-angle NAFA-3S/25 cameras. (auth)

39962 GENERAL PATTERNS OF PEARL-TYPE PULSATIONS. Matveeva, E. T.; Troitskaya, V. A. (Inst. of Terrestrial Physics, Academy of Sciences, USSR). Geomagn. Aeronomy (USSR) (Engl. Transl.), 5: 846-50(1965).

Translated from Geomagn. Aeronomiya, 5: 1078-84 (1965).

The morphological properties of pulsations of the Pc 1 type are described on the basis of long-period observations. There is an inverse relationship between the amplitude of Pc 1, the duration of their series, and the number of excitations and solar activity. The characteristics of the planetary distribution of Pc 1 pulsations are described. (auth)

39963 ROLE OF THE MAGNETIC FIELDS OF SOLAR CORPUSCULAR STREAMS AND THEIR EFFECT ON THE EARTH'S MAGNETOSPHERE. Zhulin, I. A.; Mogilevskiy, E. I. (Inst. of Terrestrial Magnetism, Ionosphere and Radio Wave Propagation, Academy of Sciences, USSR). Geomagn. Aeronomy (USSR) (Engl. Transl.), 5: 858-60 (1965).

Translated from Geomagn. Aeronomiya, 5: 1095-7(1965).

Considerations are given to the effect of the magnetic fields of solar corpuscular streams on processes in interplanetary space and on the interaction of the streams with the earth's magnetosphere. (J.H.M.)

39964 KINETIC INSTABILITY OF THE OUTER RADIATION ZONE OF THE EARTH. Trakhtengerts, V. Yu. (Gorkii State Univ., USSR). Geomagn. Aeronomy (USSR) (Engl. Transl.), 5: 865-7(1965).

Translated from Geomagn. Aeronomiya, 5: 1103-4(1965).

The kinetic instability for the outer radiation zone of the earth is computed. The presence of a "loss cone" is taken into account. The computations indicate that kinetic instability can play an important role in the dynamics of the entire outer radiation zone of the earth. (J.H.M.)

39965 CHARACTERISTICS OF f_0F_2 VARIATIONS AT HIGH SOLAR ACTIVITY. Vasil'eva, T. N. (Inst. of Terrestrial Magnetism, Ionosphere and Radio Wave Propagation, Academy of Sciences, USSR). Geomagn. Aeronomy (USSR) (Engl. Transl.), 5: 870-2(1965).

Translated from Geomagn. Aeronomiya, 5: 1108-10 (1965).

The percentage distribution of the various types of dependences of f_0F_2 on R (sunspot numbers) is examined. Cases were selected and analyzed when the growth of f_0F_2 decreased with increasing solar activity and when the dependence of f_0F_2 on R had an inverse pattern in years of high solar activity. (J.H.M.)

39966 RELATIONSHIP BETWEEN E_s AND THE F REGION OF THE IONOSPHERE. Ovezgel'dev, O.; Lezhneva, A. V. (Dept. of Geophysics and Seismology, Academy of Sciences, Turkmen SSR). Geomagn. Aeronomy (USSR) (Engl. Transl.), 5: 873-5(1965).

Translated from Geomagn. Aeronomiya, 5: 1111-12 (1965).

Results of an analysis of experimental data obtained from 1959-1963 on the relationship between E_s and the F region of the ionosphere are presented. During this period, 141 cases of transformation of a secondary formation in the F region into an E_s were detected. It was found that transformation occurs during the daytime from 8 to 17 hr with a maximum at about 12–13 hr LT and most frequently in the equinoctical months and less frequently in summer. Also, to some extent, the process of transformation depends on the solar activity level. (J.H.M.)

39967 POSITION OF THE EQUATORIAL BOUNDARY OF THE REGION WHERE ANOMALOUS IONIZATION APPEARS AS A FUNCTION OF PLANETARY MAGNETIC ACTIVITY. Yudovich, L. A. (Inst. of Terrestrial Magnetism, Ionosphere and Radio Wave Propagation, Academy of Sciences, USSR). Geomagn. Aeronomy (USSR) (Engl. Transl.), 5: 875-6(1965).

Translated from Geomagn. Aeronomiya, 5: 1113-14 (1965).

To determine the position of the equatorial boundary of the region where anomalous ionization appears as a function of the intensity of planetary magnetic activity, three meridional chains of stations were selected: Baker Lake, Churchill, Meanook, Winnipeg, Victoria, Fort Monmouth, and Washington in the Western Hemisphere and Tikhaya, Dixon, Murmansk, Sverdlovsk, and Moscow in the Eastern Hemisphere. Since the possibilities for the selection of stations in the Southern Hemisphere are limited, a profile was made through the American Continent and the Antarctic: Byrd, Ellsworth, Halley Bay, Deception, and Port Lockroy. Results indicate that the position of the equatorial boundary changes substantially in all three profiles. The boundary occupies its most poleward position on magnetically quiet days when anomalous ionization is observed at Churchill, Byrd, and Dixon, and not recorded at Meanook, Murmansk, and Ellsworth. As magnetic activity increases the boundary shifts toward the equator. The equatorial boundary of the region of anomalous ionization is located at the same corrected geomagnetic latitudes for all three chains of stations for the same ΣKp. (J.H.M.)

39968 POSSIBLE DISTRIBUTION OF ION DENSITY IN THE IONO-EXOSPHERE WITH A DIPOLE MAGNETIC FIELD. Kamiyama, Hiroshi; Takaki, Hideo (Tohoku Univ., Sendai). J. Geomagnet. Geoelec., 18: 1-11(1966).

The base of the iono-exosphere is defined as the level where the mean free path of ionized particles in a horizontal direction equals the scale height for the ionized gas. It is assumed that an ionized particle moving upward from this base level spirals up along a line of magnetic force without suffering any collision until it returns back to the starting base or goes across the equatorial plane and reaches its conjugate base on the other hemisphere. Due to external forces such as the gravitation, an ion with low velocity at the base can not pass across the equatorial plane but turns back at a certain point on the line of force. The critical velocity at the base for an ion which turns back at any given point on a line of force is calculated as a function of pitch angle and the magnetic latitude assuming a dipole magnetic field. Thus, ionized particles with velocities exceeding the critical velocity at the base contribute to the ion density at farther points. The computed result shows a steeper vertical gradient of the ion density at the equator than at a high latitude. The ion density at 5 earth radii in the equatorial plane is estimated to be about 9 ions cm^{-3}. (auth)

39969 DECLINATION-CHANGE OF SC, ITS LOCAL-TIME AND SEASONAL DEPENDENCE AT KAKIOKA, JAPAN. Fukushima, Naoshi (Tokyo Univ.). J. Geomagnet. Geoelec., 18: 99-101(1966).

A systematic eastward and westward deviation found in the direction of the main impulse of the sudden commencement of a magnetic storm recorded at Kakioka, Japan, is discussed. The local-time dependence of the angular deviation of the SC-vector from the local magnetic north for 183 SCs in all seasons of 15 years is shown and deviation angles of the main impulses of SCs are plotted separately for summer and winter seasons. (J.H.M.)

39970 RING CURRENT EFFECTS ON TRAPPED PARTICLES. McIlwain, Carl E. (Univ. of California, San Diego, La Jolla). J. Geophys. Res., 71: 3623-8 (Aug. 1, 1966).

Dessler and Karplus have predicted that measurable changes in trapped particle fluxes should accompany the betatron acceleration and radial movement of the particles due to time-dependent diamagnetic ring currents. The adiabatic deceleration and reacceleration of trapped protons were observed by a detector on the Explorer 26 satellite. The measured time dependence of the particle fluxes are shown to follow the variations expected theoretically. (auth)

39971 LATITUDE OF THE DAYSIDE AURORA. Bates, Howard F. (Unv. of Alaska, College). J. Geophys. Res., 71: 3629-33(Aug. 1, 1966).

The aurora, as determined from the College h-f multifrequency backscatter records, was present somewhere on the College geomagnetic meridian during 1965 a minimum of 65% of the time at any hour on the dayside of the earth, and 95% on the nightside. The southern boundary of the aurora (1) occurred at approximately 77° geomagnetic latitude during midday periods when K_p, the planetary magnetic activity index, was less than 4, (2) during midnight periods occurred at approximately 70° when K_p was 0_0 and 68° when K_p was less than 2, and (3) in general extended farther south at any hour as magnetic activity increased. The midday aurora on magnetically quiet days ($K_p < 4$) during the 1965 summer solstice was approximately 1.5° north of that during the winter solstice. The 1965 backscatter results agree closely with 1957 to 1959 optical results; thus, the position and the rate of occurrence of the dayside aurora for a given level of magnetic activity are almost independent of both season and solar activity. (auth)

39972 ION TEMPERATURE IN THE IONOSPHERE OBTAINED FROM CYCLOTRON DAMPING OF PROTON WHISTLERS. Gurnett, Donald A. (Univ. of Iowa, Iowa City); Brice, Neil M. J. Geophys. Res., 71: 3639-52 (Aug. 1, 1966).

A method of determining ion temperature in the ionosphere from cyclotron damping of proton whistlers is discussed. These whistlers are dispersed forms of lightning impulses, observed by satellites as propagating left-hand polarized (ion cyclotron) waves. It is found that the amplitude of the proton whistler decreases abruptly at a wave frequency slightly below the proton gyrofrequency at the satellite. Of several factors considered, it is found that only cyclotron damping can satisfactorily explain this abrupt cutoff. The theory of cyclotron damping of proton whistlers is developed, and the difference between the wave frequency at cutoff and the proton gyrofrequency at the satellite is related to the proton temperature. Sample proton temperatures in the ionosphere are determined, using proton whistlers observed by the Injun 3 and Alouette 1 satellites. The temperatures found are comparable to those obtained previously by other experimenters. The method of observing ion temperatures developed here has inherent advantages in that the parameters measured are independent of electron temperature and ion composition. (auth)

39973 OCCURRENCE PATTERNS OF TOPSIDE SPREAD F ON ALOUETTE IONOGRAMS. Hice, James D.; Frank, Bernadine (Stanford Research Inst., Menlo Park, Calif.). J. Geophys. Res., 71: 3653-64(Aug. 1, 1966).

The extent and frequency of occurrence of spread F, as shown on 8400 ionograms taken by the Alouette satellite, were investigated. These ionograms were taken during the solstice periods of December 1962 and June 1963. The spread F observed was found to be consistent with three proposed qualitative radio-propagation models. These models involve: aspect-sensitive scattering from thin magnetic-field-aligned irregularities, waveguide-like action—called ducting—along wide irregularities, and refraction due to large-scale reductions in electron density. The three types of spread F were found to exhibit markedly different occurrence patterns during the two observation periods. (auth)

39974 STEEP HORIZONTAL ELECTRON-DENSITY GRADIENTS IN THE TOPSIDE F LAYER. Calvert, W. (Inst. for Telecommunication Sciences and Aeronomy, Boulder, Colo.). J. Geophys. Res., 71: 3665-9(Aug. 1, 1966).

Very steep latitudinal electron-density gradients are found to occur in the topside F layer at high latitudes. They occur either associated with the trough (>6% km^{-1}) or within the auroral zone (>60% km^{-1}). The electron-density scale height at 1000 km may be nearly constant across these gradients. (auth)

39975 MEASUREMENT OF ELECTRON CONTENT AT THE MAGNETIC EQUATOR. Ross, William J. (Pennsylvania State Univ., University Park). J. Geophys. Res., 71: 3671-6(Aug. 1, 1966).

Values of the vertical column electron content of the ionosphere at Huancayo, Peru, are presented for an 18-month interval. These data were obtained from an analysis of Faraday rotation data from a radio beacon satellite (Transit 4A). The daytime electron content is found to vary with the 10.7-cm solar radio flux, and, after normalization for this dependence, the average diurnal variation is found to be quite regular with a range of about 20:1. A biannual variation in the daytime electron content is found also, with maxima near the equinoxes and with a range of about 2:1. (auth)

39976 CORRELATION OF MAGNETIC FIELDS AND ENERGETIC ELECTRONS ON THE IMP 1 SATELLITE. Anderson, K. A. (Univ. of California, Berkeley); Ness, N. F. J. Geophys. Res., 71: 3705-27(Aug. 1, 1966).

A study of simultaneous magnetic field and energetic particle records from the IMP 1 satellite on the dark side of the earth has shown several distinct correlations that can be understood as diamagnetic effects of charged particle populations. Depression of the magnetic field in the closed magnetic field line configuration of the particle cusp region is observed on most orbits. A small but significant portion of this effect can be attributed to the diamagnetic effects of electrons >45 kev. In the geomagnetic tail region, large depressions of the magnetic field having radial extent ~10 R_E are observed when the satellite approaches the neutral sheet to within ~5 R_E. Energetic electron fluxes appear throughout this volume and show no strong preference to occur immediately adjacent to the neutral sheet. In this region, less than 1% of the diamagnetic effect is due to electrons >45 kev. Finally, there are examples of intense, energetic electron fluxes closely associated with reduction of the magnetic field magnitude. In one case, an electron flux of 3×10^6 cm^{-2} sec^{-1} >45 kev was associated with a field change from 20 γ to 8 γ. (auth)

39977 PROPAGATION OF Pc 1 MICROPULSATIONS FROM HIGH TO LOW LATITUDES. Manchester, R. N. (Univ. of Newcastle, New South Wales, Australia). J. Geophys. Res., 71: 3749-54(Aug. 1, 1966).

It is shown, for typical profiles of ionospheric parameters, that a duct exists in the F region of the ionosphere in which hydromagnetic waves are efficiently guided. The duct has a low-frequency cutoff at about 0.5 cps, showing that the observed variation of emission frequency with latitude is largely a propagation effect. Duct attenuation is small during the night hours, when the majority of Pc 1 events are observed at middle and low latitudes, but it is large during the day. The calculated duct group velocity is of the same order as that given in initial reports of experimental observations. (auth)

39978 LOW-ENERGY ELECTRONS MEASURED ON IMP 2. Serbu, G. P.; Maier, E. J. R. (Goddard Space Flight Center, Greenbelt, Md.). J. Geophys. Res., 71: 3755-66(Aug. 1, 1966).

The integral spectrum for low-energy electrons was measured with detailed definition of temperature and number density throughout the IMP 2 orbit. Electrons are found to have a Maxwellian distribution at energies below 2.0 ev with a component of higher energy. The electron temperature typically increases from above the ionosphere as the square of the radial distance, whereas the number density decreases approximately as the inverse cube of the distance out to 5 R_E. From 5 to 15.9 R_E (apogee) the temperature remains between 1.0 and 2.0 ev, and the number density remains between 25 and 50 electrons/cm^{-3}. It is verified that the observed positive ion density of 25–50 cm^{-3} is in agreement with the number of electrons observed per unit volume in the solar wind region. The location of the magnetopause is not evident in the low-energy electrons; however, a small temperature increase is noted at the shock boundary. An intensity increase is noted in the energetic electron component in the magnetosheath. Data for a six-month period covering a 180° sector of the earth's environment are reported on. These observations constitute the first integral measurements in the solar wind region of charged particle spectra in the energy range 0 to 45 ev. The observations of the number density are in disagreement with presently accepted solar wind theory but are not inconsistent with previous measurements of the streaming ions. (auth)

39979 GEOMAGNETIC AND SOLAR DATA. Lincoln, J. Virginia (Inst. for Telecommunication Sciences and Aeronomy, Boulder, Colo.). J. Geophys. Res., 71: 3793-8 (Aug. 1, 1966).

Data collected during 1964, 1965, and January through March 1966 on principal magnetic storms are tabulated. Observatories, Greenwich date, storm time, sudden commencement information, activity observations, and ranges are shown. Selected geomagnetic and solar data collected during March 1966 are included. (J.H.M.)

39980 THEORETICAL TIME-DEPENDENT THERMAL BEHAVIOR OF THE IONOSPHERIC ELECTRON GAS. da Rosa, A. V. (Stanford Univ., Calif.). J. Geophys. Res., 71: 4107-20(Sept. 1, 1966).

The considerable theoretical work done on the thermal behavior of the ionospheric plasma by Hanson, Dalgarno, Geisler and Bowhill, and other authors is extended here from the steady-state solutions found by them to a time-dependent solution that allows the examination of the temperature changes in the ionosphere at dawn. Physical consideration of this problem leads to models that can be mathematically represented by a second-order, nonlinear, partial differential equation, the numerical integration of which presents serious stability difficulties. An unconditionally stable form of the equivalent difference equation is used in solving numerical examples worked out for models that attempt to represent the dawn ionosphere at summer and winter for both solar cycle maximum and conditions, and the following conclusions are drawn: (a) very substantial heating occurs in the ionosphere before any perceptible increase in ionization. Experimental evidence shows that a measurable increase of ionization begins at a solar zenithal angle of about 95°, while considerable heating starts at angles larger than 110°. (b) As the sun begins to shine on the high atmosphere, the competing effects of increasing heat production and growing heat capacity of the electron gas result in an electron gas temperature that initially rises fast, reaches a peak, and then declines. This peak is more pronounced the higher the altitude and predominates in the winter when the electron concentration buildup is faster. (c) Owing to smaller electron concentration in the summer, the temperatures during this season are higher than in the winter. (d) The much slower rate of increase of electron concentration during the solar cycle minimum period results in a tendency for the temperatures in this period to be higher than during the solar cycle maximum. (e) In most models it is observed that up to the time when the temperature reaches its peak, it is practically height independent at levels above the altitude of maximum heat production. Later a "bulge" is formed at the altitude of maximum heat production, and a negative gradient of temperature exists in the higher levels resulting in an upward heat flow. (auth)

39981 RADIATION FROM POSITIVE PARTICLES PENETRATING THE AURORAL ATMOSPHERE. Eather, R. H. (Rice Univ., Houston, Tex.). J. Geophys. Res., 71: 4133-40(Sept. 1, 1966).

Recently published cross-sectional information is used to set upper and lower limits to the expected Hα, Hβ, and He I λ5876 emissions due to fast protons and α particles penetrating the atmosphere in the auroral zones. The calculated λ5876 emission per incident α particle is about two times the Hβ emission per incident proton. If the ratio of precipitating α particles to protons in the auroral zones is of the order 0.1, the λ5876 line should be detectable in auroras. (auth)

39982 THE LUNAR PERIOD, THE SOLAR PERIOD, AND K_p. Rassbach, M. E. (Rice Univ., Houston, Tex.); Dressler, A. J.; Cameron, A. G. W. J. Geophys. Res., 71: 4141-6(Sept. 1, 1966).

The variation of geomagnetic activity with the phase of the moon was tested for statistical significance. The fluctuations in K_p at the lunar period are typical of the periods near it and in fact are within one standard deviation of the average fluctuation amplitude. Furthermore, these K_p fluctuations appear to be due to the sun. The so-called 27-day peak due to the sun (the well-known M-region effect) has a width of about a week and thus is not a sharp peak but contributes to periods between about 24 and 31 days. Any narrow-banded detection system, such as the superposed epoch analysis, will sense the solar effect anywhere within this broad interval. The 29.5-day lunar period falls within the interval; K_p analyses at the lunar period should take into account the nonrandom variation in K_p caused by the broad solar peak. It is shown that previous analyses concluding that there is a significant lunar-K_p effect have treated the data so as to disregard the possible solar origin of the effects found. When the solar peak is included in the analyses, the hypothesized lunar effect falls well within the limits of chance occurrence. It is concluded that the available data do not indicate any statistically significant lunar influence on geomagnetic activity; the effect at 29.53-days periodicity that was attributed to the moon is actually due to the sun. (auth)

39983 BEHAVIOR OF TRAPPED ELECTRONS AND PROTONS AT THE LOWER EDGE OF THE INNER RADIATION BELT. Imhof, W. L.; Smith, R. V. (Lockheed Missiles and Space Co., Palo Alto, Calif.). J. Geophys. Res., 71: 4157-71(Sept. 1, 1966).

Fluxes and energy distributions of trapped electrons and fluxes of trapped protons were measured at the lower edge of the inner radiation belt following two different energy selective redistributions of electrons at 1.34 Mev and at 0.74 Mev. Each of the two groups of electrons decayed at a rate that was in agreement with atmospheric scattering calculations. Thus it is concluded that at the observations in October–November 1963, scattering by atmospheric collisions was the dominant over-all loss mechanism for electrons trapped on magnetic shells with $1.145 \lesssim L \lesssim 1.160$. All electrons on a given L shell with $0 \lesssim h_{min} \lesssim 350$ km decayed at approximately the same rate, consistent with theoretical calculation. The unexpectedly large fluxes of electrons for $0 \lesssim h_{min} \lesssim 150$ km and for $1.145 \lesssim L \lesssim 1.160$ indicate a rather steady injection of electrons at high B values by processes in addition to small-angle atmospheric scattering. The time behavior and the energy spectrum variations suggest that these electrons originated from a pitch-angle redistribution of some of the electrons trapped at higher altitudes on the same or nearby magnetic field lines. The integral fluxes of protons above ~70 Mev trapped on magnetic field lines with $1.145 \lesssim L \lesssim 1.160$ were steady during this same

time period. For 200 km $\lesssim h_{min} \lesssim$ 350 km, the measured proton spatial distribution is consistent with that calculated using a source that is uniform in time and space (in this region) and a loss mechanism consisting of atmospheric ionization and excitation. For $h_{min} \lesssim$ 200 km the fluxes of trapped protons did not fall off with decreasing h_{min} as rapidly as predicted. (auth)

39984 ISOTOPIC COMPOSITION OF XENON FROM Ca-POOR ACHONDRITES. Rowe, M. W.; Bogard, D. D. (Univ. of Arkansas, Fayetteville). J. Geophys. Res., 71: 4183-8(Sept. 1, 1966).

The isotopic composition of xenon extracted from six samples of five Ca-poor achondrites is presented. The data suggest that the principal component in all the samples studied (except Shallowater) is probably atmospheric xenon, which is simply adsorbed onto the meteorite, presumably during the terrestrial life of the sample. A quite high $^{129}Xe/^{130}Xe$ ratio is observed in xenon from the Shallowater enstatite achondrite, which contained relatively large amounts of primordial xenon compared to the other Ca-poor achondrites. The large special anomaly is thought to imply a genetic relationship between the enstatite achondrites and enstatite chondrites. (auth)

39985 VARIATIONS IN f_0E AND f_0F_2 AT WASHINGTON, D. C., NEAR DAYS OF INCREASED GEOMAGNETIC ACTIVITY. Noonkester, V. R. (Navy Electronics Lab., San Diego, Calif.). J. Geophys. Res., 71: 4192-5(Sept. 1, 1966).

Simultaneous long-term variations in midday averages of f_0E and f_0F_2 at Washington, D. C., before and after large increases in geomagnetic activity, are examined. The variation f_0F_2 near days of large increases appears to depart from the accepted variation of hourly values of f_0F_2 near sudden commencements of magnetic storms. Also, the present theories do not appear to explain large predisturbance values of ⟨fF⟩ or the absence of a response in ⟨fF⟩ during sunspot minimum. (J.H.M.)

39986 EVIDENCE FOR CONNECTION OF GEOMAGNETIC TAIL LINES TO THE INTERPLANETARY FIELD. Lin, R. P.; Anderson, K. A. (Univ. of California, Berkeley). J. Geophys. Res., 71: 4213-17(Sept. 1, 1966).

Recent observations of electrons with kinetic energy above 40 kev in interplanetary space following solar flares are discussed and the properties of the solar fluxes are summarized. Measurements on these events using the IMP-3 satellite are reported. Several possible ways exist to account for the remarkable result that electrons with low magnetic rigidity readily appear in the geomagnetic tail. After eliminating several of these possibilities it is concluded that at least some of the lines of force in the geomagnetic tail connect directly into interplanetary field lines behind the earth. An upper limit is proposed on the goecentric distance behind the earth that this field line connection takes place. Consequences to models of the geomagnetic tail are discussed and future observations bearing on the problem are mentioned. (W.D.M.)

39987 GALACTIC DEUTERIUM AND ITS ENERGY SPECTRUM ABOVE 20 Mev PER NUCLEON. Fan, C. Y.; Gloeckler, George; Simpson, J. A. (Univ. of Chicago). Phys. Rev. Lett., 17: 329-33(Aug. 8, 1966).

The fluxes and energy spectra of deuterium, protons, and helium were measured on the IMP-III satellite at a time near minimum solar activity. The deuterium differential energy spectrum in the range 17-63 Mev/nucleon is $\propto E^{+2}$ and, at 60 Mev/nucleon, the relative abundance ratios are $^2H/^4He = 0.15$ and $^2H/^1H = 0.05$. If present values of experimental cross sections for the production of ^2H from nucleon interactions with ^4He are used, the observed deuterium abundance may be accounted for by the traversal of ^4He through 4 to 6 g/cm^2 of matter is cosmic-ray sources and the interstellar medium. (auth)

39988 DIRECTIONAL VARIATION OF GEOMAGNETIC CUT-OFF RIGIDITY AROUND HYDERABAD, INDIA. Daniel, R. R.; Stephens, S. A. (Tata Inst. of Fundamental Research, Bombay). Proc. Indian Acad. Sci., Sect. A, 63: 275-83(May 1966).

The geomagnetic cutoff rigidities for cosmic ray particles arriving at the top of the atmosphere over Hyderabad, India (geographic latitude 17.6°N and longitude 78.5°E), as a function of zenith and azimuthal angles and the vertical cutoff rigidities for a few neighboring locations, were made using the sixth degree simulation of the geomagnetic field by the CDC 3600 computer. (auth)

39989 MAGNETIC COORDINATES. McIlwain, Carl E. (Univ. of California, San Diego, La Jolla). Space Sci. Rev., 5: 585-98(Aug. 1966).

The definitions and properties of the magnetic coordinates B, L, K, Φ_0, R, λ and Λ are reviewed. The roles these parameters play in the study of geomagnetically trapped particles are discussed in detail. The intrinsic accuracy of the magnetic shell parameter L is examined as are the accuracies which are desired, available, and possible. A plea is made for the adoption of standard methods of presenting results. (auth)

39990 BALLOON OBSERVATIONS OF INFRARED AND X-RAY INTENSITIES IN THE AURORAL ZONE. Wax, Robert LeRoy. Berkeley, Calif., Univ. of California, 1965. 73p.

Thesis.

During September and October, 1964, a series of eight balloon flights were flown in the northern auroral zone at Fairbanks, Alaska. These balloons carried x-ray scintillation counters for the observation of aurorally associated bremsstrahlung and lead sulfide photodetectors for the observation of the total intensity of infrared radiation emitted by the sky in the spectral region from 0.7 to 2.7 microns. Rapid and irregular fluctuations of the infrared intensity indicated the presence of auroras on several of the flights. The brightest aurora observed was nearly an IBC Class III. The infrared nightglow from OH was observed also. During extended periods of auroral activity, the intensity of the nightglow was enhanced to a level as much as four times background. The x-ray fluxes and the infrared intensities did not have detailed time correlations, but in general, on a night that showed enhancement of the infrared intensity, the x-ray rate also was above background. Correlations of the infrared auroral intensity with cosmic noise absorption, visible auroras, and magnetic activity are considered. The total energy input of an auroral display is calculated from the direct knowledge of the infrared intensity. This total energy is compared to the amount of energy carried by the electrons of energy greater than 25 kev, which produced the observed bremsstrahlung, and it is found that these electrons carry less than 1% of the total auroral energy. (Dissertation Abstr.)

39991 COSMIC RAY PRODUCED PHOSPHORUS ISOTOPES IN ATMOSPHERE. Rao, M. N.; Husain, L.; Kuroda, P. K. (Univ. of Arkansas, Fayetteville). 12p. (CONF-660401-10). ORAU. Gmelin, AED-CONF-66-061-17.

From American Meteorological Society, American Geophysical Union, Annual Joint Meeting, Washington, D. C.

Concentrations of ^{33}P and ^{32}P isotopes produced in the atmosphere by interactions of secondary neutrons from cosmic rays with argon atoms in atmosphere are determined radiochemically by isolating them from about 100 liters of rain water. The experimental $^{33}P/^{32}P$ ratios vary from 0.8 to 1.7. The experimental values are compared with the calculated ones for mid-latitudes by the method of Lal, Malhotra and Peters (1958). The calculated and observed annual deposition rates are compared for ^{32}P and ^{33}P isotopes. (auth)

39992 CHARGED PARTICLE FLUXES IN THE INNER VAN ALLEN BELT PRIOR TO THE JULY 9, 1962, HIGH ALTITUDE NUCLEAR TEST. Kuck, George A. (Cambridge Research Labs., L. G. Hanscom Field, Mass.). 37p. (CONF-651067-1). ORAU. Gmelin, AED-CONF-65-351-1.

From 12th Annual Air Force Science and Engineering Symposium, Brooks AFB, Tex.

Charged particles were measured in the inner Van Allen belt on December 19, 1961. The instrument was carried on a ballistic trajectory by an Atlas Pod. A phoswich scintillator arrangement was used in which a thin CsI(Tl) crystal was placed over a thick plastic scintillator. Pulse-height analysis was done on the scintillators to give fluxes at different energies. The data perpendicular to the magnetic field at L = 1.25 ± .05, B = .190 ± .002 was fit to exponential form. The reanalysis of this pre-Starfish data showed that the electron spectrum was $N_e(E) = 3.3 \times 10^6\ e^{-2.8E}$ electrons-cm^{-2}-sec^{-1}-ster^{-1}-Mev^{-1}. The proton spectrum obtained was $N_P(E) = 44e^{-.09E}$ protons-cm^{-2}-sec^{-1}-ster^{-1}-Mev^{-1}. From these parameters it was determined that the number of electrons E > 1 Mev was approximately 10^5 electrons-cm^{-2}-sec^{-1}-ster^{-1} perpendicular to B. (auth)

39993 GRADIENT INSTABILITIES AS POSSIBLE CAUSES OF IRREGULARITIES IN THE IONOSPHERE. Liu, C. H.; Yeh, K. C. (Univ. of Illinois, Urbana). 22p. (CONF-660443-2). ORAU. Gmelin, AED-CONF-66-142-5.

From International Scientific Radio Union Conference, Washington, D. C.

A theory is proposed to explain the production of certain irregularities in the ionosphere. It is found that the region of the ionosphere below the peak of the electron distribution may become unstable because of the joint effect of the gravitational field and the positive electron density gradient there. The unstable modes are found to correspond to quasi-transverse modes. For the case when only plasma is considered, the condition for instability to occur is $g\rho_p'/\nu\rho_p > \xi$, where g is the gravity, ρ_p the plasma density, ρ_p' its height gradient, ν ion-neutral collisional frequency and ξ is the effective attachment coefficient. When the coupling between plasma and neutral particles is taken into account, additional instability condition may occur when the neutral particle distribution has a positive density gradient. This quasi-transverse unstable mode is proposed as a possible causative mechanism for the formation of irregularities in the ionosphere. When either one of the instability criteria is satisfied, spontaneous generation of irregularities is possible. Some experimental evidences are presented and discussed. (auth)

39994 ELECTRON TEMPERATURES IN THE D REGION. Dalgarno, A.; Henry, R. J. W. (Queen's Univ., Belfast). 27p. (CONF-660439-1). ORAU. Gmelin, AED-CONF-66-063-3.

From Conference on Ground-Based Aeronomic Studies of the Lower Ionosphere, Ottawa, Ontario, Canada.

Detailed estimates are made of the rates of energy loss of electrons moving in the D region and it is argued that the electron gas has a negligible non-thermal component. The Maxwellian velocity distribution of the thermal component is brought about by collisions with molecular nitrogen involving rotational transitions and the distribution is determined by the neutral particle gas temperature. (auth)

39995 D-REGION ELECTRON DENSITY DISTRIBUTIONS DEDUCED FROM THE REFLECTION OF LOW- AND VERY-LOW-FREQUENCY RADIO WAVES. May, B. R. (Radio and Space Research Station, Slough, Eng.). 23p. (CONF-660439-3). ORAU. Gmelin, AED-CONF-66-063-4.

From Conference on Ground-Based Aeronomic Studies of the Lower Ionosphere, Ottawa.

Results of the determination of the height distribution of electron density in the D region from observations of the reflection of low- and very-low-frequency radio waves are given. The electron distributions were obtained using a "trial and error" process, in which a search was made for distributions whose calculated reflection properties were in agreement with observations. The reflection properties of the distributions were calculated using the "full-wave integration" technique. The D region electron density distribution and the way in which it varies during the day, the year, the sunspot cycle, and during an eclipse and a "sudden ionospheric disturbance" is shown. (auth)

39996 TRANSVERSE HYDROMAGNETIC DISTURBANCES AT 1100 km IN THE AURORAL REGION. Zmuda, A. J.; Martin, J. H.; Heuring, F. T. (Johns Hopkins Univ., Silver Spring, Md.). 43p. (CONF-660443-1). ORAU. Gmelin, AED-CONF-66-142-2.

From International Scientific Radio Union Conference, Washington, D. C.

Transverse hydromagnetic disturbances are regularly observed at 1100 km altitude in the auroral region with the magnetically oriented satellite 1963-38C. For the dayside period 1000–1400 LT the lower-latitude boundary of the disturbance region has an average invariant latitude Λ_b of 76° during magnetic quiet ($K_p < 40$) and shifts southward to $\Lambda_b = 68°$ during periods of magnetic activity ($K_p \geq 40$). For 2300–0100 LT, this latitude is 67° when $K_p < 40$ and 63° when $K_p \geq 40$. The hydromagnetic amplitudes range from about 30 γ (the minimum here detectable) to 380 γ, or about 1% of the local geomagnetic field. Such variations are absent between $\Lambda = 31°$ (the minimum sampled) and the Λ_b appropriate to the local time and K_p. The results indicate that the transverse variations propagate along the auroral field lines, with little or no energy being transmitted in other directions. The quiet-time location and diurnal variation of the hydromagnetic disturbance region correspond to those for the auroral oval and the trapping cutoff for electrons ≥40 kev; all three phenomena have a nightside position comparable to the trapping cutoff for electrons ≥280 kev and ≥1.2 Mev, whose dayside displacement is also toward higher latitudes but with a smaller diurnal shift, ≈2°. The location and diurnal variation of the region containing most of these geophysical properties are reflected in the surface values of magnetic intensity recorded at the Baker Lake ($\Lambda = 75°$) and Fort Churchill ($\Lambda = 70°$) observatories: around local noon the Baker Lake values exceed those for Fort Churchill while the reverse is true at local midnight. It is suggested that the hydromagnetic variations on the dayside have their origin in the particles and surface currents on the magnetopause; and on the nightside, in the particles and currents from the neutral sheet. The transverse hydromagnetic disturbances occur on L shells which also contain the polar electrojet as determined by surface observations. (auth)

Gravitation, Quantum Mechanics, and Relativity Theory

39997 (JINR-P-2758) METOD FAZOVYKH FUNKTSII V KVANTOVOI MEKHANIKE. (Method of Phase Functions in Quantum Mechanics). Babikov, V. V. (Joint Inst. for Nuclear Research, Dubna (USSR). Lab. of Theoretical Physics). 1966. 30p. Dep. mn.

A brief review is given of a method for solving the problems of quantum mechanics in nuclear and atomic physics, which is widely developed of late. The method of phase functions proved to be very convenient in practical calculations as well as in a number of general problems of quantum mechanics. (auth)

39998 (KAPL-3147) A MATHEMATICAL FOUNDATION FOR EMPIRICAL SCIENCE, WITH SPECIAL REFERENCE TO QUANTUM THEORY. PART I. A CALCULUS OF EXPERIMENTAL PROPOSITIONS. Randall, C. H. (Knolls Atomic Power Lab., Schenectady, N. Y.). June 1966. Contract W-31-109-eng-52. 223p. Dep. mn. CFSTI $6.00 cy, $1.25 mn.

The aim of an empirical science is to order, explain and predict the observable events associated with certain physical situations or experiments. As such its mathematical foundations ought to be erected on a formal language capable of describing these physical occurrences with adequate precision. The direct approach is to synthesize a formal symbolic logic from the real physical operations employed in an empirical science. In this regard formal symbolic logic is a collection of propositions partly ordered by some implication relation. The operational point of view has the virtue of providing such a logic without first committing itself to some model of reality. The calculus of experimental propositions is investigated. Topics discussed are histori-

cal review; experiments (events and operation); lattice of events (objective implication and simultaneous observability); conditioning (temporal order); operational, perspective, and translational equivalence; free operational logic; and sublogics. (B.G.D.)

39999 EQUATION OF MOTION OF A POINT MASS UNDER CONSIDERATION OF GRAVITATIONAL RADIATION TERMS. Schmutzer, Ernst (Friedrich-Schiller-Univ., Jena, Ger.). Ann. Physik (7), 17: 107-12(1966). (In German).

The equation of motion obtained by Havas and Goldberg for a point mass under consideration of the gravitational radiation terms was derived by using the Galilean proper time as a parameter. The effect of energy absorption in respect to radiation of negative energy of the particles is neglected, if the general relativistic proper time is used consequently as the parameter. The radiation terms then contain in part, other coefficients and signs. (tr-auth)

40000 STUDY OF THE ORBITAL DEGENERACY OF THE COULOMB POTENTIAL IN GROUP THEORY. I. Antoine, J.-P. (Univ., Louvain, Belg.). Ann. Soc. Sci. Brux. Ser. I, 80: 169-84(July 16, 1966). (In French).

The angular degeneracies of the Schrödinger equation with a central potential in f dimensions are studied. In the Coulomb case the known results of Fock and Bargmann are obtained. The geometric aspect of the method is emphasized using explicity not only the Lie algebra, but also the Lie group generated by this algebra, i.e., the full symmetry group. The discrete spectrum is considered. (auth)

40001 SOME COLLAPSING CYLINDERS AND THEIR EXTERIOR VACUUM METRICS IN GENERAL RELATIVITY. Cocke, W. J. (Institut Henri Poincare, Paris. Aerospace Corp., El Segundo, Calif.). Contract AF 04(695)-669. J. Math. Phys. (N. Y.), 7: 1171-8(July 1966).

A cylindrical form of the Friedman metric is used to obtain nonstatic infinite cylinders of incoherent fluid. The vacuum metrics exterior to the cylinders are determined from the hypothesis that the metric tensor and its first partial derivatives be continuous. This hypothesis is applied by requiring the continuity of the first and second fundamental forms of the boundaries of the cylinders. The exterior metrics are nonstatic and may be expressed in the Einstein–Rosen form, and equations governing their behavior are derived. It is found that the exterior metric carries a flux of gravitational "C energy," the direction of which in the Einstein–Rosen frame is the same as that of the surface of the cylinders. (auth)

40002 COVARIANT CONSERVATION LAWS FOR GENERAL RELATIVISTIC EXPLODING MATTER. Droz-Vincent, Philippe H. (Centre National de la Recherche Scientifique, Paris. Univ. of North Carolina, Chapel Hill). J. Math. Phys. (N. Y.), 7: 1179-84(July 1966).

A general relativistic extension of some simple notions, e.g., total angular momentum, so far correctly defined only in the frame of special relativity is attempted. The mathematical aspect of the problem leads to the question of how to construct an integral object, conserved in time and covariant given a tensor of vanishing divergence. A formalism based upon bitensors ensures the covariance, while the assumption of an exploding (or imploding) schema of matter seems to be the only available means to preserve conservation when the space-time is curved. This can be formulated in a general theorem then applied to different physical situations. The total linear momentum occurs as a vector fixed at the point of explosion (or implosion). Its length turns out (at least when a pure matter schema is concerned) to be superior to the total mass of the fluid. The excess appears as the energy carried by the explosion. The case of a so called "uncompressible" holonomic fluid gives a quite analogous result. In order to find a nontrivial angular momentum the case of a fluid possessing an intrinsic spin density is also considered. Both linear and angular momenta are conserved and covariantly defined. Moreover, they reduce to the conventional ones when the curvature vanishes. (auth)

40003 ELECTROMAGNETIC FIELDS OF MOVING DIPOLES AND MULTIPOLES. Ellis, J. R. (Bedford Coll., London). J. Math. Phys. (N. Y.), 7: 1185-97(July 1966).

A method of invariant Green's functions which is frequently used to find the fields of a moving charge is applied to evaluate the fields of dipoles and multipoles. Concise expressions are obtained from the integrals by successively integrating by parts. Two well-known methods for finding the radiation field on the world line of charge are repeated for a dipole. It is found that a nonrotating (Fermi-Walker propagated) electric dipole has vanishing radiation field on the world line when it moves hyperbolically, as in the corresponding case for a charge. Radiation on the world lines of multipoles is also discussed (with particular reference to quadrupoles and octupoles), and the problem of evaluating the radiation reaction for a dipole is described within the context of the methods here given. It is further shown that a classical description of mass renormalization is possible to within the approximation of first-order terms, but not beyond. (auth)

40004 WICK POLYNOMIALS AT A FIXED TIME. Jaffe, Arthur (Princeton Univ., N. J.). J. Math. Phys. (N. Y.), 7: 1250-5(July 1966).

In general, a Wick polynomial must be smeared with a test function depending on both time and space in order to yield an operator in Hilbert space. However, in space time of two dimensions, it is sufficient to smear in the space direction alone. This statement is proved by an application of Weinberg's asymptotic theorem. Operators formed in this manner are candidates for approximate interaction hamiltonians. (auth)

40005 EXACT INVARIANTS FOR A CLASS OF NON-LINEAR WAVE EQUATIONS. Kruskal, Martin D. (Princeton Univ., N. J.); Zabusky, Norman J. J. Math. Phys. (N. Y.), 7: 1256-67(July 1966).

A method is given for obtaining explicitly an infinite number of exact invariants for a physical system described by the coupled set of first-order hyperbolic partial differential equations $\partial u_i/\partial t = A_{ij}(u_0, u_1, \ldots u_n)\,\partial u_j/\partial x$ (i,j = 0, 1, . . ., n). (A1) Temporal and spatial invariants are constructed as integrals of temporally and spatially invariant densities T and X, over appropriate spatial and temporal intervals, respectively. For physical systems the energy and momentum densities are temporal invariant densities. These invariant densities are solutions of the hodograph transformed equations corresponding to (A1). For the case n = 1 every invariant density T satisfies an equation in conservation form: $(T_{u_x})_t - (T_{u_t})_x = 0$. The methods are applied to the equation $y_{tt} - (1 + \epsilon y_x)^\alpha y_{xx} = 0$, and a denumerable infinity of invariant densities, each expressible as a polynomial, are calculated in two equivalent cases: the first when (A2) (with $\alpha = 1$) is expressed in zero diagonal form $u_t = v_x$, $v_t = (1 + \epsilon u)u_x$, where $u = y_t$ and $v = y_t$; and the second when (A2) is expressed in diagonal form $r_t - \Phi r_x = 0$, $s_t + \Phi s_x = 0$, where $\Phi = (\tfrac{1}{2}\epsilon(2 + \alpha)(r + s))^{\alpha/(2+\alpha)}$ and r and s, the Riemann invariants of (A2), are related to u and v. A theorem of Noether is used to construct from the invariant densities continuous transformation groups that leave the action functional invariant. Using the methods of Kruskal the adiabatic invariant is derived for the continuous system (A2) ($\alpha = 1$) which has nearly periodic solutions. To order ϵ the adiabatic invariant is identical with one of the exact invariants and gives no new information about the system. (auth)

40006 CLASSICAL FIELD THEORY AND GRAVITATION IN A DE SITTER WORLD. Roman, P.; Aghassi, J. J. (Boston Univ.). J. Math. Phys. (N. Y.), 7: 1273-83(July 1966).

The algebra and the calculus pertaining to a certain class of representations of the de Sitter group is developed. This permits a formulation of covariant field equations in de Sitter space, and, in particular, the construction of quantum mechanical equations of motion associated with particles of given spin. The gauge principle is invoked and a spin-two field emerges, which is identified with the

gravitational field. Its coupling to sources is discussed and conservation laws are derived. The emerging nongeometric theory of gravitation is compared with both the Einstein–Riemann type and other previously proposed nongeometrical theories. (auth)

40007 GLOBAL COVARIANT CONSERVATION LAWS IN RIEMANNIAN SPACES. [PART] I. Shepelavey, Bohdan (General Electric Co., Syracuse, N. Y.). J. Math. Phys. (N. Y.), 7: 1303-9(July 1966).

It is demonstrated that in the theory of general relativity integral conservation laws can be obtained from a vanishing covariant divergence of a tensor in a completely covariant form. This is achieved by introducing into tensor calculus a new operation, namely, tensor integration which is defined as an inverse of tensor differentiation. In particular, a one-dimensional absolute integration of a tensor along a curve is defined as an inverse operation to the same type of differentiation. A representation of absolute integration is developed by a perturbation method as an infinite series where each term consists of ordinary integrations only. As an example of absolute integration, a vector field is obtained whose components can be employed as a coordinate frame having a very close resemblance to the Riemannian coordinates. Covariant integration is then introduced as an inverse of covariant differentiation; however, its usefulness is severely limited by the conditions of integrability which have to be satisfied to make covariant integration possible. A set of unspecified covariantly constant base vectors is used to explain the idea of a covariantly constant tensor and to express symbolically absolute integration in terms of the ordinary integration. The one-dimensional absolute integration is then extended to higher dimensions in such a way that it is independent of the order of integrations. Finally, Gauss' theorem is proved for the absolute integration which enables one to convert a volume integral of a covariant divergence of a tensor into a corresponding surface integral of the same tensor. (auth)

40008 GLOBAL COVARIANT CONSERVATION LAWS IN RIEMANNIAN SPACES. [PART] II. Shepelavey, Bohdan (General Electric Co., Syracuse, N. Y.). J. Math. Phys. (N. Y.), 7: 1310-20(July 1966).

Using the idea of tensor integration, the vector field developed previously and the full Bianchi identities, it is shown that in a general Riemannian space there are four global covariantly conserved tensors. The ranks of these tensors are three, four, five, and six. The traces of the first two of these tensors yield the generally covariant equivalent of the familiar linear and angular momentum. The remaining four traceless tensors describe, residually, the gravitational field. With each covariantly conserved tensor one can associate a number of independent invariants. Such invariants are conserved in the ordinary sense. Among these are two types of rest energies and two types of angular momentum magnitudes obtained from the trace and traceless tensors. Examples of global, conserved tensors are derived for a Schwarzschild metric with the electron mass, and a metric of a point electron. It is shown that the rest energy of the Coulomb field diverges as $\ln(1/r)$ at the origin and the second rest energy, that is, the rest energy of the gravitational field diverges as $\ln r$ as r approaches infinity. When cutoffs are introduced at the Schwarzschild radius r_0, at the classical electron radius r_1, and at the radius of the visible universe r_2, the rest energy of the gravitational field contained in the shell of thickness $r_1 - r_0$ is approximately 100 times that of the electron rest energy. It is twice this value in the entire visible universe. Since the gravitational field is described by the traceless tensors and the former forms a heavy, compact cloud around the point particle, it is conjectured that the traceless tensors represent the internal degrees of freedom of the elementary particles. (auth)

40009 CYLINDRICAL GRAVITATIONAL NEWS. Stachel, John J. (Boston Univ.). J. Math. Phys. (N. Y.), 7: 1321-31(July 1966).

The concepts of news function and mass aspect are generalized to a class of cylindrically symmetric metrics containing both degrees of freedom of the gravitational field. It is proved that the mass/unit length always decreases if there is any cylindrical news. The asymptotic behavior of the Riemann tensor in the cylindrical case is analyzed and a peeling theorem proved for this case. An example is given to show that asymptotic conditions on the metric or the Riemann tensor which are analogous to the conditions used in the asymptotically spherical case do not exclude certain infinite incoming radiation trains in the cylindrical case. Pure incoming and outgoing solutions are defined for the cylindrical case, and their generalization to the asymptotically spherical case is suggested. An exactly conserved quantity is shown to exist which may be the cylindrical analog of the ten exactly conserved quantities recently discovered by Newman and Penrose. (auth)

40010 RAYSKI FORMULATION OF THE LAWS OF CONSERVATION FOR THE EXACT STATIC METRIC. Horsky, J. (Brno Univ.). Phys. Lett., 22: 282-3(Aug. 15, 1966).

Rayski's method of formulating the laws of conservation in general relativity by tetrad fields is discussed. (B.G.D.)

40011 mTH-ORDER ADIABATIC INVARIANCE FOR QUANTUM SYSTEMS. Sancho, F. J. (Univ. de Navarra, San Sebastian, Spain. Instituto de Fisica Teorica, Barcelona, Spain). Proc. Phys. Soc. (London), 89: 1-5(Sept. 1966).

The approximate validity of the quantum adiabatic theorem is established without the restriction of considering the spectrum of the discrete and non-degenerate Hamiltonian, provided that the assumptions made in a previous paper are fulfilled. (auth)

Low Temperature Physics

Refer also to abstract 39733.

40012 (COO–1198-364) ION MOBILITY IN LIQUID ^{3}He BELOW 1 DEG K. Kuchnir, Moyses (Illinois Univ., Urbana). May 1966. Contract AT(11-1)-1198. 104p. Dep. mn. CFSTI $4.00 cy, $1.00 mn.

Thesis.

The low field mobility of positive and negative ions in liquid ^{3}He was measured for temperatures between 0.03°K and 1°K and pressures of 27.9 atm, 7.5 atm, and less than 0.35 atm. Ions in the liquid were produced by a radioactive tritiated titanium source and their mobility was obtained by directly measuring their drift velocity using a time of flight technique which involved a multigrid system of electrodes. Details of the experimental procedures as well as of the experimental apparatus and its construction are given. The positive ion mobility, μ_+, was found to be larger than the negative, μ_-, except at 27.9 atm above 0.3°K, where both are $\approx$0.036 cm^2/V sec. By increasing the pressure, μ_- was observed to increase while μ_+ decreased. Furthermore, μ_- was found to be a continuous function of the temperature, reproducible within 1% throughout the entire temperature range of the measurements, while μ_+ presented hysteresis in a temperature range that depended on the pressure. The experimental results are presented in both graph and table forms. Some typical mobility values are given. The "cluster" model for the positive ion and the "bubble" model for the negative ion in liquid helium are discussed and applied for liquid ^{3}He. The temperature and pressure dependence of μ_- between 0.03°K and 0.07°K is in agreement with the theoretical prediction for the mobility of an electron localized in a bubble that undergoes Brownian motion in a Fermi gas. No theoretical calculation available predicts μ_- between 0.07°K and 1°K or μ_+ correctly. (auth)

40013 (IS-T-84) THE HEAT CAPACITY OF SOLID ^{3}He. Sample, Howard Harshaw (Ames Lab., Iowa State Univ. of Science and Tech.). July 1966. Contract W-7405-eng-82. 139p. Dep. mn. CFSTI $4.00 cy, $1.00 mn.

Thesis.

Specific heat measurements were made from 0.2°K to the

melting line for solid ^{3}He at nine densities and for solid ^{4}He at one density. The results, which cover molar volumes from 23.80 cm^3 to 11.42 cm^3, everywhere were accurate to better than 1% in an equivalent θ_D. The relatively high precision of these experiments and their wide temperature range enabled a determination of the thermal equations of state of both hcp and bcc solid ^{3}He quite unambiguously. The $\theta_0(V)$ relationship which was obtained for hcp ^{3}He gave values of γ which varied from 2.0 at 11.42 cm^3/mole to 2.6 at 19.05 cm^3/mole. For hcp ^{4}He, the value of $\theta_{04}(V)$ and previous data can be obtained from the simple relationship $\theta_{04}(V) = \theta_{03}(V)/1.18$. The constant in this relationship was quite close to the "Debye" value of 1.154. In all other aspects, hcp ^{3}He and hcp ^{4}He appeared to behave quite like the heavier more classical inert gas solids argon and krypton, with a Grüneisen γ which increased slowly with temperature. The results for bcc ^{3}He indicated that the specific heat contains a large, apparently exponential anomalous contribution which is superimposed on a Debye-like behavior as reported previously. Low-temperature anomalies (smaller than but resembling the "linear" anomalies in previous work) were found in all the data, and are believed to be due to unknown apparatus problems. (auth)

40014 (ORNL–3989, pp 109-27) MAGNETICS AND SUPERCONDUCTIVITY. (Oak Ridge National Lab., Tenn.).

For various applications it appeared necessary to calculate new tables of the ratio B_0/B_{max} for magnet coils with rectangular cross section and uniform current density. A short description of the work needed to reach this goal is presented. The 7-MW 13-in.-ID "D coil," which produces in Helmholtz configuration a field of 62 kG and which can be operated in cusp configuration, was assembled. Electrical and mechanical tests preceding regular operation are progressing. Development work on the "ribbon coil" was continued. This new design is supposed to be used for plasma physics experiments in which the restricted space calls for magnet coils with very high current densities. The test arrangements described here consider carefully the necessity to use small header volumes. For various applications the use of iron to shape magnet fields is very convenient. Recent work in this line is the development of ferromagnetic flux tube spreaders for the Beam Plasma Facility; test results are described here. Superconductivity research was continued. Surface current phenomena on cylindrical samples of hard superconductors in longitudinal external fields were studied. Experiments were made with Nb–Zr and Pb–In samples, with sample surfaces unpolished, polished, and plated after polishing. (M.O.W.)

40015 (ORNL-TM–1598) EXPERIMENTAL SIMULATION OF LARGE, HIGH FIELD, SUPERCONDUCTING MAGNET OPERATION. Period Covered: December 1, 1965–July 31, 1966. Gauster, W. F.; Efferson, K. R.; Hendricks, J. B.; Kernohan, R. H.; Koppe, H. W.; Ullmaier, H. A.; Wilkes, W. R. (Oak Ridge National Lab., Tenn.). Aug. 19, 1966. Contract W-7405-eng-26. 80p. Dep. mn. CFSTI $3.00 cy, $0.75 mn.

Under certain conditions, stable performance of superconductors partly in normal and partly in superconducting state can be achieved even without a "stabilizer," i.e., normal material which is in close electrical and thermal connection with the superconductor. This occurs only at very low current densities; experiments and related calculations are described ("post quenching performance"). For higher current densities "compound conductors" with stabilizers of relatively large cross sections are necessary. The performance of these compound conductors is described first under the condition that the superconductor is in a perfectly resistanceless state. A useful equivalent network is described. For current densities above the critical values flux flow and thermal phenomena must be taken into account. However, if the cross section of the stabilizer is very large, it is sufficient to consider flux flow alone. Relevant experiments are discussed. A presentation is made which attempts in a simplified way to consider both flux flow and thermal performance. In this it is necessary to take into account the different modes of heat transfer to the liquid helium bath. Finally the influence of flaws of the superconductors is discussed. Several appendices describe additional work which is in part directly related to the main subjects reported. (auth)

40016 FARADAY UNIPOLAR INDUCTION IN A NONIDEAL TYPE II SUPERCONDUCTOR. LeBlanc, M. A. R.; Fletcher, E. L. (Aerospace Corp., Los Angeles). Appl. Phys. Lett., 9: 161-4(Aug. 15, 1966).

A Faraday unipolar inductor using a solid cylinder of a nonideal type II superconductor (unannealed Nb) constitutes a zero internal impedance generator capable of supplying appreciable electrical power and permits continuous study of the behavior of the average internal magnetic field vs the applied field. The various contributions to the observed emf are discussed in terms of the relativistic interpretation of Faraday unipolar induction. (auth)

40017 ENERGY DEPENDENCE OF THE EFFECTIVE INTERACTION IN SUPERCONDUCTIVITY. Ailawadi, N. K.; Radhakrishnan, V. (Tata Inst. of Fundamental Research, Bombay). Austral. J. Phys., 19: 509-18(Aug. 1966).

The effective interaction in the BCS model of superconductivity is usually approximated by a constant. The interaction is expanded in a power series in $\epsilon_k/\hbar\omega$ and the energy-dependent terms to first order are treated. This introduces one more parameter in the theory. The gap, which now becomes energy dependent, is obtained by solving an integral equation by iteration. The critical field and specific heat are calculated. The value of $2\Delta(0,0)/k_BT_c$ and the jump in the electronic specific heat at the critical temperature T_c are now dependent on the parameters of the superconductor. Calculated values for the energy gap and the critical field H_c agree rather well with the experimental data. (auth)

40018 WORLD'S LARGEST SUPERCONDUCTING MAGNET. Cryog. Eng. News, 1: No. 9, 18-19(July 1966).

The development of a 40,000-gauss superconducting magnet, 5 ft by 12 in., is discussed in terms of materials, construction, testing, equipment, and economics. Since the MHD generator application requires that the field be perpendicular to the axis of a duct carrying hot gas, the magnet windings are in a saddle-shaped configuration. The winding consists of 4450 turns of ½-inch-wide by 0.40 inch inch-thick composite-strip conductor composed of nine Nb–Zr superconducting wires embedded in high-purity copper. (W.D.M.)

40019 METHODS AND COSTS OF TESTING AT LIQUID HELIUM TEMPERATURES. Bernert, R. E. (Avco-Everett Research Lab., Everett, Mass.). Cryog. Eng. News, 1: No. 9, 24; 26; 28; 30(July 1966).

Operating costs of different methods are compared with the cost of the standard system which has only a 77°K beat station provided with liquid N_2. Topics briefly discussed include facility costs, cooldown—N_2 subcooling, operation N_2 subcooling, cooldown H_2, operation H_2, and a minimum cost system. It is concluded that significant savings are possible by using the most complex system, i.e., subcooled N_2/H_2/He. (W.D.M.)

40020 EFFECT OF MICROHETEROGENEITY ON THE CHARACTERISTICS OF SUPERCONDUCTIVITY OF Nb–Zr–Ta ALLOY. Shmulevich, R. S.; Baranov, I. A.; Karasik, V. R.; Kurganov, G. B. Fiz. Metal. Metalloved., 21: 379-83(Mar. 1966). (In Russian).

In a search for new superconducting materials, a niobium-base alloy containing 35% zirconium and 15% tantalum was tested for the effect of structural microheterogeneity on the magnitude of critical current density. Two alloy ingots were melted in an electron-beam furnace and cooled at different rates. The slowly cooled ingot had a homogenous structure and a resistivity of 49.9 μohm · cm. In the rapidly cooled ingots the dendrites were niobium- and tantalum-rich and the matrix was zirconium-rich; the resistivity of this ingot was 54.4 μohm cm. Both ingots were conditioned by machining to a diame-

ter of 4 mm, preforged, and cold drawn into wire 0.2 mm in diameter. The size of heterogeneous areas in the wire obtained from the rapidly cooled ingot was 1000 to 1500Å, i.e., of the same order as the depth of magnetic field penetration into a superconductor. The heterogeneous alloy was found to have a considerably higher critical current density than that of homogeneous alloy. The upper critical field of the former exceeds, apparently, 70 koe. (ATD)

40021 RELATIONSHIP BETWEEN THE CHARACTERISTICS OF SUPERCONDUCTIVITY AND STRUCTURE OF ZIRCONIUM–4 NIOBIUM ALLOY. Sudareva, S. V.; Buinov, N. N.; Vozilkin, V. A.; Romanov, E. P.; Rakin, V. G. (Inst. of Metal Physics, Academy of Sciences, Ukrainian SSR). Fiz. Metal. Metalloved., 21: 388-95 (Mar. 1966). (In Russian).

Zirconium-base alloy containing 4% niobium melted from 99.8%-pure zirconium and 99.4%-pure niobium, rolled at 600 to 700°C into bars, homogenized at 1280°C for 50 hr, annealed at 1200°C and water quenched, aged at 550°C for up to 1000 min, and rolled at 550°C with a reduction of 93% was tested for the effect of structure on the characteristics of superconductivity. It was found that alloy annealed at 1200°C is not superconductive at 4.2°K. Aging of annealed alloy at 550°C for 15 min brings about a precipitation of the finely dispersed β phase and the alloy becomes superconductive with a critical current density of 5000 amp/cm^2. The β-phase particles precipitate mainly at the boundaries of the martensitic needles and form a system of superconductive fibers in the nonsuperconductive matrix. Such a structure appears to have a favorable effect on the magnitude of the critical current density. Prolonged aging of annealed alloy has no additional effect on the critical current density. Alloy which, after annealing, was rolled at 550°C also became superconductive after aging at 550°C for 3 hr, but its critical current density was found to be 50,000 amp/cm^2 (one order higher than that of alloy aged without rolling). The structure of alloy in this condition is distinguished by a network of dislocations decorated by rather large (50 to 100 Å) particles of β phase and forming a system of superconducting fibers. Such a structure appears to be a specific feature of all niobium–zirconium alloys with high values of critical current density. (ATD)

40022 SIZE EFFECT IN THE INTERMEDIATE-STATE THERMAL RESISTIVITY MAXIMA IN INDIUM AND LEAD. Olsen, J. L.; Waldvogel, A.; Wyder, P. (Swiss Federal Inst. of Tech., Zurich). Helv. Phys. Acta, 39: 361-8(1966).

The size dependence of the intermediate-state thermal resistivity maxima in superconducting lead and indium was measured. At temperatures near 2°K phonon conduction is dominant in the intermediate state in lead while electron conduction dominates in indium. For the phonon case, the maximum resistivity is inversely proportional to the square root of the specimen diameter. In the electron conduction case, the ratio of maximum resistivity to the resistivity in the superconducting state is independent of specimen size at temperatures above ca. $T_c/2$. (auth)

40023 NEAR-SURFACE EFFECTS IN SUPERCONDUCTING NIOBIUM–ZIRCONIUM ALLOYS. Love, Gordon R. (Oak Ridge National Lab., Tenn.). J. Appl. Phys., 37: 3361-6(Aug. 1966). (ORNL-P–1620).

At a given magnetic field, critical currents may be induced to flow in the surface layers of a superconductor by the application of a relatively small-amplitude alternating-current field. Many measurements of this induced current have been made as a function of the intensity of the direct-current field, and the frequency and amplitude of the alternating-current field. The results of these measurements may be interpreted by assuming that there is a near-surface layer of a few hundred angstroms thickness which is able to carry extraordinary current densities from 3 to 20 times the bulk current densities at a given field. Current densities calculated for this surface layer exceed 10^7 A/cm^2 at low fields. Details of the observations vary with sample history, but the general features of these measurements have been observed in all samples tested. (auth)

40024 FERROMAGNETIC PARTICLES IN A TYPE-II SUPERCONDUCTOR. Alden, T. H.; Livingston, J. D. (General Electric Research and Development Center, Schenectady, N. Y.). J. Appl. Phys., 37: 3551-6(Aug. 1966).

A dispersion of fine, single-domain, iron particles in a superconducting Hg–13% In alloy was found to produce considerably magnetic hysteresis that was dependent on the sense of the applied field. When the applied field was parallel to the remanent particle magnetization, and particles attract and pin flux threads, the observed hysteresis was always larger than in the antiparallel case, where particles repelled flux threads. Significant sense-dependent properties were observed for particles from 20 to 200 Å in diameter, and for volume fractions from 0.01% to 1%. The results demonstrated the effectiveness of ferromagnetic particles in increasing superconducting critical currents, the superiority of attractive centers over repulsive ones, and the possibility of "directional superconductors" whose properties depend on the sense of the applied magnetic field. (auth)

40025 EFFECT OF INTERSTITIAL GASES ON THE SUPERCONDUCTING CRITICAL TEMPERATURE OF COLUMBIUM. Wiseman, Carl D. (Arlington State Coll., Tex.). J. Appl. Phys., 37: 3599-3602(Aug. 1966).

High-purity electron-beam-melted niobium was doped up to levels of 15 at.% with nitrogen, hydrogen, or oxygen, the precision lattice spacing measured, and the superconducting transition temperatures determined. The relationship between transition temperature and volume change developed for substitutional alloys was shown to be valid also for interstitial gaseous impurities. Beyond the effect each gas had upon lattice distortion, no critical temperature characteristics were observed which were dependent upon the specific element. (auth)

40026 OSCILLATIONS OF THE INTERMEDIATE STATE OF SUPERCONDUCTORS. Andreev, A. F. (Inst. of Physics Problems, Academy of Sciences, USSR). JETP Lett. (USSR) (Engl. Transl.), 4: 4-7(July 1, 1966).

Translated from Zh. Eksp. Teor. Fiz., Pis'ma Redaktsiyu, 4: 7-11(July 1, 1966).

In the intermediate state, the volume of a superconductor constitutes a system of alternating layers of normal and superconducting phases. The regular arrangement of the layers corresponds to a minimum of energy, and therefore if the layers are bent by external forces, the system will ultimately return to the unperturbed state. Small oscillations of the intermediate state, the wavelength of which greatly exceeds the dimensions of the layers of the normal phase, are described. (M.O.W.)

40027 MAGNETORESISTANCE OF BISMUTH IN FIELDS UP TO 450 kOe AT HELIUM TEMPERATURES. Brandt, N. B.; Svistova, E. A.; Tabieva, G. Kh. (Moscow State Univ.). JETP Lett. (USSR) (Engl. Transl.), 4: 17-20(July 1, 1966).

Translated from Zh. Eksp. Teor. Fiz., Pis'ma Redaktsiyu, 4: 27-32(July 1, 1966).

The results are presented for electric conductivity measurements for various Bi crystal orientations to a 450-kOe magnetic field at liquid helium temperatures. (M.O.W.)

40028 "NON-JOSEPHSON" RADIATION FROM JOSEPHSON TUNNEL JUNCTIONS. Langenberg, D. N.; Parker, W. H.; Taylor, B. N. (Univ. of Pennsylvania, Philadelphia). Phys. Lett., 22: 259-60(Aug. 15, 1966).

Josephson tunnel junctions are observed to emit microwave radiation which does not obey the generalized Josephson frequency-voltage relation $\nu = 2$ eV/nh. (auth)

40029 DISTRIBUTION OF CURRENT IN A TYPE-II SUPERCONDUCTOR. Jones, R. G.; Rose-Innes, A. C. (Univ. of Manchester, Eng.). Phys. Lett., 22: 271-2 (Aug. 15, 1966).

Experiments show that resistanceless transport current along a cylinder of very pure type II superconductors in the mixed state is concentrated into two surface bands that lie at the ends of a diameter perpendicular to the direction of the applied magnetic field. (auth)

40030 GROUND STATE OF LIQUID ^{4}He. Chester, G. V.; Reatto, L. (Cornell Univ., Ithaca, N. Y.). Contract AT(30-1)-2391. Phys. Lett., 22: 276-7(Aug. 15, 1966). (NYO-2391-31).

A new trial function for the ground state of liquid ^{4}He is proposed. This function accounts correctly for the low-lying phonon modes in the system. (auth)

40031 HELICON-LIKE RESONANCES IN SUPERCONDUCTING NIOBIUM. Druyvesteyn, W. F.; Van Gurp, G. J.; Greebe, C. A. A. J. (Philips' Gloeilampenfabrieken, Eindhoven, Netherlands). Phys. Lett., 22: 248-9(Aug. 15, 1966).

From helicon-type resonances in the mixed state of pure niobium formal resistivities are obtained, showing a dynamic Hall effect which varies linearly with the applied magnetic field. (auth)

40032 ^{4}He MELTING CURVE BELOW 1 DEG K. Straty, G. C.; Adams, E. D. (Univ. of Florida, Gainesville). Phys. Rev. Lett., 17: 290-2(Aug. 8, 1966).

Using a capacitive method of measuring pressure with a sensitivity of 10^{-4} atm, the melting curve of ^{4}He was determined below 1°K. The minimum was found at 0.775°K with an increase in pressure of 7.5×10^{-3} atm on cooling to 0.35°K. (auth)

40033 TEMPERATURE DEPENDENCE OF THE CRITICAL VELOCITY OF POSITIVE IONS IN LIQUID HELIUM. Bruschi, L.; Mazzoldi, P.; Santini, M. (Univ., Padua. Istituto Nazionale di Fisica Nucleare, Padua). Phys. Rev. Lett., 17: 292-4(Aug. 8, 1966).

It is pointed out that the critical velocity, $\langle v_c \rangle$, is no longer temperature independent above 1.1°K. Experiments were carried out at higher temperatures and it was found that: $\langle v_c \rangle$ is a temperature-dependent quantity from 1.1°K upwards; it goes through a strong minimum around 1.3°K; and from 1.4°K it decreases slowly, approaching zero at the λ point. Diagrams of the results are given. (M.O.W.)

40034 BRILLOUIN SCATTERING IN LIQUID HELIUM II. Woolf, Michael A.; Platzman, P. M.; Cohen, M. G. (Bell Telephone Labs., Murray Hill, N. J.). Phys. Rev. Lett., 17: 294-7(Aug. 8, 1966).

Using the technique of Brillouin scattering, the attenuation and velocity of high frequency (556 and 732 Mc/sec) acoustic phonons were measured in liquid helium below the lambda point. Data are given. (M.O.W.)

40035 RADIATION-INDUCED STRUCTURE IN THE d-c JOSEPHSON CURRENT. Scalapino, D. J.; Wu, T. M. (Univ. of Pennsylvania, Philadelphia). Phys. Rev. Lett., 17: 315-18(Aug. 8, 1966).

A method is analyzed for measuring the temperature dependence of the imaginary part of the gap at the gap edge, $\Delta_2(T) = \Delta_2(\Delta_0(T),T)$, based upon the behavior of the critical d-c Josephson current carried by a superconducting tunnel junction in the presence of a high-frequency electromagnetic field. It is shown that the form of this temperature dependence provides a low-frequency probe of the effective electron-phonon coupling. (auth)

40036 ENTHALPY OF IMPURE NIOBIUM IN THE MIXED SUPERCONDUCTIVE STATE. Goedemoed, S. H.; Van Kolmeschate, C.; Kes, P. H.; De Klerk, D. (Kamerlingh Onnes Laboratorium, Leiden). Physica, 32: 1183-8(June 1966).

From the simultaneous measurements of the magnetization and the heat development during the magnetization process of a second type superconductor it is possible to calculate the enthalpy. This is done for an impure niobium sample. As a result Gorter's criterion for flux jumping can be checked. It appears that this criterion holds in the first quadrant of the hysteresis loop. (auth)

40037 TWO-FLUID MODEL OF SUPERCONDUCTIVITY. Rickayzen, G. (Univ. of Kent, Canterbury, England). Proc. Phys. Soc. (London), 89: 129-34(Sept. 1966).

The basis of the two-fluid model of superconductivity is discussed especially for dirty superconductors. It is shown that for the free-electron model of a medal the superfluid velocity can be defined by $v_s = p_s/m$ where the macroscopic order parameter depends on position through the phase factor $p_s \cdot r$, and where m is the band mass. With this definition of v_s the energy and current densities have the same form in pure and impure materials. It is shown further that, for consistency with the conservation of energy, the time development of v_s is given by the usual macroscopic equation even in very impure material. (auth)

40038 THE DE GENNES METHOD OF CORRELATION FUNCTIONS IN THE THEORY OF SUPERCONDUCTIVITY. Lueders, Gerhart (Univ., Goettingen, Ger.). Z. Naturforsch., 21a: 680-8(June 1966). (In German).

At a second order transition, gap function and transition temperature of a superconductor can be determined from a linear integral equation. According to de Gennes, the kernel of this integral equation may be obtained from a correlation function. This relation between correlation function and kernel is critically discussed. It is shown that the quantum mechanical correlation function is to be replaced by its slowly varying part, and it is suggested that the latter may be calculated from classical mechanics. The classical correlation function can be expressed as a momentum integral over a distribution in phase space developing with time according to the laws of classical mechanics. In the presence of statistically distributed impurities, the distribution function obeys the Boltzmann equation. Finally, the mathematical formulation of reflection properties of surfaces is discussed. (auth)

40039 SUPERCONDUCTIVITY OF GERMANIUM AND SILICON UNDER HIGH PRESSURE. Wittig, Joerg (Technische Hochschule, Karlsruhe, Ger.). Z. Phys., 195: 215-27(1966). (In German).

High pressure metallic modifications of germanium and silicon formed at room temperature are investigated for superconductivity. The zero-field transition temperatures are $T_c(p = 115 \text{ kbar}) = 5.35 \pm 0.1$°K for Ge and $T_c(p = 120 \text{ kbar}) = 6.70 \pm 0.1$°K for Si. Both artificial metals showed "normal behavior" in exhibiting negative values of the quantity dT_c/dp. A comparison of the critical temperatures of group IV elements Si, Ge, and Sn at corresponding points of their isomorphous phase diagrams gives a striking proportionality between T_c and the Grüneisen characteristic temperature of the lattice which was received from the temperature dependence of the electrical resistance. A detailed description of experimental procedure is enclosed. (auth)

40040 SUPERCONDUCTIVITY OF TIN AND LEAD UNDER VERY HIGH PRESSURE. Wittig, Joerg (Technische Hochschule, Karlsruhe, Ger.). Z. Phys., 195: 228-38(1966). (In German).

The dependence of the critical temperature T_c upon pressure P is measured in the pressure range up to 160 kbar. The experimental technique developed for very high pressure-low temperature experiments is improved by introducing a double-sample electrical resistance cell. An internal pressure calibration is therefore possible at some well-established room temperature pressure reference points commonly used. Both metals, tetragonal white tin and fcc lead, show a monotonic decrease of T_c vs. P with upward curvature. The results recommend the use of Pb as a secondary standard for very high pressure experiments at helium temperatures. In addition, high pressure polymorphic modifications of Sn and Pb are found to show superconductivity with $T_c = (5.30 \pm 0.10)$°K for Sn III at P = 113 kbar and $T_c = (3.55 \pm 0.10)$°K for Pb II at P = 160 kbar. (auth)

40041 EFFECTS OF ANISOTROPY OF THE SUPERCONDUCTING ENERGY GAP. Clem, John Richard. [Urbana], Ill., Univ. of Illinois, 1965. 145p.

Thesis.

In order to estimate the effects of anisotropy upon the thermodynamic properties of pure single-crystal superconductors, a factorable BCS-like model for the effective electron-electron matrix element $V_{pp'} = [1 + a(\underline{p})]\, v\, [1 + a(\underline{p}')]$ is used. The effects of anisotropy upon the tempera-

ture dependence of the gap parameter Δ_p, the critical field, and the specific heat near the critical temperature are shown to be small and proportional to the mean-squared anisotropy $\langle a^2 \rangle$, which is of the order of 0.02 for typical superconductors. A number of processes, such as those involved in low-temperature specific heat, nuclear spin-lattice relaxation time, tunneling, surface resistance, and longitudinal ultrasonic attenuation are more sensitive to the details of the anisotropy than are the above thermodynamic properties. Theoretical expressions, which explicitly include the anisotropy of a general gap parameter, are given for these processes. In order to simplify the description of these effects, two quantities, the anisotropy distribution function P(a) and the reduced anisotropic effective density of states, are introduced. The influence of the presence of nonmagnetic impurities upon the anisotropy of the superconducting energy gap parameter and the experimental manifestations of the reduction of the anisotropy by impurity scattering are considered. The thermodynamic properties are discussed in terms of the behavior of quantities of the order of the mean-squared anisotropy; the more sensitive experimental processes are discussed in terms of the impurity concentration-dependent behavior of the effective density of states. (TCO)

40042 FLUX-TRAPPING MODEL FOR R-F LOSSES IN SUPERCONDUCTORS. Haden, Clovis Roland. Austin, Tex., Univ. of Texas, 1965. 136p.

Thesis.

Both theoretical and experimental investigations are made into the residual r-f losses at temperatures well below the critical value in superconductors. Pulse techniques are used to measure the Q, which is a direct indication of the surface losses, of superconductive resonant circuits. The experimental measurements are made in the frequency range 10–1000 Mc at temperatures below 4.2°K. The measurements are restricted to r-f fields below the bulk critical value. A critical review of existing superconducting surface resistance theories is made in order to determine whether surface resistance can account for the observed losses. Other possible loss mechanisms, such as eddy-current losses in normal surface regions are considered. It is concluded that these are not responsible for the observed losses. Flux-trapping of the r-f magnetic fields is proposed as the responsible loss mechanism. A simple model for flux-trapping on a local basis is developed, and an expression for the equivalent surface resistance is obtained. This resistance is shown to be proportional to frequency and to the density of flux-trapping centers. It has a characteristic dependence on r-f field magnitude. This dependence is a function of the model assumptions, and predicts critical behavior with field magnitude. Experimental data are shown, which indicate full verification for the dependences predicted in the local model. These data are taken on various materials, including lead, tin, tantalum, and the indium-tin alloy system. Frequency and temperature measurements are made, which verify these respective dependences. Measurements on the indium-tin system indicate little or no dependence of the density of trapping centers on the impurity content. Inspection of the decaying r-f pulses at the circuit output reveals a "break" corresponding to the predicted "critical" behavior. (TCO)

40043 INVESTIGATION OF THE ELECTRICAL AND SUPERCONDUCTING PROPERTIES OF THIN INDIUM FILMS. Garland, Michael McKee. [Clemson, S. C.], Clemson Univ., 1965. 70p.

Thesis.

The superconducting transition temperatures of indium films of varying thicknesses were measured and a relation was sought between the transition temperature and film thickness. An attempt was made to explain the normal electrical conductivity and the change in resistivity with temperature for thin indium films. The films were deposited in groups of five onto substrates held at 77°K; the films were then allowed to anneal by raising the temperature slowly to about 300°K. During this anneal values of resistance versus temperature were recorded. The film resistivities at 300°K were compared to the theory of Fuchs for totally diffuse scattering. Film thicknesses were obtained by the change of resistivity that resulted from cooling the films from 300 to 77°K. Film thicknesses were also measured by timing the deposition and by multiple beam interferometry. Superconducting transition temperatures were observed for indium films ranging in thickness from 95 Å to about 1000 Å deposited on quartz and glass substrates. A comparison was made of transition temperatures for several films both before and after annealing. Transition temperatures obtained for indium films deposited onto quartz substrates were in good agreement with the theoretical predictions of Toxen. It was also found that the data could be explained on the basis of a Ginzburg surface layer. In both cases stresses were believed to be responsible for the observed shifts in transition temperature relative to the bulk value. Transition temperature data for indium films deposited on glass substrates could not be accounted for by either theory. It was found that resistivities of films below about 250 Å could not be accounted for entirely on the basis of diffuse scattering at the film surfaces. (Dissertation Abstr.)

40044 EFFECT OF A MAGNETIC FIELD ON THE FAR INFRARED ABSORPTION SPECTRUM OF THIN FILM SUPERCONDUCTORS. Martin, William Sonderman. Berkeley, Calif., Univ. of California, 1965. 121p.

Thesis.

The change in absorption of far infrared radiation by superconducting lead films as a function of magnetic field was measured. The experiments were conducted over a frequency range of 8 to 60 cm^{-1} on films of the order of 100 Å thick and primarily with the magnetic field parallel to the plane of the film. Second-order phase transitions as predicted by the theories of Gingzburg and Landau and of Maki were observed. The angular dependence of the critical field was measured by observing the d-c resistive transition and it agreed well with the theory of Tinkham. The perpendicular and parallel critical fields were also reasonably consistent with theoretical values. With the field close to parallel to the film plane, considerable amount of absorption below the gap frequency and apparently extending to very low frequencies even for fields well below the critical field was noted. This absorption is inexplicable in terms of a magnetic field strictly parallel to the film. It is suggested that the small perpendicular field component due to misalignment and imperfections in the flatness of the film forces the film into a mixed state with order parameter varying from 0 at the normal core of each vortex to a maximum value ω_m at the outer perimeter of the vortex. The major effect of the parallel field component is to depress ω_m. Thus the absorption below the anticipated gap frequency is attributed to the gap variation caused by the mixed state. The amount of absorption at any frequency depends upon the geometric fraction of the film having a gap small enough to allow excitations by the incident infrared radiation. A phenomenological theory was constructed to treat the effect of a simultaneous parallel and perpendicular component of magnetic field upon the absorption spectrum of a very thin superconducting film. It successfully accounts for the major qualitative and many of the quantitative features of the observed spectrum. (Dissertation Abstr.)

40045 ISOTHERMAL CALORIMETRY ON TYPE II SUPERCONDUCTORS. Otter, F. A. Jr.; Yntema, G. B. (United Aircraft Corp., East Hartford, Conn.). 11p. (CONF-660107–64). ORAU. Gmelin, AED-CONF-66-003-152.

From American Physical Society Meeting, New York.

A low-temperature calorimeter, built with provision for monitoring the magnetic moment of a superconducting specimen as well as the heat added or subtracted during an isothermal transition in a slowly changing magnetic field, was used to determine the thermodynamic critical fields of type-II superconductors in which the magnetic transitions are not reversible. The experimental arrangement

is outlined and results are given for 60Pb–40Tl and 40Pb–60In. (W.D.M.)

40046 FULDE-FERRELL EFFECT IN TYPE II SUPERCONDUCTORS. Gruenberg, Leonard W. (Massachusetts Inst. of Tech., Cambridge); Gunther, Leon. 11p. (CONF-660327-7). ORAU. Gmelin, AED-CONF-66-050-23.

From American Physical Society Meeting, Durham, N. C.

The effect of Pauli spin paramagnetism on the mixed state was studied. It was found that for a pure superconductor, in which the ratio between the Gor'kov upper critical field H_{c20} and the paramagnetically limited upper critical field H_P exceeds 1.28, a new kind of superconducting state can exist. At the nucleation field H_{c2}, the Cooper pairs find themselves in the lowest Landau orbit; in addition, they have a drift velocity along the direction of the applied field. This result is a generalization of the one found by Fulde and Ferrell (Phys. Rev., 135: A550(1964)) who considered the problem of a uniform magnetic field acting only on the electron spins. It is concluded that, although the orbital effects of a real magnetic field are detrimental to the Fulde-Ferrell state, such a state can exist in a type-II superconductor, for example, V_3Ga, at sufficiently low temperatures and high fields. (W.D.M.)

40047 SUPERCONDUCTIVITY IN THE TRANSITION METALS AT VERY LOW TEMPERATURES. Jensen, M. Anthony (Univ. of California, La Jolla, San Diego). 174p. (CONF-758-61). ORAU. Gmelin, AED-CONF-65-003-131.

From American Physical Society Meeting, New York, Jan. 1965.

The results are presented of an investigation of the occurrence of superconductivity in certain transition elements and alloys. The experimental results are from the beginning and end of the transition metals. These results are discussed in terms of the properties of all the transition metals and also in terms of the theory for the transition temperature which is presented. It is concluded that the behavior (decrease) of superconductivity near Pd, Pt, and Rh is a real effect which also manifests itself in a greatly enhanced spin susceptibility. Also, in this region the superconductivity, electronic specific heat and spin susceptibility all seem to depend only on the electron density. The behavior (no superconductivity) near Sc, Y, and Lu may be affected by the presence of impurities. (auth)

40048 BOILING HEAT TRANSFER TO LIQUID HELIUM. Cummings, Richard D. (General Electric Missile and Space Div., Philadelphia); Smith, Joseph L. Jr. 21p. (CONF-660628-5). ORAU. Gmelin, AED-CONF-66-173-5.

From International Inst. of Refrigeration Commission I Meeting, Boulder, Colo.

Liquid helium at atmospheric pressure was boiled above a fixed geometry, horizontal test surface. The heat flux was determined as a function of the temperature difference. The influence of surface finish on the boiling was investigated for a pure copper test surface. A light dusting of H_2O crystals was shown to produce a significant improvement in the heat transfer. The properties of the sub-surface metal were shown to influence appreciably the peak heat flux for nucleate boiling. (auth)

40049 FACILITY FOR TESTING LARGE SUPERCONDUCTING MAGNETS. de Winter, T. A. (Avco-Everett Research Lab., Everett, Mass.). 20p. (CONF-660628-6). ORAU. Gmelin, AED-CONF-66-173-10.

From International Inst. of Refrigeration Commission I Meeting, Boulder, Colo.

A facility was designed, built, and used to test a large superconducting magnet. The facility was built around a 1.524 m inside diameter, multilayer insulated, and liquid nitrogen shielded vertical liquid helium dewar with a depth of over 4.5 m. Multiple precooling provisions were built into the facility. Multiple liquid helium transfer lines were provided for filling the dewar at various stages of a magnet test. Pressure, temperature, and helium gas flow rate measurements were made during a test. The magnet assemblies to be tested were supported by tension members connected to the top dewar cover assembly. The cover assembly was fitted with a liquid nitrogen cooled horizontal shield, and rigid foam was used on both sides of the shield as a filler and insulator. A safety ventoff system was designed and installed with several separate pressure relief circuits. (auth)

40050 SUPERCONDUCTING CRITICAL FIELD MEASUREMENTS IN CERIUM DOPED LEAD BETWEEN 4.1 DEG K AND 1.8 DEG K. Monroe, John J.; Leinhardt, T. E. (Virginia Polytechnic Inst., Blacksburg). 24p. (CONF-660547-3). ORAU. Gmelin, AED-CONF-66-122-3.

From Virginia Academy of Science, 44th Annual Meeting, Harrisonburg, Va.

Ballistic measurements were made of the critical magnetic fields of superconducting cylinders of cerium-doped lead. Within the accuracy of the measurements, the introduction of the paramagnetic impurity, cerium, in lead has no effect other than a slight broadening of the transition. The samples, containing 0.00, 0.10, 1.0, and 1.5 at. % cerium in lead, were vacuum cast in pyrex tubes. The relative fractions of the cerium in these samples and their final purities were tested by the techniques of neutron activation analysis. (auth)

40051 SYMPOSIUM ON EVALUATION OF METALLIC MATERIALS IN DESIGN FOR LOW-TEMPERATURE SERVICE. Presented at the Sixty-Fourth Annual Meeting, American Society for Testing and Materials, Atlantic City, N. J., June 27–28, 1961. Amer. Soc. Test. Mater., Spec. Tech. Pub., No. 302, 1-245(1962). (CONF-610602).

Fourteen papers and a panel discussion were presented on metallic materials for low-temperature service. Review papers presented theories which have been proposed in the field of crack propagation, indicating areas where work is essential to verify or modify the mathematical proposals so that they might be useful in designing of safe structures. The subject of severe service conditions created in the handling of low-temperature liquefied gases was treated. (W.D.M.)

Neutron Physics

See also REACTOR TECHNOLOGY — Criticality Studies

Refer also to abstracts 39542, 39546, 40378, and 40455.

40052 STEADY STATE DISTRIBUTION OF NEUTRONS IN AN INFINITE MEDIUM. Kozachok, I. A. Geofiz. Sb., Akad. Nauk Ukr. SSR, Inst. Geofiz., No. 7, 163-75(1964). (In Russian).

The steady-state distribution of neutrons at the time of their moderation in infinite media is studied. (D.C.W.)

40053 DIFFUSION LENGTH CALCULATIONS IN WATER. Goyal, I. C.; Ghatak, A. K. (Univ. of Delhi). J. Nucl. Energy: Pt. A and B, 20: 659-65(Aug. 1966).

An extensive series of calculations was performed to determine the asymptotic neutron energy spectra and diffusion lengths in water poisoned by absorbers like boron, cadmium, and gadolinium at different concentrations. The effect of chemical binding was studied by comparing the results obtained by using the well-known Nelkin model of water with the free-gas model for hydrogen. Diffusion theory was used in making the calculations; however, to test the validity of the diffusion approximation, some transport theory calculations were also made for a few cases. It was found that even for fairly large absorptions (i.e., for $\kappa/\Sigma_{min} \approx 0.7$-$0.8$) diffusion theory gives results which compare well with those obtained by using transport theory. (auth)

40054 REAL EIGENVALUES OF THE MONOENERGETIC TRANSPORT OPERATOR FOR A HOMOGENEOUS MEDIUM. Ukai, Seiji (Kyoto Univ.). J. Nucl. Sci. Technol. (Tokyo), 3: 263-6(July 1966).

The eigenvalue problem of the monoenergetic neutron transport operator is studied mathematically under the assumptions of homogeneity and boundedness of the medium and of isotropy of scattering. It is shown that the spectrum involves a countable infinity of real eigenvalues with an accumulation point at minus infinity. Each eigenvalue has a finite multiplicity. (auth)

40055 MEASUREMENT AND CALCULATION OF NEUTRON-DIFFUSION PARAMETERS IN WATER. Kobayashi, Keisuke; Seki, Yuji; Mizoo, Nobutatsu; Watanabe, Takao; Watanabe, Takashi; Nishihara, Hiroshi (Kyoto Univ.). J. Nucl. Sci. Technol. (Tokyo), 3: 275-88(July 1966).

Neutron diffusion parameters in water at a room temperature of 10°C were measured by the pulsed neutron method for the range of geometrical buckling from 0.093 to 1.36 cm^{-2}. The results are 205 ± 4 μsec for the neutron mean life time due to absorption, 34.120 ± 610 $cm^2 \cdot sec^{-1}$ for the diffusion coefficient and 3.350 ± 560 $cm^4 \cdot sec^{-1}$ for the diffusion cooling coefficient. The decay constant was calculated as a function of buckling for the Nelkin and the Radkowsky scattering models of water on the assumption of linear anisotropic scattering. The calculated diffusion coefficients, 36.290 $cm^2 \cdot sec^{-1}$ for the Nelkin model and 37.610 $cm^2 \cdot sec^{-1}$ for the Radkowsky model, are somewhat higher than the experimental result. It is shown that the calculated diffusion coefficient approaches the experimental value if $\bar{\mu}(E)$, the mean value of cosine of scattering angle obtained from the Beyster's experiment is used instead of that for the Nelkin model. (auth)

40056 EXTENSION OF A COMMON APPROXIMATING EQUATION FOR THE COLLISION DENSITY. Wilkins, Coleridge A. (Wollongong Univ. Coll., N. S. W.). J. Nucl. Sci. Technol. (Tokyo), 3: 298-9(July 1966).

The integral equation for the collision density in an infinite homogeneous mixture of n species is $F(u) = S(u) + \Sigma_1^n \int_0^u F(u')h_i(u')f_i(u-u')du'$. Here, F(u) is the collision density per unit lethargy, S(u) the source term, $h_i(u)$ the ratio of the macroscopic scattering cross section of the i-th species to the total macroscopic scattering cross section, and $f_i(u-u')$ the scattering kernel of the i-th species. The equation is described for sets of Wigner and Greuling-Goertzel kernels. (M.O.W.)

40057 CHOICE OF THE OPTIMUM SHAPE OF A NEUTRON HOWITZER FOR NEUTRON ABSORPTION METHODS. Janczyszyn, Jerzy; Kwiecinski, Stanislaw; Loska, Ludwik (Instytut Techniki Jadrowej AGH, Krakow). Nukleonika, 11: 67-9(1966). (In Polish).

The apparatus consists of a neutron source (Ra–Be) surrounded by a paraffin moderator, with cadmium shielding, a Pb plug, and a shaped paraffin collimator that directs the slow-neutron flux to a neutron-absorption sample. The Pb plug reduces the gammas and fast neutrons which travel down the collimator. Behind the sample is located a scintillation counter with a scintillator that is sensitive to thermal neutrons. The paraffin collimator is replacable so that the thermal neutron flux distribution across the neutron-absorption sample can be preselected. The angular distribution of neutrons at the center of the absorption-sample location is given for several collimator geometries. It was measured with a goniometer-type of neutron detection device. The overall geometric factors were selected to maximize the usable thermal neutron flux at the location of the absorption sample. (TTT)

40058 CALCULATION OF NEUTRON FLUX IN HYDROGENOUS MEDIUM ROUND A FAST POINT SOURCE FOR APPLICATION TO MOISTURE MEASUREMENTS BY NEUTRONS. Kasi, Servo (State Inst. for Technical Research, Helsinki). Valtion Tek. Tutkimuslaitos, 99: 1-19(1966).

A method of calculating the thermal-neutron flux around a point source of fast neutrons in an infinite hydrogenous medium is outlined. The calculations are based on the use of an Ac–Be source as the neutron emitter. At energies above 0.75 Mev, the Monte Carlo method is used; but below this limit the use of the nine-group Selengut-Goertzel modification of the age-diffusion approximation is satisfactory. (D.C.W.)

40059 TIME-DEPENDENT NEUTRON-DIFFUSION THEORY OF PLANE HETEROGENEOUS SYSTEMS. Liner, Robert Thayer Jr. Raleigh, N. C., Univ. of North Carolina, 1965. 212p.

Thesis.

The one-group time-dependent diffusion equation is formulated for one-dimensional bare systems with thin heterogeneities at arbitrary positions. The equations are solved exactly for the case of a single heterogeneity and, in the case of multiplying systems, one delayed neutron group. The solution is discussed in considerable detail with particular attention to the physical significance of the various features of the theory. The greatest emphasis is on the relationship between the spatial flux dependence in transient and critical systems and the nonseparability of the space and time dependence. Most of the results obtained are analogous in a qualitative sense to the results obtained from the theory of homogeneous systems. One exception occurs in systems with a sink-type heterogeneity, in which case the flux contains an anomalous exponential term. This term is associated with the net diffusion of delayed neutrons toward the heterogeneity. The effect is small and is probably negligible for all practical purposes. The equations are also solved for nonmultiplying multiplate systems. However, the solution is not discussed in detail. The initial phase of the solution for multiplying multiplate systems is presented. In order to estimate errors involved in the one-group theory and to provide a possible means of making improvements to the theory, a modified one-group model that is intermediate in accuracy between the one- and two-group models is formulated and solved for critical systems. The solution should be useful in obtaining more accurate spatial eigenfunctions than are obtained from the one-group model. In addition, the two-group diffusion equations are formulated and a method of solution is outlined. (Dissertation Abstr.)

40060 INSCATTERING APPROXIMATIONS IN DISCRETE VARIABLE TRANSPORT THEORY. Craven, Clyde Wesley Jr. [Knoxville], Tenn., Univ. of Tennessee, 1965. 107p.

Thesis.

The extension of existing discrete variable transport theory models to adequately treat highly anisotropic systems at practical costs is investigated. The one-dimensional form of the discrete variable transport theory model is developed from the Boltzmann equation in order to define the form of the inscatter source term. The development is accomplished by subdividing each phase space into a set of subspaces. In each of these subspaces the neutron density $n(\vec{r}, E, \vec{\Omega}, t)$ is assumed separable in each variable. The continuous variables are replaced with sets of discrete variables in each phase space, and the Boltzmann equation is reduced to a finite difference form amenable to digital computation. The definitions used in developing the discrete equation are used to develop the explicit form of the discrete transfer matrix, which defines the probability per neutron path length of a neutron being scattered from a given energy group and angular segment to any other energy group and angular segment. The Gegenbauer (generalized Legendre) polynomial approximation to the discrete transfer matrix is developed for both the "diamond difference" and "step function" models. This approximation allows an arbitrary weighting of angular space, which may be used to increase the polynomial approximation accuracy in the forward direction. The effect of the polynomial weight functions on the root mean square error and the endpoint error is examined to determine whether other classical polynomials provide a more acurate approximation than Legendre polynomials for low order truncations. It is concluded that the Tchebycheff polynomials provide a more accurate approximation in the forward direction when cal-

culating the discrete transfer matrix, and that the increase in root mean square error above that of the Legendre polynomials is negligible. Results of reactivity calculations performed using the discrete transfer matrix are presented for several metallic systems reflected by heavy water. A comparison is made between this model and the "isotropic" and "linearly anisotropic" models. The machine code developed to perform the reactivity calculations using the discrete transfer matrix exhibited running times in the neighborhood of 13.8 min on the 7090 for a 19-group, 125-space point, two-region problem converged to 10^{-5} in multiplication factor. (TCO)

40061 PULSED-NEUTRON MEASUREMENTS OF THE DIFFUSION PARAMETERS OF HEAVY AND LIGHT WATER MIXTURES AT SEVERAL TEMPERATURES. Salaita, George Nicola. Blacksburg, Va., Virginia Polytechnic Inst., 1966. 55p.

Thesis.

Thermal neutron diffusion parameters of 0, 20, 50, 80, and 100 percent D_2O in mixtures of light and heavy water were measured by the pulsed neutron technique at room temperature (21°C), near the freezing point of the mixture in the liquid state, and at –20°C in the solid state (ice). A 250-kv pulsed Cockcroft-Walton accelerator, using neutrons from the $_1H^2(d,n)_2He^3$ reaction, was used to generate fast neutron bursts. The values of the infinite medium decay constant, λ_0, were computed by a least squares fit of λ versus B^2 data to the expression $\lambda = \lambda + D_0B^2 - CB^4$. The parameters D_0, C and λ_{tr} were determined from the above expression after rearranging: $\lambda - \lambda_0 = D_0B^2 - CB^4$. The resulting values of D_0, C, λ, and λ_{tr} at several temperatures are tabulated. (TCO)

40062 GEOMETRICAL EFFECTS ON THE RESONANCE ABSORPTION OF NEUTRONS. Ludewig, Hans. Pasadena, Calif., California Inst. of Tech., 1966. 143p.

Thesis.

An investigation was conducted to estimate the error when the flat-flux approximation is used to compute the resonance integral for a single absorber element embedded in a neutron source. The investigation was initiated by assuming a parabolic flux distribution in computing the flux-averaged escape probability that occurs in the collision density equation. Also assumed were both wide resonance and narrow resonance expressions for the resonance integral. The fact that this simple model demonstrated a decrease in the resonance integral motivated the more detailed investigation. An integral equation describing the collision density as a function of energy, position, and angle is constructed and is subsequently specialized to the case of energy and spatial dependence. This equation is further simplified by expanding the spatial dependence in a series of Legendre polynomials (since a one-dimensional case is considered). In this form, the effects of slowing down and flux depression may be accounted for to any degree of accuracy desired. The resulting integral equation for the energy dependence is thus solved numerically, considering the slowing-down model and the infinite-mass model as separate cases. From the solution obtained by the above method, the error ascribable to the flat-flux approximation is obtained. The error introduced in the resonance integral in assuming no slowing down in the absorber is deduced. Results by Chernick for bismuth rods, and by Corngold for uranium slabs, are compared to the latter case, and these agree to within the approximations made. (Dissertation Abstr.)

40063 COMPUTER EVALUATION OF NEUTRON SCATTERING ANGULAR DISTRIBUTION DATA. Horsley, A. (Atomic Weapons Research Establishment, Aldermaston, Eng.). 12p. (CONF-660303–47). ORAU. Gmelin, AED-CONF-66-034-38.

From American Physical Society, Conference of Neutron Cross Section Technology, Washington, D. C.

A Fortran program is described which produces evaluated angular distribution data for incident neutron energies up to 30 Mev for a given nuclide from the experimental differential cross section data which are available. (auth)

40064 CONSISTENT P-3 THEORY OF NEUTRON WAVE PROPAGATION. Kunaish, Hassan H. (Univ. of Florida, Gainesville). 20p. (CONF-660206–19). ORAU. Gmelin, AED-CONF-66-014-23.

From Symposium on Neutron Noise, Waves, and Pulse Propagation, Gainesville, Fla.

A P-3 spherical harmonics expansion of the Boltzmann neutron transport equation was used with the heavy gas scattering kernel to obtain the complex inverse relaxation length, ρ, of a thermal neutron wave propagating through a semi-infinite rectangular block of homogeneous material. The results are compared with measurements of thermal neutron propagation through type-AGOT graphite. Good agreement exists between theory and experiment for frequencies below 300 cps. Going from a P-1 approximation to a P-3 approximation yielded a definite improvement in the predicted value of ξ, the imaginary part of ρ, but made very little difference in the value of α, the real part. The derivation of the theoretical calculations from experimental measurements at high frequencies is attributed primarily to two factors: the possibility of spatial and background contaminations in the measurements; and the sensitivity of the problem to the scattering kernel. It is suggested that a more detailed kernel should be used. (S.F.L.)

Nuclear Properties and Reactions

Refer also to abstracts 38838, 39203, 39216, 39774, and 39828.

40065 (BMWF-FB-K–66-01) JAHRESBERICHT 1964. (Annual Report, 1964). (Max-Planck-Institut fuer Kernphysik, Heidelberg (West Germany)). Feb. 1966. 159p. Dep. mn.

The studies made at the Max Planck Institute for Nuclear Physics in Heidelberg on tandem accelerators, cosmochemistry and space research, cyclotrons, and nuclear spectroscopy are summarized. Results were reported on studies of the $^4He(\alpha,\alpha)^4He$ reaction, p + D → p + p + n, ^{14}N-induced nuclear reactions, statistical fluctuations in the cross sections of $^{26}Mg(p,p)$, $^{26}Mg(p,\alpha)$, $^{37}Cl(p,\alpha)$, $^{45}Sc(p,\alpha)^{42}Ca$, $^{56}Fe(p,p)(p,\alpha)$, and $^{54}Cr(p,p)$ and (p,α) reactions, isobaric analog states, stripping reactions producing ^{53}Cr, ^{55}Cr, ^{31}Si, ^{53}Mn, ^{51}Cr, ^{39}Ca, and ^{41}Sc, subcoulomb stripping, high-resolution γ spectrometer, target chambers, isotope analysis and age determination of meteorites, diffusion of rare gases and tritium in meteorites, chemical distinction of the bright-dark structure of primordial rare-gas containing stone meteorites, rare gas isotopes of stone meteorites, K–Ar determination in iron meteorites, fission ^{40}Ar in iron meteorites, production of K and Ni and Fe targets by proton bombardment, isotopic frequency and concentration of Li in stone meteorites, detection of single ions in mass spectrometers, mineral existence of meteorites and cosmic spheroids, meteorite craters and tectite problem, age determinations and rare gas isotope measurements in terrestrial stones, collection and recording of cosmic dust, mass spectrometry of the outer atmosphere, registration of cosmic radiation, radioactive aerosols of the atmosphere, elastic and inelastic scattering of deuterons, (d,α) reactions on light nuclei, (d,n) reactions and total reaction cross section for medium heavy nuclei at 11.8 Mev, (d,t) reactions, correlation measurements on ^8Li and ^8B, apparatus for measurement of two-particle correlations, apparatus for measurement of particle correlations, recoil proton spectrometer, dE/dx telescope for ^3He, dE × E particle separation with a multiplication stage, measurement of the form of the β spectra of ^{45}Ca, ^{90}Sr, ^{90}Y, ^{144}Ce, ^{144}Pr, and ^{166}Ho, β decay of ^{144}Pr, β-γ directional correlations of ^{126}I, ^{130}I, ^{144}Ce, ^{170}Tm, and ^{203}Hg, effect of solid-body effects on the β-γ directional correlation of ^{166}Ho, β-γ circular polarization correlations in β transitions of ^{58}Co, ^{95}Zr, ^{95}Nb, and ^{203}Hg, β-γ circular polarization correlation on ^{133}Xe, measurements of γ spectra, measurements on conversion lines with high resolution and transmission β spectrometer, proposal for measurement of neutretto mass, development of β spectrometer, construc-

tion of devices for measurement of circular polarization of γ radiation, measurement of β-γ circular polarization as function of energy and angle, principle of magnetic Compton spectrometer, and development of spark chambers, magnetic flasks, helix field spectrometer, and focusing properties of azimuthal changing magnetic fields. (J.S.R.)

40066 (BMWF-FBK-66-15) BERICHT UEBER EINIGE ARBEITEN AUF DEM GEBIET DER NIEDER-ENERGIE-KERNPHYSIK ANLAESSLICH EINES STUDIENAUFENTHALTES IN JAPAN. (Report About Some Investigations in Low Energy Physics Performed in Japan). Breuer, G. (Hamburg Univ. (West Germany). I. Institut fuer Experimentalphysik). June 1966. 50p. Dep. mn.

Separate abstracts were prepared for 3 of the 4 sections presented. One section on the construction of a ^{3}He gas circuit for induced ^{3}He reactions with cyclotrons was not abstracted for NSA. (B.G.D.)

For abstracts of individual sections see: 39477, 40067, and 40068.

40067 (BMWF-FBK-66-15, pp 20-37) BERICHT UEBER DIE MESSUNGEN DER REAKTION ^{40}Ca(d,α)^{39}Ca FUER 24 Mev EINSCHUSSENERGIE. (Report on the Measurements of the Reaction ^{40}Ca(d,α)^{39}Ca for 24 Mev Impact Energy). Yagi, K.; Ejiri, H.; Ishimatsu, T.; Breuer, G. (Institute for Nuclear Study, Tokyo Univ. (Japan)).

Using particle analyzer and a ^{3}He gas circuit, cross sections of the ^{40}Ca(^{3}He,α)^{39}Ca reaction were measured at $E_{^3He}$ = 24 Mev. The results are compared with DWBA calculations and the shell model. (auth)

40068 (BMWF-FBK-66-15, pp 38-46) WINKEL-VERTEILUNGEN DER REAKTION ^{10}B(d,α)^{8}Be ZWISCHEN 1,6 U.3,0 Mev. (Angular Distribution and Effective Cross Section of the Reaction ^{10}B(d,α)^{8}Be Between 1.6 and 3.0 Mev). Breuer, G. (Institute for Nuclear Study, Tokyo Univ. (Japan)).

Reactions (d,d) and (d,α) on ^{10}B were investigated in the energy range between 1 to 3 Mev. At E_d < 2 Mev, a deuteron pickup is to be seen with l_d = 2. At $E_d \geq$ 2 Mev, compound nuclear processes contribute, as already observed in the (d,p) reaction. However, elastic scattering of deuterons does not show any influence of resonances. (auth)

40069 (EANDC(E)-66(U)) PROGRESS REPORT ON NUCLEAR DATA RESEARCH IN THE EURATOM COMMUNITY FOR THE PERIOD JANUARY 1-DECEMBER 31, 1965. (European-American Nuclear Data Committee). Feb. 1966. 211p. Dep. mn.

A progress report is presented on nuclear data research concentrated mainly on neutron reactions. Also included in the report are technological advances in instrumentation and experimental techniques. (B.G.D.)

40070 (IEA-111) PROGRAMACAO DIGITAL PARA O CALCULO DAS ATIVIDADES DOS PRODUTOS DE FISSAO DE MEIAS-VIDAS LONGAS. (Digital Program for Calculation of Activities of Fission Products of Long Half Life). Nastasi, Maria Jose C.; Caceres, C. (Instituto de Energia Atomica, Sao Paulo (Brazil)). Dec. 1965. 98p. (CONF-650974-2). Dep. mn.

From 15th Brazilian Congress, Rio de Janeiro, Brazil.

A program in FORTRAN II was developed for the Model 2 IBM 1620 digital computer to calculate the activities of long-lived fission products formed during reactor irradiation of natural uranium, for several irradiation and cooling times. The values of activities formed in continuous and discontinuous irradiations are given. (S.F.L.)

40071 (JINR-E-2774) ^{8}He PRODUCTION IN NEGATIVE PION CAPTURE BY CARBON AND OXYGEN NUCLEI. Batusov, Yu. A.; Bunyatov, S. A.; Sidorov, V. M.; Yarba, V. A. (Joint Inst. for Nuclear Research, Dubna (USSR). Lab. of Nuclear Problems). 1966. 8p. Dep. mn.

The events of ^{8}He production and decay in negative pion capture by carbon and oxygen nuclei were detected in photoemulsion. The probability of ^{8}He production is (2-3) 10^{-6}. The mass of ^{8}He was measured to M_{He^8} = (7481.3 ± 0.9) Mev. (auth)

40072 (LA-DC-8061) A COMPARISON OF ROTATIONAL M1 TRANSITION RATES BETWEEN HIGH AND LOW SPIN STATES. Seaman, G. G.; Bernstein, E. M.; Palms, J. M. (Los Alamos Scientific Lab., Univ. of California, N. Mex.). [1966]. Contract W-7405-eng-36. 9p. (CONF-660906-11). Dep. mn. CFSTI $1.00 cy, $0.50 mn.

From International Conference on Nuclear Physics, Gatlinburg, Tenn.

Measurements were made of branching ratios from rotational states in ^{153}Eu, ^{159}Tb, ^{165}Ho, ^{169}Tm, ^{171}Yb, ^{173}Yb, ^{175}Lu, and ^{181}Ta populated by multiple Coulomb excitation with oxygen ions. The relative B(M1) values calculated from these ratios are in good agreement in all cases with the collective model. (auth)

40073 (LA-DC-8065) FURTHER EVIDENCE FOR EFFECTIVE NUCLEON SPIN g-FACTORS. Palms, J. M.; Bernstein, E. M.; Seaman, G. G. (Los Alamos Scientific Lab., Univ. of California, N. Mex.). [1963]. Contract W-7405-eng-36. 6p. (CONF-660906-12). Dep. mn. CFSTI $1.00 cy, $0.50 mn.

From International Conference on Nuclear Physics, Gatlinburg, Tenn.

In order to obtain agreement between experimental and theoretical values for magnetic moments in deformed nuclei, it is necessary to use an effective spin g-factor. For K = $\frac{1}{2}$ nuclei, it is possible to obtain three independent determinations of $g_{s,eff}$. Agreement of these independent determinations for ^{171}Yb appears to provide further evidence that the concept of an effective nucleon spin g-factor is valid. (auth)

40074 (LA-DC-8069) A HIGH-RESOLUTION STUDY OF INELASTIC PROTON SCATTERING FROM NUCLEI IN THE Pb REGION: THE 2.6-Mev OCTUPOLE STATE. Hafele, J. C.; Woods, Richard (Los Alamos Scientific Lab., Univ. of California, N. Mex.). [1966]. Contract W-7405-eng-36. 8p. (CONF-660906-10). Dep. mn. CFSTI $1.00 cy, $0.50 mn.

From International Conference on Nuclear Physics, Gatlinburg, Tenn.

The magnetic analysis of 21-Mev protons inelastically scattered from the 2.6-Mev octupole state of ^{206}Pb, ^{207}Pb, ^{208}Pb, and ^{209}Bi is reported. In the odd-A nuclei, this state splits into a close multiplet with the number of levels in agreement with the predictions of the weak-coupling model. Energies and spins for the multiplet levels are assigned, and multipole strengths for the interaction are derived. (auth)

40075 (LNF-66/30) CHARGED PION PHOTOPRODUCTION ON LIGHT NUCLEI. Note No. 324. Ferroni, S.; Gracco, V.; Lehmann, P.; Merkel, B.; Schaerf, C. (Laboratoire Nazionali di Frascati, Comitato Nazionale per l'Energia Nucleare (Italy)). June 6, 1966. 8p. Dep. mn.

The differential cross section for the photoproduction of charged pions on light nuclei was measured for different values of the photon energy using the excitation curve method. Hydrogen, Lithium-6, Lithium-7 and Carbon were studied. No correlation with the detailed structure of the final nuclei were found. The data seem consistent with a model where the nucleons are considered as independent emission centers and where reabsorption from the other nucleons in the nucleus is taken into account. This appears to be valid both for single and double pion photoproduction. (auth)

40076 (MIT-2098-255) GENERALIZED HARTREE-FOCK CALCULATION FOR ^{90}Zr USING AN EFFECTIVE INTERACTION. Waghmare, Y. R.; Shakin, C. M.; Svenne, J. P. (Massachusetts Inst. of Tech., Cambridge). July 22, 1966. Contract AT(30-1)-2098. 9p. (CONF-660906-6). Dep. mn. CFSTI $1.00 cy, $0.50 mn.

From International Conference on Nuclear Physics, Gatlinburg, Tenn.

Hartree-Fock calculations have been performed for ^{90}Zr

using an effective interaction derived from the Yale potential. Results are presented for the binding energy, r.m.s. radius, and single-particle energies. Comparison is made with similar calculations using the nonlocal Tabakin potential. (auth)

40077 (MIT-2098-256) SHELL EFFECTS IN THE HIGH ENERGY PHOTOPROTON SPECTRA FROM ^{6}Li. Matthews, J. L.; Bertozzi, W.; Kowalski, S.; Sargent, C. P.; Turchinetz, W. (Massachusetts Inst. of Tech., Cambridge). July 1966. Contract AT(30-1)-2098. 8p. (CONF-660906-5). Dep. mn. CFSTI $1.00 cy, $0.50 mn.

From International Conference on Nuclear Physics, Gatlinburg, Tenn.

Measurements were made of the energy spectra and angular distributions of protons from the ^{6}Li(γ,p) reaction. The experiment was performed at the Saskatchewan Accelerator Laboratory using a bremsstrahlung beam of maximum energy ~100 Mev. Structure observed in the photoproton spectra can be interpreted on the basis of a single-particle direct-interaction model. (auth)

40078 (NP-16203) OPREDELENIE VYKHODA REAKTSII D(d,n)^{3}He I T(d,n)^{4}He V TOLSTYKH MISHENYAKH PRI ENERGIYAKH DO 100 KEV. (Determination of the Yield of D(d,n)^{3}He and T(d,n)^{4}He Reactions in Thick Targets at Energies up to 100 Kev). Vasil'ev, R. D. (Gosudarstvennyi Komitet po Ispol'zovaniyu Atomnoi Energii SSSR, Moscow. Soyuznyi Nauchno-Issledovatel'skii Institut Priborostroeniya. Gosudarstvennyi Komitet po Ispol'zovaniyu Atomnoi Energii SSSR, Obninsk. Fiziko-Tekhnicheskii Institut). 1966. 8p. Dep. mn.

There are no known data on measurements of the D(d,n)^{3}He reaction yields from thick TiD and ZrD targets at low neutron energies. Consequently, yield determinations were carried out for D(d,n^{3}He and T(d,n)^{4}He reactions on thick, industrially produced targets for deuterons up to 100 kev. The measured values for reaction yields were subsequently used for the calculation of neutron flux densities at distances from the target at which the authors calibrated various detection equipment. It was assumed during the yield determination that (1) the deuterium flow is constant over the depth of the target; (2) that the concentration of absorbed deuterium and tritium is uniform over the target; and (3) that one can neglect absorption and scattering within the target of charged particles leaving in the detector direction. The results are given in the form of graphs representing (a) the momentum spectrum of the charged nuclear reaction products, (b) the excitation function of the D(d,n)^{3}He and T(d,n)^{4}He reactions, and (c) the efficiency of the long neutron counter as a function of neutron energy. (JPRS)

40079 (ORO-3346-2) NEUTRON REACTION CROSS SECTIONS OF Se AND Fe AT 14.4 Mev. Rao, P. Venugopala; Fink, R. W. (Georgia Inst. of Tech., Atlanta. School of Chemistry). July 22, 1966. Contract AT(40-1)-3346. 7p. (CONF-660906-2). Dep. mn. CFSTI $1.00 cy, $0.50 mn.

From International Conference on Nuclear Physics, Gatlinburg, Tenn.

An improved technique for the measurement of activation cross sections was developed which takes advantage of high resolution of Ge(Li) detectors. Neutron-induced activities in samples of natural Se and Fe were studied by this method. The following reactions of isotopes of these natural elements resulting in gamma-emitting activities were determined simultaneously: (n,2n) cross sections on ^{74}Se, ^{76}Se, ^{80}Se, ^{82}Se, and ^{54}Fe; (n,p) cross sections on ^{74}Se, ^{76}Se, ^{78}Se, and ^{54}Fe; and (n,α) cross sections on ^{78}Se, ^{80}Se, and ^{54}Fe. The method was used successfully with chemical compounds and with mixtures of powders in which one of the constituents was employed as a monitoring activity. A careful determination of these cross sections in the region Z = 30 to Z = 35 at 14.4 ± 0.3 Mev was undertaken in view of their importance in studying shell structure effects on (n,α) and (n,2n) cross section systematics. (auth)

40080 (ORO-3346-3) MEASUREMENT OF (n,2n), (n,p), AND (n,α) CROSS SECTIONS OF Ge AT 14.4 Mev. Wood, R. E.; Cook, W. S.; Goodgame, J. R.; Fink, R. W. (Georgia Inst. of Tech., Atlanta. School of Chemistry). July 22, 1966. Contract AT(40-1)-3346. 7p. (CONF-660906-3). Dep. mn. CFSTI $1.00 cy, $0.50 mn.

For Presentation at International Conference on Nuclear Physics, Gatlinburg, Tenn.

The nuclides ^{75}Ge, ^{69}Ge, ^{72}Ga, ^{73}Ga, ^{74}Ga, ^{69m}Zn, and ^{71m}Zn were produced by irradiating natural germanium with 14.4 ± 0.3-Mev neutrons. A mixture of iron, aluminum, and germanium powders also was irradiated. The activities were identified from the gamma spectra taken with a Ge(Li) detector, and the cross sections were measured using the improved technique described by Rao and Fink (this conference). The reactions for which cross sections have been measured are as follows: ^{70,76}Ge(n,2n); ^{72,73,74}Ge(n,p); and ^{72,74}Ge(n,α). The results are compared with previously published work on the systematics of (n,2n), (n,p), and (n,α) cross sections at 14 to 15 Mev. (auth)

40081 (PAEC(D)IS-653) ON THE PREPARATION OF 2.56-HOUR ^{65}Ni. Davila, A. T.; Eugenio, M. R. (Philippine Atomic Energy Commission, Manila). June 1965. 15p. Dep. mn.

Ni-65 is produced by neutron irradiation of NiO in the PRR-1 by the reaction Ni-64(n,γ)Ni-65. Co-58 is also formed by an (n,p) reaction on the Ni-58 isotope which occurs naturally, and is 67.76% abundant. The two radioisotopes are separated by anion exchange using a Dowex 1 × 8 resin (100–200 mesh), with 7 M HCl as an eluant. The irradiated sample is first dissolved in concentrated HCl; this converts the cobalt present to $CoCl_4^{2-}$ complex while the nickel remains as Ni^{2+} and $NiCl^{+}$ ions. On passing through the anion exchange resin, previously converted into the chloride form, the $CoCl_4^{2-}$ exchanges with the Cl^{-} of the resin and is retained in the column. The Ni^{2+} and $NiCl^{+}$ pass through and are collected. The R_2CoCl_4 complex is then broken up when water is passed through, and Co^{2+} comes down. Ni-65 was identified by its gamma spectrum and half life. Co-58 was identified by its gamma spectrum and by the addition of Co-60 to the solution of irradiated NiO. When this was passed through the column, both Co-58 and Co-60 were found to be in the same fraction. (auth)

40082 COMPLETE CLASSIFICATION OF THE STATES OF NUCLEAR CONFIGURATIONS j^{K} FOR j = 9/2. Darling, J. D. (Univ. of Kentucky, Henderson); Seyler, R. G. Acta Phys. Acad. Sci. Hung., 21: 33-54(1966).

The techniques of group theory were first applied by Flowers (Proc. Roy. Soc., A212: 248(1952)) to the problem of classifying the states of systems of equivalent nucleons in jj-coupling. Flowers completely classified the states of equivalent nucleon configurations for the cases j = 3/2, j = 5/2, and j = 7/2. These classifications are extended to the case j = 9/2. In addition, formulas are obtained for the dimensionalities N[λ] and N(σ) of the partitions [λ] and (σ) associated with the irreducible representations of the unitary unimodular group SU (2j + 1) and the symplectic group Sp (2j + 1) respectively. These formulas reduce considerably the computations required to obtain the values of the dimensionalities N[λ] and N(σ) for the various partitions [λ] and (σ). Furthermore, the formula for N(σ) provides for the interpretation of non-standard partitions (σ) on the basis of dimensionality. This formula is used to deduce several general rules regarding these interpretations. (S.F.L.)

40083 NUCLEAR REACTIONS INDUCED BY INTERACTIONS OF 200-Mev ^{20}Ne IONS WITH NUCLEI OF IONOGRAPHIC EMULSIONS. Pfohl, Raymond (Centre de Recherches Nucleaires, Strasbourg). Ann. Phys. (Paris), 1: 353-90(May-June 1966). (In French).

The results of an investigation of the reactions of 200-Mev ^{20}Ne ions with light (C,N,O) and heavy (Br and Ag) nuclei in Ilford G2 and G5 emulsions are presented, together with an interpretation of the results. The emphasis in the study was on the reaction mechanisms involved. 82 references. (D.C.W.)

40084 NEW LEVELS IN ^{97}Tc. Cretzu, T. (Univ., Bucharest); Hohmuth, K.; Winter, G.; Schlintlmeister, J. Ann. Physik (7), 17: 1-6(1966). (In German).

The decay of ^{97}Ru was investigated using a scintillation spectrometer, a proportional counter, and a two-dimensional coincidence apparatus. New gamma lines of energies 460, 670 and 780 kev were found. For the classification of these transitions two new levels at 786 and 995 kev were introduced. The relative intensities of the gamma lines were found for the first time. The results are summarized in a new decay scheme for ^{97}Ru. The transition energy was found to be $Q_{\epsilon_0} \geq 1050$ kev. (tr-auth)

40085 ELECTRON POLARIZATION OF ^{144}Pr. Daniel, H.; Zaidi, S. A. A. (Max-Planck-Institut fuer Kernphysik, Heidelberg). Ann. Physik (7), 17: 33-41(1966). (In German).

The electron longitudinal polarization of the $(0^- \rightarrow 0^+)$ transitions of ^{144}Pr was measured at different energies. The measuring arrangement, consisting of a magnetic Doppler-line monochromator, a Pb converter, and an analyzer for the circular polarization of the bremsstrahlung, is described in detail and compared with other arrangements. The following polarizations P/(v/c) were measured relative to ^{32}P: 0.988 ± 0.037 (904 kev), 1.012 ± 0.029 (1215) kev), and 1.022 ± 0.045 (1532 kev). Together with new data concerning the spectral form it follows as upper limits for pure and pseudo-induced pseudoscalar coupling: $|C_P/C_A| < 5$, $|C'_P/C_A| < 5$. (tr-auth)

40086 THRESHOLD STATES AND REDUCED CLUSTER WIDTHS IN LIGHT NUCLEI. Rotter, I.; Zhusupov, M. A. (Vereinigtes Institut fuer Kernforschung, Dubna, USSR). Ann. Physik (7), 17: 57-67(1966). (In German).

The reduced cluster widths $A_{g.s.} + a \rightarrow B$ are found to be comparable for the various levels of the nucleus B. The number of shell model levels and the number of thresholds in a certain energy interval increase with increasing (but not too high) excitation energy. Therefore, in the framework of the shell model, frequently, one may observe an accidental correlation between a maximum in the spectrum of reduced cluster widths and the position of thresholds. With regard to this a large reduced cluster width in the neighborhood of the corresponding cluster threshold is not considered as an indication of a threshold effect. The existence of threshold effects will be seen in systematic deviations from the reduced widths and energies calculated without account of threshold effects. By means of lithium induced reactions effects of such a kind may be investigated. In general, they have large Q-values and conclusions to be drawn about the cluster structure of nuclei. The reduced cluster widths calculated in the framework of the shell model are given for some nuclei of the 1 p-shell. (auth)

40087 INTERMEDIATE STRUCTURE IN ^{41}Ca. Deconninck, G. (Univ., Namur, Belg.); Husain, M. Ann. Soc. Sci. Brux. Ser. I, 80: 185-92(July 16, 1966). (In French).

The neutron total cross section of ^{41}Ca was measured between 1 and 2 Mev, as was the cross section for elastic scattering. The total cross section revealed a strong resonance at 1.5 Mev, which was interpreted as a doorway state ($J = \frac{1}{2}^+$, $\Gamma = 300$ kev) and was compared with states recently observed in ^{41}K. (D.C.W.)

40088 OPTICAL MODEL ANALYSIS OF NEUTRON SCATTERING ON ^{12}C FROM 16 TO 20 Mev. Deconninck, G. (Univ., Namur, Belg.); Meulders, J. P. Ann. Soc. Sci. Brux. Ser. I, 80: 193-205(July 16, 1966). (In French).

The results of optical-model and Monte Carlo calculations are presented and discussed. The aim of this work is the study of resonances occurring in ^{9}Be$(\alpha,n)^{12}$C and ^{12}C$(n,n)^{12}$C reactions corresponding to states in ^{13}C. Preliminary experimental results are compared with calculation. It is also shown that discrepancies between optical-model calculations and measurements of elastic scattering of 14-Mev neutrons can not be explained by the presence of those resonances. (auth)

40089 SPIN-ORBIT POTENTIAL IN ^{9}Be(α,α) ELASTIC SCATTERINGS. Gregoire, G. (Centre de Physique Nucleaire, Louvain, Belg.). Ann. Soc. Sci. Brux. Ser. I, 80: 206-11(July 16, 1966). (In French).

The influence of a coupling potential between the angular momentum and the sign of the target nucleus is calculated in the distorted-wave Born approximation. The results are compared with experimental data. Some suggestions are made for an accurate determination of this coupling term. (auth)

40090 EXPERIMENTAL STUDY OF SCATTERING OF ALPHA PARTICLES BY ^{31}P. Gregoire, G. (Centre de Physique Nucleaire, Louvain, Belg.). Ann. Soc. Sci. Brux. Ser. I, 80: 212-17(July 16, 1966). (In French).

The elastic alpha particle scattering data on ^{31}P at 18.1 and 24 Mev are analyzed using the DWBA method. Some results relative to inelastic scattering are presented. Comparison with ^{32}S (α,α) data at the same energies indicates the validity of the weak-coupling approximation at least for the low-lying excited states (Q < 4 Mev). But the application of the collective models seems to be of doubtful value in explaining the level sequence and the gamma transition probabilities. (auth)

40091 INVESTIGATION OF A BOUND NEUTRON-NEUTRON STATE IN THE REACTION ^{9}Be(n,2n)^{8}Be. Roturier, Jacques; Irigaray, Jean-Leon; Petit, Georges-Yves (Faculte des Sciences de Bordeaux, Gironde, France). Compt. Rend., Ser. B, 1735-8(June 27, 1966). (In French).

From direct measurements of the distribution in time-of-flight of neutrons scattered by ^{9}Be and of the energy distribution of these neutrons for a given time of flight, the upper limit of the differential cross section of the reaction leading to the formation of a bound neutron-neutron state was determined to be 2 mb/sr. (tr-auth)

40092 STUDY OF THE ISOMERS ^{236g}Np AND ^{236m}Np BY THE INTERACTION OF DEUTERONS WITH ^{238}U. Lavollee, Philippe; Simonoff, Gabriel; Chenouard, Jean (Faculte des Sciences de Bordeaux, Gironde, France. CEN de Saclay, Gif-sur-Yvette, France). Compt. Rend., Ser. B, 1739-41(June 27, 1966). (In French).

After extraction by chemical separation, the ^{236g}Np produced was identified and measured with the aid of its descendant ^{236}Pu. The detection of ^{236m}Np was made by mass spectrometry. The value of the isomeric ratios of ^{236m}Np to ^{236g}Np increases rapidly with the increase of the angular momentum of the ^{240}Np compound nucleus formed. (tr-auth)

40093 INTENSITY OF THE 1.114-Mev GAMMA TRANSITION IN THE DECAY OF ^{65}Zn TO ^{65}Cu. Rao, P. S. (Atomic Energy Establishment, Trombay, India). Curr. Sci. (India), 35: 384(Aug. 5, 1966).

The intensity of the gamma transition from the 1.114-Mev level to the ground state of ^{65}Cu was evaluated by measuring a standard sample of ^{65}Zn using a 4π gamma chamber. A value of 51.3 ± 1.5% was obtained for the intensity of the transition. (S.F.L.)

40094 LIFETIMES OF 1554- AND 1289-kev LEVELS OF ^{182}W. Narasimha Rao, B. V.; Jnanananda, Swami (Andhra Univ., Waltair, India). Curr. Sci. (India), 35: 384-5(Aug. 5, 1966).

Measurements were made of the lifetimes of the 1289- and 1554-kev levels of ^{182}W using a delayed-coincidence spectrometer. The average values of the lifetimes of the 1289- and 1554-kev levels obtained from three sets of experiments are 1.08 ± 0.04 ns and 5.07 ± 0.16 ns, respectively. These values include an error of 3% arising from the instrument calibration and measurement of cable lengths. (S.F.L.)

40095 MEASUREMENT OF THE INTERNAL CONVERSION COEFFICIENT OF THE 800 kev TRANSITION OF Ba-134. Raja Rao, M.; Jnanananda, S. (Andhra Univ., Waltair, India). Curr. Sci. (India), 35: 435-6(Sept. 5, 1966).

The internal conversion coefficient of the 800-kev transition in ^{134}Ba was measured using an internal-external conversion technique. The total conversion coefficient was obtained, and the K-conversion coefficient was derived using K/L = 7. The values for the K-conversion coefficient were

compared with other experimental values and with theoretical values. The E2 nature of the radiation was confirmed by the agreement of the values. (D.C.W.)

40096 SOME REGULARITIES IN THE ANGULAR DISTRIBUTION OF NEUTRONS EMITTED IN POLARIZED μ-MESON CAPTURE BY NUCLEI. Bobodzhanov, I. B.; Kashkarov, L. L. Dokl. Akad. Nauk Tadzh. SSR, 7: No. 4, 12-15(1964). (In Russian).

The reaction $\mu^- + (A,Z) \rightarrow (A-1, Z-1) + n + \nu$ with polarized mesons (μ^-) on Cu, Fe, and Pb was investigated using cosmic radiation. The coefficient of asymmetry $a_n = b(1 - C)/(1 + C)$, where b accounts for the experimental geometry and C is the ratio of neutrons emitted in the same direction and the opposite direction as the mesons (μ^-), was -0.062 ± 0.054, -0.066 ± 0.81, and -0.079 ± 0.010, for Cu, Fe, and Pb, respectively. The coefficients a_n are approximately the same as the values of the coefficient of e asymmetry in the $(\mu^- - e^-)$ decay. (D.C.W.)

40097 CIRCULARLY POLARIZED β-γ CORRELATION IN THE DECAY OF ^{188}Re(17h). Gygax, F.; Hess, R. (EPF, Zurich). Helv. Phys. Acta, 39: 209-10(1966). (In French).

The circularly polarized β-γ correlation in the decay of ^{188}Re was calculated at β energies of 1.2 Mev for angles of 180 and 135°. The results obtained were $\overline{P}_\gamma = -0.17 \pm 0.06$ and 0.21 ± 0.08, respectively. (J.S.R.)

40098 THE CROSS SECTION OF THE ^{73}Ge(n,α)^{70}Zn REACTION AT 14-Mev NEUTRON ENERGY. Huber, P.; Hunn, W.; Steiner, E.; Wagner, R. (Univ., Basel). Helv. Phys. Acta, 39: 217-18(1966). (In German).

The cross section of the ^{73}Ge(n,α)^{70}Zn reaction at 14-Mev neutron energy was measured as 0.13 ± 0.02 mb. (J.S.R.)

40099 Q VALUE OF THE REACTION ^{27}Al(p,α)^{24}Mg. Reichart, W.; Von Sengbusch, G.; Staub, H. H.; Zamboni, F. (Univ., Zurich). Helv. Phys. Acta, 39: 219-21(1966). (In German).

Direct measurements were made of the Q value of the ^{27}Al(p,α)^{24}Mg reaction in order to discover the source of the discrepancies in previous measurements. The value obtained was $Q = 1598^{+3.3}_{-1.3}$ kev. The discrepancies were ascribed to simple combined errors in the measurement. (J.S.R.)

40100 STUDY OF THE REACTIONS ^{40}Ca(n,α)^{37}Ar AND ^{19}F(n,α)^{16}N WITH 6-Mev NEUTRONS. Knellwolf, T.; Rossel, J. (Univ., Neuchatel, Switzerland). Helv. Phys. Acta, 39: 376-96(1966). (In French).

The differential cross section for the group α_0 and the group $\alpha_1 + \alpha_2$ corresponding to the ground and first two excited states in the reaction ^{40}Ca(n,α)^{37}Ar and for the 4 unresolved lower states in the reaction ^{19}F(n,α)^{16}N were measured with 6 Mev neutrons and both CaF_2 and Ca targets. The directional detector composed of two proportional and one solid state counter in coincidence, which allows E versus dE/dx proton-α discrimination, is described and the different checks and corrections needed are discussed. The angular distribution for the α_0 group is found to be symmetrical about 90° whereas it is not for the $\alpha_1\alpha_2$ group. For ^{19}F, the measurement in a limited angular range allows no definite conclusion. The total cross sections obtained by integration are as follows: $\sigma(n,\alpha_0) = (60.5 \pm 7.2)$ mb, $\sigma(n,\alpha_1\alpha_2) = (47.8 \pm 5.8)$ mb for ^{40}Ca and $\sigma(n,\alpha) = (121 \pm 14)$ mb for ^{19}F. It is argued that the difference in character of the two angular distributions for ^{40}Ca is due to fluctuations and that direct interaction is improbable. An attempt is made to evaluate the probability of preformation of the α particle in the compound nucleus, the difference in nucleon configuration for ^{40}Ca and ^{19}F being particularly pronounced. Some results concerning this point are presented. (auth)

40101 ^{27}Al(p,α)^{24}Mg REACTION STUDIES WITH A 30-Mev AVF CYCLOTRON. Put, L. W. (Univ., Groningen, Netherlands); Roeders, J. D. A.; van der Woude, A.; Hagedoorn, H.; Kramer, P. IEEE (Inst. Elec. Electron. Eng.), Trans. Nucl. Sci., NS-13: No. 4, 349-52(Aug. 1966).

The experimental arrangement and results of an investigation of the excitation function for the ^{27}Al(p,α)^{24}Mg reaction from 11 to 19.7 Mev are described, which point to the usefulness of AVF cyclotrons as a very suitable tool for high resolution nuclear physics experiments. (L.B.S.)

40102 INFLUENCE OF BLOCKING EFFECTS ON NUCLEAR MOMENTS OF INERTIA. Safarov, R. Kh. (Inst. of Nuclear Physics, Academy of Sciences, Uzbek SSR). Izv. Akad. Nauk Uz. SSR, Ser. Fiz.-Mat. Nauk, No. 1, 69-73 (Jan.-Feb. 1966). (In Russian).

Application of the superfluid model to calculations of the moments of inertia of strongly deformed nuclei indicated that the blocking effect, which changes the superfluid properties, must be taken into account. Pairing of nucleons in the ground state of an even system causes changes in the Fermi distribution, resulting in the blurring of the pairs near the chemical potential. These changes are especially strong at levels near the Fermi surface; with increasing excitation energy, the superfluid properties increase and approach the value of the ground state. An attempt was made to extend these blocking effects to the moments of inertia of even-even nuclei at any arbitrary low-excitation state and to odd nuclei. It was found that consideration of the blocking effect causes a reduction of the moment of inertia values obtained without consideration of blocking; this indicates that the wave function is involved in this effect. (TTT)

40103 NUCLEAR MAGNETIC DOUBLE RESONANCE OF A SINGLE NUCLEUS OF SPIN 1/2. Gordon, Sidney L. (Georgia Inst. of Tech., Atlanta). J. Chem. Phys., 45: 1145-51(Aug. 15, 1966).

The nuclear magnetic double-resonance spectrum of a single nucleus of spin $\frac{1}{2}$ is theoretically described by perturbation theory and by the Bloch equations. The perturbation theory correctly predicts all experimental features except line shapes and saturation effects. The description in terms of the Bloch equations provides a clear physical picture of the spin-$\frac{1}{2}$ problem. The analysis shows that the macroscopic moment is aligned with the effective field when the strong r-f field is not in the immediate vicinity of the Larmor frequency. When the strong r-f field is at the Larmor frequency, however, the macroscopic moment is perpendicular to the effective field. This produces considerable changes in line shapes and intensities as the strong r-f field approaches the Larmor frequency. The spectrum in this region is sensitive to the relaxation times and provides a steady-state method for measurement of relatively short relaxation times. The theory is confirmed by frequency-sweep double-resonance experiments on chloroform saturated with oxygen. (auth)

40104 CALCULATION OF THE DIRECT REACTION ^{12}C(n,n')^{12}*C(2+) BY THE DISPERSION METHOD. Kaminskii, V. A. (Inst. of Physics and Chemistry, USSR). JETP Lett. (USSR) (Engl. Transl.), 4: 43-5(July 15, 1966).

Translated from Zh. Eksp. Teor. Fiz., Pis'ma Redaktsiyu, 4: 64-8(July 15, 1966).

The angular distribution of neutrons inelastically scattered by ^{12}C at 14 Mev was calculated taking into account the interaction in the initial and final states. The results show that, in the case considered, the amplitude with allowance for the virtual-scattering effects can be expressed in terms of the initial amplitude and the scattering phases in the physical region without using a model for the scattering. The results do not exclude the possibility of explaining the experimental data small angles by considering diagrams that do not take into account the virtual scattering and have amplitudes differing from zero at $\theta = 0$. (auth)

40105 LIFETIMES OF THE EXCITED LEVELS OF ^{151}Pm. Begzhanov, R. B.; Gladyshev, D. N.; Sadykov, Kh. M.; Teshabaev, K. (Inst. of Nuclear Physics, Uzbek SSR). JETP Lett. (USSR) (Engl. Transl.), 4: 48-50 (July 15, 1966).

Translated from Zh. Eksp. Teor. Fiz., Pis'ma Redaktsiyu, 4: 71-4(July 15, 1966).

The lifetimes of the excited states of ^{151}Pm were investi-

gated using a delayed coincidence method. Evidence that the 256-kev level is l-forbidden with multipolarity M1 and spin $7/2^+$ was obtained. (D.C.W.)

40106 VORTEX ISOMERS OF NUCLEI. Zel'dovich, Ya. B. JETP Lett. (USSR) (Engl. Transl.), 4: 53-4 (July 15, 1966).

Translated from Zh. Eksp. Teor. Fiz., Pis'ma Redaktsiyu, 4: 78-80(July 15, 1966).

If nuclear matter is a superfluid liquid, then a state corresponding to a drop of this liquid is possible (a nucleus with a quantized vortex passing along the axis of the drop). It is shown that the vortical state can be regarded as isomeric. The experimental realization of such states is briefly considered, particularly the smallest number of bosons above which the concepts of superfluidity and quantum vortex can be used. It is shown that an isomeric state with angular momentum $I = z\hbar_0/2$ can be realized, in principle, in a relatively light nucleus. (D.C.W.)

40107 MEASUREMENT OF RADIOACTIVE DISINTEGRATION RATE BY THE COINCIDENCE METHOD. Baerg, A. P. (National Research Council, Ottawa). Metrologia, 2: 23-32(Jan. 1966).

The principles of radioactive disintegration rate measurement by the coincidence method are reviewed. It is shown that the basic equations for complex decay can be translated into formulas suitable for deducing absolute rates from observed counting data without requiring any knowledge of the decay scheme constants. The formulas are generally valid for β-γ emitters under conditions attainable in practical $4\pi\beta$-γ coincidence systems. Currently used techniques and various factors which influence the accuracy of measurement are discussed. (auth)

40108 WHY SHOULD WE INVESTIGATE NUCLIDES FAR OFF THE STABILITY LINE. Bergstroem, I. (Royal Inst. of Tech. and Research Inst. for Physics, Stockholm). Nucl. Instrum. Methods, 43: 116-28(Aug. 1, 1966).

An analysis of the nuclear chart shows that there should exist more beta-unstable nuclides (including neutron-, proton-, and alpha-emitters) than hitherto observed. The half lives of these radioactive nuclides fall in the region 10^{-3}–10^2 sec, which is the experimental reason that they have not been studied very much so far. It is emphasized that new double magic regions will be found among these nuclides as well as new regions of stable deformation. Q_β-values far off the stability line as well as a careful mapping of delayed neutron- and proton-emitters and alpha emitters will be of great importance for the semi-empirical mass formula. In addition half lives and neutron separation energies are of astrophysical interest. Because of the high Q_β-values expected, highly excited states will be populated and beta decay yields information which usually is reserved for nuclear reactions. The extension of the systematics of fission and spallation yields into the regions of very short half lives may increase our understanding of fission as well as other nuclear reaction processes. (auth)

40109 HOW SHOULD WE INVESTIGATE NUCLIDES FAR OFF THE STABILITY LINE. Bergstroem, I. (Royal Inst. of Tech. and Research Inst. for Physics, Stockholm). Nucl. Instrum. Methods, 43: 129-45(Aug. 1, 1966).

An extension of nuclear spectroscopy to beta unstable nuclides all the way to the limit for which the neutron- and proton-separation energies are zero, will require new experimental approaches, because of the fact that the half lives for beta decay will fall in the region 10^{-3}–10^2 sec. One possible way is to use a complete so called on-line system having irradiation, chemical separation, transport to an ion source, electromagnetic mass separation, collection and detection as well as data handling in a continuous chain. The expected difficulties and limitations of such systems are discussed and the projects and preliminary results presented. As much as possible the analysis is based on information which has become available during the last two years. (auth)

40110 LIFETIMES OF THE 87 AND 105 kev LEVELS IN ^{155}Gd. McAdams, R. E.; Hatch, E. N. (Ames Lab., Ames, Iowa). Nucl. Phys., 82: 372-84(July 1966). (IS-1306).

The half lives of the 87- and 105-kev levels in ^{155}Gd were measured using fast coincidence techniques in a study of the decay of ^{155}Eu. In addition, the half lives of the 89-kev level in ^{156}Gd and the 122-kev level in ^{152}Sm were determined as a check on the experimental equipment and the method used in the measurements. (D.C.W.)

40111 LEVELS IN ^{11}B FROM ^{7}Li$(\alpha,\alpha)^7$Li AND ^{7}Li$(\alpha,\alpha')^7$Li*(0.48). Cusson, R. Y. (California Inst. of Tech., Pasadena). Nucl. Phys., 86: 481-508(1966).

The absolute differential cross sections for the reactions ^{7}Li$(\alpha,\alpha)^7$Li and ^{7}Li$(\alpha,\alpha')^7$Li*(0.48) were measured in the range of energies and angles, $1.6 \leqq E_{\alpha L} \leqq 12.0$ Mev, $20° \leqq \theta_{\alpha L} \leqq 150°$, using thin ^{7}Li targets. Solid-state detectors were were used to detect the scattered α particles. A total of 19 scattering anomalies was observed in this energy range. In the excitation energy range $9.88 \leqq E_x(^{11}B) \leqq 11.27$ Mev, in which six levels were observed, the measured cross sections were fitted by using a multi-level R-matrix-theory program for the 7094 computer. The best fits were obtained with the spin and parity assignments 9.88 ($3/2^+$), 10.26 ($3/2^-$), 10.32 ($5/2^-$), 10.60 ($7/2^+$), 11.0 ($5/2^-$), 11.27 ($7/2^+$, $9/2^+$). Some alternatives for these assignments are discussed. These results are consistent with what is known of the level structure of the analogue nucleus ^{11}C. (auth)

40112 THE REACTIONS ^{11}B$(^3$He,n$)^{13}$N AND ^{7}Li$(^3$He,n$)^9$B FROM 1.5 TO 5.5 Mev BOMBARDING ENERGY. Din, G. U. (Rice Univ., Houston, Tex.); Weil, J. L. Nucl. Phys., 86: 509-27(1966). (TID–22724).

Excitation functions for the ^{11}B$(^3$He,n$)^{13}$N in the ground state were measured at lab angles of 0, 90, and 145° in the energy range of 1.5 to 5.6 Mev. A very broad peak in the 0° yield curve at 4.15-Mev, together with other evidence, indicates the existence of a 1-Mev wide state in ^{14}N at an excitation energy of about 23.9 Mev. Seven angular distributions were measured at 2.03, 2.70, 3.47, 3.83, 4.10, 4.76, and 5.27 Mev. The shapes of these angular distributions do not change rapidly as a function of energy. Each angular distribution shows a broad peak at 0°, and a secondary maximum at about 130° is seen in those measured above 4 Mev. Excitation functions were studied for the reaction ^{7}Li$(^3$He,n$)^9$B at $\theta_{lab} = 0$, 90, and 160° in the energy range of 1.5 to 5.5 Mev. Resonances are seen in the 0 and 160° curves near 2.2 Mev with widths of about 270 kev. There is also a resonance in the 0° yield at 3.25 Mev with a width of 500 kev. The 90° yield curve stays roughly constant in the range of bombarding energy studied. Eleven angular distributions were measured at 1.56, 1.95, 2.20, 2.56, 2.94, 3.27, 3.62, 3.97, 4.35, 4.86 and 5.27 Mev. All angular distributions have a single broad minimum around 90° and broad peaks at 0° and/or 180°. Despite the general similarity of the angular distributions, analysis in terms of sums of Legendre polynomials indicates the presence of a state near 2.2-Mev bombarding energy. No information on a possible neutron group leaving ^{9}B in a state of excitation of about 1.7 Mev could be obtained because of a continuum background of neutrons from many-body breakup of ^{10}B. (auth)

40113 PROBABILITY DISTRIBUTION OF MAXIMA AND MINIMA OF NUCLEAR CROSS SECTIONS. Ericson, M.; Couchoud, S. (Univ., Lyon). Nucl. Phys., 86: 528-34(1966).

The probability distributions of maxima and minima of nuclear cross sections are derived assuming a random scattering amplitude in the one-channel case. The probability distributions are similar to χ^2 distributions, of one of degree of freedom for minima and of three degrees of freedom for maxima. (auth)

40114 DISTORTED WAVE CALCULATIONS OF LOW-ENERGY DEUTERON STRIPPING REACTIONS. Strobel, G. L. (Univ. of California, Davis). Nucl. Phys., 86: 535-44(1966). (UCD-CNL-45).

Distorted-wave calculations for low-energy deuteron stripping reaction cross sections are compared to experiment. Possible competition of various direct reaction mechanisms is considered for various parameterizations of the distorting optical potentials. (auth)

40115 PROBLEMS IN NUCLEAR SATURATION. I. STATISTICAL TREATMENT OF FINITE NUCLEI. Macke, W.; Rennert, P.; Schiller, W. (Technical Univ., Dresden). Nucl. Phys., 86: 545-60(1966).

For momentum-dependent, nonsingular nuclear forces, a statistical method is developed which allows the simple calculation of density distribution, binding energy, separation energy, and average one-particle potential for nuclear matter and finite nuclei. Equations are set up for spin- and isospin-dependent central forces. They correspond to the Thomas-Fermi approximation with exchange and inhomogeneity corrections. For one test potential, the nuclear density of ^{40}Ca and ^{197}Au is determined by various approximations. Good agreement with the experimentally measured density is obtained. (auth)

40116 ELECTRIC MONOPOLE TRANSITIONS AND BETA BANDS IN EVEN NUCLEI. Davidson, J. P. (Naval Radiological Defense Lab., San Francisco). Nucl. Phys., 86: 561-73(1966).

Reduced transition probabilities for electric monopole transitions ρ^2 were calculated using a collective model with deformation vibrations but no asymmetry vibrations. Both ρ^2 and $X = \rho^2 e^2 R_0^4/B(E2)$ were evaluated within the context of the model by exact numerical methods for transitions within positive as well as negative parity rotational bands of even nuclei. Comparison of experiment with theory shows quite good agreement in the actinide deformed region; however, for the rare earths theoretical predictions are generally an order of magnitude greater than the measured values. (auth)

40117 THEORETICAL PROTON ENERGY-LOSS DISTRIBUTIONS FROM THIN CARBON FOILS. Butler, J. W. (Naval Research Lab., Washington, D. C.). Nucl. Phys., 86: 574-80(1966).

The Landau solution of the problem of fluctuations in energy losses of charged particles in penetrating thin foils is compared with the experimental data of Morsell, who measured the energy-loss distributions of 992-kev protons in penetrating carbon foils in the thickness range of 222 to 2013 ev. The theoretical distributions so computed agree with the experimental data within experimental precision. This agreement is interpreted to confirm the applicability of Landau's solution to the problem of computing nuclear reaction yield curves for 1-Mev protons impinging on low-Z foils in the kev thickness range. (auth)

40118 THE γ-VIBRATIONS IN ODD-MASS RARE-EARTH NUCLEI. Bes, D. R. (NORDITA, Copenhagen); Cho, Yi-chung. Nucl. Phys., 86: 581-610(1966).

The calculations of γ vibrations are extended to odd-mass nuclei. The essential assumptions of the even case are maintained, including the harmonic approximation. In the construction of the phonons, care is taken of the Pauli principle. It is concluded that the quadrupole correlations provide a useful way of explaining the present experimental material, although, as in the even case, some difficulties remain unexplained. (auth)

40119 CALCULATION OF BINDING ENERGY OF ^{16}O NUCLEUS. Koehler, H. S.; McCarthy, R. J. (Rice Univ., Houston, Tex.). Nucl. Phys., 86: 611-24(1966). (TID-22933).

A method to calculate binding energies of nuclei by K-matrix theory is presented and is applied to ^{16}O. A first-order approximation to the K-matrix is obtained by neglecting the Pauli principle and potential energies in intermediate states. Thus to first order, the Puff-Mohling reaction matrix is considered. In light of recent work on the effect of the three-body interaction it seems a reasonable approximation to neglect potential energies in intermediate states. Thus the only correction term is due to the Pauli principle. The method is however easily extended to a more general energy spectrum. It can be applied to finite nuclei as well as to infinite nuclear matter. Formally, the method used to calculate the K-matrix is similar to the "reference spectrum" method of Bethe, Brandow and Petschek applied by them to infinite nuclear matter. The method is applied to ^{16}O using harmonic oscillator single-particle wave functions and a nucleon-nucleon interaction represented by a spin independent exponential potential giving infinite scattering length and 2.5 fm effective range (Moszkowski-Scott potential) acting only in relative s-states. A binding energy of 2.77 Mev/nucleon is obtained. The Puff-Mohling K-matrix (the first-order K-matrix) gives 1.7 Mev/nucleon more binding. Comparison with the, in principle, more approximate separation method calculation gives perfect agreement. (auth)

40120 DIAGRAMMATIC REPRESENTATION AND UTILIZATION OF ROTATION MATRICES. El-Baz, E.; Massot, J.-N.; Lafoucriere, J. (Univ., Lyon). Nucl. Phys., 86: 625-37(1966). (In French).

It is shown that rotation matrices can be represented by a diagrammatic method. The diagram representing a rotation matrix is given, and the rules of integration and summation on these diagrams are presented. (D.C.W.)

40121 ON THE OCTUPOLE DEFORMABILITY OF THE NUCLEUS ^{19}F. Zaikin, D. A. (Lebedev Inst. of Physics, Moscow). Nucl. Phys., 86: 638-48(1966).

The nucleus ^{19}F is considered within the framework of the unified model. It is shown that experimental data on the excited states and γ transitions indicate that this nucleus is rather soft for octupole deformations, mainly for the non-axial ones. (auth)

40122 DISTORTED WAVE ANALYSIS OF THE REACTION $^{14}N(d,p)^{15}N$ AT LOW BOMBARDING ENERGIES. Robson, B. A. (Australian National Univ., Canberra). Nucl. Phys., 86: 649-56(1966).

Several transitions in the reaction $^{14}N(d,p)^{15}N$ at low bombarding energies are analyzed using the distorted-wave theory of deuteron stripping. It is found that the dominating reaction mechanism, even when the Q-value is not low, is a direct interaction. Under certain conditions, resonance behavior, typical of compound nucleus formation, may occur through a direct process. (auth)

40123 HALF-LIFE OF THE 453.08 kev LEVEL IN ^{183}W. Hoenig, V.; Loebner, K. E. G.; Vetter, M. (Univ., Freiburg i. B.). Nucl. Phys., 86: 657-67(1966).

The half life of the $7/2\ 7/2^-[503]$ level at 453.08 kev in ^{183}W was measured from the decay of ^{183}Re to be $T_{1/2} = 19.0 \pm 0.6$ ns, yielding the absolute gamma transition probabilities of transitions to seven different levels. The half life of the 453.08-kev level, in connection with the upper limit given for the gamma transition to the 309.49-kev state, suggests the interpretation of the 309.49-kev level as the $11/2\ 11/2^+[615]$ Nilsson level instead of $9/2\ 9/2^+[624]$. (auth)

40124 SINGLE-PARTICLE MATRIX ELEMENTS jj-COUPLING FOR FIRST-FORBIDDEN BETA TRANSITIONS. Delabaye, M.; Lipnik, P. (Centre de Physique Nucleaire, Louvain, Belg.). Nucl. Phys., 86: 668-76 (1966).

Reduced single particle matrix elements are tabulated for the first-forbidden beta transitions. These computations are made in the framework of the jj-coupling scheme for the single-particle wave functions. (auth)

40125 ON CIRCULAR POLARIZATION MEASUREMENTS IN γ-γ PERTURBED ANGULAR CORRELATIONS. Beltrametti, E. G. (Univ., Genoa). Nucl. Phys., 86: 677-80(1966).

The role of circular polarization measurements in γ-γ perturbed angular correlations is examined. It is shown, in particular, that g-factors of spin-1/2 excited nuclear states could be measured by allowing circular polarization detection. (auth)

40126 LEVEL STRUCTURE OF OXYGEN ISOTOPES IN THE SU_3 SCHEME. Trlifaj, L.; Gmitro, M.; Sotona, M.

(Inst. for Nuclear Research, Czechoslovak Academy of Sciences, Rez). Nucl. Phys., 86: 681-94(1966).

The lowest ^{20}O levels are calculated in the L-S coupling using the SU_3 classification. The residual interaction is taken as a mixture of two-body Gaussian potentials and the spin-orbit force. After fitting the energy spectrum, the spectroscopic factors of the reaction $^{18}O(t,p)^{20}O$ and E2 transition probabilities are calculated. Overall agreement with experiment is obtained. (auth)

40127 HALF LIFE AND SPECIFIC ACTIVITY OF ^{226}Ra. Ramthun, Heinz (Physikalisch-Technische Bundesanstalt, Brunswick). Nukleonik, 8: 244-7(June 1966). (In German).

Microcalorimetric measurements on the heating effects of three radium standards prepared by Honigschmid are combined with a calculated value for the mean energy transfer to the calorimeter cell per radium disintegration. The derived values for the specific disintegration rate ζ, the half life τ, and the disintegration constant λ of ^{226}Ra seem to be more reliable than any other value previously published: $\zeta = 3.659 \pm 0.015 \times 10^{10}\ s^{-1}\ g^{-1}$; $\tau = 1599 \pm 7$ yr; and $\lambda = 4.33 \pm 0.02 \times 10^{-4}\ a^{-1}$. The confidence limits are given for a statistical significance of 99.7%. (auth)

40128 MAGNETIC MOMENT OF THE LOWEST 2^+ VIBRATIONAL STATE IN ^{122}Te. Johansson, K.; Karlsson, E.; Sommerfeldt, R. W. (Inst. of Physics, Uppsala). Phys. Lett., 22: 297-9(Aug. 15, 1966).

The nuclear g factor of the 564 kev 2^+ state in ^{122}Te was measured by observation of the rotation of the 656-564 kev γ-γ angular correlation in the internal field acting on the nuclei of tellurium when dissolved into an iron matrix. The result was $g = 0.386 \pm 0.060$, or $\mu = 0.77 \pm 0.12$ mm. The result is discussed in terms of current theories for vibrational states. Furthermore, the M1 admixture in the $2^{+\prime} \rightarrow 2^+$ transition was obtained with improved accuracy from the angular correlation measurements. (auth)

40129 MEASUREMENT OF THE ELECTRON-NEUTRON INTERACTION BY THE ASYMMETRICAL SCATTERING OF THERMAL NEUTRONS BY NOBLE GASES. Krohn, V. E.; Ringo, G. R. (Argonne National Lab., Ill.). Phys. Rev., 148: 1303-11(Aug. 26, 1966).

The electron-neutron interaction was obtained from measurements of thermal neutron scattering by argon, krypton, and xenon. In terms of the slope of the electric structure factor of the neutron at zero momentum transfer, the values obtained were $0.0196 \pm 0.0013\ ^2F$ from Ar, $0.0197 \pm 0.0007\ ^2F$ from Kr, and $0.0190 \pm 0.0005\ ^2F$ from Xe. The final result is $0.0193 \pm 0.0004\ ^2F$, which corresponds to an electron-scattering length of $-1.34 \pm 0.03 \times 10^{-16}$ cm and an effective potential of -3720 ± 90 ev. During the course of the experiment, the neutron-absorption cross sections of krypton and xenon (at 2200 m/sec) were measured by transmission and found to be 25.0 ± 0.8 b and 25.1 ± 1.0 b, respectively. Also, some free-atom thermal-neutron scattering cross sections were measured. The results were 2.415 ± 0.010 b for neon, 0.647 ± 0.003 b for argon, 7.61 ± 0.04 b for krypton, 4.30 ± 0.02 b for xenon, 73.7 ± 0.4 b for ^{36}Ar, 1.705 ± 0.009 b for ^{22}Ne, and 5.1 ± 0.3 b for ^{21}Ne. (auth)

40130 ALMOST EXACT SUM RULES FOR NUCLEON MOMENTS FROM AN INFINITE-DIMENSIONAL ALGEBRA. Beg, M. A. B. (Brookhaven National Lab., Upton, N. Y. Rockefeller Univ., New York). Phys. Rev. Lett., 17: 333-6(Aug. 8, 1966).

A set of sum rules which follow from an infinite-dimensional algebra, which contains (and may be regarded as the most natural extension of) an algebra suggested by Gell-Mann (Physics 1: 63(1964)) is presented for nucleon moments. Besides providing a means for calculation of the magnetic moments, these sum rules, taken together with the Adler-Weisberger (Phys. Rev. Letters 14: 1047, 1051(1965)) sum rule, constitute a useful tool for investigating the nature of the dynamical approximations that underlie higher symmetry schemes. (S.F.L.)

40131 PROMETHIUM-140. Aten, A. H. W. Jr.; Kapteijn, Johanna C. (Instituut voor Kernphysisch Onderzoek, Amsterdam). Physica, 32: 1159-60(June 1966).

Previous experiments on the proton irradiation of rare earths are discussed and it is concluded that the reactions; $^{142}Nd(p,3n)^{140}Pm$ and $^{144}Sm(p,\alpha n)^{140}Pm$ were observed. The half-life observed in the present experiments with the proton irradiation of ^{142}Nd was 6 ± 1 min. The γ energies of the ^{140}Pm decay were measured with a germanium detector and found to be 418 kev, 775 kev, and 1027. After the rare earth fraction was separated from ^{15}O by a fluoride precipitation, the decay of the annihilation line also showed a component of about 6 min., which indicated that positrons are also emitted by ^{140}Pm. (W.D.M.)

40132 MEASUREMENT OF THE LIFETIME OF THE 14.4 kev LEVEL OF ^{57}Fe. Eckhause, M.; Harris, R. J. Jr.; Shuler, W. B.; Welsh, R. E. (Coll. of William and Mary, Williamsburg, Va.). Proc. Phys. Soc. (London), 89: 187-8(Sept. 1966).

The half-life of the 14.4 kev level of ^{57}Fe was measured with scintillation detectors and a digital timer. The value obtained was 97.7 ± 0.2 nsec. (auth)

40133 RESONANCES IN THE $^{41}K(p,\gamma)^{42}Ca$ REACTION AT PROTON ENERGIES 1740-2170 kev. Simons, L.; Anttila, A.; Bergstroem, S.; Luukko, A. (Univ. of Helsinki). Soc. Sci. Fenn., Comment. Phys.-Math., 32: No. 3, 1-7 (1966).

The reaction $^{41}K(p,\gamma)^{42}Ca$ was investigated in the energy range from 1.74 to 2.17 Mev; 80 resonances were observed. Gamma spectra from some of the strongest resonances were recorded. The intensity ratios of the gamma rays follow approximately the Weisskopf estimates for single-particle excitations. (D.C.W.)

40134 INTERNAL PAIR FORMATION IN ^{22}Ne FOLLOWING THE POSITRON DECAY OF ^{22}Na. Spring, E. (Univ. of Helsinki). Soc. Sci. Fenn., Comment. Phys.-Math., 32: No. 9, 1-7(1966).

The internal pair formation of the 127-Mev transition in ^{22}Ne was studied by measuring quadrupole coincidences between NaI(Tl) detectors. The annihilation radiation originating from the internal pair formation was measured in coincidence with the corresponding radiation caused by the positron decay of ^{22}Na. The internal pair formation coefficient was determined to be $3.5 \pm 1.0 \times 10^{-5}$. (D.C.W.)

40135 INFLUENCE OF THE CRYSTAL LATTICE ON SOME ATOMIC AND NUCLEAR PROCESSES. Tulinov, A. F. Usp. Fiz. Nauk, 87: 585-98(Dec. 1965). (In Russian).

A review is given of the influence of the lattice on the nature of motion of fast particles in a crystalline medium. The study includes an analysis of problems connected with the motion of particles introduced into a crystalline sample from the outside, as well as problems involving particles generated in the crystal itself, particularly those emerging directly from the lattice sites. Only the motion of charged particles is considered. In the case of particles incident on a single crystal from the outside, special attention is paid to the channeling of the captured particles inside a crystal, the distribution of the electrons belonging to different atomic shells within the channel, the decrease in the probability of reactions caused by the channeled particles, the reduction in the energy lost by the particles, and the yield of characteristic x rays resulting from such reactions. In the case of charged particles which are products of nuclear reactions and interact with the lattice, the emphasis is on the shadow effect in which certain directions along the crystallographic axes are closed to particles leaving the lattice sites so that characteristic shadows can be observed along these directions. Possible applications of the shadow effect to determine the duration of nuclear reactions and to investigate some properties of crystals, as well as in investigations of the alpha decay of nuclei introduced in the crystal lattice are described. The use of shadow patterns connected with the presence of numerous crystallographic directions for the study of crystalline structure is described. (ATD)

40136 NUCLEAR SHAPE, DEFORMABILITY, AND EXCITED STATES OF ATOMIC NUCLEI. Davydov, A. S. Usp. Fiz. Nauk, 87: 599-614(Dec. 1965). (In Russian).

A review is given of recent developments in the study of the symmetry of the self-consistent field acting on the nucleons within the nucleus, which governs the nuclear shape and its deformability and is a very important factor in the classification of single-nucleon and collective excited states. The relation between recent theories of nuclear deformations and rotational states in nonspherical nuclei is discussed briefly in light of the most recent experimental data. This is followed by a description of several nuclear models proposed for the theoretical calculations of the equilibrium nuclear shape, including both axial and nonaxial models. (ATD)

40137 HYPERFINE STRUCTURE OF ^{65}Cu TRANSITIONS, $5s^2S_{1/2} - 4p^2P_{1/2}$ AND $3d^{10}4p^2P_{1/2} - 3d^94s^2m^2D_{3/2}$ AND THE QUADRUPOLE MOMENT OF ^{65}Cu. Fischer, Wolfgang; Huehnermann, Harry; Kollath, Klaus-Johannes (Univ., Marburg, Ger.). Z. Phys., 194: 417-24(1966). (In German).

The hyperfine structure of the ^{65}Cu transitions, $5s^2S_{1/2} - 4p^2P_{1/2}$ and $3d^{10}4p^2P_{1/2} - 3d^94s^2m^2D_{3/2}$, was investigated by interference spectroscopy using isotopic-pure ^{65}Cu. From the B-factor of the terms $m^2D_{3/2}$ the value $Q(^{65}Cu) = 10.16 \pm 0.01) \times 10^{-24}$ cm^2 was obtained for the quadrupole moment. (tr-auth)

40138 HARTREE-FOCK CALCULATIONS WITH PARITY MIXING IN ONE-PARTICLE FUNCTIONS. Ebenhoeh, Wolfgang (Univ., Heidelberg). Z. Phys., 195: 171-92 (1966). (In German).

A mixture of one-particle states of opposite parities introduced into the framework of the Hartree-Fock theory leads to an additional spin-dependent potential in the Hartree-Fock equation, which provides a j-splitting similar to the shell model prediction. This splitting depends strongly on the strength of the nucleon-nucleon tensor force. For an effective two-body potential with a tensor part like the Hamada-Johnston potential the calculated splitting agrees in sign and magnitude with the observed values. The calculations are carried through for the nuclei ^{5}He, ^{12}C, ^{15}N, ^{16}O and, ^{17}O. (auth)

40139 PERSPEKTIVY SINTEZA TRANSURANOVYKH ELEMENTOV. (Perspectives in Synthesis of Transuranium Elements). Chernov, A. G. (ed.). Novoye v Zhizni, Nauke, Tekhnike. Ser. 9, Fizika, Matematika, Astronomiya, 1965, No. 10. Besedy po Aktual'nym Probleman Nauki, No. 9. Moscow, Izdatel'stvo Znanie, 1965. 41p.

Separate abstracts were prepared for the 8 lectures presented. (B.G.D.)

For abstracts of individual papers see: 38913, 39116, and 40140–40145.

40140 PERSPECTIVES OF SYNTHESIS AND STUDIES OF PROPERTIES OF TRANSURANIUM ELEMENTS. Flerov, G. N. pp 3-7 of Perspektivy Sinteza Transuranovykh Elementov. Moscow, Izdatel'stvo Znanie, 1965. (In Russian).

The laws governing the 1500 known nuclei are shown to be inadequate as compared to those controlling the periodic table. The synthesis of new nuclei possessing a Z number higher than known previously and a high A number and the preparation of new proton-rich radioisotopes of known elements are discussed. Results show that beyond element-100 addition of a neutron results in spontaneous fission. (B.G.D.)

40141 ON ONE OF THE METHODS OF SYNTHESIS. Polikanov, S. M. pp 7-9 of Perspektivy Sinteza Transuranovykh Elementov. Moscow, Izdatel'stvo Znanie, 1965. (In Russian).

A method of synthesis of transuranium elements or new isotopes of known elements by means of the heavy-ion method, involving use of accelerated nuclei, heavier than helium followed by neutron capture is described. The fusion of two complex nuclei is another approach described. In order to overcome the Coulomb barrier, the nuclei must be brought together with great velocity; therefore, the nuclei must be accelerated and the conditions must favor neutron evaporation, rather than fission. Unfortunately, these processes take place with a low probability and the lifetime of the transuranium elements, if formed, is very short. The Dubna cyclotron, used for the synthesis of transuranium elements, is more than two times larger than the usual proton, deuteron or α-particle accelerator. The oxygen, neon, argon, and calcium ion beams obtained with this cyclotron make it possible to synthetize isotopes, for which the probability of formation is extremely low. (TTT)

40142 SYNTHESIS OF A HEAVY ISOTOPE ^{256}102. Donets, E. D. pp 9-13 of Perspektivy Sinteza Transuranovykh Elementov. Moscow, Izdatel'stvo Znanie, 1965. (In Russian).

Element 102 was synthetized on the basis of the following reaction: $^{238}U + {}^{22}Ne \rightarrow {}^{260*}102 \rightarrow {}^{256}102 + 4n$. Determination of the α decay, resulting in the formation of ^{252}Fm was found to be an excellent method to determine whether the synthesis was successful. The operation involves bombardment of the U target with accelerated neon ions. Under such conditions, the ^{256}102 ions are knocked out of the target and enter the gas phase where they are slowed down and are spread on the walls of the chamber. After the new element is removed from the zone of irradiation, it is identified by means of its β decay and is collected electrically. The α-activity halflife of the element was found to be 8 seconds. The nucleus is relatively stable; its spontaneous fission half life was found to amount to about 1500 seconds, although the theoretically predicted value was only 0.01 second. (TTT)

40143 THE ELEMENT 104. Oganesyan, Yu. Ts. pp 14-22 of Perspektivy Sinteza Transuranovykh Elementov. Moscow, Izdatel'stvo Znanie, 1965. (In Russian).

In view of its short half life, a physical, rather than chemical method was used for the synthesis of Element 104. The physical method required to carry a large number of logically developed experiments, establishing whether the element has indeed been synthetized on the basis of its radioactive decay characteristics. The following reaction was used for the synthesis: $^{242}Pu + {}^{22}Ne \rightarrow {}^{260}104 + 4n$. The fusion results in the formation of the highly excited nucleus ^{264*}104 which subsequently emits neutrons. The probability is 1 nucleus formed in 10^9 to 10^{10} interactions between the target nuclei and the bombarding ions. The newly-formed nucleus may be identified from his propensity of undergoing spontaneous fission. Care must be taken to avoid confusion with fissioning uranium reacting with the emitted neutron beam; therefore, special, uranium-free phosphate glass detectors were used. Maximum yield was obtained when the energy of the bombarding particles was 115 Mev. After 6 hours of irradiation, only one event of synthesis was recorded; subsequent experiments were extended to 50 to 60 hours. The half life of the new element was found to be 0.3 second. (TTT)

40144 KEY TO SYNTHESIS. Flerov, G. N. pp 26-30 of Perspektivy Sinteza Transuranovykh Elementov. Moscow, Izdatel'stvo Znanie, 1965. (In Russian).

High-density neutron beams were used with good success for the synthesis of the first eight transuranium elements but during the subsequent years, not a single new element was synthetized by that method. Accelerated heavy ions were used for the next elements, but serious difficulties were encountered already with Element 102, and synthesis of Element-104 required a five-hour long operation of the accelerator. Therefore, synthesis of even heavier elements by such methods appears highly improbable. The spontaneous fission requires much higher neutron densities. In a pulsed, controlled thermonuclear reaction, the flux density may be increased to 10^{22} n/cm^2. Subsequent neutron capture could increase the mass of the nucleus, without changing the atomic number; β decay will decrease it. According to the $\alpha - \beta + \gamma$ (Alfvén-Bethe-Gamov) hypothesis, all elements are created by the interaction of deuterium and tritium in catastrophic stellar flareups. Historic α Chinese documents describing changes in the luminosity of a celestial body 600 years ago gave values agreeing with the 55-day half life of californium. If heavier elements were formed in such stellar reactions, their existence possibly could be ascertained from x-ray or γ spectra. (TTT)

40145 MORE ON TRANSURANIC ELEMENTS. Flerov, G. N. pp 33-6 of Perspektivy Sinteza Transuranovykh Elementov. Moscow, Izdatel'stvo Znanie, 1965. (In Russian).

Extrapolation of the half lives of the known elements indicates that the half lives of elements beyond No. 110 must be shorter than 10^{-15} seconds. Theoretical studies are in progress to determine the region of stability of such nuclei, in order to synthesize isotopes that may be used meaningfully with respect to the human scale, possessing half lives of months and years, as is the case of ^{238}Pu, with a half-life of 80 years, used as an energy source. Transuranium elements may be created on the basis of the spontaneous fission of high-mass transuranium elements, as the Z value of the fragments increase and decrease as a result of the fission. However, irradiation of uranium targets with uranium ions would require 1600 Mev. Fusion of uranium with uranium nuclei would thus yield elements both above and below uranium in the periodic table, possessing both proton and neutron radioactivity. The chief problem lies in the required acceleration of the uranium ions. (TTT)

40146 MEASUREMENT OF INFINITE DILUTION CAPTURE RESONANCE INTEGRALS WITH A MOXON-RAE DETECTOR. LeSage, L.; Sher, R. (Stanford Univ., Calif.). 26p. (CONF-660204-20). ORAU. Gmelin, AED-CONF-66-017-13.

From American Nuclear Society Meeting, San Diego, Calif.

Neutron capture resonance integrals for Co, Hf, Ho, In, Mo, Nb, Pd, Pt, Rh, Ag, and Ta were measured in reaction beam geometry using a Moxon-Rae counter to detect the prompt capture gamma rays. The counter and the experimental method are described, and the formulas used in the reduction of the data are given. The results are compared with other measurements and with theoretical predictions. (D.C.W.)

40147 RESONANCES IN $^{40}Ar(p,p)$ NEAR 1.1 Mev. Winkler, H.; Pixley, R. E.; Bloch, R. (Univ., Zurich). 10p. (CONF-651213-13). ORAU. Gmelin, AED-CONF-65-400-34.

From American Physical Society, Winter Meeting in the West, Los Angeles.

Elastic-scattering anomalies due to two resonances near a proton energy of 1.1 Mev were observed using a stabilized beam, a thin gas target, and a gamma counter in addition to four particle counters. The data for the 1.102-Mev resonance were fitted with $J^{\pi} = 3/2^-$ and $\Gamma = 17$ ev; the best fit for the 1.086-Mev resonance was obtained with $J^{\pi} = 1/2^-$ and $\Gamma = 10$ ev, although $J^{\pi} = 3/2^-$ and $\Gamma = 5$ ev can not be ruled out completely. (D.C.W.)

40148 SEARCH FOR EVIDENCE OF POSITRON EMISSION IN THE DECAY OF ^{36}Cl. Tolbert, W. R.; Shrum, E. V.; Hutcheson, E. T.; Diana, L. M. 8p. (CONF-650653-28). ORAU. Gmelin, AED-CONF-65-170-68.

From American Physical Society, Summer Meeting, New York.

The decay of ^{36}Cl was investigated using a scintillation spectrometer. A peak at 0.51 Mev was observed; under the assumption that the 0.51-Mev peak results from positron annihilation, a value of 1×10^{-5} was obtained for the branching ratio for positron emission in the decay of ^{36}Cl. (D.C.W.)

40149 CROSS SECTION FOR THE REACTIONS $^{65}Cu(n,p)^{65}Ni$, $^{65}Cu(n,2n)^{64}Cu$, AND $^{65}Cu(n,n\alpha)^{61}Co$. Butler, J.P.; Santry, D. C. 11p. (CONF-650570-1). ORAU. Gmelin, AED-CONF-65-237-2.

From 48th Canadian Chemical Conference and Exhibition, Montreal.

The cross sections for the reactions $^{65}Cu(n,n\alpha)^{61}Co$, $^{65}Cu(n,2n)^{64}Cu$, and $^{65}Cu(n,p)^{65}Ni$ were measured in the range of neutron energies from 2 to 20.3 Mev. At a given neutron energy, the yields of the reactions were obtained by absolute counting of the radioactive products. (D.C.W.)

40150 PARTIAL WAVE ANALYSIS OF INELASTIC ELECTRON SCATTERING IN THE LOW-ENERGY REGION. Tuan, S. T.; Wright, L. E. (Duke Univ., Durham, N. C.). 7p. (CONF-660411-50). ORAU. Gmelin, AED-CONF-66-060-94.

From American Physical Society Meeting, Washington, D. C.

To investigate the validity of the Born approximation for low-energy (1 to 10 Mev) electron scattering, a partial wave analysis was performed for comparison. The energy loss of the scattered electrons was included since at these energies the energy loss is comparable to the incoming electron energy. The liquid drop model which assumes incompressible irrotational fluid flow was used in the calculation. The ground state charge distribution was taken to be the Fermi distribution characterized by a half-density radius and a skin thickness. (W.D.M.)

40151 MUON CAPTURE AND NUCLEAR GIANT RESONANCES. Ueberall, H. (Catholic Univ. of America, Washington, D. C.). 60p. (CONF-660209-2). ORAU. Gmelin, AED-CONF-66-023-2.

From Williamsburg Conference on Intermediate Energy Physics, Va.

A selected number of ways in which effects of the structure of the final nucleus, and particularly of its giant dipole resonances can become manifest in the process of muon capture is discussed. At the same time, a unified picture is presented of both weak and electromagnetic excitations of the giant resonances (which may be calculated in terms of nuclear form factors with a good degree of confidence), their similarities and their mutual interdependence. The collective aspects of the giant resonance states as described by the Goldhaber-Teller model and its spin-wave generalization are stressed in some detail. (auth)

40152 MOTIONAL NARROWING OF MAGNETIC HYPERFINE MOESSBAUER SPECTRA. Dash, J. G.; Dunlap, B. D. (Univ. of Washington, Seattle). 13p. (CONF-660107-49). ORAU. Gmelin, AED-CONF-66-003-104.

From American Physical Society 1966 Annual Meeting, New York.

Magnetic hyperfine spectra of Mossbauer radiation are analyzed in the case of fluctuating hyperfine fields due to transitions between the electronic levels of the ion. A simple approximation is developed for ions of spin greater than $1/2$, when the electronic polarization is sufficiently great for only the lowest two electronic levels to be appreciably populated. The theory is found to provide a good representation of the experimental spectra of ^{57}Fe in iron ammonium alum obtained by Obenshain, Roberts, Coleman, Forester, and Thomson at low temperatures and in moderate magnetic fields. The relaxation frequency between the $m_s = 5/2$ and $m_s = 3/2$ electronic levels is found to be $2.6 \pm 0.4 \times 10^8$ sec^{-1}, and appears to be independent of H and T in the experimental range. (auth)

40153 COMPARISON OF ALLOWED M/L ORBITAL ELECTRON CAPTURE RATIOS WITH THEORY. Fink, R. W.; Ledingham, K. W. D. (Georgia Inst. of Tech., Atlanta). 7p. (CONF-660411-7). ORAU. Gmelin, AED-CONF-66-060-33.

From American Physical Society Meeting, Washington, D. C.

All reasonably precise experimental values of allowed M/L capture ratios are compared with theoretical results (Bahcall, Phys. Rev., 131: 1756 (1963); Robinson, Nuclear Phys., 64: 197 (1965)) with and without exchange-overlap corrections. In medium- and low-Z nuclides, the experiments are exceedingly difficult due to the low energies of the M radiations. Two experimental methods are reviewed: direct measurement of M/L capture, which requires accuracies, in order to verify the Bahcall corrections, of approximately 30% at Z = 18, 20% at Z = 25, 15% at Z = 36, 10% at Z = 55, and 6% at Z = 90; and indirect evaluation of M/L ratios from experimental (L + M +/K) or (K/Total) capture ratios in nuclides with well established experimental or theoretical L/K capture ratios. To use the second

method for a critical verification of the Bahcall corrections, an accuracy of 1 or 2% is required. The most precise experimental values generally lie lower than either corrected or uncorrected theoretical predictions. More experimental results with accuracies given above are necessary before a definite disagreement with theory can be established. (auth)

40154 SPIN OF ^{48}V. Redi, Olav. 15p. (CONF-660107–50). ORAU. Gmelin, AED-CONF-66-003-108.

From American Physical Society 1966 Annual Meeting, New York.

A measurement of the spin of ^{48}V is outlined, together with shell-model calculations for the energy levels and wave functions of this nucleus. (D.C.W.)

40155 STUDIES OF SOME DEUTERON STRIPPING REACTIONS. Wait, G. D. Edmonton, Alta., Univ. of Alberta, 1964. 36p.

Thesis.

The original purpose of the experiment was the determination of the contribution of exchange stripping in the ^{17}O(d,n)^{18}F reaction. However, the absolute cross section of the ^{17}O(d,p)^{18}O reaction was found to be so small as to discourage this. It was necessary to determine the angular distributions of ^{12}C(d,p)^{13}C and ^{13}C(d,p)^{14}C from a natural carbon target in order to get a measure of the angular distribution of ^{17}O(d,p)^{18}O since the ^{13}C contamination swamped the peak from the ^{18}O ground state. The absolute cross sections of ^{12}C(d,p)^{13}C, ^{13}C(d,p)^{14}C, and ^{17}O(d,p)^{18}O were subsequently measured at bombarding energies of 1 and 1.5 Mev for comparison purposes. The angular distribution of ^{16}O(d,n)^{17}F was also measured at a bombarding energy of 3.5 Mev for comparison with the ^{16}O(d,p)^{17}O reaction. (auth)

40156 PROPERTIES OF STATES OF ^{21}Ne FROM ^{18}O(α,nγ)^{21}Ne. Pronko, J. G. Edmonton, Alta., Univ. of Alberta, 1965. 154p.

Thesis.

Spectroscopic parameters of ^{21}Ne were measured using the reaction ^{18}O(α,nγ)^{21}Ne. The method of triple angular correlations was used to determine the spins of the 0.35, 1.75 and 2.87 Mev levels as well as the multipole mixing ratios of the gamma rays emitted from these states. The target used was approximately 20 kev thick at 2.50 Mev and consisted of isotopically separated ^{18}O. At a bombarding energy of 4.43 Mev, the gamma rays from the 0.35 and 1.75 Mev levels were observed and three types of correlation experiments were performed: neutron-gamma angular correlations with the neutron counter at zero degrees, gamma distributions with the intermediate radiation unobserved, and gamma-gamma correlations. These yielded spin assignments of $\frac{5}{2}$ and $\frac{7}{2}$ for the 0.35 and 1.75 Mev levels, respectively, and multipole mixing ratios for the gamma rays of $\delta_{0.35} = +0.08 \pm 0.02$, $\delta_{1.40} = +0.18 \pm 0.02$, and $\delta_{1.75} = +0.034 \pm 0.04$. The 1.75 Mev level was found to decay 4.6% to the ground state. At a bombarding energy of 5.50 Mev, neutron-gamma correlations yielded a spin of $\frac{9}{2}$ as most probable for the 2.87 Mev level with $\delta_{1.12} = +0.13 \pm 0.06$ and $\delta_{2.52} = +0.035 \pm 0.045$. This level was found to decay at least 37% to the 1.75 Mev level. (auth)

40157 NUCLEAR REACTION RATES IN EXTREMELY DENSE MATTER. Van Horn, Hugh Moody. Ithaca, N. Y., Cornell Univ., 1966. 139p.

Thesis.

The problem of calculating nuclear reaction rates at high densities is considered. It is shown that under conditions in which the "pycnonuclear" reactions dominate, the microscopic structure of the plasma is that of a crystalline lattice rather than that of a gas. Approximations are derived for the effective interaction potential of two ions within the crystal structure, and a serious error is pointed out in some of the previous work on this subject. A three dimensional version of the WKB approximation is developed in order to deal with the non-separable potential, and the method is then used to calculate the wave function at the nuclear surface. The extremes of very low and very high temperature are considered, and suitable formulas for the reaction rates are obtained in each of these regions. Finally, it is shown that these calculations are closely connected with the strong screening approximation in the conventional thermonuclear case. As specific illustrations of the calculations the proton-proton and carbon-carbon reactions are considered. The results are written in such a way that the reaction rate for any pair of identical nuclei can be directly obtained from the general formulas. (Dissertation Abstr.)

40158 TIME OF EMISSION AND THE YIELD OF X RAYS FROM THERMAL NEUTRON FISSION OF ^{235}U AND ^{239}Pu. Bridwell, Lynn Boyd. [Urbana], Ill., Univ. of Illinois, 1965. 85p.

Thesis.

The time and energy characteristics of K x rays from fission fragments of two fissionable isotopes, ^{235}U and ^{239}Pu, were studied. Delayed coincidence techniques using time-to-amplitude conversion were employed to obtain time spectra of the light and heavy fragment x rays separately. The x-ray detector was a 1 mm thick NaI(Tl) scintillation crystal. Fission fragments were detected with a thin plastic scintillation detector. Thermal neutrons from the thermal column of the University of Illinois Triga Mark II reactor were confined to a small slit profile by a collimator constructed of B_4C and paraffin. In every case approximately 50% of the x rays were found to have half lives greater than 4 nsec. On the basis of these results it was concluded that the x rays were emitted as a result of the process of internal conversion during de-excitation of low energy nuclear states of the primary fission fragments. A model for predicting the x-ray energy spectra was constructed. Good agreement was obtained by assuming equal charge displacement for the primary charge yield when the type of transitions was assumed to be 50% M1 and 50% E2 at an average energy of 100 kev for fragments of ^{235}U. A 50% mixture of M1 and E2 at an average energy of 50 kev resulted in a good fit for fragments of ^{239}Pu. For ^{235}U a yield of 0.43 ± 0.04 x rays per fission was measured for the heavy fragments, and 0.19 ± 0.02 x rays per fission for the light fragments. ^{239}Pu experiments yielded 0.26 ± 0.03 and 0.15 ± 0.02 x rays per fission for the heavy and light fragment groups. (Dissertation Abstr.)

40159 NUCLEAR ENERGY-LEVEL STRUCTURES OF ^{117}In, ^{117}Sn AND ^{143}Pr. Mancuso, Richard V. Buffalo, State Univ., 1965. 125p.

Thesis.

From the results of coincidence experiments performed on various regions of the gamma-ray spectrum, the prominent energy levels of ^{117}In were established at 310, 400, 590, 745, 860, 1070, 1710, 1880, 1975, 2120, and 2320 kev. The gamma-ray relative intensities were measured from which the percent beta feeding of the ^{117}In levels from ^{117}Cd and ^{117m}Cd, the log ft values of the beta decay, and the ratio of slow-neutron cross sections for ^{117}Cd and ^{117m}Cd were determined. Two directional correlation measurements were performed from which the allowable spins and types of radiation were obtained for the levels and gamma rays involved. The experimental results are compared to the theoretical predictions of the superfluid model. The level structure of ^{117}Sn previously reported was confirmed with levels at 160, 319, 720, 865, and 1030 kev. A directional correlation experiment was performed on the 560 kev-160 kev cascade that connects the 720- and 160-kev levels and the ground state. From the result of this measurement, unique spins of $\frac{3}{2}$ and $\frac{1}{2}$ were assigned to the 160- and 720-kev levels, respectively. The 560-kev gamma ray is pure E2, while the 160-kev gamma ray is M1 + E2 with an E2 content of $1.2 \pm 0.5\%$. The experimental results are in close agreement with the theoretical predictions of the superfluid model. Levels were established in ^{143}Pr at 57, 350, 493, 725, 945, and 1167 kev. An additional level may possibly be at 1395 kev. The gamma-ray relative intensities were measured from which the percent beta feeding of the ^{143}Pr levels from ^{143}Ce and log ft values of the beta decay were determined. Three directional correlation experiments were performed and the allowable spins and

types of radiation determined for the levels and gamma rays involved. The predictions of the superfluid model, which treats spherical nuclei, do not agree too well with the experimental results since ^{143}Pr is close to the deformed region. (TCO)

40160 STATISTICAL METHOD FOR INVESTIGATION OF DELAYED TRIPLE NUCLEAR CASCADES. Mink, Lawrence Albright. Raleigh, N. C., Univ. of North Carolina, 1966. 84p.

Thesis.

A statistical correlation method is presented, which allows determination of the half lives of the two daughters, the source strength, and the absolute efficiencies of the three counters for ranges of half lives for which triple coincidence methods are not suitable. The correlation method has no restrictions, in principal, on source strength and background. Counts per sample interval are recorded for a large number of intervals of short duration. Simple correlation functions are computed using these counts. The desired half lives, source strengths, and efficiencies are readily determined from the correlation functions. Theoretical expressions are obtained for the expectation of the correlation functions and the variances. Simplified expressions are developed for computing the fractional standard deviation. These expressions are used to estimate the accuracy of the source strength, efficiency, and half-life determinations under typical experimental conditions. (Dissertation Abstr.)

40161 REACTIONS $^{17}O(d,p)^{18}O$, $^{18}O(d,p)^{19}O$ AND THE NUCLEAR STRUCTURE OF ^{18}O AND ^{19}O. Wiza, Joseph Ladislaus. Philadelphia, Univ. of Pennsylvania, 1965. 108p.

Thesis.

A target enriched to 40% in ^{17}O was bombarded with 10-Mev deuterons, and the emitted protons were analyzed with a broad-range single-gap magnetic spectrograph. Angular distributions of the groups corresponding to the ground and twelve excited states of ^{18}O were measured and analyzed using plane wave theory. The predicted 3^+ state arising from the $(d_{\frac{5}{2}}s_{\frac{1}{2}})$ configuration was found to be at 5.37 Mev excitation. Relative reduced widths and spectroscopic factors were determined from the stripping analysis, and were found to be in good agreement with recent theoretically predicted wave function amplitudes. This implies that several states of ^{18}O have an appreciable collective component. In addition, a tungsten oxide target enriched to 30% in ^{17}O was bombarded with 12.0-Mev tritons, and a similar target enriched to 50% in ^{18}O was bombarded with 12.0-Mev deuterons. In both cases, emitted protons were analyzed using a broad-range multi-angle spectrograph. The $^{18}O(d,p)^{19}O$ reaction was also studied at a bombarding energy of 11 Mev using a gas target and magnetic analysis. Energy levels up to 6.3 Mev excitation in ^{19}O were determined and no evidence was found for the recently reported levels at 0.348 and 2.617 Mev excitation. Angular distributions were measured and several new spin and parity assignments were made. (Dissertation Abstr.)

40162 ELASTIC SCATTERING OF 45-Mev PROTONS. Willmes, Henry. Los Angeles, Univ. of California, 1966. 70p.

Thesis.

Measurements of the differential elastic scattering cross section were carried out using the negative ion beam of the UCLA cyclotron, as part of a program of optical model studies. The methods of data taking and of the reduction of the raw data are discussed in detail. Brief outlines of the history of the optical model and of its mathematical formulation are included. Results of the cross section measurements are given for beryllium-9, carbon-12, nickel-58, and nickel-60 for a series of angles ranging from 15° to 150°. (Dissertation Abstr.)

40163 ON THE SU_3 NUCLEAR SHELL MODEL. Bernier, Jean-Pierre. Edmonton, Alta., Univ. of Alberta, 1963. 146p.

Thesis.

Elliott's SU_3 classification of nuclear shell model wave functions in LS coupling is extended and relations between related formalisms are examined, with emphasis on the group-theoretical techniques. To this end, the use of Young Diagrams to classify many-particle wave functions according to representations of various symmetric and linear groups is reviewed and illustrated. Operations such as inner and outer products and plethysms of representations of these different groups are redefined as operations on the Young Diagrams themselves, allowing the same data to be used with different interpretations for different groups. These techniques are used to review the supermultiplet classification of Wigner and Feenberg, as applied to harmonic oscillator wave functions in the nuclear shell model in LS coupling, with emphasis on the dual interpretation of this classification in terms of the unitary group SU_s as well as the symmetric group S_k. This classification and the corresponding supermultiplet model are applied to excited configurations. Elliott's SU_3 classification (which extends to all shells in LS coupling an interesting property that the above-mentioned supermultiplet classification possesses in the p shell only, namely the property of predicting bands of eigenstates typical of the rotational model) is then introduced, exploiting an analogy with the SU_s classification: the r-quanta harmonic oscillator eigenfunctions, which correspond to homogeneous polynomials of degree r in three creation operators, are compared to the k-particle eigenfunctions, which are homogeneous polynomials of degree k in s variables, namely the s possible single-particle eigenfunctions. The SU_3 model, using Moszkowski's quadrupole-quadrupole interaction, is presented, and it is shown that in the p shell its predictions are identical to those of the supermultiplet model provided the parameters L and K of the latter are suitably related to the "moment of inertia" of the SU_3 model. The SU_3 model is then extended to excited configurations and applied to the experimental energy spectrum of ^{20}Ne. A qualitative fit to the position of all fifteen observed states, belonging to five bands and to two or three configurations can be obtained with a single adjustable parameter. It is pointed out in particular that the SU_3 model provides for a lowering of the excitation energy of the leading excited-configuration state below the value predicted by the unperturbed harmonic oscillator hamiltonian; this effect, which has no counterpart in the supermultiplet model, accounts for 40% of the 10 Mev observed lowering in ^{20}Ne. Kretzschmar's alternative approach to the SU_3 classification is then described, and his technique for identifying spurious states is used to verify that the previously mentioned state of ^{20}Ne is not spurious. Finally, the pseudo-spin of Bargmann and Moshinsky is related to the reduction of a representation of SU_2 introduced by Moshinsky as a generalization of his transformation brackets, and the formalism of Kretzschmar is used to explain the identity of the SU_A classification of Bargmann and Moshinsky to the SU_3 classification of Elliott. (auth)

40164 NEUTRON TIME-OF-FLIGHT STUDIES OF ^{10}B, ^{11}C, AND ^{20}Ne. Riley, Peter Julian. Edmonton, Alta., Univ. of Alberta, 1962. 112p.

Thesis.

The $^9Be(d,n)^{10}B$ reaction was studied using time-of-flight techniques. Neutron groups leading to the 5.11- and 5.16-, Mev states in ^{10}B were resolved. Angular distribution measurements were made on neutrons leading to the 5.16-, 5.11-, and 4.77-Mev states in ^{10}B. Analysis of these distributions in terms of plane-wave Butler stripping theory is given. Partial width measurements indicate that the 5.11- and 4.77-Mev levels of ^{10}B decay almost entirely by alpha emission, and that the 5.16-Mev level decays almost entirely by gamma emission. The results are consistent with the respective assignments of $J^\pi = 2^+$, $T = 1$; $J^\pi = 2^-$, $T = 0$, and $T = 0$ for the 5.16-, 5.11-, and 4.77-Mev states. No evidence was seen for the broad 5.18-Mev level in ^{10}B. The decay of the 6.48-Mev level in ^{11}C was studied by means of the $^{10}B(d,n\gamma)^{11}C$ reaction. Gamma rays from the decay of this state were observed using a collimated 4-inch by 4-inch NaI crystal. The NaI crystal was gated by neutrons leading to the 6.48-Mev state. The results give a value of the branching ratio for direct ground-state transi-

tions relative to cascades through the 4.26-Mev level of $8 \pm 1 : 1$. This measurement is in good agreement with the intermediate-coupling-model prediction. Preliminary $^{19}F(d,n)^{20}Ne$ neutron time-of-flight spectra were recorded. Using a pulsed beam, neutron groups leading to states in ^{20}Ne at 1.63, 4.97, 5.64, 6.75, 9.34, and 9.97 Mev were tentatively identified. Neutron-gamma coincidence spectra indicated states in ^{20}Ne at 9.34, 9.97, and 10.9 Mev. Unsuccessful attempts were made to bunch at low energy an ion beam obtained from an rf-excited ion source. A method of ion-pulsing by means of a grid arrangement located immediately after the ion-source extractor canal was investigated. The pulse duration obtained was not as short as that obtainable from a pre-acceleration deflector plate system. (auth)

Plasma Physics and Thermonuclear Processes

See also Fluid Physics and Thermodynamics

Refer also to abstracts 39567, 39569, 39655, 39656, 39659, 39662, 39665, 39666, 39670–39673, 39677, 39683, 39684, 39691, 39699, 39700, 39714, 39715, 39721, 39722, 39727, 39734, 39738, and 39739.

40165 (AD–637710) CYCLOTRON HARMONIC RADIATION FROM ELECTRON BEAM INJECTION INTO AN AFTERGLOW PLASMA. Scientific Report No. 86. Marshall, T. C.; Bradford, P. V.; Schlesinger, S. P. (Columbia Univ., New York. Dept. of Electrical Engineering). Jan. 1966. Contract AF19(628)-2461. 31p. (AFCRL–66-204; CU–18-65-AF-2461-EE). CFSTI $2.00 cy, $0.50 mn.

A pulsed electron beam was injected into an afterglow produced by a P.I.G. discharge in low pressure argon. The beam and the afterglow formed concentric posts in χ-band waveguide on which accurate microwave measurements were made. Radiation at the cyclotron harmonics was observed from the simultaneous beam and afterglow plasmas when the beam was too low to generate its own radiating plasma. Radiation was enhanced when the experimental parameters were consistent with the Bernstein electrostatic dispersion relations. Observations of the width of the third harmonic radiation resonance as the plasma frequency was varied were in qualitative agreement with the theory of Auer and Stone. Space charge fluctuations at the receiver frequency (9.2 Gc) were also observed when the radiation occurred. (auth)

40166 (AD–637711) ELECTROMAGNETIC: ACOUSTIC WAVE PROPAGATION ALONG WARM PLASMA COLUMNS. Scientific Report No. 88. Diament, Paul; Granatstein, V. L.; Schlesinger, S. P. (Columbia Univ., New York. Dept. of Electrical Engineering). Dec. 1965. Contract AF19(628)-2461. 47p. (AFCRL–66-161). CFSTI $2.00 cy, $0.50 mn.

Dispersion relations for waves propagating along homogeneous, isotropic, warm plasma columns surrounded by a dielectric medium were obtained. A steady state, linearized model with temperature introduced through a scalar pressure was analyzed both quasistatically and more rigorously from Maxwell's equations. The results show effects of temperature on the cold-plasma surface wave and predict a new series of propagating modes above the plasma frequency, related to the Tonks-Dattner scattering resonances near cutoff and to the Bohm-Gross longitudinal plasma waves for large wave numbers. Warm and cold plasmas, large and small columns, and quasistatic and rigorous predictions are contrasted. Regions of the Brillouin diagram corresponding to different bound and radiating wave types are delineated and related to their physical properties. (auth)

40167 (IC–65/90) ON CONSTANTS OF THE LINEARIZED MOTION OF VLASOV PLASMAS. De Barbieri, O.; Nocentini, A. (International Centre for Theoretical Physics, Trieste (Italy)). Dec. 1965. 34p. Dep. mn.

A one-specie Vlasov plasma is considered with an equilibrium distribution function spatially homogeneous. The method of Oberman and Kruskal (J. Math. Phys. 6: 327 (1965)) is used in order to find the quadratic constant of its linearized motion, taking into account the full electromagnetic interaction. Equations are presented for the coefficients of the quadratic constant of the motion and it is shown that the system of equations splits into two separate systems, one for the symmetric and one for the antisymmetric part of the coefficients. (W.D.M.)

40168 (NASA-CR–559) TRANSPORT PHENOMENA IN IONIZED GASES AS AN INITIAL VALUE PROBLEM. Huchital, D. A.; Holt, E. H. (Rensselaer Polytechnic Inst., Troy, N. Y.). Sept. 1966. 10p. CFSTI $1.00 cy, $0.50 mn.

Transport phenomena in plasmas in terms of initial value problems are discussed. Plasma diffusion is discussed from two points of view. If the moments of the Boltzmann equation are taken, there results the macroscopic equations. This approach is shown to yield a diffusion equation which differs from the conventional equation which is based on Fick's law. Some gross aspects of the appropriate initial value problem are thereby revealed. A second point of view is developed by solving the Boltzmann equation using Fourier and Laplace transform techniques which permit the initial conditions to be inserted into the solution. This latter approach is shown to be the superior one. It is also used to study plasma transport in the presence of an applied electric field. In treating the collision operator a Lorentz gas model of the plasma is chosen. The solution is obtained in terms of odd and even components of the distribution function. It is shown that the initial condition propagates along a single particle orbit in phase space but the number of particles is depleted at the rate exp (–νt/2) where ν is the electron collision frequency. Those particles which have suffered a collision are deposited in a residue in phase space. An asymptotic formula for the solution for relatively long times was obtained. The collisional residue then contains the following elements: the Maxwell-Boltzmann distribution, (2) a term describing the diffusion in configuration space independent of the electric field and (3) a term describing the heating of the electron gas by the electric field and the resulting diffusion in velocity space (auth)

40169 (NASA-TN–D-3595) SUPERCONDUCTING MAGNETIC BOTTLE FOR PLASMA PHYSICS EXPERIMENTS. Coles, Willard D.; Fakan, John C.; Laurence, James C. (National Aeronautics and Space Administration, Cleveland, Ohio. Lewis Research Center). Aug. 1966. 14p. CFSTI $1.00 cy, $0.50 mn.

A superconducting magnetic bottle consisting of two mirror coils, a central field coil, and a cylindrical cusp field coil was designed and constructed of seven-strand niobium–25% zirconium cable. The configuration was designed to investigate the problems involved in using superconductive materials to produce magnets useful for experiments in plasma physics. Mirror fields as intense as 5 teslas were produced in the bore of the 10-centimeter-inside-diameter coil assembly with a superimposed quadrupole cusp field of 5 to 10% of the center field and a mirror ratio of 2. (auth)

40170 (ORNL–3989) THERMONUCLEAR DIVISION SEMIANNUAL PROGRESS REPORT FOR PERIOD ENDING APRIL 30, 1966. (Oak Ridge National Lab., Tenn.). Aug. 1966. Contract W-7405-eng-26. 164p. Dep. mn. CFSTI $5.00 cy, $1.00 mn.

Separate abstracts were prepared for the eleven included sections. (M.O.W.)

For abstracts of individual sections see: 39097, 39580, 39581, 40014, and 40171–40177.

40171 (ORNL–3989, pp 1-13) INJECTION AND ACCUMULATION: SINGLE-PASS EXPERIMENTS (DCX-1). Dunlap, J. L.; Edwards, R. S.; Massengill, L. A.; Postma, H.; Reinhardt, R. G.; Schill, W. G.; Wells, E. R. (Oak Ridge National Lab., Tenn.).

The flexibility of variable magnetic field gradient acquired by the earlier installation of an additional coil pair

was employed to obtain data for comparison with properties of the DCX-2 plasma. The properties of the two plasmas became more nearly alike as the DCX-1 field was flattened, but this mockup of the DCX-2 plasma omitted features required for unambiguous comparisons. A variety of reactive end walls was installed in the plasma chamber, and studies were made of the effects of these boundaries on plasma instability. The effects were negligible unless the walls were advanced into a portion of the volume normally occupied by the fast-proton plasma. A historical review of the principal lines of investigations to which the facility has been devoted since its inception is presented. (M.O.W.)

40172 (ORNL–3989, pp 14-30) INJECTION AND ACCUMULATION: MULTIPLE-PASS EXPERIMENTS (DCX-2). **Bell, P. R.; Culver, J. S.; Davis, R. C.; (and others) (Oak Ridge National Lab., Tenn.).**

Gas dissociation experiments were performed, to study plasmas which may be related in a simple way to theoretical models, and to study the mechanism which results in the highly anisotropic, but relatively stable, plasmas which are produced. Since the large volume ($\sim 7 \times 10^4$ cm^3), highly anisotropic ($T_\perp/T_{||} \sim 10^3$) central-peak-dominant plasma fits theoretical models, these plasmas were used to demonstrate the limitations of the current theories of ion-cyclotron instabilities through studies of the r-f behavior following turnoff of the molecular-ion beam. It is found that when r-f activity occurs after beam turnoff, it is associated with the streaming side-lobe plasmas. The central-peak plasma by itself is shown to be stable against ion-cyclotron instabilities after beam turnoff at densities about a factor of 40 above the usual rule of thumb instability threshold predicted by the infinite medium theory ($\omega_{pe} > \omega_{ci}$). Measurements of the cold-plasma density were made with a microwave interferometer as well as with gridded probes, but the two measurements yield inconsistent results. Experiments were started with an axially injected 200-mA beam of 100-kev protons. Initial experiments show no trapping. The r-f generated does not include ion-cyclotron lines, and there is anomalous ion transmission at the mirrors. (M.O.W.)

40173 (ORNL–3989, pp 31-42) ELECTRON-CYCLOTRON HEATING. **(Oak Ridge National Lab., Tenn.).**

The injected 20-kev neutral beam was used for further proton trapping studies in the INTEREM facility. The energy spectrum of the trapped protons was measured. No energy spread was observed either with trapping on hydrogen gas or with electron-cyclotron plasma (ECP). The axial distribution of the trapped protons was also measured. A slight amount of spreading occurs in the presence of the ECP, but this may be due to normal scattering processes rather than to an instability. An experiment in the ELMO facility is described. An 8-mm ECP was formed in a 3.6-liter stainless steel cavity arranged to permit the measurement of fairly fast diamagnetic perturbations. This diagnostic along with a radial profile measurement of cold plasma streaming axially out of the hot plasma region has shown the principal electron constituent of the density to be of the order of 10^{12} electrons/cm^3 and to have an average energy of ~1.5 kev. Instabilities observed after turnoff are well correlated with the decay of the conductivity-stabilizing cold plasma. Further work on the PTF is described. The large radial loss of hot electrons that is observed in the PTF plasma under some conditions is associated with perturbations that propagate azimuthally around the plasma surface with a phase velocity that is near the gradient-B drift velocity of 25-kev electrons. When the perturbations are fully developed, their wavelength is one-half the circumference of the plasma. However, it appears that the perturbations that grow initially are of much shorter wavelength. The instability can be suppressed by increasing the density of the cold plasma between the hot plasma and the conducting end walls. Stability is obtained when the cold plasma density is about 5×10^{-2} times the hot plasma density. (auth)

40174 (ORNL–3989, pp 43-77) PLASMA PHYSICS. **(Oak Ridge National Lab., Tenn.).**

Brief summaries of research work are presented for the following: beam-plasma interactions, beam-excited ion-cyclotron oscillations, electron-collecting probe as an ion wave detector, plasma density measurement in a hollow-cathode arc by arc reversal, use of ordinary camera as a streak camera, a cesium plasma with no short-circuit effects at the end electrodes, varying plasma electron temperature in discharge tubes by a simple auxiliary electrode, hot-electron plasma blanket, a curved arc, boundary wall treatment in the Penning ion gage, and excitation heating of ions. (M.O.W.)

40175 (ORNL–3989, pp 89-94) HIGH-CURRENT ION-BEAM PRODUCTION AND INJECTION. **Davis, R. C.; Hall, R. R.; Kelley, G. G.; Morgan, O. B.; Stratton, R. F. (Oak Ridge National Lab., Tenn.).**

The four-electrode H_2^+ ion source was studied over an energy range of 10 to 600 kev. A 100-kv non-PIG accelerator was designed and successfully tested, and a similar 600-kv accelerator was designed. The DCX-2 end injector (100 kev, ~500 mA) was installed and tested. The ion source and accelerator for a 150-kv, 500-mA d-c neutron generator was completed and operated successfully for typical 4-h operation periods. A low-energy (0 to 40 kev) ion beam test stand was completed. In conjunction with the DCX-1 group, a program was started to evaluate various neutral-forming cells with intense hydrogen ion beams in the energy range 20 to 60 kev. (auth)

40176 (ORNL–3989, pp 95-108) PLASMA THEORY AND COMPUTATION. **(Oak Ridge National Lab., Tenn.).**

The principal theoretical investigations were centered on questions raised by two aspects of the DCX-2 program: (1) the detailed study of radio-frequency emissions during steady-state operation and (2) studies of the stability properties of the "central-peak plasma" after the beam is turned off. The analysis required to determine the important characteristics of the unstable waves is lengthy, difficult, and almost entirely numerical, so that work in this area was concerned largely with the development of computer codes. A number of rather specific questions relating to plasma stability was investigated, several of which are reported. The possible importance of an instability related to the relativistic change in gyrofrequency for fast ions was explored, even though for ion energies of interest to controlled fusion plasmas such relativistic shifts would be very small. New insight into one class of "drift-cyclotron" modes was obtained by studying the region of overlap of two very dissimilar models of the diamagnetic response of a plasma of finite radial extent. The stabilizing effects of cold plasma were analyzed for those experiments which might shed light on the accuracy of the model under study, and substantial agreement between theoretical predictions and experimental observations was found. Theoretical calculations reveal that transverse electron plasma oscillations can be set up by parametric longitudinal oscillations at other than the plasma frequency. A number of computations related to design problems in the proposed DCX-3 configuration was carried out by the computer group. (M.O.W.)

40177 (ORNL–3989, pp 135-43) DESIGN AND ENGINEERING: NOTES. **(Oak Ridge National Lab., Tenn.).**

Progress in the consideration of a few technological problems is briefly discussed. Development of high-temperature coaxial probes has continued, and means were found to pyrolytically deposit boron nitride on wires down to 0.1 mm diameter and then deposit tungsten on the boron nitride, resulting in very small probes which can withstand a 3000°K environment. Further progress in the understanding of early failure of copper tubing used in DCX-1 liners is discussed. Additional improvements in the design of hollow-conductor water-cooled electromagnets are described, including the progress of a cast-to-shape copper crossover and some techniques for Heliarc brazing of conductors in the proximity of insulating materials. Additionally, some general improvements in welding, braze-welding, and brazing of CTR equipment are discussed. (auth)

40178 (SIT–2582-19) EXPERIMENTAL INVESTIGATION OF CUSPED CONTAINMENT GEOMETRIES. Annual

Report, 1965–1966. Yevick, George J. (Stevens Inst. of Tech., Hoboken, N. J. Dept. of Physics). Contract AT (30-1)-2582. 205p. (SIT–187). Dep. mn. CFSTI $6.00 cy, $1.25 mn.

Experimental results from the performance of the Chalice system are discussed and their analyses, which include data with preheater and cusp bank and preheater alone, are given. Information is also included on the following: diagnostics, including optical, improvements in the bank system, the suppression of r-f noise, magnetic fields, vacuum systems and θ-pinch guns, the snow-plow model for fast pinches, and collective coordinates for inhomogeneous plasmas. Results indicate fairly accurate repeatability in the performance of the Chalice system. (J.H.M.)

40179 (SU-IPR–49) GROWTH OF FLUCTUATIONS IN A COLLISIONLESS PLASMA SUBJECTED TO AN ELECTRIC FIELD. Linson, Lewis M. (Stanford Univ., Calif. Inst. for Plasma Research). May 1966. Contract AT (04-3)-326. 225p. Dep. mn. CFSTI $6.00 cy, $1.25 mn.

An analytic representation of the time-behavior of the fluctuating fields $E_k(t)$ in a non-stationary, collisionless plasma is derived. The specific case treated is that of a uniform, constant electric field E_0 which is large enough to excite the two-stream instability when applied to a uniform plasma. The basic equation solved is the inhomogeneous Volterra integral equation for the fluctuating electric fields derived by Fried et al., on the basis of the linearized Vlasov equation. The technique developed is applicable for plasmas whose velocity distribution functions lead to a polynomial dispersion function; the integral equation can then be converted into an inhomogeneous differential equation for the fluctuating fields. Cold plasma and a plasma whose velocity distribution functions are resonance-shaped are discussed; the resulting differential equations are of fourth order. Besides being capable of dealing with more general distribution functions, the technique can also be generalized to include non-steady applied fields as well as situations in which the relative velocity between the species comprising the plasma has arbitrary time behavior. (M.O.W.)

40180 (SU-IPR–69) STUDY OF THE DIFFUSION PROCESS IN A TOROIDAL DISCHARGE. LeBail, R.; Pigache, D. (Stanford Univ., Calif. Inst. for Plasma Research). May 1966. Contract AT(04-3)-326. 27p. Dep. mn. CFSTI $2.00 cy, $0.50 mn.

The diffusion rate of a plasma across a magnetic field was measured in a toroidal, pulsed d.c. discharge, and also during the afterglow. During the pulse the measured diffusion coefficient decreases by about a factor 2 when the magnetic field is increased from 200 gauss to 400 gauss and remains approximately constant between 400 gauss and 800 gauss. It appears to be higher than it should be according to collisional diffusion theory, by a factor 10 at 200 gauss and 100 at 800 gauss. During the afterglow, the diffusion rate is definitely one order of magnitude slower than during the discharge. The poor accuracy of the measurement during the afterglow does not permit, however, to decide whether the diffusion is purely collisional or somewhat faster. (auth)

40181 (TID–23307) THE KINETIC EQUATION FOR AN UNSTABLE PLASMA IN PARALLEL ELECTRIC AND MAGNETIC FIELDS. Fried, Burton D.; Ossakow, Sidney L. (California Univ., Los Angeles. Plasma Physics Group). Nov. 1965. Contract AT(04-1)-Gen-12. 28p. (R–3). Dep.

The response of a homogeneous plasma, in a strong uniform magnetic field, $\underline{B}_0$, to the sudden application of a strong, uniform electric field is studied in a self-consistent formulation which treats the coupled equations for the one-particle and two-particle distribution functions resulting from neglect of three-particle correlations. As in earlier work on the case $\underline{B}_0 = 0$, the electric field is assumed to be large compared to that which produces a "runaway current", so that particle-wave interactions should dominate. In the limit of strong magnetic field, use of the Bernstein-Kulsrud expansion in $k_\perp R_{ic}$ makes the problem effectively one-dimensional, eliminating the need for factorization assumptions of the form $f(v) = f_{||}(v_{||})f_\perp(v_\perp)$ used in the $\underline{B}_0 = 0$ case. Only the dominant contributions to the diffusion in velocity space, arising from the fastest growing waves, are retained. Other simplifications result from the assumption of unequal electron and ion temperatures, but it proves necessary to specify the ratio T_e/T_i, rather than simply assuming it to be large. In sharp contrast to the case $\underline{B}_0 = 0$, it is found that the diffusion affects only those electrons which have, in the ion rest frame, velocities of order $(m/M)^{1/3}$ of the electron thermal speed. No appreciable "quasi-linear" effects, such as the current limitation found in the $\underline{B}_0 = 0$ case, are therefore to be expected; the results of numerical calculations confirming this are summarized. (auth)

40182 NEW DATA ON THE SPECTRAL LINES SHIFT MECHANISM IN THE PLASMA OF AN ELECTRIC SPARK DISCHARGE. Iova, I. An. Univ. Bucuresti, [Ser.] Stiint. Nat. Fiz., 13: 51-67(1964). (In Rumanian).

The broadening and shifting phenomena of spectral lines have been emphasized by means of a Fabry-Perot interferometer and by a Q 24 Zeiss spectrograph. Convergent light has been admitted into the interferometer in order to avoid surface flaws. A tangent line of the comparison spectra has not been derived by projecting the light through the spectrograph slit from three different sources, but the three comparison spectra are all obtained following one single fitting, in identical geometrical conditions, by placing the three sources inside the same tube. Helium at 462 mm Hg pressure is introduced into the vacuum tube. The discharge electrodes, placed 4 mm apart, are made of iron. Water-cooling of the tube prevents thermal effects from occurring in operating conditions. Iron spectrum obtained from the tube electrodes has been used as reference spectrum to evaluate the irradiated platinum spectrum. Ornstein's method of intensity ratios has been used in deriving electron temperature $-33,500°C$. The different behavior of the spectral line profiles in the two physical media is illustrated graphically. It is established that in the case of the excitation of the helium lines in the plasma, the interference ring profiles superimposed on the line corresponding to various orders of interference, is broadened symmetrically according to the collision theory and shifted towards greater wavelengths. The fact that the shifting and broadening processes are achieved in the studied case by nonadiabatic collision is confirmed. The greatest part of the apparent He lines are atomic lines pointing to a low ionization. In cases of high ionization, an asymmetrical profile is derived by the statistical theory. The absence of a noticeable influence of the electrode impurities on the He-ray profiles has been observed. (auth)

40183 TRANSPORT PROPERTIES OF AN ELECTRON GAS IN A MAGNETIC FIELD. II. THE OSCILLATORY TRANSPORT COEFFICIENTS. Dworin, Lowell (Columbia Univ., New York). Ann. Phys. (N. Y.), 39: 43-71(Aug. 1966).

The theory of the Shubnikov-de Haas effect for a system of free electrons interacting with a set of fixed, but randomly located, impurity centers is presented. The transport equation satisfied by the lowest order term of a gauge-invariant function $f_k^{\gamma(-1)}$ in an expansion in powers of the density of impurity centers, and ω/μ, the ratio of the magnetic energy $\omega = |e|H/m$ to the chemical potential is obtained in the limit $\kappa_B T/\mu \to 0$ (κ_B is Boltzmann's constant), although nothing need be said about the relative magnitude of ω and $\kappa_B T$ or of ω and n_i. The oscillatory part of the transport coefficients, $\tilde{S}_k^{\alpha\gamma(-1)}$ may be obtained from $\tilde{f}_k^{\gamma(-1)}$ by the relationship

$$\tilde{S}_{ij}^{\alpha\gamma(-1)} = \sum_k \frac{k_\alpha}{m} (\epsilon_k)^{i-1} \tilde{I}_k^{\gamma(-1)}$$

It is shown that the oscillatory parts of the thermal and electrical conductivities obey a relationship similar to the Wiedemann-Franz relationship. (auth)

40184 EXACT DETERMINATION OF THE ELECTRON DENSITY DISTRIBUTION IN AN INFINITE ANISOTROPIC PLASMA. Fischer, M. (Philipps-Univ., Marburg, Ger.). Ann. Physik (7), 17: 7-32(1966). (In German).

If a microwave cavity containing an anisotropic, inhomogeneous plasma is excited with a nonresonant frequency ω, the electron density distribution inside the plasma can be obtained from a knowledge of the tangential electrical field on a surface enclosing the plasma. The main step is the derivation of an integral equation relating the tangential field to the high-frequency plasma current. An experimental setup is discussed. The obtainable precision is limited by the noise like density fluctuations in the plasma itself and is about 1% for $\delta N/\bar{N}$ for a spatial resolution in the same order of magnitude. (auth)

40185 VARYING PLASMA ELECTRON TEMPERATURE IN DISCHARGE TUBES BY A SIMPLE AUXILIARY ELECTRODE. Alexeff, I.; Jones W. D. (Oak Ridge National Lab., Tenn.). Appl. Phys. Lett., 9: 77-9(July 15, 1966). (ORNL-P-2205).

A simple auxiliary electrode is described, that, when inserted into a simple discharge tube, allows a variation of the electron temperature of rare-gas plasmas over a wide range. The electrode is essentially a hot probe that when heated, becomes a strong emitter of electrons, and approaches plasma potential. A schematic of the experimental apparatus is shown and typical experimental results obtained with the apparatus are given. Possible applications of this technique for varying plasma electron temperature are mentioned. (W.D.M.)

40186 TIME AND SPATIALLY RESOLVED INTERFEROMETRY ON PULSED-LASER-INDUCED PLASMAS. Bruce, C. W.; Deacon, J.; Vonderhaar, D. F. (Kirtland Air Force Base, Albuquerque, N. Mex.). Appl. Phys. Lett., 9: 164-6(Aug. 15, 1966).

A technique is described for the measurement of plasma density. Multiple beam interferometry gives simultaneous time and position information on the state of the laser-induced plasma. Experiments using a single interferometric probe at various distances from the target surface along the incident laser axis indicates that the leading edge of the blowoff absorbs a portion of the incident energy and hence additional fringe shifts are observed. (auth)

40187 PLASMA ENERGY MEASUREMENT ON TOKAMAK BY OBSERVATION OF LONGITUDINAL MAGNETIC FLUX VARIATION. Razumova, K. A. At. Energ. (USSR), 20: 459-64(June 1966). (In Russian).

The results of the measurement of the magnitude of the transverse plasma energy in Tokamak by diamagnetic signals are described. It is shown that, for regimes in which the flux axis at the precision limits of the experiment corresponds with the axis of the discharge chamber, the measurements of the electron temperature correspond with the temperatures calculated from the conductivity. Divergences were observed in those cases where the discharge occurred at low initial hydrogen pressures and the flux axis was displaced to the interior wall of the chamber. (tr-auth)

40188 EXCITATION OF CYCLOTRON ELECTROMAGNETIC WAVES IN A MAGNETOACTIVE PLASMA BY A STREAM OF CHARGED PARTICLES, INCLUDING TEMPERATURE EFFECTS IN THE STREAM. Fung, P. C. W. (Univ. of Tasmania, Australia). Austral. J. Phys., 19: 489-99(Aug. 1966).

The dispersion equation for cyclotron electromagnetic waves in a system comprising a charged particle stream injected at an angle to the static magnetic field of a magnetoactive plasma is derived for a general wave-normal angle θ when the temperature of the stream was taken into account. The expression for the growth rate is derived in general for all cyclotron waves. (auth)

40189 PROPAGATION OF HELICON WAVES IN A NON-UNIFORM PLASMA. Blevin, H. A.; Christiansen, P. J. (Univ. of New England, Armidale, N. S. W.). Austral. J. Phys., 19: 501-8(Aug. 1966).

Theoretical results are obtained for the dispersion of helicon waves in a non-uniform cylindrical plasma. Although a direct comparison with the experimental data of Lehane and Thonemann cannot be made (due to simplifying assumptions in the present theory), a qualitative explanation is given for some of the discrepancies between their experimental results and the uniform plasma theory. (auth)

40190 EXPERIMENTAL STUDY OF THE IONIZATION OF GASES BY A VERY INTENSE LUMINOUS BEAM. MEASUREMENT OF THE ABSORPTION OF THE ENERGY IN THE IONIZED ZONE. Fecan, Jean-Claude; Floux, Francis; Veyrie, Pierre (Centre d'Etudes de Limeil, Villeneuve-Saint-Georges, France). Compt. Rend., Ser. B, 262: 1613-16(June 20, 1966). (In French).

In order to interpret the experimental results obtained with a very high-powered laser, it is necessary to know the variation of some parameters as a function of time. The parameters studied are the power transmitted and the intensity absorbed by the plasma. (tr-auth)

40191 ON THE TURBULENT DIFFUSION OF PLASMA IN AN OSCILLATING DISCHARGE. Vaclavik, J. (Inst. of Plasma Physics, Czechoslovak Academy of Sciences, Prague). Czech. J. Phys., 16: 676-80(1966).

An investigation was made of the turbulent diffusion of plasma caused by instabilities in an oscillating discharge. The coefficients of turbulent diffusion of plasma are approximately determined by means of the quasi-linear theory. (auth)

40192 INFLUENCE OF THE INCREASE IN INDUCTANCE AT THE ACCELERATION OF PLASMA IN AN EXTERNAL MAGNETIC FIELD. Jelen, J. (Czech Technical Univ., Podebrady). Czech. J. Phys., 16: 662-75 1966).

The accelerating influence of an external perpendicular constant magnetic field on the acceleration of plasma clusters is discussed. Assuming that the increase in inductance, caused by the motion of the cluster, plays a relatively small role, approximate solutions are found for the current and velocity by expanding the solution into power series with respect to a small parameter which characterizes the increase in inductance. (auth)

40193 ON THE MOTION OF PARTICLES IN NON-RESONANT H-F AND MAGNETIC FIELDS. Klima, R. Czech. J. Phys., 16: 681-96(1966). (In Russian).

The smoothed motion of a particle along the lines of force of a magnetic field in the presence of a high-frequency field is analyzed. Small gradients of all the fields and non-resonant frequency of the h-f field are assumed. A certain conservativeness of motion is derived which permits further development of the kinetic theory. A qualitative evaluation of the possibility of trapping a rapid cluster of plasma by means of a h-f field is made. (auth)

40194 ON THE CONFINEMENT OF A HIGH-TEMPERATURE PLASMA IN A TRAP WITH MAGNETIC MIRRORS. Dubovoi, L. V.; Fedyakov, V. P. Dokl. Akad. Nauk SSSR, 167: 553-5(Mar. 21, 1966). (In Russian).

The confinement time was measured for a plasma with hot electrons in a mirror-type trap (probkotron). The trap was filled with high temperature particles by the method of turbulently heating the plasma with a direct discharge. The experiments were made in a quartz tube 1.2 meters long and 12 cm in diameter, in deuterium, at a gas pressure 1 to 2×10^{-5} mm Hg. The longitudinal magnetic field in the homogeneous part of the trap ranged from 2 to 10 kOe at a constant mirror ratio 1.5. The field half cycle was 6 msec long. The direct discharge current was applied at the maximum of the magnetic field. The discharge current could be varied from 1 to 45 ka, with a half-cycle duration of 5 μsec. The results show that with increasing electron temperature the time of plasma confinement increased monotonically, reaching values of the order of 1 millisecond at a temperature of 10^4 ev. The relative change in the longitudinal magnetic field reached a maximum of 0.04,

corresponding to an electron temperature of 10 to 20 kev. Satisfactory agreement is obtained between the measured and theoretical values. It is concluded that further research on turbulent heating of plasma in a direct discharge with subsequent capturing of the plasma in magnetic traps of different types can lead to promising results with respect to plasma containment. (ATD)

40195 FLUTE INSTABILITY IN AN UNCOMPENSATED PLASMA. Dnestrovskii, Yu. N.; Kostomarov, D. P. (Moscow State Univ.). Dokl. Akad. Nauk SSSR, 167: 1032-4(Apr. 11, 1966). (In Russian).

The influence was investigated of the plasma proper electric fields on the plasma stability, starting with a second-order differential equation for the plasma potential, first derived by M. N. Rosenbluth and N. Simon. The differential equation is solved by the Galerkin method and a solution is obtained in the form of a series of basis functions. An estimate is presented for the value of the dimensionless distance at which the plasma becomes unstable. It is shown that a uniform electric field causing drift in a plasma as a whole, does not give rise to instability, which arises only when individual layers of the plasma move relative to one another. When the electric field gradients are positive, the stabilization of the plasma oscillations resulting from the finite value of the Larmor radius becomes weaker and the critical dimensionless distance increases sharply. At small negative gradients, the stabilization improves somewhat. (ATD)

40196 INFLUENCE OF COLLISIONS ON WHISTLER PROPAGATION. Hedvall, P.; Sjoegren, L. (Royal Inst. of Tech., Stockholm). Electron Lett., 1: 54-5(May 1965).

Some numerically calculated dispersion curves for whistler waves propagating along a magnetized plasma slab with a non-zero collision frequency taken into account are presented. The plasma structure examined is an infinitely extended plasma slab in the x,z plane, with thickness $2y_0$, magnetized in the z direction. The whistler waves are assumed to propagate in the positive z direction, and the longitudinal field components are assumed to be antisymmetrical in the y direction. Furthermore, all field components are assumed to have no x variation. The dispersion equation for these whistler waves are obtained from Maxwell's equations by means of the tensor dielectric model of the plasma. The results show that, if the wavelength of the whistler waves is much smaller than the transverse dimensions of the plasma slab, a non-zero collision frequency can have a large influence on the dispersion characteristics. For such small wavelengths it would be expected that the whistler dispersion is close to that of the corresponding plane waves, but this is, for certain parameter values, true only if the collision frequency is assumed to be non-zero. (BBB)

40197 ELECTRIC FIELD AND STRUCTURE OF PLASMA IN THE VICINITY OF A CHARGED CYLINDER OF SMALL RADIUS. Moskalenko, A. M. (Inst. of Terrestrial Magnetism, Ionosphere and Radio Wave Propagation, Academy of Sciences, USSR). Geomagn. Aeronomy (USSR) (Engl. Transl.), 5: 867-70(1965).

Translated from Geomagn. Aeronomiya, 5: 1105-7 (1965).

Equations are given to determine the electric field and plasma structure in the vicinity of a charged cylinder of small radius. An infinite absorbing cylinder, located in a very rarefied plasma, so that the radius of the cylinder is small compared to the Debye radius, is examined. The analysis is performed on the assumption that the Debye radius is very large, so that the electric field from the surface of the cylinder is weak because of the Coulomb potential drop. Concentration patterns of attracted and repelled particles in the vicinity of the cylinder are given. (J.H.M.)

40198 ON THE STABILITY OF A CYLINDRICAL PLASMA. Zickert, D.; Ruedisuehli, P.; Schneider, H. (Univ., Freiburg i. B.). Helv. Phys. Acta, 39: 177-8 (1966). (In German).

The stability diagram of Rosenbluth was used to determine the confined flux of a cylindrical plasma. The fraction of the magnetic flux present in the plasma was determined as a function of the compression and it is shown that this flux fraction is a function of the compression. (J.S.R.)

40199 RADIATION FROM AN ELECTROMAGNETIC SOURCE IN A HALF-SPACE OF COMPRESSIBLE PLASMA-SURFACE WAVES. Seshadri, S. R. (Harvard Univ., Cambridge, Mass.). IEEE (Inst. Elec. Electron. Engrs.) Trans. Antennas Propagation, AP-12: 340-8(May 1964).

Radiation characteristics of a line source of magnetic current, situated in a compressible plasma medium of semi-infinite extent and bounded on one side by a perfectly conducting, rigid planar screen, are investigated. The special case for which the line source is on the screen becomes equivalent to the problem of radiation into a plasma half-space from an infinitely long slot radiator whose width is very small in comparison to the wavelength. A previous analysis, of an incompressible plasma in which the longitudinal plasma waves cannot be sustained, was extended to the case of a compressible plasma which is capable of supporting both the transverse electromagnetic waves and the longitudinal plasma waves. Earlier studies of the radiation from sources in a compressible plasma are considered. For a line source of magnetic current situated in a half-space of isotropic, compressible plasma which is bounded on one side by a perfectly conducting, rigid plane screen, in addition to the electromagnetic and plasma space waves, the line source excites a boundary wave. This boundary wave is a coupled wave. It has associated with it both a magnetic field component and the pressure term. This is in contrast to the space waves which can be decomposed into an electromagnetic (EM) mode with no pressure term and a plasma (P) mode with no magnetic field associated with it. The characteristics of this boundary wave are evaluated. The boundary wave propagates for all frequencies and the power carried by the boundary wave becomes smaller as the frequency is increased. (BBB)

40200 SURFACE WAVES AT A PLANE INTERFACE BETWEEN VACUUM AND PLASMA WITH THE MAGNETOSTATIC FIELD NORMAL TO THE INTERFACE. Seshadri, S. R. (Sylvania Electronics Systems, Waltham, Mass.). IEEE (Inst. Elec. Electron. Eng.) Trans. Antennas Propagation, AP-14: 297-302(May 1966).

A basic problem in the theory of electromagnetic wave propagation in plane stratified magneto-plasma layers is that of the guided waves at a plane interface which separates semi-infinite regions of free space and homogeneous plasma without and with an external static magnetic field, B_0. The spectrum of guided waves at a plane interface between vacuum and isotropic plasma shows that plane surface waves exist for wave angular frequencies, ω, below $1/\sqrt{2}$ times the plasma angular frequency ω_p. The effect on the characteristics of the surface waves guided along a vacuum-plasma interface due to a B_0 normal to the interface is studied. If B_0 is normal to the interface, a low-frequency cutoff is introduced and the surface waves propagate only for frequencies which lie between the gyromagnetic angular frequency ω_c and $1/\sqrt{2}$ times the upper hybrid resonant frequency. The phase velocity of the surface waves is always less than the velocity of electromagnetic waves in free space, and it decreases monotonically with the increase in the frequency and goes to zero at $1/\sqrt{2}$ times the upper hybrid resonant frequency. The attenuation rates normal to the interface of the surface wave fields are examined, and numerical results of the surface wave characteristics are given for one typical case. (BBB)

40201 TRANSVERSE ELECTROMAGNETIC WAVE PROPAGATION IN A CYLINDRICALLY STRATIFIED MAGNETOPLASMA. Burman, R. (Victoria Univ. of Wellington, New Zealand). IEEE (Inst. Elec. Electron.

Eng.) Trans. Microwave Theory Tech., MTT-14: 253-4 (May 1966).

A study of the transverse propagation of electromagnetic waves in a cylindrically stratified, axially magnetized plasma showed that in a continuously varying plasma, the fields can be described by two uncoupled wave equations. Thus, the total field can be expressed as the sum of two partial fields which propagate independently. These are called E-parallel and H-parallel fields, with the electric and magnetic vectors, respectively, having only axial components. The differential equation describing E-parallel fields is unaffected by the static magnetic field. The equation describing H-parallel fields was derived, and its normal form is considered. (BBB)

40202 PROBE DATA OF DUOPLASMATRON PLASMA. Bose, D. K.; Majumdar, N. K.; Sengupta, S. N. (Saha Inst. of Nuclear Physics, Calcutta). Indian J. Phys., 40: 147-50(Mar. 1966).

A Langmuir probe was placed at the mouth of the anode orifice of a duoplasmatron source to study the effect of magnetic field on the plasma state in this region under different operating conditions. Current-voltage characteristics obtained from the probe technique are given. A table listing various other probe data is included. (M.O.W.)

40203 DETERMINATION OF IONIZATION POTENTIAL OF Gd AND Ho BY SURFACE IONIZATION METHOD. Dey, S. D.; Karmohapatro, S. B. (Saha Inst. of Nuclear Physics, Calcutta). Indian J. Phys., 40: 151-3(Mar. 1966).

Ionization potential values for Gd and Ho were determined directly by the surface ionization method using a new and simple technique. (M.O.W.)

40204 ELECTROMAGNETIC FIELD PENETRATION INTO MAGNETO ACTIVE PLASMA. Bogomolov, Yu. V. (Radio-Technical Inst., Academy of Sciences, USSR). Izv. Vyssh. Ucheb. Zaved., Radiofiz., 9: 462-8(1966). (In Russian).

By Dnestrovsky and Kostomarov's method a total surface impedance of magnetoactive plasma was calculated. A constant magnetic field the pressure of which is greater as compared with a gas one is directed along the plasma surface. The plasma boundary is modeled under the condition of the mirror reflection of electrons. (auth)

40205 NONLINEAR WAVE INTERACTION IN PLASMA IN THE PRESENCE OF INTENSIVE TRANSVERSE WAVES. Liperovskii, V. A.; Tsytovich, V. N. (Lebedev Inst. of Physics, Academy of Sciences, USSR). Izv. Vyssh. Ucheb. Zaved., Radiofiz., 9: 469-78(1966). (In Russian).

Four-plasma processes leading in some cases to the nonlinear pumping of the longitudinal wave spectrum were considered towards the great wave numbers. (auth)

40206 THEORY OF ELECTROMAGNETIC WAVE PROPAGATION IN LIMITED PLASMA. Kormilitsin, B. T. Izv. Vyssh. Ucheb. Zaved., Radiofiz., 9: 479-88(1966). (In Russian).

The conditions were obtained for an electromagnetic wave on plasma boundary, taking into account the electron collision with the boundary in the case when the thermal velocities of electrons are much less than the phase one of an electromagnetic wave. The comparison was made with the results published elsewhere. Possible experiments were proposed of investigation of the character of electron reflection from the boundary. (auth)

40207 DISINTEGRATED WAVE INTERACTION IN MAGNETOACTIVE PLASMA. Giorgadze, N. P.; Khirseli, E. M.; Tsintsadze, N. L. (Inst. of Physics, Academy of Sciences, Georgian SSR). Izv. Vyssh. Ucheb. Zaved., Radiofiz., 9: 489-96(1966). (In Russian).

The disintegrated wave interactions in a magnetoactive plasma were considered under the condition when the wave vectors are directed along a magnetic field. An average power of disintegrated generation was calculated. (auth)

40208 PECULIARITIES OF THE RAY THEORY OF CYLINDRICAL AND SPHERICAL WAVES PROPAGATING IN A WEAK NONHOMOGENEOUS PLASMA. [PART] I. Orlov, Yu. I. (Inst. of Power Engineering, Moscow). Izv. Vyssh. Ucheb. Zaved., Radiofiz., 9: 497-506(1966). (In Russian).

By ray-optics method the problem was considered of the incidence of a cylindrical (spherical) local-plane electromagnetic wave on a weak nonhomogeneous plane-stratified plasma without losses. It is shown that the finite divergence of an incident wave front leads to the peculiarities of the ray picture, caustics, and hence, to the field peculiarities. The coordinates of peculiar caustic points were determined and calculated for the case of linear and nonlinear changes of the electron density. The deformation of the ray picture and caustic surface was estimated when changing parameters of the problem. (auth)

40209 PRODUCTION OF CARBON PLASMAS. Rutowski, R. W.; Weimer, D.; Marlow, W. C. (Lockheed Palo Alto Research Lab., Calif.). J. Appl. Phys., 37: 3483-6 (Aug. 1966).

An experimental technique for the production of high-temperature, high-density plasmas in a shocktube-like configuration was developed. The device consists of an arc chamber (8.6 cm) analogous to a shocktube driver and a test chamber (25.6 cm) analogous to a shocktube receiver. Both sections have the same diameter (2.54 cm) and are joined without a separating diaphragm. Capacitively stored energy (120 000 J) is delivered over a period of 75 μsec to the arc chamber. This energy flow is initiated by introducing a low-pressure gas (100 μ) into the entire system so that the voltage (7000 V) across the arc chamber electrodes causes a discharge. The discharge produces a shock wave in the trigger gas (usually argon) followed by the flow of the arc chamber electrode material, primarily carbon, which acts, in analogy to the shock tube, as a hot-dense driver gas. In analyzing the subsequent flow, the low-density trigger gas is ignored and the dense carbon plasma is treated as if it were the flow behind an incident shock. This incident carbon plasma is reflected from the end wall of the test chamber producing the plasma of principal interest. The properties of the plasma behind the reflected shock were studied and indicated that temperatures on the order of 25 000°K, pressures of 800 atm, and electron densities of 10^{20} cm^{-3}. (auth)

40210 TRANSPORT PHENOMENA IN LOW-ENERGY PLASMAS. Wilkins, Daniel R.; Gyftopoulos, Elias P. (Massachusetts Inst. of Tech., Cambridge). Contract DA36-039-AMC-03200(E). J. Appl. Phys., 37: 3533-40 (Aug. 1966).

An extended Chapman-Cowling formalism is used to derive transport differential equations for the charged-particle species in low-energy, three-component, two-temperature plasmas consisting of electrons, ions, and neutrals. The analysis is developed in two parts: (a) the charged-particle Boltzmann equations are solved for the charged-particle distribution functions; (b) these distribution functions are used to reduce the charged-particle hydrodynamic equations into a system of differential equations involving the densities, temperatures, and electrostatic potential of the plasma, and a set of transport coefficients which depend upon the prevailing collision laws. A general procedure for the computation of the transport coefficients is given, and illustrative numerical results are presented for specific collision laws. (auth)

40211 LANDAU DAMPING IN PLASMAS WITH FINITE TRANSVERSE DIMENSIONS. Gunshor, R. L. (Rensselaer Polytechnic Inst., Troy, N. Y.). J. Appl. Phys., 37: 3630-1(Aug. 1966).

A theory developed for longitudinal plasma waves in finite-diameter, uniform-density, cylindrical plasmas is used, in conjunction with recently reported experimental results, to plot curves of the real part of the frequency versus experimental temperature range and the e-folding distance for power versus the square of the phase velocity. (W.D.M.)

40212 PRELIMINARY RESULTS FROM THE PIONEER 6 M.I.T. PLASMA EXPERIMENT. Lazarus, A. J.; Bridge, H. S.; Davis, J. (Massachusetts Inst. of Tech., Cambridge). J. Geophys. Res., 71: 3787-90(Aug. 1, 1966).

Preliminary interplanetary plasma data obtained by the M.I.T. plasma experiment aboard Pioneer 6 are presented. The plasma sensor, a Faraday cup with an energy-determining grid, is shown. The data-taking sequence is illustrated, and a sample of positive ion data is included. (J.H.M.)

40213 A THEORY OF INCOHERENT SCATTERING OF RADIO WAVES BY A PLASMA. 4. THE EFFECT OF UNEQUAL ION AND ELECTRON TEMPERATURES. Farley, D. T. (Jicamarca Radar Observatory, Lima). J. Geophys. Res., 71: 4091-8(Sept. 1, 1966).

The theory is extended to include the effects of unequal ion and electron temperatures and a magnetic field. Two approximate formulas for the total scattered power are derived, which, with certain restrictions, are applicable (1) when $T_e/T_i \lesssim 1$, (2) when $T_e/T_i \gg 1$. For moderately large values of the temperature ratio, a full numerical calculation is necessary. In contrast to the equilibrium case, the total scattered power is not independent of the magnetic field when T_e/T_i is not unity. In the interesting case in which the ion cyclotron radius is large compared to wave-lengths of interest, but the electron cyclotron radius is small, the mass ratio m_e/m_i is replaced by an effective ratio $(m_e/m_i)\sec^2 \alpha$, where α is the angle between the propagation vector k and the magnetic field. As α approaches 90°, the effective mass ratio ceases to be small, and the scattering is significantly altered. The general behavior of the scattering has a simple physical explanation. The scattering can be considered to be from acoustic waves that are in equilibrium with the particles that contribute most of their Landau damping. (auth)

40214 LOW-ELECTRON-DENSITY MEASUREMENTS OF TRANSIENT PLASMAS BY OPTICAL INTERFEROMETERS. Takeda, Susumu; Minami, Kazuo (Univ. of Nagoya, Japan). Jap. J. Appl. Phys., 5: 696-700(Aug. 1966).

A simple and sensitive optical interferometer system was developed to extend the lower limit of measurable electron densities for time varying plasmas. This technique, which can eliminate the effect of mechanical vibrations of the building floor and/or the drift, was tested and compared with that of an 8 mm microwave measurement. The electron density decay from 10^{15} cm^{-3} down to 4×10^{13} cm^{-3} for a plasma length of 20 cm was detected by a wave of 0.5463μ from a mercury lamp. (auth)

40215 SPECTROSCOPIC MEASUREMENT OF ELECTRON DENSITY AND TEMPERATURE IN ARGON–HYDROGEN PLASMA JET. Terasawa, Yoshio (Hitachi Ltd., Japan). Jap. J. Appl. Phys., 5: 711-18(Aug. 1966).

Measurements were made of electron densities and temperatures in an argon–hydrogen gas mixture plasma jet using the Griem-Kolb-Shen theory for the Stark profile of the H_β line and Inglis-Teller's formula in the Balmer lines. The true intensity distribution for the H_β line was obtained by taking into account the background spectrum due to argon. Both the electron densities and temperatures determined by the two different methods were in reasonable agreement. Under operating conditions of the plasma jet of an arc current of 100A, arc voltage of 62v, and gas flow rate of 23 l/min (Ar : H_2 = 2 : 1), the electron densities of the plasma jet at distances of 2, 7, and 12 mm from the head of an anode were $7.25 \pm 1.10 \times 10^{16}$ cm^{-3}, $4.16 \pm 0.62 \times 10^{16}$ cm^{-3}, and $2.25 \pm 0.33 \times 10^{16}$ cm^{-3}, respectively, and the corresponding temperatures were 12,100 ± 300°K, 11,100 ± 200°K, and 10,300 ± 200°K, respectively. (auth)

40216 LOAD SUPPORTING CAPACITY OF A VERTICAL PLASMA CYLINDER. Ramanaiah, Gundala (Indian Inst. of Tech., Kharagpur, India). Jap. J. Appl. Phys., 5: 730(Aug. 1966).

It was shown previously [Wear, 5: 198(1962)] that the use of an applied axial current increases the load capacity of a hydrostatic thrust bearing without affecting the frictional drag on the bearing surfaces. In this note, the load-supporting capacity of a vertical cylinder is discussed. The physical situation consisted of a plasma cylinder contained between ideally conducting plates and between which a voltage was applied. The load-supporting capacity is given as a function of the radii of plasma and plates. (W.D.M.)

40217 INSTABILITY OF PLASMA ON TRAPPED PARTICLES. Kadomtsev, B. B. JETP Lett. (USSR) (Engl. Transl.), 4: 10-12(July 1, 1966).

Translated from Zh. Eksp. Teor. Fiz., Pis'ma Redaktsiyu, 4: 15-19(July 1, 1966).

A discussion is presented of the plasma flute instabilities in magnetic-mirror traps and in toroidal traps with closed force lines. The density and type of plasma were considered. (M.O.W.)

40218 STABILIZATION OF LOW-FREQUENCY PLASMA INSTABILITIES. Fainberg, Ya. B.; Shapiro, V. D. (Ukrainian Inst. of Physics and Tech.). JETP Lett. (USSR) (Engl. Transl.), 4: 20-3(July 1, 1966).

Translated from Zh. Eksp. Teor. Fiz., Pis'ma Redaktsiyu, 4: 32-6(July 1, 1966).

The possibility is discussed for stabilizing drift instability of an inhomogeneous plasma by superimposing an external high-frequency electric field parallel to the magnetic field. The effects of the high-frequency field are theoretically described. (M.O.W.)

40219 CYCLOTRON RADIATION FLASHES. Timofeev, A. V. JETP Lett. (USSR) (Engl. Transl.), 4: 32-5 (July 15, 1966).

Translated from Zh. Eksp. Teor. Fiz., Pis'ma Redaktsiyu, 4: 48-51(July 15, 1966).

Cyclotron radiation accompanied by ejection of particles, in the form of periodic bursts spaced in time, was observed in a number of experiments on adiabatic plasma containment. An investigation was made to relate the explosive character of the radiation with certain singularities in the development of cyclotron oscillations with negative energy. The mathematical technique is described. (M.O.W.)

40220 INSTRUMENTATION FOR PLASMA DIAGNOSTICS. Eubank, Harold P. (Princeton Univ., N. J.). Phys. Today, 19: No. 7, 91-4; 96-7; 99-101; 103-5(July 1966).

Developments in diagnostic techniques for measuring plasma properties are reviewed, which include interactions with electromagnetic waves, particle beams, probes, lasers, and spectroscopy. (L.B.S.)

40221 STABILITY OF HOMOGENEOUS STATES. Kulikovskii, A. G. Prikl. Mat. Mekh., 30: 148-53(1966). (In Russian).

A linear system with certain homogeneous boundary conditions is considered. To show that it leads to a stable homogeneous system independent of time, the boundaries of the system, $x = \pm L$, are assumed to be far apart. It is shown that for very large L there exist two nontrivial solutions to the boundary value problem. One of these constitutes a one-sided solution in which the complex frequency ω is determined from boundary conditions on one side only, the other is a "global" solution analogous to the quasi-classical solution in which ω is independent of the boundary conditions. For the global (or universal) instability, the frequency is obtained from the solution $\mathrm{Im}\ \omega > 0$, $\mathrm{Im} k(\omega) = 0$. A connection is then established between global instabilities and absolute instabilities (the unbounded problem). (ATD)

40222 EFFECTS OF COLLISION ON THE PROPAGATION OF ELECTROMAGNETIC WAVE IN A PLASMA. I. HOMOGENEOUS ISOTROPIC PLASMA. Ogasawara, Masatada (Keio Univ., Tokyo); Kajiura, Toshihiro. Proc. Fujihara Mem. Fac. Eng., Keio Univ. (Tokyo), 19: 1-13 (June 1966).

Propagation constant, attenuation constant, index of refraction, and velocity of energy transfer were calculated for an isotropic homogeneous plasma. It is explicitly shown that in the lossy plasma not the group velocity but the ve-

locity of energy transfer satisfies the relativity requirement. These two velocities coincide only when the collision is absent. (NSA of Japan)

40223 STUDY BY MOVING ELECTRIC PROBES OF DIFFERENT PARAMETERS OF A CESIUM PLASMA OBTAINED BY CONTACT IONIZATION IN A MACHINE WITH VARIABLE GEOMETRY. Felden, Marceau; Patou, Claude; Haug, Robert (Faculte des Sciences, Nancy, France). Rev. Phys. Appl., 1: No. 1, 48-60(Mar. 1966). (In French).

A cesium plasma machine is studied. It is made of metal and is entirely demountable which allows different structures to be used for various problems. The geometry is variable and two moving probes analyze the region created by contact ionization. The measurements are made at different pressures for variable hot surface temperatures. Electrodes of which the polarization may be changed, are situated at some distance. The machine and results of several experiments are presented and discussed. (auth)

40224 PLASMA WAVES IN THE FREQUENCY RANGE 0.001-10 CPS IN THE EARTH'S MAGNETOSPHERE AND IONOSPHERE. Hultqvist, Bengt (Kiruna Geophysical Observatory, Sweden). Space Sci. Rev., 5: 599-695(Aug. 1966).

The plasma model for the magnetosphere and ionosphere is first discussed. A review of some parts of the theory for a warm collisionless plasma of interest in the magnetosphere in connection with waves of periods between 0.1 and 1000 seconds is given. The theory for magnetohydrodynamic waves in a slightly ionized gas is then summarized. The available observational data about magnetospheric and ionospheric phenomena, which may be interpreted in terms of waves with periods between 0.1 and 1000 seconds, are briefly surveyed and some theoretical applications to the ionosphere and magnetosphere are finally discussed. The theory of shock phenomena and transients in the magnetosphere is not included. (auth)

40225 SURFACE PLASMON DISPERSION RELATION FOR AN ELECTRON GAS. Ritchie, R. H.; Marusak, A. L. (Oak Ridge National Lab., Tenn.). Surface Sci., 4: 234-40(May-June 1966). (ORNL-P-1674).

The dispersion and damping of surface plasmons in a semi-infinite free electron gas were examined using a specular reflection model for electrons at the bounding surface. The approach employed is equivalent to the use of a classical Boltzmann-Vlasov equation for the motion of electrons in a free electron plasma under the influence of electrical forces generated by the displacement of other electrons from their equilibrium positions. It is assumed that a plane boundary separates a semi-infinite free electron gas from vacuum and supposed that electrons impinging upon this surface from the interior of the electron gas are reflected from it in a specular fashion. It is assumed that a polarization wave with wave vector K propagates along this surface. The characteristic frequency of oscillation of the polarization wave is sought for this value of K. A transcendental equation involving the longitudinal dielectric constant of an infinite free electron gas of the same density is obtained and is solved numerically. This approach predicts a nonzero damping rate for surface polarization waves. It was found that this dispersion relation agrees well with the predictions of the hydrodynamical model for small wave numbers. The damping rate, which is predicted to be zero on the hydrodynamical model, is found to be $\leq 1\%$ of the plasmon frequency over a substantial range of wave numbers. These results on dispersion and damping of surface plasmons are being employed in a calculation of the cross section for surface plasmon excitation by low-energy electrons. This cross section is of importance in the theory of photoelectric emission from metals and secondary emission from metals under charged particle bombardment. (BBB)

40226 OPTICAL INTERFEROMETER WITH LASER FOR PLASMA DIAGNOSIS. Adamov, I. Yu.; Dushin, L. A.; Pavlichenko, O. O. (Kharkov Physico-Technical Inst.). Ukr. Fiz. Zh., 11: 615-18(1966). (In Ukrainian).

A single sideband interferometer for the measurement of plasma density using a laser is described. (auth)

40227 EFFECT OF SPIN-ORBITAL INTERACTION ON THE FREQUENCIES OF PLASMA OSCILLATIONS IN SEMICONDUCTORS. Marinchuk, M. E. Vestn. Moskov. Univ., Ser. III, Fiz. Astron., No. 4, 44-9(July-Aug. 1965). (In Russian).

Plasma oscillations are studied in materials where spin-orbital interaction takes place in the absence of a magnetic field. Spin-orbital interaction affects on the frequencies of plasma oscillations are described. The method of Green functions is used in solving this problem. In approximating the effective mass, a single-band model is used—the conduction band for the electrons. Spin-orbital interaction manifests itself in various ways in crystals, depending on whether or not a given crystal has an inversion center. When there is no spin-orbital interaction, all bands are double degenerate throughout the k-space. If the crystal has a center of inversion, spin-orbital interaction does not cancel this degeneration, and the electron energy depends only on the band number and on the crystal momentum. In crystals which have no center of inversion (e.g., InSb), spin-orbital interaction cancels this double degeneration, causing a small but finite divergence in bands, and the electron energy still depends on the spin in the absence of a magnetic field. In the latter case, the spin is not an integral motion and the eigenfunctions of the Hamiltonian are linear combinations of wave functions for states with "upward" and "downward" spin. Crystals of the second type are studied. The correction is found for the limiting frequency of plasma oscillations due to spin-orbital interaction in a semiconductor electron plasma in the absence of a magnetic field. It is found that spin-orbital interaction in InSb gives a small contribution to the "optical" effective mass and has little effect on the frequencies of plasma oscillations. (ATD)

40228 THEORY OF THE FREQUENCY MULTIPLIER IN A GAS DISCHARGE IN A STRONGLY NONUNIFORM SHF FIELD. Brandt, A. A.; Tyagunov, A. V. Vestn. Moskov. Univ., Ser. III, Fiz. Astron., No. 4, 92-3(July-Aug. 1965). (In Russian).

A study was made on the possibilities of the mechanism of frequency multiplication for gas discharge multipliers with a nonuniform field. The model examined is a cylindrical condenser filled with a plasma. An a-c voltage $\mu = U_0 \sin\omega t$ is applied to the linings of this condenser. The entire system is located in an axially symmetric magnetic field directed along the axis of the condenser. In order to increase the amplitude of electron oscillations in the plasma, the magnetic field strength is chosen in such a way that the Larmor frequency of electron rotation is equal to the frequency of the applied voltage. It is assumed that an electron loses energy only by collisions with molecules. The shape of the induced current signal is calculated and an example is given with specific parameters. It is found that conversion (multiplication) efficiency is increased as pressure is reduced, since energy losses due to collisions are reduced. With operation using electron beams, where there are no collisions and the power of the fundamental frequency depends only on electron recoil, the multiplication efficiency of any harmonic approaches 100%. (ATD)

40229 VARIATION OF THE ADIABATIC INVARIANT OF THE HARMONIC OSCILLATOR. Knorr, G. (Institut fuer Plasmaphysik, Garching, Ger.); Pfirsch, D. Z. Naturforsch., 21a: 688-93(June 1966).

The variation of the adiabatic invariant μ of a harmonic oscillator or gyrating particle in a time-varying homogeneous magnetic field is given as an absolutely converging series. This solution is used to discuss the behavior of the adiabatic invariant for slow and fast as well as small and large variations of the oscillator strength. General estimates are obtained for the dependence of the oscillator strength which is twice differentiable or which is analytic. For the latter case it is found that $\Delta\mu$ tends to zero at least as $\exp[-(2\,d - \epsilon)/\alpha]$ for $\alpha \to 0$; $2\,d$ is the width of the analytic strip of $\omega(\alpha\, t)$; α characterizes the slowness of the variation and ϵ is any number $2\,d > \epsilon > 0$. (auth)

40230 THEORY OF THE COLLISION-FREE PLASMA COLUMN WITH REGARD TO WALL LOSSES. Ecker, G. (Univ., Bochum, Ger.); Kanne, H. Z. Naturforsch., 21a: 719-25(June 1966). (In German).

The collision-free plasma column was investigated without a magnetic field in the normal and subnormal region, neglecting wall losses. This simplifies the analysis appreciably since it allows the electron description by a Boltzmann distribution. However, in the subnormal region and in strong magnetic fields, the wall loss is a decisive factor. Therefore the investigation extends the theory, including this effect. Starting from the transport equations, particle density and potential distributions, as well as the current-voltage characteristic, are found by numerical integration. With increasing magnetic field, the particle density profiles grow wider, whereas the potential distribution grows flatter. These effects are particularly pronounced in the subnormal region. In this region the I/V characteristic shows a negative slope, which for a given current decreases with increasing magnetic field. (auth)

40231 INTERACTION OF A PLASMA JET WITH AN AXISYMMETRIC MAGNETIC FIELD. Ragaller, K. (Technische Hochschule, Munich). Z. Naturforsch., 21a: 725-32(June 1966). (In German).

The interaction of a plasma jet with an axisymmetric magnetic field is calculated in linear approximation for a periodic and for a convergent or divergent field configuration. The solution depends on the Mach number, the magnetic pressure number, and the magnetic Reynolds number. In the convergent field, the plasma is decelerated. If the flow is supersonic, this is connected with a contraction of the jet leading beyond equilibrium and therefore being followed by an expansion. In the subsonic case, the stopping is accompanied by a broadening of the jet. With increasing magnetic Reynolds number, "wakes" appear which extend upstream or downstream, depending on the values of the magnetic pressure number and the Mach number. (auth)

40232 CATHODE JETS AND THE RETROGRADE MOTION OF ARCS IN MAGNETIC FIELDS. Hermoch, V.; Teichmann, J. (Inst. of Physics, Prague). Z. Phys., 195: 125-45(1966).

The influence of a transverse magnetic field on the jets of an impulse discharge was investigated. It was found that the jet trajectories show a curvature. The amount of the curvature depends on the pressure, the magnetic field intensity, the discharge current, the material, and the polarity of the electrodes. The curvature of the jets was explained as a result of the action of forces arising in a plasma flow through a magnetic and electric field; their analysis was carried out on the bases of a MHD model. On hand of a derived solution, a possible influence of the jets on the origin of a retrograde motion is discussed. It is shown that the existence of certain discharge parameters and of a certain magnitude of the magnetic field brings about, in a plasma flying through a magnetic field, an induction of fields and currents under the action of which, on the one hand, the plasma itself flows in a retrograde direction and, on the other hand, there are influenced the trajectories of the carriers (particularly those of ions) of the current in the channel of discharge in front of the cathode spot. The proposed model of the retrograde motion is discussed and compared to the known results. (auth)

40233 STUDIES OF CHARACTERISTIC FLASH X-RAY LINES. Bergfeldt, J.; Haendel, S. K. (Uppsala Univ.). Z. Phys., 195: 193-200(1966).

Time resolved spectroscopic detection of characteristic x radiation as well as bremsstrahlung from flash x-ray discharges and simultaneous recording of the dI/dt waveform showed that both kinds of x radiation were produced during dI/dt minima. The Mo $K\alpha_1$ line could be detected with an initial capacitor voltage right down to only 70% of the excitation potential. The investigation supports the theory that the plasma in the flash x-ray discharge is pinched, causing high voltages in the discharge. (auth)

40234 THERMAL AND REACTIVE NONEQUILIBRIUM OF MAGNETOACTIVE PLASMA FLOWS. Wilhelm, H. E.; Schneider, R. T. (Univ. of Florida, Gainesville). Z. Phys., 195: 300-15(1966).

Based on multifluid equations derived from the Boltzmann equation under inclusion of ionization and recombination reactions, the following convective processes magnetoactive plasma flows transverse to homogeneous magnetic fields are investigated: The buildup of the nonuniform plasma state, the intercomponent thermal nonequilibrium and the reactive nonequilibrium in dependence of the flow coordinate. Due to the complexity of the problem, a numerical approach is used, parallel to which an approximate analytical theory is developed. (auth)

40235 THEORY OF NONLINEAR WAVES IN A PLASMA. Berezin, Yu. A.; Sagdeev, R. Z. Zh. Prikl. Mekh. Tekh. Fiz., No. 2, 3-6(Mar.-Apr. 1966). (In Russian).

Nonlinear waves propagating across a magnetic field in a cold rarefied quasi-neutral plasma consisting of electrons and two types of ions were studied. Dispersion curves are given for low-amplitude waves in a three-component plasma. The lower branch of the dispersion curve describes nonlinear waves at relatively low velocities. As velocity increases, the upper branch of the curve describes nonlinear wave profiles. Electron velocity is determined by drift approximation. An expression is given for the velocity of an isolated wave in terms of the maximum magnetic field in the wave. The lower the concentration of light component in the plasma the greater is the deviation from linearity. The lower velocity limit of the wave is equal to the speed of sound and the upper limit is equal to the phase velocity of low oscillation at high frequencies. As the wave approaches the upper limit the light component drops out. Dispersion effects which compensate nonlinear spiraling appear at higher frequencies due to electron inertia. The critical velocity of the wave and the maximum magnetic field in the wave decrease with the reduction in concentration of the light component. The ion energy in the wave is estimated. It is shown that light ions are accelerated in a direction perpendicular to the wave motion when an isolated wave passes through a three-component plasma. If friction between the plasma components is introduced into the original calculations, the result is a shock wave having an oscillator structure with a steep front. (ATD)

40236 ANISOTROPIC DRIFT INSTABILITY IN A PLASMA AND ANOMALOUS TRANSFER PROCESSES. Galeev, A. A. Zh. Prikl. Mekh. Tekh. Fiz., No. 2, 7-13 (Mar.-Apr. 1966). (In Russian).

A nonlinear theory is proposed for the instability of a weakly nonhomogeneous plasma assuming a "cone of losses" in their velocity distribution. Channel type ($k_z \equiv 0$) perturbations are considered which may build up even in short traps with magnetic mirrors when the nonhomogeneity is sufficiently strong. It is shown that the total ion flow across the magnetic mirrors due to turbulent diffusion into the cone of losses exceeds the flow of ions across the magnetic field due to diffusion in the coordinate space $\underline{n}$ by $(2n/R_H\nabla n)^{1/2}$ where R_H is the Larmor radius of the ions. The ion diffusion time in the cone of losses is of the order of $\tau = 10\Omega_H^{-1}(2n/R_H\nabla n)^{1/2}$ where Ω_H is the Larmor frequency. (ATD)

40237 SELF-SIMILAR SOLUTION TO THE PROBLEM OF EXPANSION OF A CYLINDRICAL COLUMN OF CONDUCTING GAS IN A LONGITUDINAL MAGNETIC FIELD. Cherepanov, A. N.; Yakovlev, V. I. Zh. Prikl. Mekh. Tekh. Fiz., No. 2, 14-20(Mar.-Apr. 1966). (In Russian).

The unsteady radial motion of an infinite cylindrical column of conducting gas along a time-variable longitudinal magnetic field is studied. The method of separating the variables was used for calculating the exact solution for a system of magnetohydrodynamic equations, assuming proportionality between the static pressure of the plasma on the boundary of the column and the external magnetic pressure. The energy characteristics of the interaction were calculated. Expressions are given for the effect of the

magnetic Reynolds number on the ratio of the work done by the gas in an infinite time interval to the initial energy of the column. A physical model of this type may be interpreted as the expansion of a compressible conducting gas column in a nonconducting incompressible fluid located in a permeable infinite cylinder. In this case the requirement of proportionality between the static and magnetic pressures reduces to the condition of a change in the external pressure at the boundary of the permeable cylinder according to a law which may be easily determined. (ATD)

40238 ELECTRON CONDUCTIVITY OF A THERMOIONIZED GAS IN AN ELECTRIC FIELD. Kunin, V. N.; Pisarev, N. M. Zh. Prikl. Mekh. Tekh. Fiz., No. 2, 21-4 (Mar.-Apr. 1966). (In Russian).

Electron conductivity of a thermoionized gas in an electric field was studied. The electron conductivity of the gas was calculated by using Drude's method and considering the drift of electrons in determining their travel time. The following are given: free electron concentration, the mean effective cross section of collisions, and mean free path. It is assumed that these quantities have a spatially isotropic distribution in the gas and are independent of time. It is further assumed that the macroscopic parameters for the state of the gas are given. The conductivity problem reduces to finding the mean drift rate of the electrons. It is shown that kinematic relationships may be used for determining conductivity without knowing the distribution function. A model is set up in which a gas particle is surrounded by a sphere of given radius. Free electrons within this sphere drift under the effect of a field which is parallel to the axis and where the electrons are scattered by a particle. After scattering, the electrons travel in the field along curved trajectories resulting in electron-ion and electron-molecule collisions. Since molecules and ions have large masses, their motion in a weak field does not depend on field intensity. Therefore the motion of electrons is limited only by the surface of the sphere. In the case of weak fields, it may be assumed that electron scattering intensity is nearly equal in all directions. An expression is given for calculating the electron drift rate within a given sphere. An improved classical formula for calculating conductivity is given. (ATD)

40239 SOME CHARACTERISTICS OF PROBLEMS IN MAGNETOHYDRODYNAMIC STABILITY THEORY REDUCIBLE TO A DIFFERENTIAL EQUATION IN WHICH THE HIGHEST DERIVATIVE HAS AN ARBITRARY PARAMETER. Erokhin, N. S.; Moiseev, S. S. Zh. Prikl. Mekh. Tekh. Fiz., No. 2, 25-9(Mar.-Apr. 1966). (In Russian).

The asymptotic properties of solutions for a fourth-order differential equation are studied, where the highest derivative has an arbitrary parameter. It is shown that similarity of asymptotic behavior is independent of the value of this parameter for values of the argument which give zero coefficients at the second derivative. The Laplace method is used in conjunction with the analytical properties of the solutions to study the problem for various values of the given parameter. It is shown that the solutions have convergent asymptotic properties to a certain degree for arbitrary values of this parameter. Specific applications of the proposed theory are considered with regard to the effect which a finite Larmor radius of the ions and ion-ion viscosity have on the development of plasma instability in a magnetic field due to longitudinal current. (ATD)

40240 THEORY OF THE SUPERSONIC PART OF A NONDISSIPATIVE BOX-TYPE ACCELERATOR. Morozov, A. I. Zh. Prikl. Mekh. Tekh. Fiz., No. 2, 30-5(Mar.-Apr. 1966). (In Russian).

A theory is developed for the supersonic part of a box-type accelerator. Calculations are given for two-dimensional flow of a two-component cold nondissipative plasma. Only low-density plasma acceleration is studied, where the density of the plasma is ($n \gtrsim 10^{14}$ cm^{-3}). Three conditions must be considered in setting up a low-density box-type accelerator: sectional electrodes must be used; conditions must be maintained to prevent interaction between the fast-particle stream and the wall; conditions have to be maintained ensuring the escape of the plasma from the magnetic field. It is shown that nondissipative plasma escapes from a magnetic field under the condition $\xi \gg 1$, where the exchange parameter ξ is the ratio of the discharge current I_0 to the intensity of ion flux I_i at the accelerator output, $\xi = I_0/I_i$, $I_i = eq/m$, where q is the mass flow of the working medium. (ATD)

40241 ELECTRIC DISCHARGE IN A CONDUCTING JET OF VISCOUS FLUID. Vulis, L. A.; Dzhaugashtin, K. E. Zh. Prikl. Mekh. Tekh. Fiz., No. 2, 36-40(Mar.-Apr. 1966). (In Russian).

Elementary problems dealing with the mode of discharge in free laminar flows that can be solved using second-order magnetic boundary layer theory are discussed. Expressions are given for a two-dimensional steady flow of a viscous incompressible fluid. An example is discussed for the case of discharge in the boundary layer at the edge of a two-dimensional stream. Self-conjugate solutions for ordinary differential equations are given for the case where conductivity is constant, assuming given boundary conditions for the magnetic field and temperature. The effect of temperature on conductivity in the problem for an incompressible fluid is also considered. The problem of a plane jet source is solved by a similar method. The energy equation for this case is solved for temperature boundary conditions which are symmetric and asymmetric with respect to velocity. The distribution of the magnetic field and current is determined for an axisymmetric jet source. (ATD)

40242 THE SOLUTION OF EQUATIONS FOR A REGULAR ELECTROSTATIC BEAM, ASSUMING EMISSION FROM AN ARBITRARY SURFACE. Kuznetsov, Yu. E.; Syrovoi, V. A. Zh. Prikl. Mekh. Tekh. Fiz., No. 2, 41-5(Mar.-Apr. 1966). (In Russian).

An analytical solution is given for the equations for a regular electrostatic beam emitting from an arbitrary surface under conditions of full space charge. A regular beam is defined as one in which the generalized particle momentum is a potential vector. It is assumed that the emitter is the coordinate surface x^1 = const in the orthogonal system x^i (i = 1,2,3) and that the density of the emission current J is a fixed function $J(x^2,x^3)$. The solution is given as series in x^1 with coefficient functions of x^2,x^3. The first correction to the Child-Langmuir $^3/_2$ law is determined by the sum of principal curvatures of the emitting surface with respect to the expansion of an arc along the length of the x^1 axis which is orthogonal to the emitter. This solution can be used to determine the shape of a collector which will provide a given emission current density distribution at a given surface. (ATD)

40243 ONE-DIMENSIONAL MOTION OF A FINITE MASS OF LIKE CHARGE PARTICLES CONCENTRATED IN A PLANE. Rykov, V. A. Zh. Prikl. Mekh. Tekh. Fiz., No. 2, 46-9(Mar.-Apr. 1966). (In Russian).

The kinetics theory was used for resolving the problem of one-dimensional motion in a vacuum of a dense gas of charged particles located at the plane x = 0 at time t = 0. The problem was resolved using the collisionless equation approximation taking into account the self-consistent electric field. A unified asymptotic of one-dimensional motion was found, and the relation between the problem of motion of a charged gas layer and the problem of motion of a point charge was established. (M.O.W.)

40244 NONLINEAR CONVERSION OF ELECTROMAGNETIC WAVES TO ION-ACOUSTIC PLASMA OSCILLATION. Liperovskii, V. A.; Tsytovich, V. N. Zh. Prikl. Mekh. Tekh. Fiz., No. 2, 116-19(Mar.-Apr. 1966). (In Russian).

The self-consistent problem of conversion of electromagnetic waves with a frequency much higher than the critical frequency to ion-acoustic oscillations in a plasma is considered, assuming that a Langmuir wave is generated as the transverse electromagnetic wave decays and that

the ion-acoustic wave is then generated by the Langmuir wave. The problem is solved with regard to ion-acoustic wave absorption as well as in the one-dimensional approximation. Examples of two-stage decay are given to illustrate application of the expressions derived. One-dimensional quasi-stationary boundary problems are also considered and solutions are given for nonlinear equations which determine the spatial distribution from the number of waves in the spectrum during the decay process. (ATD)

40245 STABILITY OF A NONHOMOGENEOUS ELECTRON BEAM. Zhvaniya, I. A.; Kucherov, R. Ya.; Rikenglaz, L. E. Zh. Prikl. Mekh. Tekh. Fiz., No. 2, 119-21 (Mar.-Apr. 1966). (In Russian).

Development of perturbation in a nonhomogeneous periodic electron beam to determine whether plasma instability in a limited space is an absolute or a convective process is considered. Theoretical expressions are derived for the perturbations in the electron beam in terms of the density, velocity, charge, and mass of the electrons, ion density, and potential. The criterion for determining whether the perturbation will increase or decrease is discussed. It is shown that the increment in perturbation is proportional to the square of the amplitude for weak disturbances. (ATD)

40246 PULSED GAS VALVE (Engineering Materials). (Lawrence Radiation Lab., Univ. of California, Livermore). (CAPE-1406).

13 drawings.

The small, bakeable, magnetically actuated, pulsed gas valve used in plasma physics attains reproducible gas pulses of from 1 to 150 μl. Valve timing is obtained by firing a trigger pulse at the time the gas pulse is to be initiated. (For details see TID-4100). (F.S.)

40247 HELIUM RECOMBINATION IN A RADIO FREQUENCY DISCHARGE. Stafford, B.; Durham, J.; Schlueter, H. (Univ. of Texas, Austin). 37p. (CONF-650833-4). ORAU. Gmelin, AED-CONF-65-315-48.

From Fourth International Conference on the Physics of Electronic and Atomic Collisions, Quebec.

The recombination in a steady-state, plasmoid-like radio frequency helium plasma is investigated spectroscopically. In an ionization-recombination balance only the radiative-collisional recombination rate involving the abundant atomic ions is of importance. This atomic recombination rate is investigated, yielding reasonable agreement with theory. The small contributions due to molecular recombination are studied for various conditions. Lower limits for the molecular collisional-radiative recombination coefficient are evaluated and found to be consistent with theory. Evidence for generally strong contributions of Hornbeck-Molnar processes to the molecular ion formation and for fast vibrational relaxation is reported. (auth)

40248 PRESSURE DEPENDENCE OF WAVE PROPAGATION IN A MAGNETOPLASMA-FILLED WAVEGUIDE. Willett, Joseph E.; Sodek, Benard A. Jr. (General Dynamics/Fort Worth, Tex.). 16p. (CONF-650220-5). ORAU. Gmelin, AED-CONF-65-022-9.

From American Physical Society, Southwest Meeting, Norman, Okla.

Propagation of magnetohydrodynamic waves in a plasma is investigated. The plasma is bounded by a rigid, perfectly conducting cylindrical waveguide. The plasma is nonviscous and completely ionized. A magnetic field is directed along the axis. The theoretical description including non-vanishing plasma pressure and resistivity has been reported previously. Maxwell's equations, two-fluid equations describing the plasma in one-fluid notation, and waveguide imposed boundary conditions are combined to yield dispersion relations. Numerical solutions are presented for the propagation characteristics of three types of wave: the transverse magnetic, TM; the transverse electric, TE (+); the transverse electric, TE (–). The TM wave is unaffected by the addition of pressure effects. The TE (+) wave is strongly pressure dependent. The most striking effect of increasing pressure appears in the increase of the cut-off frequency of the TE (–) wave. (auth)

40249 KINETIC EQUATION FOR AN UNSTABLE PLASMA IN PARALLEL ELECTRIC AND MAGNETIC FIELDS. Fried, Burton D.; Ossakow, Sidney L. (Univ. of California, Los Angeles). 30p. (CONF-651213-4). ORAU. Gmelin, AED-CONF-65-400-12.

From American Physical Society, Winter Meeting in the West, Los Angeles.

The response of a homogeneous plasma, in a strong uniform magnetic field $\underline{B}_0$, to the sudden application of a strong uniform electric field is studied in a self-consistent formulation which treats the coupled equations for the one-particle and two-particle distribution functions resulting from neglect of three-particle correlations. As in earlier work on the case $\underline{B}_0 = 0$, the electric field is assumed to be large compared to that which produces a "runaway current", so that particle-wave interactions should dominate. In the limit of strong magnetic field, use of the Bernstein-Kulsrud expansion in $k_\perp R_{ic}$ makes the problem effectively one-dimensional, eliminating the need for factorization assumptions of the form $f(v) = f_{||}(v_{||})f_\perp(v_\perp)$ used in the $\underline{B}_0 = 0$ case. Only the dominant contributions to the diffusion in velocity space, arising from the fastest growing waves, are retained. Other simplifications result from the assumption of unequal electron and ion temperatures, but it proves necessary to specify the ratio T_e/T_i, rather than simply assuming it to be large. In sharp contrast to the case $\underline{B}_0 = 0$, it is found that the diffusion affects only those electrons which have, in the ion rest frame, velocities of order $(m/M)^{1/4}$ of the electron thermal speed. No appreciable "quasi-linear" effects, such as the current limitation found in the $\underline{B}_0 = 0$ case, are therefore to be expected; the results of numerical calculations confirming this are summarized. (auth)

40250 EXPERIMENTAL STUDY OF THE DYNAMICS OF A LARGE INVERSE PINCH. Kolpin, M. A. (Aerospace Corp., El Segundo, Calif.). New York, American Inst. of Aeronautics and Astronautics, 1966, Preprint No. 66-482, 18p., $1.50. (CONF-660632-2). ORAU.

From American Inst. of Aeronautics and Astronautics, 4th Aerospace Sciences Meeting, Los Angeles, Calif.

An experimental study was made of the dynamics, stability and long-time behaviors of an unrestrained current sheet. The device selected for this study is an inverse pinch discharge of large dimension. The pressure of the test gas is varied from 100 to 1000 μ Hg. As a basis for comparison, the dynamics of the current sheet were calculated on a digital computer. Measurements of the position of the luminous front with a streak camera indicate only fair agreement. Velocities of the order of 1 to 5 cm/μsec are recorded. Other diagnostics performed to date indicate that the current sheet is stable for monatomic gases but unstable for diatomic gases. In the stable mode, the current sheet remains stable for long times and displacement, although it becomes very thick and diffused. No shock detachment from the electromagnetic piston is observed. The conductivity in the current sheet is not high enough to prevent leakage of the driving magnetic field that results in poor energy transfer. (auth)

40251 SPECTROSCOPIC STUDIES OF LASER-PRODUCED HYDROGEN PLASMA. Litvak, M. M.; Edwards, David F. (Massachusetts Inst. of Tech., Lexington). 27p. (CONF-660438-1). ORAU. Gmelin, AED-CONF-66-078-6.

From International Quantum Electronics Conference, Phoenix, Ariz.

Time-resolved intensity and Stark-width measurements were made for the radiation emitted during the decay of the hydrogen plasma produced by a 0.2-joule ruby laser. The electron density and temperature decay are determined from the spectroscopic data assuming local thermodynamic equilibrium for excited states. The electron loss is shown to occur by collision-radiative recombination for these observation times. When volume expansion and electron production by thermal ionization are taken into account, the experimentally determined recombination coefficient agrees with computed values. (M.O.W.)

40252 ELECTROMAGNETIC INTERACTION WITH A PLASMA COLUMN. Gal, G.; Gibson, W. (Avco Research and Development Div., Wilmington, Mass.). 19p. (CONF-660107-62). ORAU. Gmelin, AED-CONF-66-003-143.

From American Physical Society Meeting, New York.

Microwave techniques are widely used to determine electron distributions in plasma columns. The amplitude of the scattered or transmitted wave is then related to the parameters of the electron distribution by means of theoretical solutions. These are available for electron distributions which have a sharp cutoff. Due to this assumption, the results are strongly influenced by the behavior of the electron distribution near cutoff as well as by the choice of cutoff radius. Furthermore, realistic electron distributions decay smoothly away from the plasma axis. A theoretical solution is given for the interaction of microwaves with a smoothly decaying electron distribution. The reflection and transmission coefficients are evaluated. Particular attention is given to the asymptotic behavior of the Fourier components of the electric field. The present results display the dependence on peak electron density, collision frequency, and overall column radius. (auth)

40253 CALCULATION OF SPACE CHARGE EFFECTS IN PULSED DISCHARGES. Ward, A. L. (Harry Diamond Labs., Washington, D. C.). 20p. (CONF-660414-3). ORAU. Gmelin, AED-CONF-66-119-1.

From 2nd International Conference on Electron and Ion Beam Science and Technology, New York.

Low-pressure glow and pulsed discharges are common sources of ion and electron beams. A computer program to calculate the temporal behavior of the current in a gas under space charge conditions is described. The combined effect of ionization, diffusion and space charge upon the motion of electron avalanches is presented in a one-dimensional analysis. The collection of electrons and ions created in a gap by ionizing radiation is used as a first illustrative example. The electron and ion pulses are not treated separately as in previous papers. A second illustrative example presents the current growth and quenching in deuterium at pressures from ~0.04 to 0.1 torr and voltages up to 50 kv. The calculated variation of the maximum current attained with applied voltage and with pressure gives good agreement with the measurements of McClure. (auth)

40254 TRANSVERSE PLASMA INJECTION INTO A MULTIPOLE MAGNETIC FIELD. Cardwell, George L.; Boyd, Jim A.; Duesterhoeft, W. C. (Univ. of Texas, Austin). 7p. (CONF-660421-1). ORAU. Gmelin, AED-CONF-66-065-1.

From 18th Annual Southwestern IEEE Conference and Show, Dallas.

An experimental arrangement is described for studying transverse injection into a linear octupole magnetic field, and preliminary results of a study of the coaxial plasma gun, which is used to produce the plasma, are given. (M.O.W.)

40255 COMPTE RENDU DU COLLOQUE INTERNATIONAL SUR L'INTERACTION DES CHAMPS H-F ASSOCIES A UN CHAMP MAGNETIQUE STATIQUE AVEC UN PLASMA, SACLAY, 16 ET 17 SEPTEMBRE, 1964. (Proceedings of the International Conference on the Interaction of h-f Fields Associated with a Static Magnetic Field in a Plasma, Saclay, September 16–17, 1964). [Paris] Presses Universitaires de France, [1965]. 207p. (CONF-564).

Separate abstracts were prepared for 24 of the 26 papers included. The remaining papers appeared previously in NSA as 18: 30892 and 18: 44855. Another conference paper, which is not included, appeared in NSA as 19: 14291. (M.O.W.)

For abstracts of individual papers see: 40256–40269 and 40274–40283.

40256 R-F HEATING OF COLLISIONLESS PLASMAS. Buneman, O. (Stanford Univ., Calif.). pp 7-10 of Compte Rendu du Colloque International sur l'Interaction des Champs H-F Associes a un Champ Magnetique Statique Avec un Plasma. [Paris] Presses Universitaires de France, [1965].

A series of paradoxes are described to illustrate that the problem of collisionless plasmas heating can not be solved in conventional manner. It is shown that oversimplification yields meaningless results. It is also shown that strict theories fail to account for irreversible deposition in a plasma. (J.S.R.)

40257 DAMPING OF TRANSVERSE PLASMA OSCILLATIONS AT THE ION CYCLOTRON RESONANCE. May, R. M.; Tendys, J. pp 11-15 of Compte Rendu du Colloque International sur l'Interaction des Champs H-F Associes a un Champ Magnetique Statique Avec un Plasma. [Paris] Presses Universitaires de France, [1965].

The damping length for an ion cyclotron wave in the neighborhood of its resonance in an infinite homogeneous plasma is known in two limiting cases: Landau-like damping in a collisionless plasma; and collisional damping in a zero temperature plasma. A simplified model was used for collisions to effect an investigation which includes both finite temperature and collisions. It is found that the limiting cases above are joined by a transition region in which damping depends on both effects. (auth)

40258 WAVES IN AN INHOMOGENEOUS PLASMA. COLLECTIVE RESONANCES. Rebut, P. H. (EURATOM-CEA, Fontenay-aux-Roses, France). pp 16-25 of Compte Rendu du Colloque International sur l'Interaction des Champs H-F Associes a un Champ Magnetique Statique Avec un Plasma. [Paris] Presses Universitaires de France, [1965]. (In French).

The waves propagated in an inhomogeneous cold plasma are calculated. In the plasma considered currents having a plasma force-free zero pressure is considered. Notations analogous to those found in stability calculations are used. The base equations are derived and the J currents are calculated. The results show that even in a cold plasma there are resonance effects and these resonance effects lead to energy absorption. (J.S.R.)

40259 SOLUTIONS OF THE DISPERSION EQUATION AND LANDAU DAMPING NEAR THE CYCLOTRON FREQUENCY. Motz, H. pp 26-7 of Compte Rendu du Colloque International sur l'Interaction des Champs H-F Associes a un Champ Magnetique Statique Avec un Plasma. [Paris] Presses Universitaires de France, [1965].

Solutions of the dispersion equation for wave propagation in a plasma parallel to the magnetic field are presented. It is shown that the cyclotron resonance is masked by strong Landau damping in all cases considered. In some cases the approach to the resonance may be observed. (tr-auth)

40260 PRELIMINARY EXPERIMENT ON THE ION CYCLOTRON RESONANCE OF HIGHLY IONIZED PLASMA. Nagao, Shigeo; Miyahara, Akira; Matsura, Kiyokata; Sato, Teruyuki; Kuroda, Tsutomu; Kojima, Chiyo; Fujiwaka, Setsuya; Masuroki, Masaru (Nagoya Univ., Japan). pp 28-37 of Compte Rendu du Colloque International sur l'Interaction des Champs H-F Associes a un Champ Magnetique Statique Avec un Plasma. [Paris] Presses Universitaires de France, [1965].

A preliminary experiment on the ion cyclotron resonance heating of a plasma in the QP machine is described. The QP machine is described and the preliminary results are reported. The shift of the frequency peak as a function of the magnetic field and the r-f frequency are shown. The peak of the loading is shifted to the higher magnetic field in comparison with that of the electrode voltage by collected ions. The results show that the mechanism of the ion collection by r-f electrodes at cyclotron resonance is simple as in an omegatron mass spectrometer. The mechanism of overtone resonances of ion cyclotron motion are not yet clarified. (J.S.R.)

40261 THREE MODES OF ENERGY TRANSFER OF A PLASMA H-F FIELD. PRELIMINARY EXPERIMENTAL RESULTS OF HEATING BY THE WHISTLER METHOD. Cadart, M.; Consoli, T.; Dupas, L.; Leroy, J.; Parlange, F.

pp 45-51 of Compte Rendu du Colloque International sur l'Interaction des Champs H-F Associes a un Champ Magnetique Statique Avec un Plasma. [Paris] Presses Universitaires de France, [1965]. (In French).

Three procedures for the energy transfer for a plasma h-f field in the vicinity of the cyclotron resonance of the electrons are discussed. These are heating in a resonating cavity, heating in a reflecting enclosure, and heating by plasma acceleration. The procedures were applicable both with stationary and progressive h-f fields. The heating of a plasma by the electromagnetic field of right circular polarization waves was described in particular. (tr-auth)

40262 ACCELERATION OF AN ELECTRON CYCLOTRON PLASMA BY SELF GENERATED ELECTRIC FIELDS. Hendel, H. W.; Ahmed, S. A.; Faith, T. J. (Radio Corp. of America, Princeton, N. J.). pp 57-61 of Compte Rendu du Colloque International sur l'Interaction des Champs H-F Associes a un Champ Magnetique Statique Avec un Plasma. [Paris] Presses Universitaires de France, [1965].

The continuous acceleration of a neutral plasma by self-generated electrostatic fields is investigated. Energy input to the plasma is achieved by selective transfer by r-f energy to the electrons at electron cyclotron resonance. Some previously reported measurements of some plasma potentials, electron temperatures, ion energies, and accelerator efficiency are summarized and new results on the relation of the plasma potential drop to the magnetic field gradient are given. (J.S.R.)

40263 RELATIVISTIC MOTION AND ENERGY GAIN OF CHARGED PARTICLES IN A STANDING WAVE NEAR CYCLOTRON RESONANCE. Hall, Richard B. (Boeing Co., Seattle). pp 62-7 of Compte Rendu du Colloque International sur l'Interaction des Champs H-F Associes a un Champ Magnetique Statique Avec un Plasma. [Paris] Presses Universitaires de France, [1965].

The relativistic equations of motion of a charged particle in an r-f standing wave and a uniform d-c magnetic field are solved by use of a computer. Curves of energy gain, ratios of transverse to longitudinal energy, and interaction times are found for particles that either are reflected from or pass through the r-f field. Some of the effects of relativistic mass increases are found to be predicted by a simple modification of the time-averaged theory. It is proved that, after its interaction with an r-f field with a space variation only along the d-c magnetic field, that the guiding center of the charged particle remains unchanged. (auth)

40264 ENERGY GAIN OF A LOW-ENERGY CHARGED PARTICLE IN A STANDING WAVE NEAR CYCLOTRON RESONANCE. Hall, Richard B. (Boeing Co., Seattle. CEN, Saclay, France). pp 68-73 of Compte Rendu du Colloque International sur l'Interaction des Champs H-F Associes a un Champ Magnetique Statique Avec un Plasma. [Paris] Presses Universitaires de France, [1965].

Approximate expressions are derived for the energy gain of a charged particle as a result of either being reflected from or of passing entirely through an r-f standing wave. It is shown that energy gain is obtained only when a d-c magnetic field is present and commences further from cyclotron resonance as the r-f field amplitude increases. The exact equations of motion are numerically solved and curves showing energy gain, ratios of perpendicular to longitudinal energy and the time required for reflection are obtained. It is found that the approximate analysis predicts closely the actual phenomena. (auth)

40265 INFLUENCE OF THE RELATIVISTIC INCREASE OF MASS ON PARTICLE ENERGY GAIN AND TRAPPING NEAR CYCLOTRON RESONANCE. Schrader, W. J. (FOM-Instituut voor Plasma-Physica, Jutphaas, Netherlands). pp 74-8 of Compte Rendu du Colloque International sur l'Interaction des Champs H-F Associes a un Champ Magnetique Statique Avec un Plasma. [Paris] Presses Universitaires de France, [1965].

The effect of the relativistic increase of mass on the energy gain and the trapping of charged particles in a constant magnetic field $\bar{B}$, by a standing electromagnetic wave, is investigated at values of B which differ slightly from the resonance value B_0. A critical value of the magnetic field, above which particles are trapped in the region of high electric field, is derived. This value lies above resonances by an amount proportional to the $^2/_3$ power of the electric field strength. It is further shown that for values of the magnetic field between resonances and this critical value, the particle can pick up more energy than at resonance. (auth)

40266 RUNAWAY ELECTRONS IN AN R-F MIRROR FIELD. Hagebeuk, H. J. L.; Weenink, M. P. H. (FOM-Instituut voor Plasma-Fysica, Jutphaas, Netherlands). pp 79-83 of Compte Rendu du Colloque International sur l'Interaction des Champs H-F Associes a un Champ Magnetique Statique Avec un Plasma. [Paris] Presses Universitaires de France, [1965].

A stationary distribution and runaway rate are derived for electrons, reflecting back and forth along a constant magnetic field between two exponentially increasing r-f electric mirror fields. The r-f field is mainly parallel to the constant magnetic field. The reflection of single electrons is numerically treated and the relation between incoming and outcoming velocities is calculated. For low velocities the electrons are reflected adiabatically and the electron distribution is dominated by collisions. At higher velocities the electrons gain, averaged over all initial phases, energy by nonadiabatic reflections and reach the escape velocity long before they collide with other electrons. The number of escaping particles is obtained and is balanced with the production by ionization. (auth)

40267 ACCELERATION OF PLASMA BY THE FIELD OF A PROGRESSIVE WAVE DAMPED IN THE VICINITY OF THE ELECTRON OR ION CYCLOTRON RESONANCE. Bardet, R.; Cadart, M.; Consoli, T.; Dupas, L.; Geller, R.; Leroy, J.; Parlange, F. pp 84-93 of Compte Rendu du Colloque International sur l'Interaction des Champs H-F Associes a un Champ Magnetique Statique Avec un Plasma. [Paris] Presses Universitaires de France, [1965]. (In French).

The principle and the theory of the acceleration of a plasma by the electromagnetic fields of waves with right circular polarization in the vicinity of the electron cyclotron resonance in a static magnetic field gradient are described. Two accelerating devices, operating with right circularly polarized waves of wave length $\lambda = 8$ and 3 cm, are described. (tr-auth)

40268 THEORETICAL AND EXPERIMENTAL STUDY OF PLASMA ACCELERATION BY MEANS OF R-F AND STATIC MAGNETIC FIELD GRADIENT. Bardet, R.; Consoli, T.; Geller, R. pp 94-122 of Compte Rendu du Colloque International sur l'Interaction des Champs H-F Associes a un Champ Magnetique Statique Avec un Plasma. [Paris] Presses Universitaires de France, [1965]. (In French).

Theory is developed for the physical mechanism of ion dragging by accelerated electrons due to the superimposition of the gradient of an electromagnetic field and the gradient of a static magnetic field. The resulting trajectory of the electrons is a helicoid and one shows the variations of the diameter and the path of the spirals along the axis as a function of the difference between the gyrofrequency and the applied r-f frequency. The ion acceleration is due to an electron space charge effect. The grouping of the equations of the electronic and ionic fluid motions leads to the introduction of a tensor mass: along the x and y direction the transverse motion of the fluid is controlled by the relativistic mass of electrons whereas along the z direction the axial motion is determined by the ionic mass. An experimental device called Pleiade is described which allows verification of some of the theoretical predictions. Pleiade produces a d-c operating plasma beam in which the electrons exhibit radially oriented energies whereas the ionic energy is mainly axial. The experimental

results indicate that the energy of the particles is in the kev range. The reflecting properties of the device are described. It is shown that r-f static magnetic field gradients are not only capable of accelerating a plasma beam along the axially decreasing magnetic field, but are also capable of stopping and reflecting such a beam when the latter is moving along an axially increasing magnetic field. A plasma accumulation experiment is described in which two symmetric structures form simultaneously an accelerator and a "dynamic mirror" for the particles. Evidence of accumulation is given. (auth)

40269 SPACE CHARGE ELECTRIC FIELD OF AN ELECTRON BEAM INJECTED IN A DECREASING MAGNETIC FIELD. ACCELERATING EFFECT. Lascar, G. pp 123-6 of Compte Rendu du Colloque International sur l'Interaction des Champs H-F Associes a un Champ Magnetique Statique Avec un Plasma. [Paris] Presses Universitaires de France, [1965]. (In French).

The electron space charge field is calculated and the results lead to axial electric field gradients that explain the acceleration of ions at high energies when the neutralization of this space charge occurs. The model adopted simulates the physical situation created spontaneously in static magnetic and transverse high-frequency field gradient accelerators. (J.S.R.)

40270 SELF-CONSISTENT INCORPORATION OF RADIATION INTO THE EQUATIONS GOVERNING THE APPROACH TO EQUILIBRIUM OF A FULLY IONIZED GAS WITH APPLICATION TO THE PROBLEM OF CYCLOTRON RADIATION. Smith, John Marlin. [Evanston, Ill.], Northwestern Univ., 1965. 122p.

Thesis.

The kinetic equation for the single-particle distribution function and the equation of radiative transport are developed for a fully ionized gas interacting via its transverse or radiation field in the presence of an externally applied magnetic field. The starting point of the analysis is with Liouville's equation for N particles and a denumerably infinite set of oscillators. The dynamical character of the system is described by the Heitler Hamiltonian. The reduction of Liouville's equation to the equation for the single-particle distribution function and the equation of radiative transport is accomplished by analogy to the perturbation technique used by Prigogine and his coworkers to reduce Liouville's equation for a plasma interacting via its longitudinal or Coulomb field. The equations obtained are to first order in the interaction parameter, which results in Fokker-Planck type equations. (Dissertation Abstr.)

40271 PROPAGATION AND INSTABILITIES IN BOUNDED AND FINITE TEMPERATURE PLASMAS. Jayson, Joel Stanley. Berkeley, Calif., Univ. of California, 1965. 118p.

Thesis.

The quasi-static analysis is used to examine propagation and instabilities in plasmas in which both the transverse bounds and the temperature are important. Initially only longitudinal thermal velocity is assumed and two stream instabilities are studied. With the introduction of transverse temperature, instabilities resulting from temperature anisotropy are also studied. The full set of Maxwell's equations is utilized for an investigation of the effects of dispersion on the synchrotron radiation spectrum. The investigation of hot plasmas with finite boundaries was undertaken initially to explain the differences between phenomena found in experimental observations and those predicted by the cold plasma theory. Longitudinal temperature is added to the model and it is found that strong cyclotron wave damping and the absence of the cyclotron interaction in a two-stream configuration are predicted by the theory. Transverse temperature is introduced into the model using the Boltzmann equation, instabilities arising from temperature anisotropy are investigated, and it is found that, for a bi-Maxwellian distribution, for low values of k_z the plasma is stable. The investigation of finite plasmas with transverse temperature is pursued by consideration of a configuration in which a boundary layer region is included and the particle density decreases to zero through this region. The potential in this region is constructed from arbitrary functions whose coefficients are determined from the boundary conditions on either side of the boundary layer. The dispersion relation is obtained and instabilities due to temperature anisotropy are investigated. The effects of dispersion on synchrotron radiation are studied and it is shown that the dispersion results in a shift of the emission spectrum from that predicted by the theory in which dispersion was not accounted for. (Dissertation Abstr.)

40272 CORRELATIONS IN AN EQUILIBRIUM PLASMA. Ramanathan, Ganapathiagraharam Visvanathan. Princeton, N. J., Princeton Univ., 1965. 57p.

Thesis.

A new method of definition of correlation functions is proposed and some of its advantages over the Mayer expansion scheme are demonstrated. A general equation for the s-particle correlation function is derived for a large classical system of particles interacting through a two-body potential at thermal equilibrium. In an equilibrium plasma the correlations are ordered in terms of the plasma parameter ϵ. It is shown that, unlike in the Mayer expansion scheme, the three-particle and higher correlations are infinitesimally small everywhere in phase space. A uniformly valid leading order solution is obtained for the s-particle function. This shows that in a large equilibrium system of particles interacting through a two-body potential that is repulsive and decreases to zero at infinity, as in a plasma, the higher correlation functions to their leading orders are functionals of the two-particle correlation, independent of the detailed nature of the potential. The solution for the three- and four-particle functions are given as illustrations. A new technique of successive approximations is developed for obtaining uniformly valid solutions for the two-particle function in an equilibrium plasma. Explicit solutions are obtained order by order up to the order of ϵ^2. It is shown that the two-particle function has a power series expansion up to the order of ϵ^2 in the finite-distance regime. In the short-distance regime however, there is an $\epsilon^2 \ln \epsilon$ term in the asymptotic series. The internal energy is calculated correct to an error of the order of ϵ^2. In the asymptotic expansion for the internal energy, there is an $\epsilon^2 \ln \epsilon$ term and, presumably, an $\epsilon^2 \ln \epsilon$ term but no $\epsilon^3 \ln \epsilon$ term. (Dissertation Abstr.)

40273 RADIATION BY A PLASMA: QUADRUPOLE BREMSSTRAHLUNG AND SYNCHROTRON EMISSION. Birmingham, Thomas Joseph. Princeton, N. J., Princeton Univ., 1965. 125p.

Thesis.

A model recently developed for computing the radiative emission from a classical, fully ionized plasma is applied to two new problems: quadrupole bremsstrahlung and synchrotron radiation. These two types of radiation are treated separately, the plasma being assumed free of external fields for the former and permeated by a static homogeneous magnetic field for the latter. For the bremsstrahlung calculation, a systematic expansion of the accelerative contribution to the plasma current density resulting from particle encounters is developed in the ratio of the electron Debye distance to the wavelength of the emitted radiation. Zeroth order terms in this expansion lead to dipole emission results previously calculated, while from the first order terms the spectra of longitudinal and transverse electric quadrupole waves arising from both electron-ion and electron-electron collisions are obtained. The quadrupole results are compared with the corresponding dipole emissions and shown to be small. From the electron-electron power emission results and Kirchoff's law an effective high frequency viscosity due to electron-electron collisions is calculated in thermal equilibrium. Synchrotron emission is considered to all multipole orders and is assumed to emanate from a small number of energetic electrons embedded in a relatively much colder plasma and gyrating about the

magnetic field. Reabsorption of the radiation by inverse processes is neglected and the modification of the radiation at high harmonics (m > 4) by the cold plasma bulk ascertained asymptotically to first order in the ratio ω_p^2/ω^2 ($\ll 1$). In this limit the effect of the plasma is to reduce the power radiated below the level predicted by vacuum radiation theory. The radiation from a single relativistic particle is computed numerically in the presence of a plasma and the plasma corrections are compared with the calculated radiation in a vacuum. (Dissertation Abstr.)

40274 ELECTRON CYCLOTRON HARMONIC RADIATION FROM A PLASMA. Kuckes, A. F.; Dawson, J. M. (Princeton Univ., N. J.). pp 129-30 of Compte Rendu du Colloque International sur l'Interaction des Champs H-F Associes a un Champ Magnetique Statique Avec un Plasma. [Paris] Presses Universitaires de France, [1965].

Calculations are presented to show that the electron cyclotron harmonic radiation from a plasma is due to energetic electrons gyrating in a region of plasma hybrid resonance. (J.S.R.)

40275 STABILITY OF A PLASMA CONFINED BY R-F FIELDS. Troyon, F. (Laboratoire de Recherches sur la Physique des Plasmas, Lausanne, Switzerland). pp 141-4 of Compte Rendu du Colloque International sur l'Interaction des Champs H-F Associes a un Champ Magnetique Statique Avec un Plasma. [Paris] Presses Universitaires de France, [1965].

The problem of the stability of a slab of plasma confined by a rotating or a combination of oscillating and static magnetic fields is examined. Two models of the plasma are considered: a continuum model and a free particle model. A potential is added which simulates an acceleration of the plasma or a curvature of the field lines. It is shown that for a sufficiently high frequency the plasma is stable. (auth)

40276 PRELIMINARY INVESTIGATIONS WITH A R-F ELECTRIC MIRROR FIELD. Hagebeuk, H. J. L. (FOM-Instituut voor Plasma-Fysica, Jutphaas, Netherlands). pp 145-8 of Compte Rendu du Colloque International sur l'Interaction des Champs H-F Associes a un Champ Magnetique Statique Avec un Plasma. [Paris] Presses Universitaires de France, [1965].

A description and discussion is given of some preliminary measurements on a r-f confinement experiment with two r-f cavities connected by a constant magnetic field. (auth)

40277 STUDY OF A CONFINEMENT OF A PLASMA IN A SPHERICAL CAVITY. Consoli, T. (CEN, Saclay, France); Mourier, G.; Slama, L.; Roux, R.; Vial, R. pp 149-67 of Compte Rendu du Colloque International sur l'Interaction des Champs H-F Associes a un Champ Magnetique Statique Avec un Plasma. [Paris] Presses Universitaires de France, [1965]. (In French).

High-frequency properties of the Te_{110} mode are reviewed. The confinement of a plasma by the high-frequency fields of the TE_{110} spherical mode is theoretically investigated under well-defined hypotheses and using solutions obtained by machine integration for various parameter values. Some typical types of the distribution of their high-frequency fields in the presence of the plasma and of the density distribution are given. The individual movements of the electrons in a configuration of mixed fields is considered. The trajectories obtained by a resolution of the motion equation are discussed and interpreted for the case where the static magnetic field is absent, and where the presence of the magnetic field considering the resonance $f_{ce} = f_{h\text{-}f}$ entrains a relativistic variation of the electron mass. Some experimental results illustrating qualitatively the conclusions of the theoretical study are given as examples. (J.S.R.)

40278 EFFECTS OF CONFINEMENT IN HIGH-FREQUENCY DISCHARGES AT LOW PRESSURE. Consoli, T. (CEN, Saclay, France); Mourier, G.; Roux, R.; Vial, P. pp 168-73 of Compte Rendu du Colloque International sur l'Interaction des Champs H-F Associes a un Champ Magnetique Statique Avec un Plasma. [Paris] Presses Universitaires de France, [1965]. (In French).

High-frequency gaseous discharges observed at pressures between 10^{-5} and 10^{-3} torr are described. The experimental devices are described. The discharge conditions are analyzed. It is shown that the discharge is controlled principally by the Boot force and the space charge. The confinement in nonaxial directions was evident and a certain axial confinement was noted when a magnetic field was added. The discharge ignition is badly understood but it probably occurs near the wall. The fact that the discharge is maintained in a low field region shows that in order to establish the plasma it is more advantageous to work with a weaker electromagnetic field even if it is then necessary to apply a stronger field with another generator in order to heat or compress a plasma. (J.S.R.)

40279 CONFINEMENT AND HEATING OF A PLASMA BY A LOW-FREQUENCY ROTATING MAGNETIC FIELD. Consoli, T.; Jacquot, B.; Le Gardeur, R.; Nakach, R. pp 174-83 of Compte Rendu du Colloque International sur l'Interaction des Champs H-F Associes a un Champ Magnetique Statique Avec un Plasma. [Paris] Presses Universitaires de France, [1965]. (In French).

A general study was made on the confinement of a plasma in closed magnetic configurations. Such a configuration can be obtained by the superposition of a static magnetic field and a low-frequency oscillating field. In the case where the static magnetic field is uniform along the axis z the trajectory of a single particle is examined without consideration of its sign and mass. The development of rotating magnetic fields is studied, and two solutions for the technological realization of the problem are given. An experimental device constituting a small scale model, where the second solution is applied to the confinement and heating of a plasma, is described. The devices whose performances have been verified experimentally in vacuum (without plasma) can be used for more intense fields. (tr-auth)

40280 STUDY OF A MIXED FIELD CONFIGURATION WITHOUT LEAKS. Consoli, T.; Le Gardeur, R.; Jacquot, B.; Slama, L. pp 184-8 of Compte Rendu du Colloque International sur l'Interaction des Champs H-F Associes a un Champ Magnetique Statique Avec un Plasma. [Paris] Presses Universitaires de France, [1965]. (In French).

A mixed structure in which the configuration of the high-frequency field is completely closed is described. It permits the capture of a beam of particles by resonant trapping. The preliminary results of the capture of a beam of electrons are given. (tr-auth)

40281 HIGH FREQUENCY MULTIMEGAWATT GENERATOR WITH AMPLITUDE AND FREQUENCY MODULATION. Keller, R. pp 189-91 of Compte Rendu du Colloque International sur l'Interaction des Champs H-F Associes a un Champ Magnetique Statique Avec un Plasma. [Paris] Presses Universitaires de France, [1965]. (In French).

High-frequency wave packets are produced by means of transmission lines, which are connected in series by spark gaps. The obtained effective power is 9.5 Mw at frequencies of several megacycles. The amplitude and the frequency can be programmed. (auth)

40282 PRODUCTION OF AN INTENSE H-F FIELD BY THE INJECTION OF AN ENERGETIC ELECTRON BEAM INTO A RESONATING STRUCTURE. Le Gardeur, R. pp 192-7 of Compte Rendu du Colloque International sur l'Interaction des Champs H-F Associes a un Champ Magnetique Statique Avec un Plasma. [Paris] Presses Universitaires de France, [1965]. (In French).

The conditions for the production of an intense high-frequency field by the injection of an energetic electron beam into a resonating cavity are calculated, and an experimental device for the production of such fields is described. (J.S.R.)

40283 SOME PROBLEMS OF TRAJECTORIES IN THE STUDIES OF INTERACTIONS OF H-F FIELDS WITH A

PLASMA. Caillet, C.; Deat, M.; List, D.; Consoli, T. pp 198-204 of Compte Rendu du Colloque International sur l'Interaction des Champs H-F Associes a un Champ Magnetique Statique Avec un Plasma. [Paris] Presses Universitaires de France, [1965]. (In French).

The analog computer study of trajectories in interactions of h-f fields with a plasma is described. The analog methods used are described, and the difficulties found are discussed. The various methods used are compared. (J.S.R.)

Shielding

Refer also to abstracts 39061–39064 and 39071.

40284 (AD-637125) EXPOSURE FIELD FROM A POINT ISOTROPIC SOURCE LOCATED AT THE SURFACE OF A THICK CONCRETE SLAB. Nuclear Radiation Shielding Studies Report No. 2. Chilton, A. B.; Fu, C. Y. (Illinois Univ., Urbana). July 1966. Contract OCD-OS-63-66. 62p. CFSTI $3.00 cy, $0.75 mn.

Results are given of computations for the exposure field from point isotropic sources of cobalt-60 and cesium-137 near the surface of a semi-infinite concrete slab. A modification of the Chilton-Huddleston differential albedo formula developed for the vacuum/concrete interface situation is used. To modify the results to include the air effect, computation was made to account for the single-scattered contribution. The higher order air scattering contribution, which is smaller, was estimated approximately from infinite buildup factors in air. The final results, with horizontal source-detector distances out to 50 feet, are presented in comparison with various experimental results. The computational results are estimated to have an uncertainty of about 1%. Agreement with previous work is good in some cases, but under some conditions appreciable discrepancies exist. The preponderance of evidence supports the theoretical results and they are recommended for future use. (auth)

40285 (BNWL-236) ISOSHLD: A COMPUTER CODE FOR GENERAL PURPOSE ISOTOPE SHIELDING ANALYSIS. Engel, R. L.; Greenborg, J.; Hendrickson, M. M. (Battelle-Northwest, Richland, Wash. Pacific Northwest Lab.). June 1966. Contract AT(45-1)-1830. 147p. Dep. mn. CFSTI $4.00 cy, $1.00 mn.

ISOSHLD is a computer code to perform gamma ray shielding calculations for isotope sources in a wide variety of source and shield configurations. Attenuation calculations are performed by point kernel integration; for most geometries by Simpson's rule numerical integration. Source strength in uniform or exponential distribution (where applicable) may be calculated by the linked fission product inventory code RIBD or by other options as desired. Buildup factors are calculated by the code based on the number of mean free paths of material between the source and detector points, the effective atomic number of a particular shield region (the last unless otherwise chosen), and the point isotropic NDA buildup data available as Taylor coefficients in the effective atomic number range of 4 to 82. Other data needed to solve most isotope shielding problems of practical interest are linked to ISOSHLD in various libraries. (auth)

40286 ANGULAR DISTRIBUTION OF FAST NEUTRONS BEHIND IRON SHIELDING. Goryachev, I. V.; Dulin, V. A.; Ermakov, S. M.; Kolyzhenkova, V. V.; Suvorov, A. P.; Trykov, L. A. At. Energ. (USSR), 20: 469-73(June 1966). (In Russian).

The angular energy distribution of fast neutrons behind iron shielding was measured. The experimental results are compared with calculations by the Monte Carlo method and with multigroup calculations by the passage matrix method in the $2P_7$ approximation. Satisfactory agreement of the experimental with the calculated results was obtained both for the absolute magnitude and for the form of the angular spectrum. (tr-auth)

40287 NEUTRON FLUX DISTRIBUTION AND SPECTRUM IN IRON–WATER SHIELDS. Miyakoshi, Junichi; Kawamoto, Setsuo (Hitachi Shipbuilding and Engineering Co., Ltd., Japan). Hitachi Zosen Giho, 27: 72-8(May 1966). (In Japanese).

The neutron flux distribution and spectrum were measured along the central axis of the iron–water shields assembled in the HTR experimental pool. The fast- and thermal-neutron distributions were measured by means of a foil-activation method. The threshold and resonance reactions were utilized to measure the fast and epithermal neutron spectra. The removal and diffusion theory were employed with each iron–water configuration. The experimental results were compared with the results of calculations. (D.C.W.)

40288 SINGLE SCATTERING CALCULATIONS OF SKY-SHINE WITH CYLINDRICAL CONTAINER PENETRATIONS. Shimamura, Akira (Nippon Electric Co. Ltd., Kawasaki, Japan). J. Nucl. Sci. Technol. (Tokyo), 3: 300-1(July 1966).

A calculation is presented for scattering in the air outside cylindrical shielded containers. (M.O.W.)

40289 THE BUILD-UP FACTOR B IN ATTENUATION CALCULATIONS OF γ RADIATION. Dumitrescu, Silvia; Marghitu, V. (Inst. of Atomic Physics, Bucharest). Stud. Cercet. Fiz., 18: 445-61(1966). (In Rumanian).

Gamma-ray experiments with radioisotopes require a careful selection of the source-absorber-detector geometry in order to describe the attenuation by a law that can be expressed analytically. In order to facilitate the design of radiation shields, a new calculation method was developed; it yielded results with an error not exceeding 20% even when considering the dose rate of sealed sources. Introduction of the buildup factor B into the calculations makes it unnecessary to use arbitrary safety coefficients. The study is based on the examination of ^{60}Co and ^{137}Cs sources with energies of 1.25 and 0.66 Mev, respectively; it involved determination of the dose rates at various distances and for various thicknesses of absorbers, such as lead, iron and concrete. The results are presented in the form of nomograms plotted with and without taking the buildup factor into consideration. Use of these nomograms allows one to avoid complex calculations. When measuring the dose rate with G-M counters, the calibration curve of the energy range in question must be taken into account. (TTT)

40290 ENERGY SPECTROGRAMS OF POINT SOURCES OF γ RAYS. Artsybashev, V. A.; Ivanyukovich, G. A. Vop. Rudn. Geofiz., Min. Geol. Okhrany Nedr. SSSR, No. 5, 52-62 (1965). (In Russian).

Models of sand, iron and lead plates were used to study spectrograms of gamma rays dispersed in these media. The resulting spectrograms and the effects of the media on the gamma spectra are described. It was found that the relation between the spectra in infinite, semi-infinite, and barrier geometry of the medium depends on the radiation filtration. Field symmetry was observed in sands while using the aluminum and iron filters, but the field geometry was destroyed by use of the lead filter. Differences between the spectra at various geometries of the absorption medium were found to decrease with increased atomic number of the medium. (J.F.P.)

40291 ANALOGUE STUDIES OF MAGNETIC SHIELDS. Levine, Samuel H.; Lepper, Richard (Northrop Space Labs., Hawthorne, Calif.). New York, American Inst. of Aeronautics and Astronautics, 1966, Preprint No. 66-513, 20p., $1.50. (CONF-660632-3). ORAU.

From American Inst. of Aeronautics and Astronautics, 4th Aerospace Sciences Meeting, Los Angeles, Calif.

Externally deflecting magnets provide a protective region around space vehicles which shields them from the hazardous space radiation. The magnetic shield simulator, MAGSIM, is an analogue device which provides a simple means for directly measuring the forbidden volume or protective region produced by externally deflecting magnets.

The MAGSIM was employed to determine the protective volume for some rather complex magnet configurations. These configurations include two coplanar current loops of different radii but having the same vertical axis, and a six coil quasi-hollow conductor configuration. In addition, the assumption of substituting an equivalent simple loop for a hollow conductor was checked. In general, the simple loop approximation predicts results found with the hollow conductor magnet, however, the outward displacement of the forbidden volume from the center of the magnet is approximately 25% larger than predicted by simple loop theory. The ability to shape the forbidden region to match the shape of the vehicle is described. (auth)

40292 MAGNETIC SPACE SHIELDS. Kash, S. W. (Aerospace Corp., San Bernardino, Calif.). 53p. (CONF-650813-3). ORAU. Gmelin, AED-CONF-65-216-10.

From 6th Biennial Gas Dynamics Symposium, Evanston, Ill.

Magnetic fields can in principle be used to protect human space travelers against energetic charged-particle radiation. It may be possible to construct a magnetic shield utilizing a superconducting coil that will be considerably less massive than an equivalent material shield. Magnetic coils may be designed in which the field is completely confined to the space ship or in which the field extends over a considerable region of space. Two of the principal problems in the design of an unconfined magnetic shield, namely the determination of the volume protected by the field and the structural mass required to support the coils producing the field, are considered in detail. A numerical method is presented which can be used to determine the shielded volume of many axially symmetric coil configurations. Means of minimizing the structural mass associated with such coils are also described. These methods are then applied to the unconfined field produced by a cylindrical coil. (auth)

Solid State Physics

See also **CHEMISTRY — Inorganic and Physical Chemistry**
METALS, CERAMICS, AND OTHER MATERIALS — Properties and Structure

Refer also to abstracts 39199, 39200, 39395, 39458, 39467, and 40135.

40293 (AD-634746) DISSOLUTION SPIRALS ON GAMMA-IRRADIATED LITHIUM FLUORIDE. Technical Report No. 6. Ives, M. B.; Ramachandran, T. R. (McMaster Univ., Hamilton (Ontario). Dept. of Metallurgy and Metallurgical Engineering). June 1966. Contract Nonr-3925(00). 18p. CFSTI $1.00 cy, $0.50 mn.

Double-spiral features were observed at high resolution on lithium fluoride {100} surfaces etched in distilled water containing from 0.1 to 9 ppm ferric ions (as ferric chloride). The models proposed for similar features on other materials are reviewed and rejected in favor of a mechanism involving the formation of prismatic loops produced by vacancy condensation following γ irradiation. In preference to the existence of dislocations in lithium fluoride with large Burgers Vector, a series of stacked loops is suggested. (auth)

40294 DEMONSTRATION OF X-RAY DIFFRACTION BY LiF USING THE Mn Kα X RAYS RESULTING FROM ^{55}Fe DECAY. Preuss, Luther E.; Toothacker, William S.; Bugenis, Claudius K. (Ford Inst. for Medical Research, Detroit). Appl. Phys. Lett., 9: 159-61(Aug. 15, 1966).

Mn K x rays from ^{55}Fe were diffracted with detectable intensity by NaCl and LiF powder. A special diffractometer incorporating a 100-mc ^{55}Fe linear source (1.5 mm × 10 mm) was used. Theoretical diffraction efficiency is about 10^{-6} (on the NaCl 200 plane). Diffractometer geometry provided 10^{-1} to 10^{1} photons per min at the detector. This order of intensity was observed with a proportional counter, linear pulse amplifiers, and a multichannel analyzer. The three most intense beams of LiF (θ = 20° to 55°) were clearly demonstrated. (auth)

40295 LOW-ENERGY BOMBARDMENT OF GOLD WITH GOLD IONS: ON INTERSTITIAL ATOM MIGRATION IN STAGE III. Thomas, L. E.; Balluffi, R. W. (Cornell Univ., Ithaca, N. Y.). Appl. Phys. Lett., 9: 171-3(Aug. 15, 1966). (NYO-3504-6).

Gold foils containing 300 to 400 Å vacancy stacking fault tetrahedra were bombarded with 270-ev gold ions to a dose of 3×10^{16} ions cm^{-2} in 10 min, and with similar dose and flux of 180-ev argon ions. The procedure used to study tetrahedron shrinkage was to photograph the same tetrahedra in specimens before and after bombardment. Changes of individual tetrahedra due to bombardment were unambiguously revealed in this way. The results are described. (M.O.W.)

40296 VALENT STATES AND INTERATOMIC DISTANCES IN METAL CRYSTALS OF THE ELEMENTS OF THE SEVENTH PERIOD. Sarkisov, E. S. (Lomonosov Inst. of Fine Chemical Tech., Moscow). Dokl. Akad. Nauk SSSR, 166: 627-30(Jan. 21, 1966). (In Russian).

There are no direct methods available at present for experimental determination of the number of valence electrons that participate in the creation of an interatomic bond in crystals. The problem was examined by extending to this case the author's earlier equation that was found applicable to lanthanides; experimental and theoretical values for rare earth elements differed only by ±1%. An equation was derived to correlate the interatomic distance with the number of 4f and 5f electrons, the number of electrons in the atom and in the core of the atom, and with the metallic interatomic distance of hydrogen, 0.965 Å. It was found that the number of valence electrons in metallic structures of francium, radium, actinium, thorium, protactinium, uranium, neptunium, plutonium, and americium is higher than 3; therefore, in a typically metallic state, they cannot be considered as lanthanides. Neptunium, which like uranium, possesses $f = 6(5f^3 6d7s^2)$ valence electrons, must be considered as the first uranoid. The metallic atomic radii of transamericium elements, including the as yet not synthesized elements 104, 105, and 107 are presented. (TTT)

40297 WORK FUNCTION OF W–Hf, Ta–Hf, Nb–Hf, Re–Zr, AND W–Re ALLOYS. Dyubua, B. Ch.; Kultashev, O. K. Fiz. Metal. Metalloved., 21: 396-402(Mar. 1966). (In Russian).

Data are presented on the work function of refractory metals in which various amounts of hafnium and zirconium were dissolved. The work function was determined from the Richardson-Dushman equation for A = 120.4 A/cm^2 deg^2. The thermionic emission measurements were carried out in a vacuum of 10^{-8}-10^{-9} mm Hg. The phase composition of the alloys was determined by microstructural analysis. The work function of pure Re, Ta, Nb, and Zr was shown to remain constant with changing temperature. The addition of hafnium and zirconium was found to decrease the work function of the refactory metals. The cause of this effect is thought to be the adsorption of hafnium and zirconium atoms on the surface of the solid solution. In the region of the σ phase of the W–Re alloy an increase in work function up to 5.0 ev was observed. This is attributed to a possible adsorption of rhenium. (ATD)

40298 ON THE INFRARED EXTINCTION OF THE SPECIFIC PHOTOCONDUCTIVITY OF GERMANIUM OF THE n-TYPE PRODUCED BY γ RAYS. Vasil'ev, A. V.; Smirnov, L. S. (Institut Fiziki Poluprovodnikov, Novosibirsk, USSR). Fiz. Tverd. Tela, 8: 603(Feb. 1966). (In Russian).

The photoconductivity spectrum of γ-irradiated n-type Ge recorded at liquid N_2 temperatures showed a system of radiation defects in the following levels: E_C, −0.22, −0.25, −0.27, −0.30, −0.33, −0.36, −0.43, −0.49, −0.52, and −0.59 ev; growth to the stationary state occurred in 12 sec; decrease occurred over a 10-min span. Infrared extinction

was observed in the whole long-wavelength region examined (1.5 to 5.5 μ). Three absorptions were found at about 0.47, 0.52, and 0.60 ev. Slight absorption was also found in the region from 0.2 to 0.4 ev; the spectrum is illustrated. Data are examined using the model of Rose. The maxima at 0.47 and 0.52 are explained by transitions of electrons from the valence zones to $E_C - 0.27$ and -0.22 ev; the max at 0.60 ev corresponds to a transition from the valence zone to -0.14 ev, which would not have been observed in the photoconductivity spectrum because of a high noise level. (BBB)

40299 LOW-ENERGY PROTON BOMBARDMENT OF GaAs AND Si SOLAR CELLS. Wysocki, J. J.; Rappaport, P.; Davison, E.; Loferski, J. J. (RCA Labs., Princeton, N. J.). IEEE (Inst. Elec. Electron. Eng.), Trans. Electron. Devices, ED-13: 420-6(Apr. 1966).

Space experiments have shown that the short-circuit current of unshielded GaAs and Si solar cells decays rapidly; in one day, for example, the current from GaAs, Si p/n, and Si n/p cells dropped by 50, 60, and 38%, respectively. Since other experiments have demonstrated the existence of a substantial flux of low-energy protons (0.040 to 1.0 Mev) in outer space, the degradation occurring in the cells is attributed in part to these particles. Experiments were therefore performed with 185- to 530-kev protons to study the effect of these particles on solar cells. Results of these experiments are presented together with a model which correlates present-day knowledge of solar cell operation with the behavior observed under low-energy proton bombardment. When GaAs, Si n/p, and Si p/n solar cells were irradiated with protons, the short-circuit current of the GaAs and the open-circuit voltage of the Si cells decreased severely as a result of bombardment. The short-circuit current of the Si cells was independent of flux at first, but it then fell rapidly. The damage produced in both the GaAs and Si cells increased with the proton energy. The model which accounts for the proton range satisfactorily predicts that the maximum damage rate in short-circuit current will occur at proton energies of 4 to 6 Mev for cells irradiated at 45° with respect to the beam. Above this energy, Rutherford-type behavior is expected. (BBB)

40300 MOESSBAUER EFFECT IN $Co_{1-x}Fe_xSi$. Wertheim, G. K.; Wernick, J. H.; Buchanan, D. N. E. (Bell Telephone Labs., Inc., Murray Hill, N. J.). J. Appl. Phys., 37: 3333-7(Aug. 1966).

It is shown on the basis of experiments with CoSi(^{57}Co) in a high magnetic field and with magnetically ordered $Co_{0.5}Fe_{0.5}Si$ that iron does not develop a magnetic moment greater than 0.1 μ_B at low temperature in the system $Co_{1-x}Fe_xSi$. The results also indicate that the magnetic properties are not directly related to the electron and hole bands pertinent to transport properties. The isomer shift shows that the configuration of Fe is independent of composition over the entire range of composition. The electron concentration dependence of the quadrupole splitting is discussed. (auth)

40301 EFFECT OF NEUTRON-INDUCED DEFECTS ON THE CURRENT-CARRYING BEHAVIOR OF VAPOR-DEPOSITED NIOBIUM STANNIDE. Cullen, G. W.; Novak, R. L. (RCA Labs., Princeton, N. J.). J. Appl. Phys., 37: 3348-52(Aug. 1966).

The current-carrying capacity of vapor-deposited Nb_3Sn can be increased by introduction of structural defects by neutron irradiation. The change in current density per unit of neutron flux is a function of the initial perfection of the material. The characteristics of low-α material ($\alpha \approx J_cH$) are altered more than high-α material by irradiation. The current capacity of the material is eventually decreased by continued irradiation. The current behavior of material exhibiting an α less than 15 kG·A/cm^2 can be described by a simple Lorentz force model. Material exhibiting an α higher than this is not adequately described by such a model. The electrical scattering cross section of a neutron-damaged area is calculated to be $\sim 4 \times 10^{-12}$ cm^2. (auth)

40302 OXYGEN-DEFECT COMPLEXES IN NEUTRON-IRRADIATED SILICON. Whan, R. E. (Sandia Lab., Albuquerque, N. Mex.). J. Appl. Phys., 37: 3378-82(Aug. 1966).

The growth and decay of infrared absorption bands in the spectra of oxygen-doped silicon irradiated with fast neutrons or 2-Mev electrons at −50°C were studied. These bands at 836, 922, 932, and 936 cm^{-1}, are associated with defect impurity complexes, and previously have been observed after electron irradiation at temperatures as low as 80°K. The gradual growth of the 836-cm^{-1} band, associated with an oxygen-vacancy complex, from the low-intensity measured immediately after neutron irradiation to approximately four fimes that intensity upon annealing to 275°C is in contrast with the gradual decay of the band observed after electron irradiation over the same temperature range. The growth of the band is attributed to an increase in the concentration of the O-V complex as additional vacancies are evolved from defect clusters produced by neutron irradiation. Shifts in the annealing curves of a band at 865 cm^{-1}, which appears upon annealing above 0°C, and the band at 936 cm^{-1} suggest that the corresponding complexes also involve vacancies. The constant intensity ratio and identical annealing behavior for the 922 and 932 cm^{-1} bands indicate that they belong to different vibrational modes of the same complex. No shift in the annealing curves for these bands was observed for the neutron irradiated sample, suggesting that the corresponding complex does not involve vacancies but rather may involve interstitial Si atoms. (auth)

40303 COMPARISON OF NEUTRON AND GAMMA-RAY DAMAGE IN n-TYPE SILICON. Stein, H. J. (Sandia Lab., Albuquerque, N. Mex.). J. Appl. Phys., 37: 3382-4 (Aug. 1966).

Fission-spectrum neutron damage of n-type, float-zone silicon is compared with ^{60}Co gamma-ray damage. The damage was measured at 293°K by the degradation of the minority-carrier lifetime. The room-temperature damage coefficients, defined as $K = (1/\Phi)[(1/\tau_{ai}) - (1/\tau_0)]$, are 5.8×10^{-6} (neutrons/cm^2)$^{-1}$ sec^{-1} for neutron irradiation and 2.8×10^{-10} (photons/cm^2)$^{-1}$ sec^{-1} for gamma-ray irradiation where τ_0 and τ_{ai} are the initial and after-irradiation carrier lifetimes, and Φ is the integrated flux. The neutron damage coefficient is found to be independent of the irradiation temperature (76–300°K) in contrast to a marked decrease with decreased irradiation temperature which has been observed in the gamma-ray damage coefficient. Neutron damage recovery is observed over a broad temperature range from 60–220°C, while gamma-ray damage recovers sharply between 150 and 210°C. These results indicate that the energy transferred to the silicon recoils by the irradiating particle influences the number and kind of primary defects produced at 76°K and also affects defect reordering at higher temperatures. (auth)

40304 POLARIZATION IN LaF_3. Solomon, R.; Sher, A.; Muller, M. W. (Varian Associates, Palo Alto, Calif.). J. Appl. Phys., 37: 3427-32(Aug. 1966).

Results of measurements of the low-frequency dielectric behavior and of persistent polarization in single-crystal LaF_3 are reported. This ionic conductor exhibits unusually large polarization effects. The measurements distinguish at least two components of polarization. One component, with a time constant of the order of milliseconds, is linear in the applied voltage; the long-term polarization is proportional to its square. The phenomena are evidently associated with surface effects, but they cannot be described by the accepted space-charge theory of ionic conductors. They appear, however, to be qualitatively consistent with an extension of the notion of ionic surface states introduced by Frenkel. (auth)

40305 ATOM EJECTION STUDIES FOR SPUTTERING OF SEMICONDUCTORS. Anderson, G. S. (Litton Systems, Inc., Minneapolis). Contract AT(11-1)-722. J. Appl. Phys., 37: 3455-8(Aug. 1966).

Atom-ejection patterns resulting from the sputtering of semiconductor single crystals were examined. The annealing temperature T_a (defined as the minimum target temperature for which single-crystal spot patterns are observed) previously reported for Ge, Si, InSb, and InAs, was determined for GaAs and CdTe. For target temperatures below T_a damage remains frozen in and the deposit indicates an amorphous or polycrystalline surface. For GaAs it was found that $T_a \sim 130°C$ for Ar^+ and Ne^+ ion bombardment; for CdTe no spot patterns were observed up to 510°C where the target begins to evaporate. No clear correlation of T_a with other physical properties was noticeable. It was previously reported that spot patterns persist even for $T < T_a$ if the bombarding-ion energy is less than some critical energy. It was demonstrated that no such critical energy existed. The ⟨111⟩ and ⟨$\bar{1}\bar{1}\bar{1}$⟩ deposits resulting from sputtering of InAs and (110) surfaces were studied. The ⟨$\bar{1}\bar{1}\bar{1}$⟩ spot [the normal to the ($\bar{1}\bar{1}\bar{1}$) face, which terminates with a triply bonded In or Ga atom] is generally slightly thicker (by ~10%) than the ⟨111⟩ spot. For GaAs the ⟨$\bar{1}\bar{1}\bar{1}$⟩ spot is slightly richer in Ga and the ⟨111⟩ spot is slightly richer in As. No compositional differences were noted for the deposits from InAs. (auth)

40306 COMBINED EFFECT OF ULTRAHIGH PRESSURE AND NUCLEAR IRRADIATION ON SOLID-SOLID PHASE TRANSFORMATIONS. Kulcinski, Gerald L.; Maynard, Charles W. (Univ. of Wisconsin, Madison). J. Appl. Phys., 37: 3519-27(Aug. 1966).

A special Bridgman opposed diamond anvil apparatus was constructed to generate useful static pressures up to 50 kbar at ambient temperatures. It was designed to function in the environment of a nuclear reactor to thermal fluxes of 10^{18} nvt. The bulk of the study deals with ZrO_2; other materials investigated to varying degrees were PbO_2, BN, B_2O_3, B, silicic acid, SiO_2, $BaTiO_3$, graphite, P, Ni, Zr, and U. The samples were exposed while under pressure to fast neutron fluxes (>2.8 Mev) of 4.1×10^{15} nvt. The boron-containing samples suffered up to 2×10^{18} fissions/cc while under pressure. PbO_2, BN, B_2O_3, silicic acid, graphite, SiO_2, and Zr were bombarded by uranium fission fragments to $6.5 \times 10^{11}/cm^2$. ZrO_2 was bombarded with 2×10^{16} nvt epithermal neutrons and 1.6×10^{14} fission fragments/cm^2. There was no evidence of any irradiation-pressure-promoted phase change. Pressure alone converted tetragonal ZrO_2 to the monoclinic form and cubic ZrO_2 transformed to tetragonal plus monoclinic phases. A PbO_2 rutile → orthorhombic transformation occurred in seconds at room temperature along with a pressure-sensitive optical absorption edge above 20 kbar. (auth)

40307 EVAPORATIVE LIFETIMES OF COPPER, CHROMIUM, BERYLLIUM, NICKEL, IRON, AND TITANIUM ON TUNGSTEN AND OXYGENATED TUNGSTEN. Shelton, H.; Cho, A. Y. H. (TRW Systems, Redondo Beach, Calif.). J. Appl. Phys., 37: 3544-8(Aug. 1966).

The evaporative lifetimes of Cu, Cr, Be, Ni, Fe, and Ti on W and O-covered W ribbon filaments at temperatures from 1250 to 1750°K were measured as a function of coverage. The low-coverage life-times of these materials on clean polycrystalline tungsten at 1500°K are Cu, 0.01; Cr, 3.0; Be, 0.05; Ni, 1.0; and Fe, 0.7 sec. Less precise measurement of the lifetime of titanium showed it to be much longer than the lifetimes of the other metals studied and extremely coverage dependent. (auth)

40308 CRYSTAL STRUCTURE OF SOLID HYDROGEN AND DEUTERIUM, AND OF NEON–HYDROGEN AND NEON–DEUTERIUM MIXTURES. Barrett, Charles S.; Meyer, Lothar; Wasserman, Judith (Univ. of Chicago). J. Chem. Phys., 45: 834-7(Aug. 1, 1966).

Solid hydrogen (normal and para), deuterium, and the systems neon–hydrogen and neon–deuterium were studied by x-ray diffraction at various temperatures with and without prior plastic deformation. Under most conditions D_2 freezes from the liquid phase as hexagonal close packed (hcp) and is stable in this form against plastic deformation; similarly H_2 usually freezes in the hcp form. When gold foil with a cube texture is present, D_2, normal H_2 and para-H_2 freeze in the face-centered-cubic (fcc) form. Plastic deformation at about 3° and 4.2° causes the addition of fcc reflections to the hcp diffraction pattern with samples of normal H_2 that previously had shown only hcp. It is concluded that normal H_2 is metastable in the hcp structure at these temperatures, and that the spontaneous transformation to cubic on cooling may often be incomplete. It was found that, in concentrations between 0.25% and 99.5% Ne, Ne and the hydrogens are immiscible. (auth)

40309 CRYSTAL-STRUCTURE EFFECTS IN HOT-ATOM CHEMISTRY OF COPPER PHTHALOCYANINE. Yoshihara, K.; Ebihara, H. (Japan Atomic Energy Research Inst., Tokyo). J. Chem. Phys., 45: 896-901(Aug. 1, 1966).

Structure sensitivity of the recoil-atom reactions and thermal annealing reactions in α and β copper phthalocyanines were studied in detail. Isothermal annealing curves were analyzed by the method of Vand and Primak. Two groups of activation-energy spectra appeared corresponding to two stages of the annealing reactions. Stage I was more sensitive to the crystal structure than Stage II. Stage I could be explained by the exchange reaction, $Cu^{2+(1+,0)*} + CuPn_4 \rightarrow Cu^*Pn_4 + Cu^{2+(1+,0)}$, and Stage II by the synthetic reaction, $Cu^{2+(1+,0)*} + 4Pn \rightarrow Cu^*Pn_4$ (Pn denotes a phthalonitrile molecule). From the analysis of the initial retentions in the α and β crystals, hot and thermal processes in the initial recoil reactions could be estimated. (auth)

40310 VIBRONIC ENERGY AND DIPOLE MOMENT OF HD. Kolos, W.; Wolniewicz, L. (Univ. of Chicago). Contract DA-11-022-ORD-3119. J. Chem. Phys., 45: 944-6(Aug. 1, 1966).

The HD molecule was treated by perturbation theory using the complete nonrelativistic four-particle Hamiltonian. In the zeroth order the calculations were carried out with a 147-term variational wave-function. The resulting energies and expectation values of several operators for the ground state and for the first vibrationally excited state are reported. The computed ground-state dissociation energy, D_0, is by 1.9 cm^{-1} larger than the experimental value. By treating the mass difference of the nuclei as the perturbation parameter, a 103-term correction function was computed which yields the second-order correction to the energy $E^{(2)} = -0.04664$ cm^{-1}, and the dipole moment of the molecule $\mu = 1.54\ 10^{-3}$ D. (auth)

40311 MOESSBAUER STUDIES OF DIVALENT AND TRIVALENT ^{57}Fe IN $CoSO_4$ AND $CoSO_4.7H_2O$. Ingalls, R. (Univ. of Illinois, Urbana); Coston, C. J.; De Pasquali, G.; Drickamer, H. G.; Pinajian, J. J. Contracts AT(11-1)-1198; 1834(05). J. Chem. Phys., 45: 1057-61(Aug. 1, 1966). (COO–1198-355).

The results of a Mössbauer study of $^{57}Co(^{57}Fe)$ in $CoSO_4$ as a function of temperature at atmospheric pressure and as a function of pressure at room temperature are reported. In addition to the expected divalent ^{57}Fe component, one also observes a trivalent component, the relative intensity of which decreases with increasing temperature or pressure. The isomer shifts of both charge states also decrease with increasing temperature or pressure. The behavior of the large quadrupole splittings observed in each charge state is analyzed using the crystal field approximation. Similar results were also found in a temperature study of $CoSO_4 \cdot 7H_2O$ at atmospheric pressure. The relative intensity of the trivalent ^{57}Fe component was considerably greater in the hydrate and also decreases with increasing temperature. (auth)

40312 EPR SPECTRA OF 1 PERCENT Nd-DOPED $La_2(SO_4)_3.9H_2O$ AND $LaBr_3$. Johnston, David R.; Wong, Eugene Y. (Univ. of California, Los Angeles). J. Chem. Phys., 45: 1073-4(Aug. 1, 1966).

The X-band EPR spectra of 1% Nd-doped in $La_2(SO_4)_3 \cdot 9H_2O$ and $LaBr_3$ crystals were measured at liquid-helium temperatures. The $La_2(SO_4)_3 \cdot 9H_2O$ crystals showed very strong resonance signals. The results summarized in a spin Hamiltonian with axial symmetry are given for both

crystals. Comparisons with other work on similar compounds are given. (W.D.M.)

40313 KINETIC EQUATION FOR THE ELECTRON-PHONON GAS. Chappell, Willard R. (Smithsonian Astrophysical Observatory, Cambridge, Mass. Harvard Univ., Cambridge, Mass.). J. Math. Phys. (N. Y.), 7: 1153-7 (July 1966).

The random phase approximation equations of motion for the electron-phonon system are solved to obtain long-time expressions for the basic operators that appear in the calculation of correlation functions. These operator expressions are used to obtain a kinetic equation for the electrons and an expression for the phonon spectral function. The kinetic equation has the same form as the Balescu-Lenard equation. Expressions for the density autocorrelation function and the two-particle correlation function are also obtained. The latter is shown to have the same form as the test-particle result for a classical plasma. (auth)

40314 FORMATION OF SiO_2 FILMS BY OXYGEN-ION BOMBARDMENT. Watanabe, Masanori; Tooi, Atsutomo (Matsushita Electric Industrial Co., Ltd., Osaka). Jap. J. Appl. Phys., 5: 737-8(Aug. 1966).

P-type silicon wafers (100 Ω-cm) were bombarded with 60-kev oxygen ions to form silicon dioxide films on mirror-lapped silicon substrates. The ion beam had a penetration depth of approximately 0.15μ. Substrates were irradiated with current density of 20μA/cm² for 200 minutes from room temperature to 300°C. Properties of the films were measured and are compared with thermally grown oxide films. (W.D.M.)

40315 EMISSION AND EXCITATION SPECTRA OF Eu_2O_3 COMPARED WITH Y_2O_3:Eu PHOSPHOR. Ozawa, Lyuji (Nippon Toryo Co., Ltd., Kanagawa, Japan). Jap. J. Appl. Phys., 5: 740-1(Aug. 1966).

The emission and excitation spectra of Eu_2O_3 and Y_2O_3:Eu phosphors at room temperature were studied. Raw materials were yttrium oxalate and europium oxalate of 99.99% purity; firing was done at 1300°C for 3 hr in air. Spectra were measured with an Hitachi Fluorescence Spectrometer (MPF-2). Comparisons of emission and excitation spectra for each phosphor are shown. (W.D.M.)

40316 INFORMATION OBTAINED WITH THE HELP OF THE CRITICAL MAGNETIC SCATTERING OF NEUTRONS. Kashcheev, V. N. (Inst. of Physics, Academy of Sciences, Latv. SSR). Latv. PSR Zinat. Akad. Vestis, Fiz. Teh. Zinat. Ser., No. 2, 22-31(1966). (In Russian).

The information deduced from the critical magnetic scattering of neutrons in a ferromagnet is considered. A number of new experiments on such scattering is proposed. (auth)

40317 EFFECT OF INTERFACES ON THE RADIATION PRODUCTION OF COLOR CENTERS IN ALKALI HALIDES. Gibbon, C. F.; Kuczynski, G. C. (Univ. of Notre Dame, Ind.). Mater. Sci. Res., 3: 131-48(1966). (COO-38-351).

The changes in optical absorption spectra induced by gamma irradiation of polycrystalline pellets pressed from KCl, KBr, and KI powders were studied and compared to the spectra of irradiated deformed single crystals. The results indicated that there is an accelerated rate of destruction of lattice defects in the presence of intercrystalline interfaces. In addition, an enhanced production of certain V-centers was observed, which is explained on the basis of the reaction of products of dissociation of water trapped in the interfaces with point defects existing in the interior of the grains. (auth)

40318 ORIGIN OF FERROMAGNETISM IN DIVALENT EUROPIUM SALTS. de Graaf, A. M.; Xavier, R. M. (Centro Brasileiro de Pesquisas Fisicas, Rio de Janeiro). Notas Fis., Cent. Brasil. Pesqui. Fis., 11: 345-7(1965).

It is shown that the Bloembergen-Rowland indirect interaction between localized magnetic moments in insulators can account for the occurrence of ferromagnetism in the salts of divalent europium. The following europium salts are considered: EuO, EuS, and EuSe. (J.H.M.)

40319 V_k CENTRE IN $SrCl_2$ CRYSTALS. Bill, H.; Suter, H.; Lacroix, R. (Univ., Geneva). Phys. Lett., 22: 241-2(Aug. 15, 1966).

The V_k center was observed in $SrCl_2$ single crystals and the constants of the spin-Hamiltonian were determined. In analogy to the V_k center in CaF_2 it shows resolved hfs with the nearest neighbors on the molecular axis. (auth)

40320 ANISOTROPY AND THERMAL INVERSION IN HIGH FIELD MAGNETIZATION OF CUBIC RARE EARTH COMPOUNDS. Cooper, B. R. (General Electric Co., Schenectady, N. Y.). Phys. Lett., 22: 244-5(Aug. 15, 1966).

Interesting effects are predicted for the high field magnetization in rare earth compounds where the crystal field gives a singlet ground state. For a magnetic field in the hard direction the predicted magnetization increases in steps and shows thermal inversion. (auth)

40321 EPR OF A CENTRE IN Y^{3+} DOPED ARTIFICIAL CaF_2 CRYSTALS. Bill, H.; Lacroix, R. (Univ., Geneva). Phys. Lett., 22: 250(Aug. 15, 1966).

A center was observed in artificial CaF_2 single crystals related to the simultaneous presence of oxygen and yttrium impurity ions. EPR measurements gave the constants of the appropriate spin-Hamiltonian. (auth)

40322 MAGNETIC FIELDS AT ^{119}Sn IN RARE EARTH METALS. Bosch, D.; Pobell, F.; Kienle, P. (Technische Hochschule, Munich). Phys. Lett., 22: 262-4(Aug. 15, 1966).

The magnetic field at ^{119}Sn nuclei in heavy rare earths are deduced from the hyperfine splitting of the 23.8 kev γ ray. (auth)

40323 HINDRANCE EFFECTS IN COLD NEUTRON SCATTERING BY ROTATING MOLECULES. Solt, G. (Central Research Inst. for Physics, Budapest). Phys. Lett., 22: 288-9(Aug. 15, 1966).

Some effects of rotational hindrance for molecules in the solid state are discussed in relation to slow neutron scattering. Numerical estimates for explaining recent data on solid methane are also given. (auth)

40324 OBSERVATION OF PROTON CHANNELING IN THIN MICA. Hamilton, G. F.; Quinton, A. R. (Univ. of lorida, Gainesville). Phys. Lett., 22: 312-13(Aug. 15, 1966).

The channeling of 3.55-Mev protons through a thin film of mica was observed. About 9.2% of the particles penetrating the mica suffered anomalously low energy losses at the channeling orientation. (auth)

40325 MAGNETIC MOMENT DISTRIBUTION OF NICKEL METAL. Mook, H. A. (Harvard Univ., Cambridge, Mass. Massachusetts Inst. of Tech., Cambridge). Phys. Rev., 148: 495-501(Aug. 12, 1966).

The magnetic form factor of nickel was determined for the first 27 Bragg reflections by the polarized-neutron-beam technique. Fourier inversion of the form factor showed that the moment density was quite asymmetric about the lattice sites and was negative in the region between the lattice sites. The measured form factor agreed well with a free-atom form factor for Ni^{++} provided a uniform negative contribution was included in the moment density. From the comparison of the free-atom and measured form factors it was found that 81 ± 1% of the 3d magnetic electrons occupied T_{2g} orbitals, compared with the 60% required for spherical symmetry. The size of the negative contribution needed for agreement between the measured and free-atom form factors agreed well with that given by the Fourier inversion, and the analysis of the data was consistent with the following model for the magnetization of nickel: 3d spin +0.656μ_B, 3d orbit +0.055μ_B, negative contribution −0.105μ_B. (auth)

40326 PRESSURE-INDUCED PHASE TRANSFORMATIONS AND MAGNETIC ORDERING IN SOME INTRA-RARE-EARTH ALLOYS AND SAMARIUM. Jayaraman,

A.; Sherwood, R. C.; Williams, H. J.; Corenzwit, E. (Bell Telephone Labs., Murray Hill, N. J.). Phys. Rev., 148: 502-8(Aug. 12, 1966).

Intra-rare-earth alloys in the system La–Y, La–Gd, Ce–Y, Gd–Y, and also the Sm-type PrY, NdY, NdTm, NdGd, $Ce_{0.30}Gd_{0.70}$, and $Ce_{0.45}Ho_{0.55}$, were investigated at 40 kbar and 450°C. Pressure-induced phase transformation in the sequence hcp → Sm-type → dhcp → fcc seemed to be a rule in these alloy systems, with the exception of Ce–Y. In all cases the high-pressure phase was retained metastably on release of pressure and temperature to the ambient. The similarity between the effect of alloying a hcp rare-earth metal from Gd to Lu or Y, with a lighter rare earth, and the effect of pressure on the former, is pointed out, and certain consequences arising therefrom are discussed. In the Ce–Y system decomposition to γ-Ce and α-Y was observed for two compositions, CeY and $Ce_{0.75}Y_{0.25}$ at the pressure and temperature conditions stated. This decomposition was interpreted as the result of 4f-5d electron promotion in Ce and the consequent size incompatibility preventing the alloy structure from being stable. Magnetic behavior of $LaGd_3$ and NdTm in their normal Sm-type structure and the pressure-induced dhcp structure, and also of the La-Gd alloys in their hcp and pressure-induced Sm-type structure, are reported. In the former two alloys the high-temperature susceptibility anomalies present in the Sm-type phase appear to be absent in the dhcp phase. Both forms however seem to be ordered at low temperatures (1–4°K) with incomplete cancellation of the moments. The La–Gd alloys are all ferromagnetic when in hcp form. In analogy with the behavior under pressure of the Sm form of Gd, it was presumed that the pressure-induced Sm form of La–Gd alloys would order antiferromagnetically. An unambiguous determination of the magnetic behavior of the Sm form is complicated by reversion to the hcp structure on cooling. Some evidence is presented to show that this somewhat unusual reversion of a metastably retained phase on cooling may be connected with magnetic ordering, and it is suggested that the exchange magneto-elastic strain energy associated with a magnetic transition could provide the driving force for the Sm-type → hcp transition. It is suggested that the magnetic-susceptibility anomalies observed in the normal as well as in the pressure-induced dhcp forms of Sm metal are connected with the ordering of the cubic-site layers (c) and the hexagonal-site layers (h) at different temperatures. (auth)

40327 THERMAL CONDUCTIVITY, SECOND SOUND, AND PHONON HYDRODYNAMIC PHENOMENA IN NONMETALLIC CRYSTALS. Guyer, R. A. (Duke Univ., Durham, N. C.); Krumhansl, J. A. Phys. Rev., 148: 778-88 (Aug. 12, 1966).

A variety of phonon-gas phenomena in nonmetals are discussed in a unified manner using a set of macroscopic equations developed from the solution of the linearized phonon Boltzmann equation. This set of macroscopic equations, appropriate for the description of a low-temperature phonon gas, is solved for a cylindrical sample in the limit $\lambda_N \ll R$; $\lambda_N\lambda_{R^2} \gg R^2$. Here λ_N is the normal-process mean free path, λ_{R^2} is the mean free path for momentum-loss scattering calculated in the Ziman limit, and R is the radius of the sample. The solution in this limit exhibits Poiseuille flow of the phonon gas as first discussed by Sussmann and Thellung. An equation for the thermal conductivity which correctly includes this phenomenon is found. Using this equation, the possible outcomes of steady-state thermal-conductivity measurements are discussed in terms of the microscopic scattering rates. Heat-pulse propagation is discussed from a similar point of view. The existence of Poiseuille flow in steady-state thermal-conductivity measurements bears directly on the possibility of observing second sound in solids. A quantitative analysis of available data on LiF suggests that the chemical purity of these samples sets very stringent limits on the observation of either of these effects. The observation of Poiseuille flow in solid ^{4}He samples by Mezov-Deglin strongly suggests that this material is a prime subject for investigations of second-sound propagation. (auth)

40328 STAGE-II RECOVERY IN ELECTRON-IRRADIATED InSb. Eisen, F. H. (Atomics International, Canoga Park, Calif.). Contract AT(11-1)-GEN-8. Phys. Rev., 148: 828-38(Aug. 12, 1966).

Isochronal and isothermal recovery studies were carried out in electron-irradiated samples of InSb following irradiation with high-energy electrons, using Hall coefficient and electrical conductivity as measures of the damage. The emphasis in this work was on the recovery in stage II, and the results show that the recovery depends strongly on the carrier concentration of the sample. The temperature of the center of the recovery stage was observed to vary from 91°K in some p-type samples to 203°K in a highly degenerate n-type sample. The activation energy for recovery changed from 0.24 to 0.71 ev over this same range of carrier concentrations. These changes were explained by assuming that the two acceptor levels associated with the radiation-produced defects must be empty in order for annihilation of the defects to occur. The details of the analysis relating these recovery parameters to the sample carrier concentration are presented. In order to fit the observed recovery kinetics, it was assumed that two close interstitial-vacancy pairs produced by the irradiation were involved, and that they annihilate by basically first-order processes with different rate constants. A model for the defects and their mode of annihilation, assuming vacancies to be the mobile species, is suggested. (auth)

40329 RECOVERY OF AN INSULATOR FROM A RADIATION PULSE. Mayburg, Sumner (Controls for Radiation, Inc., Cambridge, Mass.). Proc. IEEE (Inst. Elec. Electron. Eng.), 54: 1013(July 1966).

Spurious voltages are often produced in insulators in a pulsed nuclear environment. These voltages arise from positive charges left in the insulator after a nuclear blast has stripped some of the electrons from the material. It is shown that a simple time constant can be calculated for recovery of the insulator. (auth)

40330 MAGNETIC MOMENT DISTRIBUTIONS FOR TRANSITION METAL IMPURITIES IN IRON. Campbell, I. A. (Univ., Paris, Orsay, France). Proc. Phys. Soc. (London), 89: 71-6(Sept. 1966).

An analysis is made of the neutron diffraction results of Low and Collins on transition metal impurities in iron. The moment values found are shown to be related to the hyperfine fields on impurity sites and on neighbor sites. (auth)

40331 ROTATIONAL ANALYSIS OF SOME NEW ABSORPTION BANDS OF SrH AND SrD IN THE ULTRAVIOLET REGION. Khan, M. Aslam (Univ. of Chicago, Univ. of Karachi, Pakistan). Proc. Phys. Soc. (London), 89: 165-72(Sept. 1966).

Two new bands of SrH at 3115 Å and 2718 Å and three new bands of SrD at 3115 Å, 2848 Å and 3001.5 Å were observed in absorption using a King-type furnace containing strontium metal and hydrogen (deuterium) at a temperature greater than 1300°C. Whereas the SrH band at 3115 Å is shown to be the (0,0) band of a new transition which may be called $G\ ^2\Sigma \leftarrow X\ ^2\Sigma$, the band at 2718 Å is analysed as the (1,0) band of the previously known system at 2927 Å. The SrD bands at 3115 Å, 3001.5 Å, and 2848 Å are analysed as the (0,0) band corresponding to the (0,0) band of SrH at 3113 Å and the (0,1) and the (1,0) bands of the previously reported system of SrD at 2928 Å, respectively. (auth)

40332 ELECTRON IRRADIATION OF III-V COMPOUNDS. Baeuerlein, Rudolf (Siemans-Schuckert Research Center, Erlangen, Ger.). Siemens Rev., 33: 111-15(Mar. 1966).

Effect of fast-electron bombardment of semiconductors was studied. Electrons of a sufficiently high energy create in the semiconductor crystal lattice defects which may act as donors or acceptors or even as recombination centers for minority carriers. These lattice defects result from the fact that a lattice atom acquires so much energy on collision with a fast electron, that it is displaced from its normal position to an interstitial position. The remaining

vacancy and the atom in the interstitial position form a vacancy-interstitial pair, a so-called Frenkel defect. Displacement energies were determined for the III-V compounds and compared with those of germanium. It was found that the displacement energies of the III-V compounds are markedly lower than those of germanium. A study of the formation mechanism of lattice defects by electron collision indicated that the binding energy in the germanium lattice is higher than in the III-V compounds. The lattice defects introduced by electron bombardment disappear if the sample is heated. The thermal vibration sets the interstitial atoms and vacancies produced by irradiation into motion so that they can recombine. In InAs this takes place at room temperature if the lattice defects have been produced at lower temperatures. The generation rate of electron-hole pairs during the electron impulse is 10^{23} cm^{-3} in GaAs. At an assumed lifetime of 10^{-9} sec, the excess carrier concentration during the electron pulse duration is 10^{14} cm^{-3}, which is large enough to enable the change in conductivity to be observed satisfactorily, even for low-resistance material. (BBB)

40333 PHOTO-STIMULATED RADIATION DOSIMETRY. **Miyashita, K.; Henisch, H. K. (Pennsylvania State Univ., University Park). Solid-State Electron., 9: 615-17(June 1966). (TID-22761).**

A method is described which permits photostimulated polarization transients in single crystals of ZnS to be used for the measurement of uv or x-ray doses previously received by the specimen. Lab-grown single crystals of ZnS were cut into platelets of 0.05 cm thickness (0.4 × 0.4 cm area) and polished on two sides. They were placed between electrodes in a vacuum chamber and exposed to uv radiation or x rays at −90°C. Before exposure to the dose, the specimen is preconditioned by the application of field and photostimulus, resulting in a polarization transient. Repetition of the procedure within a reasonable period of time leads only to a very minor current peak. If the same procedure is repeated after the dose, it results in a sharp current peak. The peak height of this pulse can be used directly as the dosimetric criterion. The response is linear over a three-decade range of doses. With the system described, it is possible to detect uv dosages as small as 0.01 μw-sec/cm^2 or, in the x-ray range, as small as a few milliroentgens at 50 kv. Several methods are open for achieving a substantial increase in sensitivity: (1) optimum doping of the crystals, (2) reduction in the thickness of the conducting glass electrode (or complete elimination), and (3) addition of an x-ray-uv converter intensifying screen. (BBB)

40334 DEFECTS IN SILICON PRODUCED BY IRRADIATION WITH FAST NEUTRONS AT 77 DEG K. **Konopleva, R. F.; Novikov, S. R.; Rubinova, E. E. (Ioffe Inst. of Physics and Tech., Leningrad). Soviet Phys.-Solid State (Engl. Transl.), 8: 264-8(Aug. 1966).**

Translated from Fiz. Tverd. Tela, 8: 321-6(Feb. 1966).

The electrical conductivity and spectral distribution of impurity photoconductivity were investigated in both n- and p-type silicon irradiated by fast neutrons in a reactor at 77°K. The samples were annealed in the temperature range 77 to 400°K; seven stages of annealing were observed, associated with the appearance and disappearance of defects. Nineteen levels were found to be associated with the radiation defects produced by irradiation with fast neutrons at 77°K and subsequent low-temperature annealing. Comparison of the electrical conductivity curves and the curves of the spectral distribution obtained during various stages of annealing permitted us to reach conclusions about the character of some of the levels which were observed. (auth)

40335 RADIATION-STIMULATED EMF IN CsI CRYSTALS. **Niyazova, O. R.; Klimkova, O. A. (Nuclear Physics Inst., Tashkent). Soviet Phys.-Solid State (Engl. Transl.), 8: 304-5(Aug. 1966).**

Translated from Fiz. Tverd. Tela, 8: 375-7(Feb. 1966).

A radiation-induced emf was observed in CsI crystals exposed to a localized irradiation by x rays having an energy threshold $E_n \simeq 30$ kev. The dose dependence, the probe characteristics, and the annealing process of the radiation-stimulated emf are all described. (auth)

40336 ABSORPTION OF ULTRASOUND IN SUPERCONDUCTORS. **Kashlev, Yu. A. (Baikov Inst. for Metallurgy, Moscow). Soviet Phys.-Solid State (Engl. Transl.), 8: 340-5(Aug. 1966).**

Translated from Fiz. Tverd. Tela, 8: 428-36(Feb. 1966).

Consideration is given to the absorption of longitudinal ultrasonic waves in superconductors containing impurity atoms for $ql \gg 1$ (q is the wave vector of the ultrasound, l is the electron mean free path). On the basis of investigation of the temperature and frequency dependence of the coefficient of ultrasonic absorption in the superconductor and of the jump in this coefficient below the transition temperature it is shown that the drag effect plays an important part in the dissipation of the acoustic wave energy. The investigation indicates that in the normal state the ratio of the absorption coefficient to q decreases with increase in ql when $ql \gg 1$. (auth)

40337 CONCERNING INFRARED QUENCHING OF INTRINSIC PHOTOCONDUCTIVITY IN n-TYPE GERMANIUM IRRADIATED BY γ RAYS. **Vasilev, A. V.; Smirnov, L. S. (Inst. of Semiconductor Physics, Novosibirsk, USSR). Soviet Phys.-Solid State (Engl. Transl.), 8: 484(Aug. 1966).**

Translated from Fiz. Tverd. Tela, 8: 603(Feb. 1966).

The photoconductivity of n-type germanium irradiated at room temperature by ^{60}Co γ rays was investigated. Examination of the photoconductivity spectrum, recorded at liquid nitrogen temperature, led to the identification of the following system of levels associated with the radiation defects: $E_c - 0.22$, -0.25, -0.27, -0.30, -0.33, -0.36, -0.43, -0.49, -0.52, and -0.59 ev. When the samples were subjected to a constant illumination by light in the intrinsic region, it was observed that infrared quenching occurred over almost all of the wavelength region under investigation (1.5 to 5.5 μ). The results indicate that the radiation introduced into the germanium a large number of defects with widely varying cross sections for the capture of electrons and holes. (J.H.M.)

40338 USE OF SLOW NEUTRONS FOR THE STUDY OF DYNAMIC PROCESSES IN LIQUIDS. **Ripeanu, S. (Inst. of Atomic Physics, Bucharest). Stud. Cercet. Fiz., 18: 463-508(1966). (In Rumanian).**

Slow and very slow reactor neutrons possess energies and wave lengths comparable with the vibrational energy and atomic distance of molecules in condensed systems. They are well suited for the study of atomic motion in liquids and solids. Experimental neutron diffraction tools adaptable to this type of research include the triaxial crystal spectrometer, the rotary crystal spectrometer, the time-of-flight method choppers, and others. It was shown both experimentally and theoretically that broadening of the quasielastically scattered neutron spectra in a liquid is the result of diffusive processes. Water and heavy water have been investigated by several authors. Lately, special attention has been turned toward radiation-resistant high-boiling organic moderators, such as glycine, pentane, oleic acid, etc.; studies were carried out also on solid methane, methyl-, ethyl-, amyl and other alcohols. Inelastic scattering of slow neutrons in the broadened spectra yields information on the various energy levels of the system under study. In most of the liquids examined, the proton is considered as the chief scatterer. (TTT)

40339 EXPERIMENTAL INVESTIGATION OF THE ZONAL STRUCTURE OF SOME CHALCOGENIDES OF RARE-EARTH ELEMENTS. **Zalevskii, B. K.; Lashkaryev, G. V.; Sobolev, V. V.; Syrbu, N. N. (Inst. of Applied Physics, Kishinev, Moldav SSR. Inst. of Problems in Material Studies, Kiev). Ukr. Fiz. Zh., 11: 638-43(1966). (In Ukrainian).**

The reflection spectra of polished polycrystalline samples of selenides of lanthanum, cerium, praseodymium, neodymium, and samarium of the Me_2Se_3 type, as

well as Sm_2S_3 and EuSe, were studied in the region of 1 to 6 ev at T = 293°K. A great similarity was found experimentally in the reflection spectr for crystals of one type and a weak difference between t sulfides and the selenides. In the region of self-absorption ($E > E_g$) reflection maxima were found in all chalcogenides of rare-earth metals. These maxima are explained in terms of the well-known group theoretical calculations of the zonal structure of crystals with a Th_3P_4 lattice, by the scheme of direct interzonal transitions at various points of the Brillouin zone. (auth)

40340 INFRARED SPECTRUM OF NEUTRON-IRRADIATED SILICON. Vakulenko, O. V.; Lisitsa, M. P.; Zaets, V. D. (Kiev State Univ. Inst. of Semiconductors, Kiev). Ukr. Fiz. Zh., 11: 653-7(1966). (In Ukrainian).

The Si absorption spectrum was investigated (specific resistance = 5 ohm cm) in the region of 1 to 25 wavelengths before and after irradiation with neutrons at an integral flow intensity of $\sim 10^{18}$ neutrons/cm^2. The number of centers responsible for absorption at $\lambda = 1.8\mu$ was calculated using the Kravets integral. The result ($\sim 2.10^{17}$ cm^{-3}) does not permit linking these centers with residual impurities, since their concentration is usually less than 10^{15} cm^{-3}. It is presumed that the $\lambda = 1.8\mu$ band arises as a result of the transition of an electron from the valent zone at the level of $E_c = 0.40$ ev. The absorption at $\lambda = 12\mu$ is explained by the existence of silicon A-centers, which appear during neutron irradiation. (auth)

40341 ABSORPTION AND EMISSION OF IRRADIATED RARE EARTH IONS IN CaF_2. Merz, J. L.; Pershan, P. S. (Harvard Univ., Cambridge, Mass.). 11p. (CONF-660411-24). ORAU. Gmelin, AED-CONF-66-060-50.

From American Physical Society Meeting, Washington, D. C.

Optical absorption and thermoluminescence measurements are used to study the charge reduction of rare earth ions in x-irradiated CaF_2. Previously reported spectra of the thermoluminescent glow peaks between 80° and 440°K indicate the site symmetry of the emitting trivalent rare earths and the nature of the holes involved in recombination. By measuring the optical absorption after each glow peak is annealed, it is found that the concentration of divalent rare earth ions decreases in contradiction to previous results. An absorption band at 3100 Å is found that is associated with the hole centers formed during irradiation. Slight shifts in this peak are observed for the holes responsible for different glow peaks. Anomalous absorption bands are found in some samples that are associated with the high-temperature glow peaks. These data support the model that divalent rare earths and holes recombine, and the resulting trivalent rare earths emit the fluorescence seen in the low-temperature glow peaks. (auth)

40342 EFFECTIVE MAGNETIC FIELDS AT Sm, Gd, AND Dy NUCLEI IN METALLIC Fe FOLLOWING COULOMB EXCITATION IMPLANTATION. Grodzine, L.; Berchers, R.; Hagemann, G. B. (Niels Bohr Inst., Copenhagen, Denmark). 14p. (CONF-660411-20). ORAU. Gmelin, AED-CONF-66-060-66.

From American Physical Society Meeting, Washington, D. C.

A technique for the study of internal fields in solids is described which utilizes Coulomb excitation by means of ^{16}O ions to both excite a nuclear state and propel the nucleus into an arbitrary host backing. The perturbed angular distribution of the de-excitation γ's with respect to the back-scattered ^{16}O ions measures the electromagnetic interaction of the nuclear state with the lattice environment. Larmor precession of the ($^{16}O,\gamma$) distribution was observed for Sm, Gd, and Dy implanted in a magnetized iron host. The deduced values of H_{eff} are approximately +1.3, −0.2, and −2.0 mOe, respectively, indicating an antiferromagnetic coupling of the rare earth-iron moments. (auth)

40343 CRYSTAL DYNAMICS OF POTASSIUM. I. PSEUDOPOTENTIAL ANALYSIS OF PHONON DISPERSION CURVES AT 9 DEG K. Cowley, R. A.; Woods, A. D. B.; Dolling, G. (Chalk River Nuclear Labs., Ontario). 34p. (CONF-660327-5). ORAU. Gmelin, AED-CONF-66-050-16.

From American Physical Society Meeting, Durham, N. C.

The frequencies of normal modes of vibration of potassium at 9°K were measured by inelastic neutron scattering techniques. Certain selected frequencies are (units 10^{12} cps) H_{15} 2.21 ± .02, P_4 1.78$_5$ ± .02, N_1' 2.40 ± .04, N_3' 1.50 ± .02$_5$ and N_4' 0.53 ± .02. The results are very similar, apart from a scale factor 1.65, to those for sodium. Analysis of the results was carried out in terms both of conventional Born-von Kármán models and of potential functions defined in reciprocal space. A fifth neighbor, axially symmetric force model was used to compute the frequency distribution function for the normal modes and the associated heat capacity. The reciprocal space analysis was performed in two ways: (a) in terms of a total potential function, whose Fourier transform is the effective interatomic potential between "neutron pseudoatoms" of potassium, and (b) in terms of the screened pseudopotential for the conduction electron-ion interaction. Analysis (a) shows that a wide variety of interatomic potentials, both with and without long range oscillatory character, can be found that give a satisfactory fit to the results. These potentials are compared with those obtained from an analysis of x-ray-scattering data for liquid potassium. The pseudopotential s obtained from analysis (b) are in good agreement with that derived by Bortolani form the Heine-Abarenkov model. A re-analysis of the phonon dispersion curves for sodium leads to very similar conclusions, confirming earlier work by Cochran. (auth)

40344 ELECTRONIC EFFECTS ON LATTICE MODES. Sjoelander, Alf (Inst. of Theoretical Physics, Gothenburg, Sweden). 39p. (CONF-650932-4). ORAU. Gmelin, AED-CONF-65-292-6.

From Symposium on the Inelastic Scattering of Neutrons by Condensed Systems, Upton, N. Y.

The essential progress made in the last few years on lattice vibrations in metals and semiconductors is reviewed. Points considered include the following: the Born-von Kármán theory, crystal symmetry, response of electrons to nuclear motion, the interaction between a single ion and a conduction electron in metals, the dielectric constant in metals, the effective ion-ion interaction in metals, Kohn anomalies, and the shell model. It is concluded that it is difficult to calculate dispersion curves accurately enough from first principles. It may be more profitable to let the experimental data give the effective forces between the atoms and then use the obtained information to calculate electron band structure, conductivity, etc. (49 references). (A.G.W.)

40345 VARIATIONS OF PHYSICAL AND ELECTRICAL CONCENTRATIONS OF DONORS DURING THERMAL ANNEALING. Glotin, Ph. (Centre d'Etudes Nucleaires, Grenoble, France); Grapa, J. 25p. (CONF-660414-5). ORAU. Gmelin, AED-CONF-66-119-9.

From Second International Conference on Electron and Ion Beam Science and Technology, New York.

Samples of p-type Si were doped by ion bombardment. The total concentration of impurity atoms implanted in the crystal was measured by a tracer technique involving the inclusion of a given proportion of ^{32}P ions in the incident ion beam. The concentration of electrically active atoms implanted was obtained from four-probe measurements. Samples were annealed at temperatures from 150 to 700°C. Evidence of the following physical phenomena was observed: disappearance of channeling for high doses (10^{15}/cm^2), decrease of the ratio of physical concentration to electrically active concentration at the surface with increasing dose, annealing of lattice defects mainly under 400°C, jumps of the P atoms to substitutional sites between 400 and 700°C, and appearance of thermal diffusion at ~700°C. (A.G.W.)

40346 MAGNETIC ANISOTROPY OF TERBIUM. Rhyne, J. J.; Clark, A. E. (Naval Ordnance Lab., White

Oak, Md.). 11p. (CONF-660327-8). ORAU. Gmelin, AED-CONF-66-050-19.

From American Physical Society Meeting, Durham, N. C.

A study of the magneto-crystalline anisotropy in the rare earth ferromagnets has been initiated at NOL. Anisotropy energies of the order 10^8 ergs/cm^3 are responsible for the anomalous magnetic states in these metals and for transitions between these states. First results on terbium represent the largest reported anisotropy measured by a direct torque method. (W.D.M.)

40347 PHYSICAL ASPECTS OF ELECTRON BEAM PENETRATION IN METALS. Meulemans, M. (Centre d'Etudes de l'Energie Nucleaire, Mol, Belg.). 22p. (CONF-660414-8). ORAU. Gmelin, AED-CONF-66-119-10.

From 2nd International Conference on Electron and Ion Beam Science and Technology, New York.

Direct visual observation of samples and metallographic examination after different stages of the electron beam cutting process led to a better understanding and detailed description of the way of an electron beam in a metal. The power density of the electron beam determines entirely the mechanism of the penetration. The momentary temperature reached on impact stems from the collisions between incident electrons and lattice ions. The crater formation then depends on the rate of temperature increase in a larger volume of the metal. At high power density (10^{+9} watt/cm^2), solid or liquid material passes into the gaseous state, changing the overall density of the material and thereby the mean free path of the electrons. The action of the surface tension will then tend to seal off the crater thus forming a plasma bubble inside the cavity. Furthermore, a pinch effect on the beam is caused by the elastic collisions of the electrons on the liquid walls. At lower power density (10^{+5} watt/cm^2), the change of overall density and the influence of capillarity are not present. The thermal conductivity is the controlling factor and a spherical liquid region will be formed around the beam spot. (auth)

40348 PARAMAGNETIC AND FERROMAGNETIC RESONANCE IN EuS. von Molnar, Stephen. Riverside, Calif., Univ. of California, 1965. 82p.

Thesis.

EuS is a cubic nonmetallic ferromagnet below 16°K. Measurements of microwave power absorption as a function of applied magnetic field strength and orientation above and below the Curie temperature yield the paramagnetic line width, spectroscopic splitting factor, g, and magnetocrystalline anisotropy field. A standard microwave spectrometer operating at 22 Gcps was employed to observe the ferromagnetic and paramagnetic resonance in single-crystal EuS. The paramagnetic line width is found to be 1200 Oe and is explained solely on the basis of magnetic dipole-dipole interactions without invoking more complicated electrostatic mechanisms. The experimental value, $g = 2.002 \pm .004$, confirms this conclusion. An upper limit on the anisotropy field in the ferromagnetic state is 30 Oe. This is to be contrasted with a field of -190 Oe in EuO. The results are understood in terms of crystal field perturbations of the magnetic Eu^{2+} ion. (Dissertation Abstr.)

40349 EFFECT OF HIGH ELECTRONIC CURRENT DENSITY ON THE MOTION OF ^{195}Au AND ^{125}Sb IN GOLD. Gilder, Howard Michael. [Urbana], Ill., Univ. of Illinois, 1965. 114p.

Thesis.

The effect of high electronic current density on the motion of the ^{195}Au and ^{125}Sb ions in gold was studied by means of a novel lathe-sectioning technique that permitted the assay of radioactive sections from a specimen only 3 mm in diameter. The mobility, v/j, of the ^{195}Au ion in gold was investigated in the temperature range 874 to 1016°C, with a corresponding variation in mobility of from 9.6×10^{-13} cm^3/sec/amp to 7.3×10^{-12} cm^3/sec/amp, and was found, within experimental uncertainty, to obey the Nernst-Einstein relation, $v/j = e^*\rho D/kT$. The effective charge, e*, was determined to be independent of temperature, with the value $(9 \pm 1)e$, indicating that the momentum exchange with the conduction electrons dominates the force arising from the direct interaction between the external electric field and the positively charged ion. The specific resistivity of the gold ion-vacancy complex was calculated to be $(1.2 \pm 0.3)\mu\Omega$ cm/% defect, using the models of either Huntington and Grone or Fiks. The electromigration of the ^{125}Sb ion in gold was studied at a temperature of 853°C, for which the mobility was 9.24×10^{-11} cm^3/sec/amp, and at 1009°C, corresponding to a mobility of 4.54×10^{-10} cm^3/sec/amp. Although only two different temperatures were investigated, there were sufficient data to estimate an effective charge and specific resistivity of the activated complex of $(140 \pm 40)e$ and (18 ± 6) $\mu\Omega$ cm/% defect, respectively. As the shift of the ^{125}Sb tracer was some 50% greater than the mean square diffusional penetration distance of the antimony, and the mobility of the antimony ion some one to two orders of magnitude greater than that of the solvent gold atoms, it appears that electromigration techniques could be adapted as a practical method for purifying metals, as an addition to, or substitute for zone refinement. (TCO)

40350 ANISOTROPIC SPIN-LATTICE RELAXATION TIMES OF TRIVALENT RARE EARTH IONS IN ANHYDROUS LANTHANUM TRICHLORIDE. Mikkelson, Raymond Charles. [Urbana], Ill., Univ. of Illinois, 1965. 174p.

Thesis.

Measurements of the temperature and angular dependence of the spin-lattice relaxation time T_1 were made for cerium, praseodymium, neodymium, samarium, terbium, and erbium in single crystals of anhydrous lanthanum trichloride. The experiments were performed on samples containing ≤ 2 at. % rare earth doping using pulse-saturation techniques at X-band frequencies. Angular measurements at constant temperature and microwave frequency were made for magnetic field orientations between 0° and 90° with respect to the crystal c-axis in the temperature range 1.65 to 4.2°K. The results are interpreted as involving an angular dependent direct process and isotropic Orbach and Raman mechanisms. They are compared with theoretically predicted rates obtained from computer calculations. Except for the ions cerium and samarium, nearly all the predicted relaxation rate temperature dependencies agree with experimental results within a factor of five or less. Theoretical treatments that involve the mixing of excited state wave functions into the ground magnetic doublet through the anisotropic Zeeman interaction are required to explain the observed angular dependence. The theoretical anisotropies are followed almost exactly in every case. One of the ions, praseodymium, exhibits a phonon limited direct process relaxation rate that is interesting because the apparent hot phonon equilibration time is about 13 nsec, corresponding to an equilibration path length of only 26 microns. Measurements made before and after a crystal was cleaved to half its original thickness gave an unaltered relaxation rate. After neutron bombardment the bottlenecked relaxation rate changed with the phonon equilibration time apparently reduced to 8 nsec. Prior irradiation of this same sample with 100 kev x rays produced no observable change in the relaxation time. (Dissertation Abstr.)

40351 INFRARED REFLECTION STUDIES OF SINGLE CRYSTAL LITHIUM HYDRIDE AND SOME OF ITS ISOTOPIC DERIVATIVES. Brodsky, Marc Herbert. Philadelphia, Univ. of Pennsylvania, 1965. 154p.

Thesis.

The physical and chemical properties of crystal lithium hydride are reviewed and the usefulness of examining its infrared reflection spectrum is discussed. An outline of the theory of the interaction of infrared radiation and vibrating ionic lattices is presented with emphasis on the effective charge characterizing the interaction. A shell model theory calculation of the effective charge is performed and yields a result in agreement with the experi-

mental value, which is also determined. The infrared reflection spectra of natural lithium hydride plus three isotopic derivatives (lithium deuteride, lithium-7 hydride, and lithium-6 hydride) are measured and analyzed using the Kramers-Kronig dispersion relation. From this analysis the long wavelength limits of the transverse and longitudinal lattice frequencies are found. With this knowledge, the low-frequency (static) dielectric constants, effective charges, and effective compressibilities are deduced. The isotopic effect on the various measured properties are discussed in terms of their interrelations as well as intrinsic significance. Of particular interest are the values of the effective charges of lithium deuteride and lithium hydride and the physical implications of the observed difference. (Dissertation Abstr.)

40352 ELECTRON SPIN RESONANCE IN CERIUM METAL. Goodrich, Roy Gordon. Riverside, Calif., Univ. of California, 1965. 61p.

Thesis.

Metallic cerium undergoes a first order phase transition at room temperature and at a pressure of 7 kilobars. The transition has been attributed to the promotion of the single 4f electron in the cerium ion to the 5d conduction band. The electron spin resonance spectrum of the 4f electron through this phase transition was studied. The results obtained at atmospheric pressure could not be accounted for on the basis of a simple theory and are at variance with a previous measurement. Efforts were directed toward an explanation of the results obtained at atmospheric pressure and at the temperatures 300°, 196°, and 77°K. The data were taken at 21.5 Gcps using a standard 1.25-cm microwave spectrometer, and the absorption spectrum was investigated in magnetic fields up to 26.5 kilogauss. In order to explain the observed results it is necessary to consider the effects of the crystalline field and the exchange interactions that act on the 4f electrons. It is found that the atmospheric pressure and room temperature cubic phase has a small trigonal distortion. In addition, the resonance spectrum from this phase exhibits a series of satellite resonances, which can be attributed to an indirect exchange interaction between the different Stark levels produced by the crystalline field. Resonances were also observed from the hexagonal phase that coexists with the cubic phase at the temperatures investigated. The spectrum from the hexagonal phase is in agreement with the results expected on the basis of the crystal field theory for this structure. The values of the measured g-factors are $g_{||} = 1.29$ and $g_{\perp} = 1.07$ for the fcc phase (trigonal distortion), $g_{||}$ 4.25, $g_{\perp} = 0.6$, $g_{||} = 1.26$, and $g_{\perp} = 2.14$ for the hexagonal phase. The 4f–conduction electron exchange energy for the fcc phase is found to be $\bar{I} = -0.062$ ev. The results obtained at 77°K suggest that the phase transition originally to be studied induces sufficient strain into the samples to completely obscure the resonance spectrum, and that no information concerning the 4f electron in the high pressure phase can be obtained with this technique. (Dissertation Abstr.)

REACTOR TECHNOLOGY

General

Refer also to abstract 39175.

40353 (ANL–7228) CATALOG OF NUCLEAR REACTOR CONCEPTS. PART I. HOMOGENEOUS AND QUASI-HOMOGENEOUS REACTORS. SECTION VI. SOLID HOMOGENEOUS (SEMIHOMOGENEOUS) REACTORS. Teeter, Charles E.; Lecky, James A.; Martens, John H. (Argonne National Lab., Ill.). June 1966. Contract W-31-109-eng-38. 71p. Dep. mn. CFSTI $3.00 cy, $0.75 mn.

Reactor concepts in which the solid fuel and moderator are in a uniform combination or mixture are cataloged. The concepts are separated into reactors designed for research and testing and for power production and breeding. (H.D.R.)

40354 (AP-Note–393) CONTROL ROD PROGRAMMING. PART I. FUNDAMENTAL ANALYSIS. Murray, R. L. (Alco Products, Inc., Schenectady, N. Y. Nuclear Power Engineering Dept.). Oct. 13, 1961. Contract AT(30-1)-2639. 34p. ORAU.

Preliminary ideas in regard to development of analytical models which may adequately describe the nuclear effects of control rod programming are presented. The desired information that is sought in an optimization of the rod operation procedure during core life is defined and a variety of analytical methods of approach are presented. (auth)

40355 (APDA-TPI–1) FACILITIES, CAPABILITIES, AND EXPERIENCE IN LIQUID METALS AND FAST REACTOR RESEARCH AND DEVELOPMENT. (Atomic Power Development Associates, Inc., Detroit, Mich.). June 1966. Contract AT(11-1)-865. 94p. Dep. mn. CFSTI $3.00 cy, $0.75 mn.

The research, design, and developmental work performed by Atomic Power Development Associates is summarized for the liquid metal-cooled fast breeder reactor concept. Most of the work is directly related to the development of the Enrico Fermi Atomic Power Plant and includes: reactor physics and related calculations, development of fuel, shielding, and reactor materials, fuel element design, reactor design, and design of the heat transport system and related system components. (H.D.R.)

40356 (EURAEC–1644) ON THE HYDRAULIC CHARACTERISTICS OF A BOILING WATER CHANNEL WITH NATURAL CIRCULATION. Spigt, C. L. (Technische Hogeschool, Eindhoven (Netherlands)). May 1966. Contract 030-64-1-TEEN (RD). 150p. (EUR–2842; WWO–16-R92). Dep. mn. CFSTI $4.00 cy, $1.00 mn.

Work Performed under United States–Euratom Joint Research and Development Program.

The results of an experimental and theoretical study are reported on the hydraulic characteristics of a single coolant channel of simple annular geometry in a boiling water nuclear reactor, with the main emphasis on the stability characteristics of the flow process in such a channel. The experimental part is restricted to operation under conditions of natural convection. Emphasis is placed on the determination of the liquid flow rate at the inlet and the void and pressure distribution along the height of the coolant channel, the occurrence and characterization of hydraulic instabilities, and the determination of the stability characteristics of a study state by means of a frequency response analysis. The experimental set-up and the measuring, recording, and analyzing equipment are described. The results are discussed and compared to those obtained from a theoretical study of a boiling channel. (H.D.R.)

40357 (NAA-SR–11766) FISSION-PRODUCT RETENTION IN SODIUM: A SUMMARY OF ANALYTICAL AND EXPERIMENTAL STUDIES AT ATOMICS INTERNATIONAL. Kunkel, W. P. (Atomics International, Canoga Park, Calif.). Aug. 8, 1966. Contract AT(11-1)-Gen-8. 94p. Dep. mn. CFSTI $3.00 cy, $0.75 mn.

Studies performed for the purpose of evaluating the release and transport characteristics of fission products in liquid Na are summarized. Results indicate that the presence of Na vapor affects the efficiency of injection and sampling methods, and mitigates chemical and physical identification of the fission product effluent. Equilibrium results for I_2 show some agreement when expressed as distribution coefficients and compared with a theoretical distribution coefficient derived from Log $K_d = 4500/T - 5.66$, where K_d is the distribution coefficient, and T is the system temperature in degrees Kelvin. Cs and Sr results show fairly logical distribution coefficients. Extensive plating and deposition on surfaces was observed throughout the experiments. The results of an examination of previously contaminated Na reactor piping indicated some correlation of fission product activity with carbonaceous impurities in the system. Application of these results to typical reactor configurations is made with the extrapolation equation developed. Release fractions are suggested as a result of this preliminary model. (auth)

40358 (ORNL-NSIC–17) ABNORMAL REACTOR OPERATING EXPERIENCES. (Oak Ridge National Lab., Tenn.). Aug. 1966. Contract W-7405-eng-26. 106p. Dep. mn. CFSTI $4.00 cy, $0.75 mn.

Information prepared by the Division of Operational Safety since 1963 in memorandum form on unusual reactor operating experiences is compiled and indexed. Seven licensed reactor experiences issued by the AEC Regulatory Staff are also included. (H.D.R.)

40359 (TID–8200(13th Rev.)) NUCLEAR REACTORS BUILT, BEING BUILT, OR PLANNED IN THE UNITED STATES AS OF DECEMBER 31, 1965. (Office of the Assistant General Manager for Reactors (AEC), Washington, D. C.). 25p. Dep. mn. CFSTI $1.00 cy, $0.50 mn.

Information on name, owner, location, principal contractor, type, and power is tabulated on facilities in the United States capable of sustaining a nuclear chain reaction. The facilities are categorized under civilian reactors, production reactors, reactors for export, and critical assembly facilities. (H.D.R.)

40360 (WAPD-T–1890) ANGLE-SPACE SYNTHESIS: AN APPROACH TO TRANSPORT APPROXIMATIONS. Kaplan, S.; Davis, J. A.; Natelson, M. (Bettis Atomic Power Lab., Pittsburgh, Pa.). May 1966. Contract AT(11-1)-Gen-14. 49p. (CONF-660606–14). Dep. mn. CFSTI $2.00 cy, $0.50 mn.

From American Nuclear Society Meeting, Denver.

Three new ideas are combined to produce an analytical approach to solution of the neutron transport equation in realistic multidimensional reactor geometries. The method is of the expansion approach type in which the flux is represented by a linear combination of known functions of angle with mixing coefficients which are unknown functions of space. The mechanics of the new approach are developed in detail and some initial numerical examples are described. (H.D.R.)

40361 NUCLEAR REACTOR OSCILLATION-MEASURING DEVICE. Efanov, A. I.; Konstantinov, L. V.; Postnikov, V. V.; Sadikov, I. P.; Sokolov, M. P. At. Energ. (USSR), 20: 437-8(May 1966). (In Russian).

A hand-operated device for measuring the natural oscillation frequency of reactors is described. The apparatus consists of a set of rods coupled to an oscillation controller and a harmonics analyzer. The controller consists of a frequency divider and two-position relays triggered by the incoming frequency-divider pulse. A sinusoidal voltage of 50 Hz is transmitted to the computing part of the frequency

divider; and the computation count is set at 128, 256, 512, 1024, or 2048. The amplitude of the periodic oscillations observed with this device did not exceed the 0.5 to 1.0% level and did not interfere with reactor performance for 1.0 to 1.5 hours. (G.O.Y.)

40362 OCEAN TECHNOLOGY AND NUCLEAR POWER. Croke, Edward J. Power Reactor Technol., 9: 1-18(Winter 1965-1966).

The potential applications of undersea nuclear power for exploration and exploitation of ocean resources are examined. Uses for reliable electric- or thermal-power supplies include undersea construction, submarine laboratories, oil drilling and production operations, mining and dredging, submersible-vehicle propulsion, navigational aids, and undersea pumping facilities for water or petroleum. Power sources available or in the planning and development stage, including isotopic thermal power, isotopic thermoelectric systems, isotopic engines, and reactor-powered systems, are reviewed. (H.D.R.)

40363 HOW COOLANT DYNAMICS AFFECT FAST REACTOR SAFETY. Singer, Ralph M. Power Reactor Technol., 9: 46-50(Winter 1965-1966).

The probable sequence of events that would follow cooling loss or a power excursion in a fast reactor is examined. Specific mechanisms relating to coolant dynamics and heat transfer, including transient core heating and single-phase behavior, coolant vaporization, generation of pressure pulses, and coolant expulsion, are discussed. (H.D.R.)

40364 TECHNOLOGY OF CHEMONUCLEAR PROCESSES AND DESIGN OF CHEMONUCLEAR REACTORS. Costea, T. (Inst. of Atomic Physics, Bucharest). Stud. Cercet. Fiz., 18: 407-44(1966). (In Rumanian).

Design methods aiming at the determination of the dimensions of the reactor and of its mass make use of approximation techniques, such as the Monte Carlo method. Actual problems arising in the design of the various types of reactors are reviewed. Chemonuclear processes, such as the fixation of N_2, radiolysis of CO_2, production of ethylene glycol, phenol, and hydrazine are reviewed in detail, making recommendations concerning the needed pure and applied research in this field. (Review article, 42 references). (TTT)

Auxiliaries and Components

40365 IMPROVEMENTS IN OR RELATING TO SUPPORT ARRANGEMENTS. Fell, Christopher Brocklebank; Lockney, Eric Victor (to Nuclear Power Plant Co. Ltd. A.E.L.-John Thompson Nuclear Energy Co. Ltd.). British Patent 1,033,641. June 22, 1966. Filed Apr. 19, 1962.

An arrangement for supporting a body upon a supporting surface, for example a charge pan upon the core of a gas-cooled graphite-moderated reactor, includes a device located between the body and the supporting surface which is adapted to permit free relative tilting movement between the surface and the device about one lateral axis and between the body and the device about a further lateral axis not parallel to the first. The device comprises a tubular member having at each end an opposed pair of arcuate shaped protrusions with the pair at one end being disposed on a line at right angles to a line joining the pair at the other end. (B.L.M.)

40366 IMPROVEMENTS RELATING TO NUCLEAR REACTORS. Prince, Norman; Triggs, Geoffrey William (to United Kingdom Atomic Energy Authority). British Patent 1,035,129. July 6, 1966. Filed June 17, 1964.

A reactor design is provided that includes a number of registers associated with resilient loading means and that are adapted to locate fuel assemblies or other articles located within fuel channels. The reactor utilizes a solid block type moderator, and the fuel channels extending through the moderator are loaded and unloaded with fuel assemblies or other articles from one end of the channels only. The register device is retractable out of the fuel channel against the action of resilient loading means and is minimally stressed when the registers are withdrawn. (B.L.M.)

40367 METAL HEAT INSULATING STRUCTURAL MEMBERS. Beck, Ainslie Rogers; Marshall, Geoffrey Peter (to Nuclear Power Plant Co. Ltd. A.E.L.-John Thompson Nuclear Energy Co. Ltd.). British Patent 1,035,134. July 6, 1966. Filed Apr. 16, 1964.

A metal heat insulating structural member is provided that finds particular application in reactors having a concrete pressure vessel in which it is necessary to support a shield wall between the heat exchangers and the reactor core and on the base of the concrete vessel. The insulating structural member comprises a boss with a number of projecting rib members. The members support a load which exerts a compressive force upon the member acting in the direction of the axis of its boss. The spaces between the ribs is packed with insulating material to provide thermal insulation against heat flow in the direction of the axis. Alternatively, two or more bosses and associated ribs may be arranged coaxially. (B.L.M.)

40368 METHOD OF FLUX SEPARATION IN NUCLEAR REACTORS AND STRUCTURE THEREFOR. Klahr, Carl N. U. S. Patent 3,255,083. June 7, 1966. Filed Dec. 26, 1962.

In a nuclear reactor with fission occurring predominantly at thermal energies and having two fuel regions of different enrichment, an internal reflector is interposed between and completely separates the two fuel regions. The reflector is of a material of sufficient thickness to maintain the thermal neutron flux within the first fuel regions adjacent to the moderator material at a level no more than one-half the thermal neutron flux within the second fuel regions adjacent to the reflector material. The first fuel regions have a maximum volumetric ratio of moderator material to fuel material of 1:2; while the same ration in the second fuel regions is 1:1. The use of the internal reflector allows the use of relatively inexpensive fuel elements without increasing the size of the reactor core and provides for a substantial increase in reactor lifetime without largely increasing the size or cost of the reactor and without increasing the difficulties in reactor control. (B.L.M.)

40369 RADIATION SHIELD ARRANGEMENT FOR NUCLEAR REACTOR. Clifford, Charles E.; Antonsen, Knud (to General Dynamics Corp.). U. S. Patent 3,255,085. June 7, 1966. Filed Jan. 31, 1961.

In a reactor system for irradiation purposes, a reactor core is supported within a tank filled with a suitable fluid, such as water, that serves as reactor coolant. An irradiation zone is provided outside the core and is exposed to fast neutron and gamma radiation from the core. A self-supporting radiation shield is so mounted that it can be moved vertically into and out of the path of the radiation from the core to the irradiation zone so that the intensity and/or character of radiation in the radiation zone may be changed. The shield is free standing upon the motive means and has no attachment to other parts of the reactor. (B.L.M.)

40370 BALL-TYPE CONTROL FOR A NUCLEAR REACTOR. Ryon, John W.; Schluderberg, Donald C. (to Babcock and Wilcox Co.). U. S. Patent 3,257,286. June 21, 1966. Filed Feb. 28, 1961.

A reactor control arrangement using balls of neutron absorbing material is described. A number of elongated conduits are positioned so that a first section of conduit is located within and passes through the core while an adjoining second section is located outside the core and above the first section. Each conduit holds a number of individual bodies composed of a neutron absorbing material which absorbs neutrons. A sufficient number of these bodies are placed in the first section of the conduit to at least partially fill it and to provide enough neutron absorber within the core to maintain it subcritical when all the bodies are located in that section of the conduit in the core. The bodies are moved by a source of pressurized fluid in communication with the conduits. By properly positioning the absorber bodies within the two sections of the conduit, the

reactor can be started up, shut down, or its reactivity controlled during reactor operation. (B.L.M.)

40371 DRIVE MECHANISM FOR A NUCLEAR REACTOR CONTROL ROD. Good, James A. (to Babcock and Wilcox Co.). U. S. Patent 3,257,287. June 21, 1966. Filed Apr. 6, 1962.

A rack and pinion control rod drive mechanism is described that does not require disassembly of the rack from the pinion for removal of the control rod. The control rod for which the drive mechanism is used is disposed in and is linearly positionable through the reactor core by means of the drive mechanism. The rack or rod drive is circular in cross section and is detachably coupled to the control rod. Teeth are cut on a helical or screw type pitch into the surface of the drive rod, and they matingly engage similar teeth cut in the surface of the pinion. The surface of the pinion engaging the drive rod is concave so that it can properly mesh with the rounded surface of the drive rod. A keeper extends into an opening in the drive rod to prevent its rotation as it is propelled by the pinion for positioning the control rod along its path of travel. (B.L.M.)

40372 NUCLEAR REACTOR CONTAINMENT SYSTEM. Malay, Frank L. (to Westinghouse Electric Corp.). U. S. Patent 3,258,403. June 28, 1966. Filed May 24, 1963.

A safety containment system for a reactor comprises two sealed liners or containers, one located within the other. The inner container contains the reactor, heat exchangers, primary cooling system, etc. The second container is spaced from the first container and encloses it. The space between the two containers is maintained at a pressure lower than that in the inner container or outside the outer container. In case of a rupture of the reactor cooling system, within the inner container, the cooling fluid and possible fission products escape from the reactor system into the inner container. The escaping fluid flashes into vapor, in the case of liquid coolant, or otherwise expands, fills and pressurizes the inner container. Any leakage from the inner container then flows into the space between the two containers and is pumped back into the inner container by means of pumps or compressors located either in the space between the two containers or outside both containers. This pumping back of any leakage creates a vacuum in the space between the two containers to prevent any leakage through the outer container to the atmosphere. (B.L.M.)

40373 BOILING DETECTOR EXPERIMENT /Q-2503/ (Engineering Materials). (Oak Ridge National Lab., Tenn.). (CAPE-1342).

1 drawing.

The boiling detector is a safety instrument used to protect the Oak Ridge Research Reactor. Two temperature controls are used to shut down heaters when the temperature is too high. Recorders provide temperature records. (For details see TID-4100). (F.S.)

Criticality Studies

Refer also to abstracts 39382, 40053, and 40384.

40374 (ACNP-63562) REACTIVITY EVALUATION OF SM-1 CORE III QUALIFICATION FUEL PLATES. Raby, T. M. (Allis-Chalmers Mfg. Co., Milwaukee, Wis. Atomic Energy Div.). June 24, 1964. Contract AT(30-1)-3106. 11p. Dep. mn. CFSTI $1.00 cy, $0.50 mn.

Production models of the SM-1 Core III stationary fuel plates were compared with the mockup elements used in initial core specification experiments. Tests were made to evaluate the reactivity difference between the mockup and qualification elements, to establish uniformity among the qualification fuel plates, and to establish that their ^{10}B loading falls within specified limits. (H.D.R.)

40375 (DP-1031) INTERACTION OF FISSILE UNITS. A COMPUTER CODE: INTERACT. Clark, Hugh K. (Du Pont de Nemours (E. I.) and Co., Aiken, S. C. Savannah River Lab.). June 1966. Contract AT(07-2)-1. 59p. Dep. mn. CFSTI $3.00 cy, $0.75 mn.

A FORTRAN code, INTERACT, is described which computes the k_{eff} for a group of fissile units surrounded by a reflector and the spacing between units required to make k_{eff} unity. A number of approximations are made to simplify the calculations. Comparisons with experiment are included and serve to normalize the calculations. The code may be used with confidence for nuclear safety applications. In addition to the dimensions and spacings of units and reflectors, the required input includes the material buckling, the bare extrapolation distance, the migration area of the fissile units, and the albedo of the reflector. (auth)

40376 THE PERSISTENT CHANGE IN THE MEASURED VALUES OF THE DECAY CONSTANT IN BERYLLIUM. Goyal, I. C.; Ghatak, A. K.; Kothari, L. S. (Univ. of Delhi). J. Nucl. Energy: Pt. A and B, 20: 667-70(Aug. 1966).

The time decay constant for a Be assembly at 30°C with a buckling $B^2 = 0.073$ cm^{-2} was studied using a multigroup approach with 30 energy groups. The time- and velocity-dependent neutron density were calculated. The results were compared with experimental observations. (D.C.W.)

40377 SEMI-EMPIRICAL FORMULA FOR THE CHANGE OF DIFFUSION COEFFICIENTS CAUSED BY EMPTY CHANNELS. Persson, R. (Aktiebolaget Atomenergi, Studsvik, Sweden). J. Nucl. Energy: Pt. A and B, 20: 671-3(Aug. 1966).

A single expression for the effect of empty channels on diffusion coefficients in reactors is derived. Theoretical predictions are compared with experimental observations on D_2O-moderated lattices of fuel assemblies with air coolant; good agreement is noted. (D.C.W.)

40378 THERMAL AND EPITHERMAL SPECTRUM MEASUREMENTS. Stanford, George S. Power Reactor Technol., 9: 80-100(Spring 1966).

The applications and limitations of differential and integral methods for measuring neutron spectra are discussed. Recent work with pulsed accelerators, mechanical choppers, and crystal spectrometers are reviewed for differential methods. Integral techniques are surveyed and available probe materials, various perturbations, and corrections required are discussed. Integral measurements in both well-moderated spectra and in hardened Maxwellian spectra are examined. The value of being able to predict accurately the neutron-energy spectrum in a reactor design is discussed and the techniques for measuring spectra in various experimental configurations are considered. (H.D.R.)

40379 MEASURING NEUTRON-FLUX DISTRIBUTION IN OPERATING REACTORS. Popper, Glenn F. Power Reactor Technol., 9: 25-34(Winter 1965-1966).

Reasons for making measurements of the neutron flux distribution within a reactor core are considered. Among the purposes are greater power, burnup uniformity, safety, and radiation monitoring. Measurement techniques, including activation methods, miniature ion chambers, gamma and neutron thermometers, and solid-state detectors, are reviewed. Advanced techniques and factors affecting the choice of methods are discussed. (H.D.R.)

40380 MULTI-GROUP COLLISION PROBABILITY THEORY IN CLUSTER GEOMETRY. COMPARISON WITH EXPERIMENTS. Jonsson, A.; Pekarek, H. (Aktiebolaget Atomenergi, Stockholm). 40p. (CONF-660204-18). ORAU. Gmelin, AED-CONF-66-017-16.

From American Nuclear Society Meeting, San Diego, Calif.

Cell calculations using multi-group collision probability theory in cluster geometry are compared with experimental thermal fine structures, spectral indices, and relative conversion ratios. The theoretical program was aimed at checking the reliability of above all thermal data for this type of calculations. Thus care was taken to avoid unnecessary approximations in the calculation of neutron transport. The cluster geometry is not homogenized and collision probabilities are calculated with a

method limited in accuracy only by the time spent on the computation. The results show that the data used are capable of reproducing experimental thermal fine structures to within their accuracy. Also, predictions of relative conversion ratios are not in contradiction with experimental evidence. (auth)

40381 UTILIZATION AND EFFECTIVENESS OF LINEAR ARRAYS OF NEUTRON-ABSORBER-FILLED TUBES AS CONTROL RODS IN WATER MODERATED NUCLEAR REACTORS. Fisher, John Raymond. College Park, Md., Univ. of Maryland, 1966. 167p.

Thesis.

An experimental and analytical investigation was made with the University of Maryland reactor to determine the reactivity worth of linear arrays of absorber-filled tubes as compared to solid slabs of the same material. Measurements were made as a function of tube diameter and spacing between the tubes in both an air and water environment. An analytical model was devised to correlate the experimental results; this was then applied to a typical water-moderated power reactor to determine the effect of spacing the absorber-filled tubes. Solid slabs of Ag–In–Cd, Boral, and cadmium and stainless steel tubes filled with Ag–In–Cd and B_4C were used for the measurements. The slabs varied in thickness and could be arranged in a close-packed linear array to form a slab, or could be arranged in a linear array with gaps between adjacent tubes. The reactivity worth of the samples was measured by placing them in a lucite box inserted into the center of the University of Maryland Reactor. Reactivity worths were determined from the difference in critical positions of the reactor regulating rod and reduced to the reactivity per unit area of an infinitely long and wide sample by means of a correction factor. The difference between the solid slab and close-packed array of tubes was found experimentally to be small, 5 percent for the smaller diameter tubes and negligible for the larger ones, in both an air and water environment. The effect of spacing was found to be a function of tube diameter as well as the width of the gap. The analytical model was applied to a typical large water reactor controlled by a solid cruciform of Ag–In–Cd and a cruciform of spaced tubes filled with Ag–In–Cd. For the particular case analyzed, it was determined that a reduction of 45 percent in absorber material could be accomplished with a reduction in the shutdown capability of only 0.8 percent Δk for the stuck rod condition. (TCO)

Fuels

Refer also to abstract 39353.

40382 (CEND–3107-267) BURNABLE POISON ADDITIONS TO UO_2. Progress Report, January 1–March 31, 1966. Brayer, R. C.; Christopher, S. S. (Combustion Engineering, Inc., Windsor, Conn. Nuclear Div.). May 1966. Contract AT(30-1)-3107. 25p. (EURAEC–1638). Dep. mn. CFSTI $1.00 cy, $0.50 mn.

Work Performed under United States–Euratom Joint Research and Development Program.

A 6% enriched UO_2 fuel rod, E-1, containing 500 ppm B_4C was irradiated in the Saxton Reactor to a peak burnup of 1070 Mwd/MTU at a peak specific power of 17.2 kw/ft. A second rod, E-4, is being irradiated to a burnup of 5000 Mwd/MTU. Nondestructive evaluation of Rod E-1 was completed and no defects or dimensional changes were found. Analyses of gases from the plenum of Rod E-1 revealed the presence of CO_2 in an amount consistent with that required to prevent the reaction, $UO_2 + B_4C \rightarrow UB_4 + CO_2$, from going to completion. Equipment was assembled to conduct the open and closed system, low temperature experimental runs aimed at confirming prior thermodynamic calculations concerning UO_2–B_4C reactions. A high temperature furnace was designed and is being fabricated for the high temperature studies. A low temperature (1150°C), short time (25 hours) open system test was completed. A thin film was found deposited on the furnace outlet and was analyzed by x-ray diffraction analysis. Of the four diffraction lines obtained on the film, two corresponded to the B_2O_3 pattern and the other two were unidentified. (auth)

40383 (EUR–2780.e) PROCEEDINGS OF THE CONFERENCE ON FUEL CYCLES ON HIGH-TEMPERATURE GAS-COOLED REACTORS, BRUSSELS, JUNE 10–11, 1965. Tytgat, D. (ed.) (European Atomic Energy Community). May 1965. 634p. (CONF-650606). Belgian American Bank and Trust Co., New York $12.00.

Separate abstracts were prepared for twenty-nine of the papers presented. Eleven abstracts were included in previous issues of NSA as 19: 22406, 25706, 25707, 25728, 25729, 33602, 34653, 38174, 44109, 20: 2226 and 14638. (H.D.R.)

For abstracts of individual papers see: 40388–40394, 40419–40421, and 40466–40473.

40384 (EURAEC–1660) NEUTRON STUDY OF PLUTONIUM IN THERMAL NEUTRON REACTORS. Final Report No. 1, December 18, 1960–August 31, 1964. (Commissariat a l'Energie Atomique, Paris (France)). Contract 037-60-12RDF. 236p. (EUR–2853). Dep. mn. CFSTI $6.00 cy, $1.25 mn.

Work Performed under Unites States–Euratom Joint Research and Development Program.

A series of theoretical and experimental studies are described on the reactivity evolution in U–Pu lattices moderated with graphite and heavy water. Experiments are carried out on the evolution of the fuel composition under known conditions of irradiation and on the effect of composition changes on the neutron balance. Preparation methods and procedures are described for the experiments and the results are tabulated. The experiments were of three basic types: irradiation of fuel followed by chemical and isotopic analysis, replacement experiments by U–Pu fuels, and oscillations of U–Pu fuels and irradiated fuels. Theoretical studies on neutron thermalization in multiplying media containing Pu are described. (H.D.R.)

40385 (ORNL-P-2327) CURRENT STATUS OF IRRADIATION TESTING OF THORIUM FUELS AT OAK RIDGE NATIONAL LABORATORY. Olsen, A. R.; Coobs, J. H.; Ullmann, J. W. (Oak Ridge National Lab., Tenn.). [1966]. Contract W-7405-eng-26. 30p. (CONF-660524-10). Dep. mn. CFSTI $2.00 cy, $0.50 mn.

From 2nd International Thorium Fuel Cycle Symposium, Gatlinburg, Tenn.

The sol-gel process production, fabrication procedures, and irradiation tests are summarized for pure or mixed compounds of Th, U, and Pu as oxides and carbides. Materials characteristics and irradiation behavior are described for both vibratorily compacted metal-clad bulk oxide fuels and pyrolytic carbon coated particle fuels. (H.D.R.)

40386 (SGAE-CH-33/1966) UNTERSUCHUNG UBER DIE SPALTPRODUKTVERTEILUNG IN DER BESCHICHTUNG VON BRENNSTOFFTEILCHEN FUR HOCHTEMPERATURREAKTOREN. (Study on the Fission Product Distribution in the Coating of Fuel Elements for High Temperature Reactors). Szterk, L.; Bildstein, H. (Oesterreichische Studiengesellschaft fuer Atomenergie G.m.b.H., Seibersdorf, Institut fuer Chemie). 1966. 28p. Dep. mn.

A method was developed for the determination of fission product distribution in the coating of fuel particles for high-temperature reactors, which permits a selective, stepwise dissolution of the various coating layers. By gamma spectrometry of the etching solutions fission product profiles can be determined. The basic development was followed by the application of the procedure on the investigation of two types of coated particles of PyC/SiC/PyC-coatings, irradiated to 16% fifa at a temperature of 1400°C max. As the cooling times of the samples were more than 1½ years, distribution could be determined only for long lived nuclides (Zr, Ru, Cs and Ce). (auth)

40387 (WAPD-T-1939) FUEL CLAD DESIGN BASIS FOR THERMAL REACTORS. Lustman, B. (Bettis Atomic

Power Lab., West Mifflin, Pa.). May 1966. Contract AT-11-1-GEN-14. 49p. (CONF-660531-1). Dep. mn. CFSTI $2.00 cy, $0.50 mn.

From 22nd High Temperature Fuels Committee Meeting, Pittsburgh.

The progress that has been made in arriving at a rotational fuel-clad design basis for Zircaloy-clad oxide fuel rods in a high temperature pressurized water environment is discussed, and existing problem areas are pointed out. Factors considered in the design are: interactions of cladding with environment, fuel-clad interactions, fuel-clad-environment interactions, and fuel operating temperature. (H.D.R.)

40388 FABRICATION METHODS AND COSTS OF FUEL ELEMENTS. Tytgat, D. (EURATOM, Brussels). pp 83-94 of EUR-2780.e.

Fabrication methods and costs of fuel elements for high temperature gas-cooled reactors are summarized from data presented in five papers on separate research projects. Two concepts of coated particle fuel elements are examined, the purged and the unpurged fuel elements, and compared both from technical and economic considerations. (H.D.R.)

40389 REPROCESSING OF NUCLEAR FUELS BY FLUORIDE VOLATILIZATION WITH SULFUR HEXAFLUORIDE. Knacke, O.; Laser, M.; Merz, E.; Riedel, H. J. (Kernforschungsanlage, Juelich, Ger.). pp 239-43 of EUR-2780.e.

A fuel reprocessing procedure based on the fact that U or U-containing fuels can be fluorinated in a single step to UF_6 with SF_6 at temperatures above 800°C was developed. The fuels are first pulverized and then fluorinated with pure SF_6 alone or in combination with oxidation agents in ovens. The procedure is simple and economical, and the SF_6 is noncorrosive up to high temperatures. The UF_6 formed can be decontaminated by the absorption-desorption technique on NaF columns. (H.D.R.)

40390 HEAD-END TREATMENT FOR THE REPROCESSING OF HIGH TEMPERATURE CARBIDE-GRAPHITE FUELS. Zuest, H.; Von Gunten, H. R.; Baertschi, P. (Eidgenoessisches Institut fuer Reaktorforschung, Wuerenlingen, Switzerland). pp 245-58 of EUR-2780.e.

Whole fuel elements are heated in an induction furnace and burned in O_2 and air. The resulting oxides of U, Th, and fission products are collected whereas the off-gases containing CO_2, O_2, N_2 and volatile fission products are cleaned in an off-gas treatment system consisting of a scrubber column, an electrostatic filter unit and an absolute filter. The installation has been successfully operated with inactive and slightly active Dragon-type fuel elements and is now ready for work with highly irradiated fuel specimens. (auth)

40391 BASIC STUDIES RELATED TO THE DEVELOPMENT OF THE SOL-GEL PROCESS. Van Der Plas, Th.; Noothout, A. J.; Hermans, M. E. A. (N. V. Kema, Arnhem, Netherlands). pp 275-88 of EUR-2780.e.

A review of the development of the KEMA Sol-Gel process is given. The external gelation method, in which NH_3 is added from the exterior to a sol droplet has been successfully used for 10 μm particles. It fails, however, for particles of larger size, viz., 250-1,000 μm. The use of an NH_3 donor, e.g., hexamethylene-tetramine, dissolved in the sol, leads to a successful preparation of particles of the larger size. A washing step, in which nitrate is removed, must be included in the procedure. Both oxide particles and oxide-carbon mixtures, ready for reaction and heat treatment can be prepared. A few data characterising hydroxide precipitates, sols and oxide particles are given, and photographs illustrate the influence of the composition of the washing liquid on the formation of defects in oxide particles. (auth)

40392 REPROCESSING AND REFABRICATION METHODS AND COSTS. Zifferero, M. (CNEN, Italy). pp 289-97 of EUR-2780.e.

Technical problems associated with reprocessing and refabrication of fuels for high temperature gas-cooled reactors are summarized, and the principal options for head end, decontamination, and refabrication processes are examined. Problems in the evaluation of fuel cycle costs are discussed. (H.D.R.)

40393 ^{235}U/THORIUM FUEL CYCLES IN GRAPHITE MODERATED SYSTEMS. Blomstrand, J. H.; Schloesser, J.; Bruneder, H.; Nyffenegger, U.; Graziani, G. pp 325-55 of EUR-2780.e.

Presented are results from calculations on both once-through and reprocessing fuel cycles. Different fuel management schemes have been considered. Fuel costs are evaluated for a wide range of values for the cost parameters involved. (auth)

40394 RANGE OF BURN-UPS AND CONVERSION FACTORS ECONOMIC ASSESSMENT. Schmidt, H. (Brown Boveri/Krupp, Mannheim, Ger.). pp 477-82 of EUR-2780.e.

Presented is a summary of data from papers on the use of Th fuel cycles in high temperature reactors and the technical and economic potentialities of this system. The implications of the use of this type of reactor in an intermediate and long range power program on a national or international basis are discussed. (H.D.R.)

40395 IMPROVEMENTS IN OR RELATING TO FUELS FOR NUCLEAR REACTORS. Glueckauf, Eugen (to United Kingdom Atomic Energy Authority). British Patent 1,033,393. June 22, 1966. Filed Jan. 30, 1962.

A reactor fuel composition for high temperature reactors consists of kernels of UC coated with a metallic carbide compatible with the UC. The term "metallic carbide" includes SiC. A thin layer of pyro-carbon can be disposed between the UC and the second metallic carbide, and/or an outer layer of pyro-carbon can be disposed over the second carbide layer. The coated kernels are disposed in a matrix of carbon or graphite to form a fuel compact or are encased in a sheath of C or graphite to form a fuel element. (B.L.M.)

40396 IMPROVEMENTS IN OR RELATING TO FUEL ELEMENTS FOR NUCLEAR REACTORS. Saunders, Alan Charles Anthony (to United Kingdom Atomic Energy Authority). British Patent 1,035,087. July 6, 1966. Filed June 3, 1965.

The fuel element sheath design described in British Patent 983,218, consisting of a herringbone fin configuration with a number of lugs projecting outward beyond the outer edges of the fins to contact the fuel channel walls to prevent bowing, is further modified to include elongated longitudinal ribs projecting beyond the edges of the fins but of less height than the lugs. The ribs function to impart added rigidity to the sheath to increase the resistance to bowing under irradiation and to improve the heat transfer by the sheath. (B.L.M.)

40397 IMPROVEMENTS IN OR RELATING TO FUEL ELEMENTS FOR NUCLEAR REACTORS. Tutte, Edward; Taylor, Anthony Francis (to United Kingdom Atomic Energy Authority). British Patent 1,035,487. July 6, 1966. Filed July 24, 1962.

An elongated fuel element for axial insertion into a coolant-conducting passageway of a graphite-moderated gas-cooled reactor carries at least three lateral-support members that are free to be displaced radially outwards by coolant flow along the passageway so as to reach the wall of the passageway and restrain any tendency toward coolant flow-induced vibration. The lateral-support members are carried at the end of the element that first enters the passageway and are provided with means biasing them radially outwards so that they move in that direction when acted upon by the coolant. (B.L.M.)

Power and Power-Breeder Reactors

Refer also to abstracts 39019, 39639, 39682, 39686, and 40374.

40398 (AEEW-M-631) A.G.R. STEAM DRUM EXPERIMENT. Collins, G. B. (Atomic Energy Establishment, Winfrith (England)). 1966. 38p. Dep. BIS $1.10. HMSO 5s. 6d.

Steady state and transient measurements made on a forced recirculation boiler steam drum are described, and conclusions are drawn concerning the steady state water subcooling and the dynamic behavior of the water and steam phases during transients. Attempts at parameter identification using a linearized model set up on an analog computer are described, and it is concluded that an asymmetric model is required to adequately describe both increasing and decreasing pressure effects. Further dynamic experiments are suggested using more refined measurement techniques. (auth)

40399 (AEEW-M-654) THE CONVERSION AND FAST FISSION RATIOS IN AN AGR CLUSTER COMPARISON OF EXPERIMENT AND THEORETICAL RESULTS. MacDougall, J. D. (Atomic Energy Establishment, Winfrith (England)). June 1966. 14p. Dep. BIS $0.50. HMSO 2s. 6d.

Comparison of calculations using the ARGOSY method with experimental buckling measurements on a large number of U and UO_2 fueled graphite lattices showed a systematic error, which could be largely removed by the expedient of decreasing the total resonance integral (4 ev to 10 kev) of the fuel by about 10% in the ARGOSY calculations. An attempt is made to confirm the validity of this reduction of the resonance integral by the interpretation of relative conversion ratio and fission ratio experiments. A reduction of 6 ± 3% in the resonance integral is found to be required to give agreement with experiment. This is in agreement with the 10% mentioned above when the hydrogen content of graphite is allowed for. (auth)

40400 (BNWL-244) FORMATION OF SELECTED FISSION PRODUCTS IN POWER REACTORS. Rohrmann, C. A.; Merrill, E. T. (Battelle-Northwest, Richland, Wash. Pacific Northwest Lab.). May 1966. Contract AT(45-1)-1830. 48p. Dep. mn. CFSTI $2.00 cy, $0.50 mn.

Revision of HW-78140.

Fission product production data are tabulated as a function of fuel exposure for specific reactor conditions. Calculated cross sections and potential large scale uses are listed for typical fission product isotopes. The production data were calculated using the ALTHAEA-MELEAGER computer code. The two groups of reactor parameters were based on a slightly enriched U PWR and on a similar PWR fueled with natural U enriched with Pu. (H.D.R.)

40401 (CEND-259) ADVANCED BONUS CORE THERMAL CYCLE TEST REPORT. Anderson, L. E.; Gibbons, J. F.; Grubelich, F. T.; Meinert, W.; Taylor, W. C.; Zuromsky, G. (Combusion Engineering, Inc., Windsor, Conn. Nuclear Div.). Dec. 1965. Contract AT(40-1)-3154. 197p. Dep. mn. CFSTI $5.00 cy, $1.00 mn.

A completely automatic thermal cycle test loop was designed and constructed to test advanced BONUS core fuel elements. A fixed tube sheet design and a floating tube sheet design of combination boiling-superheating fuel elements were fabricated and thermal cycle tested. The fuel elements were exposed to thermal cycles whose severity equalled or exceeded that which would occur in a normal reactor startup to full power and subsequent shutdown. The fuel elements performed satisfactorily for more than 2000 superheated steam temperature cycles from 500 to 1200°F without failure. (H.D.R.)

40402 (EUR-2993.d) ANALYSE DER ANLAGEKOSTEN VON KERNKRAFTWERKEN UND DIE MOEGLICHKEITEN IHRER SENKUNG. TEIL I UND II. (Analysis of Nuclear Power Plants Construction Costs and Possibilities of Reducing Them. Part I and II). (Technische Hochschule, Aachen (West Germany). Institut fuer Elektrische Anlagen und Energiewirtschaft). 1966. 332p. Dep. mn.

Direct construction costs are analyzed for nuclear power plants equipped with PWRs and BWRs in the 250–1200 Mw(e) range. Relations based on the construction cost estimates of plants being built or planned are developed for the estimation of costs within a certain power range. The cost of single construction elements dependent on the installed power of a plant is investigated, and possibilities to lower construction costs are discussed. Results of detailed analyses are given for six plants of different installed powers, and possible cost reductions are estimated. (H.D.R.)

40403 (EURAEC-1464) HYDRODYNAMIC INSTABILITIES LIMITING THE POWER OF BOILING WATER REACTORS. VOLUMES I AND II. Final Report. Boure, J. (Commissariat a l'Energie Atomique, Grenoble (France). Centre d'Etudes Nucleaires). June 1965. Contract 006-64-1TEEF. 509p. (EUR-2389). Dep. mn. CFSTI $7.00 cy, $2.25 mn.

Work Performed under United States–Euratom Joint Research and Development Program.

A bibliographic study is presented on the hydrodynamic oscillations phenomenon. This phenomenon occurs, under some conditions, in heated channels in which boiling of the fluid is allowed (such as nuclear reactors channels). It is shown that the understanding of the mechanism of these oscillations can only be obtained by means of very simplified models. Two such models are proposed but only one, the density effect model is studied here. A dimensional analysis is made on the equations of the model. The mechanism of the oscillations is demonstrated. Oscillations are sustained owing to the delays introduced by the density effect between a disturbance and its consequences on the mass, the center of mass, and the moment of inertia of the mass of fluid in the channel. This is shown on the integrated momentum equation. (auth)

40404 (GEAP-4496) CORE PERFORMANCE AND TRANSIENT FLOW TESTING [OF] BIG ROCK POINT BOILING WATER REACTOR. Hodde, J. A. (General Electric Co., San Jose, Calif. Atomic Power Equipment Dept.). July 1965. Contract AT(04-3)-361. 265p. Dep. mn. CFSTI $6.00 cy, $1.50 mn.

The results of extensive testing are presented. The tests included flow transient tests and measurements of the steady-state thermal-hydraulic performance of the reactor. The plant gross efficiency increased from 29.8% at 800 psia to 33.5% at 1500 psia at the expense of a reduction in the minimum critical heat flux ratio from 2.5 to 1.8. Quantitative measurements were made of power and flow distributions in the core. Pump trip tests were performed which showed the manner in which power and flow coast down to their natural circulation levels. Flow control and load following tests demonstrated that the automatic control of the reactor power by varying the recirculation flow is feasible and attractive. Schemes were developed for computing the steady-state core performance parameters and the transient following the loss of pumps for the Big Rock Point Plant. (auth)

40405 (HIT-3583-27) LOW ENRICHED PM REPLACEMENT CORE. EVALUATION OF CORE DESIGNS USING ALTERNATE PRESSURE VESSEL HEADS. (Hittman Associates, Inc., Baltimore, Md.). May 12, 1966. Contract AT(30-1)-3583. 37p. Dep. mn. CFSTI $2.00 cy, $0.50 mn.

Preliminary physics, heat transfer, and hydraulic analyses were performed on two alternate core concepts and compared to the reference design of the Low Enriched PM Replacement Core. An economic analysis of each alternate core design was prepared and compared to the reference design. The comparisons indicate that the alternate designs are generally inferior to the reference design in regard to cost, lifetime, and thermal performance. (H.D.R.)

40406 (NP-16181(Exh,B)(Vol.1)) INDIAN POINT NUCLEAR GENERATING UNIT NO. 2. PRELIMINARY SAFETY ANALYSIS REPORT. DESCRIPTION OF SITE AND ENVIRONMENT. (Consolidated Edison Co. of New York, Inc., New York). [1965]. 240p. (DOCKET-50-247(Exh.B)(Vol.1)). Dep. mn. CFSTI $6.00 cy, $1.50 mn.

The site and environmental data which together form a basis for the criteria for designing the Indian Point Unit No. 2 and for evaluating the routine and accidental release

of radioactive liquids and gases to the environment are presented. Extensive information is included on the location, topography, population and land usage, hydrology, meteorology, geology, seismology, and environmental radioactivity. (H.D.R.)

40407 (NP–16181(Exh.B)(Vol.2)(Pt.A)) INDIAN POINT NUCLEAR GENERATING UNIT NO. 2. PRELIMINARY SAFETY ANALYSIS REPORT. PLANT DESIGN DESCRIPTION AND SAFETY ANALYSIS. (Consolidated Edison Co. of New York, Inc., New York). [1965]. 248p. (DOCKET–50-247(Exh.B)(Vol.2)(Pt.A)). Dep. mn. CFSTI $6.00 cy, $1.25 mn.

Summary descriptions are given of the principal structures and equipment necessary for the safe operation of the Indian Point Unit No. 2. Extensive design and safety analysis data are presented for the reactor, reactor coolant system, containment system, and engineered safeguards systems. (H.D.R.)

40408 (NP–16181(Exh.B)(Vol.2)(Pt.B)) INDIAN POINT NUCLEAR GENERATING UNIT NO. 2. PRELIMINARY SAFETY ANALYSIS REPORT. PLANT DESIGN DESCRIPTION AND SAFETY ANALYSIS. (Consolidated Edison Co. of New York, Inc., New York). [1965]. 306p. (DOCKET–50-247(Exh.B)(Vol.2)(Pt.B)). Dep. mn. CFSTI $7.00 cy, $1.50 mn.

Descriptions are given of the principal structures and equipment necessary for the safe operation of the Indian Point Unit No. 2. Extensive design and safety analysis data are presented for the plant instrumentation and control systems, electrical system, auxiliary and emergency systems, steam and power conversion system, waste disposal system, and radiation protection systems. The safety of various plant systems under hypothetical accident conditions is evaluated. Appendices are included on high power level fuel rods, reactivity coefficients, and spatial stability of pressurized water reactors. (H.D.R.)

40409 (NP–16230) O.E.C.D. HALDEN REACTOR PROJECT. Sixth Annual Report, 1964/65. (Institutt for Atomenergi, Halden (Norway). OECD Halden Reaktor Prosjekt). 194p. Dep. mn.

The experimental operation of the HBWR is covered for the period July 1, 1964 to December 31, 1965. Reactivity calculations were performed and a power level of 16 Mw was chosen to ensure sufficient excess core reactivity to mid 1966. A burnup program was undertaken to verify the validity of physics calculational schemes. Measurements of the spectral indices in the coolant channel were performed on two modified standard second charge fuel assemblies, and spectral indices inside the canning were measured for unirradiated fuel. Isotopic analysis of a burned fuel assembly was initiated. A dynamics program to investigate the hydrodynamic instability mechanism of boiling channels was undertaken. Boiling loop experiments were conducted with mockups of thin-walled U metal tubular fuel assemblies. Water chemistry experiments were conducted with a neutral moderator to investigate heavy water decomposition effects of D_2, O_2, N_2, and air. Heavy NH_3 was added to the moderator to observe NO_3^- formation in the coolant channels, the D_2 concentration below which NO_3^- formation starts, the ND_3 decomposition rate, and the effect of D_2 from decomposed ND_3 on the heavy water decomposition. Test fuel assemblies from the United Kingdom, Sweden, and Norway were irradiated under the experimental irradiation test program. Active fuel handling facilities were modified and a handling pond was constructed. In-core instruments were developed and used to measure assembly power, coolant velocity, void, steam quality, and slip ratio. Calibration techniques were developed, a high-speed data logger was purchased, and electronic equipment for data read-out was designed and constructed. The reactor operation was largely dictated by the test fuel irradiation program. Reactor availability was 64%. Modifications were made to control stations and improvements were made to plant and instrumentation. (H.D.R.)

40410 (NP–16251(Vol.1)) BROWNS FERRY NUCLEAR POWER STATION, TENNESSEE VALLEY AUTHORITY DESIGN AND ANALYSIS REPORT. (Tennessee Valley Authority, Knoxville). [1966]. 358p. Dep. mn. CFSTI $7.00 cy, $1.75 mn.

The description and analysis of a two-unit nuclear power plant to be located at the Browns Ferry site in Limestone County, Alabama, is presented. The plant will use single cycle, forced circulation, boiling water reactors with a gross power output of approximately 1,098Mw(e) per unit. Technical data descriptive of the plant design and an analysis of operational effects on the environs are presented in Vol. 1. Applicable pictures, drawings, plot and building elevation plans, sketches, and electrical and piping diagrams are presented in Vol. 2. (H.D.R.)

40411 (NP–16251(Vol.2)) BROWNS FERRY NUCLEAR POWER STATION, TENNESSEE VALLEY AUTHORITY DESIGN AND ANALYSIS REPORT. (Tennessee Valley Authority, Knoxville). [1966]. 296p. Dep. mn. CFSTI $6.00 cy, $1.50 mn.

Pictures, drawings, plot and building elevation plans, sketches, and electrical and piping diagrams of the proposed power plant are presented. Technical data descriptive of the plant design and an analysis of operational effects on the environs are presented in Vol. 1. (H.D.R.)

40412 (ORNL-TM–497) ANALYSIS OF FILLING ACCIDENTS IN MSRE. Engel, J. R.; Haubenreich, P. N.; Ball, S. J. (Oak Ridge National Lab., Tenn.). Aug. 16, 1966. Contract W-7405-eng-26. 36p. Dep. mn. CFSTI $2.00 cy, $0.50 mn.

During MSRE shut down, the fuel salt is drained from the core. Then, during a normal startup, the graphite and fuel are preheated and the control rods are positioned so that the reactor remains subcritical while it is being filled. Certain abnormal circumstances could result in criticality and a power excursion in the partially filled core. Various postulated incidents were surveyed and the worst case was analyzed in detail. This case involved selective freezing in the drain tanks to concentrate the U in the molten salt fraction. Physical restrictions on the fill rate and safety actions of control rods and gas control valves limited the calculated power and temperature excursions so that any damage to the reactor would be prevented. (auth)

40413 (TID–23257(Vol.1)) ENGINEERING STUDY FOR LARGE STEAM-ELECTRIC GENERATING UNITS APPLIED TO ARGONNE FAST BREEDER REACTOR STUDIES. VOLUME 1. PLANT DESCRIPTION. (United Engineers and Constructors Inc., Philadelphia, Pa.). Nov. 1, 1964. Contract W-31-109-eng-38; Subcontract 31-109-38-1717. 135p. Dep. mn. CFSTI $4.00 cy, $1.00 mn.

For Argonne National Lab., Ill.

The consulting engineering services in support of the Argonne Fast Breeder Reactor evaluation program are described. The objective was to develop the design and related costs for the steam-electric portion of large nuclear powered central stations. The general design, arrangement, thermal performance and installed cost for eight steam-electric generating visits are summarized. (R.C.K.)

40414 (TID–23257(Vol.2)) ENGINEERING STUDY FOR LARGE STEAM-ELECTRIC GENERATING UNITS APPLIED TO ARGONNE FAST BREEDER REACTOR STUDIES. VOLUME 2. DRAWINGS AND DIAGRAMS EQUIPMENT LIST. (United Engineers and Constructors Inc., Philadelphia, Pa.). Nov. 1, 1964. Contract W-31-109-eng-38; Subcontract 31-109-38-1717. 45p. Dep. mn. CFSTI $2.00 cy, $0.50 mn.

For Argonne National Lab., Ill.

Drawings and diagrams, arrangement drawings, systems diagrams and electrical single line diagrams for the various generation units contained in the Argonne fast breeder reactor study are presented. (R.C.K.)

40415 (TID–23257(Vol.3)) ENGINEERING STUDY FOR LARGE STEAM-ELECTRIC GENERATING UNITS

APPLIED TO ARGONNE FAST BREEDER REACTOR STUDIES. VOLUME 3. COST SUMMARY. (United Engineers and Constructors Inc., Philadelphia, Pa.). Nov. 1, 1964. Contract W-31-109-eng-38; Subcontract 31-109-38-1717. 32p. Dep. mn. CFSTI $2.00 cy, $0.50 mn.

For Argonne National Lab., Ill.

Cost estimates are given for four 500-Mw(e) and four 1000-Mw(e) steam-electric generating units operating at various temperatures and pressures. It was concluded that a 1000-Mw(e) unit operating at 2400 psig and 1000°F would be most economical. It was estimated that the cost per kilowatt (net) for this visit would be $44.98. (R.C.K.)

40416 (WCAP-2222-P) 1000 MWe SUPERCRITICAL PRESSURE NUCLEAR REACTOR POWER PLANT. Interim Report. (Westinghouse Electric Corp., Pittsburgh, Pa. Atomic Power Div.). [1963]. Contract AT(30-1)-2948. 109p. Dep. mn. CFSTI $4.00 cy, $0.75 mn.

Progress in the design of two types of reactor power plant is described for the Supercritical Once-Thru Tube Reactor concept. The condensing steam reheat reactor power plant has a heat rate of 8000 Btu/kwh and 540 annular fuel charged supercritical steam pressure tubes. The in-core reheat reactor power plant has a heat rate of 7,796 Btu/kwh, 440 annular fuel charged supercritical steam pressure tubes, and 208 rodded reheat pressure tubes. (H.D.R.)

40417 TECHNICAL REPORT ON THE WELDING OF A REACTOR FOR AN ELECTROTHERMONUCLEAR POWER PLANT. Tissi, C.; Popoli, G.; Paris, G. Acciaio Inossidabile, 29: 153-88(Nov.-Dec. 1962). (In Italian).

The pressure vessel constructed for the enriched U boiling water reactor of SENN is described. The welding techniques used are discussed. Basic considerations are made on the effect of dilution of the base metal of the pressure vessel. The effects of the pre- and post-welding temperatures are also considered. The welding techniques and temperatures for union welding are reported. Quality control of the welds is discussed. (J.S.R.)

40418 BASIC PRINCIPLES OF THE DESIGN AND PERFORMANCE OF THE GARIGLIANO NUCLEAR POWER PLANT. Lepore, R. Calore, 36: 256-70(1965). (In Italian).

The basic principles followed for the final plant design, their practical application, and the consequent most important decisions are examined. Design estimates are compared with the experimental results obtained during the startup tests and the first operating period. (auth)

40419 STUDIES ON THE REPROCESSING AND REFABRICATION OF HTGR FUELS IN THE OECD DRAGON PROJECT. Horsley, G. W.; Podo, L. A.; Wood, F. C. pp 121-44 of EUR-2780.e.

The aims of the Dragon Project fuel reprocessing studies are broadly outlined. Preliminary results of assessment and experimental studies on the head-end treatment of spent fuel elements commensurate with the centralized reprocessing requirements of an integrated HTGR power system of 10,000 Mw(t) are presented. Proposals for the decontamination of irradiated Th-U fuels by solvent extraction at the rate of 60-70 kg (Th-U) per day to produce either $UO_2(NO_3)_2$ solution for rapid fuel fabrication in a lightly shielded facility or $Th(NO_3)_4-UO_2(NO_3)_2$ solution for conversion to fuel in a heavily shielded facility are presented and discussed. Relevant results of experimental studies on the preparation of particulate oxide and carbide fuels by powder metallurgical and sol-gel techniques are presented and schemes for the refabrication of such fuels from high enrichment $UO_2(NO_3)_2$ and $UO_2(NO_3)_2-Th(NO_3)_4$ solutions are outlined. (auth)

40420 FUTURE FUEL REQUIREMENTS FOR ATOMIC POWER PLANTS. Wagemann, K. (Kernforschungsanlage, Juelich Ger.). pp 413-45 of EUR-2780.e.

Relations between the available reserves of fissile material and the expected requirements of nuclear energy are given. The amount of fuel necessary to cover these energy requirements is studied without taking into consideration certain reactor types. Calculational parameters are specific power, conversion ratio or doubling time, and date at which breeders will be available. The results are given as diagrams. (auth)

40421 PLUTONIUM FUEL CYCLE STUDIES FOR A LARGE HIGH TEMPERATURE GRAPHITE MODERATED REACTOR. Bruneder, H.; Haubert, P. pp 519-49 of EUR-2780.e.

Physics and optimization studies of large (1250 Mw; 10 Mw/m^3) Pu-fueled reactors are carried out. Either ^{238}U or Th is considered as fertile material. Complete core replacement is assumed. (auth)

40422 NUCLEAR ELECTRICAL POWER FOR CANAL CONSTRUCTION. McDonald, G. Corry (Sandia Corp., Albuquerque, N. Mex.). Mech. Eng., 88: No. 8, 22-8(Aug. 1966).

The use of nuclear reactors to furnish a portion of the electrical power required for the construction of a sea-level Isthmian canal is described. Interactions of nuclear and electrical power with the mining processes are also described. Cost estimates for electric power from nuclear reactors and conventional fuels are presented. It was concluded that nuclear power reactors can be used economically to furnish a minor portion of the electrical power required for sea-level canal construction. At the present time it appears that only about 20 to 30 Mw of reactor-generated power of a total required load of 3000 to 4000 Mw, may be economically furnished by nuclear reactors. (R.C.K.)

40423 NEAR-OPTIMUM SHUTDOWNS FOR NUCLEAR REACTORS. Fredsall, J. R. (Australian Atomic Energy Commission, New South Wales). Nucl. Appl., 2: 89-93 (Apr. 1966).

The general problem of determining the optimum-power reduction function for a reactor is a complex one that depends on the desired startup time, the Xe and I_2 concentrations, the variations in reactivity, and the purpose of the reactor in question. An analysis method embodied in the digital computer code SHUTDOWN makes possible the determination of near-optimum shutdown modes for most reactors. Determined functions compare favorably with available data for the Canadian NRU reactor and with solutions for the minimization of peak Xe problem found by using Pontryagin's maximum principle. (auth)

40424 SODIUM HEATED STEAM GENERATOR (Engineering Materials). (Babcock and Wilcox Co., Lynchburg, Va.). (CAPE-1363).

6 drawings.

The once-through Na-heated steam generator is the prototype of a 1000-Mw(e) steam generator. Operating Na pressure is 20 psig max. The full-power capacity is 25.2 Mw(e) with a design and operating load of ~86,750 lb/hr at full load. (For details see TID-4100). (F.S.)

40425 FUEL ELEMENT ASSEMBLY FOR THE ELK RIVER REACTOR (Engineering Materials). (Allis-Chalmers Mfg. Co., Milwaukee, Wis. Atomic Energy Div.). (CAPE-1437).

5 drawings.

The element is fabricated from borated stainless steel and the fuel material is sintered thoria-urania ceramic pellets. (For details see TID-4100 Suppl. 36). (F.S.)

40426 POWER REACTOR TECHNOLOGY. Volume 9, Number 2. Dutton, James J.; Lennox, David H.; Brown, Karl K.; Croke, Edward J.; Gold, Raymond; Schmeh, Barbara A. (eds.). One of the five Quarterly Technical Progress Reviews published for the Division of Technical Information, USAEC. Argonne National Lab., Ill., Spring 1966. 100p. GPO $0.70 Domestic, $0.90 Foreign.

Recent developments in reactor technology are reviewed. Included are new concepts and applications and research results, analysis, and experience with existing or new components and systems. (H.D.R.)

For abstracts of individual sections see: 40378 and 40427-40429.

40427 COMPRESSIBILITY AFFECTS FLOW INSTABILITY AND BURNOUT. Fauske, Hans K. Power Reactor Technol., 9: 65-8(Spring 1966).

Problems in evaluating accurately the burnout heat flux and flow instabilities in forced-convection boiling systems are examined. The importance of including compressibility effects when interpreting two-phase flow data is discussed. (H.D.R.)

40428 INTERPRETING THE FRENCH LIQUID-METAL-HEATED STEAM-GENERATOR PROGRAM. Smith, Fred A. Power Reactor Technol., 9: 69-73(Spring 1966).

Three designs to be tested in the U.S. liquid-metal steam-generator program are examined and compared to the French steam generator design. Basic differences in the French design are in a configuration of pipe headers and tubes rather than tubes and tube sheets in a shell design and in the construction materials for both water and sodium sides. Leak tests on NaK-water reactions are also discussed. (H.D.R.)

40429 DESIGN FORESIGHT CAN SIMPLIFY REACTOR MODIFICATION. Martens, Frederick H. Power Reactor Technol., 9: 74-9(Spring 1966).

Major modifications made to the Sodium Reactor Experiment, Big Rock Point Reactor, and the Heavy Water Components Test Reactor are examined. Two general lessons in reactor design are apparent from these experiences. The reactor-coolant inlet and outlet pipes should be sized to handle the maximum power that the reactor can accommodate and reactor-vessel internals should be designed to be removable. (H.D.R.)

40430 POWER REACTOR TECHNOLOGY. Volume 9, Number 1. Dutton, James J.; Lennox, David H.; Croke, Edward J.; Gold, Raymond; Schmeh, Barbara A. (eds.). One of the five Quarterly Technical Progress Reviews published for the Division of Technical Information, USAEC. Argonne National Lab., Ill., Winter 1965-1966. 63p. GPO $0.70 Domestic, $0.90 Foreign.

Recent developments in reactor technology are reviewed. Included are new concepts and applications and research results, analysis, and experience with existing or new components and systems. (H.D.R.)

For abstracts of individual sections see: 39941, 40362, 40363, 40379, 40431, and 40474.

40431 ADVANCES IN POWER-REACTOR SHIELD ANALYSIS. Mittelman, Philip S. Power Reactor Technol., 9: 19-24(Winter 1965-1966).

Techniques available for the analysis of reactor bulk shields are examined. Neutron- and gamma-leakage doses are studied using a variety of computer programs which combine a removal theory and multigroup diffusion theory. The RASH, NRN, MAC, NIOBE, and P_1MG methods are compared. Analysis of complex-geometry problems associated with ducts, plugs, and structural heating are handled using a point-kernel or Monte Carlo method. Principle characteristics of the 05R, FMC, ADONIS, and UNC-SAM programs are tabulated. (H.D.R.)

40432 METHOD AND APPARATUS FOR CONTROL OF A NUCLEAR POWER PLANT. Doroszlai, Pal (to Sulzer Brothers Ltd.). U. S. Patent 3,255,084. June 7, 1966. Priority date May 17, 1963, Switzerland.

A method is provided for controlling a nuclear power plant that includes a reactor, a heat exchanger, means to circulate reactor coolant in a closed cycle through the reactor and through the primary side of the heat exchanger, and means to drive a vaporizable working fluid through the secondary side of the exchanger and to a heat-engine load. The flow of the coolant in the cycle is changed directly with changes in the reactor exit coolant temperature. The flow of working substance through the exchanger is changed directly with changes in exchanger exit coolant temperature, and means are provided to vary directly the flow of working substance through the exchanger with the flow of reactor coolant. These flow controls serve to control the reactivity of the reactor. (B.L.M.)

40433 INTEGRAL NUCLEAR REACTOR-STEAM GENERATOR UNIT. Sprague, Theodore S.; Ammon, Johannes H. (to Babcock and Wilcox Co.). U. S. Patent 3,255,088. June 7, 1966. Filed Sept. 20, 1963.

A nuclear reactor for use in a steam generating system includes an upright wall forming a vertically elongated pressure vessel having an opening in the upper end. The opening is fitted with a removable closure, and an upright tubular baffle arranged in the pressure vessel is removable through the opening. The baffle coacts with the pressure vessel wall to form a downcomer passage and an upright central riser chamber. The baffle provides communication between the riser chamber and the downcomer passage at the upper and lower ends. A number of heterogeneous fuel elements are arranged as a core in the riser chamber. A fluid coolant circulates upwardly through the core and riser chamber and downwardly through the downcomer passage. A tube bundle is disposed in the downcomer passage and is at least partially offset from the perimeter of the pressure vessel upper end opening. The tube bundle has a maximum radial diameter less than the diameter of the pressure vessel opening and is so arranged to permit its radial inward movement upon removal of only the baffle. A vapor-liquid drum is attached to and supported by the pressure vessel at a position above the heat exchanger tube bundles to provide for the circulation of the secondary fluid in closed circuit between the tube bundles and the drum. (B.L.M.)

40434 NUCLEAR POWER REACTOR HAVING A HIGH, PROMPT NEGATIVE TEMPERATURE COEFFICIENT OF REACTIVITY. Clifford, Charles E.; Hopkins, George R.; West, Gordon B. (to General Dynamics Corp.). U. S. Patent 3,257,285. June 21, 1966. Filed Feb. 18, 1963.

A pressurized water power reactor having a high prompt negative temperature coefficient of reactivity comprises a pressure vessel, a quantity of water in the pressure vessel, and a reactive core within the water in the vessel. The reactive core includes a number of fluid-tight elongated tubes, each containing a solid homogeneous mixture of ZrH_4, fully enriched U, and lumped Er in the form of a wire disposed centrally in the solid homogeneous mixture. The ZrH_4 comprises a major proportion by weight of the mixture with the ratio of H atoms to Zr atoms being at least approximately 1.5 to 1. Tubes are spaced within the core to provide passageways surrounding each tube. A fuel-free region is provided in the core and means are included for causing water to flow through the fuel-free region and through the passageways in heat exchange relation with the tubes. (B.L.M.)

40435 NUCLEAR REACTOR HYDROPULSE SYSTEM. Silvers, John P. (to Avco Corp.). U. S. Patent 3,258,405. June 28, 1966. Filed Aug. 22, 1961.

A system is provided that will perform pumping or propelling functions in remote locations which would be difficult to achieve by conventional methods. The system, also capable of generating rotational power, includes a nuclear reactor having a fluid inlet and outlet opening and a core. The core of the reactor comprises a number of parallel, elongated fuel elements defining a number of fluid passages between them. The fuel elements are subcritical in the absence of liquid moderator and sufficiently critical in the presence of the moderator to cause a very rapid power rise, concomitant violent heating in the moderator and consequent high pressure in the reactor. A source of liquid moderator with means for permitting the moderator to flow into the core when it is subcritical and for permitting it to flow out of the core when it is critical are provided. A hydraulic motor having a fluid inlet and outlet opening is included in the system. First fluid conduit means interconnect the reactor fluid outlet opening and the hydraulic motor fluid inlet opening for supplying liquid moderator to the hydraulic motor, and a surge tank is in communication with this first conduit means. Second fluid

conduit means couple the hydraulic motor fluid outlet opening and the reactor inlet opening for supplying liquid moderator to the reactor. Heat exchange means are interposed in the second fluid conduit means for removing heat from the liquid moderator. This design provides a closed loop hydraulic system, such as a power generating system, which does not require a steam boiler, condenser, or turbine. (B.L.M.)

40436 OYSTER CREEK NUCLEAR STATION: DESIGN CONCEPT, CONSTRUCTION, AND TRAINING PROGRAM. Rees, D. R. (Jersey Central Power and Light Co., Morristown, N. J.); Huggins, R. A. 13p. (CONF-660429-3). ORAU. Gmelin, AED-CONF-66-098-1.

From American Power Conference, 28th Annual Meeting, Chicago.

The general design, plant layout, construction, and operation criteria are briefly described for the 540 Mw(e) Oyster Creek plant. The training program for operating personnel of the station is also discussed. (H.D.R.)

40437 USE OF A DIGITAL CONTROL COMPUTER IN A NUCLEAR POWER PLANT. Siddall, E.; Smith, J. E. (Atomic Energy of Canada Ltd., Toronto). 11p. (CONF-651063-1). ORAU. Gmelin, AED-CONF-65-330-1.

From Canadian Electronics Conference, Toronto.

The design and installation of a Control Data 636 digital computer to handle control and monitoring functions at the Douglas Point plant are discussed. (H.D.R.)

40438 AN ANALYSIS OF THE DYNAMIC BEHAVIOR OF DUAL PURPOSE POWER/DESALINATION NUCLEAR PLANTS. Saphier, D.; Wolberg, J. R.; Yiftah, S. 19p. (CONF-651005-7). ORAU.

From 1st International Symposium on Water Desalination, Washington, D. C.

A model of a dual purpose power/desalination nuclear plant is described and used to simulate operation for a variety of control systems and disturbances in the operating conditions. A comparison of the dynamic behavior of the plant to nuclear single purpose plants indicates the model is in working order. (H.D.R.)

40439 REACTOR STEAM CYCLES FOR DESALINATION. Chambers, S.; Hitchcock, A. 10p. (CONF-651005-5). ORAU.

From 1st International Symposium on Water Desalination, Washington, D. C.

The principles involved in the optimization of nuclear dual-purpose power-water plants are discussed assuming only modest advances in reactor and flash distillation plant technology. Comparisons between reactor types as sources of heat and economic considerations are examined. (H.D.R.)

40440 2ND FORATOM CONGRESS 1965. Nuclear Energy in Europe. From Raw Material to Electricity Grid, 29 September–1 October, 1965, Frankfurt on Main. Forum Atomique Europeen FORATOM. Bonn, Deutsches Atomforum e. V., 1965. 272p. (CONF-650976).

Information presented at the congress is summarized in five sections. Separate abstracts were prepared for each section. (J.R.D.)

For abstracts of individual papers see: 39101, 39332, and 40441–40443.

40441 PRESENT TYPES OF NUCLEAR POWER STATIONS. Jaroschek, K. (Technische Hochschule, Darmstadt, Ger.). pp 83-134 of 2nd FORATOM Congress 1965. Bonn, Deutsches Atomforum e. V., 1965.

A review of power stations in United Kingdom, France, Germany, Belgium, Austria, Switzerland, and Spain is presented. (J.R.D.)

40442 USE OF NUCLEAR POWER STATIONS IN THE ELECTRICITY GRID. Mandel, H. pp 135-88 of 2nd FORATOM Congress 1965. Bonn, Deutsches Atomforum e. V., 1965.

Discussions are summarized concerning replies to questionaires by FORATOM member countries on use of nuclear power. Most countries anticipate increase of nuclear power use by the seventies. It is noted that present development of nuclear power sources is less pronounced in countries where hydroelectric resources are greater. (J.R.D.)

40443 CONCLUSIONS CONCERNING THE FUTURE UTILIZATION OF NUCLEAR ENERGY IN EUROPE. Wirtz, K. (Kernforschungszentrum, Karlsruhe, Ger. Technische Hochschule, Karlsruhe, Ger.). pp 189-266 of 2nd FORATOM Congress 1965. Bonn, Deutsches Atomforum e. V., 1965.

The conclusions presented are based on surveys of national reports on nuclear power use and development, data on nuclear fuel requirements, and the cost structure of nuclear energy development. Future prospects for nuclear power are analyzed. (J.R.D.)

Propulsion and Space

See also ENGINEERING — Space Propulsion

Refer also to abstract 39023.

40444 (AED-C-22-06) BIBLIOGRAPHIES IN NUCLEAR SCIENCE AND TECHNOLOGY. SECTION 22: NUCLEAR SHIP PROPULSION. Paro, J. N. (comp.) (Zentralstelle fuer Atomkernenergie-Dokumentation, Gmelin-Institut fuer Anorganische Chemie und Grenzgebiete, Frankfurt am Main (West Germany)). June 1966. 48p. Dep. mn.

A compilation of 113 references is presented on the application of nuclear reactors and radioisotopes to surface and underwater ship propulsion. Author, report number, and subject indexes are included. (H.D.R.)

40445 (BAW-1225) ZERO POWER TESTS ON NS SAVANNAH CORE II. Batch, M. L.; Ball, R. M.; Farrar, J. P.; Poston, J. W. (Babcock and Wilcox Co., Lynchburg, Va. Critical Experiment Lab.). Feb. 1962. Contract AT(30-1)-2534. 255p. Dep. mn. CFSTI $6.00 cy, $1.25 mn.

The techniques used in performing a series of tests on Savannah Core II fuel elements are presented. Eight items were measured and are compared to similar zero power tests on Core I where appropriate. Measurements were made on: uniformity of elements, subcriticality of core, response of service instrumentation during core loading, rod pattern, shape of rod group sensitivity as a function of position, temperature coefficient, neutron flux mapping with specified rod patterns, and stuck rod margin. Detailed flux maps are presented for two rod patterns, and the partial water height method is compared with the B poisoning method of rod evaluation. (H.D.R.)

40446 (NAA-SR-11879) SNAP-10A THERMOELECTRIC PUMP. Final Report. Davis, K. A. (Atomics International, Canoga Park, Calif.). July 15, 1966. Contract AT(11-1)-Gen-8. 82p. Dep. mn. CFSTI $3.00 cy, $0.75 mn.

The pump used to circulate the NaK from the SNAP-10A reactor to the thermoelectric converter is described. The liquid metal dc conduction pump is powered by an integrally mounted thermoelectric generator. The development, manufacture, testing, post-test examination, and application in flight systems are described. (H.D.R.)

40447 (NAA-SR-11913) THE APPLICATION OF K-FACTORS FOR RELIABILITY EVALUATION OF TEST PROGRAMS. Anderson, R. H. (Atomics International, Canoga Park, Calif.). July 15, 1966. Contract AT(11-1)-Gen-8. 16p. Dep. mn. CFSTI $1.00 cy, $0.50 mn.

The basic concepts of K-factors are presented along with information on their application, and the constraints that must be considered in their use for reliability prediction. Their application in the reliability prediction for SNAP fuel elements is discussed in detail as well as case histories of their effective use in other work. The extensive trend towards the use of K-factors for the reliability prediction of space systems is reviewed. (J.R.P.)

40448 (NP–16217) PROVISIONAL GUIDE FOR THE CLASSIFICATION OF NUCLEAR SHIPS. (Nippon Kaiji Kyokai, Tokyo). 1964. 44p. Dep. mn.

Basic requirements are presented for the construction and survey of ships equipped with a nuclear reactor or reactors for main propulsion. (H.D.R.)

40449 (SAN–650–1) ORGANIC RANKINE CYCLE FEASIBILITY DEMONSTRATION PROGRAM. Quarterly Report, April 15–June 30, 1966. Linhardt, H. D. (Aeronutronic Div., Philco Corp., Newport Beach, Calif.). Contract AT(04-3)-650. 39p. Dep. mn. CFSTI $2.00 cy, $0.50 mn.

The performance potential of the organic Rankine cycle working fluid monoisopropylbiphenyl (MIPB) for long duration space power applications was evaluated. For durations less than 100 hours, the feasibility of achieving high component and cycle efficiencies when using MIPB as Rankine cycle working fluid was demonstrated. A 65-watt, 16-pound prototype engine demonstrated a high degree of confidence in overall performance for the development of 1.5 to 20 kw(e) MIPB power plants. Component efficiencies increase with increased power levels and the fundamental design of the organic MIPB power plant remains unchanged. This design consists of the forced recirculation boiler and the turbinemotor driven recirculation and system pump unit. Both were selected for prevention and control of fluid hot spots, and the minimization of connections and welds in order to eliminate oxygen loop contamination during ground testing. The analysis and preliminary design effort connected with the fluid properties evaluation are presented. Test loops have been sized to correspond to the operating conditions of 1.5 kw(e) power conversion system having a boiler exit temperature of 650°F and a condenser pressure of 1 psia. Each test loop consists of a forced circulation boiler with separator, regenerator, condenser, turbine-motor driven multipump, controls, instrumentation and a turbine simulation device. The test loops are designed for hermetic, unmonitored and continuous operation for 10,000 hours. The preliminary design of the 1000-hour endurance loop is presented, including cycle analysis and discussion of component selection. Finally, the test facility, the preliminary test plan, and the program schedule are discussed. (F.S.)

40450 (TIM–911) SNAP-50/SPUR ELECTROMAGNETIC PUMP PROGRAM: CONCEPT SELECTION AND STATUS REPORT. McConville, J. H.; Walton, J. W. (Pratt and Whitney Aircraft, Middletown, Conn. Connecticut Advanced Nuclear Engineering Lab.). May 28, 1965. Contract AT(30-1)-2789. 27p. Dep. mn. CFSTI $2.00 cy, $0.50 mn.

A 3200 cycle rectifier/conduction pump unit was selected as the most logical alternative to the frequency converter/motor pump under development for the SNAP-50/SPUR reactor coolant pump application. A direct-current conduction pump incorporating contoured magnetic pole pieces will be combined with a rectifier featuring high-current tunnel rectifiers to produce a light-weight, efficient, reactor coolant pump. (auth)

40451 ENERGETICS. 3. THERMOELECTRIC POWER. Klem, R. L.; Dingwall, A. G. F. (Radio Corp. of America, Somerville, N. J.). Mech. Eng., 88: No. 8, 36-40(Aug. 1966).

The integration of the thermocouple into devices that produce serious amounts of power is described. The use of semiconductors in place of "dissimilar metals" raises the efficiency to practical levels. Silicon-germanium thermoelements provide reliable sources of electrical power. The SNAP-10A power system is an important example of the use of SiGe thermoelements for space applications. (R.C.K.)

40452 CRITERIA FOR DESIGN OF ADVANCED DYNAMIC POWER GENERATING SYSTEMS. Lee, H. S. (Douglas Aircraft Co., Inc., Huntington Beach, Calif.). New York, Inst. of Electrical and Electronics Engineers, 1966, Paper No. 31PP66-364, 35p., $1.00. (CONF-660708–4). ORAU.

From IEEE Summer Power Meeting, New Orleans.

An analysis and evaluation of the Rankine and Brayton cycle conversion units for space applications and interplanetary vehicles demonstrate that the Brayton cycle system is less efficient than the Rankine system when operating between the same temperatures. The Rankine power-conversion cycle appears attractive for space application because of its high-operating efficiency, relatively low heat source temperatures, and rejection of waste heat at relatively high temperature. These features minimize radiator area thereby reducing the probability of meteoroid penetration. (F.S.)

40453 60 KW ALTERNATOR FOR THE SNAP 8 PROGRAM. Luddy, Charles T. (General Electric Co., Erie, Pa.); Nice, William A. New York, Inst. of Electrical and Electronics Engineers, 1966, Paper No. 31PP66-499, 26p. (CONF-660708–6). ORAU.

From IEEE Summer Power Meeting, New Orleans.

A reliable, long-life 80-kva alternator suitable for operation in a space environment was developed. The alternator is a solid rotor, brushless, homopolar conductor operating at 12,000 rpm and producing 120/208-v, 3 phase a-c power with a frequency of 400 cps. The alternator has a hermetically sealed frame. The angular contact ball bearings are oil lubricated with non-contacting dynamic seals. Other design features include: welded electrical connections, all metallic seals in the oil system, and the polyimideepoxy insulation system. (auth)

Research and Test Reactors

40454 (AD–636542) FAST NEUTRON SPECTRUM OF THE AFRRI TRIGA REACTOR. (General Dynamics Corp., San Diego, Calif. General Atomic Div.). Jan. 1966. Contract DA-49-146-XZ-337. 106p. (AFRRI-CR–66-2). CFSTI $4.00 cy, $0.75 mn.

Report originally issued June 1965.

The angular flux spectrum was measured in a non-multiplying spherical mockup of the TRIGA reactor. Measurements were made at various angular positions in the energy range of 0.1–15 Mev. The experimental techniques and equipment are discussed. Calculations of the spectrum are done with the S_n transport code GAPSLN and compared to the experimental data to decide on the angular mesh, order of anisotropic scattering approximation, energy grouping, and cross sections for a similar calculation of the critical TRIGA reactor spectrum. Results of the calculated cylindrical geometry, cross sections, angular flux spectrum, and total leakage spectrum at the surface of the reflector are tabulated. (H.D.R.)

40455 (BNL–10454) ENGINEERING PROBLEMS IN PULSED NEUTRON SOURCES. Hoffman, K. C.; Parsick, R.; Reich, M.; Levine, M. (Brookhaven National Lab., Upton, N. Y.). Aug. 1966. Contract AT(30-2)-Gen-16. 21p. (CONF-660914–1). Dep. mn. CFSTI $1.00 cy, $0.50 mn.

For Presentation at Seminar on Intense Neutron Sources, Los Alamos, N. Mex.

Design studies were made for two high-performance repetitively pulsed neutron sources; an advanced pulsed fast reactor, and an advanced accelerator-booster system. The major engineering problems associated with each type of device, a description of the method of analysis, and a summary of the analytical results are discussed. The advanced pulsed reactor studied has an average power of 30 Mw in a 20 liter core producing 1.1 Mw-sec bursts of energy with a repetition rate of 22 bursts/sec. The total leakage neutron yield per burst is 5×10^{16} with a burst width at half power of 60 μsec. The advanced booster concept has an average power of 9 Mw in a 6 liter core producing 160 bursts per second with .044 Mw sec of energy in each burst. The core assembly has a prompt multiplication of 250 and is driven by an electron accelerator that develops a 33 amp average current of 30 Mev electrons for 3 microseconds. The total leakage neutron yield is 2×10^{15} per burst with a burst width at half power of 6.5 μsec. Thermal, hydraulic, me-

chanical, and physics analyses of both systems are presented. The major engineering problems are encountered in the fuel elements and in the rotating assemblies containing fuel and reflector pieces for reactivity pulsing. Performance requirements for these components are evaluated and discussed. (auth)

40456 (DP–1049) THE HEAVY WATER COMPONENTS TEST REACTOR: SAFETY SYSTEMS, FUEL FAILURE DETECTION, AND STANDBY CONDITION. (Du Pont de Nemours (E. I.) and Co., Aiken, S. C. Savannah River Lab.). May 1966. Contract AT(07-2)-1. 38p. Dep. mn. CFSTI $2.00 cy, $0.50 mn.

Three papers describing separate phases of the HWCTR operating program are included. Separate abstracts were prepared for two of the papers and the third was abstracted previously as NSA 19: 35846. (H.D.R.)

For abstracts of individual papers see: 40457 and 40458.

40457 (DP–1049, pp 1-19) PERFORMANCE OF THE HWCTR SAFETY SYSTEMS. Ross, C. P. (Du Pont de Nemours (E. I.) and Co., Aiken, S. C. Savannah River Lab.). (CONF-650710-3)

From American Nuclear Society, Meeting on Reactor Operating Experience, Jackson Lake Lodge, Wyo., July 28-30, 1965.

The role of HWCTR safety systems that provide a defense against abnormal operation accidents are discussed. The design features, testing procedures, and possible areas of concern for the safety rods, poison injection, pressure relief, and containment systems are described. (H.D.R.)

40458 (DP–1049, pp 21-31) AN INSTRUMENT FOR LOCATING FAILED FUEL ELEMENTS IN THE HWCTR. Vandervelde, V. D. (Du Pont de Nemours (E. I.) and Co., Aiken, S. C. Savannah River Lab.).

Four of the instrument systems to detect the existence and position of foiled fuel elements in the original HWCTR design are described and their deficiencies are noted. A prototype instrument, the fixed window gamma monitor (FWGM), was installed and tested in the HWCTR for eight months. The FWGM used a photomultiplier probe to monitor the sample stream from the effluent of each test element in sequence and properly identified the location of two oxide fuel element failures. Design of an improved failure location instrument that incorporated the FWGM electronic system was completed shortly before HWCTR shutdown. (H.D.R.)

40459 (GEMP-152) NUCLEAR TEST GAUGE SAFETY ANALYSIS REPORT. Bermanis, H. L. (General Electric Co., Cincinnati, Ohio. Nuclear Materials and Propulsion Operation). Dec. 28, 1962. Contract AT(40-1)-2847. 52p. Dep. mn. CFSTI $3.00 cy, $0.50 mn.

The Nuclear Test Gauge (NTG) is a subcritical assembly used to measure nuclear characteristics of reactor materials. The NTG is described and the operational and administrative features designed to assure its safe operation are outlined. Estimates of the biological consequences of an accidental NTG power excursion are given which indicate that the operation of the NTG does not constitute an unacceptable hazard to the public. The biological insult following a maximum credible accident is estimated to produce no lethal or even clinically provable injury to the public. (auth)

40460 (IDO–17191) NUCLEAR TECHNOLOGY BRANCHES QUARTERLY REPORT, OCTOBER 1–DECEMBER 31, 1965. (Phillips Petroleum Co., Idaho Falls, Idaho. Atomic Energy Div.). June 1966. Contract AT (10-1)-205. 56p. Dep. mn. CFSTI $3.00 cy, $0.50 mn.

Detailed measurements in the ATR Critical Facility (ATRC) show that flux depression in ATR fuel plates is insignificant. Replacing the 35 kg ^{235}U core in the ATRC with a new 39 kg core resulted in a net increase in excess reactivity of 3.8$, 0.4$ of which was due to the side plate vents in the new fuel elements. A high-temperature, high-pressure loop was installed in the ATRC, and all operational tests were completed. The average temperature coefficient of this loop is approximately $4 \times 10^{-4}$$/°F. Analyses of the thermal-hydraulic-structural performance of the ATR driver fuel elements indicate that an element operating at the maximum power density in either a 40 or 50 Mw lobe probably will be satisfactory. The performance of that element operating at the maximum power density in a 60 Mw lobe is questionable since the yield stress of the unirradiated cladding material is exceeded over the span of the hot plate. Further efforts to assess this result are underway. An attempt to measure the channel thickness in a spent ETR fuel element was made. Pb shielding was introduced in the microprobe and was found to reduce the background noise level from radioactive specimens by 80 to 90 percent. Maximum benefits from the shielding require the selection of the proper spectrometer crystals to diffract the desired x-ray wavelengths in the intermediate-to-high 2θ range. Electron fractography of MTR lattice Be tested under both compressive and Izod loading showed no effect due to the manner of testing, but post-irradiation, pretest annealing caused a slight decrease in the amount of He observed within the grains and a marked increase in the amount of He observed in the grain boundaries. Two versions of the Monte Carlo Program, PMC, are presently complete and are available to solve difficult transport theory problems. Both versions have the same geometry subroutines which enable the program to handle difficult three-dimensional geometries without approximation. In the first version, constant multigroup or few-group cross sections are supplied from pre-calculated data. In the second version, a resonance calculation is performed for particles which traverse the resonance range based on single-level, Breit-Wigner resonance parameters supplied in the input. In both versions, a statistical analysis of all data is incorporated with the output subroutines. The program is written for the IBM 7040 computer. (auth)

40461 (NASA-TN–D-3552) HEAT-TRANSFER ANALYSIS OF THE PLUM BROOK REACTOR. Reilly, Harry J.; Baumeister, Kenneth J.; Altomare, Salvi (National Aeronautics and Space Administration, Cleveland, Ohio. Lewis Research Center). Aug. 1966. 32p. CFSTI $2.00 cy, $0.50 mn.

A heat-transfer analysis of the Plum Brook Reactor core was performed to determine fuel-plate surface temperatures, heat fluxes, and the departure-from-nucleate-boiling ratio during full power operation. The hot-spot–hot-channel method was employed. The heat-flux distributions in the coolant channels were based on the measured low-power neutron-flux distributions in the cold clean core and in cores containing partially depleted elements. A statistical method was employed to determine the effects of engineering uncertainties on the reactor heat transfer. The calculations include the effects of asymmetrical cooling of the fuel plates and fuel lumping at the ends of the fuel plates. A flow coastdown study was performed to determine the required responses of reactor instrumentation following a loss of the main coolant pumps. The calculations were done for the hot spot located by the steady-state analysis. The results indicate that the analytical methods described give more realistic estimates of the heat-transfer margin during operation at 60 Mw(t) than would be obtained with conventional methods. The observed performance of the reactor indicates that the methods used are sufficiently conservative to ensure the safety of the reactor. (auth)

40462 (NIJS-R–474) HAZARDS SUMMARY REPORT FOR THE TRIGA MARK II REACTOR AT THE NUCLEAR INSTITUTE JOZEF STEFAN IN LJUBLJANA. Gabrovsek, Z. (ed.) (Nuklearni Institut Jozef Stefan, Ljubljana (Yugoslavia)). Jan. 1966. 69p. Dep. mn.

A hazards analysis is presented for the TRIGA Mark II training and research reactor to be installed at the Reactor Center in Ljubljana. Characteristics of the site and environment, reactor building design, reactor description and operational hazards, external hazards, operational procedures, radiation protection, and administrative control procedures are discussed. (H.D.R.)

40463 (UCRL–14413) THE FRAN PROMPT BURST REACTOR. Stillman, D. B.; Mead, S. W. (Lawrence Radiation Lab., Univ. of California, Livermore). Sept. 29, 1965. Contract W-7405-eng-48. 37p. Dep. mn. CFSTI $2,00 cy, $0.50 mn.

The FRAN Prompt Burst Reactor is a cylindrical oralloy assembly that can be driven super-critical for the production of short self-limiting fission bursts. Its characteristic feature is an internal annular void into which samples can be introduced for irradiation. Burst operation was begun in the latter part of 1962 and interrupted for an indefinite period in April 1965 after approximately 180 bursts. The largest burst resulted in a central fuel temperature increase of 375°C and a total yield of 5.6×10^{16} fissions. (auth)

40464 (UJV–1180/64) WASSERAUFBEREITUNG DURCH DIREKTE LiOH-ZUGABE. (Water Treatment by Direct LiOH Addition). Rypar, V. (Ustav Jaderneho Vyzkumu, Ceskoslovenska Akademie Ved, Rez). 1964. 6p. (CONF-641134–1). Dep. mn.

From Symposium on Water Problems in Nuclear Reactors, Rossendorf, Ger.

The water of the open primary circuit shows a tendency to acidification during operation with damaging results. Three methods are discussed for pH control. Direct LiOH addition was used as the simplest means for the pH control of the water. This precaution does not essentially modify the water conductivity. (tr-auth)

40465 (UJV–1181/64) DIE VORBEREITUNG VON WASSERWIRTSCHAFT FUER LEISTUNGSERHOEHUNG DES REAKTORS WWR-S. (Water Management for Power Increase in the WWR-S Reactor). Rypar, V. (Ustav Jaderneho Vyzkumu, Ceskoslovenska Adademie Ved, Rez). [1964]. 6p. (CONF-641134–2). Dep. mn.

From Symposium on Water Problems in Nuclear Reactors, Rossendorf, Ger.

The water parameters are affected by power increases. The O_2-H_2 gas formation was considered in connection with the power. For continuous water filtration, an arrangement and construction of the filter is given. On the basis of the discussion of methods of surface preparation of Al constituents the boiling of the Al construction pieces in water to form a thin protective layer is described. For protection against corrosion in the secondary circuit ordinary water with inhibitors is used. (tr-auth)

40466 THE COST OF COATED PARTICLE FUEL FOR A HIGH TEMPERATURE REACTOR PROGRAMME. Huddle, R. A. U.; Price, M. S. T.; Houdaille, M.; Popp, W. G. pp 1-26 of EUR–2780.e.

In order to indicate the areas where further experimental effort is likely to prove most effective in reducing fuel costs, a cost estimate based on the experience gained during the manufacture of fuel for the first charge of the Dragon Reactor Experiment has been carried out. A typical fuel specification has been selected for detailed cost analysis. It involves the fabrication of green particles by a powder metallurgy route, reaction sintering and coating with a complex layer of pyrocarbon/SiC/pyrocarbon deposited in a fluidized bed. If fueled compacts are to be employed, the coated particles are overcoated with an appropriate matrix material and pressed directly to the required shape. The detailed cost estimate is based on feed of such a fuel in a 2,000 Mw(e) reactor program. (auth)

40467 FUEL DEVELOPMENT FOR THTR. Spener, G.; Hrovat, M.; Rachor, L. (Nuklear-Chemie und-Metallurgie G.m.b.H., Wolfgang, Ger.). pp 51-60 of EUR–2780.e.

Several types of spherical graphite fuel elements are under development for the Thorium High Temperature Reactor. Pyrolytic carbon coated particles serve as fuel. One type is a graphite sphere with an annular or spherical gap which is loosely filled with coated particles. A second type is a hollow sphere which contains a thin layer of coated particles on the inner wall of the sphere and graphite in the remaining hole. The shell consists of electrographite with high strength, especially high drop strength, and good heat conductivity. A synthetic fuel ball prepared by heating a molded mixture of coated particles, graphite powder and binder to 1600°C is the third type element. A graphite matrix of good properties was developed. Irradiation experiments in the Risø Reactor in Denmark performed with hollow sphere fuel elements at 2.4 kw and a burn-up to 20%, showed good stability and low temperature differences between the surface and the center. (auth)

40468 DESIGN AND FABRICATION OF THE ARBEITS-GEMEINSCHAFT VERSUCH-REAKTOR (AVR) INJECTION-MOLDED FUEL ELEMENT. Eatherly, W. P.; Burkett, M. N. (Union Carbide Corp., Lawrenceburg, Tenn.). pp 71-81 of EUR–2780.e.

A description of the evaluation of various coated particle fuel element designs in terms of unique AVR requirements, previous reactor tests on materials to be used, present state-of-the-art, economics, and AVR time schedule are discussed. It is concluded that, within the above parameters, the injection-molded element has the greatest potential for success. The injection-molding process and its unique features which make it so suitable for use in fabricating the AVR fuel elements are described in some detail. Advantages of one modification of the injection-molded element, the unfueled-center design, are also discussed. A number of cost considerations in fuel fabrication are pointed out, emphasizing the role payed by quality assurance provisions, either in design, specifications, or testing requirements. (auth)

40469 ^{235}U FUELED THERMAL HIGH TEMPERATURE REACTOR WITH ^{233}U IN EQUILIBRIUM STATE WITH ^{232}Th AS THE FERTILE SPECIES. Brandes, S. (Kernforschungsanlage, Juelich, Ger.). pp 371-88 of EUR–2780.e.

Presented are the description and the results of calculations for favorable operating conditions of a ^{235}U fueled, graphite-moderated, He cooled high temperature reactor with ^{232}Th as fertile material supposing equilibrium state of ^{233}U in Th at all times (THTR-Project). The conversion factors and special defined fifa-values are calculated on the basis of present nuclear cross-section data. (auth)

40470 FUEL CYCLES OF THE THORIUM-HIGH-TEMPERATURE-REACTOR THTR. Giesser, W. (Brown Boveri, Krupp Reaktorbau G.m.b.H., Duesseldorf, Ger.). pp 389-99 of EUR–2780.e.

Equilibrium fuel cycles of the U–Th-graphite system are studied. The fuel cycle costs are estimated for different specific fabrication and reprocessing costs. (auth)

40471 BREEDING IN PEBBLE-BED REACTORS. Dreisvogt, H.; Schulten, R. (Technische Hochschule, Aachen). pp 399-412 of EUR–2780.e.

The conversion factor of a high temperature thorium reactor of the pebble-bed type is given with respect to the produced daughter elements, the poisioning by the fission products and the neutron leakage. The separate consideration of fissile and fertile materials allows the computation of the conversion factor as a function of the distinct life-time of these two element types. For a fuel element life-time of half a year and a breeding element life-time of one year, the conversion factor was calculated as $C = 1.04$. The proper doubling time for the fissile material is less than 20 years. (auth)

40472 REVIEW OF THE STUDIES MADE ON THE UTILISATION OF PLUTONIUM IN THE HIGH TEMPERATURE REACTOR. Gratton, C. P. (United Kingdom Atomic Energy Authority, Winfrith, Eng.). pp 559-66 of EUR–2780.e.

Discussed are the reactor physics studies carried out during 1961-1962 at A. E. E. Winfrith on the utilization of Pu in the High Temperature Reactor. The calculational model is described with particular reference to the ^{240}Pu isotope. Temperature coefficients, long term reactivity changes and fuel cycle aspects of the design are considered. (auth)

40473 SOME ASPECTS OF THE USE OF Pu IN HIGH-TEMPERATURE REACTORS. Massimo, L. (Euratom Joint Nuclear Research Center, Ispra, Italy). pp 567-82 of EUR-2780.e.

Physical problems involved in the study of Pu fuel in High Temperature Graphite Reactors and the methods of calculation used are examined. Batch loading fuel cycles in this type of reactor are studied, considering different moderation ratios and fuel lumpings. (auth)

40474 UHTREX OPERATION NEAR. Hoglund, Barton M. Power Reactor Technol., 9: 51-63(Winter 1965-1966).

The Ultra High Temperature Reactor Experiment, a 3 Mw(t) He-cooled graphite moderated reactor, is described. Unique features of its design are: a rotatable annular core to facilitate refueling during reactor operation, articulated control rods that can be inserted directly into the core regardless of its angular position, simple graphite fuel elements that promise fuel economies and lead to normal operation with a contaminated primary coolant, and use of an extensive on-line coolant-cleanup system. (H.D.R.)

40475 DESCRIPTION OF THE DYNAMIC BEHAVIOR OF A TRIGA REACTOR. Hornyik, Karl. [Urbana], Ill., Univ. of Illinois, 1965. 162p.

Thesis.

The nuclear, thermal, and hydraulic phenomena and a number of coupling mechanisms between them are described. These are heat generation by nuclear fission, temperature feedback of reactivity, convective cooling and finally, the buoyancy driving force due to temperature-induced density changes in the coolant. The nuclear flux states of the reactor are described by the well-known point model, whereas a suitable cell structure was chosen to represent the core in both the thermal as well as the hydraulic model. Distribution coefficients were introduced to describe the space dependency of the heat source. The total feedback reactivity was calculated from a weighted sum over all cell temperatures. The analytic formulation of the description resulted in a system of nonlinear ordinary differential equations. General solutions were obtained by numerical integration using a digital computer. A predictor-corrector method and a flexible scheme of approximation of the point kinetics equations were combined into a new, efficient, and general technique, which permits a severe reduction of computing time with practically no loss of accuracy. The experimental investigations carried out along with the development of the model were centered around direct reactivity measurements by analog computer techniques, water flow rate measurements at the flow channel exits with a rotor-type flow meter, and a number of temperature measurements in all parts of the core. It is concluded that the analytic description is in good qualitative agreement with all aspects of the actual system. (TCO)

WASTE DISPOSAL AND PROCESSING

See also BIOLOGY AND MEDICINE — Ecology
CHEMISTRY — Radiochemistry
CHEMISTRY — Separation Processes and Procedures
HEALTH AND SAFETY

Refer also to abstracts 38998 and 39103.

40476 (BNWL-267) FIXATION OF RADIOACTIVE RESIDUES. Quarterly Progress Report, January–March 1966. Platt, A. M. (ed.) (Battelle-Northwest, Richland, Wash. Pacific Northwest Lab.). May 1966. Contract AT(45-1)-1830. 30p. Dep. mn. CFSTI $2.00 cy, $0.50 mn.

A survey of properties of melts and solid products in the system PW-1 waste-Na_2O-P_2O_5 was made. The data obtained aided in defining flowsheets for spray calciner-melter processing of PW-1 waste with and without addition of melting-temperature-lowering constituents to the melter. A statistical study of the effects of variation in composition of a Purex-type waste has been completed but the data are only partially analyzed. All major Waste Solidification Engineering Prototype (WSEP) equipment has been installed in the Chemical and Materials Engineering Laboratory. Installation of services is 80% complete and preliminary equipment tests are underway. Plugging of the prototype immersion heater-circulator in plant tests resulted in an expedited experimental investigation of the causes, and the development of instrumentation for detecting flow in the circulator. An empirical correlation was developed relating maximum temperature in waste storage tanks to thermal conductivities and thicknesses of the salt cake and soil cover. Scintillation measurements with a prototype detector indicates this system can indicate sludge deposits in waste storage tanks. Quantitative extraction of strontium and rare earths from a Zirflex-type waste were achieved with D2EHPA solvent in pulse column studies. Two techniques for measuring ion exchange resin level are being developed. (auth)

40477 (HW-80056) THE EFFECTIVENESS OF A FINNED CIRCULATOR-EVAPORATOR FOR CONCENTRATING RADIOACTIVE WASTE. McElfresh, A. J. (General Electric Co., Richland, Wash. Hanford Atomic Products Operation). Dec. 23, 1963. Contract AT(45-1)-1350. 22p. Dep. mn. CFSTI $1.00 cy, $0.50 mn.

In-tank solidification of intermediate level wastes is accomplished initially using prototype equipment in a 200-E underground tank. Air at 1200°F provides the heat necessary to concentrate the solution by about a factor of 4, so that it solidifies on cooling. The heated air is forced down an annulus and rises outside and inside concentric pipes, acting as an airlift circulator. Heat transfer takes place through the walls of the pipes and by direct transfer from the air bubbles after the air enters the solution at the bottom of the annulus. The temperature of the air entering the liquid must be reduced to about 700°F to minimize entrainment in the off-gas. Heat transfer calculations and mock-up studies were performed to establish the design basis for the annular heat exchange surface. On the basis of this work, a finned surface was found necessary to provide adequate heat transfer rates. A fin design was developed and has subsequently been incorporated in the prototype design. (auth)

40478 (IN-1011) LEACHABILITY OF ALUMINA CALCINE PRODUCED IN THE IDAHO WASTE CALCINING FACILITY. Paige, B. E. (Idaho Nuclear Corp., Idaho Falls). July 1966. Contract AT(10-1)-1230. 26p. Dep. mn. CFSTI $2.00 cy, $0.50 mn.

Granular alumina calcine produced in the Waste Calcining Facility (WCF) at the Idaho Chemical Processing Plant (ICPP) was leached continuously in laboratory experiments with distilled water at 25°C and 80 to 90°C and in dilute (0.25 to 0.5M) nitric acid at 25°C. In a seven-week period, greater than 95% of the Cs and 33% of the Sr were leached from the amorphous WCF calcine with distilled water at 25°C. This leachability does not represent a hazard at the National Reactor Testing Station (NRTS) where the calcine is stored in stainless steel bins under dry climate conditions. The high leaching rate for Cs and Sr with distilled water does make recovery of these fission products potentially feasible because less than 0.01% of the Al is leached in a seven-week period. Based on initial rates, the leaching rates for Ce and Ru are estimated to be the same as the rate for aluminum from the calcine. At 80 to 90°C, the initial leaching rate for Al was the same as that at 25°C, but the total amount of Al leached was two to three times higher at the higher temperature after the first two days. The amount of Al leached is low enough that practical recovery of Cs and Sr appears feasible at the higher temperature. During six weeks of leaching the calcine with 0.5M HNO_3, the calcine disintegrated and more than 99% of the alumina dissolved; nearly 90% was dissolved in the first two days. Apparently, this reagent cannot be used for selective recovery of fission products from the amorphous calcine currently being produced in the WCF. Cesium, Sr, and Ce were leached at the same rate as Al, showing that these fission products were uniformly distributed in the calcine. (auth)

40479 (ORNL-P-2328) DILUTION, DISPERSION, AND MASS TRANSPORT OF RADIONUCLIDES IN THE CLINCH-TENNESSEE RIVERS. Parker, F. L.; Churchill, M. A.; Andrew, R. W.; Frederick, B. J.; Carrigan, P. H. Jr.; Cragwall, J. S. Jr.; Jones, S. L.; Struxness, E. G.; Morton, R. J. (Oak Ridge National Lab., Tenn.). [1966]. Contract W-7405-eng-26. 33p. (SM-72/3; CONF-660507-33). Dep. mn. CFSTI $2.00 cy, $0.50 mn.

From Symposium for the Disposal of Radioactive Wastes into Sea, Oceans, and Surface Waters, Vienna.

A comprehensive cooperative study, by state and Federal agencies and the Oak Ridge National Laboratory, of the fate of nuclides discharged to the Clinch River has been successfully concluded. Analyses of water samples indicated that the major radionuclides discharged to the Clinch River in the 20 years, 1944 through 1963, were ^{90}Sr, 1110 C; ^{137}Cs, 660 C; ^{106}Ru, 6600 C; TRE, 1240 C; and ^{60}Co, 270 C. A mass-balance analysis of the ^{90}Sr, ^{137}Cs, ^{60}Co, and ^{106}Ru in Clinch and Tennessee rivers below ORNL was made, covering a period of 2 years and 160 river miles. Water samples proportional to flow were analyzed for both radioactive and stable chemical elements. A good balance was found in the Clinch River between the input and output of radionuclides, except for ^{137}Cs. Tracer tests in the river show that dispersion at all flow rates causes practically uniform distribution of the radionuclides before reaching the water intake of the Oak Ridge Gaseous Diffusion Plant. Diffusion coefficients were calculated and a mathematical model formulated for the movement of radioactive materials through the Clinch River. By theoretical analyses and field tests, it was shown that the momentary minimum dilution of ORNL wastes in the Clinch River was reduced to a dilution factor of 54 for summer conditions and 17 for winter conditions at ORGDP. These minimum dilutions persist for very short periods of time. Results of the study were compared with those for other streams receiving low-level radioactive wastes. For the rivers investigated with low organic content and comparable velocities, it can be concluded that a catastrophic large-scale release of radioactive material already stored in the river system would not occur, even

as a result of major changes in flow, in pH, or in oxidation-reduction potential. (auth)

40480 (STI-PUB-119) THE MANAGEMENT OF RADIOACTIVE WASTES PRODUCED BY RADIOISOTOPE USERS. TECHNICAL ADDENDUM. Safety Series No. 19. (International Atomic Energy Agency, Vienna (Austria)). 1966. 86p. IAEA: $2.00; S42.-; 12/-stg; F Fr 8,-; DM 6,40.

Processes and procedures involved in the handling of relatively small quantities of waste arising from the use of radioisotopes in laboratories, hospitals, and industry are presented. Topics discussed are: types of waste associated with a number of radioisotopes; waste collection containers and systems; direct disposal of radioactives wastes to sewers; liquid-waste treatment techniques suitable for users of radioisotopes; solid-waste treatment and disposal by individual users of radioisotopes; and air-borne waste management. (32 references). (J.G.B.)

40481 (WAPD-T-1851) SHIPPINGPORT ATOMIC POWER STATION DISPOSITION OF RADIOACTIVE WASTE FROM UNDERGROUND STORAGE TANKS. Suchoza, B. P. (Bettis Atomic Power Lab., West Mifflin, Pa.). Nov. 1965. Contract AT(11-1)-Gen-14. 31p. (CONF-651101-52). Dep. mn. CFSTI $2.00 cy, $0.50 mn.

From 13th Conference on Remote Systems Technology, Washington, D. C.

The design of a station for the economical removal and subsequent disposition of radioactive wastes from the Shippingport Atomic Power Station is described. The station design includes the capability of temporarily storing some 3100 ft^3 of radioactive wastes in two underground storage tanks. The radioactive waste is basically spent demineralizer resin with some incinerator ash resulting from plant operations. The system design applies primarily to the removal of solid demineralizer resin. Any removal of incinerator ash is a consequence of the basic operation. After approximately seven years of plant operation, the underground storage tanks were essentially full and it was necessary to remove the radioactive waste in order to provide space for the acceptance and storage of additional waste discharges. In addition, performing this operation successfully made available a proven method for the transfer of such radioactive wastes from readily inaccessible underground tanks. (R.C.K.)

40482 SOME ASPECTS OF THE PUBLIC HEALTH HAZARD ASSOCIATED WITH THE STORAGE OR DISPOSAL OF GLASSES INCORPORATING HIGHLY ACTIVE FISSION PRODUCT WASTES. Freke, A. M. (United Kingdom Atomic Energy Authority, Harwell, Eng.). Health Phys., 12: 1077-86(Aug. 1966).

The continuing search for safer methods of storage or disposal of high active fission product wastes has led to techniques involving their incorporation in low leach matrices. One method under development at Harwell is the incorporation of fission product wastes, from the processing of irradiated fuel elements, in cylinders of borosilicate glass. That such a method should be superior, and adopted in preference to current methods of liquid storage, primarily depends upon the ability of the resultant glass to withstand the leaching action of water, thus permitting cheap storage under conditions of minimum maintenance. Conditions in the United Kingdom require guaranteed maintenance for some hundreds of years for storage of high activity fission products in liquid or soluble form. The degree of resistance to leaching action which the glass must possess may be calculated, so that any activity leached by water and subsequently returned to man does not expose him to a radiation hazard. Consideration of various methods of storage or disposal indicates that resistance to leaching needs to be several orders of magnitude greater than that currently obtainable in relation to proposed underground tunnel storage, unless sufficient maintenance is provided to ensure the absence of ground water from the tunnels for some hundreds of years or the control or dilution of any contaminated ground water leaving the tunnels. Current values are however adequate for pond storage with a bleed of contaminated pond-water to sea, and for disposal into areas of deep sea. (auth)

40483 REMOVAL OF LOW-LEVEL RADIOISOTOPES FROM WASTEWATER BY AEROBIC TREATMENT. Lawrence, C. H. (Univ. of Oklahoma Medical Center, Oklahoma City); Gilcreas, F. W. J. Water Pollut. Contr. Federation, 37: 1289-301(Sept. 1965).

A pilot-size waste-water treatment plant employing primary sedimentation, trickling filtration, secondary sedimentation, and lagooning was used to study extraction of ^{32}P, ^{131}I, ^{42}K, ^{141}Ce, ^{144}Ce, ^{59}Fe, ^{58}Co, ^{89}Sr, and mixed fission products (MFP). Primary sedimentation was relatively ineffective, less than 10% being extracted. The treatment efficiency of the overall process of trickling filtration, controlled by the removal accomplished by secondary sedimentation, was 60 to 70% for ^{59}Fe and ^{58}Co; 40 to 50% for ^{141}Ce, ^{144}Ce, and MFP; 25% for ^{42}K and ^{89}Sr; and less than 5% for ^{131}I and ^{32}P. The concentration of radioactive materials by zoogleal slimes in a trickling filter was also examined. The comparatively long detention time and algal-bacterial contact provided by lagoons are effective in diluting, delaying, and, in most cases, substantially removing slugs of low-level radioactive materials. Basins employing effective detention times of 2 to 3 days attain the following removals: 90% for ^{141}Ce, ^{144}Ce, and ^{59}Fe; 70% for ^{89}Sr; 50 to 60% for ^{32}P, ^{58}Co, and MFP; and less than 1% for ^{131}I. The mechanisms effective in the removal of radioactive materials by lagooning are precipitation by chemical, physical, and biological means, and ion-exchange reactions. These mechanisms are most effective in removing trivalent materials in their colloidal form and divalent elements biologically significant in trace amounts. To minimize groundwater contamination and to facilitate the removal of the accumulated radionuclides, lagoons used to treat radioactive wastes should be provided with impervious bottoms. (BBB)

40484 STUDIES OF THE APPLICATION OF VARIOUS METHODS FOR DECONTAMINATION OF RADIOACTIVE RESERVOIR WATER IN A HIGH POWER FAST FILTER SYSTEM. Baumgaertel, F. Brunswick, Technische Hochschule, 1964. 76p. $2.00 Gmelin, AED-Diss. 64-1086. Thesis.

Various methods for water decontamination are compared in regard to their application for high flow rate fast-filter decontamination. Decontamination factors with precipitation were lower than 50% for Sr nuclides. A combination of a sand filter with an ion exchanger is proposed giving a decontamination factor larger than 99.8%. (Gmelin Inst.)

GENERAL AND MISCELLANEOUS

40485 (AD–636091) RESEARCH IN PROGRESS, 1965. (Army Research Office, Durham, N. C.). 355p. CFSTI $7.00 cy, $1.75 mn.

A compilation is presented that describes research sponsored by the Chief of Research and Development. Other research described includes projects sponsored through this office by the Advanced Research Projects Agency, the Army Material Command, and the Defense Atomic Support Agency. The fields covered include: physics; chemistry; mathematics; engineering; and metallurgy and ceramics. Extensive principal investigator and subject indexes are included. (P.C.H.)

40486 (NASA-SP–82) PROCEEDINGS OF THE FIFTH NATIONAL CONFERENCE ON THE PEACEFUL USES OF SPACE HELD IN ST. LOUIS, MISSOURI, MAY 26-28, 1965. (National Aeronautics and Space Administration, Washington, D. C.). 1966. 199p. (CONF-650578). GPO $1.50.

Twenty-nine papers are presented on space exploration accomplishments, the space challenge, space exploration goals and future programs, space research influences on industry and the economy, space communication, space research impact on science and education, political implications of space exploration, impact on communications, the challenge of space, and space exploration opportunities and implications. (W.D.M.)

40487 (NP–16229) ATOMIC ENERGY PROSPECTS: THE OUTLOOK FOR BRAZIL AND FOR THE DEVELOPING COUNTRIES. do Prado, L. Cintra (International Atomic Energy Agency, Vienna (Austria)). 1966. 98p. Dep. mn.

A collection of papers is presented on prospects for the development of nuclear power in Brazil. Some general and specific problems are discussed with major emphasis placed on the economics of nuclear energy development. (H.D.R.)

40488 (ORNL–3957) ECOSYSTEMS, SYSTEMS ECOLOGY, AND SYSTEMS ECOLOGISTS. Van Dyne, George M. (Oak Ridge National Lab., Tenn.). June 1966. Contract W-7405-eng-26. 33p. Dep. mn. CFSTI $2.00 cy, $0.50 mn.

This paper defines and discusses ecosystems, systems ecology, and systems ecologists, in that order. Some properties of ecosystems and the ecosystem concept are given as a basis for defining the area of study called systems ecology. Problems, methods, tools, and approaches of systems ecology are considered in defining tasks, problems, and training of systems ecologists. The interdisciplinary nature of systems ecology research and the importance of computers in this research are considered. Examples of methods, concepts, and applications are drawn from a diverse body of ecological, natural resource management, and mathematical literature, which further illustrate the interdisciplinary nature of systems ecology. Advantages and limitations, with respect to total-ecosystem problems, of research by ecologists in universities, in state and federal experiment stations, and in national laboratories are compared. An example is given wherein, possibly under International Biological Program support, the skills and resources of these three groups of ecologists might be combined for integrated attack on nationally important ecosystem problems. (120 references.) (auth)

40489 (SC-DC–66-1118) CLEAN ASSEMBLY PRACTICES GUIDE. Fjelseth, D. E.; Davis, D. M.; Jones, L. K.; Schroeder, C. F. (Sandia Corp., Albuquerque, N. Mex.). Oct. 1965. Contract AT(29-1)-789. 56p. Dep. mn. CFSTI $3.00 cy, $0.75 mn.

A practical guide to clean assembly practices relating to manufacturing processes for high reliability precision components is described. Process requirements cannot be stated with the same precision as can dimensions, material characteristics, and their associated tolerances, but the guide does point out recurrent areas of process difficulties related to cleaning and suggests controls to minimize contamination. (R.C.K.)

40490 (Y–1483) AN INVESTIGATION OF THE MAGNETIC-PULSE FORMING PROCESS [Thesis]. Jones, F. W. (Union Carbide Corp., Oak Ridge, Tenn. Y-12 Plant). Dec. 2, 1965. Contract W-7405-eng-26. 111p. Dep. mn. CFSTI $4.00 cy, $0.75 mn.

Submitted to Univ. of Tennessee, Knoxville.

An investigation of the magnetic-pulse forming process, which is one of the newest methods of forming metals at high strain rates is described. A simple method is presented for measuring strain rates of tubular-shaped parts. The strain rate of the magnetic-pulse forming process has been determined and compared with other high-strain-rate processes such as explosive forming. Tubing has been bulged with the magnetic-pulse forming process from which calculations were made to determine the efficiency of the process. This efficiency has been compared with other high-strain-rate forming processes. The equations necessary for predicting the performance of this new forming process are summarized. Graphs of forming pressure versus stored energy are also presented. The problem of design and manufacture of forming coils is discussed in detail along with examples of coils that have been constructed and the experimental results of these coils. The limitations of this new forming process are presented along with examples of parts that are ideally suited for this manufacture process. (auth)

40491 PROGRESS IN NUCLEAR ENERGY. SERIES X. LAW AND ADMINISTRATION. VOLUME 4. Weinstein, Jerry L. (ed.). Progr. Nucl. Energy, Ser. X, 4: 1-402 (1966).

The new atomic laws in Western Europe and Japan are analyzed and the new international liability conventions — both world-wide and regional — are reviewed. Special emphasis is given to international developments since 1962. Among the more important topics discussed are criteria for reactor sites, the new U.S. law providing for private ownership of special nuclear material, and the application and experience of international safeguards systems. Full texts of all the international conventions and recent national laws on nuclear liability are given in the appendixes. (W.D.M.)

40492 THERMAL POWER STATIONS FOR THE ELECTRICITY AGE OF TOMORROW. Schroeder, Karl. Siemens-Z., 40: 379-90(May 1966). (In German).

The most important development lines of power technology up to its economic limits are outlined. Cost problems in the 1980's are summarized. An analysis is presented of energy conversion methods. The volume-limited outputs are derived. (J.S.R.)

CORPORATE AUTHOR INDEX

This index contains entries for this period for all report literature and, in addition, for certain published literature items for which it is felt that a corporate approach is especially desirable, e.g., symposia, conference proceedings, and meetings.

Each entry under a corporate author is a shortened version of the title of the publication, followed by the *NSA* volume and abstract number. Report numbers are given in parentheses.

The phrase "Progress report" is abbreviated as "Prog. rpt.," permitting a more rapid and complete alphabetical arrangement of the titles without changing the location of the progress report titles in relation to the other titles.

A

AERONUTRONIC DIV., PHILCO CORP., NEWPORT BEACH, CALIF.
Prog. rpt. on organic Rankine cycle feasibility demonstration, 4–6/66, 20: 40449 (SAN-650-1)

AEROSPACE RESEARCH LABS., WRIGHT-PATTERSON AFB, OHIO.
Lozier tube for ionization studies not involving mass analysis, · 20: 39167 (AD-636927)

AEROSPACE TECHNOLOGY DIV., LIBRARY OF CONGRESS, WASHINGTON, D. C.
Bibliography on high-purity metals, 20: 39328 (AD-624997)

AKTIEBOLAGET ATOMENERGI, STOCKHOLM (SWEDEN).
DETEC subprogram for simulation of fast-neutron detection process in hydro-carbonous plastic scintillator, 20: 39196 (AE-236)
Optimal linear air filters for pulse height measurements in presence of noise, · 20: 39195 (AE-235)
Prog. rpt. on nuclear chemistry, annual, 1965, 20: 38994 (AE-232)

ALBERT EINSTEIN MEDICAL CENTER, PHILADELPHIA, PA.
Prog. rpt. on lysosomes and lysosomal enzymes in normal and beta-irradiated albino guinea pig epidermis, 8/65–4/66, 20: 38591 (NYO-3445-7)

ALCO PRODUCTS, INC., SCHENECTADY, N. Y. NUCLEAR POWER ENGINEERING DEPT.
Control rod programing. I., · 20: 40354 (AP-Note-393)

ALLIS-CHALMERS MFG. CO., MILWAUKEE, WIS. ATOMIC ENERGY DIV.
Reactivity evaluation of SM-1 Core III qualification fuel plates, · 20: 40374 (ACNP-63562)

AMES LAB., IOWA STATE UNIV. OF SCIENCE AND TECH.
Combined effect of mean stress and stress concentrations on fatigue properties of 2011-T3 alloy, 20: 39396 (IS-T-60)
Heat capacity of solid ^3He, · 20: 40013 (IS-T-84)
Heats of dilution of aqueous rare-earth chloride solutions at 25°C, 20: 38870 (IS-1356)

ARGONNE NATIONAL LAB., ILL.
Catalog of nuclear reactor concepts, Pt. I, Sect. VI, 20: 40353 (ANL-7228)
Long range speculations on isotopic power, · 20: 39304 (DP-1066(Vol.1), pp 19-28)
Neutron diffraction study of ordered Ni–Mn alloys, · 20: 39407 (ANL-Trans-344)
Steam-electric generating units applied to Argonne fast breeder reactor studies: plant description, · 20: 40413 (TID-23257(Vol.1))
Steam-electric generating units applied to Argonne fast breeder reactor studies: drawings and diagrams equipment list, · 20: 40414 (TID-23257 (Vol.2))
Steam-electric generating units applied to Argonne fast breeder reactor studies: cost summary, · 20: 40415 (TID-23257(Vol.3))

ARIZONA STATE UNIV., TEMPE.
Anion diffusion in samarium sesquioxide, 20: 38865 (COO-1109-22, Paper 4)
High-temperature x-ray diffraction studies in selected rare earth oxide–oxygen systems, 20: 38864 (COO-1109-22, Paper 3)
On the lower oxides of the rare earths, 20: 38867 (COO-1109-22, Paper 6)
Prog. rpt. on solid-state chemistry of rare earth oxides, annual, 1965–66, 20: 38861 (COO-1109-22)
Rare earth carbonate system, 20: 38868 (COO-1109-22, Paper 7)
Some tensimetric studies in the mixed ceria–terbia system, · 20: 38862 (COO-1109-22, Paper 1)
Spectroscopic and x-ray studies in region PrO_x $1.5 \leq x \leq 1.714$, 20: 38866 (COO-1109-22, Paper 5)
Tensimetric study of terbia and praseodymia system and mixed praseodymia–terbia system, 20: 38863 (COO-1109-22, Paper 2)
X-ray diffraction studies on rare earth carbonates, 20: 38869 (COO-1109-22, Paper 8)

ARMED FORCES RADIOBIOLOGY RESEARCH INST., BETHESDA, MD.
Procedure for minimizing personnel hazards while changing tritium targets in accelerators, · 20: 39476 (AD-636185)

ARMY MATERIALS RESEARCH AGENCY, WATERTOWN, MASS. MATERIALS ENGINEERING DIV.
Petch analysis of hydrogenated tantalum sheet, 20: 39378 (AD-635596)

ARMY NATICK LABS., MASS.
Food preservation, 20: 39284 (DP-1066(Vol.1), pp IV.3-25)

ARMY RESEARCH OFFICE, DURHAM, N. C.
Prog. rpt., 1965, · 20: 40485 (AD-636091)

ATOMIC ENERGY CENTRE, DACCA (PAKISTAN).
Dual-purpose unit for high vacuum pumping system and leak detection in vaccuum chambers, 20: 39096 (AECD-EP-11)

ATOMIC ENERGY COMMISSION, WASHINGTON, D. C.
Plutonium and other radioisotope sources: discovery to demand, 20: 39314 (DP-1066(Vol.1), pp 29-39)

ATOMIC ENERGY ESTABLISHMENT, WINFRITH (ENGLAND).
Analysis of uranium metal-graphite systems using multi-group code "WIMS", 20: 39382 (AEEW-R-473)
Burnout in a channel with non-uniform circumferential heat flux, 20: 39046 (AEEW-R-477)
Conversion and fast fission ratios in AGR cluster, · 20: 40399 (AEEW-M-654)
Measurement of radial voltage distribution in two-phase flow by isokinetic sampling, 20: 39045 (AEEW-M-650)
Steam drum experiment (A.G.R.), · 20: 40398 (AEEW-M-631)

ATOMIC ENERGY OF CANADA LTD., CHALK RIVER (ONTARIO).
Cosmic ray NM-64 neutron monitor data-III, · 20: 39623 (AECL-2598)
Effect of density and grain size on thermal conductivity of UO_2 during irradiation, · 20: 39446 (AECL-2564)
Effect of TiO_2 additions on defect structure, sintering, and gas release of UO_2, 20: 39381 (AECL-2585)
Electron probe microanalysis of Al-clad Zy-2 specimens after heat treatments, · 20: 39380 (AECL-2570)
Note on fast fracture of a pressure vessel, 20: 39329 (AECL-2432)
Short duration irradiation behavior of UO_2, 20: 39447 (AECL-2581)
Terminal solid solubility of H in Zy-2, 20: 39379 (AECL-2453)

ATOMIC ENERGY OF CANADA LTD., CHALK RIVER (ONTARIO). CHALK RIVER NUCLEAR LABS.
Use of Ge(Li) detectors in γ-γ coincidence experiments, 20: 39197 (AECL-2565)

ATOMIC ENERGY OF CANADA LTD., OTTAWA (ONTARIO).
Canadian program on large scale production and application of radioisotopes, · 20: 39282 (DP-1066(Vol.1), pp III.3-32)

ATOMIC ENERGY RESEARCH ESTABLISHMENT, HARWELL (ENGLAND).
Effects of self-irradiation damage on electrical resistivity of alpha and delta stabilized Pu, U, and Np, · 20: 39448 (AERE-X-PR-2596-9)

Pressure-drop characteristics for flow of subcooled water in heated channels. I., 20: 39047 (AERE-M-1739)
Radioisotope powered generator development in UK, 20: 39309 (DP-1066 (Vol.2), pp III.39-48)

ATOMIC POWER DEVELOPMENT ASSOCIATES, INC., DETROIT, MICH.
Facilities, capabilities, and experience in liquid metals and fast reactor research and development, 20: 40355 (APDA-TPI-1)

ATOMICS INTERNATIONAL, CANOGA PARK, CALIF.
Application of K-factors for reliability evaluation of test programs, 20: 40447 (NAA-SR-11913)
Computer study of dynamics of MRP shaft-bearing system, 20: 39022 (NAA-SR-11943)
Fission-product retention in Na, 20: 40357 (NAA-SR-11766)
SNAP-10A expansion compensator, 20: 39023 (NAA-SR-11952)
SNAP-10A thermoelectric pump, 20: 40446 (NAA-SR-11879)

B

BABCOCK AND WILCOX CO., LYNCHBURG, VA. CRITICAL EXPERIMENT LAB.
Zero power tests on NS Savannah Core II, 20: 40445 (BAW-1225)

BALLISTIC RESEARCH LABS., ABERDEEN PROVING GROUND, MD.
Application of fast neutron activation analysis to polymer dosimetry, 20: 38937 (AD-635655)
Broad range magnetic neutron spectrometer, 20: 39194 (AD-638137)

BATTELLE INSTITUT E. V., FRANKFURT AM MAIN (WEST GERMANY).
Bibliography on deposition of layers of Mo, W, Rh, 20: 39354 (BMWF-FBK-66-09)
Evaluations on chemical reactions of carbides and oxides suitable for construction of nuclear-fueled thermionic emitters, 20: 39353 (BMWF-FBK-66-07)
High-temperature tests on tungsten-coated UO_2–Mo–cermets for thermionic nuclear fuel elements, 20: 39383 (BMWF-FBK-66-08)

BATTELLE-NORTHWEST, RICHLAND, WASH. PACIFIC NORTHWEST LAB.
Advanced alpha-beta-gamma hand and shoe contamination monitor, 20: 39198 (BNWL-250)
Formation of selected fission products in power reactors, 20: 40400 (BNWL-244)
Geology and hydrology, 20: 39099 (BNWL-235-3, pp 1-23)
Irradiation brewing of UO_2, 20: 39449 (BNWL-SA-272)
ISOSHLD: computer code for general purpose isotope shielding analysis, 20: 40285 (BNWL-236)
Mineral chemistry, 20: 38858 (BNWL-235-3, pp 23-51)
Particles and gases, 20: 39103 (BNWL-235-3, pp 51-69)
Prog. rpt. on earth sciences, annual, 1965, 20: 38857 (BNWL-235-3)
Prog. rpt. on fixation of radioactive residues, 1–3/66, 20: 40476 (BNWL-267)
Structural analysis of hexagonal tube or ring under internal pressure, 20: 39384 (BNWL-263)
Sulfur determination supporting waste solidification program, 20: 38795 (BNWL-265)

BETTIS ATOMIC POWER LAB., PITTSBURGH, PA.
Angle-space synthesis: an approach to transport approximations, 20: 40360 (WAPD-T-1890)
CYGRO-1: stress analysis of growth of concentric cylinders, 20: 39460 (WAPD-TM-514(Add.1))
Fabrication of fuel pellets from pot-process denitrated ThO_2 powder, 20: 39362 (WAPD-TM-577)
Fatigue properties of irradiated pressure vessel steels, 20: 39406 (WAPD-T-1864)
Theory and mechanism of Zircaloy pressure bonding, 20: 39361 (WAPD-305)

BETTIS ATOMIC POWER LAB., WEST MIFFLIN, PA.
Fuel clad design basis for thermal reactors, 20: 40387 (WAPD-T-1939)
Shippingport Atomic Power Station disposition of radioactive waste from underground storage tanks, 20: 40481 (WAPD-T-1851)

BOEING SCIENTIFIC RESEARCH LABS., SEATTLE, WASH. GEOASTROPHYSICS LAB.
Experimental evaluation of various rigidity models, 20: 39624 (D-1-82-0529)

BOLOGNA UNIV. (ITALY). ISTITUTO DI FISICA.
Pion-proton elastic scattering, 20: 39744 (CERN-66-18)

BRANDEIS UNIV., WALTHAM, MASS. GRADUATE DEPT. OF BIOCHEMISTRY.
Prog. rpt. on mutagenic and lethal effects of ultraviolet irradiation, 9/65–6/66, 20: 38574 (NYO-3449-1)

BROOKHAVEN NATIONAL LAB., UPTON, N. Y.
Engineering problems in pulsed neutron sources, 20: 40455 (BNL-10454)
High-temperature liquid-metal technology review, 20: 39330 (BNL-962)
Magnetic fields in superconducting quadrupole lens, 20: 39479 (BNL-10495)
Measurements on multistem drift tube structure for proton accelerators, 20: 39478 (BNL-10376)
Mixed β-diketones, 20: 38855 (BNL-10350)
Physical and chemical properties of dilute alloys of Cd in Na, 20: 38856 (BNL-10372)
200 Bev accelerator employing a separated function magnet lattice, 20: 39480 (BNL-10508)

BUREAU OF MINES, ALBANY, OREG. ALBANY METALLURGY RESEARCH CENTER.
High-energy-rate extrusion of low-density tungsten powder billets, 20: 39352 (BM-RI-6817)

BUREAU OF MINES, BARTLESVILLE, OKLA. BARTLESVILLE PETROLEUM RESEARCH CENTER.
Prog. rpt. on application of nuclear explosives to create underground storage reservoirs, 1/66, 20: 39014 (TID-23184)

BUREAU OF MINES, RENO, NEV. RENO METALLURGY RESEARCH CENTER.
Extraction and separation of selected lanthanides with tertiary amine, 20: 38995 (BM-RI-6809)

C

CALIFORNIA INST. OF TECH., PASADENA.
Topics of interest in π and η photoproduction, 20: 39743 (CALT-68-92)

CALIFORNIA UNIV., DAVIS. DEPT. OF ENGINEERING.
Irradiation of fruits and vegetables, 20: 39289 (UCD-34P73-9)

CALIFORNIA UNIV., LOS ANGELES.
Prog. rpt. on irradiation effects on brain wave correlates of conditioned behavior, final, 1960–65, 20: 38602 (UCLA-34P60-1)

CALIFORNIA UNIV., LOS ANGELES. LAB OF NUCLEAR MEDICINE AND RADIATION BIOLOGY.
FORTRAN IV program for evaluation of thyroidal assimilation of radioiodine, 20: 38549 (UCLA-12-592)
Radiation effects on lizards in a Puerto Rican forest, 20: 38601 (UCRL-12-567)

CALIFORNIA UNIV., LOS ANGELES. PLASMA PHYSICS GROUP.
Kinetic equation for unstable plasma in parallel electric and magnetic fields, 20: 40181 (TID-23307)

CAMBRIDGE ELECTRON ACCELERATOR, MASS.
Prog. rpt. semiannual, 7–12/65, 20: 39481 (CEAL-1031)

CASE INST. OF TECH., CLEVELAND, OHIO.
Conference on a deep underground laboratory, Johannesburg, South Africa, 10/65, 20: 39016 (COO-818-94)

CENTRE D'ETUDE DE L'ENERGIE NUCLEAIRE, BRUSSELS (BELGIUM).
Production and application of ^{227}Ac for direct conversion sources, 20: 39277 (DP-1066(Vol.1), pp III.63-9)

CENTRE D'ETUDE DE L'ENERGIE NUCLEAIRE, MOL (BELGIUM).
Irradiation damage in beryllium oxide, 20: 39453 (EUR-3054.e)
Irradiation damage in beryllium, 20: 39454 (EUR-3055.e)
Irradiation damage in graphite, 20: 39455 (EUR-3056.e)

COLUMBIA UNIV., NEW YORK. DEPT. OF CHEMICAL ENGINEERING.
Viscosity of Cs up to 5 bars and 1000°C, 20: 39392 (CU-2660-29)

COLUMBIA UNIV., NEW YORK. DEPT. OF ELECTRICAL ENGINEERING.
Cyclotron harmonic radiation from electron beam injection into an afterglow plasma, 20: 40165 (AD-637710)
Electromagnetic: acoustic wave propagation along warm plasma columns, 20: 40166 (AD-637711)

COMBUSTION ENGINEERING, INC., WINDSOR, CONN. NUCLEAR DIV.
Advanced BONUS core thermal cycle test, 20: 40401 (CEND-259)
Prog. rpt. on burnable poison additions to UO_2, 1–3/66, 20: 40382 (CEND-3107-267)

COMISION NACIONAL DE ENERGIA ATOMICA, BUENOS AIRES (ARGENTINA).
Prog. rpt. on ^{90}Sr levels in diets and bones of children, annual, 1965, 20: 39150 (NYO-2753-4)

COMMISSARIAT A L'ENERGIE ATOMIQUE, FONTENAY-AUX-ROSES (FRANCE). CENTRE D'ETUDES NUCLEAIRES.
Contribution to the analytic study of ferrates, 20: 38859 (CEA-R-2895)
Variation in hematocrit of rat after gamma irradiation, 20: 38587 (CEA-R-2909)

COMMISSARIAT A L'ENERGIE ATOMIQUE, GRENOBLE (FRANCE). CENTRE D'ETUDES NUCLEAIRES.
Hydrodynamic instabilities limiting power of boiling water reactors, 20: 40403 (EURAEC-1464)
Oxidation risks during sintering of uranium dioxide, and characterization of excess O, 20: 39390 (CEA-R-3003)
Study of point defects in pure iron by means of electric resistivity, 20: 39386 (CEA-R-2905)

COMMISSARIAT A L'ENERGIE ATOMIQUE, PARIS (FRANCE).
Prog. rpt. on neutron study of Pu in thermal neutron reactors, final, 12/18/60–8/31/64, 20: 40384 (EURAEC-1660)

COMMISSARIAT A L'ENERGIE ATOMIQUE, SACLAY (FRANCE). CENTRE D'ETUDES NUCLEAIRES.

$\beta \rightarrow \alpha$ isothermal transformation in pure and weakly alloyed U, 20: 39388 (CEA-R-2956)
Cobalt-60 production in graphite gas cooled reactors, 20: 39317 (DP-1066(Vol.2), pp I.67-77)
Coulometric determination of C in Pu and in U–Mo alloys, 20: 38796 (CEA-R-2968)
ELAN: installation for recovery and packaging of ^{137}Cs in France, 20: 39319 (DP-1066(Vol.2), pp II.33-44)
Electron microscope study of irradiated beryllium oxide, 20: 39450 (CEA-R-2963)
Influence of O, N, and C on lattice parameter of uranium monocarbide, 20: 39385 (CEA-R-2852)
Orientational relationships between phases in the $\gamma \rightarrow \alpha$ transformations for U–Mo alloys, 20: 39389 (CEA-R-2973)
Production and utilization of radioisotopes in continental Europe, 20: 39276 (DP-1066(Vol.1), pp III.45-50)
Radioisotope converters, 20: 39633 (CEA-R-2788)
Texture study of divided solids by gas adsorption, 20: 39387 (CEA-R-2947)

CONSOLIDATED EDISON CO. OF NEW YORK, INC., NEW YORK.
Indian Point Nuclear Generating Unit No. 2. Description of site and environment, 20: 40406 (NP-16181(Exh.B)(Vol.1))
Indian Point Nuclear Generating Unit No. 2. Plant design description and safety analysis, 20: 40407 (NP-16181(Exh.B)(Vol.2)(Pt.A))
Indian Point Nuclear Generating Unit No. 2. Plant design description and safety analysis, 20: 40408 (NP-16181(Exh.B)(Vol.2)(Pt.B))

D

DANISH ATOMIC ENERGY COMMISSION, RISOE. RESEARCH ESTABLISHMENT.
Dispersion-strengthened Al products, 20: 39359 (RISO-113)
Prog. rpt. on electronics, 1–3/66, 20: 39170 (RISO-M-423)

DAVID SARNOFF RESEARCH CENTER, PRINCETON, N. J.
Prog. rpt. on photomultiplier investigation, 2/15–5/14/66, 20: 39212 (NYO-3421-7)

DELAWARE UNIV., NEWARK. DEPT. OF CHEMISTRY.
Prog. rpt. on primary chemical processes in radiolysis of liquids, 9/65–9/66, 20: 38939 (NYO-2668-13)

DEPARTMENT OF MINES AND TECHNICAL SURVEYS (CANADA). MINES BRANCH.
Effect of heat treatment on corrosion behavior of two Zr–Cu–Mo alloys, 20: 39347 (NP-16239)

DIVISION OF BIOLOGY AND MEDICINE (AEC), WASHINGTON, D. C.
Radiotherapy, 20: 38744 (DP-1066(Vol.1), pp IV.47-66)

DIVISION OF ISOTOPES DEVELOPMENT (AEC), WASHINGTON, D. C.
Atomic Energy Commission's role in the process radiation industry, 20: 39281 (DP-1066(Vol.1), pp 13-18)
Food preservation, 20: 39284 (DP-1066(Vol.1), pp IV.3-25)

DIVISION OF MATERIALS AND LICENSING (AEC), WASHINGTON, D. C.
Safety of isotopic power sources for terrestrial applications, 20: 39307 (DP-1066(Vol.1), pp V.35-40)

DIVISION OF SPACE NUCLEAR SYSTEMS (AEC), WASHINGTON, D. C.
USAEC isotopic power applications, 20: 39305 (DP-1066(Vol.1), pp V.3-16)

DU PONT DE NEMOURS (E. I.) & CO., AIKEN, S. C. SAVANNAH RIVER LAB.
Application of radioisotope heat source interior to tubular thermoelectric generator, 20: 39308 (DP-1066(Vol.2), pp III.3-16)
Atomic Energy Commission's role in the process radiation industry, 20: 39281 (DP-1066(Vol.1), pp 13-18)
Canadian program on large scale production and application of radioisotopes, 20: 39282 (DP-1066(Vol.1), pp III.3-32)
Cobalt-60 production in graphite gas cooled reactors, 20: 39317 (DP-1066(Vol.2), pp I.67-77)
Conference on large scale production and applications of radioisotopes, Augusta, Ga., 3/66. I., 20: 39275 (DP-1066(Vol.1))
Conference on large scale production and applications of radioisotopes, Augusta, Ga., 3/66. II., 20: 39278 (DP-1066(Vol.2))
ELAN: installation for recovery and packaging of ^{137}Cs in France, 20: 39319 (DP-1066(Vol.2), pp II.33-44)
Food preservation, 20: 39284 (DP-1066(Vol.1), pp IV.3-25)
Heavy water components test reactor: safety systems, fuel failure detection, and standby condition, 20: 40456 (DP-1049)
In-place nondestructive leak test for iodine adsorbers, 20: 39018 (DP-MS-66-46)
Instrument for locating failed fuel elements in the HWCTR, 20: 40458 (DP-1049, pp 21-31)
Interaction of fissile units computer code: INTERACT, 20: 40375 (DP-1031)
Large scale application of radioisotopes to sterilization, 20: 39285 (DP-1066(Vol.1), pp IV.33-42)
Large scale processing and source preparation of neutron-produced isotopes, 20: 39316 (DP-1066(Vol.1), pp II.3-14)
Large scale production and utilization of radioisotopes in the United Kingdom, 20: 39283 (DP-1066(Vol.1), pp III.33-44)
Large scale separation of ^{210}Po from Bi, 20: 38996 (DP-1066(Vol.2), pp II.79-102)
Long range speculations on isotopic power, 20: 39304 (DP-1066(Vol.1), pp 19-28)
Performance of the HWCTR safety systems, 20: 40457 (DP-1049, pp I-19)
Plutonium and other radioisotope sources: discovery to demand, 20: 39314 (DP-1066(Vol.1), pp 29-39)
Production and application of ^{227}Ac for direct conversion sources, 20: 39277 (DP-1066(Vol.1), pp III.63-9)
Production and utilization of radioisotopes in continental Europe, 20: 39276 (DP-1066(Vol.1), pp III.45-50)
Production of radioisotopes in power reactors, 20: 39315 (DP-1066 (Vol.1), pp I.29-52)
Production of ^{60}Co in the BR2 reactor, Belgium, 20: 39318 (DP-1066 (Vol.2), pp I.93-101)
Prog. rpt. on nondestructive test of C beds for reactor confinement applications, 10/64–1/66, 20: 39017 (DP-1053)
Projected large scale use of radioisotopes by NASA, 20: 39306 (DP-1066(Vol.1), pp V.17-25)
Radiography, Vol. I., 20: 39286 (DP-1066(Vol.1), pp IV.43-5)
Radioisotope powered generator development in UK, 20: 39309 (DP-1066 (Vol.2), pp III.39-48)
Radiotherapy, 20: 38744 (DP-1066(Vol.1), pp IV.47-66)
Safety of isotopic power sources for terrestrial applications, 20: 39307 (DP-1066(Vol.1), pp V.35-40)
USAEC isotopic power applications, 20: 39305 (DP-1066(Vol.1), pp V.3-16)

DUKE UNIV., DURHAM, N. C.
Evidence concerning C violation in eta decay, 20: 39766 (ORO-3065-10)
Three-pion production by 1.95 Bev/c positive pions on protons, 20: 39767 (TID-23278)

E

EDGERTON, GERMESHAUSEN AND GRIER, INC., SANTA BARBARA, CALIF.
Field detector station for fallout and transit dose rate measurement system, 20: 39192 (AD-636206)
Prog. rpt. on Linac adaption for weapons simulation, 1/65, 20: 39487 (EGG-1183-2009)
Prog. rpt. on Linac adaptation for weapons simulation, 4/65, 20: 39488 (EGG-1183-2027)
Prog. rpt. on Linac adaptation for weapons simulation, subharmonic buncher, 10/65, 20: 39489 (EGG-1183-2050)
Prog. rpt. on Linac adaptation for weapons simulation, high current gun, 10/65, 20: 39490 (EGG-1183-2051)

EDSEL B. FORD INST. FOR MEDICAL RESEARCH, DETROIT, MICH.
Prog. rpt. on effects of x radiation on metabolism of ^{15}N from ammonium citrate and glycine in rats, 9/65–4/66, 20: 38600 (TID-23034)

ETHICON, INC., SOMERVILLE, N. J.
Large scale application of radioisotopes to sterilization, 20: 39285 (DP-1066(Vol.1), pp IV.33-42)

EUROPEAN-AMERICAN NUCLEAR DATA COMMITTEE.
Prog. rpt. on nuclear data research in Euratom community, annual, 1965, 20: 40069 (EANDC(E)-66(U))

EUROPEAN ATOMIC ENERGY COMMUNITY.
Analysis of nuclear power plants construction costs. I and II, 20: 40402 (EUR-2993.d)
Conference on fuel cycles of high temperature gas-cooled reactors, Brussels, 6/65, 20: 40383 (EUR-2780.e)
Contribution to enhanced diffusion of ^{63}Ni in alpha-irradiated pure Cu, 20: 39451 (EUR-2968.e)
Fine structure of thermal flux and end-effect in tubular composite U fuel elements cooled by an organic compound, 20: 39452 (EUR-2981.f)
Irradiation damage in beryllium oxide, 20: 39453 (EUR-3054.e)
Irradiation damage in beryllium, 20: 39454 (EUR-3055.e)
Irradiation damage in graphite, 20: 39455 (EUR-3056.e)
Obtaining an impermeable graphite by impregnation with molten metals, 20: 39355 (EUR-2988.f)
Phase locked frequency multiplier for a speed- and phase synchronization system between a d.c.- and synchronous motor, 20: 39201 (EUR-2999.e)
Production of ^{60}Co in the BR2 reactor, Belgium, 20: 39318 (DP-1066 (Vol.2), pp I.93-101)
Prog. rpt. on mutagenic substances, annual, 1/10/64–9/30/65, 20: 38589 (EUR-2761.f)
Statistical techniques and analysis in corrosion measurements of Zr alloys in terphenyls, 20: 39344 (EUR-2997.e)

EUROPEAN ATOMIC ENERGY COMMUNITY, ISPRA (ITALY). JOINT NUCLEAR RESEARCH CENTER.

Contribution to enhanced diffusion of ^{63}Ni in alpha-irradiated pure Cu, 20: 39451 (EUR-2968.e)
Fine structure of thermal flux and end-effect in tubular composite U fuel elements cooled by an organic compound, · 20: 39452 (EUR-2981.f)
Obtaining an impermeable graphite by impregnation with molten metals, 20: 39355 (EUR-2988.f)
Phase locked frequency multiplier for a speed- and phase synchronization system between a d.c.- and synchronous motor, 20: 39201 (EUR-2999.e)
Statistical techniques and analysis in corrosion measurements of Zr alloys in terphenyls, 20: 39344 (EUR-2997.e)

EUROPEAN ORGANIZATION FOR NUCLEAR RESEARCH, GENEVA (SWITZERLAND).
Creation of particles at cosmic-ray energies, · 20: 39745 (CERN-66-22)
Introduction to beam optics, 20: 39484 (CERN-66-21, pp 1-30)
Layout of the new CERN neutrino beam, · 20: 39746 (CERN-66-24)
Lectures on beam optics, · 20: 39483 (CERN-66-21)
Low-energy separated beams, · 20: 39485 (CERN-66-21, pp 31-42)
Pion-proton elastic scattering, · 20: 39744 (CERN-66-18)
Radio-frequency separated beams, · 20: 39486 (CERN-66-21, pp 43-54)

G

GENERAL DYNAMICS CORP., SAN DIEGO, CALIF. GENERAL ATOMIC DIV.
Fast neutron spectrum of AFRRI TRIGA reactor, · 20: 40454 (AD-636542)
GADOSE and DOSET: programs to calculate environmental consequences of radioactivity release, 20: 39148 (GA-6511)
Test evaluation of SNAP-15A generator, 20: 39310 (GA-5781)

GENERAL ELECTRIC CO., CINCINNATI, OHIO. NUCLEAR MATERIALS AND PROPULSION OPERATION.
DEFCOT: plane-strain plastic-viscoelastic deformation of a composite tube, 20: 39394 (GEMP-415)
Nuclear test gauge safety analysis report, 20: 40459 (GEMP-152)

GENERAL ELECTRIC CO., PLEASANTON, CALIF. NUCLEAR TECHNOLOGY DEPT.
Uranium oxide powder and pellet thermal conductivity during irradiation, 20: 39456 (GEAP-5100-1)

GENERAL ELECTRIC CO., PLEASANTON, CALIF. VALLECITOS ATOMIC LAB.
Mechanical property changes in Zircaloy-2, Inconel and Incoloy from neutrons, · 20: 39457 (GEAP-5100-9)
Solid-liquid phase diagram for the UO_2–PuO_2 system, 20: 39393 (GEAP-4878)

GENERAL ELECTRIC CO., RICHLAND, WASH. HANFORD ATOMIC PRODUCTS OPERATION.
Finned circulator-evaporator for concentrating radioactive waste, 20: 40477 (HW-80056)

GENERAL ELECTRIC CO., SAN JOSE, CALIF. ADVANCED PRODUCTS OPERATION.
Improved heat transfer performance with boundary layer turbulence promoters, 20: 39048 (GEAP-5115)

GENERAL ELECTRIC CO., SAN JOSE, CALIF. ATOMIC POWER EQUIPMENT DEPT.
Behavior of selected steels exposed in flowing sodium test loops, 20: 39345 (GEAP-4831)
Core performance and transient flow testing of Big Rock Point Boiling Water Reactor, · 20: 40404 (GEAP-4496)
Prog. rpt. on radial vane steam separator, 1–3/66, 20: 39019 (GEAP-5149)

GENERAL ELECTRIC CO., SAN JOSE, CALIF. VALLECITOS ATOMIC LAB.
Prog. rpt. on specific Zr alloy design program, 4/66, 20: 39356 (GEAP-5134)

GEORGIA INST. OF TECH., ATLANTA. SCHOOL OF CHEMISTRY.
Measurement of (n,2n), (n,p), and (n,α) cross sections of Ge at 14.4 Mev, 20: 40080 (ORO-3346-3)
Neutron reaction cross sections of Se and Fe at 14.4 Mev, 20: 40079 (ORO-3346-2)

GOSUDARSTVENNYI KOMITET PO ISPOL'ZOVANIYU ATOMNOI ENERGII SSSR, MOSCOW. SOYUZNYI NAUCHNO-ISSLEDOVATEL'SKII INSTITUT PRIBOROSTROENIYA.
Yield of D(d,n)^{3}He and T(d,n)^{4}He reactions in thick targets at energies up to 100 kev, 20: 40078 (NP-16203)

GOSUDARSTVENNYI KOMITET PO ISPOL'ZOVANIYU ATOMNOI ENERGII SSSR, OBNINSK. FIZIKO-TEKHNICHESKII INSTITUT.
Yield of D(d,n)^{3}He and T(d,n)^{4}He reactions in thick targets at energies up to 100 kev, · 20: 40078 (NP-16203)

GRENOBLE UNIV. (FRANCE).
Study of point defects in pure iron by means of electric resistivity, 20: 39386 (CEA-R-2905)

H

HAMBURG UNIV. (WEST GERMANY). I. INSTITUT FUER EXPERIMENTALPHYSIK.
Angular distribution and effective cross section of reaction $^{10}B(d,\alpha)^8Be$ between 1.6 and 3.0 Mev, · 20: 40068 (BMWF-FBK-66-15, pp 38-46)
Broad range magnetic analyzer of the Institute for Nuclear Study, University of Tokyo, 20: 39477 (BMWF-FBK-66-15, pp 1-15)
Investigations in low energy physics performed in Japan, · 20: 40066 (BMWF-FBK-66-15)
Report on measurements of reaction $^{40}Ca(d,\alpha)^{39}Ca$ for 24 Mev impact energy, 20: 40067 (BMWF-FBK-66-15, pp 20-37)

HAWAII UNIV., HONOLULU.
Prog. rpt. on effect of radiation on processes of cellular proliferation, megasporogenesis, and embryo-sac development, 5/66, 20: 38597 (TID-23057)

HEIDELBERG UNIV. (WEST GERMANY). ZWEITES PHYSIKALISCHES INSTITUT.
Concentration of radioactive substances in precipitation, 20: 39106 (BMwF-FBK-65-05)

HELSINKI UNIV. (FINLAND). RESEARCH INST. FOR THEORETICAL PHYSICS.
Introductory lectures on SU_3 symmetry, 20: 39862 (NP-16242)

HITTMAN ASSOCIATES, INC., BALTIMORE, MD.
Evaluation of PM core designs alternate pressure vessel heads, 20: 40405 (HIT-3583-27)

I

IDAHO NUCLEAR CORP., IDAHO FALLS.
Leachability of alumina calcine produced in Idaho Waste Calcining Facility, · 20: 40478 (IN-1011)

ILLINOIS UNIV., URBANA.
Exposure field from a point isotropic source located at surface of thick concrete slab, · 20: 40284 (AD-637125)
Ion mobility in liquid ^{3}He below 1°K, 20: 40012 (COO-1198-364)

INSTITUT ATOMNOI ENERGII, GOSUDARSTVENNYI KOMITET PO ISPO'.'ZOVANIYU ATOMNOI ENERGII SSSR, MOSCOW.
Theory of electrical conductance of metals with nonmagnetic impurities, 20: 39395 (IAE-1028)

INSTITUT NATIONAL AGRONOMIQUE, PARIS (FRANCE).
Prog. rpt. on mutagenic substances, annual, 1/10/64–9/30/65, 20: 38589 (EUR-2761.f)

INSTITUT NATIONAL DES SCIENCES ET TECHNIQUES NUCLEAIRES, SACLAY (FRANCE).
Introduction to the study of linear accelerators, · 20: 39482 (CERN-66-20)

INSTITUTE FOR NUCLEAR STUDY, TOKYO UNIV. (JAPAN).
Angular distribution and effective cross section of reaction $^{10}B(d,\alpha)^8Be$ between 1.6 and 3.0 Mev, · 20: 40068 (BMWF-FBK-66-15, pp 38-46)
Report on measurements of reaction $^{40}Ca(d,\alpha)^{39}Ca$ for 24 Mev impact energy, · 20: 40067 (BMWF-FBK-66-15, pp 20-37)
Single RACE spectrometer, 20: 39206 (INSJ-99)

INSTITUTE OF MATHEMATICAL SCIENCE, MADRAS (INDIA).
Selected topics in weak interactions, · 20: 39764 (NP-16232)

INSTITUTE OF NUCLEAR PHYSICS, KRAKOW (POLAND).
Equal time commutators and scalar mesons decays, · 20: 39852 (INP-480/PL)
Large permanent magnet semicircular beta ray spectrograph, 20: 39203 (INP-476/PL)

INSTITUTE OF NUCLEAR RESEARCH, WARSAW (POLAND).
Determination of coincidence-circuit statistical parameters by means of point method, 20: 39205 (INR-703/III/PL)
Influence of channel width of multichannel analyzer on spectrometer resolution, 20: 39204 (INR-694/III)

INSTITUTO DE ENERGIA ATOMICA, SAO PAULO (BRAZIL).
Digital program for calculation of activities of fission products of long half life, · 20: 40070 (IEA-111)

INSTITUTT FOR ATOMENERGI, HALDEN (NORWAY). OECD HALDEN REAKTOR PROSJEKT.
Prog. rpt. on Halden Reactor Project, annual, 1964–65, · 20: 40409 (NP-16230)

INSTITUTUL DE FIZICA ATOMICA, ACADEMIA R. P. R., BUCHAREST (ROMANIA).
Relations between kinetics of development of emulsion sensitivity and illumination, 20: 39202 (IFA-PN-17)

INTERNATIONAL ATOMIC ENERGY AGENCY, VIENNA (AUSTRIA).
Atomic energy prospects for Brazil and for developing countries, 20: 40487 (NP-16229)
Management of radioactive wastes produced by radioisotope users (addendum), · 20: 40480 (STI-PUB-119)
Prog. rpt. on application of cloned haemopoietic cells in radiation protection, final, 1965–66, 20: 38708 (IAEA-3173-5)

INTERNATIONAL CENTRE FOR THEORETICAL PHYSICS, TRIESTE (ITALY).

Constants of linearized motion of Vlasov plasmas, · 20: 40167 (IC-65/90)
Degenerate representations of the symplectic groups. I., · 20: 39850 (IC-66/77)
Refined solution of two-dimensional model theories, 20: 39851 (IC-66/96)

ISRAEL ATOMIC ENERGY COMMISSION, YAVNE. SOREQ NUCLEAR RESEARCH CENTER.
H/D isotope effects in formation of H from combination of two radicals in aqueous solutions, 20: 38938 (IA-1074)

ISTITUTO NAZIONALE DI FISICA NUCLEARE, BOLOGNA (ITALY).
Pion-proton elastic scattering, · 20: 39744 (CERN-66-18)

ISTITUTO SUPERIORE DI SANITA', ROME (ITALY). LABORATORI DI FISICA.
Automatic apparatus for measurement of weak currents, 20: 39169 (ISS-66/17)
Measurement of electrons momentum by spark chambers in magnetic field, 20: 39207 (ISS-66/18)

J

JACKSON LAB., BAR HARBOR, MAINE.
Prog. rpt. on quantitative population genetics of mice under irradiation, annual, 7/65–5/66, 20: 38590 (NYO-1979-13)

JAPAN ATOMIC ENERGY RESEARCH INST., TOKYO.
Statistical analysis of mechanical strength of graphite, · 20: 39408 (NSJ-tr-46)

JET PROPULSION LAB., CALIF. INST. OF TECH., PASADENA.
Comparison of liquid-metal magnetohydrodynamic power conversion cycles, 20: 39634 (JPL-32-946)

JOINT INST. FOR NUCLEAR RESEARCH, DUBNA (USSR). LAB OF HIGH ENERGY.
Application of B counter with CH_2 moderator in neutron dosimetry, 20: 39214 (NP-tr-1394)
Identification of charged particles by ionization and delta-electrons in a propane bubble chamber, 20: 39211 (JINR-P-2842)
Inelastic π^-p-interactions at energy 7.5 Bev. II., · 20: 39758 (JINR-P-2773)
Investigation of interaction of π^--mesons with Xe nuclei at 5 and 9 Bev/c, 20: 39755 (JINR-P-2736)
Observation of the $\Lambda\gamma^0$ resonance in π^--p interactions at 4.0 Bev/c, 20: 39754 (JINR-E-2858)
Test of CP-invariance in $K_S^0 \to 3\pi$ decays in correlation experiments with $K^0\bar{K}^0$ pairs, · 20: 39763 (JINR-P-2850)
The search for "long-lived" Λ^0-particles, · 20: 39762 (JINR-P-2849)

JOINT INST. FOR NUCLEAR RESEARCH, DUBNA (USSR). LAB OF NUCLEAR PROBLEMS.
Accumulation of particles in a 680-Mev synchrocyclotron, · 20: 39492 (JINR-P-2811)
Decay of neutral pions into three photons, · 20: 39757 (JINR-P-2763)
Helium-8 production in negative pion capture by C and O nuclei, 20: 40071 (JINR-E-2774)
Inelastic interactions of 19.8-Bev/c protons with neutrons, · 20: 39761 (JINR-P-2809)
Measurement of the cascade time of negative pions in gaseous ^{3}He, 20: 39579 (JINR-P-2838)
Measurements of half-life ratio of π^+ and π^- mesons, · 20: 39760 (JINR-P-2802)
Momentum spectra of secondary particles in (π^-,N) interactions at 7 Bev, 20: 39751 (JINR-E-2738)
Phase-shift analysis of nucleon-nucleon scattering at 14.5 Mev, 20: 39756 (JINR-P-2742)
Planning of n-p scattering experiments above pion-production threshold, 20: 39752 (JINR-E-2765)
Programming the accelerating voltage amplitude of a model of circular proton phasotron r.f. system, · 20: 39491 (JINR-P-2732-1)
Requirements on the optical units of stereoscopic cameras used in bubble chambers, 20: 39209 (JINR-P-2728)
Spark and streamer chambers and methods of data derivation from these chambers, · 20: 39210 (JINR-P-2745)
Spin correlation in elastic scattering of 605-Mev polarized protons on protons, · 20: 39759 (JINR-P-2776)
Structure of Ar K-series during atomic capture of negative muons in pure gas and in mixture with H, · 20: 39578 (JINR-P-2807)

JOINT INST. FOR NUCLEAR RESEARCH, DUBNA (USSR). LAB OF NUCLEAR REACTIONS.
Use of mica and quartz glass for nuclear fission detection at high temperature, 20: 39208 (JINR-P-2705)

JOINT INST. FOR NUCLEAR RESEARCH, DUBNA (USSR). LAB OF THEORETICAL PHYSICS.
Adler-Weisberger relation and dispersion sum rules in theory of strong interactions, 20: 39857 (JINR-E-2876)
Approximate calculation of nearest poles of functions S_l and Δ_l in case of strong $\bar{\psi}\psi\phi$ coupling, · 20: 39859 (JINR-P-2761)
Calculation of co-efficients of mass operators, · 20: 39855 (JINR-E-2771)
Configuration mixing in quark model, 20: 39861 (JINR-P-2821)
Consistent relativization of SU(6) for two-particle reactions, · 20: 39856 (JINR-E-2826)
Existence of certain baryon and meson unitary multiplets, · 20: 39860 (JINR-P-2790)
Method of phase functions in quantum mechanics, · 20: 39997 (JINR-P-2758)
Properties of cluster expansions of the causal S-matrix, · 20: 39858 (JINR-P-2760)
Ratio of axial and vector constants in dynamical quark model, · 20: 39753 (JINR-E-2827)
S-matrix, non-compact symmetry groups and their collinear subgroups, 20: 39854 (JINR-E-2754)
Time correlation of the emission and absorption of exchange photon, 20: 39577 (JINR-P-2791)

JUNTA DE ENERGIA NUCLEAR, MADRID (SPAIN). DIVISION DE FISICA.
Free fields for Nass less particles, 20: 39853 (JEN-157-DF/I-48)

K

KNOLLS ATOMIC POWER LAB., SCHENECTADY, N. Y.
Mathematical foundation for empirical science with special reference to quantum theory. I., · 20: 39998 (KAPL-3147)

L

LABORATORI NAZIONALI DI FRASCATI, COMITATO NAZIONALE PER L'ENERGIA NUCLEARE (ITALY).
Charged pion photoproduction on light nuclei, 20: 40075 (LNF-66/30)
Evaluation of background around the Adone, · 20: 39495 (LNF-66/22)
Optical properties of strong-focusing magnet, · 20: 39494 (LNF-66/15)

LAWRENCE RADIATION LAB., UNIV. OF CALIFORNIA, BERKELEY.
Analysis of strange-particle resonant states from π^-p interactions, 20: 39770 (UCRL-16788)
Convective transfer processes in laminar gas-liquid channel flow, 20: 39050 (UCRL-16535)
Elementary guide to the elementary particles, 20: 39768 (UCRL-11100 (Rev.1))
Magnetostatic computer program TRIM operations manual, · 20: 39499 (UCRL-16959)
Pion-pion interactions from π^-p collisions at 3 and 4 Bev/c, 20: 39769 (UCRL-16655)
Prog. rpt. on bevatron operation and development, 1/3/66, · 20: 39498 (UCRL-16809)
Reaction of $\eta \to \pi^+\pi^-\gamma$, · 20: 39771 (UCRL-16923)
Sign of the K_1^0–K_2^0 mass difference, · 20: 39772 (UCRL-17007)
Strength in two-phase model system with fiber reinforcement, · 20: 39405 (UCRL-16844)
Thermionic emission from planar monocrystalline tungsten, · 20: 39635 (UCRL-16699)

LAWRENCE RADIATION LAB., UNIV. OF CALIFORNIA, LIVERMORE.
Economics of nuclear explosives in developing underground gas storage, 20: 39015 (UCRL-14877)
FRAN prompt burst reactor, · 20: 40463 (UCRL-14413)
High-temperature testing and evaluation of graphite helical-screw expanders and compressors, 20: 39026 (UCRL-14660(Rev.1))
Isotopic disproportionation reaction between light and heavy water using pulsed-molecular-beam mass spectrometer, 20: 38875 (UCRL-14703-T)
Significance of thermal effects in manufacturing and metrology, 20: 39009 (UCRL-14944)
TRUMP: computer program for transient and steady state temperature distributions in multidimensional systems, 20: 39049 (UCRL-14754)
Washout of particulate matter in long-term clouds produced by nuclear explosions, 20: 39107 (UCRL-14700)

LOS ALAMOS SCIENTIFIC LAB., UNIV. OF CALIFORNIA, N. MEX.
Comparison of rotational M1 transition rates between high and low spin states, · 20: 40072 (LA-DC-8061)
Contributions to feasibility study of early lunar flare, · 20: 39469 (LA-3453)
Further evidence for effective nucleon spin g-factors, · 20: 40073 (LA-DC-8065)
Gaussian iterative least squares techniques for modern computers, 20: 39327 (LA-3362)
Hard tube modulators for Los Alamos Meson Facility, · 20: 39493 (LA-DC-7776)
High-resolution study of inelastic proton scattering from nuclei in Pb region, · 20: 40074 (LA-DC-8069)
Leaching of uranium by hydrogen chloride, 20: 39346 (LA-3488)

LOUISIANA STATE UNIV., BATON ROUGE. DEPT. OF FOOD SCIENCE AND TECHNOLOGY.
Prog. rpt. on radiation pasteurization of shrimp and oysters, final, 1–12/65, 20: 39288 (ORO-636)

LOUISVILLE UNIV., KY. DEPT. OF CHEMISTRY.

Thermal degradation of styrene and methylmethacrylate copolymers with pure m- and p-divinylbenzene isomers, 20: 38930 (TID-23264)

M

MCMASTER UNIV., HAMILTON (ONTARIO). DEPT. OF METALLURGY AND METALLURGICAL ENGINEERING.
Dissolution spirals on gamma-irradiated lithium fluoride, 20: 40293 (AD-634746)
MARTIN CO., BALTIMORE, MD.
Prog. rpt. on radiation effects on integrated circuits, 1–3/66, 20: 39273 (AD-635198)
MARTIN CO., BALTIMORE, MD. NUCLEAR DIV.
Final safety analysis five-watt radiostrontium-fueled generator for unattended meteorological station, 20: 39311 (MND-SR-2586)
MARYLAND UNIV., COLLEGE PARK. DEPT. OF PHYSICS AND ASTRONOMY.
Baryon-baryon reactions and SU3 symmetry, 20: 39765 (ORO-2504-91)
MASSACHUSETTS GENERAL HOSPITAL, BOSTON. NEUROSURGICAL SERVICE.
Prog. rpt. on use of isotopes and slow neutrons in diagnosis and treatment of neoplasms, 6/65–5/66, 20: 38745 (NYO-3267-3)
MASSACHUSETTS GENERAL HOSPITAL, BOSTON. PHYSICS RESEARCH LAB.
Prog. rpt. on use of isotopes and slow neutrons in diagnosis and treatment of neoplasms, 6/65–5/66, 20: 38745 (NYO-3267-3)
MASSACHUSETTS INST. OF TECH., CAMBRIDGE.
Generalized Hartree-Fock calculation for ^{90}Zr using an effective interaction, 20: 40076 (MIT-2098-255)
Shell effects in high energy photoproton spectra from ^{6}Li, 20: 40077 (MIT-2098-256)
MATERIALS ADVISORY BOARD, NATIONAL ACADEMY OF SCIENCES–NATIONAL RESEARCH COUNCIL, WASHINGTON, D. C.
Summary report of the Refractory Metals Sheet Rolling Panel, 20: 39357 (MAB-212A-M)
MAX-PLANCK-INSTITUT FUER KERNPHYSIK, HEIDELBERG (WEST GERMANY).
Prog. rpt., annual, 1964, 20: 40065 (BMWF-FB-K-66-01)
MICHIGAN STATE UNIV., EAST LANSING. DEPT. OF BOTANY AND PLANT PATHOLOGY.
Prog. rpt. on radiosensitivity of embryonic tissues, annual, 1965–66, 20: 38588 (COO-1400-10)
MOREHEAD STATE UNIV., KY.
Prog. rpt. on ecological significance of radiation on tree seed and seedlings, 1966, 20: 38594 (ORO-2066-10)
MOUND LAB., MIAMISBURG, OHIO.
Prog. rpt., 11/65, 20: 39320 (MLM-1311)
Prog. rpt., 12/65, 20: 39321 (MLM-1312)
MSA RESEARCH CORP., EVANS CITY, PA.
Prog. rpt. on measurement of impurities in Na, 4–6/66, 20: 38797 (MSAR-66-150)

N

NATIONAL AERONAUTICS AND SPACE ADMINISTRATION, CLEVELAND, OHIO. LEWIS RESEARCH CENTER.
Cold reduction as a means of reducing embrittlement of a cobalt-base alloy (L-605), 20: 39399 (NASA-TN-D-3528)
Effect of alloying on grain refinement of electron-beam-melted tungsten, 20: 39400 (NASA-TN-D-3531)
Effect of orientation on ductile-to-brittle transition of tungsten single crystals, 20: 39397 (NASA-TM-X-1252)
Heat-transfer analysis of Plum Brook reactor, 20: 40461 (NASA-TN-D-3552)
Metallographic study of dispersion-strengthened alloys after failure in stress rupture, 20: 39398 (NASA-TN-D-3527)
Projected large scale use of radioisotopes by NASA, 20: 39306 (DP-1066(Vol.1), pp V.17-25)
Superconducting magnetic bottle for plasma physics experiments, 20: 40169 (NASA-TN-D-3595)
NATIONAL AERONAUTICS AND SPACE ADMINISTRATION, WASHINGTON, D. C.
Conference on peaceful uses of space, 5th, St. Louis, 5/65, 20: 40486 (NASA-SP-82)
NATIONAL LEAD CO. OF OHIO, CINCINNATI.
Prog. rpt., 4–6/66, 20: 38799 (NLCO-980)
NAVAL CIVIL ENGINEERING LAB., PORT HUENEME, CALIF.
Resistance of tubular structures to dynamic loading, 20: 39007 (AD-636914)
NAVAL RADIOLOGICAL DEFENSE LAB., SAN FRANCISCO, CALIF.
Computer-coupled quality control procedure for γ scintillation spectrometry, 20: 39193 (AD-636736)
NEW YORK UNIV., N. Y. DEPT. OF PHYSICS.
Prog. rpt. on measurement of environmental radiation, annual, 9/65–8/66, 20: 38735 (NYO-1704-13)
NIELS BOHR INSTITUTET, COPENHAGEN (DENMARK).
Creation of particles at cosmic-ray energies, 20: 39745 (CERN-66-22)
NIPPON KAIJI KYOKAI, TOKYO.
Provisional guide for classification of nuclear ships, 20: 40448 (NP-16217)
NORTH CAROLINA STATE UNIV., RALEIGH. DEPT. OF SOIL SCIENCE.
Prog. rpt. on Cs and Sr uptake and assimilation by higher plants, annual, 5/65–2/6, 20: 38548 (ORO-2410-1)
NUKLEARNI INSTITUT "JOZEF STEFAN," LJUBLJANA (YUGOSLAVIA).
Flame photometric determination of Li, Na, K, Ca, Mg and Sr in natural and mineral waters, 20: 38798 (NIJS-R-465)
Hazards summary report for Triga Mark II reactor in Ljubljana, 20: 40462 (NIJS-R-474)
Separation of ^{99m}Tc from ^{99}Mo sorbed on aluminum oxide, 20: 38997 (NIJS-R-483)

O

OAK RIDGE GASEOUS DIFFUSION PLANT, TENN.
Gravimetric gas flow standard. II., 20: 39020 (K-1632(Pt.2))
Peripheral compressor, 20: 39021 (K-1665)
OAK RIDGE NATIONAL LAB., TENN.
Abnormal reactor operating experiences, 20: 40358 (ORNL-NSIC-17)
Analysis of filling accidents in MSRE, 20: 40412 (ORNL-TM-497)
Appropriate values for thermal conductivity of UO_2 for use in design of BONUS superheaters, 20: 39403 (ORNL-TM-1450)
Atomic and molecular cross sections, 20: 39580 (ORNL-3989, pp 78-88)
Cytogenetic methods: somatic chromosome aberrations in occupationally irradiated humans, 20: 38593 (ORNL-P-2175)
Design and engineering: notes, 20: 40177 (ORNL-3989, pp 135-43)
Electrical safety of health physics instruments, 20: 39213 (ORNL-TM-1578)
Electron-cyclotron heating, 20: 40173 (ORNL-3989, pp 31-42)
Escosystems, systems ecology, and systems ecologists, 20: 40488 (ORNL-3957)
Examination of hydrous U dioxide precipitates and sols, 20: 39401 (ORNL-3963)
Forming method for curved ATR fuel plates, 20: 39358 (ORNL-3983)
Functional and morphological characterization of stem cells, 20: 38592 (ORNL-P-2158)
High-current ion-beam production and injection, 20: 40175 (ORNL-3989, pp 89-94)
Injection and accumulation: single-pass experiments (DCX-1) 20: 40171 (ORNL-3989, pp 1-13)
Injection and accumulation: multiple-pass experiments (DCX-2), 20: 40172 (ORNL-3989, pp 14-30)
Irradiation testing of Th fuels at ORNL, 20: 40385 (ORNL-P-2327)
Large scale processing and source preparation of neutron-produced isotopes, 20: 39316 (DP-1066(Vol.1), pp II.3-14)
Magnetics and superconductivity, 20: 40014 (ORNL-3989, pp 109-27)
Methods of reduction of texture data to inverse pole figures, 20: 39402 (ORNL-3979)
ORNL facilities capable of contributing to Pu fuel cycle development, 20: 39024 (ORNL-TM-1268)
Oxidation of H and CO in He stream by CuO, 20: 38874 (ORNL-TM-1540)
Plasma physics, 20: 40174 (ORNL-3989, pp 43-77)
Plasma theory and computation, 20: 40176 (ORNL-3989, pp 95-108)
Production of radioisotopes in power reactors, 20: 39315 (DP-1066 (Vol.1), pp I.29-52)
Prog. rpt. on experimental simulation of large, high field, superconducting magnet operation, 12/65–7/66, 20: 40015 (ORNL-TM-1598)
Prog. rpt. on physics, annual, 1965, 20: 39470 (ORNL-3924)
Prog. rpt. on thermonuclear research, semiannual, 10/65–4/66, 20: 40170 (ORNL-3989)
Prog. rpt. on unit operations, 10–12/65, 20: 38998 (ORNL-3958)
Radionuclides in Clinch-Tennessee Rivers, 20: 40479 (ORNL-P-2328)
Repair of molecular damage to DNA, 20: 38575 (ORNL-P-2267)
Sputtering of Cu, Mo, 304 stainless steel, and W by deuterium ions, 20: 39581 (ORNL-3989, pp 134)
Vacuum studies, 20: 39097 (ORNL-3989, pp 128-33)
OESTERREICHISCHE STUDIENGESELLSCHAFT FUER ATOMENERGIE G.M.B.H., SEIBERSDORF. INSTITUT FUER CHEMIE.
Fission product distribution in coating of fuel elements for high temperature reactors, 20: 40386 (SGAE-CH-33/1966)
OESTERREICHISCHE STUDIENGESELLSCHAFT FUER ATOMENERGIE G.M.B.H., SEIBERSDORF. INSTITUT FUER STRAHLENSCHUTZ.
Comparison between methods for measurement of radioactive samples, 20: 38983 (SGAE-SS-3/1966)
OFFICE OF THE ASSISTANT GENERAL MANAGER FOR REACTORS

(AEC), WASHINGTON, D. C.
Nuclear reactors built, being built, or planned in U.S.A. as of December 31, 1965, 20: 40359 (TID-8200(13th Rev.))
OREGON UNIV., EUGENE.
Prog. rpt. on electrophoretic and histochemical studies of tissues and body fluids of x-irradiated hamsters, 1966, 20: 38598 (TID-22955)
OXFORD UNIV. (ENGLAND)
Effects of self-irradiation damage on electrical resistivity of alpha and delta stabilized Pu, U, and Np, 20: 39448 (AERE-X-PR-2596-9)

P

PARIS UNIV. (FRANCE).
Contribution to the analytic study of ferretes, 20: 38859 (CEA-R-2895)
Orientational relationships between phases in the $\gamma \rightarrow \alpha$ transformations for U–Mo alloys, 20: 39389 (CEA-R-2973)
Texture study of divided solids by gas adsorption, 20: 39387 (CEA-R-2947)
PARIS UNIV. (FRANCE). FACULTE DES SCIENCES.
Electron microscope study of irradiated beryllium oxide, 20: 39450 (CEA-R-2963)
Influence of O, N, and C on lattice parameter of uranium monocarbide, 20: 39385 (CEA-R-2852)
PENNSYLVANIA UNIV., PHILADELPHIA. ELECTROCHEMISTRY LAB.
Prog. rpt. on properties and structure of molten salts, annual, 1964–65, 20: 38871 (NYO-1769-54)
Prog. rpt. on properties and structure of molten salts, annual, 1965–66, 20: 38872 (NYO-1769-68)
PHILCO CORP., BLUE BELL, PA.
Radiation-resistant device phenomena, 20: 39274 (N-66-18175)
PHILIPPINE ATOMIC ENERGY COMMISSION, MANILA.
Preparation of high specific activity ^{51}Cr, 20: 38982 (PAEC(D)IS-652)
Preparation of 2.56-hour ^{68}Ni, 20: 40081 (PAEC(D)IS-653)
Water analysis, 12/63–11/64, 20: 38800 (PAEC(C)RE-652)
PHILLIPS PETROLEUM CO. IDAHO FALLS, IDAHO., ATOMIC ENERGY DIV.
Prog. rpt. on nuclear technology, 10–12/65, 20: 40460 (IDO-17191)
PICKER X-RAY CORP., CLEVELAND, OHIO.
Radiography, Vol.I., 20: 39286 (DP-1066(Vol.1), pp IV.43-5)
PRATT AND WHITNEY AIRCRAFT, MIDDLETOWN, CONN. CONNECTICUT ADVANCED NUCLEAR ENGINEERING LAB.
SNAP-50/SPUR electromagnetic pump program, 20: 40450 (TIM-911)
PRODUCTION GROUP, UNITED KINGDOM ATOMIC ENERGY AUTHORITY, SELLAFIELD (ENGLAND).
Absorptiometric determination of Fe in high purity Pu metal, 20: 38801 (PG-Report-729)

R

RADIATION RESEARCH LABS., MELLON INST., PITTSBURGH, PA.
Prog. rpt. on radiation research, 4–6/66, 20: 38941 (RRL-2310-182)
RADIOCHEMICAL CENTRE, AMERSHAM (ENGLAND).
Large scale production and utilization of radioisotopes in the United Kingdom, 20: 39283 (DP-1066(Vol.1), pp III.33-44)
REACTOR GROUP, UNITED KINGDOM ATOMIC ENERGY AUTHORITY, CULCHETH (ENGLAND).
Method for gas-hydriding zirconium alloys at 400°C, 20: 39360 (TRG-Report-1255)
REACTOR GROUP, UNITED KINGDOM ATOMIC ENERGY AUTHORITY, SPRINGFIELDS (ENGLAND).
Mechanism of failure in UO_2/stainless steel cermets, 20: 39459 (TRG-Report-1278)
RENSSELAER POLYTECHNIC INST., TROY, N. Y.
Transport phenomena in ionized gases as initial value problem, 20: 40168 (NASA-CR-559)
REYNOLDS ELECTRICAL AND ENGINEERING CO., INC., MERCURY, NEV. MANAGEMENT ENGINEERING DEPT.
Safety involving detonation of nuclear devices, 20: 39149 (NVO-28)
RHODE ISLAND UNIV., PROVIDENCE.
Effects of gamma irradiation on two cyclic carbonates, 20: 38940 (NYO-3410-2)
ROSWELL PARK MEMORIAL INST., BUFFALO, N. Y. DEPT. OF EXPERIMENTAL BIOLOGY.
Functional and morphological characterization of stem cells, 20: 38592 (ORNL-P-2158)
RUTHERFORD HIGH ENERGY LAB., SCIENCE RESEARCH COUNCIL, CHILTON (ENGLAND).
Plunging magnet system for the NIMROD extracted proton beam, 20: 39496 (RHEL-R-117)

S

SAN DIEGO STATE COLL., CALIF.
Prog. rpt. on x-ray induced changes in Drosophila germ cells, 9/65–8/66, 20: 38596 (SAN-590-1)
SANDIA CORP., ALBUQUERQUE, N. MEX.
Chemical integrity of radioisotope containment materials in launch abort environments, 20: 39312 (SC-CR-66-2044)
Clean assembly practices guide, 20: 40489 (SC-DC-66-1118)
SCRIPPS INSTITUTION OF OCEANOGRAPHY, LA JOLLA, CALIF.
Urechis program: rapid survey of fallout Cs in the ocean, 20: 39147 (CONF-660401-6)
SOUTHWEST RESEARCH INST., SAN ANTONIO, TEX.
Low-cycle fatigue strengths of dissimilar weldments, 20: 39404 (SWRI-1228-4-20)
SOUTHWEST RESEARCH INST., SAN ANTONIO, TEX. DEPT. OF AEROSPACE PROPULSION RESEARCH.
Prog. rpt. on liquid-metal lubricated journal bearings, 4–7/66, 20: 39008 (SWRI-1228-8-24)
STANFORD LINEAR ACCELERATOR CENTER, STANFORD UNIV., CALIF.
Prog. rpt. on two-mile accelerator project, 1–3/66, 20: 39497 (SLAC-65)
STANFORD RESEARCH INST., MENLO PARK, CALIF.
Industrial recovery techniques, 20: 39146 (AD-636947)
STANFORD UNIV., CALIF. HIGH-ENERGY PHYSICS LAB.
Relativistic two-body kinematics: program for Burroughs 220 computer, 20: 39750 (HEPL-236)
STANFORD UNIV., CALIF. INST. FOR PLASMA RESEARCH.
Diffusion process in toroidal discharge, 20: 40180 (SU-IPR-69)
Growth of fluctuations in collisionless plasma subjected to electric field, 20: 40179 (SU-IPR-49)
STATE UNIV. OF NEW YORK, BUFFALO. DEPT. OF CHEMISTRY.
Prog. rpt. on studies in solution and nuclear chemistry, 10/65–9/66, 20: 38873 (NYO-2269-9)
STATENS RADIOLOGISK-FYSISKE LABORATORIUM, OSLO (NORWAY).
Radiation exposure of gonads during betatron therapy at 31 Mev, 20: 38746 (NYO-3364-19)
STEVENS INST. OF TECH., HOBOKEN, N. J. DEPT. OF PHYSICS.
Prog. rpt. on cusped containment geometries, annual, 1965–1966, 20: 40178 (SIT-2582-19)

T

TECHNISCHE HOCHSCHULE, AACHEN (WEST GERMANY). INSTITUT FUER ELEKTRISCHE ANLAGEN UND ENERGIEWIRTSCHAFT.
Analysis of nuclear power plants construction costs. I and II, 20: 40402 (EUR-2993.d)
TECHNISCHE HOGESCHOOL, EINDHOVEN (NETHERLANDS).
Hydraulic characteristics of boiling water channel, 20: 40356 (EURAEC-1644)
TENNESSEE UNIV., KNOXVILLE.
Magnetic-pulse forming process, 20: 40490 (Y-1483)
Oxidation of H and CO in He stream by CuO, 20: 38874 (ORNL-TM-1540)
Prog. rpt. on effects of hormones, x rays, and cerium compounds on rat liver cells, 10/65–9/66, 20: 38595 (ORO-3295-2)
TENNESSEE UNIV., MEMPHIS. DEPT. OF BIOCHEMISTRY.
Final rpt. on effects of radiation on metabolism of ascites tumor cells, 20: 38599 (TID-22968)
TENNESSEE VALLEY AUTHORITY, KNOXVILLE.
Browns Ferry Nuclear Power Station, TVA design and analysis report, 20: 40410 (NP-16251(Vol.1))
Browns Ferry Nuclear Power Station, TVA design and analysis report, 20: 40411 (NP-16251(Vol.2))
TEXAS NUCLEAR CORP., AUSTIN.
An on line nuclear analysis facility, 20: 39025 (ORO-2980-12)
TRW SPACE TECHNOLOGY LABS., THOMPSON RAMO WOOLDRIDGE INC., REDONDO BEACH, CALIF.
Radiation damage in semiconductors. XII., 20: 39458 (NP-16225)
TRW SYSTEMS, REDONDO BEACH, CALIF.
Chemical integrity of radioisotope containment materials in launch abort environments, 20: 39312 (SC-CR-66-2044)
Creep of axisymmetric shells, 20: 39391 (CONF-660629-1)

U

UED EARTH SCIENCES DIV., TELEDYNE, INC., ALEXANDRIA, VA.
Seismic measurements of Red Hot, 20: 39124 (AD-632957)
UNION CARBIDE CORP., OAK RIDGE, TENN. Y-12 PLANT.
Magnetic-pulse forming process, 20: 40490 (Y-1483)
Power requirements for single-point tools, 20: 39027 (Y-DA-1287)
UNION MINIERE DU HAUT-KATANGA, BRUSSELS (BELGIUM).
Production and application of ^{227}Ac for direct conversion sources, 20: 39277 (DP-1066(Vol.1), pp III.63-9)
UNITED ENGINEERS AND CONSTRUCTORS INC., PHILADELPHIA, PA.
Steam-electric generating units applied to Argonne fast breeder reactor

studies: plant description, · 20: 40413 (TID-23257(Vol.1))
Steam-electric generating units applied to Argonne fast breeder reactor studies: drawings and diagrams equipment list, · 20: 40414 (TID-23257 (Vol.2))
Steam-electric generating units applied to Argonne fast breeder reactor studies: cost summary, · 20: 40415 (TID-23257(Vol.3))

UNITED STATES–EURATOM JOINT RESEARCH AND DEVELOPMENT PROGRAM.
Hydraulic characteristics of boiling water channel, · 20: 40356 (EURAEC-1644)
Hydrodynamic instabilities limiting power of boiling water reactors, 20: 40403 (EURAEC-1464)
Mechanical property changes in Zircaloy-2, Inconel and Incoloy from neutrons, · 20: 39457 (GEAP-5100-9)
Prog. rpt. on burnable poison additions to UO_2, 1–3/66, 20: 40382 (CEND-3107-267)
Prog. rpt. on radial vane steam separator, 1–3/66, 20: 39019 (GEAP-5149)
Prog. rpt. on specific Zr alloy design program, 4/66, 20: 39356 (GEAP-5134)
Uranium oxide powder and pellet thermal conductivity during irradiation, 20: 39456 (GEAP-5100-1)

UNIVERSITY OF WESTERN ONTARIO, LONDON.
Prog. rpt. on neutron study of Pu in thermal neutron reactors, final, · 12/18/60–3/31/64, 20: 40384 (EURAEC-1660)

USTAV JADERNEHO VYZKUMU, CESKOSLOVENSKA AKADEMIE VED, REZ.
Radiation-induced oxidation of methanol, 20: 38942 (UJV-1457)
Vaporization of actinides and their compounds. I., 20: 38876 (UJV-1598)
Water management for power increase in WWR-S reactor, · 20: 40465 (UJV-1181/64)
Water treatment by direct LiOH addition, · 20: 40464 (UJV-1180/64)

V

VIENNA UNIV. (AUSTRIA). ANALYTISCHES INSTITUT.
Ion exchange separation of U and Th in mixed and non-aqueous solvents, 20: 38999 (TID-23229)

VIRGINIA UNIV., CHARLOTTESVILLE. RADIOBIOLOGY AND BIOPHYSICS LAB.
Variation of radiation dose and its relationship to depression of DNA synthesis, 20: 38576 (TID-22103)

VITRO ENGINEERING CO., NEW YORK.
Engineering and evaluation study for the manufacture of wood-plastic composites, 20: 39287 (KLX-1876)

W

WESTERN RESERVE UNIV., CLEVELAND, OHIO. DEPT. OF PHYSICS.
Chemical effects of lead ions on positronium, 20: 38860 (COO-1297-6)

WESTINGHOUSE ELECTRIC CORP., PITTSBURGH, PA. ASTRONUCLEAR LAB.
Application of radioisotope heat source interior to tubular thermoelectric generator, · 20: 39308 (DP-1066(Vol.2), pp III.3-16)

WESTINGHOUSE ELECTRIC CORP., PITTSBURGH, PA. ATOMIC POWER DIV.
Engineering and metallurgical evaluation of an irradiated Yankee Core I control rod, · 20: 39461 (WCAP-6074)
Supercritical pressure nuclear reactor power plant (1000 MWe), 20: 40416 (WCAP-2222-P)

WESTINGHOUSE RESEARCH LABS., PITTSBURGH, PA.
Prog. rpt. on ultrahigh vacuum techniques, semiannual, 12/65–5/66, 20: 39098 (WERL-2823-21)
Theory of electron collision experiments, 20: 39576 (AD-636533)

WISCONSIN UNIV., MADISON. DEPT. OF PHYSICS.
Effect of quality of radiation on thermoluminescence of LiF(TLD-100), 20: 39199 (COO-1105-117)
Effects of irradiation temperature in LiF(TLD-100), 20: 39200 (COO-1105-118)
Evidence for a Σ-η enhancement near threshold, · 20: 39747 (COO-881-75)
Polarization of the neutron from $\Sigma^+ \rightarrow n^+ + n$, 20: 39748 (COO-881-76)
Regge recurrence parity assignments for S = 0 Regge recurrences, 20: 39749 (COO-881-77)

WORCESTER FOUNDATION FOR EXPERIMENTAL BIOLOGY, SHREWSBURY, MASS.
Prog. rpt. on steroid synthesis, analysis, and metabolism, 5/65–4/66, 20: 38547 (NYO-918-15)

Z

ZENTRALSTELLE FUER ATOMKERNENERGIE-DOKUMENTATION, GMELIN-INSTITUT FUER ANORGANISCHE CHEMIE UND GRENZGEBIETE, FRANKFURT AM MAIN (WEST GERMANY).
Bibliography on instruments and measuring techniques in nuclear physics, No. 14, 5/66, 20: 39168 (AED-C-06-14)
Bibliography on nuclear ship propulsion, No. 6, 6/66, · 20: 40444 (AED-C-22-06)

PERSONAL AUTHOR INDEX

Each entry after an author's name is a shortened version of the title of the report or article, followed by the *NSA* volume and abstract number. Report numbers are given in parentheses.

The phrase "Progress report" is abbreviated as "Prog. rpt.," permitting a more rapid and complete alphabetical arrangement of the titles without changing the location of the progress report titles in relation to the other titles.

Because of problems involving the mechanical preparation of this index, all accent marks are omitted. The following changes in spelling have been introduced to reduce some of the confusion which might result from omitting the accents:

ä	becomes	ae
ö		oe
ø		oe
ü		ue (except in transliterated Chinese names)

A

ABATUROVA, E. A., Therapeutic effects of selachyl alcohol during experimental radiation sickness, 20: 38731

ABBAS, A. A. M., Electrical measurements on a moving argon plasma, 20: 39655

ABDEL-WAHAB, M. F., Preparation of radio-iodinated tyrosines and thyroxine and separation on Sephadex G 25, 20: 38992

ABDEL-WAHAB, M. F., Variations in ascorbic acid content of gramineae during germination and effect of β- and γ-radiation, 20: 38583

ABDULLAH, E., Preparation of diiodo-^{131}I fluorescein and tetraiodo-^{131}I phenolphthalein for diagnostic purposes, 20: 38985

ABELES, F., Optical properties and electronic structure of metals and alloys, 20: 39339

ABELEVA, L. G., Behavior of impurities and admixtures during sintering of W, 20: 39363

ABERLE, J. A., Procedure for minimizing personnel hazards while changing tritium targets in accelerators, 20: 39476 (AD-636185)

ABRAMOVA, K. B., Magnetohydrodynamic instabilities in electrical explosion, 20: 39010

ABRAMS, I. A., Determining γ radiation of spherical source with cylindrical channel, 20: 38989

ACERBI, E., Acceleration of H$^-$ ions and extracted beam measurements in Milan cyclotron, 20: 39550

ADAMOV, I. Yu., Interferometer for plasma diagnosis, 20: 40226

ADAMS, E. D., Helium-4 melting curve below 1°K, 20: 40032

ADEY, W. R., Prog. rpt. on irradiation effects on brain wave correlates of conditioned behavior, final, 1960-65, 20: 38602 (UCLA-34P60-1)

AFONIN, A. A., Allowance for the influence of m scattering annihilation channels in reaction N(π,2π)N, 20: 39776

AGAMOVA, K. A., Megakaryocytes of bone marrow in patients with milk-duct and lung carcinoma during ^{198}Au therapy, 20: 38643

AGHASSI, J. J., Classical field theory and gravitation in a de Sitter world, 20: 40006

AHMED, S. A., Acceleration of electron cyclotron plasma by self-generated electric fields, 20: 40262

AIKENS, A. Jr., Safety of isotopic power sources for terrestrial applications, 20: 39307 (DP-1066(Vol.1), pp V.35-40)

AILAWADI, N. K., Energy dependence of effective interaction in superconductivity, 20: 40017

AIRAPETYAN, G. M., Mechanism of radioprotective action of indolylalkylamines, 20: 38725

AITABAEV, T. Kh., Changes in biochemical and physiological indices in guinea pigs during internal chronic irradiation, 20: 38662

AKAMINE, Ernest K., Gamma radiation as a quarantine treatment for Hawaiian fruit flies, 20: 39293

AKERMAN, K., Industrial application of tracer isotopes in Poland, 20: 39290

AKIYOSHI, Study on Co phase composition contained in WC–Co base cemented carbides, 20: 39427

ALBERS, L. U., Electron distribution function and state populations in non-equilibrium MHD plasmas, 20: 39711

ALDEN, T. H., Ferromagnetic particles in type-II superconductor, 20: 40024

ALEKSANDROV, Yu. M., Determination of quantometer constant at 650 Mev, 20: 39248

ALEKSEEV, V. A., Analogy between a high-density plasma and metal-ammonia solutions, 20: 39656

ALEXEFF, I., Varying plasma electron temperature in discharge tubes by simple auxiliary electrode, 20: 40185

ALIAGA-KELLY, D., Recent developments in scintillation detectors, 20: 39233

ALLEAU, Thierry, Radioisotope converters, 20: 39633 (CEA-R-2788)

ALLINGER, J. E., 200 Bev accelerator employing a separated function magnet lattice, 20: 39480 (BNL-10508)

ALLISON, D. C., Collision-induced de-activation of metastable helium, 20: 39609

ALTMANN, Hans, Use of neutron activation analysis in determination of trace elements in tobacco mosaic virus, 20: 38846

ALTOMARE, Salvi, Heat-transfer analysis of Plum Brook reactor, 20: 40461 (NASA-TN-D-3552)

AL'TSHULER, L. V., Peculiarities of shock compression of lanthanides, 20: 39425

ALYEA, E. D. Jr., Interactions (π^--p) at 460 Mev, 20: 39793

AMBROZHII, N. M., Europium and gadolinium hydroxides and products of their thermal decomposition, 20: 38923

AMME, Robert C., Charge-exchange cross sections for Ar ions in H_2 and D_2 below 1 kev, 20: 39592

AMMON, Johannes H., Integral nuclear reactor-steam generator unit, 20: 40433

AMOSOV, I. S., Pulmonary circulation during acute and chronic radiation sickness, 20: 38657

AMOSOV, V. M., Behavior of impurities and admixtures during sintering of W, 20: 39363

ANBAR, M., H/D isotope effects in formation of H from combination of two radicals in aqueous solutions, 20: 38938 (IA-1074)

ANDERS, L. R., Ion-cyclotron double resonance, 20: 38902

ANDERSON, G. S., Atom ejection studies for sputtering on semiconductors, 20: 40305

ANDERSON, J. R., Performance of ion engines and systems for satellite control, 20: 39092

ANDERSON, K. A., Correlation of magnetic fields and energetic electrons on the IMP 1 satellite, 20: 39976

ANDERSON, K. A., Evidence for connection of geomagnetic tail lines to interplanetary field, 20: 39986

ANDERSON, K. D., Antiferromagnetism of uranium monophosphide, 20: 39422

ANDERSON, L. E., Advanced BONUS core thermal cycle test, 20: 40401 (CEND-259)

ANDERSON, R. H., Application of K-factors for reliability evaluation of test programs, 20: 40447 (NAA-SR-11913)

ANDREEV, A. F., Oscillations of intermediate state of superconductors, 20: 40026

ANDREEV, E. M., Requirements on the optical units of stereoscopic cameras used in bubble chambers, 20: 39209 (JINR-P-2728)

ANDREEV, S. V., Separate determination of daughter products of radon and

thoron during alpha therapy, 20: 38775
ANDREW, R. W., Radionuclides in Clinch-Tennessee Rivers, 20: 40479 (ORNL-P-2328)
ANDREWS, A. E., Cesium ion sputtering of aluminum, 20: 39585
ANDRIENKO, D. A., Some vertical distribution patterns, 20: 39961
ANDRZEJEWSKI, St., Study of cycle diagrams of power plants with MHD generators, 20: 39732
ANIKINA, M., The search for "long-lived" Λ^0-particles, 20: 39762 (JINR-P-2849)
ANTHONY, A. M., Insulators and conductors for MHD flow, 20: 39657
ANTOINE, J.-P., Orbital degeneracy of the Coulomb potential in group theory. I., 20: 40000
ANTONI, F., Effects of gamma rays on vitamin B_6, 20: 38580
ANTONSEN, Knud, Radiation shield arrangement for nuclear reactor, 20: 40369
ANTTILA, A., Resonances in the $^{41}K(p,\gamma)^{42}Ca$ reaction at proton energies 1740–2170 kev, 20: 40133
APELGOT, Sonia, Comparative lethal action of x and β of tritium on E. coli, 20: 38630
APITZSCH, Ursula, RBE of fast neutrons by release of mutations in Drosophila, 20: 38645
APOLLONSKII, S. M., Calculation of boundary layer on insulator walls in MHD generator channel, 20: 39933
APTEL, J., Recovery of residual enthalpy of gases at outlet of MHD duct, 20: 39658
ARAGONES, M., Effect of density and grain size on thermal conductivity of UO_2 during irradiation, 20: 39446 (AECL-2564)
ARCHAMBAULT, Y., Effect of gaseous impurities on conductivity of an alkali metal plasma, 20: 39659
ARENS, J., Polarization parameter in p-p scattering from 328 to 736 Mev, 20: 39791
ARENS, J., Polarization parameter in p-p scattering from 1.7 to 6.1 Bev, 20: 39702
ARISTOV, A. I., Hall effect in low-temperature plasma in non-homogeneous magnetic field, 20: 39740
ARKHANGEL'SKAYA, G. V., Preparations conducive to removal of radioactive isotopes from an organism, 20: 38733
ARMSTRONG, J. F., MHD generator operation as affected by electrode current saturation, 20: 39660
ARONSON, S., Gibbs free energies of formation of thorium phosphides from solid-state electromotive force measurements, 20: 38907
ARTANDI, C., Large scale application of radioisotopes to sterilization, 20: 39285 (DP-1066(Vol.1), pp IV.33-42)
ARTSYBASHEV, V. A., Energy spectrograms of point sources of γ rays, 20: 40290
ARTYKOV, I. Z., Interactions of 1- to 30-Bev elementary particles with atomic nuclei, 20: 39828
ARYKOVA, M. A., Changes in biochemical and physiological indices in guinea pigs during internal chronic irradiation, 20: 38662
ARZUMANOV, A. A., Conversion of Kazakhstan cyclotron to a variable energy isochronous cyclotron, 20: 39553
ASINOVSKII, E. I., Electric conductivity of argon plasma with ionizing additive, 20: 39670
ASNER, A., Layout of the new CERN neutrino beam, 20: 39746 (CERN-66-24)
ASPELUND, O., DETEC subprogram for simulation of fast-neutron detection process in hydro-carbonous plastic scintillator, 20: 39196 (AE-236)
ATEN, A. H. W. Jr., Determination of fast neutron flux densities by activation of phosphorus compounds, 20: 39222
ATEN, A. H. W. Jr., Promethium-140, 20: 40131
ATKINSON, C. H., Prog. rpt. on application of nuclear explosives to create underground storage reservoirs, 1/66, 20: 39014 (TID-23184)
AUBERT, Henri, $\beta \rightarrow \alpha$ isothermal transformation in pure and weakly alloyed U, 20: 39388 (CEA-R-2956)
AUDOIN, Claude, Field distribution in useful region of magnetic lens, 20: 39011
AUFAURE, M., Conformal transformation investigations on MHD ducts of finite length and segmentation, 20: 39661
AUGUST, Henry, Plasma properties induced in air by alpha radiation, 20: 39662
AULT, John Douglas, Improvements in or relating to illumination of timepieces, 20: 39296
AURAND, K., Preparation of representative mixed samples of tap water with simple continuous sampling device, 20: 39218
AUXIER, John, ICHIBAN: dosimetry program for nuclear bomb survivors of Hiroshima and Nagasaki, 20: 39064
AVAKYAN, S. O., Influence of x irradiation on the yield and chemical composition of potatoes, 20: 38690
AVAKYAN, V. A., Influence of x irradiation on the yield and chemical composition of potatoes, 20: 38690
AVERY, Robert T., Design of AVF cyclotrons above 100 Mev, 20: 39539
AVGUSTINIK, A. I., Reactions of oxides and carbides with metals, 20: 39331 (UCRL-Trans-10044)
AVGUSTINIK, A. I., Structure of Zr–C–Nb system, 20: 39434
AYERS, B. O., Apparent molal volumes of some aqueous rare earth chloride and nitrate solutions at 25°, 20: 38905
AYSCOUGH, P. B., Room-temperature ESR spectrum of irradiated polypropylene, 20: 38954
AZALBERT, Jean-Paul, Conditions for use of ducts of disk geometry in MHD conversion, 20: 39663
AZALBERT, Jean-Paul, Minimum-volume conversion duct, 20: 39664
AZARENKO, T. G., Use of alkyl phosphoric acids in analytical chemistry. IV., 20: 38828
AZIMOV, S. A., Inelastic π^--p interactions with slow-recoil protons at 17 Bev, 20: 39830

B

BABIKOV, V. V., Method of phase functions in quantum mechanics, 20: 39997 (JINR-P-2758)
BABU, P., Further consequences of Sugawara's theory of hyperon nonleptonic decays, 20: 39895
BACON, G. E., Neutron diffraction and its applications in inorganic chemistry, 20: 38882
BACQ, Z. M., Inhibition of O consumption of liver homogenates from mice injected with radioprotectors in presence of pyruvate, 20: 38713
BADIELLO, Roberto, Preparation of selenosure-^{75}Se by neutron activation and its radiolytic decomposition, 20: 38991
BAERG, A. P., Measurement of radioactive disintegration rate by coincidence method, 20: 40107
BAERTSCHI, P., Head-end treatment for the reprocessing of high temperature carbide–graphite fuels, 20: 40390
BAEUERLEIN, Rudolf, Electron irradiation of III-V compounds, 20: 40332
BAGINSKI, Willi A., Columbium–Hf base alloys with Y addition, 20: 39445
BAGNALL, K. W., Existence of Cm(VI), 20: 38917
BAGRAMYAN, E. R., Radiation effects on hypophysis-suprarenal system, 20: 38661
BAIER, V. N., Emission of two photons into given angle in electron collisions, 20: 39836
BAILEY, L. E., Use of ^{241}Am alphas to measure properties of thin films, 20: 39298
BAILY, Norman A., Radiation dosimetry aboard manned space vehicles, 20: 39158
BAILY, W. E., Solid-liquid phase diagram for the UO_2–PuO_2 system, 20: 39393 (GEAP-4878)
BAIN, A. S., Short duration irradiation behavior of UO_2, 20: 39447 (AECL-2581)
BAIRD, J., Electron probe microanalysis of Al-clad Zy-2 specimens after heat treatments, 20: 39380 (AECL-2570)
BAISOGOLOV, G. D., Correlation of local tissue changes and general reactions at different stages of acute radiation sickness in man, 20: 38774
BAKANOVA, A. A., Peculiarities of shock compression of lanthanides, 20: 39425
BAKER, F., Test evaluation of SNAP-15A generator, 20: 39310 (GA-5781)
BAKHTADZE, A. K., Influence of polarization of medium on electron-photon showers, 20: 39829
BALDESCHWIELER, John D., Ion-cyclotron double resonance, 20: 38902
BALFOUR, D., Ionization and temperature measurement in MPD experiments, 20: 39665
BALL, R. M., Zero power tests on NS Savannah Core II, 20: 40445 (BAW-1225)
BALL, S. J., Analysis of filling accidents in MSRE, 20: 40412 (ORNL-TM-497)
BALLUFFI, R. W., Low-energy bombardment of Au with Au ions: on interstitial atom migration in stage III, 20: 40295
BALMUKHANOV, S. B., Changes in biochemical and physiological indices in guinea pigs during internal chronic irradiation, 20: 38662
BALOCK, J. W., Gamma radiation as a quarantine treatment for Hawaiian fruit flies, 20: 39293
BALYA, E., Inelastic π^-p-interactions at energy 7.5 Bev. II., 20: 39758 (JINR-P-2773)
BAL\A, O., Inelastic π^-p-interactions at energy 7.5 Bev. II., 20: 39758 (JINR-P-2773)
BANDIRALI, G. R., Radiotherapy of carcinoma of uterine neck, 20: 38786
BANNIK, B. P., Observation of the $\Lambda\eta^0$ resonance in π^--p interactions at 4.0 Bev/c, 20: 39754 (JINR-E-2858)
BARABOI, V. A., Use of gallic acid in prophylaxis and therapy of acute radiation sickness, 20: 38728
BARAKAT, M. F., Labeling of insulin with ^{131}I, 20: 38933
BARAKAT, M. Z., Variations in ascorbic acid content of gramineae during germination and the effect of β- and γ-radiation, 20: 38583
BARANOV, I. A., Effect of microheterogeneity on characteristics of superconductivity of Nb–Zr–Ta alloy, 20: 40020
BARANOV, V. Yu., Electric arc in a flow of ionized and non-ionized gas, 20: 39666
BARASHENKOV, V. S., Interactions of 1- to 30-Bev elementary particles

with atomic nuclei, 20: 39828
BARCATTA, F. A., Surface tension storage and feed systems for ion engines, 20: 39091
BARCLAY, F. R., Analysis of uranium metal–graphite systems using multigroup code "WIMS", 20: 39382 (AEEW-R-473)
BARDET, R., Acceleration of plasma by field of progressive wave damped in vicinity of electron or ion cyclotron resonance, · 20: 40267
BARDET, R., Plasma acceleration by means of r-f and static magnetic field gradient, · 20: 40268
BARGER, V., Regge recurrence parity assignments for S = 0 Regge recurrences, 20: 39749 (COO-881-77)
BARGER, V., Regge-pole model and total cross sections in intermediate laboratory momentum range 2–6 Bev/c, 20: 39801
BARKOVSKII, V., Experiments on ion acceleration at 685-mm sector cyclotron, 20: 39549
BARKOVSKII, V. N., Ion optical studies of extraction transport and analysis systems for 240 cm cyclotron, 20: 39545
BARNETT, C. F., Atomic and molecular cross sections, 20: 39580 (ORNL-3989, pp 78-88)
BARRETT, Charles S., Crystal structure of solid H and deuterium, 20: 40308
BARROS, Ramon E., Radiation and dentistry, 20: 38793
BARTHELEMY, Robert R., Experimental evaluation of MHD generators operating at high Hall coefficients, 20: 39667
BARTHELEMY, Robert R., Optimum magnets for MHD generators, 20: 39668
BARTHOLIN, H., Magnetic study of the intermetallic compound $NdCo_5$, 20: 39424
BARTHOLOMEW, G. A., Research possibilities with intense neutron generator, 20: 39542
BARTON, G. W. Jr., Isotopic disproportionation reaction between light and heavy water using pulsed-molecular-beam mass spectrometer, 20: 38875 (UCRL-14703-T)
BARTSCH, J., Observation of a (K $\pi\pi$) resonance near 1800 Mev, 20: 39788
BARUT, A. O., Tensor operators and mass formula in minimal extension of U_3 by charge conjugation, · 20: 39916
BARUT, A. O., Two uses of non-compact groups in particle physics and their relations, 20: 39915
BASARGIN, Yu. G., Ion optical studies of extraction transport and analysis systems for 240 cm cyclotron, 20: 39545
BASHKIN, S., Collisional excitation of atomic spectra in accelerated beams of light elements, 20: 39593
BASLER, E., Prefabricated blast-resistant shelter, 20: 39075
BASOV, S. N., Injection of liquid metals in MHD converters, 20: 39669
BASU, D., Solar and solar-terrestrial events in relation to solar cycle, 20: 39563
BATCH, M. L., Zero power tests on NS Savannah Core II, 20: 40445 (BAW-1225)
BATCHELOR, A. L., Clinical and pathological response of goats to whole-body irradiation by gamma rays and fission neutrons, 20: 38629
BATCHELOR, A. L., Comparison of the mutagenic effectiveness of chronic neutron and γ irradiation of mouse spermatogonia, 20: 38647
BATE, L. C., Adsorption and elution of trace elements on human hair, 20: 38543
BATEMAN, G. H., Trans-sphenoidal hypophysectomy, 20: 38758
BATENIN, V. M., Electric conductivity of argon plasma with ionizing additive, 20: 39670
BATES, Howard F., Latitude of the dayside aurora, 20: 39971
BATES, J. L., Irradiation brewing of UO_2, 20: 39449 (BNWL-SA-272)
BATHOW, G., Measurement of synchrotron radiation in x-ray region, 20: 39473
BATRA, T. L., Effect of π and Σ molecular states in Ne^+-Ne scattering, 20: 39601
BATUSOV, Yu. A., Helium-8 production in negative pion capture by C and and O nuclei, 20: 40071 (JINR-E-2774)
BAUER, D. J., Extraction and separation of selected lanthanides with tertiary amine, 20: 38995 (BM-RI-6809)
BAUMANN, M., Lifetimes of the excited states $(6s6p)^1P_1$ and $(6s6p)^3P_1$ of Yb, 20: 39597
BAUMEISTER, Kenneth J., Heat-transfer analysis of Plum Brook reactor, 20: 40461 (NASA-TN-D-3552)
BAUMGAERTEL, F., Application of various methods for decontamination of radioactive reservoir water in high power fast filter system, 20: 40484
BAYANOV, A. P., Rare earth metal and Y distribution during Zn crystallization in lead melt, 20: 39435
BEAUCHAMP, J. L., Ion-cyclotron double resonance, 20: 38902
BECARUD, Nicole, Contribution to the analytic study of ferrates, 20: 38859 (CEA-R-2895)
BECK, Ainslie Rogers, Metal heat insulating structural members, 20: 40367
BECKETT, A., Effect of deuterium substitution on radioniess decay of anthracene triplet, 20: 38958
BEDENIG, D., Experimental methods for flow in spherical bodies, 20: 39051
BEG, M. A. B., Almost exact sum rules for nucleon moments from infinite-dimensional algebra, · 20: 40130
BEGZHANOV, R. B., Lifetimes of the excited levels of ^{151}Pm, 20: 40105
BEHRENS, H., Preparation of representative mixed samples of tap water with simple continuous sampling device, 20: 39218
BELAI, V. E., Prophylaxis of diseases caused by multiple external gamma irradiation, 20: 38726
BELINFANTE, J. G., Ambiguity of meson-baryon couplings in bootstrap static model of SU(6) symmetry, 20: 39813
BELL, P. R., Injection and accumulation: multiple-pass experiments (DCX-2), · 20: 40172 (ORNL-3989, pp 14-30)
BELL, R. J., Stopping powers and straggling in rare gases, 20: 39611
BELMONT, J. L., Axial injection for the Grenoble cyclotron, 20: 39532
BELOUSOV, A. S., Photoproduction of π^0 mesons on ^4He near to threshhold, 20: 39822
BELOUSOV, V. N., Ionization instability and turbulent conductivity of non-equilibrium plasma, 20: 39671
BELTRAMETTI, E. G., Circular polarization measurements in γ-γ perturbed angular correlations, · 20: 40125
BELTRAMI, Mario, Tolerance of the heart to ionizing radiations, 20: 38675
BELTYUKOVA, S. V., Spark method for spectrographic determination of rare earths in solutions, 20: 38832
BELYAKOV, V. A., Inelastic π-p-interactions at energy 7.5 Bev. II., 20: 39758 (JINR-P-2773)
BEM, J., Production of electron-positron pairs by high-energy gamma quanta, 20: 39594
BEM, Yu., Identification of charged particles by ionization and δ-electrons in a propane bubble chamber, 20: 39211 (JINR-P-2842)
BENAKSAS, D., Deuteron electromagnetic form factors for $3\ F^{-2} < q^2 < 6\ F^{-2}$, 20: 39795
BENAROYA, R., Superconducting plates as magnetic shields, 20: 39523
BENDER, Carl M., Peculiarities of free massless spin-½ field theory, 20: 39890
BENDER, Charles F., Natural orbital based energy calculation for helium hydride and lithium hydride, 20: 38910
BENDER, M. A., Cytogenetic methods: somatic chromosome aberrations in occupationally irradiated humans, 20: 38593 (ORNL-P-2175)
BENES, Petr, Substoichiometric determination of amount of carrier in a "carrier-free" ^{65}Zn preparation, 20: 38814
BENJAMIN, Thomas Livingston, Radiobiological and biochemical investigations of Polyoma virus-cell interactions, 20: 38702
BENNETT, Michael, Functional and morphological characterization of stem cells, 20: 38592 (ORNL-P-2158)
BENSON, R. H., Apparatus for precise metering of radioactive gases or solutions, 20: 39172
BENUSKA, K. L., Resistance of tubular structures to dynamic loading, 20: 39007 (AD-636914)
BERBANO, Mario C., Preparation of high specific activity ^{51}Cr, 20: 38982 (PAEC(D)IS-652)
BERCHERS, R., Effective magnetic fields at Sm, Gd, and Dy nuclei in metallic Fe following Coulomb excitation implantation, 20: 40342
BEREZIN, Yu. A., Theory of nonlinear waves in plasma, · 20: 40235
BERG, R. E., Control of the Michigan State University cyclotron, 20: 39552
BERGER, Edmond Louis, Deuteron and bound states of nucleon-antinucleon system, 20: 39841
BERGER, Harold, Characteristics of thermal neutron television imaging system, 20: 39174
BERGER, M. S., Results of experiments with 100-kw MHD generator model, 20: 39672
BERGER, R., Determination of americium by controlled-potential coulometry, 20: 38854
BERGFELDT, J., Studies of characteristic flash x-ray lines, · 20: 40233
BERGHAUS, Bernard, Anti-corrosion treatment of nuclear reactor fuel rod envelopes, 20: 39350
BERGKVIST, K.-E., Scheme for high luminosity, high resolution internal and external conversion measurements, 20: 39234
BERGSTROEM, I., Nuclides far off the stability line, · 20: 40108
BERGSTROEM, I., Nuclides far off the stability line, 20: 40109
BERGSTROEM, I., Why nuclear spectroscopists should know about recent development in atomic stopping, 20: 39595
BERGSTROEM, S., Resonances in the $^{41}K(p,\gamma)^{42}Ca$ reaction at proton energies 1740–2170 kev, · 20: 40133
BERLIN, L. B., Mechanism of protective action of aminothiols, 20: 38723
BERMANIS, H. L., Nuclear test gauge safety analysis report, 20: 40459 (GEMP-152)
BERNARD, Jean, Effect of ionization saturation and duct shape on losses near walls, 20: 39673
BERNARDINI, M., Evaluation of background around the Adone, 20: 39495 (LNF-66/22)
BERNERT, R. E., Large experimental superconducting magnet for MHD power generation, 20: 39643

BERNERT, R. E., Methods and costs of testing at liquid helium temperatures, 20: 40019
BERNIER, Jean-Pierre, SU_3 nuclear shell model, 20: 40163
BERNSTEIN, E. M., Comparison of rotational M1 transition rates between high and low spin states, 20: 40072 (LA-DC-8061)
BERNSTEIN, E. M., Further evidence for effective nucleon spin g-factors, 20: 40073 (LA-DC-8065)
BERNSTEIN, Gustave, Method and arrangement for burning fuel containing hydrogen at very high temperature, 20: 39013
BERRY, Roger J., Effects of metabolic inhibitors on x-ray-dose-response curves for survival of mammalian cells in vitro, 20: 38710
BERSENEV, P. A., Conversion of Kazakhstan cyclotron to a variable energy isochronous cyclotron, 20: 39553
BERTANZA, L., Interactions (π^--p) at 775 Mev, 20: 39780
BERTHELET, Jacqueline, Variation in hematocrit of rat after gamma irradiation, 20: 38587 (CEA-R-2909)
BERTOLINI, E., CNEN He–Cs blow-down MPD facility and experiments with prototype duct, 20: 39675
BERTOLINI, E., Relaxation phenomena in MPD generators, 20: 39674
BERTOZZI, W., Shell effects in high energy photoproton spectra from ^{6}Li, 20: 40077 (MIT-2098-256)
BES, D. R., Gamma vibrations in odd-mass rare-earth nuclei, 20: 40118
BETER, E. V., Diffraction dissociation $\pi \to 3\pi$ in field of heavy nuclei, 20: 39774
BETHARD, W. F., Neutron activation analysis for quantitation of selected cations in blood, 20: 38852
BETZ, F., Polarization parameter in p-p scattering from 328 to 736 Mev, 20: 39791
BETZ, F., Polarization parameter in p-p scattering from 1.7 to 6.1 Bev, 20: 39792
BEURTEY, R., New injection method for cyclotrons, 20: 39530
BEZUSY, L. G., Electrical parameters of synchronous MHD generator with pulsating electric conductivity of medium, 20: 39676
BHAT, T. R., Retardation of oxidation rates of Nb, Ta, and W by fluoride coating, 20: 39348
BHATKI, K. S., Radiochemical separation and purification of ^{140}Ba and rapid milking of ^{140}La from ^{140}Ba, 20: 39001
BIBERMAN, L. M., Energy exchange between electron and molecular gases, 20: 39677
BICK, J. H., Computer study of dynamics of MRP shaft-bearing system, 20: 39022 (NAA-SR-11943)
BIDARD, René, MHD generator using an emulsion, 20: 39678
BIEDENHARN, Lawrence C. Jr., Complex angular momenta and the groups SU(1,1) and SU(2), 20: 39863
BIETH, C., Heavy ion injection for stripping in the central region of the CEVIL, 20: 39531
BIETH, C., Operation of the Orsay CEVIL and its extraction systems, 20: 39551
BIGI, A., Interactions (π^--p) at 775 Mev, 20: 39780
BILDSTEIN, H., Fission product distribution in coating of fuel elements for high temperature reactors, 20: 40386 (SGAE-CH-33/1966)
BILENKAYA, S. I., Polarization tensor in scattering of polarized nucleons on polarized proton target, 20: 39909
BILL, H., Center (V_k) in $SrCl_2$ crystals, 20: 40319
BILL, H., EPR of a center in Y^{3+} doped artificial CaF_2 crystals, 20: 40321
BIRARELLI, B., Effect of cysteamine on ultrastructural modifications of liver of rabbits exposed to whole-body x irradiation, 20: 38716
BIRGENEAU, R. J., Temperature variation and separation dependence of exchange interactions of Gd^{3+} pairs in $LaCl_3$, 20: 38914
BIRISOV, M. S., Complexing of trivalent actinides and lanthanides in phosphoric acid solutions, 20: 38878 (ORNL-tr-1257)
BIRMINGHAM, Thomas Joseph, Radiation by a plasma: quadrupole bremsstrahlung and synchrotron emission, 20: 40273
BIROT, André, Concentration of natural radioactive gas and of equilibrium between this gas and its daughter products in air at ground level, 20: 39114
BISSON, Auguste-André, Electron microscope study of irradiated beryllium oxide, 20: 39450 (CEA-R-2963)
BISWAS, S., Solar cosmic-ray multiply charged nuclei and July 18, 1961, solar event, 20: 39564
BJORKEN, J. D., Applications of the chiral U(6) × U(6) algebra of current densities, 20: 39896
BLACK, K. M., Engineering and evaluation study for the manufacture of wood-plastic composites, 20: 39287 (KLX-1876)
BLACKMAN, Vernon H., Magnetically induced ionization in rare gas mixtures, 20: 39679
BLAIR, I. M., Search for resonant π-π interaction in process π^-p→ $\pi^+\pi^-$n near threshold, 20: 39779
BLAKE, Kenneth R., An on-line nuclear analysis facility, 20: 39025 (ORO-2980-12)
BLANC, Daniel, Concentration of natural radioactive gas and of equilibrium between this gas and its daughter products in air at ground level, 20: 39114
BLANKS, J. R., Power requirements for single-point tools, 20: 39027 (Y-DA-1287)
BLASE, E. F., Prototype thermoluminescent dosimetry system for personnel monitoring, 20: 39224
BLASER, J. P., Progress report on the 500-Mev isochronous cyclotron meson factory of ETH Zurich, 20: 39533
BLECHER, Melvin, Synthesis and characterization of 3-ketohexadecanoic acid-1-^{14}C, DL-3-hydroxyhexadecanoic acid-1-^{14}C, and trans-2-hexadecenoic acid-1-^{14}C, 20: 38987
BLEVIN, H. A., Propagation of helicon waves in non-uniform plasma, 20: 40189
BLOCH, R., Resonances in ^{40}Ar(p,p) near 1.1 Mev, 20: 40147
BLOEDORN, Fernando G., Rationale and benefit of preoperative irradiation in lung cancer, 20: 38755
BLOMQVIST, Goeran, Further age measurements on radioactive minerals from Sweden, 20: 39125
BLOMQVIST, Goeran, Rubidium–strontium whole rock age data on some Swedish precambrian rocks, 20: 39126
BLOMSTRAND, J. H., Uranium-235/Th fuel cycles in graphite moderated systems, 20: 40393
BLOOD, R. E., Prog. rpt. on specific Zr alloy design program, 4/66, 20: 39356 (GEAP-5134)
BLOSSER, H. G., Control of the Michigan State University cyclotron, 20: 39552
BLOSSER, H. G., Phase space density studies on cyclotron ion sources, 20: 39528
BLOSSER, H. G., Problems and performance in the cyclotron central region, 20: 39511
BLUMENTHAL, J. L., Chemical integrity of radioisotope containment materials in launch abort environments, 20: 39312 (SC-CR-66-2044)
BOBODZHANOV, I. B., Regularities in angular distribution of neutrons emitted in polarized μ-meson capture by nuclei, 20: 40096
BOCHKAREV, V. V., Scintillation dosimeter for rating beta applicators, 20: 38777
BOCKRIS, John O'M., Prog. rpt. on properties and structure of molten salts, annual, 1964–65, 20: 38871 (NYO-1769-54)
BOCKRIS, John O'M., Prog. rpt. on properties and structure of molten salts, annual, 1965–66, 20: 38872 (NYO-1769-68)
BODDY, K., Mobile shadow-shield whole-body monitor for medical research, 20: 38753
BODENHEIMER, Peter Herman, Problems in pre-main-sequence stellar evolution, 20: 39574
BOECK, W. L., Effect of surface micropatches on average thermionic constants of metallic emitters, 20: 39642
BOESCH, R., Compton effect on bound K electrons, 20: 39773
BOETTCHER, A., Fuel elements, 20: 39332
BOEUF, A., Fine structure of thermal flux and end-effect in tubular composite U fuel elements cooled by an organic compound, 20: 39452 (EUR-2981.f)
BOGACHEV, N. P., Inelastic interactions of 19.8-Bev/c protons with neutrons, 20: 39761 (JINR-P-2809)
BOGARD, D. D., Isotopic composition of Xe from Ca-poor achondrites, 20: 39984
BOGOLUBOV, N. N., Adler-Weisberger relation and dispersion sum rules in theory of strong interactions, 20: 39857 (JINR-E-2876)
BOGOLYUBOV, P. N., Ratio of axial and vector constants in dynamical quark model, 20: 39753 (JINR-E-2827)
BOGOMOLOV, YU. V., Electromagnetic field penetration into magnetoactive plasma, 20: 40204
BOHN, Th., Analysis of essential characteristics for closed MHD power stations, 20: 39682
BOHN, Th., Closed MHD-loop ARGAS, 20: 39680
BOHN, Th., Layout data of homogeneous closed-cycle 300-Mw MHD generator, 20: 39681
BOHNE, F., Diminution of radiocesium body-burden in dogs and human beings by Prussian Blue, 20: 38557
BOHNE, Felicitas, Excretion of ^{85}Zn-DTPA in the rat, 20: 38556
BOKK, M. I., Preparations conducive to removal of radioactive isotopes from an organism, 20: 38733
BOMAN, L. H., Application of radioisotope heat source interior to tubular thermoelectric generator, 20: 39308 (DP-1066(Vol.2), pp III.3-16)
BOND, V. P., Intranuclear ^{3}H thymidine: dosimetric, radiobiological and radiation protection aspects, 20: 38624
BONFIELD, William, Beryllium alloy and process, 20: 39374
BONHAM, Kolshaw, Effects of low-level chronic irradiation of Chinook and Coho salmon eggs and alevins, 20: 38698
BONILLA, C. F., Viscosity of Cs up to 5 bars and 1000°C, 20: 39392 (CU-2660-29)
BOORSTEIN, Seth A., Theory of slow atomic collisions. II., 20: 39620
BORCHERT, C., Large experimental superconducting magnet for MHD power generation, 20: 39643
BORDYUKOVA, M. A., Dosage loads in medical staff dealing with colloidal ^{198}Au, 20: 39159

BORGIA, B., Optical properties of strong-focusing magnet, 20: 39494 (LNF-66/15)
BORLERA, Maria Lucce, Niobium oxide–titanium dioxide system, 20: 39411
BOROS, I., Influence of ionizing radiations on cortico-suprarenal system evaluated on basis of potassium in rabbits, 20: 38697
BOSCH, D., Magnetic fields at ^{119}Sn in rare earth metals, 20: 40322
BOSE, D. K., Probe data of duoplasmatron plasma, 20: 40202
BOSE, Shubha, Sum rules for strangeness-changing axial-vector coupling constants, 20: 39809
BOUISSIERES, Georges, Protactinium peroxide compounds in basic media, 20: 38890
BOUNDEN, J. E., High-output neutron tube for activation analysis, 20: 38839
BOURE, J., Hydrodynamic instabilities limiting power of boiling water reactors, 20: 40403 (EURAEC-1464)
BOURGAREL, M. P., Operation of the Orsay CEVIL and its extraction systems, 20: 39551
BOWEN, H. J. M., Necessity of biological standards for activation analysis, 20: 38844
BOYCE, Richard P., Loci in E. coli K-12 that control mutagen products from DNA, 20: 38620
BOYD, Jim A., Transverse plasma injection into multipole magnetic field, 20: 40254
BOYER, T. H., Operators for symmetry transformations in canonically quantized field theories, 20: 39876
BRADFORD, P. V., Cyclotron harmonic radiation from electron beam injection into an afterglow plasma, 20: 40165 (AD-637710)
BRANDELA, Maxime, Oxidation risks during sintering of uranium dioxide, and characterization of excess O, 20: 39390 (CEA-R-3003)
BRANDES, S., Uranium-235 fueled thermal high temperature reactor with ^{233}U in equilibrium state with ^{232}Th as a fertile species, 20: 40469
BRANDMAIER, Harold E., Performance characteristics of an electrogasdynamic power generator, 20: 39649
BRANDT, A. A., Theory of frequency multiplier in a gas discharge in strongly nonuniform shf field, 20: 40228
BRANDT, N. B., Magnetoresistance of Bi in fields up to 450 kOe at He temperatures, 20: 40027
BRANSDEN, B. H., Positron scattering by H and adiabatic potential, 20: 39817
BRASKI, David N., Dynamic modulus of stabilized zirconia, 20: 39438
BRAUN, J., Measurement of the electrical conductivity of ^{3}He induced by neutron irradiation, 20: 39683
BRAYER, R. C., Prog. rpt. on burnable poison additions to UO_2, 1–3/66, 20: 40382 (CEND-3107-267)
BRDAR, B., Patterns of nucleic acid and protein synthesis during modification of lethal ultraviolet lesion, 20: 38562
BRDAR, B., Survival of uv-irradiated E. coli in presence of chloramphenicol and in absence of essential metabolite, 20: 38563
BREARTON, Denis Stanislas, Preparation of dense uranium oxide, 20: 39373
BRECCIA, Alberto, Preparation of selenoures-^{75}Se by neutron activation and its radiolytic decomposition, 20: 38991
BREDERLOW, G., Non-equilibrium conductivity in Ar–K plasma in crossed electric and magnetic fields, 20: 39684
BREEV, V. V., Development of flow of a viscous fluid in duct of MHD generator, 20: 39685
BREGADZE, Yu. I., Calculation of absorbed doses in plant seeds during irradiation with fast neutrons, 20: 38693
BRESLAVETS, K. G., Separation of neon isotopes in film fractionating column, 20: 39322
BRESSAT, Rene, Preparation and properties of the double salt $2Th(C_2O_4)_2 \cdot (NH_4)_2C_2O_4 \cdot 7H_2O$, 20: 38886
BREUER, G., Angular distribution and effective cross section of reaction $^{10}B(d,\alpha)^{8}Be$ between 1.6 and 3.0 Mev, 20: 40068 (BMWF-FBK-66-15, pp 38-46)
BREUER, G., Investigations in low energy physics performed in Japan, 20: 40066 (BMWF-FBK-66-15)
BREUER, G., Report on measurements of reaction $^{40}Ca(d,\alpha)^{39}Ca$ for 24 Mev impact energy, 20: 40067 (BMWF-FBK-66-15, pp 20-37)
BREUIL, Lucien, Variation in hematocrit of rat after gamma irradiation, 20: 38587 (CEA-R-2909)
BREWEN, J. G., Nonrandom rejoining of chromatid breaks and its relation to origin of sister-chromatid exchanges, 20: 38649
BREZIKOVA, D., Internal contamination with ^{90}Sr and ^{226}Ra in man in relation to clinical findings, 20: 38623
BRIANTI, G., Strong-focusing ring, as beam stretcher for synchrocyclotrons, 20: 39538
BRICE, Neil M., Ion temperature in ionosphere obtained from cyclotron damping of proton whistlers, 20: 39972
BRICKWEDDE, F. G., Comparison of saturated-liquid viscosities of low molecular substances, 20: 39940
BRIDGE, H. S., Preliminary results from the Pioneer 6 M.I.T. plasma experiment, 20: 40212
BRIDWELL, Lynn Boyd, Time of emission and yield of x rays from thermal neutron fission of ^{235}U and ^{239}Pu, 20: 40158
BRIGGS, Russell C., Quantitative radiosensitivity studies of solid carcinomas in vivo, 20: 38635
BRIGHT, A. W., Recent developments in electrostatics, 20: 39472
BRIN, M. L., Megakaryocytes of bone marrow in patients with milk-duct and lung carcinoma during ^{198}Au therapy, 20: 38643
BRITT, Harold C., Instrumentation for fission studies, 20: 39242
BROBECK, William M., Design of AVF cyclotrons above 100 Mev, 20: 39539
BROCHER, E., MHD generator with pulsating flow in a pre-heated gas, 20: 39686
BROCHER, E., Shock-wave MHD generator using nuclear reactor as energy source, 20: 39639
BRODE, Harold, Blast and other threats, 20: 39055
BRODSKY, Marc Herbert, Infrared reflection studies of single-crystal lithium hydride derivatives, 20: 40351
BROERSE, J. J., Dosimetry for fast-neutron irradiations of cultured cells and intact animals. I., 20: 39227
BROERSE, J. J., Dosimetry for fast-neutron irradiations of cultured cells and intact animals. II., 20: 39228
BROGAN, Thomas R., Magnetohydrodynamic power plant, 20: 39043
BROWN, D. A., Determination of ^{55}Fe and ^{59}Fe in blood by liquid scintillation counting, 20: 38555
BROWN, Karl K., Power Reactor Technology. Vol. 9, No. 2, 20: 40426
BROWN, R., CNEN He–Cs blow-down MPD facility and experiments with prototype duct, 20: 39675
BROWN, R., Further development, operation, and experiments with IRD closed-cycle MPD loop, 20: 39687
BROWN, Stephen L., Industrial recovery techniques, 20: 39146 (AD-636947)
BROWNE, J. C., Collision-induced de-activation of metastable helium, 20: 39609
BRUCE, C. W., Time and spatially resolved interferometry on pulsed-laser-induced plasmas, 20: 40186
BRUN, Gilbert, Orientational relationships between phases in the $\gamma \rightarrow \alpha$ transformations for U–Mo alloys, 20: 39389 (CEA-R-2973)
BRUNEDER, H., Plutonium fuel cycle studies for large high temperature graphite moderated reactor, 20: 40421
BRUNEDER, H., Uranium-235/Th fuel cycles in graphite moderated systems, 20: 40393
BRUNER, H. D., Radiotherapy, 20: 38774 (DP-1066(Vol.1), pp IV. 47-66)
BRUNTON, Donald C., Mass determination of fluent material by radioactive measuring means, 20: 39189
BRUSCHI, L., Temperature dependence of critical velocity of positive ions in liquid helium, 20: 40033
BRUYERE, P., Veterinary medicine and nuclear science, 20: 38748
BRZOZOWSKI, W. S., Open-cycle power generation experiment with high preheat temperature of air, 20: 39689
BRZOZOWSKI, W. S., Operating experience of an open-cycle MHD test facility, 20: 39688
BRZOZOWSKI, W. S., Production and investigation of materials for MHD generator, 20: 39690
BUBELEV, E. G., Observation of the $\Lambda\eta^0$ resonance in π^--p interactions at 4.0 Bev/c, 20: 39754 (JINR-E-2858)
BUCHANAN, D. H. E., Moessbauer effect in $Co_{1-x}Fe_xSi$, 20: 40300
BUCHANAN, Robert F., Anion exchange in nitrate solutions, 20: 38820
BUCKLEY, John D., Dynamic modulus of stabilized zirconia, 20: 39438
BUDYASHOV, Yu. G., Structure of Ar K-series during atomic capture of negative muons in pure gas and in mixture with H, 20: 39578 (JINR-P-2807)
BUECKEN, R., General formulation of postulate for minimum volume of MHD generator duct with fixed outer boundary values, 20: 39703
BUERKHOLZ, A., Irradiation damage in beryllium, 20: 39454 (EUR-3055.e)
BUERKHOLZ, A., Irradiation damage in beryllium oxide, 20: 39453 (EUR-3054.e)
BUERKHOLZ, A., Irradiation damage in graphite, 20: 39455 (EUR-3056.e)
BUGENIS, Claudius K., Demonstration of x-ray diffraction by LiF using the Mn Kα x rays resulting from ^{55}Fe decay, 20: 40294
BUGRYSHEV, P. F., Toxicity of tritium oxide in mice and rats subjected to intraperitoneal injection, 20: 38568
BUINOV, N. N., Relationship between superconductivity and structure of Zr–4Nb alloy, 20: 40021
BUKHMAN, N. D., Effect of vitamins and phosphatides on resistance to radiation, 20: 38721
BUKHVOSTOV, A. P., Depolarization of μ^- mesons in the creation of μ-mesicatoms, 20: 39616
BULATSKII, N. P., X-ray effects on esterase activity in white rat blood serum, 20: 38682
BUNEMAN, O., Radio-frequency heating of collisionless plasmas, 20: 40256
BUNYATOV, S. A., Helium-8 production in negative pion capture by C

and O nuclei, 20: 40071 (JINR-E-2774)
BURAGGI, G. L., Improvement in techniques of metabolic radiotherapy of thyroid disorders, 20: 38785
BURDESE, Aurelio, Niobium oxide–titanium dioxide system, 20: 39411
BURDITT, A. K. Jr., Gamma radiation as a quarantine treatment for Hawaiian fruit flies, 20: 39293
BURENKOV, D. K., Choice of optimum Mach number for flow of non-equilibrium He–Cs plasma in MHD generator duct, 20: 39691
BURENKOV, D. K., Effect of inhomogeneity of the magnetic field on flow of conducting fluid in Hall-type MHD generators, 20: 39692
BURG, C., Synergetic effect of x rays and of vincaleucoblastine on solid isologous tumor of mouse C^3H, 20: 38613
BURG, H., Obtaining an impermeable graphite by impregnation with molten metals, 20: 39355 (EUR-2988.f)
BURGER, R., Machine development at the Berkeley 88-inch cyclotron, 20: 39547
BURGETT, R., Prog. rpt., 4–6/66, 20: 38799 (NLCO-980)
BURK, W., Ammonolysis of U halides. I., 20: 38920
BURKETT, M. N., Design and fabrication of (AVR) injection-molded fuel element, 20: 40468
BURKHARDT, H., Reduction of the dimensions of induction converters by skin-heating, 20: 39693
BURMAN, R., Transverse electromagnetic wave propagation in cylindrically stratified magnetoplasma, 20: 40201
BURNEY, G. A., Analytical chemistry of neptunium, 20: 38821
BURNHAM, D. Arthur, Prog. rpt. on solid-state chemistry of rare earth oxides, annual, 1965–66, 20: 38861 (COO-1109-22)
BURNHAM, Marvin W., Influence of a curved duct on explosive-driven MHD converters, 20: 39694
BURTON, R. A., Prog. rpt. on liquid-metal lubricated journal bearings, 4–7/66, 20: 39008 (SWRI-1228-8-24)
BUSCHOW, K. H. J., Magnetic properties of rare-earth aluminum compounds, 20: 39433
BUTLER, J. P., Cross section for reactions $^{65}Cu(n,p)^{65}Ni$, $^{65}Cu(n,2n)^{64}Cu$, and $^{65}Cu(n,n\alpha)^{61}Co$, 20: 40149
BUTLER, J. W., Theoretical proton energy-loss distributions from thin carbon foils, 20: 40117
BUXBAUM, Piroska, Solvent effects in isotope exchange reactions. VI., 20: 38936
BYERS, Charles Harry, Convective transfer processes in laminar gas-liquid channel flow, 20: 39050 (UCRL-16535)
BYRNE, Thomas J., Zirconia based foam insulating material and method, 20: 39375

C

CABRESPINE, A., Heavy ion injection for stripping in the central region of the CEVIL, 20: 39531
CABRESPINE, A., Operation of the Orsay CEVIL and its extraction systems, 20: 39551
CACACE, Fulvio, Reactions of energetic carbon atoms in methylamine, 20: 38964
CACERES, C., Digital program for calculation of activities of fission products of long half life, 20: 40070 (IEA-111)
CADART, M., Acceleration of plasma by field of progressive wave damped in vicinity of electron or ion cyclotron resonance, 20: 40267
CADART, M., Three modes of energy transfer of a plasma h-f field, 20: 40261
CAILLET, C., Trajectories in studies of interactions of h-f fields with plasma, 20: 40283
CALDERWOOD, J. H., Effect of radiation on electric conduction in n-hexane, 20: 38971
CALDWELL, Richard A., Triplet states in radiation chemistry, 20: 38948
CALLAWAY, Joseph, Comparison of approximate polarization potentials, 20: 39621
CALLEBAUT, D. K., Ion density in electron beams. II., 20: 39605
CALVERT, W., Steep horizontal electron-density gradients in topside F layer, 20: 39974
CAMBI, Silvano, Progress on the PCUT program, 20: 39006
CAMERON, A. G. W., Lunar period, solar period, and K_p, 20: 39982
CAMERON, J. R., Effect of quality of radiation on thermoluminescence of LiF(TLD-100), 20: 39199 (COO-1105-117)
CAMERON, J. R., Effects of irradiation temperature in LiF(TLD-100), 20: 39200 (COO-1105-118)
CAMPANA, R. J., Test evaluation of SNAP-15A generator, 20: 39310 (GA-5781)
CAMPBELL, G. M., Thermodynamic properties of plutonium mononitride from electromotive force measurements, 20: 38911
CAMPBELL, I. A., Magnetic moment distributions for transition metal impurities in iron, 20: 40330
CAPALNA, Simion, Protective effect of glycine in x irradiation, 20: 38714
CAPPIS, John H., Leaching of uranium by hydrogen chloride, 20: 39346 (LA-3488)
CAPPS, Richard H., $SU(6)_w$-symmetric meson bootstrap model, 20: 39885
CARDWELL, George L., Transverse plasma injection into multipole magnetic field, 20: 40254
CAREY, Walter E., Neutron radiography of pyrotechnic cartridges, 20: 39334
CARIBBO, N., Algebra of scalar and vector vertex strengths in Regge residues, 20: 39881
CARLESON, G., Prog. rpt. on nuclear chemistry, annual, 1965, 20: 38994 (AE-232)
CARO, Paul, Prog. rpt. on solid-state chemistry of rare earth oxides, annual, 1965–66, 20: 38861 (COO-1109-22)
CARPENTER, R. T., USAEC isotopic power applications, 20: 39305 (DP-1066(Vol.1), pp V.3-16)
CARR, Donald E., Irradiation of oil shale–polyolefin articles, 20: 38974
CARRARA, R., Interactions (π^--p) at 775 Mev, 20: 39760
CARRASSE, J., Chemical recovery of energy in combined MHD/steam power station, 20: 39695
CARRIGAN, P. H. Jr., Radionuclides in Clinch-Tennessee Rivers, 20: 40479 (ORNL-P-2328)
CARROLL, David I., Missile scoring systems utilizing nuclear radiation, 20: 39190
CARTER, J. R., Radiation damage in semiconductors. XII., 20: 39458 (NP-16225)
CASALI, R., Interactions (π^--p) at 775 Mev, 20: 39780
CASON, Neal M., A_1 and A_2 production in the reaction $\pi^- + p \to \pi^- + \pi^- + \pi^+ + p$ at 7.0 Bev/c, 20: 39790
CASTIGLIONI, M., Acceleration of H^- ions and extracted beam measurements in Milan cyclotron, 20: 39550
CATES, Phillip Stephen, Peripheral compressor, 20: 39021 (K-1665)
CATSCH, Alexander, Excretion of ^{65}Zn-DTPA in the rat, 20: 38556
CATSCH, Alexander, RBE of fast neutrons by release of mutations in Drosophila, 20: 38645
CAWLEY, Robert Gerald, Integral equation for anomalous deuteron vertex and comparison of two normalization conditions, 20: 39843
CELINSKI, Z. N., Effect of finite-length electrodes on electrical parameters in MHD generator, 20: 39697
CELINSKI, Z. N., Electrical equivalent circuits of d-c MHD generators, 20: 39696
CELINSKI, Z. N., Operating experience of an open-cycle MHD test facility, 20: 39688
CERINI, D. J., Theoretical and experimental investigation of liquid–metal MHD power generation, 20: 39716
CHADRAA, B., Observation of the $A\eta^0$ resonance in π^--p interactions at 4.0 Bev/c, 20: 39754 (JINR-E-2858)
CHADWICK, B. M., Transition metal cyanides and their complexes, 20: 38881
CHALOV, P. I., Comparative oxidation rate of ^{234}U and ^{238}U atoms in certain minerals, 20: 38894
CHALOV, P. I., Washout of radioactive aerosols from atmospheric fallout in layer below clouds, 20: 39113
CHAMBERLAIN, O., Polarization parameter in p-p scattering from 328 to 736 Mev, 20: 39791
CHAMBERLAIN, O., Polarization parameter in p-p scattering from 1.7 to 6.1 Bev, 20: 39792
CHAMBERS, S., Reactor steam cycles for desalination, 20: 40439
CHANG, L. O., Variation radiation dose and its relationship to depression of DNA synthesis, 20: 38576 (TID-22103)
CHANG, Shau-Jin, Quantization of spin-2 fields, 20: 39884
CHANTRY, P. J., Theory of electron collision experiments, 20: 39576 (AD-636533)
CHAPMAN, J. W., Evidence concerning C violation in eta decay, 20: 39766 (ORO-3065-10)
CHAPMAN, J. W., Three-pion production by 1.95 Bev/c positive pions on protons, 20: 39767 (TID-23278)
CHAPOROVA, I. N., Preparation of the carbides (Ti,W,Cr)C and study of their properties, 20: 39431
CHAPPELL, Willard R., Kinetic equation for electron-phonon gas, 20: 40313
CHASSEUR, Philippe, Coulometric determination of C in Pu and in U–Mo alloys, 20: 38796 (CEA-R-2968)
CHEKHOVSKII, V. Ya., Thermal conductivity of heat-resisting high-alumina concretes, 20: 39698
CHEKMAREV, I. B., Problems of MHD conversion: experimental results, 20: 39707
CHEMERIS, V. T., Hall effect in low-temperature plasma in non-homogeneous magnetic field, 20: 39740
CHEN, Ji, Assignments of baryon resonances in $SU(12)$ and their strong decays, 20: 39907
CHENG, David, Nucleon-nucleon polarization at 700, 600, 500, and 400 Mev, 20: 39844
CHENG, Shao-chang, Role of autoinfection in development of the hemorrhagic syndrome during acute radiation sickness, 20: 38656
CHENOUARD, Jean, Study of isomers ^{236}Np and ^{236m}Np by interaction

of deuterons with ^{238}U, 20: 40092
CHEREPANOV, A. N., Expansion of cylindrical column of conducting gas in longitudinal magnetic field, 20: 40237
CHERKASSKII, L. A., Roentgeno-morphological investigation of skeleton subsequent to radiation therapy of pelvic tumors, 20: 38767
CHERNENKO, G. T., Prophylaxis of diseases caused by multiple external gamma irradiation, 20: 38726
CHERNOV, A. G., Perspectives in synthesis of transuranium elements, 20: 40139
CHERNOV, A. G., Problems in elementary particle theory, 20: 39917
CHESTER, G. V., Ground state of liquid ^4He, 20: 40030
CHEVALLEY, J. L., MHD generator with pulsating flow in a pre-heated gas, 20: 39686
CHEVALLEY, J. L., Shock-wave MHD generator using nuclear reactor as energy source, 20: 39639
CHEZEM, C. G., Gaussian iterative least squares techniques for modern computers, 20: 39327 (LA-3362)
CHHABRA, A. S., Cesium-137 content of man in India, 20: 39154
CHILDRESS, J. D., Composite particles in separable-potential models, 20: 39889
CHILTON, A. B., Exposure field from a point isotropic source located at surface of thick concrete slab, 20: 40284 (AD-637125)
CHILTON, A. B., Shielding experiments, 20: 39062
CHILTON, FRANK, Theory of W production in nucleon-nucleon collisions, 20: 39797
CHINNOV, V. F., Experimental investigation of the radiation of an Ar/K plasma, 20: 39699
CHIOTAN, C., Chemical and radiochemical purity of radioactive Ca, 20: 38827
CHKHAIDZE, L., The search for "long-lived" Λ^0-particles, 20: 39762 (JINR-P-2849)
CHO, A. Y. H., Evaporative lifetimes of Cu, Cr, Be, Ni, Fe, and Ti on W and oxygenated W, 20: 40307
CHO, Kyu Suk, Study of $\bar{K}N$ and KN interactions, 20: 39840
CHO, Yi-chung, Gamma vibrations in odd-mass rare-earth nuclei, 20: 40118
CHOPRA, K. L., Growth of sputtered vs. evaporated metal films, 20: 39587
CHOQUET, Claudine, Effect of whole body irradiated and methyl-hydrazine in eradicating transplant leukaemia 1210, 20: 38794
CHORNII, V. A., Determination of rare-earth on electrode, 20: 38811
CHORVAT, Karol, Preparation of radioisotopes, radiation sources, and labeled compounds in Czechoslovak SSR, 20: 39279
CHOW, Yutze, Majorization of Feynman graphs, 20: 39867
CHRIST, N., Reciprocity relations in photopion reactions, 20: 39810
CHRISTEN, Michel, Ceramic materials for magnetoaerodynamic conversion duct electrodes, 20: 39708
CHRISTIANSEN, P. J., Propagation of helicon waves in non-uniform plasma, 20: 40189
CHRISTOPHER, S. S., Prog. rpt. on burnable poison additions to UO_2, 20: 40382 (CEND-3107-267)
CHUDAKOV, V. M., Inelastic π^--p interactions with slow-recoil protons at 17 Bev, 20: 39830
CHUKHLANTSEV, V. G., Subsolidus formation in ternary compounds of the system $BaO–ZrO_2–SiO_2$, 20: 38899
CHUN, Byong Doo, Properties of colloidal thoria. I to V., 20: 38926
CHUPAKHIN, M. S., Measurement of difference in isotopic ratios in small volumes of gases, 20: 38831
CHURCHILL, M. A., Radionuclides in Clinch-Tennessee Rivers, 20: 40479 (ORNL-P-2328)
CIALELLA, C. M., Broad range magnetic neutron spectrometer, 20: 39194 (AD-638137)
CICCARONE, P., Inhibition of O consumption of liver homogenates from mice injected with radioprotectors in presence of pyruvate, 20: 38713
CIERJACKS, S., Novel deflection-bunching system at the Karlsruhe isochronous cyclotron, 20: 39546
CIFKA, J., Distribution of radioactive Se between modifications of Se in neutron-irradiated red crystalline Se, 20: 38961
CIGNA, Arrigo A., Cesium-137 and ^{90}Sr levels in diet and urine of an Italian children's community, 20: 39152
CIPLEA, I., Chemical and radiochemical purity of radioactive Ca, 20: 38827
CLARK, A. E., Magnetic anisotropy of terbium, 20: 40346
CLARK, D. J., Machine development at the Berkeley 88-inch cyclotron, 20: 39547
CLARK, Hugh K., Interaction of fissile units computer code: INTERACT, 20: 40375 (DP-1031)
CLARKE, George A., Prog. rpt. on studies in solution and nuclear chemistry, 10/65–9/66, 20: 38873 (NYO-2269-9)
CLAUDEL, Bernard, Preparation and properties of the double salt $2Th(C_2O_4)_2 \cdot (NH_4)_2C_2O_4 \cdot 7H_2O$, 20: 38886
CLEARFIELD, Abraham, Process for production of zirconia, 20: 38929
CLEM, John Richard, Effects of anisotropy of the superconducting energy gap, 20: 40041
CLIFFORD, Charles E., Nuclear power reactor having high, prompt negative temperature coefficient of reactivity, 20: 40434
CLIFFORD, Charles E., Radiation shield arrangement for nuclear reactor, 20: 40369
CLIFTON, Kelly H., Quantitative radiosensitivity studies of solid carcinomas in vivo, 20: 38635
CLINE, D., Evidence for a $\Sigma^- \eta$ enhancement near threshold, 20: 39747 (COO-881-75)
CLINE, D., Polarization of the neutron from $\Sigma^+ \to \pi^+ + n$, 20: 39748 (COO-881-76)
CLINE, D., Regge recurrence parity assignments for S = 0 Regge recurrences, 20: 39749 (COO-881-77)
CLOOS, H., Uranium resources, 20: 39101
CLOSE, E., Machine development at the Berkeley 88-inch cyclotron, 20: 39547
COATES, Arthur D., Application of fast neutron activation analysis to polymer dosimetry, 20: 38937 (AD-635655)
COCCHI, M., Statistical techniques and analysis in corrosion measurements of Zr alloys in terphenyls, 20: 39344 (EUR-2997.e)
COCKE, W. J., Collapsing cylinders and their exterior vacuum metrics in general relativity, 20: 40001
COE, E. H. Jr., Properties, origin, and mechanism of conversion-type inheritance at B locus in maize, 20: 38617
COHEN, Edward, Blast-closure systems, 20: 39073
COHEN, M. G., Brillouin scattering in liquid He II, 20: 40034
COHEN, Martin J., Missile scoring systems utilizing nuclear radiation, 20: 39190
COHEN, R., Nevis synchrocyclotron conversion project, 20: 39536
COKAL, E. J., Controlled-potential coulometric determination of rare earths in acetonitrile, 20: 38812
COKAL, E. J., Controlled-potential electrolysis of Eu, Yb, and Sm and their mixtures in acetonitrile solutions, 20: 38813
COLEMAN, E. W., Radiography, 20: 39286 (DP-1066(Vol.1), pp IV.43-5)
COLEMAN, J. P., Transition probabilities for electron capture, 20: 39606
COLEMAN, Paul J. Jr., Evidence for hydromagnetic waves in interplanetary plasma, 20: 39569
COLEMAN, Paul Jerome Jr., Irregularities in interplanetary magnetic field, 20: 39575
COLES, Willard D., Superconducting magnetic bottle for plasma physics experiments, 20: 40169 (NASA-TN-D-3595)
COLLIN, J. E., Ionization, dissociation, and intramolecular rearrangements in aliphatic amines under electron bombardment, 20: 38887
COLLIN, J. E., Ionization, dissociation, and intramolecular rearrangements in aliphatic amines under electron bombardment, 20: 38888
COLLINS, G. B., Steam drum experiment (A.G.R.), 20: 40398 (AEEW-M-631)
COLLINS, Russell L., Selective Moessbauer detector and use thereof, 20: 39250
COLLINS, W. T., Gravimetric gas flow standard, 20: 39020 (K-1632(Pt.2))
COLONIAS, John S., Magnetostatic computer program TRIM operations manual, 20: 39499 (UCRL-16959)
COMAR, D., Determination of iodine by radioactivation analysis, 20: 38849
CONGDON, C. C., Shift in relative distribution of body nitrogen between skin and carcass in mouse radiation chimeras, 20: 38636
CONGDON, Charles C., Destructive effect of radiation on lymphatic tissue, 20: 38612
CONSOLI, T., Confinement and heating of a plasma by low-frequency rotating magnetic field, 20: 40279
CONSOLI, T., Effects of confinement in high-frequency discharges at low pressure, 20: 40278
CONSOLI, T., Mixed-field configuration without leaks, 20: 40280
CONSOLI, T., Plasma acceleration by means of r-f and static magnetic field gradient, 20: 40268
CONSOLI, T., Study of a confinement of a plasma in spherical cavity, 20: 40277
CONSOLI, T., Three modes of energy transfer of a plasma h-f field, 20: 40261
CONSOLI, T., Trajectories in studies of interactions of h-f fields with plasma, 20: 40283
CONSTANT, R., Problems posed in Belgium for pharmaceutical control of radioelements for medical usage, 20: 39156
CONTE, Madeleine, Oxidation risks during sintering of uranium dioxide, and characterization of excess O, 20: 39390 (CEA-R-3003)
COOBS, J. H., Irradiation testing of Th fuels at ORNL, 20: 40385 (ORNL-P-2327)
COOK, Charles F., Selective Moessbauer detector and use thereof, 20: 39250
COOK, W. S., Measurement of (n,2n), (n,α) cross sections of Ge at 14.4 Mev, 20: 40080 (ORO-3346-3)
COOMES, E. A., Effect of surface micropatches on average thermionic constants of metallic emitters, 20: 39642
COOPER, B. R., Anisotropy and thermal inversion in high field magnetiza-

tion of cubic rare earth compounds, 20: 40320
COOPER, Robert F., Experimental evaluation of MiD generators operating at high Hall coefficients, 20: 39667
COPLIN, D. H., Mechanical property changes in Zircaloy-2, Inconel and Incoloy from neutrons, 20: 39457 (GEAP-5100-9)
COPLIN, D. H., Uranium oxide powder and pellet thermal conductivity during irradiation, 20: 39456 (GEAP-5100-1)
CORENZWIT, E., Pressure-induced phase transformations and magnetic ordering in intrarare-earth alloys and Sm, 20: 40326
CORNECI, I., Influence of ionizing radiations on cortico-suprarenal system evaluated on basis of potassium in rabbits, 20: 38697
CORTI, F., Automatic apparatus for measurement of weak currents, 20: 39169 (ISS-66/17)
COSTEA, T., Chemonuclear processes and design of chemonuclear reactors, 20: 40364
COSTON, C. J., Moessbauer studies of divalent and trivalent ^{57}Fe in $CoSO_4$ and $CoSO_4 \cdot 7H_2O$, 20: 40311
COTTIER, H., Acute whole-body irradiation syndrome, 20: 38700
COUCHOUD, S., Probability distribution of maxima and minima of nuclear cross sections, 20: 40113
COUCOURDE, F., Radiotherapy of carcinoma of uterine neck, 20: 38786
COUROUBLE, J. M., ELAN: installation for recovery and packaging of ^{137}Cs in France, 20: 39319 (DP-1066(Vol.2), pp II.33-44)
COVELL, D. F., Computer-coupled quality control procedure for γ scintillation spectrometry, 20: 39193 (AD-636736)
COWAN, Arthur, Improvements relating to low alloy steels, 20: 39444
COWLEY, R. A., Crystal dynamics of K. I., 20: 40343
COWPER, George, Radiation dosimeter for measuring exposure to high and low energy radiation, 20: 39251
CRADDOCK, M. K., Polarized ion sources for cyclotrons, 20: 39525
CRAGWALL, J. S. Jr., Radionuclides in Clinch-Tennessee Rivers, 20: 40479 (ORNL-P-2328)
CRAIG, Doris L., Prog. rpt. on Cs and Sr uptake and assimilation by higher plants, annual, 5/65–2/6, 20: 38548 (ORO-2410-1)
CRAVEN, Clyde Wesley Jr., Inscattering approximations in discrete variable transport theory, 20: 40060
CRAWFORD, J. V., Management of cerebral tumors, 20: 38783
CREBBIN, Kenneth C., Prog. rpt. on bevatron operation and development, 1/3/66, 20: 39498 (UCRL-16809)
CRETZU, T., New levels in ^{97}Tc, 20: 40084
CRITTENDEN, R. R., Isotopic spin of the η^* (960 Mev) meson, 20: 39786
CROCHET, Marie-Francoise, Effect of whole body irradiated and methylhydrazine in eradicating transplant leukaemia 1210, 20: 38794
CROCKER, G. R., Physical and radiochemical properties of fallout particles, 20: 39115
CROENI, Jack G., High-energy-rate extrusion of low-density tungsten powder billets, 20: 39352 (BM-RI-6817)
CROITORU, Z., Conformal transformation investigations on MHD ducts of finite length and segmentation, 20: 39661
CROITORU, Z., Relaxation phenomena in rare gases seeded with alkali-metal substances, 20: 39700
CROKE, Edward J., Ocean technology and nuclear power, 20: 40362
CROKE, Edward J., Power Reactor Technology. Vol. 9, No. 2, 20: 40426
CROKE, Edward J., Power Reactor Technology, Vol. 9, No. 1, 20: 40430
CSEJKA, D. A., Heats of dilution of aqueous rare earth chloride solutions at 25°, 20: 38903
CUDDIHY, Richard G., Thyroidal ^{131}I uptake, turnover and blocking in adults and adolescents, 20: 38553
CUDKOWICZ, Gustave, Functional and morphological characterization of stem cells, 20: 38592 (ORNL-P-2158)
CULLEN, G. W., Effect of neutron-induced defects on current-carrying behavior of vapor-deposited niobium stannide, 20: 40301
CULVER, J. S., Injection and accumulation: multiple-pass experiments (DCX-2), 20: 40172 (ORNL-3989, pp 14-30)
CUMMINGS, Richard D., Boiling heat transfer to liquid helium, 20: 40048
CUSHING, James T., Internal symmetries in coupled-channel soluble model with inelasticity, 20: 39902
CUSSON, R. Y., Levels in ^{11}B from $^7Li(\alpha,\alpha)^7Li$ and $^7Li(\alpha,\alpha')^7Li^*(0.48)$, 20: 40111
CZECH, Zbigniew, Registration of state of decatron counting systems by means of teleprinter code, 20: 39178
CZOWNICKI, Z., Long-term results and complications after irradiation of haemangiomas in children, 20: 38787

D

DAGAN, S., Evidence concerning C violation in eta decay, 20: 39766 (ORO-3065-10)
DAGONNIER, R., Comments on Brownian motion theory, 20: 39596
DALGARNO, A., Collision-induced de-activation of metastable helium, 20: 39609
DALGARNO, A., Electron temperatures in the D region, 20: 39994
DALGARNO, A., Stopping powers and straggling in rare gases, 20: 39611
DAMAN, E. L., Electrogasdynamic central power stations, 20: 39701
DANBY, G. T., 200 Bev accelerator employing a separated function magnet lattice, 20: 39480 (BNL-10508)
DANETSKAYA, E. V., Effect of vitamins and phosphatides on resistance to radiation, 20: 38721
DANIEL, A. R., Terminal solid solubility of H in Zy-2, 20: 39379 (AECL-2453)
DANIEL, H., Electron polarization of ^{144}Pr, 20: 40085
DANIEL, R. R., Directional variation of geomagnetic cut-off rigidity around Hyderabad, India, 20: 39988
DANILOV, V. I., Accumulation of particles in a 680-Mev synchrocyclotron, 20: 39492 (JINR-P-2811)
DARLING, J. D., Complete classification of the states of nuclear configurations j^n for $j = 9/2$, 20: 40082
DA ROSA, A. V., Theoretical time-dependent thermal behavior of ionospheric electron gas, 20: 39980
DAS GUPTA, M. K., Solar and solar-terrestrial events in relation to solar cycle, 20: 39563
DASH, J. G., Motional narrowing of magnetic hyperfine Moessbauer spectra, 20: 40152
DASHEN, Roger, Representation of local current algebra at infinite momentum, 20: 39903
DASHKEVICH, N., Investigation of interaction of π^--mesons with Xe nuclei at 5 and 9 Bev/c, 20: 39755 (JINR-P-2736)
DASS, Guru Vachan, Absorptive model for $\bar{K}N$ charge-exchange reaction, 20: 39805
DATZ, S., Determination of interatomic potentials and stopping powers from channeled-ion energy-loss spectra, 20: 39602
DATZ, Sheldon, Reflection and thermal accommodation of helium beams on platinum, 20: 39590
DAUBY, J. J., Preparation of sources for alpha spectrometry, 20: 38990
DAUCH, Fritz, RBE of fast neutrons by release of mutations in Drosophila, 20: 38645
DAVIDSON, Ernest R., Natural orbital based energy calculation for helium hydride and lithium hydride, 20: 38910
DAVIDSON, J. P., Electric monopole transitions and beta bands in even nuclei, 20: 40116
DAVIES, D. Roy, Acriflavine inhibition of dark repair and late generation death, 20: 38611
DAVIES, Hywel A., Physical and chemical properties of dilute alloys of Cd in Na, 20: 38856 (BNL-10372)
DAVIES, I. Ll., Model analysis (protective structures), 20: 39071
DAVILA, A. T., Preparation of 2.56-hour ^{65}Ni, 20: 40081 (PAEC(D)IS-653)
DAVIS, D. M., Clean assembly practices guide, 20: 40489 (SC-DC-66-1118)
DAVIS, J., Preliminary results from the Pioneer 6 M.I.T. plasma experiment, 20: 40212
DAVIS, K. A., SNAP-10A thermoelectric pump, 20: 40446 (NAA-SR-11879)
DAVIS, R. C., High-current ion-beam production and injection, 20: 40175 (ORNL-3989, pp 89-94)
DAVIS, R. C., Injection and accumulation: multiple-pass experiments (DCX-2), 20: 40172 (ORNL-3989, pp 14-30)
DAVISON, E., Low-energy proton bombardment of GaAs and Si solar cells, 20: 40299
DAVYDOV, A. S., Nuclear shape, deformability, and excited states of atomic nuclei, 20: 40136
DAWSON, J. M., Electron cyclotron harmonic radiation from a plasma, 20: 40274
DEACON, J., Time and spatially resolved interferometry on pulsed-laser-induced plasmas, 20: 40186
DEAT, M., Trajectories in studies of interactions of h-f fields with plasma, 20: 40283
DE BARBIERI, O., Constants of linearized motion of Vlasov plasmas, 20: 40167 (IC-65/90)
DEBERTIN, K., Bibliography on instruments and measuring techniques in nuclear physics, No. 14, 5/66, 20: 39168 (AED-C-06-14)
DE BONTE, W. J., Kaon-nucleon scattering and threshold K* production, 20: 39778
DEBRAY, P., Operation of the Orsay CEVIL and its extraction systems, 20: 39551
DE CASTRO FARIA, N. V., Monte-Carlo calculation of intrinsic double-escape peak efficiency of cylindrical Li-drift Ge gamma rays detectors, 20: 39271
DECKART, H., Comparative scintigraphic determinations of thyroid weight for dose determination in radioiodine therapy, 20: 38789
DECONNINCK, G., Intermediate structure in ^{41}Ca, 20: 40087
DECONNINCK, G., Optical model analysis of neutron scattering on ^{12}C from 16 to 20 Mev, 20: 40088
DEGENKOLB, John G., Fire-safe shelter design, 20: 39065
DE GRAAF, A. M., Origin of ferromagnetism in divalent europium salts, 20: 40318
DE HALAS, D. R., Irradiation brewing of UO_2, 20: 39449 (BNWL-SA-272)
DE HEER, F. J., Transition probabilities for electron capture, 20: 39606

DEJONGHE, P., Production and application of ^{227}Ac for direct conversion sources, 20: 39277 (DP-1066(Vol.1), pp III.63-9)
DE KLERK, D., Enthalpy of impure niobium in mixed superconductive state, 20: 40036
DEKNOCK, R., Survey of devices to measure fuel element coolant channels, 20: 39175
DE KOCK, C. W., Heats of dilution of aqueous rare-earth chloride solutions at 25°C, 20: 38870 (IS-1356)
DE KOCK, C. W., Heats of dilution of aqueous rare earth chloride solutions at 25°, 20: 38903
DELABAYE, M., Single-particle matrix elements jj-coupling for first-forbidden beta transitions, 20: 40124
DEMAINE, Peter Darien, Improvements in or relating to magnesium base alloys, 20: 39443
DE MEESTER, P., Survey of devices to measure fuel element coolant channels, 20: 39175
DENEKAMP, J., Response of irradiated mouse skin, 20: 38627
DENISENKO, A. N., Determination of tracer deposition depth by method involving simultaneous measurement of two values, 20: 39770
DENZEL, D. L., Evaluation of performance characteristics for Faraday generator, 20: 39645
DENZEL, P., General formulation of postulate for minimum volume of MHD generator duct with fixed outer boundary values, 20: 39703
DEODHAR, G. B., New forbidden lines in the L spectrum of lutetium, 20: 39613
DE PASQUALI, G., Moessbauer studies of divalent and trivalent ^{57}Fe in $CoSO_4$ and $CoSO_4 \cdot 7H_2O$, 20: 40311
DEPCZYK, D., High-strontium diet and radiostrontium retention in rats, 20: 38566
DEPTULA, Czeslaw, Spectrophotometric determination of U(VI) in solutions of tri-n-octylamine sulfate, 20: 38809
DE RAAD, B., Introduction to beam optics, 20: 39484 (CERN-66-21, pp 1-30)
DE RAAD, B., Lectures on beam optics, 20: 39483 (CERN-66-21)
DE SOUZA, Patrick D., Baryon-baryon reactions and SU3 symmetry, 20: 39765 (ORO-2504-91)
DESSLER, A. J., Lunar period, solar period, and K_p, 20: 39982
DETERLING, Ralpha A. Jr., Tumoricidal effect of laser energy on experimental and human malignant tumors, 20: 38780
DE TROYER, A., Production and application of ^{227}Ac for direct conversion sources, 20: 39277 (DP-1066(Vol.1), pp III.63-9)
DEUBERT, Angela, Notation and formulae for dose specification and calculations in radiotherapy, 20: 38750
DEUTSCHMANN, M., Observation of a (K $\pi\pi$) resonance near 1800 Mev, 20: 39788
DEVIDE, Z., Precipitation and hydrolysis of uranium (VI) in aqueous systems. IV., 20: 38928
DEVIME, R., Evaluation of Rayleigh-Taylor instability and turbulent diffusion effects in inhomogeneous flow conversion, 20: 39704
DEVIN, Bernard, Radioisotope converters, 20: 39633 (CEA-R-2788)
DE WERD, L. A., Effects of irradiation temperature in LiF(TLD-100), 20: 39200 (COO-1105-118)
DE WINTER, T. A., Facility for testing large superconducting magnets, 20: 40049
DE WINTER, T. A., Large experimental superconducting magnet for MHD power generation, 20: 39643
DEWS, Jon Robert, Search for isotopic anomalies in Ag and Li from meteorites, 20: 39102
DEY, S. D., Ionization potential of Gd and Ho by surface ionization method, 20: 40203
DHANESHWAR, M. R., Extraction of protactinium by long-chain amines from hydrochloric acid solutions, 20: 39003
DIAMANT, E. S., Creep of axisymmetric shells, 20: 39391 (CONF-660629-1)
DIAMENT, Paul, Electromagnetic: acoustic wave propagation along warm plasma columns, 20: 40166 (AD-637711)
DIANA, L. M., Search for evidence of positron emission in the decay of ^{36}Cl, 20: 40148
DI CARLO, R., Radioprotection of sulfurated mineral waters, 20: 38709
DICKS, J. B. Jr., Comparison of performance of diagonal wall generators, Faraday generators, and Hall current generators, 20: 39702
DIENSTBIER, Z., Effect of 19-nor-testosterone phenylpropionate on post-irradiation syndrome, 20: 38610
DIETERLE, B., Polarization parameter in p-p scattering from 1.7 to 6.1 Bev, 20: 39792
DIETRICH, Helmut, Measurements of beam behavior in the Karlsruhe cyclotron, 20: 39515
DIETRICH, R. V., Mineral tables (hand specimen properties of 1500 minerals), 20: 39100
DIN, G. U., Reactions $^{11}B(^3He,n)^{13}N$ and $^7Li(^3He,n)^9B$ from 1.5 to 5.5 Mev, 20: 40112
DINELLI, G., Effect of various parameters on efficiency of the MHD power stations, 20: 39705
DINGWALL, A. G. F., Energetics. III., 20: 40451
DITTRICH, Wolfgang, Radiobiological action mechanisms, 20: 38616
DIXON, C. F., Effect of heat treatment on corrosion behavior of two Zr–Cu–Mo alloys, 20: 39347 (NP-16239)
DMITRIEV, K. I., Investigation of MHD flow of liquid metal in rectangular duct with conducting walls, 20: 39706
DMITRIEVSKII, V. P., Development and prospects for application of meson factories, 20: 39534
DMITRIEVSKII, V. P., Modified resonance extraction method from relativistic cyclotron, 20: 39520
DNESTROVSKII, Yu. N., Flute instability in an uncompensated plasma, 20: 40195
DODGE, Marilyn J., Radiation-induced instability in refractive properties of some optical glasses, 20: 39468
DOERING, John P., Low-energy large-angle electron scattering spectrum of helium, 20: 39591
DOLEN, Richard, Vacuum Regge trajectory in conventional field theory, 20: 39925
DOLLING, G., Crystal dynamics of K. I., 20: 40343
DOLMATOV, S. A., Kinetics of radiation-induced allyl polymerization. III., 20: 38956
DOMANSKI, T., High-strontium diet and radiostrontium retention in rats, 20: 38566
DOMEIJ, B., Why nuclear spectroscopists should know about recent development in atomic stopping, 20: 39595
DOMSHLAK, M. P., Mechanism of death of animals with most acute form of radiation sickness, 20: 38666
DONALDSON, Lauren R., Effects of low-level chronic irradiation of Chinook and Coho salmon eggs and alevins, 20: 38698
DONETS, E. D., Synthesis of a heavy isotope $^{256}102$, 20: 40142
DONNACHIE, A., New evidence for sigma meson, 20: 39782
DONNELLY, R. G., Weldability evaluation of advanced refractory alloys, 20: 39366
DONNET, Jean-Baptiste, Determination of surface carboxylic and hydroxyl groups of carbon black by radiochemical method, 20: 38805
DONSKOI, K. V., Problems of MHD conversion: experimental results, 20: 39707
DORMAN, L. I., Complex amplitude-phase modulation of periodic cosmic-ray variations, 20: 39629
DORMAN, L. I., Solar-diurnal and semidiurnal variations of cosmic rays and their spectra as function of solar activity, 20: 39628
DOROSHENKO, A. V., Neutron diffraction study of ordered Ni–Mn alloys, 20: 39407 (ANL-Trans-344)
DOROSZLAI, Pal, Method and apparatus for control of nuclear power plant, 20: 40432
DOST, H., Polarization parameter in p-p scattering from 328 to 736 Mev, 20: 39791
DOWNING, R. G., Radiation damage in semiconductors. XII., 20: 39458 (NP-16225)
DRAGANIC, Ivan, Radiation-induced water decomposition, 20: 38959
DRAGANIC, Zorica, Radiation-induced water decomposition, 20: 38959
DRAKE, C. W. Jr., Polarized negative ions produced by charge exchange process, 20: 39584
DRAKULIC, M., Patterns of nucleic acid and protein synthesis during modification of lethal ultraviolet lesion, 20: 38562
DRAKULIC, M., Survival of uv-irradiated E. coli in presence of chloramphenicol and in absence of essential metabolite, 20: 38563
DREISVOGT, H., Breeding in pebble-bed reactors, 20: 40471
DRICKAMER, H. G., Moessbauer studies of divalent and trivalent ^{57}Fe in $CoSO_4$ and $CoSO_4 \cdot 7H_2O$, 20: 40311
DRICKEY, D., Deuteron electromagnetic form factors for 3 $F^{-2} < q^2 <$ 6 F^{-2}, 20: 39795
DROZ-VINCENT, Phillippe H., Covariant conservation laws for general relativistic exploding matter, 20: 40002
DRUCKER, Eugene E., Ventilation and air cooling in protective structures, 20: 39074
DRUIN, V. A., Transuranic elements in nature, 20: 39116
DRUTMAN, R. D., Correlation of local tissue changes and general reactions at different stages of acute radiation sickness in man, 20: 38774
DRUYVESTEYN, W. F., Helicon-like resonances in superconducting niobium, 20: 40031
DRYAGINA, I. V., Cytological disturbances in appletree roots following irradiation of seeds, 20: 38692
DUBOIS, Andre, Ceramic materials for magnetoaerodynamic conversion duct electrodes, 20: 39708
DUBOIS, Andre, Magnetoaerodynamic conversion test rig with subatmospheric operating conditions, 20: 39709
DUBOIS, P., Analysis of the volatile constituents of irradiated apple juice, 20: 39300
DUBOIS, Pierre, Magnetoaerodynamic conversion test rig with subatomspheric operating conditions, 20: 39709
DUBOVOI, L. V., Confinement of high-temperature plasma, 20: 40194
DUBROVINA, Z. V., Absorption of Ca compounds from stomach and

intestines and effects on assimilation of Sr in rats, 20: 38569
DUDOLADOV, I. P., Peculiarities of shock compression of lanthanides, 20: 39425
DUELLI, B., Novel deflection-bunching system at the Karlsruhe isochronous cyclotron, 20: 39546
DUESTERHOEFT, W. C., Transverse plasma injection into multipole magnetic field, · 20: 40254
DUFOUR, Louis-Claude, Preparation, composition, and stability of β-phase W, 20: 39412
DUGAN, J. V. Jr., Electron distribution function and state populations in non-equilibrium MHD plasmas, 20: 39711
DUKES, E. K., Analytical chemistry of neptunium, 20: 38821
DUL, J., Open-cycle power generation experiment with high preheat temperature of air, 20: 39689
DULAR, M., Flame photometric determination of Li, Na, K, Ca, Mg, and Sr in natural and mineral waters, 20: 38798 (NIJS-R-465)
DULIN, V. A., Angular distribution of fast neutrons behind iron shielding, 20: 40286
DUMITRESCU, Rodica, Blood and bone marrow disorders occurring in radiology-service personnel, 20: 38781
DUMITRESCU, Silvia, Build-up factor B in attenuation calculations of γ radiation, · 20: 40289
DUNAITSEV, A. A., Measurement of π^+-meson lifetime, 20: 39821
DUNBAR, R. C., Ion-cyclotron double resonance, 20: 38902
DUNLAP, B. D., Motional narrowing of magnetic hyperfine Moessbauer spectra, 20: 40152
DUNLAP, J. L., Injection and accumulation: single-pass experiments (DCX-1), · 20: 40171 (ORNL-3989, pp 1–13)
DUPAS, L., Acceleration of plasma by field of progressive wave damped in vicinity of electron or ion cyclotron resonance, · 20: 40267
DUPAS, L., Three modes of energy transfer of a plasma h-f field, · 20: 40261
DUPONT, H., Diffusion of triplet excitons produced by ionizing radiation in aromatic materials, 20: 38957
DURGAPAL, M. C., Gravitation and the abundance of hydrogen, 20: 39560
DURHAM, J., Helium recombination in radio frequency discharge, · 20: 40247
DUSHIN, L. A., Interferometer for plasma diagnosis, · 20: 40226
DUTOV, A. G., Determination of dysprosium in samples of yttrium oxide and ferrite garnets by radioactivation method, 20: 38833
DUTT, J. C., Dual-purpose unit for high vacuum pumping system and leak detection in vacuum chambers, 20: 39096 (AECD-EP-11)
DUTTO, G., Acceleration of H^- ions and extracted beam measurements in Milan cyclotron, 20: 39550
DUTTON, James J., Power Reactor Technology. Vol. 9, No. 2, 20: 40426
DUTTON, James J., Power Reactor Technology, Vol. 9, No. 1, 20: 40430
DUXBURY, Donald, Improvements in or relating to production of uranium metal, 20: 39342
DVORNIKOVA, L. M., Europium and gadolinium hydroxides and products of their thermal decomposition, 20: 38923
DWORIN, Lowell, Transport properties of an electron gas in a magnetic field. II., · 20: 40183
DYUBUA, B. Ch., Work function of W–Hf, Ta–Hf, Nb–Hf, Re–Zr, and W–Re alloys, · 20: 40297
DZHAGATSPANYAN, R. V., Calculation of efficiency of radiation-chemical apparatus with plane beta sources, 20: 38943
DZHARAK'YAN, T. K., Mechanism of protective action of aminothiols, 20: 38723
DZHAUGASHTIN, K. E., Electric discharge in conducting jet of viscous fluid, · 20: 40241
DZHAUGASHTIN, K. E., Propagation of plane jet of conducting liquid in magnetic field, 20: 39934
DZHELEPOV, V. P., Development and prospects for application of meson factories, 20: 39534
DZHELEPOV, V. P., Formation of charged π mesons in collisions between 600-Mev neutrons and protons, 20: 39834
DZUNG, L. S., Influence of wall conductance on performance of MHD generators with segmented electrodes, 20: 39712
DZUNG, L. S., MHD generators with ion slip and finite electrode segments, 20: 39713

E

EAKINS, J. D., Determination of ^{55}Fe and ^{59}Fe in blood by liquid scintillation counting, 20: 38555
EANDI, Richard D., Polarization in proton-proton scatterings at 735 Mev, 20: 39789
EASEY, J. F., Existence of Cm(VI), 20: 38917
EATHER, R. H., Radiation from positive particles penetrating auroral atmosphere, 20: 39981
EATHERLY, W. P., Design and fabrication of (AVR) injection-molded fuel element, 20: 40468
EBENHOEH, Wolfgang, Hartree-Fock calculations with parity mixing in one-particle functions, · 20: 40138
EBERHAGEN, Dietrich, Lipoid changes in various rat organs after whole-body irradiation with lethal x-ray doses. III., 20: 38701
EBIHARA, H., Crystal-structure effects in hot-atom chemistry of copper phthalocyanine, 20: 40309
ECKER, G., Theory of collision-free plasma column with regard to wall losses, · 20: 40230
ECKHAUSE, M., Measurement of the lifetime of the 14.4 kev level of ^{57}Fe, 20: 40132
EDMONDSON, P. W., Clinical and pathological response of goats to whole-body irradiation by gamma-rays and fission neutrons, 20: 38629
EDWARDS, Arthur L., TRUMP, computer program for transient and steady state temperature distributions in multidimensional systems, 20: 39049 (UCRL-14754)
EDWARDS, David F., Spectroscopic studies of laser-produced hydrogen plasma, · 20: 40251
EDWARDS, R. S., Injection and accumulation: single-pass experiments (DCX-1), 20: 40171 (ORNL-3989, pp 1-13)
EFANOV, A. I., Nuclear reactor oscillation-measuring device, 20: 40361
EFFERSON, K. R., Prog. rpt. on experimental simulation of large, high field, superconducting magnet operation, 12/65-7/66, 20: 40015 (ORNL-TM-1598)
EGANA, Enrique, Relation of internal β irradiation and biochemical effects in the CNS, 20: 38651
EGGEBRAATEN, V. L., Precision neutron activation analysis of zinc and titanium oxides in organic coating pigments, 20: 38853
EHRENPREIS, Stanley N., Flux mapping system for measuring radiation, 20: 39252
EICHELBERGER, J. F., Prog. rpt., 11/65, 20: 39320 (MLM-1311)
EICHELBERGER, J. F., Prog. rpt., 12/65, 20: 39321 (MLM-1312)
EICHERT, K., Influence of non-equilibrium excitation on electron density in one-dimensional MFD channel flow, 20: 39714
EICHLER, Roland, Deuterium-isotope geochemistry of ground and surface waters, 20: 39127
EINMAHL, Gerd, Strength in two-phase model system with fiber reinforcement, 20: 39405 (UCRL-16844)
EISEN, F. H., Stage-II recovery in electron-irradiated InSb, 20: 40328
EJIRI, H., Report on measurements of reaction ^{40}Ca(d,α)^{38}Ca for 24 Mev impact energy, 20: 40067 (BMWF-FBK-66-15, pp 20-37)
EJIRI, H., Single RACE spectrometer, 20: 39206 (INSJ-99)
EL-ASRAG, H. A., Labeling of insulin with ^{131}I, 20: 38933
EL-BAZ, E., Diagrammatic representation and utilization of rotation matrices, 20: 40120
EL BINDARI, A., Large experimental superconducting magnet for MHD power generation, 20: 39643
ELESIN, A. A., Complexing of trivalent actinides and lanthanides in phosphoric acid solutions, 20: 38878 (ORNL-tr-1257)
ELFENBAUM, Arthur, Cancer of the lower lip, 20: 38752
ELIASZ, W., Snoek peaks and their stability in annealed and deformed tantalum, 20: 39420
ELION, H. A., Analytical chemistry. Vol. 6, 20: 38817
ELISEEV, S. M., Interactions of 1- to 30-Bev elementary particles with atomic nuclei, 20: 39828
ELISEEV, V. V., Ionization instability and turbulent conductivity of non-equilibrium plasma, 20: 39671
EL-KINAWY, S. A., Preparation of radio-iodinated tyrosines and thyroxine and separation on Sephadex G 25, 20: 38992
ELLINGTON, H. I., Atmospheric pressure discharges in inert gases seeded with alkali metal vapor, 20: 39715
ELLIOTT, D. G., Theoretical and experimental investigation of liquid–metal MHD power generation, 20: 39716
ELLIOTT, James H., Antibody production in corneal hypersensitivity, 20: 38608
ELLIS, J. R., Electromagnetic fields of moving dipoles and multipoles, 20: 40003
ELLO, J. G., Modification of Eberline PAC-3G and FM-3G survey meters to detect low-energy beta activity, 20: 39220
ELPAT'EVSKAYA, G. N., Therapeutic effects of selachyl alcohol during experimental radiation sickness, 20: 38731
EMELEUS, H. J., Advances in inorganic chemistry and radiochemistry. Vol. 8, 20: 38880
ENCHEVICH, I. B., Accumulation of particles in a 680-Mev synchrocyclotron, 20: 39492 (JINR-P-2811)
ENGEL, J. R., Analysis of filling accidents in MSRE, 20: 40412 (ORNL-TM-497)
ENGEL, R. L., ISOSHLD: computer code for general purpose isotope shielding analysis, · 20: 40285 (BNWL-236)
ENGELN, F., End effects on the linear induction MHD generator calculated by two-sided Laplace transform, 20: 39717
ENGLISH, R. E., Projected large scale use of radioisotopes by NASA, 20: 39306 (DP-1066(Vol.1), pp V.17-25)
ENKOVSKII, L., Existence of certain baryon and meson unitary multiplets, 20: 39860 (JINR-P-2790)
EPHRAIM, D. C., Radiochemical separation and purification of ^{140}Ba and rapid milking of ^{140}La from ^{140}Ba, 20: 39001

ERBE, W., Increase in RNase and DPNase activities in ascites tumor cells induced by cytostatic agents, 20: 38578
ERICSON, M., Probability distribution of maxima and minima of nuclear cross sections, 20: 40113
ERMAKOV, S. M., Angular distribution of fast neutrons behind iron shielding, 20: 40286
ERMOLAEVA, E. V., Dose distributions in homologous phantoms in distance gamma-therapy, 20: 38762
ERMOLOV, P. F., Structure of Ar K-series during atomic capture of negative muons in pure gas and in mixture with H, 20: 39578 (JINR-P-2807)
EROKHIN, N. S., Characteristics of problems in MHD stability theory, 20: 40239
ERRINGTON, R. F., Canadian program on large scale production and application of radioisotopes, 20: 39282 (DP-1066(Vol.1), pp III.3-32)
ERWIN, A. R., Search for the kappa meson, 20: 39784
ERWIN, J. H., Forming method for curved ATR fuel plates, 20: 39358 (ORNL-3983)
ESKUCHE, Irmo, Effect of gamma irradiation on response to erythropoietin of non-fasted rats, 20: 38673
EUBANK, Harold P., Instrumentation for plasma diagnostics, 20: 40220
EUGENIO, M. R., Preparation of 2.56-hour ^{65}Ni, 20: 40081 (PAEC(D)IS-653)
EUSTIS, R. H., Calculation of idealized MHD generator performance with non-equilibrium electron heating, 20: 39647
EWAN, G. T., Use of Ge(Li) detectors in γ-γ coincidence experiments, 20: 39197 (AECL-2565)
EYRE-BROOK, A. L., Management of malignant tumors of bone, 20: 38784
EYRING, Leroy, Prog. rpt. on solid-state chemistry of rare earth oxides, annual, 1965–66, 20: 38861 (COO-1109-22)

F

FADEEVA, L. A., Spark method for spectrographic determination of rare earths in solutions, 20: 38832
FADIN, V. S., Emission of two photons into given angle in electron collisions, 20: 39836
FAINBERG, Ya. B., Stabilization of low-frequency plasma instabilities, 20: 40218
FAITH, T. J., Acceleration of electron cyclotron plasma by self-generated electric fields, 20: 40262
FAKAN, John C., Superconducting magnetic bottle for plasma physics experiments, 20: 40169 (NASA-TN-D-3595)
FAKHRUTDINOV, G. F., Absorption and removal of ^{131}I from the thyroid gland, 20: 38734
FALLAIS, C., Problems posed in Belgium for pharmaceutical control of radioelements for medical usage, 20: 39156
FALOMKIN, I. V., Recording of particle paths in streamer high-pressure chamber filled with helium, 20: 39245
FAN, C. Y., Galactic deuterium and its energy spectrum above 20 Mev per nucleon, 20: 39987
FARCHI, G., Measurement of electrons momentum by spark chambers in magnetic field, 20: 39207 (ISS-66/18)
FARHATAZIZ, Radiolysis of aerated 0.8 N sulfuric acid solutions of K bromide with ~15-Mev electrons, 20: 38952
FARIS, John, Anion exchange in nitrate solutions, 20: 38820
FARLEY, D. T., Theory of incoherent scattering of radio waves by a plasma. IV., 20: 40213
FARNSWORTH, Philo T., Electric discharge device for producing interactions between nuclei, 20: 39509
FARRAR, J. P., Zero power tests on NS Savannah Core II, 20: 40445 (BAW-1225)
FARRELL, Kenneth G., Passing parade of shielding-analysis methods, 20: 39063
FAST, J. F., Magnetic properties of rare-earth aluminum compounds, 20: 39433
FAUSKE, Hans K., What's new in two-phase flow, 20: 39941
FECAN, Jean-Claude, Ionization of gases by very intense luminous beam, 20: 40190
FEDERBUSH, Paul G., Existence of spurious solutions to many-body Bethe-Salpeter equations, 20: 39900
FEDOROV, Anatol F., Radiation doses for some types of marine biota under present-day conditions, 20: 38741
FEDOROV, V. V., Planning of n-p scattering experiments above pion-production threshold, 20: 39752 (JINR-E-2765)
FEDOTOVA, M. I., Restoration of bone marrow tissue in acute radiation sickness, 20: 38663
FEDYAKOV, V. P., Confinement of high-temperature plasma, 20: 40194
FEHER, Imre, Agents influencing granulocyte output and production in irradiated rabbits, 20: 38633
FEINBERG, E. L., Possible presence of relic quarks in cosmic rays, 20: 39631
FEINENDEGEN, L. E., Intranuclear ^{3}H thymidine: dosimetric, radiobiological and radiation protection aspects, 20: 38624
FEIST, Ivan, Application of high sensitive integrator in gas chromatography, 20: 38815
FELDEN, Marceau, Parameters of Cs plasma obtained by contact ionization, 20: 40223
FELDMAN, Michael, Prog. rpt. on application of cloned haemopoietic cells in radiation protection, final, 1965–66, 20: 38708 (IAEA-3173-5)
FELDMANN, Hans-Helmut, Non-intercepting ion phase measuring equipment of isochronous cyclotrons at Karlsruhe and Juelich, 20: 39514
FELICI, C., Automatic apparatus for measurement of weak currents, 20: 39169 (ISS-66/17)
FELL, Christopher Brocklebank, Improvements in or relating to support arrangements, 20: 40365
FELMLEE, Theron L., Prog. rpt. on solid-state chemistry of rare earth oxides, annual, 1965–66, 20: 38861 (COO-1109-22)
FENEBERG, W., Non-equilibrium conductivity in Ar–K plasma in crossed electric and magnetic fields, 20: 39684
FENTON, A. G., Time delays in Ar–propane proportional and Geiger counters, 20: 39215
FENTON, K. B., Time delays in Ar–propane proportional and Geiger counters, 20: 39215
FERNANDEZ, L. P., Large scale separation of ^{210}Po from Bi, 20: 38996 (DP-1066(Vol.2), pp II.79-102)
FERREIRA, Erasmo M., Poles of S matrix for long-range potentials, 20: 39868
FERRO-LUZZI, Anna, Cesium-137 and ^{90}Sr levels in diet and urine of an Italian children's community, 20: 39152
FERRONI, S., Charged pion photoproduction on light nuclei, 20: 40075 (LNF-66/30)
FETZER, Homer Donald, Scattering of electrons by iodine monochloride, 20: 39622
FILIMONOV, V. T., Complexing of trivalent actinides and lanthanides in phosphoric acid solutions, 20: 38878 (ORNL-tr-1257)
FINK, D., Collisional excitation of atomic spectra in accelerated beams of light elements, 20: 39593
FINK, R. W., Comparison of allowed M/L orbital electron capture ratios with theory, 20: 40153
FINK, R. W., Measurement of (n,2n), (n,p), and (n,α) cross sections of Ge at 14.4 Mev, 20: 40080 (ORO-3346-3)
FINK, R. W., Neutron reaction cross sections of Se and Fe at 14.4 Mev, 20: 40079 (ORO-3346-2)
FINK, Richard W., Selective Moessbauer detector and use thereof, 20: 39250
FINKELSTEIN, David, Kinks, 20: 39869
FISCHER, F. W., Experimental determination of current distribution in a simulated MHD generator, 20: 39718
FISCHER, M., Determination of electron density distribution in infinite anisotropic plasma, 20: 40184
FISCHER, Wolfgang, Hyperfine structure and quadrupole moment of ^{65}Cu, 20: 40137
FISHER, C., Production and utilization of radioisotopes in continental Europe, 20: 39276 (DP-1066(Vol.1), pp III.45-50)
FISHER, John Raymond, Linear arrays of neutron-absorber-filled tubes as, 20: 40381
FISHER, Philip Andrew, Improvements in or relating to magnesium base alloys, 20: 39443
FISZDON, J., Production and investigation of materials for MHD generator, 20: 39690
FITCH, Frederick T., Rare earth actinide metal sols, 20: 39341
FITCH, Frederick T., Sols of zirconia and hafnia with actinide oxides, 20: 39442
FITE, Lloyd E., Use of high-speed automatic systems for medical and biologic activation analysis, 20: 38843
FITZ SIMONS, Neal, Engineering approach to protective structures, 20: 39069
FJELSETH, D. E., Clean assembly practices guide, 20: 40489 (SC-DC-66-1118)
FLANAGAN, T. B., H–Pd system, 20: 39428
FLECKENSTEIN, A., Biological application of activation analysis of ^{18}O, 20: 38848
FLEROV, G. N., Key to synthesis, 20: 40144
FLEROV, G. N., More of transuranic elements, 20: 40145
FLEROV, G. N., Perspectives of synthesis and studies of properties of transuranium elements, 20: 40140
FLESCHER, H. L., Prog. rpt. on radiation effects on integrated circuits, 1–3/66, 20: 39273 (AD-635198)
FLETCHER, E. L., Faraday unipolar induction in a nonideal type II superconductor, 20: 40016
FLICKER, H., Radiation damage in semiconductors. XII., 20: 39458 (NP-16225)
FLINT, H. M., Effects of gamma radiation on mating competitiveness and fecundity of Hippelates pusio loew, 20: 38632
FLORENTIN, Irene, Effect of whole body irradiated and methyl-hydrazine in eradicating transplant leukaemia 1210, 20: 38794

FLOUX, Francis, Ionization of gases by very intense luminous beam, 20: 40190
FLOWERS, C. D., Structural analysis of hexagonal tube or ring under internal pressure, 20: 39384 (BNWL-263)
FLYAGIN, V. B., Formation of charged π mesons in collisions between 600-Mev neutrons and protons, 20: 39834
FOCACCI, M. N., Pion-proton elastic scattering, 20: 39744 (CERN-66-18)
FODOROV, A., Experiments on ion acceleration at 685-mm sector cyclotron, 20: 39549
FOERSTER, S., Analysis of essential characteristics for closed MHD power stations, 20: 39682
FOERSTER, S., Closed MHD-loop ARGAS, 20: 39680
FOEX, M., Insulators and conductors for MHD flow, 20: 39657
FOKIN, A. V., Radiation-induced polymerization of fluoroolefins, 20: 38946
FOLEY, Dennis D., Production of age hardenable tantalum-based alloys, 20: 39441
FOLLMER, William C., Radiation-resistant device phenomena, 20: 39274 (N-66-18175)
FOLSOM, T. R., Urechis program: rapid survey of fallout Cs in the ocean, 20: 39147 (CONF-660401-6)
FONTAN, Jacques, Concentration of natural radioactive gas and of equilibrium between this gas and its daughter products in air at ground level, 20: 39114
FORD, John Brian Malpas, Improvements in or relating to containers for radioactive members, 20: 39040
FORGAN, R., Pressure-drop characteristics for flow of subcooled water in heated channels. I., 20: 39047 (AERE-M-1739)
FORRESTER, A. Theodore, Surface tension storage and feed systems for ion engines, 20: 39091
FORTNEY, L. R., Evidence concerning C violation in eta decay, 20: 39766 (ORO-3065-10)
FORTNEY, L. R., Three-pion production by 1.95 Bev/c positive pions on protons, 20: 39767 (TID-23278)
FOSCHI, G. C., Changes in antiinsulin antibodies subjected to radioactivity, 20: 38579
FOSS, M. H., Possible improvements to the Carnegie Institute of Technology synchrocyclotron, 20: 39537
FOWLER, E. C., Evidence concerning C violation in eta decay, 20: 39766 (ORO-3065-10)
FOWLER, E. C., Three-pion production by 1.95 Bev/c positive pions on protons, 20: 39767 (TID-23278)
FOWLER, E. E., Atomic Energy Commission's role in the process radiation industry, 20: 39281 (DP-1066(Vol.1), pp 13-18)
FOWLER, J. F., Response of irradiated mouse skin, 20: 38627
FRADIN, J., ELAN: installation for recovery and packaging of ^{137}Cs in France, 20: 39319 (DP-1066(Vol.2), pp II.33-44)
FRANK, Bernadine, Occurrence patterns of topside spread F on Alouette ionograms, 20: 39973
FRANK, Edmund, Apparatus with vertical and lateral movable means for handling groups of radioactive samples, 20: 39041
FRANKFORT, J. H., Engineering and evaluation study for the manufacture of wood-plastic composites, 20: 39287 (KLX-1876)
FRANKHOUSER, W. L., Theory and mechanism of Zircaloy pressure bonding, 20: 39361 (WAPD-305)
FRANKLIN, Jerrold, Study of the ρ and B mesons in π-ω scattering, 20: 39807
FRANSKIN, M. J., Ionization, dissociation, and intramolecular rearrangements in aliphatic amines under electron bombardment, 20: 38887
FRANSKIN, M. J., Ionization, dissociation, and intramolecular rearrangements in aliphatic amines under electron bombardment, 20: 38888
FRANTSEVICH, I.N., Young's modulus of carbides of some transition metals, 20: 39430
FRATINO, P., Changes in antiinsulin antibodies subjected to radioactivity, 20: 38579
FRAUENFELDER, R., Prog. rpt. on ultrahigh vacuum techniques, semiannual, 12/65–5/66, 20: 39098 (WERL-2823-21)
FRAUSKE, Hans K., Compressibility affects flow instability and burnout, 20: 40427
FREDERICK, B. J., Radionuclides in Clinch-Tennessee Rivers, 20: 40479 (ORNL-P-2328)
FREDSALL, J. R., Near-optimum shutdowns for nuclear reactors, 20: 40423
FREEDMAN, A. H., High remelt temperature brazing of columbium honeycomb structures, 20: 39365
FREIFELDER, David, Mechanism of x-ray sensitization of bacteriophage T_7 by 5-bromouracil, 20: 38712
FREIFELDER, Dorothy Read, Mechanism of x-ray sensitization of bateriophage T_7 by 5-bromouracil, 20: 38712
FREILING, E. C., Physical and radiochemical properties of fallout particles, 20: 39115
FREKE, A. M., Public health hazard associated with storage or disposal of glasses incorporating highly active fission product wastes, 20: 40482
FRENCH, Norman R., FORTRAN IV program for evaluation of thyroidal assimilation of radioiodine, 20: 38549 (UCLA-12-592)
FRERE JACQUE, D., Deuteron electromagnetic form factors for 3 F^{-2} < q^2 < 6 F^{-2}, 20: 39795
FREYMAN, Robert W., Hard tube modulators for Los Alamos meson facility, 20: 39493 (LA-DC-7776)
FREYTAG, E., Measurement of synchrotron radiation in x-ray region, 20: 39473
FRIAS, Robert, Prog. rpt. on Bevatron operation and development, 1/3/66, 20: 39498 (UCRL-16809)
FRIED, Burton D., Kinetic equation for unstable plasma in parallel electric and magnetic fields, 20: 40181 (TID-23307)
FRIED, Burton D., Kinetic equation for an unstable plasma in parallel electric and magnetic fields, 20: 40249
FRIEDMAN, Irving, Fractionation of $^{18}O/^{16}O$ between coexisting calcite and dolomite, 20: 39129
FRIEDRICH, C. M., CYGRO-1: stress analysis of growth of concentric cylinders, 20: 39460 (WAPD-TM-514(Add.1))
FRITZE, K., Extraction of Mo into acetylacetone and use in analysis of fission products, 20: 38824
FROST, K. J., Search for the quiet-time solar gamma rays from balloon altitudes, 20: 39565
FU, C. Y., Exposure field from a point isotropic source located at surface of thick concrete slab, 20: 40284 (AD-637125)
FUEREDI, H., Precipitation and hydrolysis of uranium (VI) in aqueous systems. IV., 20: 38928
FUJINO, Moriji, Modification of perivascular subcutaneous connective tissue reaction following x-ray irradiation, 20: 38640
FUJITA, Akira, Effect of radioactive fallout upon electric conductivity of lower atmosphere, 20: 39111
FUJITA, Akira, Fallout in soil particles, 20: 39112
FUJITA, Akira, Observation of fallout around the laboratory, 20: 39106
FUJITA, Akira, X-ray microanalysis of fallout from first Chinese nuclear explosion, 20: 39110
FUJIWAKA, Setsuya, Preliminary experiment on ion cyclotron resonance of highly ionized plasma, 20: 40260
FUKSIEWICZ, E., Open-cycle power generation experiment with high preheat temperature of air, 20: 39689
FUKUDA, Makoto, Radiometric titration of trace amounts of cobalt using EDTA, 20: 38806
FUKUSHIMA, Naoshi, Declination change of SC, its local time, and seasonal dependence at Kakioka, Japan, 20: 39969
FUNG, P. C. W., Excitation of cyclotron electromagnetic waves in magnetoactive plasma by stream of charged particles, 20: 40188
FUNG, Yun-Tong, Potential calculations with the N/D method and bootstrap of the rho resonance, 20: 39927

G

GABROVSEK, Z., Hazards summary report for Triga Mark II reactor in Ljubljana, 20: 40462 (NIJS-R-474)
GAEBLER, Oliver H., Prog. rpt. on effects of x radiation on metabolism of ^{15}N from ammonium citrate and glycine in rats, 9/65–4/66, 20: 38600 (TID-23034)
GAL, G., Electromagnetic interaction with plasma column, 20: 40252
GALANIN, A. D., Quantum field theory with indefinite metric in Hilbert space, 20: 39912
GALATZEANU, I., Effects of gamma rays on vitamin B_6, 20: 38580
GALEEV, A. A., Anisotropic drift instability in plasma and anomalous transfer processes, 20: 40236
GALINA, L. S., Dosimetric specifications of gamma therapy unit "Luch-1", 20: 38771
GALKIN, Yu. M., Subsolidus formation in ternary compounds of the system $BaO–ZrO_2–SiO_2$, 20: 38899
GALLOWAY, Kenneth Franklin, Pion-neutron interactions at 3.5 Bev/c, 20: 39842
GARLAND, Michael McKee, Electrical and superconducting properties of In films, 20: 40043
GARLICK, Ralph G., Effect of orientation on ductile-to-brittle transition of tungsten single crystals, 20: 39397 (NASA-TM-X-1252)
GARNER, R. J., Metabolism of radium in dairy cows, 20: 38552
GARNER, R. J., Radioactivity and dairy products, 20: 39157
GASIOROWICZ, S., Adler-Weisberger sum rules for higher spin particles, 20: 39883
GASPERIN, Madeleine, Synthesis of a new double oxide of niobium and uranium, 20: 38892
GATES, W. E., Resistance of tubular structures to dynamic loading, 20: 39007 (AD-636914)
GATTI, E., Review of theories and experiments of resolving time with scintillation counters, 20: 39239
GAUGER, J., Experimental evaluation of various rigidity models, 20: 39624 (D-1-82-0529)
GAUK, W., Production and investigation of materials for MHD generator, 20: 39690
GAUSTER, W. F., Prog. rpt. on experimental simulation of large, high field,

superconducting magnet operation, 12/65-7/66, 20: 40015 (ORNL-TM-1598)
GAUTIER, Francoise, Electron efficiency of fast film emulsified on two faces, 20: 39216
GAVRYUCHENKOV, F. G., Composition of vapor in $ErCl_3$–CsCl and $NdCl_3$–CsCl systems, 20: 38919
GAZZA, George E., Petch analysis of hydrogenated tantalum sheet, 20: 39378 (AD-635596)
GEBEL, R., Optimization of open-cycle MHD power plants, 20: 39719
GEFFEN, D. A., Adler-Weisberger sum rules for higher spin particles, 20: 39883
GEHLOT, G. L., Gravitation and the abundance of hydrogen, 20: 39560
GEIGER, Eric L., Radon film badge, 20: 39272
GELLER, R., Acceleration of plasma by field of progressive wave damped in vicinity of electron or ion cyclotron resonance, 20: 40267
GELLER, R., Plasma acceleration by means of r-f and static magnetic field gradient, 20: 40268
GELL-MANN, Murray, Representation of local current albebra at infinite momentum, 20: 39903
GEORGE, D. W., MHD generator operation as affected by electrode current saturation, 20: 39660
GEORGE, W., Prog. rpt. on Linac adaptation for weapons simulation, 1/65, 20: 39487 (EGG-1183-2009)
GERASIMOV, S. B., Electromagnetic properties of baryons and mesons in a nonrelativistic quark model, 20: 39835
GETOFF, N., Carboxylation of formate under radiation effects of radon, 20: 38966
GHATAK, A. K., Diffusion length calculations in water, 20: 40053
GHATAK, A. K., Persistent change in measured values of decay constant in Be, 20: 40376
GHIORDANESCU, N., Determination of constants for geometric reconstruction of tracks on np films from neutron irradiated 24-l bubble chamber, 20: 39247
GHIZARI, Eugenio, Protective effect of glycine in x irradiation, 20: 38714
GIACOMELLI, G., Pion-proton elastic scattering, 20: 39744 (CERN-66-18)
GIBBON, C. F., Effect of interfaces on radiation production of color centers in alkali halides, 20: 40317
GIBBONS, J. F., Advanced BONUS core thermal cycle test, 20: 40401 (CEND-259)
GIBBONS, W. G., Fatigue properties of irradiated pressure vessel steels, 20: 39406 (WAPD-T-1864)
GIBBS, Alan G., Modified kinetic model for calculation of $G_g(r,t)$ in dense fluids, 20: 39946
GIBSON, Henry C. Jr., Missile scoring systems utilizing nuclear radiation, 20: 39190
GIBSON, W., Electromagnetic interaction with plasma column, 20: 40252
GIDALI, Julio, Agents influencing granulocyte output and production in irradiated rabbits, 20: 38633
GIESBRECHT, Ernesto, Phosphates and polyphosphates of the lanthanide elements. VIII., 20: 38883
GIESSER, W., Fuel cycle of the Th-high-temperature-reactor THTR, 20: 40470
GILCREAS, F. W., Removal of low-level radioisotopes from wastewater by aerobic treatment, 20: 40483
GILDER, Howard Michael, Effect of high electronic current density on motion of ^{195}Au and ^{125}Sb in gold, 20: 40349
GILLET, C., Relation between modifications of water content of barley seeds and radioprotection by saline solutions, 20: 38736
GILLI, P. V., Evaluating thermodynamic parameters and selecting flow schemes for closed cycle MHD power plants, 20: 39720
GILMAN, Frederick Joseph, Baryon electromagnetic mass differences, 20: 39928
GINGERICH, K. A., Gibbs free energies of formation of thorium phosphides from solid-state electromotive force measurements, 20: 38907
GIORDANO, S., Measurements on multistem drift tube structure for proton accelerators, 20: 39478 (BNL-10376)
GIORGADZE, N. P., Disintegrated wave interaction in magnetoactive plasma, 20: 40207
GIRARD, V., Synergetic effect of x rays and of vincaleucoblastine on solid isologous tumor of mouse C^{3}H, 20: 38613
GIRARDI, Francesco, Determination of Mg in Al by neutron activation, 20: 38804
GIRULSKI, Ryszard, Stabilized power supply of the type ZNN 4, 20: 39177
GITTUS, J. H., Mechanism of failure in UO_2/stainless steel cermets, 20: 39459 (TRG-Report-1278)
GLADTKE, E., Kinetic studies with radioactive (^{59}Fe) and nonradioactive (^{56}Fe) iron in serum, 20: 38573
GLADYSHEV, D. N., Lifetimes of the excited levels of ^{151}Pm, 20: 40105
GLADYSHEVSKII, E. I., Crystal structure of $EuNi_5$, $TmNi_5$, and $LuNi_5$ compounds, 20: 39415
GLAZOV, A. A., Programming the accelerating voltage amplitude of a model of circular proton phasotron r.f. system, 20: 39491 (JINR-P-2732-1)
GLAZOV, O. A., Magnetohydrodynamic boundary layer of rotative liquids over stationary base, 20: 39936
GLEESON, Austin Michael, Pion-nucleon collisions and pion production, 20: 39839
GLOECKLER, George, Galactic deuterium and its energy spectrum above 20 Mev per nucleon, 20: 39987
GLONTI, G. L., Movement of ^{90}Sr in Georgian soils, 20: 39117
GLOTIN, Ph., Variations of physical and electrical concentrations of donors during thermal annealing, 20: 40345
GLUECKAUF, Eugen, Improvements in or relating to fuels for nuclear reactors, 20: 40395
GMITRO, M., Level structure of oxygen isotopes in the SU_3 scheme, 20: 40126
GODDARD, Judy, Inactivation of tobacco mosaic virus by ultraviolet light, 20: 38584
GOEDEMOED, S. H., Enthalpy of impure niobium in mixed superconductive state, 20: 40036
GOGOSOV, V. V., Boundary layers in two-temperature plasma, 20: 39721
GOLD, Raymond, Power Reactor Technology. Vol. 9, No. 2, 20: 40426
GOLD, Raymond, Power Reactor Technology, Vol. 9, No. 1, 20: 40430
GOLDANSKII, V. I., Annihilation of slow positrons in ionic media, 20: 39819
GOLDBERG, Edward D., Uranium-234/U-238 ratios in seawater, 20: 39133
GOL'DBERG, M. B., Inborn radiation syndrome induced experimentally, 20: 38665
GOLDBLITH, Samuel A., Historical development of the irradiation of foodstuffs, 20: 39297
GOLDSTEIN, Ch., Heavy ion injection for stripping in the central region of the CEVIL, 20: 39531
GOLEB, Joseph A., Determination of B natural abundance ratio, $^{11}B/^{10}B$, by atomic absorption spectrophotometry, 20: 38803
GOLINSKI, Marek, Crystallization of double ammonium lanthanide nitrates, 20: 38915
GOLOVIN, B. M., Spin correlation in elastic scattering of 605-Mev polarized protons on protons, 20: 39759 (JINR-P-2776)
GONSHERY, Marvin E., Radiation-induced instability in refractive properties of some optical glasses, 20: 39468
GOOCH, P. C., Cytogenetic methods: somatic chromosome aberrations in occupationally irradiated humans, 20: 38593 (ORNL-P-2175)
GOOD, James A., Drive mechanism for nuclear reactor control rod, 20: 40371
GOODGAME, J. R., Measurement of (n,2n), (n,p), and (n,α) cross sections of Ge at 14.4 Mev, 20: 40080 (ORO-3346-3)
GOODRICH, Roy Gordon, Electron spin resonance in cerium metal, 20: 40352
GORDEEVA, V. A., Effects of ionizing radiation and other factors on rate of topochemical decomposition of various inorganic compounds, 20: 38955
GORDON, M. M., Control of the Michigan State University cyclotron, 20: 39552
GORDON, M. M., Single turn extraction [in MSU cyclotron], 20: 39517
GORDON, Milton P., Inactivation of tobacco mosaic virus by ultraviolet light, 20: 38584
GORDON, Sidney L., Nuclear magnetic double resonance of single nucleus of spin ½, 20: 40103
GORENC, B., Separation of ^{99m}Tc from ^{99}Mo sorbed on aluminum oxide, 20: 38997 (NIJS-R-483)
GORIZONTOV, P. D., Results of experimental study of radiation pathology, 20: 38653
GORLA, P., Szilard-Chalmers recoil of ^{60}Co and ^{60m}Co, 20: 38962
GORODETSKII, A. A., Use of gallic acid in prophylaxis and therapy of acute radiation sickness, 20: 38728
GOROKHOV, L. N., Mass spectrometric investigation of gaseous compounds of alkali metals, 20: 39724
GORYACHEV, I. V., Angular distribution of fast neutrons behind iron shielding, 20: 40286
GOSHAW, A. T., Search for the kappa meson, 20: 39784
GOTTLIEB, Leonard S., Tumoricidal effect of laser energy on experimental and human malignant tumors, 20: 38780
GOUGH, D. O., Influence of a magnetic field on Schwarzschild's criterion for convective instability in an ideally conducting fluid, 20: 39939
GOULDING, F. S., Semiconductor detectors for nuclear spectrometry. I., 20: 39230
GOURDIN, M., General methods in current algebra, 20: 39882
GOURDINE, M. C., Electrogasdynamic central power stations, 20: 39701
GOURDINE, M. C., Prospect for electrogasdynamic power, 20: 39648
GOYAL, I. C., Diffusion length calculations in water, 20: 40053
GOYAL, I. C., Persistent change in measured values of decay constant in Be, 20: 40376
GRACCO, V., Charged pion photoproduction on light nuclei, 20: 40075 (LNF-66/30)
GRAHAM, R. L., Use of Ge(Li) detectors in γ-γ coincidence experiments,

20: 39197 (AECL-2565)
GRANATSTEIN, V. L., Electromagnetic: acoustic wave propagation along warm plasma columns, 20: 40166 (AD-637711)
GRANNIS, P., Polarization parameter in p-p scattering from 328 to 736 Mev, 20: 39791
GRANNIS, P., Polarization parameter in p-p scattering from 1.7 to 6.1 Bev, 20: 39792
GRANSTROEM, Sune, Swedish 200-psi blast-resistant seven-man shelter, 20: 39077
GRAPA, J., Variations of physical and electrical concentrations of donors during thermal annealing, 20: 40345
GRATTON, C. P., Utilisation of Pu in high temperature reactor, 20: 40472
GRAZIANI, G., Uranium-235/Th fuel cycles in graphite moderated systems, 20: 40393
GREEBE, C. A. A. J., Helicon-like resonances in superconducting niobium, 20: 40031
GREEN, Earl L., Prog. rpt. on quantitative population genetics of mice under irradiation, annual, 7/65–5/66, 20: 38590 (NYO-1979-13)
GREEN, J. K., Prog. rpt. on earth sciences, annual, 1965, 20: 38857 (BNWL-235-3)
GREENBAUM, G. A., Creep of axisymmetric shells, 20: 39391 (CONF-660629-1)
GREENBORG, J., ISOSHLD: computer code for general purpose isotope shielding analysis, 20: 40285 (BNWL-236)
GREENSPAN, Jacob, Structural, high strength U alloys, 20: 39440
GREGOIRE, G., Scattering of alpha particles by ^{31}P, 20: 40090
GREGOIRE, G., Spin-orbit potential in $^{9}Be(\alpha,\alpha)$ elastic scatterings, 20: 40089
GREMION, Robert, Methods and devices for determining the mean radius of pores in microporous barriers, 20: 39012
GRICE, Karl R. Jr., Missile scoring systems utilizing nuclear radiation, 20: 39190
GRIDNEVA, S. M., Boundary layers in two-temperature plasma, 20: 39721
GRIGOR'EV, V. N., Separation of neon isotopes in film fractionating column, 20: 39322
GRIGOR'EV, Yu., Radiation safety, 20: 38603 (AD-629422)
GRILLI, M., Optical properties of strong-focusing magnet, 20: 39494 (LNF-66/15)
GRINEV, V. S., Mathematical model of accumulation and elimination of radioactive isotopes, 20: 38571
GRISHIN, V. G., Identification of charged particles by ionization and δ-electrons in a propane bubble chamber, 20: 39211 (JINR-P-2842)
GRISHIN, V. G., Possible experiments checking isotopic structure of electromagnetic interactions, 20: 39824
GRISHIN, V. G., Production of electron-positron pairs by high-energy gamma quanta, 20: 39594
GRODZINE, L., Effective magnetic fields at Sm, Gd, and Dy nuclei in metallic Fe following Coulomb excitation implantation, 20: 40342
GROH, H. J., Analytical chemistry of neptunium, 20: 38821
GROMOVA, A. I., Corrosion resistance of reactor materials, 20: 39349
GROPP, A., Chromosome anomalies after radiation exposure, 20: 38615
GROSSMAN, Lawrence, Prog. rpt. on mutagenic and lethal effects of ultraviolet irradiation, 9/65–6/66, 20: 38574 (NYO-3449-1)
GROSSMAN, Leonard N., High-temperature thermal analysis of ceramic systems, 20: 39437
GROVE, G. R., Prog. rpt., 11/65, 20: 39320 (MLM-1311)
GROVE, G. R., Prog. rpt., 12/65, 20: 39321 (MLM-1312)
GROZDENSKII, D. E., Radiation effects on hypophysis-suprarenal system, 20: 38661
GRUBELICH, F. T., Advanced BONUS core thermal cycle test, 20: 40401 (CEND-259)
GRUENBERG, Leonard W., Fulde-Ferrell effect in type II superconductors, 20: 40046
GRUENEWALD, T., Experiences with machine sources in food irradiation, 20: 39303
GRUNDER, H. A., Survey of isochronous cyclotron technology, 20: 39548
GRUSHIN, V. F., Determination of quantometer constant at 650 Mev, 20: 39248
GRUZDEV, G. P., Restoration of bone marrow tissue in acute radiation sickness, 20: 38663
GUBAREV, A. V., Development of flow of a viscous fluid in duct of MHD generator, 20: 39685
GUERRERO, H., Effect of density and grain size on thermal conductivity of UO_2 during irradiation, 20: 39446 (AECL-2564)
GUILLON, H., Review of multichannel and multiparameter analyzer systems, 20: 39176
GUILLON, H., Review of basic instruments and trends, 20: 39238
GUILLOT, J. C., New forms of irreducible unitary representations of Poincare group. I., 20: 39864
GUILLOT, J. C., New forms of irreducible unitary representations of Poincare group. II., 20: 39865
GUILLOU, Michel, Electrochemical criteria for selecting MHD electrode materials research on electronically-conducting zirconium oxide, 20: 39723
GUINET, Philippe, Isotherm section at room temperature of U–C–Si diagram, 20: 39413
GUINN, VINCENT P., Neutron-activation determination of traces of Se, V, Sr, and As in biological samples, 20: 38837
GUITTARD, Micheline, Selenides ML_xSe_y of structural type Y_5S_7 (L = rare earth and M = Mg, Cr^{2+}, Mn, Fe^{2+}), 20: 38884
GUKASYAN, L. A., Influence of x irradiation on the yield and chemical composition of potatoes, 20: 38690
GULYAMOV, U. G., Diffraction dissociation $\pi \rightarrow 3\pi$ in field of heavy nuclei, 20: 39774
GUNSHOR, R. L., Landau damping in plasmas with finite transverse dimensions, 20: 40211
GUNTHER, Leon, Fulde-Ferrell effect in type II superconductors, 20: 40046
GUPTA, K. C., Free convection flow of electrically conducting fluid past porous flat plate under transverse magnetic field, 20: 39929
GUPTA, Sharda Das, Radiation resistant lubricants, 20: 38973
GUPTA, V., Sum rules for K-meson decays with CP nonconservation, 20: 39812
GURNETT, Donald A., Ion temperature in ionosphere obtained from cyclotron damping of proton whistlers, 20: 39972
GURSKAYA, S. F., Rare earth metal and Y distribution during Zn crystallization in lead melt, 20: 39435
GUSAROV, A. V., Mass spectrometric investigation of gaseous compounds of alkali metals, 20: 39724
GUSEV, Yu. K., Formation of XeO_3 in β decay of ^{131}I, 20: 38984
GUSKOVA, A. K., Correlation of local tissue changes and general reactions at different stages of acute radiation sickness in man, 20: 38774
GUSTAFSSON, B., DETEC subprogram for simulation of fast-neutron detection process in hydro-carbonous plastic scintillator, 20: 39196 (AE-236)
GUTAY, Laszlo Janos, Study of the N*(1920) resonance, 20: 39845
GUYER, R. A., Thermal conductivity, second sound, and phonon hydrodynamic phenomena in nonmetallic crystals, 20: 40327
GYFTOPOULOS, Elias P., Transport phenomena in low-energy plasmas, 20: 40210
GYGAX, F., Circularly polarized β-γ correlation in decay of $^{188}Re(17h)$, 20: 40097

H

HAAS, P. A., Prog. rpt. on unit operations, 10–12/65, 20: 38998 (ORNL-3958)
HABERSBERGEROVA, A., Radiation-induced oxidation of methanol, 20: 38942 (UJV-1457)
HADEN, Clovis Roland, Flux-trapping model for r-f losses in superconductors, 20: 40042
HAENDEL, S. K., Studies of characteristic flash x-ray lines, 20: 40233
HAENSEL, R., Measurement of synchrotron radiation in x-ray region, 20: 39473
HAFELE, J. C., High-resolution study of inelastic proton scattering from nuclei in Pb region, 20: 40074 (LA-DC-8069)
HAGEBEUK, H. J. L., Preliminary investigations with a r-f electric mirror field, 20: 40276
HAGEBEUK, H. J. L., Runaway electrons in an r-f mirror field, 20: 40266
HAGEDOORN, H., Reaction $^{27}Al(p,\alpha)^{24}Mg$ studies with a 30-Mev AVF cyclotron, 20: 40101
HAGEDOORN, H. L., Beam properties of Philips' A.V.F. cyclotrons, 20: 39516
HAGEDOORN, H. L., Extraction studies in an AVF cyclotron, 20: 39518
HAGEMANN, G. B., Effective magnetic fields at Sm, Gd, and Dy nuclei in metallic Fe following Coulomb excitation implantation, 20: 40342
HAGENMULLER, Paul, System As_2O_5–ThO_2, 20: 38885
HAKE, G., Note on fast fracture of a pressure vessel, 20: 39329 (AECL-2432)
HALEVY, E., Health physics implications in choice of radioactive tracers for hydrological investigations, 20: 39155
HALL, Hugh E. Jr., Epithermal neutron well logging, 20: 39138
HALL, R. R., High-current ion-beam production and injection, 20: 40175 (ORNL-3989, pp 89-94)
HALL, Richard B., Energy gain of a low-energy charged particle in standing wave near cyclotron resonance, 20: 40264
HALL, Richard B., Relativistic motion and energy gain of charged particles in standing wave near cyclotron resonance, 20: 40263
HALL, Wayne E., Fractionation of $^{18}O/^{16}O$ between coexisting calcite and dolomite, 20: 39129
HALLABA, E., Preparation of diiodo-^{131}I fluorescein and tetraiodo-^{131}I phenolphthalein for diagnostic purposes, 20: 38985
HALLE-PANNENKO, Olga, Effect of whole body irradiated and methylhydrazine in eradicating transplant leukaemia 1210, 20: 38794
HALLIDAY, F. O., Use of ^{241}Am alphas to measure properties of thin films, 20: 39298

HALLIWELL, James, Nuclear reactor fuel elements, 20: 39377
HALPERN, Martin B., Solution of very singular N/D equations: approach to nonrenormalizable field theory, 20: 39870
HALS, F., High-temperature regenerative air preheater for MHD power plants, 20: 39725
HAMILTON, G. F., Observation of proton channeling in thin mica, 20: 40324
HAMMITT, A. G., Magnetohydrodynamic liquid metal power conversion systems, 20: 39726
HAMMOND, George S., Triplet states in radiation chemistry, 20: 38948
HAMPL, J., Contribution to estimation of radiosensitivity in domestic fowl, 20: 38676
HANGEA, N., Determination of constants for geometric reconstruction of tracks on np films from neutron irradiated 24-l bubble chamber, 20: 39247
HANKINS, Denis, Dynamical calculation of the Regge-pole parameters, 20: 39924
HANNER, D. W., High-temperature testing and evaluation of graphite helical-screw expanders and compressors, 20: 39026 (UCRL-14660(Rev.1))
HANSEN, Niels, Dispersion-strenghened Al products, 20: 39358 (RISO-113)
HANSEN, Richard Otto, Isotopic distribution of U and Th in soils weathered from granite and alluvium, 20: 39144
HANSROUL, M., Polarization parameter in p-p scattering from 328 to 736 Mev, 20: 39791
HANST, K., Prog. rpt. on Linac adaptation for weapons simulation, 1/65, 20: 39487 (EGG-1183-2009)
HANST, K., Prog. rpt. on Linac adaptation for weapons simulation, 4/65, 20: 39488 (EGG-1183-2027)
HANST, K., Prog. rpt. on Linac adaptation for weapons simulation, subharmonic buncher, 10/65, 20: 39489 (EGG-1183-2050)
HANST, K., Prog. rpt. on Linac adaptation for weapons simulation, high current gun, 10/65, 20: 39490 (EGG-1183-2051)
HARA, Akio, Study on Co phase composition contained in WC–Co base cemented carbides, 20: 39427
HARADA, Y., Fabrication and characterization of metal carbide-graphite composites, 20: 39367
HARADA, Yoshishige, Method for producing thermoplastic resins of ternary copolymers, 20: 38978
HARDY, C. J., Examination of hydrous U dioxide precipitates and sols, 20: 39401 (ORNL-3963)
HARDY, Lyndon Maurice, Analysis of strange-particle resonant states from π-p interactions, 20: 39770 (UCRL-16788)
HARE, G. E., Radioisotope powered generator development in UK, 20: 39309 (DP-1066(Vol.2), pp III.39-48)
HARMUTH-HOENE, Anno-Elisabeth, Excretion of ^{65}Zh-DTPA in the rat, 20: 38556
HARRENSTIEN, Howard P., Risk-oriented solution for target community, 20: 39089
HARRIS, D., Non-steady modulated MHD systems, 20: 39730
HARRIS, I. R., Effect of cold work on x-ray diffraction patterns of rare-earth metals, 20: 39421
HARRIS, R. J. Jr., Measurement of the lifetime of the 14.4 kev level of ^{57}Fe, 20: 40132
HARRISON, Kenneth, Management of glottic carcinoma of larynx, 20: 38782
HASEGAWA, Masayoshi, Ternary alloys of iron and boron, 20: 39426
HASSELTINE, E. H., Cesium ion sputtering of aluminum, 20: 39585
HATCH, A. M., Large experimental superconducting magnet for MHD power generation, 20: 39643
HATCH, E. N., Lifetimes of the 87 and 105 kev levels in ^{155}Gd, 20: 40110
HAUBENREICH, P. N., Analysis of filling accidents in MSRE, 20: 40412 (ORNL-TM-497)
HAUBERT, P., Plutonium fuel cycle studies for large high temperature graphite moderated reactor, 20: 40421
HAUG, Robert, Parameters of Cs plasma obtained by contact ionization, 20: 40223
HAUSNER, H., Uranium oxide powder and pellet thermal conductivity during irradiation, 20: 39456 (GEAP-5100-1)
HAVA, M., Effect of 19-nor-testosterone phenylpropionate on postirradiation syndrome, 20: 38610
HAYASHI, Koichiro, Polymerization of cyclic ethers in presence of maleic anhydride. I., 20: 38953
HAYMAKER, W., Astroglial reactions to ionizing radiation, 20: 38674
HAYS, L. G., Comparison of liquid-metal magnetohydrodynamic power conversion cycles, 20: 39634 (JPL-32-946)
HAYS, L. G., Theoretical and experimental investigation of liquid–metal MHD power generation, 20: 39716
HEASLIP, Margaret B., Prog. rpt. on ecological significance of radiation on tree seed and seedlings, 1966, 20: 38594 (ORO-2066-10)
HEATH, R. L., Computer techniques for the analysis of gamma-ray spectra obtained with NaI and Li-ion drifted Ge detectors, 20: 39237
HEBEL, W., Production of ^{60}Co in the BR2 Reactor, Belgium, 20: 39318 (DP-1066(Vol.2), pp I.93-101)
HEDVALL, P., Influence of collisions on whistler propagation, 20: 40196
HEINZ, R. M., New evidence for sigma meson, 20: 39782
HENDEL, H. W., Acceleration of electron cyclotron plasma by self-generated electric fields, 20: 40262
HENDRICKS, J. B., Prog. rpt. on experimental simulation of large, high field, superconducting magnet operation, 12/65-7/66, 20: 40015 (ORNL-TM-1598)
HENDRICKSON, M. M., ISOSHLD: computer code for general purpose isotope shielding analysis, 20: 40285 (BNWL-236)
HENISCH, H. K., Photo-stimulated radiation dosimetry, 20: 40333
HENNING, Gerhart R., Decoration of individual lattice vacancies in graphite, 20: 39439
HENRY, R., Cobalt-60 production in graphite gas cooled reactors, 20: 39317 (DP-1066(Vol.2), pp I.67-77)
HENRY, R. J. W., Electron temperatures in the D region, 20: 39994
HENTZ, Robert R., Method of performing a radiation-induced chemical reaction, 20: 38972
HERMANS, M. E. A., Basic studies related to the development of the Sol-Gel process, 20: 40391
HERMOCH, V., Cathode jets and retrograde motion of arcs in magnetic fields, 20: 40232
HERNEGGER, F., Carboxylation of formate under radiation effects of radon, 20: 38966
HEROLD, C., Localization of interface reactions in metal–aqueous solution systems. I., 20: 39336
HEROLD, C., Localization of boundary reactions in metal–aqueous solution systems. II., 20: 39337
HERRING, F. G., Electron spin resonance spectrum and electronic structure of PO_2^{2-} radical in irradiated crystal of ammonium fluorophosphate, 20: 38949
HERRINGTON, Arthur C., Process for impregnating an adsorbent catalyst with a radioactive metal isotope, 20: 38993
HESLOT, H., Molecular mechanisms of mutagenesis and nature of mutations, 20: 38542 (UCRL-Trans-10029)
HESS, R., Circularly polarized β-γ correlation in decay of ^{188}Re(17h), 20: 40097
HESSE, John Lambom, Impact and hardness properties of irradiated beryllium, 20: 39436
HEURING, F. T., Transverse hydromagnetic disturbances at 1100 km in auroral region, 20: 39996
HEUSCH, Clemens A., Topics of interest in π and η photoproduction, 20: 39743 (CALT-68-92)
HICE, James D., Occurrence patterns of topside spread F on Alouette ionograms, 20: 39973
HILS, D., Remeasurement of the total cross section for excitation of hydrogen 2 $^2S_{1/2}$ state by electron impact, 20: 39608
HILZ, H., Increase in RNase and DPNase activities in ascites tumor cells induced by cytostatic agents, 20: 38578
HINO, Koichi, Study on Co phase composition contained in WC–Co base cemented carbides, 20: 39427
HIRAMOTO, Tatsumi, Flow velocities, seeding ratios and electrical conductivities in seeded Ar plasmas, 20: 39727
HITCHCOCK, A., Reactor steam cycles for desalination, 20: 40439
HIYAMA, Yoshio, Gamma emitters in marine organisms. I., 20: 38560
HLINIAK, A., Long-term results and complications after irradiation of haemangiomas in children, 20: 38787
HOBSON, D. O., Influence of neutron irradiation twinning in a Nb–V alloy (40% V), 20: 39462
HODDE, J. A., Core performance and transient flow testing of Big Rock Point Boiling Water Reactor, 20: 40404 (GEAP-4496)
HODGSON, George, Effect of gamma irradiation on response to erythropoietin of non-fasted rats, 20: 38673
HODGSON, R., Non-equilibrium conductivity in Ar–K plasma in crossed electric and magnetic fields, 20: 39684
HOENIG, V., Half-life of the 453.08 kev level in ^{183}W, 20: 40123
HOFFMAN, Charles A., Metallographic study of dispersion-strengthened alloys after failure in stress rupture, 20: 39398 (NASA-TN-D-3527)
HOFFMAN, K. C., Engineering problems in pulsed neutron sources, 20: 40455 (BNL-10454)
HOGLUND, Barton M., UHTREX operation near, 20: 40474
HOHMUTH, K., New levels in ^{97}Tc, 20: 40084
HOLLADAY, W. G., Application of π-N scattering results to Λ-K^0 production, 20: 39803
HOLLANDER, J. M., Impact of semiconductor detectors on gamma-ray and electron spectroscopy, 20: 39232
HOLLOWAY, L., Polarization parameter in p-p scattering from 328 to 736 Mev, 20: 39791
HOLM, S., Proposal for sector-focusing synchrocyclotron, 20: 39535
HOLMAN III, Wayne J., Complex angular momenta and the groups SU(1,1) and SU(2), 20: 39863
HOLMES, J. J., Multiprocess creep in uranium deduced from literature data, 20: 39410

HOLT, E. H., Transport phenomena in ionized gases as initial value problem, · 20: 40168 (NASA-CR-559)
HOLTON, C. S., Effect of x-radiation on spore germination and stability of virulence in Ustilago avenae, 20: 38672
HOLZAPFEL, C., Closed MHD-loop ARGAS, 20: 39680
HOLZAPFEL, C., Layout data of homogeneous closed-cycle 300-Mw MHD generator, 20: 39681
HOOPER, A. T., Closed-cycle nuclear MHD studies using dust suspensions, 20: 39728
HOPKINS, George R., Nuclear power reactor having high, prompt negative temperature coefficient of reactivity, 20: 40434
HORETS, T. A., Preparations conducive to removal of radioactive isotopes from an organism, 20: 38733
HORI, Shiro, Genetic studies on radio-resistant strain of Chlorella ellipsoidea. I., 20: 38605
HORI, Yasuharu, Observations on thymus of mice after x irradiation, 20: 38606
HORI, Yoshimichi, Method for producing tetrafluoroethylene polymers, 20: 38980
HORN, G. R., Irradiation brewing of UO_2, 20: 39449 (BNWL-SA-272)
HORNYIK, Karl, Dynamic behavior of a TRIGA reactor, 20: 40475
HORSKY, J., Rayski formulation of laws of conservation for exact static metric, 20: 40010
HORSLEY, A., Computer evaluation of neutron scattering angular distribution data, 20: 40063
HORSLEY, G. W., Studies on the reprocessing and refabrication of HTGR fuels in OECD Dragon Project, 20: 40419
HORSLEY, Geoffrey Winton, Improvements in or relating to processes for production of pellets from particulate material, 20: 39368
HORTON, R. W., Prog. rpt. on unit operations, 10–12/65, 20: 38998 (ORNL-3958)
HORWITZ, L., Algebra of scalar and vector vertex strengths in Regge residues, 20: 39881
HOSTE, J., Determination of Cu, Cr, Zn, Co, Na, and K in blood serum, 20: 38851
HOUDAILLE, M., Cost of coated particle fuel for a high temperature reactor program, 20: 40466
HOUSKOVA, M., Internal contamination with ^{90}Sr and ^{226}Ra in man in relation to clinical findings, 20: 38623
HOUSTON, John M., Survey of theory and laboratory performance of cesium thermionic converters, 20: 39651
HOWARD-FLANDERS, Paul, Loci in E. coli K-12 that control mutagen products from DNA, 20: 38620
HOWARD-FLANDERS, Paul, Mutants of E. coli K-12 defective in DNA repair and genetic recombination, 20: 38621
HOWATSON, A. M., Electrical measurements on a moving argon plasma, 20: 39655
HOWE, John S. Jr., High-energy-rate extrusion of low-density tungsten powder billets, 20: 39352 (BM-RI-6817)
HOWIE, Donald L., Review of the U. S. Army wholesomeness of irradiated food program 1955–1966, 20: 39302
HOYER, F., Simultaneous scintillation spectrometry of α and β rays by cesium iodide, 20: 39217
HRADECNA, Zdenka, X-ray inactivation of lambda phages. I., 20: 38628
HRISTEV, P. Anatolie, Commutators of covariant bilinear forms of quantified spinorial field, 20: 39906
HROVAT, M., Fuel development for THTR, 20: 40467
HRUSKOVA, I., Space and time variations of long wave ionospheric absorption at small solar heights and at night, 20: 39960
HSU, Y. C., Prog. rpt. on liquid-metal lubricated journal bearings, 4–7/66, 20: 39008 (SWRI-1228-8-24)
HUBER, P., Cross section of $^{73}Ge(n,\alpha)^{70}Zn$ reaction at 14 Mev, 20: 40098
HUBER, P., Neutron flux determination with thick $(CH_2)_n$ radiators, 20: 39223
HUCHITAL, D. A., Transport phenomena in ionized gases as initial value problem, · 20: 40168 (NASA-CR-559)
HUDDLE, R. A. U., Cost of coated particle fuel for a high temperature reactor program, 20: 40466
HUDDLESTON, Charles M., Gamma-ray streaming through ducts, 20: 39060
HUDGINS, Arthur J., Cooperative group shelter near Livermore, California, 20: 39085
HUDSON, E. D., Operating characteristics of ORIC beam extraction system, 20: 39521
HUEHNERMANN, Harry, Hyperfine structure and quadrupole moment of ^{65}Cu, · 20: 40137
HUENDORF, B., Experimental methods for flow in spherical bodies, 20: 39051
HUETTER, Godfrey Thomas, Analysis of 3587 τ^+ decays, 20: 39846
HUFF, H. L., Sputtering of Cu, Mo, 304 stainless steel, and W by deuterium ions, 20: 39581 (ORNL-3989, pp 134)
HUGGINS, R. A., Oyster Creek nuclear station: design concept, construction, and training program, 20: 40436
HULTQVIST, Bengt, Negative ions in lowest ionosphere with special reference to experimental evidence from upper atmosphere research, 20: 39949
HULTQVIST, Bengt, Plasma waves in frequency range 0.001–10 CPS in Earth's magnetosphere and ionosphere, · 20: 40224
HUMMEL, R. W., Acetylene production in the radiolysis of methane, 20: 38951
HUMMER, D. G., Introduction to radiative transfer problems in stellar atmospheres, 20: 39570
HUNN, W., Cross section of $^{73}Ge(n,\alpha)^{70}Zn$ reaction at 14 Mev, 20: 40098
HUNT, J. C. R., Fluid dynamic effects in large-scale MHD generators, 20: 39729
HUNT, J. C. R., Stability of parallel flows with parallel magnetic fields, 20: 39943
HUNTER, James H. Jr., Thermal instabilities in solar chromosphere, 20: 39562
HUSAIN, L., Cosmic ray produced phosphorus isotopes in atmosphere, 20: 39991
HUSAIN, M., Intermediate structure in ^{41}Ca, 20: 40087
HUTCHESON, E. T., Search for evidence of positron emission in the decay of ^{36}Cl, 20: 40148
HUTCHINGS, M. T., Temperature variation and separation dependence of exchange interactions of Gd^{3+} pairs in $LaCl_3$, 20: 38914
HUYSKENS, P., New apparatus for irradiating liquids and gases by means of accelerated electrons, 20: 38947
HWANG, J. H., Electron spin resonance spectrum and electronic structure of PO_3^{2-} radical in irradiated crystal of ammonium fluorophosphate, 20: 38949

I

IBBERSON, V. J., Non-steady modulated MHD systems, 20: 39730
ICHII, Shogo, Alterations in functional state of rat adrenal following the lethal and sub-lethal, whole-body x-irradiations, 20: 38638
IL'IN, L. A., Preparations conducive to removal of radioactive isotopes from an organism, 20: 38733
ILINA, N. P., Angular distributions of muons in ground and under water and their generation mechanism, 20: 39831
IL'INSKII, D. A., Changes in blood vessels during acute radiation sickness, 20: 38658
IL'INSKII, D. A., Mechanism of protective action of aminothiols, 20: 38723
IMARISIO, G. C., Statistical techniques and analysis in corrosion measurements of Zr alloys in terphenyls, 20: 39344 (EUR-2997.e)
IMHOF, W. L., Behavior of trapped electrons and protons at lower edge of inner radiation belt, 20: 39983
INAGAKI, Eiichi, Comparison of frequency patterns between whole-body and fractional mutations induced by x rays in Drosophila, 20: 38650
INGALLS, R., Moessbauer studies of divalent and trivalent ^{57}Fe in $CoSO_4$ and $CoSO_4 \cdot 7H_2O$, 20: 40311
IOVA, I., New data on spectral lines shift mechanism in plasma of an electric spark discharge, · 20: 40182
IRIGARAY, Jean-Leon, Investigation of bound neutron-neutron state in reaction $^9Be(n,2n)^8Be$, 20: 40091
ISAEV, B. M., Calculation of absorbed doses in plant seeds during irradiation with fast neutrons, 20: 38693
ISAEV, P. S., Cross sections for generating $K\bar{K}$ pairs in $\pi\pi$ collisions at low energies, 20: 39833
ISELIN, Ch., Layout of the new CERN neutrino beam, 20: 39746 (CERN-66-24)
ISHIBACHI, T., Singularities in coherent diffuse scattering of x rays, 20: 39586
ISHIBASHI, Nobuhiko, Radiometric titration of trace amounts of cobalt using EDTA, 20: 38806
ISHIBASHI, Nobuhiko, Radioisotopic dilution analysis of trace amount of cobalt, 20: 38807
ISHIDA, Koji, Determination of Re by neutron activation, 20: 38802
ISHIHARA, M., Single RACE spectrometer, 20: 39206 (INSJ-99)
ISHIMATSU, T., Report on measurements of reaction $^{40}Ca(d,\alpha)^{39}Ca$ for 24 Mev impact energy, 20: 40067 (BMwF-FBK-66-15, pp 20-37)
ISOMURA, Shohei, Separation of ^{10}B by distillation of BF_3–CH_3F, 20: 39325
ISTOMIN, V. G., Observational results on atmospheric ions in region of outer ionosphere, 20: 39950
ISTOMINA, A. G., Toxicity of tritium oxide in mice and rats subjected to intraperitoneal injection, 20: 38568
ITO, Toshio, Analysis of thermodynamic properties of high-temperature gas, 20: 39938
ITO, Toshio, Seeded combustion gas of MHD generation, 20: 39636
IVANENKO, I. P., Influence of polarization of medium on electron-photon showers, 20: 39829
IVANENKO, T. I., Radiation effects on hypophysis-suprarenal system, 20: 38661

IVANOV-KHOLODNYI, G. S., Rocket data on behavior of electron concentration in ionosphere at heights of 100-300 km. I., 20: 39958
IVANTER, I. G., Four-fermion interaction and lepton masses, 20: 39832
IVANYUKOVICH, G. A., Energy spectrograms of point sources of γ rays, 20: 40290
IVES, M. B., Dissolution spirals on gamma-irradiated lithium fluoride, 20: 40293 (AD-634746)
IWASHITA, Fumio, Method for preparation of adhesive films, 20: 38979
IZUTSU, Kosaku, Effects of ultraviolet microbeam irradiations on mitosis studied in Tradescantia cells in vivo, 20: 38614

J

JACKSON, C. N. Jr., Enrichment tester for 0.15 to 3.0 wt.% ^{235}U U fuel, 20: 39335
JACKSON, J. W., 200 Bev accelerator employing a separated function magnet lattice, 20: 39480 (BNL-10508)
JACKSON, W. D., Material limitations in the MHD induction generator, 20: 39731
JACKSON, William A., Prog. rpt. on Cs and Sr uptake and assimilation by higher plants, annual, 5/65-2/6, 20: 38548 (ORO-2410-1)
JACQUOT, B., Confinement and heating of a plasma by low-frequency rotating magnetic field, . 20: 40279
JACQUOT, B., Mixed-field configuration without leaks, . 20: 40280
JAFFE, Arthur, Wick polynomials at fixed time, 20: 40004
JAGER, Frederick William, Detector of radioactivity, 20: 39249
JAGGER, J., Photoreactivation of mutation to prototrophy in E. coli, 20: 38669
JAKOBSON, Kurt, Method of pickling and chemically milling zirconium and zirconium alloys, 20: 39351
JANCZYSZYN, Jerzy, Choice of optimum shape of neutron howitzer for neutron absorption methods, 20: 40057
JANKE, J., Biological application activation analysis of ^{18}O, 20: 38848
JANOUT, Z., Planning of n-p scattering experiments above pion-production threshold, 20: 39752 (JINR-E-2765)
JANOVSKY, I., Radiation-induced oxidation of methanol, 20: 38942 (UJV-1457)
JANSSEN, Norbert, Influencing properdin and agglutinin formation by whole-body irradiation, 20: 38695
JAROSCHEK, K., Present types of nuclear power stations, 20: 40441
JAUCH, J. M., Unitarity of the S matrix for multichannel scattering, 20: 39866
JAYARAMAN, A., Pressure-induced phase transformations and magnetic ordering in intrarare-earth alloys and Sm, 20: 40326
JAYSON, Joel Stanley, Propagation and instabilities in bounded and finite temperature plasmas, . 20: 40271
JEDRZEJOWSKI, Zb., Study of cycle diagrams of power plants with MHD generators, 20: 39732
JEFFRIES, R. A., Contributions to feasibility study of early lunar flare, 20: 39469 (LA-3453)
JELEN, J., Influence of the increase in inductance at acceleration of plasma in external magnetic field, . 20: 40192
JELINEK, J. M., Effect of 19-nor-testosterone phenylpropionate on post-irradiation syndrome, 20: 38610
JENNINGS, A. S., Large scale separation of ^{210}Po from Bi, 20: 38996 (DP-1066(Vol.2), pp II.79-102)
JENSEN, M. Anthony, Superconductivity in transition metals at very low temperatures, 20: 40047
JENSSEN, Arnfinn, Public shelters in Norway: protection against ground shock, 20: 39084
JESENAK, Viktor, Radioactive kryptonates in science and technology, 20: 39294
JEZDIC, Vojislav, Synthesis of malathion labeled with ^{35}S or ^{32}P and dipterex-^{32}P, 20: 38931
JNANANANDA, S., Measurement of the internal conversion coefficient of the 800 kev transition of ^{134}Ba, 20: 40095
JNANANANDA, Swami, Lifetimes of 1554- and 1289-kev levels of ^{182}W, 20: 40094
JOHANSSON, B., Proposal for sector-focusing synchrocyclotron, 20: 39535
JOHANSSON, K., Magnetic moment of the lowest 2$^+$ vibrational state in ^{122}Te, 20: 40128
JOHNSON, E., Prog. rpt. on Linac adaptation for weapons simulation, 4/65, 20: 39488 (EGG-1183-2027)
JOHNSON, Frank Fawcett, High resolution apparatus using γ source and detector for investigating earth formations, 20: 39139
JOHNSON, J. Enoch, Fire and noxious gases: effect on internal environments of protective shelters, 20: 39059
JOHNSON, Keith H., Multiple-scattering model for polyatomic molecules, 20: 39618
JOHNSON, R. G. R., Fabrication of fuel pellets from pot-process denitrated ThO_2 powder, 20: 39362 (WAPD-TM-577)
JOHNSTON, David R., EPR spectra of 1% Nd-doped $La_2(SO_4)_3 \cdot 9H_2O$ and $LaBr_3$, 20: 40312
JONES, Daniel T., Protection against fallout by core shelters in typical British house, 20: 39083
JONES, F. W., Magnetic-pulse forming process, 20: 40490 (Y-1483)
JONES, John A., Synthesis and characterization of 3-ketohexadecanoic acid-1-^{14}C, DL-3-hydroxyhexadecanoic acid-1-^{14}C, and trans-2-hexadecenoic acid-1-^{14}C, 20: 38987
JONES, K. C., Heat capacities of aqueous rare earth chloride solutions at 25°, 20: 38906
JONES, L. K., Clean assembly practices guide, 20: 40489 (SC-DC-66-1118)
JONES, L. V., Prog. rpt., 11/65, 20: 39320 (MLM-1311)
JONES, L. V., Prog. rpt., 12/65, 20: 39321 (MLM-1312)
JONES, Malcolm S. Jr., Magnetically induced ionization in rare gas mixtures, 20: 39679
JONES, P. R., Effect of π and Σ molecular states in Ne$^+$-Ne scattering, 20: 39601
JONES, R. G., Distribution of current in type-II superconductor, 20: 40029
JONES, S. L., Radionuclides in Clinch-Tennessee Rivers, 20: 40479 (ORNL-P-2328)
JONES, W. D., Varying plasma electron temperature in discharge tubes by simple auxiliary electrode, . 20: 40185
JONSSON, A., Multi-group collision probability theory in cluster geometry, 20: 40380
JOOS, P., Optical properties of strong-focusing magnet, 20: 39494 (LNF-66/15)
JORDAN, P., Simultaneous determination of ^{3}H and ^{14}C in proportional counters, 20: 38823
JOSEPHSON, E. S., Food preservation, 20: 39284 (DP-1066(Vol.1), pp IV.3-25)
JUNDI, Z., Positron scattering by H and adiabatic potential, 20: 39817
JUNGERMAN, J. A., Central region studies for incorporating an axial ion source in the Davis 76-inch cyclotron, 20: 39512
JUNOD, E., Isotopic analysis of ^{48}Ca by neutron activation, 20: 38850

K

KADENATSKI, B. M., Effects of ionizing radiation and other factors on rate of topochemical decomposition of various inorganic compounds, 20: 38955
KADNER, M., Bibliography on deposition of layers of Mo, W, Rh, 20: 39354 (BMwF-FBK-66-09)
KADOMTSEV, B. B., Instability of plasma on trapped particles, . 20: 40217
KADYKOV, B. I., Effect of vitamins and phosphatides on resistance to radiation, 20: 38721
KAEPPELER, H. J., Influence of non-equilibrium excitation on electron density in one-dimensional MFD channel flow, 20: 39714
KAGAN, Yu., Theory of electrical conductance of metals with nonmagnetic impurities, 20: 39395 (IAE-1028)
KAGAN, Yu. M., Probe measurements at intermediate and high pressures, 20: 39734
KAHN, Bernard, Performance characteristics of an electrogasdynamic power generator, 20: 39649
KAINDL, K., Analysis of the volatile constituents of irradiated apple juice, 20: 39300
KAINDL, Karl, Use of neutron activation analysis in determination of trace elements in tobacco mosaic virus, 20: 38846
KAJANTIE, Keijo, Introductory lectures on SU_6 symmetry, 20: 39862 (NP-16242)
KAJIURA, Toshihiro, Effects of collision on propagation of electromagnetic wave in a plasma. I., . 20: 40222
KALENDO, G. S., Effects of γ irradiation influence on synthesis and decay of RNA in HeLa cells, 20: 38683
KALINICHENKO, I. M., Cytological disturbances in appletree roots following irradiation of seeds, 20: 38692
KALININA, E. V., Mathematical model of accumulation and elimination of radioactive isotopes, 20: 38571
KALIS, Kh. E., Determining γ radiation of spherical source with cylindrical channel, 20: 38989
KALISZ, J., Determination of coincidence-circuit statistical parameters by means of point method, 20: 39205 (INR-703/III/PL)
KALISZ, Jozef, Influence of channel width of multichannel analyzer on spectrometer resolution, 20: 39204 (INR-694/III/PL)
KAMBOUROV, Christo, Comparison between methods for measurement of radioactive samples, 20: 38983 (SGAE-SS-3/1966)
KAMINSKII, V. A., Calculation of direct reaction ^{12}C(n,n′)^{12*}C (2+) by dispersion method, 20: 40104
KAMIYAMA, Hiroshi, Possible distribution of ion density in iono-exosphere with dipole magnetic field, 20: 39968
KANE, John V., Instrumentation for nuclear-structure analysis, 20: 39240
KANG, Kyungsik, Study of the ρ and B mesons in π-ω scattering, 20: 39807
KANNE, H., Theory of collision-free plasma column with regard to wall losses, . 20: 40230
KANTOR, Poul B., Application of partial-wave analyticity to nucleon-nucleon scattering, 20: 39799

KANTROWITZ, Arthur R., Magnetohydrodynamic power plant, 20: 39043
KANTROWITZ, Arthur, Model MHD type superconducting magnet, 20: 39733
KAO, K. C., Effect of radiation on electric conduction in n-hexane, 20: 38971
KAPLAN, R. W., Mixed clones of uv-induced mutants in kappa phage, 20: 38670
KAPLAN, S., Angle-space synthesis: an approach to transport approximations, 20: 40360 (WAPD-T-1890)
KAPLAN, Selig N., Polarization in proton-proton scatterings at 735 Mev, 20: 39789
KAPLIT, M., Models for electron emission from metals with adsorbed monolayers, 20: 39641
KAPTEIJN, Johanna C., Promethium-140, 20: 40131
KAPUSTSIK, A., Use of mica and quartz glass for nuclear fission detection at high temperature, 20: 39208 (JINR-P-2705)
KARALOVA, Z. K., Separation of ionium (^{230}Th) from U, Pa, Fe, Mn, and Eu by cation exchange, 20: 38834
KARAPETYANTS, M. Kh., Heat of formation of lanthanum selenites, 20: 38900
KARAPETYANTS, M. Kh., Heat of formation of praseodymium selenites, 20: 38901
KARASIK, V. R., Effect of microheterogeneity on characteristics of superconductivity of Nb–Zr–Ta alloy, 20: 40020
KAREEV, Yu. A., Quasi-one-dimensional movement of plasma in Hall-type MHD generator ducts, 20: 39735
KARELIN, O. N., Protective measures for medical personnel and patients during operation of superhighfrequency physiotherapy apparatus, 20: 38622
KARIBOV, Yu. I., X-ray therapy of carcinoma of stomach through lead grating, 20: 38763
KARLSSON, E., Magnetic moment of the lowest 2^+ vibrational state in ^{122}Te, 20: 40128
KARMANOVA, Z. P., Role of autoinfection in development of the hemorrhagic syndrome during acute radiation sickness, 20: 38656
KARMOHAPATRO, S. B., Ionization potential of Gd and Ho by surface ionization method, 20: 40203
KARPENKO, L. I., Spark method for spectrographic determination of rare earths in solutions, 20: 38832
KARPOV, V. L., Radiation chemistry of polypropylene, 20: 38945
KARPUKHIN, V. T., High-melting metal electrodes for MHD generators with non-equilibrium conductivity, 20: 39736
KARR, C., Estimation of the efficiency of inhomogeneous-flow MHD generator, 20: 39737
KARR, C., Evaluation of Rayleigh-Taylor instability and turbulent diffusion effects in inhomogeneous flow conversion, 20: 39704
KARYAGIN, S. V., Determination of local field parameters in Moessbauer hyperfine spectra, 20: 39615
KARZMARK, C. J., Notation and formulae for dose specification and calculations in radiotherapy, 20: 38750
KASABOV, G. A., Investigation of Hg–Cs plasma with non-equilibrium conductivity, 20: 39738
KASABOV, G. A., Spectroscopic investigation of Ar–Cs plasma, 20: 39722
KASH, S. W., Magnetic space shields, 20: 40292
KASHCHEEV, V. N., Information obtained with help of critical magnetic scattering of neutrons, 20: 40316
KASHKAROV, L. L., Regularities in angular distribution of neutrons emitted in polarized μ-meson capture by nuclei, 20: 40096
KASHLEV, Yu. A., Absorption of ultrasound in superconductors, 20: 40336
KASI, Servo, Neutron flux in hydrogenous medium round fast point source, 20: 40058
KASTNER, Jacob, LiF thermoluminescent response to fast neutrons, 20: 39219
KASTRUP, H. A., Method of determining electromagnetic form factors of nucleons by cosmic ray experiments, 20: 39781
KATO, H., High-energy-rate extrusion of low-density tungsten powder billets, 20: 39352 (BM-RI-6817)
KATOCH, D. S., Cesium-137 content of man in India, 20: 39154
KATSANOS, Nicholas A., Effects of isomeric transition and (n,γ) activation of Br atoms in n-propyl bromide, 20: 38963
KATULKINA, N. N., Transfusions of blood and leukocytes to gynecological cancer patients for prevention of leukopenia in radiation therapy, 20: 38768
KAULENAS, A. A., Thermal conductivity of heat-resisting high-alumina concretes, 20: 39698
KAWAMOTO, Setsuo, Neutron flux distribution and spectrum in Fe–water shields, 20: 40287
KAWASAKI, Shoji, Effect of whole body x-irradiation on swelling of rat liver mitochondria, 20: 38639
KAZACHEVSKAYA, T. V., Rocket data on behavior of electron concentration in ionosphere at heights of 100-300 km. I., 20: 39958
KAZAEVA, F. M., Changes in biochemical and physiological indicies in guinea pigs during internal chronic irradiation, 20: 38662
KAZARINOV, Yu. M., Phase-shift analysis of nucleon-nucleon scattering at 14.5 Mev, 20: 39756 (JINR-P-2742)
KAZARINOV, Yu. M., Pion production in np collisions at 600 Mev, 20: 39826
KEEFE, L., High-temperature regenerative air preheater for MHD power plants, 20: 39725
KEENAN, Thomas K., Lattice constants of 7:6 Na-actinide(IV) fluorides, 20: 38898
KEGELMANN, G., Concentration of radioactive substances in precipitation, 20: 39106 (BMwF-FBK-65-05)
KEIL, E., Lectures on beam optics, 20: 39483 (CERN-66-21)
KEIL, E., Radio-frequency separated beams, 20: 39486 (CERN-66-21, pp 43-54)
KEISCH, B., Neutron activation analysis studies of ^{129}I in the biosphere, 20: 38564
KELLER, R., High-frequency multimegawatt generator with amplitude and frequency modulation, 20: 40281
KELLERSHOHN, C., Determination of iodine by radioactivation analysis, 20: 38849
KELLEY, G. G., High-current ion-beam production and injection, 20: 40175 (ORNL-3989, pp 89-94)
KELLY, B. T., Dimensional changes in pyrolytic graphite under fast-neutron irradiation, 20: 39465
KELLY, B. T., Dimensional changes in polycrystalline graphites under fast-neutron irradiation, 20: 39466
KELLY, J. C., Focusons in potassium chloride, 20: 39600
KENNEDY, Peter, Improvements in or relating to production of spheroids, 20: 39376
KENNETT, Terence J., Instrumentation for gamma-ray spectroscopy, 20: 39243
KENNEY, J. F., Experimental evaluation of various rigidity models, 20: 39624 (D-1-82-0529)
KENNY, Peter J., Analysis of digital Anger camera with three-dimensional resolution for positron emitters, 20: 39181
KEPPEL, E., Observation of a (K $\pi\pi$) resonance near 1800 Mev, 20: 39788
KERNOHAN, R. H., Prog. rpt. on experimental simulation of large, high field, superconducting magnet operation, 12/65-7/66, 20: 40015 (ORNL-TM-1598)
KERR, G. D., Application of solid-state nuclear track detectors to Hurst threshold detector system, 20: 39221
KES, P. H., Enthalpy of impure niobium in mixed superconductive state, 20: 40036
KEVAN, Larry, Radiolysis of frozen solutions. VI., 20: 38950
KHAIT, M. M., Transfusions of blood and leukocytes to gynecological cancer patients for prevention of leukopenia in radiation therapy, 20: 38768
KHAN, I. A., Retardation of oxidation rates of Nb, Ta, and W by fluoride coating, 20: 39348
KHAN, M. Aslam, Rotational analysis of new absorption bands of SrH and SrD in ultra-violet region, 20: 40331
KHELASHVILI, A. A., Analytical properties and asymptotic behavior of multichannel, quasi-potential scattering amplitude, 20: 39905
KHIRSELI, E. M., Disintegrated wave interaction in magnetoactive plasma, 20: 40207
KHMELEVA, N. N., Accumulation of radioactive Sr, Y, and Ce isotopes by filamentous algae in presence of EDTA and dissolved organic compounds, 20: 38570
KHODZHAEV, L. Sh., Properties of cluster expansions of the causal S-matrix, 20: 39858 (JINR-P-2760)
KHOE, T., Superconducting plates as magnetic shields, 20: 39523
KHOLIN, V. V., Experimental data on thymus state during acute radiation syndrome, 20: 38685
KHOROZOV, S., The search for "long-lived" Λ^0-particles, 20: 39762 (JINR-P-2849)
KHOZE, V. A., Emission of two photons into given angle in electron collisions, 20: 39836
KHUSSAR, Yu. P., Changes in thymus during acute radiation sickness in animals, 20: 38720
KIBBE, L. J., Central region studies for incorporating an axial ion source in the Davis 76-inch cyclotron, 20: 39512
KIENLE, P., Magnetic fields at ^{119}Sn in rare earth metals, 20: 40322
KIKHTIN, V. V., Existence of certain baryon and meson unitary multiplets, 20: 39860 (JINR-P-2790)
KIM, H., Machine development at the Berkeley 88-inch cyclotron, 20: 39547
KIM, K. I., Electromagnetic phenomena in dense plasma with non-equilibrium electric conductivity in variable magnetic field, 20: 39739
KIM, K. I., Hall effect in low-temperature plasma in non-homogeneous magnetic field, 20: 39740
KIM, Sedong, Measurement of the N^{*-}-N^{*++} mass difference, 20: 39847
KIMBERLIN, Jerome, Determination by neutron activation of gallium and germanium in iron meteorites, 20: 38825
KING, C. Judson, Convective transfer processes in laminar gas-liquid channel flow, 20: 39050 (UCRL-16535)
KING, Paul A., Ionizing radiation of water solution of polyalkylene oxide

and product thereof, 20: 38976
KING, T. A., Diffusion of triplet excitons produced by ionizing radiation in aromatic materials, 20: 38957
KINGSTON, A. E., Classical electron ionization cross sections, 20: 39612
KIRBY, W. H., Preparation of sources for alpha spectrometry, 20: 38990
KIRILLIN, V. A., Operation of MHD generator plants, 20: 39741
KIRILLOV, P. L., Injection of liquid metals in MHD converters, 20: 39669
KIRILLOV, P. L., Measuring electrical conductivity of a liquid–vapor K mixture, 20: 39742
KIRIN, I. S., Formation of XeO_3 in β decay of ^{131}I, 20: 38984
KIRSCH, M., Decontamination vessels for contaminated sewage of ward for radioisotope patients taking idealized premises as base, 20: 38790
KISELEV, P. N., Role of autoinfection in development of the hemorrhagic syndrome during acute radiation sickness, 20: 38656
KISELEV, V. S., Formation of charged π mesons in collisions between 600-Mev neutrons and protons, 20: 39834
KISELEV, V. S., Spin correlation in elastic scattering of 605-Mev polarized protons on protons, 20: 39759 (JINR-P-2776)
KISHKOVSKII, A. N., Alterations in bronchio-pulmonary system and G-I tract during radiation sickness, 20: 38659
KISTENEV, E. P., Production of electron-positron pairs by high-energy gamma quanta, 20: 39594
KIVINIITTY, K., Exact measurement of gamma-ray doses in ureter, 20: 38778
KLADNITSKAYA, E. N., Inelastic π^-p-interactions at energy 7.5 Bev. II., 20: 39758 (JINR-P-2773)
KLAHR, Carl N., Method of flux separation in nuclear reactors and structure therefor, 20: 40368
KLAUBER, William A., Pregnancy complicated by carcinoma of the cervix, 20: 38759
KLEINERT, H., Tensor operators and mass formula in minimal extension of U_3 by charge conjugation, 20: 39916
KLEINPOPPEN, H., Remeasurement of the total cross section for excitation of hydrogen $2\,^2S_{1/2}$ state by electron impact, 20: 39608
KLEM, R. L., Energetics. III., 20: 40451
KLEMPARSKAYA, N. N., Autoflora as test of clinical study of immunological reactivity in radiation injuries, 20: 38644
KLEMPARSKAYA, N. N., Effect of novocaine on course of acute radiation sickness and immunogenesis, 20: 38727
KLENER, V., Internal contamination with ^{90}Sr and ^{226}Ra in man in relation to clinical findings, 20: 38623
KLEPFER, H. H., Prog. rpt. on specific Zr alloy design program, 4/66, 20: 39356 (GEAP-5134)
KLIMA, R., Motion of particles in non-resonant h-f and magnetic fields, 20: 40193
KLIMENKO, A. A., Hematopoietic changes in patients with malignant tumors following beam therapy, 20: 38766
KLIMKOVA, O. A., Radiation-stimulated emf in CsI crystals, 20: 40335
KLIMOVSKAYA, L. D., Mechanisms of disturbance of central regulation of automatic functions in irradiated animals, 20: 38654
KLINGEMAN, Peter Clayton, Transport of radionuclides in surface and estuarine waters, 20: 39121
KLINKENBERG, P. F. A., Structure of the spectrum of neutral Tb, Tb I, 20: 39604
KLOTZ, P., Mixed β-diketones, 20: 38855 (BNL-10350)
KLYZHUK, K. N., Effectiveness of bone marrow transplantation in relation to time of administration, 20: 38740
KNACKE, O., Reprocessing of nuclear fuels by fluoride volatilization with sulfur hexafluoride, 20: 40389
KNAPP, Harold, Intensity and distribution of initial and residual radiation, 20: 39056
KNAPP, Harold A., Targeting assumptions for attacks against populations, 20: 39087
KNELLWOLF, T., Reactions $^{40}Ca(n,\alpha)^{37}Ar$ and $^{19}F(n,\alpha)^{16}N$ with 6-Mev neutrons, 20: 40100
KNORR, G., Variation of adiabatic invariant of harmonic oscillator, 20: 40229
KNOTT, David Howard, Effect of irradiation on response of dog to standardized hemorrhagic stress, 20: 38703
KOBAYASHI, Keisuke, Neutron-diffusion parameters in water, 20: 40055
KOBAYASHI, Shigeru, Alterations in functional state of rat adrenal following the lethal and sub-lethal, whole-body x-irradiations, 20: 38638
KOCH, R. C., Neutron activation analysis studies of ^{129}I in the biosphere, 20: 38564
KOCHETOV, N. K., Radiation chemistry of carbohydrates. VII., 20: 38969
KOEHLER, H. S., Calculation of binding energy of ^{16}O nucleus, 20: 40119
KOEHLY, G., Determination of americium by controlled-potential coulometry, 20: 38854
KOENIG, K.-H., Simultaneous scintillation spectrometry of α and β rays by cesium iodide, 20: 39217
KOENIG, W., Decontamination vessels for contaminated sewage of ward for radioisotope patients taking idealized premises as base, 20: 38790
KOHARA, Hitoshi, Radiometric titration of trace amounts of cobalt using EDTA, 20: 38806
KOHARA, Hitoshi, Radioisotopic dilution analysis of trace amount of cobalt, 20: 38807
KOIDE, Minoru, Uranium-234/U-238 ratios in seawater, 20: 39133
KOIKE, Hiroyuki, Changes in blood lipids induced by roentgen irradiation, 20: 38652
KOIKE, Nobuyuki, Changes in blood lipids induced by roentgen irradiation, 20: 38652
KOJIMA, Chiyo, Preliminary experiment on ion cyclotron resonance of highly ionized plasma, 20: 40260
KOKES, R. J., Hydrogenation of ethylene and propylene over palladium hydride, 20: 38908
KOLB, G., Closed MHD-loop ARGAS, 20: 39680
KOLB, G., Layout data of homogeneous closed-cycle 300-Mw MHD generator, 20: 39681
KOLESNIKOVA, G. S., Cellular elements in parametrial and paracervical tissue during preoperative beam therapy of cervical carcinoma, 20: 38769
KOLGA, V. V., Development and prospects for application of meson factories, 20: 39534
KOLGA, V. V., Modified resonance extraction method from relativistic cyclotron, 20: 39520
KOLLATH, Klaus-Johannes, Hyperfine structure and quadrupole moment of ^{65}Cu, 20: 40137
KOLOMEETS, E. V., Solar-diurnal and semidiurnal variations of cosmic rays and their spectra as function of solar activity, 20: 39628
KOLOMIETS, V. M., Analytical properties of relativistic multichannel scattering amplitude, 20: 39911
KOLOS, W., Vibronic energy and dipole moment of HD, 20: 40310
KOLPIN, M. A., Dynamics of large inverse pinch, 20: 40250
KOLYZHENKOVA, V. V., Angular distribution of fast neutrons behind iron shielding, 20: 40286
KOMAROV, V. I., Measurements of half-life ratio of π^+ and π^- mesons, 20: 39760 (JINR-P-2802)
KONAKH, V. F., Investigation of Hg–Cs plasma with non-equilibrium conductivity, 20: 39738
KONDO, S., Photoreactivation of mutation to prototrophy in E. coli, 20: 38669
KONIN, A. D., Structure of Ar K-series during atomic capture of negative muons in pure gas and in mixture with H, 20: 39578 (JINR-P-2807)
KONNOV, B. A., Doses in organs and tissues of head in x-ray therapy of cancer of facial skin, 20: 38765
KONOPLEVA, R. F., Defects in silicon produced by irradiation with fast neutrons at 77°K, 20: 40334
KONSTANTINOV, L. V., Nuclear reactor oscillation-measuring device, 20: 40361
KONSTANTINOVIC, Stanimir, Synthesis of malathion labeled with ^{35}S or ^{32}P and dipterex-^{32}P, 20: 38931
KOPPE, H. W., Prog. rpt. on experimental simulation of large, high field, superconducting magnet operation, 12/65-7/66, 20: 40015 (ORNL-TM-1598)
KORDIS, J., Prog. rpt. on solid-state chemistry of rare earth oxides, annual, 1965–66, 20: 38861 (COO-1109-22)
KORENKOV, I. P., Choice of a dominant radiation in calculating the protection against electron accelerators, 20: 39160
KORENKOV, I. P., Dosage loads in medical staff dealing with colloidal ^{198}Au, 20: 39159
KORKISCH, J., Ion exchange separation of U and Th in mixed and non-aqueous solvents, 20: 38999 (TID-23229)
KORKISCH, Johann, Ion exchange in mixed and non-aqueous media, 20: 38818
KORMICKI, Jan, Large permanent magnet semicircular beta ray spectrograph, 20: 39203 (INP-476/PL)
KORMILITSIN, B. T., Theory of electromagnetic wave propagation in limited plasma, 20: 40206
KORMILITSYN, D. V., Behavior of impurities and admixtures during sintering of W, 20: 39363
KORNEV, I. I., Radium therapy of cancer of cardial region of stomach with 25-Mev betatron, 20: 38772
KOROES, Endre, Solvent effects in isotope exchange reactions. VI., 20: 38936
KOROLEV, G. K., Mathematical model of accumulation and elimination of radioactive isotopes, 20: 38571
KOROSIN, J., Flame photometric determination of Li, Na, K, Ca, Mg, and Sr in natural and mineral waters, 20: 38798 (NIJS-R-465)
KOS, E., Patterns of nucleic acid and protein synthesis during modification of lethal ultraviolet lesion, 20: 38562
KOS, E., Survival of uv-irradiated E. coli in presence of chloramphenicol and in absence of essential metabolite, 20: 38563
KOSCHMIEDER, H., Remeasurement of the total cross section for excitation of hydrogen $2\,^2S_{1/2}$ state by electron impact, 20: 39608
KOSHIKA, M., Irradiation flavor and the volatile components of beef, 20: 39299

KOSMOWSKI, A., Gaging and controlling of basis weight and thickness using radionuclides, 20: 39292
KOSTOMAROV, D. P., Flute instability in an uncompensated plasma, 20: 40195
KOTHARI, L. S., Persistent change in measured values of decay constant in Be, 20: 40376
KOTLYAREVSKII, D., The search for "long-lived" Λ^0-particles, 20: 39762 (JINR-P-2849)
KOTOV, A. G., Energy transfer mechanism in radiolysis of ammonia adsorbed on zeolites, 20: 38944
KOURIS, C. B., High-energy large-angle scattering by strongly singular complex potential, 20: 39777
KOVALEV, E., Radiation safety, 20: 38603 (AD-629422)
KOVALEVSKAYA, T. N., Transfusions of blood and leukocytes to gynecological cancer patients for prevention of leukopenia in radiation therapy, 20: 38768
KOWALSKI, S., Shell effects in high energy photoproton spectra from ^{6}Li, 20: 40077 (MIT-2098-256)
KOZACHOK, I. A., Steady state distribution of neutrons in infinite medium, 20: 40052
KOZLOV, V. F., Dosage loads in medical staff dealing with colloidal ^{198}Au, 20: 39159
KOZLOVA, A. V., Hematopoietic changes in patients with malignant tumors following beam therapy, 20: 38766
KOZLOVA, A. V., Immediate and remote reactions in beam therapy of cervical malignant neoplasms, 20: 38773
KOZLOWSKI, T., Open-cycle power generation experiment with high preheat temperature of air, 20: 39689
KOZLOWSKI, T., Operating experience of an open-cycle MHD test facility, 20: 39688
KRAMER, P., Beam properties of Philips' A.V.F. cyclotrons, 20: 39516
KRAMER, P., Extraction studies in an AVF cyclotron, 20: 39518
KRAMER, P., Reaction ^{27}Al(p,α)^{24}Mg studies with a 30-Mev AVF cyclotron, 20: 40101
KRANTZ, Frank M., Structure for atomic blast resistance, 20: 39053
KRANYS, M., Postulate of relaxation of nonstationary processes caused by finite transport velocity of interaction in matter, 20: 39475
KRASNYKH, I. G., Mechanism of radioprotective action of indolylalkylamines, 20: 38725
KRAUSE, M. O., Atomic and molecular cross sections, 20: 39580 (ORNL-3989, pp 78-88)
KREPS, R. E., Asymptotic behavior of inelasticity parameter, 20: 39884
KRESHKOV, A. P., Analysis of alloys of rare earth elements with magnesium in nonaqueous solutions, 20: 38830
KRETCHMAR. A. L., Shift in relative distribution of body nitrogen between skin and carcass in mouse radiation chimeras, 20: 38636
KRETZSCHMAR, Robert M., Isotope placental localization, 20: 38757
KRIEGEL, W. Wurth, Materials science research. Vol. 3, 20: 39338
KRILL, Arthur M., Influence of a curved duct on explosive-driven MHD converters, 20: 39694
KRIPYAKEVICH, P. I., Crystal structure of $EuNi_5$, $TmNi_5$, and $LuNi_5$ compounds, 20: 39415
KRIPYAKEVICH, P. I., New rare earth compounds with zinc and their crystal structure, 20: 39417
KRISHNA Prasad, N. S., Stability constants of lanthanide phthalates from potentiometric data, 20: 38896
KRISHNAMURTHY, M., Stability constants of lanthanide phthalates from potentiometric data, 20: 38896
KRIVENTSOVA, A. G., Identification of charged particles by ionization and δ-electrons in a propane bubble chamber, 20: 39211 (JINR-P-2842)
KRIVY, I., Vaporization of actinides and their compounds. I., 20: 38876 (UJV-1598)
KROHN, V. E., Measurement of electron-neutron interaction by asymmetrical scattering of thermal neutrons by noble gases, 20: 40129
KROKOWSKI, Ernst, Radiogenic radiation protection effect, 20: 38696
KROPP, L., Novel deflection-bunching system at the Karlsruhe isochronous cyclotron, 20: 39546
KROTKOV, R. V., Polarized negative ions produced by charge exchange process, 20: 39584
KROTOVA, L. V., Determination of Pr, Nd, Ho, and Er in fluorite monocrystals, 20: 38829
KROUSE, H. R., Oxygen-18/oxygen-16 in snow and ice of the Hubbard and Kaskawulsh Glaciers, 20: 39123
KROUSE, H. R., Tellurium isotope fractionation study, 20: 39122
KRUGER, P. Gerald, Magnetic fields in superconducting quadrupole lens, 20: 39479 (BNL-10495)
KRUGLOV, S. P., Determination of quantometer constant at 650 Mev, 20: 39248
KRUMHANSL, J. A., Thermal conductivity, second sound, and phonon hydrodynamic phenomena in nonmetallic crystals, 20: 40327
KRUSKAL, Martin D., Exact invariants for class of nonlinear wave equations, 20: 40005
KUCHEROV, R. Ya., Stability of nonhomogeneous electron beam, 20: 40245
KUCHIN, I. A., Suppression of large transfers in peripheral interactions as effect of nucleon diffuseness, 20: 39820
KUCHNIR, Moyses, Ion mobility in liquid ^{3}He below 1°K, 20: 40012 (COO-1198-364)
KUCK, George A., Charged particle fluxes in inner Van Allen belt prior to 7/9/62 high-altitude nuclear test, 20: 39992
KUCKES, A. F., Electron cyclotron harmonic radiation from a plasma, 20: 40274
KUCZYNSKI, G. C., Effect of interfaces on radiation production of color in alkali halides, 20: 40317
KUDRYASHOV, L. I., Radiation chemistry of carbohydrates. VII., 20: 38969
KUENZLY, J. D., Chemical integrity of radioisotope containment materials in launch abort environments, 20: 39312 (SC-CR-66-2044)
KULCINSKI, Gerald L., Combined effect of ultrahigh pressure and nuclear irradiation on solid-solid phase transformations, 20: 40306
KULIKOVSKII, A. G., Stability of homogeneous states, 20: 40221
KULLANDER, S., Proposal for sector-focusing synchrocyclotron, 20: 39535
KULLANDER, S., Regenerative beam extraction in synchrocyclotrons, 20: 39522
KULTASHEV, O. K., Work function of W–Hf, Ta–Hf, Nb–Hf, Re–Zr, and W–Re alloys, 20: 40297
KULYUKIN, M. M., Accumulation of particles in a 680-Mev synchrocyclotron, 20: 39492 (JINR-P-2811)
KULYUKIN, M. M., Recording of particle paths in streamer high-pressure chamber filled with helium, 20: 39245
KUMAGAI, Michikazu, Formation of hydrogen negative ions in mercury vapor, 20: 39500
KUMAR, Arvind, Decoupling of a multichannel problem in static model, 20: 39887
KUMAR, Sushil, Post-irradiation centrifugation and radiation-induced chromosome aberrations in barley, 20: 38618
KUMOK, V. N., Complexes of La, Y, Lu, and Sc with xylenol orange, 20: 38924
KUNAISH, Hassan H., Consistent P-3 theory of neutron wave propagation, 20: 40064
KUNIN, V. N., Electron conductivity of thermoionized gas in electric field, 20: 40238
KUNKEL, W. P., Fission-product retention in Na, 20: 40357 (NAA-SR-11766)
KURATA, Sueno, Study on Co phase composition contained in WC–Co base cemented carbides, 20: 39427
KURBATOVSKII, Yu. N., Results of experiments with 100-kw MHD generator model, 20: 39672
KURGANOV, G. B., Effect of microheterogeneity on characteristics of superconductivity of Nb–Zr–Ta alloy, 20: 40020
KURODA, P. K., Cosmic ray produced phosphorus isotopes in atmosphere, 20: 39991
KURODA, Tsutomu, Preliminary experiment on ion cyclotron resonance of highly ionized plasma, 20: 40260
KURSHAKOV, N. A., Correlation of local tissue changes and general reactions at different stages of acute radiation sickness in man, 20: 38774
KUSHAKOVSKII, M. S., Evaluation of models for initial selection of radioprotective compounds, 20: 38729
KUSHWAKE, Ram S., Electron and ion temperature in solar corona, 20: 39572
KUZHEVSKII, B. M., Generation of deuterium nuclei in cosmic rays, 20: 39825
KUZIN, A. M., Effects of γ irradiation influence on synthesis and decay of RNA in HeLa cells, 20: 38683
KUZIN, A. M., Role of toxins in radiation-induced cell injury, 20: 38664
KUZ'MA, Yu. B., Crystal structure of compounds $Zr_2Ni_{21}B_6$ and $Zr_6Co_{21}B_6$, 20: 39416
KUZ'MA, Yu. B., New rare earth compounds with zinc and their crystal structure, 20: 39417
KUZNETSOV, B. G., What is an elementary particle?, 20: 39918
KUZNETSOV, V. I., Changes in blood vessels during acute radiation sickness, 20: 38658
KUZNETSOV, Yu. E., Solution of equations for regular electrostatic beam, 20: 40242
KUZNETSOVA, E. S., Inelastic π^- p-interactions at energy 7.5 Bev. II., 20: 39758 (JINR-P-2773)
KUZNETSOVA, V. N., Corrosion resistance of reactor materials, 20: 39349
KVARATSKHELIA, N. T., Movement of ^{90}Sr in Georgian soils, 20: 39117
KWIECINSKI, Jan, Equal time commutators and scalar mesons decays, 20: 39852 (INP-480/PL)
KWIECINSKI, Stanislaw, Choice of optimum shape of neutron howitzer for neutron absorption methods, 20: 40057
KYUNEL, A., Approximate calculation of nearest poles of functions S_f and Δ_f in case of strong $\psi\psi\phi$ coupling, 20: 39859 (JINR-P-2761)

L

LA BAHN, R. W., Comparison of approximate polarization potentials, 20: 39621

LACROIX, R., Center (V_k) in $SrCl_2$ crystals, 20: 40319

LACROIX, R., EPR of a center in Y^{3+} doped artificial CaF_2 crystals, 20: 40321

LADANYI, Laszlo, Solvent effects in isotope exchange reactions. VI., 20: 38936

LAFOUCRIERE, J., Diagrammatic representation and utilization of rotation matrices, 20: 40120

LAGERQUIST, R., Prototype thermoluminescent dosimetry system for personnel monitoring, 20: 39224

LAHR, Thomas N., Auto-canning of radiation sources, 20: 39371

LAKH, V. I., Crystal structure of compounds $Zr_2Ni_{21}B_6$ and $Zr_6Co_{21}B_6$, 20: 39416

LAKOS, J., Influence of x-irradiation on course of adrenalin-lymphocytosis, 20: 38678

LAMB, E., Large scale processing and source preparation of neutron-produced isotopes, 20: 39316 (DP-1066(Vol.1), pp II.3-14)

LAMBERT, M., Compton effect on bound K electrons, 20: 39773

LAMIC, Jacques, System As_2O_5–ThO_2, 20: 38885

LAND, David J., Study of the ρ and B mesons in π-ω scattering, 20: 39807

LANG, Gerard, Preparation and properties of the double salt $2Th(C_2O_4)_2 \cdot (NH_4)_2C_2O_4 \cdot 7H_2O$, 20: 38886

LANG, J., Compton effect on bound K electrons, 20: 39773

LANGE, Robert C., Analytical chemistry of polonium, 20: 38822

LANGE, W. J., Prog. rpt. on ultrahigh vacuum techniques, semiannual, 12/65–5/66, 20: 39098 (WERL-2823-21)

LANGENBERG, D. N., "Non-Josephson" radiation from Josephson tunnel junctions, 20: 40028

LANGLEY, R. A., Atomic and molecular cross sections, 20: 39580 (ORNL-3989, pp 78-88)

LANGLEY, Robert A., Instrument for varying angle of incidence between ion beams and spectrometer, 20: 39029

LANZA, F., Obtaining an impermeable graphite by impregnation with molten metals, 20: 39355 (EUR-2988.f)

LAPERASHVILI, L. V., SU(6) symmetry and correlations between cross sections of meson-baryon processes, 20: 39904

LA PORTE, M., Estimation of the efficiency of inhomogeneous-flow MHD generator, 20: 39737

LAPOSTOLLE, P., Introduction to the study of linear accelerators, 20: 39482 (CERN-66-20)

LARANJEIRA, M. F., Temperature assignment to thermal diffusion factor, 20: 39326

LASCAR, G., Space charge electric field of an electron beam injected in decreasing magnetic field, 20: 40269

LASER, M., Reprocessing of nuclear fuels by fluoride volatilization with sulfur hexafluoride, 20: 40389

LASHKAREV, G. V., Selenides and tellurides of rare earth metals and actinides, 20: 38927

LASHKARYEV, G. V., Zonal structure of chalcogenides of rare-earth elements, 20: 40339

LATHAM, W. N., Large experimental superconducting magnet for MHD power generation, 20: 39643

LAUGHLIN, John S., Analysis of digital Anger camera with three-dimensional resolution for positron emitters, 20: 39181

LAURENCE, James C., Superconducting magnetic bottle for plasma physics experiments, 20: 40169 (NASA-TN-D-3595)

LAUTER, E. A., Space and time variations of long wave ionospheric absorption at small solar heights and at night, 20: 39960

LAUTER, E. A., Survey of A3: absorption measurements at low and medium frequencies, 20: 39952

LAUTRUP, B., Two-baryon approximation to decay of neutral pseudoscalar mesons, 20: 39783

LAVERLOCHERE, J., Isotopic analysis of ^{48}Ca by neutron activation, 20: 38850

LAVERLOCHERE, J., Radioactivation analysis by means of 14-Mev neutrons, 20: 38840

LAVOLLEE, Philippe, Study of isomers ^{236g}Np and ^{236m}Np by interaction of deuterons with ^{238}U, 20: 40092

LAVRENT'EVA, G. M., Accumulation of radioactive Sr, Y, and Ce isotopes by filamentous algae in presence of EDTA and dissolved organic compounds, 20: 38570

LAWRENCE, C. H., Removal of low-level radioisotopes from wastewater by aerobic treatment, 20: 40483

LAZAREVA, L. S., Europium and gadolinium hydroxides and products of their thermal decomposition, 20: 38923

LAZARUS, A. J., Preliminary results from the Pioneer 6 M.I.T. plasma experiment, 20: 40212

LAZZARINI, E., Szilard-Chalmers recoil of ^{60}Co and ^{60m}Co, 20: 38962

LEADER, Elliot, General analysis of nucleon-nucleon scattering, 20: 39806

LEARY, J. A., Thermodynamic properties of plutonium mononitride from electromotive force measurements, 20: 38911

LE BAIL, R., Diffusion process in toroidal discharge, 20: 40180 (SU-IPR-69)

LEBEDEV, I. A., Complexing of trivalent actinides and lanthanides in phosphoric acid solutions, 20: 38878 (ORNL-tr-1257)

LEBEDEVA, D. A., Substantiation of peroral ingestion of radon water in alpha therapy, 20: 38776

LEBEDEVA, G. A., Liver cirrhosis development under influence of radioactive cerium, 20: 38567

LEBEDEVA, M. A., Effect of vitamins and phosphatides on resistance to radiation, 20: 38721

LEBEDINSKII, A. V., Pathogenesis, experimental prophylaxis and therapy of radiation injuries, 20: 38718

LE BLANC, M. A. R., Faraday unipolar induction in a nonideal type II superconductor, 20: 40016

LECKY, James A., Catalog of nuclear reactor concepts, Pt. I, Sect. VI, 20: 40353 (ANL-7228)

LECROART, H., Evaluation of Rayleigh-Taylor instability and turbulent diffusion effects in inhomogeneous flow conversion, 20: 39704

LEDINGHAM, K. W. D., Comparison of allowed M/L orbital electron capture ratios with theory, 20: 40153

LEE, D. H., Burnout in a channel with non-uniform circumferential heat flux, 20: 39046 (AEEW-R-477)

LEE, D. I., Viscosity of Cs up to 5 bars and 1000°C, 20: 39392 (CU-2660-29)

LEE, E., GADOSE and DOSET: programs to calculate environmental consequences of radioactivity release, 20: 39148 (GA-6511)

LEE, H. S., Criteria for design of advanced dynamic power generating systems, 20: 40452

LEE, T. D., Reciprocity relations in photopion reactions, 20: 39810

LEE, T. D., Space inversion, time reversal, and other discrete symmetries in local field theories, 20: 39891

LEE, W. R., Partial-body radiation of queen honeybees, 20: 38631

LEEDY, R., Test evaluation of SNAP-15A generator, 20: 39310 (GA-5781)

LEESON, Jeffrey Sanford, Chemical effects of lead ions on positronium, 20: 38860 (COO-1297-6)

LEE-WHITING, G. E., Improved beta-spectrometers, 20: 39235

LEE-WHITING, G. E., Proposed electrostatic correction of the Chalk River $\pi\sqrt{2}$ beta spectrometer, 20: 39236

LEFEVRE, H., Myometrial blood flow in pregnancy measured with xenon, 20: 38747

LEFEVRE, J., ELAN: installation for recovery and packaging of ^{137}Cs in France, 20: 39319 (DP-1066(Vol. 2), pp II.33-44)

LE FLEM, Gilles, System As_2O_5–ThO_2, 20: 38885

LEGAR, F., Momentum spectra of secondary particles in (π^-,N) interactions at 7 Bev, 20: 39751 (JINR-E-2738)

LEGAR, F., Phase-shift analysis of nucleon-nucleon scattering at 14.5 Mev, 20: 39756 (JINR-P-2742)

LEGAR, F., Polarization tensor in scattering of polarized nucleons on polarized proton target, 20: 39909

LE GARDEUR, R., Confinement and heating of a plasma by low-frequency rotating magnetic field, 20: 40279

LE GARDEUR, R., Mixed-field configuration without leaks, 20: 40280

LE GARDEUR, R., Production of an intense h-f field by injection of an energetic electron beam into resonating structure, 20: 40282

LEHAR, F., Planning of n-p scattering experiments above pion-production threshold, 20: 39752 (JINR-E-2765)

LEHMANN, P., Charged pion photoproduction on light nuclei, 20: 40075 (LNF-66/30)

LEIBOWITZ, Howard M., Antibody production in corneal hypersensitivity, 20: 38608

LEIGHTY, Robert D., Snow density profiling by nuclear means, 20: 39130

LEIKIN, E. M., Determination of quantometer constant at 650 Mev, 20: 39248

LEINHARDT, T. E., Superconducting critical field measurements in Ce-doped lead between 4.1°K and 1.8°K, 20: 40050

LEITTEN, C. F. Jr., Forming method for curved ATR fuel plates, 20: 39358 (ORNL-3983)

LELONG, Claude, $\beta \rightarrow \alpha$ isothermal transformation in pure and weakly alloyed U, 20: 39388 (CEA-R-2956)

LEMAIRE, J., Evaporative and hydrodynamical atmospheric models, 20: 39556

LEMAIRE, R., Magnetic study of the intermetallic compound $NdCo_5$, 20: 39424

LEMARD, A., One-dimensional impenetrable bosons in thermal equilibrium, 20: 39474

LENIHAN, J. M. A., Trace elements in human disease, 20: 38847

LENNOX, David H., Power Reactor Technology. Vol. 9, No. 2, 20: 40426

LENNOX, David H., Power Reactor Technology, Vol. 9, No. 1, 20: 40430

LEONARD, L., Cold reduction as a means of reducing embrittlement of a cobalt-base alloy (L-605), 20: 39399 (NASA-TN-D-3528)

LEONOVA, V. G., X-irradiation effects on cytochrome systems of yeast

organisms, 20: 38680
LEPORE, R., Design and performance of Garigliano nuclear power plant, 20: 40418
LEPPER, Richard, Analogue studies of magnetic shields, 20: 40291
LEROY, J., Acceleration of plasma by field of progressive wave damped in vicinity of electron or ion cyclotron resonance, 20: 40267
LEROY, J., Three modes of energy transfer of a plasma h-f field, 20: 40261
LE SAGE, L., Measurement of infinite dilution capture resonance integrals with Moxon-Rae detector, 20: 40146
LESHCHENKO, S. S., Radiation chemistry of polypropylene, 20: 38945
LE THOMAS, M., Ceramic materials for magnetoaerodynamic conversion duct electrodes, 20: 39708
LEUSHKINA, G. V., Determination of dysprosium in samples of yttrium oxide and ferrite garnets by radioactivation method, 20: 38833
LEUTZ, Hermann, Fireproof shelters with secured ventilating systems, 20: 39066
LEUTZ, Hermann, Possibilities of occurrence of area conflagrations and firestorms with respect to fuel density, 20: 39057
LEVESQUE, R. J. A., Monte-Carlo calculation of intrinsic double-escape peak efficiency of cylindrical Li-drift Ge gamma rays detectors, 20: 39271
LEVI, H. W., Exchange adsorption of cations on $TiO_2 \cdot aq$, 20: 39002
LEVIN, I. S., Use of alkyl phosphoric acids in analytical chemistry. IV., 20: 38828
LEVINE, M., Engineering problems in pulsed neutron sources, 20: 40456 (BNL-10454)
LEVINE, Samuel H., Analogue studies of magnetic shields, 20: 40291
LEVINSON, Warren Edward, Radiation studies of large RNA viruses and chick embryo cells, 20: 38707
LEVIS, F., Effect of cysteamine on ultrastructural modifications of liver of rabbits exposed to whole-body x irradiation, 20: 38716
LEZHNEVA, A. V., Relationship between E_s and the F region of the ionosphere, 20: 39966
LIBINZON, R. E., Mechanism of inhibition of nucleic acid synthesis in irradiated animals, 20: 38585
LIBMAN, G., Requirements on the optical units of stereoscopic cameras used in bubble chambers, 20: 39209 (JINR-P-2728)
LIN, R. P., Evidence for connection of geomagnetic tail lines to interplanetary field, 20: 39986
LIN, Tsing Ko, Enrichment of ^{64}Cu by the Szilard-Chalmers process, 20: 38988
LIN, W. C., Electron spin resonance spectrum and electronic structure of PO_3^{2-} radical in irradiated crystal of ammonium fluorophosphate, 20: 38949
LINCOLN, J. Virginia, Geomagnetic and solar data, 20: 39979
LINDBAECK, S., Regenerative beam extraction in synchrocyclotrons, 20: 39522
LINDEMAN, H., Plateau of a GM counter at higher intensities, 20: 39244
LINDLEY, B. C., CNEN He–Cs blow-down MPD facility and experiments with prototype duct, 20: 39675
LINDLEY, B. C., Further development, operation, and experiments with IRD closed-cycle MPD loop, 20: 39687
LINER, Robert Thayer Jr., Time-dependent neutron-diffusion theory of plane heterogeneous systems, 20: 40059
LINGENFELTER, R. E., Galactic cosmic-ray electrons, 20: 39630
LINHARDT, H. D., Prog. rpt. on organic Rankine cycle feasibility demonstration, 4–6/66, 20: 40449 (SAN-650-1)
LINIECKI, J., High-strontium diet and radiostrontium retention in rats, 20: 38566
LINQUETTE, M., Treatment of Basedow's disease with radioactive iodine, 20: 38760
LINSON, Lewis M., Growth of fluctuations in collisionless plasma subjected to electric field, 20: 40179 (SU-IPR-49)
LIPEROVSKII, V. A., Nonlinear wave interaction in plasma in presence of intensive transverse waves, 20: 40205
LIPEROVSKII, V. A., Nonlinear conversion of electromagnetic waves to ion-acoustic plasma oscillation, 20: 40244
LIPINSKI, Stanislaw, Method of assaying ^{36}Cl in studies on kinetics of Cl metabolism in body, 20: 38550
LIPKAN, N. F., Radiation biology and biochemistry, 20: 38544
LIPKIN, H. J., Current algebras and matrix elements of axial-vector current, 20: 39892
LIPNIK, P., Single-particle matrix elements jj-coupling for first-forbidden beta transitions, 20: 40124
LIPSKI, Slawomir, Method of assaying ^{36}Cl in studies on kinetics of Cl metabolism in body, 20: 38550
LISITSYA, M. P., Infrared spectrum of neutron-irradiated silicon, 20: 40340
LISKOVICH, V. A., Behavior of impurities and admixtures during sintering of W, 20: 39363
LIST, D., Trajectories in studies of interactions of h-f fields with plasma, 20: 40283
LISZKA, Ludwik, Scintillation-rate spectrum observed in auroral zone, 20: 39954
LITUNOVSKII, R., Central region of 240 cm variable energy cyclotron, 20: 39513
LITUNOVSKII, R., Experiments on ion acceleration at 685-mm sector cyclotron, 20: 39549
LITUNOVSKII, R. N., Ion optical studies of extraction transport and analysis systems for 240 cm cyclotron, 20: 39545
LITVAK, M. M., Spectroscopic studies of laser-produced hydrogen plasma, 20: 40251
LITVINA, N. M., Transfusions of blood and leukocytes to gynecological cancer patients for prevention of leukopenia in radiation therapy, 20: 38768
LIU, C. H., Gradient instabilities as possible causes of irregularities in ionosphere, 20: 39993
LIU, Lien-sou, Assignments of baryon resonances in SU(12) and their strong decays, 20: 39907
LIUZZO, Joseph A., Prog. rpt. on radiation pasteurization of shrimp and oysters, final, 1–12/65, 20: 39288 (ORO-636)
LIVINGSTON, J. D., Ferromagnetic particles in type-II superconductor, 20: 40024
LLOYD, James Elgie, Improvements in or relating to coating with beryllia, 20: 39370
LO, Shui-yin, Meson production from electron-positron annihilation, 20: 39802
LOBANOV, E. M., Determination of dysprosium in samples of yttrium oxide and ferrite garnets by radioactivation method, 20: 38833
LOBODZIEC, W., Comparison of theoretical and experimental investigations of influence of bone on depth dose distribution in irradiated medium, 20: 38791
LOCKNEY, Eric Victor, Improvements in or relating to support arrangements, 20: 40365
LOEBNER, K. E. G., Half-life of the 453.08 kev level in ^{183}W, 20: 40123
LOESEL, M., Novel deflection-bunching system at the Karlsruhe isochronous cyclotron, 20: 39546
LOEVINGER, R., Notation and formulae for dose specification and calculations in radiotherapy, 20: 38750
LOFERSKI, J. J., Low-energy proton bombardment of GaAs and Si solar cells, 20: 40299
LOMAN, E. L., Kaon-nucleon scattering and threshold K* production, 20: 39778
LOMER, P. D., High-output neutron tube for activation analysis, 20: 38839
LONG, D. M., Prog. rpt. on radiation effects on integrated circuits, 1–3/66, 20: 39273 (AD-635198)
LOONEY, W. B., Variation radiation dose and its relationship to depression of DNA synthesis, 20: 38576 (TID-22103)
LOPANTSEVA, G. B., Analogy between a high-density plasma and metal-ammonia solutions, 20: 39656
LOPATIN, I. V., Determination of quantometer constant at 650 Mev, 20: 39248
LORD, R. S., Operating characteristics of ORIC beam extraction system, 20: 39521
LOSKA, Ludwik, Choice of optimum shape of neutron howitzer for neutron absorption methods, 20: 40057
LOSTY, Howard Harold Walter, Improvements in or relating to production of carbon tubes, 20: 39369
LOTHROP, Fred H. G., Prog. rpt. on bevatron operation and development, 1/3/66, 20: 39498 (UCRL-16809)
LOVE, Gordon R., Near-surface effects in superconducting Nb–Zr alloys, 20: 40023
LOVELACE, C., New evidence for sigma meson, 20: 39782
LOWELL, A. F., World's U resources, 20: 39145
LOZHKINA, V. G., Cytological disturbances in appletree roots following irradiation of seeds, 20: 38692
LUBAS, B., Comparison of theoretical and experimental investigations of influence of bone on depth dose distribution in irradiated medium, 20: 38791
LUCAS, Jacques, Sulfides and oxysulfides of uranium and potassium, 20: 38891
LUDDY, Charles T., Alternator for the SNAP 8 program, 20: 40453
LUDEWIG, Hans, Geometrical effects on resonance absorption of neutrons, 20: 40062
LUEDERS, Gerhart, de Gennes correlation functions in theory of superconductivity, 20: 40038
LUKASH, N. I., Preparations conducive to removal of radioactive isotopes from an organism, 20: 38733
LUKSTYN'SH, Yu., Test of CP-invariance in $K_S^0 \to 3\pi$ decays in correlation experiments with $K^0\bar{K}^0$ pairs, 20: 39763 (JINR-P-2850)
LUKSTYN'SH, Yu., The search for "long-lived" Λ^0-particles, 20: 39762 (JINR-P-2849)
LUMBA, Linda G., Preparation of high specific activity ^{51}Cr, 20: 38982 (PAEC(D)IS-652)
LUNDY, Arvid, Analysis of digital Anger camera with three-dimensional resolution for positron emitters, 20: 39181

LUNELLI, Bruno, Improved method of H isotopic exchange with deuterium sulfate, and preparation of 9,10-anthraquinone-d_8, 20: 38889
LUSCHER, Ulrich, Footings for protective structures, 20: 39068
LUST, L. F., Sulfur determination supporting waste solidification program, 20: 38795 (BNWL-265)
LUSTMAN, B., Fuel clad design basis for thermal reactors, 20: 40387 (WAPD-T-1939)
LUTZ, H. O., Determination of interatomic potentials and stopping powers from channeled-ion energy-loss spectra, 20: 39602
LUUKKO, A., Resonances in the $^{41}K(p,\gamma)^{42}Ca$ reaction at proton energies 1740–2170 kev, 20: 40133
LYAPIDEVSKII, V. K., Determination of tracer deposition depth by method involving simultaneous measurement of two values, 20: 38770
LYASHCHENKO, A. B., Young's modulus of carbides of some transition metals, 20: 39430
LYASKIN, Yu. G., Calculation of efficiency of radiation-chemical apparatus with plane beta sources, 20: 38943
LYKOUREZOS, A. P., Simultaneous determination of ^{3}H and ^{14}C in proportional counters, 20: 38823
LYMAN, F. A., Electron distribution function and state populations in non-equilibrium MHD plasmas, 20: 39711
LYON, W. L., Solid-liquid phase diagram for the UO_2–PuO_2 system, 20: 39393 (GEAP-4878)
LYONS, M. F., Mechanical property changes in Zircaloy-2, Inconel and Incoloy from neutrons, 20: 39457 (GEAP-5100-9)
LYONS, M. F., Uranium oxide powder and pellet thermal conductivity during irradiation, 20: 39456 (GEAP-5100-1)
LYSGAARD, H., Myometrial blood flow in pregnancy measured with xenon, 20: 38747
LYUBOSHITS, V. L., Possible experiments checking isotopic structure of electromagnetic interactions, 20: 39824

M

MA, Chung-chi, Assignments of baryon resonances in SU(12) and their strong decays, 20: 39907
MABBOUX, Claude, Sidereal variation of cosmic muon component at 440-m depth, 20: 39626
MAC DONALD, A. R., Procedure for minimizing personnel hazards while changing tritium targets in accelerators, 20: 39476 (AD-636185)
MAC DOUGALL, J. D., Conversion and fast fission ratios in AGR cluster, 20: 40399 (AEEW-M-654)
MACH, P., Contribution to question of breed-specific radiosensitivity, 20: 38677
MACK, G., Method of determining electromagnetic form factors of nucleons by cosmic ray experiments, 20: 39781
MACK, R. J., GADOSE and DOSET: programs to calculate environmental consequences of radioactivity release, 20: 39148 (GA-6511)
MACKE, W., Statistical treatment of finite nuclei, 20: 40115
MACKENZIE, I. K., Use of Ge(Li) detectors in γ-γ coincidence experiments, 20: 39197 (AECL-2565)
MAC LEAN, Margaret A., Carcinoma of the cervix, 20: 38751
MACPHERSON, D. S., Oxygen-18/oxygen-16 in snow and ice of the Hubbard and Kaskawulsh Glaciers, 20: 39123
MADONIA, G., Radiotherapy of carcinoma of uterine neck, 20: 38786
MADSHUS, K., Diminution of radiocesium body-burden in dogs and human beings by Prussian Blue, 20: 38557
MADUEV, V. L., Radiometric equipment on the Cosmos 41 satellite, 20: 39171
MAELAND, A., H–Pd system, 20: 39428
MAGGI, G., Changes in antiinsulin antibodies subjected to radioactivity, 20: 38579
MAGNIER, Pierre, Influence of O, N, and C on lattice parameter of uranium monocarbide, 20: 39385 (CEA-R-2852)
MAIER, A. I., Heat of formation of lanthanum selenites, 20: 38900
MAIER, A. I., Heat of formation of praseodymium selenites, 20: 38901
MAIER, E. J. R., Low-energy electrons measured on IMP 2, 20: 39978
MAIER, Ludwig, Organic phosphorus compounds. XXVI., 20: 38895
MAILLARD, R., New injection method for cyclotrons, 20: 39530
MAIOROVA, N. F., Investigation of reflectory stimulation of solar plexus ganglions following x irradiation, 20: 38687
MAJOR, J. H., Plunging magnet system for the NIMROD extracted proton beam, 20: 39496 (RHEL-R-117)
MAJUMDAR, N. K., Probe data of duoplasmatron plasma, 20: 40202
MAKAROVA, I. A., Transfusions of blood and leukocytes to gynecological cancer patients for prevention of leukopenia in radiation therapy, 20: 38768
MALAY, Frank L., Nuclear reactor containment system, 20: 40372
MALCOLM, D. H., Prospect for electrogasdynamic power, 20: 39648
MALITSON, Irving H., Radiation-induced instability in refractive properties of some optical glasses, 20: 39468
MALLORY, M. L., Phase space density studies on cyclotron ion sources, 20: 39528
MALMBERG, P. R., Collisional excitation of atomic spectra in accelerated beams of light elements, 20: 39593
MALPLAT, J., Evaluation of Rayleigh-Taylor instability and turbulent diffusion effects in inhomogeneous flow conversion, 20: 39704
MALTSEV, V. N., Characteristics of reaction to bacterial antigens after irradiation, 20: 38641
MALYSHEVA, M. S., Correlation of local tissue changes and general reactions at different stages of acute radiation sickness in man, 20: 38774
MAMURO, Tetsuo, Alpha activity of highly radioactive fallout particles, 20: 39109
MAMURO, Tetsuo, Observation of fallout around the laboratory, 20: 39108
MAMURO, Tetsuo, X-ray microanalysis of fallout from first Chinese nuclear explosion, 20: 39110
MANCHESTER, R. N., Propagation of Pc 1 micropulsations from high to low latitudes, 20: 39977
MANCUSO, Richard V., Nuclear energy-level structures of ^{117}In, ^{117}Sn and ^{143}Pr, 20: 40159
MANDEL, H., Use of nuclear power stations in electricity grid, 20: 40442
MANI, R. S., Preparation of isotopically labeled organic iodo compounds for medical use, 20: 38932
MANTENIEKS, M. A., Current-voltage measurements in supersonic MHD generator with arc heated Ar plasma, 20: 39646
MAOR, U., Analysis of photoproduction of vector mesons, 20: 39811
MARBLE, Georges, Variation in hematocrit of rat after gamma irradiation, 20: 38587 (CEA-R-2909)
MARCHAND, J.-P., Unitarity of the S matrix for multichannel scattering, 20: 39866
MARCOPOULOS, Christos A., Isotopic exchange between 1-iodo-2,4-dinitronaphthalene and iodides in acetone, 20: 38916
MARENGO, G., Obtaining an impermeable graphite by impregnation with molten metals, 20: 39355 (EUR-2988.f)
MARGHITU, V., Build-up factor B in attenuation calculations of γ radiation, 20: 40289
MARIANI, Aldo, Cesium-137 and ^{90}Sr levels in diet and urine of an Italian children's community, 20: 39152
MARIANO, Maria Helena, Reduction of ceric sulfate in presence of thallous ions by 5-Mev α particles, 20: 38967
MARINCHUK, M. E., Effect of spin-orbital interaction on frequencies of plasma oscillations in semiconductors, 20: 40227
MARINKOVIC, D., Hereditary hypochromic microcytic anemia in laboratory rat, 20: 38619
MARINSKY, Jacob A., Prog. rpt. on studies in solution and nuclear chemistry, 10/65–9/66, 20: 38873 (NYO-2269-9)
MARKOVSKII, N. V., Hall effect in low-temperature plasma in non-homogeneous magnetic field, 20: 39740
MARLE, C., Evaluation of Rayleigh-Taylor instability and turbulent diffusion effects in inhomogeneous flow conversion, 20: 39704
MARLOW, W. C., Production of carbon plasmas, 20: 40209
MARMIER, P., Analysis by nuclear reaction, 20: 38841
MARSCH, W., Chromosome anomalies after radiation exposure, 20: 38615
MARSHALL, Geoffrey Peter, Metal heat insulating structural members, 20: 40367
MARSHALL, Scott J., Influence of a curved duct on explosive-driven MHD converters, 20: 39694
MARSHALL, T. C., Cyclotron harmonic radiation from electron beam injection into an afterglow plasma, 20: 40165 (AD-637710)
MARTENS, Frederick H., Design foresight can simplify reactor modification, 20: 40429
MARTENS, John H., Catalog of nuclear reactor concepts, Pt. I, Sect. VI, 20: 40353 (ANL-7228)
MARTIN, E., Operation of the Orsay CEVIL and its extraction systems, 20: 39551
MARTIN, Frank E., Thermal degradation of styrene and methylmethacrylate copolymers with pure m- and p- divinylbenzene isomers, 20: 38930 (TID-23264)
MARTIN, Frederick Samuel, Improvements in or relating to coating with beryllia, 20: 39379
MARTIN, H. J. Jr., Interactions (π^-p) at 460 Mev, 20: 39793
MARTIN, H. J. Jr., Isotopic spin of the η^* (960 Mev) meson, 20: 39786
MARTIN, J. A., Separated-orbit cyclotron, 20: 39541
MARTIN, J. H., Transverse hydromagnetic disturbances at 1100 km in auroral region, 20: 39996
MARTIN, James Edward, Correlation of wind tunnel and field measurements of gas diffusion using ^{85}Kr as tracer, 20: 39105
MARTIN, Troy C., An on-line nuclear analysis facility, 20: 39025 (ORO-2980-12)
MARTIN, W. H., Dimensional changes in pyrolytic graphite under fast-neutron irradiation, 20: 39465
MARTIN, W. H., Dimensional changes in polycrystalline graphites under fast-neutron irradiation, 20: 39466
MARTIN, Willion Sonderman, Effect of magnetic field on far infrared absorption spectrum of thin-film superconductors, 20: 40044
MARTINOVIC, J., Hereditary hypochromic microcytic anemia in laboratory

rat, 20: 38619
MARTINOVITCH, P. N., Hereditary hypochromic microcytic anemia in laboratory rat, 20: 38619
MARTRES, M.-J., Morphological study of the magnetic structure in active regions with relation to chromospheric phenomena and solar flares. I., 20: 39557
MARTRES, M.-J., Morphological study of the magnetic structure in active regions with relation to chromospheric phenomena and solar flares. II., 20: 39558
MARUSAK, A. L., Surface plasmon dispersion relation for electron gas, 20: 40225
MARUYAMA, Yosh, Current concepts of radiation biology as relevant to radiation therapy, 20: 38634
MARUYAMA, Yosh, Leukemic cell growth, host death, and response to x-irradiation, 20: 38699
MASLOVA, A. F., Mechanisms of disturbance of central regulation of automatic functions in irradiated animals, 20: 38654
MASSE, J., Effect of various parameters on efficiency of the MHD power stations, 20: 39705
MASSENGILL, L. A., Injection and accumulation: single-pass experiments (DCX-1), 20: 40171 (ORNL-3989, pp 1-13)
MASSIMO, L., Use of Pu in high-temperature reactors, 20: 40473
MASSOT, J.-N., Diagrammatic representation and utilization of rotation matrices, 20: 40120
MASTILLO, J. A., Orthovoltage radiation therapy, 20: 38792
MASUDA, Seizo, Formation of hydrogen negative ions in mercury vapor, 20: 39500
MASURAKI, Masaru, Preliminary experiment on ion cyclotron resonance of highly ionized plasma, 20: 40260
MATSUNAGA, Sakuro, Flow velocities, seeding ratios and electrical conductivities in seeded Ar plasmas, 20: 39727
MATSUNAMI, Todao, Alpha activity of highly radioactive fallout particles, 20: 39109
MATSUNAMI, Todao, Observation of fallout around the laboratory, 20: 39108
MATSUNAMI, Todao, X-ray microanalysis of fallout from first Chinese nuclear explosion, 20: 39110
MATSUOKA, Masaru, Instruments for observation of galactic x rays, 20: 39229
MATSURA, Kiyokata, Preliminary experiment on ion cyclotron resonance of highly ionized plasma, 20: 40260
MATSUZAWA, Toiju, Chemical prevention of radiation-induced leukemia in mice, 20: 38715
MATTAUSCH, Herbert, Biological radiation protection. LXX., 20: 38717
MATTHEWS, J. L., Shell effects in high energy photoproton spectra from ^{6}Li, 20: 40077 (MIT-2098-256)
MATVEEV, B. V., Evaluation of models for initial selection of radioprotective compounds, 20: 38729
MATVEEV, V. A., Adler-Weisberger relation and dispersion sum rules in theory of strong interactions, 20: 39857 (JINR-E-2876)
MATVEEV, V. A., Configuration mixing in quark model, 20: 39861 (JINR-P-2821)
MATVEEV, V. A., Cross sections for generating $K\bar{K}$ pairs in $\pi\pi$ collisions at low energies, 20: 39833
MATVEEVA, E. T., General patterns of pearl-type pulsations, 20: 39962
MATZKE, Hj., Effect of TiO_2 additions on defect structure, sintering, and gas release of UO_2, 20: 39381 (AECL-2585)
MAUTE, R. L., Apparatus for precise metering of radioactive gases or solutions, 20: 39172
MAXIE, E. C., Irradiation of fruits and vegetables, 20: 39289 (UCD-34P73-9)
MAXIMILIAN, Stefania, Blood and bone marrow disorders occurring in radiology-service personnel, 20: 38781
MAY, B. R., D-region electron density distributions deduced from reflection of radio waves, 20: 39995
MAY, F., Phase locked frequency multiplier for a speed- and phase synchronization system between a d-c and synchronous motor, 20: 39201 (EUR-2999.e)
MAY, J. P., Treatment of Basedow's disease with radioactive iodine, 20: 38760
MAY, R. M., Damping of transverse plasma oscillations at ion cyclotron resonance, 20: 40257
MAYBURG, Sumner, Recovery of insulator from radiation pulse, 20: 40329
MAYER, J. W., Semiconductor detectors for nuclear spectrometry. II., 20: 39231
MAYNARD, Charles W., Combined effect of ultrahigh pressure and nuclear irradiation on solid-solid phase transformations, 20: 40306
MAZARYU, E. A., Complex amplitude-phase modulation of periodic cosmic-ray variations, 20: 39629
MAZDA, Rumi N., Effects of gamma irradiation on two cyclic carbonates, 20: 38940 (NYO-3410-2)
MAZITOV, R. K., Relaxation of protons and deuterons in aqueous solutions of pentavalent molybdenum, 20: 38893
MAZZOLDI, P., Temperature dependence of critical velocity of positive ions in liquid helium, 20: 40033
MC ADAMS, R. E., Lifetimes of the 87 and 105 kev levels in ^{155}Gd, 20: 40110
MC ARTHUR, W. H., Shift in relative distribution of body nitrogen between skin and carcass in mouse radiation chimeras, 20: 38636
MC CALLUM, Robert E., Chlorine logging apparatus with temperature compensation circuit, 20: 39136
MC CARROLL, Ronald, Excitation of hydrogen by protons, 20: 39583
MC CARTHY, R. J., Calculation of binding energy of ^{16}O nucleus, 20: 40119
MC CLURE, Eldon Roy, Significance of thermal effects in manufacturing and metrology, 20: 39009 (UCRL-14944)
MC CONVILLE, J. H., SNAP-50/SPUR electromagnetic pump program, 20: 40450 (TIM-911)
MC COY, Barry M., Peculiarities of free massless spin-½ field theory, 20: 39890
MC COY, H. E., Influence of neutron irradiation twinning in a Nb–V alloy (40% V), 20: 39462
MC DONALD, G. Corry, Nuclear electrical power for canal construction, 20: 40422
MC DONALD, J., Low-cycle fatigue strengths of dissimilar weldments, 20: 39404 (SWRI-1228-4-20)
MC DOWELL, C. A., Electron spin resonance spectrum and electronic structure of PO_3^{2-} radical in irradiated crystal of ammonium fluorophosphate, 20: 38949
MC DOWELL, M. R. C., Classical impulse approximations, 20: 39607
MC DOWELL, M. R. C., Transition probabilities for electron capture, 20: 39606
MC ELFRESH, A. J., Finned circulator-evaporator for concentrating radioactive waste, 20: 40477 (HW-80056)
MC ELROY, J. L., High-temperature testing and evaluation of graphite helical-screw expanders and compressors, 20: 39026 (UCRL-14660(Rev.1))
MC GREW, John W., Method of pickling and chemically milling zirconium and zirconium alloys, 20: 39351
MC GUFF, Paul E., Tumoricidal effect of laser energy on experimental and human malignant tumors, 20: 38780
MC ILLWAIN, Carl E., Ring current effects on trapped particles, 20: 39970
MC ILWAIN, Carl E., Magnetic coordinates, 20: 39989
MC ILWAIN, John F., Charge-exchange cross sections for Ar ions in H_2 and D_2 below 1 kev, 20: 39592
MC MANIGAL, Paul G., Polarization in proton-proton scatterings at 735 Mev, 20: 39789
MC MULLEN, James M., Mass determination of fluent material by radioactive measuring means, 20: 39189
MC NAB, I. R., CNEN He–Cs blow-down MPD facility and experiments with prototype duct, 20: 39675
MC NAB, I. R., Further development, operation, and experiments with IRD closed-cycle MPD loop, 20: 39687
MC NAB, I. R., Relaxation phenomena in MPD generators, 20: 39674
MEAD, S. W., FRAN prompt burst reactor, 20: 40463 (UCRL-14413)
MEADS, Philip F. Jr., Design of AVF cyclotrons above 100 Mev, 20: 39539
MEDVED, S. V., Spin correlation in elastic scattering of 605-Mev polarized protons on protons, 20: 39759 (JINR-P-2776)
MEDYNSKA, A., Long-term results and complications after irradiation of haemangiomas in children, 20: 38787
MEERSON, G. A., Behavior of impurities and admixtures during sintering of W, 20: 39363
MEGAHED, Y. M., Variations in ascorbic acid content of gramineae during germination and effect of β- and γ-radiation, 20: 38583
MEGUMI, Tsuneo, Effect of ^{137}Cs and ^{90}Sr on growth and reproduction of mice. III., 20: 38551
MEIER, Walter, Radioactive sample changing and measuring apparatus, 20: 39044
MEINEL, A. B., Collisional excitation of atomic spectra in accelerated beams of light elements, 20: 39593
MEINERT, W., Advanced BONUS core thermal cycle test, 20: 40401 (CEND-259)
MEINKE, W. Wayne, Rapid radiochemical separations and activation analysis of biological samples, 20: 38842
MEISNER, Gerald Warren, Sign of the K_1^0–K_2^0 mass difference, 20: 39772 (UCRL-17007)
MEKSYN, David, Magnetohydrodynamic flow past semi-infinite plate, 20: 39945
MELARDI, Ebe Barbieri, Phosphates and polyphosphates of the lanthanide elements. VIII., 20: 38883
MELCHING, Hans-Joachim, Biological radiation protection. LXX., 20: 38717
MELIK-MUSYAN, A. B., Morphological and functional changes of retina during radiation syndrome in rabbits, 20: 38689
MENKES, Cirel K., Dosimetry for large animal experiments using multiple

^{60}Co sources and 1 mvp x-rays, 20: 38625
MEREKOV, Yu. P., Inelastic interactions of 19.8-Bev/c protons with neutrons, 20: 39761 (JINR-P-2809)
MERICLE, L. W., Prog. rpt. on radiosensitivity of embryonic tissues, annual, 1965–66, 20: 38588 (COO-1400-10)
MERICLE, R. P., Prog. rpt. on radiosensitivity of embryonic tissues, annual, 1965–66, 20: 38588 (COO-1400-10)
MERKEL, B., Charged pion photoproduction on light nuclei, 20: 40075 (LNF-66/30)
MERKOVA, M. A., Immediate and remote reactions in beam therapy of cervical malignant neoplasms, 20: 38773
MERKULOVA, K. I., Comparative oxidation rate of ^{234}U and ^{238}U atoms in certain minerals, 20: 38894
MERRILL, E. T., Formation of selected fission products in power reactors, 20: 40400 (BNWL-244)
MERRITT, Charles Jr., Chemical changes induced by irradiation in meats and meat components, 20: 39301
MERZ, E., Reprocessing of nuclear fuels by fluoride volatilization with sulfur hexafluoride, 20: 40389
MERZ, J. L., Absorption and emission of irradiated rare earth ions in CaF_2, 20: 40341
MESHKOV, S., Current algebras and matrix elements of axial-vector current, 20: 39892
MESSERLE, H. K., MHD generator operation as affected by electrode current saturation, 20: 39660
MESTEL, L., Problems of star formatica. II., 20: 39568
MEULDERS, J. P., Optical model analysis of neutron scattering on ^{12}C from 16 to 20 Mev, 20: 40088
MEULEMANS, M., Physical aspects of electron beam penetration in metals, 20: 40347
MEYER, Lothar, Crystal structure of solid H and deuterium, 20: 40308
MEYER, Ph., Selected topics in weak interactions, 20: 39764 (NP-16232)
MEYER-HEINE, A., Cobalt-60 production in graphite gas cooled reactors, 20: 39317 (DP-1066(Vol.2), pp I.67-77)
MEYERSTEIN, D., H/D isotope effects in formation of H from combination of two radicals in aqueous solutions, 20: 38938 (IA-1074)
MICHARD, R., Morphological study of the magnetic structure in active regions with relation to chromospheric phenomena and solar flares. I., 20: 39557
MICHARD, R., Morphological study of the magnetic structure in active regions with relation to chromospheric phenomena and solar flares. II., 20: 39558
MICKEVICIUS, V. V., Polarization capacity of certain ions, 20: 38879 (UCRL-Trans-1325)
MICU, D., Blood and bone marrow disorders occurring in radiology-service personnel, 20: 38781
MIJNHEER, B. J., Determination of fast neutron flux densities by activation of phosphorus compounds, 20: 39222
MIKELSON, Yu. Yu., Effect of toothed inductor on electromagnetic-field distribution in conducting slab, 20: 39937
MIKELSONS, J., Effect of toothed inductor on electromagnetic-field distribution in conducting slab, 20: 39937
MIKHAILOV, Yu. M., Investigation of MHD flow of liquid metal in rectangular duct with conducting walls, 20: 39706
MIKHIN, V. V., Results of experiments with 100-kw MHD generator model, 20: 39672
MIKHLIN, V. E., Effects of ionizing radiation and other factors on rate of topochemical decomposition of various inorganic compounds, 20: 38955
MIKHUL, A., Inelastic π^- p-interactions at energy 7.5 Bev. II., 20: 39758 (JINR-P-2773)
MIKKELSON, Raymond Charles, Anisotropic spin-lattice relaxation times of trivalent rare earth ions in anhydrous lanthanum trichloride, 20: 40350
MIKOLEIT, A. E., Fatigue properties of irradiated pressure vessel steels, 20: 39406 (WAPD-T-1864)
MIKUS, E. B., High remelt temperature brazing of columbium honeycomb structures, 20: 39365
MILAEV, S. M., Analysis of alloys of rare earth elements with magnesium in nonaqueous solutions, 20: 38830
MILEY, G. H., Gamma-electric cell theory and experiment, 20: 39652
MILLER, C. D., Lozier tube for ionization studies not involving mass analysis, 20: 39167 (AD-636927)
MILLER, Donald G., Application of irreversible thermodynamics to electrolyte solutions. I., 20: 38909
MILLER, L. E., Precision neutron activation analysis of zinc and titanium oxides in organic coating pigments, 20: 38853
MILLER, Robert W., Etiology of childhood leukemia: epidemiologic evidence, 20: 38668
MILLET, Jacques, Electrochemical criteria for selecting MHD electrode materials research on electronically-conducting zirconium oxide, 20: 39723
MINAEV, O., Experiments on ion acceleration at 685-mm sector cyclotron, 20: 39549
MINAEV, O. A., Ion optical studies of extraction transport and analysis systems for 240 cm cyclotron, 20: 39545
MINAMI, Kazuo, Low-electron-density measurements of transient plasmas by optical interferometers, · 20: 40214
MINIER-CASSAYRE, Colette, Study of point defects in pure iron by means of electric resistivity, 20: 39386 (CEA-R-2905)
MINK, Lawrence Albright, Statistical method for investigation of delayed triple nuclear cascades, · 20: 40160
MINTEN, A., Lectures on beam optics, 20: 39483 (CERN-66-21)
MINTEN, A., Low-energy separated beams, 20: 39485 (CERN-66-21, pp 31-42)
MIQUEL, J., Astroglial reactions to ionizing radiation, 20: 38674
MISHINA, I. M., Protective measures for medical personnel and patients during operation of superhighfrequency physiotherapy apparatus, 20: 38622
MITAMURA, Noritsugu, Production of Al–U alloy nuclear fuel by direct reduction, 20: 39333
MITTLEMAN, Philip S., Advances in power-reactor shield analysis, 20: 40431
MIYAHARA, Akira, Preliminary experiment on ion cyclotron resonance of highly ionized plasma, · 20: 40260
MIYAKOSHI, Junichi, Neutron flux distribution and spectrum in Fe–water shields, · 20: 40287
MIYASHITA, K., Photo-stimulated radiation dosimetry, 20: 40333
MIYOSHI, Study on Co phase composition contained in WC–Co base cemented carbides, 20: 39427
MIZOO, Nobutatsu, Neutron-diffusion parameters in water, 20: 40055
MIZUTANI, J., Irradiation flavor and the volatile components of beef, 20: 39299
MLCKOVSKY, Miloslav, Parameters of radioisotope relay instruments, 20: 39173
MNATSAKANYAN, A. Kh., Energy exchange between electron and molecular gases, 20: 39677
MOAK, C. D., Determination of interatomic potentials and stopping powers from channeled-ion energy-loss spectra, 20: 39602
MOEN, R. H., Prog. rpt. on radial vane steam separator, 1–3/66, 20: 39019 (GEAP-5149)
MOGILEVSKIY, E. I., Role of magnetic fields of solar corpuscular streams and their effect on magnetosphere, 20: 39963
MOGILEVSKIY, E. I., Variability of fluxes of magnetic fields of sunspots and faculae, 20: 39561
MOISEEV, S. S., Characteristics of problems in MHD stability theory, 20: 40239
MOKHOVA, E. N., X-irradiation effects on cytochrome systems of yeast organisms, 20: 38680
MONROE, John J., Superconducting critical field measurements in Ce-doped lead between 4.1°K and 1.8°K, 20: 40050
MONTEITH, Larry King, Spontaneous discharge from electron-irradiated polyethylene terephthalate films, 20: 39467
MOOK, H. A., Magnetic moment distribution of nickel metal, 20: 40325
MOORE, David, Liquid-protected electrodes, 20: 39094
MOORE, George E., Reflection and thermal accommodation of helium beams on platinum, 20: 39590
MOORE, R. H., Gaussian iterative least squares techniques for modern computers, 20: 39327 (LA-3362)
MORGAN, Ira Lon, An on-line nuclear analysis facility, 20: 39025 (ORO-2980-12)
MORGAN, O. B., High-current ion-beam production and injection, · 20: 40175 (ORNL-3989, pp 89-94)
MORI, Shigeyuki, Genetic studies on radio-resistant strain of Chlorella ellipsoidea. I., 20: 38605
MORNEL, E., Plateau of a GM counter at higher intensities, 20: 39244
MOROZOV, A. E., Choice of optimum Mach number for flow of non-equilibrium He–Cs plasma in MHD generator duct, 20: 39691
MOROZOV, A. I., Theory of supersonic part of nondissipative box-type accelerator, · 20: 40240
MOROZOVA, I. K., Corrosion resistance of reactor materials, 20: 39349
MORRISON, D. J. T., Excitation of atomic hydrogen by electron impact, 20: 39610
MORTON, R. J., Radionuclides in Clinch-Tennessee Rivers, 20: 40479 (ORNL-P-2328)
MOSKALENKO, A. M., Electric field and structure of plasma in vicinity of charged cylinder of small radius, · 20: 40197
MOSKALEV, Yu. I., Mathematical model of accumulation and elimination of radioactive isotopes, 20: 38571
MOSRIN, Pierre, Sidereal variation of cosmic muon component at 440-m depth, 20: 39626
MOTZ, H., Solutions of dispersion equation and Landau damping near cyclotron frequency, · 20: 40259
MOURIER, G., Effects of confinement in high-frequency discharges at low pressure, · 20: 40278
MOURIER, G., Study of a confinement of a plasma in spherical cavity, 20: 40277
MOUTINHO, A., Temperature assignment to thermal diffusion factor,

20: 39326
MOYER, Burton J., Polarization in proton-proton scatterings at 735 Mev, 20: 39789
MOZZHUKHIN, A. S., Changes in blood vessels during acute radiation sickness, 20: 38658
MOZZHUKHIN, A. S., Chemical structure and radioprotective properties of aminothiols and derivatives, 20: 38724
MUELLER, J., Internal contamination with ^{90}Sr and ^{226}Ra in man in relation to clinical findings, 20: 38623
MUELLER, R., Compton effect on bound K electrons, 20: 39773
MUHLBAIER, D. R., In-place nondestructive leak test for iodine adsorbers, 20: 39018 (DP-MS-66-46)
MUHLBAIER, David R., Prog. rpt. on nondestructive test of C beds for reactor confinement applications, 10/64–1/66, 20: 39017 (DP-1053)
MUKHIN, A. I., Structure of Ar K-series during atomic capture of negative muons in pure gas and in mixture with H, 20: 39578 (JINR-P-2807)
MUKSINOVA, K. N., Effectiveness of transplantations of bone marrow in hypoplastic anemia, 20: 38711
MUKSINOVA, K. N., Effectiveness of bone marrow transplantation in relation to time of administration, 20: 38740
MUKSINOVA, K. N., Relation between effects of marrow transfusion during radiation sickness and transplanted cells, 20: 38730
MUKUNDA, N., Equal-time commutators and photoproduction sum rules, 20: 39879
MULLEN, James G., New results on the question of Auger aftereffects, 20: 39603
MULLER, M. W., Polarization in LaF_3, 20: 40304
MUMINOV, M. M., Identification of charged particles by ionization and δ-electrons in a propane bubble chamber, 20: 39211 (JINR-P-2842)
MUNARI, S., Room-temperature ESR spectrum of irradiated polypropylene, 20: 38954
MUNN, Alfred A., Radioactivity level detecting apparatus for samples carried by portable trays, 20: 39042
MUNZEL, Fritz, Process of modifying cellulosic materials with ionizing radiation, 20: 38975
MURAI, Yutaka, Analysis of thermodynamic properties of high-temperature gas, 20: 39938
MURAKAMI, Akio, Relative biological effectiveness of 14-Mev neutrons to γ rays for inducing mutations in mature sperm of silkworm, 20: 38626
MURAKAMI, Masahiro, X-ray microanalysis of fallout from first Chinese nuclear explosion, 20: 39110
MURRAY, E., Irradiation flavor and the volatile components of beef, 20: 39299
MURRAY, K., Use of neutron activation in characterization of small quantities of nucleic acids, 20: 38816
MURRAY, Peter, Improvements in or relating to heat treatment of refractory materials, 20: 39343
MURRAY, R. L., Control rod programming. I., 20: 40354 (AP-Note-393)
MUS, K. F., Determination of quantometer constant at 650 Mev, 20: 39248
MUXART, Roland, Protactinium peroxide compounds in basic media, 20: 38890
MUZYCHENKO, A. D., High-melting metal electrodes for MHD generators with non-equilibrium conductivity, 20: 39736

N

NAGAO, Shigeo, Preliminary experiment on ion cyclotron resonance of highly ionized plasma, 20: 40260
NAGARAJAN, G., Mean amplitudes of thermal motion and shrinkages of chemical bonds: octahedral hexafluorides, 20: 38897
NAIDU, P. S., Inverse problem of particle motion and its application, 20: 39471
NAKACH, R., Confinement and heating of a plasma by low-frequency rotating magnetic field, 20: 40279
NAKANE, Ryohei, Separation of ^{10}B by distillation of BF_3–CH_3F, 20: 39325
NAKAO, Yoshio, Comparison of frequency patterns between whole-body and fractional mutations induced by x rays in Drosophila, 20: 38650
NAKATSUKA, Haruo, Modification of perivascular subcutaneous connective tissue reaction following x-ray irradiation, 20: 38640
NARASIMHA RAO, B. V., Lifetimes of 1554- and 1289-kev levels of ^{182}W, 20: 40094
NARCISI, R. S., Ion composition measurements and related ionospheric processes in D and lower E regions, 20: 39948
NARDON, P., Use of radiations in control of insects, 20: 38671
NARIBOLI, Gundo A., Blast waves in magnetogasdynamics with finite electrical conductivity, 20: 39944
NARVER, David L. Jr., Metropolitan-area blast-shelter system, 20: 39088
NASTASI, Maria Jose C., Digital program for calculation of activities of fission products of long half life, 20: 40070 (IEA-111)
NATARAJAN, A. T., Post-irradiation centrifugation and radiation-induced chromosome aberrations in barley, 20: 38618
NATELSON, M., Angle-space synthesis: an approach to transport approximations, 20: 40360 (WAPD-T-1890)
NATH, Amar, Thermal annealing of recoil damage in Co chelates, 20: 38965
NATH, P., Asymptotic behavior of inelasticity parameter, 20: 39884
NAUMANN, D., Ammonolysis of U halides. I., 20: 38920
NAVARRO, Alain, Preparation and properties of the double salt $2Th(C_2O_4)_2 \cdot (NH_4)_2C_2O_4 \cdot 7H_2O$, 20: 38886
NEDOBOROVA, L. I., Radiation chemistry of carbohydrates. VII., 20: 38969
NE'EMAN, Y., Algebra of scalar and vector vertex strengths in Regge residues, 20: 39881
NEMENOV, L. L., Reaction $\pi N \to \pi_1\pi_2 N'$ in energy region up to 1 Bev, 20: 39827
NEMENOV, L. M., Conversion of Kazakhstan cyclotron to a variable energy isochronous cyclotron, 20: 39553
NESIS, E. I., Boiling of liquids, 20: 39052
NESS, N. F., Correlation of magnetic fields and energetic electrons on the IMP 1 satellite, 20: 39976
NESTOROV, G., Space and time variations of long wave ionospheric absorption at small solar heights and at night, 20: 39960
NETTLEY, P. T., Dimensional changes in pyrolytic graphite under fast-neutron irradiation, 20: 39465
NETTLEY, P. T., Dimensional changes in polycrystalline graphites under fast-neutron irradiation, 20: 39466
NEUMANN, W., Velocity dependence of atom-atom total scattering cross sections in the 7–500 ev energy range, 20: 39599
NEVSKAYA, G. F., Mechanism of death of animals with most acute form of radiation sickness, 20: 38666
NEVSTRUEVA, M. A., Third scientific and working conference on radiation protection, Leningrad, Apr. 16–20, 1963, 20: 39166
NEWBURY, R. S., Isotopic disproportionation reaction between light and heavy water using pulsed-molecular-beam mass spectrometer, 20: 38875 (UCRL-14703-T)
NEWBY, D., Closed-cycle nuclear MHD studies using dust suspensions, 20: 39728
NEWMAN, L., Mixed β-diketones, 20: 38855 (BNL-10350)
NEWMARK, Nathan M., State of art for design of underground protective construction, 20: 39070
NEWTON, D., Case of accidental inhalation of ^{227}Ac, 20: 38554
NGUYEN DUC, X., Evaluation of Rayleigh-Taylor instability and turbulent diffusion effects in inhomogeneous flow conversion, 20: 39704
NGUYEN DUC, X., Radiation of flames used in MHD, 20: 39710
NGUYEN THI HONG, Existence of certain baryon and meson unitary multiplets, 20: 39860 (JINR-P-2790)
NGUYEN VAN HIEU, S-matrix, non-compact symmetry groups and their collinear subgroups, 20: 39854 (JINR-E-2754)
NHUONG, Doan, Possibility of determining electromagnetic form factors of the W meson, 20: 39823
NICE, William A., Alternator for SNAP 8 program, 20: 40453
NICHOLL, D. R., Recent developments in scintillation detectors, 20: 39233
NICHOLS, L. D., Current-voltage measurements in supersonic MHD generator with arc heated Ar plasma, 20: 39646
NICHOLS, Roy Woodward, Improvements relating to low alloy steels, 20: 39444
NICOLAE, M., Relations between kinetics of development of emulsion sensitivity and illumination, 20: 39202 (IFA-PN-17)
NIEDERALT, G., Chromosome anomalies after radiation exposure, 20: 38615
NIEH, H. T., Form factors (K_{13}) and the pion charge form factor, 20: 39796
NIEPOLOMSKA, W., Squamous-cell carcinoma of skin in child treated by radium-gamma-rays, 20: 38788
NIEWODNICZANSKI, Henryk, Large permanent magnet semicircular beta ray spectrograph, 20: 39203 (INP-476/PL)
NIGROVIC, V., Diminution of radiocesium body-burden in dogs and human beings by Prussian Blue, 20: 38557
NIGROVIC, Vladimir, Excretion of ^{65}Zn-DTPA in the rat, 20: 38556
NIKANOROV, V. I., Spin correlation in elastic scattering of 605-Mev polarized protons on protons, 20: 39759 (JINR-P-2776)
NIKISHIN, B. K., Inelastic π^--p interactions with slow-recoil protons at 17 Bev, 20: 39830
NIKITINA, K. I., Role of autoinfection in development of the hemorrhagic syndrome during acute radiation sickness, 20: 38656
NIKOLAEV, V., Central region of 240 cm variable energy cyclotron, 20: 39513
NIKOLAEV, V., Experiments on ion acceleration at 685-mm sector cyclotron, 20: 39549
NILAN, R. A., Effect of x-radiation on spore germination and stability of virulence in Ustilago avenae, 20: 38672
NIR, A., Isotope methods applied to groundwater hydrology, 20: 39142
NISHIHARA, Hiroshi, Neutron-diffusion parameters in water, 20: 40055
NISHIO, Kazuo, Effect of ^{137}Cs and ^{90}Sr on growth and reproduction of mice. III., 20: 38551

NISHIO, Kazuo, Observations on thymus of mice after x irradiation, 20: 38606
NIVINSKAYA, M. M., Radiosensitivity of malignant melanoma, 20: 38764
NIYAZOVA, O. R., Radiation-stimulated emf in CsI crystals, 20: 40335
NOACK, G., Analysis of essential characteristics for closed MHD power stations, 20: 39682
NOACK, G., Closed MHD-loop ARGAS, 20: 39680
NOBLE, Carl M. Jr., Pion-pion interactions from π–p collisions at 3 and 4 Bev/c, 20: 39769 (UCRL-16655)
NOBLE, Julian V., Discussion of a note by Federbush on spurious solutions of three-particle equations, 20: 39901
NOCENTINI, A., Constants of linearized motion of Vlasov plasmas, 20: 40167 (IC-65/90)
NOGGLE, T. S., Determination of interatomic potentials and stopping powers from channeled-ion energy-loss spectra, 20: 39602
NOMOFILOV, A. A., Measurement of real part of π–p elastic scattering amplitude in Coulomb interference region at 3.5 Bev/c, 20: 39785
NOONKESTER, V. R., Variations in f_0E and f_0F_2 at Washington, D. C., near days of increased geomagnetic activity, 20: 39985
NOOTHOUT, A. J., Basic studies related to the development of the Sol-Gel process, 20: 40391
NORRIS, N., Prog. rpt. on Linac adaptation for weapons simulation, 1/65, 20: 39487 (EGG-1183-2009)
NORRIS, N., Prog. rpt. on Linac adaptation for weapons simulation, 4/65, 20: 39488 (EGG-1183-2027)
NORRIS, N., Prog. rpt. on Linac adaptation for weapons simulation, sub-harmonic buncher, 10/65, 20: 39489 (EGG-1183-2050)
NORRIS, N., Prog. rpt. on Linac adaptation for weapons simulation, high current gun, 10/65, 20: 39490 (EGG-1183-2051)
NOVAIS, Horacio Maggiolli, Reduction of ceric sulfate in presence of thallous ions by 5-Mev α particles, 20: 38967
NOVAK, Arthur F., Prog. rpt. on radiation pasteurization of shrimp and oysters, final, 1–12/65, 20: 39288 (ORO-636)
NOVAK, J., Separation of ^{99m}Tc from ^{99}Mo sorbed on aluminum oxide, 20: 38997 (NIJS-R-483)
NOVAK, R. L., Effect of neutron-induced defects on current-carrying behavior of vapor-deposited niobium stannide, · 20: 40301
NOVIKOV, G. I., Composition of vapor in $ErCl_3$–CsCl and $NdCl_3$–CsCl systems, 20: 38919
NOVIKOV, S. R., Defects in silicon produced by irradiation with fast neutrons at 77°K, 20: 40334
NOVIKOVA, L. V., Doses in organs and tissues of head in x-ray therapy of cancer of facial skin, 20: 38765
NUNEZ-LAGOS ROGLA, Rafael, Free fields for Nass less particles, 20: 39853 (JEN-157-DF/I-48)
NYFFENEGGER, U., Uranium-235/Th fuel cycles in graphite moderated systems, 20: 40393
NYGAARD, K., Measurement of the electrical conductivity of ^{3}He induced by neutron irradiation, 20: 39683
NYGAARD, K., Optimal linear filters for pulse height measurements in presence of noise, 20: 39195 (AE-235)

O

OBERLY, Charles E., Optimum magnets for MHD generators, 20: 39668
OBOLONCHIK, V. A., Selenides and tellurides of rare earth metals and actinides, 20: 38927
O'CONNOR, J. D., Physical and radiochemical properties of fallout particles, 20: 39115
ODLAND, L. T., Effects of pulsed fission spectrum neutron irradiation, 20: 38637
O'DONNELL, W. J., Fatigue properties of irradiated pressure vessel steels, 20: 39406 (WAPD-T-1864)
OEGELMAN, Hakki Boran, Search for discrete sources of high-energy cosmic gamma rays, 20: 39632
OEHME, Reinhard, Current algebras and form factors, 20: 39898
OFFORD, R. E., Use of neutron activation in characterization of small quantities of nucleic acids, 20: 38816
OGANESYAN, K. O., Formation of charged π mesons in collisions between 600-Mev neutrons and protons, 20: 39834
OGANESYAN, Yu. Ts., Element 104, 20: 40143
OGASAWARA, Masatade, Effects of collision on propagation of electromagnetic wave in a plasma. I., · 20: 40222
OGIEVETSKII, V. I., Consistent relativization of SU(6) for two-particle reactions, 20: 39856 (JINR-E-2826)
OGIEVETSKII, V. I., Possible experiments checking isotopic structure of electromagnetic interactions, 20: 39824
OHARA, Akira, Radiolytic decomposition and radiation sensitivity of amino acids in aqueous solution by gamma irradiation, 20: 38582
OK, Hong Nam, New results on the question of Auger aftereffects, 20: 39603
OKAMOTO, Masafumi, Ternary alloys of iron and boron, 20: 39426
OKAMURA, Seizo, Polymerization of cyclic ethers in presence of maleic anhydride. I., 20: 38953
OKONOV, E., Test of CP-invariance in $K_S^0 \to 3\pi$ decays in correlation experiments with $K^0\bar{K}^0$ pairs, 20: 39763 (JINR-P-2850)
OKONOV, E., The search for "long-lived" Λ^0-particles, 20: 39762 (JINR-P-2849)
O'LAUGHLIN, Jerome W., Some neutral bifunctional organophosphorus compounds as solvent extractants, 20: 38819
OLEHY, D. A., Neutron activation analysis for quantitation of selected cations in blood, 20: 38852
OLESEN, P., Two-baryon approximation to decay of neutral pseudoscalar mesons, 20: 39783
OLIVER, D. A., Calculation of idealized MHD generator performance with non-equilibrium electron heating, 20: 39647
OLIVIERI, G., Nonrandom rejoining of chromatid breaks and its relation to origin of sister-chromatid exchanges, 20: 38649
OLSEN, A. R., Irradiation testing of Th fuels at ORNL, 20: 40385 (ORNL-P-2327)
OLSEN, J. L., Size effect in thermal resistivity maxima in In and Pb, 20: 40022
OLSEN, Raymond Edgar, Effects of whole-body gamma irradiation on blood constituents and hemopoietic organs of calf, 20: 38706
OLSON, H. Thomas, Cesium ion sputtering of aluminum, 20: 39585
OLSSON, M., Evidence for a $\Sigma^-\eta$ enhancement near threshold, 20: 39747 (COO-881-75)
OLSSON, M., Regge-pole model and total cross sections in intermediate laboratory momentum range 2–6 Bev/c, 20: 39801
OLTMAN, B. G., LiF thermoluminescent response to fast neutrons, 20: 39219
OMATA, Saburo, Alterations in functional state of rat adrenal following the lethal and sub-lethal, whole-body x-irradiations, 20: 38638
OMHOLT, A., Physical composition of aurora, 20: 39947
ONTKO, Joseph A., Final rpt. on effects of radiation on metabolism of ascites tumor cells, 20: 38599 (TID-22968)
ORBAN, Miklos, Solvent effects in isotope exchange reactions. VI., 20: 38936
ORDAN'YAN, S. S., Structure of Zr–C–Nb system, 20: 39434
ORLOV, Yu. I., Peculiarities of theory of cylindrical and spherical waves in plasma. I., · 20: 40208
ORSENIGO, Giuseppe, Progress on the PCUT program, 20: 39006
OSSAKOW, Sidney L., Kinetic equation for unstable plasma in parallel electric and magnetic fields, · 20: 40181 (TID-23307)
OSSAKOW, Sidney L., Kinetic equation for an unstable plasma in parallel electric and magnetic fields, · 20: 40249
OSTRETSOV, L. A., Dosimetric specifications of gamma therapy unit "Luch-1", 20: 38771
OTH, D., Synergetic effect of x rays and of vincaleucoblastine on solid isologous tumor of mouse C^3H, 20: 38613
OTTER, F. A. Jr., Isothermal calorimetry on type II superconductors, 20: 40045
OVCHARENKO, V. A., Choice of optimum Mach number for flow of non-equilibrium He–Cs plasma in MHD generator duct, 20: 39691
OVEZGEL'DEV, O., Relationship between E_s and the F region of the ionosphere, 20: 39966
OZAWA, Lyuji, Emission and excitation spectra of Eu_2O_3 compared with Y_2O_3 : Eu phosphor, 20: 40315

P

PABOT, J. L., Axial injection for the Grenoble cyclotron, 20: 39532
PACINI, Franco, Gravitational collapse and scalar interaction in superdense matter, 20: 39555
PACKARD, L. E., Radioactivity level detecting apparatus for samples carried by portable trays, 20: 39042
PADIOU, Jean, Sulfides and oxysulfides of uranium and potassium, 20: 38891
PAGNINI, G., Radioprotection of sulfurated mineral waters, 20: 38709
PAIGE, B. E., Leachability of alumina calcine produced in Idaho Waste Calcining Facility, 20: 40478 (IN-1011)
PAJAS, P., Degenerate representations of the symplectic groups. I., 20: 39850 (IC-66/77)
PALEI, P. N., Separation of ionium (^{230}Th) from U, Pa, Fe, Mn, and Eu by cation exchange, 20: 38834
PALIBRODA, N., Theory of separating columns with successive exchange between three fluids, 20: 39005
PALMER, R. C., Prototype thermoluminescent dosimetry system for personnel monitoring, 20: 39224
PALMER, R. C., Prototype LiF radiation dosimeter for personnel monitoring, 20: 39225
PALMOUR III, Hayne, Materials science research. Vol. 3, 20: 39338
PALMS, J. M., Comparison of rotational M1 transition rates between high and low spin states, 20: 40072 (LA-DC-8061)
PALMS, J. M., Further evidence for effective nucleon spin g-factors, 20: 40073 (LA-DC-8065)

PANZHAUSER, E., Technical aspects of the Austrian shelter program, 20: 39081
PAPASTAMATIOU, N. J., Broken relativistic supermultiplet symmetries and weak currents, 20: 39877
PAPIRER, Eugene, Determination of surface carboxylic and hydroxyl groups of carbon black by radiochemical method, 20: 38805
PARFENOV, B. G., Corrosion resistance of reactor materials, 20: 39349
PARFENOV, Yu. D., Mathematical model of accumulation and elimination of radioactive isotopes, 20: 38571
PARIS, G., Welding of a reactor for an electrothermonuclear power plant, 20: 40417
PARIZOT, Daniel, Magnetoaerodynamic conversion test rig with sub-atmospheric operating conditions, 20: 39709
PARK, Keung Shik, Preparation of carrier-free ^{59}Fe by Korean TRIGA Mark II reactor, 20: 39324
PARKER, C. Vorren Jr., An on-line nuclear analysis facility, 20: 39025 (ORO-2980-12)
PARKER, F. L., Radionuclides in Clinch-Tennessee Rivers, 20: 40479 (ORNL-P-2328)
PARKER, W. H., "Non-Josephson" radiation from Josephson tunnel junctions, 20: 40028
PARLANGE, F., Acceleration of plasma by field of progressive wave damped in vicinity of electron or ion cyclotron resonance, 20: 40267
PARLANGE, F., Three modes of energy transfer of a plasma h-f field, 20: 40261
PARO, J. N., Bibliography on nuclear ship propulsion, No. 6, 6/66, 20: 40444 (AED-C-22-06)
PARSHIKOVA, S. M., Radiosensitivity of malignant melanoma, 20: 38764
PARSICK, R., Engineering problems in pulsed neutron sources, 20: 40456 (BNL-10454)
PARTOLIN, O. F., Dosimetric specifications of gamma therapy unit "Luch-1", 20: 38771
PARWEL, Alexander, Rubidium–strontium whole rock age data on some Swedish precambrian rocks, 20: 39126
PASCHKA, W., End effects on the linear induction MHD generator calculated by two-sided Laplace transform, 20: 39717
PASCU, L., Determination of constants for geometric reconstruction of tracks on np films from neutron irradiated 24-l bubble chamber, 20: 39247
PASHOS, T. J., Mechanical property changes in Zircaloy-2, Inconel and Incoloy from neutrons, 20: 39457 (GEAP-5100-9)
PASHOS, T. J., Uranium oxide powder and pellet thermal conductivity during irradiation, 20: 39456 (GEAP-5100-1)
PASSELL, T. O., Use of ^{241}Am alphas to measure properties of thin films, 20: 39298
PATIL, Sharashchandra H., Ghost in scalar state, 20: 39808
PATOU, Claude, Parameters of Cs plasma obtained by contact ionization, 20: 40223
PAUL, Arthur C., Variable energy extraction from negative ion cyclotrons, 20: 39519
PAULY, H., Velocity dependence of atom-atom total scattering cross sections in the 7–500 ev energy range, 20: 39599
PAULY, Jules, Determination of Mg in Al by neutron activation, 20: 38804
PAVIC, D., Hereditary hypochromic microcytic anemia in laboratory rat, 20: 38619
PAVLICHENKO, O. O., Interferometer for plasma diagnosis, 20: 40226
PAVLOV, A. S., Dose distributions in homologous phantoms in distance gamma-therapy, 20: 38762
PAVLOVA, F. S., Corrosion resistance of reactor materials, 20: 39349
PAVLOVA, T. G., Dose distributions in homologous phantoms in distance gamma-therapy, 20: 38762
PAXSON, E., Engineering and metallurgical evaluation of an irradiated Yankee Core I control rod, 20: 39461 (WCAP-6074)
PAYNTER, D. A., Field detector station for fallout and transit dose rate measurement system, 20: 39192 (AD-636206)
PEARCE, D. W., Prog. rpt. on earth sciences, annual, 1965, 20: 38857 (BNWL-235-3)
PEARSON, Charles James, Approximation methods for Regge parameters in potential scattering, 20: 39923
PEARSON, John Edwin James, Improvements in or relating to containers for radioactive members, 20: 39040
PECILE, Cesare, Improved method of H isotopic exchange with deuterium sulfate, and preparation of 9,10-anthraquinone-d_8, 20: 38889
PEEK, N. F., Central region studies for incorporating an axial ion source in the Davis 76-inch cyclotron, 20: 39512
PEKAREK, H., Multi-group collision probability theory in cluster geometry, 20: 40380
PELEKIS, L. L., Determining γ radiation of spherical source with cylindrical channel, 20: 38989
PELLEGRINI, G., Changes in antiinsulin antibodies subjected to radio-activity, 20: 38579
PENAS, N. P. Jr., Water analysis, 12/63–11/64, 20: 38800 (PAEC(C)RE-652)
P'ENG, Pi-hsien, Some problems of rare earths catalysis, 20: 38877 (JPRS-35594)
PEREBASKINE, C., ELAN: installation for recovery and packaging of ^{137}Cs in France, 20: 39319 (DP-1066(Vol.2), pp II.33-44)
PEREGUD, B. P., Magnetohydrodynamic instabilities in electrical explosion, 20: 39010
PERELYGIN, V. P., Use of mica and quartz glass for nuclear fission detection at high temperature, 20: 39208 (JINR-P-2705)
PERSHAN, P. S., Absorption and emission of irradiated rare earth ions in CaF_2, 20: 40341
PERSSON, R., Semi-empirical formula for change of diffusion coefficients caused by empty channels, 20: 40377
PESTIEAU, J., n-Body scattering amplitude: separation of total angular momentum, 20: 39897
PETELINA, V. V., Effects of functional condition of the hypothalamus on the course of radiation sickness, 20: 38688
PETERKOP, R. K., Electron exchange in electron-atom collisions, 20: 39582 (AERE-Trans-1053)
PETERS, B., Creation of particles at cosmic-ray energies, 20: 39745 (CERN-66-22)
PETERSEN, Allen H., Washout of particulate matter in long-term clouds produced by nuclear explosions, 20: 39107 (UCRL-14700)
PETERSEN, M. C. E., Focusons in potassium chloride, 20: 39600
PETERSON, Jorgen Otzen, Hydrogen-burning models for stars in the horizontal branch of globular clusters, 20: 39566
PETERSON, Lawrence E., Search for the quiet-time solar gamma rays from balloon altitudes, 20: 39565
PETERSON, S. W., Neutron-diffraction determination of the structure of $CH_3CN \cdot 2HCl$, 20: 38935
PETERSON, Sigfred, Forming method for curved ATR fuel plates, 20: 39358 (ORNL-3983)
PETIT, Georges-Yves, Investigation of bound neutron-neutron state in reaction $^9Be(n,2n)^8Be$, 20: 40091
PETIT, J. L., New forms of irreducible unitary representations of Poincare group. I., 20: 39864
PETIT, J. L., New forms of irreducible unitary representations of Poincare group. II., 20: 39865
PETRESCU, D., Influence of ionizing radiations on cortico-suprarenal system evaluated on basis of potassium in rabbits, 20: 38697
PETROV, R. V., Mechanism of death of animals with most acute form of radiation sickness, 20: 38666
PETRUKHIN, V. I., Measurements of half-life ratio of π^+ and π^- mesons, 20: 39760 (JINR-P-2802)
PETRZHILKA, V., Momentum spectra of secondary particles in (π^-,N) interactions at 7 Bev, 20: 39751 (JINR-E-2738)
PETTIT, Donald Ethan, Combined effect of mean stress and stress concentrations on fatigue properties of 2011-T3 Al alloy, 20: 39396 (IS-T-60)
PFIRSCH, D., Variation of adiabatic invariant of harmonic oscillator, 20: 40229
PFOHL, Raymond, Nuclear reactions induced by interactions of 200-Mev ^{20}Ne ions with nuclei of ionographic emulsions, 20: 40083
PHAHLE, A. M., Effect of radiation on electric conduction in n-hexane, 20: 38971
PHELPS, A. V., Theory of electron collision experiments, 20: 39576 (AD-636533)
PHILLIPS, R. J. S., Comparison of the mutagenic effectiveness of chronic neutron and γ irradiation of mouse spermatogonia, 20: 38647
PICHOTIN, Bernard, Coulometric determination of C in Pu and in U–Mo alloys, 20: 38796 (CEA-R-2968)
PIERSON, E. S., Material limitations in the MHD induction generator, 20: 39731
PIGACHE, D., Diffusion process in toroidal discharge, 20: 40180 (SU-IPR-69)
PIJCK, J., Determination of Cu, Cr, Zn, Co, Na, and K in blood serum, 20: 38851
PIKAL, M. J., Apparent molal volumes of some aqueous rare earth chloride and nitrate solutions at 25°, 20: 38905
PIKAL, M. J., Relative viscosities of some aqueous rare earth chloride solutions at 25°, 20: 38904
PIKHTELEV, R. N., Measurement of π^+-meson lifetime, 20: 39821
PILLAT, L., Blood and bone marrow disorders occurring in radiology-service personnel, 20: 38781
PINAJIAN, J. J., Moessbauer studies of divalent and trivalent ^{57}Fe in $CoSO_4$ and $CoSO_4 \cdot 7H_2O$, 20: 40311
PINCET, J., Correlation between mortality due to tumors and dietary radioactivity in man, 20: 38739
PINCUS, Gregory, Prog. rpt. on steroid synthesis, analysis, and metabolism, 5/65–4/66, 20: 38547 (NYO-918-15)
PINK, Erwin, Dislocation etching of deformed molybdenum, 20: 39432
PINSLEY, Edward A., Preliminary design considerations of high-performance Hall-current accelerator, 20: 39090
PIONTKOVSKII, I. A., Inborn radiation syndrome induced experimentally,

20: 38665
PIROUE, P. A., Particle production by 2.9-Bev protons incident on Be and Pt, 20: 39794
PISAREV, A. F., Spark and streamer chambers and methods of data derivation from these chambers, 20: 39210 (JINR-P-2745)
PISAREV, A. F., Spin correlation in elastic scattering of 605-Mev polarized protons on protons, 20: 39759 (JINR-P-2776)
PISAREV, N. M., Electron conductivity of thermoionized gas in electric field, 20: 40238
PIXLEY, R. E., Resonances in $^{40}Ar(p,p)$ near 1.1 Mev, 20: 40147
PLANTIN, Lars-Olof, Assessment of trace elements of blood and tissues by radioactivation, 20: 38845
PLATT, A. M., Prog. rpt. on fixation of radioactive residues, 1–3/66, 20: 40476 (BNWL-267)
PLATZMAN, P. M., Brillouin scattering in liquid He II, 20: 40034
PLETTE, Gisela, Lipoid changes in various rat organs after whole-body irradiation with lethal x ray doses. III., 20: 38701
PLUMLEE, D. E., Behavior of selected steels exposed in flowing sodium test loops, 20: 39345 (GEAP-4831)
POBELL, F., Magnetic fields at ^{119}Sn in rare earth metals, 20: 40322
PODGORETSKII, M. I., Possible experiments checking isotopic structure of electromagnetic interactions, 20: 39824
PODO, L. A., Studies on the reprocessing and refabrication of HTGR fuels in OECD Dragon Project, 20: 40419
PODOBNIK, B., Flame photometric determination of Li, Na, K, Ca, Mg, and Sr in natural and mineral waters, 20: 38798 (NIJS-R-465)
POESCHEL, E., Evaluations on chemical reactions of carbides and oxides suitable for construction of nuclear-fueled thermionic emitters, 20: 39353 (BMwF-FBK-66-07)
POGORELKO, M. A., Effect of vitamins and phosphatides on resistance to radiation, 20: 38721
POIRIER, C. P., Interactions (π^-p) at 460 Mev, 20: 39793
POLFEROV, E. A., Accumulation of particles in a 680-Mev synchrocyclotron, 20: 39492 (JINR-P-2811)
POLIC, Edward F., Apparatus with vertical and lateral movable means for handling groups of radioactive samples, 20: 39041
POLIC, Edward F., Radioactivity level detecting apparatus for samples carried by portable trays, 20: 39042
POLIKANOV, S. M., On one of the methods of synthesis, 20: 40141
POLLARD, Morris, Chemical prevention of radiation-induced leukemia in mice, 20: 38715
POLUBARINOV, I. V., Consistent relativization of SU(6) for two-particle reactions, 20: 39856 (JINR-E-2826)
POLUBOYARINOVA, Z. I., Changes of kidneys in animals during radiation sickness when treated with unithiol, 20: 38719
POLUMORDVINOVA, N. I., Modified resonance extraction method from relativistic cyclotron, 20: 39520
POMERANCHUK, I. Ya., Interactions of elementary particles, 20: 39919
POMOSHNIKOVA, N. A., X-irradiation effects on cytochrome systems of yeast organisms, 20: 38680
PONTEKORVO, D. B., Recording of particle paths in streamer high-pressure chamber filled with helium, 20: 39245
POPOLI, G., Welding of a reactor for an electrothermonuclear power plant, 20: 40417
POPOV, A. V., Ion optical studies of extraction transport and analysis systems for 240 cm cyclotron, 20: 39545
POPP, W. G., Cost of coated particle fuel for a high temperature reactor program, 20: 40466
POPPER, Glenn F., Measuring neutron-flux distribution in operating reactors, 20: 40379
PORTE, R., Estimation of the efficiency of inhomogeneous-flow MHD generator, 20: 39737
PORTE, R., Evaluation of Rayleigh-Taylor instability and turbulent diffusion effects in inhomogeneous flow conversion, 20: 39704
PORTER, S. W. Jr., Procedure for minimizing personnel hazards while changing tritium targets in accelerators, 20: 39476 (AD-636185)
POSTMA, H., Injection and accumulation: single-pass experiments (DCX-1), 20: 40171 (ORNL-3989, pp 1-13)
POSTNIKOV, V. V., Nuclear reactor oscillation-measuring device, 20: 40361
POSTON, J. W., Zero power tests on NS Savannah Core II, 20: 40445 (BAW-1225)
POTAPENKO, T. G., Evaluation of models for initial selection of radioprotective compounds, 20: 38729
POWELL, W. B., Ion injection from external sources, 20: 39526
POWER, Derek John, Improvements in or relating to containers for radioactive members, 20: 39040
PRAMANICK, Dinabandhu, Photosensitized polymerization of methyl methacrylate using uranyl, vanadyl and molybdenyl salts, 20: 38934
PREISS, J., Increase in RNase and DPNase activities in ascites tumor cells induced by cytostatic agents, 20: 38578
PREISS, Kenneth, Design of a neutron scattering water content gage for soils, 20: 39141
PRESNYAKOV, V. S., Investigation of MHD flow of liquid metal in rectangular duct with conducting walls, 20: 39706
PRESSON, A. G., Computer study of dynamics of MRP shaft-bearing system, 20: 39022 (NAA-SR-11943)
PREUSS, Luther E., Demonstration of x-ray diffraction by LiF using the Mn Kα x rays resulting from ^{55}Fe decay, 20: 40294
PRICE, LeRoy Raymond, Reaction of $\eta \to \pi^+\pi^-\gamma$, 20: 39771 (UCRL-16923)
PRICE, M. S. T., Cost of coated particle fuel for a high temperature reactor program, 20: 40466
PRIGENT, Jacques, Sulfides and oxysulfides of uranium and potassium, 20: 38891
PRINCE, Norman, Improvements relating to nuclear reactors, 20: 40366
PRITCHETT, William C., Chlorine logging apparatus with temperature compensation circuit, 20: 39136
PROCHAZKA, Z., Contribution to estimation of radiosensitivity in domestic fowl, 20: 38676
PROCTOR, J. F., Large scale separation of ^{210}Po from Bi, 20: 38996 (DP-1066(Vol.2), pp II.79-102)
PROKHOROV, V. M., Relationship between diffusion rate of ^{90}Sr and soil moisture content, 20: 38918
PROKOPEV, E. P., Annihilation of slow positrons in ionic media, 20: 39819
PROKOSHKIN, Yu. D., Measurement of π^0-meson lifetime, 20: 39821
PRONKO, J. G., Properties of states of ^{21}Ne from $^{18}O(\alpha,n\gamma)^{21}Ne$, 20: 40156
PSHEZHETSKII, S. Ya., Energy transfer mechanism in radiolysis of ammonia adsorbed on zeolites, 20: 38944
PURO, Jaakko, Mutational response of premeiotic germ-cell stages of adult Drosophila melanogaster males to x irradiation, 20: 38607
PUT, L. W., Reaction $^{27}Al(p,\alpha)^{24}Mg$ studies with a 30-Mev AVF cyclotron, 20: 40101
PYPER, J. W., Isotopic disproportionation reaction between light and heavy water using pulsed-molecular-beam mass spectrometer, 20: 38875 (UCRL-14703-T)
PYTLINSKI, J., Relaxation phenomena in rare gases seeded with alkali-metal substances, 20: 39700
PYZHOVA, Z. I., Separation of ionium (^{230}Th) from U, Pa, Fe, Mn, and Eu by cation exchange, 20: 38834

Q

QUAIFE, M. A., Effects of pulsed fission spectrum neutron irradiation, 20: 38637
QUINTON, A. R., Observation of proton channeling in thin mica, 20: 40324
QURESHI, Zafar Ahmad, Effects of γ radiation on grain moth, Sitotroga cerealella, 20: 38705

R

RABSON, Thomas A., Temperature stabilized radioactivity well logging unit, 20: 39140
RABSON, William R., Temperature stabilized radioactivity well logging unit, 20: 39140
RABY, T. M., Reactivity evaluation of SM-1 Core III qualification fuel plates, 20: 40374 (ACNP-63562)
RACHINSKII, F. Yu., Chemical structure and radioprotective properties of aminothiols and derivatives, 20: 38724
RACHINSKII, F. Yu., Evaluation of models for initial selection of radioprotective compounds, 20: 38729
RACHOR, L., Fuel development for THTR, 20: 40467
RACZKA, R., Degenerate representations of the symplectic groups. I., 20: 39850 (IC-66/77)
RADBILL, John R., Ion propulsion device, 20: 39095
RADHA, T. K., Equal-time commutators and photoproduction sum rules, 20: 39879
RADHAKRISHNAN, V., Energy dependence of effective interaction in superconductivity, 20: 40017
RAEVA, N. V., Effect of novocaine on course of acute radiation sickness and immunogenesis, 20: 38727
RAGALLER, K., Interaction of plasma jet with axisymmetric magnetic field, 20: 40231
RAGGENBRASS, A., ELAN: installation for recovery and packaging of ^{137}Cs in France, 20: 39319 (DP-1066(Vol.2), pp II.33-44)
RAHMAN, M., Dual-purpose unit for high vacuum pumping system and leak detection in vacuum chambers, 20: 39096 (AECD-EP-11)
RAICA, Nicholas Jr., Review of the U. S. Army wholesomeness of irradiated food program 1955–1966, 20: 39302
RAINBOW, M. T., Time delays in Ar–propane proportional and Geiger counters, 20: 39215
RAJA RAO, M., Measurement of the internal conversion coefficient of the 800 kev transition of ^{134}Ba, 20: 40095
RAKIN, V. G., Relationship between superconductivity and structure of Zr–4Nb alloy, 20: 40021

RALPH, J. C., Atmospheric pressure discharges in inert gases seeded with alkali metal vapor, 20: 39715
RAMACHANDRAN, T. R., Dissolution spirals on gamma-irradiated lithium fluoride, 20: 40293 (AD-634746)
RAMANAIAH, Gundala, Load supporting capacity of vertical plasma cylinder, 20: 40216
RAMANATHAN, Ganapathiagraharam Visvanathan, Correlations in an equilibrium plasma, 20: 40272
RAMATY, R., Galactic cosmic-ray electrons, 20: 39630
RAMLER, W. J., Superconducting plates as magnetic shields, 20: 39523
RAMSKILL, Eugene A., Fire and noxious gases: effect on internal environments of protective shelters, 20: 39059
RAMTHUN, Heinz, Half life and specific activity of ^{226}Ra, 20: 40127
RANDALL, C. H., Mathematical foundation for empirical science with special reference to quantum theory. I., 20: 39998 (KAPL-3147)
RANGA, H. A., Effect of π and Σ molecular states in Ne^+-Ne scattering, 20: 39601
RAO, K. A., Thermal annealing of recoil damage in Co chelates, 20: 38965
RAO, M. N., Cosmic ray produced phosphorus isotopes in atmosphere, 20: 39991
RAO, P. S., Intensity of the 1.114-Mev gamma transition in the decay of ^{65}Zn to ^{65}Cu, 20: 40093
RAO, P. Venugopala, Neutron reaction cross sections of Se and Fe at 14.4 Mev, 20: 40079 (ORO-3346-2)
RAPPAPORT, P., Low-energy proton bombardment of GaAs and Si solar cells, 20: 40299
RARATY, L. E., Correlation of fatigue properties of Magnox AL80 in terms of plastic strain range, 20: 39419
RASSBACH, M. E., Lunar period, solar period, and K_p, 20: 39982
RATCLIFFE, C. A., Advanced alpha-beta-gamma hand and shoe contamination monitor, 20: 39198 (BNWL-250)
RAUSCH, W., Experimental methods for flow in spherical bodies, 20: 39051
RAVNIK, V., Separation of ^{99m}Tc from ^{99}Mo sorbed on aluminum oxide, 20: 38997 (NIJS-R-483)
RAY, A. E., Crystal structure of $CeFe_7$, $PrFe_7$, $NdFe_7$, and $SmFe_7$, 20: 39409
RAY, J. A., Atomic and molecular cross sections, 20: 39580 (ORNL-3989, pp 78-88)
RAYNOR, G. V., Effect of cold work on x-ray diffraction patterns of rare-earth metals, 20: 39421
RAZUMOVA, K. A., Plasma energy measurement in Tokamak, 20: 40187
REATTO, L., Ground state of liquid ^4He, 20: 40030
REBUT, P. H., Waves in an inhomogeneous plasma, 20: 40258
RECHITSKII, I. V., Inelastic π^--p interactions with slow-recoil protons at 17 Bev, 20: 39830
REDI, Olav, Spin of ^{48}V, 20: 40154
REDIES, M., Determination of total K in soils using gamma emission of ^{40}K, 20: 39280
REED, Dale H., Chlorine logging apparatus with temperature compensation circuit, 20: 39136
REES, D. R., Oyster Creek nuclear station: design concept, construction, and training program, 20: 40436
REICH, M., Engineering problems in pulsed neutron sources, 20: 40456 (BNL-10454)
REICHART, W., Q value of reaction $^{27}Al(p,\alpha)^{24}Mg$, 20: 40099
REICHENBACH, H., Behavior of shock waves in ducts and when entering entrance structures, 20: 39072
REID, G. C., Cesium electron bombardment ion engines, 20: 39093
REILLY, Harry J., Heat-transfer analysis of Plum Brook reactor, 20: 40461 (NASA-TN-D-3552)
REINES, Frederick, Conference on a deep underground laboratory, Johannesburg, South Africa, 10/65, 20: 39016 (COO-818-94)
REINHARDT, R. G., Injection and accumulation: single-pass experiments (DCX-1), 20: 40171 (ORNL-3989, pp 1-13)
REISER, Martin, Space charge effects and current limitations in cyclotrons, 20: 39529
REMIZOVA, I. V., Adrenaline influence on leukocytic and glycemic reactions in irradiated rabbits, 20: 38686
RENNARD, R. J. Jr., Hydrogenation of ethylene and propylene over palladium hydride, 20: 38908
RENNERT, P., Statistical treatment of finite nuclei, 20: 40115
RENNINGER, G. H., Ambiguity of meson-baryon couplings in bootstrap static model of SU(6) symmetry, 20: 39813
RESIBOIS, P., Comments on Brownian motion theory, 20: 39596
RESMINI, F., Acceleration of H^- ions and extracted beam measurements in Milan cyclotron, 20: 39550
RESNIKOFF, M., Meson mass formulas for the 405 multiplet of SU(6), 20: 39886
REUSCHL, H., Gamma radiolysis of 5-bromouracil, 20: 38968
RHODE, J. I., Interactions (π-p) at 460 Mev, 20: 39793
RHODES, Buck A., Are iodotyrosines normal constituents of plasma?, 20: 38561
RHOTEN, Merle L., Neutron radiography of pyrotechnic cartridges, 20: 39334
RHYNE, J. J., Magnetic anisotropy of terbium, 20: 40346
RICATEAU, Pierre, Effect of ionization saturation and duct shape on losses near walls, 20: 39673
RICATEAU, Pierre, Minimum-volume conversion duct, 20: 39664
RICH, H. W., Public shelters in Denmark, 20: 39079
RICHARDS, P., Comments on ^{99m}Tc, 20: 38986
RICHARDSON, D. M., Vacuum studies, 20: 39097 (ORNL-3989, pp 128-33)
RICHARDSON, J. Reginald, Meson facility (H^-), 20: 39540
RICKAYZEN, G., Two-fluid model of superconductivity, 20: 40037
RIEDEL, H. J., Reprocessing of nuclear fuels by fluoride volatilization with sulfur hexafluoride, 20: 40389
RIKENGLAZ, L. E., Stability of nonhomogeneous electron beam, 20: 40245
RILEY, P. J., Measurement of radial voidage distribution in two-phase flow by isokinetic sampling, 20: 39045 (AEEW-M-650)
RILEY, Peter Julian, Neutron time-of-flight studies of ^{10}B, ^{11}C, and ^{20}Ne, 20: 40164
RINEHART, Robert R., Prog. rpt. on x-ray induced changes in Drosophila germ cells, 9/65–8/66, 20: 38596 (SAN-590-1)
RINGNES, Truls S., Secular variations in the magnetic field strength of sunspot groups, 20: 39559
RINGO, G. R., Measurement of electron-neutron interaction by asymmetrical scattering of thermal neutrons by noble gases, 20: 40129
RIPEANU, S., Use of slow neutrons for study of dynamic processes in liquids, 20: 40338
RIPOUTEAU, F. A., Polarized protons and deuterons source for axial injection into Grenoble isochronous cyclotron, 20: 39527
RITCHIE, R. H., Surface plasmon dispersion relation for electron gas, 20: 40225
RIVIERE, R., Determination of iodine by radioactivation analysis, 20: 38849
RIZZITANO, Fortunato J., Structural, high strength U alloys, 20: 39440
ROBASCHIK, D., Calculation of coefficients of mass operators, 20: 39855 (JINR-E-2771)
ROBERT, J., Synergetic effect of x rays and of vincaleucoblastine on solid isologous tumor of mouse C^3H, 20: 38613
ROBERTS, M., Dual-purpose unit for high vacuum pumping system and leak detection in vacuum chambers, 20: 39096 (AECD-EP-11)
ROBINSON, E., High-temperature testing and evaluation of graphite helical-screw expanders and compressors, 20: 39026 (UCRL-14660(Rev.1))
ROBINSON, J., Polarization of the neutron from $\Sigma^+ \rightarrow \pi^+ + n$, 20: 39748 (COO-881-76)
ROBINSON, Loyd R. Jr., Monitoring streams for radioactive wastes, 20: 38742
ROBSON, B. A., Distorted wave analysis of the reaction $^{14}N(d,p)^{15}N$ at low bombarding energies, 20: 40122
ROCHOW, H., Evaluations on chemical reactions of carbides and oxides suitable for construction of nuclear-fueled thermionic emitters, 20: 39353 (BMwF-FBK-66-07)
RODARI, T., Changes in antiinsulin antibodies subjected to radioactivity, 20: 38579
RODCHENKOV, B. S., Corrosion resistance of reactor materials, 20: 39349
RODERICK, Thomas H., Longevity and body weights of mice with ancestral spermatogonial x irradiation, 20: 38648
RODERICK, Thomas H., Prog. rpt. on quantitative population genetics of mice under irradiation, annual, 7/65–5/66, 20: 38590 (NYO-1979-13)
ROEDERS, J. D. A., Reaction $^{27}Al(p,\alpha)^{24}Mg$ studies with a 30-Mev AVF cyclotron, 20: 40101
ROEMBKE, James, Actual versus hypothetical fallout-shelter case studies, 20: 39086
ROESSLER, K., Chlorine-36 and ^{82}Br isotopic exchange in solid Co and Rh dihalobis halogenides, 20: 38960
ROESSNER, W., Effect of radiomimetics and x rays on permeability of blood-brain barrier, 20: 38609
ROGERS, John D., Comparison of saturated-liquid viscosities of low molecular substances, 20: 39940
ROHRMANN, C. A., Formation of selected fission products in power reactors, 20: 40400 (BNWL-244)
ROLNICK, William B., Phase of scattering amplitude for charged bosons, 20: 39899
ROMAN, P., Classical field theory and gravitation in a de Sitter world, 20: 40006
ROMANOV, E. P., Relationship between superconductivity and structure of Zr–4Nb alloy, 20: 40021
ROMANTSEV, E. F., Formation of organic peroxides as one of first biochemical reactions to radiation, 20: 38660
ROSE-INNES, A. C., Distribution of current in type-II superconductor, 20: 40029
ROSEN, Gerald, Unitary irreducible representations of SL(3,R), 20: 39871
ROSENFELD, Arthur H., Elementary guide to the elementary particles, 20: 39768 (UCRL-11100(Rev.1))
ROSENKOVITCH, Emma, Effect of whole body irradiated and methylhydrazine in eradicating transplant leukaemia 1210, 20: 38794

ROSS, C. P., Performance of the HWCTR safety systems, 20: 40457 (DP-1049, pp 1-19)
ROSS, William J., Measurement of electron content at magnetic equator, 20: 39975
ROSSEL, J., Reactions $^{40}Ca(n,\alpha)^{37}Ar$ and $^{19}F(n,\alpha)^{16}N$ with 6-Mev neutrons, 20: 40100
ROTHE, E. D., Search for the quiet-time solar gamma rays from balloon altitudes, 20: 39565
ROTTER, I., Threshold states and reduced cluster widths in light nuclei, 20: 40086
ROTURIER, Jacques, Investigation of bound neutron-neutron state in reaction $^{9}Be(n,2n)^{8}Be$, 20: 40091
ROUQUEROL, Francoise, Texture study of divided solids by gas adsorption, 20: 39387 (CEA-R-2947)
ROUX, R., Effects of confinement in high-frequency discharges at low pressure, 20: 40278
ROUX, R., Study of a confinement of a plasma in spherical cavity, 20: 40277
ROWE, M. W., Isotopic composition of Xe from Ca-poor achondrites, 20: 39984
ROWLAND, M. C., Behavior of selected steels exposed in flowing sodium test loops, 20: 39345 (GEAP-4831)
ROY, D. K., Radiotherapy in treatment of carcinoma of cervix and its complications, 20: 38754
ROZYCHI, Cezary, Thiocyante ions in colorimetric analysis, 20: 38808
RUBIN, C. P., Creep of axisymmetric shells, 20: 39391 (CONF-660629-1)
RUBIN, G. A., Fabrication and characterization of metal carbide-graphite composites, 20: 39367
RUBINOVA, E. E., Defects in silicon produced by irradiation with fast neutrons at 77°K, 20: 40334
RUBINSTEIN, H. R., Current algebras and matrix elements of axial-vector current, 20: 39892
RUDEE, M. L., Singularities in coherent diffuse scattering of x rays, 20: 39586
RUDGE, M. R. H., Excitation of atomic hydrogen by electron impact, 20: 39610
RUDRAIAH, N., Pulsating MHD flow in annular channel, 20: 39942
RUEDISUEHLI, P., Stability of a cylindrical plasma, 20: 40198
RUEHL, W., Multilinear invariant forms built of an arbitrary number of unitary representations of SL_{nC}, 20: 39878
RUEHL, W., Relativistically invariant model of SU_6 symmetry, 20: 39875
RUHS, N., Reduction of the dimensions of induction converters by skin-heating, 20: 39693
RUPP, A. F., Production of radioisotopes in power reactors, 20: 39315 (DP-1066(Vol.1), pp I.29-52)
RUPP, W. Dean, Photochemistry of iodouracil and survival of uv-irradiated T1 bacteriophage, 20: 38704
RUSAKOV, S. V., Photoproduction of π^0 mesons on ^{4}He near to threshold, 20: 39822
RUSH, J. E., Application of π-N scattering results to Λ-K^0 production, 20: 39803
RUSSELL, A. H., Closed-cycle nuclear MHD studies using dust suspensions, 20: 39728
RUSSELL, F. M., Super-SOC, 20: 39543
RUTLAND, D., Prototype thermoluminescent dosimetry system for personnel monitoring, 20: 39224
RUTOWSKI, R. W., Production of carbon plasmas, 20: 40209
RUYTERS, P. J. M., Protective recommendations, measures, and construction in the Netherlands, 20: 39076
RUZICKA, Jaromir, Substoichiometric determination of amount of carrier in a "carrier-free" ^{65}Zn preparation, 20: 38814
RYAN, K. R., Lozier tube for ionization studies not involving mass analysis, 20: 39167 (AD-636927)
RYBALCHENKO, R. V., Preparation of the carbides (Ti,W,Cr)C and study of their properties, 20: 39431
RYBALKO, V. S., Modified resonance extraction method from relativistic cyclotron, 20: 39520
RYKOV, V. A., One-dimensional motion of finite mass of like charge particles concentrated in plane, 20: 40243
RYON, A. D., Prog. rpt. on unit operations, 10–12/65, 20: 38998 (ORNL-3958)
RYON, John W., Ball-type control for nuclear reactor, 20: 40370
RYPAR, V., Water treatment by direct LiOH addition, 20: 40464 (UJV-1180-64)
RYPAR, V., Water management for power increase in WWR-S reactor, 20: 40465 (UJV-1181/64)

S

SABBIONI, Enrico, Determination of Mg in Al by neutron activation, 20: 38804
SABEU, M., Inelastic π^- p-interactions at energy 7.5 Bev. II., 20: 39758 (JINR-P-2773)
SABINA, A. C., Water analysis, 12/63–11/64, 20: 38800 (PAEC(C)RE-652)
SABININ, A. A., Corrosion resistance of reactor materials, 20: 39349
SABIR, A., Dual-purpose unit for high vacuum pumping system and leak detection in vacuum chambers, 20: 39096 (AECD-EP-11)
SACHITHANANTHAN, C., Gamma emitters in marine organisms. I., 20: 38560
SADIKOV, I. P., Nuclear reactor oscillation-measuring device, 20: 40361
SADOUNE, Joseph, Ceramic materials for magnetoaerodynamic conversion duct electrodes, 20: 39708
SADYKOV, Kh. M., Lifetimes of the excited levels of ^{151}Pm, 20: 40105
SAFAROV, R. Kh., Influence of blocking effects on nuclear moments of inertia, 20: 40102
SAFRONOVA, M. V., Radiation protection during operation of x-ray devices, 20: 38737
SAGDEEV, R. Z., Theory of nonlinear waves in plasma, 20: 40235
SAHA, Mihir K., Photosensitized polymerization of methyl methacrylate using uranyl, vanadyl and molybdenyl salts, 20: 38934
SAIBEKOV, T., Changes in biochemical and physiological indices in guinea pigs during internal chronic irradiation, 20: 38662
SAKAI, M., Single RACE spectrometer, 20: 39206 (INSJ-99)
SAKAI, Masako, Modification of perivascular subcutaneous connective tissue reaction following x-ray irradiation, 20: 38640
SAKMAR, Ismail A., Crossing problem for backward cone and threshold, 20: 39798
SAKSONOV, P. P., Prophylaxis of diseases caused by multiple external gamma irradiation, 20: 38726
SALAITA, George Nicola, Pulsed-neutron measurements of diffusion parameters of heavy and light water mixtures, 20: 40061
SALAM, Abdus, Relativistic U(6,6) theory, 20: 39888
SALIN, Antoine, Excitation of hydrogen by protons, 20: 39583
SAMPLE, Howard Horshaw, Heat capacity of solid ^{3}He, 20: 40013 (IS-T-84)
SAMPSON, H. T., Gamma-electric cell theory and experiment, 20: 39652
SAMPSON, W. B., Magnetic fields in superconducting quadrupole lens, 20: 39479 (BNL-10495)
SANCHO, F. J., Adiabatic invariance for quantum systems, 20: 40011
SANDARS, P. G. H., Enhancement factor for electric dipole moment of the valence electron in an alkali atom, 20: 39598
SANDERS, J. P., Appropriate values for thermal conductivity of UO_2 for use in design of BONUS superheaters, 20: 39403 (ORNL-TM-1450)
SANDROCK, Gary D., Cold reduction as a means of reducing embrittlement of a cobalt-base alloy (L-605), 20: 39399 (NASA-TN-D-3528)
SANGIUST, V., Szilard-Chalmers recoil of ^{60}Co and ^{60m}Co, 20: 38962
SANSOM, B. F., Metabolism of radium in dairy cows, 20: 38552
SANTINI, M., Temperature dependence of critical velocity of positive ions in liquid helium, 20: 40033
SANTRY, D. C., Cross section for reactions $^{65}Cu(n,p)^{65}Ni$, $^{65}Cu(n,2n)^{64}Cu$, and $^{65}Cu(n,n\alpha)^{61}Co$, 20: 40149
SANTY, M. J., Chemical integrity of radioisotope containment materials in launch abort environments, 20: 39312 (SC-CR-66-2044)
SAPERSTEIN, A. M., Theory of W production in nucleon-nucleon collisions, 20: 39797
SAPHIER, D., Analysis of dynamic behavior of dual purpose power/desalination nuclear plants, 20: 40438
SARGENT, C. P., Shell effects in high energy photoproton spectra from ^{6}Li, 20: 40077 (MIT-2098-256)
SARKAR, N. H., Analytical expression for mass-scattering cross section of carbon, 20: 39588
SARKISOV, E. S., Valent states and interatomic distances in metal crystals of elements of seventh period, 20: 40296
SARKISYAN, L. A., Modified resonance extraction method from relativistic cyclotron, 20: 39520
SARTELL, Jack A., Beryllium alloy and process, 20: 39374
SARYCHEVA, L. I., Angular distributions of muons in ground and under water and their generation mechanism, 20: 39831
SATO, Sennosuke, Statistical analysis of mechanical strength of graphite, 20: 39408 (NSJ-tr-46)
SATO, Teruyuki, Preliminary experiment on ion cyclotron resonance of highly ionized plasma, 20: 40260
SAUNDERS, Alan Charles Anthony, Improvements in or relating to fuel elements for nuclear reactors, 20: 40396
SAUVARD, Sandra, Action of reticulin on accumulation of ^{32}P in various organs and endocrine glands, 20: 38572
SAVCHENKO, O. V., Measurements of half-life ratio of π^+ and π^- mesons, 20: 39760 (JINR-P-2802)
SAVENKO, I. A., Radiometric equipment on the Cosmos 41 satellite, 20: 39171
SAVIN, V. N., Changes in barley plant growth and leaf-forming rate following γ irradiation of seed, 20: 38691
SAVITSKII, I. V., Contents of glycogen and ribonucleic acid and phagocytic activity of leukocytes during x irradiation of rabbits, 20: 38681
SAVUN, O. I., Radiometric equipment on the Cosmos 41 satellite,

20: 39171
SAWYER, James O., Prog. rpt. on solid-state chemistry of rare earth oxides, annual, 1965–66, 20: 38861 (COO-1109-22)
SAXENA, S. C., Isotope separation by thermal diffusion columns, 20: 39323
SAXENA, V. K., Isotope separation by thermal diffusion columns, 20: 39323
SCALAPINO, D. J., Radiation-induced structure in d-c Josephson current, 20: 40035
SCANDRETT, J. H., Interations (π^-p) at 460 Mev, 20: 39793
SCHAERF, C., Charged pion photoproduction on light nuclei, 20: 40075 (LNF-66/30)
SCHARDIN, H., Behavior of shock waves in ducts and when entering entrance structures, 20: 39072
SCHEAR, W., Digital computer program for calculation of extent of exchange from liquid scintillation counting data, 20: 39226
SCHECHTER, J., Nonleptonic decays of hyperons in broken SU(3) × SU(3), 20: 39893
SCHERB, Maurice V., Compensated nuclear radiation fluid analyzer, 20: 39191
SCHERER, Maurice, Sidereal variation of cosmic muon component at 440-m depth, 20: 39626
SCHIAU, S., Influence of ionizing radiations on cortico-suprarenal system evaluated on basis of potassium in rabbits, 20: 38697
SCHIEWER, E., Exchange adsorption of cations on TiO_2 · aq, 20: 39002
SCHILL, W. G., Injection and accumulation: single-pass experiments (DCX-1), 20: 40171 (ORNL-3989, pp 1-13)
SCHILLER, W., Statistical treatment of finite nuclei, 20: 40115
SCHLAGER, Gunther, Longevity and body weights of mice with ancestral spermatogonial x irradiation, 20: 38648
SCHLAGER, Gunther, Prog. rpt. on quantitative population genetics of mice under irradiation, annual, 7/65–5/66, 20: 38590 (NYO-1979-13)
SCHLESINGER, S. P., Cyclotron harmonic radiation from electron beam injection into an afterglow plasma, 20: 40165 (AD-637710)
SCHLESINGER, S. P., Electromagnetic: acoustic wave propagation along warm plasma columns, · 20: 40166 (AD-637711)
SCHLINDLER, G., Examples of Swiss protective structures, 20: 39082
SCHLINTLMEISTER, J., New levels in ^{97}Tc, 20: 40084
SCHLOESSER, J., Uranium-235/Th fuel cycles in graphite moderated systems, 20: 40393
SCHLUDERBERG, Donald C., Ball-type control for nuclear reactor, 20: 40370
SCHLUETER, H., Helium recombination in radio frequency discharge, 20: 40247
SCHMEH, Barbara A., Power Reactor Technology. Vol. 9, No. 2, 20: 40426
SCHMEH, Barbara A., Power Reactor Technology, Vol. 9, No. 1, 20: 40430
SCHMIDT, G. B., Chlorine-36 and ^{82}Br isotopic exchange in solid Co and Rh dihalobis halogenides, 20: 38960
SCHMIDT, H., Range of burn-ups and conversion factors economic assessment, 20: 40394
SCHMIDT, Juergen, Hematological changes after irradiation of normal and damaged liver tissue, 20: 38694
SCHMIDT, Theodor, Measurement of small doses in radiation protection supervision, 20: 39246
SCHMITT, R. A., Neutron activation analysis for quantitation of selected cations in blood, 20: 38852
SCHMUTZER, Ernst, Equation of motion of point mass under consideration of gravitational radiation terms, 20: 39999
SCHNEIDER, H., Stability of a cylindrical plasma, · 20: 40198
SCHNEIDER, R. T., Thermal and reactive nonequilibrium of magnetoactive plasma flows, · 20: 40234
SCHNEIDER, Rudolf, Hematological changes after irradiation of normal and and damaged liver tissue, 20: 38694
SCHOENBRUN, R. L., Prog. rpt. on irradiation effects on brain wave correlates of conditioned behavior, final, 1960-65, 20: 38602 (UCLA-34P60-1)
SCHOLZ, A., Kinetic studies with radioactive (^{59}Fe) and nonradioactive (^{56}Fe) iron in serum, 20: 38573
SCHONFELD, Ernest, Effect of temperature on rare earth separations on cation resin columns with lactate, 20: 39004
SCHOPPER, H., Research with AVF cyclotrons in Europe, 20: 39544
SCHRADER, W. J., Influence of relativistic increase of mass on particle energy gain and trapping near cyclotron resonance, · 20: 40265
SCHREINER, Sheldon Ira, Thermionic emission from planar monocrystalline tungsten, 20: 39635 (UCRL-16699)
SCHRENK, G. L., Models for electron emission from metals with adsorbed monolayers, 20: 39641
SCHROEDER, C. F., Clean assembly practices guide, 20: 40489 (SC-DC-66-1118)
SCHROEDER, Karl, Thermal power stations for electricity age of tomorrow, 20: 40492
SCHROEDER, L. S., Isotopic spin of the η^* (960 Mev) meson, 20: 39786
SCHROEDER, Wilfried, Geographical spread of polar lights, 20: 39956
SCHROEDER, Wilfried, Morphology of polar lights, 20: 39955
SCHUELE, W., Contribution to enhanced diffusion of ^{63}Ni in alpha-irradiated pure Cu, 20: 39451 (EUR-2968.e)
SCHULER, W. B., Measurement of the lifetime of the 14.4 kev level of ^{57}Fe, 20: 40132
SCHULTE, John H., Problem of radioactive contamination of the skin, 20: 39151
SCHULTEN, R., Breeding in pebble-bed reactors, 20: 40471
SCHULTZ, C., Polarization parameter in p-p scattering from 328 to 736 Mev, 20: 39791
SCHULTZ, C., Polarization parameter in p-p scattering from 1.7 to 6.1 Bev, 20: 39792
SCHULTZ-GRUNOW, F., Evaluation of performance characteristics for Faraday generator, 20: 39645
SCHULZ, G. J., Theory of electron collision experiments, 20: 39576 (AD-636533)
SCHULZE, Werner, Fast neutrons in activation analysis, 20: 38838
SCHUSTER, K., High-temperature tests on tungsten-coated UO_2–Mo–cermets for thermionic nuclear fuel elements, 20: 39383 (BMwF-FBK-66-08)
SCHWABE, K., Localization of boundary reactions in metal–aqueous solution systems. II., 20: 39337
SCHWABL, F., Refined solution of two-dimensional model theories, 20: 39851 (IC-66/96)
SCHWEICKERT, H., Novel deflection-bunching system at the Karlsruhe isochronous cyclotron, 20: 39546
SCHWEIZER, J., Magnetic study of the intermetallic compound $NdCo_5$, 20: 39424
SCHWENTEK, Heinrich, Determination of absorption in ionosphere, 20: 39951
SCOTT, Charles D., Oxidation of H and CO in He stream by CuO, 20: 38874 (ORNL-TM-1540)
SCOTT, W. P., Orthovoltage radiation therapy, 20: 38792
SEAMAN, G. G., Comparison of rotational M1 transition rates between high and low spin states, 20: 40072 (LA-DC-8061)
SEAMAN, G. G., Further evidence for effective nucleon spin g-factors, 20: 40073 (LA-DC-8065)
SEARLE, A. G., Comparison of the mutagenic effectiveness of chronic neutron and γ irradiation of mouse spermatogonia, 20: 38647
SECREST, Bruce G., Blast waves in magnetogasdynamics with finite electrical conductivity, 20: 39944
SEDGLEY, D. B., GADOSE and DOSET: programs to calculate environmental consequences of radioactivity release, 20: 39148 (GA-6511)
SEDOV, V. V., Mechanism of death of animals with most acute form of radiation sickness, 20: 38666
SEIFERT, R., Increase in RNase and DPNase activities in ascites tumor cells induced by cytostatic agents, 20: 38578
SEKI, Yoshitatsu, Production of Al–U alloy nuclear fuel by direct reduction, 20: 39333
SEKI, Yuji, Neutron-diffusion parameters in water, 20: 40055
SELBY, T. W., Gravimetric gas flow standard, 20: 39020 (K-1632(Pt.2))
SELIVANOV, G. I., Requirements on the optical units of stereoscopic cameras used in bubble chambers, 20: 39209 (JINR-P-2728)
SEMASHKO, G. L., Spin correlation in elastic scattering of 605-Mev polarized protons on protons, 20: 39759 (JINR-P-2775)
SEN, Hari K., Electron and ion temperature in solar corona, 20: 39572
SENCHENKOVA, T. M., Radiation chemistry of carbohydrates. VII., 20: 38969
SENGUPTA, S. N., Probe data of duoplasmatron plasma, · 20: 40202
SEO, Stanley T., Gamma radiation as a quarantine treatment for Hawaiian fruit flies, 20: 39293
SERBU, G. P., Low-energy electrons measured on IMP 2, 20: 39978
SEREBRENNIKOV, V. V., Complexes of La, Y, Lu, and Sc with xylenol orange, 20: 38924
SEREBRENNIKOV, V. V., Rare earth metal and Y distribution during Zn crystallization in lead melt, 20: 39435
SERGEEVA, G. A., Solar-diurnal and semidiurnal variations of cosmic rays and their spectra as function of solar activity, 20: 39628
SERMONS, G., Effect of toothed inductor on electromagnetic-field distribution in conducting slab, 20: 39937
SERMONS, G. Ya., Effect of toothed inductor on electromagnetic-field distribution in conducting slab, 20: 39937
SERVETNIK-CHALAYA, G. K., Changes in biochemical and physiological indices in guinea pigs during internal chronic irradiation, 20: 38662
SESHADRI, S. R., Radiation from an electromagnetic source in a half-space of compressible plasma-surface waves, · 20: 40199
SESHADRI, S. R., Surface waves at plane interface between vacuum and plasma with magnetostatic field normal to interface, · 20: 40200
SESMA, J., Chakrabarti transformation, 20: 39872
SETLOW, R. B., Repair of molecular damage to DNA, 20: 38575 (ORNL-P-2267)
SHABANSKII, V. P., Radiation belts, 20: 39957
SHAFRAN, L. M., Contents of glycogen and ribonucleic acid and phago-

cytic activity of leukocytes during x irradiation of rabbits, 20: 38681
SHAKHNOV, I. I., Problems of MHD conversion: experimental results, 20: 39707
SHAKIN, C. M., Generalized Hartree-Fock calculation for ^{90}Zr using an effective interaction, 20: 40076 (MIT-2098-255)
SHALASHOV, V. A., Singularities of radiation-thermal treatment of white cast iron, 20: 39464
SHAL'NOVA, G. A., Microflora of oral cavity mucus membrane in dogs suffering from radiation sickness, 20: 38667
SHANKLAND, Donn G., Hartree-Fock scheme for obtaining electronic wavefunctions, 20: 39617
SHANKLIN, R. V., Comparison of performance of diagonal wall generators, Faraday generators, and Hall current generators, 20: 39702
SHAPIRO, G., Polarization parameter in p-p scattering from 328 to 736 Mev, 20: 39791
SHAPIRO, G., Polarization parameter in p-p scattering from 1.7 to 6.1 Bev, 20: 39792
SHAPIRO, I. S., Conservation law in elementary particle physics, 20: 39921
SHAPIRO, V. D., Stabilization of low-frequency plasma instabilities, 20: 40218
SHARMA, R. C., Cesium-137 content of man in India, 20: 39154
SHARPE, A. G., Advances in inorganic chemistry and radiochemistry. Vol. 8, 20: 38880
SHARPE, A. G., Transition metal cyanides and their complexes, 20: 38881
SHATALOVA, A. A., Use of alkyl phosphoric acids in analytical chemistry. IV., 20: 38828
SHCHERBAKOV, Yu. A., Recording of particle paths in streamer high-pressure chamber filled with helium, 20: 39245
SHCHERBININ, E. V., Problems of MHD boundary layer, 20: 39935
SHCHERBOVA, E. N., Restoration of bone marrow tissue in acute radiation sickness, 20: 38663
SHEA, K. G., Food preservation, 20: 39284 (DP-1066(Vol.1), pp IV.3-25)
SHEA, M. A., Experimental evaluation of various rigidity models, 20: 39624 (D-1-82-0529)
SHEA, R. F., Conference on isochronous cyclotrons, Gatlinburg, 5/66, 20: 39510
SHEARD, H., Large scale production and utilization of radioisotopes in the United Kingdom, 20: 39283 (DP-1066(Vol.1), pp III.33-44)
SHEEN, E. M., Advanced alpha-beta-gamma hand and shoe contamination monitor, 20: 39198 (BNWL-250)
SHEINDLIN, A. E., Electric conductivity of argon plasma with ionizing additive, 20: 39670
SHEINDLIN, A. E., Operation of MHD generator plants, 20: 39741
SHELEPIN, L. A., Theory of Clebsch-Gordan coefficients for SU_n groups, 20: 39913
SHELTON, H., Evaporative lifetimes of Cu, Cr, Be, Ni, Fe, and Ti on W and oxygenated W, 20: 40307
SHEPARD, Harvey Kenneth, Influence of the NN* channel on elastic NN scattering, 20: 39848
SHEPELAVEY, Bohdan, Global covariant conservation laws in Riemannian spaces. I., 20: 40007
SHEPELAVEY, Bohdan, Global covariant conservation laws in Riemannian spaces. II., 20: 40008
SHER, A., Polarization in LaF_3, 20: 40304
SHER, R., Measurement of infinite dilution capture resonance integrals with Moxon-Rae detector, 20: 40146
SHERMA, Joseph, Inorganic chromatography on impregnated ion-exchange papers, 20: 39000
SHERWOOD, R. C., Pressure-induced phase transformations and magnetic ordering in intrarare-earth alloys and Sm, 20: 40326
SHEVCHENKO, A. N., Mechanism of radioprotective action of indolylalkylamines, 20: 38725
SHIBAEA, N. P., Separation of ionium (^{230}Th) from U, Pa, Fe, Mn, and Eu by cation exchange, 20: 38834
SHIBATA, E., Observation of $\omega^0 \to \pi^0 + \gamma$, 20: 39787
SHIMAMURA, Akira, Single scattering calculations of sky-shine with cylindrical container penetrations, 20: 40288
SHIMANOVSKII, K. B., Roentgeno-morphological investigation of skeleton subsequent to radiation therapy of pelvic tumors, 20: 38767
SHIPUK, I. Ya., Ionization instability and turbulent conductivity of non-equilibrium plasma, 20: 39671
SHIRAI, Shogo, X-ray microanalysis of fallout from first Chinese nuclear explosion, 20: 39110
SHIRAKATA, Hirofumi, Flow velocities, seeding ratios and electrical conductivities in seeded Ar plasmas, 20: 39727
SHIRES, G. L., Measurement of radial voidage distribution in two-phase flow by isokinetic sampling, 20: 39045 (AEEW-M-650)
SHIROKOV, M. I., Time correlation of the emission and absorption of exchange photon, 20: 39577 (JINR-P-2791)
SHIUE, James C., Performance characteristics of an electrogasdynamic power generator, 20: 39649
SHKHINEK, E. K., Whole-body x-irradiation effects on content of 17-oxycorticosteroids in peripheral blood of dogs, 20: 38684
SHMULEVICH, R. S., Effect of microheterogeneity on characteristics of superconductivity of Nb–Zr–Ta alloy, 20: 40020
SHORES, Richard Dale, Reactions of hot tritium atoms produced by electron impact on T_2 with solid propene and propane, 20: 38970
SHRAUNER, E., Theory of W production in nucleon-nucleon collisions, 20: 39797
SHRUM, E. V., Search for evidence of positron emission in the decay of ^{36}Cl, 20: 40148
SHTUKKENBERG, Yu. M., Correlation of local tissue changes and general reactions at different stages of acute radiation sickness in man, 20: 38774
SHUBINA, A. V., Therapeutic effects of selachyl alcohol during experimental radiation sickness, 20: 38731
SHUTOV, A. A., Changes in barley plant growth and leaf-forming rate following γ irradiation of seed, 20: 38691
SHUVALOV, V. A., Corrosion resistance of reactor materials, 20: 39349
SICK, I., Neutron flux determination with thick $(CH_2)_n$ radiators, 20: 39223
SIDDALL, E., Use of digital control computer in nuclear power plant, 20: 40437
SIDHU, S. S., Antiferromagnetism of uranium monophosphide, 20: 39422
SIDOROV, S. K., Neutron diffraction study of ordered Ni–Mn alloys, 20: 39407 (ANL-Trans-344)
SIDOROV, V. M., Helium-8 production in negative pion capture by C and O nuclei, 20: 40071 (JINR-E-2774)
SIEBERG, Robert, An on-line nuclear analysis facility, 20: 39025 (ORO-2980-12)
SILBAR, R. R., Meson mass formulas for the 405 multiplet of SU(6), 20: 39886
SILBERBERG, Rein, Cosmic ray modulations in solar system and in interstellar space, 20: 39571
SILVERS, John P., Nuclear reactor hydropulse system, 20: 40435
SILVERSTEIN, Martin Louis, Many-particle processes, 20: 39926
SIMMONS, J. H. W., Radiation damage in graphite, 20: 39463
SIMMONS, L. M. Jr., Dispersion relation for axial-vector vertex and sum rule for axial-vector coupling-constant renormalization, 20: 39814
SIMON, P., Ionospheric absorption of emissions of radio sources and its application to knowledge of the ionosphere, 20: 39953
SIMONOFF, Gabriel, Study of isomers ^{236g}Np and ^{236m}Np by interaction of deuterons with ^{238}U, 20: 40092
SIMONOV, Yu. N., Measurement of π^+-meson lifetime, 20: 39821
SIMONOV, Yu. N., Pion production in np collisions at 600 Mev, 20: 39826
SIMONS, L., Resonances in the $^{41}K(p,\gamma)^{42}Ca$ reaction at proton energies 1740–2170 kev, 20: 40133
SIMPSON, J. A., Galactic deuterium and its energy spectrum above 20 Mev per nucleon, 20: 39987
SIMPSON, Stuart Douglas, Radiation dosimeter for measuring exposure to high and low energy radiation, 20: 39251
SINGER, Ralph M., Combined thermal convective magnetohydrodynamic flow, 20: 39930
SINGER, Ralph M., How coolant dynamics affect fast reactor safety, 20: 40363
SINGH, R. B., New forbidden lines in the L spectrum of lutetium, 20: 39613
SINGH, S. N., Magnetohydrodynamic flow in curved pipe, 20: 39931
SINGLER, A., Harmonic analysis of the diurnal variation of critical F_2-layer frequencies, 20: 39959
SINGLETON, J. H., Prog. rpt. on ultrahigh vacuum techniques, semiannual, 12/65–5/66, 20: 39098 (WERL-2823-21)
SINILA, Alexander, Radioactive sample changing and measuring apparatus, 20: 39044
SISAKYAN, I. Sh., Influence of x irradiation on the yield and chemical composition of potatoes, 20: 38690
SITNIK, I. M., Measurement of real part of π^-p elastic scattering amplitude in Coulomb interference region at 3.5 Bev/c, 20: 39785
SJOEGREN, L., Influence of collisions on whistler propagation, 20: 40196
SJOELANDER, Alf, Electronic effects on lattice modes, 20: 40344
SKAKUN, Miroslave, Synthesis of malathion labeled with ^{35}S or ^{32}P and dipterex-^{32}P, 20: 38931
SKAREK, P., Strong-focusing ring, as beam stretcher for synchro-cyclotrons, 20: 39538
SKELLY, H. M., Effect of heat treatment on corrosion behavior of two Zr–Cu–Mo alloys, 20: 39347 (NP-16239)
SKHVABE, E., Programming the accelerating voltage amplitude of a model of circular proton phasotron r.f. system, 20: 39491 (JINR-P-2732-1)
SKOBETS, E. M., Determination of rare-earth on electrode, 20: 38811
SLADIC-SIMIC, D., Hereditary hypochromic microcytic anemia in laboratory rat, 20: 38619
SLAMA, L., Mixed-field configuration without leaks, 20: 40280
SLAMA, L., Study of a confinement of a plasma in spherical cavity, 20: 40277

SLANSKY, Richard C., General analysis of nucleon-nucleon scattering, 20: 39806
SLAUGHTER, G. M., Weldability evaluation of advanced refractory alloys, 20: 39366
SLAVACHEVSKAYA, N. M., Chemical structure and radioprotective properties of aminothiols and derivatives, 20: 38724
SLAVACHEVSKAYA, N. M., Evaluation of models for initial selection of radioprotective compounds, 20: 38729
SLAVIN, L. G., Dosimetric substantiation of roentgenotherapeutic methods in dealing with hypophyseal tumors, 20: 38761
SLEPETS, L. A., Measurement of real part of π^-p elastic scattering amplitude in Coulomb interference region at 3.5 Bev/c, 20: 39785
SLOBODIAN, James Theodore, Radiation-resistant lubricants, 20: 38973
SLOVINSKII, B., Investigation of interaction of π^--mesons with Xe nuclei at 5 and 9 Bev/c, 20: 39755 (JINR-P-2736)
SLUTSKINA, S. I., Dosage loads in medical staff dealing with colloidal ^{198}Au, 20: 39159
SMAL, Z., Decontamination of fabrics intended for use in production of protective clothing, 20: 39161
SMALLEY, W. R., Engineering and metallurgical evaluation of an irradiated Yankee Core I control rod, 20: 39461 (WCAP-6074)
SMART, D. F., Experimental evaluation of various rigidity models, 20: 39624 (D-1-82-0529)
SMIRNOV, A. D., Mechanism of protective action of aminothiols, 20: 38723
SMIRNOV, L. S., Infrared extinction of specific photoconductivity of germanium of the n-type produced by γ rays, 20: 40298
SMIRNOV, L. S., Infrared quenching of intrinsic photoconductivity in n-type Ge irradiated by γ rays, 20: 40337
SMIRNOV, O. P., Influence of gaseous media on injuries induced in mice by various radiation doses, 20: 38642
SMIRNOV, V. V., Corrosion resistance of reactor materials, 20: 39349
SMITH, A. J. S., Particle production by 2.9-Bev protons incident on Be and Pt, 20: 39794
SMITH, Fred A., Interpreting the French liquid-metal-heated steam-generator program, 20: 40428
SMITH, H. M. Jr., Prog. rpt. on photomultiplier investigation, 2/15–5/14/66, 20: 39212 (NYO-3421-7)
SMITH, Harold P. Jr., Cesium ion sputtering of aluminum, 20: 39585
SMITH, J., Approximate solution to the multichannel N/D equations, 20: 39880
SMITH, J. E., Use of digital control computer in nuclear power plant, 20: 40437
SMITH, Jean G., Rare earth actinide metal sols, 20: 39341
SMITH, Jean G., Sols of zirconia and hafnia with actinide oxides, 20: 39442
SMITH, John Marlin, Self-consistent incorporation of radiation into equations governing equilibrium of fully ionized gas, 20: 40270
SMITH, Joseph L. Jr., Boiling heat transfer to liquid helium, 20: 40048
SMITH, Lewis Taylor, Resonance production in K-p interactions at 1.80 to 1.96 Bev/c, 20: 39838
SMITH, Maynard E., Leaching of uranium by hydrogen chloride, 20: 39346 (LA-3488)
SMITH, R. V., Behavior of trapped electrons and protons at lower edge of inner radiation belt, 20: 39983
SMITH, Roy E., Radioactivity level detecting apparatus for samples carried by portable trays, 20: 39042
SMITHERS, R. M., Tellurium isotope fractionation study, 20: 39122
SMITT, Goesta, Fire-safe shelter design: Swedish views, 20: 39067
SMORODINSKII, Ya. A., Particles, predicted by theory, 20: 39920
SNYDER, J. N., Magnetic fields in superconducting quadrupole lens, 20: 39479 (BNL-10495)
SOBOLEV, V. V., Zonal structure of chalcogenides of rare-earth elements, 20: 40339
SODEK, Benard A. Jr., Pressure dependence of wave propagation in magnetoplasma-filled waveguide, 20: 40248
SODERQUIST, Charles E. Jr., Radioactive sample changing and measuring apparatus, 20: 39044
SOEREMARK, Rune, Concentration of V in biological specimens, 20: 38565
SOGA, Naohiro, Comparison of measured and predicted bulk moduli of Ta and W, 20: 39418
SOHL, G., Cesium electron bombardment ion engines, 20: 39093
SOJKA, Bohumil, Application of high sensitive integrator in gas chromatography, 20: 38815
SOKOLOV, M. P., Nuclear reactor oscillation-measuring device, 20: 40361
SOLOMON, R., Polarization in LaF_3, 20: 40304
SOLT, G., Hindrance effects in cold neutron scattering by rotating molecules, 20: 40323
SOMERVILLE, W. B., Ground state of H_2^-, 20: 39614
SOMMER, N. F., Irradiation of fruits and vegetables, 20: 39289 (UCD-34P73-9)
SOMMERFELDT, R. W., Magnetic moment of the lowest 2^+ vibrational state in ^{122}Te, 20: 40128
SONDHAUS, Charles A., Radiation dosimetry aboard manned space vehicles, 20: 39158
SONG, Xing-chang, Weak interactions in the SU(6) symmetry theory, 20: 39908
SOOLE, Bernard Walter, Detector of radioactivity, 20: 39249
SOROKIN, Yu. A., Energy transfer mechanism in radiolysis of ammonia adsorbed on zeolites, 20: 38944
SOROKINA, Yu. D., Effect of radioprotective agents on frequency of leukemia induced by radiation, 20: 38722
SORU-ISCOVICI, I., Morphological study of the magnetic structure in active regions with relation to chromospheric phenomena and solar flares. I., 20: 39557
SORU-ISCOVICI, I., Morphological study of the magnetic structure in active regions with relation to chromospheric phenomena and solar flares. II., 20: 39558
SOSOVA, V. F., Microflora of oral cavity mucus membrane in dogs suffering from radiation sickness, 20: 38667
SOTONA, M., Level structure of oxygen isotopes in the SU_3 scheme, 20: 40126
SOULEAU, Charles, Selenides ML_qSe_7 of structural type Y_5S_7 (L = rare earth and M = Mg, Cr^{2+}, Mn, Fe^{2+}), 20: 38884
SPADONI, Maria Antonietta, Cesium-137 and ^{90}Sr levels in diet and urine of an Italian children's community, 20: 39152
SPAETH, Albert E., Perfusion with T_2O to measure hepatic lipogenesis and lipid secretion, 20: 38559
SPEDDING, F. H., Apparent molal volumes of some aqueous rare earth chloride and nitrate solutions at 25°, 20: 38905
SPEDDING, F. H., Heat capacities of aqueous rare earth chloride solutions at 25°, 20: 38906
SPEDDING, F. H., Heats of dilution of aqueous rare-earth chloride solutions at 25°C, 20: 38870 (IS-1356)
SPEDDING, F. H., Heats of dilution of aqueous rare earth chloride solutions at 25°, 20: 38903
SPEDDING, F. H., Relative viscosities of some aqueous rare earth chloride solutions at 25°, 20: 38904
SPEISER, R. C., Cesium electron bombardment ion engines, 20: 39093
SPENCER, Lewis V., Problems of shielding against initial radiations, 20: 39061
SPENER, G., Fuel development for THTR, 20: 40467
SPIGT, C. L., Hydraulic characteristics of boiling water channel, 20: 40356 (EURAEC-1644)
SPINRAD, B. I., Long range speculations on isotopic power, 20: 39304 (DP-1066(Vol.1), pp 19-28)
SPRAGUE, Theodore S., Integral nuclear reactor-steam generator unit, 20: 40433
SPRATT, James P., Radiation-resistant device phenomena, 20: 39274 (N-66-18175)
SPRENGER, K., Space and time variations of long wave ionospheric absorption at small solar heights and at night, 20: 39960
SPRING, E., Internal pair formation in ^{22}Ne following the positron decay of ^{22}Na, 20: 40134
SREEKUMARAN, C., Urechis program: rapid survey of fallout Cs in the ocean, 20: 39147 (CONF-660401-6)
STABROVSKII, A. I., Polarography of uranium in hydrochloric acid solutions, 20: 38922
STACHEL, John J., Cylindrical gravitational news, 20: 40009
STACHURA, Zbigniew, Large permanent magnet semicircular beta ray spectrograph, 20: 39203 (INP-476/PL)
STADNIK, B. I., Crystal structure of compounds $Zr_2Ni_{21}B_6$ and $Zr_6Co_{21}B_6$, 20: 39416
STAFFORD, B., Helium recombination in radio frequency discharge, 20: 40247
STAFFURTH, J. S., Thyroid cancer after ^{131}I therapy for thyrotoxicosis, 20: 38749
STAKHANOV, I. P., Measuring electrical conductivity of a liquid–vapor K mixture, 20: 39742
STAMBACH, Th., Neutron flux determination with thick $(CH_2)_n$ radiators, 20: 39223
STAMOULI, Maria I., Effects of isomeric transition and (n,γ) activation of Br atoms in n-propyl bromide, 20: 38963
STANCU-ARDELEANU, Alexandru, Action of reticulin on accumulation of ^{32}P in various organs and endocrine glands, 20: 38572
STANFORD, George S., Thermal and epithermal spectrum measurements, 20: 40378
STAUB, H. H., Q value of reaction ^{27}Al(p,α)^{24}Mg, 20: 40099
STAVITSKII, R. V., Dosimetric substantiation of roentgenotherapeutic methods in dealing with hypophyseal tumors, 20: 38761
STCHOUZKOY, Tatiana, Protactinium peroxide compounds in basic media, 20: 38890
STEED, Patricia R., Notation and formulae for dose specification and calculations in radiotherapy, 20: 38750
STEELE, Edgar L., Use of high-speed automatic systems for medical and biologic activation analysis, 20: 38843

STEFAN, Maria, Protective effect of glycine in x irradiation, 20: 38714
STEHLIK, G., Analysis of the volatile constituents of irradiated apple juice, 20: 39300
STEHLIK, Gerhard, Use of neutron activation analysis in determination of trace elements in tobacco mosaic virus, 20: 38846
STEIN, H. J., Comparison of neutron and gamma-ray damage in n-type silicon, 20: 40303
STEIN, William E., Instrumentation for fission studies, 20: 39242
STEINER, E., Cross section of $^{73}Ge(n,\alpha)^{70}Zn$ reaction at 14 Mev, 20: 40098
STEINER, H., Polarization parameter in p-p scattering from 1.7 to 6.1 Bev, 20: 39792
STEKERT, James Joseph, Traveling-wave nature of Cherenkov interaction, 20: 39501
STEKLY, Z. J. J., Large experimental superconducting magnet for MHD power generation, 20: 39643
STEKLY, Z. J. J., Model MHD type superconducting magnet, 20: 39733
STELJES, J. F., Cosmic ray NM-64 neutron monitor data-III, 20: 39623 (AECL-2598)
STENDER, Hans-Stephan, Hematological changes after irradiation of normal and damaged liver tissue, 20: 38694
STENDER, Hans-Stephan, Influencing properdin and agglutinin formation by whole-body irradiation, 20: 38695
STEPANOV, A., Experiments on ion acceleration at 685-mm sector cyclotron, 20: 39549
STEPANOV, A. V., Ion optical studies of extraction transport and analysis systems for 240 cm cyclotron, 20: 39545
STEPHAN, Brian G., Experimental evaluation of MHD generators operating at high Hall coefficients, 20: 39667
STEPHENS, D. R., Phase diagram and compressibility of neptunium, 20: 39423
STEPHENS, S. A., Directional variation of geomagnetic cut-off rigidity around Hyderabad, India, 20: 39988
STERESCU, N., Action of reticulin on accumulation of ^{32}P in various organs and endocrine glands, 20: 38572
STERLINI, Jacques, MHD generator using an emulsion, 20: 39678
STEWART, D. C., Analytical chemistry. Vol. 6, 20: 38817
STEWART, D. C., Effect of temperature on rare earth separations on cation resin columns with lactate, 20: 39004
STILLMAN, D. B., FRAN prompt burst reactor, 20: 40463 (UCRL-14413)
STOCKWELL, Norman David, Extraction of He ion beam from an optically polarized He source gas, 20: 39619
STOECKLIN, Gerhard, Reactions of energetic carbon atoms in methylamine, 20: 38964
STONE, G. Duane, Prog. rpt. on solid-state chemistry of rare earth oxides, annual, 1965–66, 20: 38861 (COO-1109-22)
STONE, Helen B., Quantitative radiosensitivity studies of solid carcinomas in vivo, 20: 38635
STONE, L. R., SNAP-10A expansion compensator, 20: 39023 (NAA-SR-11952)
STONESCU, R., Influence of ionizing radiations on cortico-suprarenal system evaluated on basis of potassium in rabbits, 20: 38697
STORER, John B., Longevity and body weights of mice with ancestral spermatogonial x irradiation, 20: 38648
STRATHDEE, J., Relativistic U(6,6) theory, 20: 39888
STRATTON, R. F., High-current ion-beam production and injection, 20: 40175 (ORNL-3989, pp 89-94)
STRATY, G. C., Helium-4 melting curve below 1°K, 20: 40032
STREETER, David, Inactivation of tobacco mosaic virus by ultraviolet light, 20: 38584
STREFFER, Christian, Biological radiation protection. LXX., 20: 38717
STREHLOW, R. A., Vacuum studies, 20: 39097 (ORNL-3989, pp 128-33)
STREL'TSOVA, V. N., Changes of kidneys in animals during radiation sickness when treated with unithiol, 20: 38719
STRICKLER, T. D., Application of solid-state nuclear track detectors to Hurst threshold detector system, 20: 39221
STRINI, G., Acceleration of H- ions and extracted beam measurements in Milan cyclotron, 20: 39550
STROBEL, G. L., Distorted wave calculations of low-energy deuteron stripping reactions, 20: 40114
STROEMME, A., Diminution of radiocesium body-burden in dogs and human beings by Prussian Blue, 20: 38557
STROEMME, Aksel, Radiation exposure of gonads during betatron therapy at 31 Mev, 20: 38746 (NYO-3364-19)
STRUGAL'SKII, Z. S., Investigation of interaction of π^--mesons with Xe nuclei at 5 and 9 Bev/c, 20: 39755 (JINR-P-2736)
STRUMINSKII, B. V., Configuration mixing in quark model, 20: 39861 (JINR-P-2821)
STRUNOV, L. N., Measurement of real part of π-p elastic scattering amplitude in Coulomb interference region at 3.5 Bev/c, 20: 39785
STRUXNESS, E. G., Radionuclides in Clinch-Tennessee Rivers, 20: 40479 (ORNL-P-2328)
STULIK, K., Amperometry with two polarizable electrodes. X., 20: 38810
SUBBOTIN, V. I., Injection of liquid metals in MHD converters, 20: 39669
SUBBOTIN, V. I., Measuring electrical conductivity of a liquid–vapor K mixture, 20: 39742
SUBRAMANYAN, V., Extraction of protactinium by long-chain amines from hydrochloric acid solutions, 20: 39003
SUBRAMANYAN, V., Paper electrophoresis of protactinium in sulfuric acid medium, 20: 38826
SUCCI, C., Acceleration of H- ions and extracted beam measurements in Milan cyclotron, 20: 39550
SUCHOZA, B. P., Shippingport Atomic Power Station disposition of radioactive waste from underground storage tanks, 20: 40481 (WAPD-T-1851)
SUDAREVA, S. V., Relationship between superconductivity and structure of Zr–4Nb alloy, 20: 40021
SUDDATH, J. C., Prog. rpt. on unit operations, 10–12/65, 20: 38998 (ORNL-3958)
SUHR, R. W., Correlation of fatigue properties of Magnox AL80 in terms of plastic strain range, 20: 39419
SUK, M., Momentum spectra of secondary particles in (π^-,N) interactions at 7 Bev, 20: 39751 (JINR-E-2738)
SULYAEV, R. M., Measurement of the cascade time of negative pions in gaseous ^3He, 20: 39579 (JINR-P-2838)
SUNDERLAND, Robert J., Ion propulsion device, 20: 39095
SUNDERLAND, Robert J., Magnetically induced ionization in rare gas mixtures, 20: 39679
SUPONITSKII, Yu. L., Heat of formation of lanthanum selenites, 20: 38900
SUPONITSKII, Yu. L., Heat of formation of praseodymium selenites, 20: 38901
SUTER, H., Center (V_k) in $SrCl_2$ crystals, 20: 40319
SUTHERLAND, Wm. A., Improved heat transfer performance with boundary layer turbulence promoters, 20: 39048 (GEAP-5115)
SUURA, H., Dispersion relation for the axial-vector vertex and sum rule for axial-vector coupling-constant renormalization, 20: 39814
SUVOROV, A. P., Angular distribution of fast neutrons behind iron shielding, 20: 40286
SUVOROV, N. N., Mechanism of radioprotective action of indolylalkylamines, 20: 38725
SVANHEDEN, A., Regenerative beam extraction in synchrocyclotrons, 20: 39522
SVELTO, V., Review of theories and experiments of resolving time with scintillation counters, 20: 39239
SVENNE, J. P., Generalized Hartree-Fock calculation for ^{90}Zr using an effective interaction, 20: 40076 (MIT-2098-255)
SVIDERSKII, V. I., Use of mica and quartz glass for nuclear fission detection at high temperature, 20: 39208 (JINR-P-2705)
SVIRIDOV, N. K., Therapeutic effects of selachyl alcohol during experimental radiation sickness, 20: 38731
SVISTOVA, E. A., Magnetoresistance of Bi in fields up to 450 kOe at He temperatures, 20: 40027
SVYATUKHIN, M. V., Effect of radioprotective agents on frequency of leukemia induced by radiation, 20: 38722
SWAIN, J. H., Plunging magnet system for the NIMROD extracted proton beam, 20: 39496 (RHEL-R-117)
SWARTOUT, John A., Oceanographic applications of nuclear energy, 20: 39313
SWEET, William H., Prog. rpt. on use of isotopes and slow neutrons in diagnosis and treatment of neoplasms, 6/65–5/66, 20: 38745 (NYO-3267-3)
SWISHER, Joe A., Application of fast neutron activation analysis to polymer dosimetry, 20: 38937 (AD-635655)
SWYNGEDAUW, J., Treatment of Basedow's disease with radioactive iodine, 20: 38760
SYRBU, N. N., Zonal structure of chalcogenides of rare-earth elements, 20: 40339
SYROVOI, V. A., Solution of equations for regular electrostatic beam, 20: 40242
SZASZ, Gy., Influence of x-irradiation on course of adrenalin-lymphocytosis, 20: 38678
SZIKLA, G., Partial amygdalo-hippocampal destruction by ^{90}Y in treatment of certain rhinencephalic types of epilepsy, 20: 38779
SZKOPIAK, Z. C., Snoek peaks and their stability in annealed and deformed tantalum, 20: 39420
SZTERK, L., Fission product distribution in coating of fuel elements for high temperature reactors, 20: 40386 (SGAE-CH-33/1966)

T

TABIEVA, G. Kh., Magnetoresistance of Bi in fields up to 450 kOe at He temperatures, 20: 40027
TACEV, T., Mechanism of protective effect of thiopental, 20: 38738
TADZHIKOV, M. M., Separate determination of daughter products of radon and thoron during alpha therapy, 20: 38775
TAENZER, Volker, Radiogenic radiation protection effect, 20: 38696
TAGLIAFERRI, G., Acceleration of H- ions and extracted beam measure-

ments in Milan cyclotron, 20: 39550
TAHA, M. O., Reduced-amplitude equations for two- and three-particle systems. I., 20: 39874
TAKAHASHI, S. K., Resistance of tubular structures to dynamic loading, 20: 39007 (AD-636914)
TAKAKI, Hideo, Possible distribution of ion density in iono-exosphere with dipole magnetic field, 20: 39968
TAKAKURA, Koichi, Polymerization of cyclic ethers in presence of maleic anhydride. I., 20: 38953
TAKEDA, Atsuhiko, Observations on thymus of mice after x irradiation, 20: 38606
TAKEDA, Susumu, Low-electron-density measurements of transient plasmas by optical interferometers, 20: 40214
TAKHTAMYSHEV, G., The search for "long-lived" Λ^0-particles, 20: 39762 (JINR-P-2849)
TALAIRACH, J., Partial amygdalo-hippocampal destruction by ^{90}Y treatment of certain rhinencephalic types of epilepsy, 20: 38779
TAMM, E. I., Photoproduction of π^0 mesons on ^4He near to threshold, 20: 39822
TAMM, I. E., Fundamental problems in contemporary physics theory, 20: 39922
TANK, L. I., Chemical structure and radioprotective properties of aminothiols and derivatives, 20: 38724
TANK, L. I., Evaluation of models for initial selection of radioprotective compounds, 20: 38729
TANKO, P., Action of reticulin on accumulation of ^{32}P in various organs and endocrine glands, 20: 38572
TAPE, G. F., Plutonium and other radioisotope sources: discovery to demand, 20: 39314 (DP-1066(Vol.1), pp 29-39)
TARASOV, A. V., Decay of neutral pions into three photons, 20: 39757 (JINR-P-2763)
TARGAMADZE, V. G., Configuration mixing in quark model, 20: 39861 (JINR-P-2821)
TASHIRO, Shigeki, Method for producing ketene polymer with ionizing radiation, 20: 38977
TASSAN, S., Fine structure of thermal flux and end-effect in tubular composite U fuel elements cooled by an organic compound, 20: 39452 (EUR-2981.f)
TATARINSKAYA, L. S., Photoproduction of π^0 mesons on ^4He near to threshold, 20: 39822
TAURE, I. Ya., Determining γ radiation of spherical source with cylindrical channel, 20: 38989
TAUTFEST, George W., Instrumentation for high-energy research, 20: 39241
TAUTZ, M., Comparative scintigraphic determinations of thyroid weight for dose determination in radioiodine therapy, 20: 38789
TAVKHELIDZE, A. N., Adler-Weisberger relation and dispersion sum rules in theory of strong interactions, 20: 39857 (JINR-E-2876)
TAYLER, R. J., Influence of a magnetic field on Schwarzschild's criterion for convective instability in an ideally conducting fluid, 20: 39939
TAYLOR, Anthony Francis, Improvements in or relating to fuel elements for nuclear reactors, 20: 40397
TAYLOR, B. N., "Non-Josephson" radiation from Josephson tunnel junctions, 20: 40028
TAYLOR, C. D., Motion of electrons scattered from an infinite slab, 20: 39775
TAYLOR, Ellison H., Reflection and thermal accommodation of helium beams on platinum, 20: 39590
TAYLOR, J. C., Broken relativistic supermultiplet symmetries and weak currents, 20: 39877
TAYLOR, John G., Relativistic three particle equations. I., 20: 39914
TAYLOR, W. C., Advanced BONUS core thermal cycle test, 20: 40401 (CEND-259)
TAZZARI, S., Evaluation of background around the Adone, 20: 39495 (LNF-66/22)
TCHOE, Yuong-Tchel, Effect of β-irradiation on deoxyribonucleoprotein, 20: 38581
TEDESCHI, Pete, LiF thermoluminescent response to fast neutrons, 20: 39219
TEETER, Charles E., Catalog of nuclear reactor concepts, Pt. I, Sect. VI, 20: 40353 (ANL-7228)
TEICHMANN, J., Cathode jets and retrograde motion of arcs in magnetic fields, 20: 40232
TEIXEIRA, Antonio F. F., Poles of S matrix for long-range potentials, 20: 39868
TELEMAN, M., Determination of constants for geometric reconstruction of tracks on np films from neutron irradiated 24-l bubble chamber, 20: 39247
TEL'TSOV, M. V., Radiometric equipment on the Cosmos 41 satellite, 20: 39171
TEMPEL, K., Effect of radiomimetics and x rays on permeability of blood-brain barrier, 20: 38609
TENDYS, J., Damping of transverse plasma oscillations at cyclotron resonance, 20: 40257
TENOSO, Harold John, Effect of irradiation and Brucella infection on malic dehydrogenase activity of rabbit peritoneal macrophages, 20: 38586
TEODORESCU, G., Methods for the measurements of atmospheric radioactivity, 20: 39104
TEPLY, J., Radiation-induced oxidation of methanol, 20: 38942 (UJV-1457)
TERASAWA, Michitaka, Formation of hydrogen negative ions in mercury vapor, 20: 39500
TERASAWA, Yoshio, Spectroscopic measurement of electron density and temperature in Ar–H plasma jet, 20: 40215
TEZAK, B., Precipitation and hydrolysis of uranium (VI) in aqueous systems. IV., 20: 38928
THERIOT, Lee, Loci in E. coli K-12 that control mutagen products from DNA, 20: 38620
THERIOT, Lee, Mutants of E. coli K-12 defective in DNA repair and genetic recombination, 20: 38621
THIRION, J., New injection method for cyclotrons, 20: 39530
THIRRING, W., Refined solution of two-dimensional model theories, 20: 39851 (IC-66/96)
THOMAS, Donald E., Thermionic converters, 20: 39637
THOMAS, J., Internal contamination with ^{90}Sr and ^{226}Ra in man in relation to clinical findings, 20: 38623
THOMAS, L. E., Low-energy bombardment of Au with Au ions: on interstitial atom migration in stage III, 20: 40295
THORSON, Walter R., Theory of slow atomic collisions. II., 20: 39620
THREEFOOT, Sam A., Shielded coil for continuous scintillation monitoring of circulating radioactivity, 20: 38558
THUERIGEN, Guenther, Influencing properdin and agglutinin formation by whole-body irradiation, 20: 38695
THURBER, David Lawrence, Variation in ratio $^{234}U/^{238}U$ potential of ^{234}U for Pleistocene chronology, 20: 39120
TIDRIKS, A., Proposal for sector-focusing synchrocyclotron, 20: 39535
TILFORD, S. G., Collisional excitation of atomic spectra in accelerated beams of light elements, 20: 39593
TILGER, C. A., Interactions (π^-p) at 460 Mev, 20: 39793
TIMOFEEV, A. V., Cyclotron radiation flashes, 20: 40219
TIMOFEEV, L. V., Scintillation dosimeter for rating beta applicators, 20: 38777
TIPA, I., Determination of constants for geometric reconstruction of tracks on np films from neutron irradiated 24-l bubble chamber, 20: 39247
TIPTON, Samuel R., Prog. rpt. on effects of hormones, x rays, and cerium compounds on rat liver cells, 10/65–9/66, 20: 38595 (ORO-3295-2)
TIRELLA, G., Changes in antiinsulin antibodies subjected to radioactivity, 20: 38579
TISSI, C., Welding of a reactor for an electrothermonuclear power plant, 20: 40417
TITOV, A. V., Evaluation of models for initial selection of radioprotective compounds, 20: 38729
TITTMAN, Jay, High resolution apparatus using γ source and detector for investigating earth formations, 20: 39139
TJON, J. A., Note on quantum theory of electrical conductivity, 20: 39873
TOERNQVIST, Nils A., Consequences of charge independence in strong interactions, 20: 39800
TOLBERT, W. R., Search for evidence of positron emission in the decay of ^{36}Cl, 20: 40148
TOLEUBAEVA, A. S., Suppression of large transfers in peripheral interactions as effect of nucleon diffuseness, 20: 39820
TOLGYESSY, Juraj, Radioactive kryptonates in science and technology, 20: 39294
TOMANA, M., Changes of content of ascorbic acid, dehydroascorbic acid, and reduced glutathion in brain of irradiated rats, 20: 38679
TOMASSI, Gianni, Cesium-137 and ^{90}Sr levels in diet and urine of an Italian children's community, 20: 39152
TOMILINA, T. N., Accumulation of particles in a 680-Mev synchrocyclotron, 20: 39492 (JINR-P-2811)
TOMINAGA, Moriyuki, Seeded combustion gas of MHD generation, 20: 39636
TOOI, Atsutomo, Formation of SiO_2 films by O-ion bombardment, 20: 40314
TOOTHACKER, William S., Demonstration of x-ray diffraction by LiF using the Mn Kα x rays resulting from ^{55}Fe decay, 20: 40294
TORELLI, G., Search for resonant π–π interaction in process $\pi^-p \rightarrow \pi^+\pi^-n$ near threshold, 20: 39779
TORGERSON, Ronald T., Columbium–Hf base alloys with Y addition, 20: 39445
TOSCHI, R., CNEN He–Cs blow-down MPD facility and experiments with prototype duct, 20: 39675
TOSCHI, R., Relaxation phenomena in MPD generators, 20: 39674
TRAKHTENGERTS, V. Yu., Kinetic instability of outer radiation zone of earth, 20: 39964
TRAMBOUZE, Yves, Preparation and properties of the double salt $2Th(C_2O_4)_2 \cdot (NH_4)_2C_2O_4 \cdot 7H_2O$, 20: 38886
TREFIL, J. S., Random-phase K-matrix approach to absorption in peripheral

interactions, 20: 39804
TREGUBOVA, N. N., Transfusions of blood and leukocytes to gynecological cancer patients for prevention of leukopenia in radiation therapy, 20: 38768
TRET'YAKOVA, S. P., Use of mica and quartz glass for nuclear fission detection at high temperature, 20: 39208 (JINR-P-2705)
TREUTING, Robert G., Nb–Zr superconductor and process of making same, 20: 39372
TRIGGS, Geoffrey William, Improvements relating to nuclear reactors, 20: 40366
TRIPATHY, K. C., Absorptive model for $\bar{K}N$ charge-exchange reaction, 20: 39805
TRIPIER, R. V., Polarized protons and deuterons source for axial injection into Grenoble isochronous cyclotron, 20: 39527
TRIPP, Robert D., Elementary guide to the elementary particles, 20: 39768 (UCRL-11100(Rev.1))
TRIPPLER, Klaus, Report on studies on the β activity of the lower atmosphere, 20: 39119
TRKA, Z., Identification of charged particles by ionization and δ-electrons in a propane bubble chamber, 20: 39211 (JINR-P-2842)
TRLIFAJ, L., Level structure of oxygen isotopes in the SU_3 scheme, 20: 40126
TROITSKAYA, V. A., General patterns of pearl-type pulsations, 20: 39962
TROYON, F., Stability of a plasma confined by r-f fields, 20: 40275
TRUMBORE, C. N., Prog. rpt. on primary chemical processes in radiolysis of liquids, 9/65–9/66, 20: 38939 (NYO-2668-13)
TRUSCOTT, J. R., Eskdalemuir Seismological Station, 20: 39128
TRYKOV, L. A., Angular distribution of fast neutrons behind iron shielding, 20: 40286
TSEKHMISTRENKO, Yu. V., Analytical properties of relativistic multichannel scattering amplitude, 20: 39911
TSEVELEVA, I. A., Mechanism of inhibition of nucleic acid synthesis in irradiated animals, 20: 38585
TSEVELOV, M. A., Washout of radioactive aerosols from atmospheric fallout in layer below clouds, 20: 39113
TSINOBER, A. B., Problems of MHD boundary layer, 20: 39935
TSINTSADZE, N. L., Disintegrated wave interaction in magnetoactive plasma, 20: 40207
TSUKERMAN, V. G., Measuring photoconductivity under strong irradiation, 20: 39179
TSUKO-SITNIKOV, V. M., Measurement of the cascade time of negative pions in gaseous ^{3}He, 20: 39579 (JINR-P-2838)
TSYBUL'SKII, B. A., Radium therapy of cancer of cardial region of stomach with 25-Mev betatron, 20: 38772
TSYPIN, A. B., Conditional reflex during ^{60}Co γ irradiation of fish and rabbits, 20: 38655
TSYTOVICH, V. N., Nonlinear wave interaction in plasma in presence of intensive transverse waves, 20: 40205
TSYTOVICH, V. N., Nonlinear conversion of electromagnetic waves to ion-acoustic plasma oscillation, 20: 40244
TUAN, S. T., Partial wave analysis of inelastic electron scattering in low-energy region, 20: 40150
TUBMAN, Philip E., Ceramic structures for direct energy conversion devices, 20: 39638
TUKHSHEERER, T., Problem of induced radioactivity in food products, 20: 39165
TULINOV, A. F., Influence of crystal lattice on atomic and nuclear processes, 20: 40135
TURALA, Michal, Registration of state of decatron counting systems by means of teleprinter code, 20: 39178
TURCHIN, N. M., Injection of liquid metals in MHD converters, 20: 39669
TURCHIN, N. M., Measuring electrical conductivity of a liquid–vapor K mixture, 20: 39742
TURCHINETZ, W., Shell effects in high energy photoproton spectra from ^{6}Li, 20: 40077 (MIT-2098-256)
TUREK, Leszek, Registration of state of decatron counting systems by means of teleprinter code, 20: 39178
TURKEVICH, E. A., Preparations conducive to removal of radioactive isotopes from an organism, 20: 38733
TURNER, Frederick B., Radiation effects on lizards in a Puerto Rican forest, 20: 38601 (UCLA-12-567)
TUSCANY, R., Internal contamination with ^{90}Sr and ^{226}Ra in man in relation to clinical findings, 20: 38623
TUTTE, Edward, Improvements in or relating to fuel elements for nuclear reactors, 20: 40397
TYAGUNOV, A. V., Theory of frequency multiplier in a gas discharge in strongly nonuniform shf field, 20: 40228
TYTGAT, D., Conference on fuel cycles of high-temperature gas-cooled reactors, Brussels, 20: 40383 (EUR-2780.e)
TYTGAT, D., Fabrication methods and costs of fuel elements, 20: 40388

U

UEBERALL, H., Muon capture and nuclear giant resonances, 20: 40151
UEDA, Y., Nonleptonic decays of hyperons in broken SU(3) × SU(3), 20: 39893
UENO, Jiroo, Method for producing foamed plastics, 20: 38981
UGRIN, N. S., New rare earth compounds with zinc and their crystal structure, 20: 39417
UHLMANN, A., Calculation of coefficients of mass operators, 20: 39855 (JINR-E-2771)
UJIHARA, Akio, Genetic studies on radio-resistant strain of Chlorella ellipsoidea. I., 20: 38605
UKAI, Seiji, Real eigenvalues of monoenergetic transport operator for homogeneous medium, 20: 40054
ULLMAIER, H. A., Prog. rpt. on experimental simulation of large, high field, superconducting magnet operation, 12/65-7/66, 20: 40015 (ORNL-TM-1598)
ULLMANN, J. W., Irradiation testing of Th fuels at ORNL, 20: 40385 (ORNL-P-2327)
ULLMANN, J. W., ORNL facilities capable of contributing to Pu fuel cycle development, 20: 39024 (ORNL-TM-1268)
ULYANOV, K. N., Electric arc in a flow of ionized and non-ionized gas, 20: 39666
UNNERUS, C-E., Exact measurement of gamma-ray doses in ureter, 20: 38778
UNSELD, H., Novel deflection-bunching system at the Karlsruhe isochronous cyclotron, 20: 39546
URRECHAGA-ALTUNA, J., Composite particles in separable-potential models, 20: 39889
USIK, P. A., Suppression of large transfers in peripheral interactions as effect of nucleon diffuseness, 20: 39820
UTO, Hiroaki, Decay asymmetries and production angular distributions of Λ^0 hyperons from $\pi^- + p \rightarrow \Lambda^0 + K^0$, 20: 39837

V

VACCA, Jacopo, Extension of some theorems of MFD to viscous fluids of finite conductivity, 20: 39932
VACEK, A., Mechanism of protective effect of thiopental, 20: 38738
VACLAVIK, J., Turbulent diffusion of plasma in oscillating discharge, 20: 40191
VAINSHTEIN, A. I., Mass formulae for particles with spin 1 and ½ in broken SU(3) symmetry, 20: 39910
VAKULENKO, O. V., Infrared spectrum of neutron-irradiated silicon, 20: 40340
VALDERAS, Ramon, Relation of internal β irradiation and biochemical effects in the CNS, 20: 38651
VALITSKII, V. P., Magnetohydrodynamic instabilities in electrical explosion, 20: 39010
VALLONE, A., Automatic apparatus for measurement of weak currents, 20: 39169 (ISS-66/17)
VAN AMMERS, H., Dosimetry for fast-neutron irradiations of cultured cells and intact animals. I., 20: 39227
VANDAKUROV, Yu. V., Magnetohydrodynamic instabilities in electrical explosion, 20: 39010
VAN DEN BOS, J., Transition probabilities for electron capture, 20: 39606
VAN DER COOK, B. P., Sulfur determination supporting waste solidification program, 20: 38795 (BNWL-265)
VAN DER PLAS, Th., Basic studies related to the development of the Sol-Gel process, 20: 40391
VANDERVELDE, V. D., Instrument for locating failed fuel elements in the HWCTR, 20: 40458 (DP-1049, pp 21-31)
VAN DER WOUDE, A., Reaction ^{27}Al(p,α)^{24}Mg studies with a 30-Mev AVF cyclotron, 20: 40101
VANDEVYVER, Michel, Radioisotope converters, 20: 39633 (CEA-R-2788)
VAN DYNE, George M., Ecosystems, systems ecology, and systems ecologists, 20: 40488 (ORNL-3957)
VAN GURP, G. J., Helicon-like resonances in superconducting niobium, 20: 40031
VAN HORN, Hugh Moody, Nuclear reaction rates in extremely dense matter, 20: 40157
VAN KOLMESCHATE, C., Enthalpy of impure niobium in mixed superconductive state, 20: 40036
VAN KRANENBURG, A. A., Beam properties of Philips' A.V.F. cyclotrons, 20: 39516
VAN LAAR, B., Magnetic study of the intermetallic compound $NdCo_5$, 20: 39424
VAN OOSTERHOUT, G. W., Identical relations between bilinear covariants of Dirac's theory of electron, 20: 39816
VAN ROSSUM, L., Polarization parameter in p-p scattering from 1.7 to

6.1 Bev, 20: 39792
VARBA, V. A., Helium-8 production in negative pion capture by C and O nuclei, 20: 40071 (JINR-E-2774)
VARDENGA, G., The search for "long-lived" Λ^0-particles, 20: 39762 (JINR-P-2849)
VARMA, P. P., New forbidden lines in the L spectrum of lutetium, 20: 39613
VARTERESZ, Vilmos, Agents influencing granulocyte output and production in irradiated rabbits, 20: 38633
VASCONCELOS, M. H., Temperature assignment to thermal diffusion factor, 20: 39326
VASIL'EV, A. V., Infrared extinction of specific photoconductivity of germanium of the n-type produced by γ rays, 20: 40298
VASILEV, A. V., Infrared quenching of intrinsic photoconductivity in n-type Ge irradiated by γ rays, 20: 40337
VASIL'EV, P. V., Prophylaxis of diseases caused by multiple external gamma irradiation, 20: 38726
VASIL'EV, R. D., Yield of D(d,n)^{3}He and T(d,n)^{4}He reactions in thick targets at energies up to 100 kev, 20: 40078 (NP-16203)
VASILEV, V., Experiments on ion acceleration at 685-mm sector cyclotron, 20: 39549
VASIL'EVA, E. D., Dosimetric specifications of gamma therapy unit "Luch-1", 20: 38771
VASILEVA, I. A., Electric arc in a flow of ionized and non-ionized gas, 20: 39666
VASIL'EVA, T. N., Characteristics of f_0F_2 variations at high solar activity, 20: 39965
VAUGOYEAU, Henri, Isotherm section at room temperature of U–C–Si diagram, 20: 39413
VEDERNIKOV, A. N., Prophylaxis of diseases caused by multiple external gamma irradiation, 20: 38726
VELIKHOV, E. P., Analogy between a high-density plasma and metal-ammonia solutions, 20: 39656
VELINOV, P., Formal derivation for electron production in the ionosphere under effects of cosmic radiation, 20: 39625
VENKATESWARLU, K. S., Extraction of protactinium by long-chain amines from hydrochloric acid solutions, 20: 39003
VENKATESWARLU, K. S., Paper electrophoresis of protactinium in sulfuric acid medium, 20: 38826
VERHAAK, R., The Thorotrast kidney, 20: 38756
VERNON, P. B., Health hazards associated with fabrication of Pu–Al fuel elements, 20: 39153
VERSTAPPEN, G., Survey of devices to measure fuel element coolant channels, 20: 39175
VESELOVSKII, R. A., Radiation chemistry of polypropylene, 20: 38945
VETTER, M., Half-life of the 453.08 kev level in ^{183}W, 20: 40123
VEYRIE, Pierre, Ionization of gases by very intense luminous beam, 20: 40190
VIAL, P., Effects of confinement in high-frequency discharges at low pressure, 20: 40278
VIAL, R., Study of a confinement of a plasma in spherical cavity, 20: 40277
VIGDERGAUZ, V. Sh., Structure of Zr–C–Nb system, 20: 39434
VIMPANY, I., Determination of total K in soils using gamma emission of ^{40}K, 20: 39280
VINKLER, A., Contribution to question of breed-specific radiosensitivity, 20: 38677
VISSONOV, Yu. V., Use of tetoxacin and unithiol in radiation sickness caused by ^{144}Ce, 20: 38732
VLADIMIROV, V. G., Mechanism of protective action of aminothiols, 20: 38723
VOEROES, I., Influence of x-irradiation on course of adrenalin-lymphocytosis, 20: 38678
VOGELSANG, W., Antiferromagnetism of uranium monophosphide, 20: 39422
VOGT, Erich W., Meson facility (H$^-$), 20: 39540
VOLKOVA, E. V., Radiation-induced polymerization of fluoroolefins, 20: 38946
VOLTZ, R., Diffusion of triplet excitons produced by ionizing radiation in aromatic materials, 20: 38957
VON DER DECKEN, C. B., Experimental methods for flow in spherical bodies, 20: 39051
VONDERHAAR, D. F., Time and spatially resolved interferometry on pulsed-laser-induced plasmas, 20: 40186
VON GUNTEN, H. R., Head-end treatment for the reprocessing of high temperature carbide–graphite fuels, 20: 40390
VON MOLNAR, Stephen, Paramagnetic and ferromagnetic resonance in EuS, 20: 40349
VON SENGBUSCH, G., Q value of reaction $^{27}Al(p,\alpha)^{24}Mg$, 20: 40099
VOROSHILOV, Yu. V., Crystal structure of compounds $Zr_2Ni_{21}B_6$ and $Zr_6Co_{21}B_6$, 20: 39416
VOROZHTSOV, S. B., Modified resonance extraction method from relativistic cyclotron, 20: 39520
VOZILKIN, V. A., Relationship between superconductivity and structure of Zr–4Nb alloy, 20: 40021
VRIENS, L., Electron exchange in binary encounter collision theory, 20: 39818
VRZHESHCH, E. Y., Preparation of the carbides (Ti,W,Cr)C and study of their properties, 20: 39431
VULIS, L. A., Electric discharge in conducting jet of viscous fluid, 20: 40241
VYDRA, F., Amperometry with two polarizable electrodes. X., 20: 38810

W

WACKERLE, Jerry, Contributions to feasibility study of early lunar flare, 20: 39469 (LA-3453)
WADA, Bungo, Effects of ultraviolet microbeam irradiations on mitosis studied in Tradescantia cells in vivo, 20: 38614
WAGEMANN, K., Future fuel requirements for atomic power plants, 20: 40420
WAGHMARE, Y. R., Generalized Hartree-Fock calculation for ^{90}Zr using an effective interaction, 20: 40076 (MIT-2098-255)
WAGNER, Guenther A., Age determination of tektites by tracks of spontaneous fission of ^{238}U, 20: 39135
WAGNER, Henry N. Jr., Are iodotyrosines normal constituents of plasma?, 20: 38561
WAGNER, J., Effect of quality of radiation on thermoluminescence of LiF(TLD-100), 20: 39199 (COO-1105-117)
WAGNER, R., Cross section of $^{73}Ge(n,\alpha)^{70}Zn$ reaction at 14 Mev, 20: 40098
WAHLIG, M., Observation of $\omega^0 \to \pi^0 + \gamma$, 20: 39787
WAINERDI, Richard E., Use of high-speed automatic systems for medical and biologic activation analysis, 20: 38843
WAIT, G. D., Deuteron stripping reactions, 20: 40155
WALDVOGEL, A., Size effect in thermal resistivity maxima in In and Pb, 20: 40022
WALKER, W. D., Search for the kappa meson, 20: 39784
WALLACE, Bruce, Natural and radiation-induced chromosomal polymorphism in Drosophila, 20: 38646
WALTER, Hans, Use of underground parking lots and garages for the protection of civilian populations, 20: 39078
WALTON, J. W., SNAP-50/SPUR electromagnetic pump program, 20: 40450 (TIM-911)
WANDEL, G., Lifetimes of the excited states $(6s6p)^1P_1$ and $(6s6p)^3P_1$ of Yb, 20: 39597
WANG, Kenneth, Analytic solution for a two-dimensional, axisymmetric EGD conversion channel, 20: 39650
WANG, R., Production and investigation of materials for MHD generator, 20: 39690
WARD, A. L., Calculation of space charge effects in pulsed discharged, 20: 40253
WARD, Don C., Prog. rpt. on application of nuclear explosives to create underground storage reservoirs, 1/66, 20: 39014 (TID-23184)
WARMKESSEL, Joyce M., Prog. rpt. on solid-state chemistry of rare earth oxides, annual, 1965–66, 20: 38861 (COO-1109-22)
WASSERMAN, Judith, Crystal structure of solid H and deuterium, 20: 40308
WASSON, John T., Determination by neutron activation of gallium and germanium in iron meteorites, 20: 38825
WATANABE, Masanori, Formation of SiO_2 films by O-ion bombardment, 20: 40314
WATANABE, Takeo, Neutron-diffusion parameters in water, 20: 40055
WATANABE, Takashi, Neutron-diffusion parameters in water, 20: 40055
WATERBURY, Glenn R., Leaching of uranium by hydrogen chloride, 20: 39346 (LA-3488)
WATERS, W. R., Classification of Canadian hospitals based on fallout exposure probabilities, 20: 39162
WATSON, C. D., Prog. rpt. on unit operations, 10–12/65, 20: 38998 (ORNL-3958)
WATSON, M. D. S., Ionization and temperature measurement in MPD experiments, 20: 39665
WATSON, P. D., Low-cycle fatigue strengths of dissimilar weldments, 20: 39404 (SWRI-1228-4-20)
WAX, Robert LeRoy, Balloon observations of infrared and x-ray intensities in auroral zone, 20: 39990
WEBER, Celia, Inactivation of tobacco mosaic virus by ultraviolet light, 20: 38584
WEBER, Gary R., Prog. rpt. on solid-state chemistry of rare earth oxides, annual, 1965–66, 20: 38861 (COO-1109-22)
WEBER, J., Theory and mechanism of Zircaloy pressure bonding, 20: 39361 (WAPD-305)
WEEKS, John R., Physical and chemical properties of dilute alloys of Cd in Na, 20: 38856 (BNL-10372)
WEENINK, M. P. H., Runaway electrons in an r-f mirror field, 20: 40266
WEETON, John W., Metallographic study of dispersion-strengthened alloys after failure in stress rupture, 20: 39398 (NASA-TN-D-3527)
WEIDENBAUM, B., Mechanical property changes in Zircaloy-2, Inconel and Incoloy from neutrons, 20: 39457 (GEAP-5100-9)

WEIDENBAUM, B., Uranium oxide powder and pellet thermal conductivity during irradiation, 20: 39456 (GEAP-5100-1)
WEIL, J. L., Reactions $^{11}B(^3He,n)^{13}N$ and $^7Li(^3He,n)^9B$ from 1.5 to 5.5 Mev, 20: 40112
WEIMER, D., Production of carbon plasmas, 20: 40209
WEINBERG, A., Search for the kappa meson, 20: 39784
WEINBERG, E., Comparison of liquid-metal magnetohydrodynamic power conversion cycles, 20: 39634 (JPL-32-946)
WEINBERG, E., Theoretical and experimental investigation of liquid–metal MHD power generation, 20: 39716
WEINBERG, Steven, Current-commutator calculation of the K_{l4} form factors, 20: 39815
WEINSTEIN, Jerry L., Law and administration. Vol. 4, 20: 40491
WEISS, N. O., Expulsion of magnetic flux by eddies, 20: 39567
WEISSMAN, Samuel, Blast-closure systems, 20: 39073
WELDON, D., Polarization parameter in p-p scattering from 1.7 to 6.1 Bev, 20: 39792
WELIN, Eric, Further age measurements on radioactive minerals from Sweden, 20: 39125
WELIN, Eric, Rubidium–strontium whole rock age data on some Swedish precambrian rocks, 20: 39126
WELLS, E. R., Injection and accumulation: single-pass experiments (DCX-1), 20: 40171 (ORNL-3989, pp 1-13)
WELLS, W. M., High-temperature testing and evaluation of graphite helical-screw expanders and compressors, 20: 39026 (UCRL-14660(Rev.1))
WELSH, R. E., Measurement of the lifetime of the 14.4 kev level of ^{57}Fe, 20: 40132
WERNICK, J. H., Moessbauer effect in $Co_{1-x}Fe_xSi$, 20: 40300
WERNICK, Jack H., Nb–Zr superconductor and process of making same, 20: 39372
WERNLUND, Roger F., Missile scoring systems utilizing nuclear radiation, 20: 39190
WERTHEIM, G. K., Moessbauer effect in $Co_{1-x}Fe_xSi$, 20: 40300
WESS, J., Refined solution of two-dimensional model theories, 20: 39851 (IC-66/96)
WEST, Gordon B., Nuclear power reactor having high, prompt negative temperature coefficient of reactivity, 20: 40434
WESTPHAL, K. O., Inverse problem of particle motion and its application, 20: 39471
WHAN, R. E., Oxygen-defect complexes in neutron-irradiated silicon, 20: 40302
WHATLEY, M. E., Prog. rpt. on unit operations, 10–12/65, 20: 38998 (ORNL-3958)
WHITAKER, W. D., SNAP-10A expansion compensator, 20: 39023 (NAA-SR-11952)
WHITE, Clayton S., Tentative biological criteria for estimating blast hazards, 20: 39058
WHITE, S. N., Canadian use of reinforced plastics in blast shelters, 20: 39080
WHITE, W. H. Jr., Operating characteristics of ORIC beam extraction system, 20: 39521
WHITEWAY, F. E., Recording and analysis of seismic waves using linear cross arrays, 20: 39134
WHITMAN, Robert V., Footings for protective structures, 20: 39068
WHITTEN, David G., Triplet states in radiation chemistry, 20: 38948
WHITTLE, R. H., Pressure-drop characteristics for flow of subcooled water in heated channels. I., 20: 39047 (AERE-M-1739)
WICK, E. L., Irradiation flavor and the volatile components of beef, 20: 39299
WICK, G. C., Space inversion, time reversal, and other discrete symmetries in local field theories, 20: 39091
WIDEROEE, R., Calculating disturbed motion of particles in cyclic accelerators, 20: 39524
WIDHOLM, O., Exact measurement of gamma-ray doses in ureter, 20: 38778
WIEGERT, Robert E., Zirconia based foam insulating material and method, 20: 39375
WIERTS, D., Beam properties of Philips' A.V.F. cyclotrons, 20: 39516
WIESEMANN, Robert A., Flux mapping system for measuring radiation, 20: 39252
WIESNER, L., Measurement methods with radioisotopes for industry and geophysics, 20: 39291
WIGLEY, D. A., Effects of self-irradiation damage on electrical resistivity of alpha and delta stabilized Pu, U, and Np, 20: 39448 (AERE-X-PR-2596-9)
WILHELM, H. E., Thermal and reactive nonequilibrium of magnetoactive plasma flows, 20: 40234
WILKES, W. R., Prog. rpt. on experimental simulation of large, high field, superconducting magnet operation, 12/65-7/66, 20: 40015 (ORNL-TM-1598)
WILKINS, Coleridge A., Extension of common approximating equation for collision density, 20: 40056
WILKINS, Daniel R., Transport phenomena in low-energy plasmas, 20: 40210
WILKINSON, A. E., Release of enzymes from lysosomes by irradiation and relation of lipid peroxide formation to enzyme release, 20: 38577
WILLAX, H. A., Progress report on the 500-Mev isochronous cyclotron meson factory of ETH Zurich, 20: 39533
WILLETT, Joseph E., Pressure dependence of wave propagation in magnetoplasma-filled waveguide, 20: 40248
WILLI, A. V., Deuterium and tritium isotope effects in methoxide-promoted elimination reaction of 2,2-diphenylethyl benzenesulfonate, 20: 38912
WILLIAMS, C. D., Electron probe microanalysis of Al-clad Zy-2 specimens after heat treatments, 20: 39380 (AECL-2570)
WILLIAMS, H. J., Pressure-induced phase transformations and magnetic ordering in intrarare-earth alloys and Sm, 20: 40326
WILLIAMS, Jack M., Neutron-diffraction determination of the structure of $CH_3CN \cdot 2HCl$, 20: 38935
WILLIAMS, R. O., Methods of reduction of texture data to inverse pole figures, 20: 39402 (ORNL-3979)
WILLMARTH, T. E., Microscopical study of structure of spherical thoria sol-gel beads, 20: 39364
WILLMES, Henry, Elastic scattering of 45-Mev protons, 20: 40162
WILLS, E. D., Release of enzymes from lysosomes by irradiation and relation of lipid peroxide formation to enzyme release, 20: 38577
WILSON, Stuart H., Origin of tritium in hydrothermal solutions, 20: 39132
WILSON, William A., Process for impregnating an adsorbent catalyst with a radioactive metal isotope, 20: 38993
WINDMUELLER, H. G., Perfusion with T_2O to measure hepatic lipogenesis and lipid secretion, 20: 38559
WINKLER, H., Resonances in $^{40}Ar(p,p)$ near 1.1 Mev, 20: 40147
WINKLEY, Donald Charles, Scandium hydrolysis as measured by chelate solvent extraction, 20: 38925
WINTENBERG, R. E., Electrical safety of health physics instruments, 20: 39213 (ORNL-TM-1578)
WINTENBERGER, Micheline, Selenides ML_4Se_7 of structural type Y_5S_7 (L = rare earth and M = Mg, Cr^{2+}, Mn, Fe^{2+}), 20: 38884
WINTER, G., New levels in ^{97}Tc, 20: 40084
WINTERNITZ, P., Polarization tensor in scattering of polarized nucleons on polarized proton target, 20: 39909
WINTON, J., Method for gas-hydriding zirconium alloys at 400°C, 20: 39360 (TRG-Report-1255)
WIRTZ, K., Future utilization of nuclear energy in Europe, 20: 40443
WISE, E. N., Controlled-potential coulometric determination of rare earths in acetonitrile, 20: 38812
WISE, E. N., Controlled-potential electrolysis of Eu, Yb, and Sm and their mixtures in acetonitrile solutions, 20: 38813
WISEMAN, Carl D., Effect of interstitial gases on superconducting critical temperature of niobium, 20: 40025
WITHERSPOON, Paul A., Economics of nuclear explosives in developing underground gas storage, 20: 39015 (UCRL-14877)
WITTIG, Joerg, Superconductivity of germanium and silicon under high pressure, 20: 40039
WITTIG, Joerg, Superconductivity of Sn and Pb under very high pressure, 20: 40040
WITTKOWER, Andrew B., Ion source having plasma control means, 20: 39039
WITZKE, Walter R., Effect of alloying on grain refinement of electron-beam-melted tungsten, 20: 39400 (NASA-TN-D-3531)
WIZA, Joseph Ladislaus, Reactions $^{17}O(d,p)^{18}O$, $^{18}O(d,p)^{19}O$ and nuclear structure of ^{18}O and ^{19}O, 20: 40161
WOELFLI, W., Compton effect on bound K electrons, 20: 39773
WOJCIESZEK, Z., Long-term results and complications after irradiation of haemangiomas in children, 20: 38787
WOLBERG, J. R., Analysis of dynamic behavior of dual purpose power/desalination nuclear plants, 20: 40438
WOLF, Alfred P., Reactions of energetic carbon atoms in methylamine, 20: 38964
WOLF, W. P., Temperature variation and separation dependence of exchange interactions of Gd^{3+} pairs in $LaCl_3$, 20: 38914
WOLNIEWICZ, L., Vibronic energy and dipole moment of HD, 20: 40310
WOLSKY, S. P., Sputtering-yields crossover in single-crystal copper, 20: 39589
WONG, Eugene Y., EPR spectra of 1% Nd-doped $La_2(SO_4)_3 \cdot 9H_2O$ and $LaBr_3$, 20: 40312
WOOD, F. C., Studies on the reprocessing and refabrication of HTGR fuels in OECD Dragon Project, 20: 40419
WOOD, J. D. L. H., High-output neutron tube for activation analysis, 20: 38839
WOOD, J. P., Sputtering of Cu, Mo, 304 stainless steel, and W by deuterium ions, 20: 39581 (ORNL-3989, pp 134)
WOOD, R. E., Measurement of (n,2n), (n,p), and (n,α) cross sections of Ge at 14.4 Mev, 20: 40080 (ORO-3346-3)
WOODS, A. D. B., Crystal dynamics of K. I., 20: 40343
WOODS, Richard, High-resolution study of inelastic proton scattering from nuclei in Pb region, 20: 40074 (LA-DC-8069)
WOOLF, Michael A., Brillouin scattering in liquid He II, 20: 40034
WORCESTER, Samuel A., Columbium–Hf base alloys with Y addition,

20: 39445
WRIGHT, Byron T., Variable energy extraction from negative ion cyclotrons, 20: 39519
WRIGHT, L. E., Partial wave analysis of inelastic electron scattering in low-energy region, 20: 40150
WRISCHER, M., Precipitation and hydrolysis of uranium (VI) in aqueous systems. IV., 20: 38928
WU, T. M., Radiation-induced strucutre in d-c Josephson current, 20: 40035
WU, Ying-chu Lin, Comparison of performance of diagonal wall generators, Faraday generators, and Hall current generators, 20: 39702
WUJEK, Joseph H. Jr., Radiation measurements in space, 20: 39627
WYDER, P., Size effect in thermal resistivity maxima in In and Pb, 20: 40022
WYSOCKI, J. J., Low-energy proton bombardment of GaAs and Si solar cells, 20: 40299

X

XAVIER, R. M., Origin of ferromagnetism in divalent europium salts, 20: 40318

Y

YAGI, K., Report on measurements of reaction $^{40}Ca(d,\alpha)^{39}Ca$ for 24 Mev impact energy, 20: 40067 (BMWF-FBK-66-15, pp 20-37)
YAKOVLEV, G. N., Complexing of trivalent actinides and lanthanides in phosphoric acid solutions, 20: 38878 (ORNL-tr-1257)
YAKOVLEV, V. I., Expansion of cylindrical column of conducting gas in longitudinal magnetic field, 20: 40237
YALCH, J. P., DEFCOT, plane-strain-viscoelastic deformation of a composite site tube, 20: 39394 (GEMP-415)
YAMAZAKI, T., Single RACE spectrometer, 20: 39206 (INSJ-99)
YAMPOL'SKAYA, L. I., Evaluation of models for initial selection of radioprotective compounds, 20: 38729
YANO, Syukuro, Flow velocities, seeding ratios and electrical conductivities in seeded Ar plasmas, 20: 39727
YANOUT, Z., Phase-shift analysis of nucleon-nucleon scattering at 14.5 Mev, 20: 39756 (JINR-P-2742)
YANOUT, Z., Polarization tensor in scattering of polarized nucleons on polarized proton target, 20: 39909
YAROVENKO, A. N., Analysis of alloys of rare earth elements with magnesium in nonaqueous solutions, 20: 38830
YASINSKAYA, G. A., Wettability of refractory carbide, boride, and nitride by molten metal, 20: 39429
YASTREBENETSKAYA, M. M., Transfusions of blood and leukocytes to gynecological cancer patients for prevention of leukopenia in radiation therapy, 20: 38768
YAZEVA, L. I., Effect of vitamins and phosphatides on resistance to radiation, 20: 38721
YEH, K. C., Gradient instabilities as possible causes of irregularities in ionosphere, 20: 39993
YEH, Si Jung, Enrichment of ^{64}Cu by the Szilard-Chalmers process, 20: 38988
YEN, K. T., Interaction between solar wind and sun's general magnetic field, 20: 39573
YEVICK, George J., Prog. rpt. on cusped containment geometries, annual, 1965–1966, 20: 40178 (SIT-2582-19)
YIFTAH, S., Analysis of dynamic behavior of dual purpose power/desalination nuclear plants, 20: 40438
YNTEMA, G. B., Isothermal calorimetry on type II superconductors, 20: 40045
YOCK, P. C. M., Analysis of photoproduction of vector mesons, 20: 39811
YONTS, O. C., Sputtering of Cu, Mo, 304 stainless steel, and W by deuterium ions, 20: 39581 (ORNL-3989, pp 134)
YOSHIHARA, K., Crystal-structure effects in hot-atom chemistry of copper phthalocyanine, 20: 40309
YOSHII, Giichi, Effect of β-irradiation on deoxyribonucleoprotein, 20: 38581
YOSHIKAWA, Kozuko, Observation of fallout around the laboratory, 20: 39108
YOSHISAKI, M. B., Water analysis, 12/63–11/64, 20: 38800 (PAEC(C)RE-652)
YOUMANS, Arthur H., Method and apparatus for identifying elements in formations penetrated by drill hole, 20: 39137
YOUNG, Kenneth Kong, Measurement of Λ^0 hyperon and K_1^0 meson lifetimes and search for coherent interference in decay $K^0 \to \pi^+\pi^-$, 20: 39849
YOUNG, R. S., Behavior of selected steels exposed in flowing sodium test loops, 20: 39345 (GEAP-4831)
YUAN, Jung-Fong, Reaction $\pi N \to \pi_1\pi_2 N'$ in energy region up to 1 Bev, 20: 39827
YUDOVICH, L. A., Position of equatorial boundary of region where anomalous ionization appears as function of planetary magnetic activity, 20: 39967
YUROVSKII, A. V., Radiometric equipment on the Cosmos 41 satellite, 20: 39171
YURTAEV, G. I., Effect of vitamins and phosphatides on resistance to radiation, 20: 38721

Z

ZABUSKY, Normen J., Exact invariants for class of nonlinear wave equations, 20: 40005
ZAETS, V. D., Infrared spectrum of neutron-irradiated silicon, 20: 40340
ZAIDI, S. A. A., Electron polarization of ^{144}Pr, 20: 40085
ZAIKIN, D. A., Octupole deformability of the nucleus ^{19}F, 20: 40121
ZAIMIDOROGA, O. A., Measurement of the cascade time of negative pions in gaseous ^3He, 20: 39579 (JINR-P-2838)
ZALEVSKII, B. K., Zonal structure of chalcogenides of rare-earth elements, 20: 40339
ZAMBONI, F., Q value of reaction $^{27}Al(p,\alpha)^{24}Mg$, 20: 40099
ZAMFIR, I., Chemical and radiochemical purity of radioactive Ca, 20: 38827
ZAMOLODCHIKOV, B. I., Development and prospects for application of meson factories, 20: 39534
ZAMOLODCHIKOV, B. I., Modified resonance extraction method from relativistic cyclotron, 20: 39520
ZANOLLA, W., Radiotherapy of carcinoma of uterine neck, 20: 38786
ZAPLATIN, N. L., Modified resonance extraction method from relativistic cyclotron, 20: 39520
ZAR, J. L., Large experimental superconducting magnet for MHD power generation, 20: 39643
ZARECHNYUK, O. S., Ternary compounds with $ThMn_{12}$ superstructure in systems Y–transition metal–Al, 20: 39414
ZARETSKAYA, I. V., Contents of glycogen and ribonucleic acid and phagocytic activity of leukocytes during x irradiation of rabbits, 20: 38681
ZARETSKII, D. F., Four-fermion interaction and lepton masses, 20: 39832
ZAUDERER, B., Electrical characteristics of linear Hall and Faraday generators at small Hall parameters, 20: 39640
ZAVARA, Ivo, Chemical behavior of a new element, 20: 38913
ZAVATTINI, E., Search for resonant π-π interaction in process $\pi^- p \to \pi^+\pi^- n$ near threshold, 20: 39779
ZDANUK, E. J., Sputtering-yields crossover in single-crystal copper, 20: 39589
ZEITLER, G., Application of alpha spectrometry to the solution of geochemical questions, 20: 39143
ZEL'DOVICH, Ya. B., Vortex isomers of nuclei, 20: 40106
ZENKLUSEN, G., Radiation-induced protein leakage into small intestine of rat, 20: 38604
ZENZ, H., Analysis of the volatile constituents of irradiated apple juice, 20: 39300
ZETTWOOG, Pierre, Conditions for use of ducts of disk geometry in MHD conversion, 20: 39663
ZETTWOOG, Pierre, Effect of ionization saturation and duct shape on losses near walls, 20: 39673
ZHABROVA, G. M., Effects of ionizing radiation and other factors on rate of topochemical decomposition of various inorganic compounds, 20: 38955
ZHAVORONKOVA, L. A., Transfusions of blood and leukocytes to gynecological cancer patients for prevention of leukopenia in radiation therapy, 20: 38768
ZHEREBCHENKO, P. G., Effect of radioprotective agents on frequency of leukemia induced by radiation, 20: 38722
ZHEREBCHENKO, P. G., Mechanism of radioprotective action of indolylalkylamines, 20: 38725
ZHERNOV, A. P., Theory of electrical conductance of metals with nonmagnetic impurities, 20: 39395 (IAE-1028)
ZHUKOV, V. A., Reaction $\pi N \to \pi_1\pi_2 N'$ in energy region up to 1 Bev, 20: 39827
ZHULANOVA, Z. I., Formation of organic peroxides as one of first biochemical reactions to radiation, 20: 38660
ZHULIN, I. A., Role of magnetic fields of solar corpuscular streams and their effect on magnetosphere, 20: 39963
ZHULIN, I. A., Variability of fluxes of magnetic fields of sunspots and faculae, 20: 39561
ZHURAVLEV, V. F., Toxicity of tritium oxide in mice and rats subjected to intraperitoneal injection, 20: 38568
ZHURAVLEVA, M., The search for "long-lived" Λ^0-particles, 20: 39762 (JINR-P-2849)
ZHUSUPOV, M. A., Threshold states and reduced cluster widths in light nuclei, 20: 40086
ZHVANIYA, I. A., Stability of nonhomogeneous electron beam, 20: 40245
ZICKERT, D., Stability of a cylindrical plasma, 20: 40198
ZIEBORAK, K., Boiling temperatures and vapor pressure of H_2O–D_2O mixtures and their azeotropes, 20: 38921
ZIFFERERO, M., Reprocessing and refabrication methods and costs,

20: 40392
ZIMAKOV, P. V., Radiation-induced polymerization of fluoroolefins, 20: 38946
ZIMMER, Karl G., RBE of fast neutrons by release of mutations in Drosophila, 20: 38645
ZINOV, V. G., Structure of Ar K-series during atomic capture of negative muons in pure gas and in mixture with H, 20: 39578 (JINR-P-2807)
ZIPF, K., Effect of radiomimetics and x rays on permeability of blood-brain barrier, 20: 38609
ZIPKIN, Morris A., Technology for large Rankine cycle space power systems, 20: 39028
ZITZOW, U., Comparison of performance of diagonal wall generators, Faraday generators, and Hall current generators, 20: 39702
ZIVKOVIC, N., Hereditary hypochromic microcytic anemia in laboratory rat, 20: 38619
ZLATIN, N. A., Magnetohydrodynamic instabilities in electrical explosion, 20: 39010
ZMUDA, A. J., Transverse hydromagnetic disturbances at 1100 km in auroral region, 20: 39996
ZOLIN, L. S., Application of B counter with CH_2 moderator in neutron dosimetry, 20: 39214 (NP-tr-1394)
ZOLIN, L. S., Measurement of real part of π^-p elastic scattering amplitude in Coulomb interference region at 3.5 Bev/c, 20: 39785
ZON, B. A., Time correlation of the emission and absorption of exchange photon, 20: 39577 (JINR-P-2791)
ZUERNER, L. V., Advanced alpha-beta-gamma hand and shoe contamination monitor, 20: 39198 (BNWL-250)
ZUEST, H., Head-end treatment for the reprocessing of high temperature carbide–graphite fuels, 20: 40390
ZUL'KARNEEV, R. Ya., Spin correlation in elastic scattering of 605-Mev polarized protons on protons, 20: 39759 (JINR-P-2776)
ZURICHENKO, Alex, Bibliography on high-purity metals, 20: 39328 (AD-624997)
ZUROMSKY, G., Advanced BONUS core thermal cycle test, 20: 40401 (CEND-259)
ZWETZIG, Gerald B., Compensated nuclear radiation fluid analyzer, 20: 39191

SUBJECT INDEX

Main entries in this index are generally specific materials, things, and processes. These are followed by modifiers that describe the properties of, and processes applied to, the main entries.

The number preceding the colon is the *NSA* volume number, and the number following is the abstract number. The designation (R) following the abstract number indicates that the abstract is of a progress report; (P) indicates a patent; and (T) indicates a translation. Abstracts for reports other than progress reports carry no letter designation. References to report numbers, where appropriate, are included after the abstract number of the citation. Published literature (journal article or book) is identifiable by the absence of a report number.

The user should bear in mind that the ideas presented in the original literature, rather than key words, have been indexed. The indexers have tried to select what seemed the most probable and logical place to look for typical information. Since it is not possible to anticipate where a user would look for information, numerous cross references are included in cumulative indexes to assist him in his search.

Experience in using an index of this type will be the best guide in obtaining the desired information, and a consideration of synonymous or closely related terms will prove valuable.

Information must be so indexed as to be of the greatest use to the greatest number of users. This requires that a topic be indexed to headings that most specifically describe it and not ordinarily to the headings that describe its ultimate use, nor to the general class headings that include the specific headings. For example, information on the treatment of thyroid disease with I-131 would be indexed under Thyroid Gland and under Iodine Isotopes I-131, but not necessarily under Radiotherapy. A study of the effects of x radiation on hair would be indexed under both X Radiation and Hair. However, the information would not be indexed under the experimental animal, e.g., Rats, unless the report discusses the effects on rat hair as compared with the effect on the hair of other animals.

The broad, general class headings are used only for general information or for comprehensive reports or articles.

Subject Heading Styles

Generally, the direct form of subject entry is used rather than inverted headings, e.g., Amino Acids rather than Acids, Amino; Helium Isotopes He-4 rather than Helium—isotopes He-4 or Helium—He-4 isotopes. Note, however, that in some cases parenthetic modifying terms or inverted headings of the form Neutrons, Fast are used in preference to a direct entry that would result in the scattering of information. Organic compounds are usually entered in the index in the inverted form so that substituted compounds can be listed near the parent compound; e.g., Benzene, Bromo- rather than Bromobenzene. In general, the style of nomenclature used is that of Chemical Abstracts, except that some items listed in that publication as subheadings are elevated to form part of the main heading; e.g., Butyric Acid, Methyl Ester rather than Butyric Acid—methyl ester.

Alphabetization

Main headings are alphabetized word-by-word. A parenthetic qualifier following a main heading is disregarded in alphabetizing unless there are two or more headings identical except for the parenthetic qualifier, in which case the qualifier determines the order. Headings involving Greek letters are arranged as if the names of the letters were spelled out.

Examples:

M-Capture
see Electron Capture
Magnesium
Magnesium Alloys
Manganese Fluorides
Manganese(II) Fluorides
Mesons
Mesons (π)
Mesons (ρ)
3-Pentanol, 2,4-Dimethyl-
2-Pentanol, 2-Methyl-
2-Pentanol, 4-Methyl-

Nomenclature of Inorganic Compounds

Inorganic compounds are indexed in the direct form, listing cations in the order of increasing valence in the case of polycationic salts of varying valence and in alphabetic order for polycationic salts in which all cations have the same valence; e.g., Sodium Aluminum Silicates and Potassium Sodium Sulfates.

Multicomponent Alloys and Other Systems

Multicomponent alloys, except well-known trade names, are indexed under a main heading in the form "element alloy" for each element in the alloy. The modifier begins with element symbols for each component arranged alphabetically as if the English name for the element were spelled out.

Example: Copper-Gold Alloy is indexed
Copper Alloys
Cu-Au...
Gold Alloys
Cu-Au...

Well-known alloys such as Zircaloy-2 are indexed directly to the trade name; cross references referring from each component of the alloy to the entry for the trade name appear in cumulative indexes.

Multicomponent systems of non-metallic elements are indexed in a manner similar to alloys except the main heading used contains the word "Systems" in place of "Alloys."

Example: Silicon–Tungsten Systems are indexed
Silicon Systems
Si-W...
Tungsten Systems
Si-W...

Multicompound systems and mixtures of compounds are indexed under the main heading for each component com-

pound; the modifiers begin with an alphabetical listing of compound formulas.

Example: Lead Titanate–Lead Zirconate is indexed

Lead Titanates
$PbTiO_3$-$PbZrO_3$...
Lead Zirconates
$PbTiO_3$-$PbZrO_3$...

A mixed system of compounds and elements is indexed using a combined form of the above conventions, e.g., a dispersion of copper and alumina would be indexed

Aluminum Oxides
Al_2O_3-Cu...
Copper Systems
Al_2O_3-Cu..

Physical States and Configurations of Materials

Specification of the physical state, if other than normal, or geometric configuration of the material is included in the modifying phrase, i.e., liquid metals would be indexed to the metal with "liquid" in the modifier, and carbon crucibles would be indexed to Carbon with "crucibles" appropriately placed in the modifier and also to Crucibles if appropriate.

Modifying Phrases

The modifiers appearing under a main heading are written specifically to describe the relation of the item being indexed to that main heading. The modifier, therefore, will generally contain more useful information about that relation than will a title or a phrase written to be used under every main heading assigned to the item. Effort is exerted to begin the modifier with the word judged to be of greatest use to the greatest number of users; this, however, does not obviate the need to consider all modifiers under the main heading(s) of interest.

Modifiers are usually intended to form a meaningful phrase when combined with the main heading. Some are intended to be read following the main heading, e.g., the entry Hydrogen—sorption by charcoal is read "hydrogen sorption by charcoal"; however, as a result of placing the important word first, many modifiers must be arranged for smooth reading, e.g., Formaldehyde—yields in radiolysis of ethyl ether, effects of deuterium on is read "effects of deuterium on formaldehyde yields in radiolysis of ethyl ether" and Uranium—crystal structure of, effect of cooling rate on allotropic transformations in is read "effect of cooling rate on allotropic transformations in crystal structure of uranium." Prepositions are sometimes omitted if no ambiguity results.

Special characters are added to modifiers in the field of physics; if the modifier does not establish the experimental or theoretical character of a reference, a symbol (E), (T), or (E/T) is placed immediately after the modifying phrase and before the journal reference number. The value of this identification has been established by the American Institute of Physics.

A

ABRASION
use of vibratory, in sphere production, 20: 39376(P)
ACCELERATORS
beam extraction systems for, superconducting niobium-tin plates as magnetic shields for, 20: 39523
beam optics for, lectures on, 20: 39483 (CERN-66-21)
beam optics in, (T), 20: 39484 (CERN-66-21, pp 1-30)
beam separation for, at low energies, 20: 39485 (CERN-66-21, pp 31-42)
beam separation for, r-f separators for, 20: 39486 (CERN-66-21, pp 43-54)
design of cesium ion, for space propulsion, 20: 39090
particle motion in cyclic, stability of, 20: 39524
radiation protection practices for, 20: 39160
storage rings for, background evaluation for Adone, 20: 39495 (LNF-66/22)
tritium targets in, use of glove boxes for changing, 20: 39476 (AD-636185)
use of proton, as intense neutron generator, 20: 39542
ACCIDENTS
analysis of filling, in MSRE, 20: 40412 (ORNL-TM-497)
computer code for calculation of environmental radioactivity from reactors after instantaneous release of radioisotopes, 20: 39148 (GA-6511)
diagnosis of radiation exposure from, by leukocyte chromosome aberration analysis, 20: 38593 (ORNL-P-2175)
ACETALDEHYDE
determination in irradiated fruit juices, chromatographic, 20: 39300
ACETALDEHYDE, PHENYL-
effects on flavor of irradiated beef, 20: 39299
ACETAMIDE, THIO-
radiosensitivity effects on rat liver and spleen, x, 20: 38694
ACETATES
radiation effects on metabolism in rats, x, 20: 38638
ACETIC ACID, [(CARBOXYMETHYLIMINO) BIS(ETHYLENENITRILO)] TETRA-
effects on elimination of radioisotopes by mice and rats, 20: 38733
excretion in rats, tracer study, 20: 38556
solvent properties with tertiary amine for rare earths, 20: 38995 (BM-RI-6809)
ACETIC ACID, (1,2-CYCLOHEXYLENEDINITRILO)TETRA- COMPLEXES
with gallium, iron, thorium, or uranium, formation of, biamperometric studies of, 20: 38810
ACETIC ACID, [ETHYLENEBIS[(CARBOXYMETHYLIMINO)ETHYLENENITRILO]]TETRA-
complexes with gallium, iron, thorium, or uranium, formation of, biamperometric studies of, 20: 38810
ACETIC ACID, (ETHYLENEDIAMINE) TETRA-
analytical use in radiometric determination of cobalt and zinc, 20: 38806
effects on uptake of cerium-144, strontium-90, and yttrium-91 by algae, 20: 38570
solvent properties with tertiary amine for rare earths, 20: 38995 (BM-RI-6809)
ACETIC ACID, (ETHYLENEDIAMINE)TETRA-, CALCIUM DISODIUM SALTS
effects on cerium-144 induced radiation sickness in rats, 20: 38732
ACETIC ACID, (ETHYLENEDIAMINE) TETRA- COMPLEXES
with gallium, iron, thorium, or uranium, formation of, biamperometric studies of, 20: 38810
ACETIC ACID, NITRILOTRI- COMPLEXES
with gallium, iron, thorium, or uranium, formation of, biamperometric studies of, 20: 38810
ACETONE
effects on annealing of recoil damage in neutron-irradiated cobalt complexes, 20: 38965
viscosity of, use of oscillating sphere device for measuring, 20: 38872(R) (NYO-1769-68)
ACETONE, THENOYL-
complexes with copper and uranyl ions in mixture with other β-diketone in benzene solution, 20: 38855 (BNL-10350)
ACETONE, THENOYLTRIFLUORO-
complexes with copper and uranyl ions in mixture with other β-diketone in benzene solution, 20: 38855 (BNL-10350)
ACETONITRILE
analytical use in coulometric determination of europium, samarium, and ytterbium, 20: 38812
effects on color production in controlled-potential coulometric reduction of rare earths, 20: 38813
molecular structure of hydrochloride of, neutron diffraction studies of, 20: 38935
ACETYLENE
yields from radiolysis of methane by electrons and gamma rays, 20: 38951
ACID PHOSPHATES
complexes with americium, cerium, promethium, and yttrium, ion exchange studies on, 20: 38878(T) (ORNL-tr-1257)
ACOUSTIC WAVES
propagation along warm plasma columns, (T), 20: 40166 (AD-637711)
ACRIDINES
effects of exposure of uv irradiated chick embryo cells to, 20: 38707
effects on DNA, 20: 38542(T) (UCRL-Trans-10029)
ACRIFLAVINE
radiosensitivity effects on bacteria, y, light, and uv, 20: 38611
ACRYLAMIDE
radioinduced polymerization of, to yield foamed plastics, 20: 38981(P)
ACRYLIC ACID
radioinduced polymerization of, to yield foamed plastics, 20: 38981(P)
acrylic monomers–aromatic vinyl monomers–polyisobutylene, radioinduced formation of thermoplastic resin of, 20: 38978(P)
ACTINIDE OXIDES
actinide oxides–HfO_2, preparation of sols of, 20: 39442(P)
actinide oxides–ZrO_2, preparation of sols of, 20: 39442(P)
actinide oxides–rare earth oxides, preparation of sols of, 20: 39341(P)
actinide oxides–Y_2O_3, preparation of sols of, 20: 39341(P)
ACTINIDES
crystal structure of, valence electrons and interatomic bonds in, 20: 40296
separation of berkelium from, efficiency and hydraulic stability of equipment rack for solvent extraction, 20: 38998(R) (ORNL-3958)
vaporization of, thermodynamics of, 20: 38876 (UJV-1598)
ACTINIUM
crystal structure of, valence electrons and interatomic bonds in, 20: 40296
ACTINIUM ISOTOPES Ac-227
alpha-beta branching ratio of, 20: 39321(R) (MLM-1312)
biological half-life in thorax of man, 20: 38554
distribution of inhaled, in tissues of man, 20: 38554
production in BR-2, 20: 39277 (DP-1066(Vol.1), pp III.63-9)
ACTINOMYCIN
effects on DNA-ase and RNA-ase activity in Ehrlich ascites cells, 20: 38578
ACTIVATION ANALYSIS
facility design for on-line, 20: 39025 (ORO-2980-12)
method for determining sputtering yields, 20: 39585
neutron tube for, high-output sealed-off, 20: 38839
quality control in, requirements for, 20: 38853
radiochemical separations for use with, of biological materials, 20: 38904
standards for, of biological materials, 20: 38844
use in biological sciences, 20: 38836
use of automated gamma spectrometers for, of biological materials, 20: 38843
use of 14-Mev neutrons in, 20: 38838
use of $^{32}S(n,p)^{32}P$ reaction for measurement of fast neutron flux densities, 20: 39222
ACTIVATION DETECTORS
design for reactor neutron flux mapping, 20: 39252(P)
performance of sulfur, for fast neutron dosimetry, 20: 39228
ADENINE
uptake of, in *Vivia faba*, effects of radioinduced toxins on, 20: 38664
ADENOSINEPHOSPHORIC ACIDS
analysis for oxygen, activation, 20: 38848
determination in erythrocytes using oxygen-18, proton activation, 20: 38841
ADRENAL GLANDS
radiation effects on function of rat, x, 20: 38638
radiation effects on rat, biochemical, x, 20: 38661
radiation effects on immune reactions of rabbit, x, 20: 38697
radiation effects on content of, in rabbits, x, 20: 38654
radiosensitivity effects of cortical, in animals, 20: 38653
radiosensitivity of dog, 20: 38684
ADRENALINE
effects on inhibition of tissue reaction in irradiated rabbit connective tissue, 20: 38640
radiation effects on content of, in rabbits, x, 20: 38654
radiosensitivity effects on lymphocytes in blood, x, 20: 38678
radiosensitivity effects on rabbits, 20: 38686
ADRENOCORTICOTROPIC HORMONE
radiation effects on content in rat blood, x, 20: 38661
ADVANCED TEST REACTOR
fuel element thermal-hydraulic-structural performance, 20: 40460(R) (IDO-17191)
fuel plates for, fabrication of curved, 20: 39358 (ORNL-3983)
neutron flux depression in fuel plates of, 20: 40460(R) (IDP-17191)
reactivity change in ATRC, core replacement effects on, 20: 40460(R) (IDO-17191)
AEROSOL GENERATORS

performance of spinning-disk type, 20: 39103(R) (BNWL-235-3, pp 51-69)
AEROSOLS
effect on radioactivity levels in air, 20: 39114
AGE ESTIMATION
method of, using fission tracks, 20: 39135
of soils from thorium and uranium distribution, 20: 39144
potassium–argon method of, for tektites, 20: 39135
rubidium–strontium and strontium-87/-86 method of, 20: 39126
use in geochronology in Sweden, 20: 39125
use of uranium-234 to uranium-238 ratio in, 20: 39120
AGING
effects of, on strontium-90 turnover rates, 20: 39150(R) (NYO-2753-4)
hemoglobin and hematocrit levels in irradiated rats, 20: 38619
AIR
effects on heavy water decomposition, 20: 40409(R) (NP-16230)
radiation effects on, plasma properties induced by alpha, (E), 20: 39662
sampling, design of IBM card holder used in, 20: 39253
air–water, voidage measurements in upward two-phase flow through tube, 20: 39045 (AEEW-M-650)
AIRCRAFT
fuel gage for, radiometric, 20: 39189(P)
ALANINE
radiolysis of, in aqueous solution, γ, 20: 38582
ALANINE, PHENYL-
radiolysis of, in aqueous solution, γ, 20: 38582
ALBUMINS
radiation effects on concentration of, in potato tubers, x, 20: 38690
ALDEHYDES
determination in irradiated fruit juices, chromatographic, 20: 39300
ALDOSTERONE
biogenesis and metabolism in elderly men, tracer study on, 20: 38547(R) (NYO-918-15)
use of carbon-14-labeled, for measurements on peripheral blood, 20: 38547(R) (NYO-918-15)
ALGAE
cerium-144 uptake by, effects of EDTA on, 20: 38570
strontium-90 uptake by, effects of EDTA on, 20: 38570
yttrium-91 uptake by, effects of EDTA on, 20: 38570
ALKALI METAL HYDROXIDES
reactions with zirconium tetrachloride to form zirconium dioxide, 20: 38929(P)
spectra of gamma-irradiated alkali benzoate- or α-naphthoate-containing glass of, ESR and optical, 20: 38941(R) (RRL-2310-182)
ALKALI METAL IONS
polarization capacities, 20: 38879(T) (UCRL-Trans-1325)
ALKALI METALS
chemical properties of, in solution, 20: 38873(R) (NYO-2269-9)
ion exchange on minerals, 20: 38858 (BNWL-235-3, pp 23-51)
spectrometry of gaseous compounds of, for MHD Generators, 20: 39724
ALKALINE EARTH METALS
chemical properties of, in solution, 20: 38873(R) (NYO-2269-9)
ALKANES
determination in irradiated meats and meat components by gas chromatography and mass spectrometry, 20: 39301
properties of N-Paraffins-175 for use in stacked-clone contactor, 20: 38998(R) (ORNL-3958)
ALKENES
determination in irradiated meats and meat components by gas chromatography and mass spectrometry, 20: 39301
oil shales–polyolefins, fabrication of molded articles of, using heat, pressure, and radiation, 20: 38974(P)
ALLOYS
analysis by electron scattering, 20: 38799(R) (NLCO-980)
book: *Optical Properties and Electronic Structure of Metals and Alloys*, 20: 39339
ALLYL ALCOHOL
radioinduced polymerization of, kinetic study of, 20: 38956
ALPHA DECAY
of nuclei in crystals, research using shadow effect, 20: 40135
ALPHA PARTICLES
density in ionosphere, energy spectra from, (E), 20: 39987
detection of, design of counter for, 20: 39254
effects on astroglial cells and blood vessels in rat brain, glycogen accumulation from, 20: 38674
effects on brain wave activity during conditioned activity of cats, 20: 38602(R) (UCLA-34P60-1)
effects on carboxylation of formate, 20: 38966
effects on cerium sulfate in presence of thallous ions, intratrack distribution of primary products of, 20: 38967
effects on luminescence of liquid phosphors, 20: 38957
effects on nickel-63 diffusion in copper, 20: 39451 (EUR-2968.e)
effects on partially dissociated and ionized air, (E), 20: 39662
reactions ($\alpha,\alpha'\gamma$) with chromium isotopes at 4 to 5.6 Mev, gamma spectra from, (E), 20: 39470(R) (ORNL-3924)
reactions ($\alpha,\alpha'\gamma$) with palladium isotopes at 9 to 10 Mev, gamma spectra from, (E), 20: 39470(R) (ORNL-3924)
reactions (α,nγ) with oxygen-18 at 4.43 Mev, neon-21 energy levels from, (E), 20: 40156
reactions with gold at 3 Mev, energy loss spectra from, (E), 20: 39602
scattering by beryllium-9, spin-orbit potential in elastic, (T), 20: 40089
scattering by helium-4 at 12 to 20 Mev, phase analysis of elastic, 20: 40065(R) (BMwF-FB-K-66-01)
scattering by lithium-7 at 1.6 to 12.0 Mev, boron-11 energy levels from, (E), 20: 40111
scattering by phosphorus-31, calculations using distorted-wave Born approximation, (T), 20: 40090
ALPHA SOURCES
activity of, in fallout from USSR and Chinese nuclear tests, 20: 39109
efficiency in radiation-chemical apparatus, method for calculating, 20: 38943
monitoring in air, 20: 39269
monitoring of, large-area scintillation detector for, 20: 39257
preparation of, for analysis by alpha spectrometry, 20: 38990
use in measurement of properties of thin films, 20: 39298
ALPHA SPECTROMETERS
alpha source preparation for use with, 20: 38990
design and performance of simultaneous alpha and beta, using cesium iodide, 20: 39217
uses in geochemistry, 20: 39143
ALUMINUM
analysis for magnesium by neutron activation methods, 20: 38804
content in fallout from Chinese atomic test, Oct. 1964, 20: 39110
determination in coal by activation, on-line, 20: 39025 (ORO-2980-12)
effects of medium of, on gamma energy spectra, (E), 20: 40290
effects on properties of magnesium-base alloys for fuel-element cladding, 20: 39443(P)
fabrication by magnetic-pulse forming, 20: 40490 (Y-1483)
reactions with oxidized Zircaloy-2 at 400 to 500°C, 20: 39380 (AECL-2570)
reactions with uranium tetrafluoride at high temperatures, production aluminum–uranium alloy by, 20: 39333
sputtering by cesium ions at 1 to 10 kev, 20: 39585
superconductivity of, 20: 40047
ALUMINUM ALLOYS
Al–Bi–Cu–Pb, fatigue failure of 2011-T3, equations for, 20: 39396 (IS-T-60)
Al–Ce, magnetic properties of intermetallic compounds of, 20: 39433
Al–Cr–Y, crystal structure of intermetallic compounds in, 20: 39414
Al–Cu–Y, crystal structure of intermetallic compounds in, 20: 39414
Al–Dy, magnetic properties of intermetallic compounds of, 20: 39433
Al–Er, magnetic properties of intermetallic compounds of, 20: 39433
Al–Fe–Y, crystal structure of intermetallic compounds in, 20: 39414
Al–Gd, magnetic properties of intermetallic compounds of, 20: 39433
Al–Ho, magnetic properties of intermetallic compounds of, 20: 39433
Al–Mg, fatigue of Magnox A180, plastic strain range at 350 to 500°C, 20: 39419
Al–Mn–Y, crystal structure of intermetallic compounds in, 20: 39414
Al–Nd, magnetic properties of intermetallic compounds of, 20: 39433
Al–Pr, magnetic properties of intermetallic compounds of, 20: 39433
Al–Pu, fabrication, hazards evaluation tests, 20: 39153
Al–Sm, magnetic properties of intermetallic compounds of, 20: 39433
Al–Tb, magnetic properties of intermetallic compounds of, 20: 39433
Al–Tm, magnetic properties of intermetallic compounds of, 20: 39433
Al–U, phase studies of uranium-base, 20: 39388 (CEA-R-2956)
Al–U, production of intermetallic compound, by direct reduction of uranium tetrafluoride, 20: 39333
Al–Yb, magnetic properties of intermetallic compounds of, 20: 39433
ALUMINUM COMPLEXES
with dipentyl pentylphosphonate, spectra of, infrared, 20: 38799(R) (NLCO-980)
ALUMINUM FLUORIDES
effect on metallurgical properties of uranium metal produced by reduction of uranium(IV) fluorides, 20: 39342(P)
ALUMINUM HYDROXIDES
radiation effects on rate of decomposition of, beta and gamma, 20: 38955
ALUMINUM ISOTOPES Al-27
neutron scattering at 14.2 Mev, cross sections for, (E), 20: 40069(R) (EANDC(E)-66(U))
proton reactions (p,α) with, Q value for, (E), 20: 40099
proton reactions (p,α) at 11 to 19.7 Mev, excitation function for, (E), 20: 40101
ALUMINUM OXIDES
determination in swimming pool reactor coolant, activation and chemical, 20: 38800 (PAEC(C)RE-652)
effects on grain size of tungsten, 20: 39400 (NASA-TN-D-3531)
electric properties of reactively evaporated films of, 20: 39274 (N-66-

18175)
leaching of fission products from, with distilled water and nitric acid, 20: 40478 (IN-1011)
surface areas of, calculation and measurement methods for, 20: 39387 (CEA-R-2947)
thermal conductivity of concretes containing, (E), 20: 39698
Al–Al_2O_3, fabrication and properties of dispersion-strengthened, 20: 39359 (RISO-113)
Al–Al_2O_3, rupture strength of, effects of microstructure on, 20: 39398 (NASA-TN-D-3527)
Al_2O_3–$AlPO_4$–ZrO_2–$Zr_3(PO_4)_4$, preparation of foam for insulating materials, 20: 39375(P)
Al_2O_3–Cu, rupture strength of, effects of microstructure on, 20: 39398 (NASA-TN-D-3527)
Al_2O_3–Gd_2O_3, phase studies, 20: 39437
Al_2O_3–W, phase diagrams, 20: 39437
ALUMINUM PHOSPHATES
Al_2O_3–$AlPO_4$–ZrO_2–$Zr_3(PO_4)_4$, preparation of foam for insulating materials, 20: 39375(P)
ALUMINUM SYSTEMS
Al–Al_2O_3, fabrication and properties of dispersion-strengthened, 20: 39359 (RISO-113)
Al–Al_2O_3, rupture strength of, effects of microstructure on, 20: 39398 (NASA-TN-D-3527)
Al–ClF_3, shock-wave compression measurements on mixtures, (E), 20: 39469 (LA-3453)
Al–Si, dispersion in graphite, optimum pressure and temperature for liquid, 20: 39355 (EUR-3988.f)
Al–Zircaloy-2–ZrO_2, phase studies, 20: 39380 (AECL-2570)
AMBERLITES
solvent properties for protactinium, 20: 39003
AMERICIUM
crystal structure of, valence electrons and interatomic bonds in, 20: 40296
determination in sulfuric acid solutions containing ammonium sulfate by controlled-potential coulometry, 20: 38854
vaporization of, thermodynamics of, 20: 38876 (UJV-1598)
AMERICIUM COMPLEXES
with acid phosphates, ion exchange studies on composition and stability of, 20: 38878(T) (ORNL-tr-1257)
AMERICIUM ISOTOPES Am-241
radiation effects on, self, 20: 39448 (AERE-X-PR-2596-9)
use in measurement of properties of thin films, 20: 39298
AMERICIUM OXIDES
AmO_2–HfO_2, preparation of sols of, 20: 39442(P)
AmO_2–rare earth oxides, preparation of sols of, 20: 39341(P)
AmO_2–Y_2O_3, preparation of sols of, 20: 39341(P)
AmO_2–ZrO_2, preparation of sols of, 20: 39442(P)
AMETHOPTERIN
radiosensitivity effects on cultured mammalian cells, x, 20: 38710
AMINES
tertiary, solvent properties with diethylenetriaminopentaacetic acid or EDTA for rare earths, 20: 38995 (BM-RI-6809)
AMINO ACIDS
activities in transfer-RNA, 20: 38998(R) (ORNL-3958)
determination in irradiated meats and meat components by gas chromatography and mass spectrometry, 20: 39301
effects of absence of essential, on nucleic acid and protein synthesis in uv-irradiated *E. coli*, 20: 38562
effects of absence of essential, on survival of uv-irradiated *E. coli*, 20: 38563
radiolysis of eleven, in aqueous solution, γ, 20: 38582
AMINO COMPOUNDS
effects as radioprotective agents in mice, relation to chemical structure, 20: 38724
AMMONIA
effects on heavy water decomposition, 20: 40409(R) (NP-16230)
metabolism in rats, tracer study, 20: 38600(R) (TID-23034)
metabolism in wheat seedlings, 20: 38548(R) (ORO-2410-1)
radiolysis of, adsorbed on zeolites, EPR studies of gamma, 20: 38944
reactions with uranium tetrabromide and tetrachloride at 20 to 700°C, products formed in, 20: 38920
AMMONIUM BROMIDES
neutron reactions at 0.025 to 0.4 ev, total cross sections for, (E), 20: 40069(R) (EANDC(E)-66(U))
AMMONIUM CHLORIDES
neutron reactions at 0.025 to 0.4 ev, total cross sections for, (E), 20: 40069(R) (EANDC(E)-66(U))
AMMONIUM FLUOPHOSPHATES
radiation effects on, ESR spectra of phosphate ion from x, 20: 38549
AMMONIUM IODIDES
neutron reactions at 0.025 to 0.4 ev, total cross sections for, (E), 20: 40069(R) (EANDC(E)-66(U))
AMMONIUM LANTHANUM NITRATES
crystallization of, 20: 38915
AMMONIUM NEODYMIUM NITRATES
crystallization of, 20: 38915
AMMONIUM PRASEODYMIUM NITRATES
crystallization of, 20: 38915
AMMONIUM SAMARIUM NITRATES
crystallization of, 20: 38915
AMMONIUM SULFATES
$(NH_4)_2SO_4$–H_2SO_4, analysis for americium by controlled-potential coulometry, 20: 38854
AMMONIUM THORIUM OXALATES
preparation and crystal structure of, 20: 38886
AMPLIFIERS
design for radiation detectors in satellites, 20: 39268
design of d-c, for use in filters, 20: 39186
design of solid-state, with fast recovery, 20: 39188
ANALYSIS
equipment and method for, of mixed flowing fluids, 20: 39191(P)
ANEMIA
radioinduced in rats, pathology of, 20: 38619
radioinduced in rats, effects of bone marrow transfusions on, 20: 38711
ANESTHETICS
effects of, on skin reactions in irradiated mice, 20: 38627
ANILINE, DIMETHYL-p-NITROSO-
radiolysis of aqueous solutions of, mechanisms of pulse, 20: 38939(R) (NYO-2668-13)
ANIMAL CELLS
chromatid exchange frequency in, 20: 38649
effects of irradiated medium on chick embryo, 20: 38707
neutron dosimetry in cultured, fast, 20: 39227
radiation effects on ribonucleic acid metabolism in cultured HeLa, γ, 20: 38683
radiation effects on interactions of Polyoma virus with mouse embryo, 20: 38702
radiation effects on cultured HeLa, effects of metabolic inhibitors on x, 20: 38710
radiation effects on, morphological, γ, 20: 38769
radiation injuries of, role of toxins in, 20: 38664
radiosensitivity of, effects of 5-bromouracil on, 20: 38968
ANIMAL REPRODUCTION
effects of gestation on blood serum proteins in hamsters, 20: 38598(R) (TID-22955)
radiation effects on mouse, whole-body x, 20: 38590(R) (NYO-1979-13)
radiation effects on, of grain moths, gamma, 20: 38705
radiation effects on mice, following administration of ^{137}Cs and ^{90}Sr in drinking water, 20: 38551
radiation effects on mouse, fast neutron and γ, 20: 38647
ANIMAL RESPIRATION
effects of osmolarity, ion concentration, and substrate on, in cultured Ascites tumor cells, 20: 38599 (TID-22968)
ANIMALS
analysis for vanadium in Swedish, activation, 20: 38565
cerium-144 metabolism in, mathematical model for, 20: 38571
chlorine metabolism in, tracer study, 20: 38550
desoxyribonucleic acid from, use of neutron activation analysis in characterization of, 20: 38816
effects of radiosterilized food on, 20: 39302
iodine-131 content in thyroid in, activation studies on, 20: 38564
medicine of, uses of radiation and radioisotopes in, 20: 38748
neutron dosimetry in, using ionization chambers, 20: 39227
nucleic acid synthesis in, mechanisms of radiosensitivity of, 20: 38585
pathology of radiation sickness in, effects of age and sexual maturity on, in whole-body x-irradiated, 20: 38685
radiation effects on, 20: 38544
radiation effects on, whole-body biological, effects of pre-irradiation on, 20: 38696
radiation effects on, protection against, 20: 38718
radiation effects on pathology of tissues in, 20: 38653
radiotherapy of skeletal muscles, alpha, 20: 38776
ANNEALING
effects on impurity-atom concentration in ion-bombarded silicon, 20: 40345
effects on irradiated graphite, survey on, 20: 39455 (EUR-3056.e)
effects on point defects in iron, model of, 20: 39386 (CEA-R-2905)
effects on white cast iron during electron irradiation, 20: 39464
ANOXIA
radiosensitivity effects on carcinoma cells, 20: 38635
radiosensitivity effects on transplanted lymphoma cells in mice, x, 20: 38699
radiosensitivity effects on blood vessels in rabbit connective tissue, 20: 38640

ANTHRACENE
phosphorescence decay kinetics in, at 298 and 77°K, effects of deuterium on, 20: 38958
radiation effects on diffusion of triplet excitons in, 20: 38957
ANTHRAQUINONE
labeling with deuterium by isotopic exchange with deuterium-labeled sulfuric acid, 20: 38889
ANTIBIOTICS
radiosensitivity effects of cycloheximide and puromycin on cultured mammalian cells, x, 20: 38710
ANTIBODIES
effects of procaine on formation of, in irradiated dogs, mice, rabbits, and rats, 20: 38727
radiation and Brucella effects on, in rabbits, 20: 38586
radiation effects on antiinsulin, loss of activity in presence of iodine-131, 20: 38579
radiation effects on production in rabbit cornea, x, 20: 38608
radiation effects on content in rat blood serum, γ, 20: 38695
ANTIFERROMAGNETIC MATERIALS
phase transitions in manganese–nickel, neutron diffraction studies on, 20: 39407(T) (ANL-Trans-344)
ANTIGENS
effects on potassium content in blood of rabbits, 20: 38697
preparation of brain tissue and tumor, 20: 38745(R) (NYO-3267-3)
radiation effects to corneal response to, x, 20: 38608
radiation effects on antibody binding of, iodine-131, 20: 38579
radiation effects on response of rabbits to bacterial, 20: 38641
ANTIMONY
separation from bismuth in acid solution by solvent extraction using alkyl phosphates, 20: 38828
ANTIMONY ALLOYS
Sb–In, plasma oscillations in, spin-orbital interaction effects on, 20: 40227
Sb–In, radiation effects in, stage-II, (E), 20: 40328
Sb–Tm, magnetization of cubic, anisotropy and thermal inversion in high-field, 20: 40320
ANTIMONY IONS
mobility in gold, effects of high electronic current density on, 20: 40349
ANTIMONY ISOTOPES Sb-122
neutron reactions at 7.8 to 64 kev, activation cross sections for, (E), 20: 40069(R) (EANDC(E)-66(U))
ANTIMONY ISOTOPES Sb-124
neutron reactions at 7.8 to 64 kev, activation cross sections for, (E), 20: 40069(R) (EANDC(E)-66(U))
ANTIMONY ISOTOPES Sb-125
tracer use in ion mobility studies, 20: 40349
ANTINEUTRINOS
field theory for, quantum, 20: 39853 (JEN-157-DF/I-48)
ANTIPROTONS
interactions with protons at 2 to 6 Bev/c, Regge-pole model for cross sections for, (E/T), 20: 39801
interactions with neutrons at 2 to 6 Bev/c, Regge-pole model for cross-sections for, (E/T), 20: 39801
APPENDIX
nucleic acid synthesis in, effects of gamma dose, 20: 38585
ARACHIDONIC ACID
radiation effects on content of, in rat tissues, x, 20: 38701
ARGENTINA
strontium-90 content in boaes and diets of children, 1965, 20: 39150(R) (NYO-2753-4)
ARGININE
radiolysis of, in aqueous solution, γ, 20: 38582
ARGON
conductivity of potassium-seeded plasma of, nonequilibrium, (T), 20: 39684
current conduction in seeded plasma of, (E), 20: 39660
current densities in cesium-seeded plasma of, (E), 20: 39736
current distribution in potassium-seeded plasma at 2000°K, 20: 39718
current-voltage curves for moving plasma of, (E), 20: 39655
effects on yields in gamma radiolysis of ethylene solutions, 20: 38941(R) (RRL-2310-182)
electric conductivity of seeded plasma of, (E), 20: 39670
electric conductivity of seeded, in MHD loops, (E), 20: 39727
electric discharge in alkali-metal seeded, (E), 20: 39715
electron beam injection into afterglow plasma of, cyclotron harmonic radiation from, 20: 40165 (AD-637710)
electron density and temperature in electric arcs in, (E), 20: 39666
ionization in MHD generators, magnetically induced, (E), 20: 39679
ionization instability in seeded plasma of, (F), 20: 39671
kinetics of liquid, calculations using self-correlation function, (T), 20: 39946
losses near walls in cesium-seeded plasma of, 20: 39673
meson (μ^-) capture by, spectra from, 20: 39578 (JINR-P-2807)
neutron scattering by, cross sections and electron-neutron interaction from thermal, (E), 20: 40129
plasma radiation properties of potassium-seeded, (E), 20: 39699
reactions with cosmic neutrons in atmosphere, phosphorus isotope production by, 20: 39991
relaxation phenomena in cesium-seeded, (T), 20: 39700
scattering by argon during thermal diffusion, 20: 39321(R) (MLM-1312)
spectra of cesium recombination continuum in plasma, 20: 39722
viscosity of, saturated-liquid, (T), 20: 39940
ARGON IONS
reactions with deuterium and hydrogen molecules, cross sections for charge-exchange, (E), 20: 39592
reactions with gold foils, interstitial atom migration in, 20: 40295
sputtering of single-crystal copper, yields crossover in, (E), 20: 39589
sputtering on potassium chloride crystals at 30 kev, angular dependence of, (E), 20: 39600
ARGON ISOTOPES
thermal diffusion factor for, temperature dependence in, 20: 39326
ARGON ISOTOPES Ar-36
neutron scattering by, cross sections for thermal, (E), 20: 40129
separation from argon-38 by thermal diffusion, 20: 39321(R) (MLM-1312)
ARGON ISOTOPES Ar-37
electron capture ratios, M/L, 20: 40153
ARGON ISOTOPES Ar-38
separation from argon-36 by thermal diffusion, 20: 39321(R) (MLM-1312)
ARGON ISOTOPES Ar-40
proton elastic scattering near 1.1 Mev, resonances in, (E), 20: 40147
ARGON SYSTEMS
Ar–H, electron density and temperature in plasma jet of, 20: 40215
Ar–H, meson (μ^-) capture by, spectra from, 20: 39578 (JINR-P-2807)
ARMY REACTORS
core design for, evaluation of PM replacement, 20: 40405 (HIT-3583-27)
ARMY REACTORS (SM-1)
fuel plates for Core III, reactivity evaluation of, 20: 40374 (ACNP-63562)
ARSENIC
determination in man, activation, 20: 38847
determination of traces of, in biological materials, activation, 20: 38837
separation from bismuth in acid solution by solvent extraction using alkyl phosphates, 20: 38828
ARTERENOL
effects on inhibition of tissue reaction in irradiated rabbit connective tissue, 20: 38640
radiation effects on content of, in rabbits, x, 20: 38654
ASCORBIC ACID
content in adrenal glands of irradiated and unirradiated rats, 20: 38661
content in Gramineae seeds, 20: 38583
effects on enzyme release from x irradiated lysosomes in rat liver, 20: 38577
radiation effects on content in germinating seeds, β and γ, 20: 38583
radiation effects on content in rat brain, whole-body x, 20: 38679
radiation effects on content of, in rat blood, dietary effects of B group vitamins, folic acid, and phosphatides on gamma and x-ray, 20: 38721
radiation stability of a complex of pyridoxine and, γ, 20: 38580
ASTRONAUTS
radiation protection during space flight, 20: 38603(T) (AD-629422)
ASTROPHYSICS
evaporative and hydrodynamical atmospheric models, 20: 39556
ATLANTIC OCEAN
uranium-234/-238 ratio in, 20: 39133
ATMOSPHERE
analysis for iodine-129, activation, 20: 38564
auroral effects on, 20: 39947
charged-particle penetration into auroral, hydrogen and helium spectra from, (T), 20: 39981
diffusion in, field and wind-tunnel measurements of, 20: 39105
electrical conductivity of, effects of fallout on, 20: 39111
monitoring for beta activity, instrument for, 20: 39259
monitoring of, equipment for alpha and beta, 20: 39269
phosphorus isotope production in, by argon-cosmic neutron reactions, 20: 39991
radioactivity content in, review of methods for measuring, 20: 39104
radioactivity of ground-level, at Toulouse, France, 20: 39114
ATOMIC CLOUDS
particulate rainout from, mathematical analysis of, 20: 39107 (UCRL-14700)
ATOMIC ENERGY, LEGAL ASPECTS
book: *Progress in Nuclear Energy, Series X, Law and Administration Vol. 4*, 20: 40491
radioisotope control in pharmaceutical industry in Belgium, 20: 39156
ATOMIC EXPLOSIONS

economics of, for underground gas storage, 20: 39015 (UCRL-14877)
effect of, atmospheric, 20: 39149 (NVO-28)
effect on ground water contamination, 20: 39149 (NVO-28)
effect on mine safety, 20: 39149 (NVO-28)
effects of, shock and seismic, 20: 39149 (NVO-28)
fallout from Chinese, Oct. 1964, 20: 39110
fallout from Chinese, 1964 and 1965, alpha activity of, 20: 39109
fallout particle size from Chinese, May 1965, 20: 39108
gamma flux from, electron interactions with, (T), 20: 39775
ground motion from, effect on structures, 20: 39149 (NVO-28)
particulate rainout from nuclear device cloud after, mathematical analysis of, 20: 39107 (UCRL-14700)
protection against, design of structure for, 20: 39053(P)
radiation from, shielding against initial, 20: 39061
safety in, geologic and hydrologic effect on, 20: 39149 (NVO-28)
seismic data from RED HOT, long-range, 20: 39124 (AD-632957)
use to create underground gas storage reservoirs, 20: 39014(R) (TID-23184)

ATOMIC WEAPONS
effects of, survey of, 20: 39055
effects on industry, study of recovery from, 20: 39146 (AD-636947)
radiation from, distribution of initial and residual, 20: 39056
simulation of, linear accelerator adaptation for, 20: 39487(R) (EGG-1183-2009)
simulation of, linear accelerator adaptation for, 20: 39488(R) (EGG-1183-2027)
simulation of, linear accelerator adaptation for, 20: 39489(R) (EGG-1183-2050)
simulation of, linear accelerator adaptation for, 20: 39490(R) (EGG-1183-2051)
targeting assumptions for attacks against U. S. population, 20: 39087

ATOMS
content of impurity, in ion-bombarded silicon, 20: 40345
detection of low-energy neutral, system for, 20: 39580(R) (ORNL-3989, pp 78-88)
electron scattering by, total cross sections for, (T), 20: 39818
gamma scattering by K electrons of, cross sections for Compton, (T), 20: 39773
interactions with electrons, electron exchange in, 20: 39582(T) (AERE-Trans-1053)
interactions with atoms, theory for slow, 20: 39620
photon emission and absorption by, time correlation for exchange, 20: 39577 (JINR-P-2791)

ATROPINE
effects on inhibition of tissue reaction in irradiated rabbit connective tissue, 20: 38640

AUGER ELECTRONS
detection in Moessbauer spectra of cobalt oxides, 20: 39603

AURORAL STORMS
distribution of, effect of atmospheric tides on vertical, 20: 39961(T)
heights as function of density at Tixie Bay during 1962–1964, 20: 39961(T)
infrared and x-ray intensities in auroral zones, balloon observations of, 20: 39990
intensity of polar, relation to magnetic disturbances of, 20: 39955
latitude of, over College, Alaska, during 1965, 20: 39971
occurrence and geographical spread of, geomagnetic and solar activity effects on, 20: 39956
properties and relationship to atmospheric phenomena, 20: 39947

AUSTRIA
nuclear power development in, 20: 40441
nuclear power use in, for electricity production, 20: 40442

AVR REACTOR
conversion rate of thorium-232 in, 20: 40469
fuel cycle costs, 20: 40470
fuel element design, 20: 40468
fuel element development for, 20: 40467

B

BACTEREMIA
radiation effects on incidence in guinea pigs, x, 20: 38656

BACTERIA
effects of Brucella and radiation on malic dehydrogenase activity of rabbit peritoneal cells, 20: 38586
radiation effects on *Micrococcus lysodeikticus*, lethal and mutagenic, molecular basis for, 20: 38574(R) (NYO-3449-1)
radiation effects on *Chlamydomonas reinhardi*, effects of acriflavine on γ, light, and uv, 20: 38611
radiation effects on buccal flora of dogs and monkeys, γ, 20: 38667
radiation effects on rabbits injected with typhoid antigens, x, 20: 38641
radiation effects on number on mucous membranes and skin of animals, 20: 38644
radioresistant, metabolism of, γ, 20: 39288(R) (ORO-636)
radiosensitivity of exogenous on oysters, 20: 39288(R) (ORO-636)

BACTERIOPHAGES
growth on *E. coli*, genetic control of, 20: 38620
growth on *E. coli*, genetic control of, 20: 38621
mutations of, molecular mechanisms for induction of, 20: 38542(T) (UCRL-Trans-10029)
radiation effects on, effects of cysteine, cysteamine, and glycerol on x, 20: 38628
radiation effects on iodouracil-substituted T1, uv, 20: 38704
radioinduced mutants in *Serratia marcescens* κ, uv, 20: 38670
radiosensitivity effects of 5-bromouracil on, x, 20: 38712

BALANCES
design of thermogravimetric, 20: 38835

BARIUM
diffusion from sodium at high temperatures, factors affecting, 20: 40357 (NAA-SR-11766)
metabolism in rats, effects of strontium content in diet, tracer study, 20: 38566
separation and purification of, from lanthanum-140, 20: 39001
superconductivity of, 20: 40047

BARIUM CHLORIDES
diffusion in, self-, 20: 38871(R) (NYO-1769-54)
ionic transport coefficients for, at 25°C, 20: 38909
$BaCl_2$–Na_2CO_3–$UO_2(NO_3)_2$, uranium precipitation in, mechanism of, 20: 38928

BARIUM FERRATES
preparation and properties of, 20: 38859 (CEA-R-2895)
separation processes for, 20: 38859 (CEA-R-2895)

BARIUM ISOTOPES Ba-134
internal conversion coefficient of 800-kev transition in, (E), 20: 40095

BARIUM ISOTOPES Ba-140
content in fallout from USSR nuclear test, Jan. 1965, 20: 39108
decay curves for precursors of, 20: 40357 (NAA-SR-11766)

BARIUM OXIDES
BaO–SiO_2–ZrO_2, phase studies, 20: 38899

BARIUM TITANATES
phase transformations, effect of pressure and irradiation on solid-solid, (E), 20: 40306

BARLEY
radiation effects on seeds of, genetic, effects of centrifugation on γ, 20: 38618
radiation effects on seedlings of, physiological, γ, 20: 38691
radiosensitivity effects of water content and calcium chloride solutions on seeds of, x, 20: 38736
radiosensitivity of embryonic tissues of, 20: 38588(R) (COO-1400-10)

BARRIERS
pure radius in, determination of mean, 20: 39012(P)

BARYONS
electromagnetic properties in non-relativistic quark model, 20: 39835
form factors of, current-algebra relations between vector and axial-vector, 20: 39898
interactions with baryons, SU(3) symmetry for, (T), 20: 39765 (ORO-2504-91)
interactions with mesons, bootstrap static model of SU(6) symmetry for, 20: 39813
interactions with mesons, multichannel calculations in static model for, 20: 39887
interactions with mesons at low-energies, nonrelativistic SU(6) symmetry for, 20: 39904
mass differences of, calculations of electromagnetic, 20: 39928

BARYONS, RESONANCE
classification in SŪ(12) representations, 20: 39907
existence of unitary multiplets of, 20: 39860 (JINR-P-2790)
mass and width difference (N^{*-}–N^{*++}), measurement of, (E), 20: 39847
parity of Regge recurrences in meson (π)-nucleon interactions, (T), 20: 39749 (COO-881-77)
production of $\Lambda\eta$, in meson (π^-)-proton interactions at 4 Bev/c, (E), 20: 39754 (JINR-E-2858)
production of N^{*0} and N^{*++}, in meson (π^-) interactions with protons at 7.0 Bev/c, 20: 39790
production of N^* and Y_1^* (1385) in meson (K^-)-proton interactions at 1.80 to 1.95 Bev/c, (E), 20: 39838
production of N^* (1236), (1518), and (1688), in meson (π)-nucleon interactions, (T), 20: 39839
production of N^* (1920) in meson (π^+)-proton interactions at 1350 Mev, (E), 20: 39845
production of $N_{3/2}^{*++}$ and $N_{3/2}^{*0}$, from meson (π^-)-proton interactions at 7.5 Bev, (E), 20: 39758 (JINR-P-2773)
production of Y_0^* (1385) and Y_1^* (1405), in meson (K)-nucleon interactions, (T), 20: 39840
production of Y^*, in meson (π^-)-proton interactions at 1.6 to 4.2 Bev/c, (E), 20: 39770 (UCRL-16788)

properties of N* (1920), (E), 20: 39845
BAUXITE
analysis of, continuous on-line activation, 20: 39025 (ORO-2980-12)
gamma spectrum from neutron-activated, 20: 39025 (ORO-2980-12)
handling system for, 20: 39025 (ORO-2980-12)
BEARINGS
development of graphite roller and needle, for turbines, 20: 39026 (UCRL-14660(Rev.1))
dynamics of MRP Combined Rotating Unit shaft-bearing system, analog study, 20: 39022 (NAA-SR-11943)
load capacity of, increase by MHD techniques of, 20: 40216
BEHAVIOR
radiation effects on brain wave activity during conditioned, of cats, α and x, 20: 38602(R) (UCLA-34P60-1)
radiation effects on male eye gnat sexual, y, 20: 38632
radiation effects on, in fish following hypothalmus removal, gamma, 20: 38655
BELGIAN REACTOR-2
actinium-227 production in, 20: 39277 (DP-1066(Vol.1), pp III-63-9)
coolant channel, gage for, 20: 39175
description of reactor and reactor facility, 20: 39318 (DP-1066(Vol.2), pp I.93-101)
BELGIUM
control of radioisotopes and radioactive pharmaceuticals for medical use in, 20: 39156
nuclear power development in, 20: 40441
nuclear power use in, for electricity production, 20: 40442
BELLOWS
design for pressure compensator, 20: 39023 (NAA-SR-11952)
BENZENE
neutron reactions at 0.025 to 0.4 ev, total cross sections for, (E), 20: 40069(R) (EANDC(E)-66(U))
viscosity of, use of oscillating sphere device for measuring, 20: 38872(R) (NYO-1769-68)
benzene–cyclopentanone, radiolysis of aqueous solutions of, mechanisms of pulse, 20: 38939(R) (NYO-2668-13)
BENZENE, DIVINYL-
thermal degradation of polymers of, with methyl methacrylate and styrene, mechanism of, 20: 38930 (TID-23264)
BENZENESULFONIC ACID, 2,2-DIPHENYLETHYL ESTER
reaction with sodium methoxide, effects of deuterium and tritium on, 20: 38912
BENZOIC ACID
separation from nitric acid into organic phases, performance of stacked-clone contactor for, 20: 38998(R) (ORNL-3958)
p-BENZOQUINONE, TRIS(1-AZIRIDINYL)-
effects on DNA-ase and RNA-ase activity in Ehrlich ascites cells, 20: 38578
BENZOYL PEROXIDE
effects on radioinduced polymerization of cyclic ethers, 20: 38953
BERKELIUM
separation from other actinides by solvent extraction, efficiency and hydraulic stability of equipment rack for, 20: 38998(R) (ORNL-3958)
BERKELIUM OXIDES
BkO_2–HfO_2, preparation of sols of, 20: 39442(P)
BkO_2–ZrO_2, preparation of sols of, 20: 39442(P)
BERYLLIUM
effects on properties of magnesium-base alloys for fuel-element cladding, 20: 39443(P)
electronic wavefunctions for crystals of, Hartree-Fock approximation for, (T), 20: 39617
energy spectra from beryllium-9–nitrogen-14 reactions at 25 Mev, 20: 40065(R) (BMwF-FB-K-66-01)
evaporative lifetime on tungsten and oxygenated tungsten from 1250 to 1750°K, (E), 20: 40307
impact properties of irradiated, 20: 40460(R) (IDO-17191)
neutron decay constant in, (T), 20: 40376
proton reactions at 2.9 Bev, particle production by, (E), 20: 39794
radiation damage of, survey on, 20: 39454 (EUR-3055.e)
radiation effects on hardness and impact properties of, neutron, 20: 39436
BERYLLIUM ALLOYS
Be–Ag, preparation of beryllium-base, for precision instruments, 20: 39374(P)
Be–Ti–V, performance in niobium alloy brazing, 20: 39365
BERYLLIUM HYDROXIDES
surface areas of, calculation and measurement methods for, 20: 39387 (CEA-R-2947)
BERYLLIUM ISOTOPES Be-8
energy levels in, reduced cluster widths for, 20: 40086
BERYLLIUM ISOTOPES Be-9
abundance in stellar atmospheres and depletion during stellar evolution, 20: 39574
alpha elastic scattering by, spin-orbit potential in, (T), 20: 40089
deuteron reactions (d,n) with, boron-10 energy levels from, (E), 20: 40164
energy levels in, reduced cluster widths for, 20: 40086
neutron reactions (n,2n) with, neutron-neutron bound state in, (E), 20: 40091
nitrogen-14 reactions at 25 Mev, beryllium, boron, carbon, and lithium spectra from, 20: 40065(R) (BMwF-FB-K-66-01)
nitrogen-14 reactions (N-14, C-13) at 20 to 30 Mev, angular distributions from, 20: 40065(R) (BMwF-FB-K-66-01)
proton scattering at 45 Mev, cross sections for elastic, (E), 20: 40162
BERYLLIUM ISOTOPES Be-10
energy levels in, reduced cluster widths for, 20: 40086
BERYLLIUM OXIDES
deposition of coatings of, on particulate material, 20: 39370(P)
radiation damage of, survey on, 20: 39453 (EUR-3054.e)
radiation effects on microstructure of, neutron, 20: 39450 (CEA-R-2963)
surface areas of, calculation and measurement methods for, 20: 39387 (CEA-R-2947)
BERYLLIUM OXIDES (IMPREGNATED)
fabrication of thermionic, materials for, 20: 39353 (BMWF-FBK-66-07)
BETA DECAY
matrix elements for first-forbidden transitions, single-particle, (T), 20: 40124
properties of, systematics of, 20: 40108
BETA PARTICLES
activity in lower atmosphere, Braunschweig, Germany, 20: 39119
content in rainfall, 20: 39113
detection and measurement of, development of proportional detector for, 20: 39220
detection and measurement of, ion chamber detector for, 20: 39249(P)
dosage levels to medical staff from gold-198, 20: 39159
dosimetry of internally-deposited in central nervous system, 20: 38651
effects of, from iodine-131 on binding of antibody to insulin, 20: 38579
effects on ascorbic acid content in germinating seeds, 20: 38583
effects on cell nuclei of, from incorporated tritium, 20: 38624
effects on chemical reactions in the presence of solid contact material, 20: 38972(P)
effects on chromosomes, genetic, from incorporated tritium, 20: 38649
effects on decomposition of aluminum hydroxide, lead oxalate, magnesium hydroxide, and nickel oxalate, 20: 38955
effects on desoxyribonucleoprotein solutions, chemical, 20: 38581
effects on developing organisms in marine environment from natural sources, 20: 38741
effects on DNase in guinea pig skin, 20: 38591(R) (NYO-3445-7)
effects on *E. coli* of, from tritiated thymidine, lethal, 20: 38630
effects on guinea pigs, biochemical and physiological, 20: 38662
effects on mice and rats of, from injected tritium oxide, pathological, 20: 38568
effects on thermoluminescence of lithium fluorides, quality of, 20: 39199 (COO-1105-117)
measurement of, from radioisotopes deposited in man, 20: 38770
monitoring of, from ground in western states of U. S., 20: 38735(R) (NYO-1704-13)
of nuclei, systematics of, 20: 40109
BETA SOURCES
efficiency in radiation-chemical apparatus, method for calculating, 20: 38943
monitoring in air, 20: 39269
production, properties, and uses of kryptonate, 20: 39294
use in aircraft fuel gages, 20: 39189(P)
BETA SPECTROMETERS
description of large permanent magnet semicircular, 20: 39203 (INP-476/PL)
design and performance of, for reaction conversion electrons, 20: 39206 (INSJ-99)
design and performance of simultaneous alpha and beta, using cesium iodide, 20: 39217
design for use in satellites, 20: 39268
design of $\pi\sqrt{2}$, 20: 39235
electrostatic correction for $\pi\sqrt{2}$, 20: 39236
performance of magnetic $\pi\sqrt{2}$, with electrostatic devices for high luminosity and resolution, 20: 39234
use for conversion ratio studies by photographic method, 20: 39216
BETA SPECTROSCOPY
detectors for, properties and performance of germanium and silicon, 20: 39232
internal and external conversion measurements in, scheme for high-luminosity high-resolution, 20: 39234
BETATRONS
use for therapy of stomach cancers, 20: 38772
BEVATRON
development and operation of, 20: 39498(R) (UCRL-16809)

magnet design for, beam-control, 20: 39508
BIBLIOGRAPHIES
on analytical chemistry of neptunium, 20: 38821
on analytical chemistry of polonium, 20: 38822
on blast-closure systems, 20: 39073
on ecology, 20: 40488 (ORNL-3957)
on gamma radiation streaming through shelter air ducts, 20: 39060
on heavy-ion reactions with nuclei, 20: 40083
on high-purity metals, 20: 39328 (AD-624997)
on instruments and measuring techniques in nuclear physics, 20: 39168 (AED-C-06-14)
on ion exchange in mixed and non-aqueous solvents, 20: 38818
on ion exchange in nitrate solutions, 20: 38820
on lattice vibrations in metals and semiconductors, 20: 40344
on neutron diffraction and its applications in inorganic chemistry, 20: 38882
on nuclear ship propulsion, 20: 40444 (AEC-C-22-06)
on radiation damage of beryllia, 20: 39453 (EUR-3054.e)
on radiation damage of beryllium, 20: 39454 (EUR-3055.e)
on radiation effects on graphite, 20: 39455 (EUR-3056.e)
on radioisotope production and uses, 20: 39275 (DP-1066(Vol.1))
on research in progress under Army Research Office, 20: 40485(R) (AD-636091)
on thiocyanate ions in colorimetric analysis, 20: 38808
on transition metal cyanides and their complexes, 20: 38881
on vapor deposition of molybdenum, tungsten, and rhenium, 20: 39354 (BMWF-FBK-66-09)
BIG ROCK POINT POWER REACTOR
coolant flow transient tests, 20: 40404 (GEAP-4496)
core performance of, steady-state thermal-hydraulic analysis, 20: 40404 (GEAP-4496)
modification of, review of procedures, 20: 40429
BIOCHEMISTRY
book: *Elements of Radiation Biology and Biochemistry*, 20: 38544
BIOLOGICAL MATERIALS
analysis for arsenic, selenium, strontium, and vanadium traces, activation, 20: 38837
analysis for iodine, activation, 20: 38849
analysis for trace elements, radiochemical separation methods for use with activation, 20: 38842
analysis for trace elements, use of automated gamma spectrometers for activation, 20: 38843
analysis for vanadium, activation, 20: 38565
analysis of, activation, 20: 38836
analysis of, standards for activation, 20: 38844
BIOLOGICAL MODELS
evaluation of, for selecting radioprotective sulfur compounds, 20: 38729
BIOLOGICAL STRESS
radiosensitivity effects on astronauts, 20: 38603(T) (AD-629422)
BIOLOGY
centrifuge design for, intermediate-speed zonal, 20: 39030
BIOMETRY
mathematical model for cerium-144 metabolism, 20: 38571
BIOSYNTHESIS
radiosensitivity of nucleic acid, in animals, 20: 38585
BIPHENYL, ISOPROPYL-
performance as working fluid in Rankine cycle plants, 20: 40449(R) (SAN-650-1)
BISMUTH
dispersion in graphite, optimum pressure and temperature for liquid, 20: 39355 (EUR-2988.f)
electric conductivity at low temperature in 450 kOe magnetic fields, 20: 40027(T)
separation from accompanying elements by solvent extraction using alkyl phosphates, 20: 38828
separation from polonium-210 by vacuum distillation, 20: 38996 (DP-1066(Vol.2), pp II.79-102)
BISMUTH ALLOYS
Al–Bi–Cu–Pb, fatigue failure of 2011-T3, equations for, 20: 39396 (IS-T-60)
BISMUTH ISOTOPES Bi-209
proton inelastic scattering at 21 Mev, (E), 20: 40074 (LA-DC-8069)
BISMUTH ISOTOPES Bi-214
concentration in air in Braunschweig, Germany, 20: 39119
content in precipitation, effects of meteorological parameters on, 20: 39106 (BMwF-FBK-65-05)
BLAST EFFECTS
hazards from, biological criteria for estimating, 20: 39058
of atomic weapons, 20: 39055
on design of seven-man shelters, 20: 39077
on prefabricated shelters, 20: 39075
on tubular towers, 20: 39007 (AD-636914)
protection against, design of structure for, 20: 39053(P)
BLOOD
analysis for copper, gold, iodine, manganese, and zinc in human, activation, 20: 38845
analysis for copper, magnesium, manganese, and zinc in erythrocytes and plasma in human, activation, 20: 38852
analysis for iodine, micro method for, 20: 38652
analysis for iron-55 and iron-59, simultaneous methods using liquid scintillation counting, 20: 38555
analysis for lipids, micro method for, 20: 38652
extracorporeal scintillation monitoring of circulating, 20: 38558
measurements on peripheral, using carbon-14-labeled aldosterone, 20: 38547(R) (NYO-918-15)
radiation effects on ACTH content in rat, 20: 38661
radiation effects on peripheral cells in circulating, gamma, 20: 38663
radiation effects on newborn, in animals given intrauterine radiation, 20: 38665
radiation effects on 17-ketosteroid content in dog, x, 20: 38684
radiation effects on constituents of calf, gamma, 20: 38706
radiation effects of ascorbic acid content in rat, dietary effects of B group vitamins, folic acid, and phosphatide on gamma and x-ray, 20: 38721
radiation effects on leukocyte and sugar content in rabbit, x, 20: 38686
role in radiation pathology, 20: 38653
BLOOD CIRCULATION
measurement in brain, use of oxygen-15 and positron scanner for, 20: 38745(R) (NYO-3267-3)
radiation sickness effects on, in rabbit lungs, 20: 38657
xenon-133 measurement of myometrial, during pregnancy, 20: 38747
BLOOD COAGULATION
radiation effects on, in guinea pigs, effects of bacterial toxin on, 20: 38656
BLOOD FORMATION
radiation effects on, liver and spleen exposure of rats, x, 20: 38694
radiation effects on, mechanisms involved in, 20: 38700
BLOOD PICTURE
radiation effects on hematocrit of rats, γ, 20: 38587 (CEA-R-2909)
radiation effects on lymphocyte, effects of adrenaline on x, 20: 38678
use for determining radiation exposure of radiology service personnel, 20: 38781
BLOOD PLASMA
analysis for copper, magnesium, manganese, and zinc in human, activation, 20: 38852
iodoamino acid composition of rat, determination by neutron activation analysis of iodine-129, 20: 38561
iodotyrosine content in rat, tracer study, 20: 38561
metabolism of steroids in sheep ovarian, tracer study on, 20: 38547(R) (NYO-918-15)
BLOOD PLATELETS
radiation effects on megakaryocytes in bone marrow, γ, 20: 38643
radiation recovery, comparison of rates in goats for gamma and fission neutron, 20: 38629
BLOOD SERUM
analysis for trace elements, activation, 20: 38851
iron-56 and iron-59 transfer kinetics in human, 20: 38573
potassium content of rabbit, effects of injected normal or irradiated serum on, 20: 38697
radiation effects on proteins in, from gestating hamsters, x, 20: 38598(R) (TID-22955)
radiation effects on myelopoietic agent in rabbit, x, 20: 38633
radiation effects on esterase content in rat, x, 20: 38682
radiation effects on agglutinin and properdin content in rat, γ, 20: 38695
radiation effects on potassium content in rabbit, effects of injected antigen on, 20: 38697
BLOOD TRANSFUSIONS
effects on leukopenia in cancer patients during radiotherapy, 20: 38768
BLOOD VESSELS
radiation effects on tonus of dog, 20: 38658
radiation injuries to cardiovascular system in animals, in death from acute radiation sickness, 20: 38666
radioinduced dilation of subcutaneous rabbit, effects of vasoconstricting drugs on x, 20: 38640
radiosensitivity of, γ, 20: 38773
BOILERS
design for nuclear reactors, 20: 40433(P)
design for sodium-heated steam, 20: 40424
design of sodium-heated, French program for, 20: 40428
design of, for isopropylbiphenyl, 20: 40449(R) (SAN-650-1)
steam drum measurements in AGR, 20: 40398 (AEEW-M-631)
testing two-fluid, single-tube, 20: 39028
BOILING
burnout measurements in tubes and annuli with circumferential heat flux tilt, 20: 39046 (AEEW-R-477)
detection in reactors, instrument for, 20: 40373
heat transfer during, review of, 20: 39052

kinetics of, review, 20: 39052

BOILING REACTORS
control system for, for power generation, 20: 40432(P)
coolant channel hydraulic characteristics in, 20: 40356 (EURAEC-1644)
power limitations in, effect of hydrodynamic instabilities on, 20: 40403 (EURAEC-1464)
steam separators for, design of radial-vane, 20: 39019(R) (GEAP-5149)

BONDING
mechanism of Zircaloy-2, on PWR core-2 fuel plates, 20: 39361 (WAPD-305)

BONE MARROW
effects of transplanted, on erythropoiesis in mice, 20: 38592 (ORNL-P-2158)
formate metabolism in rabbit, effects of blood serum from x irradiated rabbits on *in vitro*, 20: 38633
nucleic acid synthesis in, effects of gamma dose, 20: 38585
radiation effects on colony formation by transplanted, in mouse spleen, 20: 38708(R) (IAEA-3173-5)
radiation effects on human, from deposited radium-226 or strontium-90, 20: 38623
radiation effects on granulocyte output from rabbit, effects of humoral agent on x, 20: 38633
radiation effects on rat, morphological, γ, 20: 38663
radiation effects on megakaryocytes in, γ, 20: 38643
radioinduced syndrome of, mechanisms involved in, 20: 38700
radiosensitivity effects of transplanted, in dogs and rats, effects of cell numbers on, 20: 38740
sampling of, for clinical studies, 20: 38781
use of transfusions of, for therapy of radioinduced anemia in rats, 20: 38711
use of transfusions of, for therapy of radiation sickness in dogs and rats, 20: 38730

BONES
gamma attenuation by, 20: 38791
radiation dose to guinea pig, calculations, 20: 38662
radiation injuries of, after therapy, 20: 38767
radiotherapy of various malignant tumors of, 20: 38784
strontium-90 content in children's, effects of age and diet on, 20: 39150(R) (NYO-2753-4)
strontium-90 content in samples collected in Great Britain, 1965, 20: 39163
x radiation attenuation by, 20: 38791

BORIDES
chemical reactions with metals at high temperatures, review on, 20: 39331(T) (UCRL-Trans-10044)
wettability of refractory, by molten metals, 20: 39429

BORON
determination in metals, activation, 20: 38840
diffusion in graphite, determination by etching and gold deposition, 20: 39439
effects on grain size of tungsten, 20: 39400 (NASA-TN-D-3531)
energy spectra from beryllium-9–nitrogen-14 reactions at 25 Mev, 20: 40065(R) (BMwF-FB-K-66-01)
incorporation into nitrogen mustards, 20: 38745(R) (NYO-3267-3)
phase transformations, effect of pressure and irradiation on solid-solid, (E), 20: 40306

BORON CARBIDES
reactivity worths of arrays of tubes filled with, 20: 40381
B_4C–UO_2, radiation effects on boron migration in, 20: 40382(R) (CEND-3107-267)

BORON COMPOUNDS
use in neutron capture therapy of brain tumors, preparation and evaluation of, 20: 38745(R) (NYO-3267-3)

BORON ISOTOPES B-10
abundance ratio to boron-11, atomic absorption spectrophotometric determination of natural, 20: 38803
deuteron reactions (d,α) at 1.6 to 3.0 Mev, angular distributions and cross sections for, (E), 20: 40068 (BMwF-FBK-66-15, pp 38-46)
deuteron reactions (d,nγ) with, carbon-11 energy levels from, (E), 20: 40164
deuteron scattering at 1.6 to 3.0 Mev, angular distributions and cross sections for elastic, (E), 20: 40068 (BMwF-FBK-66-15, pp 38-46)
energy levels, (E), 20: 40112
energy levels in, reduced cluster widths for, 20: 40086
energy-level quantum numbers and transitions, (E), 20: 40164
preparation of highly enriched, by low-temperature distillation of boron fluoride–methyl fluoride complex, 20: 39325
use for neutron capture therapy of brain tumors, 20: 38745(R) (NYO-3267-3)

BORON ISOTOPES B-11
abundance ratio to boron-10, atomic absorption spectrophotometric determination of natural, 20: 38803
energy levels in, reduced cluster widths for, 20: 40086
energy levels of, spin and parity of, (E), 20: 40111
helium-3 reactions (He-3,n) at 1.5 to 5.5 Mev, nitrogen-14 energy levels from, (E), 20: 40112

BORON NITRIDES
phase transformations, effect of pressure and irradiation on solid-solid, (E), 20: 40306

BORON OXIDES
phase transformations, effect of pressure and irradiation on solid-solid, (E), 20: 40306

BORON STEEL
properties of, effects of additive metals on, 20: 39426

BORON SYSTEMS
B–Co–Zr, crystal structure of stoichiometric, 20: 39416
B–Ni–Zr, crystal structure of stoichiometric, 20: 39416

BOSONS
form factors for mesons (ω), electromagnetic, 20: 39823
interactions of charged, phase of amplitudes for, (T), 20: 39899
models of interacting, separable-potential, 20: 39889
production of W, in nucleon-nucleon interactions, (T), 20: 39797
wave functions for impenetrable one-dimensional, in thermal equilibrium, 20: 39474

BOUNDARY LAYER
effects on mass transfer in two-phase flow, 20: 39050 (UCRL-16535)

BRAIN
antigen preparation from tissues of, 20: 38745(R) (NYO-3267-3)
blood circulation in, tracer study using oxygen-15, 20: 38745(R) (NYO-3267-3)
radiation dose to, from x radiation therapy of facial tumors, 20: 38765
radiation effects on electrical activity during conditioned behavior in cat, α and x, 20: 38602(R) (UCLA-34P60-1)
radiation effects on astroglial cells and blood vessels in rat, glycogen accumulation from alpha and x, 20: 38674
radiation effects on ascorbic acid and glutathione content in rat, whole-body x, 20: 38679
radiation effects on electrically stimulated hypothalamus in rabbit, x, 20: 38654
radiosensitivity effects of hypothalamus functional state of, in dogs and rabbits, 20: 38688
yttrium-90 implants in, use in control of epilepsy, 20: 38779

BRAIN TUMORS
antigen preparation from tissues of, 20: 38745(R) (NYO-3267-3)
radiodiagnosis by positron scanning technique, 20: 38745(R) (NYO-3267-3)
radiosensitivity of various types of, effectiveness of radiotherapy for, 20: 38783
radiotherapy of using boron-10 neutron capture, 20: 38745(R) (NYO-3267-3)

BRAZIL
nuclear power development in, prospects for, 20: 40487 (NP-16229)

BRAZING
technique for, high remelt temperature, 20: 39365

BRAZING ALLOYS
performance of, for niobium honeycomb structures, 20: 39365

BREEDER REACTORS
conversion factor of high temperature thorium, 20: 40471
fuel cycle costs of AVR, 20: 40470
fuel cycles in, costs of thorium, 20: 40394
operating conditions of AVR, determination of favorable, 20: 40469

BREMSSTRAHLUNG
detection and measurement in beta applicators, design of scintillation detector for, 20: 38777
effects on bromine-82 and chlorine-36 exchange between ethylenediamine cobalt or rhodium complexes and hydrobromic or hydrochloric acids, 20: 38960
emission of quadrupole, from plasma, (T), 20: 40273
reactions with helium-4 at 159 to 209 Mev, meson (π^0) production in, (E), 20: 39822
reactions with light nuclei, differential cross sections for meson ($\pi^\pm$) production in, (E), 20: 40075 (LNF-66/30)
spectra of, from flash discharges, (E), 20: 40233

BROMINE
meson (π^-) reactions with, diffraction dissociation for meson (ρ^0) production from, (E), 20: 39774
neon-20 reactions at 200 Mev, in emulsions, (E), 20: 40083

BROMINE ISOTOPES Br-81
neutron reactions with, in propyl bromide, chemical effects from, 20: 38963

BROMINE ISOTOPES Br-82
decay of isomeric, in neutron-irradiated propyl bromide, chemical effects from, 20: 38963
localization in aqueous solution–metal systems, beta/gamma ratio measurements for determining, 20: 39336

radiation effects on exchange of, between ethylenediamine cobalt complexes and hydrobromic acid, bremsstrahlung, gamma, and x, 20: 38960
sorption by nickel sheets, beta attenuation in, 20: 39357
BROWNIAN MOVEMENT
quantum mechanics of, validity of Fokker-Planck equation for, 20: 39596
BROWNS FERRY POWER REACTOR
design, 20: 40410 (NP-16251(Vol.1))
design, 20: 40411 (NP-16251(Vol.2))
BUBBLE CHAMBERS
cameras for, specifications for optical units of stereoscopic, 20: 39209 (JINR-P-2728)
charged-particle interactions in propane, method of identification of, (E), 20: 39211 (JINR-P-2842)
development for high-energy physics, 20: 39241
film projector for, 20: 39182
film scanning system for, design of computer-controlled, 20: 39767 (TID-23278)
particle tracks on films from, constants for geometric reconstruction of, 20: 39247
BUBBLES
formation in boiling, 20: 39052
1,3-BUTANEDIONE, 1-PHENYL- COMPLEXES
with copper and uranyl ions in mixture with other β-diketone in benzene solution, 20: 38855 (BNL-10350)
1,3-BUTANEDIONE, 4,4,4-TRIFLUORO-1-PHENYL-
complexes with copper and uranyl ions in mixture with other β-diketone in benzene solution, 20: 38855 (BNL-10350)
1-BUTANOL
effects on yield of oxalate in radioinduced carboxylation of formate, 20: 38966
2-BUTANONE
determination in irradiated fruit juices, chromatographic, 20: 39300
BUTYRALDEHYDE
determination in irradiated fruit juices, chromatographic, 20: 39300

C

CADMIUM
determination in kidneys in arthritic and healthy patients, activation, 20: 38845
determination in mosaic virus and nucleic acids in tobacco plants, activation, 20: 38846
superconductivity of, 20: 40047
CADMIUM ALLOYS
Cd–In–Ag, radiation effects on silver-base, in-reactor, 20: 39461 (WCAP-6074)
Cd–In–Ag, reactivity worths of arrays of tubes filled with, 20: 40381
Cd–Na, properties of, chemical and physical, 20: 38656 (BNL-10372)
CADMIUM CHLORIDES
diffusion in, self-, 20: 38871(R) (NYO-1769-54)
CADMIUM ISOTOPES Cd-109
electron capture ratios, M/L, 20: 40153
CADMIUM ISOTOPES Cd-111
proton reactions (p,n) at 3.0 to 5.8 Mev, strength functions for, (E), 20: 39470(R) (ORNL-3924)
CADMIUM ISOTOPES Cd-112
proton scattering at 13 Mev, differential cross sections for elastic and inelastic, (E), 20: 39470(R) (ORNL-3924)
CADMIUM ISOTOPES Cd-117
beta decay, (E), 20: 40159
CADMIUM TELLURIDES
performance for alpha spectrometry, 20: 39231
sputtering of single-crystal, atom-ejection patterns for, (E), 20: 40305
CALCINATION
fission product incorporation into borosilicate glass, public health aspects of, 20: 40482
CALCITES
oxygen-16/-18 fractionation between dolomites and, 20: 39129
CALCIUM
analysis for calcium-48 in natural, activation, 20: 38850
content in fallout from Chinese atomic test, Oct. 1964, 20: 39110
content in milk of, 20: 39157
determination in mineral and natural waters, flame photometric, 20: 38798 (NIJS-R-465)
effects on properties of magnesium-base alloys for fuel-element cladding, 20: 39443(P)
effects on strontium retention in rats of dietary, 20: 38566
metabolism in dairy cows, 20: 38552
reduction of uranium(IV) fluoride, process for, 20: 39342(P)
superconductivity of, 20: 40047
uptake by desoxyribonucleoproteins in solution, tracer study, 20: 38581
CALCIUM CARBONATES
analysis for calcium-48, activation, 20: 38850
determination in swimming pool reactor coolant, activation and chemical, 20: 38800 (PAEC(C)RE-652)
leaching fission products from, 20: 40478 (IN-1011)
CALCIUM CHLORIDES
diffusion in, self-, 20: 38871(R) (NYO-1769-54)
ionic transport coefficients for, at 25°C, 20: 38909
radiosensitivity effects on barley seeds, 20: 38736
$CaCl_2$–Na_2CO_3–$UO_2(NO_3)_2$, uranium precipitation in, mechanism of, 20: 38928
CALCIUM COMPOUNDS
effects on strontium-90 absorption from gastrointestinal tract of rats, 20: 38569
CALCIUM FLUORIDES
analysis for erbium, holmium, neodymium, and praseodymium, spectrophotometric, 20: 38829
radiation effects on rare earth ions in, x, (E), 20: 40341
radioinduced color center in yttrium-doped crystals of, EPR of x, 20: 40321
CALCIUM ISOTOPES Ca-40
deuteron reactions (d,p) at 2 Mev, distorted-wave calculations for, (T), 20: 40114
helium-3 reactions (He-3,α) at 24 Mev, cross sections for, (E), 20: 40067 (BMwF-FBK-66-15, pp 20-37)
neutron reactions (n,α) at 6 Mev, cross sections for, (E), 20: 40100
CALCIUM ISOTOPES Ca-41
neutron elastic scattering at 1 to 2 Mev, cross sections for, (E), 20: 40087
neutron total cross section at 1 to 2 Mev, (E), 20: 40087
CALCIUM ISOTOPES Ca-42
energy levels from potassium-41 (p,γ) reaction, (E), 20: 40133
CALCIUM ISOTOPES Ca-45
analysis for impurities, chromatographic, 20: 38827
radiation effects with ^{226}Ra on dairy cattle metabolism, 20: 38552
CALCIUM ISOTOPES Ca-47
analysis for impurities, chromatographic, 20: 38827
CALCIUM ISOTOPES Ca-48
determination in natural calcium medium, activation, 20: 38850
CALCIUM NITRATES
$Ca(NO_3)_2$–D_2O, phase diagram of, 20: 38994(R) (AE-232)
$Ca(NO_3)_2$–H_2O, phase diagram of, 20: 38994(R) (AE-232)
CALCIUM OXIDES
effects on elastic properties of zirconia, 20: 39438
CALIBRATION
equipment for photographic film detector, design of mobile, 20: 39266
CALIFORNIA
environmental radiation measurements in, 20: 38735(R) (NYO-1704-13)
CALIFORNIUM ISOTOPES Cf-252
fission of, prompt neutron emission in spontaneous, (E), 20: 39470(R) (ORNL-3924)
use in radiotheraphy, 20: 38744 (DP-1066(Vol.1), pp IV.47-66)
CALIFORNIUM OXIDES
CfO_2–HfO_2, preparation of sols of, 20: 39442(P)
CfO_2–ZrO_2, preparation of sols of, 20: 39442(P)
CALORIMETERS
design of adiabatic, containing thermistor thermometer, 20: 38906
CAMBRIDGE SYNCHROTRON
development program, July 1, 1965–Dec. 31, 1965, 20: 39481(R) (CEAL-1031)
CANADA
computer study of radiation dose probability for hospitals throughout, following nuclear attack on North America, 20: 39162
oxygen-16 to oxygen-18 ratio in St. Elias Mountain, 20: 39123
CANDU REACTOR
control of, use of digital computer for, 20: 40437
CARBIDES
chemical reactions with metals at high temperatures, review on, 20: 39331(T) (UCRL-Trans-10044)
fabrication of, sintered pellets of, 20: 39368(P)
wettability of refractory, by molten metals, 20: 39429
CARBOHYDRATES
effects of level of, on uptake of Cs and Sr in wheat seedlings, 20: 38548(R) (ORO-2410-1)
CARBON
determination in coal by activation, on-line, 20: 39025 (ORO-2980-12)
determination in earth formations, neutron-gamma well logging method for, 20: 39137(P)
determination in molybdenum–uranium alloys and plutonium coulometric, 20: 38796 (CEA-R-2968)
determination in sodium, development of techniques for, 20: 38797(R) (MSAR-66-150)
effect on properties of low-alloy steels for reactor pressure vessels, 20: 39444(P)
effects on grain size of tungsten, 20: 39400 (NASA-TN-D-3531)

effects on internal friction of electron-beam refined tantalum, 20: 39420
electron mass-scattering cross section for, (T), 20: 39588
energy spectra from beryllium-9–nitrogen-14 reactions at 25 Mev, 20: 40065(R) (BMwF-FB-K-66-01)
fabrication of tubes of low permeability, 20: 39369(P)
neon-20 reactions at 200 Mev, in emulsions, (E), 20: 40083
photon reactions with, differential cross sections for meson ($\pi^{\pm}$) production in, (E), 20: 40075 (LNF-66/30)
plasma properties of, in shock tubes, (E), 20: 40209
proton energy-loss distributions from thin foils of, (T), 20: 40117
reactions with carbon at high densities, rate calculations for, 20: 40157
sorptive properties for iodine, 20: 39017(R) (DP-1053)
use in fission product sorption beds, 20: 39017(R) (DP-1053)

CARBON BLACK
analysis for carboxyl and hydroxyl groups, using carbon-14-labeled diazomethane, 20: 38805

CARBON DIOXIDES
production in radioinduced oxidation of methanol, effects of dose rate on, 20: 38942 (UJV-1457)
reactions with radioisotope-containment materials in launch pad abort environment, 20: 39312 (SC-CR-66-2044)
CO_2–ethanol–O, man transfer of, in channel flow, 20: 39050 (UCRL-16535)
CO_2–ethyl ether–helium, man transfer in channel flow, 20: 39050 (UCRL-16535)

CARBON IONS
heating of, excitation method for, 20: 40174(R) (ORNL-3989, pp 43-77)

CARBON ISOTOPES
separation of carbon-13 from, by chemical exchange in alcoholic solutions of monoethanolamine, 20: 39320(R) (MLM-1311)
separation of carbon-13 from, by chemical exchange in monoethanolamine solutions, 20: 39321(R) (MLM-1312)

CARBON ISOTOPES C-11
energy level transitions in, branching ratio for, (E), 20: 40164
reactions of recoiling, in proton-irradiated methylamine, 20: 38964

CARBON ISOTOPES C-12
deuteron reactions (d,p) at 1.0 and 1.5 Mev, cross sections for, (E), 20: 40155
energy levels of, Hartree-Fock calculations for, (T), 20: 40138
meson (π^-) capture at 80 Mev, helium-8 production in, (E), 20: 40071 (JINR-E-2774)
neutron elastic scattering at 16 to 20 Mev, optical-model analysis of, (E/T), 20: 40088
neutron inelastic scattering at 14 Mev, calculations by dispersion method, (T), 20: 40104(T)
proton scattering at 45 Mev, cross sections for elastic, (E), 20: 40162

CARBON ISOTOPES C-13
deuteron reactions (d,n) at 2 to 7 Mev, distorted-wave calculations for, (T), 20: 40114
deuteron reactions (d,p) at 1.0 and 1.5 Mev, cross sections for, (E), 20: 40155
separation from carbon isotopes by chemical exchange in alcoholic solutions of monoethanolamine, 20: 39320(R) (MLM-1311)
separation from carbon isotopes by chemical exchange in monoethanolamine solutions, 20: 39321(R) (MLM-1312)

CARBON ISOTOPES C-14
determination of, in proportional counter, simultaneously with tritium, 20: 38823
incorporation in 3-hydroxy- and 3-oxo-, hexadecanoic acids and *trans*-2-hexadecenoic acid, 20: 38987
use as tracer for DTPA excretion in rats, 20: 38556
use as tracer in analysis of carbon black for carboxyl and hydroxyl groups, 20: 38805

CARBON MONOXIDES
reactions with copper oxide pellets in differential and deep beds, 20: 38874 (ORNL-TM-1540)
reactions with radioisotope-containment materials in launch pad abort environment, 20: 39312 (SC-CR-66-2044)

CARBON STEEL
fatigue strength of weldments of, to type 304 stainless steel, 20: 39404 (SWRI-1228-4-20)
fracture of pressure-vessel, under reactor startup conditions, 20: 39329 (AECL-2432)
radiation effects on fatigue of A212B, neutron, 20: 39406 (WAPD-T-1864)

CARBON SULFIDES
reactions with potassium diuranates, 20: 38891
viscosity of, use of oscillating sphere device for measuring, 20: 38872(R) (NYO-1769-68)

CARBON SYSTEMS
C–Nb–Zr, phase diagrams, 20: 39434
C–N–O–U, crystal structure of solid-solutions, 20: 39385 (CEA-R-2852)
C–Si–U, phase studies of, at room temperature, 20: 39413

CARBON TETRACHLORIDE
effects on hydridation of zirconium alloys at 400°C, 20: 39360 (TRG-Report-1255)
spectra of, laser excitation of Raman, 20: 38872(R) (NYO-1769-68)
viscosity of, use of oscillating sphere device for measuring, 20: 38872(R) (NYO-1769-68)

CARBONATES
uranium-234 to uranium-238 ratio in, deposits of, 20: 39120

CARBONIC ACID, CYCLIC ETHYLENE ESTER
radiolysis of, γ, 20: 38940 (NYO-3410-2)

CARBOXYL GROUP
determination of surface, in carbon black, using carbon-14-labeled diazomethane, 20: 38805

CARCINOGENESIS
effects of radiation, drugs, and viruses on etiology of childhood leukemia, review of, 20: 38668

CARCINOMAS
effects of dietary radioactivity on incidence in human populations, 20: 38739
radioinduced in children treated for hemangiomas by radium, 20: 38787
radioinduced thyroid, after iodine-131 therapy of goiter, 20: 38749
radioinduced, after radium therapy of hemangioma, 20: 38788
radiosensitivity of, effects of anoxia on γ, 20: 38635
radiotherapy of cervical, effects on cellular composition of tissues, 20: 38769
radiotherapy of facial, absorbed dose in brain from x, 20: 38765
radiotherapy of stomach, use of lead grating for x, 20: 38763
radiotherapy of uterine, nursing case of patients receiving radium, 20: 38751
radiotherapy of uterine, x, 20: 38786
radiotherapy of, effects of blood transfusions on leukopenia induced by, 20: 38768
radiotherapy using gold-198 colloids, 20: 38643
radiotherapy, effects of immunotherapy on, 20: 38612

CAST IRON
radiation and thermal effects on white, simultaneous, 20: 39464

CATALYSTS
loss of solid, from fluid catalytic conversion unit, impregnation with radioactive isotope for study of, 20: 38993(P)
preparation of labeled, for loss-rate studies, 20: 38993(P)
properties and uses of rare earth, 20: 38877(T) (JPRS-35594)

CATHEPSIN
release of acid, from lysosomes of x irradiated rat liver, 20: 38577

CATHODES
protection of thermionic-converter, using halogen gas, 20: 39637(P)

CATIONS
metabolism in wheat seedlings, 20: 38548(R) (ORO-2410-1)

CATS
radiation effects on brain wave electrical activity during conditioned behavior, α and x, 20: 38602(R) (UCLA-34P60-1)

CATTLE
calcium metabolism in dairy cows, tracer study, 20: 38552
radiation effects on blood constituents and hematopoietic organs of calves, gamma, 20: 38706
radium metabolism in dairy cows, tracer study, 20: 38552

CAVES
passout system for, engineering drawings of, 20: 39036

CELLOPHANE
radiation effects on color of blue films of, 20: 38941(R) (RRL-2310-182)

CELLULOSE
radioinduced crosslinking in presence of sensitizing agent, 20: 38975(P)

CENTRIFUGATION
effects on yield and kinetics of radiation-induced chromosome aberrations in barley seeds, 20: 38618

CENTRIFUGES
design of intermediate-speed zonal, 20: 39030
rotor design for zonal, 20: 39037

CERAMIC COATINGS
deposition on reactor fuel particles, 20: 39370(P)

CERAMIC MATERIALS
book: *Materials Science Research*, Vol. 3, role of grain boundaries and surfaces in, 20: 39338
effects of oxide, on grain size of tungsten, 20: 39400 (NASA-TN-D-3531)
fabrication and physical properties of composite graphite-metal carbide, 20: 39367
research in progress under Army Research Office, 20: 40485(R) (AD-636091)
use in components of thermionic diode system, 20: 39638

CERIUM
determination using amalgamated silver electrode, oscillographic, 20: 38811
electron spin resonance of metallic, (E), 20: 40352

separation from lanthanum by solvent extraction using tertiary amines and diethylenetriaminopentaacetic acid or EDTA, 20: 38995 (BM-RI-6809)
shock compression of, 20: 39425(T)
x-ray-diffraction patterns of, effects of cold working on, 20: 39421

CERIUM ALLOYS
Al–Ce, magnetic properties of intermetallic compounds of, 20: 39433
Ce–Fe, crystal structure of intermetallic compound, 20: 39409
Ce–Gd, phase transformations and magnetic ordering in, pressure-induced, 20: 40326
Ce–Ho, phase transformations and magnetic ordering in, pressure-induced, 20: 40326
Ce–Pb–Zn, component distribution in recrystallized, 20: 39435
Ce–Y, phase transformations and magnetic ordering in, pressure-induced, 20: 40326

CERIUM COMPLEXES
with acid phosphates, ion exchange studies on composition and stability of, 20: 38878(T) (ORNL-tr-1257)
with dipentyl pentylphosphonate, spectra of, infrared, 20: 38799(R) (NLCO-980)

CERIUM COMPOUNDS
effects of, on rat liver cells, 20: 38595(R) (ORO-3295-2)

CERIUM IONS
spin-lattice relaxation time in lanthanum trichloride, angular and temperature effects on, 20: 40350

CERIUM ISOTOPES Ce-141
separation from waste-water by aerobic treatment, 20: 40483

CERIUM ISOTOPES Ce-143
beta decay, (E), 20: 40159

CERIUM ISOTOPES Ce-144
effects on rat liver, pathological, 20: 38567
metabolism in animals, mathematical model for, 20: 38571
release from simulated high-level wastes, 20: 40476(R) (BNWL-267)
separation from waste-water by aerobic treatment, 20: 40483
separation using mixed oxide scavenger, 20: 40476(R) (BNWL-267)
uptake by algae, effects of EDTA on, 20: 38570
use as heat source in SNAP-7 device, radiological hazards of, 20: 39307 (DP-1066(Vol.1), pp V.35-40)
use as heat source in thermoelectric generators, 20: 39308 (DP-1066 (Vol.2), pp III.3-16)

CERIUM OXIDES
actinide oxides–CeO_2, preparation of sols of, 20: 39341(P)
Ce_2O_3–Tb_2O_3, phase studies of, tensimetric, 20: 38862(R) (COO-1109-22, Paper 1)
Ce_2O_3–Tb_2O_3, phase studies of, in oxidation-reduction cycles, 20: 38864(R) (COO-1109-22, Paper 3)

CERIUM SELENIDES
crystal structure of, reflection spectra for zonal, (E), 20: 40339

CERIUM SULFATES
radiolysis of, in presence of thallous ions, intratrack distribution of distribution of primary products of alpha, 20: 38967

CERMETS
failure of stainless steel–urania, model of, 20: 39459 (TRG-Report-1278)
formation by reactions of metals with refractory materials at high temperatures, 20: 39331(R) (UCRL-Trans-10044)
reactions of molybdenum–urania, at 1800°C, 20: 39383 (BMWF-FBK-66-08)
rupture strength of, effects of microstructure on, 20: 39398 (NASA-TN-D-3527)

CESIUM
determination in gases, design of GM monitor for, 20: 39264
diffusion from sodium at high temperatures, factors affecting, 20: 40357 (NAA-SR-11766)
diffusion in molten cesium and sodium nitrates, coefficients of, 20: 38871(R) (NYO-1769-54)
electric dipole moments of, ratio of atomic to electron, 20: 39598
electron interactions with atomic, electron exchange in, 20: 39582(T) (AERE-Trans-1053)
electron temperatures in positive column of, (E), 20: 39659
handling of, for ion engines, 20: 39091
ion exchange on minerals, 20: 38858 (BNWL-235-3, pp 23-51)
metabolism in wheat seedlings, 20: 38548(R) (ORO-2410-1)
production and diagnostics of plasma of, contact ionization, 20: 40223
scattering by mercury beams at 7 to 500 ev, cross sections for, 20: 39599
separation from alumina calcine by leaching with dilute nitric acid or distilled water, 20: 40478 (IN-1011)
separation from uranium by ion exchange on zirconium phosphate gel, 20: 38994(R) (AE-232)
sorption by ion exchange on titanium oxide, 20: 39002
sorption by zirconium silicate phosphate gel, 20: 38994(R) (AE-232)
sorption on potassium cobalt ferrocyanides, fallout sampling by, 20: 39147 (CONF-660401-6)
spectra of recombination continuum in argon plasma, 20: 39722
superconductivity of, 20: 40047
use in two-phase MHD cells, (T), 20: 39634 (JPL-32-946)
viscosity of vapor of, to 1000°C and 0.4 to 5 bars, 20: 39392 (CU-2660-29)

CESIUM CARBONATES
heat and free energy of formation of, 20: 39724

CESIUM CHLORIDES
CsCl–$ErCl_3$, phase studies, 20: 38919
CsCl–$NdCl_3$, phase studies, 20: 38919

CESIUM ERBIUM CHLORIDES
production of vapors of, 20: 38919

CESIUM IODATES
iodine-131 beta decay in, properties of xenon oxide compounds formed by, 20: 38984

CESIUM IODIDES
radioinduced emf in crystals of, x, 20: 40335(T)
use in simultaneous alpha and beta spectrometers, 20: 39217

CESIUM IONS
acceleration of, production of thrust by, 20: 39090
acceleration of, production of thrust by, 20: 39093
sputtering effects on aluminum at 1 to 10 kev, 20: 39585

CESIUM ISOTOPES Cs-134
diffusion in molten cesium nitrate at constant volume, 20: 38872(R) (NYO-1769-68)
diffusion in molten sodium nitrate at constant volume, 20: 38872(R) (NYO-1769-68)
release from simulated high-level wastes, 20: 40476(R) (BNWL-267)

CESIUM ISOTOPES Cs-137
content in Clinch River, 20-year analysis of, 20: 40479 (ORNL-P-2328)
content in diet of Italian children, 20: 39152
content in man in India, 1962 through 1965, 20: 39154
content in milk, methods for reducing, 20: 39157
content in urine of Italian children, 20: 39152
content in whales, 20: 38560
distribution in sea water, sampling method for measuring, 20: 39147 (CONF-660401-6)
effects on mice, biological, of chronic ingestion of, 20: 38551
excretion in dogs and man, effects of Prussian Blue on biological half-life, 20: 38557
fixation in glasses, 20: 39319 (DP-1066(Vol.2), pp II.33-44)
gamma field from source at surface of thick concrete slab, (T), 20: 40284 (AD-637125)
half-life and metabolism of, 20: 38743
production and use in United Kingdom, 20: 39283 (DP-1066(Vol.1), pp III.33-44)
release from simulated high-level wastes, 20: 40476(R) (BNWL-267)
removal from fabrics using citric acid, detergents, or water, 20: 39161
separation from fission products in France, 20: 39319 (DP-1066(Vol.2), pp II.33-44)
separation using mixed oxide scavenger, 20: 40476(R) (BNWL-267)
use as heat source in SNAP-7 device, radiological hazards of, 20: 39307 (DP-1066(Vol.1), pp V.35-40)
use in mobile irradiators in Europe, 20: 39276 (DP-1066(Vol.1), pp III.45-50)
use in radiotheraphy, 20: 38744 (DP-1066(Vol.1), pp IV.47-66)

CESIUM ISOTOPES Cs-144
effects on radiation sickness induction in rats, protective effects of tetoxacin and unithiol against, 20: 38732
elimination by mice and rats, effects of DTPA, pectin, and zirconium phosphate on, 20: 38733

CESIUM NEODYMIUM CHLORIDES
production of vapors of, 20: 38919

CESIUM NITRATES
diffusion of cesium in, coefficient of, 20: 38871(R) (NYO-1769-54)
diffusion of cesium-134 in molten, at constant volume, 20: 38872(R) (NYO-1769-68)
radiolysis of frozen, at 77°K, yields of nitrite ion from gamma, 20: 38950

CESIUM OXIDES
heat and free energy of formation of, 20: 39724

CHARGED PARTICLE BEAMS
control of, design of step magnet for, 20: 39508
momentum analysis of, bending magnets for, (T), 20: 39484 (CERN-66-21, pp 1-30)
optics of, lectures on, 20: 39483 (CERN-66-21)
position monitor for, 20: 39506
separation of low-energy, mass and momentum, (E/T), 20: 39485 (CERN-66-21, pp 31-42)
separation of, r-f separators for, 20: 39486 (CERN-66-21, pp 43-54)
spectrometer for, 20: 39502
use for therapy of stomach cancers, 20: 38772

CHARGED PARTICLES
distribution function in low-energy plasma, (T), 20: 40210

energy losses in thin foils, (T), 20: 40117
excitation of cyclotron waves in plasma by streams of, (T), 20: 40188
interactions in propane bubble chambers, method of identification of, (E), 20: 39211 (JINR-P-2842)
magnetic moment of gyrating, in magnetic field, (T), 20: 40229
motion in crossed electric and magnetic fields, (T), 20: 40243
motion in crystals, lattice-structure effects on, 20: 40135
motion in non-resonant h-f and magnetic fields, 20: 40193
motion of, theory of inverse problem of, 20: 39471
reactions with rare gases, stopping powers and straggling in, (T), 20: 39611
stopping in matter, atomic, 20: 39595
trajectories in plasma interactions with h-f fields, (T), 20: 40283
trapping in geomagnetic field, magnetic coordinates for analyzing, 20: 39989

CHEMICAL ANALYSIS
book: *Progress in Nuclear Energy* Series IX, *Analytical Chemistry*, Vol. 6, 20: 38817
use of neutron scattering in, 20: 38882

CHEMISTRY
book: *Advances in Inorganic Chemistry and Radiochemistry*, Vol. 8, 20: 38880
research in mineral, 20: 38857(R) (BNWL-235-3)
research in progress under Army Research Office, 20: 40485(R) (AD-636091)
research progress on solution, 20: 38873(R) (NYO-2269-9)

CHERENKOV RADIATION
emission by electrons in waveguides, traveling wave nature of, 20: 39501

CHICKENS
effects of breed on radiosensitivity of, x, 20: 38677
radiation dosimetry in, lethal, x, 20: 38676
radiation effects on, biological, whole-body x, 20: 38677

CHIMERAS
radiation mouse, nitrogen balance in, 20: 38636

CHLORAMPHENICOL
effects of, on viability of uv-irradiated *E. coli*, 20: 38562
effects on survival of uv-irradiated *E. coli*, 20: 38563

CHLORELLA
radiation effects on, genetic, γ, 20: 38605

CHLORINE
determination by radiometric well logging, temperature compensation circuit for equipment for, 20: 39136(P)
metabolism in animals, tracer study, 20: 38550

CHLORINE FLUORIDES
Al–ClF_3, shock-wave compression measurements on mixtures, (E), 20: 39469 (LA-3453)

CHLORINE ISOTOPES Cl-36
decay of, positron emission in, (E), 20: 40148
determination in aqueous tissue extracts, 20: 38550
radiation effects on exchange of, between ethylenediamine cobalt or rhodium complexes and hydrochloric acid, bremsstrahlung, gamma, and x, 20: 38960

CHLORINE ISOTOPES Cl-37
proton reactions (p,α) at 11 and 12 Mev, statistical fluctuations in cross sections for, 20: 40065(R) (BMwF-FB-K-66-01)

CHLORINE ISOTOPES Cl-38
determination in swimming pool reactor coolant, activation and chemical, 20: 38800 (PAEC(C)RE-652)

CHLOROFORM
viscosity of, use of oscillating sphere device for measuring, 20: 38872(R) (NYO-1769-68)

CHLOROGRAPHIN
labeling with iodine-131, 20: 38932

CHOLESTEROL
determination in blood, micro method, 20: 38652
metabolism in rat liver, effects of tritium oxide perfusion on, 20: 38559

CHOLESTEROL ESTERS
radiation effects on content of, in rat tissues, x, 20: 38701

CHOLINE, ACETYL-
radiation effects on content of, in rabbit nervous system, 20: 38654

CHROMATOGRAPHY
efficiency of impregnated ion-exchange paper in, 20: 39000
equipment for gas, use of integrator with, 20: 38815

CHROMIUM
deposition on fuel rods for corrosion protection, method for, 20: 39350(P)
determination in blood serum, activation, 20: 38851
effect on properties of low-alloy steels for reactor pressure vessels, 20: 39444(P)
effects on properties of boron steel, 20: 39426
evaporative lifetime on tungsten and oxygenated tungsten from 1250 to 1750°K, (E), 20: 40307
superconductivity of, 20: 40047

CHROMIUM ALLOYS
Al–Cr–V, crystal structure of intermetallic compounds in, 20: 39414
Cr–Co–Fe–Mn–Ni–W, tensile properties of L-605, effects of cold deformation on, 20: 39399 (NASA-TN-D-3528)
Cr–Fe–Zr, corrosion of zirconium-base, by steam at 300 to 500°C, 20: 39356(R) (GEAP-5134)
Cr–Fe–Zr, properties of zirconium base, for fuel cladding, 20: 39356(R) (GEAP-5134)
Cr–Ti, performance in niobium alloy brazing, 20: 39365
Cr–U, phase studies of uranium-base, 20: 39388 (CEA-R-2956)

CHROMIUM CARBIDES
effects on properties of titanium–tungsten carbides, 20: 39431
elastic properties of stoichiometric, 20: 39430
Cr_2C_3–TiC–WC, preparation and properties of, 20: 39431

CHROMIUM DYSPROSIUM SELENIDES
preparation and crystal structure, 20: 38884

CHROMIUM ISOTOPES Cr-50
alpha reactions (α,$\alpha'\gamma$) at 4 to 5.6 Mev, gamma spectra from, (E), 20: 39470(R) (ORNL-3924)
oxygen-16 reactions (O-16, O-16 γ) at 30 to 39 Mev, gamma spectra from, (E), 20: 39470(R) (ORNL-3924)

CHROMIUM ISOTOPES Cr-51
production by Szilard-Chalmers reaction, 20: 38982 (PAEC(D)IS-652)
use as tracer for ground water research, 20: 39155

CHROMIUM ISOTOPES Cr-52
alpha reactions (α,$\alpha'\gamma$) at 4 to 5.6 Mev, gamma spectra from, (E), 20: 39470(R) (ORNL-3924)
deuteron reactions (d,p) at 10 Mev, differential cross section for, 20: 40065(R) (BMwF-FB-K-66-01)
helium-3 reactions (He-3,α) and (He-3,d) at 18 Mev, differential cross sections for, 20: 40065(R) (BMwF-FB-K-66-01)
oxygen-16 reactions (O-16, O-16 γ) at 30 to 39 Mev, gamma spectra from, (E), 20: 39470(R) (ORNL-3924)

CHROMIUM ISOTOPES Cr-53
alpha reactions (α,$\alpha'\gamma$) at 4 to 5.6 Mev, gamma spectra from, (E), 20: 39470(R) (ORNL-3924)
oxygen-16 reactions (O-16, O-16 γ) at 30 to 39 Mev, gamma spectra from, (E), 20: 39470(R) (ORNL-3924)

CHROMIUM ISOTOPES Cr-54
alpha reactions (α,$\alpha'\gamma$) at 4 to 5.6 Mev, gamma spectra from, (E), 20: 39470(R) (ORNL-3924)
deuteron reactions (d,p) at 10 Mev, differential cross section for, 20: 40065(R) (BMwF-FB-K-66-01)
oxygen-16 reactions (O-16, O-16 γ) at 30 to 39 Mev, gamma spectra from, (E), 20: 39470(R) (ORNL-3924)
proton scattering at 9.3 to 10.2 Mev, statistical fluctuations in cross sections for elastic, 20: 40065(R) (BMwF-FB-K-66-01)

CHROMIUM STEEL
Cr–Mo, corrosion and mass transfer in flowing sodium, 20: 39345 (GEAP-4831)
Cr–Mo–Ti, corrosion and mass transfer in flowing sodium, 20: 39345 (GEAP-4831)

CHROMOSOMES
analysis of animal cell, for chromatid exchange frequency, 20: 38649
analysis of Drosophila, 20: 38596(R) (SAN-590-1)
analysis of maize, 20: 38617
analysis of, in x radiation induced mutants of Drosophila, 20: 38646
radiation effects on human bone marrow, β and γ, 20: 38623
radioinduced aberrations in leukocyte, 20: 38593 (ORNL-P-2175)
radioinduced aberrations of barley root, effects of post-irradiation centrifugation of seeds on γ, 20: 38618
radioinduced aberrations in apple root, fast neutron and γ, 20: 38692
radioinduced aberrations in mouse, fast neutron and γ, 20: 38647
radioinduced aberrations of, in animal cells, β, 20: 38649
radioinduced anomalies of, in human lymphocytes, x, 20: 38615

CIRCUITS
design of printed, for amplifiers, 20: 39188

CITIES
shelter for large, blast-resistant tunnel design for, 20: 39088

CITRIC ACID
use in decontaminating protective clothing, 20: 39161

CIVILIAN DEFENSE
fallout exposure probabilities for Canadian hospitals, use of computer for rating, 20: 39162
industrial recovery from nuclear attack, study of techniques for, 20: 39146 (AD-636947)

CLAYS
sorptive properties for strontium-90, 20: 39117(T)

CLEANING
equipment for ultrasonic and noncavitating, 20: 40489 (SC-DC-66-1118)

CLINCH RIVER
radioactivity dilution and dispersal in, 20: 40479 (ORNL-P-2338)

CLOTHING
contamination monitor for shoes, design of alpha, beta, and gamma, 20: 39198 (BNWL-250)
COAL
analysis on-line for carbon, oxygen, aluminum and silicon, activation, 20: 39025 (ORO-2980-12)
combustion in oxygen to produce plasma, 20: 39043(P)
handling system for, 20: 39025 (ORO-2980-12)
radioactivity induced in, during activation analysis, 20: 39025 (ORO-2980-12)
COATINGS
analysis for titanium and zinc in organic, activation, 20: 38853
corrosion of nickel, by water at high temperatures, 20: 39461 (WCAP-6074)
deposition of chromium, nickel, and silicon, on fuel rods, method for, 20: 39350(P)
development and testing chromium–iron–zirconium alloy, for fuel elements, 20: 39356(R) (GEAP-5134)
performance of fluoride, for protection of refractory metals from oxidation, 20: 39348
properties of magnesium-alloy, for reactor fuel elements, 20: 39443(P)
radiation effects on nickel, for control rods, 20: 39461 (WCAP-6074)
welding of end cap-to-sheath, 20: 39377
COBALT
determination in blood serum, activation, 20: 38851
determination of trace amounts of, using paper chromatography and isotope dilution, 20: 38807
determination of, in presence of zinc by radiometric titration using EDTA, 20: 38806
neutron capture resonance integrals, (E), 20: 40146
COBALT ALLOYS
reactions with combustion gas species in launch pad abort environments, 20: 39312 (SC-CR-66-2044)
Co–Nd, magnetic properties of intermetallic compound $NdCo_5$ in, 20: 39424
Cr–Co–Fe–Mn–Ni–W, tensile properties of L-605, effects of cold deformation on, 20: 39399 (NASA-TN-D-3528)
COBALT COMPLEXES
cobalt-60 and cobalt-60m recoil reactions in irradiated, 20: 38962
radiation effects on bromine-82 and chlorine-36 exchange with hydrochloric acids, bremsstrahlung, gamma, and x, 20: 38960
salicylaldehyde–triethylenetetramine, radiation effects on, annealing of recoil damage in neutron, 20: 38965
with 2-nitroso-1-naphthol, paper chromatographic separation of, 20: 38807
COBALT ISOTOPES Co-58
use as tracer for ground water research, 20: 39155
COBALT ISOTOPES Co-60
content in Clinch River, 20-year analysis of, 20: 40479 (ORNL-P-2328)
evaluation of, for space heat source, 20: 39306 (DP-1066(Vol.1), pp V.17-25)
gamma field from source at surface of thick concrete slab, (T), 20: 40284 (AD-637125)
production and use in United Kingdom, 20: 39283 (DP-1066(Vol.1), pp III.33-44)
production in BR2, 20: 39318 (DP-1066(Vol.2), pp I.93-101)
production in gas-cooled reactors, 20: 39317 (DP-1066(Vol.2), pp I.67-77)
production in NRX or NRU reactors, 20: 39282 (DP-1066(Vol.1), pp III.3-32)
production in power reactors in Europe, 20: 39276 (DP-1066(Vol.1), pp III.45-50)
reactions of recoil isomers of, in irradiated cobalt nitrate complexes, 20: 38962
separation from waste-water by aerobic treatment, 20: 40483
separation using mixed oxide scavenger, 20: 40476(R) (BNWL-267)
use as heat source in SNAP-7 device, radiological hazards of, 20: 39307 (DP-1066(Vol.1), pp V.35-40)
use as tracer for ground water research, 20: 39155
use in combination with orthovoltage x radiation therapy, economics and effectiveness of, 20: 38792
use in industry in Europe, 20: 39317 (DP-1066(Vol.2), pp I.67-77)
use in industry, medicine, and food preservation in Canada, 20: 39282 (DP-1066(Vol.1), pp III.3-32)
use in radiography, 20: 39286 (DP-1066(Vol.1), pp IV.43-5)
use in radiotheraphy, 20: 38744 (DP-1066(Vol.1), pp IV.47-66)
COBALT OXIDES
Moessbauer spectra in, Auger aftereffects from, 20: 39603
COBALT SULFATES
iron-57 Mössbauer effect in, 20: 40311
COBALT SYSTEMS
B–Co–Zr, crystal structure of stoichiometric, 20: 39416
Co–Fe–Si, Mössbauer effect in, 20: 40300
Co–Wc, phases in, determination by chemical analysis, 20: 39427
COINCIDENCE CIRCUITS
performance of, point method for determining statistical parameters of, 20: 39205 (INR-703/III/PL)
COINCIDENCE COUNTERS
performance for radioactive decay rate measurements, 20: 40107
COLCHICINE
effects on DNA-ase and RNA-ase activity in Ehrlich ascites cells, 20: 38578
COLLIDINES
effects on iodine-131 exchange between elementary iodine and phenyl-dimethyliodopyrazolone, 20: 38936
COLLOIDS
preparation of actinide oxide–rare earth oxide, 20: 39341(P)
preparation of hafnia and zirconia, with actinide oxides, 20: 39442(P)
COLORADO
environmental radiation measurements in, 20: 38735(R) (NYO-1704-13)
COLORIMETRY
use of thiocyanate ions in, review on, 20: 38808
COMPLEXES
book: *Advances in Inorganic Chemistry and Radiochemistry*, Vol. 8, 20: 38880
COMPRESSORS
design and performance of peripheral, 20: 39021 (K-1665)
efficiency of, at speeds to 14,100 rpm, 20: 39026 (UCRL-14660(Rev.1))
COMPTON EFFECT
cross sections for, on bound K electrons, 20: 39773
COMPUTER PROGRAMS
calculation of gamma dose to Canadian hospitals from fallout, 20: 39162
CYGRO-1, for stress analysis of concentric cylinders undergoing irradiation growth and thermal strains, 20: 39460 (WAPD-TM-514 (Add.1))
DEFCOT for deformation of composite tubes, 20: 39394 (GEMP-415)
DETEC, for simulation of fast neutron detection in plastic scintillators, FORTRAN IV for IBM 7044, 20: 39196 (AE-236)
for analysis of gamma spectra from sodium-iodide and lithium-drifted germanium detectors, 20: 39237
for calculating molecular beam scattering intensities, 20: 39321(R) (MLM-1312)
for calculation of extent of exchange from liquid scintillation counting data, in FORTRAN IV, 20: 39226
for calculations in relativistic two-body kinematics, for Burroughs 220, 20: 39750 (HEPL-236)
for calculations of iodine-131 uptake by thyroid of mammals, FORTRAN IV, 20: 38549 (UCLA-12-592)
for determining optical potential for deuterons, 20: 39470(R) (ORNL-3924)
for evaluation of neutron-scattering angular distributions, 20: 40063
for fission-product activities in irradiated natural uranium, FORTRAN II for IBM 1620 model 2, 20: 40070 (IEA-111)
for ion orbit and magnetic field calculations for synchrocyclotrons, 20: 39537
for reactor shield analysis, 20: 40431
GADOSE, for calculation of environmental radioactivity after instantaneous release of radioisotopes from reactors, FORTRAN for IBM 7044, 20: 39148 (GA-6511)
INTERACT, for fissile unit interaction analysis, 20: 40375 (DP-1031)
ISOSHLD, for isotope shielding analysis, FORTRAN IV, 20: 40285 (BNWL-236)
PMC, for neutron transport problems, 20: 40460(R) (IDO-17191)
SETOP, for operation of MSU cyclotron, 20: 39552
SHUTDOWN, for reactor shutdown optimization, 20: 40423
STREAM, for waste transport analysis, 20: 39099(R) (BNWL-235-3, pp 1-23)
SURFER, for analysis of interphase mass transfer, 20: 39050 (UCRL-16535)
TRIM, for solving mathematical models of two-dimensional magnets, FAP for IBM 7094, 20: 39499 (UCRL-16959)
TRUMP, for transient and steady state temperature distribution, 20: 39049 (UCRL-14754)
WIMS, for reactor lattice calculations, 20: 39382 (AEEW-R-473)
COMPUTERS
use for processing of positron radioisotope scan data, 20: 38745(R) (NYO-3267-3)
use for recording Raman spectra of molten salts, 20: 38872(R) (NYO-1769-68)
use for solution of interphase mass transfer problems, 20: 39050 (UCRL-16535)
use in gamma spectroscopy, 20: 39243
use in high-energy physics research, 20: 39241
use in nuclear power plant control, 20: 40437
use in reactivity calculations using discrete transfer matrix, 20: 40060
use of time-sharing, for nuclear structure analysis, 20: 39240
CONCRETES

gamma attenuation calculations for, build-up factor effects on, 20: 40289
gamma exposure field from point source at surface of thick slab of, (T), 20: 40284 (AD-637125)
thermal conductivity of high-alumina, at 200 to 1500°C, (E), 20: 39698

CONDENSERS
design for fast-breeder reactors, 20: 40413 (TID-23257(Vol.1))
design of, for isopropylbiphenyl, 20: 40449(R) (SAN-650-1)
testing of forced-convection, 20: 39028

CONFERENCES
see also introduction to Report Number Index
Evaluation of Metallic Materials in Design for Low-Temperature Service, Atlantic City, N. J., June 27–28, 1961, 20: 40051
Radioactivation Analysis and Its Applications in Biological Sciences, Saclay, September 1963, 20: 38836

CONNECTIVE TISSUE
radiation effects on rabbit, effects of vasoconstricting drugs on x, 20: 38640
radiation effects on pathology of, in animals, 20: 38653

CONTACTORS
operation and performance of stacked-clone, 20: 38998(R) (ORNL-3958)

CONTAMINATION
control during manufacturing processes, 20: 40469 (SC-DC-66-1118)

CONVECTION
magnetohydrodynamic, in compressible conducting fluid, 20: 39939

CONVERSION ELECTRONS
detection and measurement of, design and performance of spectrometer for, 20: 39206 (INSJ-99)

COPPER
determination in blood in arthritic and healthy patients, activation, 20: 38845
determination in blood serum, activation, 20: 38851
determination in erythrocytes and plasma in human blood, activation, 20: 38852
determination in mosaic virus and nucleic acids in tobacco plants, activation, 20: 38846
deuterium ion reactions at 40 and 50 kev, sputtering from, 20: 39581(R) (ORNL-3989, pp 134)
electric discharge explosion of wires of, MHD instabilities in, 20: 39010
electron beam reactions with, physical aspects of penetrations from, 20: 40347
evaporation lifetime on tungsten and oxygenated tungsten from 1250 to 1750°K, (E), 20: 40307
fabrication by magnetic-pulse forming, 20: 40490 (Y-1483)
meson (μ^-) capture by, neutron angular distributions from, (E), 20: 40096
radioinduced diffusion of nickel-63 in, model of alpha, 20: 39451 (EUR-2968.e)
sputtering-yields crossover in single-crystal, (E), 20: 39589
superconductivity of, 20: 40047

COPPER ALLOYS
Al–Bi–Cu–Pb, fatigue failure of 2011-T3, equations for, 20: 39396 (IS-T-60)
Al–Cu–Y, crystal structure of intermetallic compounds in, 20: 39414
Cu–Au–Ni, gold-197 hyperfine structure coupling in, (E), 20: 39470(R) (ORNL-3924)
Cu–Mo–Zr, corrosion by steam, effects of heat treatments on copper-base and zirconium-base, 20: 39347 (NP-16239)

COPPER COMPLEXES
with mixed β-diketones in benzene solution, 20: 38855 (BNL-10350)

COPPER ISOTOPES Cu-63
neutron reactions (n,d) at 14.08 Mev, angular distributions from, (E), 20: 40069(R) (EANDC(E)-66(U))

COPPER ISOTOPES Cu-64
preparation of high-specific-activity, by Szilard-Chalmers reactions, 20: 38988

COPPER ISOTOPES Cu-65
gamma transition in beta decay of zinc-65, intensity of 1.114-Mev, (E), 20: 40093
hyperfine structure and quadrupole moment of, (E), 20: 40137
neutron reactions (n,d) at 14.08 Mev, angular distributions from, (E), 20: 40069(R) (EANDC(E)-66(U))
neutron reactions (n,nα), (n,2n), and (n,p) at 2 to 20.3 Mev, cross sections for, (E), 20: 40149

COPPER OXIDES
reactions with carbon monoxide and hydrogen in helium flow in differential and deep beds, 20: 38874 (ORNL-TM-1540)

COPPER PHTHALOCYANINE
annealing reactions in α- and β-, thermal, 20: 40309
structure sensitivity of recoil-atom reactions in α- and β-, 20: 40309

COPPER SYSTEMS
Al_2O_3–Cu, rupture strength of, effects of microstructure on, 20: 39398 (NASA-TN-D-3527)

CORROSION
book: *Corrosion Resistance of Reactor Materials, Handbook*, 20: 39349

CORROSION FILMS
reactions of zirconium oxide, with carbon tetrachloride, 20: 39360 (TRG-Report-1255)

CORROSION LOOPS
design for liquid potassium, 20: 39028

CORROSION-RESISTANT ALLOYS
development for alkali metal containment, 20: 39028

CORTICOSTEROIDS
determination in urine using paper chromatography, 20: 38547(R) (NYO-918-15)

CORTICOSTERONES
radiation effects on synthesis in rats of, x, 20: 38638

COSMIC ALPHA PARTICLES
intensity variations in solar system and interstellar space, 20: 39571
interactions with interstellar gas, secondary electrons from, 20: 39630
penetration into auroral atmosphere, helium spectra from, (T), 20: 39981

COSMIC ELECTRONS
production of secondary, in galaxy, 20: 39630

COSMIC MESONS (μ)
angular distribution in ground and under water, generation mechanism from, (T), 20: 39831
capture by copper, iron, and lead, neutron angular distributions from, (E), 20: 40096
production of, mechanisms for, (T), 20: 39831
sidereal variation at 440-m depth, (E), 20: 39626

COSMIC NEUTRINOS
detection underground, laboratory for, 20: 39016 (COO-818-94)

COSMIC NEUTRONS
counting rates from Canadian stations, 20: 39623 (AECL-2598)
energy spectra during solar activity, 20: 39628(T)
intensity variations of, energy spectrum of solar-diurnal and semidiurnal, 20: 39628(T)
reactions with argon in atmosphere, phosphorus isotope production by, 20: 39991

COSMIC NUCLEONS
interactions of, nucleon form factors determination by analysis of momentum transfer in, 20: 39781

COSMIC PARTICLES
abundance of helium and heavier nuclei in solar, during July 18, 1961 event, 20: 39564
energy in magnetosphere, cut-off rigidity, 20: 39988

COSMIC PHOTONS
interactions with interstellar gas, secondary electrons from, 20: 39630

COSMIC PROTONS
fluxes of trapped, ring current effects on, 20: 39970
intensity variations in solar system and interstellar space, 20: 39571
penetration into auroral atmosphere, hydrogen spectra from, (T), 20: 39981

COSMIC RADIATION
detection and measurement of galactic x, instrumentation for, 20: 39229
detection and measurement of gamma, balloon-borne equipment for, 20: 39632
deuterons in, generation of, 20: 39825
effects on ionosphere, height dependence of electron production from, (T), 20: 39625
gamma flux in, from quiet sun, (E), 20: 39565
intensity variations on earth's surface, rigidity models for ordering data on, 20: 39624 (D-1-82-0529)
magnetic field of solar, effect on magnetosphere, 20: 39963(T)
measurements in space, 20: 39627
monitoring of, in first 10,000 ft. in western states of U. S., 20: 38735(R) (NYO-1704-13)
quark generation in, mechanisms of, 20: 39631(T)
radiation hazards to astronauts from, 20: 38603(T) (AD-629422)
reactions in atmosphere during quiet sun, 20: 39565
research on, deep underground laboratory for, 20: 39016 (COO-818-94)
shielding space vehicles against, using superconducting magnet coils, 20: 40292
sources of high-energy gamma, search for discrete, 20: 39632
variations in, complex amplitude-phase modulation of, (T), 20: 39629(T)
variations of neutron component of, solar-diurnal and semidiurnal, 20: 39628(T)

COSMOLOGY
formation of elements, gravitation effects on, (T), 20: 39560
gravitational collapse and scalar interaction in superdense matter, 20: 39555
star formation in rotating magnetic clouds, 20: 39568

COUNTING DEVICES
design of, for Neurospora colonies, 20: 38546

CREATINEPHOSPHORIC ACID
analysis for oxygen, activation, 20: 38848

CREEP
effects on pressurized shells, analytical method for, 20: 39391 (CONF-

660629-1)
CRITICAL ASSEMBLIES
built, being built, or planned in the U. S., 20: 40359 (TID-8200(13th Rev.))
CRITICALITY STUDIES
of graphite–uranium lattices using WIMS code, 20: 39382 (AEEW-R-473)
CROSS SECTIONS
probability distribution of maxima and minima of nuclear, (T), 20: 40113
CRUSTACEA
radioactivity in fresh-water, from nuclear plant wastes, 20: 38742
CRYOGENICS
materials evaluation for, metallic, 20: 40051
testing at liquid helium temperatures, methods and costs of, 20: 40019
CRYSTAL STRUCTURE
effects on charged-particle motion in crystals, 20: 40135
effects on rupture strength of dispersion strengthened alloys, 20: 39398 (NASA-TN-D-3527)
radioinduced changes in urania, use in determining thermal conductivity, 20: 39456 (GEAP-5100-1)
CRYSTALLOGRAPHY
use of shadow effect in research on crystal structure, 20: 40135
CRYSTALS
charged-particle motion in, lattice-structure effects on, 20: 40135
electronic wavefunctions for, Hartree-Fock approximation for, (T), 20: 39617
phonon hydrodynamic phenomena in non-metalic, (T), 20: 40327
preferred orientation data on, conversion to inverse pole figures, 20: 39402 (ORNL-3979)
second sound propagation in non-metallic, (T), 20: 40327
thermal conductivity in non-metallic, (T), 20: 40327
CULTURE MEDIA
effects of x-irradiated, on chick embryo cells, 20: 38707
CURIUM
separation of, from other rare earths, by lactate elution from cation resin columns, 20: 39004
vaporization of, thermodynamics of, 20: 38876 (UJV-1598)
CURIUM IONS
oxidation of trivalent, in ozonized solutions, tracer studies of, 20: 38917
CURIUM ISOTOPES Cm-242
production and use in United Kingdom, 20: 39283 (DP-1066(Vol.1), pp III.33-44)
production in reactors, 20: 39316 (DP-1066(Vol.1), pp II.3-14)
separation from irradiated targets at ORNL, 20: 39316 (DP-1066(Vol.1), pp II.3-14)
use in thermionic converters, 20: 39633 (CEA-R-2788)
use in thermoelectric converters, 20: 39633 (CEA-R-2788)
CURIUM ISOTOPES Cm-244
evaluation of, for space heat source, 20: 39306 (DP-1066(Vol.1), pp V.17-25)
production and use in United Kingdom, 20: 39283 (DP-1066(Vol.1), pp III.33-44)
separation from irradiated targets at ORNL and Savannah River, 20: 39316 (DP-1066(Vol.1), pp II.3-14)
CURIUM ISOTOPES Cm-246
use as heat source in thermoelectric generators, 20: 39308 (DP-1066 (Vol.2), pp III.3-16)
CURIUM OXIDES
CmO_2–HfO_2, preparation of sols of, 20: 39442(P)
CmO_2–rare earth oxides, preparation of sols of, 20: 39341(P)
CmO_2–Y_2O_3, preparation of sols of, 20: 39341(P)
CmO_2–ZrO_2, preparation of sols of, 20: 39442(P)
CURRENT INTEGRATORS
design for ORIC beam monitoring, 20: 39507
CYANIDE COMPLEXES
with transition metals, review on preparation, properties, and structure of, 20: 38881
CYCLOBUTANE
decomposition of deuterated and normal, effects of added gases on photosensitized, 20: 38941(R) (RRL-2310-182)
CYCLOHEXANE
neutron reactions at 0.025 to 0.4 ev, total cross sections for, (E), 20: 40069(R) (EANDC(E)-66(U))
cyclohexane–iodomethane, radiolysis of, methyl radical yields in, 20: 38941(R) (RRL-2310-182)
CYCLOPENTANONE
benzene–cyclopentanone, radiolysis of aqueous solutions of, mechanisms of pulse, 20: 38939(R) (NYO-2668-13)
CYCLORATORS
conference on isochronous, 20: 39510
CYCLOTRON RADIATION
emission by plasma, (T), 20: 40273
emission from plasma, dispersion effects on, (T), 20: 40271
emission of, in x-ray region, 20: 39473
excitation in plasma by charged particle streams, (T), 20: 40188
incorporation into equations for fully ionized plasma, 20: 40270
CYCLOTRONS
beam analysis of proton, characteristics of broad range magnetic analyzer for, 20: 39477 (BMwF-FBK-66-15, pp 1-15)
beam deflection-bunching system at Karlsruhe, for use with neutron spectrometer, 20: 39546
beam extraction and transport systems of 240-cm, ion-optical studies of, 20: 39545
beam extraction from UCLA and Manitoba, variable energy negative-ion, 20: 39519
beam extraction in AVF, 20: 39518
beam extraction system for MSU, single-turn, 20: 39517
beam extraction system and operation of Orsay CEVIL, 20: 39551
beam injection method for, 20: 39530
beam optics in central region of 240-cm variable-energy, 20: 39513
beam orbit properties in Karlsruhe, 20: 39515
beam properties in central region of, 20: 39511
beam properties of Philip's AVF, 20: 39516
beam resonance extraction method for relativistic, modified, 20: 39520
betatron frequency in, current limitations and space charge effects on, 20: 39529
control of MSU, computer program for, 20: 39552
design and development of separated-orbit, 20: 39541
design concept of super separated-orbit, 20: 39543
design modifications and developments for Berkeley 88-inch, 20: 39547
design modifications for Kazakhstan, 20: 39553
design of AVF, above 100 Mev, 20: 39539
design specifications, status, and progress summaries of isochronous, 20: 39554
development at ETH Zurich, as meson factory, 20: 39533
development for meson production, 20: 39534
development of negative hydrogen-ion, as meson factory, 20: 39540
ion acceleration and beam extraction measurements in Milan, negative hydrogen, 20: 39550
ion acceleration in 685-mm sector, 20: 39549
ion injection for stripping into central region of CEVIL, heavy-, 20: 39531
ion injection in Grenoble, axial, 20: 39532
ion injection in, external, 20: 39526
ion phase measuring equipment at Karlsruhe and Jülich isochronous, 20: 39514
ion source design for, 20: 39505
ion source for Davis 76-in., central region studies for axial, 20: 39512
ion source trap design for, 20: 39504
ion sources for Grenoble isochronous, construction of polarized hydrogen and deuterium, 20: 39527
ion sources for, polarized, 20: 39525
ion sources for, phase space density of, 20: 39528
particle motion in, stability of, 20: 39524
performance of AVF, for high-resolution nuclear physics experiments, 20: 40101
research with AVF, in Europe, 20: 39544
technology of isochronous, survey of, 20: 39548
CYLINDERS
deformation of concentric, computer program for, 20: 39394 (GEMP-415)
gravitational collapse of incoherent fluid, exterior metrics in general relativity for, 20: 40001
response of tubular towers to static and dynamic loads, 20: 39007 (AD-636914)
stress analysis of concentric, computer program for, 20: 39460 (WAPD-TM-514(Add.1))
CYSTEIC ACID
radiolysis of, in aqueous solution, γ, 20: 38582
CYSTEINE
effects on organic peroxy compound synthesis in x irradiated mice, 20: 38660
radioprotective effects on bacteriophage, 20: 38628
radiosensitivity effects on iodouracil-substituted T1 bacteriophage, 20: 38704
radiosensitivity effects on bacteriophage, x, 20: 38712
radiosensitivity effects on mice, 20: 38717
CYSTINE
radiolysis of, in aqueous solution, γ, 20: 38582
CYTOCHROMES
radiosensitivity of yeast, x, 20: 38680
CYTOLOGY
cell separator for design, 20: 38545
effects of cysteamine on rabbit liver, 20: 38716
radiation effects on tumor and other cells, mechanisms for, 20: 38616
radiation effects as a function of cellular level responses, relevance to radiotherapy, review of, 20: 38634
radiation effects on rat liver mitochondria, x, 20: 38639

CZECHOSLOVAKIA
genesis of moldonites in, 20: 39135
radioisotope, labeled compound, and radiation source preparation and use in, 20: 39279

D

DATA RECORDING SYSTEMS
design for 100-channel pulse analyzer, 20: 39183
design of automatic, for sample counting apparatus, 20: 39044(P)
design of punched-card for film badge exposures, 20: 39258
DATA TABULATIONS
cosmic-ray NM-64 neutron monitor data-3, 20: 39623 (AECL-2598)
on geomagnetic and solar data, 20: 39979
on hand specimen properties of 1500 minerals, 20: 39100
DECONTAMINATING SOLUTIONS
use on skin, evaluation of, 20: 39151
DECONTAMINATION
equipment for, of radioactive reservoir water, 20: 40484
DECONTAMINATION OF PERSONNEL
methods for skin, 20: 39151
DEHYDROASCORBIC ACID
radiation effects on content in rat brain, whole-body x, 20: 38679
DEHYDROGENASES
radiation and Brucella effects on activity of malic, in rabbit peritoneal cells, 20: 38586
DENSITOMETERS
properties of neutron, in snow and ice density measurements, 20: 39130
use of radioisotopic, in industry, 20: 39291
DETERGENTS
use in protective clothing decontamination, 20: 39161
DEUTERIUM
abundance in stellar atmospheres and depletion during stellar evolution, 20: 39574
argon ion reactions with molecules of, cross sections for charge-exchange, (E), 20: 39592
containment of plasma of, in magnetic mirror traps, 20: 40194
crystal structure of solid, (E), 20: 40308
density in ionosphere, energy spectra from, (E), 20: 39987
deuteron reactions (d,n) up to 100 kev, yields of, (E), 20: 40078 (NP-16203)
effects of, on sodium methoxide-promoted elimination reaction of 2,2-diphenylethyl benzenesulfonate, 20: 38912
effects on heavy water decomposition, 20: 40409(R) (NP-16230)
effects on hydrogen production in gamma radiolysis of heavy water–water mixtures, 20: 38938 (IA-1074)
effects on radiationless decay of anthracene triplet, 20: 38958
electron elastic scattering by, electromagnetic form factors of deuterons and neutrons from, (E), 20: 39795
incorporation in anthraquinone by isotopic exchange with deuterium-labeled sulfuric acid, 20: 38889
isotope effects on crystal properties of lithium hydride, 20: 40351
proton scattering at 8.9 Mev, mechanisms for, 20: 40065(R) (BMwF-FB-K-66-01)
spectra of high-speed excited atomic, at 2700 to 6600 A, (E), 20: 39593
use in percolation and evaporation studies, 20: 39127
viscosity of molecular, saturated-liquid, 20: 39940
yields in radiolysis of hexane, effects of hydriodic acids on, 20: 38941(R) (RRL-2310-182)
DEUTERIUM COMPOUNDS
production of N_2O^* in mass spectrometer ion source, 20: 38902
DEUTERIUM HYDRIDES
magnetic dipole moment of, (T), 20: 40310
vibronic energy of, (T), 20: 40310
yields in radiolysis of hexane, effects of hydriodic acids on, 20: 38941(R) (RRL-2310-182)
DH–H, combustion at very high temperatures, 20: 39013(P)
DEUTERIUM IONS
production of polarized negative, by charge exchange, 20: 39584
reactions with tritium to produce gamma-free neutrons for well logging, 20: 39137(P)
sputtering on copper, molybdenum, stainless steel-304, and tungsten at 28 to 50 kev, 20: 39581(R) (ORNL-3989, pp 134)
DEUTERIUM SYSTEMS
D–H, combustion at very high temperatures, 20: 39013(P)
D–Ne, crystal structure of solid, (E), 20: 40308
DEUTERON SOURCES
development of polarized, for Grenoble isochronous cyclotron, 20: 39527
DEUTERONS
effects on coloring in blue cellophane films, 20: 38941(R) (RRL-2310-182)
exchange in bound nucleon-antinucleon systems, (T), 20: 39841
form factors from electron scattering by deuterium, electromagnetic, (E), 20: 39795
interactions with mesons (π^+) at 3.29 Bev/c, A_1 (1090) and A_2 (1310) production in, (E), 20: 39470(R) (ORNL-3924)
interactions with mesons (K^-) at 0.9 to 1.12 Bev/c, $\Sigma^-\eta$ enhancement in, (E), 20: 39747 (COO-881-75)
interactions with photons at 0.4 to 1.0 Bev, computer program for determining quantities in, 20: 39750 (HEPL-236)
production in cosmic radiation, 20: 39825
production in proton reactions with beryllium and platinum at 2.9 Bev, (E), 20: 39794
reactions (d,α) with magnesium isotopes, angular distributions from, 20: 40065(R) (BMwF-FB-K-66-01)
reactions (d,α) with boron-10 at 1.6 to 3.0 Mev, angular distributions and cross sections for, (E), 20: 40068 (BMwF-FBK-66-15, pp 38-46)
reactions (d,nγ) with boron-10, carbon-11 energy levels from, (E), 20: 40164
reactions (d,n) with deuterium and tritium up to 100 kev, yields of, (E), 20: 40078 (NP-16203)
reactions (d,n) with carbon-13 at 2 to 7 Mev, distorted-wave calculations for, (T), 20: 40114
reactions (d,n) with oxygen-16 at 3.5 Mev, angular distribution for, (E), 20: 40155
reactions (d,n) with beryllium-9, boron-10 energy levels from, (E), 20: 40164
reactions (d,n) with fluorine-19, neon-20 energy levels from, (E), 20: 40164
reactions (d,p) with nuclei, differential cross sections for, 20: 40065(R) (BMwF-FB-K-66-01)
reactions (d,p) with lead-208 at 4 to 7 Mev, subcoulomb stripping, 20: 40065(R) (BMwF-FB-K-66-01)
reactions (d,p) with calcium-40 at 2 Mev, distorted-wave calculations for, (T), 20: 40114
reactions (d,p) with nitrogen-14 at low energy, distorted-wave analysis of, (T), 20: 40122
reactions (d,p) with carbon-12, carbon-13, and oxygen-17, (E), 20: 40155
reactions (d,p) with oxygen-18 at 11 Mev, oxygen-19 energy levels from, (E), 20: 40161
reactions (d,p) with oxygen-17 at 10 Mev, oxygen-18 energy levels from, (E), 20: 40161
reactions with nuclei, computer program for determining optical potential for, 20: 39470(R) (ORNL-3924)
reactions with nuclei at 11.8 Mev, energy spectra from, 20: 40065(R) (BMwF-FB-K-66-01)
reactions with uranium-238, production of isomeric neptunium-236 in, (E), 20: 40092
relaxation times of, in aqueous pentavalent molybdenum solutions, 20: 38893
scattering by boron-10 at 1.6 to 3.0 Mev, angular distributions and cross sections for elastic, (E), 20: 40068 (BMwF-FBK-66-15, pp 38-46)
vertex of, integral equation for anomalous, 20: 39843
DIET
cesium-137 and strontium-90 content of children's, in Italy, 20: 39152
content of cesium-137, iodine-131, strontium-89, and strontium-90 in U. S., 1965, 20: 38743
effects of B group vitamins, folic acid, and phosphatide on radiation resistance in rats, 20: 38721
effects of calcium, phosphorus, or strontium content of, on barium and strontium retention in rats, 20: 38566
effects of drinking high sulfur-content mineral water on radiosensitivity of mice to x rays, 20: 38709
effects on iodine-131 uptake by thyroid gland of mammals, 20: 38549 (UCLA-12-592)
radioactivity in, effects on carcinoma incidence in human populations, 20: 38739
strontium-90 content in Argentina, 20: 39150(R) (NYO-2753-4)
DIETHYLAMINE
dissociation, intramolecular rearrangements, and ionization of deuterated and normal, by electron bombardment in mass spectrometer, 20: 38888
DIFFERENTIAL THERMAL ANALYSIS
equipment and procedures for high-temperature, uses in ceramic research, 20: 39437
DIFFUSION PUMPS
performance of glass, using DC-705 silicone oil, 20: 39098(R) (WERL-2823-21)
DIKETONES
complexes with copper and uranyl ions in pairs in benzene solution, 20: 38855 (BNL-10350)
DIODRAST
labeling with iodine-131, 20: 38932
DIOXANE
hydrogen scattering cross sections in, (E), 20: 40069(R) (EANDC(E)-66(U))
2,3-DIPHOSPHOGLYCERIC ACID

determination in erythrocytes using oxygen-18, proton activation, 20: 38841
DIRECT ENERGY CONVERSION DEVICES
development of, for oceanographic applications, 20: 39313
DISEASES
analysis for trace elements in human, activation, 20: 38847
radiotherapy of epilepsy using yttrium-90 implants, 20: 38779
DISPLACEMENT GAGES
design for reactor fuel channel gaps, 20: 39175
DISTILLATION APPARATUS
design for separating bismuth and polonium-210, 20: 38996 (DP-1066(Vol.2), pp II.79-102)
DISULFIDES
effects as radioprotective agents in mice, relation to chemical structure, 20: 38724
DODECANE
yields in gamma radiolysis of *n*-hexane–silica gel, 20: 38994(R) (AE-232)
DOGS
cesium-137 excretion by, effects of Prussian Blue on biological half-life, 20: 38557
iodine-131 uptake and elimination from thyroid of, effects of potassium iodide and thiouracil on, 20: 38734
pathology of radiation sickness in, effects of functional state of hypothalamous on, 20: 38688
radiation effects on buccal flora of, γ, 20: 38667
radiation effects on 17-ketosteroid content in blood of, whole-body, x, 20: 38684
radiation effects on response of, to hemorrhagic stress, x, 20: 38703
radiation effects on tonus of blood vessels of, 20: 38658
radiation protection of, using sodium gallate, 20: 38728
radiation sickness in newborn, by exposure during intrauterine development, 20: 38665
radiation sickness effects on kidney function and morphology in, protective effects of unithiol against, 20: 38719
radiation sickness in, protective effects of procaine against, 20: 38727
radioprotective effects of selachyl alcohol, 20: 38731
radiosensitivity effects of bone marrow transplants in, effects of cell number on, 20: 38740
use of bone marrow for therapy of radiation sickness in, 20: 38730
DOLOMITES
oxygen-16/-18 fractionation between calcites and, 20: 39129
oxygen-16/-18 fractionation between limestones and, 20: 39129
DOORS
design for blast shelters, 20: 39073
DOSIMETERS
calibration of film, design of unit for, 20: 39266
design of boron polyethylene-moderated, for neutrons, 20: 39214(T) (NP-tr-1394)
design of thermoluminescent, 20: 39224
design of thermoluminescent, 20: 39225
design parameters for space-flight, 20: 39158
development of neutron, 20: 39221
filter design for photographic film, 20: 39251(P)
small dose measurement by, in personnel monitoring, 20: 39246
DROSOPHILA
effects of diet containing irradiated food on, genetic, 20: 38596(R) (SAN-590-1)
helium effects on, genetic, 20: 38596(R) (SAN-590-1)
radiation effects on, genetic, x, 20: 38596(R) (SAN-590-1)
radiation effects on spermatogenesis in, x, 20: 38607
radiation effects on, genetic, fast neutron, 20: 38645
radiation effects on, genetic, x, 20: 38646
radiation effects on, genetic, x, 20: 38650
DRUGS
effects of anti-metabolic, on metabolism of iodine-131 in thyroid, 20: 38785
radiosensitivity effects of vasoconstricting, on blood vessels in rabbit connective tissue, 20: 38640
DUSTS
use of suspensions in closed-cycle MHD nuclear loops, (T), 20: 39728
DYSPROSIUM
determination in biological materials, use of automated gamma spectrometers in activation, 20: 38843
determination in ferrite garnets and yttrium oxide, activation, 20: 38833
determination in solutions, spark method for spectrographic, 20: 38832
magnetic field at nuclei of, implanted in iron, 20: 40342
magnetic fields at tin-119 in, deduction from gamma hyperfine splitting, 20: 40322
neutron activation of, use in measuring thermal flux fine structure, 20: 39452 (EUR-2981.f)
shock compression of, 20: 39425(T)
DYSPROSIUM ALLOYS
Al–Dy, magnetic properties of intermetallic compounds of, 20: 39433
Dy–Pb–Zn, component distribution in recrystallized, 20: 39435
Dy–Zn, crystal structure of intermetallic compounds Dy_6Zn_{23} in, 20: 39417
DYSPROSIUM CHLORIDES
heat of dilution of aqueous, at 25°C, 20: 38903
specific gravity and apparent molal volume of aqueous solutions of, at 25°C, 20: 38905
thermal capacity of aqueous solutions of, at 25°C, 20: 38906
viscosity of aqueous solutions of, at 25°C, 20: 38904
DYSPROSIUM OXIDES
actinide oxides–Dy_2O_3, preparation of sols of, 20: 39341(P)

E

EARTH
density of, well logger for determination of, 20: 39139(P)
ECOLOGY
bibliography, 20: 40488 (ORNL-3957)
radiation effects on deciduous forest, γ and neutron, 20: 38594(R) (ORO-2066-10)
radiation effects on, of Puerto Rican forest, γ, 20: 38601 (UCLA-12-567)
systems, review of, 20: 40488 (ORNL-3957)
EGGS
radiation effects on eye gnat production of, γ, 20: 38632
radiation effects on salmon, biological, chronic γ, 20: 38698
radiation effects on grain moth, gamma, 20: 38705
radiation effects on marine, natural β, 20: 38741
ELASTICITY
moduli of transition metal carbides, 20: 39430
ELECTRIC ARCS
electron density and temperature in, in argon, (E), 20: 39666
motion in magnetic fields, retrograde, (E), 20: 40232
ELECTRIC CHARGES
electromagnetic field of moving dipole and multipole, (T), 20: 40003
ELECTRIC CONDENSERS
design for chalice, 20: 40178(R) (SIT-2582-19)
ELECTRIC CONDUCTIVITY
cryogenic effects on actinides, 20: 39448 (AERE-X-PR-2596-9)
effects of fallout on atmospheric, 20: 39111
of metals, effects of nonmagnetic impurities on, 20: 39395 (IAE-1028)
theory for, quantum, 20: 39873
use in studies of point defects in iron, 20: 39386 (CEA-R-2905)
ELECTRIC CURRENTS
measurement of weak, instrument for, 20: 39169 (ISS-66/17)
ELECTRIC DISCHARGE
electron and ion emission in pulsed, space charge effects on, 20: 40253
electron temperature in tubes, variation of plasma, 20: 40185
frequency multiplier for gaseous, in nonuniform shf fields, (T), 20: 40228
in low-pressure gases, confinement effects on, 20: 40278
plasma diffusion across magnetic fields in toroidal, (E/T), 20: 40180 (SU-IPR-69)
plasma turbulent diffusion in oscillating, (Y), 20: 40191
radioinduced in capacitor-type polyethylene terephthalate structures, 20: 39467
spectral shift mechanism in plasma of, 20: 40182
use in producing nuclear reactions, device for, 20: 39509(P)
ELECTRIC FIELDS
charged-particle motion in magnetic and non-resonant h-f, 20: 40193
charged-particle motion in crossed magnetic and, (T), 20: 40243
effects on collisionless plasma oscillations, growth, 20: 40179 (SU-IPR-49)
effects on conductivity of ionized gases, (T), 20: 40238
electron motion in r-f mirror, (T), 20: 40266
plasma containment in magnetic and non-resonant h-f, 20: 40193
plasma containment in closed mixed magnetic and, 20: 40280
plasma kinetics in strong magnetic and, 20: 40249
plasma properties in r-f, (E/T), 20: 40276
ELECTRIC GENERATORS
design for ANL fast breeder reactors, 20: 40414 (TID-23257(Vol.2))
design of 60-kw alternator for SNAP-8, 20: 40453
ELECTRIC INSULATORS
development of radiation resistant, 20: 39274 (N-66-18175)
properties of oxide, for MHD generators, 20: 39657
radioinduced voltage in, recovery of, 20: 40329
ELECTRIC POWER
generation of, methods and economics of future, 20: 40492
generation of, using nuclear and conventional fuels, 20: 40422
protection using fast-breeder reactors, economics of, 20: 40415 (TID-23257(Vol.3))

ELECTRIC PROBES
design for reactor fuel channel gaps, 20: 39175
development of coaxial, 20: 40177(R) (ORNL-3989, pp 135-43)
use of Langmuir, for duoplasmatron diagnostics, 20: 40202
ELECTRODES
current saturation effects in MHD generator, (E), 20: 39660
design for beam divergence and intensity control in ion sources, 20: 39039(P)
design for velocity spectrometer, 20: 39502
development of liquid-protected, for ion engine, 20: 39094
effects on electrical parameters of MHD generators, (T), 20: 39697
electrochemical properties of, for MHD loops, (E), 20: 39723
electron emission from cesiated-copper, 20: 39092
electron temperature variation in discharge tubes with auxiliary, 20: 40185
materials for MHD generator, (T), 20: 39708
materials testing for, 20: 39093
performance of segmented, in MHD ducts, 20: 39661
use of segmented, in MHD generators, (T), 20: 39712
ELECTROHYDRODYNAMIC CELLS
design of, (T), 20: 39650
performance of, (E), 20: 39649
properties and uses of, 20: 39648
uses in power generation, 20: 39701
ELECTROMAGNETIC FIELDS
calculation for moving dipole and multipole charges, 20: 40003
effects on Josephson current in superconductors, 20: 40035
interactions with plasma, particle trajectories in, (T), 20: 40283
penetration in magnetoplasma, analysis of, 20: 40204
plasma heating in h-f, properties of, 20: 40261
ELECTROMAGNETIC LENSES
magnetic field calculations for, (T), 20: 39011
magnetic fields in quadrupole superconducting, digital calculations of, 20: 39479 (BNL-10495)
ELECTROMAGNETIC PUMPS
development for SNAP-10A, 20: 40446 (NAA-SR-11879)
development for SNAP-50/SPUR powerplant, 20: 40450 (TIM-911)
performance in Rankine cycle test loops, 20: 39028
ELECTROMAGNETIC WAVES
absorption in ionosphere, solar height and night variations of, 20: 39960(T)
conversion to ion-acoustic plasma oscillations, (T), 20: 40244
interactions in magnetoplasma, dispersions from, 20: 40207
interactions in plasma with transverse waves present, 20: 40205
plasma acceleration from, near cyclotron resonance, 20: 40267
propagation along warm plasma columns, (T), 20: 40166 (AD-637711)
propagation in cold plasma, resonance effects on, (T), 20: 40258
propagation in cylindrical magnetoplasma, transverse, (T), 20: 40201
propagation in plasma, collision effects on, (T), 20: 40222
propagation in plasma, dispersion equations and Landau damping from, 20: 40259
propagation in plasma, charged particle motion and energy gain in standing, (T), 20: 40263
propagation in plasma, charged particle energy gain in standing, (T), 20: 40264
propagation in plasma, mass effects on charged particle energy gain in standing, (T), 20: 40265
propagation in plasma, ray theory for cylindrical and spherical, 20: 40208
propagation in plasma, theory for, 20: 40206
propagation of surface, along plane vacuum-plasma interface, 20: 40200
ELECTRON BEAMS
Cherenkov radiation from, in waveguides, 20: 39501
density of ions in, at pressure below breakdown, (T), 20: 39605
effects on liquid aliphatic hydrocarbons, ESR spectra of products of, 20: 38941(R) (RRL-2310-182)
effects on white cast iron during heat treatments, 20: 39464
emission from arbitrary surfaces, equations for, 20: 40242
injection into afterglow plasma, cyclotron harmonic radiation from, (E), 20: 40165 (AD-637710)
interactions with gas slabs, (T), 20: 39576 (AD-636533)
interactions with plasma, diagnostics from, 20: 40174(R) (ORNL-3989, pp 43-77)
interactions with plasma, ion cyclotron frequency excitation from, 20: 40174(R) (ORNL-3989, pp 43-77)
interactions with magnetoplasma, ion acceleration from, (T), 20: 40269
interactions with rotating magnetic fields, intensification properties of, 20: 40282
production in pulsed discharges, space charge effects on, 20: 40253
radiation protection practices for accelerators, 20: 39160
reactions with metals, physical aspects of penetrations from, 20: 40347
stability of nonhomogeneous periodic, (T), 20: 40245
uses in metallography of aluminum–Zircaloy-2–zirconia phases, 20: 39380 (AECL-2570)
ELECTRON CAPTURE
by low- and medium-Z nuclei, M/L ratios for, 20: 40153
ELECTRON MICROSCOPES
modification for use with radioactive materials, 20: 39038
resolution of, methods for high, 20: 39470(R) (ORNL-3924)
ELECTRON MICROSCOPY
of irradiated beryllia, 20: 39450 (CEA-R-2963)
ELECTRON PAIRS
photoproduction of, high-energy, 20: 39594(T)
ELECTRON SHOWERS
properties of, effect of polarization of medium on, (T), 20: 39829
ELECTRON SOURCES
design of high-current electron gun, for linear accelerators, 20: 39490(R) (EGG-1183-2051)
incorporation in thermionic fuel elements, 20: 39353 (BMWF-FBK-66-07)
ELECTRONIC EQUIPMENT
description of, for data analysis system, 20: 39025 (ORO-2980-12)
design for measurement of weak currents, 20: 39169 (ISS-66/17)
design of transistorized, for decatron counting system state registration, 20: 39178
development of nuclear, review of, 20: 39238
performance of chamber for irradiated high-ohmic material conductivity measurements, 20: 39179
ELECTRONS
capture by fast protons from hydrogen atoms, cross sections for, (T), 20: 39606
density and temperature profiles in magnetosphere, 20: 39978
density distribution in infinite anisotropic plasma, 20: 40184
density distribution in equatorial ionosphere at Huancayo, Peru, 20: 39975
density distribution in ionospheric D region, l-f and v-l-f reflection for determining, 20: 39995
density in F2 layer, season and solar activity effects on, 20: 39959(T)
density in ionosphere, solar and geomagnetic effects on, 20: 39958(T)
density in ionospheric topside F layer, steep horizontal, 20: 39974
density in solar wind-magnetosphere region, 20: 39978
effects on coloring in blue cellophane films, 20: 38941(R) (RRL-2310-182)
effects on enzyme release from rat liver lysosomes, 20: 38577
effects on fast photographic film at 24 to 500 kev, blackening, (E), 20: 39216
effects on indium antimonide, stage-II recovery of, 20: 40328
effects on liquids and gases at dose rates to 10^7 rad/sec, 20: 38947
effects on methane, production of acetylene in, 20: 38951
effects on mouse skin, biological, 20: 38627
effects on oxygen-doped silicon at 2 Mev, (E), 20: 40302
effects on polypropene, ESR spectral studies on, 20: 38954
effects on production of induced radioactivity in food, methods for predicting, 20: 39165
effects on semiconductor compounds of fast, (E), 20: 40332
effects on silicon at 1 Mev, (E), 20: 39458 (NP-16225)
effects on sulfur fluorides in presence of phosphorus fluorides, ESR spectra of products of, 20: 38941(R) (RRL-2310-182)
effects on wholesomeness of food at 10 Mev, 20: 39302
effects on yields of hydrogen peroxide from sulfuric acid solutions of potassium bromide, 20: 38952
electric dipole moment of, 20: 39598
emission from alloys containing dissolved hafnium and zirconium, 20: 40297
emission from metals with adsorbed monolayers, models for, 20: 39641
emission from planar monocrystalline tungsten, work function for thermionic, 20: 39635 (UCRL-16699)
emission from thermionic emitters, surface micropatch effects on, 20: 39642
energy distribution and flux in lower edge of inner radiation belt, 20: 39983
energy levels in polyatomic molecules, multiple-scattering model for, (T), 20: 39618
energy loss in ionospheric D region, (T), 20: 39994
flow of free, from thermoionized gases in electric fields, 20: 40238
flux in geomagnetic tail of 40-kev, 20: 39986
flux in inner Van Allen Belt on Dec. 19, 1961, (E), 20: 39992
flux of geomagnetically trapped, diagnostic effects of, 20: 39976
gamma scattering by bound K, differential cross sections for Compton, (T), 20: 39773
gases of, energy exchange between nitrogen and, 20: 39677
intensity in radiation belts, 20: 39957(T)
interactions in metals, effects on lattice vibrations, (T), 20: 40344
interactions of system of, quantum theory of electric conductivity for, 20: 39873

interactions of, cross section for two-photon emission in, (T), 20: 39836
interactions with gamma flux from nuclear explosions, 20: 39775
interactions with positrons, cross sections for meson production in, (T), 20: 39802
interactions with electrons, cross sections for, (T), 20: 39818
interactions with atoms, electron exchange in, 20: 39582(T) (AERE-Trans-1053)
interactions with neutrons from thermal neutron scattering by rare gases, (E), 20: 40129
kinetics of electron-phonon gas, (T), 20: 40313
momentum measurements using spark chambers in magnetic fields, precision of, 20: 39207 (ISS-66/18)
motion in r-f mirror fields, (T), 20: 40266
production in ionosphere, height dependence of cosmic ray-induced, (T), 20: 39625
reactions with atoms, ionization cross sections for, (T), 20: 39607
scattering by atoms, total cross sections for, (T), 20: 39818
scattering by carbon, mass-scattering cross sections for, 20: 39588
scattering by deuterium, deuteron and neutron electromagnetic form factors from, (E), 20: 39795
scattering by helium, phase shifts and cross sections for, 20: 39621
scattering by hydrogen, excitation cross sections for, (E), 20: 39608
scattering by hydrogen, ionization cross sections for, (T), 20: 39612
scattering by hydrogen, excitation cross sections for elastic, (T), 20: 39610
scattering by infinite slab, motion from, (T), 20: 39775
scattering by iodine monochloride, (E/T), 20: 39622
scattering by metals, effects of nonmagnetic impurities on, 20: 39395 (IAE-1028)
scattering by nuclei at 1 to 10 Mev, partial wave analysis of inelastic, (T), 20: 40150
scattering on helium at large angles and low energies, (E), 20: 39591
synchrotron radiation from, at 4.0 to 6.3 Bev(E), 20: 39473
temperature in completely ionized plasma, boundary-layer equations for, (T), 20: 39721
temperature in ionospheric D region, (T), 20: 39994
theory of, Dirac's relativistic quantum, 20: 39816
transport properties in magnetic field, (T), 20: 40183
trapping in irradiated polyethylene terephthalate films, 20: 39467

ELECTROSTATIC FIELDS
plasma structure and, in vicinity of charged cylinders, (T), 20: 40197(T)

ELECTROSTATIC GENERATORS
development of insulating medium for, 20: 39472

ELECTROSTATIC PRECIPITATORS
design of, for sol dispersion, 20: 38998(R) (ORNL-3958)

ELECTROSTATICS
beam emission from arbitrary surfaces, equations for, 20: 40242
developments in, 20: 39472

ELEMENT ONE HUNDRED AND FOUR
chemical properties, 20: 38913
production of, from neon-22 reactions with plutonium-242, 20: 40143

ELEMENTARY PARTICLES
angular momenta of, SU(1,1) and SU(2) groups for complex, 20: 39863
classification of, algebra of SU(3) × SU(3) for, (T), 20: 39903
conservation laws for, 20: 39921
existence of, theoretical prediction of, 20: 39920
field theory for, kinks in, 20: 39869
field theory for, very singular N/D equations solutions for nonrenormalizable, 20: 39870
interactions at cosmic-ray energies, particle creation in, 20: 39745 (CERN-66-22)
interactions at high energies, algebra of vertex strengths in Regge residues for predictions in, 20: 39881
interactions in local field theory, symmetry properties of, 20: 39891
interactions of two- and three-body systems of, reduced-amplitude equations for, 20: 39874
interactions of, Adler-Weisberger sum rules for strong, (T), 20: 39857 (JINR-E-2876)
interactions of, Adler-Weisberger sum rules for, 20: 39883
interactions of, asymptotic behavior of inelasticity parameter for strong, 20: 39894
interactions of, analytical properties of amplitudes for relativistic multichannel, 20: 39911
interactions of, Bethe–Salpeter equations for three-body, 20: 39901
interactions of, consistent relativization of SU(6) symmetry for, (T), 20: 39856 (JINR-E-2826)
interactions of, current algebras and axial-vector current matrix elements for, 20: 39892
interactions of, chiral U(6) ⊗ U(6) algebra of current densities for, 20: 39896
interactions of, lectures on weak, (T), 20: 39764 (NP-16232)
interactions of, means for testing $\Delta T = 0$ or 1 rule in electromagnetic, 20: 39824
interactions of, multichannel N/D equation approximate solution for S-wave bound states in, 20: 39880
interactions of, methods in current algebra for, 20: 39882
interactions of, many-body Bethe-Salpeter equations for, 20: 39900
interactions of, SU(6) symmetry theory for weak, 20: 39908
interactions of, weak, electromagnetic, and strong, 20: 39919
kinetics of, probabilities for many-body processes in, 20: 39926
magnetic moments in quark model, axial and vector constants of, 20: 39753 (JINR-E-2827)
mass formula and tensor operations in minimal extension of U(3), 20: 39916
mass formulas for spin 1 and ⅜, in broken SU(3) symmetry, 20: 39910
mass operators for, coefficients for SU(3) and SU(6), 20: 39855 (JINR-E-2771)
photoproduction of, sum rules from equal-time commutators for amplitudes of, 20: 39879
production of quarks, in cosmic radiation, 20: 39631(T)
properties of, 20: 39918
properties of composite, in separable-potential models, 20: 39889
quark model of, configuration mixing in, (T), 20: 39861 (JINR-P-2821)
Regge pole parameters for, dynamical calculation of, 20: 39924
research on, instrumentation for, 20: 39241
symmetries for, weak currents in broken relativistic supermultiplet, 20: 39877
symmetries of, coupled-channel solubie model for internal, 20: 39902
symmetry for, irreducible unitary representations of Poincare group, 20: 39865
symmetry for, lectures on SU(3), 20: 39862 (NP-16242)
symmetry for, multilinear invariant forms from arbitrary number of unitary representations of SL(n,C), 20: 39878
symmetry for, relativistically invariant model of SU(6), 20: 39875
symmetry for, unitary representations of Poincare group, 20: 39864
symmetry for, unitary irreducible representations of SL(3,R), 20: 39871
symmetry group U(6,6) for, relativistic, 20: 39888
symmetry groups for, degenerate representations of Sp(n), 20: 39850 (IC-66/77)
symmetry groups for, theory of Clebsch-Gordon coefficients for SU_n, 20: 39913
symmetry groups for, noncompact, 20: 39915
symmetry transformations in canonically quantized field theory for, operators for, 20: 39876
theory for, Chakrabarti transformation in, 20: 39872
theory of, elementary guide to, 20: 39768 (UCRL-11100(Rev.1))
theory of, lectures on problems in, 20: 39917

ELEMENTS
absorption and elution of trace elements from human hair, 20: 38543

ELK RIVER POWER REACTOR
fuel elements, design for, 20: 40425

EMBRYOS
radiosensitivity of plant, γ, uv, and x, 20: 38588(R) (COO-1400-10)

ENDOCRINE GLANDS
phosphorus metabolism in rat, effects of reticulin on, tracer study, 20: 38572
radiation effects on, in animals, 20: 38653
radiation effects on regulatory function of rabbit, x, 20: 38654

ENGINEERING
research in progress under Army Research Office, 20: 40485(R) (AD-636091)

ENGINEERING TEST REACTOR
fuel element channel thickness, measurement of spent, 20: 40460(R) (IDO-17191)

ENGINES
performance of ion, for satellite attitude control, 20: 39092
performance testing of ion, for space missions, 20: 39093

ENVIRONMENT
radioactivity from reactors after instantaneous release of radioisotopes to, computer code for calculation of, 20: 39148 (GA-6511)

ENZYMES
effects of mutations on bacteriophage, 20: 38542(T) (UCRL-Trans-10029)
effects of photoreactivating, on recovery of uv-irradiated *E. coli*, 20: 38669
genetic control of *E. coli*, 20: 38620
radiation effects on RNA polymerase system, uv, 20: 38574(R) (NYO-3449-1)
radiation effects on DNase in guinea pig skin, beta, 20: 38591(R) (NYO-3445-7)
radiation effects on release from rat liver lysosomes of, mechanisms for electron beam and x, 20: 38577
radiation effects on activity of lactic dehydrogenase in mouse thymus, x, 20: 38606
radiosensitivity effects on *E. coli*, 20: 38621

EPIDEMIOLOGY
leukemia in children, 20: 38668
EQUIPMENT AND PROCEDURES
description of, for earth removal, 20: 40422
design of electrical, for ANL fast breeder reactors, 20: 40414 (TID-23257(Vol.2))
design of mechanical, for ANL fast breeder reactors, 20: 40414 (TID-23257(Vol.2))
guide for cleaning and assembly, 20: 40489 (SC-DC-66-1118)
ERBIUM
determination in fluorite monocrystals, spectrophotometric, 20: 38829
determination in solutions, spark method for spectrographic, 20: 38832
magnetic fields at tin-119 in, deduction from gamma hyperfine splitting, 20: 40322
neutron reactions (n,γ), yields from, 20: 39316 (DP-1066(Vol.1), pp II.3-14)
shock compression of, 20: 39425(T)
ERBIUM ALLOYS
Al–Er, magnetic properties of intermetallic compounds of, 20: 39433
Er–Pb–Zn, component distribution in recrystallized, 20: 39435
Er–Zn, crystal structure of intermetallic compound Er_2Zn_{17} in, 20: 39417
ERBIUM CHLORIDES
specific gravity and apparent molal volume of aqueous solutions of, at 25°C, 20: 38905
thermal capacity of aqueous solutions of, at 25°C, 20: 38906
viscosity of aqueous solutions of, at 25°C, 20: 38904
CsCl–$ErCl_3$, phase studies, 20: 38919
ERBIUM IONS
spin-lattice relaxation time in lanthanum trichloride, angular and temperature effects on, 20: 40350
ERBIUM NITRATES
specific gravity and apparent molal volume of aqueous solutions of, at 25°C, 20: 38905
ERBIUM OXIDES
actinide oxides–Er_2O_3, preparation of sols of, 20: 39341(P)
ERBIUM PHOSPHATES
preparation and properties of, conductometric and potentiometric studies on, 20: 38883
ERYTHROCYTES
analysis for ATP and 2,3-diphosphoglyceric acid using oxygen-18, proton activation, 20: 38841
analysis for copper, magnesium, manganese, and zinc in human, activation, 20: 38852
levels of, in irradiated rats, 20: 38619
radiation effects on hematocrit of rat, γ, 20: 38587 (CEA-R-2909)
radiation effects on agglutination of human, β and γ, 20: 38623
ERYTHROPOIESIS
changes in, in x-irradiated thioacetamide damaged rat liver, 20: 38694
effects of anoxia, erythropoietin, polycythemia, and transfused erythrocytes on erythroid clone formation by transplanted bone marrow in rat spleen, 20: 38708(R) (IAEA-3173-5)
effects of bone marrow transplants on mouse, 20: 38592 (ORNL-P-2158)
radiation effects on formation of erythroid clones from transplanted bone marrow in mouse spleen, 20: 38708(R) (IAEA-3173-5)
radiation effects on response to erythropoietin of rat, γ, 20: 38673
ERYTHROPOIETIN
radiation effects on erythropoietic response of rats to, 20: 38673
ESCHERICHIA COLI
effects of absence of an essential amino acid on synthesis of nucleic acids and proteins following uv irradiation, 20: 38562
radiation effects on DNA in, repair mechanisms for, 20: 38575 (ORNL-P-2267)
radiation effects on, survival difference in presence of chloramphenicol and in absence of the essential metabolite, uv, 20: 38563
radiation effects on DNA repair synthesis on uv, 20: 38621
radiation effects on, lethal, β and x, 20: 38630
radiation effects on growth in mouth of dogs and monkeys, 20: 38667
radioinduced mutants of, action spectra for photoreactivation of uv, 20: 38669
radiosensitivity of mutations of, uv, 20: 38620
separation of transfer-RNA from, engineering method for, 20: 38998(R) (ORNL-3958)
ESTERASES
radiation effects on content in rat blood, x, 20: 38682
ESTR-4-EN-3-ONE, 17β-HYDROXY-, PHENYLPROPIONATE
effects on radiation and shock effects on survival of mice, 20: 38610
ETHANE, 1,1,2,2-TETRACHLORO-1,2-DIFLUORO-
use as tracer for nondestructive leak test for airborne activity confinement filters, 20: 39018 (DP-MS-66-46)
1,2-ETHANEDIOL, TETRAPHENYL-, CYCLIC CARBONATE
radiolysis of, γ, 20: 38940 (NYO-3410-2)
ETHANETHIOL, 2-AMINO-
effects on organic peroxy compound synthesis in x irradiated mice, 20: 38660
effects on rabbit liver, cytological, 20: 38716
radioprotective effects on bacteriophage, 20: 38628
radioisensitivity effects on *E. coli*, 20: 38630
radiosensitivity effects on iodouracil-substituted T1 bacteriophage, 20: 38704
radiosensitivity effects on rabbits, 20: 38716
radiosensitivity effects on mice, 20: 38717
ETHANOL
effects on annealing of recoil damage in neutron-irradiated cobalt complexes, 20: 38965
evaporation into carbon dioxide and oxygen, 20: 39050 (UCRL-16535)
neutron inelastic scattering by, dynamic processes in slow, 20: 40338
radiosensitivity effects on iodouracil-substituted T1 bacteriophage, 20: 38704
CO_2–ethanol–O, man transfer of, in channel flow, 20: 39050 (UCRL-16535)
ETHANOL, 2-AMINO-
carbon-13 exchange between isopropanol or isopropanol–methanol and, 20: 39320(R) (MLM-1311)
ETHANOL, MERCAPTO-
radiosensitivity effects on iodouracil-substituted T1 bacteriophage, 20: 38704
ETHERS
evaporation into carbon dioxide, 20: 39050 (UCRL-16535)
ETHYL ACETATE
viscosity of, use of oscillating sphere device for measuring, 20: 38872(R) (NYO-1769-68)
ETHYL ETHER
CO_2–ethyl ether–helium, man transfer in channel flow, 20: 39050 (UCRL-16535)
ETHYL RADICALS
spectra of carbon-13-labeled, ESR, 20: 38941(R) (RRL-2310-182)
ETHYLAMINE, 2,2'-DITHIOBIS-
effects as radioprotective agent in rats, mechanism of, 20: 38723
effects as radioprotective agent in mice and rats, 20: 38725
effects as radioprotective agent in mice and rats, 20: 38726
effects on mice, pharmacological, 20: 38713
effects with phenatine as radioprotective agent in mice and rats, 20: 38726
radiosensitivity effects on rat thymus, 20: 38720
ETHYLENE
effects of deuterated, on photosensitized decomposition of deuterated and normal cyclobutane, 20: 38941(R) (RRL-2310-182)
hydrogenation of, over palladium hydride, effects of deuterium on kinetics of, 20: 38908
radiolysis of solutions of, effects of argon on yields in gamma, 20: 38941(R) (RRL-2310-182)
ETHYLENE, CHLOROTRIFLUORO-
radioinduced polymerization of, kinetics of, 20: 38946
ETHYLENE, DIFLUORO-
radioinduced polymerization of, kinetics of, 20: 38946
ETHYLENE, DIPHENYL-
production from elimination reaction of 2,2-diphenylethyl benzenesulfonate, effects of deuterium and tritium on, 20: 38912
ETHYLENE, FLUORO-
radioinduced polymerization of, kinetics of, 20: 38946
ETHYLENE GLYCOL
production in radioinduced oxidation of methanol, effects of dose rate on, 20: 38942 (UJV-1457)
ETHYLENE OXIDE POLYMERS
properties of cross-linked, 20: 38976(P)
radioinduced cross-linking of, process for, 20: 38976(P)
ETHYLENE POLYMERS
radiation dosimetry of films of, by activation analysis, 20: 38937 (AD-635655)
ETHYLENE, TETRAFLUORO-
radioinduced polymerization, 20: 38980(P)
radioinduced polymerization of, kinetics of, 20: 38946
yields in radiolysis of propene, competitive electron capture between nitrous oxide and, 20: 38941(R) (RRL-2310-182)
ETHYLENE, TRIFLUORO-
radioinduced polymerization of, kinetics of, 20: 38946
EUROPIUM
determination in magnesium alloys by successive potentiometric titration, 20: 38830
determination in rare earths using acetonitrile, controlled-potential coulometric, 20: 38812
determination in solutions, spark method for spectrographic, 20: 38832
reduction in acetonitrile solutions, color production in controlled-potential coulometric, 20: 38813

separation of thorium-230 from, by ion exchange, 20: 38834
separation of, from other rare earths, by lactate elution from cation resin columns, 20: 39004
x-ray-diffraction patterns of, effects of cold working on, 20: 39421

EUROPIUM ALLOYS
Eu–Ni, crystal structure of intermetallic compounds in, 20: 39415
Eu–Pb–Zn, component distribution in recrystallized, 20: 39435
Eu–Zn, crystal structure in intermetallic compound $EuZn_{13}$ in, 20: 39417

EUROPIUM HYDROXIDES
thermal decomposition, 20: 38923

EUROPIUM ISOTOPES
conversion electron spectra of, spectrometer for measuring, 20: 39203 (INP-476/PL)

EUROPIUM ISOTOPES Eu-152
decay, (E), 20: 40110

EUROPIUM ISOTOPES Eu-153
energy levels of, M1 transitions of rotational, (E), 20: 40072 (LA-DC-8061)

EUROPIUM ISOTOPES Eu-155
decay, (E), 20: 40110

EUROPIUM ISOTOPES Eu-156
decay, (E), 20: 40110

EUROPIUM OXIDES
ferromagnetism in, origin of, (T), 20: 40318
luminescence of, emission and excitation spectra studies of, (E), 20: 40315
actinide oxides–Eu_2O_3, preparation of sols of, 20: 39341(P)
Eu_2O_3–UO_2, phase diagrams, 20: 39437

EUROPIUM SELENIDES
crystal structure of, reflection spectra for zonal, (E), 20: 40339
ferromagnetism in, origin of, (T), 20: 40318

EUROPIUM SULFIDES
ferromagnetism in, origin of, (T), 20: 40318
magnetic resonance in, ferro- and para-, 20: 40348

EVAPORATORS
design and performance of electron bombardment, 20: 39180
design of finned, for concentrating liquid waste, 20: 40477 (HW-80056)
performance of wiped-film, for Purex waste solutions, 20: 40476(R) (BNWL-267)

EXCRETORY SYSTEMS
radiation dose to ureter during γ implant therapy, measurement of, 20: 38778

EXHAUST SYSTEMS
filter nondestructive leak test in, use of Freon-112 tracers for, 20: 39018 (DP-MS-66-46)

EXOSPHERE
ion density distribution in iono-, (T), 20: 39968

EXPLODING WIRE PHENOMENA
magnetohydrodynamic instabilities in, 20: 39010

EXPLOSIVES
shock-wave compression measurements on chlorine trifluoride–aluminum mixture, (E), 20: 39469 (LA-3453)
testing of, radiographic methods for nondestructive, 20: 39334
use in MHD generators, curved duct effects on, (E), 20: 39694

EXPONENTIAL PILES
neutron diffusion in plane heterogeneous systems, time-dependent equations for, 20: 40059
safety analysis of Nuclear Test Gauge, 20: 40459 (GEMP-152)

EXTRUSION
equipment and methods for tungsten sintered billets, 20: 39352 (BM-RI-6817)

EYES
radiation effects on immune reactions in rabbit, x, 20: 38608
radiation effects on rabbit retina, pathological, x, 20: 38689
radioinduction of conjunctivitis in rabbit, x, 20: 38689

F

FALLOUT
alpha activity of, from USSR and Chinese nuclear tests, 1962, 1964, and 1965, 20: 39109
analysis for iodine-129, activation, 20: 38564
analysis of, from Chinese test of Oct. 1964, 20: 39110
chemical and physical properties of particles of, 20: 39115
contamination of milk by, 20: 39157
content in rainfall, 20: 39113
content in soil in Japan, effects of soil particle size on, 20: 39112
deposition and transport in river-estuary systems, 20: 39121
dose rate measurement system for, development of solid-state, 20: 39192 (AD-636206)
effects on electric conductivity of lower atmosphere, 20: 39111
monitoring guides for cesium-137, iodine-131, strontium-89, and strontium-90, 20: 38743
monitoring in Japan, 1965, 20: 39108
monitoring in Japan, 1962, 20: 39109
monitoring in Japan, 1962 and 1964, 20: 39110
monitoring in Japan, 1961 to 1963, 20: 39111
monitoring in Netherlands, 1963, 20: 39118
particle size of, from Chinese nuclear test, May 1965, 20: 39108
probability of a given integrated radiation dose from, at Canadian hospitals, computer derived, 20: 39162
protection against, by core shelters in typical British house, 20: 39083
rainout from nuclear device clouds, mathematical analysis, 20: 39107 (UCRL-14700)
sampling in ocean water, method for cesium, 20: 39147 (CONF-660401-6)

FAST REACTORS
coolant loss in, dynamic analysis of, 20: 40363
design of electric generators for use with, 20: 40414 (TID-23257(Vol.2))
development of breeder, at ANL, 20: 40413 (TID-23257(Vol.1))
development of, by Atomic Power Development Associates, 20: 40355 (APDA-TPI-1)
economics of, for power production, 20: 40415 (TID-23257(Vol.3))
engineering problems in pulsed, 20: 40455 (BNL-10454)

FATIGUE
of carbon steel–stainless steel weldments, 20: 39404 (SWRI-1228-4-20)
of 2011-T3 aluminum alloy, equations for, 20: 39396 (IS-T-60)

FATTY ACIDS
determination in blood, micro method, 20: 38652
metabolism in rat liver, effects of tritium oxide perfusion on, 20: 38559
radiation effects on content of, in rat tissues, x, 20: 38701

FERMI FAST BREEDER REACTOR
development of, by Atomic Power Development Associates, 20: 40355 (APDA-TPI-1)

FERMIONS
interactions of, indefinite metric in Hilbert space for four-body, 20: 39912
interactions of, lepton masses from four-body, (T), 20: 39832
wave functions for impenetrable one-dimensional, in thermal equilibrium, 20: 39474

FERMIUM ISOTOPES Fm-256
production of, from neon-22 reactions with uranium-238, 20: 40142

FERRATES
determination of, polarographic, 20: 38859 (CEA-R-2895)

FERRITES
analysis for dysprosium, activation, 20: 38833

FERROMAGNETIC MATERIALS
neutron scattering by, properties from critical magnetic, 20: 40316
phase transitions in manganese–nickel, neutron diffraction studies on, 20: 39407(T) (ANL-Trans-344)

FETUSES
radiation sickness induced in dog, rabbit, and rat, by exposure during intrauterine development, 20: 38665
radiotherapy technique to safeguard, during use for cervical carcinoma during pregnancy, 20: 38759

FIELD THEORY
Bethe-Salpeter equations in, solutions to many-body, 20: 39900
Bethe–Salpeter equations in, solutions to three-particle, 20: 39901
elementary particle interactions in local, symmetry properties of, 20: 39891
equations for quantum, using indefinite metric in Hilbert space, 20: 39912
field interactions in, refined solution of two-dimensional model theories for, 20: 39851 (IC-66/96)
formulation of quantum, problems in, 20: 39922
Green's function for scalar and spinor fields, calculation of, 20: 39859 (JINR-P-2761)
properties of free massless spin-½ fields in, 20: 39890
quantization of spin-2 fields in, 20: 39884
Regge pole parameters in, dynamical calculation of, 20: 39924
Regge trajectory in conventional, vacuum, 20: 39925
spinor fields in, commutators of covariant bilinear forms of quantized, 20: 39906
Wick polynomials at fixed time in, 20: 40004

FILMS
formation of silicon dioxide, by oxygen ion bombardment of silicon, 20: 40314
production of small cross-section, use of alpha sources in, 20: 39298

FILTERS
design for photographic film detectors, 20: 39251(P)
design of linear pulse height analyzer, for measurements in presence of noise, 20: 39195 (AE-235)
testing for airborne activity confinement, use of Freon-112 tracers for nondestructive leak, 20: 39018 (DP-MS-66-46)
use of high-flow-rate, for water decontamination, 20: 40484

FINNED TUBES

design for liquid waste evaporator, 20: 40477 (HW-80056)
design with herringbone pattern, longitudinal ribs, and lugs for reactor fuel elements, 20: 40396(P)

FIRES
effects in internal environment of shelters, 20: 39059
effects of, protection of populations from, 20: 39057

FISH
radiation effects on salmon eggs, biological, chronic γ, 20: 38698
radiation effects on, natural β, 20: 38741
radiation effects on conditioned reflex in, γ, 20: 38655
radioactivity in, from nuclear plant wastes, 20: 38742

FISSION
detection at high temperatures, use of mica and quartz glass for, 20: 39208 (JINR-P-2705)
effects on failure of stainless steel–urania cermets, 20: 39459 (TRG-Report-1278)

FISSION CHAMBERS
design of parallel-plate, engineering drawings for, 20: 39256
design of parallel-plate, for capture-to-fission ratio measurements, 20: 39263

FISSION FRAGMENTS
detection and measurement of, instrumentation and semiconductor detectors for, 20: 39242
effects on solid-solid phase transformations, (E), 20: 40306
effects on uranium atom emission from uranium dioxide and metal, 20: 38994(R) (AE-232)
x-ray emission by, from plutonium-239 and uranium-235 fission, 20: 40158

FISSION PRODUCTS
activities in irradiated natural uranium, computer program for calculation of, 20: 40070 (IEA-111)
analysis for sulfur in solid wastes of, by combustion and colorimetry, 20: 38795 (BNWL-265)
content in precipitation, effects of meteorological parameters on, 20: 39106 (BMwF-FBK-65-05)
diffusion from irradiated urania fuels, mechanisms of, 20: 39449 (BNWL-SA-272)
diffusion from sodium at high temperatures, factors affecting, 20: 40357 (NAA-SR-11766)
distribution in fuel particle coatings, 20: 40386 (SGAE-CH-33/1966)
production in power reactors, calculation of, 20: 40400 (BNWL-244)
release from simulated high-level wastes, 20: 40476(R) (BNWL-267)
separation from alumina calcine by leaching, 20: 40478 (IN-1011)
separation from waste solutions using mixed iron oxide–manganese oxide scavenger, 20: 40476(R) (BNWL-267)
separation of molybdenum from, by extraction into acetylacetone, 20: 38824
separation of uranium from, combined ion exchange-solvent extraction method for, 20: 38999 (TID-23229)
separation of uranium from, freezing method for, 20: 38994(R) (AE-232)
separation of, in Europe, 20: 39276 (DP-1066(Vol.1), pp III.45-50)

FISSIONABLE MATERIAL
analysis of future needs for power production, 20: 40420
criticality of, computer program for, 20: 40375 (DP-1031)

FLAMES
thermal radiation flux from potassium-seeded, (E), 20: 39710

FLOWMETERS
design for metering radioactive gases or solutions, 20: 39172

FLUID FLOW
analysis of, in peripheral compressors, 20: 39021 (K-1665)
characteristics of, on circular wall, 20: 39019(R) (GEAP-5149)
equations of MHD, past semi-infinite plate, (T), 20: 39945
hydrodynamic instabilities in heated channels, model for, 20: 40403 (EURAEC-1464)
hydrodynamics of waste transport in soils, 20: 39099(R) (BNWL-235-3, pp 1-23)
instabilities in boiling systems, compressibility effects on, 20: 40427
investigation of, methods of, 20: 39051
magnetohydrodynamic, natural and forced thermal convective, (T), 20: 39930
magnetohydrodynamic, theorems for highly conducting, 20: 39932
magnetohydrodynamic, boundary layer at insulator walls in, (T), 20: 39933
magnetohydrodynamic jet, temperature effects on, 20: 39934
magnetohydrodynamic, stability in parallel magnetic fields of, (T), 20: 39943
magnetohydrodynamic, with changing electric conductivity, (T), 20: 39676
magnetohydrodynamic, development in Hall-type MHD generators, 20: 39685
magnetohydrodynamic, in Hall-type generators, field effects on, (T), 20: 39692
magnetohydrodynamic, instability and turbulence effects on inhomogeneous, (E), 20: 39704
magnetohydrodynamic, in rectangular duct, (E), 20: 39706
magnetohydrodynamic, electron density in, (T), 20: 39714
magnetohydrodynamic, models for MHD generators, (T), 20: 39729
pressure-drop characteristics of subcooled water at atmospheric pressure in narrow heat channels, 20: 39047 (AERE-M-1739)
stability in BWR coolant channels, 20: 40356 (EURAEC-1644)
tracer techniques for, 20: 39290
two-phase, review of developments in, 20: 39941
two-phase, voidage distribution measurement using isokinetic probe, 20: 39045 (AEEW-M-650)

FLUID FLOW (LAMINAR)
convective transfer processes in two-phase, 20: 39050 (UCRL-16536)
magnetohydrodynamic, electric discharge of viscous incompressible, (T), 20: 40241
magnetohydrodynamic incompressible, in annular channel, (T), 20: 39942
mass transfer in two-phase, between parallel walls, 20: 39050 (UCRL-16535)

FLUID FLOW (TURBULENT)
effects on heat transfer in parallel rod arrays, 20: 39048 (GEAP-5115)

FLUIDS
analysis of flowing, by x-ray absorption, 20: 39191(P)
gravitational collapse of cylinders of incoherent, exterior metrics in general relativity for, 20: 40001
kinetics of dense, calculations using self-correlation function, (T), 20: 39946
thermal convection in conducting, magnetic effects on, 20: 39939

FLUORESCEIN, DIIODO-
preparation of iodine-131-labeled, 20: 38985

FLUORIDE VOLATILITY PROCESSES
development of, for reprocessing uranium fuels, 20: 40389

FLUORINATION
equipment design for, 20: 38835

FLUORINE
determination in metals, activation, 20: 38840

FLUORINE ISOTOPES F-19
deformation of, octupole, (T), 20: 40121
deuteron reactions (d,n) with, neon-20 energy levels from, (E), 20: 40164
neutron reactions (n,α) at 6 Mev, cross sections for, (E), 20: 40100
neutron scattering at 14.2 Mev, cross sections for, (E), 20: 40069(R) (EANDC(E)-66(U))

FOILS
charged-particle energy losses in thin, (T), 20: 40117
production of small cross-section, use of alpha sources in, 20: 39298
thickness gage for, radiometric, 20: 39292

FOLIC ACID
effects on radiation resistance in rats, dietary, 20: 38721

FOOD
comparison of MPC for nuclides and induced radioactivity for single elements in, 20: 39165
effects of irradiated, on Drosophila, genetic, 20: 38596(R) (SAN-590-1)
radiation processing in Canada, 20: 39282 (DP-1066(Vol.1), pp III.3-32)
radiation processing of, review of, 20: 39284 (DP-1066(Vol.1), pp IV.3-25)
radiation processing of fruits and vegetables, 20: 39289 (UCD-34P73-9)
radioactivity induced in, methods for predicting, 20: 39165
radioactivity monitoring in Netherlands, 1963, 20: 39118
radiopreservation of, history of, 20: 39297
radiosterilization effects on wholesomeness of, 20: 39302
radiosterilization of, machine sources for, 20: 39303

FORENSIC SCIENCE
identification of hair samples by trace element content, 20: 38543

FORESTS
radiation effects on ecology of deciduous, γ and neutron, 20: 38594(R) (ORO-2066-10)
radiation effects on lizard population in Puerto Rican, γ, 20: 38601 (UCLA-12-567)

FORMALDEHYDE
production in radioinduced oxidation of methanol, effects of dose rate on, 20: 38942 (UJV-1457)

FORMATES
radioinduced carboxylation of, alpha, 20: 38966

FORMIC ACID
production in radioinduced oxidation of methanol, effects of dose rate on, 20: 38942 (UJV-1457)

FRANCE
nuclear industry in, review of, 20: 39295
nuclear power use in, for electricity production, 20: 40442

FRANCIUM
crystal structure of, valence electrons and interatomic bonds in, 20: 40296
electric dipole moments of, ratio of atomic to electron, 20: 39598

FREE RADICALS

radioinduced in polypropene, ESR spectral studies on, 20: 38954
FREONS
use in measuring leaks in carbon beds, 20: 39017(R) (DP-1053)
FREQUENCY CONVERTERS
design of phase locked frequency multiplier, for phase synchronization system of neutron rotating crystal spectrometer, 20: 39201 (EUR-2999.e)
FRUITS
analysis of irradiated juices of, for volatile constituents, 20: 39300
radiation effects on development of orchid, x, 20: 38597(R) (TID-23057)
radiation effects on juices of, chemical analysis of volatile materials resulting from, 20: 39300
radiation processing of, effects on storage life, 20: 39289 (UCD-34P73-9)
FUELS
combination of hydrogen-containing, at very high temperatures, 20: 39013(P)
FUNGI
radiation effects on spore germination and stability of virulence in *Ustilago avenae*, x, 20: 38672
FURAN
determination in irradiated fruit juices, chromatographic, 20: 39300
FURAN, TETRAHYDRO-
HNO_3–tetrahydrofuran, effects on ion exchange of uranium, 20: 38999 (TID-23229)
FURFURYL ALCOHOLS
thermal decomposition of, for preparation of low-permeability carbon tubes, 20: 39369(P)
FURNACES
design for plutonium fluorination, 20: 38835
design for temperatures of 800–2700°C, 20: 39033
design temperatures approaching 3000°C, 20: 39034
FUSED SALTS
density and viscosity at high pressure and temperature, apparatus and method for measuring, 20: 38871(R) (NYO-1769-54)
spectra of, method for laser excitation of Raman, 20: 38872(R) (NYO-1769-68)
spectra of, use of computer for recording Raman, 20: 38872(R) (NYO-1769-68)
viscosity measurements on, pressure vessel design for high-pressure, 20: 38871(R) (NYO-1769-54)

G

GADOLINIUM
determination in solutions, spark method for spectrographic, 20: 38832
ionization potential of, determination using surface ionization technique, 20: 40203
magnetic field at nuclei of, implanted in iron, 20: 40342
magnetic fields at tin-119 in, deduction from gamma hyperfine splitting, 20: 40322
GADOLINIUM ALLOYS
Al–Gd, magnetic properties of intermetallic compounds of, 20: 39433
Ce–Gd, phase transformations and magnetic ordering in, pressure-induced, 20: 40326
Gd–La, phase transformations and magnetic ordering in, pressure-induced, 20: 40326
Gd–Nd, phase transformations and magnetic ordering in, pressure-induced, 20: 40326
Gd–Pb–Zn, component distribution in recrystallized, 20: 39435
Gd–Y, phase transformations and magnetic ordering in, pressure-induced, 20: 40326
Gd–Zn, crystal structure of intermetallic compounds Gd_6Zn_{23} and $GdZn_{12}$ in, 20: 39417
GADOLINIUM CHLORIDES
heat of dilution of aqueous, at 25°C, 20: 38903
specific gravity and apparent molal volume of aqueous solutions of, at 25°C, 20: 38905
GADOLINIUM COMPLEXES
with dipentyl pentylphosphonate, spectra of, infrared, 20: 38799(R) (NLCO-980)
GADOLINIUM HYDROXIDES
thermal decomposition, 20: 38923
GADOLINIUM IONS
interactions in lanthanum chlorides, effects of, on pair exchange, 20: 38914
GADOLINIUM ISOTOPES
conversion electron spectra of, spectrometer for measuring, 20: 39203 (INP-476/PL)
GADOLINIUM ISOTOPES Gd-155
energy levels at 87 and 105 kev, lifetime of, (E), 20: 40110
GADOLINIUM ISOTOPES Gd-156
energy level at 89 kev, lifetime of, (E), 20: 40110
GADOLINIUM OXIDES
actinide oxides–Gd_2O_3, preparation of sols of, 20: 39341(P)
Al_2O_3–Gd_2O_3, phase studies, 20: 39437
GAGES
design of diameter, 20: 39032
design of radiometric, for aircraft fuel, 20: 39189(P)
survey of radiometric, in West German industry, 20: 39292
GALAXIES
contribution to cosmic muon variation at 440-m depth, 20: 39626
cosmic particle interactions with, secondary electrons from, 20: 29630
GALLIC ACID, PROPYL ESTER
use for prophylaxis and therapy of radiation sickness in mice and rats, 20: 38728
GALLIUM
determination of, simultaneously with germanium in iron meteorites by neutron activation analysis, 20: 38825
superconductivity of, 20: 40047
GALLIUM ALLOYS
radioinduced defects in, fast electron, 20: 40332
Ga–V, effects of orbital field on Fulde-Ferrell state in, 20: 40046
GALLIUM ARSENIDES
radiation effects on short-circuit current of, proton, (E), 20: 40299
sputtering of single-crystal, atom-ejection patterns for, (E), 20: 40305
GALLIUM COMPLEXES
with nitrilotriacetic acid and polyamino polycarbooxylic acids, formation of, biamperometric studies of, 20: 38810
GAMETES
Mendelian segregation of, in maize hybrids, 20: 38617
GAMMA CAMERAS
design of imaging system using digital Anger, for measurement of distributions of positron-emitting radioisotopes, 20: 39181
GAMMA RADIATION
attenuation calculations for, build-up factor effects on, 20: 40289
detection and measurement of, ion chamber detector for, 20: 39249(P)
detection and measurement using semiconductor detector, 20: 38771
detection and measurement of, from potassium-40 in soils, 20: 39280
detection and measurement in ureter during implant therapy, 20: 38778
dosage levels to medical staff from gold-198, 20: 39159
dose distribution measurements in phantoms of, use of lead filters for, 20: 38762
dose distribution in tissue, effects of bone dimensions on, 20: 38791
dosimetry in polyethylene films using activation analysis, 20: 38937 (AD-635655)
dosimetry in sheep, 20: 38625
dosimetry of, performance of thermoluminescent detector for, 20: 39224
dosimetry of, performance of thermoluminescent detector for, 20: 39225
effects of chronic, on salmon eggs, biological, 20: 38698
effects of dose level on nucleic acid synthesis in animals, 20: 38585
effects of, from iodine-131 on binding of antibody to insulin, 20: 38579
effects on alkali hydroxide glass containing alkali benzoate or α-naphthoate, ESR and optical spectral studies on, 20: 38941(R) (RRL-2310-182)
effects on ammonia adsorbed on zeolites, 20: 38944
effects on apple tree roots, genetic, 20: 38692
effects on ascorbic acid content in germinating seeds, 20: 38583
effects on bacterial count, taste, and vitamin content of oysters and shrimp, 20: 39288(R) (ORO-636)
effects on bacteria, biological, effects of acriflavine on, 20: 38611
effects on barley seeds, genetic, effects of centrifugation on, 20: 38618
effects on barley seeds, physiological, 20: 38691
effects on blood constituents and hematopoietic organs of calves, 20: 38706
effects on blood vessels and nervous system of therapeutic doses of, 20: 38773
effects on bone marrow in rats, morphological, 20: 38663
effects on bones and soft tissues in children, pathological, 20: 38787
effects on bromine-82 and chlorine-36 exchange between ethylenediamine cobalt or rhodium complexes and hydrobromic or hydrochloric acids, 20: 38960
effects on buccal flora of dogs and monkeys, 20: 38667
effects on carcinomas, effects of anoxia on, 20: 38635
effects on cellular composition of tissues, therapeutic doses, 20: 38769
effects on chemical and biological properties of vitamin B, 20: 38580
effects on chlorella, genetic, 20: 38605
effects on cobalt complexes, 20: 38962
effects on color center production in alkali halides, (E), 20: 40317
effects on conditioned reflex in fish and rabbits, 20: 38655
effects on decomposition of aluminum hydroxide, lead oxalate, magnesium hydroxide, and nickel oxalate, 20: 38955
effects on dissolution spirals on etched lithium fluorides surfaces, 20: 40293 (AD-634746)

effects on dogs and rats, pathological, 20: 38730
effects on electric conductivity of n-hexane, 20: 38971
effects on eleven amino acids in aqueous solution, 20: 38582
effects on erythropoietic response to erythropoietin in rats, 20: 38673
effects on ethylene carbonate and tetraphenylethylene carbonate, 20: 38940 (NYO-3410-2)
effects on ethylene, effects of argon on yields in, 20: 38941(R) (RRL-2310-182)
effects on fruit flies infesting various fruits and vegetables in Hawaii, 20: 39293
effects on fruit juices, chemical analysis of volatile materials resulting from, 20: 39300
effects on glucosamine and its derivatives in aqueous solutions, 20: 38969
effects on goats, pathological, 20: 38629
effects on grain moths, biological, 20: 38705
effects on heavy water–water mixtures, isotope effects in hydrogen production in, 20: 38938 (IA-1074)
effects on hematocrit values of rats, 20: 38587 (CEA-R-2909)
effects on hematopoietic system of therapeutic doses, 20: 38766
effects on immune reactions in rats, 20: 38695
effects on isomerization of olefins in benzene solutions, 20: 38948
effects on lizard population in Puerto Rican forest, 20: 38601 (UCLA-12-567)
effects on megakaryocytes of bone marrow, γ, 20: 38643
effects on methane, production of acetylene in, 20: 38951
effects on mice and rats, protective effects of chemical agents against, 20: 38726
effects on mice, biological, effects of environmental oxygen on, 20: 38642
effects on mice, genetic, RBE of fast neutrons, 20: 38647
effects on n-hexane–silica gel, ESR spectral studies on yields in, 20: 38994(R) (AE-232)
effects on n-type silicon at 293°K, 20: 40303
effects on n-type germanium, infrared quenching of, 20: 40337(T)
effects on nitrate ices, 20: 38950
effects on oxidation of methanol, products of, 20: 38942 (UJV-1457)
effects on photoconductivity of n-type germanium, (E), 20: 40298
effects on physiology of fruits and vegetables, 20: 39289 (UCD-34P73-9)
effects on plant embryos, biological, 20: 38588(R) (COO-1400-10)
effects on plants, genetic, 20: 38589(R) (EUR-2761.f)
effects on polymerization of cyclic ethers, 20: 38953
effects on polypropene, ESR spectral studies on, 20: 38954
effects on production of induced radioactivity in food, methods for predicting, 20: 39165
effects on rats, dietary effects of B group vitamins, folic acid, and phosphatide on, 20: 38721
effects on rats, hematological, 20: 38711
effects on refractive index of optical glasses, 20: 39468
effects on reproduction of eye gnats, 20: 38632
effects on ribonucleic acid metabolism in cultured HeLa cells, 20: 38683
effects on seeds of deciduous trees, RBE neutrons, 20: 38594(R) (ORO-2066-10)
effects on skin, delayed, carcinogenic, 20: 38788
effects on sperms of silkworm, genetic, RBE to fast neutron, 20: 38626
effects on structural changes in polypropene, mechanism of, 20: 38945
effects on thermoluminescence of lithium fluorides, quality of, 20: 39199 (COO-1105-117)
effects on thermoluminescence of lithium fluoride, temperature effects on, 20: 39200 (COO-1105-118)
effects on water, free radical model for, 20: 38959
effects on wholesomeness of food, 20: 39302
effects on yields of hydrogen peroxide from sulfuric acid solutions of potassium bromide, 20: 38952
effects on 5-bromouracil, under nitrogen, nitrous oxide, and oxygen, kinetic study of, 20: 38968
exposure field from point isotropic sources of, at surface of thick concrete slab, (T), 20: 40284 (AD-637125)
flux from quiet sun, (E), 20: 39565
interactions with electrons from nuclear explosions, (T), 20: 39775
monitoring of, in western states of U. S., 20: 38735(R) (NYO-1704-13)
reactions (γ,p) with lithium-6 at 100 Mev, proton energy spectra and angular distribution from, (E), 20: 40077 (MIT-2098-256)
scattering by bound K electrons, differential cross sections for Compton, (T), 20: 39773
shielding parameters for, computer program for, 20: 40285 (BNWL-236)
transmission through shelter air pipes, review of, 20: 39060
use in control of insects infesting cereals, 20: 38671

GAMMA SOURCES
dosimetry of cobalt-60 therapeutic, 20: 38771
dosimetry of spherical, method for determining, 20: 38989
energy spectra of point, media effects on, (E), 20: 40290
properties for production of plastic–wood composites, 20: 39287 (KLX-1876)
use of cobalt-60 as, for radiotheraphy, 20: 38744 (DP-1066(Vol.1), pp IV.47-66)
use of cobalt-60, in fluid flow investigation, 20: 39051

GAMMA SPECTRA
analysis of complex, computer programs for, 20: 39237
measurement of, from radioisotopes deposited in man, 20: 38770
shapes of delayed and prompt, in activation analysis of coal, 20: 39025 (ORO-2980-12)

GAMMA SPECTROMETERS
design for Mössbauer spectra, 20: 39250(P)
development and use of automated, for use in activation analysis of biological materials, 20: 38843
efficiency of lithium-drifted germanium, Monte-Carlo calculation of double-escape peak, (T), 20: 39271
performance of lithium-drifted germanium, 20: 39243
quality control procedure for scintillation, computer coupled, 20: 39193 (AD-636736)
shielding design for, 20: 39260

GAMMA SPECTROSCOPY
data analysis in, computer techniques for, 20: 39237
detectors for, properties and performance of germanium and silicon, 20: 39232
instrumentation for, 20: 39243

GARIGLIANO POWER REACTOR
design and performance, 20: 40418
pressure vessel of, fabrication and welding, method for, 20: 40417

GARNETS
analysis for dysprosium, activation, 20: 38833

GAS COOLED REACTORS
cobalt-60 production in, 20: 39317 (DP-1066(Vol.2), pp I.67-77)
efficiency of MHD converters with, as power plants, (T), 20: 39682
fuel cycle economics of high temperature, 20: 40392
fuel element design for graphite-moderated, to prevent coolant flow-induced vibration, 20: 40397(P)
fuel element development for high temperature, conference on, 20: 40383 (EUR-2780.e)
fuel element fabrication methods and costs, 20: 40388
fuel element reprocessing and refabrication, 20: 40419
heat transfer in, effects of turbulence promoters on, 20: 39084 (GEAP-5115)
loading apparatus for graphite-moderated, support arrangement for charge pan for, 20: 40365(P)
use with shock-wave MHD generator for power source, 20: 39639

GAS FLOW
calibration of, performance of gravimetric standard for, 20: 39020 (K-1632(Pt.2))
magnetohydrodynamic, in longitudinal magnetic field, 20: 40237
magnetohydrodynamic, enthalpy recovery at outlet duct in, (T), 20: 39658

GAS FLOW (LAMINAR)
measurement of, in rectangular channels, 20: 39050 (UCRL-16535)

GASES
collision integrals for molecular, (E/T), 20: 39321(R) (MLM-1312)
diffusion from irradiated uranium fuels, mechanisms of, 20: 39449 (BNWL-SA-272)
diffusion in atmosphere, field and wind-tunnel measurements of, 20: 39105
electric conductivity of thermoionized, in electric fields, 20: 40238
electric discharge frequency multiplier for, in nonuniform shf fields, (T), 20: 40228
electric discharges in, low-pressure, confinement effects on, 20: 40278
electron beam interactions with, (T), 20: 39576 (AD-636533)
energy exchange between electron and molecular, (T), 20: 39677
evaluation of, for use in tissue-equivalent ionization chambers, 20: 39227
ionization by fast neutrons, measurement of, 20: 39227
isotopic ratios in, measurement of difference in, 20: 38831
kinetics of dense, calculations using self-correlation function, (T), 20: 39946
metering radioactive, design of flowmeter for, 20: 39172
monitoring for iodine, equipment for, 20: 39264
plasmon dispersion relations for electron, surface, 20: 40225
properties of seeded combustion, as MHD working fluid, 20: 39636
research on, 20: 38857(R) (BNWL-235-3)
sorption by porous solids, calculation and measurement methods for, 20: 39387 (CEA-R-2947)
superheating for MHD generators, shock-wave, (T), 20: 39686
thermodynamic properties of high-temperature, for MHD generator, 20: 39938
transport properties in magnetic field of electron, (T), 20: 40183
gas–liquid, convective transfer processes in flow of, 20: 39050 (UCRL-16535)

GASTROINTESTINAL TRACT
radiation effects on function of rabbit, x, 20: 38659
strontium-90 absorption from rat, effects of various calcium compounds on, 20: 38569
GEIGER-MUELLER TUBES
design of, for monitoring iodine, 20: 39264
modification for low energy beta, 20: 39259
performance of, for beta counting, 20: 39228
plateau curves at high intensities, 20: 39244
time delays between spark and counter pulse, (E), 20: 39215
GELATIN
effects on polarographic reduction of uranyl ions in hydrochloric acid, 20: 38922
GENERATORS
performance testing of SNAP-15A, 20: 39310 (GA-5781)
safety analysis of 5-watt radiostrontium-fueled, for meteorological station, 20: 39311 (MND-SR-2586)
GENES
effects on DNA in *E. coli*, 20: 38620
radiosensitivity effects on *E. coli*, uv and x, 20: 38621
GENETICS
consequences of radiation exposure during radiotherapy, 20: 38746 (NYO-3364-19)
properties, origin and mechanism of conversion-type inheritance in maize, 20: 38617
radiation effects on animal, 20: 38544
role of DNA and RNA in, 20: 38542(T) (UCRL-Trans-10029)
GEOCHEMISTRY
alpha spectrometry in, 20: 39143
GEOLOGY
research in, 20: 38857(R) (BNWL-235-3)
research on, in Hanford area, 20: 39099(R) (BNWL-235-3, pp 1-23)
GEOMAGNETIC FIELDS
activity correlations with variations in E and F2 regions, 20: 39985
activity variation in, solar and lunar effects on, (E/T), 20: 39982
auroral zone of, charged particle effects on propagation of radiowaves in, 20: 39954
charged particle trapping in, magnetic coordinates for analyzing, 20: 39989
charged-particle transport in, cut-off rigidity for, 20: 39988
connection of tail lines to interplanetary field, 20: 39986
disturbances of, effects on auroral displays of, 20: 39955
effects on electron flux, diamagnetic, 20: 39976
effects on fluxes of particles mirroring at equator, ring current, 20: 39970
ionization as function of, position of equatorial boundary of anomalous, 20: 39967(T)
pulsations in, patterns of pearl-type, 20: 39962(T)
pulsations in, propagation of Pc 1 micro-, 20: 39977
variations of, correlation with auroras, 20: 39956
GEOMAGNETIC STORMS
data for 1964, 1965, and Jan.–Mar. 1966, 20: 39979
effects on variations in ionospheric E and F2 region, 20: 39985
ionospheric absorption at small solar heights and at night during, 20: 39960(T)
properties of, sunspot cycle relation to, 20: 39563
sudden commencement declination change, time and seasonal dependence of, 20: 39969
GEOPHYSICS
radioisotopic measurements used in, review on, 20: 39291
GERMANIUM
determination of, simultaneously with gallium in iron meteorites by neutron activation analysis, 20: 38825
properties and use of semiconductor detectors of, for electron and gamma spectroscopy, 20: 39232
properties of semiconductor detectors of, 20: 39230
radioinduced photoconductivity of n-type, infrared extinction of, gamma, (E), 20: 40298
radioinduced photoconductivity in n-type, quenching of γ, 20: 40337(T)
superconductivity under high pressure, (E), 20: 40039
use of detectors of lithium-drifted, in γ-γ coincidence experiments, 20: 39197 (AECL-2565)
GERMANIUM ISOTOPES Ge-70
neutron reactions (n,2n) at 14.4 Mev, cross sections of, (E), 20: 40080 (ORO-3346-3)
GERMANIUM ISOTOPES Ge-71
electron capture ratios, M/L, 20: 40153
GERMANIUM ISOTOPES Ge-72
neutron reactions (n,p) at 14.4 Mev, cross sections of, (E), 20: 40080 (ORO-3346-3)
neutron reactions (n,α) at 14.4 Mev, cross sections of, (E), 20: 40080 (ORO-3346-3)
GERMANIUM ISOTOPES Ge-73
neutron reactions (n,p) at 14.4 Mev, cross sections of, (E), 20: 40080 (ORO-3346-3)
neutron reactions (n,α) at 14 Mev, cross sections for, (E), 20: 40098
GERMANIUM ISOTOPES Ge-74
neutron reactions (n,p) at 14.4 Mev, cross sections of, (E), 20: 40080 (ORO-3346-3)
neutron reactions (n,α) at 14.4 Mev, cross sections of, (E), 20: 40080 (ORO-3346-3)
GERMANIUM ISOTOPES Ge-76
neutron reactions (n,2n) at 14.4 Mev, cross sections of, (E), 20: 40080 (ORO-3346-3)
GERMANIUM SYSTEMS
Ge–Si, thermoelectric properties, 20: 40451
GERMANY
nuclear power development in, 20: 40441
nuclear power use in, for electricity production, 20: 40442
GERMINATION
effects on ascorbic acid content of seeds, 20: 38583
GLASS
age of natural, fission-track estimation of, 20: 39135
leaching of incorporated fission products from, 20: 40482
radiation effects on refractive index of optical, gamma, 20: 39468
spectra of alkali benzoate- or alpha-naphthoate-containing alkali hydroxide, ESR and optical, 20: 38941(R) (RRL-2310-182)
strength and structure of nickel- and tungsten-fiber reinforced, 20: 39405 (UCRL-16844)
GLOBULIN
electrophoretic determination of blood serum, from irradiated hamsters, 20: 38598(R) (TID-22955)
radiation effects on blood serum, x, 20: 38598(R) (TID-22955)
GLOVE BOXES
design and performance of cryogenic, 20: 39448 (AERE-X-PR-2596-9)
use in changing tritium targets in accelerators, 20: 39476 (AD-636185)
GLUCOSAMINE
derivatives of, radiolysis of aqueous solutions of, gamma, 20: 38969
radiolysis of aqueous solutions of, gamma, 20: 38969
GLUCURONIDASE
distribution in rat liver subcellular fractions, 20: 38595(R) (ORO-3295-2)
release of acid, from lysosomes of x irradiated rat liver, 20: 38577
GLUTATHIONE
radiation effects on content in rat brain, whole-body x, 20: 38679
GLYCEROL
effects on yield of oxalate in radioinduced carboxylation of formate, 20: 38966
neutron inelastic scattering by, dynamic processes in slow, 20: 40338
neutron reactions at 0.025 to 0.4 ev, total cross sections for, (E), 20: 40069(R) (EANDC(E)-66(U))
radioprotective effects on bacteriophage, 20: 38628
GLYCINE
metabolism in rats, tracer study, 20: 38600(R) (TID-23034)
radiosensitivity effects on mice, 20: 38714
GLYCOGEN
accumulation in astroglial cells of rat brain, 20: 38674
radiation effects on content in rabbit leukocytes, x, 20: 38681
GOATS
radiation effects on, pathological, RBE of fission neutron and γ, 20: 38629
GOITER
radiotherapy using iodine-131, late carcinogenic effects, 20: 38749
GOLD
alpha particle channeling at 3 Mev, energy loss spectra from, (E), 20: 39602
antimony and gold ion mobility in, effects of high electronic current density on, 20: 40349
argon and gold ion reactions with foils of, interstitial atom migration in, 20: 40295
deposition in graphite by vapor diffusion, for lattice vacancy determination, 20: 39439
deposition in graphite by vapor diffusion, for trace-boron determination, 20: 39439
determination in blood in arthritic and healthy patients, activation, 20: 38845
iodine-137 ion channeling at 60 Mev, energy loss spectra from, (E), 20: 39602
superconductivity of, 20: 40047
GOLD ALLOYS
Au–Fe, gold-197 hyperfine structure spectra in, (E), 20: 39470(R) (ORNL-3924)
Au–Mn, gold-197 hyperfine structure coupling in, (E), 20: 39470(R) (ORNL-3924)
Cu–Au–Ni, gold-197 hyperfine structure coupling in, (E), 20: 39470(R) (ORNL-3924)

GOLD IONS
mobility in gold, effects of high electronic current density on, 20: 40349
reactions with gold foils, interstitial atom migration in, 20: 40295
GOLD ISOTOPES Au-195
tracer use in ion mobility studies, 20: 40349
GOLD ISOTOPES Au-197
gamma energy of, pressure dependence of resonance, (E), 20: 39470(R) (ORNL-3924)
hyperfine structure spectra in gold–iron alloys, (E), 20: 39470(R) (ORNL-3924)
hyperfine structure coupling and isomer shift in copper–gold–nickel alloys, (E), 20: 39470(R) (ORNL-3924)
hyperfine structure coupling in gold–manganese alloys, (E), 20: 39470(R) (ORNL-3924)
neutron reactions at 30 and 64 kev, activation cross section for, (E), 20: 40069(R) (EANDC(E)-66(U))
neutron reactions (n,γ) with, resonance activation integral cross sections for, (E), 20: 40069(R) (EANDC(E)-66(U))
GOLD ISOTOPES Au-198
distribution in tissues, measurement of, 20: 38770
effects on cambium cells and macrocytes in patients, 20: 38769
radiation monitoring of medical personnel using, 20: 39159
use for therapy of carcinoma, 20: 38643
use in therapy, effects on radioactivity of patients and wastes, 20: 38790
use in trans-sphenoidal hypophysectomy, results compared with use of yttrium-90, 20: 38758
GONADAL HORMONES
metabolism in blood plasma in sheep ovaries, tracer study on, 20: 38547(R) (NYO-918-15)
GONADS
radiation dose to, during therapeutic exposure to 31 Mev x radiation, 20: 38746 (NYO-3364-19)
radiation effects on queen honeybee, x, 20: 38631
radiation effects on testes size of eye gnats, variations with age at irradiation, γ, 20: 38632
radiosensitivity of mouse, x, 20: 38590(R) (NYO-1979-13)
radiosensitivity of male, in mice, fast neutron and γ, 20: 38647
radiosensitivity of male, in mice, x, 20: 38648
transplantation of ovaries in sheep, method for auto-, 20: 38547(R) (NYO-918-15)
GRAIN STRUCTURE
book: *Materials Science Research*, Vol. 3, role of grain boundaries and surfaces in, 20: 39338
effects of additives on tungsten, 20: 39400 (NASA-TN-D-3531)
effects on radiation resistance of beryllia, 20: 39453 (EUR-3054.e)
GRANITES
age of Swedish, 20: 39125
age of Swedish, rubidium–strontium and strontium-87/-86 estimation of, 20: 39126
GRAPHITE
book: *Radiation Damage in Graphite*, 20: 39463
crystal structure of, determination of lattice vacancies in, 20: 39439
diffusion of boron in, by deposition of gold and etching, 20: 39439
neutron transport in, calculations using P-3 approximation, 20: 40064
phase transformations, effect of pressure and irradiation on solid-solid, (E), 20: 40306
preparation of impermeable, by liquid metal impregnation, 20: 39355 (EUR-2988.f)
processing reactor fuels of, grind-leach method for, 20: 38998(R) (ORNL-3958)
properties in high-temperature helical-screw expanders and compressors, 20: 39026 (UCRL-14660(Rev.1))
radiation effects on, survey of, 20: 39455 (EUR-3056.e)
radiation effects on physical properties of, book on, 20: 39463
radiation effects on dimensions of pyrolytic, fast neutron, 20: 39465
radiation effects on polycrystalline, fast neutron, 20: 39466
tensile properties of, statistical analysis of, 20: 39408(T) (NSJ-tr-46)
graphite–TiC, fabrication and mechanical properties of, 20: 39367
graphite–ZrC, fabrication and mechanical properties of, 20: 39367
graphite–HfC, fabrication and physical properties of, 20: 39367
graphite–VC, fabrication and physical properties of, 20: 39367
graphite–NbC, fabrication and physical properties of, 20: 39367
graphite–TaC, fabrication and physical properties of, 20: 39367
graphite–MoC, fabrication and physical properties of, 20: 39367
graphite–WC, fabrication and physical properties of, 20: 39367
GRAPHITE MODERATED REACTORS
fuel channel registers for, 20: 40366(P)
fuel cycle costs in, evaluation of thorium–uranium-235, 20: 40393
fuel cycle studies for high temperature plutonium-fueled, 20: 40421
fuel cycles in, study of plutonium, 20: 40473
fuel element design for gas-cooled, to prevent coolant flow-induced vibration, 20: 40397(P)
loading apparatus for gas-cooled, support arrangement for charge pan for, 20: 40365(P)
reactivity evolution in plutonium–uranium fueled, 20: 40384(R) (EURAEC-1660)
GRAVITATION
collapse of cylinders of incoherent fluid, exterior metrics in, 20: 40001
conservation laws for general relativistic exploding matter in, covariant, 20: 40002
effects on hydrogen abundance in universe, (T), 20: 39560
equation of motion of point mass in, 20: 39999
fields of, mass aspect and news function for cylindrical, 20: 40009
theory of, in de Sitter world, 20: 40006
GREAT BRITAIN
nuclear power development in, 20: 40441
nuclear power use in, for electricity production, 20: 40442
strontium-90 content in bone samples in, 1965, 20: 39163
GRINDING
equipment design for, 20: 39340
GROUND WATERS
analysis of, evaluation of isotope methods for use in, 20: 39142
contamination by nuclear explosions, 20: 39149 (NVO-28)
flow measurements on, using computers, 20: 39099(R) (BNWL-235-3, pp 1-23)
hydrogen isotope ratios in, effect of rain and spring water on, 20: 39127
tracer studies of, 20: 39155
GUANIDINES
effects as radioprotective agents in mice, relation to chemical structure, 20: 38724
GUINEA PIGS
effects of radiation on biochemical and physiological indexes in, β, 20: 38662
radiation effects on urinary excretion and production of cortisols in, 20: 38547(R) (NYO-918-15)
radiation injuries of skin of, pathology of β, 20: 38591(R) (NYO-3445-7)
radioinduced hemmorrhage in, effects of autoinfection on, 20: 38656
strontium-90 distribution in, 20: 38662
GULONIC ACID, DIKETO-
radiation effects on content in rat brain, whole-body x, 20: 38679
GUNDREMMINGEN POWER REACTOR
steam separator development for, 20: 39019(R) (GEAP-5149)

H

HAFNIUM
effects on grain size of tungsten, 20: 39400 (NASA-TN-D-3531)
neutron capture resonance integrals, (E), 20: 40146
superconductivity of, 20: 40047
HAFNIUM ALLOYS
Hf–Nb, work function for, 20: 40297
Hf–Nb–W–Y, properties for high-temperature service, 20: 39445(P)
Hf–Nb–W–Y, weldability evaluation of, 20: 39366
Hf–Ta, work function for, 20: 40297
Hf–Ta–W, weldability evaluation of, 20: 39366
Hf–W, work function for, 20: 40297
HAFNIUM CARBIDES
effects on grain size of tungsten, 20: 39400 (NASA-TN-D-3531)
graphite–HfC, fabrication and physical properties of, 20: 39367
HAFNIUM ISOTOPES Hf-181
incorporation in solid cracking catalyst, process for, 20: 38993(P)
HAFNIUM OXIDES
actinide oxides–HfO_2, preparation of sols of, 20: 39442(P)
HAFNIUM SYSTEMS
Hf–MoC–Ta, preparation and properties of dispersion-hardened, 20: 39441(P)
Hf–Ta–Wc, preparation and properties of dispersion-hardened, 20: 39441(P)
HAIR
occurrence of epilation in neutron and gamma-irradiated rats, 20: 38629
trace element adsorption and elution on, tracer study, 20: 38543
HALDEN BOILING REACTOR
development and operation, July 1964–Dec. 1965, 20: 40409(R) (NP-16230)
HALL EFFECT
accelerator using, performance of, 20: 39090
HALOGENS
use to prevent thermionic converter cathode failure, 20: 39637(P)
HAMSTERS
radiation effects on blood serum proteins in gestating, whole-body x, 20: 38598(R) (TID-22955)
radiation effects on transplanted experimental tumors in, laser, 20: 38780
HANDBOOKS AND MANUALS

book: *Corrosion Resistance of Reactor Materials, Handbook*, 20: 39349
guide for cleaning and assembly, 20: 40489 (SC-DC-66-1118)
protective action guides for fallout cesium-137, iodine-131, strontium-89, and strontium-90, 20: 38743
HANDLING AND STORAGE
of fissile material, safety calculations for, 20: 40375 (DP-1031)
of radioactive materials by personnel, 20: 39166
HANDS
contamination monitor for, design of alpha, beta, and gamma, 20: 39198 (BNWL-250)
monitoring for alpha sources, instrument for, 20: 39254
HARDNESS
testing of beryllium, equipment for, 20: 39436
HARWELL SYNCHROTRON
beam extraction from, design of plunging magnet system for, 20: 39496 (RHEL-R-117)
HASTELLOY C
reactions with combustion gas species in launch pad abort environments, 20: 39312 (SC-CR-66-2044)
HASTELLOY X
reactions with combustion gas species in launch pad abort environments, 20: 39312 (SC-CR-66-2044)
HAWAIIAN ISLANDS
use of gamma radiosterilization as a quarantine treatment for fruit flies infesting fruits and vegetables from, 20: 39293
HAYNES 25 ALLOY
reactions with combustion gas species in launch pad abort environments, 20: 39312 (SC-CR-66-2044)
HEAD
use of phantoms of, for x radiation dosimetry, from facial therapy, 20: 38765
HEALTH PHYSICS
conference on, 20: 39166
HEART
radiation effects on normal and pathological, during radiotherapy, 20: 38675
radiation injuries to cardiovascular system in animals, in death from acute radiation sickness, 20: 38666
radiosensitivity of, review of, 20: 38675
HEAT-RESISTING ALLOYS
properties of hafnium–niobium based, 20: 39445(P)
HEAT TRANSFER
analysis and theory of, during boiling of liquids, 20: 39052
analysis of, design of equipment for, 20: 39050 (UCRL-16535)
burnout flux in boiling systems, compressibility effects on, 20: 40427
improvement of, in parallel rod arrays using turbulence promoters, 20: 39048 (GEAP-5115)
in boiling channels, model for, 20: 40403 (EURAEC-1464)
in shelters, development of systems for, 20: 39074
measurement at wall of MHD combustion chamber and electrode surface, 20: 39636
to liquid helium, boiling, 20: 40048
transient and steady state, TRUMP computer program for, 20: 39049 (UCRL-14754)
HEAT TRANSFER SYSTEMS
design for two-phase flow analysis, 20: 39050 (UCRL-16535)
design of 3000-kw, for liquid metal turbine tests, 20: 39028
HEAT TREATMENT
effects on corrosion of copper–molybdenum–zirconium alloys, 20: 39347 (NP-16239)
method of, using induction-coupled plasma, 20: 39343(P)
HEATERS
design for preheating in MHD open-cycle converters, (T), 20: 39653
performance of, for CNEN blow-down MPD facility, 20: 39675
HEAVY WATER REACTORS
reactivity evolution in plutonium–uranium fueled, 20: 40384(R) (EURAEC-1660)
HELIUM
boiling heat transfer to liquid, 20: 40048
collision integrals for, (E/T), 20: 39321(R) (MLM-1312)
effects on Drosophila, genetic, 20: 38596(R) (SAN-590-1)
electric discharge in alkali-metal seeded, (E), 20: 39715
electron density and temperature of cesium-seeded plasma of, (E), 20: 39665
electron interactions with atomic, electron exchange in, 20: 39582(T) (AERE-Trans-1053)
electron scattering spectrum of, large-angle low-energy, (E), 20: 39591
electron scattering by, phase shifts and cross sections for, 20: 39621
ion velocity in liquid, temperature dependence on critical, 20: 40033
ionization in MHD generators, magnetically induced, (E), 20: 39679
light scattering in liquid II, acoustic phonon attenuation and velocity from, 20: 40034
plasma of, MHD flow in ducts of cesium-seeded, 20: 39691
polarization potentials for atomic, 20: 39621
production in auroral atmosphere from cosmic alpha particles, 20: 39981
radioinduced production in beryllium, embrittling effects of, 20: 39454 (EUR-3055.e)
reactions with charged particles, stopping powers and straggling in, (T), 20: 39611
reflection and thermal accommodation of beams of, by platinum, (E), 20: 39590
scattering on helium, cross section for thermal collision-produced radiative de-activation process in, (T), 20: 39609
spectra of high-speed excited atomic, at 2700 to 6600 A, (E), 20: 39593
spectral shift mechanism in plasma of, 20: 40182
transport properties for, during thermal diffusion flow, 20: 39321(R) (MLM-1312)
HELIUM HYDRIDES
molecular structure of, calculation of natural orbital-based energy for, 20: 38910
HELIUM IONS
content in outer ionosphere, 20: 39950
effects on coloring in blue cellophane films, 20: 38941(R) (RRL-2310-182)
emission from optically polarized plasma, 20: 39619
mobility in liquid helium-3 below 1°K, 20: 40012 (COO-1198-364)
recombination in r-f discharge plasma, 20: 40247
HELIUM ISOTOPES
abundance in solar cosmic particles from July 18, 1961 event, 20: 39564
HELIUM ISOTOPES He-3
ion mobility in liquid, below 1°K, 20: 40012 (COO-1198-364)
mesons (π^-) cascade time in gaseous, measurement of, 20: 39579 (JINR-P-2838)
neutron induced conductivity in plasma of, thermal, (E), 20: 39683
production in proton reactions with beryllium and platinum at 2.9 Bev, (E), 20: 39794
purification of, nitrogen-cooled trap for, 20: 39504
reactions (He-3,α) and (He-3,d) with chromium-52, differential cross sections for, 20: 40065(R) (BMwF-FB-K-66-01)
reactions (He-3,α) with calcium-40 at 24 Mev, cross sections for, (E), 20: 40067 (BMwF-FBK-66-15, pp 20-37)
reactions (He-3,n) with boron-11 and lithium-7 at 1.5 to 5.5 Mev, (E), 20: 40112
separation from helium-4 by thermal diffusion, 20: 39320(R) (MLM-1311)
specific heat of solid, 20: 40013 (IS-T-84)
vapor pressure of, thermomolecular, 20: 39320(R) (MLM-1311)
viscosity of, saturated-liquid, (T), 20: 39940
HELIUM ISOTOPES He-4
alpha scattering at 12 to 20 Mev, phase analysis of elastic, 20: 40065(R) (BMwF-FB-K-66-01)
bremsstrahlung reactions at 159 to 209 Mev, meson (π^0) production in, (E), 20: 39822
flow in solid, Poiseville, (E), 20: 40327
melting curve below 1°K, 20: 40032
properties of liquid, ground state, 20: 40030
separation from helium-3 by thermal diffusion, transport properties for, 20: 39320(R) (MLM-1311)
specific heat of solid, 20: 40013 (IS-T-84)
vapor pressure of, thermomolecular, 20: 39320(R) (MLM-1311)
viscosity of, saturated-liquid, (T), 20: 39940
HELIUM ISOTOPES He-5
energy levels of, Hartree-Fock calculations for, (T), 20: 40138
HELIUM ISOTOPES He-8
production in meson (π^-) capture by carbon and oxygen at 80 Mev, (E), 20: 40071 (JINR-E-2774)
HELIUM SYSTEMS
CO_2–ethyl ether–helium, man transfer in channel flow, 20: 39050 (UCRL-16535)
HEMATOPOIETIC SYSTEM
radiation effects on growth of transplanted cells of mouse, x, 20: 38592 (ORNL-P-2158)
radiation effects on sheep, fission neutrons, 20: 38637
radiation effects on calf, gamma, 10: 38706
radiation effects on, γ, 20: 38766
HEMATOPOIESIS
restoration of, in irradiated animals using bone marrow transplants, 20: 38740
HEMOGLOBIN
levels of, in irradiated rats, 20: 38619
HEMOLYSIN
effects of procaine on formation of, in irradiated dogs, mice, rabbits, and rats, 20: 38727
HEMORRHAGE
radiation effects on response of dogs to, 20: 38703
radioinduced in guinea pigs, x, 20: 38656
HEXADECANOIC ACID, 3-HYDROXY-

preparation and properties of carbon-14-labeled, 20: 38987
HEXADECANOIC ACID, 3-OXO-
preparation and properties of carbon-14-labeled, 20: 38987
2-HEXADECENOIC ACID
trans-, preparation and properties of carbon-14-labeled, 20: 38987
HEXANE
neutron reactions at 0.025 to 0.4 ev, total cross sections for, (E), 20: 40069(R) (EANDC(E)-66(U))
radiation effects on electric conductivity of, gamma and uv, 20: 38971
radiolysis of, effects of deuterated and normal hydriodic acid on yields in, 20: 38941(R) (RRL-2310-182)
hexane–SiO_2, radiolysis of, ESR spectral studies on yields in gamma, 20: 38994(R) (AE-232)
1-HEXANOL, 2-ETHYL-
properties for use in stacked-clone contactor, 20: 38998(R) (ORNL-3958)
HIGH ENERGY INJECTION DEVICES
plasma ion cyclotron instabilities in DCX-2, 20: 40172(R) (ORNL-3989, pp 14-30)
plasma properties in DCX-1, 20: 40171(R) (ORNL-3989, pp 1-13)
plasma properties in DCX-2, (E/T), 20: 40176(R) (ORNL-3989, pp 95-108)
HIGH TEMPERATURE GAS COOLED REACTOR EXPERIMENT
fuel element reprocessing and refabrication, 20: 40419
fuel fabrication for, cost analysis of coated particle, 20: 40466
HIPPURIC ACID, AMINO-, SODIUM SALTS
labeling with iodine-131, 20: 38932
HIPPURIC ACID, *o*-IODO-, SODIUM SALTS
labeling with iodine-131, 20: 38932
HIROSHIMA
radiation dosimetry of bomb survivors, Ichiban program for, 20: 39064
HISTIDINE
radiolysis of, in aqueous solution, γ, 20: 38582
synthesis in plants, 20: 38589(R) (EUR-2761.f)
HOLMIUM
determination in fluorite monocrystals, spectrophotometric, 20: 38829
determination in solutions, spark method for spectrographic, 20: 38832
ionization potential of, determination using surface ionization technique, 20: 40203
magnetic fields at tin-119 in, deduction from gamma hyperfine splitting, 20: 40322
neutron capture resonance integrals, (E), 20: 40146
HOLMIUM ALLOYS
Al–Ho, magnetic properties of intermetallic compounds of, 20: 39433
Ce–Ho, phase transformation and magnetic ordering in, pressure-induced, 20: 40326
Ho–Zn, crystal structure of intermetallic compound $HoZn_{12}$ in, 20: 39417
Ho–Pb–Zn, component distribution in recrystallized, 20: 39435
HOLMIUM CHLORIDES
heat of dilution of aqueous solutions of, 20: 38870 (IS-1356)
heat of dilution of aqueous, at 25°C, 20: 38903
heat of solution of hexahydrate of, 20: 38870 (IS-1356)
specific gravity and apparent molal volume of aqueous solutions of, at 25°C, 20: 38905
viscosity of aqueous solutions of, at 25°C, 20: 38904
HOLMIUM ISOTOPES Ho-165
energy levels of, M1 transitions of rotational, (E), 20: 40072 (LA-DC-8061)
HOLMIUM OXIDES
actinide oxides–Ho_2O_3, preparation of sols of, 20: 39341(P)
HOLMIUM PHOSPHATES
preparation and properties of, conductometric and potentiometric studies on, 20: 38883
HOMOGENEOUS REACTORS
characteristics of solid, catalog, 20: 40353 (ANL-7228)
HORMONES
biogenesis and metabolism in elderly men, tracer study on, 20: 38547(R) (NYO-918-15)
effects of, on rat liver cells, 20: 38595(R) (ORO-3295-2)
HOSPITALS
classification of Canadian, based on fallout exposure probabilities, 20: 39162
sewage disposal for radioisotope wards, 20: 38790
HUMIDITY
effect on radioactivity levels in air, 20: 39114
HYDRAZINE, METHYL-
effects on response of leukemic mice to immunotherapy, 20: 38794
HYDRIODIC ACID
effects of deuterated and normal, on yields in radiolysis of hexane, 20: 38941(R) (RRL-2310-182)
HYDROCARBONS
radiation effects on, electron, 20: 38947
radioinduced polymerization of, with styrene, for radioresistant lubricants, 20: 38973(P)
radiolysis of liquid aliphatic, ESR spectra of products of electron, 20: 38941(R) (RRL-2310-182)
HYDROCHLORIC ACID
analytical use for separation of molybdenum-99 from technetium-99m sorbed on aluminum oxide, 20: 38997 (NIJS-R-483)
effects on carbon-coated uranium dicarbide beads at 1600 to 2100°C, 20: 39346 (LA-3488)
effects on polarographic reduction of uranium ions, 20: 38922
ionic transport coefficients for, at 25°C, 20: 38909
HYDROGEN
abundance in universe, gravitation effect on, (T), 20: 39560
argon ion reactions with molecules of, cross sections for charge-exchange, (E), 20: 39592
chemical reactions with zirconium alloys at 400°C, effects of carbon tetrachloride on, 20: 39360 (TRG-Report-1255)
crystal structure of solid, (E), 20: 40308
determination in sodium, development of techniques for, 20: 38797(R) (MSAR-66-150)
effects on ductility of tantalum at low temperatures, Petch analysis of, 20: 39378 (AD-635596)
effects of interstitial, on superconducting critical temperature of niobium, (E), 20: 40025
electron elastic scattering by, excitation cross sections for, (T), 20: 39610
electron energy levels of atomic, diatomic, and triatomic, 20: 39580(R) (ORNL-3989, pp 78-88)
electron interactions with atomic, electron exchange in, 20: 39582(T) (AERE-Trans-1053)
electron scattering by, ionization cross sections for, (T), 20: 39612
electron scattering by, ionization cross sections for, (T), 20: 39607
electron scattering by, excitation cross sections for, (E), 20: 39608
energy levels in ionized molecular, ground-state, (T), 20: 39614
excitation by protons, 20: 39583
permeation through molybdenum and tungsten, 20: 39098(R) (WERL-2823-21)
photon reactions with, differential cross sections for meson ($\pi^{\pm}$) production in, (E), 20: 40075 (LNF-66/30)
positron scattering by, sensitivity of phase shifts for, (T), 20: 39817
production in auroral atmosphere from cosmic protons, 20: 39981
production in radioinduced oxidation of methanol, effects of dose rate on, 20: 38942 (UJV-1457)
proton reactions in, electron capture cross section for, (T), 20: 39606
proton scattering by, ionization cross sections for, (T), 20: 39607
radiations from laser-produced plasma of, spectra of, 20: 40251
reactions with copper oxide pellets in differential and deep beds, 20: 38874 (ORNL-TM-1540)
reactions with radioisotope-containment materials in launch pad abort enrichment, 20: 39312 (SC-CR-66-2044)
scattering by dioxane, cross sections for, (E), 20: 40069(R) (EANDC(E)-66(U))
solubility in Zircaloy-2, effects of temperature on, 20: 39379 (AECL-2453)
viscosity of molecular, saturated-liquid, 20: 39940
yields in gamma radiolysis of heavy water–water mixtures, isotope effects in, 20: 38938 (IA-1074)
yields in radiolysis of hexane, effects of hydriodic acids on, 20: 38941(R) (RRL-2310-182)
HYDROGEN IONS
content in outer ionosphere, 20: 39950
formation of negative, from charge-exchange collisions in mercury vapor, 20: 39500
production of H_2^-, properties of four-electrode source for, 20: 40175(R) (ORNL-3989, pp 89-94)
HYDROGEN ISOTOPES
content ratios in ground and surface waters, 20: 39127
HYDROGEN PEROXIDES
production in radioinduced oxidation of methanol, effects of dose rate on, 20: 38942
yields from radiolysis of sulfuric acid solutions of potassium bromide, effects of dosage of electrons and gamma on, 20: 38952
HYDROGEN SYSTEMS
Ar–H, electron density and temperature in plasma jet of, 20: 40215
Ar–H, meson (μ^-) capture by, spectra from, 20: 39578 (JINR-P-2807)
D–H, combustion at very high temperatures, 20: 39013(P)
DH–H, combustion at very high temperatures, 20: 39013(P)
H–Ne, crystal structure of solid, (E), 20: 40308
H–Pd, kinetics and structures of, diffraction studies on, 20: 39428
HYDROLOGY
isotope methods of analysis of ground water, evaluation of, 20: 39142
research in, 20: 38857(R) (BNWL-235-3)
tracer studies of ground water, choice of tracers for, 20: 39155

HYDROMAGNETIC WAVES
propagation at 1100 km in auroral region, 20: 39996
propagation from source in half-space of compressible plasma, 20: 40199
propagation in interplanetary plasma, evidence for, 20: 39569
propagation in ionosphere and magnetosphere, low-frequency, 20: 40224
propagation in ionosphere, waveguide theory for, 20: 39977
propagation in waveguide-filled magnetoplasma, pressure effects on, 20: 40248
pulsations of pearl-type, in geomagnetic field, 20: 39962(T)

HYDROPEROXIDE, HYDROXYMETHYL-
production in radioinduced oxidation of methanol, effects of dose rate on, 20: 38942 (UJV-1457)

HYDROXYL RADICAL
determination of surface, in carbon black, using carbon-14-labeled diazomethane, 20: 38805

HYDROXYLAMINE
effects on *Micrococcus lysodeikticus*, lethal and mutagenic, 20: 38574(R) (NYO-3449-1)

HYPERFINE STRUCTURE
field parameters in Mössbauer, local, 20: 39615(T)

HYPERONS
decays in broken SU(3) × SU(3), nonleptonic, 20: 39893
decays of, group-theoretical interpretation of Sugawara theory for nonleptonic, 20: 39895
mass differences of, calculations of electromagnetic, 20: 39928

HYPERONS (Λ^0)
decay asymmetries of, from meson (π^-)-proton interactions, 20: 39837
decay of long-lived, 20: 39762 (JINR-P-2849)
lifetime of, (E), 20: 39849
production angular distributions of, from meson (π^-)-proton interactions, 20: 39837

HYPERONS (Σ^-)
interactions with protons, cross sections for, (T), 20: 39765 (ORO-2504-91)
production in deuteron-meson (K−) interactions at 0.9 to 1.12 Bev/c, (E), 20: 39747 (COO-881-75)

HYPERONS (Σ^+)
decay of, neutron polarization from, (E), 20: 39748 (COO-881-76)
interactions with protons, cross sections for, (T), 20: 39765 (ORO-2504-91)

HYPERONS (Ξ^-)
decay of, sum rules for strangeness-changing axial-vector coupling constants for beta, 20: 39809

HYPERONS (Ξ^0)
decay of, sum rules for strangeness-changing axial-vector coupling constants for beta, 20: 39809

HYPERTHYROIDISM
radiotherapy of Basedow's disease using iodine-131, 20: 38760
therapy using iodine-131, dose determination for, 20: 38785

I

ICE
density profile measurement in, using nuclear techniques, 20: 39130
oxygen-16 to oxygen-18 ratio in St. Elias Mountain, Canada, 20: 39123

IGNEOUS ROCKS
age of, rubidium–strontium determination of, 20: 39126

IMAGE BRIGHTNESS INTENSIFIERS
design of thermal-neutron, 20: 39174

IMIDAZOLE
radiosensitivity effects on rat thymus, 20: 38720

IMMUNE REACTIONS
effects on nitrogen balance in mouse radiation chimeras, 20: 38636
radiation effects on, in rabbit eyes, x, 20: 38608
radiation effects on tissue transplant, 20: 38612
radiation effects on Brucella agglutinin formation and properdin content in rats, γ, 20: 38695
radiation effects on, in rabbit adrenal cortex, x, 20: 38697
radiation effects on, in rabbits, x, 20: 38641
radiation effects on, in animals and man, 20: 38644
radioimmunoassay of insulin, iodine-131 effects on antibodies in, 20: 38579
use for study of brain tumor proteins, 20: 38745(R) (NYO-3267-3)

IMMUNITY
effects of procaine on, in irradiated mice, 20: 38727

IMPACT SHOCK
protection of public shelters against ground, 20: 39084
testing of beryllium, equipment for, 20: 39436

IMPELLERS
performance of, influence of geometry on, 20: 39021 (K-1665)

IN-PILE LOOPS
operation in ATRC, 20: 40460(R) (IDO-17191)

INCOLOY
radiation effects on mechanical properties of type-800, fast neutron, 20: 39457 (GEAP-5100-9)

INCONEL
radiation effects on mechanical properties of type-600, fast neutron, 20: 39457 (GEAP-5100-9)

INDIA
cesium-137 content in man, 1962 through 1965, 20: 39154

INDIAN POINT POWER REACTOR
safety of Unit No. 2, plant design analysis, 20: 40407 (NP-16181(Exh.B)(Vol.2)(Pt.A))
safety of Unit No. 2, plant design analysis, 20: 40408 (NP-16181(Exh.B)(Vol.2)(Pt.B))
safety of Unit No. 2, site and environment analysis, 20: 40406 (NP-16181(Exh.B)(Vol.1))

INDIUM
electric properties of thin films of, temperature effects on, 20: 40043
neutron capture resonance integrals, (E), 20: 40146
superconducting transition temperatures of thin films of, 20: 40043
thermal resistivity in intermediate-state superconducting, size effect in, (E), 20: 40022

INDIUM ALLOYS
Cd–In–Ag, radiation effects on silver-base, in-reactor, 20: 39461 (WCAP-6074)
Cd–In–Ag, reactivity worths of arrays of tubes filled with, 20: 40381
In–Hg, superconductivity of, effect of iron particles on, (E), 20: 40026
In–Pb, calorimetry on superconducting, isothermal, (E), 20: 40045
In–Sn, surface resistance of superconducting, (E), 20: 40042
Sb–In, plasma oscillations in, spin-orbital interaction effects on, 20: 40227
Sb–In, radiation effects in, stage-II recovery of, (E), 20: 40328

INDIUM ARSENIDES
radioinduced defects in, fast electron, 20: 40332

INDIUM ISOTOPES In-114
neutron reactions at 7.8 to 64 kev, activation cross sections for, (E), 20: 40069(R) (EANDC(E)-66(U))

INDIUM ISOTOPES In-115
proton reactions (p,n) at 3.0 to 5.8 Mev, strength functions for, (E), 20: 39470(R) (ORNL-3924)

INDIUM ISOTOPES In-116
neutron reactions at 7.8 to 64 kev, activation cross sections for, (E), 20: 40069(R) (EANDC(E)-66(U))

INDIUM ISOTOPES In-117
energy level structure of, (E), 20: 40159

INDOLE,3-(2-AMINOETHYL)-
effects as radioprotective agent in mice and rats, 20: 38725

INDOLE, 3-(2-AMINOETHYL)-5-METHOXY-
effects on radioinduced leukemia in mice, protective, 20: 38722
effects with cystamine as radioprotective agent in mice and rats, 20: 38725

5-INDOLOL, 3-(2-AMINOETHYL)-
effects on mice, pharmacological, 20: 38713

INDUSTRIAL HYGIENE
hazards evaluation tests of Pu–Al fuel fabrication facility, 20: 39153

INFECTIONS
effects of auto-, on development of hemorrhagic syndrome by irradiated guinea pigs, 20: 38656

INFRARED RADIATION
absorption by superconducting lead films, effects of magnetic fields on, 20: 40044
intensity in auroral zones, balloon observations of, 20: 39990
reflection by lithium hydride crystals, isotope effects on, 20: 40351

INSECTICIDES
content of residues of, in Gulf oysters and shrimp, 20: 39288(R) (ORO-636)
preparation of phosphorus-32- and sulfur-35-labeled Malathion and phosphorus-32-labeled Dipterex, 20: 38931

INSECTS
radiation effects on reproductive system of queen honeybee, x, 20: 38631
radiation effects on reproduction of eye gnats, γ, 20: 38632
radiation effects as means of population control of, infesting cereals, 20: 38671
radiation effects on grain moth *Sitotroga cerealella*, gamma, 20: 38705
radiation effects on various fruit flies infecting fruits and vegetables in Hawaii, 20: 39293

INSTRUMENTATION
design for determining strain rates, 20: 40490 (Y-1483)
design for fast-breeder power plants, 20: 40413 (TID-23257(Vol.1))
development for Halden fuel irradiation tests, 20: 40409(R) (NP-16230)
development of biomedicine, data processing, and reactor engineering, 20: 39170(R) (RISO-M-423)
use in nuclear structure analysis, 20: 39240

INSTRUMENTS

bibliography on nuclear physics, 20: 39168 (AED-C-06-14)
design for varying angle of incidence of ion beams, 20: 39029
development for plasma diagnostics, 20: 40220
fabrication of precision, beryllium–silver alloys for, 20: 39374(P)

INSULIN
labeling with iodine-131, 20: 38933
radioimmunoassays of, effects of radioactivity of iodine-131 label, 20: 38579

INTERFEROMETERS
design for use in machining, 20: 39031
development of optical, for plasma electron density measurement, 20: 40214
performance for density measurements in laser-induced plasmas, 20: 40186

INTESTINE
radiation effects on DNA synthesis in tissues of, 20: 38576 (TID-22103)
radiation effects on permeability of rat, x, 20: 38604
radiation injuries to animal, in death from acute radiation sickness, 20: 38666

IODIDES
oxidation of, for generation of molecular iodine vapors, 20: 39103(R) (BNWL-235-3, pp 51-69)

IODINE
determination in blood, micro colorimetric method for, 20: 38652
determination in blood in arthritic and healthy patients, activation, 20: 38845
determination in biological materials, activation, 20: 38849
determination in gases, design of GM monitor for, 20: 39264
diffusion from sodium at high temperatures, factors affecting, 20: 40357 (NAA-SR-11766)
iodine-131 exchange between, and 1-phenyl-2, 3-dimethyl-4-iodopyrazolone, effects of aromatic azines on, 20: 38936
radiation effects on content in blood, 20: 38652
sorption by carbon, 20: 39017(R) (DP-1053)

IODINE CHLORIDES
electron scattering by, (E/T), 20: 39622

IODINE IONS
reactions with gold at 60 Mev, energy loss spectra from, (E), 20: 39602

IODINE ISOTOPES
dose determinations for thyroid disease therapy, 20: 38789

IODINE ISOTOPES I-125
electron capture ratios, M/L, 20: 40153

IODINE ISOTOPES I-129
determination in animal and human thyroid, activation, 20: 38564
determination in biosphere, activation, 20: 38564

IODINE ISOTOPES I-131
beta decay of, in alkali metal iodates, properties of xenon oxide compounds formed by, 20: 38984
content in milk, methods for reducing, 20: 39157
decay curves for precursors of, 20: 40357 (NAA-SR-11766)
determination of effective biological half life, 20: 38549 (UCLA-12-592)
effects of radiation of, on binding of antibody to insulin, 20: 38579
elimination by mice and rats, effects of DTPA, pectin, and zirconium phosphate on, 20: 38733
exchange between elementary iodine and phenyldimethyliodopyrazolone, effects of aromatic azines on, 20: 38936
exchange between 1-iodo-2,4-dinitronaphthalene and potassium iodide, 20: 38916
generation of molecular vapor of, for field release use, 20: 39103(R) (BNWL-235-3, pp 51-69)
half-life and metabolism of, 20: 38743
incorporation in diiodofluorescein, 20: 38985
incorporation in insulin, 20: 38933
incorporation in organic iodo compounds and purity studies of, 20: 38932
incorporation in thyroxine and tyrosine, method for, 20: 38992
incorporation in tetraiodophenolphthalein, 20: 38985
separation from waste-water by aerobic treatment, 20: 40483
uptake by thyroid gland of mammals, effects of diet on, 20: 38549 (UCLA-12-592)
uptake by thyroid gland in adolescents and adults, 20: 38553
use for therapy of goiter, late carcinogenic effects, 20: 38749
use for therapy of hyperthyroidism, dose determination for, 20: 38785
use in therapy, effects on radioactivity of patients and wastes, 20: 38790
use in treatment of Basedow's disease, 20: 38760

ION BEAMS
control by source electrodes, 20: 39039(P)
density and pressures below breakdown, (T), 20: 39605
extraction of negative, from Manitoba and UCLR cyclotrons, 20: 39519
production in pulsed discharges, space charge effects on, 20: 40253
production of positive or negative equipment design for, 20: 39095(P)
space charge effects in cyclotrons, 20: 39529
variation of angle of incidence of, 20: 39029

ION EXCHANGE
solvents for, properties of mixed and non-aqueous, 20: 38818
use with solvent extraction for separation of uranium from elements and fission products, 20: 38999 (TID-23229)

ION EXCHANGE MATERIALS
properties of minerals for use as, 20: 38858 (BNWL-235-3, pp 23-51)
radiolysis of ammonia adsorbed on zeolites, EPR studies of gamma, 20: 38944
thermodynamic properties of weakly acidic, 20: 38873(R) (NYO-2269-9)
use in mixtures with sand for water decontamination, 20: 40484

ION EXCHANGE PROCESSES
book: *Progress in Nuclear Energy* Series IX, *Analytical Chemistry*, Vol. 6, 20: 38817
use of minerals in, 20: 38857(R) (BNWL-235-3)
use of nitrate solutions in, 20: 38820

ION SOURCES
charged-particle motion in, theory of, 20: 39471
design for beam control, 20: 39039(P)
design for cyclotrons, 20: 39505
design for producing nuclear reactions, 20: 39509(P)
development of negative, for tandem electrostatic accelerator, 20: 39500
development of polarized deuterium and hydrogen, for Grenoble isochronous cyclotron, 20: 39527
phase space density of cyclotron, 20: 39528
properties of duoplasmatron, Langmuir probe analysis of, 20: 40202
properties of four-electrode H_2^+, 20: 40175(R) (ORNL-3989, pp 89-94)
properties of helium, from optically polarized plasma, 20: 39619
purification trap for helium-3, 20: 39504
use of polarized, for cyclotrons, 20: 39525

IONIZATION
patterns of spread F from field-aligned, during solstice period of Dec. 1962 and June 1963, 20: 39973

IONIZATION CHAMBERS
design and construction of modified Lozier tube, 20: 39167 (AD-636927)
design for detection of beta, gamma, or x radiations, 20: 39249(P)
design for use in aircraft fuel gages, 20: 39189(P)
design of tissue equivalent, for fast neutron dosimetry, 20: 39227
performance of tissue equivalent, for fast neutron dosimetry, 20: 39227
performance of tissue-equivalent, for neutron dosimetry, 20: 39228
performance, for fast neutron dosimetry in seeds, 20: 38693
use of small attached or inserted, for x radiation dosimetry of gonads during therapy, 20: 38746 (NYO-3364-19)

IONOSPHERE
alpha particle energy spectra in, 20: 39987
critical frequencies of, solar activity effects on, 20: 39965(T)
critical frequency of F2 layer of, season and solar activity effects on diurnal variation of, 20: 39959(T)
deuterium energy spectra in, 20: 39987
disturbances in, transformation of secondary formations of F region into E_s during, 20: 39966(T)
electromagnetic wave absorption in, solar height and night variations of, 20: 39960(T)
electron concentration in, solar and geomagnetic effects on, 20: 39958(T)
electron density distribution in D region of, l-f and v-l-f reflection for determining, 20: 39995
electron density in topside F layer of, steep horizontal, 20: 39974
electron density in equatorial, at Huancayo, Peru, 20: 39975
electron energy loss rate in D region of, (T), 20: 39994
electron production in, height dependence of cosmic ray-induced, (T), 20: 39625
electron temperatures in D region of, (T), 20: 39994
hydrodynamic wave propagation in, low-frequency, 20: 40224
hydromagnetic wave propagation in, waveguide theory for, 20: 39977
hydromagnetic wave disturbances at 1100 km in auroral region of, 20: 39996
ion composition in D and lower E regions of, (E), 20: 39948
ion composition in outer, (E), 20: 39950
ion density in lowermost, variations of negative, (E), 20: 39949
ion temperature in, from cyclotron damping of proton whistlers, 20: 39972
ionization as function of geomagnetic activity, position of equatorial boundary of anomalous, 20: 39967(T)
ionization in F region of, patterns of topside spread during solstice of Dec. 1962 and June 1963 of, 20: 39973
plasma temperature in, time-dependent, (T), 20: 39980
plasma variations in D region of, radio-wave absorption for determining, (E), 20: 39952
proton energy spectra in, 20: 39987
radio-wave absorption in, A3 method for measuring, 20: 39951
radio-wave absorption in, cosmic, (E), 20: 39953
structure irregularities in, gradient instability effects on, 20: 39993
variations in E and F2 region of, before and after increases in geomagnetic activity, 20: 39985

IONS

abundances of positive, in ionospheric D and lower E regions, (E), 20: 39948
content of single-charged, in outer ionosphere, (E), 20: 39950
density distribution in iono-exosphere with dipole magnetic field, (T), 20: 39968
density in lowermost ionosphere, variations of negative, (E), 20: 39949
density in solar wind-magnetosphere region, 20: 39978
flow across magnetic mirrors due to turbulent diffusion, (T), 20: 40236
interactions in metals, effects on lattice vibrations, (T), 20: 40344
motion in liquid helium, temperature dependence on critical, 20: 40033
paths in ion sources, theory of, 20: 39471
polarization capacities, 20: 38879(T) (UCRL-Trans-1325)
reactions with molecules, ion-cyclotron double resonance in, 20: 38902
temperature in completely ionized plasma, boundary-layer equations for, (T), 20: 39721
temperature of ionospheric, from cyclotron damping of proton whistlers, 20: 39972

IOPANOIC ACID
labeling with iodine-131, 20: 38932

IRIDIUM
superconductivity of, 20: 40047

IRIDIUM ALLOYS
Ir–Os, superconductivity, 20: 40047
Ir–Pt, superconductivity, 20: 40047
Ir–Rh, superconductivity, 20: 40047

IRIDIUM FLUORIDES
molecular structure of, mean amplitudes of vibration at 0 and 298°K in, 20: 38897

IRIDIUM ISOTOPES Ir-192
use in radiography, 20: 39286 (DP-1066(Vol.1), pp IV.43-5)

IRON
content in fallout from Chinese atomic test, Oct. 1964, 20: 39110
defects in, annealing observation, and production of point, 20: 39386 (CEA-R-2905)
determination in high-purity plutonium, absorptiometric, 20: 38801 (PG-Report-729)
effects of medium of, on gamma energy spectra, (E), 20: 40290
effects on superconductivity of Hg–13% In alloy, (E), 20: 40024
evaporative lifetime on tungsten and oxygenated tungsten from 1250 to 1750°K, (E), 20: 40307
gamma attenuation calculations for, build-up factor effects on, 20: 40289
magnetic fields at dysprosium, gadolinium, and samarium nuclei implanted in, 20: 40342
magnetic moment distributions for impurities in, neutron-diffraction study of, (T), 20: 40330
meson (μ^-) capture by, neutron angular distributions from, (E), 20: 40096
neutron angular distributions behind shielding of, fast, 20: 40286
neutron inelastic scattering at 5 Mev, cross sections for, (E), 20: 39470(R) (ORNL-3924)
neutron reactions at 54 to 250 kev, total cross sections for, (E), 20: 40069(R) (EANDC(E)-66(U))
radioinduced defects in, effects of metallic impurities on point, 20: 39386 (CEA-R-2905)
separation of thorium-230 from, by ion exchange, 20: 38834

IRON ALLOYS
Al–Fe–Y, crystal structure of intermetallic compounds in, 20: 39414
Au–Fe, gold-197 hyperfine structure spectra in, (E), 20: 39470(R) (ORNL-3924)
Ce–Fe, crystal structure of intermetallic compound, 20: 39409
Cr–Co–Fe–Mn–Ni–W, tensile properties of L-605, effects of cold deformation on, 20: 39399 (NASA-TN-D-3528)
Cr–Fe–Zr, corrosion of zirconium-base, by steam at 300 to 500°C, 20: 39356(R) (GEAP-5134)
Cr–Fe–Zr, properties of zirconium base, for fuel cladding, 20: 39356(R) (GEAP-5134)
Fe–Nd, crystal structure of intermetallic compound, 20: 39409
Fe–Pr, crystal structure of intermetallic compound, 20: 39409
Fe–Rh, iron-57 hyperfine structure coupling in, (E), 20: 39470(R) (ORNL-3924)
Fe–Sm, crystal structure of intermetallic compound, 20: 39409
Fe–U, phase studies of uranium-base, 20: 39388 (CEA-R-2956)

IRON COMPLEXES
with nitrilotriacetic acid and polyamino polycarbooxylic acids, formation of, biamperometric studies of, 20: 38810

IRON DYSPROSIUM SELENIDES
preparation and crystal structure, 20: 38884

IRON FLUORIDES
effect on metallurgical properties of uranium metal produced by reduction of uranium(IV) fluorides, 20: 39342(P)

IRON IONS
effects on mitochondrial swelling, 20: 38639

IRON ISOTOPES Fe-55
determination in blood using liquid scintillation counting, 20: 38555

IRON ISOTOPES Fe-56
kinetics of transfer in human serum, comparison with iron-59, 20: 38573
neutron reactions (n,α), (n,p), and (n,2n) at 14.4 Mev, cross sections for, (E), 20: 40079 (ORO-3346-2)
proton reactions (p,α) and (p,p) at 9 and 12 Mev, statistical fluctuations in cross sections for, 20: 40065(R) (BMwF-FB-K-66-01)

IRON ISOTOPES Fe-57
energy level at 14.4 kev, half life of, (E), 20: 40132
hyperfine structure coupling in iron–rhodium alloys, (E), 20: 39470(R) (ORNL-3924)
Mössbauer effect in cobalt iron silicides, 20: 40300
Mössbauer effect in cobalt sulfates, 20: 40311

IRON ISOTOPES Fe-59
determination in blood using liquid scintillation counting, 20: 38555
kinetics of transfer in human serum, comparison with iron-56, 20: 38573
preparation of carrier-free, using Korean TRIGA Mark II reactor, 20: 39324
separation from waste-water by aerobic treatment, 20: 40483

IRON OXIDES
Fe_2O_3–MnO_2, sorptive properties for fission products, 20: 40476(R) (BNWL-267)

IRON(III) OXIDES
determination in swimming pool reactor coolant, activation and chemical, 20: 38800 (PAEC(C)RE-652)

IRON SYSTEMS
Co–Fe–Si, Mössbauer effect in, 20: 40300
Fe–H_2O, neutron flux distributions and spectra in shielding of, (E/T), 20: 40287

IRRADIATION FACILITIES
description of FRAN Prompt Burst Reactor, 20: 40463 (UCRL-14413)
design for food processing and sterilization of medical supplies, 20: 39282 (DP-1066(Vol.1), pp III.3-32)
design for radiosterilization, 20: 39285 (DP-1066(Vol.1), pp IV.33-42)
design of UK, 20: 39283 (DP-1066(Vol.1), pp III.33-44)
design of, for liquids and gases, using electrons to 10^7 rad/sec, 20: 38947
operation of FRAN Prompt Burst Reactor, 20: 40463 (UCRL-14413)
shielding design for reactor, variable, 20: 40369(P)

IRRADIATIONS
control of accelerator, equipment for, 20: 39507

ISOBUTYRALDEHYDE
determination in irradiated fruit juices, chromatographic, 20: 39300

ISOTOPE EFFECTS
of deuterium on radiationless decay of anthracene triplet, 20: 38958
on crystal properties of lithium hydride, 20: 40351
on hydrogenation of ethylene and propylene over palladium deuteride and hydride, 20: 38908
on sodium methoxide-promoted elimination reaction of 2,2-diphenylethyl benzenesulfonate, 20: 38912

ISOTOPE SEPARATION METHODS
columns with successive exchange among three fluids for continuous, theory of, 20: 39005
performance of hot-wire thermal diffusion, 20: 39323

ISOTOPES
uses of, in ground-water hydrology, evaluation of, 20: 39142

ISOTOPIC EXCHANGE
between iodine and 1-phenyl-2, 3-dimethyl-4-iodopyrazolone, effects of aromatic azines on, 20: 38936
columns with successive exchange among three fluids for continuous, theory of, 20: 39005
of iodine-131 between 1-iodo-2,4-dinitronaphthalene and potassium iodide, 20: 38916

ITALY
levels of cesium-137 and strontium-90 in the diet and urine in children in, 20: 39152
nuclear power development in, 20: 40441
nuclear power use in, for electricity production, 20: 40442

J

JAPAN
fallout content in soil of, effects of soil particle size on, 20: 39112
fallout monitoring, 1965, 20: 39108
fallout monitoring, 1962, 20: 39109
fallout monitoring, 1962 and 1964, 20: 39110
fallout monitoring, 1961 to 1963, 20: 39111
nuclear ship classification guide, 20: 40448 (NP-16217)

JOURNAL BEARINGS
properties of liquid-metal-lubricated, 20: 39008(R) (SWRI-1228-8-24)

K

KEROSENE
properties for use in stacked-clone contactor, 20: 38998(R) (ORNL-3958)
KETENE
radioinduced polymerization of, 20: 38977(P)
KIDNEYS
analysis for cadmium in human, activation, 20: 38845
effects of Thorotrast administration on human, 20: 38756
radiation sickness effects on function and morphology of dog, protective effects of unithiol against, 20: 38719
KRYPTON
diffusion from sodium at high temperatures, factors affecting, 20: 40357 (NAA-SR-11766)
neutron scattering by, cross sections and electron-neutron interaction from thermal, (E), 20: 40129
proton scattering at 3 to 6 Mev, differential cross sections for elastic and inelastic, (E), 20: 39470(R) (ORNL-3924)
release rate from pools of water, 20: 39103(R) (BNWL-235, pp 51-69)
KRYPTON ISOTOPES
thermal diffusion factor for, temperature dependence in, 20: 39326
KRYPTON ISOTOPES Kr-79
electron capture ratios, M/L, 20: 40153
KRYPTON ISOTOPES Kr-84
separation from krypton-86 by thermal diffusion, 20: 39321(R) (MLM-1312)
KRYPTON ISOTOPES Kr-85
preparation for use as beta source, 20: 39294
separation from xenon by chromatography, 20: 39321(R) (MLM-1312)
tracer use in atmospheric diffusion studies, 20: 39105
use in gaging foil thickness, 20: 39292
KRYPTON ISOTOPES Kr-86
separation from krypton-84 by thermal diffusion, 20: 39321(R) (MLM-1312)

L

LABORATORIES
design at ORNL for plutonium fuel cycle development, 20: 39024 (ORNL-TM-1268)
design for ANL fast breeder reactors, 20: 40414 (TID-23257(Vol.2))
radiation protection in, conference on, 20: 39166
use for neutrino and cosmic-ray research, deep underground, 20: 39016 (COO-818-94)
LABORATORY EQUIPMENT
design of automatic handling and measuring equipment, 20: 39044(P)
design specifications for radioisotope, in France, 20: 39295
LANTHANUM
determination in magnesium alloys by successive potentiometric titration, 20: 38830
diffusion from sodium at high temperatures, factors affecting, 20: 40357 (NAA-SR-11766)
separation and purification of barium-140 from, 20: 39001
separation from cerium by solvent extraction using tertiary amines and diethylenetriaminopentaacetic acid or EDTA, 20: 38995 (BM-RI-6809)
shock compression of, 20: 39425(T)
superconductivity of, 20: 40047
LANTHANUM ALLOYS
Gd–La, phase transformations and magnetic ordering in, pressure-induced, 20: 40326
La–Pb–Zn, component distribution in recrystallized, 20: 39435
La–Y, phase transformations and magnetic ordering in, pressure-induced, 20: 40326
La–Zn, crystal structure of intermetallic compound $LaZn_{13}$ in, 20: 39417
LANTHANUM BROMIDES
electron paramagnetic resonance spectrum of neodymium-doped, 20: 40312
LANTHANUM CHLORIDES
gadolinium ion exchange interactions in, temperature and separation effects on, 20: 38914
heat of dilution of aqueous solutions of, 20: 38870 (IS-1356)
ionic transport coefficients for, at 25°C, 20: 38909
radiation effects on spin-lattice relaxation time of praseodymium ions in, neutron and x, 20: 40350
specific gravity and apparent molal volume of aqueous solutions of, at 25°C, 20: 38905
spin lattice relaxation times of rare earth ions in, 20: 40350
thermal capacity of aqueous solutions of, at 25°C, 20: 38906
viscosity of aqueous solutions of, at 25°C, 20: 38904
LANTHANUM COMPLEXES
with Xylenol Orange, composition and chemical properties of, 20: 38924
LANTHANUM FLUORIDES
dielectric behavior of single-crystal, (E), 20: 40304
polarization in single-crystal, (E), 20: 40304
LANTHANUM ISOTOPES La-138
neutron reactions at 0.2 ev to 2 kev, resonance parameters from, (E), 20: 39470(R) (ORNL-3924)
LANTHANUM ISOTOPES La-140
content in fallout from USSR nuclear test, Jan. 1965, 20: 39108
decay curves for precursors of, 20: 40357 (NAA-SR-11766)
LANTHANUM NITRATES
specific gravity and apparent molal volume of aqueous solutions of, at 25°C, 20: 38905
LANTHANUM OXIDES
diffusion of oxygen in, tracer studies of, 20: 38865(R) (COO-1109-22, Paper 4)
electrical measurements on, for MHD generator electrodes, (T), 20: 39708
actinide oxides–La_2O_3, preparation of sols of, 20: 39341(P)
LANTHANUM SELENIDES
crystal structure of, reflection spectra for zonal, (E), 20: 40339
LANTHANUM SELENITES
heat of formation of, at 298°C, 20: 38900
LANTHANUM SULFATES
electron paramagnetic resonance spectrum of neodymium-doped, 20: 40312
heat of solution, 20: 38900
LARYNX
radiotherapy of cancer of, late pathological effects of γ, 20: 38773
radiotherapy of cancer, of x, 20: 38782
LEACHING
method for grind-, of graphite-matrix fuels, 20: 38998(R) (ORNL-3958)
method for shear, of metal-clad uranium dioxide fuels, 20: 38998(R) (ORNL-3958)
LEAD
content in minerals in Sweden, 20: 39125
dispersion in graphite, optimum pressure and temperature for liquid, 20: 39355 (EUR-2988.f)
effects of medium of, on gamma energy spectra, (E), 20: 40290
electric discharge explosion of wires of, MHD instabilities in, 20: 39010
electron inelastic scattering at 1 to 10 Mev, partial wave analysis of, (T), 20: 40150
gamma attenuation calculations for, build-up factor effects on, 20: 40289
infrared absorption by superconducting films of, effects of magnetic fields on, (E), 20: 40044
meson (μ^-) capture by, neutron angular distributions from, (E), 20: 40096
neutron reactions at 30 kev, effective cross sections for, (E), 20: 40069(R) (EANDC(E)-66(U))
separation from bismuth in acid solution by solvent extraction using alkyl phosphates, 20: 38828
superconducting critical field in cerium-doped, 20: 40050
superconductivity up to 160 kbar, (E), 20: 40040
superconductivity of, 20: 40047
surface resistance of superconducting, 20: 40042
thermal resistivity in intermediate-state superconducting, size effect in, (E), 20: 40022
LEAD ALLOYS
Al–Bi–Cu–Pb, fatigue failure of 2011-T3, equations for, 20: 39396 (IS-T-60)
In–Pb, calorimetry on superconducting, isothermal, (E), 20: 40045
Pb–rare earths–Zn, component distribution in recrystallized, 20: 39435
Pb–Tl, calorimetry of superconducting, isothermal, (E), 20: 40045
LEAD IONS
effects on positronium formation, 20: 38860 (COO-1297-6)
LEAD ISOTOPES Pb-206
content in minerals in Sweden, 20: 39125
proton inelastic scattering at 21 Mev, 20: 40074 (LA-DC-8069)
LEAD ISOTOPES Pb-207
content in minerals in Sweden, 20: 39125
proton inelastic scattering at 21 Mev, 20: 40074 (LA-DC-8069)
LEAD ISOTOPES Pb-208
content in minerals in Sweden, 20: 39125
deuteron reactions (d,p) at 4 to 7 Mev, subcoulomb stripping, 20: 40065(R) (BMwF-FB-K-66-01)
proton inelastic scattering at 21 Mev, (E), 20: 40074 (LA-DC-8069)
LEAD ISOTOPES Pb-212
concentration in air in Braunschweig, Germany, 20: 39119
LEAD ISOTOPES Pb-214
concentration in air in Braunschweig, Germany, 20: 39119
content in precipitation, effects of meteorological parameters on, 20: 39106 (BMwF-FBK-65-05)
LEAD OXALATES
radiation effects on rate of decomposition of, beta and gamma, 20: 38955
LEAD OXIDES
phase transformations, effects of pressure and irradiation on solid-solid, (E), 20: 40306

LEAK DETECTORS
design and operation of vacuum pump-leak detection system, 20: 39096 (AECD-EP-11)
design for measuring Freon concentration, 20: 39017(R) (DP-1053)
LEAKS
detection of, in or around carbon beds, 20: 39017(R) (DP-1053)
LECTURES
on charged particle beam optics, 20: 39483 (CERN-66-21)
on problems in elementary particle theory, 20: 39917
on properties and synthesis of transuranic elements, 20: 40139
on SU(3) symmetry, 20: 39862 (NP-16242)
LEUKEMIA
effects of methylhydrazine on response to immunotherapy of mice with, 20: 38794
etiology of childhood, review of, 20: 38668
radiation effects on growth of injected lymphoma cells in mice, x, 20: 38699
radiation effects on response to immunotherapy of mice with, 20: 38794
radioinduced in mice, effects of AET and endotoxin on x, 20: 38715
radioinduced in mice, protective effects of 5-methoxytryptamine and propamine against, 20: 38722
LEUKOCYTES
granulocytic migration in irradiated rabbit connective tissue, 20: 38640
radiation effects on granulocyte output from bone marrow in rabbits, effects of humoral agent on x, 20: 38633
radiation effects on content in blood, effects of adrenaline on x, 20: 38678
radiation effects on rabbit, biochemical and morphological, x, 20: 38681
radiation effects on content in rabbit blood of, x, 20: 38686
radioinduced chromosome aberrations in, 20: 38593 (ORNL-P-2175)
LEUKOPENIA
effects of blood transfusions on, in cancer patients during radiotherapy, 20: 38768
LEVEL INDICATORS
design of radiometric, 20: 39042(P)
LIFE SPANS
radiation effects on mouse, whole-body life, 20: 38590(R) (NYO-1979-13)
radiation effects on, in genetically homogeneous mouse populations, x, 20: 38648
shortening of, in irradiated mice given ^{137}Cs and ^{90}Sr in drinking water, 20: 38551
LIGHT
effects on bacteria, biological, effects of acriflavine on, 20: 38611
effects on plant embryos, biological, 20: 38588(R) (COO-1400-10)
scattering by liquid helium II, acoustic phonon attenuation and velocity from, 20: 40034
LIGHT SOURCES
design of, using gaseous radionuclide and phosphor for timepieces, 20: 39296(P)
LIMESTONE
oxygen-16/-18 fractionation between dolomites and, 20: 39129
LINEAR ACCELERATORS
beam injection system for, design and construction of, 20: 39489(R) (EGG-1183-2050)
development for simulation of weapons, 20: 39487(R) (EGG-1183-2009)
development for simulation of weapons, 20: 39489(R) (EGG-1183-2050)
development for weapons simulation, 20: 39488(R) (EGG-1183-2027)
development for weapons simulation, 20: 39490(R) (EGG-1183-2051)
drift tube for proton, operation of multistem, 20: 39478 (BNL-10376)
electron gun for, design of high current, 20: 39490(R) (EGG-1183-2051)
engineering problems of, for pulsed neutron source, 20: 40455 (BNL-10454)
modulator system for Los Alamos 800 Mev proton, 20: 39493 (LA-DC-7776)
operational theory of, 20: 39482 (CERN-66-20)
properties of, for use in food sterilization studies, 20: 39303
LIPIDS
determination in blood, micro colorimetric method for, 20: 38652
peroxides of, formation in mitochondria, effects of iron on, 20: 38639
radiation effects on formation of peroxide, in lysosomes of rat liver, x, 20: 38577
radiation effects on content of rat adrenal, x, 20: 38701
radiation effects on rat metabolism of, dietary effects of B group vitamins, folic acid, and phosphatides on gamma and x-ray, 20: 38721
radiation effects on content in blood, 20: 38652
radiation effects on, in meats and meat components, 20: 39301
LIQUID FLOW
magnetohydrodynamic, in curved pipe, (T), 20: 39931
LIQUID JETS
propagation of conducting, in magnetic field, 20: 39934
LIQUID METAL COOLED REACTORS
boiler design for, 20: 40424
design of electric generators for use with, 20: 40414 (TID-23257(Vol.2))
development of power breeder, at ANL, 20: 40413 (TID-23257(Vol.1))
development of, by Atomic Power Development Associates, 20: 40355 (APDA-TPI-1)
economics of fast power breeder, 20: 40415 (TID-23257(Vol.3))
steam generator design for sodium-cooled, French program for, 20: 40428
LIQUIDS
infiltration of, into porus solids, 20: 39099(R) (BNWL-235-3, pp 1-23)
neutron inelastic scattering by, dynamic processes in slow, 20: 40338
vaporization of wetting and nonwetting, 20: 39091
gas–liquid, convective transfer processes in flow of, 20: 39050 (UCRL-16535)
LITHIUM
determination in mineral and natural waters, flame photometric, 20: 38798 (NIJS-R-465)
electric dipole moments of, ratio of atomic to electron, 20: 39598
electron interactions with atomic, electron exchange in, 20: 39582(T) (AERE-Trans-1053)
electron scattering by, ionization cross sections for, (T), 20: 39607
energy spectra from beryllium-9–nitrogen-14 reactions at 25 Mev, 20: 40065(R) (BMwF-FB-K-66-01)
neutron reactions at 4.2 to 6.1 Mev, total cross sections for, (E), 20: 40069(R) (EANDC(E)-66(U))
proton scattering by, ionization cross sections for, (T), 20: 39607
use in two-phase MHD cells, (T), 20: 39634 (JPL-32-946)
LITHIUM CHLORIDES
ionic transport coefficients for, at 25°C, 20: 38909
LITHIUM FLUORIDES
radiation effects on dissolution spirals on surfaces of etched, gamma, 20: 40293 (AD-634746)
radioinduced thermoluminescence of, effects of radiation quality on beta and gamma, 20: 39199 (COO-1105-117)
radioinduced thermoluminescence of, temperature effects on gamma, 20: 39200 (COO-1105-118)
second sound in solid, 20: 40327
x-ray diffraction analysis at 5.898 kev, 20: 40294
LITHIUM HYDRIDES
crystal properties of, infrared reflection studies of, 20: 40351
molecular structure of, calculation of natural orbital-based energy for, 20: 38910
LITHIUM IODATES
iodine-131 beta decay in, properties of xenon oxide compounds formed by, 20: 38984
LITHIUM ISOTOPES
abundance in Bjurbole and Bruderheim meteorites, 20: 39102
LITHIUM ISOTOPES Li-6
abundance in stellar atmospheres and depletion during stellar evolution, 20: 39574
gamma reactions (γ,p) at 100 Mev, proton energy spectra and angular distributions from, (E), 20: 40077 (MIT-2098-256)
isotope effects on crystal properties of lithium hydride, 20: 40351
photon reactions with, differential cross sections for meson ($\pi^{\pm}$) production in, (E), 20: 40075 (LNF-66/30)
reactions with light nuclei, reduced cluster widths for, 20: 40086
LITHIUM ISOTOPES Li-7
abundance in stellar atmospheres and depletion during stellar evolution, 20: 39574
alpha elastic and inelastic scattering at 1.6 to 12.0 Mev, boron-11 energy levels from, (E), 20: 40111
helium-3 reactions (He-3,n) at 1.5 to 5.5 Mev, boron-10 energy levels from, (E), 20: 40112
isotope effects on crystal properties of lithium hydride, 20: 40351
photon reactions with, differential cross sections for meson ($\pi^{\pm}$) production in, (E), 20: 40075 (LNF-66/30)
reactions with light nuclei, reduced cluster widths for, 20: 40086
LITHIUM NITRATES
effects on separation of rare earths by solvent extraction, 20: 38995 (BMI-6809)
radiolysis of frozen, at 77°K, yields of nitrite ion from gamma, 20: 38950
$LiNO_3$–D_2O, phase diagram of, 20: 38994(R) (AE-232)
$LiNO_3$–H_2O, phase diagram of, 20: 38994(R) (AE-232)
LIVER
cholesterol metabolism in rat, effects of tritium oxide perfusion on, 20: 38559
effects of hepatectomy on phosphorus metabolism in rats, effects of reticulin on, 20: 38572
fatty acid metabolism in rat, effects of tritium oxide perfusion on, 20: 38559
glucuronidase and phosphatase content in subcellular fractions of rat, 20: 38595(R) (ORO-3295-2)
pathology of cerium-144-induced cirrhosis in rat, 20: 38567

radiation effects on DNA synthesis in tissues of, 20: 38576 (TID-22103)
radiation effects on mitochondria of rat, biochemical and morphological, x, 20: 38639
radiation effects on ultrastructure of rabbit, effects of cysteamine on, x, 20: 38716
radiation effects on rat, dietary effects of B group vitamins, folic acid, and phosphatide on gamma and x-ray, 20: 38721
radiation injuries to animal, in death from acute radiation sickness, 20: 38666
radioinduced enzyme release from lysosomes of rat, electron beam and x, 20: 38577
radiosensitivity of rat, effects of thioacetamide on x, 20: 38694

LOOPS
design and operation of, for evaluating isopropylbiphenyl working fluids, 20: 40449(R) (SAN-650-1)

LOS ALAMOS TURRET REACTOR
description of, 20: 40474

LUBRICANTS
preparation of radioresistant, 20: 38973(P)
radiation effects on hydrocarbon–styrene polymeric, 20: 38973(P)

LUMINESCENT DETECTORS
performance of metaphosphate glass for γ dosimetry during implant therapy, 20: 38778
response of lithium fluoride, to fast neutrons, 20: 39219

LUNGS
actinium 227 clearance from, biological half-life for, 20: 38554
radiation effects on megakarocytes of patients with carcinoma of, γ, 20: 38643
radiation sickness effects on blood circulation in rabbit, 20: 38657
radiotherapy in conjunction with surgery for cancer of, 20: 38755

LUTETIUM
determination in solutions, spark method for spectrographic, 20: 38832
superconductivity of, 20: 40047
x-ray absorption spectra of, (E), 20: 39613

LUTETIUM ALLOYS
Lu–Ni, crystal structure of intermetallic compounds in, 20: 39415
Lu–Zn, crystal structure of intermetallic compounds Lu_6Zn_{23}, Lu_2Zn_{17}, and $LuZn_{12}$ in, 20: 39417
Pb–Lu–Zn, component distribution in recrystallized, 20: 39435

LUTETIUM COMPLEXES
with Xylenol Orange, composition and chemical properties of, 20: 38924

LUTETIUM ISOTOPES Lu-175
energy levels of, M1 transitions of rotational, (E), 20: 40072 (LA-DC-8061)

LUTETIUM OXIDES
actinide oxides–Lu_2O_3, preparation of sols of, 20: 39341(P)

LUTETIUM PHOSPHATES
preparation and properties of, conductometric and potentiometric studies on, 20: 38883

LYMPH
phosphate uptake by ribonucleotides of, effects of gamma dose, 20: 38585

LYMPH CELLS
radiation effects on formation in lymphatic tissue, 20: 38612
radiation effects on content in blood, effects of adrenaline on x, 20: 38678
radioinduced chromosome anomalies in human, x, 20: 38615

LYMPH SYSTEM
radiation effects on, biological, x, 20: 38612
radiosensitivity of, γ, 20: 38773
uptake of Thorotrast into, following pyelography, 20: 38756

LYSOSOMES
radioinduced enzyme release from rat liver, mechanisms for electron beam and x, 20: 38577

M

MACHINE TOOLS
diameter gage for, 20: 39032
power requirements of, for uranium, 20: 39027 (Y-DA-1287)

MACHINING
interferometer design for, 20: 39031
temperature effects on accuracies in, 20: 39009 (UCRL-14944)

MAGNESIUM
content in fallout from Chinese atomic test, Oct. 1964, 20: 39110
determination in aluminum by neutron activation methods, 20: 38804
determination in biological materials, radiochemical separation methods for activation, 20: 38842
determination in biological materials, use of automated gamma spectrometers in activation, 20: 38843
determination in erythrocytes and plasma in human blood, activation, 20: 38852
determination in mineral and natural waters, flame photometric, 20: 38798 (NIJS-R-465)
dispersion in graphite, optimum pressure and temperature for liquid, 20: 39355 (EUR-2988.f)
reduction of uranium(IV) fluoride, process for, 20: 39342(P)

MAGNESIUM ALLOYS
analysis for rare earths by successive potentiometric titration, 20: 38830
properties as fuel-element cladding, 20: 39443(P)
Al–Mg, fatigue of Magnox Al80, plastic strain range at 350 to 500°C, 20: 39419

MAGNESIUM CHLORIDES
spectra of liquid, Raman, 20: 38871(R) (NYO-1769-54)
$MgCl_2$–KCl, spectra of liquid, Raman, 20: 38871(R) (NYO-1769-54)
$MgCl_2$–Na_2CO_3–$UO_2(NO_3)_2$, uranium precipitation in, mechanism of, 20: 38928

MAGNESIUM HYDROXIDES
radiation effects on rate of decomposition of, beta and gamma, 20: 38955

MAGNESIUM ISOTOPES Mg-24
deuteron reactions (d,α) at 11.45 to 12.1 Mev, angular distributions from, 20: 40065(R) (BMwF-FB-K-66-01)

MAGNESIUM ISOTOPES Mg-25
deuteron reactions (d,α) at 11.45 to 12.1 Mev, angular distributions from, 20: 40065(R) (BMwF-FB-K-66-01)

MAGNESIUM ISOTOPES Mg-26
proton reactions (p,p) at 8.34 and 14 Mev, statistical fluctuations in cross section for, 20: 40065(R) (BMwF-FB-K-66-01)
proton reactions (p,α) at 11 and 13.26 Mev, statistical fluctuations in cross sections for, 20: 40065(R) (BMwF-FB-K-66-01)

MAGNET COILS
design and performance of superconducting, for MHD power generation, 20: 39643
design for electromagnetic metal forming, 20: 40490 (Y-1483)
design of superconducting, for, 20: 40169 (NASA-TN-D-3595)
development of superconducting, 20: 40014(R) (ORNL-3989, pp 109-27)
performance of niobium–zirconium superconducting, 20: 40015(R) (ORNL-TM-1598)
testing of large superconducting, facility for, 20: 40049

MAGNETIC FIELDS
calculation for synchrocyclotrons, computer program for, 20: 39537
charged particle motion in non-resonant h-f and, 20: 40193
charged particles in, magnetic moment of gyrating, (T), 20: 40229
charged-particle motion in quadrupole, equations for, 20: 39484 (CERN-66-21, pp 1-30)
charged-particle motion in crossed electric and, (T), 20: 40243
determination for magnetic lenses, (T), 20: 39011
effect on cathode jets in impulse discharge of transverse, (E), 20: 40232
effects of inhomogeneities of, on flow in Hall-type MHD generators, (T), 20: 39692
effects on flow of jet of conducting liquid, 20: 39934
effects on infrared absorption by superconducting lead films, (E), 20: 40044
effects on parallel fluid flow, (T), 20: 39943
effects on thermal convection in conducting fluid, 20: 39939
electron gas transport properties in, (T), 20: 40183
fluid flow past porous flat plate under transverse, (T), 20: 39929
flux explosion of by eddies, (T), 20: 39567
flux trapping in, effects on r-f losses in superconductors, 20: 40042
flux variations in, of sunspots and faculae, 20: 39561(T)
intensity variations in sun spot groups, (T), 20: 39559
interaction of solar wind with sun's, (T), 20: 39573
interactions with plasma, particle trajectories in, (T), 20: 40283
interplanetary, connection of geomagnetic tail lines to, 20: 39986
measurement of internal, in solids, 20: 40342
model for quiet interplanetary, 20: 39575
plasma acceleration in external, induction effects on, (T), 20: 40192
plasma acceleration in, theory of supersonic, (T), 20: 40240
plasma acceleration in r-f and static, (E/T), 20: 40268
plasma column expansion in longitudinal, (T), 20: 40237
plasma containment in spherical cavity, (T), 20: 40277
plasma containment and heating in low-frequency rotating, (E/T), 20: 40279
plasma containment in closed mixed electric and, 20: 40280
plasma injection in multipole, transverse, (E), 20: 40254
plasma instabilities due to longitudinal, (T), 20: 40239
plasma jet interaction with, (T), 20: 40231
plasma kinetics in strong electric and, 20: 40249
plasma stability in, flute, 20: 40217(T)
production of intense, from electron beam injection in rotating, 20: 40282
shielding of space vehicles with, 20: 40292
star formation in rotating, (T), 20: 39568
structure of solar, flare effects on, 20: 39557

structure of solar, flare effects on, 20: 39558
variations in interplanetary, (E), 20: 39575
wave propagation across, theory of nonlinear, (T), 20: 40235

MAGNETIC MIRROR MACHINES
plasma containment in Probkatron, properties of, 20: 40194
plasma electron cyclotron heating in ELMO, 20: 40173(R) (ORNL-3989, pp 31-42)
plasma heating in QP, ion cyclotron resonance, 20: 40260
plasma stability in, flute, 20: 40217(T)

MAGNETIC MIRRORS
ion flow in, due to turbulent diffusion, (T), 20: 40236
plasma containment by, superconducting magnetic coils for, 20: 40169 (NASA-TN-D-3595)

MAGNETO-OPTICAL ROTATION
induction in type II superconductors, Faraday unipolar, 20: 40016

MAGNETOHYDRODYNAMIC CELLS
air preheater for power plants, high-temperature regenerative, (E), 20: 39725
air preheating for open-cycle, (T), 20: 39653
alkali metal gaseous compounds for, spectrometry of, 20: 39724
characteristics of closed-cycle, for reactor power conversion, (T), 20: 39682
characteristics of sub-atmospheric, (E), 20: 39709
characteristics of linear and turbulent, (T), 20: 39707
conductivity of helium-3 plasma in, neutron-induced, 20: 39683
conductivity of potassium-seeded argon plasma in, nonequilibrium, (T), 20: 39684
current distribution in, with segmented electrodes, (F/T), 20: 39718
design of ARGAS closed-loop, 20: 39680
design of high efficiency, using coal burned in oxygen to produce plasma, 20: 39043(P)
design of large combustion-fired generator, 20: 39654
design of open-cycle, with high preheat temperature of air, 20: 39689
dimensions of induction, reduction by skin heating of, (T), 20: 39693
duct design for, conditions for minimum volume, (T), 20: 39664
duct volume minimization in, 20: 39703
efficiency and thermodynamic, parameters for closed-loop, (T), 20: 39720
efficiency of close-cycle nuclear, (T), 20: 39728
efficiency of liquid-metal, (E), 20: 39716
efficiency of power plants with, (T), 20: 39732
efficiency of power stations using, effect of various parameters on, (T), 20: 39705
efficiency of two-phase liquid-metal, (T), 20: 39634 (JPL-32-946)
electric conductivity of two-phase potassium mixture for, (E), 20: 39742
electric conductivity in seeded argon plasma in, (E), 20: 39727
electric parameters of synchronous, (T), 20: 39676
electric properties of linear Hall- and Faraday-type, 20: 39640
electric properties of supersonic, with arc-heated argon plasma, 20: 39646
electrical equivalent circuits of, (T), 20: 39696
electrical insulation of, high-alumina concrete for, (E), 20: 39698
electrode effects on electrical parameters of, (T), 20: 39697
electrode materials for, electrochemical properties of, (E), 20: 39723
electrode performance in, high-melting, (E), 20: 39736
electrodes for, material testing for, (T), 20: 39708
electromagnetic properties of dense plasma in variable field, (E), 20: 39739
electron temperature and density in, relaxation lengths of, (T), 20: 39674
end effects in induction, (T), 20: 39717
energy conversion in, use of ducts of disk geometry for, (T), 20: 39663
explosive-driven, effects of curved duct on, (E), 20: 39694
flow conversion in, effects of instability and turbulence on inhomogeneous, (E), 20: 39704
flow in Hall-type, effects of field inhomogeneities on, (T), 20: 39692
flow of conductivity fluid in Hall-type, (T), 20: 39685
flow processes in, efficiency of striated-, (T), 20: 39737
fluid dynamics in large, (T), 20: 39729
fuel for, thermodynamic properties of oil combustion products for, 20: 39938
gas as working fluid in, properties of seeded combustion, 20: 39636
gas flow at duct outlet, recovery of residual enthalpy in, (T), 20: 39658
gas superheating in, use of shock waves for, (T), 20: 39686
Hall phenomena in combustion-product plasma in, (E), 20: 39740
injection of liquid metals in, 20: 39669
liquid-metal cycles in, properties of, 20: 39726
liquid-metal emulsions for, (T), 20: 39678
losses near walls in, effects of ionization saturation and geometry on, (F), 20: 39673
magnet design optimization for MHD generators, 20: 39668
magnets for, design and performance of superconducting, 20: 39643
materials for walls and electrodes, production and testing of, 20: 39690
materials limitations in induction, (T), 20: 39731
operation at large Hall parameters and Mach numbers, 20: 39667
operation in nonequilibrium mode without seeding, (E), 20: 39679
operation of closed-loop, at International Research and Development Co., Ltd., 20: 39687
operation of CNEN blow-down loop, 20: 39675
operation of open-cycle kerosene-burning, (E), 20: 39688
operation of 100-kw model, 20: 39672
operation of, power plants with, (T), 20: 39741
operation with potassium-seeded fossil fuel, 20: 39695
optimization of open-cycle power plants, (T), 20: 39719
performance calculation of idealized, with nonequilibrium electron heating, 20: 39647
performance of diagonal-wall, (E), 20: 39702
performance of Faraday-type, 20: 39645
performance of open-cycle, facility for evaluating, 20: 39667
performance of segmented-electrode, effect of wall conductance on, (T), 20: 39712
performance of, effects of ion slip and electrode segmentation on, (T), 20: 39713
performance of, electrode current saturation effects on, (E), 20: 39660
performance of, with electrodes of finite length and segmentation, (T), 20: 39661
plasma dynamics in Hall-type, (T), 20: 39735
plasma flow in, boundary layer on insulator walls for, (T), 20: 39933
plasma flow in, optimum Mach number for, (T), 20: 39691
power density in non-steady modulated, (T), 20: 39730
properties of high-density plasma working fluid, (T), 20: 39656
radiative losses in closed-cycle 300-Mw, 20: 39681
relaxation phenomena in, (T), 20: 39700
superconducting magnet for, (E), 20: 39733
thermal radiation flux from potassium-seeded flames, (E), 20: 39710
use of shock-wave, with high-temperature gas-cooled reactor for power source, 20: 39639

MAGNETOHYDRODYNAMICS
conductivity of cesium plasma, effect of gaseous impurities on, (E), 20: 39659
current-voltage curves for moving argon plasma, (E), 20: 39655
electric discharge in conducting jet of viscous fluid, (T), 20: 40241
electric discharge experiments on alkali-seeded inert gases, (E), 20: 39715
electrical insulators for MHD flow, (E), 20: 39657
electromagnetic field distribution in conducting slab, effect of toothed inductor on, (T), 20: 39937
electron density and temperature of cesium-seeded helium plasma, (E), 20: 39665
electron density in one-dimensional channel flow, non-equilibrium excitation effects on, (T), 20: 39714
electron distribution function and state populations in non-equilibrium, (T), 20: 39711
flow of cylindrical conducting gas column in longitudinal magnetic field, 20: 40237
flow of sodium in rectangular duct, (E), 20: 39706
flow of viscous electrically conducting fluid past semi-infinite plate, (T), 20: 39945
fluid flow boundary layer around body in magnetic fields, 20: 39935
fluid flow boundary layer over stationary base, rotational, 20: 39936
fluid flow in annular channel, incompressible electrically conducting, (T), 20: 39942
fluid flow in magnetic field, natural and forced thermal convective, (T), 20: 39930
fluid flow in, theorems for highly conducting viscous, 20: 39932
fluid flow past porous flat plate under transverse field, (T), 20: 39929
liquid flow in curved pipe, (T), 20: 39931
plasma stability theory in, (T), 20: 40239
shock waves with finite electrical conductivity in, 20: 39944
use for increasing load capacity of bearings, 20: 40216

MAGNETOSPHERE
charged particle trapping in, magnetic coordinates for analyzing, 20: 39989
charged-particle geomagnetic cut-off rigidities in, 20: 39988
electron density and temperature profiles in, 20: 39978
hydrodynamic wave propagation in, low-frequency, 20: 40224
interaction of solar corpuscular streams with, magnetic field effects on, 20: 39963(T)
structure, 20: 39957(T)

MAGNETS
design for space vehicle shielding, 20: 40291
design for velocity spectrometer, 20: 39502
design of pulsed step, for Bevatron beam control, 20: 39508
design of superconducting, for magnetic bottle, 20: 40169 (NASA-TN-D-3595)
design of 40,000-gauss superconducting, 20: 40018

design optimization for MHD generators, 20: 39668
development for ion engines, 20: 39093
magnetic center of, equipment for measuring, 20: 39503
performance of superconducting, for MHD generators, (E), 20: 39733
properties of strong-focusing, 20: 39494 (LNF-66/15)
properties of two-dimensional, computer program for solving mathematical models for, 20: 39499 (UCRL-16959)

MAGNOX ALLOYS
fatigue of A180, plastic strain range at 350 to 500°C, 20: 39419

MAIZE
radiation effects on, genetic, uv and x, 20: 38617

MALATHION
labeling with phosphorus-32 and sulfur-35, 20: 38931

MALEIC ANHYDRIDE
effects on radioinduced polymerization of cyclic ethers, 20: 38953

MAMMALS
cesium-137 content in whales,, 20: 38560
iodine-131 uptake by thyroid gland of, effects of diet on, 20: 38549 (UCLA-12-592)
manganese-54 content in whales, 20: 38560
zinc-65 content in whales, 20: 38560

MAMMARY GLAND
radiation injuries of, in children treated for hemangiomas by radium, 20: 38787

MAN
actinium-227 distribution in, 20: 38554
analysis for trace elements in diseases in, activation, 20: 38847
biogenesis and metabolism of aldosterone in elderly, tracer study on, 20: 38547(R) (NYO-918-15)
cesium-137 content in India, 1962 through 1965, 20: 39154
cesium-137 excretion by, effects of Prussian Blue on biological half-life, 20: 38557
content of cesium-137, iodine-131, strontium-89, and strontium-90 in U. S., 1965, 20: 38743
determination of daughter products of radon and thoron in, following alpha radiotherapy, 20: 38775
effects of radioactivity in diet on carcinoma incidence in, 20: 38739
effects of radiosterilized food on, 20: 39302
iodine-131 content in thyroid in, activation studies on, 20: 38564
iodine-137 uptake by thyroid gland in adolescent and adult, 20: 38553
microwave effects on, pathological, 20: 38622
radiation dose from internally deposited strontium-90 in, effects on clinical findings, 20: 38623
radiation dose from internally deposited radium-226 in, effects on clinical findings, 20: 38623
radiation effects on, protection against, 20: 38718
radiation exposure, determination of LET in manned space vehicles, 20: 39158
radiation injuries of, diagnosis using leukocyte chromosome aberration analysis, 20: 38593 (ORNL-P-2175)
radiation injury in children treated for hemangiomas by radium, 20: 38787
radiation sickness diagnosis and therapy in, 20: 38774
radioactivity in diet of, effects of cesium-137, iodine-131, and strontium-90 in milk on, 20: 39157
radioactivity of, undergoing radioisotope therapy, 20: 38790
radioinduced carcinoma in children following radium therapy of hemangioma, 20: 38788
radiotherapy of malignant tumors of, using laser beams, 20: 38780
respiration and oxygen stores in, oxygen-18 isotopic dilution studies on, 20: 38941 (RRL-2310-182)
trace element adsorption and elution on hair of, tracer study, 20: 38543

MANGANESE
determination in blood in arthritic and healthy patients, activation, 20: 38845
determination in erythrocytes and plasma in human blood, activation, 20: 38852
determination in mosaic virus and nucleic acids in tobacco plants, 20: 38846
effect on properties of low-alloy steels for reactor pressure vessels, 20: 39444(P)
effects on properties of boron steel, 20: 39426
effects on properties of magnesium-base alloys for fuel-element cladding, 20: 39443(P)
neutron reactions at 50 to 260 kev, total cross sections for, (E), 20: 40069(R) (EANDC(E)-66(U))
separation of thorium-230 from, by ion exchange, 20: 38834

MANGANESE ALLOYS
Al–Mn–Y, crystal structure of intermetallic compounds in, 20: 39414
Au–Mn, gold-197 hyperfine structure coupling in, (E), 20: 39470(R) (ORNL-3924)
Cr–Co–Fe–Mn–Ni–W, tensile properties of L-605, effects of cold deformation on, 20: 39399 (NASA-TN-D-3528)
Mn–Ni, crystal structure of, neutron diffraction studies on, 20: 39407(T) (ANL-Trans-344)
Mn–Ni, phase studies, 20: 39407(T) (ANL-Trans-344)

MANGANESE DYSPROSIUM SELENIDES
preparation and crystal structure, 20: 38884

MANGANESE ISOTOPES Mn-54
content in whales, 20: 38560
electron capture ratios, M/L, 20: 40153

MANGANESE ISOTOPES Mn-55
neutron reactions (n,γ) with, resonance activation integral cross sections for, (E), 20: 40069(R) (EANDC(E)-66(U))
x-ray emission from, Kα, 20: 40294

MANGANESE OXIDES
preparation for controlled sorptive properties, methods for, 20: 40476(R) (BNWL-267)
sorptive properties of, effects of competing ions on, 20: 40476(R) (BNWL-267)
Fe_2O_3–MnO_2, sorptive properties for fission products, 20: 40476(R) (BNWL-267)

MANGANESE STEEL
radiation effects on fatigue of A302B, neutron, 20: 39406 (WAPD-T-1864)

MARITIME PRESSURIZED WATER REACTOR
fuel elements for, zero power testing of Core II, 20: 40445 (BAW-1225)

MARITIME REACTORS
bibliography on, 20: 40444 (AED-C-22-06)

MASERS (OPTICAL)
effects on tumors, use in radiotherapy, 20: 38780
excitation of Raman spectra of molten salts, method for, 20: 38872(R) (NYO-1769-68)
ionization of gases by intense, (E), 20: 40190
use in plasma electron density measurement, 20: 40226

MASS SPECTROMETERS
angle of incidence instrument for, 20: 39029

MASS TRANSFER
analysis of, design of equipment for, 20: 39050 (UCRL-16535)

MATERIALS TESTING
hardness, equipment for testing beryllium by impact, 20: 39436
method of, for installed carbon beds, 20: 39017(R) (DP-1053)
methods for explosive cartridges, radiographic, 20: 39334

MATHEMATICS
coordinates for charged particle trapping in geomagnetic fields, magnetic, 20: 39989
curve fitting in, Gaussian iterative least square techniques for, 20: 39327 (LA-3362)
formulae for calculation of rate of particle rainout from nuclear device cloud, 20: 39107 (UCRL-14700)
foundation for empirical science, 20: 39998 (KAPL-3147)
methods for reduction of crystal texture data to inverse pole figures, 20: 39402 (ORNL-3979)
research in progress under Army Research Office, 20: 40485(R) (AD-636091)
use of K-factors for reliability evaluation of test programs, 20: 40447 (NAA-SR-11913)

MATING
radiation effects on male eye gnat competitiveness in, 20: 38632

MATTER
particle reactions in, relaxation of nonstationary processes from finite transport velocity of, 20: 39475

MEATS
analysis for volatile compounds in irradiated, 20: 39301
radiation effects on flavor of beef, review of, 20: 39299
radiation effects on chemical changes in, 20: 39301

MECHANICAL ENGINEERING
analysis of creep in axisymmetric pressurized copper shells, 20: 39391 (CONF-660629-1)

MEDICAL PERSONNEL
determination of radiation exposure in radiology service, use of blood studies for, 20: 38781
nursing care of radium-implanted patients, 20: 38751
protection of, during operation of microwave equipment, 20: 38622
radiation monitoring of, using gold-198, 20: 39159

MEDICAL SUPPLIES
radiosterilization in Canada, 20: 39282 (DP-1066(Vol.1), pp III.3-32)

MEDICINE
radiation protection in the practice of dentistry, x, 20: 38793
veterinary, principles and use of radioisotopes in, 20: 38748

MEDITERRANEAN SEA
uranium-234/-238 ratio in, 20: 39133

MELAMINE, TRIETHYLENE-
effects on permeability of the blood-brain barrier in rats, 20: 38609

MEMBRANES
effects of radiomimetics on permeability of blood-brain barrier, 20: 38609

radiation effects on permeability of blood-brain barrier, x, 20: 38609
radiation effects on microflora of mucous, 20: 38644
MEMORY DEVICES
design for 100-channel pulse analyzer, 20: 39183
MERCURY
alkali atomic beam scattering at 7 to 500 ev, cross sections for, 20: 39599
current densities in cesium-seeded plasma of, (E), 20: 39736
dispersion in graphite, optimum pressure and temperature for liquid, 20: 39355 (EUR-2988.f)
electric properties of cesium-seeded plasma of, (E), 20: 39738
reactions of positive hydrogen ions with vaporous, formation of negative hydrogen ions from, (E), 20: 39500
superconductivity of, 20: 40047
MERCURY ALLOYS
Hg–Ag, uses as electrode in oscillographic determination of rare earths, 20: 38811
In–Hg, superconductivity of, effect of iron particles on, (E), 20: 40024
MESIC ATOMS
meson (μ) depolarization in, of spin-one nuclei, (T), 20: 39616
MESONS
decay of scalar, current commutation relations for determining coupling constants for, (T), 20: 39852 (INP-480/PL)
electric quadrupole moments of vector, 20: 39835
electromagnetic properties in non-relativistic quark model, 20: 39835
interactions of, $SU(6)_w$-symmetric bootstrap model of, 20: 39885
interactions with baryons, bootstrap static model of SU(6) symmetry for, 20: 39813
interactions with baryons, multichannel calculations in static model for, 20: 39887
interactions with baryons at low energies, nonrelativistic SU(6) symmetry for, 20: 39904
mass formulas in 405 multiplet of SU(6), 20: 39886
masses of, four-fermion-interaction theory for, 20: 39832
production in electron interactions with positrons, cross sections for, (T), 20: 39802
production in meson (π^-)-neutron interactions at 3.5 Bev/c, cross sections for, (E), 20: 39842
production of, accelerator development for, 20: 39534
production of, development of ETH Zurich cyclotron for, 20: 39533
production of, development of negative-hydrogen-ion cyclotron for, 20: 39540
MESONS, RESONANCE
existence of unitary multiplets of, 20: 39860 (JINR-P-2790)
production of A_1 (1090) and A_2 (1310) in deuteron-meson (π^+) interactions at 3.29 Bev/c, (E), 20: 39470(R) (ORNL-3924)
production of A_1 and A_2, in meson (π^-) interactions with protons at 7.0 Bev/c, 20: 39790
production of η^* (960), in meson (K^-)-neutron interactions at 2.24 Bev/c, (E), 20: 39786
production of K* in meson (K^-)-proton interactions at 1.80 to 1.95 Bev/c, 20: 39838
production of K*, in meson (π^-)-proton interactions at 1.6 to 4.2 Bev/c, (E), 20: 39770 (UCRL-16788)
production of K*, from meson (K)-nucleon interactions, (T), 20: 39778
production of L (1789), in meson (K^-)-proton interactions at 10 Bev/c, (E), 20: 39788
MESONS (B)
exchange in meson (π)-meson (ω) interactions, 20: 39807
MESONS (η)
decay of, C violation in $\pi^+\pi^0\gamma^-$, (E), 20: 39766 (ORO-3065-10)
decay of, $\pi^+\pi^-\gamma$, (E), 20: 39771 (UCRL-16923)
decay widths of, two-baryon approximation method for determining, 20: 39783
photoproduction on protons, lecture on, (E), 20: 39743 (CALT-68-92)
production in deuteron-meson (K^-) interactions at 0.9 to 1.12 Bev/c, (E), 20: 39747 (COO-881-75)
MESONS (K)
decay of, current-commutator calculation of four-body leptonic, (T), 20: 39815
decay of, Lagrangian model for form factors of three-body leptonic, 20: 39796
decay of, sum rules for CP-nonconserving, 20: 39812
interaction with nucleons, (T), 20: 39840
interactions with nucleons, K* production threshold from, (T), 20: 39778
pair production in meson (π)-meson (π) interactions at low energies, (T), 20: 39833
production in meson (K^+)-proton interactions at 3.52 Bev/c, (E), 20: 39784
production in proton reactions with beryllium and platinum at 2.9 Bev, (E), 20: 39794
MESONS (K^-)
interactions with deuterons at 0.9 to 1.12 Bev/c, $\Sigma^-\eta$ enhancement in, (E), 20: 39747 (COO-881-75)
interactions with neutrons at 2.24 Bev/c, η^* (960) production in, (E), 20: 39786
interactions with protons at 10 Bev/c, mesons (L) production in, 20: 39788
interactions with protons at 2 to 6 Bev/c, Regge-pole model for cross sections for, (E/T), 20: 39801
interactions with protons, absorptive peripheral model for charge-exchange, 20: 39805
interactions with protons at 1.80 to 1.95 Bev/c, resonance production in, (E), 20: 39838
MESONS (K^0)
decay of K_2^0, CP invariance in 3π, (T), 20: 39763 (JINR-P-2850)
decay of, coherent interference in $\pi^+\pi^-$, (E), 20: 39849
lifetime of K_2^0, (E), 20: 39849
mass difference K_2^0–K_1^0, sign of, (E), 20: 39772 (UCRL-17007)
MESONS (K^+)
decay of, energy spectra from 3π, 20: 39846
interactions with protons at 3.52 Bev/c, meson (κ) production in, (E), 20: 39784
interactions with protons, graphical method for charge independence in strong, 20: 39800
interactions with protons at 2 to 6 Bev/c, Regge-pole model for cross sections for, (E/T), 20: 39801
MESONS ($K^+_{\mu 3}$)
decay of, meson (π) energy spectra in, (E), 20: 39846
MESONS (L)
production in meson (K^-)-proton interactions at 10 Bev/c, 20: 39788
MESONS (μ)
capture by complex nuclei, effects of giant resonances in, 20: 40151
polarization in mesic atoms of spin-one nuclei, (T), 20: 39616
MESONS (μ^-)
capture by argon and argon–hydrogen gases, spectra from, 20: 39578 (JINR-P-2807)
capture of polarized, by copper, iron, and lead nuclei, neutron angular distributions from, (E), 20: 40096
MESONS (ω)
interactions with mesons (π), reciprocal bootstrap of mesons (ρ) and (B) in, 20: 39807
MESONS (ω^0)
decay of, $\pi^0 + \gamma$, (E), 20: 39787
photo-production on protons, mechanism of, 20: 39811
MESONS (π)
form factor for, Lagrangian models for charge, 20: 39796
interactions of, from meson (π^-)-proton interactions at 3 and 4 Bev/c, (E), 20: 39769 (UCRL-16655)
interactions with nucleons, Regge recurrence parity assignments in, (T), 20: 39749 (COO-881-77)
interactions with protons at high energies, review on elastic, (E/T), 20: 39744 (CERN-66-18)
interactions with nucleons, effect of m-scattering annihilation channels on, 20: 39776(T)
interactions with protons, strongly singular complex potential for high-energy large-angle, (T), 20: 39777
interactions with nucleons, crossing in backward cone and threshold region in, 20: 39798
interactions with nucleons, graphical method for charge independence in strong, 20: 39800
interactions with nucleons, analysis for Λ-K^0 production, (E/T), 20: 39803
interactions with mesons (ω), reciprocal bootstrap of mesons (ρ) and (B) in, 20: 39807
interactions with protons, S-wave $m\pi$ scattering length from, (T), 20: 39808
interactions with nucleons, sum rule for axial-vector coupling-constant renormalization in, 20: 39814
interactions with nucleons at 290 to 905 Mev, cross sections for N_{33}^* production in, (E/T), 20: 39827
interactions with mesons (π) at low energies, meson (K) pair production in, (T), 20: 39833
interactions with nucleons, model for, 20: 39839
interactions with mesons (ρ) Adler-Weisberger sum rules for, 20: 39883
interactions with mesons (π) in meson (π^-)-proton interactions at 276 Mev, (E), 20: 39779
interactions with protons, meson (σ) production in, (E), 20: 39782
photoproduction on protons, lecture on, (E), 20: 39743 (CALT-68-92)
photoproduction on nucleons, reciprocity relation as test of C and T invariance in, 20: 39810
production from meson (π^-)-proton interactions at 775 Mev, 20: 39780
production in meson (π)-nucleon interactions, (T), 20: 39839
production in proton reactions with beryllium and platinum at 2.9 Bev, (E), 20: 39794
theory of, as bound nucleon-antinucleon systems, 20: 39841

MESONS (π^-)
capture by carbon and oxygen at 80 Mev, helium-8 production in, (E), 20: 40071 (JINR-E-2774)
capture in gaseous helium-3, measurement of cascade time in, 20: 39579 (JINR-P-2838)
interactions with protons at 1.6 to 4.2 Bev/c, strange-particle resonant states from, (E), 20: 39770 (UCRL-16788)
interactions with protons at 3 and 4 Bev/c, π-π final-state interactions from, (E), 20: 39769 (UCRL-16655)
interactions with nucleons at 7 Bev, momentum spectra of secondary particles from, (E/T), 20: 39751 (JINR-E-2738)
interactions with protons at 7.5 Bev, cross sections for, (E), 20: 39758 (JINR-P-2773)
interactions with protons at 7.5 Bev, angular and momentum distributions from, (E), 20: 39758 (JINR-P-2773)
interactions with mesons (π^+), annihilation channels in, 20: 39776(T)
interactions with protons at 276 Mev, resonant meson (π)-meson (π) interactions in, (E), 20: 39779
interactions with protons at 775 Mev, single meson (π) production from, (E), 20: 39780
interactions with protons at 3.5 Bev/c, elastic differential cross sections for, (E), 20: 39785
interactions with protons at 10 Bev/c, observation of $\omega^0 \rightarrow \pi^0 + \gamma$ in, (E), 20: 39787
interactions with protons at 7.0 Bev/c, mesons (A_1) and (A_2) production in, (E), 20: 39790
interactions with protons at 460 Mev, cross sections for elastic and inelastic, (E), 20: 39793
interactions with protons at 2 to 6 Bev/c, Regge-pole model for cross sections for, (E/T), 20: 39801
interactions with protons at 900 Mev, Λ-K^0 production in, (E/T), 20: 39803
interactions with protons, random-phase K-matrix formalism for peripheral, 20: 39804
interactions with protons at 17 Bev, angular correlations for inelastic, (E), 20: 39830
interactions with protons at 900 to 1050 Mev/c, hyperon (Λ^0) production in, 20: 39837
interactions with neutrons at 3.5 Bev/c, (E), 20: 39842
interactions with protons at 7.5 Bev, N^*_{33}, N^*_{11}, and ρ^0 production from, (E), 20: 39758 (JINR-P-2773)
interactions with protons at 4 Bev/c, $\Lambda\eta$ resonance production in, (E), 20: 39754 (JINR-E-2858)
lifetime of, relative to mesons (π^+), (E), 20: 39760 (JINR-P-2802)
photoproduction on light nuclei, differential cross sections for, (E), 20: 40075 (LNF-66/30)
production from meson (π^-) reactions with bromine, diffraction dissociation in, (E), 20: 39774
production in neutron-proton interactions at 600 Mev, (E), 20: 39826
production in neutron-proton interactions at 600 Mev, cross sections for, (E/T), 20: 39834
reactions with bromine, diffraction disociation for meson (ρ^0) production from, (E), 20: 39774
reactions with xenon at 5 and 9 Bev/c, angular, energy, and multiplicity distributions of mesons (π^0) produced in, 20: 39755 (JINR-P-2736)

MESONS (π^0)
decay of, 3γ, 20: 39757 (JINR-P-2763)
decay widths of, two-baryon approximation method for determining, 20: 39783
photoproduction on helium-4 near threshold, differential and total cross sections for, (E), 20: 39822
production in neutron-proton interactions at 600 Mev, (E), 20: 39826

MESONS (π^+)
interactions in propane bubble chambers, method of identification of, (E), 20: 39211 (JINR-P-2842)
interactions with deuterons at 3.29 Bev/c, A_1 (1090) and A_2 (1310) production in, (E), 20: 39470(R) (ORNL-3924)
interactions with protons at 1.95 Bev/c, cross sections for, (E), 20: 39767 (TID-23278)
interactions with mesons (π^-), annihilation channels in, 20: 39776(T)
interactions with protons at 2 to 6 Bev/c, Regge-pole model for cross sections for, (E/T), 20: 39801
interactions with protons, random-phase K-matrix formalism for peripheral, 20: 39804
interactions with protons at 1350 Mev, properties of N* (1920) in, (E), 20: 39845
lifetime, (E), 20: 39821
lifetime of, relative to mesons (π^-), (E), 20: 39760 (JINR-P-2802)
photoproduction on light nuclei, differential cross sections for, (E), 20: 40075 (LNF-66/30)
production from meson (π^-) reactions with bromine, diffraction dissociation in, (E), 20: 39774
production in neutron-proton interactions at 600 Mev, (E), 20: 39826
production in neutron-proton interactions at 600 Mev, cross sections for, (E/T), 20: 39834

MESONS (ρ)
exchange in meson (π)-meson (ω) interactions, 20: 39807
interactions with mesons (π), Adler-Weisberger sum rules for, 20: 39883
trajectories of, bootstrap calculations of, 20: 39927

MESONS (ρ^0)
photo-production on protons, mechanism of, 20: 39811
production from meson (π^-) reactions with bromine, diffraction dissociation in, (E), 20: 39774
production in meson (π^-)-proton interactions at 7.5 Bev, (E), 20: 39758 (JINR-P-2773)
production in meson (π^-) interactions with protons at 7.0 Bev/c, (E), 20: 39790

MESONS (σ)
production in meson (π)-proton interactions, (E), 20: 39782

MESONS (X^0)
production in meson (K^-)-neutron interactions at 2.24 Bev/c, (E), 20: 39786

METABOLISM
effects of anti-metabolic drugs on thyroid, 20: 38785
mathematical model for cerium-144, in animals, 20: 38571
photoreactivation of prototrophic, in uv-induced mutants of *E. coli*, 20: 38669
radiation effects on, in Ascites tumor cells, x, 20: 38599 (TID-22968)
radiation effects on, in rats, x, 20: 38600(R) (TID-23034)
radiation effects on animal, 20: 38544
radiation effects on, of dairy cows, ^{45}Ca and ^{226}Ra, 20: 38552
trace elements in human, activation analysis for, 20: 38847

METAL COATINGS
deposition of, by chloride and fluoride reduction, 20: 39354 (BMwF-FBK-66-09)

METALLIC FILMS
growth of evaporated and sputtered, (E), 20: 39587

METALLOGRAPHY
dislocation etching of deformed molybdenum, equipment and methods for, 20: 39432
equipment design for, 20: 39340

METALLURGICAL EQUIPMENT
development for magnetic-pulse process, 20: 40490 (Y-1483)

METALLURGY
research in progress under Army Research Office, 20: 40485(R) (AD-636091)

METALS
analysis for boron, fluorine, nitrogen, and oxygen, activation, 20: 38840
bibliography on high-purity, 20: 39328 (AD-624997)
book: *Optical Properties and Electronic Structure of Metals and Alloys*, 20: 39339
bromine-82 localization in aqueous solutions of, beta/gamma ratio measurements for determining, 20: 39336
chemical reactions with borides, carbides, nitrides, and oxides, review on high-temperature, 20: 39331(T) (UCRL-Trans-10044)
chemical reactions of molten, with refractory materials, 20: 39429
crystal lattice vibrations in, review, (T), 20: 40344
defects in, annealing observation, and production of point, 20: 39386 (CEA-R-2905)
electric conductivity of, model for nonmagnetic impurity-containing, 20: 39395 (IAE-1028)
electron beam reactions with, physical aspects of penetrations from, 20: 40347
electron emission models for, with adsorbed monolayers, 20: 39641
electron scattering by, effects of nonmagnetic impurities on, 20: 39395 (IAE-1028)
emulsion of gas and liquid, for MHD generators, (T), 20: 39678
evaluation for low-temperature design applications, 20: 40051
forming by magnetic-pulse process, 20: 40490 (Y-1483)
injection of liquid, in MHD generators, (T), 20: 39669
properties of liquid, in MHD generator cycles, 20: 39726
superconductivity, two-fluid model of, 20: 40037
technology of high-temperature liquid, review, 20: 39330 (BNL-962)

METEORITES
analysis of iron, for gallium and germanium simultaneously, by neutron activation analysis, 20: 38825
isotopic composition of xenon from calcium-poor achondritic, (E), 20: 39984
lithium isotopic content of Bjurbole and Bruderheim, 20: 39102
silver isotopic content of Canyon Diablo, 20: 39102

METEOROLOGY
effects on particulate rainout from nuclear device cloud, 20: 39107 (UCRL-14700)

METHACRYLAMIDE
radioinduced polymerization of, to yield foamed plastics, 20: 38981(P)

METHACRYLIC ACID

radioinduced polymerization of, to yield foamed plastics, 20: 38981(P)
METHACRYLIC ACID, METHYL ESTER
polymerization of, at various pH's use of molybdenyl, uranyl, and vandyl, salts as photosensitizers in, 20: 38934
methyl methacrylate–wood, radioinduced polymerization of, economics and properties of products from, 20: 39287 (KLX-1876)
METHACRYLIC ACID, METHYL ESTER POLYMERS
thermal degradation of, with divinylbenzene, mechanism of, 20: 38930 (TID-23264)
METHANE
neutron inelastic scattering by, dynamic processes in slow, 20: 40338
neutron scattering by solid, effects on molecular rotation from, (T), 20: 40323
production in radioinduced oxidation of methanol, effects of dose rate on, 20: 38942 (UJV-1457)
radiolysis at various dosages, yields of acetylene from electron and gamma, 20: 38951
METHANE, IODO-
cyclohexane–iodomethane, radiolysis of, methyl radical yields in, 20: 38941(R) (RRL-2310-182)
METHANOL
neutron inelastic scattering by, dynamic processes in slow, 20: 40338
neutron reactions at 0.025 to 0.4 ev, total cross sections for, (E), 20: 40069(R) (EANDC(E)-66(U))
radioinduced oxidation of, effects of dose rate on yields in, 20: 38942 (UJV-1457)
methanol–2-propanol, carbon-13 exchange between monoethanolamine and, 20: 39320(R) (MLM-1311)
METHIONAL
effects on flavor of irradiated beef, 20: 39299
METHIONINE
effects of absence of, on viability of uv-irradiated *E. coli*, 20: 38562
radiolysis of, in aqueous solution, γ, 20: 38582
METHYL RADICALS *(Free Radicals)*
spectra of carbon-13-labeled deuterated and normal, ESR, 20: 38941(R) (RRL-2310-182)
yields in radiolysis of cyclohexane–iodomethane, 20: 38941(R) (RRL-2310-182)
METHYLAMINE
dissociation, intramolecular rearrangements, and ionization of deuterated and normal, by electron bombardment in mass spectrometer, 20: 38887
radiation effects on, reactions of recoiling carbon-11 in, 20: 38964
METHYLENE BLUE
methylene blue–uranin, particle deposition and reentrainment in long vertical tubes, 20: 39103(R) (BNWL-235-3, pp 51-69)
methylene blue–uranin, use of solutions of, in aerosol generators, 20: 39103(R) (BNWL-235-3, pp 51-69)
METROLOGY
temperature effects on gaging in machining, 20: 39009 (UCRL-14944)
MICA
proton channeling in foils of, at 3.55 Mev, (E), 20: 40324
use for fission detection at high temperatures, 20: 39208 (JINR-P-2705)
MICE
effects of cesium-137 chronic ingestion on life span and reproduction of, 20: 38551
effects of cystamine and serotonin on, pharmacological, 20: 38713
effects of injected tritium oxide on, pathological, 20: 38568
effects of shock and stress on survival of, effects of 19-nor-testosterone phenylpropionate on, 20: 38610
effects of strontium-90 chronic ingestion on life span and reproduction of, 20: 38551
effects of thiopentobarbital on oxygen tension in, 20: 38738
elimination of cerium-144, iodine-131, thallium-204, zinc-65, and isotope mixtures by, effects of DTPA, pectin, and zirconium phosphate on, 20: 38733
iodine-131 uptake and elimination from thyroid of, effects of potassium iodide and thiouracil on, 20: 38734
pharmacological effects on tumors in, of sulfhydryl-containing boron hydrides, 20: 38745(R) (NYO-3267-3)
radiation chimeras, nitrogen balance in, 20: 38636
radiation effects on populations of, genetic, whole-body x, 20: 38590(R) (NYO-1979-13)
radiation effects on growth of transplanted hematopoietic cells in, x, 20: 38592 (ORNL-P-2158)
radiation effects on colony formation by transplanted bone marrow cells in spleen of, 20: 38708(R) (IAEA-3173-5)
radiation effects on thymus of, metabolic, whole-body x, 20: 38606
radiation effects on survival of, effects of 19-nor-testosterone phenylpropionate on x, 20: 38610
radiation effects on tumors in, combined vincaleucoblastine, x, 20: 38613
radiation effects on, biological, 20: 38627
radiation effects on growth of transplanted lymphoma cells in mice, effects of anoxia on, 20: 38699
radiation effects on interactions of Polyoma virus with cells of, 20: 38702
radiation effects on taurine excretion in, effects of AET and cysteine on, whole-body x, 20: 38717
radiation effects on, protective effects of aminothiols and their derivatives against, 20: 38724
radiation effects on, biological, effects of environmental oxygen on γ, 20: 38642
radiation effects on, genetic, fast neutron and γ, 20: 38647
radiation effects on, biological, x, 20: 38648
radiation effects on response to immunotherapy of leukemic, effects of methylhydrazine on, 20: 38794
radiation injuries in, protective effects of indolylalkylamines against, 20: 38725
radiation injuries in, protective effects of chemical agents against, 20: 38726
radiation sickness in, mechanism of death from, 20: 38666
radiation sickness in, protective effects of procaine against, 20: 38727
radioinduced formation of organic peroxy compounds in tissues of, x, 20: 38660
radioinduced leukemia in, effects of AET and endotoxin on, 20: 38715
radioinduced leukemia in, protective effects of 5-methoxytryptamine and propamine against, 20: 38722
radiosensitivity alteration by drinking sulfurated mineral water, 20: 38709
radiosensitivity effects of glycine on, 20: 38714
radiosensitivity effects of thiopentobarbital on, 20: 38738
use of sodium gallate prophylaxis and therapy of radiation sickness in, 20: 38728
MICROÖRGANISMS
radiation effects on genetic mutations in, tritium, 20: 38624
MICROWAVE EQUIPMENT
Cherenkov radiation from electron beams in waveguides, traveling wave nature of, 20: 39501
protection of patients and personnel during operation of medical, 20: 38622
MICROWAVES
effects on man, pathological, 20: 38622
emission from Josephson tunnel junctions, 20: 40028
interactions with plasma, reflection and transmission coefficients for, (T), 20: 40252
MILK
content of cesium-137, iodine-131, strontium-89, and strontium-90 in U. S., 1965, 20: 38743
dietary importance as a calcium source for young children, 20: 39157
radioactivity of, effects of environmental cesium-137, iodine-131, and strontium-90 on, 20: 39157
MINERALS
book: *Mineral Tables (Hand Specimen Properties of 1500 Minerals)*, 20: 39100
ion exchange properties of, for alkali and alkaline earth metals, 20: 38858 (BNWL-235-3, pp 23-51)
oxidation rate of uranium-234 and uranium-238 in, 20: 38894
MISSILES
scoring system for, using radiation sources, 20: 39190(P)
MITOCHONDRIA
radiation effects on rat liver, biochemical and morphological, x, 20: 38639
MITOSIS
radiation effects on, in Tradescantia cells, microbeam uv, 20: 38614
radiation effects on, in rat bone marrow cells, gamma, 20: 38663
radiation effects on, in rat thymus, x, 20: 38720
MOLECULAR BEAMS
scattering during thermal diffusion, computer program for calculating, 20: 39321(R) (MLM-1312)
MOLECULES
electron energy levels in polyatomic, multiple-scattering model for, (T), 20: 39618
reactions with ions, ion-cyclotron double resonance in, 20: 38902
MOLTEN SALT REACTOR EXPERIMENT
accidents during filling, analysis, 20: 40412 (ORNL-TM-497)
MOLYBDENITES
analysis for rhenium by neutron activation methods, 20: 38802
MOLYBDENUM
deposition of coatings of, by chloride reduction using hydrogen, 20: 39354 (BMwF-FBK-66-09)
deuterium ion reactions at 29 and 50 kev, sputtering from, 20: 39581(R) (ORNL-3989, pp 134)
effect on properties of low-alloy steels for reactor pressure vessels, 20: 39444(P)
effects on grain size of tungsten, 20: 39400 (NASA-TN-D-3531)

effects on properties of boron steel, 20: 39426
electric discharge explosion of wires of, MHD instabilities in, 20: 39010
electron emission in MHD generators from electrodes of, (E), 20: 39736
electron emission from filaments of, surface micropatch effects on, 20: 39642
etching of dislocations in deformed, equipment for electrolytic, 20: 39432
neutron capture resonance integrals, (E), 20: 40146
permeability to hydrogen, 20: 39098(R) (WERL-2823-21)
production of high-quality sheet, panel summary on, 20: 39357 (MAB-212A-M)
separation of, from other fission products, by extraction into acetylacetene, 20: 38824
superconductivity of, 20: 40047

MOLYBDENUM ALLOYS
Cu–Mo–Zr, corrosion by steam, effects of heat treatments on copper-base and zirconium-base, 20: 39347 (NP-16239)
Mo–Nb, superconductivity, 20: 40047
Mo–Nb–Ti–U–Zr, mechanical properties of high-strength uranium-base, 20: 39440(P)
Mo–Nb–V–Zr, weldability evaluation of, 20: 39366
Mo–Re, superconductivity, 20: 40047
Mo–U, analysis for carbon, coulometric, 20: 38796 (CEA-R-2968)
Mo–U, phase studies of uranium-base, 20: 39388 (CEA-R-2956)
Mo–U, phase transformations in, effects of lattice orientation on, 20: 39389 (CEA-R-2973)

MOLYBDENUM CARBIDES
elastic properties of stoichiometric, 20: 39430
graphite–MoC, fabrication and physical properties of, 20: 39367
Hf–MoC–Ta, preparation and properties of dispersion-hardened, 20: 39441(P)
MoC–Ta–Zr, preparation and properties of dispersion-hardened, 20: 39441(P)

MOLYBDENUM CHLORIDES
reduction for coating deposition using hydrogen, 20: 39354 (BMwF-FBK-66-09)

MOLYBDENUM COMPOUNDS
use as photosensitizer for polymerization of methyl methacrylate at various pH's, 20: 38934

MOLYBDENUM FLUORIDES
molecular structure of, mean amplitudes of vibration at 0 and 298°K in, 20: 38897

MOLYBDENUM IONS
effects of pentavalent, on deuteron and proton relaxation times in aqueous solutions, 20: 38893

MOLYBDENUM ISOTOPES Mo-99
separation from technetium-99m sorbed on aluminum oxide using physiologic solution, 20: 38997 (NIJS-R-483)
use as source of technetium-99, for medical uses, 20: 38986

MOLYBDENUM STEEL
radiation effects on fatigue of A302B, neutron, 20: 39406 (WAPD-T-1864)
Cr–Mo, corrosion and mass transfer in flowing sodium, 20: 39345 (GEAP-4831)
Cr–Mo–Ti, corrosion and mass transfer in flowing sodium, 20: 39345 (GEAP-4831)

MOLYBDENUM SYSTEMS
Mo–UO_2, chemical reactions of tungsten coated at 1800°C, 20: 39383 (BMwF-FBK-66-08)

MONAZITES
age of, in Sweden, 20: 39125

MONKEYS
radiation effects on buccal flora of, γ, 20: 38667

MONTE CARLO METHOD
for neutron transport problems, 20: 40460(R) (IDO-17191)

MONTMORILLONITES
ion exchange properties for cesium, sodium, and strontium, 20: 38858 (BNWL-235-3, pp 23-51)

MOON
effects on geomagnetic activity variations, (E/T), 20: 39982
surface properties, chemical flare study of, (T), 20: 39469 (LA-3453)

MÖSSBAUER EFFECT
in transition metal silicides, 20: 40300
measurement of iron-57, in cobalt sulfate, 20: 40311
measurement of, spectrometer for, 20: 39250(P)
spectra in cobalt oxides, Auger aftereffects from, 20: 39603
spectra of nuclei with fluctuating hyperfine magnetic fields, (T), 20: 40152
spectra of, hyperfine structure, 20: 39615(T)

MOUTH
radiation effects on flora of dogs and monkeys, γ, 20: 38667

MULTIPLICATION FACTOR
calculation for fissile units, computer program for, 20: 40375 (DP-1031)
calculation using discrete transfer matrix, 20: 40060

MUSCLES
radiation effects on electrical parameters of skeletal, α, 20: 38776
radiation injuries of, in children treated for hemangiomas by radium, 20: 38787

MUTAGENS
effects of chemical, on DNA synthesis in plants, 20: 38589(R) (EUR-2761.f)
effects of chemical, on *Escherichia coli*, 20: 38620
effects of various chemical, on plants, 20: 38589(R) (EUR-2761.f)
effects on DNA in *E. coli*, 20: 38620
effects on DNA of chemical, 20: 38542(T) (UCRL-Trans-10029)
radiation effects on reaction mechanisms of hydroxylamine, uv, 20: 38574(R) (NYO-3449-1)

MUTATIONS
effects on enzymes and proteins, 20: 38542(T) (UCRL-Trans-10029)
induction in bacteriophages, molecular mechanisms for, 20: 38542(T) (UCRL-Trans-10029)
radioinduced in apple trees, fast neutron and γ, 20: 38692
radioinduced in chlorella, γ, 20: 38605
radioinduced in Drosophila, x, 20: 38596(R) (SAN-590-1)
radioinduced in *Drosophila melanogaster*, mechanisms of, x, 20: 38607
radioinduced in Drosophila, fast neutron, 20: 38645
radioinduced in Drosophila, x, 20: 38646
radioinduced in Drosophila, x, 20: 38650
radioinduced in maize, 20: 38617
radioinduced in mice, fast neutron and γ, 20: 38647
radioinduced in phage κ of *Serratia marcescens*, uv, 20: 38670
radioinduced in rats, x, 20: 38619
radioinduced in silkworms, RBE of fast neutron and x, 20: 38626
radioinduced lethal, in honeybee gametes, x, 20: 38631
radioinduced prototrophic *E. coli*, action spectra for photoreactivation of uv, 20: 38669
radioinduced, in mice, x, 20: 38590(R) (NYO-1979-13)
radiosensitivity of *E. coli*, uv, 20: 38620
radiosensitivity of radioinduced *E. coli*, uv and x, 20: 38621

N

NAGASAKI
radiation dosimetry of bomb survivors, Ichiban program for, 20: 39064

NAPHAZOLINE
effects on inhibition of tissue reaction in irradiated rabbit connective tissue, 20: 38640

NAPHTHALENES, IODO-
iodine-131 exchange with potassium iodide, kinetic studies of, 20: 38916

1-NAPHTHOL, 2-NITROSO-
complexes with cobalt, paper chromatographic separation of, 20: 38807

NASA RESEARCH REACTOR
heat transfer analysis during full power operation, 20: 40461 (NASA-TN-D-3552)

NATURAL GAS
storage in underground reservoirs created by nuclear explosions, 20: 39014(R) (TID-23184)
storage underground, economics of nuclear explosives in developing, 20: 39015 (UCRL-14877)

NATURAL WATERS
analysis for alkali and alkaline earth metals, flame photometric, 20: 38798 (NIJS-R-465)
monitoring for radioactive wastes, 20: 38742
radioactivity monitoring in Netherlands, 1963, 20: 39118
uranium-234 to uranium-238 ratio in, 20: 39120

NEODYMIUM
determination in fluorite monocrystals, spectrophotometric, 20: 38829
determination in magnesium alloys by successive potentiometric titration, 20: 38830
x-ray-diffraction patterns of, effects of cold working on, 20: 39421

NEODYMIUM ALLOYS
Al–Nd, magnetic properties of intermetallic compounds of, 20: 39433
Co–Nd, magnetic properties of intermetallic compound $NdCO_5$ in, 20: 39424
Fe–Nd, crystal structure of intermetallic compound, 20: 39409
Gd–Nd, phase transformations and magnetic ordering in, pressure-induced, 20: 40326
Nd–Tm, phase transformations and magnetic ordering in, pressure-induced, 20: 40326
Nd–Y, phase transformations and magnetic ordering in, pressure-induced, 20: 40326
Nd–Zn, crystal structure of intermetallic compound Nd_2Zn_{17} in, 20: 39417
Pb–Nd–Zn, component distribution in recrystallized, 20: 39435

NEODYMIUM CHLORIDES
specific gravity and apparent molal volume of aqueous solutions of, at 25°C, 20: 38905
thermal capacity of aqueous solutions of, at 25°C, 20: 38906

viscosity of aqueous solutions of, at 25°C, 20: 38904
$CsCl–NdCl_3$, phase studies, 20: 38919
NEODYMIUM IONS
electron paramagnetic resonance spectra in lanthanum compounds, 20: 40312
spin-lattice relaxation time in lanthanum trichloride, angular and temperature effects on, 20: 40350
NEODYMIUM ISOTOPES Nd-142
proton reactions (p,3n) with, energy levels from, 20: 40131
NEODYMIUM NITRATES
specific gravity and apparent molal volume of aqueous solutions of, at 25°C, 20: 38905
NEODYMIUM OXIDES
diffusion of oxygen in, tracer studies of, 20: 38865(R) (COO-1109-22, Paper 4)
actinide oxides–Nd_2O_3, preparation of sols of, 20: 39341(P)
NEODYMIUM SELENIDES
crystal structure of, reflection spectra for zonal, (E), 20: 40339
NEON
electric discharge in alkali-metal seeded, (E), 20: 39715
neon ion scattering on atomic, effects of π and Σ molecular states in, 20: 39601
separation from xenon, thermal diffusion factors for, 20: 39321(R) (MLM-1312)
transport properties for, during thermal diffusion flow, 20: 39321(R) (MLM-1312)
viscosity of, saturated-liquid, (T), 20: 39940
NEON IONS
scattering on neon, effects of π and Σ molecular states in, 20: 39601
NEON ISOTOPES
separation by fractionation in film columns, 20: 39322
separation of neon-20 and -22 from, using tube bundle as function of pressure, 20: 39320(R) (MLM-1311)
separation using hot-wire thermal diffusion columns, 20: 39323
thermal diffusion factor for, temperature dependence in, 20: 39326
NEON ISOTOPES Ne-20
energy levels, (E), 20: 40164
energy levels in SU(3) shell model, (T), 20: 40163
reactions with emulsion nuclei at 200 Mev, (E), 20: 40083
separation from neon isotopes using tube bundle as function of pressure, 20: 39320(R) (MLM-1311)
separation from neon-22 by thermal diffusion, transport properties for, 20: 39320(R) (MLM-1311)
separation from neon isotopes, performance of extraction column for, 20: 39321(R) (MLM-1312)
NEON ISOTOPES Ne-21
energy-level spins and transitions, (E), 20: 40156
neutron scattering by, cross sections for thermal, (E), 20: 40129
separation from neon isotopes, performance of extraction column for, 20: 39321(R) (MLM-1312)
NEON ISOTOPES Ne-22
electron pair formation in, following positron decay of sodium-22, (E), 20: 40134
neutron scattering by, cross sections for thermal, (E), 20: 40129
reactions with plutonium-242, element-104 production from, 20: 40143
reactions with uranium-238, fermium-256 production from, 20: 40142
separation from neon isotopes using tube bundle as function of pressure, 20: 39320(R) (MLM-1311)
separation from neon-20 by thermal diffusion, transport properties for, 20: 39320(R) (MLM-1311)
separation from neon isotopes, performance of extraction column for, 20: 39321(R) (MLM-1312)
NEON SYSTEMS
D–Ne, crystal structure of solid, (E), 20: 40308
H–Ne, crystal structure of solid, (E), 20: 40308
NEPTUNIUM
compressibility and phase diagram of, 20: 39423
crystal structure of, valence electrons and interatomic bonds in, 20: 40296
determination of, review of methods for, 20: 38821
properties of, at low temperatures, 20: 39448 (AERE-X-PR-2596-9)
radiation effects on low-temperature electric conductivity of, self, 20: 39448 (AERE-X-PR-2596-9)
vaporization of, thermodynamics of, 20: 38876 (UJV-1598)
NEPTUNIUM FLUORIDES
molecular structure of, mean amplitudes of vibration at 0 and 298°K in, 20: 38897
NEPTUNIUM ISOTOPES Np-236
production of isomeric, in deuteron reactions with uranium-238, (E), 20: 40092
NEPTUNIUM ISOTOPES Np-237
radiation effects on, self, 20: 39448 (AERE-X-PR-2596-9)
NEPTUNIUM OXIDES
preparation of sols of, with yttrium oxides, 20: 39341(P)
$HfO_2–NpO_2$, preparation of sols of, 20: 39442(P)
NpO_2–rare earth oxides, preparation of sols of, 20: 39341(P)
$NpO_2–ZrO_2$, preparation of sols of, 20: 39442(P)
NERVES
radiation effects on excitability of ganglions of solar plexus, x, 20: 38687
NERVOUS SYSTEM
dosimetry of beta particles from internally deposited phosphorus-32 in, central, 20: 38651
radiation effects on stimulation of solar plexus, x, 20: 38687
radiation effects on, in animals, 20: 38653
radiation effects on regulatory function of rabbit, x, 20: 38654
radiation effects on conditioned reflex in fish and rabbits, 20: 38655
radiosensitivity of, γ, 20: 38773
NETHERLANDS
radioactivity monitoring in biosphere, 1963, 20: 39118
NEUROSPORA
counter design for, 20: 38546
NEUTRINO BEAMS
production of, description of CERN layout for, 20: 39746 (CERN-66-24)
NEUTRINOS
field theory for, quantum, 20: 39853 (JEN-157-DF/I-48)
NEUTRON-ABSORPTION ANALYSIS
method for pyrotechnic cartridges, 20: 39334
NEUTRON CAPTURE CROSS SECTIONS
measurement of infinitely dilute resonance integrals, method for, 20: 40146
NEUTRON CROSS SECTIONS
date on 14-Mev, for stable isotopes, (E/T), 20: 38838
measurement of, parallel-plate fission chamber for, 20: 39256
NEUTRON-DIFFRACTION ANALYSIS
developments in, for use in inorganic chemistry, 20: 38882
of hydrogen–palladium systems, 20: 39428
of ordering in manganese–nickel alloys, 20: 39407(T) (ANL-Trans-344)
use in magnetic moment distributions for impurities in iron, (T), 20: 40330
NEUTRON SOURCES
design of high-output sealed-off, for activation analysis, 20: 38839
design of howitzer, for neutron absorption studies, 20: 40057
development of intense, using proton accelerators, 20: 39542
energy spectra of americium-241–beryllium, 20: 40069(R) (EANDC(E)-66(U))
engineering problems of pulsed, 20: 40455 (BNL-10454)
image intensifier television system for, 20: 39174
use in soil moisture measurements, 20: 39131
NEUTRON SPECTRA
measurement in reactors, review of methods for, 20: 40378
NEUTRON SPECTROMETERS
design, 20: 39255
design and construction of broad range magnetic, 20: 39194 (AD-638137)
design of fast and slow, 20: 39261
operation of time-of-flight, with deflection-bunching system at Karlsruhe cyclotron, 20: 39546
synchronization system for rotating crystal, design of phase locked frequency multiplier for, 20: 39201 (EUR-2999.e)
NEUTRONS
absorption of, geometrical effects on resonance, (T), 20: 40062
angular distributions from capture of polarized mesons (μ^-) by copper, iron, and lead, (E), 20: 40096
capture resonance integrals for, method for measuring infinitely dilute, 20: 40146
decay constant in beryllium, 20: 40376
development of detectors for, 20: 39221
diffusion coefficients in reactors with empty channels, 20: 40377
diffusion in plane heterogeneous systems, time-dependent equations for, 20: 40059
diffusion lengths in poison-bearing water, calculations using diffusion theory and transport theory, 20: 40053
diffusion parameters in water, measurement and calculation of, (E/T), 20: 40055
distribution in infinite medium, steady-state, (T), 20: 40052
dosimetry of, design on boron polyethelene-moderated counters for, 20: 39214(T) (NP-tr-1394)
effects on beryllia microstructure, 20: 39450 (CEA-R-2963)
effects on cobalt complexes, annealing of, 20: 38965
effects on current capacity of niobium stannide, (E), 20: 40301
effects on distribution of radioactive selenium between red and gray allotropic modifications, 20: 38961
effects on fatigue of A212 and A302B steels, 20: 39406 (WAPD-T-1864)
effects on hardness and impact properties of beryllium, 20: 39436
effects on infrared absorption spectrum of silicon, (E), 20: 40340
effects on n-type silicon at 293°K, 20: 40303

effects on seeds of deciduous trees, RBE gamma, 20: 38594(R) (ORO-2066-10)
effects on solid-solid phase transformations, (E), 20: 40306
effects on spin-lattice relaxation time of praseodymium ions in lanthanum chloride, 20: 40350
effects on twinning in niobium–vanadium alloys, 20: 39462
electric dipole moment of, (E), 20: 39470(R) (ORNL-3924)
electric structure factor from thermal neutron scattering by rare gases, (E), 20: 40129
flux distribution in reactors, measurement techniques for, 20: 40379
flux distributions and spectra in iron–water shielding, (E/T), 20: 40287
flux mapping in reactors, 20: 39252(P)
form factors from electron scattering by deuterium, electromagnetic, (E), 20: 39795
interactions with mesons (K−) at 2.24 Bev/c, η^* (960) production in, (E), 20: 39786
interactions with protons at 2 to 6 Bev/c, Regge-pole model for cross sections for, (E/T), 20: 39801
interactions with mesons (K±) at 2 to 6 Bev/c, Regge-pole model for cross sections for, (E/T), 20: 39801
interactions with antiprotons at 2 to 6 Bev/c, Regge-pole model for cross sections for, (E/T), 20: 39801
interactions with protons at 600 Mev, meson (π) production in, (E), 20: 39826
interactions with protons at 600 Mev, cross sections for meson ($\pi^\pm$) production in, (E/T), 20: 39834
interactions with mesons (π^-) at 3.5 Bev/c, (E), 20: 39842
interactions with protons at 400 and 630 Mev, optimal experiments for measuring parameters of, 20: 39752 (JINR-E-2765)
interactions with protons at 19.8 Bev/c, angular and energy distributions of secondary particles from inelastic, (E), 20: 39761 (JINR-P-2809)
interactions with electrons from thermal neutron scattering by rare gases, (E), 20: 40129
polarization in hyperon (Σ^+) decay, (E), 20: 39748 (COO-881-76)
polarization in two-nucleon systems at 310 to 700 Mev, (E/T), 20: 39844
properties for use in activation analysis, 20: 38838
reactions (n,α), (n,p), and (n,2n) with iron-54 and selenium isotopes at 14.4 Mev, cross sections for, (E), 20: 40079 (ORO-3346-2)
reactions (n,α) and (n,p) with nuclei, cross sections for, (E), 20: 40069(R) (EANDC(E)-66(U))
reactions (n,α) with nuclei, resonance activation integral cross sections for, (E), 20: 40069(R) (EANDC(E)-66(U))
reactions (n,α) with sodium-23 at 12.6 to 18.7 Mev, cross sections for, (E), 20: 40069(R) (EANDC(E)-66(U))
reactions (n,α) and (n,p) with nuclei, cross sections for, (E), 20: 40069(R) (EANDC(E)-66(U))
reactions (n,α) with germanium-73 at 14 Mev, cross sections for, (E), 20: 40098
reactions (n,α) with calcium-40 and fluorine-19 at 6 Mev, cross sections for, (E), 20: 40100
reactions (n,d) with copper isotopes at 14.08 Mev, angular distributions from, (E), 20: 40069(R) (EANDC(E)-66(U))
reactions (n,d) with zinc-64, angular distributions from, (E), 20: 40069(R) (EANDC(E)-66(U))
reactions (n,γ) with tungsten isotopes, energy levels from, (E), 20: 39470(R) (ORNL-3924)
reactions (n,γ) with tin isotopes, gamma spectra of, (E), 20: 39470(R) (ORNL-3924)
reactions (n,γ) with nickel-64, nickel-65 production in, 20: 40081 (PAEC(D)IS-653)
reactions (n,2n) with beryllium-9, neutron-neutron bound state in, (E), 20: 40091
reactions with calcium-41 at 1 to 2 Mev, total cross sections for, (E), 20: 40087
reactions with copper phthalocyanine, crystal-structure effects on recoil atoms after, 20: 40309
reactions with hydrogeneous compounds at 0.025 to 0.4 ev, total cross sections for, (E), 20: 40069(R) (EANDC(E)-66(U))
reactions with iron, manganese, and vanadium at 18 to 260 kev, total cross sections for, (E), 20: 40069(R) (EANDC(E)-66(U))
reactions with lanthanum-138 at 0.2 ev to 2 kev, resonance parameters from, (E), 20: 39470(R) (ORNL-3924)
reactions with lead and uranium-238 at 7.5 to 30 kev, effective cross sections for, (E), 20: 40069(R) (EANDC(E)-66(U))
reactions with lithium at 4.2 to 6.1 Mev, total cross sections for, (E), 20: 40069(R) (EANDC(E)-66(U))
reactions with nuclei at 7.8 to 64 kev, activation cross sections for, (E), 20: 40069(R) (EANDC(E)-66(U))
reactions with tin isotopes, strong p-wave resonances from, (E), 20: 39470(R) (ORNL-3924)
reactions with tungsten-180 at 0.1 to 400 ev, resonance parameters from, (E), 20: 39470(R) (ORNL-3924)
reactions with tungsten isotopes, resonance parameters from, (E), 20: 39470(R) (ORNL-3924)
reactions with vanadium at 21.65 to 152.6 kev, resonance parameters for, (E), 20: 40069(R) (EANDC(E)-66(U))
scattering by aluminum-27 and fluorine-19 at 14.2 Mev, cross sections for, (E), 20: 40069(R) (EANDC(E)-66(U))
scattering by calcium-41 at 1 to 2 Mev, cross sections for elastic, (E), 20: 40087
scattering by carbon-12 at 16 to 20 Mev, optical-model analysis of elastic, (E/T), 20: 40088
scattering by carbon-12 at 14 Mev, calculations by dispersion method for inelastic, (T), 20: 40104(T)
scattering by ferromagnetic materials, critical magnetic, 20: 40316
scattering by iron and yttrium-89 at 5 Mev, cross sections for inelastic, (E), 20: 39470(R) (ORNL-3924)
scattering by liquids, dynamic processes in slow inelastic, 20: 40338
scattering by nitrogen-14 at 1.78 to 3.21 Mev, differential cross sections for, (E), 20: 39470(R) (ORNL-3924)
scattering by silicon at 0.57 to 2.28 Mev, differential cross sections for, (E), 20: 40069(R) (EANDC(E)-66(U))
scattering by solid methane, effects on molecular rotation from, (T), 20: 40323
scattering equation for, extension of, 20: 40056
scattering of, computer program for evaluation of angular distributions for, 20: 40063
scattering of, use of, in analysis of soil for water content, 20: 39141
thermalization in multiplying media containing plutonium, 20: 40384(R) (EURAEC-1660)
thermalization in infinite medium, (T), 20: 40052
transport in homogeneous media, calculations of using P-3 approximation, 20: 40064
transport in three-dimensional geometry, computer codes for, 20: 40460(R) (IDO-17191)
transport operator for homogeneous medium, real eigenvalues of monoenergetic, (T), 20: 40054
transport theory for, inscattering approximations in, 20: 40060

NEUTRONS, EPITHERMAL
detectors for, in well logging, 20: 39138(P)

NEUTRONS, FAST
angular distributions behind iron shielding, 20: 40286
detection in plastic scintillators, computer program for simulation of, 20: 39196 (AE-236)
detection using lithium fluoride thermoluminescence, 20: 39219
dosimetry in animals and cultured cells using ionization chambers, 20: 39227
dosimetry in seeds, 20: 38693
dosimetry using activation detectors and ionization chambers, 20: 39228
effects on apple tree roots, genetic, 20: 38692
effects on beryllium, 20: 39454 (EUR-3055.e)
effects on cobalt complexes, 20: 38962
effects on Drosophila, genetic, RBE effects of x, 20: 38645
effects on mechanical properties of Incoloy-800, Inconel-600, and Zircaloy-2, 20: 39457 (GEAP-5100-9)
effects on mice, genetic, RBE of y, 20: 38647
effects on n- and p-type silicon, 20: 40334(T)
effects on oxygen-doped silicon, (E), 20: 40302
effects on polycrystalline graphite, 20: 39466
effects on pyrolytic graphite, 20: 39465
effects on sperm of silkworms, genetic, RBE to gamma, 20: 38626
flux density measurements using activation of P compounds, 20: 39222
flux of monochromatic, thick organic radiators for determining absolute, 20: 39223
reactions (n,α), (n,2n), (n,p), and (n,t) with nuclei, cross sections for, (E), 20: 40069(R) (EANDC(E)-66(U))
reactions (n,nα), (n,2n), and (n,p) with copper-65 at 2 to 20.3 Mev, cross sections for, (E), 20: 40149
reactions (n,p) with sulfur-32, neutron dosimetry using, 20: 39228
reactions with nuclei for activation analysis, 20: 38838
scattering by coal, inelastic, 20: 39025 (ORO-2980-12)
spectra in AFRRI TRIGA, 20: 40454 (AD-636542)
transport equation in multidimensional geometries, angle-space synthesis method for, 20: 40360 (WAPD-T-1890)

NEUTRONS, FISSION
effects on goats, pathological, 20: 38629
effects on hematopoietic system in sheep, 20: 38637

NEUTRONS, PROMPT
emission in spontaneous fission of californium-252, (E), 20: 39470(R) (ORNL-3924)

NEUTRONS, THERMAL
diffusion in water–water-d_2 mixtures, parameters for, (E), 20: 40061
dosimetry in tissue-equivalent phantoms using activated gold wires, 20: 38745(R) (NYO-3267-3)
effects on cobalt complexes, 20: 38962

effects on conductivity of helium-3 plasma, (E), 20: 39683
flux distribution around point source of fast neutrons in infinite hydrogenous medium, (T), 20: 40058
image intensifier for, 20: 39174
reactions with plutonium isotopes, fission fragment energy correlations for thermal, 20: 39470(R) (ORNL-3924)
scattering by rare gases, electron-neutron interaction from, (E), 20: 40129
separation from reactor flux, design of structure for, 20: 40368(P)
spectra in heavy-water-moderated natural uranium elements, 20: 39452 (EUR-2981.f)
transport in graphite, calculations using P-3 approximation, (T), 20: 40064

NICKEL
deposition on fuel rods for corrosion protection, method for, 20: 39350(P)
determination in mosaic virus and nucleic acids in tobacco plants, activation, 20: 38846
effect on properties of low-alloy steels for reactor pressure vessels, 20: 39444(P)
effects on properties of boron steel, 20: 39426
evaporative lifetime on tungsten and oxygenated tungsten from 1250 to 1750°K, (E), 20: 40307
magnetic moment distribution of, polarized neutron-beam technique for, 20: 40325
mechanical properties of composites of, with glass, 20: 39405 (UCRL-16844)
phase transformations, effect of pressure and irradiation on solid-solid, (E), 20: 40306
radiation effects on, as control rod coating, 20: 39461 (WCAP-6074)
sorptive properties for bromine-82, 20: 39337

NICKEL ALLOYS
Cr–Co–Fe–Mn–Ni–W, tensile properties of L-605, effects of cold deformation on, 20: 39399 (NASA-TN-D-3528)
Cu–Au–Ni, gold-197 hyperfine structure coupling in, (E), 20: 39470(R) (ORNL-3924)
Eu–Ni, crystal structure of intermetallic compounds in, 20: 39415
Lu–Ni, crystal structure of intermetallic compounds in, 20: 39415
Mn–Ni, crystal structure of, neutron diffraction studies on, 20: 39407(T) (ANL-Trans-344)
Mn–Ni, phase studies, 20: 39407(T) (ANL-Trans-344)
Ni–Tm, crystal structure of intermetallic compounds in, 20: 39415

NICKEL ISOTOPES Ni-58
proton scattering at 45 Mev, cross sections for elastic, (E), 20: 40162

NICKEL ISOTOPES Ni-60
proton scattering at 45 Mev, cross sections for elastic, (E), 20: 40162

NICKEL ISOTOPES Ni-63
radioinduced diffusion in copper, model of alpha, 20: 39451 (EUR-2968.e)

NICKEL ISOTOPES Ni-64
neutron reactions (n,γ) with, nickel-65 production in, 20: 40081 (PAEC(D)IS-653)

NICKEL ISOTOPES Ni-65
production by neutron reactions (n,γ) with nickel-64, 20: 40081 (PAEC(D) IS-653)

NICKEL OXALATES
radiation effects on rate of decomposition of, beta and gamma, 20: 38955

NICKEL SYSTEMS
B–Ni–Zr, crystal structure of stoichiometric, 20: 39416
Ni–ThO_2, rupture strength of, effects of microstructure on, 20: 39398 (NASA-TN-D-3527)

NIOBIUM
diffusion from sodium at high temperatures, factors affecting, 20: 40357 (NAA-SR-11766)
effect on properties of low-alloy steels for reactor pressure vessels, 20: 39444(P)
effects on grain size of tungsten, 20: 39400 (NASA-TN-D-3531)
effects on properties of boron steel, 20: 39426
electric conductivity of superconducting, from helicon-like resonances, (E/T), 20: 40031
electron emission in MHD generators from electrodes of, (E), 20: 39736
Faraday unipolar induction in type II superconductors of, 20: 40016
magnetization of impure superconducting, (T), 20: 40036
neutron capture resonance integrals, (E), 20: 40146
oxidation of, effects of fluoride coating on, 20: 39348
production of high-quality sheet, panel summary on, 20: 39357 (MAB-212A-M)
solubility in cobalt–tungsten carbide systems, chemical determination of, 20: 39427
superconducting critical temperature of, effect of interstitial gases on, (E), 20: 40025
superconductivity of, 20: 40047

NIOBIUM ALLOYS
brazing honeycomb structures of, remelt temperature techniques for, 20: 39365
corrosion by liquid potassium at high temperatures, 20: 39028
Hf–Nb, work function for, 20: 40297
Hf–Nb–W–Y, properties for high-temperature service, 20: 39445(P)
Hf–Nb–W–Y, weldability evaluation of, 20: 39366
Mo–Nb, superconductivity, 20: 40047
Mo–Nb–Ti–U–Zr, mechanical properties of high-strength uranium-base, 20: 39440(P)
Mo–Nb–V–Zr, weldability evaluation of, 20: 39366
Nb–Sn, current capacity, neutron irradiation effects on, 20: 40301
Nb–Sn, magnetic shielding properties of superconducting, for accelerator extraction systems, 20: 39523
Nb–Ta, current distribution in type II superconductors of, 20: 40029
Nb–Ta–W–Zr, weldability evaluation of, 20: 39366
Nb–Ta–Zr, superconducting critical current density in, effect of microheterogeneity on, 20: 40020
Nb–V, radioinduced twinning in, neutron, 20: 39462
Nb–W–Zr, weldability evaluation of, 20: 39366
Nb–Zr, fabrication of superconductors of, 20: 39372(P)
Nb–Zr, superconductivity for magnets, 20: 40015(R) (ORNL-TM-1598)
Nb–Zr, superconducting critical current density in, effect of structure on, 20: 40021
Nb–Zr, superconductivity in surface layers of, (E), 20: 40023
Nb–Zr, superconductivity, 20: 40047

NIOBIUM CARBIDES
elastic properties of stoichiometric, 20: 39430
properties for matrix material in particulate uranium carbide fuels, 20: 39353 (BMwF-FBK-66-07)
graphite–NbC, fabrication and physical properties of, 20: 39367

NIOBIUM ISOTOPES Nb-93
deuteron reactions at 11.8 Mev, energy spectra from, 20: 40065(R) (BMwF-FB-K-66-01)
proton reactions (p,n) at 3.0 to 5.8 Mev, strength functions for, (E), 20: 39470(R) (ORNL-3924)

NIOBIUM ISOTOPES Nb-95
sorption on sediments in river-estuary systems, 20: 39121
transport in river-estuary systems, 20: 39121

NIOBIUM OXIDES
effects on irradiation performance of uranía, 20: 39447 (AECL-2581)
Nb_2O_5–TiO_2, phase diagrams, 20: 39411

NIOBIUM SYSTEMS
C–Nb–Zr, phase diagrams, 20: 39434

NIOBIUM URANIUM OXIDES
preparation of single crystals of $U_{2/3}Nb_2O_7$, 20: 38892

NITRATES
determination in colloidal thoria by uv absorption, 20: 38926
metabolism in wheat seedlings, 20: 38548(R) (ORO-2410-1)
properties for ion exchange in solutions of, 20: 38820

NITRIC ACID
separation of benzoic acid from, performance of stacked-clone contactor for, 20: 38998(R) (ORNL-3958)
use in leaching fission products from alumina calcine, 20: 40478 (IN-1011)
HNO_3–tetrahydrofuran, effects on ion exchange of uranium, 20: 38999 (TID-23229)
HNO_3–$UO_2(NO_3)_2$–H_2O, phase diagram, 20: 38994(R) (AE-232)

NITRIDES
chemical reactions with metals at high temperatures, review on, 20: 39331(T) (UCRL-Trans-10044)
wettability of refractory, by molten metals, 20: 39429

NITRITE IONS
yields from gamma radiolysis of nitrate solutions, at 77°K, 20: 38950

NITROGEN
balance in mouse radiation chimeras, 20: 38636
determination in metals, activation, 20: 38840
determination in solids, mass spectrographic, 20: 38831
effects on crystal structure of uranium monocarbide, 20: 39385 (CEA-R-2852)
effects on enzyme release from x irradiated lysosomes in rat liver, 20: 38577
effects on heavy water decomposition, 20: 40409(R) (NP-16230)
effects on internal friction of electron-beam refined tantalum, 20: 39420
effects of interstitial, on superconducting critical temperature of niobium, (E), 20: 40025
effects on radioinduced decomposition of 5-bromouracil, 20: 38968
energy exchange between electron gas and, (T), 20: 39677
neon-20 reactions at 200 Mev, in emulsions, (E), 20: 40083
radiosensitivity effects on bacteriophage, x, 20: 38712
reactions with radioisotope-containment materials in launch pad abort environment, 20: 39312 (SC-CR-66-2044)
solubility in tungsten, 20: 39098(R) (WERL-2823-21)
spectra of high-speed excited atomic, at 2700 to 6600 A, (E), 20: 39593
viscosity of molecular, saturated-liquid, 20: 39940

NITROGEN COMPOUNDS
production of N_2O^+ in mass spectrometer ion source, 20: 38902
NITROGEN IONS
content in outer ionosphere, 20: 39950
NITROGEN ISOTOPES N-14
deuteron reactions (d,p) at low energy, distorted-wave analysis of, (T), 20: 40122
energy levels, (E), 20: 40112
neutron scattering at 1.78 to 3.21 Mev, differential cross sections for, (E), 20: 39470(R) (ORNL-3924)
reactions (N-14, C-13) with beryllium-9 at 20 to 30 Mev, angular distributions from, 20: 40065(R) (BMwF-FB-K-66-01)
reactions with beryllium-9 at 25 Mev, beryllium, boron, carbon, and lithium spectra from, 20: 40065(R) (BMwF-FB-K-66-01)
NITROGEN ISOTOPES N-15
energy levels of, Hartree-Fock calculations for, (T), 20: 40138
incorporation of, into rat proteins from labeled glycine, 20: 38600(R) (TID-23034)
NITROGEN MUSTARDS
preparation of boron-containing, 20: 38745(R) (NYO-3267-3)
NITROGEN OXIDES
effects on annealing of recoil damage in neutron-irradiated cobalt complexes, 20: 38965
effects on photosensitized decomposition of deuterated and normal cyclobutane, 20: 38941(R) (RRL-2310-182)
effects on radioinduced decomposition of 5-bromouracil, 20: 38968
reaction with radioisotope containment materials in launch pad abort environments, 20: 39312 (SC-CR-66-2044)
yields in radiolysis of propene, competitive electron capture between tetrafluoroethylene and, 20: 38941(R) (RRL-2310-182)
NITROGEN SYSTEMS
C–N–O–U, crystal structure of solid-solutions, 20: 39385 (CEA-R-2852)
NITROUS ACID
effects on cytolytic and transforming abilities of Polyoma virus, 20: 38702
NONANAL
effects on flavor of irradiated beef, 20: 39299
NOZZLES
performance of, influence of geometry on, 20: 39021 (K-1665)
use in isokinetic sampling of particles in air streams, 20: 39103(R) (BNWL-235-3, pp 51-69)
welding of stainless steel to carbon steel pipes, fatigue strength of, 20: 39404 (SWRI-1228-4-20)
NRU REACTOR
radioisotope production in, 20: 39282 (DP-1066(Vol.1), pp III.3-32)
shutdown of, mode optimization for planned startup, 20: 40423
NRX REACTOR
radioisotope production in, 20: 39282 (DP-1066(Vol.1), pp III.3-32)
NUCLEAR BATTERIES
burnup at high altitudes, contamination of troposphere by, 20: 39306 (DP-1066(Vol.1), pp V.17-25)
properties of, comparison with solar cells, 20: 39306 (DP-1066(Vol.1), pp V.17-25)
NUCLEAR EMULSIONS
neon-20 reactions with nuclei in, at 200 Mev, (E), 20: 40083
processing of, exposure and sensitivity effects on, 20: 39202 (IFA-PN-17)
proton reactions at 1 to 30 Bev in, calculations for, 20: 39828
NUCLEAR ISOMERS
existence with quantized vortices in superfluid model, (T), 20: 40106(T)
NUCLEAR MAGNETIC MOMENTS
measurement of dipole, using perturbed γ–γ angular correlations, (T), 20: 40125
spin gyromagnetic ratio for nucleons, effective, (E), 20: 40073 (LA-DC-8065)
NUCLEAR MAGNETIC RESONANCE
spectra of double, for nuclei with spin ½, (T), 20: 40103
NUCLEAR MODELS
description of, for calculation of equilibrium nuclear shape, (T), 20: 40136
nuclear isomers with quantized vortices in superfluid, (T), 20: 40106(T)
nuclear moments of inertia in superfluid, (T), 20: 40102
superfluid, comparison with energy level structures of indium-117, praseodymium-143, and tin-117, (E), 20: 40159
NUCLEAR MODELS (OPTICAL)
formulation and history, review, 20: 40162
NUCLEAR MODELS (SHELL)
Hartree-Fock calculations with parity mixing, (T), 20: 40138
wave-function classification using SU(3) group, (T), 20: 40163
NUCLEAR PHYSICS
representation of rotation matrices, graphical method for, 20: 40120
NUCLEAR POWER
development for undersea uses, review of, 20: 40362
development in Brazil, prospects for, 20: 40487 (NP-16229)
NUCLEAR POWER PLANTS
construction cost analysis, 20: 40402 (EUR-2993.d)
control system for, 20: 40432(P)
development and future use in Europe, analysis of, 20: 40443
development data on western European, 20: 40441
use for production of electricity in western Europe, 20: 40442
NUCLEAR REACTIONS
cross sections for, probability distribution of maxima and minima of, (T), 20: 40113
production of, electron discharge device for, 20: 39509(P)
rates at high densities, calculation of, 20: 40157
NUCLEAR SPECTRA
stability in, 20: 40108
NUCLEAR STRUCTURE
analysis of, instrumentation for, 20: 39240
NUCLEAR THEORY
moments of nucleons, sum rules for, 20: 40130
NUCLEI
alpha decay in crystals, research using shadow effect, 20: 40135
beta transitions in, single-particle matrix elements for first-forbidden, (T), 20: 40124
binding energies of, calculation using K-matrix theory, 20: 40119
decay of, systematics of, 20: 40108
deformation of, review of theory of, 20: 40136
description using statistical approximation with momentum-dependent forces, (T), 20: 40115
electron capture ratios, M/L, 20: 40153
electron inelastic scattering at 1 to 10 Mev, partial wave analysis of, (T), 20: 40150
energy level transitions in even-even, EO, (T), 20: 40116
energy level transitions in, statistical method for study of triple cascades, 20: 40160
energy levels of deformed, M1 transitions of rotational, (E), 20: 40072 (LA-DC-8061)
energy levels of equivalent j = ½ nuclear configurations, classification using group theory, 20: 40082
energy levels of odd-A rare-earth, vibrational, (T), 20: 40118
existence of isomeric, with quantized vortices in superfluid model, (T), 20: 40106(T)
magnetic dipole moments of, measurement using perturbed γ–γ angular correlations, (T), 20: 40125
meson (μ^-) capture by, neutron angular distributions from, (E), 20: 40096
meson (μ) capture by complex, effects of giant resonances in, 20: 40151
moments of inertia of deformed, (T), 20: 40102
Mössbauer spectra with fluctuating hyperfine magnetic fields, (T), 20: 40152
neon-20 reactions with emulsion, at 200 Mev, (E), 20: 40083
neutron reactions (n,α), (n,2n), (n,p), and (n,t) with nuclei, cross sections for, (E), 20: 40069(R) (EANDC(E)-66(U))
neutron reactions (n,α) and (n,p) with, cross sections for, (E), 20: 40069(R) (EANDC(E)-66(U))
neutron reactions (n,α) and (n,p) with, cross sections for, (E), 20: 40069(R) (EANDC(E)-66(U))
nuclear magnetic double-resonance spectra of spin ½, (T), 20: 40103
properties of beta-unstable, methods for investigating, 20: 40109
proton reactions at 1 to 30 Bev with emulsion, calculations for, 20: 39828
reactions with 14-Mev neutrons for activation analysis, 20: 38838
stability of, 20: 40108
NUCLEI (CELLS)
radiation effects from incorporated tritium on, biological, 20: 38624
NUCLEONS
energy levels of equivalent j = ½ configurations, classification using group theory, 20: 40082
form factors of, determination by cosmic particle momentum transfer analysis, 20: 39781
interactions in nuclei, symmetry of self-consistent field, (T), 20: 40136
interactions with mesons (π), Regge recurrence parity assignments in, (T), 20: 39749 (COO-881-77)
interactions with mesons (π^-) at 7 Bev, momentum spectra of secondary particles from, (E/T), 20: 39751 (JINR-E-2738)
interactions with nucleons at 14.5 Mev, phase-shift analysis of, 20: 39756 (JINR-P-2742)
interactions with mesons (K), K* production threshold from, (T), 20: 39778
interactions with nucleons in double-peripheral model, cross section for W-meson production in, (T), 20: 39797
interactions with mesons (π), crossing in backward cone and threshold regions in, 20: 39798
interactions with nucleons, analyticity of partial-wave amplitudes for, 20: 39799

interactions with mesons (π), graphical method for charge independence in strong, 20: 39800
interactions with mesons (π), analysis for Λ-K^0 production, (E/T), 20: 39803
interactions with nucleons, Regge-pole model for cross-channel amplitudes of, (E/T), 20: 39806
interactions with photons, reciprocity relation as test of C and T invariance in, 20: 39810
interactions with mesons (π), sum rule for axial-vector coupling-constant renormalization in, 20: 39814
interactions with mesons (π) at 290 to 905 Mev, cross sections for $N^*_{3/2}$ production in, (E/T), 20: 39827
interactions with mesons (π), model for, 20: 39839
interactions with mesons (K), (T), 20: 39840
interactions with antinucleons, deuteron exchange effect in, (T), 20: 39841
interactions with nucleons, cross sections and polarization parameters for, (E/T), 20: 39844
interactions with nucleons, effects of NN* channel on elastic, (T), 20: 39848
interactions with polarized protons at 23.1 to 630 Mev, polarization tensor, 20: 39909
interactions with mesons (π), effect of m-scattering annihilation channels on, 20: 39776(T)
interactions with nucleons in nuclei, (T), 20: 40115
magnetic moments of, sum rules for photoproduction amplitude correlations with, 20: 39879
moments of, sum rules for, 20: 40130
spin gyromagnetic ratio for, effective, (E), 20: 40073 (LA-DC-8065)

NUCLEOPROTEINS
desoxy, radiation effects on solutions of, β, 20: 38581

NUCLEOTIDES
determination of, in enzymatic digests of DNA by neutron activation, 20: 38816
gamma dose effects on phosphate uptake by, in lymphoid tissue, 20: 38585
structure of, computer program for calculating three-dimensional, 20: 39470(R) (ORNL-3924)

O

OCEANOGRAPHY
nuclear energy applications in, 20: 39313
nuclear power uses in, 20: 40362

OIL SHALES
oil shales–polyolefins, fabrication of molded articles of, using heat, pressure, and radiation, 20: 38974(P)

OILS
combustion products as fuel for MHD generator, thermodynamic properties of, 20: 39938

OLEIC ACID
neutron inelastic scattering by, dynamic processes in slow, 20: 40338

ORES
analysis for rhenium by neutron activation methods, 20: 38802

ORGANIC COMPOUNDS
performance of thick slabs of, for fast neutron flux determination, 20: 39223

ORGANISMS
radiation effects on tissues in, review on, 20: 38653

ORGANS
phosphorus metabolism in rat, effects of reticulin on, tracer study, 20: 38572

ORNL RELATIVISTIC ISOCHRONOUS CYCLOTRON
beam extraction system for, operation and performance of, 20: 39521
beam monitor design, 20: 39507

ORNL RESEARCH REACTOR
boiling detector design for, 20: 40373

OROTIC ACID
effects on hepatic fatty acid synthesis in rats, 20: 38559

OSMIUM
superconductivity of, 20: 40047

OSMIUM ALLOYS
Ir–Os, superconductivity, 20: 40047
Os–Ru, superconductivity, 20: 40047

OSMIUM FLUORIDES
molecular structure of, mean amplitudes of vibration at 0 and 298°K in, 20: 38897

1,3,4-OXADIAZOLE, 2-(4-BIPHENYLYL)-5-PHENYL-
radioinduced luminescence of, determination of triplet exciton diffusion from alpha, 20: 38957

OXETANE, 3,3-BIS(CHLOROMETHYL)-
radioinduced polymerization of, in presence of maleic anhydride, gamma and uv, 20: 38953

OXIDES
chemical reactions with metals at high temperatures, review on, 20: 39331(T) (UCRL-Trans-10044)

OXYGEN
content in irradiated polyethylene films, gamma dosimetry by activation analysis of, 20: 38937 (AD-635655)
content in pools in man, isotopic dilution studies on, 20: 38941(R) (RRL-2310-182)
determination in coal by activation, on-line, 20: 39025 (ORO-2980-12)
determination in earth formations, neutron-gamma well logging method for, 20: 39137(P)
determination in metals, activation, 20: 38840
determination in organic phosphorus compounds in cardiac and skeletal muscles, activation, 20: 38848
determination in sodium, development of techniques for, 20: 38797(R) (MSAR-66-150)
determination in solids, mass spectrographic, 20: 38831
diffusion in rare earth oxides, tracer studies of, 20: 38865(R) (COO-1109-22, Paper 4)
effects on annealing of recoil damage in neutron-irradiated cobalt complexes, 20: 38965
effects on crystal structure of uranium monocarbide, 20: 39385 (CEA-R-2852)
effects on grain size of tungsten, 20: 39400 (NASA-TN-D-3531)
effects on heavy water decomposition, 20: 40409(R) (NP-16230)
effects on internal friction of electron-beam refined tantalum, 20: 39420
effects of interstitial, on superconducting critical temperature of niobium, 20: 40025
effects on photosensitized decomposition of deuterated and normal cyclobutane, 20: 38941(R) (RRL-2310-182)
effects on radioinduced decomposition of 5-bromouracil, 20: 38968
neon-20 reactions at 200 Mev, in emulsions, (E), 20: 40083
production from air in MHD power plant, 20: 39043(P)
radioinduced reactions with methanol, effects of dose rate on yields in, 20: 38942 (UJV-1457)
radiosensitivity effects on tumor cells, 20: 38699
radiosensitivity effects of environmental, on mice, γ, 20: 38642
reactions with radioisotope-containment materials in launch pad abort environment, 20: 39312 (SC-CR-66-2044)
spectra of high-speed excited atomic, at 2700 to 6600 A, (E), 20: 39593
tension in mice of, effects of thiopentobarbital on, 20: 38738

OXYGEN IONS
content in outer ionosphere, 20: 39950
effects on silicon wafers at 60 kev, formation of oxide films, (E), 20: 40314

OXYGEN ISOTOPES
energy level structure of, calculations using SU(3) model, (T), 20: 40126
fractionation in coexisting dolomites and limestones, 20: 39129

OXYGEN ISOTOPES O-15
use for cerebral blood flow measurement, 20: 38745(R) (NYO-3267-3)

OXYGEN ISOTOPES O-16
binding energy of, calculation using K-matrix theory, 20: 40119
content ratio to oxygen-18 in ice and snow of St. Elias Mountain, Canada, 20: 39123
deuteron reactions (d,n) at 3.5 Mev, angular distribution for, (E), 20: 40155
energy levels of, Hartree-Fock calculations for, (T), 20: 40138
meson (π^-) capture at 80 Mev, helium-8 production in, (E), 20: 40071 (JINR-E-2774)
reactions (O-16, O-16 γ) with chromium isotopes at 30 to 39 Mev, gamma spectra from, (E), 20: 39470(R) (ORNL-3924)
reactions (O-16, O-16 γ) with palladium isotopes at 42 to 49 Mev, gamma spectra from, (E), 20: 39470(R) (ORNL-3924)

OXYGEN ISOTOPES O-17
deuteron reactions (d,p) at 1.0 and 1.5 Mev, cross sections for, (E), 20: 40155
deuteron reactions (d,p) at 10 Mev, oxygen-18 energy levels from, (E), 20: 40161
energy levels of, Hartree-Fock calculations for, (T), 20: 40138
triton reactions (t,p) at 12 Mev, oxygen-19 energy levels from, (E), 20: 40161

OXYGEN ISOTOPES O-18
alpha reactions (α,nγ) at 4.43 Mev, neon-21 energy levels from, (E), 20: 40156
content ratio to oxygen-16 in ice and snow of St. Elias Mountain, Canada, 20: 39123
deuteron reactions (d,p) at 11 Mev, energy levels of oxygen-19 from, (E), 20: 40161
energy level structure of, calculations using SU(3) model, (T), 20: 40126
energy levels of, from oxygen-17 (d,p) reaction, (E), 20: 40161
respiration rate in man, isotopic dilution studies on, 20: 38941(R) (RRL-2310-182)

tracer use in studies on oxygen body stores, 20: 38941(R) (RRL-2310-182)
triton reactions (t,p) with, spectroscopic factors of, (T), 20: 40126
use for determination of ATP and 2,3-diphosphoglyceric acid in erthrocytes by proton activation, 20: 38841
use in determination of oxygen in organic phosphorus compounds by activation, 20: 38848

OXYGEN ISOTOPES O-19
energy levels of, from oxygen-18 (d,p) reaction, (E), 20: 40161
energy levels of, from oxygen-17 (t,p) reaction, (E), 20: 40161

OXYGEN SYSTEMS
C–N–O–U, crystal structure of solid-solutions, 20: 39385 (CEA-R-2852)
CO_2–ethanol–O, man transfer of, in channel flow, 20: 39050 (UCRL-16535)

OYSTER CREEK POWER REACTOR
construction of, 20: 40436
design of, 20: 40436
operation of, personnel training program, 20: 40436

OYSTERS
radiation effects on vitamin content in, γ, 20: 39288(R) (ORO-636)
radiosensitivity of exogenous bacteria of, 20: 39288(R) (ORO-636)

P

PACIFIC OCEAN
uranium-234/-238 ratios in, 20: 39133

PAINTS
preparation of luminous, in Czechoslovakia, 20: 39279

PALLADIUM
neutron capture resonance integrals, (E), 20: 40146
superconductivity of, 20: 40047

PALLADIUM DEUTERIDES
effects on hydrogenation of propylene, kinetics of, 20: 38908
effects on hydrogenation of ethylene, kinetics of, 20: 38908

PALLADIUM HYDRIDES
effects on hydrogenation of ethylene, effects of deuterium on kinetics of, 20: 38908
effects on hydrogenation of propylene, effects of deuterium on kinetics of, 20: 38908

PALLADIUM ISOTOPES Pd-105
proton reactions (p,n) at 3.0 to 5.8 Mev, strength functions for, (E), 20: 39470(R) (ORNL-3924)

PALLADIUM ISOTOPES Pd-106
alpha reactions ($\alpha,\alpha'\gamma$) at 9 to 10 Mev, gamma spectra from, (E), 20: 39470(R) (ORNL-3924)
oxygen-16 reactions (O-16, O-16′γ) at 42 to 49 Mev, gamma spectra from, (E), 20: 39470(R) (ORNL-3924)

PALLADIUM ISOTOPES Pd-108
alpha reactions ($\alpha,\alpha'\gamma$) at 9 to 10 Mev, gamma spectra from, (E), 20: 39470(R) (ORNL-3924)
oxygen-16 reactions (O-16, O-16′γ) at 42 to 49 Mev, gamma spectra from, (E), 20: 39470(R) (ORNL-3924)

PALLADIUM ISOTOPES Pd-110
alpha reactions ($\alpha,\alpha'\gamma$) at 9 to 10 Mev, gamma spectra from, (E), 20: 39470(R) (ORNL-3924)
oxygen-16 reactions (O-16, O-16′γ) at 42 to 49 Mev, gamma spectra from, (E), 20: 39470(R) (ORNL-3924)

PALLADIUM SYSTEMS
H–Pd, kinetics and structures of, diffraction studies on, 20: 39428

PAPER
processing of, radioisotope gages used in, 20: 39292

PARAFFIN
neutron reactions at 0.025 to 0.4 ev, total cross sections for, (E), 20: 40069(R) (EANDC(E)-66(U))

PARAMAGNETIC MATERIALS
scattering in, neutron diffraction studies on, 20: 38882

PARTICLE STATISTICS
many-body processes, probabilities in, 20: 39926

PARTICLE TRACKS
use in age estimations on natural glasses and tektites, 20: 39135

PARTICLES
chemical and physical properties of fallout, 20: 39115
deposition and reentrainment of methylene blue–uranin, in long vertical tubes, 20: 39103(R) (BNWL-235-3, pp 51-69)
reactions in matter, relaxation of nonstationary processes from finite transport velocity of, 20: 39475
research on aerosol, 20: 38857(R) (BNWL-235-3)
sampling of, in air streams, subisokinetic, 20: 39103(R) (BNWL-235-3, pp 51-69)
sampling of, in air streams, use of nozzles in isokinetic, 20: 39103(R) (BNWL-235-3, pp 51-69)
separation of biological on nonbiological, equipment for, 20: 38545
size control of, using spinning-disk generator, 20: 39103(R) (BNWL-235-3, pp 51-69)

PEBBLE BED REACTORS
conversion factor of high temperature thorium, 20: 40471

PECTINS
effects on elimination of radioisotopes by mice and rats, 20: 38733

1,3-PENTADIENE
radioinduced isomerization of, in benzene, gamma, 20: 38948

2,4-PENTANEDIONE
solvent properties for molybdenum, 20: 38824

2,4-PENTANEDIONE COMPLEXES
with copper and uranyl ions in mixture with other β-diketone in benzene solution, 20: 38855 (BNL-10350)

PENTANES
neutron inelastic scattering by, dynamic processes in slow, 20: 40338

1-PENTANOL
neutron inelastic scattering by, dynamic processes in slow, 20: 40338

PENTOBARBITAL
thio-, effects on oxygen tension in mice, 20: 38738
thio-, radioprotective effects on mice, 20: 38738

PERMEABILITY
calculation of, in soil, 20: 39099(R) (BNWL-235-3, pp 1-23)

PEROXIDES
effects on radioinduced polymerization of cyclic ethers, 20: 38953
lipid, formation in mitochondria, effects of iron on, 20: 38639
radioinduced in tissues of mice, x, 20: 38660

PERSONNEL
radiation hazards to, conference on, 20: 39166
radiation monitoring of, economics, efficiency, and sensitivity of various instruments for, 20: 39246
radiation protection of personnel servicing industrial x-ray equipment, 20: 38737

PERTURBATION THEORY
uses in calculating electromagnetic mass differences, 20: 39928

PETROLEUM
analysis of, equipment and method for, 20: 39191(P)
properties for use in stacked-clone contactor, 20: 38998(R) (ORNL-3958)

PHANTOMS
gamma and x radiation dosimetry for sheep, 20: 38625
use for gamma dose distribution measurements, 20: 38762
use of head, for x radiation dosimetry, from facial therapy, 20: 38765
use of tissue equivalent, for γ dosimetry measurements, 20: 38771
use of water, for γ and x dosimetry studies, 20: 38791
x ray dose determination in, for use in chicken irradiation studies, 20: 38676

PHARMACEUTICALS
control of radioactive, in Belgium, 20: 39156

PHASE STUDIES
use of chemical analyses in, 20: 39427

PHENATINE
effects with AET on cystamine as radioprotective agent in mice and rats, 20: 38726

PHENOL, DINITRO-
radiosensitivity effects on cultured mammalian cells, x, 20: 38710

PHENOLPHTHALEIN
tetraiodo-, preparation of iodine-131-labeled, 20: 38985

PHENYLEPHRINE
effects on inhibition of tissue reaction in irradiated rabbit connective tissue, 20: 38640

PHILIPPINE RESEARCH REACTOR
coolant analysis for corrosives and solids in, activation and chemical, 20: 38800 (PAEC(C)RE-652)

PHONONS
dispersion curves for potassium at 9°K, 20: 40343
kinetics of electron-phonon gas, (T), 20: 40313
motion in liquid helium II, Brillouin-induced, 20: 40034
spectra in metals, effects of nonmagnetic impurities on, 20: 39395 (IAE-1028)

PHOSPHATASES
distribution in rat liver subcellular fractions, 20: 38595(R) (ORO-3295-2)
radiation effects on distribution in retina, 20: 38689
release of acid, from lysosomes of x irradiated rat liver, 20: 38577

PHOSPHATE IONS
effects on sorption of americium, cerium, promethium, and yttrium by ion exchange material, 20: 38878(T) (ORNL-tr-1257)
electron spin resonance of, in irradiated ammonium fluorophosphate single crystals, 20: 38949

PHOSPHATES
analysis for oxygen, activation, 20: 38848

metabolism in wheat seedlings, 20: 38548(R) (ORO-2410-1)
PHOSPHATIDES
determination in blood, micro method, 20: 38652
effects on radiation resistance in rats, dietary, 20: 38721
radiation effects on, *in vivo*, x, 20: 38660
PHOSPHINE
phosphorus-31 chemical shifts in, calculation of, 20: 38895
PHOSPHONIC ACID, PENTYL-, DIPENTYL ESTER
complexes with metals, spectra of, infrared, 20: 38799(R) (NLCO-980)
PHOSPHONIC ACID, (2,2,2-TRICHLORO-1-HYDROXYETHYL)-, DIMETHYL ESTER
labeling with phosphorus-32, 20: 38931
PHOSPHORIC ACID
incorporation during nucleic acid synthesis in animals, radiosensitivity of, 20: 38585
PHOSPHORIC ACID, ALKYL ESTERS
solvent properties for bismuth in acid solutions, 20: 38828
PHOSPHORS
radioinduced luminescence of liquid, determination of diffusion of triplet excitons from, 20: 38957
scintillation performance of inorganic and organic, 20: 39233
use of radioisotope-excited, to illuminate timepieces, 20: 39296(P)
PHOSPHORUS
effects on strontium retention in rats of dietary, 20: 38566
metabolism in rats, effects of reticulin on, tracer study using phosphorus-32, 20: 38572
phase transformations, effects of pressure and irradiation on solid-solid, (E), 20: 40306
uptake of, in *Vicia faba*, effects of radioinduced toxins on, 20: 38664
PHOSPHORUS COMPOUNDS
organic, analysis for oxygen, activation, 20: 38848
organo-, solvent extraction properties of neutral bifunctional, 20: 38819
PHOSPHORUS FLUORIDES
PF_3–SF_6, radiolysis of, ESR spectra of products of, 20: 38941(R) (RRL-2310-182)
PHOSPHORUS ISOTOPES P-31
alpha elastic and inelastic scattering by, calculations using distorted-wave Born approximation, (T), 20: 40090
chemical shifts in organic phosphines from, calculation of, 20: 38895
PHOSPHORUS ISOTOPES P-32
beta dose distribution in polyethylene from, 20: 38777
effects of incorporated, on cytolytic and transforming abilities of Polyoma virus, 20: 38702
incorporation during nucleic acid synthesis in animals, radiosensitivity of, 20: 38585
incorporation in Malathion and Dipterex, 20: 38931
production in atmosphere by cosmic neutron reactions with argon, 20: 39991
separation from waste-water by aerobic treatment, 20: 40483
tracer use in study of annealing effects on ion-bombarded silicon, 20: 40345
uptake by central nervous system of, 20: 38651
use in therapy, effects on radioactivity of patients and wastes, 20: 38790
PHOSPHORUS ISOTOPES P-33
production in atmosphere by cosmic neutron reactions with argon, 20: 39991
PHOSPHORUS SYSTEMS
P–Th, thermodynamic properties of, solid-state EMF measurements at 800 to 950°C of, 20: 38907
PHOTOCHEMISTRY
reactivation of γ and uv irradiated *Chlamydomonas reinhardi* by light, 20: 38611
PHOTOCONDUCTIVITY
radioinduced in n-type germanium, infrared extinction of, (E), 20: 40298
PHOTOELECTRIC CELLS
theory for gamma-electric cell, 20: 39652
PHOTOGRAPHIC FILM
blackening by 24- to 500-kev electrons, 20: 39216
projector for bubble-chamber, 20: 39182
PHOTOGRAPHIC FILM DETECTORS
application of solid-state nuclear track detector to threshold detector system for neutron dosimetry, 20: 39221
calibration unit for, 20: 39266
design and fabrication for radon gas, 20: 39272
filter design for, 20: 39251(P)
performance for conversion electron studies, 20: 39216
reader design for, 20: 39258
PHOTOGRAPHY
projector design, 20: 39182
PHOTOMULTIPLIER TUBES
cooling system for, in well loggers, 20: 39140(P)
performance of, effects of dark current pulses and temperature on, 20: 39212(R) (NYO-3421-7)
PHOTON SHOWERS
properties of, effect of polarization of medium on, (T), 20: 39829
PHOTONS
emission and absorption by atoms, time correlation in exchanges, 20: 39577 (JINR-P-2791)
emission in electron interactions, (T), 20: 39836
field theory for, quantum, 20: 39853 (JEN-157-DF/I-48)
interactions with protons, meson (η) and (π) production in, (T), 20: 39743 (CALT-68-92)
interactions with protons at 0.4 to 1.0 Bev, computer program for determining quantities in, 20: 39750 (HEPL-236)
interactions with deuterons at 0.4 to 1.0 Bev, computer program for determining quantities in, 20: 39750 (HEPL-236)
interactions with nucleons, reciprocity relation as test of C and T invariance in, 20: 39810
interactions with protons, mechanism of neutral vector meson production in, 20: 39811
PHTHALIC ACID, RARE EARTH SALTS
stability constants for, potentiometric determination of, 20: 38896
PHYSICS
research in progress under Army Research Office, 20: 40485(R) (AD-636091)
PHYSIOLOGY
radiation effects on cat brain, 20: 38602(R) (UCLA-34P60-1)
radiation effects on fruit and vegetable, 20: 39289 (UCD-34P73-9)
PICOLINE
effects on iodine-131 exchange between elementary iodine and phenyl-dimethyliodopyrazolone, 20: 38936
PINCH DEVICES
development of chalice cusp-containment, 20: 40178(R) (SIT-2582-19)
plasma diagnostics in chalice, 20: 40178(R) (SIT-2582-19)
plasma stability in large inverse, current sheet, 20: 40250
radio-frequency noise in chalice, 20: 40178(R) (SIT-2582-19)
PINCH EFFECT
model for fast, snow-plow, 20: 40178 (SIT-2582-19)
voltage levels in flash x-ray discharges, 20: 40233
PIPES
fracture of defected, effects of pressure increase on, 20: 39329 (AECL-2432)
gamma radiation streaming through shelter air, review of, 20: 39060
shock wave propagation in, 20: 39072
welding of carbon steel to stainless steel nozzles, fatigue strength of, 20: 39404 (SWRI-1228-4-20)
PITUITARY GLAND
radiation effects on rat, biochemical, x, 20: 38661
radioinduced ablation of, use of yttrium-90 versus gold-198 for control of metastatic breast cancer, 20: 38758
radiosensitivity effects of frontal lobe, in animals, 20: 38653
radiotherapy of cancer of, use of yttrium-90 beads in, 20: 38744 (DP-1066(Vol.1), pp IV.47-66)
radiotherapy of tumors, dosimetry of x for, 20: 38761
PLACENTA
localization by radioisotope techniques, evaluation of hazards from, 20: 38757
PLANETS
atmospheres of, evaporative and hydrodynamic models for, 20: 39556
PLANT CELLS
radiation injuries of, role of toxins in, 20: 38664
radiosensitivity of, effects of 5-bromouracil on, 20: 38968
PLANT METABOLISM
reaction mechanisms for cation uptake, 20: 38548(R) (ORO-2410-1)
PLANT PHYSIOLOGY
radiation effects on barley, γ, 20: 38691
PLANTS
analysis for vanadium in Swedish, activation, 20: 38565
effects of chemical mutagens on, 20: 38589(R) (EUR-2761.f)
radiation effects on seedlings of Gramineae, β and γ, 20: 38583
radiation effects on cell division in chlorella, 20: 38605
radiation necrosis on reproduction of, orchid, x, 20: 38597(R) (TID-23057)
radioinduced mutations in, γ, 20: 38589(R) (EUR-2761.f)
radionuclide distribution in, from nuclear plant wastes, 20: 38742
radiosensitivity of, 20: 38588(R) (COO-1400-10)
PLASMA
acceleration by electromagnetic waves, (T), 20: 40267
acceleration by self-generated electric fields, near electron cyclotron resonance, 20: 40262
acceleration in decreasing magnetic fields, space charge electric field effects on, (T), 20: 40269
acceleration in external magnetic fields, induction effects on, (T), 20: 40192
acceleration in r-f and static magnetic fields, (E/T), 20: 40268
acceleration of low-density, theory of supersonic, (T), 20: 40240

boundary-layer equations for completely ionized, (T), 20: 39721
bremsstrahlung emission from classical, calculation of quadrupole, 20: 40273
charged-particle interactions with magneto-, cyclotron wave excitation from, (T), 20: 40188
collision-free column of, theory of wall losses in, 20: 40230
conductivity of cesium, gaseous impurity effects on, (E), 20: 39659
conductivity of helium, neutron-induced, (E), 20: 39683
conductivity of potassium-seeded argon, nonequilibrium, (T), 20: 39684
containment and heating in low-frequency rotating magnetic fields, (E/T), 20: 40279
containment in closed mixed-field configurations, properties of, (T), 20: 40280
containment in non-resonant h-f and magnetic fields, 20: 40193
containment in spherical cavity magnetic fields, (T), 20: 40277
containment of cylindrical, increasing load capacity of bearings by, 20: 40216
containment of deuterium, in magnetic mirror traps, 20: 40194
correlation functions of equilibrium, (T), 20: 40272
current-voltage curves for moving argon, (E), 20: 39655
cyclotron radiation from, effects of negative energy oscillations on, 20: 40219(T)
density measurements on laser-induced, optical interferometry for, 20: 40186
diagnostics of duoplasmatron using Langmuir probes, 20: 40202
diagnostics of, instrumentation for, 20: 40220
diffusion across magnetic fields in toroidal discharge, (E/T), 20: 40180 (SU-IPR-69)
diffusion in oscillating discharges, turbulent, (T), 20: 40191
diffusion in strong electric and magnetic fields, kinetic equation for, 20: 40249
distribution of, for improved ion engine performance, 20: 39093
dynamics of inhomogeneous, application of collective coordinates to, 20: 40178(R) (SIT-2582-19)
electric conductivity of magneto-, surface, 20: 40204
electric conductivity of, in electric field, (T), 20: 40238
electric conductivity of seeded argon, (E), 20: 39670
electric conductivity of seeded argon, (E), 20: 39727
electric discharge frequency multiplier for, in nonuniform shf fields, (T) 20: 40228
electric field of, in vicinity of charged cylinder, (T), 20: 40197(T)
electric properties of mercury–cesium, (E), 20: 39738
electromagnetic field penetration in magneto-, analysis of, 20: 40204
electromagnetic field interactions with, particle trajectories in, (T), 20: 40283
electromagnetic properties of dense, with nonequilibrium conductivity, 20: 39739
electromagnetic wave propagation in layer of magneto-, 20: 40200
electromagnetic wave propagation in cylindrical magneto-, transverse, (T), 20: 40201
electromagnetic wave interactions in, with transverse waves present, 20: 40205
electromagnetic wave propagation in limited, theory for, 20: 40206
electromagnetic wave interactions in magneto-, dispersions from, 20: 40207
electromagnetic wave propagation in, ray theory for cylindrical and spherical, 20: 40208
electromagnetic wave propagation in, collision effects on, (T), 20: 40222
electromagnetic wave propagation in cold, resonance effects on, (T), 20: 40258
electromagnetic wave propagation in, dispersion equations and Landau damping from, 20: 40259
electromagnetic waves in, charged particle motion and energy gain in standing, (T), 20: 40263
electromagnetic waves in, charged particle energy gain in standing, (T), 20: 40264
electromagnetic waves in, mass effects on charged particle energy gain standing, (T), 20: 40265
electron and ion density in magnetospheric, 20: 39978
electron beam injection into afterglow, cyclotron harmonic radiation from, (E), 20: 40165 (AD-637710)
electron beam interactions with, diagnostics from, 20: 40174(R) (ORNL-3989, pp 43-77)
electron beam interactions in magneto-, ion acceleration from, (T), 20: 40269
electron currents and temperatures in, probe measurements of, (T), 20: 39734
electron cyclotron heating of, research on, 20: 40173(R) (ORNL-3989, pp 31-42)
electron cyclotron radiations from, harmonics of, 20: 40274
electron density and temperature of cesium-seeded helium, (E), 20: 39665
electron density and temperature in argon and cesium-seeded argon, (E), 20: 39666
electron density distribution in infinite anisotropic, 20: 40184
electron density in one-dimensional channel flow, non-equilibrium excitation effects on, 20: 39714
electron density of transient, optical interferometer for measuring, 20: 40214
electron density, laser interferometer for measuring, 20: 40226
electron distribution function and state populations in non-equilibrium, (T), 20: 39711
electron temperature in discharge tube, electrode variation of, 20: 40174(R) (ORNL-3989, pp 43-77)
electron temperature of rare gas, auxiliary electrode for varying, 20: 40185
energy absorption from intense laser beam, (E), 20: 40190
energy exchange between electrons and molecules in nonequilibrium, (T), 20: 39677
energy measurement in Tokamak by magnetic flux variation, 20: 40187
flow in MHD cells, boundary layer on insulator walls for, (T), 20: 39933
flow in MHD duct, optimum Mach number for, 20: 39691
flow of magneto-, thermal and reactive nonequilibrium, 20: 40234
Hall effect in, in non-homogeneous fields, (E), 20: 39740
heating in h-f electromagnetic fields, properties of, 20: 40261
heating of collisionless, description of r-f, (T), 20: 40256
helicon-wave dispersion in non-uniform cylindrical, (T), 20: 40189
hydrodynamic wave propagation in waveguide-filled, pressure effects on, 20: 40248
injection in multipole magnetic fields, transverse, (E), 20: 40254
ion beam emission from optically polarized helium, 20: 39619
ion cyclotron frequency excitation from electron beam interactions, 20: 40174(R) (ORNL-3989, pp 43-77)
ion cyclotron instabilities in DCX-2, 20: 40172(R) (ORNL-3989, pp 14-30)
ion cyclotron oscillations in, damping of transverse, (T), 20: 40257
ion cyclotron resonance heating in QP machine, properties of, 20: 40260
ion recombination in r-f discharge, helium, 20: 40247
ionization instability of non-equilibrium argon, (E), 20: 39671
kinetic equations for unstable, in strong electric and magnetic fields, 20: 40181 (TID-23307)
Landau damping in, with finite transverse dimensions, (T), 20: 40211
magnetic field effects on cathode jets, (E), 20: 40232
magnetic field interactions with, particle trajectories in, (T), 20: 40283
magnetic fields in solar corpuscular stream, effect on magnetosphere of, 20: 39963(T)
magnetic flux of cylindrical, compression dependence of, (T), 20: 40198
microwave interactions with, reflection and transmission coefficients for, (T), 20: 40252
motion of Vlasov, constants of linearized, (T), 20: 40167 (IC-65/90)
movement in Hall-type MHD ducts, (T), 20: 39735
oscillations in cylindrical, moving along longitudinal fields, (T), 20: 40237
oscillations in electric field immersed, growth of, (T), 20: 40179 (SU-IPR-49)
oscillations in semiconductors, spin-orbital interaction effects on, 20: 40227
oscillations, conversion of electromagnetic waves to ion-acoustic, (T), 20: 40244
particle density and potential distributions in, magnetic effects on, (T), 20: 40230
particle distribution function for fully ionized, single, (T), 20: 40270
plasmon dispersion relations for electron, surface, 20: 40225
production and diagnostics of cesium, contact ionization, 20: 40223
production by burning pulverized coal in oxygen, 20: 39043(P)
production of dense carbon, (E), 20: 40209
properties as MHD working fluid, (T), 20: 39656
properties in r-f electric fields, (E/T), 20: 40276
properties of alpha-irradiated air, (E), 20: 39662
proton density and drift in interplanetary, 20: 40212
radiation emission from electromagnetic source in half-space of compressible, 20: 40199
radiation properties of alkali metal and argon–potassium, (E), 20: 39699
radiations from laser-produced hydrogen, spectra of, 20: 40251
radiative transport in fully ionized, equation for, 20: 40270
radio-wave absorption for determining variations of ionospheric, (E), 20: 39952
radio-wave scattering by, ion and electron temperature effects on, (T), 20: 40213
relaxation phenomena in cesium-seeded argon, (T), 20: 39700
spectra of cesium recombination continuum in argon, 20: 39722
spectra of characteristic x rays from flash discharges, (E), 20: 40233
spectral shift mechanism in, of electric spark discharge, 20: 40182
stability in DCX-2, (E/T), 20: 40176(R) (ORNL-3989, pp 95-108)
stability in magnetic fields, longitudinal current effects on, (T),

20: 40239
stability of homogeneous, (T), 20: 40221
stability of large inverse pinch, current sheet, 20: 40250
stability of magneto-, cyclotron under charged-particle injection, (T), 20: 40188
stability of nonhomogeneous periodic electron beam, (T), 20: 40245
stability of r-f magnetic field confined, models for, (T), 20: 40275
stability of trapped, properties of, 20: 40217(T)
stability of weakly nonhomogeneous, nonlinear theory of, (T), 20: 40236
stability of, electric field effects on, 20: 40195
stability of, temperature effects on, (T), 20: 40271
stabilization using h-f electric fields, low-frequency, 20: 40218(T)
structure at high densities, microscopic, (T), 20: 40157
structure of, in vicinity of charged cylinder, (T), 20: 40197(T)
synchrotron radiation in, dispersion effects on, (T), 20: 40271
synchrotron radiation from classical, calculation of, 20: 40273
thermal behavior of ionospheric, time-dependent, (T), 20: 39980
transport phenomena in low-energy, (T), 20: 40210
transport phenomena in, initial value problem, 20: 40168 (NASA-CR-559)
turbulent conductivity of non-equilibrium argon, (E), 20: 39671
use of induction-coupled, in heat treatment of particulate refractory materials, 20: 39343(P)
valve for, design for pulsed, 20: 40246
wave propagation along magnetized, effects of collisions on whistler, (T), 20: 40196
wave propagation along columns of, electromagnetic-acoustic, (T), 20: 40166 (AD-637711)
wave propagation in cold quasi-neutral, theory of nonlinear, (T), 20: 40235

PLASMA JETS
electron density and temperature in argon–hydrogen, 20: 40215
interaction with magnetic field, (T), 20: 40231
properties of external magnetic field, induction effects of, (T), 20: 40192
properties of r-f and static magnetic field, (E/T), 20: 40268
properties of, electron space charge electric field effects on, (T), 20: 40269

PLASTIC DEFORMATION
effects of cold working on room-temperature ductility of cobalt-base L-605 alloy, 20: 39399 (NASA-TN-D-3528)

PLASTIC FILMS
preparation of adhesive, by radioinduced graft-copolymerization of hydroxyl group-containing resin with copolymer of epoxy and polyamide resins, 20: 38979(P)

PLASTICS
preparation of foamed, 20: 38981(P)
use in blast shelters in Canada, 20: 39080
welder design for, engineering drawings of, 20: 39036

PLATINUM
neutron capture resonance integrals, (E), 20: 40146
proton reactions at 2.9 Bev, particle production by, (E), 20: 39794
reflection and thermal accommodation of helium beams by, (E), 20: 39590
superconductivity of, 20: 40047

PLATINUM ALLOYS
Ir–Pt, superconductivity, 20: 40047

PLOWSHARE PROJECT
excavation of gas storage area with nuclear explosion, 20: 39015 (UCRL-14877)
excavation of sea-level Istmian Canal, cost studies of, 20: 40422
underground gas storage reservoirs, 20: 39014(R) (TID-23184)

PLUTONIUM
analysis for carbon, coulometric, 20: 38796 (CEA-R-2968)
analysis of high-purity, for iron, absorptiometric, 20: 38801 (PG-Report-729)
crystal structure of, valence electrons and interatomic bonds in, 20: 40296
handling of, equipment design for, 20: 38835
monitoring in air, 20: 39269
monitoring in wounds, instrument for, 20: 39267
properties of, at low temperatures, 20: 39448 (AERE-X-PR-2596-9)
radiation damage in, effects of annealing on, 20: 39448 (AERE-X-PR-2596-9)
radiation effects on low-temperature electric conductivity of, self, 20: 39448 (AERE-X-PR-2596-9)
use in graphite moderated reactors, fuel cycle studies of, 20: 40421
use in high temperature reactors, physics studies on, 20: 40472
use in high temperature reactors, fuel cycle analysis, 20: 40473
use in thermal neutron reactors, 20: 40384(R) (EURAEC-1660)
vaporization of, thermodynamics of, 20: 38876 (UJV-1598)

PLUTONIUM ALLOYS
Al–Pu, fabrication, hazards evaluation tests, 20: 39153
Pu–U, irradiation testing of fuels of, 20: 40384(R) (EURAEC-1660)

PLUTONIUM FLUORIDES
molecular structure of, mean amplitudes of vibration at 0 and 298°K in, 20: 38897

PLUTONIUM ISOTOPES
preparation for use as alpha source, 20: 38990

PLUTONIUM ISOTOPES Pu-238
evaluation of, for space heat source, 20: 39306 (DP-1066(Vol.1), pp V.17-25)
production and use in United Kingdom, 20: 39283 (DP-1066(Vol.1), pp III.33-44)
use as heat source in SNAP-7 device, radiological hazards of, 20: 39307 (DP-1066(Vol.1), pp V.35-40)
use in thermoelectric converters, 20: 39633 (CEA-R-2788)

PLUTONIUM ISOTOPES Pu-239
content in fallout from USSR nuclear test, 1962, 20: 39109
content in fallout from Chinese nuclear tests, 1964 and 1965, 20: 39109
neutron fission of, fragment energy correlations for thermal, (E), 20: 39470(R) (ORNL-3924)
neutron fission of, time of emission and yield of x radiation from thermal, (E), 20: 40158

PLUTONIUM ISOTOPES Pu-240
content in fallout from USSR nuclear test, 1962, 20: 39109
content in fallout from Chinese nuclear tests, 1964 and 1965, 20: 39109

PLUTONIUM ISOTOPES Pu-241
neutron fission of, fragment energy correlations for thermal, (E), 20: 39470(R) (ORNL-3924)

PLUTONIUM ISOTOPES Pu-242
neon-22 reactions with, element-104 production from, 20: 40143

PLUTONIUM NITRIDES
thermodynamic properties of PuN, emf studies of, 20: 38911

PLUTONIUM OXIDES
PuO_2–rare earth oxides, preparation of sols of, 20: 39341(P)

PLUTONIUM(IV) OXIDES
HfO_2–PuO_2, preparation of sols of, 20: 39442(P)
PuO_2–ThO_2, irradiation testing of fuels of, 20: 40385 (ORNL-P-2327)
PuO_2–UO_2, phase diagrams, 20: 39393 (GEAP-4878)
PuO_2–Y_2O_3, preparation of sols of, 20: 39341(P)
PuO_2–ZrO_2, preparation of sols of, 20: 39442(P)

PLUTONIUM SELENIDES
preparation, properties, and uses of, book on, 20: 38927

PLUTONIUM TELLURIDES
preparation, properties, and uses of, book on, 20: 38927

PLUTONYL NITRATES
preparation and properties of hexahydrate of, 20: 39320(R) (MLM-1311)

PLYWOOD
design and testing of containers of, for isotope shipping containers, 20: 39164

POLISHING
equipment design for, 20: 39340

POLONIUM
determination of, review of methods for, 20: 38822

POLONIUM ISOTOPES
preparation for use as alpha source, 20: 38990

POLONIUM ISOTOPES Po-210
effects on radiation sickness induction in dogs, protective effects of unithiol against, 20: 38719
evaluation of, for space heat source, 20: 39306 (DP-1066(Vol.1), pp V.17-25)
half life determination by decaying pairs, 20: 39320(R) (MLM-1311)
separation from bismuth by vacuum distillation, 20: 38996 (DP-1066 (Vol.2), pp II.79-102)
use as heat source in thermoelectric generators, 20: 39308 (DP-1066 (Vol.2), pp III.3-16)
use in thermionic converters, 20: 39633 (CEA-R-2788)

POLYCYTHEMIA
effects of induced, on erythropoiesis suppression, 20: 38592 (ORNL-P-2158)

POLYMERS
radioinduced preparation of cross-linked, 20: 38976(P)

POPULATIONS
atomic weapons effects on, 20: 39055
effects of radioactivity in diet on carcinoma incidence in human, 20: 38739
protective action guides for uptake of cesium-137, iodine-131, strontium-89, and strontium-90 by, 20: 38743
radiation effects on 16-generation mouse, genetic, x, 20: 38590(R) (NYO-1979-13)
radiation effects on lizard, in Puerto Rican forest, γ, 20: 38601 (UCLA-12-567)
radioinduced mutations in Drosophila, x, 20: 38646
shelters for civilian, conference on, 20: 39054

POROUS MATERIALS

pore radius in, determination of mean, 20: 39012(P)
POSITRONIUM
effects of lead ions on formation of, 20: 38860 (COO-1297-6)
POSITRONS
annihilation in crystals, gamma angular correlations from, 20: 38745(R) (NYO-3267-3)
annihilation in ionic media, 20: 39819(T)
interactions with electrons, cross sections for meson production in, (T), 20: 39802
scattering by hydrogen, sensitivity of phase shifts for, (T), 20: 39817
use in localization of brain tumors after administration of appropriate isotopes, 20: 38745(R) (NYO-3267-3)
POTASSIUM
content in fallout from Chinese atomic test, Oct. 1964, 20: 39110
corrosive effects on niobium alloys at high temperatures, 20: 39028
determination in blood serum, activation, 20: 38851
determination in mineral and natural waters, flame photometric, 20: 38798 (NIJS-R-465)
determination of, in soils using γ emission of potassium-40, 20: 39280
electric conductivity of liquid-vapor mixtures of, in MHD ducts, (E), 20: 39742
electric dipole moments of, ratio of atomic to electron, 20: 39598
electron interactions with atomic, electron exchange in, 20: 39582(T) (AERE-Trans-1053)
heat transfer properties of condensing, 20: 39028
phonon dispersion curves at 9°K, pseudopotential analysis of, 20: 40343
plasma radiation properties of, (E), 20: 39699
radiation effects on content in blood of rabbits, x, 20: 38697
scattering by mercury beams at 7 to 500 ev, cross sections for, 20: 39599
superconductivity of, 20: 40047
POTASSIUM ACID FLUORIDES
properties of, for protective coatings on refractory metals, 20: 39348
POTASSIUM ALLOYS
K–Na, circulation in MHD ducts, (E), 20: 39716
K–Na, erosive effects on stainless steel, 20: 39023 (NAA-SR-11952)
POTASSIUM BROMIDES
effects on vapor pressure of heavy and light water solutions, 20: 38994(R) (AE-232)
radioinduced production of color centers in, γ, (E), 20: 40317
radiolysis of sulfuric acid solutions of, effects of dosage of electrons and gamma on yields of hydrogen peroxide from, 20: 38952
POTASSIUM CARBONATES
heat and free energy of formation of, 20: 39724
K_2CO_3–D_2O, phase diagram of, 20: 38994(R) (AE-232)
K_2CO_3–H_2O, phase diagram of, 20: 38994(R) (AE-232)
POTASSIUM CHLORIDES
effects on polarographic reduction of uranium ions, 20: 38922
effects on vapor pressure of saturated heavy and light water solutions, 20: 38994(R) (AE-232)
ionic transport coefficients for, at 25°C, 20: 38909
radioinduced production of color centers in γ, (E), 20: 40317
sputtering by argon ions at 30 kev, angular dependence of, (E), 20: 39600
$MgCl_2$–KCl, spectra of liquid, Raman, 20: 38871(R) (NYO-1769-54)
POTASSIUM COBALT FERROCYANIDES
sorptive properties for ocean fallout cesium, 20: 39147 (CONF-660401-6)
POTASSIUM FERRATES(VI)
preparation and properties of, 20: 38859 (CEA-R-2895)
separation processes for, 20: 38859 (CEA-R-2895)
POTASSIUM FLUORIDES
properties of aqueous sulfamic acid solutions of, for etching and pickling zirconium alloys, 20: 39351(P)
POTASSIUM IODATES
iodine-131 beta decay in, properties of xenon oxide compounds formed by, 20: 38984
POTASSIUM IODIDES
effects on iodine-131 uptake and elimination by thyroid in dogs, mice, and rats, 20: 38734
effects on vapor pressure of heavy and light water solutions, 20: 38994(R) (AE-232)
iodine-131 exchange with 1-iodo-2,4-dinitronaphthalene, kinetic studies of, 20: 38916
radioinduced production of color centers in, γ, (E), 20: 40317
POTASSIUM ISOTOPES K-40
determination of, in soil, 20: 39280
POTASSIUM ISOTOPES K-41
energy levels, (E), 20: 40147
neutron reactions (n,γ) with, resonance activation integral cross sections for, (E), 20: 40069(R) (EANDC(E)-66(U))
proton reactions (p,γ) at 1.74 to 2.17 Mev, calcium-42 energy levels from, (E), 20: 40133
POTASSIUM ISOTOPES K-42
determination in calcium-47, chromatographic, 20: 38827
separation from waste-water by aerobic treatment, 20: 40483
POTASSIUM NITRATES
radiolysis of frozen, at 77°K, yields of nitrite ion from gamma, 20: 38950
viscosity of, use of vertically oscillating cylinder for measuring, 20: 38872(R) (NYO-1769-68)
POTASSIUM OXIDES
heat and free energy of formation of, 20: 39724
POTASSIUM THIOCYANATES
use of, with 6 methyl thiouracil for iodine-131 removal from the thyroid gland, 20: 38734
POTASSIUM URANATES
reactions with carbon disulfide, 20: 38891
POTASSIUM URANIUM SULFIDES
formation of, from reactions of potassium diuranate with carbon disulfide, 20: 38891
POTATOES
radiation effects on tubers on chemical composition and yield of, x, 20: 38690
POWDER METALLURGY
process for preparation of beryllium–silver alloys, 20: 39374(P)
POWDERS
compaction and extrusion of tungsten, equipment and methods for high-energy-rate, 20: 39352 (BM-RI-6817)
POWER BREEDER REACTORS
design of electric generators for use with, 20: 40414 (TID-23257(Vol.2)
development at ANL, 20: 40413 (TID-23257(Vol.1))
development of, by Atomic Power Development Associates, 20: 40355 (APDA-TPI-1)
economic of fast, 20: 40415 (TID-23257(Vol.3))
POWER CYCLES
feasibility of Rankine and Brayton, for SNAP application, 20: 40452
POWER PLANTS
chemical recovery of energy in combined MHD/steam, 20: 39695
design of MHD, 20: 39043(P)
design of MHD combustion-fired, 20: 39654
design of Rankine cycle, using isopropylbiphenyl working fluid, 20: 40449(R) (SAN-650-1)
development of thermal, economics of future, 20: 40492
efficiency and thermodynamic parameters for closed-loop MHD, 20: 39720
efficiency of combined MHD converters and gas-cooled reactors, (T), 20: 39682
efficiency of MHD, 20: 39732
efficiency of MHD, effect of various parameters on, 20: 39705
efficiency of open-cycle MHD, 20: 39719
efficiency of, using MHD cycles, (T), 20: 39728
electrogasdynamic central, using fossil fuels, 20: 39701
evaluation of Rankine- and Brayton-cycles, for space application, 20: 40452
feasibility of shock-wave MHD generator plus gas-cooled reactor for, 20: 39639
magnetohydrodynamic utilizing reactor preheating and shock wave heating of gas, 20: 39666
magnetohydrodynamic, regenerative air preheater for, 20: 39725
operation of MHD, problems in, 20: 39741
technology of Rankine cycle, for space, 20: 39028
POWER REACTORS
boiler design for sodium-cooled, 20: 40424
construction cost analysis, 20: 40402 (EUR-2993.d)
control system for gas-cooled, 20: 40432(P)
core design for, evaluation of PM replacement, 20: 40405 (HIT-3583-27)
design of pressurized-water, with high prompt negative temperature coefficient, 20: 40434(P)
design of water-cooled and -moderated thermal, boiler- and turbine-less, 20: 40435(P)
development for undersea uses, 20: 40362
development of, review, 20: 40426
development of, review, 20: 40430
economics of dual-purpose, optimization studies of, 20: 40439
economics of, for sea-level canal construction, 20: 40422
fission product production in pressurized water, 20: 40400 (BNWL-244)
fuel compacts for, fabrication of uranium(IV) oxides, 20: 39373(P)
fuel requirements of, analysis of future, 20: 40420
heat transfer and fluid flow in boiling channels of, 20: 40427
operation of dual-purpose, analysis of dynamic behavior, 20: 40438
shield analysis for, computer programs for, 20: 40431
steam generator design for sodium-cooled, French program for, 20: 40428
steam separators for, design of radial-vane, 20: 39019(R) (GEAP-5149)
use in radioisotope production, 20: 39315 (DP-1066(Vol.1), pp I.29-52)

POWER SUPPLIES
design and performance of stabilized ZNN 4-type, 20: 39177
design for vacuum gage, 20: 39187
design for 100-channel pulse analyzer, 20: 39183
development of RIPPLE I + II radioisotope, in United Kingdom, 20: 39309 (DP-1066(Vol.2), pp III.39-48)
evaluation of isotopic, 20: 39304 (DP-1066(Vol.1), pp 19-28)
PRASEODYMIUM
determination in fluorite monocrystals, spectrophotometric, 20: 38829
determination in magnesium alloys by successive potentiometric titration, 20: 38830
x-ray-diffraction patterns of, effects of cold working on, 20: 39421
PRASEODYMIUM ALLOYS
Al–Pr, magnetic properties of intermetallic compounds of, 20: 39433
Fe–Pr, crystal structure of intermetallic compound, 20: 39409
Pb–Pr–Zn, component distribution in recrystallized, 20: 39435
Pr–Y, phase transformations and magnetic ordering in, pressure-induced, 20: 40326
Pr–Zn, crystal structure of intermetallic compound Pr_2Zn_{17} in, 20: 39417
PRASEODYMIUM CARBONATES
crystal structure of, x-ray diffraction studies of, 20: 38869(R) (COO-1109-22, Paper 8)
PRASEODYMIUM CHLORIDES
heat of dilution of aqueous solutions of, 20: 38870 (IS-1356)
heat of dilution of aqueous, at 25°C, 20: 38903
heat of solution, 20: 38901
specific gravity and apparent molal volume of aqueous solutions of, at 25°C, 20: 38905
PRASEODYMIUM IONS
radiation effects on spin-lattice relaxation time in lanthanum chloride, neutron and x, 20: 40350
spin-lattice relaxation time in lanthanum trichloride, angular and temperature effects on, 20: 40350
PRASEODYMIUM ISOTOPES Pr-143
energy level structure of, (E), 20: 40159
PRASEODYMIUM ISOTOPES Pr-144
beta transitions in, longitudinal polarization of, 20: 40085
PRASEODYMIUM OXIDES
phase studies of, in oxidation-reduction cycles, 20: 38864(R) (COO-1109-22, Paper 3)
phase studies of, at $PrO_{1.5}$ to $PrO_{1.714}$, 20: 38866(R) (COO-1109-22, Paper 5)
actinide oxides–Pr_2O_3, preparation of sols of, 20: 39341(P)
Pr_2O_3–Tb_2O_3, phase studies of, tensimetric, 20: 38863(R) (COO-1109-22, Paper 2)
PRASEODYMIUM PHOSPHATES
preparation and properties of, conductometric and potentiometric studies on, 20: 38883
PRASEODYMIUM SELENIDES
crystal structure of, reflection spectra for zonal, (E), 20: 40339
PRASEODYMIUM SELENITES
heat of formation of, at 298°C, 20: 38901
PRECIPITATION, ATMOSPHERIC
fission product, bismuth-214, and lead-214 contents in, effects of meteorological parameters on, 20: 39106 (BMwF-FBK-65-05)
PREFERRED ORIENTATION
conversion of data on, to inverse pole figures, 20: 39402 (ORNL-3979)
effects on ductile-brittle transitions in tungsten, 20: 39397 (NASA-TM-X-1252)
effects on phase transformations in molybdenum–uranium alloys, 20: 39389 (CEA-R-2973)
PREGNANCY
effects on albumen-globulin ratio in blood serum from irradiated hamsters, 20: 38598(R) (TID-22955)
radiotherapy for cervical carcinoma during, successful case report, 20: 38759
xenon-133 measurement of myometrial blood flow during, 20: 38747
PRESSURE
control in SNAP-10A coolant system, 20: 39023 (NAA-SR-11952)
effects on sodium-22 diffusion in sodium nitrate, 20: 38872(R) (NYO-1769-68)
function of capillary, in measuring permeability, 20: 39099(R) (BNWL-235-3, pp 1-23)
measurement in peripheral compressor, 20: 39021 (K-1665)
PRESSURE DROP
flow characteristics of subcooled water at atmospheric pressure in narrow heated channels, 20: 39047 (AERE-M-1739)
PRESSURE SYSTEMS
design of compensation, for SNAP-10A, 20: 39023 (NAA-SR-11952)
PRESSURE VESSELS
design for steam generators, 20: 40424
design of, for viscosity measurements in molten salts at high pressures, 20: 38871(R) (NYO-1769-54)
fracture of defected, effects of pressure increase on, 20: 39329 (AECL-2432)
materials for, design of low-alloy steel, 20: 39444(P)
radiation effects on steels for, neutron, 20: 39406 (WAPD-T-1864)
testing SNAP-10A expansion compensator, of 347 stainless steel, 20: 39023 (NAA-SR-11952)
welding methods for Senn reactor, 20: 40417
PRESSURIZED WATER REACTORS
design with high prompt negative temperature coefficient, 20: 40434(P)
fuel elements for, design of Zircaloy-clad oxide, 20: 40387 (WAPD-T-1939)
PROCAINE
radiosensitivity and therapeutic effects on dogs, mice, rabbits, and rats, 20: 38727
PROCESS HEAT REACTORS
economics of dual-purpose, optimization studies of, 20: 40439
operation of dual-purpose, analysis of dynamic behavior, 20: 40438
PROGESTERONE
metabolism in blood plasma in sheep ovaries, tracer study on, 20: 38547(R) (NYO-918-15)
PROLINE
radiolysis of, in aqueous solution, γ, 20: 38582
PROMETHIUM
x-ray-diffraction patterns of, effects of cold working on, 20: 39421
PROMETHIUM ALLOYS
Pb–Pm–Zn, component distribution in recrystallized, 20: 39435
PROMETHIUM COMPLEXES
with acid phosphates, ion exchange studies on composition and stability of, 20: 38878(T) (ORNL-tr-1257)
PROMETHIUM ISOTOPES Pm-140
gamma decay of, energy levels from, 20: 40131
half life, 20: 40131
PROMETHIUM ISOTOPES Pm-144
use as heat source in SNAP-7 device, radiological hazards of, 20: 39307 (DP-1066(Vol.1), pp V.35-40)
PROMETHIUM ISOTOPES Pm-147
beta dose distribution in polyethylene from, 20: 38777
evaluation of, for space heat source, 20: 39306 (DP-1066(Vol.1), pp V.17-25)
PROMETHIUM ISOTOPES Pm-151
energy levels of, lifetimes of, (E), 20: 40105(T)
PROMETHIUM OXIDES
actinide oxides–Pm_2O_3, preparation of sols of, 20: 39341(P)
PROPANE
reactions of solid, with electron-excited tritium atoms, 20: 38970
PROPANE, 1-BROMO-
radiation effects on, from neutron irradiation and isomeric transition, 20: 38963
1,3-PROPANEDIONE, 1,3-DIPHENYL-
complexes with copper and uranyl ions in mixture with other β-diketone in benzene solution, 20: 38855 (BNL-10350)
1-PROPANESULFONIC ACID, 2,3-DIMERCAPTO-
effects on cerium-144 excretion in rats, 20: 38732
effects on radiation injuries in dog kidneys, 20: 38719
effects with cystamine as radioprotective agent in mice and rats, 20: 38725
1-PROPANETHIOL, 2-AMINO-
effects on radioinduced leukemia in mice, protective, 20: 38722
2-PROPANETHIOL, 1-AMINO-
effects on organic peroxy compound synthesis in x irradiated mice, 20: 38660
2-PROPANOL
carbon-13 exchange between monoethanolamine and, 20: 39320(R) (MLM-1311)
methanol–2-propanol, carbon-13 exchange between monoethanolamine and, 20: 39320(R) (MLM-1311)
PROPELLANTS
feed and storage system for ion-engine, 20: 39091
PROPENE
effects on yields of acetylene from radiolysis of methane, 20: 38951
hydrogenation of, over palladium hydride, effects of deuterium on kinetics of, 20: 38908
radiolysis of, competition for electrons between nitrous oxide and tetrafluoroethylene yields in, 20: 38941(R) (RRL-2310-182)
reactions of solid, with electron-excited tritium atoms, 20: 38970
PROPENE, HEXAFLUORO-
radioinduced polymerization of, kinetics of, 20: 38946
PROPENE, 2-METHYL- POLYMERS
acrylic monomers–aromatic vinyl monomers–polyisobutylene, radioinduced formation of thermoplastic resin of, 20: 38978(P)
PROPENE, PENTAFLUORO-2-(TRIFLUOROMETHYL)-
radioinduced polymerization of, kinetics of, 20: 38946

PROPENE POLYMERS
radiation effects on, ESR spectral studies on electron and gamma, 20: 38954
radiolysis of, mechanism of structural changes in gamma, 20: 38945
PROPERDIN
radiation effects on content in rat blood serum, γ, 20: 38695
PROPIONIC ACID
labeling with iodine-131, 20: 38932
PROPORTIONAL DETECTORS
design for alpha monitor, 20: 39254
design for epithermal neutrons used in well logging, 20: 39138(P)
development for use as β monitor, 20: 39220
time delays between spark and counter pulse, (E), 20: 39215
PROPULSION
ion engine for space, using applied axial electric field, 20: 39090
ion engine for space, development of cesium, 20: 39093
ion engine for space, liquid-protected electrodes for, 20: 39094
ion engine for space, design, 20: 39095(P)
ion engines for space, surface tension storage and feed systems for, 20: 39091
ion engines for space, performance of, 20: 39092
PROTACTINIUM
crystal structure of, valence electrons and interatomic bonds in, 20: 40296
electrophoretic properties of, in sulfuric acid, 20: 38826
separation from hydrochloric acid solutions by solvent extraction using long-chain amines, 20: 39003
separation of thorium-230 from, by ion exchange, 20: 38834
PROTACTINIUM ISOTOPES Pa-231
preparation for use as alpha source, 20: 38990
radiation effects on, self, 20: 39448 (AERE-X-PR-2596-9)
PROTACTINIUM PEROXIDES
formation of, in basic media, 20: 38890
PROTECTIVE CLOTHING
decontamination using citric acid, detergents, or water, 20: 39161
PROTEINS
effects of absence of an essential amino acid on synthesis of, after uv irradiation of *E. coli* cultures, 20: 38562
immune reactions to brain tumor, in rabbits, 20: 38745(R) (NYO-3267-3)
radiation effects on synthesis in rat tissues, effects of thyroid hormone on x, 20: 38595(R) (ORO-3295-2)
radiation effects on blood serum, x, 20: 38598(R) (TID-22955)
radiation effects on binding to RNA, as mechanism of tobacco mosaic virus inactivation, uv, 20: 38584
radiation effects on permeation of intestinal wall of rats by, x, 20: 38604
radiation effects on, in meats and meat components, 20: 39301
structure of, computer program for calculating three-dimensional, 20: 39470(R) (ORNL-3924)
synthesis of, effects of chloramphenicol and uracil in uv-irradiated *E. coli*, 20: 38563
synthesis of, tracer study, 20: 38542(T) (UCRL-Trans-10029)
PROTON SOURCES
development of polarized, for Grenoble isochronous cyclotron, 20: 39527
PROTON SPECTROMETERS
design for use in satellites, 20: 39268
PROTONS
density and drift in interplanetary plasma, 20: 40212
density in ionosphere. energy spectra from, (E), 20: 39987
effects on gallium arsenide and silicon solar cells at 185 to 530 kev, 20: 40299
effects on methylamine, 20: 38964
energy-loss distributions from thin carbon foils, (T), 20: 40117
flux in inner Van Allen Belt on Dec. 19, 1961, (E), 20: 39992
flux in lower edge of inner radiation belt, (E), 20: 39983
flux in radiation belts, 20: 39957(T)
interactions in propane bubble chambers, method of identification of, (E), 20: 39211 (JINR-P-2842)
interactions with photons, meson (η) and (π) production in, (T), 20: 39743 (CALT-68-92)
interactions with photons at 0.4 to 1.0 Bev, computer program for determining quantities in, 20: 39750 (HEPL-236)
interactions with hyperons ($\Sigma^{\pm}$), cross sections for, (T), 20: 39765 (ORO-2504-91)
interactions with mesons (π^{+}) at 1.95 Bev/c, cross sections for, (E), 20: 39767 (TID-23278)
interactions with mesons (π^{-}) at 3 and 4 Bev/c, π-π final-state interactions from, (E), 20: 39769 (UCRL-16655)
interactions with mesons (π^{-}) at 1.6 to 4.2 Bev/c, strange-particle resonant states from, (E), 20: 39770 (UCRL-16788)
interactions with mesons (π) at high energies, review on elastic, (E/T), 20: 39744 (CERN-66-18)
interactions with neutrons at 400 and 630 Mev, optimal experiments for measuring parameters of, 20: 39752 (JINR-E-2765)
interactions with mesons (π^{-}) at 4 Bev/c, $\Lambda\eta$ resonance production in, (E), 20: 39754 (JINR-E-2858)
interactions with mesons (π^{-}) at 7.5 Bev, cross sections for, (E), 20: 39758 (JINR-P-2773)
interactions with protons at 605 Mev, spin correlations in elastic, (E), 20: 39759 (JINR-P-2776)
interactions with neutrons at 19.8 Bev/c, angular and energy distributions of secondary particles from inelastic, (E), 20: 39761 (JINR-P-2809)
interactions with protons, strongly singular complex potential for high-energy large-angle, (T), 20: 39777
interactions with mesons (π), strongly singular complex potential for high-energy large-angle, (T), 20: 39777
interactions with mesons (π) at 276 Mev, resonant meson (π)-meson (π) interactions in, (E), 20: 39779
interactions with mesons (π^{-}) at 775 Mev, single meson (π) production from, (E), 20: 39780
interactions with mesons (π), meson (σ) production in, (E), 20: 39782
interactions with mesons (K^{+}) at 3.52 Bev/c, meson (κ) production in, (E), 20: 39784
interactions with mesons (π^{-}) at 10 Bev/c, observation of $\omega^{0} \rightarrow \pi^{0} + \gamma$ in, (E), 20: 39787
interactions with mesons (K^{-}) at 10 Bev/c, mesons (L) production in, 20: 39788
interactions with protons at 735 Mev, polarization in, (E/T), 20: 39789
interactions with mesons (π^{-}) at 7.0 Bev/c, mesons (A_1) and (A_2) production in, (E), 20: 39790
interactions with protons at 328 to 736 Mev, polarization in elastic, (E), 20: 39791
interactions with protons at 1.7 to 6.1 Bev, polarization in, (E), 20: 39792
interactions with mesons (π^{-}) at 460 Mev, cross sections for elastic and inelastic, (E), 20: 39793
interactions with mesons (K^{+}), graphical method for charge independence in strong, 20: 39800
interactions with protons at 2 to 6 Bev/c, Regge-pole model for cross sections for, (E/T), 20: 39801
interactions with mesons ($\pi^{\pm}$) and ($K^{\pm}$) at 2 to 6 Bev/c, Regge-pole model for cross sections for, (E/T), 20: 39801
interactions with mesons (π^{-}) at 900 Mev, Λ-K^{0} production in, (E/T), 20: 39803
interactions with mesons ($\pi^{\pm}$), random-phase K-matrix formalism for peripheral, 20: 39804
interactions with mesons (K^{-}), absorptive peripheral model for charge-exchange, 20: 39805
interactions with mesons (π), S-wave $\pi\pi$ scattering length from, (T), 20: 39808
interactions with photons, mechanism of neutral vector meson production in, 20: 39811
interactions with protons at 1 to 3 Bev, peripheral model for inelastic, 20: 39820
interactions with neutrons at 600 Mev, meson (π) production in, (E), 20: 39826
interactions with mesons (π^{-}) at 17 Bev, angular correlations for inelastic, (E), 20: 39830
interactions with neutrons at 600 Mev, cross sections for meson ($\pi^{\pm}$) production in, (E/T), 20: 39834
interactions with mesons (π^{-}) at 900 to 1050 Mev/C, hyperon (Λ^{0}) production in, 20: 39837
interactions with mesons (K^{-}) at 1.80 to 1.95 Bev/c, resonance production in, (E), 20: 39838
interactions with mesons (π^{+}) at 1350 Mev, properties of N^{*} (1920) in, (E), 20: 39845
interactions with mesons (π^{-}) at 7.5 Bev, $N^{*}_{\frac{3}{2}\frac{3}{2}}$, $N^{*}_{\frac{3}{2}\frac{1}{2}}$, and ρ^{0} production from, (E), 20: 39758 (JINR-P-2773)
interactions with polarized nucleons at 23.1 to 630 Mev, polarization tensor for, 20: 39909
interactions with mesons (π^{-}) at 7.5 Bev, angular and momentum distributions from, (E), 20: 39758 (JINR-P-2773)
interactions with mesons (π^{-}) at 3.5 Bev/c, elastic differential cross sections for, (E), 20: 39785
interactions with protons at high densities, rate calculations for, 20: 40157
magnetic moment of, (T), 20: 39753 (JINR-E-2827)
polarization in two-nucleon systems at 310 to 700 Mev, (E/T), 20: 39844
production in proton reactions with beryllium and platinum at 2.9 Bev, (E), 20: 39794
propagation of solar-flare, in interplanetary magnetic field, (T), 20: 39575
radiation hazards to astronauts from, 20: 38603(T) (AD-629422)
reactions (p,α) with nuclei, statistical fluctuations in cross sections for, 20: 40065(R) (BMwF-FB-K-66-01)
reactions (p,α) with aluminum-27, Q value for, (E), 20: 40099

reactions (p,α) with aluminum-27 at 11 to 19.7 Mev, excitation function for, (E), 20: 40101
reactions (p,γ) with potassium-41 at 1.74 to 2.17 Mev, calcium-42 energy levels from, (E), 20: 40133
reactions with atoms, ionization cross sections for, (T), 20: 39607
reactions with beryllium and platinum at 2.9 Bev, particle production by, (E), 20: 39794
reactions with hydrogen, excitation, 20: 39583
reactions with hydrogen gas, electron capture cross sections for, (T), 20: 39606
reactions with nuclei (89 < A < 130) at 3.0 to 5.8 Mev, strength functions for, (E), 20: 39470(R) (ORNL-3924)
reactions with nuclei at 1 to 30 Bev, calculations for, 20: 39828
relaxation times of, in aqueous pentavalent molybdenum solutions, 20: 38893
scattering by argon-40 near 1.1 Mev, resonances in elastic, (E), 20: 40147
scattering by beryllium-9, carbon-12, nickel-58, and nickel-60 at 45 Mev, cross sections for elastic, (E), 20: 40162
scattering by bismuth-209, lead-206, lead-207, and lead-208 at 21 Mev, inelastic, (E), 20: 40074 (LA-DC-8069)
scattering by cadmium-112 and silver-107 at 13 Mev, differential cross sections for elastic and inelastic, (E), 20: 39470(R) (ORNL-3924)
scattering by deuterium at 8.9 Mev, mechanisms for, 20: 40065(R) (BMwF-FB-K-66-01)
scattering by krypton at 3 to 6 Mev, differential cross sections for elastic and inelastic, (E), 20: 39470(R) (ORNL-3924)
scattering by nuclei, statistical fluctuations in cross sections for elastic, 20: 40065(R) (BMwF-FB-K-66-01)
transmission through mica foils at 3.55 Mev, chenneling in, (E), 20: 40324

PRUSSIAN BLUE
effects on biological half-life of cesium-137 excretion in dogs and man, 20: 38557

PSEUDOUREA, 2-(2-AMINOETHYL)-2-THIO-
effects with phenatine as radioprotective agent in mice and rats, 20: 38726
radiosensitivity effects in mice, x, 20: 38715
radiosensitivity effects on mice, 20: 38717

PUERTO RICO POWER REACTOR
fuel element design, thermal conductivity values for urania, 20: 39403 (ORNL-TM-1450)
fuel elements for, thermal cycle testing of, 20: 40401 (CEND-259)

PULSE ANALYZERS
channel width of, effects on spectrometer resolution, 20: 39204 (INR-694/III/PL)
design of linear filters for, for amplitude measurements in presence of noise, 20: 39195 (AE-235)
design of single channel, 20: 39184
design of 100-channel transistorized, 20: 39183
development for scintillation measurement of uranium-235 enrichment in fuels, 20: 39335
review of multichannel and multiparameter, 20: 39176

PULSE COLUMNS
operation and performance of, in Tramex solvent extraction process, 20: 38998(R) (ORNL-3958)

PULSE GENERATORS (ELECTRONICS)
design for spark chamber, 20: 39270
design of high-frequency, for plasma studies, 20: 40281

PUMPS
design and performance of peripheral, for incompressible fluids, 20: 39021 (K-1665)
design and testing of, for radioactive waste removal, 20: 40481 (WAPD-T-1851)
design of 13.5 l/sec, for gases, 20: 39035
design of, for isopropylbiphenyl, 20: 40449(R) (SAN-650-1)

PUPAE
radiation effects on grain moth, gamma, 20: 38705

PUREX PROCESS
waste (PW-1) processing for, properties of input melts for fixation, 20: 40476(R) (BNWL-267)
waste fixation in glasses by calcination, efficiency of, 20: 38998(R) (ORNL-3958)

PURINES
synthesis in plants, 20: 38589(R) (EUR-2761.f)

PYRAZOLONES
1-phenyl-2, 3-dimethyl-4-iodo-, iodine-131 exchange between, and iodine, effects of aromatic azines on, 20: 38936

PYRIDINES
effects on iodine-131 exchange between elementary iodine and phenyl-dimethyliodopyrazolone, 20: 38936

PYRIDOXINE
effects on radiation resistance in rats, dietary, 20: 38721

PYRROLIDONE, VINYL- POLYMERS
radiation effects on permeation through rat intestinal wall of iodine-131 labeled, x, 20: 38604

Q

QUALITY CONTROL
reliability of test programs by use of K-factors, 20: 40447 (NAA-SR-11913)
requirements for, in activation analysis, 20: 38853

QUANTOMETERS
constants at 650 Mev, 20: 39248

QUANTUM MECHANICS
adiabatic invariance for quantum systems, high-order, 20: 40011
angular momentum in, SU(1,1) and SU(2) groups for complex, 20: 39863
electron energy levels in polyatomic molecules, multiple-scattering model for, (T), 20: 39618
phase functions in, methods of, (T), 20: 39997 (JINR-P-2758)
representation of rotation matrices, graphical method for, 20: 40120
Schroedinger equation with central Coulomb potential, orbital degeneracy of, 20: 40000
theory of, mathematical foundation for, 20: 39998 (KAPL-3147)
wave equations in, exact invariants for nonlinear, 20: 40005
Wick polynomials at fixed time in, 20: 40004

QUARTZ
use for fission detection at high temperatures, 20: 39208 (JINR-P-2705)

QUINOLINES
effects on iodine-131 exchange between elementary iodine and phenyl-dimethyliodopyrazolone, 20: 38936

R

RABBITS
effects of cysteamine on liver of, cytological, 20: 38716
immune reactions to human brain tumor proteins, 20: 38745(R) (NYO-3267-3)
pathology of radiation sickness in, effects of functional state of hypothalamous on, 20: 38688
pharmacological effects on tumors in, of sulfhydryl-containing boron hydrides, 20: 38745(R) (NYO-3267-3)
radiation and Brucella effects on malic dehydrogenase activity in peritoneal cells of, 20: 38586
radiation effects on immune reactions in eyes of, x, 20: 38608
radiation effects on granulocyte output from bone marrow in, effects of humoral agent on x, 20: 38633
radiation effects on connective tissue of, effects of vasoconstricting drugs on x, 20: 38640
radiation effects on function of gastrointestinal and respiratory tracts of, 20: 38659
radiation effects on leukocytes in, x, 20: 38681
radiation effects on eyes of, pathological, x, 20: 38689
radiation effects on potassium content in blood of, effects of injected antigen on, 20: 38697
radiation effects on immune reactions in adrenal cortex of, x, 20: 38697
radiation effects on, biochemical and hematological, effects of adrenaline on x, 20: 38686
radiation effects on immune reactions in, x, 20: 38641
radiation effects on lipid and iodine content of blood of, 20: 38652
radiation effects on central regulation of automatic functions in, x, 20: 38654
radiation effects on conditioned reflex in, γ, 20: 38655
radiation sickness in newborn, by exposure during intrauterine development, 20: 38665
radiation sickness in, mechanism of death from, 20: 38666
radiation sickness in, protective effects of procaine against, 20: 38727
radiation sickness effects on pulmonary circulation in, 20: 38657
radioprotective effects of selachyl alcohol, 20: 38731
radiosensitivity effects of cysteamine on, exposed to whole-body x irradiation, 20: 38716

RADIATION
detection and measurement in circulating blood, design of shielded coil for scintillation detector, 20: 38558
distribution of initial and residual, from nuclear weapons, 20: 39056
dosimetry in space, 20: 39158
effects in etiology of childhood leukemia, review of, 20: 38668
effects of Brucella and, on malic dehydrogenase activity of rabbit peritoneal cells, 20: 38586
effects of ionizing, on crosslinking of cellulose in presence of sensitizing agent, 20: 38975(P)
effects of whole-body ionizing, mechanisms involved in the bone marrow syndrome from, 20: 38700
effects on animal organisms, book on, 20: 38544
effects on animals, whole-body biological, effects of pre-irradiation on, 20: 38696

effects on animals and man, protection against, 20: 38718
effects on bacterial flora of mucous membranes and skin, 20: 38644
effects on beryllium impact properties, 20: 40460(R) (IDO-17191)
effects on beryllia, survey of, 20: 39453 (EUR-3054.e)
effects on beryllium, survey of, 20: 39454 (EUR-3055.e)
effects on blood vessel tonus in dogs, 20: 38658
effects on chemical changes in meats and meat components, 20: 39301
effects on cyclohexane-iodomethane, methyl radical yields in, 20: 38941(R) (RRL-2310-182)
effects on decomposition of selenium-75-labeled-selenourea, 20: 38991
effects on graphite, survey of, 20: 39455 (EUR-3056.e)
effects on graphite, book on, 20: 39463
effects on hexane, effects of deuterated and normal hydriodic acid on yields in, 20: 38941(R) (RRL-2310-182)
effects on insulators, recovery from induced voltage from, 20: 40329
effects on ketene, 20: 38977(P)
effects on leukemia development in mice, protective effects of 5-methoxytryptamine and propamine against, 20: 38722
effects on lung tumors, use in conjunction with surgery, 20: 38755
effects on man, conference on, 20: 39166
effects on man, effects of dose and dose rate on, 20: 39158
effects on molded oil shale–polyolefin articles, 20: 38974(P)
effects on pathology of animal tissues, 20: 38653
effects on polymerization of gaseous, liquid, and solid fluoroalkenes, kinetics of, 20: 38946
effects on response of leukemic mice to immunotherapy, 20: 38794
effects on sulfur fluorides, ESR spectra of products of, 20: 38941(R) (RRL-2310-182)
effects on ternary copolymer systems, 20: 38978(P)
effects on thermal conductivity of urania, 20: 39403 (ORNL-TM-1450)
effects on thermal conductivity of urania, in-reactor, 20: 39456 (GEAP-5100-1)
effects on tissues of human heart, review of, 20: 38675
effects on tumor and other cells, mechanism of action for ionizing, 20: 38616
permissible exposure, 20: 39166
shielding against nuclear-explosion initial, problems in, 20: 39061
use in control of insects infesting cereals, ionizing, 20: 38671
use in industry, 20: 39281 (DP-1066(Vol.1), pp 13-18)
use of ionizing, in preparation of cross-linked ethylene oxide polymers, 20: 38976(P)

RADIATION CHEMISTRY

equipment with alpha and beta sources for studies in, method for calculating efficiency of, 20: 38943
method for radioinduced chemical reaction, 20: 38972(P)

RADIATION DETECTION INSTRUMENTS

calibration of, used in radium medical appliances for, 20: 39169 (ISS-66/17)
description of, for fuel failure detection, 20: 40458 (DP-1049, pp 21-31)
design for use in satellites, 20: 39268
design of alpha, beta, gamma hand and shoe monitor, 20: 39198 (BNWL-250)
development of, review of, 20: 39238
electric shock hazards of, 20: 39213 (ORNL-TM-1578)
performance of spherical gas-filled chambers, 20: 38735(R) (NYO-1704-13)
performance of, during Cosmos 41 flight, 20: 39171(T)
shield design for beta-gamma, 20: 39262
use for environmental monitoring, 20: 38735(R) (NYO-1704-13)
use in personnel monitoring, dose range, economics, and efficiency of various types, 20: 39246
use in radiation measurements in space, 20: 39627

RADIATION DETECTION INSTRUMENTS (PULSE TYPE)

design for measurement of galactic x rays, 20: 39229
design for monitoring atmospheric beta activity, 20: 39259
design of G-M, for iodine monitoring, 20: 39264
design of miniature, for alpha monitoring, 20: 39254
design of scintillation, using 72-in.^{2} phosphor, 20: 39257
design of scintillation, for whole-body scanning, 20: 39265
design of scintillation, for Pu detection in wounds, 20: 39267
design of scintillation, used in monitoring air for alpha and beta particles, 20: 39269
performance for fast neutron absolute flux determinations, using organic compounds, 20: 39223
plateau curves of G-M counters at high intensity, 20: 39244
resolving time of scintillation, 20: 39239
time delays in proportional and Geiger counters, (E), 20: 39215

RADIATION DETECTORS

development for space vehicles, 20: 39158

RADIATION EXPOSURE CHAMBERS

design of, for partial-body x radiation of queen honeybee, 20: 38631

RADIATION INJURIES

acute whole-body irradiation syndrome, mechanisms of, 20: 38700
diagnosis in man, use of leukocyte chromosome aberration analysis for, 20: 38593 (ORNL-P-2175)
diagnosis of, by skin microflora number, 20: 38644
diagnosis of, use of adrenaline-lymphocytosis test for x, 20: 38678
diagnosis of, use of blood lipid and iodine determinations for, 20: 38652
effects of indolylalkylamines against, in mice and rats, 20: 38725
effects on function of gastrointestinal and respiratory tracts of rabbits, 20: 38659
pathology of bone, induced by radiotherapy, 20: 38767
pathology of goat, RBE of fission neutron and γ, 20: 38629
pathology of liver cirrhosis in rats induced by cerium-144, 20: 38567
pathology of rabbit eye retina, x, 20: 38689
pathology of skin, in guinea pigs, β, 20: 38591(R) (NYO-3445-7)
pathology of, in children treated for hemangioma with radium, 20: 38787
pathology of, role of toxin formation in, 20: 38664
protection against, effects of glycine in mice, 20: 38714
protection against, in animals and man, 20: 38718
protection against, effects of cystamine and ethylnorantiffeinine, 20: 38720
protection against, effects of thiopentobarbital in mice, 20: 38738
protection against, effects of bone marrow transplants in dogs and rats, 20: 38740
reaction mechanisms for, in mice, 20: 38714
repair processes in DNA, 20: 38575 (ORNL-P-2267)

RADIATION MONITORING

card holder design for, of air, 20: 39253
environment of western states of U. S., 20: 38735(R) (NYO-1704-13)
equipment design for alpha, 20: 39254
equipment for alpha, beta, and gamma, of hands and shoes, 20: 39198 (BNWL-250)
equipment for alpha, 20: 39257
equipment for alpha and beta, 20: 39269
equipment for beta, 20: 39259
equipment for beta-gamma, shielding for, 20: 39262
equipment for fallout, 20: 38743
equipment for personnel, economics, efficiency, and sensitivity of various types of, 20: 39246
methods for, in industrial plants and laboratories, 20: 39166
of tap water, sampling device for, 20: 39218

RADIATION PROTECTION

conference on, 20: 39166
cost factors for environmental fallout, 20: 38743
effects of cystamine on, in rats, mechanism of, 20: 38723
effects of drugs on, in animals and man, 20: 38718
hazard reduction methods in dental radiography, x, 20: 38793
measures in tracer studies of ground water, 20: 39155
measures taken in waste disposal, 20: 40482
measures taken to ensure safety of industrial radiography servicing personnel, 20: 38737
nurses during radiotherapy of cervical cancer, 20: 38751
practices for accelerator operation, 20: 39160
problems in space, 20: 38603(T) (AD-629422)
properties of aminothiols and their derivatives for, relation of chemical structure to, 20: 38724

RADIATION SICKNESS

changes in buccal flora of dogs and apes during severe, 20: 38667
diagnosis and therapy in man, 20: 38774
effects of cystamine against, in rats, mechanism of, 20: 38723
effects of intrauterine exposure on induction of, in newborn dogs, rabbits, and rats, 20: 38665
effects of procaine novocaine on, in dogs, mice, rabbits, and rats, 20: 38727
effects of selachyl alcohol on dog, rabbit, and rat, therapeutic, 20: 38731
effects of tetoxacin and unithiol on cerium-144 induction of, in rats, 20: 38732
effects on blood vessel tonus in dogs, 20: 38658
effects on function and morphology in dogs, protective effects of unithiol against, 20: 38719
effects on pulmonary circulation in rabbits, 20: 38657
effects on rat bone marrow, 20: 38663
induction by injected tritium oxide in mice and rats, 20: 38568
mechanism of death from, in mice, rabbits, and rats, 20: 38666
pathology of dog and rabbit, effects of functional state of hypothalamous on, 20: 38688
pathology of, effects of age and sexual maturity of animals on, 20: 38685
pathology of, in dogs, x, 20: 38684
use of bone marrow transfusions for therapy of dog and rat, 20: 38730
use of sodium gallate in prophylaxis and therapy of mouse and rat, 20: 38728

RADIATION SOURCES

characteristics, cost, and future of, 20: 39304 (DP-1066(Vol.1), pp 19-

28)
evaluation for radiosterilization, 20: 39285 (DP-1066(Vol.1), pp IV.33-42)
fabrication of encapsulated ceramic, method for, 20: 39371(P)
preparation and use of, in Czechoslovakia, 20: 39279
use in missile scoring, 20: 39190(P)
use of, in industry and geophysics, review on, 20: 39291

RADIATION TARGETS
design, 20: 39316 (DP-1066(Vol.1), pp II.3-14)

RADIATORS
development for space power systems, 20: 39028

RADIO WAVES
absorption for determining plasma variations in ionospheric D region, (E), 20: 39952
absorption in ionosphere, A3 method for measuring, 20: 39951
absorption of cosmic, in ionosphere, (E), 20: 39953
propagation in auroral zone, charged particle effects on, 20: 39954
scattering by plasma, ion and electron temperature effects on, (T), 20: 40213

RADIOACTIVE CONTAMINATION
of skin, 20: 39151
of water supplies, sampling device for monitoring, 20: 39218

RADIOACTIVE MATERIALS
handling of, automatic device for, 20: 39041(P)
handling of, automatic apparatus for sequential, 20: 39042(P)
handling of, conference on hazards in, 20: 39166
measurement of, comparison of sensitivity and time of methods for, 20: 38983 (SGAE-SS-3/1966)
microscopy of, modification of electron microscope for, 20: 39038
sample changing and measuring device for, automatic, 20: 39044(P)
sealing in plastic bags, system design for, 20: 39036
storage of, design of double-wall container for, 20: 39040(P)

RADIOACTIVE MINERALS
age of Swedish, 20: 39125

RADIOACTIVE WATERS
use of radon-containing, for therapy, 20: 38776

RADIOACTIVITY
computer program for calculation of environmental, following reactor accident, 20: 39148 (GA-6511)
content in atmosphere, review of methods for measuring, 20: 39104
production in food, methods for predicting, 20: 39165
variations in ground-level atmospheric, factors influencing, 20: 39114

RADIOAPPLICATORS
design of radium, for cancer of the lower lip, 20: 38752
dose distributions from tissue-implanted, scintillation detector for, 20: 38777
dosimetry of cobalt-60 and radium implanted, use of implanted metaphosphate glass detectors, 20: 38778

RADIOBIOLOGY
book: *Elements of Radiation Biology and Biochemistry*, 20: 38544
mechanisms of, in radiotherapy, review of, 20: 38634

RADIOCHEMICAL PROCESSING PLANTS
capacities of, review of, 20: 39332
development of PCUT, for thorium–uranium fuels, 20: 39006
hazards associated with plutonium–aluminum fuel element fabrication, 20: 39153

RADIOCHEMISTRY
book: *Advances in Inorganic Chemistry and Radiochemistry*, Vol. 8, 20: 38880

RADIODERMATITIS
induced by deposited radium-226 or strontium-90, in man, 20: 38623

RADIODIAGNOSIS
hazard reduction methods in dental radiography, x, 20: 38793
myometrial blood flow in pregnancy using xenon-133, 20: 38747
placental localization using radioisotopes, 20: 38757

RADIOGRAPHY
equipment for gamma, 20: 39295
of explosive cartridges, 20: 39334
radiation protection of personnel engaged in industrial, 20: 38737
radiation protection in dental practice of x, 20: 38793
review of radioisotopic, 20: 39286 (DP-1066(Vol.1), pp IV.43-5)

RADIOISOTOPES
book: *The Management of Radioactive Wastes Produced by Radioisotope Users*, 20: 40480 (STI-PUB-119)
characteristics, cost, and future of, 20: 39304 (DP-1066(Vol.1), pp 19-28)
control of medical uses in Belgium, 20: 39156
decay of, coincidence methods for measuring, 20: 40107
diffusion from sodium coolants, research on mechanisms of, 20: 40357 (NAA-SR-11766)
distribution in tissues, measurement of, 20: 38770
distribution of position-emitting, imaging system for measurement of, 20: 39181
metabolism of, 20: 39166
preparation and use of, in Czechoslovakia, 20: 39279
production and uses of, large-scale, 20: 39275 (DP-1066(Vol.1))
production and use in Europe, 20: 39276 (DP-1066(Vol.1), pp III.45-50)
production and use of, large-scale, 20: 39278 (DP-1066(Vol.2))
production and use in United Kingdom, 20: 39283 (DP-1066(Vol.1), pp III.33-44)
production by (n,γ) reactions, large-scale, 20: 39316 (DP-1066(Vol.1), pp II.3-14)
production in NRX or NRU reactors, 20: 39282 (DP-1066(Vol.1), pp III.3-32)
production in power reactors, 20: 39315 (DP-1066(Vol.1), pp I.29-52)
production in reactors, 20: 39314 (DP-1066(Vol.1), pp 29-39)
use for ship propulsion, bibliography on, 20: 40444 (AED-C-22-06)
use in food preservation, 20: 39284 (DP-1066(Vol.1), pp IV.3-25)
use in industry, 20: 39281 (DP-1066(Vol.1), pp 13-18)
use in industry, 20: 39314 (DP-1066(Vol.1), pp 29-39)
use in industry in Poland, 20: 39290
use in industry in France, 20: 39295
use in industry, medicine, and food preservation in Canada, 20: 39282 (DP-1066(Vol.1), pp III.3-32)
use in radiography, 20: 39286 (DP-1066(Vol.1), pp IV.43-5)
use in sterilization, review of, 20: 39285 (DP-1066(Vol.1), pp IV.33-42)
use in veterinary medicine, principles and operational techniques for, tables, 20: 38748
use of gaseous, with phosphor to illuminate timepieces, 20: 39296(P)

RADIOLOGICAL TELEMETERING SYSTEMS
design for scoring missiles or projectiles, 20: 39190(P)

RADIOLOGY
use of blood studies for determining radiation exposure to personnel working in, 20: 38781

RADIOMETERS
design and performance of, on Cosmos 41 satellite, 20: 39171(T)

RADIOMETRIC ANALYSIS
computer program for calculation of extent of exchange for liquid scintillation counting data, 20: 39226
method for simultaneous determination of iron-55 and iron-59 in blood using liquid scintillation counting, 20: 38555
sample changing and measuring device for, automatic, 20: 39044(P)
use of, in industry and geophysics, review on, 20: 39291

RADIOMIMETIC SUBSTANCES
effects of trichlortriethylamine and triethylenemelamine on blood-brain barrier permeability in rats, 20: 38609
effects on plants, genetic, 20: 38589(R) (EUR-2761.f)

RADIOOPAQUE AGENTS
labeling with iodine-131, 20: 38932

RADIOPROTECTIVE COMPOUNDS
effects of cysteamine on ultrastructure of rabbit liver, 20: 38716
effects of drinking mineral water of high sulfur content on radiosensitivity of mice to x rays, 20: 38709
effects of glycine in mice, 20: 38714
effects of pharmacological properties on biological effects in mice, 20: 38713
effects of sodium pyruvate and serum on uv irradiated chick embryo cells, 20: 38707
effects of tetoxacin as, in rats, 20: 38732
effects of thiopental on mice, 20: 38738
effects on mice and rats, 20: 38726
properties of aminothiols and their derivatives for use as, relation of chemical structure to, 20: 38724
properties of indolylalkylamines for use as, 20: 38725
selection of sulfur, evaluation of biological models for, 20: 38729

RADIOSENSITIVITY
comparison of, of brain tumors of various types, 20: 38783
effects of strain on chlorella, γ, 20: 38605
factors responsible for changes in, of embryonic tissues, 20: 38588(R) (COO-1400-10)
genetic factors of *E. coli* uv, 20: 38620
genetic factors of *E. coli*, uv and x, 20: 38621
nucleic acid synthesis in animals, 20: 38585
of animals to whole body ionizing radiation, 20: 38544
of liver and intestinal cells of rats, 20: 38576 (TID-22103)

RADIOSTERILIZATION
effects on fruit flies infesting various fruits and vegetables in Hawaii, gamma, 20: 39293
effects on insects infesting cereals, 20: 38671
effects on storage life and wholesomeness of Gulf oysters and shrimp, 20: 39288(R) (ORO-636)
effects on storage life of fruits and vegetables, 20: 39289 (UCD-34P73-9)
effects on wholesomeness of food, 20: 39302
history of food, 20: 39297
program for food, in Canada, 20: 39282 (DP-1066(Vol.1), pp III.3-32)
radioisotopes in large-scale, 20: 39285 (DP-1066(Vol.1), pp IV.33-42)
use of machine sources for food, 20: 39303

RADIOTHERAPY
advantages of, compared with surgery for treatment of laryngeal cancer, 20: 38782
determination of radioiodine dose in, by scintigraphic determination of thyroid weight, 20: 38789
dose calculations for, notations and formulae for, 20: 38750
effectiveness of various types of cerebral tumors, 20: 38783
effects in producing chromosome anomalies in human lymphocytes, 20: 38615
effects on normal and pathological heart, 20: 38675
equipment design for, 20: 39282 (DP-1066(Vol.1), pp III.3-32)
equipment for, cesium-137, 20: 38744 (DP-1066(Vol.1), pp IV.47-66)
equipment for, cobalt-60, 20: 38744 (DP-1066(Vol.1), pp IV.47-66)
equipment for, radium-226, 20: 38744 (DP-1066(Vol.1), pp IV.47-66)
injuries from cervical carcinoma, statistical analysis of, 20: 38754
injuries to vagina following use for cervical carcinoma, radium and x, 20: 38751
iodine-131 use in, of Basedow's disease, 20: 38760
leukopenia in cancer patients induced by, effects of blood transfusions on, 20: 38768
methods evaluation for treatment of uterine carcinoma, 20: 38786
program of, in Canada, 20: 39282 (DP-1066(Vol.1), pp III.3-32)
radiation dose to gonads during 31 Mev x radiation, 20: 38746 (NYO-3364-19)
radiation sources for, californium-252 and yttrium-90, 20: 38744 (DP-1066(Vol.1), pp IV.47-66)
radioapplicator for cancer of lower lip, 20: 38752
response mechanisms at the cellular level, review of, 20: 38634
technique for displacing fetus while x-irradiating cervical carcinoma during pregnancy, 20: 38759
technique of, for cardial region of stomach using a betatron, 20: 38772
use as preoperative procedure for lung cancer, effectiveness of, 20: 38755
use in malignant tumors of bone of differing radiosensitivity, 20: 38784
use of lasers for tumor, 20: 38780
use of orthovoltage x radiation therapy combined with cobalt-60 therapy, economics and effectiveness of, 20: 38792
use of yttrium-90 compared with gold-198 for trans-sphenoidal hypophysectomy, 20: 38758
yttrium-90 use in, of epilepsy, 20: 38779
RADIUM
content in diet, effects on carcinoma incidence in human populations, 20: 38739
crystal structure of, valence electrons and interatomic bonds in, 20: 40296
effects of use in therapy of hemangiomas in children, 20: 38787
metabolism in dairy cows, 20: 38552
radioinduced injuries from use of, in therapy of cervical cancer, 20: 38751
radioinduced injuries following use for uterine cancer, 20: 38754
use for therapy of hemangiomas in children, 20: 38788
use in uterine carcinoma radiotherapy, hazard to nursing personnel from, 20: 38751
use of new applicator for, in cancer of the lower lip, 20: 38752
RADIUM ISOTOPES Ra-226
decay constants, (E), 20: 40127
effects of internally deposited in man, biological, 20: 38623
radiation effects with ^{45}Ca on dairy cattle, 20: 38552
use in radiotheraphy, 20: 38744 (DP-1066(Vol.1), pp IV.47-66)
RADON
content in air at ground level in Toulouse, France, 20: 39114
content in diet, effects on carcinoma incidence in human populations, 20: 38739
content in ground-level air, effect of convection and turbulence on, 20: 39114
daughter product determination of, in man following radiotherapy, 20: 38775
reactions with charged particles, stopping powers and straggling in, (T), 20: 39611
use of water containing, for therapy, 20: 38776
RADON ISOTOPES Rn-220
content in air at ground level in Toulouse, 20: 39114
content in ground-level air, effect of convection and turbulence on, 20: 39114
daughter product determination of, in man following radiotherapy, 20: 38775
RADON ISOTOPES Rn-222
concentration in soil of Harz Mountains, 20: 39119
detection of, design and fabrication of film badge for, 20: 39272
RAIN WATER
effect on radioactivity levels in air, 20: 39114
phosphorus isotope content of, cosmic-ray produced, 20: 39991
RAMAN EFFECT
excitation of molten salt, method for laser, 20: 38872(R) (NYO-1769-68)
RARE EARTH ALLOYS
Pb–rare earths–Zn, component distribution in recrystallized, 20: 39435
rare earths–Zn, crystal structure of intermetallic compounds in, 20: 39417
RARE EARTH BROMIDES
behavior in nonaqueous tetraethylammonium hydroxide solutions, 20: 38830
RARE EARTH CARBONATES
crystal structure of, x-ray diffraction studies of, 20: 38869(R) (COO-1109-22, Paper 8)
preparation and spectra of, 20: 38868(R) (COO-1109-22, Paper 7)
RARE EARTH CHLORIDES
behavior in nonaqueous tetraethylammonium hydroxide solutions, 20: 38830
RARE EARTH COMPLEXES
with heterocyclics, energy transfer processes in, 20: 38873(R) (NYO-2269-9)
RARE EARTH IONS
radiation effects on, in calcium fluorides, (E), 20: 40341
RARE EARTH NITRATES
behavior in nonaqueous tetraethylammonium hydroxide solutions, 20: 38830
RARE EARTH OXIDES
chemistry of, research progress on solid-state, 20: 38861(R) (COO-1109-22)
actinide oxides–rare earth oxides, preparation of sols of, 20: 39341(P)
RARE EARTH SELENIDES
preparation, properties, and uses of, book on, 20: 38927
RARE EARTH TELLURIDES
preparation, properties, and uses, book on, 20: 38927
RARE EARTHS
analysis for europium, samarium, and ytterbium using acetonitrile, coulometric, 20: 38812
chemical properties of, in solution, 20: 38873(R) (NYO-2269-9)
determination in magnesium alloys by successive potentiometric titration, 20: 38830
determination using amalgamated silver electrode, oscellographic, 20: 38811
energy levels of odd-A, vibrational, (T), 20: 40118
properties for use as catalysts, 20: 38877(T) (JPRS-35594)
salts of, with phthalic acid, potentiometric determination of stability constants for, 20: 38896
separation by solvent extraction using tertiary amines and diethylenetriaminopentaacetic acid or EDTA, 20: 38995 (BM-RI-6809)
separation of, by lactate elution from cation resin columns, 20: 39004
RARE GASES
electron temperature of plasmas of, 20: 40185
reactions with charged particles, stopping powers and straggling in, (T), 20: 39611
thermal diffusion factors for, 20: 39321(R) (MLM-1312)
thermal diffusion of, cascade theory for, 20: 39321(R) (MLM-1312)
RATE METERS
development of solid-state, for fallout monitoring, 20: 39192 (AD-636206)
RATS
barium and strontium retention in, effects of dietary content of calcium, phosphorus, and strontium on, tracer study, 20: 38566
DTPA excretion in, tracer study, 20: 38556
effects of injected tritium oxide on, pathological, 20: 38568
effects of radiomimetics on permeability of blood-brain barrier, 20: 38609
effects of thyroid hormone on protein synthesis in, 20: 38595(R) (ORO-3295-2)
effects of tritium oxide perfusion on cholesterol and fatty acid metabolism in liver of, 20: 38559
elimination of cerium-144, iodine-131, thallium-204, zinc-65, and isotope mixtures by, effects of DTPA, pectin, and zirconium phosphate on, 20: 38733
hormone content in subcellular liver fractions of, 20: 38595(R) (ORO-3295-2)
iodine-131 uptake and elimination from thyroid of, effects of potassium iodide and thiouracil on, 20: 38734
iodotyrosine content in blood of, tracer study using iodine-129 and iodine-131, 20: 38561
pathology of cerium-144-induced cirrhosis in liver of, 20: 38567
phosphorus metabolism in, effects of reticulin on, tracer study, 20: 38572
phosphorus metabolism in hepatectomized, effects of reticulin on, tracer study, 20: 38572
radiation effects on astroglial cells and blood vessels in brain of, glycogen accumulation from alpha and x, 20: 38674
radiation effects on DNA synthesis in tissues of, 20: 38576 (TID-22103)
radiation effects on protein synthesis in, x, 20: 38595(R) (ORO-3295-2)

radiation effects on metabolism of ammonium citrate and glycine in, x, 20: 38600(R) (TID-23034)
radiation effects on enzyme release from liver lysosomes of, electron beam and x, 20: 38577
radiation effects on hematocrit values of, γ, 20: 38587 (CEA-R-2909)
radiation effects on permeability of intestine of, x, 20: 38604
radiation effects on permeability of blood-brain barrier, x, 20: 38609
radiation effects on, hematological, x, 20: 38619
radiation effects on adrenal function of, tracer study, whole-body x, 20: 38638
radiation effects on liver mitochondria of, biochemical and morphological, whole-body x, 20: 38639
radiation effects on adrenal and pituitary glands of, biochemical, x, 20: 38661
radiation effects on bone marrow of, morphological, γ, 20: 38663
radiation effects on erythropoietic response to erythropoietin in, γ, 20: 38673
radiation effects on ascorbic acid and glutathione content in brain of, whole-body x, 20: 38679
radiation effects on esterase content of blood of, x, 20: 38682
radiation effects on liver and spleen of, hematological, effects of thioacetamide on x, 20: 38694
radiation effects on agglutinin formation and properdin content in blood serum of, γ, 20: 38695
radiation effects on content of various lipids in tissues of, x, 20: 38701
radiation effects on mitosis in thymus gland of, x, 20: 38720
radiation effects on, effects of B group vitamins, folic acid, and phosphatide on gamma and x-ray, 20: 38721
radiation injuries in, protective effects of indolylalkylamines against, 20: 38725
radiation injuries in, protective effects of chemical agents against, 20: 38726
radiation sickness in newborn, by exposure during intrauterine development, 20: 38665
radiation sickness in, mechanism of death from, 20: 38666
radiation sickness effects on kidney function and morphology in, protective effects of unithiol against, 20: 38719
radiation sickness in, mechanism of protective effects of cystamine against, 20: 38723
radiation sickness in, protective effects of procaine against, 20: 38727
radiation sickness in, protective effects of tetoxacin and unithiol against cerium-144 induced, 20: 38732
radioinduced anemia in, effects of bone marrow transfusions on, 20: 38711
radioprotective effects of selachyl alcohol, 20: 38731
radiosensitivity effects of bone marrow transplants in, effects of cell number on, 20: 38740
strontium-90 absorption from gastrointestinal tract of, effects of various calcium compounds on, 20: 38569
use of bone marrow for therapy of radiation sickness in, 20: 38730
use of sodium gallate prophylaxis and therapy of radiation sickness in, 20: 38728

REACTION MECHANISMS
radioinduced in materials containing carbon–carbon and carbon–hydrogen bonds, 20: 38972(P)

REACTOR CONTROL RODS
drive mechanism for, design of rack and pinion, 20: 40371(P)
operation of, analysis of optimization of, 20: 40354 (AP-Note-393)
performance of neutron-absorber-filled tubes as, (E/T), 20: 40381
radiation effects on cadmium–indium–silver alloy, 20: 39461 (WCAP-6074)

REACTOR CONTROL SYSTEMS
design for gas-cooled power reactors, 20: 40432(P)
design using ball-shaped neutron absorbers in conduits, 20: 40370(P)

REACTOR COOLANTS
acidity control in WWR-S, 20: 40464 (UJV-1180/64)
corrosive effects of water, on nickel coatings, 20: 39461 (WCAP-6074)
fission product retention by sodium, survey on, 20: 40357 (NAA-SR-11766)
loss of, analysis of pressure tube and vessel failures in, 20: 39329 (AECL-2432)

REACTOR COOLING SYSTEMS
coolant flow in boiling water, stability of, 20: 40356 (EURAEC-1644)
coolant flow in Halden, hydrodynamic instability analysis of, 20: 40409(R) (NP-16230)
coolant loss in, effects on fast reactor safety, 20: 40363
water management in WWR-S, 20: 40465 (UJV-1181/64)

REACTOR FUEL ALLOYS
production of aluminum–uranium, by direct reduction of uranium tetrafluoride, 20: 39333

REACTOR FUEL ELEMENTS
burnup analysis of Halden assemblies, 20: 40409(R) (NP-16230)
channel thickness in spent ETR, 20: 40460(R) (IDO-17191)
cladding for, properties of chromium–iron–zirconium alloy, 20: 39356(R) (GEAP-5134)
costs of coated particle, for high temperature gas-cooled reactors, 20: 40388
design for Advanced BONUS Core, 20: 40401 (CEND-259)
design of finned, ribbed sheath with lugs for, 20: 40396(P)
design of injection-molded, for AVR, 20: 40468
design of Zircaloy-clad oxide, factors affecting, 20: 40387 (WAPD-T-1939)
design to prevent coolant flow-induced vibration, 20: 40397(P)
development of, for high temperature gas-cooled reactors, conference on, 20: 40383 (EUR-2780.e)
engineering problems of, for pulsed fast reactor, 20: 40455 (BNL-10454)
fabrication for Advanced BONUS Core, 20: 40401 (CEND-259)
fabrication of coated particle, for high temperature gas-cooled reactors, 20: 40388
fabrication of injection-molded, for AVR, 20: 40468
fabrication of reprocessed, from high temperature gas-cooled reactors, 20: 40419
failure of cermet, effects of fission on, 20: 39459 (TRG-Report-1278)
failure, detection device for HWCTR, 20: 40458 (DP-1049, pp 21-31)
fission product distribution in coating of, 20: 40386 (SGAE-CH-33/1966)
irradiation testing in Halden reactor, 20: 40409(R) (NP-16230)
neutron flux depression in plates of ATR, 20: 40460(R) (IDO-17191)
performance of ATR thermal-hydraulic-structural analysis of, 20: 40460(R) (IDO-17191)
processing of, in plutonium fuel cycle, facilities for, 20: 39024 (ORNL-TM-1268)
reprocessing of carbide-graphite, head-end treatment for, 20: 40390
reprocessing of irradiated, from high temperature gas-cooled reactors, 20: 40419
testing of NS Savannah Core II, 20: 40445 (BAW-1225)
testing of SNAP-10A, program evaluation using K-factors, 20: 40447 (NAA-SR-11913)
thermal testing of Advanced BONUS Core, 20: 40401 (CEND-259)
welding of, end cap-to-sheath, 20: 39377

REACTOR FUEL ELEMENTS (CERAMIC)
design for Elk River Power Reactor, 20: 40425
fabrication of thoria pellets for, 20: 39362 (WAPD-TM-577)
fabrication of urania, effects on radioinduced gas release at high temperatures, 20: 39449 (BNWL-SA-272)
preparation of, actinide oxide–rare earth oxide sols for, 20: 39341(P)
processing graphite, grind-leach method for, 20: 38998(R) (ORNL-3958)
processing metal clad uranium dioxide, temperatures in shear-leach method for, 20: 38998(R) (ORNL-3958)
radiation effects on gas release from urania, 20: 39449 (BNWL-SA-272)
radiation effects on thermal conductivity of Zircaloy-2-clad urania, 20: 39456 (GEAP-5100-1)
radioinduced swelling in, stress analysis of, 20: 39460 (WAPD-TM-514 (Add.1))
thermal conductivity of Zircaloy-2-clad urania, 20: 39403 (ORNL-TM-1450)

REACTOR FUEL ELEMENTS (DISPERSION)
design of carbide, 20: 40395(P)

REACTOR FUEL ELEMENTS (THERMOELECTRIC)
materials for coated-particle, properties of, 20: 39353 (BMWF-FBK-66-07)
testing of tungsten coated molybdenum–urania, at high temperatures, 20: 39383 (BMWF-FBK-66-08)

REACTOR FUEL PLATES
cladding of PWR core-2, bonding mechanism for Zircaloy-2 for, 20: 39361 (WAPD-305)
fabrication of curved ATR, methods for, 20: 39358 (ORNL-3983)
reactivity of SM-1 Core III, 20: 40374 (ANCP-63562)

REACTOR FUEL RODS
coating with chromium, nickel, and silicon for corrosion protection, method for, 20: 29350(P)
radiation effects on thermal conductivity of Zircaloy-2-clad urania, 20: 39456 (GEAP-5100-1)
radiation effects on boron migration in uranium dioxide, 20: 40382(R) (CEND-3107-267)

REACTOR FUEL SPHERES
fabrication of graphite containing coated uranium–thorium particles, 20: 40467
fabrication of thoria, from pot-processed denitrated powders, 20: 39362 (WAPD-TM-577)
irradiation testing of hollow graphite containing coated uranium–thorium particles, 20: 40467
preparation by vibratory abrasion, 20: 39376(P)
radiation effects on thermal conductivity of Zircaloy-2-clad urania, 20: 39456 (GEAP-5100-1)
sintering of urania, oxidizing effects of impurities on, 20: 39390 (CEA-R-3003)

REACTOR FUEL TUBES
neutron flux at functions of natural uranium, with heavy water moderation, 20: 39452 (EUR-2981.f)

REACTOR FUELS
analysis for uranium-235 by gamma scintillation, tester for, 20: 39335
coating particulate, with beryllia, 20: 39370(P)
cycle analysis in high temperature reactors, use of plutonium in, 20: 40472
cycle aspects of, review on, 20: 39332
cycle costs for AVR, 20: 40470
cycle costs for thorium–uranium-235, in graphite moderated systems, 20: 40393
cycle costs of thorium, for high temperature reactors, 20: 40394
cycle studies for high temperature graphite moderated reactors, 20: 40421
cycles in high temperature reactors, use of plutonium in, 20: 40473
decontamination of irradiated thorium–uranium, 20: 40419
enrichment and ownership of, review of, 20: 39332
fabrication and testing of thorium-base pyrolytic carbon coated particles, 20: 40385 (ORNL-P-2327)
fabrication of coated particle, cost analysis for, 20: 40466
fabrication of thorium-base, 20: 40385 (ORNL-P-2327)
fabrication of uranium dioxide, 20: 39373(P)
neutron flux distribution in natural uranium, 20: 39452 (EUR-2981.f)
performance of thorium-base, under irradiation, 20: 40385 (ORNL-P-2327)
preparation of carbide-coated uranium carbide, 20: 40395(P)
processing of thorium–uranium, design and development of PCUT facility for, 20: 39006
production of, plant capacities for, 20: 39332
radioinduced swelling in, effects of gases on, 20: 39449 (BNWL-SA-272)
refabrication of coated particles, methods and costs, 20: 40392
reprocessing by fluoride volatilization with sulfur hexafluoride, 20: 40389
reprocessing of coated particles, methods and costs, 20: 40392
requirements for power production, analysis of future, 20: 40420
testing of plutonium–uranium, in thermal neutron reactors, 20: 40384(R) (EURAEC-1660)
thermal conductivity of urania, effects of density and grain size on, 20: 39446 (AECL-2564)

REACTOR MATERIALS
book: *Corrosion Resistance of Reactor Materials, Handbook*, 20: 39349

REACTOR MATRICES
calculations of cell parameters for heavy-water-cooled and -moderated, using multigroup collision probability theory in cluster geometry, 20: 40380
conversion ratios in uranium and uranium dioxide fueled, 20: 40399 (AEEW-M-654)
fission ratios in uranium and uranium dioxide fueled, fast, 20: 40399 (AEEW-M-654)
neutron diffusion coefficients in, with empty channels, 20: 40377
reactivity of graphite–uranium, analysis using WIMS code, 20: 39382 (AEEW-R-473)

REACTOR REFLECTORS
design for thermal flux separation, 20: 40368(P)
design for thermal flux separation, 20: 40368(P)

REACTOR SAFETY
accident analyses compilation, 20: 40358 (ORNL-NSIC-17)
accident analysis in MSRE, 20: 40412 (ORNL-TM-497)
analysis for Indian Point Unit No. 2, site and environment, 20: 40406 (NP-16181(Exh.B)(Vol.1))
analysis for Indian Point Unit No. 2, plant design, 20: 40407 (NP-16181 (Exh.B)(Vol.2)(Pt.A))
analysis for Indian Point Unit No. 2, plant design, 20: 40408 (NP-16181 (Exh.B)(Vol.2)(Pt.B))
analysis for Nuclear Test Gauge, 20: 40459 (GEMP-152)
boiling detector design for, 20: 40373
containment structure design, 20: 40372(P)
coolant loss analysis in fast reactors, 20: 40363
fission product diffusion and retention by sodium coolants, 20: 40357 (NAA-SR-11766)
hazards analysis for Yugoslavian TRIGA Mark II, 20: 40462 (NIJS-R-474)
radioactivity of environment after release of radioisotopes, computer code for calculation of, 20: 39148 (GA-6511)
systems for, performance of HWCTR, 20: 40457 (DP-1049, pp 1-19)

REACTOR SAFETY EXPERIMENTS
transient heating of fuel disks in KEWB, model of, 20: 40357 (NAA-SR-11766)

REACTOR SHIELDING
analysis of, computer programs for, 20: 40431
design of variable, 20: 40369(P)
support for, within concrete pressure vessel, metal heat-insulating, 20: 40367(P)

REACTOR TUBES
deformation and stress analysis of hexagonal, 20: 39384 (BNWL-263)
fracture of defected, effects of pressure increase on, 20: 39329 (AECL-2432)

REACTORS
atmospheric diffusion at sites of, measurement of, 20: 39105
built, being built, or planned in the U. S., 20: 40359 (TID-8200(13th Rev.))
containment system for, 20: 40372(P)
control rod operation in, optimization analysis for, 20: 40354 (AP-Note-393)
coolant channels in, devices for measuring, 20: 39175
design of chemonuclear, 20: 40364
design of, provision for future modifications in, 20: 40429
design with integral steam generator, 20: 40433(P)
neutron diffusion coefficients in, with empty channels, 20: 40377
neutron flux distribution in, measurement techniques for, 20: 40379
neutron flux measuring device for, 20: 39252(P)
neutron flux separation in multi-region, design of structure for, 20: 40368(P)
neutron spectra in, measurement methods for, 20: 40378
neutron transport in, angle-space synthesis analysis of, 20: 40360 (WAPD-T-1890)
operation of, unusual experiences in, 20: 40358 (ORNL-NSIC-17)
reactivity evolution in plutonium–uranium fueled, 20: 40384(R) (EURAEC-1660)
reactivity oscillations in, device for measuring, 20: 40361
shutdown modes for, optimization of, 20: 40423

REFRACTION
radiation effects on refractive index of optical glasses, gamma, 20: 39468

REFRACTORY MATERIALS
effects of boride and carbide, on grain size of tungsten, 20: 39400 (NASA-TN-D-3531)
fabrication and physical properties of composite graphite-metal carbide, 20: 39367
heat treatment of particulate, method for, 20: 39343(P)
production of high-quality metallic, panel summary on, 20: 39357 (MAB-212A-M)
reactions with combustion gas species in launch pad abort environments, 20: 39312 (SC-CR-66-2044)
weldability of alloys, evaluation of, 20: 39366
wettability of boride, carbide, and nitride, by molten metals, 20: 39429

RELATIVITY THEORY
conservation laws for exploding matter in general, covariant, 20: 40002
conservation laws in Riemannian spaces in general, tensor integration for global, 20: 40007
conservation laws in Riemannian spaces in general, four global tensor, 20: 40008
conservation laws in general, Rayski's formulation of, 20: 40010

RELAYS
design and performance parameters for radiometric, 20: 39173

REMOTE-CONTROL EQUIPMENT
design for radioactive materials in electron microscope, 20: 39038
design for sequential handling of radioactive samples carried by portable trap, 20: 39042(P)
design for vertical and lateral movement of radioactive materials, 20: 39041(P)

REPTILES
radiation effects on lizard population in Puerto Rican forest, γ, 20: 38601 (UCLA-12-567)

RESEARCH REACTORS
control rods for, performance of neutron-absorber-filled tubes as, (E/T), 20: 40381
coolant water treatment in WWR-S, 20: 40464 (UJV-1180/64)
dynamic behavior of TRIGA, model for, (E/T), 20: 40475
fuel development for AVR, 20: 40467
neutron spectra in AFRRI TRIGA, fast, 20: 40454 (AD-636542)
physics of high temperature, effect of plutonium use on, 20: 40472
power increase in WWR-S, water management for, 20: 40465 (UJV-1181/64)
safety hazards of Yugoslavian TRIGA Mark II, 20: 40462 (NIJS-R-474)
shield design for, variable, 20: 40369(P)

RESINS
preparation of thermoplastic, of ternary copolymers using ionizing radiation, 20: 38978(P)
radioinduced grafting of hydroxyl-containing and epoxy-polyamide, 20: 38979(P)

RESISTANCE FURNACES
heat loss tests of, 20: 40476(R) (BNWL-267)

RESPIRATION
tracer studies on human, oxygen-18 use in, 20: 38941(R) (RRL-2310-182)

RESPIRATORY TRACTS
radiation effects on function of rabbit, x, 20: 38659
RETICULIN
effects on phosphorus metabolism in rats, tracer study, 20: 38572
RHENIUM
deposition of coatings of, by chloride and fluoride reduction using hydrogen, 20: 39354 (BMWF-FBK-66-09)
determination of, in rocks and ores by neutron activation methods, 20: 38802
effects on grain size of tungsten, 20: 39400 (NASA-TN-D-3531)
superconductivity of, 20: 40047
thermoelectric properties, 20: 39353 (BMWF-FBK-66-07)
RHENIUM ALLOYS
Mo–Re, superconductivity, 20: 40047
Re–W, work function for, 20: 40297
Re–Zr, work function for, 20: 40297
RHENIUM CHLORIDES
reduction for coating deposition using hydrogen, 20: 39354 (BMWF-FBK-66-09)
RHENIUM FLUORIDES
molecular structure of, mean amplitudes of vibration at 0 and 298°K in, 20: 38897
reduction for coating deposition using hydrogen, 20: 39354 (BMWF-FBK-66-09)
RHENIUM ISOTOPES Re-183
decay by electron capture, (E), 20: 40123
RHENIUM ISOTOPES Re-188
beta decay of, circularly polarized $\beta-\gamma$ correlation in, (E), 20: 40097
RHODIUM
neutron capture resonance integrals, (E), 20: 40146
superconductivity of, 20: 40047
RHODIUM ALLOYS
Fe–Rh, iron-57 hyperfine structure coupling in, (E), 20: 39470(R) (ORNL-3924)
Ir–Rh, superconductivity, 20: 40047
Rh–Ru, superconductivity, 20: 40047
RHODIUM COMPLEXES
radiation effects on chlorine-36 exchange with hydrochloric acid, bremsstrahlung, gamma, and x, 20: 38960
RHODIUM FLUORIDES
molecular structure of, mean amplitudes of vibration at 0 and 298°K in, 20: 38897
RHODIUM ISOTOPES Rh-103
proton reactions (p,n) at 3.0 to 5.8 Mev, strength functions for, (E), 20: 39470(R) (ORNL-3924)
RIBONUCLEASE
effects of cytostatics on activity of, in Ehrlich ascites cells, 20: 38578
radiation effects on activity of Ehrlich ascites cell, x, 20: 38578
RIBONUCLEASE, DEOXY-
effects of cytostatics on activity of, in Ehrlich ascites cells, 20: 38578
radiation effects on activity of, in guinea pig skin, β, 20: 38591(R) (NYO-3445-7)
radiation effects on activity of Ehrlich ascites cell, x, 20: 38578
RIBONUCLEIC ACID
analysis for amino acid activity in, 20: 38998(R) (ORNL-3958)
analysis for trace elements in tobacco plant, activation, 20: 38846
effects of absence of an essential amino acid on synthesis of, after uv irradiation of *E. coli* cultures, 20: 38562
inhibition of synthesis of, mechanisms in irradiated animals, 20: 38585
nature and structure of, 20: 38542(T) (UCRL-Trans-10029)
production of virus-specific, in mouse kidney cells infected by Polyoma virus, 20: 38702
radiation effects on synthesis of, uv, 20: 38574(R) (NYO-3449-1)
radiation effects on binding to proteins, as mechanism of tobacco mosaic virus inactivation, uv, 20: 38584
radiation effects on content in rabbit leukocytes, x, 20: 38681
radiation effects on metabolism of, in cultured HeLa cells, γ, 20: 38683
separation from *E. coli*, engineering method for, 20: 38998(R) (ORNL-3958)
synthesis of, effects of absence of uracil in uv-irradiated *E. coli*, 20: 38563
RIBONUCLEIC ACID, DESOXY-
analysis of enzymatic digests of, by neutron activation methods, 20: 38816
effects of absence of an essential amino acid on synthesis of, after uv irradiation of *E. coli* cultures, 20: 38562
effects of acridines on, 20: 38542(T) (UCRL-Trans-10029)
effects of chemical mutagens on, 20: 38542(T) (UCRL-Trans-10029)
effects of chemical mutagens on *E. coli*, 20: 38620
inhibition of synthesis of, mechanisms in irradiated animals, 20: 38585
nature and structure of, 20: 38542(T) (UCRL-Trans-10029)
radiation effects on synthesis of, uv, 20: 38574(R) (NYO-3449-1)
radiation effects on, x, 20: 38575 (ORNL-P-2267)
radiation effects on synthesis in rat tissues, 20: 38576 (TID-22103)
radiation effects on content in mouse thymus, x, 20: 38606
radiation effects on thymine dimer excision in *E. coli*, 20: 38620
radiation effects on *E. coli*, uv and x, 20: 38621
radiation effects on bacteriophage, x, 20: 38628
radiation effects on bacteriophage, effects of 5-bromouracil on x, 20: 38712
radiation effects, uv and x, 20: 38542(T) (UCRL-Trans-10029)
ROCKET REACTORS
power conversion equipment for, 20: 40449(R) (SAN-650-1)
ROCKS
analysis for rhenium by neutron activation methods, 20: 38802
geologic studies on extent and continuity of, 20: 39099(R) (BNWL-235-3, pp 1-23)
RODS
extrusion from compacted tungsten powders, equipment and methods for, 20: 39352 (BM-RI-6817)
heat transfer in parallel arrays of, effects of boundary layer turbulence promoters on, 20: 39084 (GEAP-5115)
ROOTS
effects of centrifugation on chromosome exchange yield in meristems of barley, grown from irradiated seeds, 20: 38618
radioinduced chromosome aberrations in apple tree, fast neutron and γ, 20: 38692
ROTORS
design for zonal centrifuges, 20: 39037
RUBIDIUM
electric dipole moments of, ratio of atomic to electron, 20: 39598
superconductivity of, 20: 40047
RUBIDIUM IODATES
iodine-131 beta decay in, properties of xenon oxide compounds formed by, 20: 38984
RUBIDIUM ISOTOPES Rb-87
content in rocks in Sweden, 20: 39126
RUPTURE
fast fracture of pressure vessels, mechanics of, 20: 39329 (AECL-2432)
RUTHENIUM
diffusion from sodium at high temperatures, factors affecting, 20: 40357 (NAA-SR-11766)
RUTHENIUM ALLOYS
Os–Ru, superconductivity, 20: 40047
Rh–Ru, superconductivity, 20: 40047
RUTHENIUM FLUORIDES
molecular structure of, mean amplitudes of vibration at 0 and 298°K in, 20: 38897
RUTHENIUM ISOTOPES Ru-97
decay of, technetium-97 levels from, (E), 20: 40084
RUTHENIUM ISOTOPES Ru-103
decay curves for precursors of, 20: 40357 (NAA-SR-11766)
RUTHENIUM ISOTOPES Ru-106
content in Clinch River, 20-year analysis of, 20: 40479 (ORNL-P-2328)
release from simulated high-level wastes, 20: 40476(R) (BNWL-267)
separation using mixed oxide scavenger, 20: 40476(R) (BNWL-267)

S

SAFETY
analysis of 5-watt radiostrontium-fueled generator for meteorological station, 20: 39311 (MND-SR-2586)
program for, in nuclear device detonation, 20: 39149 (NVO-28)
SALICYLALDEHYDE
complexes with cobalt, radiation effects on, annealing of recoil damage in neutron, 20: 38965
SAMARIUM
determination in magnesium alloys by successive potentiometric titration, 20: 38830
determination in rare earths using acetonitrile, controlled-potential coulometric, 20: 38812
magnetic field at nuclei of, implanted in iron, 20: 40342
reduction in acetonitrile solutions, color production in controlled-potential coulometric, 20: 38813
shock compression of, 20: 39425(T)
x-ray-diffraction patterns of, effects of cold working on, 20: 39421
SAMARIUM ALLOYS
Al–Sm, magnetic properties of intermetallic compounds of, 20: 39433
Fe–Sm, crystal structure of intermetallic compound, 20: 39409
Pb–Sm–Zn, component distribution in recrystallized, 20: 39435
Sm–Zn, crystal structure of intermetallic compound $SmZn_{12}$ in,

20: 39417
SAMARIUM CARBONATES
crystal structure of, x-ray diffraction studies of, 20: 38869(R) (COO-1109-22, Paper 8)
SAMARIUM CHLORIDES
heat of dilution of aqueous, at 25°C, 20: 38903
specific gravity and apparent molal volume of aqueous solutions of, at 25°C, 20: 38905
viscosity of aqueous solutions of, at 25°C, 20: 38904
SAMARIUM IONS
spin-lattice relaxation time in lanthanum trichloride, angular and temperature effects on, 20: 40350
SAMARIUM ISOTOPES Sm-150
energy levels of, parity and spin of, (E), 20: 40069(R) (EANDC(E)-66(U))
SAMARIUM ISOTOPES Sm-152
energy level at 122 kev, lifetime of, (E), 20: 40110
SAMARIUM OXIDES
diffusion of oxygen in, tracer studies for determining activation energies for, 20: 38865(R) (COO-1109-22, Paper 4)
preparation of lower, 20: 38867(R) (COO-1109-22, Paper 6)
actinide oxides–Sm_2O_3, preparation of sols of, 20: 39341(P)
SAMARIUM SELENIDES
crystal structure of, reflection spectra for zonal, (E), 20: 40339
SAMARIUM SILICIDES
preparation of lower, 20: 38867(R) (COO-1109-22, Paper 6)
SAMARIUM SULFIDES
crystal structure of, reflection spectra for zonal, (E), 20: 40339
SAMPLING
card holder design for air, 20: 39253
equipment and methods for fallout, 20: 38743
equipment for river-water, 20: 39185
isokinetic, of particles in air streams, use of nozzles in, 20: 39103(R) (BNWL-235-3, pp 51-69)
method for cesium, in sea water, 20: 39147 (CONF-660401-6)
subisokinetic, of particles in air streams, 20: 39103(R) (BNWL-235-3, pp 51-69)
SANDS
effects of medium of, on gamma energy spectra, (E), 20: 40290
use in mixtures with ion exchangers for water decontamination, 20: 40484
SAP (SINTERED ALUMINUM PRODUCTS)
fabrication and properties of, 20: 39359 (RISO-113)
SATELLITES
control of, performance of ion engines for, 20: 39092
SAVANNAH RIVER COMPONENTS TEST REACTOR
fuel element failure in, design of detection device, 20: 40458 (DP-1049, pp 21-31)
modification of, review of procedures, 20: 40429
operating program, 20: 40456 (DP-1049)
safety systems performance, 20: 40457 (DP-1049, pp 1-19)
SCALERS
design for ORIC beam monitoring, 20: 39507
registration of state of decatron, design of transistorized electronic system for, 20: 39178
use for environmental monitoring, 20: 38735(R) (NYO-1704-13)
SCANDIUM
hydrolysis constant of, measurement of, by chelate solvent extraction, 20: 38925
superconductivity of, 20: 40047
SCANDIUM ALLOYS
Sc–Zr, superconductivity, 20: 40047
SCANDIUM COMPLEXES
with Xylenol Orange, composition and chemical properties of, 20: 38924
SCANDIUM ISOTOPES Sc-45
proton reactions (p,α) at 8.5 to 9.4 Mev, statistical fluctuations in cross sections for, 20: 40065(R) (BMwF-FB-K-66-01)
SCANDIUM ISOTOPES Sc-46
incorporation in solid cracking catalyst, process for, 20: 38993(P)
use as tracer for ground water research, 20: 39155
SCATTERING
amplitude for relativistic multichannel, analytical properties of, 20: 39911
amplitudes for multichannel quasi-potential, asymptotic behavior of, 20: 39905
amplitudes for n-body system, separation of total angular momentum for, 20: 39897
amplitudes in, asymptotic behavior of inelasticity parameter for, 20: 39894
amplitudes of, effects of vacuum Regge trajectory on, (T), 20: 39925
amplitudes of, relativistic equations for three-particle, 20: 39914
Bethe–Salpeter equations for three-particle, solutions to, 20: 39900
Bethe–Salpeter equations for three-particle, solutions to, 20: 39901
Feynman graphs for, majorization of, 20: 39867
molecular beam, computer program for calculating, 20: 39321(R) (MLM-1312)
potential, calculation by determinental and N/D methods, 20: 39927
Regge parameters in potential, approximation methods for, 20: 39923
S-matrix elements for, cluster expansions of causal, 20: 39858 (JINR-P-2760)
S-matrix for long-range potential, poles of, 20: 39868
S-matrix for multichannel, unitarity of, 20: 39866
S-matrix theory of, relativistic U(6,6) symmetry group for, 20: 39888
S-matrix with noncompact symmetry groups in, 20: 39854 (JINR-E-2754)
SCINTILLATION DETECTORS
cooling system for well-logging, 20: 39140(P)
counting data analysis, computer program for, 20: 39226
data analysis of gamma spectra from, computer programs for, 20: 39237
design for dosimetry of beta applicators in tissues, 20: 38777
design for epithermal neutrons used in well logging, 20: 39138(P)
design for monitoring plutonium in wounds, 20: 39267
design for well logging, 20: 39139(P)
design for whole-body scanning, 20: 39265
design of alpha, using 72-in.² phosphor, 20: 39257
design of whole-body counter using, 20: 38753
design of, for monitoring air for alpha and beta particles, 20: 39269
design of, used with fission chamber, 20: 39256
development for uranium-235 enrichment measurement in fuels, 20: 39335
development of inorganic and organic, 20: 39233
neutron detection process in plastic, computer program for simulation of, 20: 39196 (AE-236)
performance for fast neutron absolute flux determinations, using organic compounds, 20: 39223
performance for measurement of gamma radiation from positron annihilation, 20: 38745(R) (NYO-3267-3)
performance of, for measurement of γ activity from potassium-40 in soils, 20: 39280
use for extracorporeal monitoring of circulating blood, design of shielded coil for, 20: 38558
SEA WATER
cesium-137 distribution in, sampling method for measuring, 20: 39147 (CONF-660401-6)
desalination of, dual purpose nuclear plant dynamic behavior analysis for, 20: 40438
desalination of, dual purpose nuclear plant optimization for, 20: 40439
radiation effects on marine life in, natural β, 20: 38741
uranium-234/-238 ratios in, 20: 39133
SEAFOOD
radiation processing of Gulf oysters and shrimp, effects on storage life and wholesomeness, 20: 39288(R) (ORO-636)
SEED
ascorbic acid content in Gramineae, 20: 38583
neutron dosimetry in, fast, 20: 38693
radiation effects on ascorbic acid content in germinating, 20: 38583
radiation effects on barley, genetic, effects of centrifugation on γ, 20: 38618
radiation effects on barley, physiological, γ, 20: 38690
radiation effects on apple, genetic, fast neutron and γ, 20: 38692
radiosensitivity effects of water content and calcium chloride solutions on barley, x, 20: 38736
radiosensitivity of deciduous tree, effects of physiological state and water content on γ and neutron, 20: 38594(R) (ORO-2066-10)
SEEDLINGS
cation metabolism in wheat, 20: 38548(R) (ORO-2410-1)
radiation effects on Gramineae, β and γ, 20: 38583
radiation effects on development of barley, γ, 20: 38691
radiation effects on growth of barley, x, 20: 38736
radiosensitivity of deciduous tree, γ and neutron, 20: 38594(R) (ORO-2066-10)
SEISMIC WAVES
detection of underground-nuclear-explosion produced, instrumentation for, 20: 39134
SEISMOLOGY
data from RED HOT explosion, long range, 20: 39124 (AD-632957)
station design and performance, Eskdalemuir, Scotland, 20: 39128
SEISMOMETERS
description of array of, in southern Scotland, 20: 39128
design of linear cross array of, for detecting underground nuclear explosions, 20: 39134
SELACHYL ALCOHOL
effects on radiation sickness in animals, therapeutic, 20: 38731
SELENIUM
determination in biological materials, use of automated gamma spectrometers in activation, 20: 38843
determination of traces of, in biological materials, activation, 20: 38837

radiation effects on distribution of radioactive, between red and gray allotropic modifications, neutron, 20: 38961
SELENIUM FLUORIDES
molecular structure of, mean amplitudes of vibration at 0 and 298°K in, 20: 38897
SELENIUM ISOTOPES Se-74
neutron reactions (n,2n) and (n,p) at 14.4 Mev, cross sections for, (E), 20: 40079 (ORO-3346-2)
SELENIUM ISOTOPES Se-76
neutron reactions (n,2n) and (n,p) at 14.4 Mev, cross sections for, (E), 20: 40079 (ORO-3346-2)
SELENIUM ISOTOPES Se-78
neutron reactions (n,α) and (n,p) at 14.4 Mev, cross sections for, (E), 20: 40079 (ORO-3346-2)
SELENIUM ISOTOPES Se-80
neutron reactions (n,α) and (n,2n) at 14.4 Mev, cross sections for, (E), 20: 40079 (ORO-3346-2)
SELENIUM ISOTOPES Se-82
neutron reactions (n,2n) at 14.4 Mev, cross sections for, (E), 20: 40079 (ORO-3346-2)
SEMICONDUCTOR DETECTORS
data analysis of gamma spectra from lithium-drifted germanium, computer programs for, 20: 39237
development for fission studies, 20: 39242
development, properties, and use for nuclear spectrometry, 20: 39231
efficiency of lithium-drifted germanium, for gamma radiation, (T), 20: 39271
performance for γ dosimetry, 20: 38771
performance of silicon, for neutral atom detection, 20: 39580(R) (ORNL-3989, pp 78-88)
properties and use of germanium and silicon, for gamma and electron spectroscopy, 20: 39232
properties of germanium and silicon, 20: 39230
response of silicon, to argon-40 and iodine-127 ions, 20: 39470(R) (ORNL-3924)
use of lithium-drifted germanium, in γ-γ coincidence experiments, 20: 39197 (AECL-2565)
use of lithium-drifted germanium, for gamma spectroscopy, 20: 39243
SEMICONDUCTORS
crystal lattice vibrations in, review, (T), 20: 40344
junction theory of, review of, 20: 39230
plasma oscillations in, spin-orbital interaction effects on, 20: 40227
properties for gamma spectrometry, 20: 39231
radioinduced conductivity in films of, performance of chamber for measuring x, 20: 39179
radioinduced defects in, fast electron, 20: 40332
sputtering of single-crystal, atom-ejection patterns, (E), 20: 40305
SEPARATION PROCESSES
radiochemical, for use with activation analysis of biological materials, 20: 38842
SEPARATORS
design of radial vane, for water and steam, 20: 39019(R) (GEAP-5149)
design of, for isopropylbiphenyl, 20: 40449(R) (SAN-650-1)
SEWAGE
disposal of, in radioisotope hospital wards, 20: 38790
radioactivity of, from radioisotope hospital wards, 20: 38790
SHEEP
gamma and x-ray dosimetry determination using phantoms, 20: 38625
metabolism of gonadal hormones in ovaries in, tracer study on, 20: 38547(R) (NYO-918-15)
radiation effects on, hematological, fission neutrons, 20: 38637
transplantation of ovaries in, method for auto-, 20: 38547(R) (NYO-918-15)
SHEETS
extrusion from compacted tungsten powders, equipment and methods for, 20: 39352 (BM-RI-6817)
SHELLS
creep effects in pressurized copper, analytical method for, 20: 39391 (CONF-660629-1)
SHELTERS
air cooling and ventilation in, 20: 39074
conference, 20: 39054
design for target community, 20: 39089
design of blast-resistant tunnel for large cities, 20: 39088
design of buildings including fallout, case studies of, 20: 39086
design of fire-safe, criteria for, 20: 39065
design of fireproof, with secured ventilation systems, 20: 39066
design of fireproof, Swedish, 20: 39067
design of ground-shock resistant, 20: 39084
design of prefabricated, blast-resistant, 20: 39075
design of public, in Denmark, 20: 39079
design of seven-man, 200 psi blast-resistant, 20: 39077
design of Swiss, 20: 39082
design of underground, effects of soil dynamics on, 20: 39070
design of, engineering approach to, 20: 39069
design specifications for Austrian, 20: 39081
development of private cooperative, 20: 39085
development status in Netherlands, 20: 39076
doors and valves for Canadian blast, use of plastic, 20: 39080
doors for blast, design of, 20: 39073
efficiency of nuclear blast, model analysis of, 20: 39071
environment of, effects of fire in internal, 20: 39059
foundations for underground, design of, 20: 39068
gamma radiation streaming through air pipes, review of, 20: 39060
shielding against nuclear-explosion initial radiations, problems in, 20: 39061
shielding calculations for, errors in, (E), 20: 39062
shielding from radioactive fallout by core, in typical British house, 20: 39083
shielding-analysis methods for, status of, 20: 39063
shock wave propagation in ducts and entrance structures of, 20: 39072
use of underground structures as, 20: 39078
ventilation valves for blast, 20: 39073
SHIELDED CONTAINERS
container for steel–lead–steel, design of plywood, 20: 39164
design for shipping high-level waste, 20: 40476(R) (BNWL-267)
design for shipping radioactive waste, 20: 40481 (WAPD-T-1851)
design of double-walled, for storage of radioactive materials, 20: 39040(P)
for storage of wastes in radioisotope hospitals, volume and number calculations for, 20: 38790
scattering outside cylindrical, sky-shine, 20: 40288
SHIELDING
against nuclear-explosion initial radiations, problems in, 20: 39061
analysis for radioisotope, computer program for, 20: 40285 (BNWL-236)
analysis methods for, status of, 20: 39063
calculations for shelters, errors in, (E), 20: 39062
design for β-γ monitor, 20: 39262
design for electron microscope, 20: 39038
design for gamma spectrometer, 20: 39260
design for whole-body counter, 20: 38753
design of lead, for coil circulating radioactive solutions during scintillation counting, 20: 38558
design of magnetic, for space vehicles, 20: 40291
efficiency of core shelters in typical British house for radioactive fallout, 20: 39083
gamma scattering from concrete, from point isotropic source at slab surface, 20: 40284 (AD-637125)
magnetic coils for, of space vehicles, 20: 40292
neutron angular distributions behind iron, fast, 20: 40286
neutron flux distributions and spectra in iron–water, (E/T), 20: 40287
properties of dwellings in Hiroshima and Nagasaki, 20: 39064
use of lead grating during x radiotherapy of stomach carcinomas, 20: 38763
use of wedge-shaped lead, for gamma dose distribution measurements in phantoms, 20: 38762
SHIELDING MATERIALS
gamma attenuation calculations for, build-up factor effects on, 20: 40289
SHIPPING
cask design for liquid waste, 20: 40476(R) (BNWL-267)
container for radioactive materials, design of, 20: 40481 (WAPD-T-1851)
container for radioisotope, design and testing of plywood, 20: 39164
hazards in solidified high-level waste, 20: 40476(R) (BNWL-267)
SHIPPINGPORT PRESSURIZED WATER REACTOR
fuel plates for core 2, bonding mechanisms for Zircaloy-2 cladding on, 20: 39361 (WAPD-305)
waste disposal at, 20: 40481 (WAPD-T-1851)
SHIPS
nuclear-powered, bibliography on, 20: 40444 (AED-C-22-06)
nuclear-powered, Japanese classification guide, 20: 40448 (NP-16217)
SHOCK WAVES
compression of lanthanides by, 20: 39425(T)
formation of magnetogasdynamic, with electrical conductivity as dissipative mechanism, 20: 39944
propagation in ducts and entrance structures of shelters, 20: 39072
use for superheating gas in MHD generators, (T), 20: 39686
SILICIC ACIDS
phase transformations, effect of pressure and irradiation on solid-solid, (E), 20: 40306
SILICIDES
reactions with combustion gas species in launch pad abort environments, 20: 39312 (SC-CR-66-2044)
SILICON
annealing of ion-bombarded, effects on impurity concentrations, (E),

20: 40345
content in fallout from Chinese atomic test, Oct. 1964, 20: 39110
deposition on fuel rods for corrosion protection, method for, 20: 39350(P)
determination in coal by activation, on-line, 20: 39025 (ORO-2980-12)
effects on properties of boron steel, 20: 39426
effects on properties of magnesium-base alloys for fuel-element cladding, 20: 39443(P)
neutron elastic scattering 0.57 to 2.28 Mev, differential cross sections for, (E), 20: 40069(R) (EANDC(E)-66(U)
properties and use of semiconductor detectors of, for electron and gamma spectroscopy, 20: 39232
properties of semiconductor detectors of, 20: 39230
radiation effects on, 1-Mev electron, (E), 20: 39458 (NP-16225)
radiation effects on short-circuit current of, proton, (E), 20: 40299
radiation effects at 293°K on n-type, neutron and gamma, (E), 20: 40303
radiation effects on, oxygen ion, (E), 20: 40314
radiation effects on infrared absorption spectrum of, neutron, (E), 20: 40340
radioinduced defects in n- and p-type, annealing of neutron, 20: 40334(T)
response of semiconductor fission detectors of, to argon-40 and iodine-127 ions, (E), 20: 39470(R) (ORNL-3924)
spectra of oxygen-doped, effects of fast neutrons and 2-Mev electrons on, (E), 20: 40302
superconductivity under high pressure, (E), 20: 40039

SILICON ISOTOPES Si-30
deuteron reactions (d,p) at 10 Mev, differential cross section for, 20: 40065(R) (BMwF-FB-K-66-01)

SILICON OXIDES
formation of films of, by oxygen ion bombardment of silicon, (E), 20: 40314
phase transformations, effect of pressure and irradiation on solid-solid, (E), 20: 40306
$BaO-SiO_2-ZrO_2$, phase studies, 20: 38899
hexane–SiO_2, radiolysis of, ESR spectral studies on yields in gamma, 20: 38994(R) (AE-232)

SILICON STEEL
radiation effects on fatigue of A212B, neutron, 20: 39406 (WAPD-T-1864)

SILICON SYSTEMS
Al–Si, dispersion in graphite, optimum pressure and temperature for liquid, 20: 39355 (EUR-2988.f)
Co–Fe–Si, Mössbauer effect in, 20: 40300
C–Si–U, phase studies of, at room temperature, 20: 39413
Ge–Si, thermoelectric properties, 20: 40451

SILICONES
performance of DC-705, in glass diffusion pumps, 20: 39098(R) (WERL-2823-21)

SILKWORMS
radiation effects on sperm of, genetic, RBE of fast neutron and γ, 20: 38626

SILTS
distribution and radionuclide sorption of, in river-estuary systems, 20: 39121
radionuclide distribution in, from nuclear plant wastes, 20: 38742

SILVER
determination in biological materials, use of automated gamma spectrometers in activation, 20: 38843
neon-20 reactions at 200 Mev, in emulsions, (E), 20: 40083
neutron capture resonance integrals, (E), 20: 40146
superconductivity of, 20: 40047

SILVER ALLOYS
Be–Ag, preparation of beryllium-base, for precision instruments, 20: 39374(P)
Cd–In–Ag, radiation effects on silver-base, in-reactor, 20: 39461 (WCAP-6074)
Cd–In–Ag, reactivity worths of arrays of tubes filled with, 20: 40381
Hg–Ag, uses as electrode in oscillographic determination of rare earths, 20: 38811

SILVER ISOTOPES
abundance in Canyon Diablo meteorite, 20: 39102

SILVER ISOTOPES Ag-107
proton scattering at 13 Mev, differential cross sections for elastic and inelastic, (E), 20: 39470(R) (ORNL-3924)

SILVER ISOTOPES Ag-109
proton reactions (p,n) at 3.0 to 5.8 Mev, strength functions for, (E), 20: 39470(R) (ORNL-3924)

SILVER ISOTOPES Ag-110
neutron reactions at 7.8 to 64 kev, activation cross sections for, (E), 20: 40069(R) (EANDC(E)-66(U))

SILVER ISOTOPES Ag-111
effects on cumbium cells and macrocytes in patients, 20: 38769

SILVER OXIDES
determination in swimming pool reactor coolant, activation and chemical, 20: 38800 (PAEC(C)RE-652)

SINGLE CRYSTALS
charged-particle reactions with, stopping power for, 20: 39595
orientation in tungsten, effects on ductile-brittle transitions, 20: 39397 (NASA-TM-X-1252)

SINTERING
process for urania, oxidizing effects of impurities on, 20: 39390 (CEA-R-3003)

SKELETON
radiation effects on, therapeutic doses, 20: 38767
radiation injuries of, in children treated for hemangiomas by radium, 20: 38787

SKIN
dose calculations for radiotherapy of, source distances from, 20: 38750
radiation effects on DNase in guinea pig, 20: 38591(R) (NYO-3445-7)
radiation effects on mouse, biological, 20: 38627
radiation effects on microflora of, 20: 38644
radiation injuries of guinea pig, pathology of β, 20: 38591(R) (NYO-3445-7)
radioactive contamination of, 20: 39151
radioinduced carcinoma of, after radium therapy, 20: 38788
radiotherapy of tumors of facial, absorbed dose in brain from x, 20: 38765
radiotherapy of, using combined orthovoltage x radiation and cobalt-60, dose curves for, 20: 38792

SNOW
density profile measurement in, using nuclear techniques, 20: 39130
oxygen-16 to oxygen-18 ratio in St. Elias Mountain, Canada, 20: 39123

SODIUM
analysis for impurities, development of techniques for, 20: 38797(R) (MSAR-66-150)
corrosion and mass transfer of low-alloy and stainless steels in flowing liquid, 20: 39345 (GEAP-4831)
determination in biological materials, radiochemical separation methods for activation, 20: 38842
determination in blood serum, activation, 20: 38851
determination in biological materials, use of automated gamma spectrometers in activation, 20: 38843
determination in mineral and natural waters, flame photometric, 20: 38798 (NIJS-R-465)
determination in mosaic virus and nucleic acids in tobacco plants, activation, 20: 38846
diffusion in molten sodium nitrate, coefficient of, 20: 38871(R) (NYO-1769-54)
diffusion of fission products from high-temperature, factor affecting, 20: 40357 (NAA-SR-11766)
electric dipole moments of, ratio of atomic to electron, 20: 39598
electron interactions with atomic, electron exchange in, 20: 39582(T) (AERE-Trans-1053)
evaporation of sodium iodide from, mechanisms of, 20: 40357 (NAA-SR-11766)
flow in rectangular duct, magnetohydrodynamic, (E), 20: 39706
ion exchange on minerals, 20: 38858 (BNWL-235-3, pp 23-51)
scattering by mercury beams at 7 to 500 ev, cross sections for, 20: 39599
superconductivity of, 20: 40047
thermal properties of liquid and vaporous, 20: 39028

SODIUM ALLOYS
Cd–Na, properties of, chemical and physical, 20: 38856 (BNL-10372)
K–Na, circulation in MHD ducts, (E), 20: 39716
K–Na, erosive effects on stainless steel, 20: 39023 (NAA-SR-11952)

SODIUM AMERICIUM FLUORIDES
crystal structure of $Na_7Am_6F_{31}$, 20: 38898

SODIUM CARBONATES
$BaCl_2-Na_2CO_3-UO_2(NO_3)_2$, uranium precipitation in, mechanism of, 20: 38928
$CaCl_2-Na_2CO_3-UO_2(NO_3)_2$, uranium precipitation in, mechanism of, 20: 38928
$MgCl_2-Na_2CO_3-UO_2(NO_3)_2$, uranium precipitation in, mechanism of, 20: 38928
$Na_2CO_3-D_2O$, phase diagram of, 20: 38994(R) (AE-232)
$Na_2CO_3-H_2O$, phase diagram of, 20: 38994(R) (AE-232)
$Na_2CO_3-SrCl_2-UO_2(NO_3)_2$, uranium precipitation in, mechanism of, 20: 38928

SODIUM CHLORIDES
analytical use for separation of molybdenum-99 from technetium-99m sorbed on aluminum oxide, 20: 38997 (NIJS-R-483)
effects on vapor pressure of saturated heavy and light water solutions, 20: 38994(R) (AE-232)
ionic transport coefficients for, at 25°C, 20: 38909
x-ray diffraction analysis at 5.898 kev, 20: 40294

SODIUM CURIUM FLUORIDES

crystal structure of $Na_7Cm_6F_{31}$, 20: 38898
SODIUM GALLATES
use for prophylaxis and therapy of radiation sickness in mice and rats, 20: 38728
SODIUM IODATES
iodine-131 beta decay in, properties of xenon oxide compounds formed by, 20: 38984
SODIUM IODIDES
evaporation from sodium, mechanisms of, 20: 40357 (NAA-SR-11766)
SODIUM ISOTOPES Na-22
beta decay of, with electron pair formation in neon-22, (E), 20: 40134
diffusion in sodium nitrates, effects of pressure on, 20: 38872(R) (NYO-1769-68)
SODIUM ISOTOPES Na-23
diffusion in molten sodium nitrate at constant volume, 20: 38872(R) (NYO-1769-68)
neutron reaction (n,α) at 12.6 to 18.7 Mev, cross sections for, (E), 20: 40069(R) (EANDC(E)-66(U))
SODIUM ISOTOPES Na-24
determination in calcium-47, chromatographic, 20: 38827
determination in swimming pool reactor coolant, activation and chemical, 20: 38800 (PAEC(C)RE-652)
use in measurement of myometrial blood flow during pregnancy, 20: 38747
SODIUM METHOXIDE
reactions with 2,2-diphenylethyl benzenesulfonate, effects of deuterium and tritium on, 20: 38912
SODIUM NEPTUNIUM FLUORIDES
crystal structure of $Na_7Np_6F_{31}$, 20: 38898
SODIUM NITRATES
diffusion of cesium and sodium in, coefficients of, 20: 38871(R) (NYO-1769-54)
diffusion of cesium-134 and sodium-23 in molten, at constant volume, 20: 38872(R) (NYO-1769-68)
diffusion of sodium-22 in, effects of pressure on, 20: 38872(R) (NYO-1769-68)
radiolysis of frozen, at 77°K, yields of nitrite ion from gamma, 20: 38950
spectra of, laser excitation of Raman, 20: 38872(R) (NYO-1769-68)
SODIUM NITRITES
$NaNO_2$–H_2SO_4, in oxidation of iodides to molecular iodine, 20: 39103(R) (BNWL-235-3, pp 51-69)
SODIUM PERPROTACTINATES
formation of insoluble, 20: 38890
SODIUM PLUTONIUM FLUORIDES
crystal structure of $Na_7Pu_6F_{31}$, 20: 38898
SODIUM REACTOR EXPERIMENT
coolant radioactivity in, effects of impurities on, 20: 40357 (NAA-SR-11766)
modification of, review of procedures, 20: 40429
SODIUM SELENITES
heat of solution, 20: 38900
heat of solution, 20: 38901
SODIUM SULFATES
crystallization from simulated glass melter condensate, 20: 40476(R) (BNWL-267)
SOILS
analysis of, for water content, by neutron scattering, 20: 39141
composition of, effect on radon gas in air, 20: 39114
fallout content in Japanese, effects of soil particle size on, 20: 39112
interactions with underground shelters, effects on shelter design, 20: 39070
moisture content of, use of neutron meters in measuring, 20: 39131
neutron flux distribution around point source of fast neutrons, thermal, (T), 20: 40058
radiation monitoring in California, 20: 38735(R) (NYO-1704-13)
radioactivity monitoring in Netherlands, 1963, 20: 39118
strontium-90 diffusion in, effects of properties on, 20: 38918(T)
strontium-90 movement in, 20: 39117(T)
thorium and uranium isotope distribution in, age estimation from, 20: 39144
SOL-GEL PROCESS
development of, for spherical UO_2–ThO_2 particle preparation, 20: 40391
flowsheets for, 20: 39006
SOLAR BATTERIES
properties of, comparison with isotope cells, 20: 39306 (DP-1066(Vol.1), pp V.17-25)
protection against radiation during Cosmos 41 flight, 20: 39171(T)
radiation effects on silicon, 1-Mev electron, (E), 20: 39458 (NP-16225)
radiation effects on gallium arsenide and silicon, proton, 20: 40299
SOLAR FLARES
cosmic-ray multiply charged nuclei from July 18, 1961, 20: 39564
effects of, and seasons on critical F2-layer frequencies, 20: 39959(T)
effects on critical frequencies of ionosphere, 20: 39965(T)
effects on solar magnetic field, 20: 39557
effects on solar magnetic field, 20: 39558
occurrence of, correlation with auroras, 20: 39956
properties of, sunspot cycle relation to, 20: 39563
proton propagation from, in interplanetary magnetic field, (T), 20: 39575
radiation hazards to astronauts from, 20: 38603(T) (AD-629422)
SOLAR RADIATION
electron and ion density in solar wind-magnetosphere region, 20: 39978
interaction with solar magnetic field, (T), 20: 39573
SOLID SOLUTIONS
formation by reactions of metals with refractory materials at high temperatures, 20: 39331(T) (UCRL-Trans-10044)
SOLIDS
analysis for nitrogen and oxygen, mass spectrometric, 20: 38831
SOLUTIONS
metering radioactive, design of flowmeter for, 20: 39172
radioactive, monitoring equipment for circulating, 20: 38558
radiolysis of aqueous, research progress on, 20: 38939(R) (NYO-2668-13)
SOLVENT EXTRACTION PROCESSES
equipment for berkelium, efficiency and hydraulic stability of, 20: 38998(R) (ORNL-3958)
organophosphorus compounds for use in, properties of neutral bifunctional, 20: 38819
use with ion exchange for separation of uranium from elements and fission products, 20: 38999 (TID-23229)
SOLVENTS
contaminant removal with, 20: 40489 (SC-DC-66-1118)
ion exchange, properties of mixed and non-aqueous, 20: 38818
properties of neutral bifunctional organophosphorus compounds for use as, 20: 38819
SONIC INSPECTION
use in reactor fuel channels, equipment for, 20: 39175
SOUTH DAKOTA
environmental radiation measurements in, 20: 38735(R) (NYO-1704-13)
SPACE
conference on peaceful uses of, 20: 40486 (NASA-SP-82)
cosmic radiation measurements in, 20: 39627
radiation transfers in interstellar, (T), 20: 39570
SPACE FLIGHT
radiation protection of astronauts during, 20: 38603(T) (AD-629422)
SPACE VEHICLES
power supplies for, evaluation of Rankine and Brayton cycles for, 20: 40452
propulsion of, design of ion engine for, 20: 39095(P)
radiation dosimetry in, 20: 39158
shielding for, design of magnetic, 20: 40291
shielding with magnetic fields, 20: 40292
SPAIN
nuclear power development in, 20: 40441
nuclear power use in, for electricity production, 20: 40442
SPARK CHAMBERS
development for high-energy physics, 20: 39241
particle track registration and data extraction in, 20: 39210 (JINR-P-2745)
performance for electron momentum measurements, 20: 39207 (ISS-66/18)
performance of high-pressure helium-filled streamer, 20: 39245
pulser design for, 20: 39270
SPECTROMETERS
design and performance of simultaneous alpha and beta, using cesium iodide, 20: 39217
design of charged particle, 20: 39502
resolution of, effects of multichannel analyzer channel width on, 20: 39204 (INR-694/III/PL)
SPERM
radiation effects on silkworm, genetic, RBE of fast neutrons and γ, 20: 38626
SPERMATOGENESIS
helium effects on Drosophila, 20: 38596(R) (SAN-590-1)
radiation effects in *Drosophila melanogaster*, x, 20: 38607
SPLEEN
radiation effects on colony formation by injected bone marrow cells in mouse, 20: 38708(R) (IAEA-3173-5)
radiosensitivity of rat, effects of thioacetamide on x, 20: 38694
SPORES
radiation effects on germination of *Ustilago avenae*, x, 20: 38672
SPUTTERING
ejection patterns for semiconductor, (E), 20: 40305
growth of, vs. evaporation in metal films, (E), 20: 39587
yields crossover in single-crystal copper, (E), 20: 39589
STAINLESS STEEL
corrosion and mass transfer of type 316, in flowing sodium, 20: 39345 (GEAP-4831)
deuterium ion reactions with 304 at 40 kev, sputtering from,

20: 39581(R) (ORNL-3989, pp 134)
electron beam reactions with, physical aspects of penetrations from, 20: 40347
erosion by liquid potassium–sodium alloy, 20: 39023 (NAA-SR-11952)
fabrication by magnetic-pulse forming, 20: 40490 (Y-1483)
fatigue strength of weldments of, to type A105 carbon steel, 20: 39404 (SWRI-1228-4-20)
reactions with combustion gas species in launch pad abort environments, 20: 39312 (SC-CR-2044)
stainless steel–UO_2, fission-induced failure model for, 20: 39459 (TRG-Report-1278)
STANDARDS
preparation of, in Czechoslovakia, 20: 39279
STANFORD LINEAR ACCELERATOR
beam position monitor for, 20: 39506
development, Jan. 1–Mar. 31, 1966, 20: 39497(R) (SLAC-65)
drift tube design, 20: 39503
magnets for, magnetic centers of quadrope, 20: 39503
thermionic diode housing for, 20: 39506
STARCHES
radiation effects on concentration of, in potato tubers, x, 20: 38690
STARS
atmospheres of, evaporative and hydrodynamic models for, 20: 39556
collapse of, (T), 20: 39555
evolution of, calculations on pre-main-sequence, 20: 39574
formation in rotating magnetic clouds, (T), 20: 39568
properties of horizontal-branch, hydrogen-burning models for, 20: 39566
transuranic element synthesis in, 20: 40144
STATISTICS
analysis of economics of nuclear cavities, 20: 39014(R) (TID-23184)
method for study of delayed triple nuclear cascades, 20: 40160
on uranium reserves, 20: 39101
STEAM
corrosive effects on chromium–iron–zirconium alloys at 300 to 500°C, 20: 39356(R) (GEAP-5134)
corrosive effects on copper–molybdenum–zirconium alloys, effects of heat treatments on, 20: 39347 (NP-16239)
separation from water, performance of radial vane separator for, 20: 39019(R) (GEAP-5149)
steam–H_2O, flow in radial-vane separators, 20: 39019(R) (GEAP-5149)
STEEL
corrosion of mild, by Purex waste solutions, 20: 40476(R) (BNWL-267)
design of low-alloy, for reactor pressure vessels, 20: 39444(P)
radiography of, using isotopes, 20: 39286 (DP-1066(Vol.1), pp IV.43-5)
STEROIDS
biogenesis and metabolism in elderly men, tracer study on, 20: 38547(R) (NYO-918-15)
determination in urine using paper chromatography, 20: 38547(R) (NYO-918-15)
preparation and uses of sulfur-35 and tritium-labeled, 20: 38547(R) (NYO-918-15)
radiation effects on excretion and production in guinea pig urine, 20: 38547(R) (NYO-918-15)
STEROIDS, 17-KETO-
determination in urine using paper chromatography, 20: 38547(R) (NYO-918-15)
radiation effects on content in dog blood, x, 20: 38684
STEROLS
radiation effects on synthesis in rats of, x, 20: 38638
STILBENE
radiation effects on diffusion of triplet excitons in, 20: 38957
radioinduced isomerization of, in benzene, gamma, 20: 38948
STILBENE, α,α'-DIMETHYL-
radioinduced isomerization of, in benzene, gamma, 20: 38948
STILBENE, α-METHYL-
radioinduced isomerization of, in benzene, gamma, 20: 38948
STOMACH
radiotherapy of carcinomas of, use of lead grating for x, 20: 38763
radiotherapy of cancers of, 20: 38772
STRAIN GAGES
design for reactor fuel channel gaps, 20: 39175
STRANGE PARTICLES
production in meson (π^-)-neutron interactions at 3.5 Bev/c, cross sections for, (E), 20: 39842
STRATIGRAPHY
measurement in basalt sequence beneath Hanford area, 20: 39099(R) (BNWL-235-3, pp 1-23)
STRESS ANALYSIS
computer program for composite tubes, 20: 39394 (GEMP-415)
of hexagonal reactor tubes, 20: 39384 (BNWL-263)
STRONTIUM
determination in mineral and natural waters, flame photometric, 20: 38798 (NIJS-R-465)
determination of traces of, in biological materials, activation, 20: 38837
diffusion from sodium at high temperatures, factors affecting, 20: 40357 (NAA-SR-11766)
effects on barium and strontium retention in rats of dietary, 20: 38566
ion exchange on minerals, 20: 38858 (BNWL-235-3, pp 23-51)
metabolism in rats, effects of calcium, phosphorus, or strontium content in diet, tracer study, 20: 38566
metabolism in wheat seedlings, 20: 38548(R) (ORO-2410-1)
separation from alumina calcine by leaching with dilute nitric acid or distilled water, 20: 40478 (IN-1011)
sorption by ion exchange on titanium oxide, 20: 39002
sorption by zirconium silicate phosphate gel, 20: 38994(R) (AE-232)
STRONTIUM CHLORIDES
diffusion in, self-, 20: 38871(R) (NYO-1769-54)
radioinduced V_k center in single crystals of, x, 20: 40319
Na_2CO_3–$SrCl_2$–$UO_2(NO_3)_2$, uranium precipitation in, mechanism of, 20: 38928
STRONTIUM DEUTERIDES
absorption bands, rotational analysis of uv, (E), 20: 40331
STRONTIUM FERRATES
preparation and properties of, 20: 38859 (CEA-R-2895)
separation processes for, 20: 38859 (CEA-R-2895)
STRONTIUM HYDRIDES
absorption bands, rotational analysis of uv, (E), 20: 40331
STRONTIUM ISOTOPES
separation from reservoir water by filtration–ion exchange, 20: 40484
STRONTIUM ISOTOPES Sr-85
removal from rat body by high strontium diets, 20: 38566
separation using mixed oxide scavenger, 20: 40476(R) (BNWL-267)
STRONTIUM ISOTOPES Sr-86
content in rocks in Sweden, 20: 39126
STRONTIUM ISOTOPES Sr-87
content in rocks in Sweden, 20: 39126
STRONTIUM ISOTOPES Sr-89
content in fallout from USSR nuclear test, Jan. 1965, 20: 39108
half-life and metabolism of, 20: 38743
separation from waste-water by aerobic treatment, 20: 40483
STRONTIUM ISOTOPES Sr-90
absorption from gastrointestinal tract of rats, effects of calcium compounds on, 20: 38569
content in bone samples in Great Britain, 1965, 20: 39163
content in bones of children in Argentina sampled in 1965, 20: 39150(R) (NYO-2753-4)
content in Clinch River, 20-year analysis of, 20: 40479 (ORNL-P-2328)
content in diet of children in Argentina, 1965, 20: 39150(R) (NYO-2750-4)
content in diet of Italian children, 20: 39152
content in milk, methods for reducing, 20: 39157
content in urine of Italian children, 20: 39152
diffusion in soils, effect of properties on, 20: 38918(T)
distribution in tissues of guinea pigs, 20: 38662
effects of internally deposited in man, biological, 20: 38623
effects on mice, biological, of chronic ingestion of, 20: 38551
evaluation of, for space heat source, 20: 39306 (DP-1066(Vol.1), pp V.17-25)
half-life and metabolism of, 20: 38743
movement in Georgian Soils, 20: 39117(T)
release from simulated high-level wastes, 20: 40476(R) (BNWL-267)
removal from fabrics using citric acid, detergents, or water, 20: 39161
removal from rat body by high strontium diets, 20: 38566
uptake by algae, effects of EDTA on, 20: 38570
use as heat source in SNAP-7 device, radiological hazards of, 20: 39307 (DP-1066(Vol.1), pp V.35-40)
use as heat source in RIPPLE I + II, 20: 39309 (DP-1066(Vol.2), pp III.39-48)
use in thermoelectric converters, 20: 39633 (CEA-R-2788)
STRUCTURES
design of metal, to withstand atomic explosion blast, 20: 39053(P)
explosion effect on, 20: 39149 (NVO-28)
response of concrete and steel tubular towers to static and dynamic loads, 20: 39007 (AD-636914)
STYRENE POLYMERS
radioinduced polymerization of, with hydrocarbons for radioresistant lubricants, 20: 38973(P)
thermal degradation of, with divinylbenzene, mechanism of, 20: 38930 (TID-23264)
SUGARS
radiation effects on content in rabbit blood of, x, 20: 38686
SULFAMIC ACID
properties of fluoride-bearing aqueous, for etching and pickling zirconium alloys, 20: 39351(P)
SULFIDES
effects as radioprotective agents in mice, relation to chemical structure,

20: 38724
SULFUR
determination in fission product waste solids by combustion and colorimetry, 20: 38795 (BNWL-265)
determination in petroleum streams, equipment and method for, 20: 39191(P)
effects of drinking water containing, on radiosensitivity of mice, 20: 38709
SULFUR COMPOUNDS
radioprotective, evaluation of models for selecting, 20: 38729
SULFUR FLUORIDES
molecular structure of, mean amplitudes of vibration at 0 and 298°K in, 20: 38897
radiolysis of, ESR spectra of products of, 20: 38941(R) (RRL-2310-182)
use of SF_6 in fuel reprocessing, 20: 40389
PF_3–SF_6, radiolysis of, ESR spectra of products of, 20: 38941(R) (RRL-2310-182)
SULFUR ISOTOPES S-32
neutron reactions (n,p) with, neutron dosimetry using, 20: 39228
SULFUR ISOTOPES S-35
incorporation in Malathion, 20: 38931
incorporation in steroids, 20: 38547(R) (NYO-918-15)
SULFURIC ACID
uses of deuterium-labeled, as deuterating agent, 20: 38889
$NaNO_2$–H_2SO_4, in oxidation of iodides to molecular iodine, 20: 39103(R) (BNWL-235-3, pp 51-69)
$(NH_4)_2SO_4$–H_2SO_4, analysis for americium by controlled-potential coulometry, 20: 38854
SUN
chromosphere of, thermal instabilities in, 20: 39562
corona electron and ion temperatures for, measurement of, 20: 39572
effects on geomagnetic activity variations, (E/T), 20: 39982
magnetic field of, connection of geomagnetic field to, 20: 39986
magnetic field of, effects of active regions on, 20: 39557
magnetic field of, effects of active regions on, 20: 39558
magnetic field of, expulsion of flux by eddies in, 20: 39567
magnetic field of, interaction of solar wind with, (T), 20: 39573
spot and faculae magnetic flux, variability of, 20: 39561(T)
spot cycle of, events from, 20: 39563
spot group magnetic field strength, secular variations in, (T), 20: 39559
spot model of, magnetic field effects on convective instability in, 20: 39939
SUPERCONDUCTIVITY
critical temperatures of germanium and silicon under high pressure, (E), 20: 40039
critical temperatures of lead and tin up to 160 kbar, (E), 20: 40040
currents in surface layers of niobium–zirconium alloys, (E), 20: 40023
effects of interstitial gases in niobium on, (E), 20: 40025
effects of orbital field on Fulde-Ferrell state in, 20: 40046
measurements for transition metals, tables of, 20: 40047
model for, two-fluid, 20: 40037
theory of, de Gennes method of correlation functions in, 20: 40038
theory of, expansion of effective interaction in BCS, 20: 40017
SUPERCONDUCTORS
colorimetry on type-II, isothermal, (E), 20: 40045
critical current density in niobium–zirconium–tantalum, effect of micro-heterogeneity on, 20: 40020
critical current density in niobium–zirconium, effect of alloy structure on, 20: 40021
critical field in cerium-doped lead, 20: 40050
current distribution in cylindrical type II, 20: 40029
current in hard, properties of surface, 20: 40014(R) (ORNL-3989, pp 109-27)
current phenomena in type II, surface, 20: 40015(R) (ORNL-TM-1598)
current-carrying capacity of hard, with zero external field, 20: 40015(R) (ORNL-TM-1598)
design and performance for MHD magnets, 20: 39643
development for magnet coils, 20: 40014(R) (ORNL-3989, pp 109-27)
electric conductivity of niobium, from helicon-like resonances, (E/T), (E/T), 20: 40031
electron tunneling in junctions of, second derivatives for conductance in, (E), 20: 39470(R) (ORNL-3924)
electron tunneling in, radiation induced structure in d-c Josephson, 20: 40035
energy gap and critical field of, (T), 20: 40017
energy gap in single-crystal, anisotropy effects on, (T), 20: 40041
fabrication from heat treated niobium–zirconium alloy, 20: 39372(P)
Faraday unipolar induction in nonideal type II, 20: 40016
ferromagnetic particle effects on type-II, (E), 20: 40024
infrared absorption by lead films, effects of magnetic fields on, (E), 20: 40044
magnetic field effect on type-II, Fulde-Ferrell, 20: 40046
magnetic fields in quadrupole lenses of, digital calculations of, 20: 39479 (BNL-10495)
magnetic flux flow in, with zero external field, 20: 40015(R) (ORNL-TM-1598)
magnetic shielding properties of niobium–tin, for accelerator extraction systems, 20: 39523
magnetization process of Type II, enthalpy from, (T), 20: 40036
microwave radiation from Josephson tunnel junctions of tin, 20: 40028
oscillations in intermediate state of, (T), 20: 40026(T)
performance of MHD generator magnets, (E), 20: 39733
performance of niobium–zirconium, for magnets, 20: 40015(R) (ORNL-TM-1598)
radiofrequency losses in, flux-trapping model for, (E/T), 20: 40042
surface resistance of, (E/T), 20: 40042
testing of large magnets of, facility for, 20: 40049
theory of compound, 20: 40015(R) (ORNL-TM-1598)
thermal resistivity in intermediate-state indium and lead, size effect in, (E), 20: 40022
thermodynamic properties of, anisotropy effects on, (T), 20: 40041
transition temperature of indium films, thickness effects on, 20: 40043
ultrasonic absorption in, 20: 40336(T)
use of niobium–zirconium, in 40,000-gauss magnet, 20: 40018
use of niobium-25 zirconium, for magnetic bottle, 20: 40169 (NASA-TN-D-3595)
SUPERCRITICAL ONCE-THRU TUBE REACTOR
design and development, 20: 40416 (WCAP-2222-P)
SUPERHEATERS (NUCLEAR)
design of fuel elements, uranía thermal conductivity values for, 20: 39403 (ORNL-TM-1450)
SURFACE-ACTIVE AGENTS
effects on mass transfer in two-phase flow, 20: 39050 (UCRL-16535)
SURFACE FRICTION
effects on heat transfer in parallel rod arrays, 20: 39084 (GEAP-5115)
SURFACE TENSION
use in liquid storage, 20: 39091
SURFACE WATERS
hydrogen isotope ratios in, effect of rain and spring water on, 20: 39127
radionuclide transport in river-estuary systems, 20: 39121
release rate of radioactive rare gases from, 20: 39103(R) (BNWL-235-3, pp 51-69)
sampling of river, engineering drawings of equipment for, 20: 39185
SURGERY
advantages of, compared with radiotherapy for treatment of laryngeal cancer, 20: 38782
radiation as a pre-operative procedure in lung cancer, effectiveness of, 20: 38755
SWEDEN
geochronology of rocks in, 20: 39126
geochronology of, from age measurements on radioactive minerals, 20: 39125
SWIMMING POOL REACTORS
coolant analysis for corrosives and solids in, activation and chemical, 20: 38800 (PAEC(C)TR-652)
SWITZERLAND
nuclear power development in, 20: 40441
nuclear power use in, for electricity production, 20: 40442
SYNCHROCYCLOTRONS
beam extraction in, regenerative, 20: 39522
beam stretcher for, strong focusing ring as, 20: 39538
design modification for Uppsala 185-Mev, sector-focusing, 20: 39535
design modifications of NEVIS, 20: 39536
design modifications for beam improvement in Carnegie, 20: 39537
ion orbit in, computer program for, 20: 39537
particle accumulation in JINR 680-Mev, method for, 20: 39492 (JINR-P-2811)
radio frequency system of proton phasotron, programming accelerating voltage amplitude of, 20: 39491 (JINR-P-2732-1)
SYNCHROTRONS
description of 200-Bev proton, employing separate function magnet lattices, 20: 39480 (BNL-10508)
particle motion in, stability of, 20: 39524
SYSTEMS FOR NUCLEAR AUXILIARY POWER
development for space terrestrial, and marine use, 20: 39305 (DP-1066 (Vol.1), pp V.3-16)
development for undersea uses, 20: 40362
development of reactor-type, for oceanographic application, 20: 39313
power cycles for, evaluation of Rankine and Brayton, 20: 40452
shaft-bearing system dynamics for MRP Combined Rotating Unit, analog study, 20: 39022 (NAA-SR-11943)
SYSTEMS FOR NUCLEAR AUXILIARY POWER (SNAP-7)
development of 7A, 20: 39313
radiological safety of, 20: 39307 (DP-1066(Vol.1), pp V.35-40)
SYSTEMS FOR NUCLEAR AUXILIARY POWER (SNAP-8)
alternator for, development out of long-life, 20: 40453

SYSTEMS FOR NUCLEAR AUXILIARY POWER (SNAP-10)
coolant pump for 10A, development of thermoelectric, 20: 40446 (NAA-SR-11879)
expansion compensator units for 10A, development, 20: 39023 (NAA-SR-11952)
fuel element testing for, program evaluation using K-factors, 20: 40447 (NAA-SR-11913)
thermoelectric arrangement of, 20: 40451
SYSTEMS FOR NUCLEAR AUXILIARY POWER (SNAP-15)
generator test evaluations for 15A, 20: 39310 (GA-5781)
SYSTEMS FOR NUCLEAR AUXILIARY POWER (SNAP-21)
development, 20: 39313
SYSTEMS FOR NUCLEAR AUXILIARY POWER (SNAP-23)
development, 20: 39313
SYSTEMS FOR NUCLEAR AUXILIARY POWER (SNAP-50)
coolant pump for SNAP-50/SPUR, development of electromagnetic, 20: 40450 (TIM-911)
SZILARD-CHALMERS REACTIONS
use in preparation of high-specific-activity chromium-51, 20: 38982 (PAEC(D)IS-652)

T

TANKS
temperatures in underground waste-storage, 20: 40476(R) (BNWL-267)
TANTALUM
bulk modulus to 500°C, adiabatic, (E), 20: 39418
ductility of hydrogenated sheets at low temperatures, Petch analysis of, 20: 39378 (AD-635596)
effects on grain size of tungsten, 20: 39400 (NASA-TN-D-3531)
electron emission in MHD generators from electrodes of, (E), 20: 39736
internal function of electron-beam refined, effects of carbon, nitrogen, and oxygen on, 20: 39420
neutron capture resonance integrals, (E), 20: 40146
oxidation of, effects of fluoride coating on, 20: 39348
production of high-quality sheet, panel summary on, 20: 39357 (MAB-212A-M)
solubility in cobalt–tungsten carbide systems, chemical determination of, 20: 39427
superconductivity of, 20: 40047
surface resistance of superconducting, 20: 40042
TANTALUM ALLOYS
Hf–Ta, work function for, 20: 40297
Hf–Ta–W, weldability evaluation of, 20: 39366
Nb–Ta, current distribution in type II superconductors of, 20: 40029
Nb–Ta–W–Zr, weldability evaluation of, 20: 39366
Nb–Ta–Zr, superconducting critical current density in, effect of micro-heterogeneity on, 20: 40020
Ta–W, reactions with combustion gas species in launch pad abort environments, 20: 39312 (SC-CR-66-2044)
TANTALUM BORIDES
effects on grain size of tungsten, 20: 39400 (NASA-TN-D-3531)
TANTALUM CARBIDES
effects on grain size of tungsten, 20: 39400 (NASA-TN-D-3531)
properties for matrix material in particulate uranium carbide fuels, 20: 39353 (BMWF-FBK-66-07)
graphite–TaC, fabrication and physical properties of, 20: 39367
Hf–MoC–Ta, preparation and properties of dispersion-hardened, 20: 39441(P)
TANTALUM ISOTOPES Ta-181
energy levels of, M1 transitions of rotational, (E), 20: 40072 (LA-DC-8061)
TANTALUM SYSTEMS
Hf–Ta–Wc, preparation and properties of dispersion-hardened, 20: 39441(P)
MoC–Ta–Zr, preparation and properties of dispersion-hardened, 20: 39441(P)
Ta–Wc–Zr, preparation and properties of dispersion-hardened, 20: 39441(P)
TAURINE
radiation effects on excretion in mice, effects of AET and cysteine on, whole-body x, 20: 38717
TECHNETIUM
superconductivity of, 20: 40047
TECHNETIUM FLUORIDES
molecular structure of, mean amplitudes of vibration at 0 and 298°K in, 20: 38897
TECHNETIUM ISOTOPES Tc-97
energy levels from ruthenium-97 decay, 20: 40084
TECHNETIUM ISOTOPES Tc-99
preparation of, by milking molybdenum-99, for medical uses, 20: 38986
separation from molybdenum-99 sorbed on aluminum oxide using physiologic solution, 20: 38997 (NIJS-R-483)
TEKTITES
age of, fission-track method for estimating, 20: 39135
TELEVISION EQUIPMENT
design of thermal-neutron sensitive, 20: 39174
TELLURIUM
determination in biological materials, use of automated gamma spectrometers in activation, 20: 38843
TELLURIUM FLUORIDES
molecular structure of, mean amplitudes of vibration at 0 and 298°K in, 20: 38897
TELLURIUM ISOTOPES
fractionation of, in laboratory reactions and natural processes, 20: 39122
TELLURIUM ISOTOPES Te-122
abundance ratio to tellurium-130 in natural samples, 20: 39122
energy levels of, magnetic moment of 564-kev 2^+ vibrational, (E), 20: 40128
TELLURIUM ISOTOPES Te-125
proton reactions (p,n) at 3.0 to 5.8 Mev, strength functions for, (E), 20: 39470(R) (ORNL-3924)
TELLURIUM ISOTOPES Te-130
abundance ratio to tellurium-122 in natural samples, 20: 39122
TEMPERATURE
calculation of, in underground waste storage tanks, 20: 40476(R) (BNWL-267)
effects on plant embryos, biological, 20: 38588(R) (COO-1400-10)
effects on radiation resistance of beryllia, 20: 39453 (EUR-3054.e)
radiosensitivity effects on *E. coli*, 20: 38630
TEMPERATURE CONTROL
circuit design for, in neutron-gamma well-logging equipment, 20: 39136(P)
equipment for, in well logging, 20: 39140(P)
TENSILE PROPERTIES
statistical methods for analysis, 20: 39408(T) (NSJ-tr-46)
TERBIUM
determination in solutions, spark method for spectrographic, 20: 38832
magnetic anisotropy of, (E), 20: 40346
magnetic fields at tin-119 in, deduction from gamma hyperfine splitting, 20: 40322
separation of, from other rare earths, by lactate elution from cation resin columns, 20: 39004
spectrum of neutral TbI, structure of optical, 20: 39604
TERBIUM ALLOYS
Al–Tb, magnetic properties of intermetallic compounds of, 20: 39433
Pb–Tb–Zn, component distribution in recrystallized, 20: 39435
TERBIUM CHLORIDES
heat of dilution of aqueous solutions of, 20: 38870 (IS-1356)
heat of dilution of aqueous, at 25°C, 20: 38903
heat of solution of hexahydrate of, 20: 38870 (IS-1356)
specific gravity and apparent molal volume of aqueous solutions of, at 25°C, 20: 38905
viscosity of aqueous solutions of, at 25°C, 20: 38904
TERBIUM IONS
spin-lattice relaxation time in lanthanum trichloride, angular and temperature effects on, 20: 40350
TERBIUM ISOTOPES
conversion electron spectra of, spectrometer for measuring, 20: 39203 (INP-476/PL)
TERBIUM ISOTOPES Tb-159
energy levels of, M1 transitions of rotational, (E), 20: 40072 (LA-DC-8061)
TERBIUM OXIDES
phase studies of, in oxidation-reduction cycles, 20: 38864(R) (COO-1109-22, Paper 3)
actinide oxides–Tb_2O_3, preparation of sols of, 20: 39341(P)
Ce_2O_3–Tb_2O_3, phase studies of, tensimetric, 20: 38862(R) (COO-1109-22, Paper 1)
Ce_2O_3–Tb_2O_3, phase studies of, in oxidation-reduction cycles, 20: 38864(R) (COO-1109-22, Paper 3)
Pr_2O_3–Tb_2O_3, phase studies of, tensimetric, 20: 38863(R) (COO-1109-22, Paper 2)
TERBIUM PHOSPHATES
preparation and properties of, conductometric and potentiometric studies on, 20: 38883
TEREPHTHALIC ACID, ETHYLENE POLYMER ESTERS
radioinduced spontaneous discharge from capacitor-type structures of, 20: 39467
TERPHENYL
corrosive effects on zirconium alloys, research on, 20: 39344 (EUR-2997.e)
radioinduced luminescence of, determination of triplet exciton diffusion from alpha, 20: 38957
use as sensitizer in cellulose textile crosslinking by radiation, 20: 38975(P)

TESTOSTERONE
determination in urine using paper chromatography, 20: 38547(R) (NYO-918-15)
metabolism in blood plasma in sheep ovaries, tracer study on, 20: 38547(R) (NYO-918-15)
TEXTILES
decontamination using citric acid, detergents, or water, 20: 39161
radiation effects on cellulosic, after treatment with sensitizing agent, 20: 38975(P)
THALLIUM
superconductivity of, 20: 40047
THALLIUM ALLOYS
Pb–Tl, calorimetry of superconducting, isothermal, (E), 20: 40045
THALLIUM CHLORIDES
viscosity of, use of vertically oscillating cylinder for measuring, 20: 38872(R) (NYO-1769-68)
THALLIUM IONS
effects on intratrack distribution of products in alpha radiolysis of ceric sulfate, 20: 38967
THALLIUM ISOTOPES Tl-202
electron capture ratios, M/L, 20: 40153
THALLIUM ISOTOPES Tl-204
elimination by mice and rats, effects of DTPA, pectin, and zirconium phosphate on, 20: 38733
THERMAL CONDUCTIVITY
measurement of, equipment for, 20: 39033
measurement of, equipment for, 20: 39034
of urania, effects of density and grain size on, 20: 39446 (AECL-2564)
of urania, survey of data for values on, 20: 39403 (ORNL-TM-1450)
radiation effects on urania, in-reactor, 20: 39456 (GEAP-5100-1)
THERMAL CYCLING APPARATUS
design, 20: 39092
THERMAL DIFFUSION
cascade theory for rare gas, 20: 39321(R) (MLM-1312)
molecular beam scattering in, computer program for calculating, 20: 39321(R) (MLM-1312)
temperature dependence in isotopic, equations for, 20: 39326
transport properties for helium and neon isotope separation by, 20: 39320(R) (MLM-1311)
transport properties for gas flow, 20: 39321(R) (MLM-1312)
THERMAL INSULATION
design for reactors with concrete pressure vessels, 20: 40367(P)
preparation of light-weight zirconia-base foams, 20: 39375(P)
THERMAL REACTORS
design of water-cooled and -moderated, with moderator control, 20: 40435(P)
THERMIONIC CELLS
ceramic structure development for, 20: 39638
design of, using halogen to prevent cathode material loss, 20: 39637(P)
emitter work function for, planar monocrystalline tungsten, 20: 39635 (UCRL-16699)
emitters of, models for electron emission from adsorbed monolayer, 20: 39641
emitters of, surface micropatch effects on, 20: 39642
properties of cesium, (E/T), 20: 39651
radioisotope heat sources for, 20: 39633 (CEA-R-2788)
THERMOCOUPLES
design and properties for use in power plants, 20: 40451
THERMODYNAMICS
calculations for fluid in peripheral compressor, 20: 39021 (K-1665)
THERMOELECTRIC CELLS
design of RIPPLE-I and -II, 20: 39309 (DP-1066(Vol.2), pp III.39-48)
design of tubular, using isotopic heat source, 20: 39308 (DP-1066(Vol.2), pp III.3-16)
development of, for oceanographic application, 20: 39313
radioisotope heat sources for, 20: 39633 (CEA-R-2788)
safety analysis of 5-watt radiostrontium-fueled, for meteorological station, 20: 39311 (MND-SR-2586)
THERMOLUMINESCENCE
radioinduced in calcium fluorides doped with rare earth ions, (E), 20: 40341
THERMOLUMINESCENT DETECTORS
design for personnel monitoring, 20: 39224
design for personnel monitoring, 20: 39225
THERMONUCLEAR EXPLOSIONS
fallout from USSR, Jan. 1965, 20: 39108
fallout from USSR, 1962, alpha activity of, 20: 39109
fallout from USSR, Oct. 1961, effects on electric conductivity of atmosphere, 20: 39111
THERMONUCLEAR REACTORS
plasma energy measurement in Tokamak, by magnetic flux variation, 20: 40187
THIAZOLIDINES
effects as radioprotective agent in mice, relation of chemical structure to, 20: 38724
THICKNESS GAGES
use of radioisotopic, review on, 20: 39291
use of radioisotope, in France, 20: 39295
THIOCYANATE IONS
properties for use in colorimetric determination of elements, review on, 20: 38808
THIOLS
effects as radioprotective agents in mice, relation to chemical structure, 20: 38724
THORIUM
content in minerals in Sweden, 20: 39125
content in soils, effect on radioactivity levels in air, 20: 39114
crystal structure of, valence electrons and interatomic bonds in, 20: 40296
determination in uranium minerals, 20: 39143
fuel cycle costs in high temperature reactors, 20: 40394
properties of, at low temperatures, 20: 39448 (AERE-X-PR-2596-9)
superconductivity of, 20: 40047
vaporization of, thermodynamics of, 20: 38876 (UJV-1598)
THORIUM ARSENATES
preparation and crystal structure of, 20: 38885
THORIUM CARBIDES
ThC_2–UC_2, irradiation testing of fuels of, 20: 40385 (ORNL-P-2327)
ThC_2–UC_2, processing reactor fuels of, grind-leach method for, 20: 38998(R) (ORNL-3958)
ThC–UC, reprocessing of fuel elements of, head-end treatment for, 20: 40390
THORIUM COMPLEXES
with dipentyl pentylphosphonate, spectra of, infrared, 20: 38799(R) (NLCO-980)
with nitrilotriacetic acid and polyamino polycarbooxylic acids, formation of, biamperometric studies of, 20: 38810
THORIUM ISOTOPES Th-230
distribution in soils, 20: 39144
preparation for use as alpha source, 20: 38990
separation from europium, iron, manganese, protactinium, and uranium by ion exchange, 20: 38834
THORIUM ISOTOPES Th-232
content in minerals in Sweden, 20: 39125
conversion rate in AVR Reactor, 20: 40469
distribution in soils, 20: 39144
THORIUM MINERALS
analysis for uranium, 20: 39143
THORIUM NITRATES
$Th(NO_3)_4$–$UO_2(NO_3)_2$, fuel fabrication from high enrichment solutions, 20: 40419
THORIUM OXIDES
analysis for nitrates by uv absorption, 20: 38926
crystal structure of sol-gel beads of, 20: 39364
properties of colloidal, 20: 38926
ThO_2–UO_2, preparation by sol-gel process, 20: 40391
THORIUM(IV) OXIDES
diffusion of gases from irradiated, effects of titania additions on, 20: 39381 (AECL-2585)
effects of Thorotrast on human kidneys, 20: 38756
effects on grain size of tungsten, 20: 39400 (NASA-TN-D-3531)
fabrication of pot-processed denitrated powders, into high-density pellets, 20: 39363 (WAPD-TM-577)
irradiation testing of reactor fuels of, 20: 40385 (ORNL-P-2327)
preparation of microspheres of, development of sol dispersers for, 20: 38998(R) (ORNL-3958)
preparation of microspheres of, performance of coated-particle facility for, 20: 38998(R) (ORNL-3958)
Ni–ThO_2, rupture strength of, effects of microstructure on, 20: 39398 (NASA-TN-D-3527)
PuO_2–ThO_2, irradiation testing of fuels of, 20: 40385 (ORNL-P-2327)
ThO_2–UO_2, irradiation testing of fuels of, 20: 40385 (ORNL-P-2327)
ThO_2–UO_2, properties of sintered, 20: 39006
THORIUM OXYCHLORIDES
formation of, in colloidal thoria, 20: 38926
THORIUM PHOSPHIDES
thermodynamics of formation of, at 1173°K, 20: 38907
THORIUM SELENIDES
preparation, properties, and uses of, book on, 20: 38927
THORIUM SYSTEMS
P–Th, thermodynamic properties of, solid-state EMF measurements at 800 to 950°C of, 20: 38907
THORIUM TELLURIDES
preparation, properties, and uses of, book on, 20: 38927
THREONINE
radiolysis of, in aqueous solution, γ, 20: 38582

THULIUM
determination in solutions, spark method for spectrographic, 20: 38832
magnetic fields at tin-119 in, deduction from gamma hyperfine splitting, 20: 40322
separation from ytterbium by solvent extraction using tertiary amines and diethylenetriaminopentaacetic acid or EDTA, 20: 38995 (BM-RI-6809)

THULIUM ALLOYS
Al–Tm, magnetic properties of intermetallic compounds of, 20: 39433
Nd–Tm, phase transformations and magnetic ordering in, pressure-induced, 20: 40326
Ni–Tm, crystal structure of intermetallic compounds in, 20: 39415
Pb–Tm–Zn, component distribution in recrystallized, 20: 39435
Sb–Tm, magnetization of cubic, anisotropy and thermal inversion in high-field, 20: 40320
Tm–Zn, crystal structure of intermetallic compounds Tm_6Zn_{23} and $TmZn_{12}$ in, 20: 39417

THULIUM CHLORIDES
heat of dilution of aqueous, at 25°C, 20: 38903

THULIUM ISOTOPES Tm-169
energy levels of, M1 transitions of rotational, (E), 20: 40072 (LA-DC-8061)

THULIUM ISOTOPES Tm-170
use in thermoelectric converters, 20: 39633 (CEA-R-2788)

THULIUM ISOTOPES Tm-171
separation from irradiated targets at Savannah River, 20: 39316 (DP-1066(Vol.1), pp II.3-14)

THULIUM OXIDES
actinide oxides–Tm_2O_3, preparation of sols of, 20: 39341(P)

THULIUM PHOSPHATES
preparation and properties of, conductometric and potentiometric studies on, 20: 38883

THYMINE
excision of dimers of, in irradiated *E. coli* mutants, 20: 38620

THYMOLS
effects on polarographic reduction of uranyl ions in hydrochloric acid, 20: 38922

THYMUS GLAND
radiation effects on metabolism in mouse, x, 20: 38606
radiation effects on, morphological, whole-body x, 20: 38685
radiation effects on mitosis in rat, x, 20: 38720

THYROID GLAND
analysis for iodine-129, activation, 20: 38564
effects of anti-metabolic drugs on metabolism of iodine-131 by, 20: 38785
iodine-131 uptake by mammalian, effects of diet on, 20: 38549 (UCLA-12-592)
iodine-131 uptake by, in adolescents and adults, 20: 38553
iodine-131 uptake and elimination from, effects of potassium iodide and thiouracil in dogs, mice, and rats, 20: 38734
radioinduced cancer of, after iodine-131 therapy of goiter, 20: 38749
radiosensitivity of, in iodine-131 therapy of Basedow's disease, 20: 38760
removal of iodine-131 by use of Tyrosine, 20: 38733
weight determination from scintograms of, for radioiodine dose determination, 20: 38789

THYRONINE, TRIIODO-
determination of, by neutron activation of iodine-129, 20: 38561
effects on protein synthesis in rat tissues, 20: 38595(R) (ORO-3295-2)

THYROXINE
determination of, by neutron activation of iodine-129, 20: 38561
preparation of iodine-131-labeled, method for, 20: 38992

TIN
dispersion in graphite, optimum pressure and temperature for liquid, 20: 39355 (EUR-2988.f)
microwave radiation from Josephson tunnel junctions of, 20: 40028
separation from bismuth in acid solution by solvent extraction using alkyl phosphates, 20: 38828
superconductivity up to 160 kbar, (E), 20: 40040
superconductivity of, 20: 40047
surface resistance of superconducting, 20: 40042

TIN ALLOYS
In–Sn, surface resistance of superconducting, (E), 20: 40042
Nb–Sn, current capacity, neutron irradiation effects on, 20: 40301
Nb–Sn, magnetic shielding properties of superconducting, for accelerator extraction systems, 20: 39523

TIN ISOTOPES Sn-113
electron capture ratios, M/L, 20: 40153

TIN ISOTOPES Sn-116
neutron reactions (n,γ) with, gamma spectra of, (E), 20: 39470(R) (ORNL-3924)

TIN ISOTOPES Sn-117
energy level structure of, (E), 20: 40159
neutron reactions (n,γ) with, gamma spectra of, (E), 20: 39470(R) (ORNL-3924)

TIN ISOTOPES Sn-118
neutron reactions with, strong p-wave resonances from, (E), 20: 39470(R) (ORNL-3924)
neutron reactions (n,γ) with, gamma spectra of, (E), 20: 39470(R) (ORNL-3924)

TIN ISOTOPES Sn-119
Mössbauer effect in rare earths, magnetic field from, 20: 40322
neutron reactions (n,γ) with, gamma spectra of, (E), 20: 39470(R) (ORNL-3924)
proton reactions (p,n) at 3.0 to 5.8 Mev, strength functions for, (E), 20: 39470(R) (ORNL-3924)

TIN ISOTOPES Sn-120
neutron reactions with, strong p-wave resonances from, (E), 20: 39470(R) (ORNL-3924)
neutron reactions (n,γ) with, gamma spectra of, (E), 20: 39470(R) (ORNL-3924)

TIN ISOTOPES Sn-122
neutron reactions (n,γ) with, gamma spectra of, (E), 20: 39470(R) (ORNL-3924)

TIN ISOTOPES Sn-124
neutron reactions with, strong p-wave resonances from, (E), 20: 39470(R) (ORNL-3924)
neutron reactions (n,γ) with, gamma spectra of, (E), 20: 39470(R) (ORNL-3924)

TISSUE CULTURES
neutron dosimetry in, using ionization detectors, 20: 39227
neutron dosimetry in, methods for, 20: 39228
radiation effects on ribonucleic acid metabolism in HeLa cells in, γ, 20: 38683
radiation effects on mammalian cells in, effects of metabolic inhibitors on x, 20: 38710
radiosensitivity of carcinoma cells in, 20: 38635
respiration of Ascites tumor cells in, 20: 38599 (TID-22968)

TISSUE TRANSPLANTS
radiation effects on growth of hematopoietic cell, in mice, 20: 38592 (ORNL-P-2158)
radiation effects on immune reactions to, 20: 38612

TISSUES
biogenesis and metabolism of steroids in elderly men, tracer study on, 20: 38547(R) (NYO-918-15)
changes in local, in acute radiation sickness, 20: 38774
radiation dose distribution in, effects of bone dimensions on, 20: 38791
radiation injuries of, in children treated for hemangiomas by radium, 20: 38787

TITANIUM
content in fallout from Chinese atomic test, Oct. 1964, 20: 39110
determination in organic coating pigments, activation, 20: 38853
effects on properties of boron steel, 20: 39426
evaporative lifetime on tungsten and oxygenated tungsten from 1250 to 1750°K, (E), 20: 40307
solubility in cobalt–tungsten carbide systems, chemical determination of, 20: 39427
superconductivity of, 20: 40047

TITANIUM ALLOYS
Be–Ti–V, performance in niobium alloy brazing, 20: 39365
Cr–Ti, performance in niobium alloy brazing, 20: 39365
Mo–Nb–Ti–U–Zr, mechanical properties of high-strength uranium-base, 20: 39440(P)
Ti–V, superconductivity, 20: 40047

TITANIUM CARBIDES
elastic properties of stoichiometric, 20: 39430
Cr_2C_3–TiC–WC, preparation and properties of, 20: 39431
graphite–TiC, fabrication and mechanical properties of, 20: 39367
TiC–WC, properties of, effects of chromium carbide additions on, 20: 39431

TITANIUM HYDRIDES
neutron reactions at 0.025 to 0.4 ev, total cross sections for, (E), 20: 40069(R) (EANDC(E)-66(U))

TITANIUM OXIDES
effects on gas diffusion and sintered density in thoria and urania, 20: 39381 (AECL-2585)
exchange capacity of, for cesium and strontium ions, 20: 39002
Nb_2O_5–TiO_2, phase diagrams, 20: 39411

TITANIUM STEEL
Cr–Mo–Ti, corrosion and mass transfer in flowing sodium, 20: 39345 (GEAP-4831)

TOBACCO
analysis for trace elements in mosaic virus and nucleic acids in, activation, 20: 38846

TOXINS
effects of *E. coli*, on blood coagulation time in guinea pigs, 20: 38656
radioinduced, in animals and plants, 20: 38664
radiosensitivity effects in mice, x, 20: 38715

TRACER TECHNIQUES
use in industry in Poland, 20: 39290
TRACER TECHNIQUES (BIOLOGY)
for determination of iodoamino-acid content in rat blood, 20: 38561
myometrial blood flow measurement, xenon-133, 20: 38747
nucleic acid synthesis in animals, phosphorus-32 studies of, 20: 38585
use for study of DTPA excretion in rats, 20: 38556
use for study of trace element adsorption and elution on hair, 20: 38543
TRACER TECHNIQUES (GEOLOGY)
tracer choice for ground water research, 20: 39155
TRACER TECHNIQUES (MEDICINE)
for thyroid weight determination, 20: 38789
measurement of deposited radioisotopes in man, 20: 38770
TRACER TECHNIQUES (METALLURGY)
beta/gamma ratio measurements in, for diffusion studies, 20: 39336
bromine-82 sorption by nickel sheets, diffusion measurements from, 20: 39337
TRACER TECHNIQUES (METEOROLOGY)
use of krypton-85 in atmospheric diffusion studies, 20: 39105
TRADESCANTIA
radiation effects on mitosis in cells of, microbeam uv, 20: 38614
radiosensitivity of embryonic tissues of, 20: 38588(R) (COO-1400-10)
TRAMEX PROCESS
pulse columns for, testing of, 20: 38998(R) (ORNL-3958)
TRANSCURIUM ELEMENTS
properties of $Z > 110$, 20: 40145
TRANSISTORS
design and properties for use in power plants, 20: 40451
radiation effects on insulated gate field effect MOS, x, 20: 39273(R) (AD-635198)
TRANSITION METALS
chemical properties of, in solution, 20: 38873(R) (NYO-2269-9)
cyanides of, review on preparation, properties, and structure of, 20: 38881
magnetic moment distributions in iron, neutron-diffraction study of, (T), 20: 40330
TRANSURANIC ELEMENTS
existence of natural, 20: 39116
production in reactors, 20: 39315 (DP-1066(Vol.1), pp I.29-52)
properties and synthesis of, lectures on, 20: 40139
properties and synthesis of, review of, 20: 40140
synthesis in stars, 20: 40144
synthesis of, method for, 20: 40141
TRAPS
design of nitrogen-cooled, for helium-3 purification, 20: 39504
TRAUMA
effects on survival of mice, effects of 19-nor-testosterone phenylpropionate on, 20: 38610
TREES
radioinduced chromosome aberrations in rootlets of apple, fast neutron and γ, 20: 38692
TRIETHYLAMINE
trichloro-, effect on permeability of blood-brain barrier in rats, 20: 38609
TRIETHYLENETETRAMINE
complexes with cobalt, radiation effects on, annealing of recoil damage in neutron, 20: 38965
TRINONYLAMINE
solvent properties for protactinium, 20: 39003
TRIOCTYLAMINE
sulfate, analysis of solutions of, for uranium, spectrophotometric, 20: 38809
TRIOXANES
radioinduced polymerization of, in presence of maleic anhydride, gamma and uv, 20: 38953
TRITIUM
determination of, in proportional counter, simultaneously with carbon-14, 20: 38823
deuteron reactions (d,n) up to 100 kev, yields of, (E), 20: 40078 (NP-16203)
effects of incorporated, on cell nuclei, 20: 38624
effects of incorporated, on chromosome aberrations in animal cells, 20: 38649
effects of, on sodium methoxide-promoted elimination reaction of 2,2-diphenylethyl benzenesulfonate, 20: 38912
handling of accelerator targets of, use of glove boxes for, 20: 39476 (AD-636185)
incorporation in steroids, 20: 38547(R) (NYO-918-15)
origin in hydrothermal solutions, 20: 39132
RBE of beta particles from, 20: 38624
reactions of electron-excited atoms of, with solid propane and propene, 20: 38970
for well logging, 20: 39137(P)
viscosity of molecular, saturated-liquid, 20: 39940
TRITONS
production in proton reactions with beryllium and platinum at 2.9 Bev, (E), 20: 39794
reactions (t,p) with oxygen-18, spectroscopic factors of, (T), 20: 40126
reactions (t,p) with oxygen-17 at 12 Mev, oxygen-19 energy levels from, (E), 20: 40161
TRYPTOPHAN
effects of absence of, on nucleic acid and protein synthesis in uv-irradiated *E. coli*, 20: 38562
radiolysis of, in aqueous solution, γ, 20: 38582
TUBES
boiling burnout in, with circumferential heat flux tilt, 20: 39046 (AEEW-R-477)
deformation of composite, computer program for, 20: 39394 (GEMP-415)
fabrication of low-permeability carbon, 20: 39369(P)
gamma radiation streaming through shelter air, review of, 20: 39060
hydridation of zirconium alloy, effects of carbon tetrachloride on high-temperature, 20: 39360 (TRG-Report-1255)
particle deposition and reentrainment in long vertical, 20: 39103(R) (BNWL-235-3, pp 51-69)
shock wave propagation in, 20: 39072
thermal effects on oxidized Zircaloy-2, with aluminum cladding, 20: 39380 (AECL-2570)
TUMORS
dose calculations for radiotherapy of, source distances from, 20: 38750
radiation effects on metabolism of cells of Ascites, x, 20: 38599 (TID-22968)
radiation effects on mouse, combined with vincaleucoblastine, x, 20: 38613
radiation effects on cells of, mechanism of action for, 20: 38616
radiation effects on growth of injected lymphoma cells in mice, x, 20: 38699
radiation effects on experimental and human malignant, laser, 20: 38780
radioapplicator for radium therapy of lower lip cancer, 20: 38752
radioinduced, after radium treatment of hemangiomas, 20: 38787
radiosensitivity of malignant melanomas, x, 20: 38764
radiosensitivity of various malignant bone, 20: 38784
radiotherapy and surgical treatment of laryngeal cancer, x, 20: 38782
radiotherapy in conjunction with surgery for lung, 20: 38755
radiotherapy of hemangiomas in children, use of radium for, 20: 38787
radiotherapy of laryngeal, late pathological effects of γ, 20: 38773
radiotherapy of malignant, effects on hematopoietic system, 20: 38766
radiotherapy of pituitary, dosimetry of x for, 20: 38761
radiotherapy of stomach, 20: 38772
radiotherapy of uterine, statistical analysis of injuries following, 20: 38754
radiotherapy of, late pathological effects of γ, 20: 38773
radiotherapy of, using combination of orthovoltage x radiation and cobalt-60, economics and effectiveness of, 20: 38792
TUNGSTEN
bulk modulus to 500°C, adiabatic, (E), 20: 39418
deposition of coatings of, by chloride and fluoride reduction using hydrogen, 20: 39354 (BMWF-FBK-66-09)
deuterium ion reactions at 28 kev, sputtering from, 20: 39581(R) (ORNL-3989, pp 134)
ductility of, effects of orientation on, 20: 39397 (NASA-TM-X-1252)
effects on properties of boron steel, 20: 39426
electric discharge explosion of wires of, MHD instabilities in, 20: 39010
electron emission from planar monocrystalline, work function for, 20: 39635 (UCRL-16699)
electron emission in MHD generators from electrodes of, (E), 20: 39736
electron emission from barium- and cesium-adsorbed, models for, 20: 39641
electron emission from filaments of, surface micropatch effects on, 20: 39642
evaporative lifetimes of metals on ribbon filaments of, at 1250 to 1750°K, (E), 20: 40307
extrusion of sintered billets of, high-energy-rate equipment and methods for, 20: 39352 (BM-RI-6817)
grain structure of, effects alloying elements and refractory additions on, 20: 39400 (NASA-TN-D-3531)
mechanical properties of composites of, with glass, 20: 39405 (UCRL-16844)
oxidation of, effects of fluoride coating on, 20: 39348
permeability to hydrogen, 20: 39098(R) (WERL-2823-21)
preparation and chemical properties of beta-phase, 20: 39412
production of high-quality sheet, panel summary on, 20: 39357 (MAB-212A-M)
reactions with combustion gas species in launch pad abort environments, 20: 39312 (SC-CR-66-2044)
sintering of, mass spectrometric studies of admixtures and impurities in,

20: 39363
solvent properties for nitrogen, 20: 39098(R) (WERL-2823-21)
superconductivity of, 20: 40047
thermoelectric properties, 20: 39353 (BMWF-FBK-66-07)
TUNGSTEN ALLOYS
Cr–Co–Fe–Mn–Ni–W, tensile properties of L-605, effects of cold deformation on, 20: 39399 (NASA-TN-D-3528)
Hf–Nb–W–Y, properties for high-temperature service, 20: 39445(P)
Hf–Nb–W–Y, weldability evaluation of, 20: 39366
Hf–Ta–W, weldability evaluation of, 20: 39366
Hf–W, work function for, 20: 40297
Nb–Ta–W–Zr, weldability evaluation of, 20: 39366
Nb–W–Zr, weldability evaluation of, 20: 39366
Re–W, work function for, 20: 40297
Ta–W, reactions with combustion gas species in launch pad abort environments, 20: 39312 (SC-CR-66-2044)
TUNGSTEN CARBIDES
elastic properties of stoichiometric, 20: 39430
Co–Wc, phases in, determination by chemical analysis, 20: 39427
Cr_2C_3–TiC–WC, preparation and properties of, 20: 39431
graphite–WC, fabrication and physical properties of, 20: 39367
Hf–Ta–Wc, preparation and properties of dispersion-hardened, 20: 39441(P)
Ta–Wc–Zr, preparation and properties of dispersion-hardened, 20: 39441(P)
TiC–WC, properties of, effects of chromium carbide additions on, 20: 39431
TUNGSTEN CHLORIDES
reduction for coating deposition using hydrogen, 20: 39354 (BMWF-FBK-66-09)
TUNGSTEN FLUORIDES
molecular structure of, mean amplitudes of vibration at 0 and 298°K in, 20: 38897
reduction for coating deposition using hydrogen, 20: 39354 (BMWF-FBK-66-09)
TUNGSTEN ISOTOPES W-180
neutron reactions at 0.1 to 400 ev, resonance parameters from, (E), 20: 39470(R) (ORNL-3924)
TUNGSTEN ISOTOPES W-182
energy levels at 1.289 and 1.554 Mev, lifetimes of, (E), 20: 40094
neutron reactions with, resonance parameters from, (E), 20: 39470(R) (ORNL-3924)
TUNGSTEN ISOTOPES W-183
energy-level transitions, (E), 20: 40123
neutron reactions with, resonance parameters from, (E), 20: 39470(R) (ORNL-3924)
neutron reactions (n,γ) with, energy levels from, (E), 20: 39470(R) (ORNL-3924)
TUNGSTEN ISOTOPES W-184
neutron reactions with, resonance parameters from, (E), 20: 39470(R) (ORNL-3924)
neutron reactions (n,γ) with, energy levels from, (E), 20: 39470(R) (ORNL-3924)
TUNGSTEN ISOTOPES W-185
neutron reactions (n,γ) with, energy levels from, (E), 20: 39470(R) (ORNL-3924)
TUNGSTEN ISOTOPES W-186
neutron reactions with, resonance parameters from, (E), 20: 39470(R) (ORNL-3924)
TUNGSTEN ISOTOPES W-187
neutron reactions (n,γ) with, energy levels from, (E), 20: 39470(R) (ORNL-3924)
TUNGSTEN SYSTEMS
Al_2O_3–W, phase diagrams, 20: 39437
W–Y_2O_3, phase diagrams, 20: 39437
TURBINES
design for fast-breeder reactors, 20: 40413 (TID-23257(Vol.1))
design of helical-screw, for space applications, 20: 39026 (UCRL-14660(Rev.1))
development of potassium vapor, for space applications, 20: 39028
shaft-bearing system dynamics for MRP Combined Rotating Unit, analog study, 20: 39022 (NAA-SR-11943)
TYROSINE
preparation of iodine-131-labeled, method for, 20: 38992
radiolysis of, in aqueous solution, γ, 20: 38582
use of, in decreasing iodine-131 in thyroid gland, 20: 38733
TYROSINE, IODO-
content in rat blood, tracer study using iodine-129 and iodine-131, 20: 38561

U

ULTRASONICS
absorption in superconductors, 20: 40336(T)
ULTRAVIOLET RADIATION
dose measurement of, using photostimulated polarization transients in zinc sulfide, (E), 20: 40333
effects on bacteria, biological, effects of acriflavine on, 20: 38611
effects on cytolytic and transforming abilities of Polyoma virus, 20: 38702
effects on DNA, 20: 38542(T) (UCRL-Trans-10029)
effects on *E. coli* cultures, synthesis of nucleic acids and proteins in absence of an essential amino acid following, 20: 38562
effects on *E. coli* cultures, survival difference with chloramphenicol and without an essential metabolite, 20: 38563
effects on *E. coli*, genetic, 20: 38620
effects on *E. coli*, genetic, effects of genetic factors on, 20: 38621
effects on *E. coli*, action spectra for photoreactivation of, 20: 38669
effects on electric conductivity of *n*-hexane, 20: 38971
effects on infectivity of viruses, 20: 38707
effects on maize, genetic, 20: 38617
effects on *Micrococcus lysodeikticus*, lethal and mutagenic, 20: 38574(R) (NYO-3449-1)
effects on mitosis in Tradescantia cells, use of microbeam, 20: 38614
effects on phage κ of *Serratia marcescens* in producing various mutations, 20: 38670
effects on plant embryos, biological, 20: 38588(R) (COO-1400-10)
effects on polymerization of cyclic ethers, 20: 38953
effects on tobacco mosaic virus inactivation, mechanisms for, 20: 38584
effects on T1 bacteriophage substituted with iodouracil, 20: 38704
ULTRAVIOLET SOURCES
design for vacuum photochemical studies, 20: 38941(R) (RRL-2310-182)
UNDERGROUND EXPLOSIONS
seismic data from RED HOT, long-range, 20: 39124 (AD-632957)
UNDERGROUND STRUCTURES
design of protective, effects of soil dynamics on, 20: 39070
foundations for protective, design of, 20: 39068
use as shelters in Germany, 20: 39078
UNDERWATER EXPLOSIONS
seismic wave detection of nuclear, instrumentation for, 20: 39134
UNITED STATES
fallout monitoring guides for cesium-137, iodine-131, strontium-89, and strontium-90, 20: 38743
URACIL
effects of absence of, on nucleic acid synthesis in *E. coli*, 20: 38562
effects of absence of, on survival of a uv-irradiated uracil-requiring strain of *E. coli*, 20: 38563
URACIL, 5-BROMO-
radiolysis of, under nitrogen, nitrous oxide, and oxygen, kinetic study of gamma, 20: 38968
radiosensitivity effects on bacteriophage, x, 20: 38712
radiosensitivity effects of, on living cells, 20: 38968
URACIL, 5-FLUORO-
effects on DNA-ase and RNA-ase activity in Ehrlich ascites cells, 20: 38578
radiosensitivity effects on cultured mammalian cells, x, 20: 38710
URACIL, 5-IODO-
photochemistry of, 20: 38704
radiation effects on T1 bacteriophage substituted with, uv, 20: 38704
URACIL, 2-THIO-
effects on iodine-131 uptake and elimination by thyroid in dogs, mice, and rats, 20: 38734
URANIN
methylene blue–uranin, particle deposition and reentrainment in long vertical tubes, 20: 39103(R) (BNWL-235-3, pp 51-69)
methylene blue–uranin, use of solutions of, in aerosol generators, 20: 39103(R) (BNWL-235-3, pp 51-69)
URANINITES
age of, in Sweden, 20: 39125
oxidation rate of uranium-234 and uranium-238 in, 20: 38894
URANITES
oxidation rate of uranium-234 and uranium-238 in black, 20: 38894
URANIUM
content in diet, effects on carcinoma incidence in human populations, 20: 38739
content in minerals in Sweden, 20: 39125
content in soils, effect on radioactivity levels in air, 20: 39114
creep mechanisms of, literature survey on, 20: 39410
crystal structure of, valence electrons and interatomic bonds in, 20: 40296
determination in thorium minerals, 20: 39143
determination in tri-*n*-octylamine sulfate solutions, spectrophotometric, 20: 38809
emission of atomic, from uranium dioxide and metal by fission fragments, 20: 38994(R) (AE-232)

fission-product activities in irradiated, computer program for calculation of, 20: 40070 (IEA-111)
leaching from carbon-coated uranium dicarbide beads by hydrochloric acid at 1600 to 2100°C, 20: 39346 (LA-3488)
machining of, power requirement for tools for, 20: 39027 (Y-DA-1287)
phase studies, 20: 39388 (CEA-R-2956)
phase transformations, effect of pressure and irradiation on solid-solid, (E), 20: 40306
preparation of billets of, by metallic reduction of uranium(IV) fluoride, 20: 39342(P)
properties of, at low temperatures, 20: 39448 (AERE-X-PR-2596-9)
radioinduced swelling of, relations with creep mechanisms of, 20: 39410
resources of natural, long-term requirements for, 20: 39101
rolling, drilling, and machining of, 20: 38799(R) (NLCO-980)
separation from cesium by ion exchange on zirconium phosphate gels, 20: 38994(R) (AE-232)
separation from elements and fission products, combined ion exchange-solvent extraction method for, 20: 38999 (TID-23229)
separation from fission products, freezing method for, 20: 38994(R) (AE-232)
separation of thorium-230 from, by ion exchange, 20: 38834
superconductivity of, 20: 40047
use prediction for, 20: 39145
vaporization of, thermodynamics of, 20: 38876 (UJV-1598)

URANIUM ALLOYS
phase studies of weakly alloyed, 20: 39388 (CEA-R-2956)
Al–U, production of intermetallic compound, by direct reduction of uranium tetrafluoride, 20: 39333
Cr–U, phase studies of uranium-base, 20: 39388 (CEA-R-2956)
Fe–U, phase studies of uranium-base, 20: 39388 (CEA-R-2956)
Mo–Nb–Ti–U–Zr, mechanical properties of high-strength uranium-base, 20: 39440(P)
Mo–U, analysis for carbon, coulometric, 20: 38796 (CEA-R-2968)
Mo–U, phase studies of uranium-base, 20: 39388 (CEA-R-2956)
Mo–U, phase transformations in, effects of lattice orientation on, 20: 39389 (CEA-R-2973)
Pu–U, irradiation testing of fuels of, 20: 40384(R) (EURAEC-1660)
U–Zr, cladding with Zircaloy-2, bonding mechanisms in, 20: 39361 (WAPD-305)
U–Zr, phase studies of uranium-base, 20: 39388 (CEA-R-2956)

URANIUM(IV) BROMIDES
reactions with ammonia at 20 to 700°C, products formed in, 20: 38920

URANIUM CARBIDES
corrosion of carbon-coated, by hydrochloric acid at 1600 to 2100°C, 20: 39346 (LA-3488)
crystal structure of, effects of nitrogen and oxygen on, 20: 39385 (CEA-R-2852)
fabrication of carbon-coated particulate, matrix materials for electron-emitting, 20: 39353 (BMWF-FBK-66-07)
preparation of carbide-coated, for reactor fuels, 20: 40395(P)
ThC_2–UC_2, irradiation testing of fuels of, 20: 40385 (ORNL-P-2327)
ThC_2–UC_2, processing reactor fuels of, grind-leach method for, 20: 38998(R) (ORNL-3958)
ThC–UC, reprocessing of fuel elements of, head-end treatment for, 20: 40390
U–UC, phase studies, 20: 39385(CEA-R-2852)

URANIUM(IV) CHLORIDES
reactions with ammonia at 20 to 700°C, products formed in, 20: 38920

URANIUM COMPLEXES
with dipentyl pentylphosphonate, spectra of, infrared, 20: 38799(R) (NLCO-980)
with mixed β-diketones in benzene solution, 20: 38855 (BNL-10350)
with nitrilotriacetic acid and polyamino polycarbooxylic acids, formation of, biamperometric studies of, 20: 38810

URANIUM FLUORIDES
molecular structure of, mean amplitudes of vibration at 0 and 298°K in, 20: 38897

URANIUM(IV) FLUORIDES
reduction to aluminum–uranium intermetallic compounds using aluminum, 20: 39333
reduction to metal using calcium or magnesium, 20: 39342(P)

URANIUM IONS
reduction of, in hydrochloric acid and potassium chloride solutions, polarographic, 20: 38922

URANIUM ISOTOPES
preparation for use as alpha source, 20: 38990
radioactive equilibrium of, in nature, 20: 39143

URANIUM ISOTOPES U-233
radiation effects on, self, 20: 39448 (AERE-X-PR-2596-9)
radiation effects on low-temperature electric conductivity of, self, 20: 39448 (AERE-X-PR-2596-9)

URANIUM ISOTOPES U-234
abundance in natural waters and carbonate deposits, 20: 39120
content ratio to uranium-238 in sea water, 20: 39133
distribution in soils, 20: 39144
oxidation rate of, compared with uranium-238 in minerals, 20: 38894
use in age estimation, 20: 39120

URANIUM ISOTOPES U-235
content in minerals in Sweden, 20: 39125
determination in fuels by gamma scintillation, tester for, 20: 39335
neutron fission of, time of emission and yield of x radiation from thermal, (E), 20: 40158

URANIUM ISOTOPES U-238
content in minerals in Sweden, 20: 39125
content ratio to uranium-234 in sea water, 20: 39133
deuteron reactions with, production of isomeric neptunium-236 in, (E), 20: 40092
distribution in soils, 20: 39144
neon-22 reactions with, fermium-256 production from, 20: 40142
neutron reactions at 7.5 to 30 kev, effective cross sections for, (E), 20: 40069(R) (EANDC(E)-66(U))
oxidation rate of, compared with uranium-234 in minerals, 20: 38894
use in fission-track dating of natural glass, 20: 39135

URANIUM MINERALS
analysis for thorium, 20: 39143

URANIUM NITRIDES
production by reactions between ammonia and uranium tetrabromide and tetrachloride at 20 to 700°C, 20: 38920

URANIUM ORES
age of Swedish, 20: 39125
age of Swedish, 20: 39126

URANIUM(IV) OXIDES
coating with beryllia, 20: 39370(P)
defects in sintered, effects of titania additions on, 20: 39381 (AECL-2585)
density of sintered, effects of titania on, 20: 39381 (AECL-2585)
diffusion of gases from irradiated, effects of titania additions on, 20: 39381 (AECL-2585)
emission of atomic uranium from, by fission fragments, 20: 38994(R) (AE-232)
fabrication of high-density sintered compacts of, 20: 39373(P)
fabrication of metal-coated particulate, matrix materials for electron-emitting, 20: 39353 (BMWF-FBK-66-07)
irradiation testing of reactor fuels of, 20: 40385 (ORNL-P-2327)
preparation of microspheres of, sol-gel process for, 20: 38998(R) (ORNL-3958)
preparation of spheroids of, by vibratory abrasion, 20: 39376(P)
processing metal-clad fuels of, temperatures in shear-leach method for, 20: 38998(R) (ORNL-3958)
properties and structure of precipitates and sols of hydrous, 20: 39401 (ORNL-3963)
radiation effects on gas release from, 20: 39449 (BNWL-SA-272)
radiation effects on thermal conductivity of dense pellets and rods of, 20: 39456 (GEAP-5100-1)
radiation effects on niobium oxide-doped, in-reactor, 20: 39447 (AECL-2581)
radiation effects on yttria-doped, in-reactor, 20: 39447 (AECL-2581)
radiation effects on, in-reactor, 20: 39447 (AECL-2581)
sintering of, oxidizing effects of impurities on, 20: 39390 (CEA-R-3003)
thermal conductivity of, 20: 39403 (ORNL-TM-1450)
thermal conductivity during irradiation, effects of density and grain size on, 20: 39446 (AECL-2564)
B_4C–UO_2, radiation effects on boron migration in, 20: 40382(R) (CEND-3107-267)
Eu_2O_3–UO_2, phase diagrams, 20: 39437
HfO_2–UO_2, preparation of sols of, 20: 39442(P)
Mo–UO_2, chemical reactions of tungsten coated at 1800°C, 20: 39383 (BMWF-FBK-66-08)
PuO_2–UO_2, phase diagrams, 20: 39393 (GEAP-4878)
rare earth oxides–UO_2, preparation of sols of, 20: 39341(P)
stainless steel–UO_2, fission-induced failure model for, 20: 39459 (TRG-Report-1278)
ThO_2–UO_2, irradiation testing of fuels of, 20: 40385 (ORNL-P-2327)
ThO_2–UO_2, preparation by sol-gel process, 20: 40391
ThO_2–UO_2, properties of sintered, 20: 39006
UO_2–ZrO_2, preparation of sols of, 20: 39442(P)

URANIUM OXYSULFIDES
formation of, 20: 38891

URANIUM PHOSPHIDES
crystal structure and magnetic properties of mono-, 20: 39422

URANIUM RESERVES
data on, review of, 20: 39101
use prediction for, 20: 39145

URANIUM SELENIDES

preparation, properties, and uses of, book on, 20: 38927

URANIUM SILICIDES
phase studies, 20: 39388 (CEA-R-2956)

URANIUM SYSTEMS
C–N–O–U, crystal structure of solid-solutions, 20: 39385 (CEA-R-2852)
C–Si–U, phase studies of, at room temperature, 20: 39413
U–UC, phase studies, 20: 39385 (CEA-R-2852)

URANIUM TELLURIDES
preparation, properties, and uses of, book on, 20: 38927

URANYL COMPOUNDS
use as photosensitizer for polymerization of methyl methacrylate at various pH's, 20: 38934

URANYL IONS
reduction of, in hydrochloric acid, effects of thymol and gelatin on polarographic, 20: 38922

URANYL NITRATES
fuel fabrication from high enrichment solutions, 20: 40419
$BaCl_2$–Na_2CO_3–$UO_2(NO_3)_2$, uranium precipitation in, mechanism of, 20: 38928
$CaCl_2$–Na_2CO_3–$UO_2(NO_3)_2$, uranium precipitation in, mechanism of, 20: 38928
HNO_3–$UO_2(NO_3)_2$–H_2O, phase diagram, 20: 38994(R) (AE-232)
$MgCl_2$–Na_2CO_3–$UO_2(NO_3)_2$, uranium precipitation in, mechanism of, 20: 38928
Na_2CO_3–$SrCl_2$–$UO_2(NO_3)_2$, uranium precipitation in, mechanism of, 20: 38928
$Th(NO_3)_4$–$UO_2(NO_3)_2$, fuel fabrication from high enrichment solutions, 20: 40419

UREA, SELENO-
preparation of selenium-75-labeled, activation method for, 20: 38991
radiolysis of selenium-75-labeled, 20: 38991

URETER
radiation dosage to, measurement during radiotherapy, 20: 38778

URIDINE
distribution of tritiated in gamma irradiated HeLa cells, 20: 38683

URINE
analysis for steroids, using paper chromatography, 20: 38547(R) (NYO-918-15)
cesium-137 and strontium-90 content in, of healthy Italian children, 20: 39152
content of carbon-14, zinc, and zinc-65 in rat, after injection of ^{65}Zn–DTPA–^{14}C, 20: 38556
radiation effects on excretion and production of cortisols in guinea pig, 20: 38547(R) (NYO-918-15)

UROKON
labeling with iodine-131, 20: 38932

UTERUS
radiotherapy for cancer of, statistical analysis of complications following, 20: 38754
radiotherapy of a cervical carcinoma in a pregnant, 20: 38759
radiotherapy of carcinoma of, nursing care during radium, 20: 38751
radiotherapy of carcinomas of, x, 20: 38786
radiotherapy of cervical cancers, effects on cellular composition of tissues, 20: 38769

V

VACCINES
radiation effects on response of rabbits to typhoid, x, 20: 38641

VACUUM GAGES
design, 20: 39187

VACUUM PUMPS
design and operation of pump-leak detection system, 20: 39096 (AECD-EP-11)

VACUUM SYSTEMS
design for chalice, 20: 40178(R) (SIT-2582-19)
development of ultrahigh, 20: 39098(R) (WERL-2823-21)
performance determination of, techniques for, 20: 39097(R) (ORNL-3989, pp 128-33)

VAGINA
radioinduced injury to, following therapy of cervical cancer, 20: 38751

VALVES
design for pulsed gas, 20: 40246
design of ventilation, for blast shelters, 20: 39073

VAN ALLEN RADIATION BELTS
charged particle flux in inver, Dec. 19, 1961, (E), 20: 39992
composition of, review of, 20: 39957(T)
electron energy distribution and flux in lower edge of inner, (E), 20: 39983
electron origin in, trapped, 20: 39957(T)
origin of trapped protons in, 20: 39957(T)
proton energy and spatial distributions in, 20: 39957(T)
proton flux in lower edge of inner, (E), 20: 39983
proton flux in, ring current effects on, 20: 39970
radiation dose from, minimizing, 20: 39158
stability of outer, kinetic, 20: 39964(T)

VAN DE GRAAFF ACCELERATORS
development status of ORNL, report on, 20: 39470(R) (ORNL-3924)
ion source for, negative, 20: 39500
properties of, for use in food sterilization studies, 20: 39303

VANADIUM
determination in biological materials and drinking water, activation, 20: 38565
determination of traces of, in biological materials, activation, 20: 38837
effect on properties of low-alloy steels for reactor pressure vessels, 20: 394..4(P)
effects on properties of boron steel, 20: 39426
neutron reactions at 18 to 220 kev, total cross sections for, (E), 20: 40069(R) (EANDC(E)-66(U))
neutron reactions at 21.65 to 152.6 kev, resonance parameters for, (E), 20: 40069(R) (EANDC(E)-66(U))
superconductivity of, 20: 40047

VANADIUM ALLOYS
Be–Ti–V, performance in niobium alloy brazing, 20: 39365
Ga–V, effects of orbital field on Fulde-Ferrell state in, 20: 40046
Mo–Nb–V–Zr, weldability evaluation of, 20: 39366
Nb–V, radioinduced twinning in, neutron, 20: 39462
Ti–V, superconductivity, 20: 40047

VANADIUM CARBIDES
elastic properties of stoichiometric, 20: 39430
graphite–VC, fabrication and physical properties of, 20: 39367

VANADIUM COMPOUNDS
use as photosensitizer for polymerization of methyl methacrylate at various pH's, 20: 38934

VANADIUM ISOTOPES V-48
spin measurement and shell-model calculations, (E/T), 20: 40154

VANADIUM ISOTOPES V-51
neutron reactions (n,γ) with, resonance activation integral cross sections for, (E), 20: 40069(R) (EANDC(E)-66(U))

VELA PROJECT
seismic data from RED HOT, long-range, 20: 39124 (AD-632957)

VENTILATION
development of systems of, for protective shelters, 20: 39074
valves for blast shelter systems, 20: 39073

VERMICULITES
diffusion of sodium in, self-, 20: 38858 (BNWL-235-3, pp 23-51)

VINCALEUKOBLASTINE
effects of, combined with x radiation on tumors in mice, 20: 38613

VINYL COMPOUNDS
acrylic monomers–aromatic vinyl monomers–polyisobutylene, radioinduced formation of thermoplastic resin of, 20: 38978(P)

VINYL RADICALS
spectra of carbon-13-labeled, ESR, 20: 38941(R) (RRL-2310-182)

VIRUSES
analysis for trace elements in tobacco mosaic, activation, 20: 38846
radiation effects in inactivation of tobacco mosaic, mechanism for uv, 20: 38584
radiation effects on interactions of Polyoma, with mouse embryo cells, 20: 38702
radiation effects on infectivity of Newcastle disease and Rous sarcoma, uv, 20: 38707

VISCOMETERS
calibration of oscillating bob, at room temperature, 20: 38871(R) (NYO-1769-54)
design for measurements on molten salts at high pressure and temperature, 20: 38871(R) (NYO-1769-54)
design of oscillating sphere, for transport studies in molten salts, 20: 38872(R) (NYO-1769-68)
design of vertically oscillating cylinder, for transport studies in molten salts, 20: 38872(R) (NYO-1769-68)
design of, for use at high pressures and temperatures, 20: 38872(R) (NYO-1769-68)

VISION
radiation effects on rabbit, x, 20: 38689

VITAMIN B
radiation effects on, biological and chemical, γ, 20: 38580

VITAMIN B_1
effects on radiation resistance in rats, dietary, 20: 38721

VITAMIN B_2
effects on radiation resistance in rats, dietary, 20: 38721

VITAMIN C
radiation effects on concentration of, in potato tubers, x, 20: 38690

VITAMIN E
effects on enzyme release from x irradiated lysosomes in rat liver, 20: 38577

VITAMINS
radiation effects on content in oysters, γ, 20: 39288(R) (ORO-636)
VOLTMETERS
design for photographic film reader, 20: 39258

W

WASTE DISPOSAL
book: *The Management of Radioactive Wastes Produced by Radioisotope Users*, 20: 40480 (STI-PUB-119)
in radioisotope hospital wards, 20: 38790
in streams, monitoring of, 20: 38742
methods for, at Shippingport Atomic Power Station, 20: 40481 (WAPD-T-1851)
public health hazards of pond storage of calcined highly active wastes, 20: 40482
WASTE PROCESSING
book: *The Management of Radioactive Wastes Produced by Radioisotope Users*, 20: 40480 (STI-PUB-119)
calcination and solidification of Purex solutions, pilot plant studies on, 20: 40476(R) (BNWL-267)
calcination, public health aspects, 20: 40482
facilities and equipment for, at Shippingport Atomic Power Station, 20: 40481 (WAPD-T-1851)
fixation in glass, properties of input melts for, 20: 40476(R) (BNWL-267)
fixation in glasses by calcination, efficiency of, 20: 38998(R) (ORNL-3958)
method of, for low-level radionuclide separation, 20: 40483
solidification, equipment and methods for, 20: 40477 (HW-80056)
WASTE SOLUTIONS
analysis for sulfur in solid, by combustion and colorimetry, 20: 38795 (BNWL-265)
concentration of intermediate-level, using finned circulator-evaporator, 20: 40477 (HW-80056)
determination of, by aerobic treatment, 20: 40483
dilution and dispersal in Clinch River, 20: 40479 (ORNL-P-2328)
handling and storage of demineralizer-resin slurries, 20: 40481 (WAPD-T-1851)
WATER
analysis for alkali and alkaline earth metals in mineral, flame photometric, 20: 38798 (NIJS-R-465)
analysis for corrosives and solids in swimming pool reactor coolant, activation and chemical, 20: 38800 (PAEC(C)RE-652)
boiling point and vapor pressure of, 20: 38921
content in soil, use of neutron meters in measuring, 20: 39131
determination of, in soils by neutron scattering, 20: 39141
monitoring of tap, sampling device for, 20: 39218
neutron diffusion lengths in poison-bearing, calculations using diffusion theory and transport theory, 20: 40053
neutron diffusion parameters in, measurement and calculation of, (E/T), 20: 40055
neutron inelastic scattering by, dynamic processes in slow, 20: 40338
pressure-drop flow characteristics of subcooled, at atmospheric pressure in narrow heated channels, 20: 39047 (AERE-M-1739)
radiation effects on, electron, 20: 38947
radiolysis of, free radical model for, 20: 38959
radioprotective effects of sulfurated mineral, 20: 38709
radiosensitivity effects on barley seeds, 20: 38736
reactions with heavy water, mass spectrometric determination of equilibrium constant for disproportionation, 20: 38875 (UCRL-14703-T)
relationship between tumor incidence and radium, uranium and radon content in, 20: 38739
sampling river, engineering drawings of equipment for, 20: 39185
sorption by colloidal thoria, 20: 38926
tritium origin in hydrothermal, 20: 39132
use in decontaminating protective clothing, 20: 39161
air–water, voidage measurements in upward two-phase flow through tube, 20: 39045 (AEEW-M-650)
$Ca(NO_3)_2$–H_2O, phase diagram of, 20: 38994(R) (AE-232)
Fe–H_2O, neutron flux distributions and spectra in shielding of, (E/T), 20: 40287
HNO_3–$UO_2(NO_3)_2$–H_2O, phase diagram, 20: 38994(R) (AE-232)
H_2O–D_2O, boiling temperature and vapor pressure of, 20: 38921
H_2O–D_2O, neutron diffusion parameters in, thermal, (E), 20: 40061
H_2O–D_2O, radiolysis of, isotope effects in hydrogen production in gamma, 20: 38938 (IA-1074)
H_2O–D_2O, vapor pressure of saturated salt solutions of, 20: 38994(R) (AE-232)
K_2CO_3–H_2O, phase diagram of, 20: 38994(R) (AE-232)
$LiNO_3$–H_2O, phase diagram of, 20: 38994(R) (AE-232)
Na_2CO_3–H_2O, phase diagram of, 20: 38994(R) (AE-232)
steam–H_2O, flow in radial-vane separators, 20: 39019(R) (GEAP-5149)
WATER-d_2
boiling point and vapor pressure of, 20: 38921
decomposition of, effects of air ammonia, deuterium, nitrogen, and oxygen, 20: 40409(R) (NP-16230)
neutron inelastic scattering by, dynamic processes in slow, 20: 40338
reactions with water, mass spectrometric determination of equilibrium constant for disproportionation, 20: 38875 (UCRL-14703-T)
$Ca(NO_3)_2$–D_2O, phase diagram of, 20: 38994(R) (AE-232)
H_2O–D_2O, boiling temperature and vapor pressure of, 20: 38921
H_2O–D_2O, neutron diffusion parameters in, thermal, (E), 20: 40061
H_2O–D_2O, radiolysis of, isotope effects in hydrogen production in gamma, 20: 38938 (IA-1074)
H_2O–D_2O, vapor pressure of saturated salt solutions of, 20: 38994(R) (AE-232)
K_2CO_3–D_2O, phase diagram of, 20: 38994(R) (AE-232)
$LiNO_3$–D_2O, phase diagram of, 20: 38994(R) (AE-232)
Na_2CO_3–D_2O, phase diagram of, 20: 38994(R) (AE-232)
WATER-t_2
effects of perfused, on cholesterol and fatty acid metabolism in rat liver, 20: 38559
effects on mice and rats of injected, pathological, 20: 38568
WATER COOLED REACTORS
design of water-moderated thermal, boiler- and turbine-less, 20: 40435(P)
fuel element cladding for, development of, 20: 39356(R) (GEAP-5134)
WATER MODERATED REACTORS
control rods for, performance of neutron-absorber-filled tubes as, (E/T), 20: 40381
design of water-cooled thermal, boiler- and turbine-less, 20: 40435(P)
WATER PURIFICATION EQUIPMENT
design for fast-breeder reactors, 20: 40413 (TID-23257(Vol.1))
efficiency in low-level waste treatment, 20: 40483
WATER SUPPLIES
analysis for vanadium in Swedish, activation, 20: 38565
WELDING
methods for Senn reactor pressure vessel, 20: 40417
WELDS
fatigue strength of carbon steel-to-stainless steel, 20: 39404 (SWRI-1228-4-20)
WELL LOGGING
equipment and method for neutron-gamma, 20: 39137(P)
equipment calibration and errors, 20: 39131
equipment design, 20: 39138(P)
equipment for gamma, 20: 39139(P)
equipment for neutron-gamma, for chlorine, temperature compensation circuit for, 20: 39136(P)
equipment for, cooling system for, 20: 39140(P)
WHALES
radioisotope content in, 20: 38560
WHEAT
cation metabolism in seedlings of, 20: 38548(R) (ORO-2410-1)
content of cesium-137, iodine-131, strontium-89, and strontium-90 in U. S., 1965, 20: 38743
WHISTLERS
cyclotron damping of proton, ionospheric temperature from, 20: 39972
propagation along magnetized plasma slab, effect of collisions on, (T), 20: 40196
WIGNER EFFECT
survey on, 20: 39455 (EUR-3056.e)
WIND TUNNELS
use in reactor-site gas diffusion studies, 20: 39105
WINDSCALE ADVANCED GAS COOLED REACTOR
fuel clusters for, conversion and fast fission ratios in, 20: 40399 (AEEW-M-654)
steam drum for, steady state and transient measurements, 20: 40398 (AEEW-M-631)
WOOD
methyl methacrylate–wood, radioinduced polymerization of, economics and properties of products from, 20: 39287 (KLX-1876)
WOUNDS
monitoring for plutonium, instrument for, 20: 39267
WYOMING
environmental radiation measurements in, 20: 38735(R) (NYO-1704-13)

X

X RADIATION
absorption spectra of L shell of lutetium, forbidden lines in, (E), 20: 39613
detection and measurement of, ion chamber detector for, 20: 39249(P)
detection of galactic, rocket-borne instrumentation for, 20: 39229
dose calculations for use in radiotherapy, 20: 38750

dose distribution in tissue, effects of bone dimensions on, 20: 38791
dose measurement of, using photostimulated polarization transients in zinc sulfide, (E), 20: 40333
dosimetry in chickens, lethal, 20: 38676
dosimetry in pituitary tumors, 20: 38761
dosimetry in sheep, 20: 38625
effects of medium exposure to, on chick embryo cells, 20: 38707
effects of whole-body, on ascorbic acid and glutathione content in rat brain, 20: 38679
effects of, with vincaleucoblastine on mouse tumors, synergetic, 20: 38613
effects on adrenal function in rats, whole-body, 20: 38638
effects on ammonium fluorophosphate, ESR studies of, 20: 38949
effects on astroglial cells and blood vessels in rat brain, glycogen accumulation from, 20: 38674
effects on bacteriophage, inactivating, 20: 38628
effects on bacteriophage, inactivating, 20: 38712
effects on blood serum proteins in gestating hamsters, 20: 38598(R) (TID-22955)
effects on bone marrow in rabbits, hematological, 20: 38633
effects on brain wave activity during conditioned activity of cats, 20: 38602(R) (UCLA-34P60-1)
effects on bromine-82 and chlorine-36 exchange between ethylenediamine cobalt or rhodium complexes and hydroboric or hydrochloric acids, 20: 38960
effects on cellular compostion of tissues, therapeutic doses, 20: 38769
effects on central regulation of automatic functions in rabbits, 20: 38654
effects on cesium monoiodide crystals, emf from, 20: 40335(T)
effects on chickens, biological, effects of breed on, whole-body, 20: 38677
effects on chromosomes of human lymphocytes, 20: 38615
effects on connective tissue of rabbits, effects of vasoconstricting drugs on, 20: 38640
effects on content of various lipids in rat tissues following lethal dose of, 20: 38701
effects on cytolytic and transforming abilities of Polyoma virus, 20: 38702
effects on development of barley seeds, 20: 38736
effects on DNA, 20: 38542(T) (UCRL-Trans-10029)
effects on DNA synthesis in rat tissues, 20: 38576 (TID-22103)
effects on DNA-ase and RNA-ase activity in Ehrlich ascites cells, 20: 38578
effects on dogs and rabbits, pathological, 20: 38688
effects on dogs, rats, and rabbits, protective effects of selachyl alcohol, 20: 38731
effects on Drosophila, genetic, 20: 38596(R) (SAN-590-1)
effects on Drosophila, genetic, 20: 38650
effects on Drosophila, genetic, RBE effects of fast neutrons, 20: 38645
effects on Drosophila, x, 20: 38646
effects on *E. coli*, genetic, effects of genetic factors on, 20: 38621
effects on *E. coli*, lethal, 20: 38630
effects on enzyme release from rat liver lysosomes, 20: 38577
effects on esterase content in rat blood, 20: 38682
effects on formation of organic peroxides in mice, 20: 38660
effects on fruit development in orchids, 20: 38597(R) (TID-23057)
effects on gastrointestinal tract function in rabbits, 20: 38659
effects on growth of transplanted hematopoietic cells in mice, 20: 38592 (ORNL-P-2158)
effects on growth of transplanted lymphoma cells in mice, effects of anoxia on, 20: 38699
effects on immune reactions in rabbit eyes, 20: 38608
effects on immune reactions in adrenal cortex of rabbits, 20: 38697
effects on incidence of bacteremia and hemorrhage in guinea pigs, 20: 38656
effects on insulated gate field effect MOS transistors, 20: 39273(R) (AD-635198)
effects on lipid and iodine content of rabbit blood, 20: 38652
effects on lymphatic tissue, biological, 20: 38612
effects on lymphocyte blood picture, effects of adrenaline on, 20: 38678
effects on maize, genetic, 20: 38617
effects on malignant melanomas, pre-operative, 20: 38764
effects on metabolism in Ascites tumor cells, 20: 38599 (TID-22968)
effects on mice and rats, protective effects of sodium gallate on pathological, 20: 38728
effects on mice, biological, 20: 38648
effects on mice, leukemogenic, 20: 38715
effects on mice, protective effects of drinking sulfurated mineral water, 20: 38709
effects on mice, protective effects of glycine on, 20: 38714
effects on morphology of thymus gland of animals, 20: 38685
effects on mortality of mice, rabbits, and rats, mechanism of, 20: 38666
effects on mouse populations, biological, 20: 38590(R) (NYO-1979-13)
effects on mouse skin, biological, 20: 38627
effects on nitrogen balance in mouse chimeras, 20: 38636
effects on permeability of blood-brain barrier in rats, 20: 38609
effects on plant embryos, biological, 20: 38588(R) (COO-1400-10)
effects on potassium content in blood of rabbits, 20: 38697
effects on potato chemical composition and yield, after tuber exposure, 20: 38690
effects on protein synthesis in rat tissues, 20: 38595(R) (ORO-3295-2)
effects on rabbit leukocytes, biochemical and morphological, 20: 38681
effects on rabbit liver, cytological, whole-body, 20: 38716
effects on rabbits, biochemical and hematological, effects of adrenaline on, 20: 38686
effects on rare earth ions in calcium fluorides, (E), 20: 40341
effects on rat intestine, physiological, 20: 38604
effects on rat liver mitochondria, biochemical and morphological, 20: 38639
effects on rat thymus, mitotic, 20: 38720
effects on rats, dietary effects of B group vitamins, folic acid, and phosphatide on, 20: 38721
effects on rats, hematological, 20: 38619
effects on rats, metabolic, 20: 38600(R) (TID-23034)
effects on reproductive system of queen honeybee, 20: 38631
effects on respiratory tract function in rabbits, 20: 38659
effects on response of dogs to hemorrhagic stress, 20: 38703
effects on response to bacterial antigens of rabbits, 20: 38641
effects on retina of rabbits eyes, pathological, 20: 38689
effects on skeleton of therapeutic doses of, 20: 38767
effects on spermatogenesis in *Drosophila melanogaster*, 20: 38607
effects on spin-lattice relaxation time of praseodymium ions in lanthanum chloride, 20: 40350
effects on spore germination and stability of virulence in *Ustilago avenae*, 20: 38672
effects on stimulation of solar plexus nerve ganglions, 20: 38687
effects on strontium chloride single crystals, V_k centers from, 20: 40319
effects on survival of mice, effects of 19-nor-testosterone phenyl-propionate on, 20: 38610
effects on survival of mammalian cells, effects of metabolic inhibitors on, 20: 38710
effects on taurine excretion in mice, effects of AET and cysteine on, whole-body, 20: 38717
effects on thymus in mice, metabolic, 20: 38606
effects on urinary excretion and production of cortisols in guinea pigs, 20: 38547(R) (NYO-918-15)
effects on yeast cytochrome systems, 20: 38680
effects on yttrium-doped calcium fluoride crystals, EPR of color centers from, 20: 40321
effects on 17-ketosteroid content in dog blood, whole-body, 20: 38684
emission by fission fragments from plutonium-239 and uranium-235, 20: 40158
emission from 4.0- to 6.3-Bev electrons, (E), 20: 39473
exposure of gonads during 31 Mev therapy, 20: 38746 (NYO-3364-19)
intensity in auroral zones, balloon observations of, 20: 39990
radioinduced injuries from use of, in therapy of cervical cancer, 20: 38751
radioinduced injuries following use for uterine cancer, 20: 38754
scattering of, singularities in coherent diffuse, (T), 20: 39586
spectra of, from flash discharges, (E), 20: 40233
use for therapy of stomach carcinomas, use of lead grating with, 20: 38763
use for therapy of facial tumors, absorbed dose in brain from, 20: 38765
use for therapy of uterine carcinomas, high voltage, 20: 38786
use in radiotherapy of laryngeal cancer, 20: 38782
use in therapy of cervical carcinoma during pregnancy, technique to safeguard fetus, 20: 38759
use of orthovoltage, combined with cobalt-60 radiotherapy, economics and effectiveness of, 20: 38792

X-RAY-ABSORPTION ANALYSIS
equipment and method for, of process streams, 20: 39191(P)

X-RAY-DIFFRACTION ANALYSIS
of hydrogen–palladium systems, 20: 39428
of lanthanides, 20: 39421
of lithium fluoride and sodium chloride powders, 20: 40294
singularities in coherent diffuse scattering, 20: 39586

X-RAY EQUIPMENT
radiation protection during operation of industrial, 20: 38737

X-RAY FLUORESCENCE ANALYSIS
use of, in industry and geophysics, review on, 20: 39291

X-RAY SPECTROMETERS
shielding effectiveness in microprobe examination of specimens, 20: 40460(R) (IDO-17191)

XENON
diffusion from sodium at high temperatures, factors affecting, 20: 40357

(NAA-SR-11766)
isotopic composition of, from calcium-poor achondrites, (E), 20: 39984
mesons (π^-) reactions at 5 and 9 Bev/c, angular, energy, and multiplicity distributions of mesons (π^0) produced in, 20: 39755 (JINR-P-2736)
neutron scattering by, cross sections and electron-neutron interaction from thermal, (E), 20: 40129
reactions with charged particles, stopping powers and straggling in, (T), 20: 39611
release rate from pools of water, 20: 39103(R) (BNWL-235-3, pp 51-69)
separation from neon, thermal diffusion factors for, 20: 39321(R) (MLM-1312)
separation of krypton-85 from, by chromatography, 20: 39321(R) (MLM-1312)

XENON ISOTOPES
separation by thermal diffusion, 20: 39321(R) (MLM-1312)
separation of xenon-124 from, by thermal diffusion, 20: 39320 (MLM-1311)
thermal diffusion factor for, temperature dependence in, 20: 39326

XENON ISOTOPES Xe-124
separation from xenon isotopes by thermal diffusion, 20: 39320(R) (MLM-1311)

XENON ISOTOPES Xe-127
electron capture ratios, M/L, 20: 40153

XENON ISOTOPES Xe-131
separation from xenon isotopes by thermal diffusion, 20: 39321(R) (MLM-1312)

XENON ISOTOPES Xe-132
separation from xenon isotopes by thermal diffusion, 20: 39321(R) (MLM-1312)

XENON ISOTOPES Xe-133
diffusion from irradiated thoria and urania, effects of titania additions on, 20: 39381 (AECL-2585)
use in measurement of myometrial blood flow during pregnancy, 20: 38747

XENON ISOTOPES Xe-134
separation from xenon isotopes by thermal diffusion, 20: 39321(R) (MLM-1312)

XENON ISOTOPES Xe-136
separation from xenon isotopes by thermal diffusion, 20: 39321(R) (MLM-1312)

XENON OXIDES
properties of, formed by beta decay of iodine-131 in alkali metal iodates, 20: 38984

XYLENOL ORANGE
complexes with lanthanum, lutetium, scandium, and yttrium, composition and chemical properties of, 20: 38924

Y

YANKEE POWER REACTOR
control rods for, radiation effects on nickel-plated cadmium–indium–silver, 20: 39461 (WCAP-6074)

YEASTS
effects of chemical mutagens on Schizosaccharomyces, 20: 38589(R) (EUR-2761.f)
radiation effects on cytochrome systems in, x, 20: 38680

YTTERBIUM
determination in rare earths using acetonitrile, controlled-potential coulometric, 20: 38812
determination in solutions, spark method for spectrographic, 20: 38832
energy levels of, lifetimes of $6s6p\,^1P_1$ and $6s6p\,^3P_1$, 20: 39597
reduction in acetonitrile solutions, color production in controlled-potential coulometric, 20: 38813
separation from thulium by solvent extraction using tertiary amines and diethylenetriaminopentaacetic acid or EDTA, 20: 38995 (BM-RI-6809)

YTTERBIUM ALLOYS
Al–Yb, magnetic properties of intermetallic compounds of, 20: 39433
Pb–Yb–Zn, component distribution in recrystallized, 20: 39435
Yb–Zn, crystal structure of intermetallic compounds Yb_2Zn_{17} and $YbZn_{13}$ in, 20: 39417

YTTERBIUM CHLORIDES
heat of dilution of aqueous solutions of, 20: 38870 (IS-1356)
heat of dilution of aqueous, at 25°C, 20: 38903
specific gravity and apparent molal volume of aqueous solutions of, at 25°C, 20: 38905
thermal capacity of aqueous solutions of, at 25°C, 20: 38906

YTTERBIUM ISOTOPES Yb-171
energy levels of, M1 transitions of rotational, (E), 20: 40072 (LA-DC-8061)
nuclear magnetic moments, (E), 20: 40073 (LA-DC-8065)

YTTERBIUM ISOTOPES Yb-173
energy levels of, M1 transitions of rotational, (E), 20: 40072 (LA-DC-8061)

YTTERBIUM NITRATES
specific gravity and apparent molal volume of aqueous solutions of, at 25°C, 20: 38905

YTTERBIUM OXIDES
preparation of lower, 20: 38867(R) (COO-1109-22, Paper 6)
actinide oxides–Yb_2O_3, preparation of sols of, 20: 39341(P)

YTTERBIUM PHOSPHATES
preparation and properties of, conductometric and potentiometric studies on, 20: 38883

YTTRIUM
determination in magnesium alloys by successive potentiometric titration, 20: 38830
determination in solutions, spark method for spectrographic, 20: 38832
effects on grain size of tungsten, 20: 39400 (NASA-TN-D-3531)
superconductivity of, 20: 40047

YTTRIUM ALLOYS
Al–Cr–Y, crystal structure of intermetallic compounds in, 20: 39414
Al–Cu–Y, crystal structure of intermetallic compounds in, 20: 39414
Al–Fe–Y, crystal structure of intermetallic compounds in, 20: 39414
Al–Mn–Y, crystal structure of intermetallic compounds in, 20: 39414
Ce–Y, phase transformations and magnetic ordering in, pressure-induced, 20: 40326
Gd–Y, phase transformations and magnetic ordering in, pressure-induced, 20: 40326
Hf–Nb–W–Y, properties for high-temperature service, 20: 39445(P)
Hf–Nb–W–Y, weldability evaluation of, 20: 39366
La–Y, phase transformations and magnetic ordering in, pressure-induced, 20: 40326
Nd–Y, phase transformations and magnetic ordering in, pressure-induced, 20: 40326
Pb–Y–Zn, component distribution in recrystallized, 20: 39435
Pr–Y, phase transformations and magnetic ordering in, pressure-induced, 20: 40326

YTTRIUM COMPLEXES
with acid phosphates, ion exchange studies on composition and stability of, 20: 38878(T) (ORNL-tr-1257)
with Xylenol Orange, composition and chemical properties of, 20: 38924

YTTRIUM ISOTOPES Y-89
deuteron reactions at 11.8 Mev, energy spectra from, 20: 40065(R) (BMwF-FB-K-66-01)
neutron inelastic scattering at 5 Mev, cross sections for, (E), 20: 39470(R) (ORNL-3924)

YTTRIUM ISOTOPES Y-90
use in radiotherapy of epilepsy, 20: 38779
use in trans-sphenoidal hypophysectomy, results compared with use of gold-198, 20: 38758
use of bead of, for pituitary cancer radiotherapy, 20: 38744 (DP-1066(Vol.1), pp IV.47-66)

YTTRIUM ISOTOPES Y-91
uptake by algae, effects of EDTA on, 20: 38570

YTTRIUM OXIDES
analysis for dysprosium, activation, 20: 38833
effects on elastic properties of zirconia, 20: 39438
effects on irradiation performance of urania, 20: 39447 (AECL-2581)
luminescence of Y_2O_3:Eu, emission and excitation spectra studies of, 20: 40315
actinide oxides–Y_2O_3, preparation of sols of, 20: 39341(P)
PuO_2–Y_2O_3, preparation of sols of, 20: 39341(P)
W–Y_2O_3, phase diagrams, 20: 39437

Z

ZINC
crystallization in lanthanide-lead melts, mechanisms of, 20: 39435
determination in blood in arthritic and healthy patients, activation, 20: 38845
determination in blood serum, activation, 20: 38851
determination in erythrocytes and plasma in human blood, activation, 20: 38852
determination in mosaic virus and nucleic acids in tobacco plants, activation, 20: 38846
determination in organic coating pigments, activation, 20: 38853
determination of, in presence of cobalt by radiometric titration using EDTA, 20: 38806
effects on properties of magnesium-base alloys for fuel-element cladding, 20: 39443(P)
superconductivity of, 20: 40047

ZINC ALLOYS
Dy–Zn, crystal structure of intermetallic compounds Dy_6Zn_{23} in, 20: 39417
Er–Zn, crystal structure of intermetallic compound Er_2Zn_{17} in, 20: 39417
Eu–Zn, crystal structure of intermetallic compound $EuZn_{13}$ in,

20: 39417
Gd–Zn, crystal structure of intermetallic compounds Gd_6Zn_{23} and $GdZn_{12}$ in, 20: 39417
Ho–Zn, crystal structure of intermetallic compound $HoZn_{12}$ in, 20: 39417
La–Zn, crystal structure of intermetallic compound $LaZn_{13}$ in, 20: 39417
Lu–Zn, crystal structure of intermetallic compounds Lu_6Zn_{23}, Lu_2Zn_{17}, and $LuZn_{12}$ in, 20: 39417
Nd–Zn, crystal structure of intermetallic compound Nd_2Zn_{17} in, 20: 39417
Pb–rare earths–Zn, component distribution in recrystallized, 20: 39435
Pr–Zn, crystal structure of intermetallic compound Pr_2Zn_{17} in, 20: 39417
Sm–Zn, crystal structure of intermetallic compound $SmZn_{12}$ in, 20: 39417
Tm–Zn, crystal structure of intermetallic compounds, Tm_6Zn_{23} and $TmZn_{12}$ in, 20: 39417
Yb–Zn, crystal structure of intermetallic compounds Yb_2Zn_{17} and $YbZn_{13}$ in, 20: 39417

ZINC CHLORIDES
spectra of liquid, Raman, 20: 38871(R) (NYO-1769-54)

ZINC ISOTOPES Zn-64
neutron reactions (n,d) with, angular distributions from, (E), 20: 40069(R) (EANDC(E)-66(U))

ZINC ISOTOPES Zn-65
analysis of, for carrier by isotopic dilution, 20: 38814
beta decay of, intensity of 1.114-Mev gamma transition in, (E), 20: 40093
content in whales, 20: 38560
electron capture ratios, M/L, 20: 40153
elimination by mice and rats, effects of DTPA, pectin, and zirconium phosphate on, 20: 38733
metabolism in rats, 20: 38556
use as tracer for DTPA excretion in rats, 20: 38556

ZINC SULFIDES
sampling of particles of, in isokinetic and subisokinetic air streams, 20: 39103(R) (BNWL-235-3, pp 51-69)
use of photostimulated crystals of, in radiation dosimetry, 20: 40333

ZIRCALOY-2
bonding to uranium–zirconium fuels, mechanisms of, 20: 39361 (WAPD-305)
hydrogen solubility in, effects of temperature on, 20: 39379 (AECL-2453)
radiation effects on mechanical properties of, fast neutron, 20: 39457 (GEAP-5100-9)
reactions of oxidized, with aluminum at 400 to 500°C, 20: 39380 (AECL-2570)
Al–Zircaloy-2–ZrO_2, phase studies, 20: 39380 (AECL-2570)

ZIRCONIUM
deuteron reactions at 11.8 Mev, energy spectra from, 20: 40065(R) (BMwF-FB-K-66-01)
diffusion from sodium at high temperatures, factors affecting, 20: 40357 (NAA-SR-11766)
effects on grain size of tungsten, 20: 39400 (NASA-TN-D-3531)
effects on properties of boron steel, 20: 39426
etching and pickling of, methods and solutions for, 20: 39351(P)
phase transformations, effect of pressure and irradiation on solid-solid, (E), 20: 40306
superconductivity of, 20: 40047

ZIRCONIUM ALLOYS
corrosion by terphenyls, research on, 20: 39344 (EUR-2997.e)
etching and pickling of, methods and solutions for, 20: 39351(P)
hydridation of, effects of carbon tetrachloride at 400°C on, 20: 39360 (TRG-Report-1255)
Cr–Fe–Zr, corrosion of zirconium-base, by steam at 300 to 500°C, 20: 39356(R) (GEAP-5134)
Cr–Fe–Zr, properties of zirconium base, for fuel cladding, 20: 39356(R) (GEAP-5134)
Cu–Mo–Zr, corrosion by steam, effects of heat treatments on copper-base and zirconium-base, 20: 39347 (NP-16239)
Mo–Nb–Ti–U–Zr, mechanical properties of high-strength uranium-base, 20: 39440(P)
Mo–Nb–V–Zr, weldability evaluation of, 20: 39366
Nb–Ta–W–Zr, weldability evaluation of, 20: 39366
Nb–Ta–Zr, superconducting critical current density in, effect of micro-heterogeneity on, 20: 40020
Nb–W–Zr, weldability evaluation of, 20: 39366
Nb–Zr, fabrication of superconductors of, 20: 39372(P)
Nb–Zr, superconductivity for magnets, 20: 40015(R) (ORNL-TM-1598)
Nb–Zr, superconductivity in surface layers of, (E), 20: 40023
Nb–Zr, superconductivity, 20: 40047
Nb–Zr, superconducting critical current density in, effect of structure on, 20: 40021
Re–Zr, work function for, 20: 40297
Sc–Zr, superconductivity, 20: 40047
U–Zr, cladding with Zirconium-2, bonding mechanisms in, 20: 39361 (WAPD-305)
U–Zr, phase studies of uranium-base, 20: 39388 (CEA-R-2956)

ZIRCONIUM CARBIDES
elastic properties of stoichiometric, 20: 39430
properties for matrix material in particulate uranium carbide fuels, 20: 39353 (BMWF-FBK-66-07)
graphite–ZrC, fabrication and mechanical properties of, 20: 39367

ZIRCONIUM CHLORIDES
reactions with alkali hydroxides to produce zirconia, 20: 38929(P)

ZIRCONIUM HYDRIDES
neutron reactions at 0.025 to 0.4 ev, total cross sections for, (E), 20: 40069(R) (EANDC(E)-66(U))

ZIRCONIUM ISOTOPES Zr-90
deuteron reactions at 11.8 Mev, energy spectra from, 20: 40065(R) (BMwF-FB-K-66-01)
nuclear properties of, generalized Hartree-Fock calculations for, (T), 20: 40076 (MIT-2098-255)

ZIRCONIUM ISOTOPES Zr-94
deuteron reactions at 11.8 Mev, energy spectra from, 20: 40065(R) (BMwF-FB-K-66-01)

ZIRCONIUM ISOTOPES Zr-95
decay curves for precursors of, 20: 40357 (NAA-SR-11766)
incorporation in solid cracking catalyst, process for, 20: 38993(P)
sorption on sediments in river-estuary systems, 20: 39121
transport in river-estuary systems, 20: 39121

ZIRCONIUM ISOTOPES Zr-96
deuteron reactions at 11.8 Mev, energy spectra from, 20: 40065(R) (BMwF-FB-K-66-01)

ZIRCONIUM OXIDES
effects on grain size of tungsten, 20: 39400 (NASA-TN-D-3531)
elastic properties of calcia-stabilized effects of temperature on, 20: 39438
elastic properties of yttria-stabilized, effects of temperature on, 20: 39438
phase transformations, effects of pressure and irradiation on solid-solid, (E), 20: 40306
preparation of crystalline, from zirconium tetrachloride or its hydrolysis products, 20: 38929(P)
use as electrodes in MHD generators, (E), 20: 39723
actinide oxides–ZrO_2, preparation of sols of, 20: 39442(P)
Al_2O_3–$AlPO_4$–ZrO_2–$Zr_3(PO_4)_4$, preparation of foam for insulating materials, 20: 39375(P)
Al–Zircaloy-2–ZrO_2, phase studies, 20: 39380 (AECL-2570)
BaO–SiO_2–ZrO_2, phase studies, 20: 38899

ZIRCONIUM PHOSPHATE SILICATES
sorptive properties for cesium and strontium in gel form, 20: 38994(R) (AE-232)

ZIRCONIUM PHOSPHATES
effects on elimination of radioisotopes by mice and rats, 20: 38733
sorptive properties for cesium and strontium in gel form, 20: 38994(R) (AE-232)
Al_2O_3–$AlPO_4$–ZrO_2–$Zr_3(PO_4)_4$, preparation of foam for insulating materials, 20: 39375(P)

ZIRCONIUM SYSTEMS
B–Co–Zr, crystal structure of stoichiometric, 20: 39416
B–Ni–Zr, crystal structure of stoichiometric, 20: 39416
C–Nb–Zr, phase diagrams, 20: 39434
MoC–Ta–Zr, preparation and properties of dispersion-hardened, 20: 39441(P)
Ta–Wc–Zr, preparation and properties of dispersion-hardened, 20: 39441(P)

ZIRFLEX PROCESS
waste processing for, strontium and rare earth recovery in, 20: 40476(R) (BNWL-267)

REPORT NUMBER INDEX

Reports, conference papers and proceedings, numbered translations, and patents abstracted during the period are included in this index. Each item is listed by report number; this is followed by the abstract number and a brief notation regarding public availability. The index entries show which reports are on file in the depository libraries, which reports have been published in open-literature journals (journal citation given), and which reports can be purchased (source and price). Whenever a report is identified by more than one number, cross references from secondary to primary report numbers are cited.

The report number codes apply to AEC reports unless designated otherwise. Non-AEC reports are identified by parenthetical notes after the report codes; e.g., (non-AEC), (British), (Canadian), (French). The note (Misc.) identifies those codes used for both USAEC and non-AEC reports. Patents are listed under the heading "PATENTS"; the country of origin is included in parentheses.

A comprehensive listing of both AEC and non-AEC report codes is contained in TID-85(5th Rev.), *Report Number Series Used by the Division of Technical Information in Cataloging Reports.* This information is also included in the Cumulative Report Number Index (issued annually).

Public Availability of USAEC Reports

All USAEC reports abstracted in *NSA* are available to the public through one or more of the following sources:

(1) Depository libraries in the United States, in other countries, and in international agencies. A list of these depositories appears on the inside covers of each issue of *NSA*.

(2) Scientific and technical journals or other publications.

(3) Microcard Editions, Inc., in Microcard and micronegative form. Orders and inquiries should be sent to: Accounting and Shipping Department, West Salem, Wisconsin 54669.

(4) Clearinghouse for Federal Scientific and Technical Information, U. S. Department of Commerce, Springfield, Virginia 22151.

(5) Superintendent of Documents, U. S. Government Printing Office, Washington, D. C. 20402.

Public Availability of Non-AEC Reports

U. S. Reports. Many reports of U. S. Government agencies are available to the public from the Clearinghouse for Federal Scientific and Technical Information (CFSTI). This availability is given when known. Such reports should be ordered by AD number or NASA-N number. If availability is not shown, inquiries may be directed to CFSTI. In the case of NP numbers, inquiries should be by title and author.

Non-U. S. Reports. Many reports of atomic energy establishments of other countries are deposited in the libraries listed on the inside covers of each issue of *NSA*.

Additionally, the following have made their reports available as indicated.

AUSTRALIA

Australian Atomic Energy Commission Research Establishment. Available upon request from the Library, Australian Atomic Research Establishment, Private Mail Bag, Sutherland, New South Wales, Australia.

BELGIUM

Centre d'Étude de l'Énergie Nucléaire. Available upon request to individuals and organizations, from the Centre d'Étude de l'Énergie Nucléaire (CEN), 31, Rue Belliard, Bruxelles, Belgium.

CANADA

Atomic Energy of Canada Limited. For sale by the Technical Information Officer, Atomic Energy of Canada Limited, Chalk River, Ontario, Canada. Copies are also deposited in libraries in the United Kingdom.

National Research Council of Canada. Available from the National Research Council of Canada, Ottawa 2, Ontario, Canada.

DENMARK

Atomic Energy Commission Research Establishment, Risø. Available on exchange from the Library, Danish Atomic Energy Commission, Risø, Roskilde, Denmark. Also for sale by Jul. Gjellerup, Booksellers, 87 Sölvgade, København K., Denmark.

Danatom. Available on loan from Research Establishment, Risø, Roskilde, Denmark. Copies are available from Danatom, Aurehøjvej 2, Hellerup, Denmark.

EURATOM

Reports from the Commission of the European Atomic Energy Community are available from: Presses academiques europeennes, 98, chaussee de Charleroi, Brussels 6, Belgium; and Office central de vente des publications des Communautes eurodeennes 2, place de Metz, Luxemburg.

FRANCE

Commissariat à l'Énergie Atomique. Inquiries for reports numbered 1-2199 should be addressed to Commissariat à l'Énergie Atomique, Service Central de Documentation, Centre d'Études Nucléaires de Saclay, Boite Postale No. 2, Gif-sur-Yvette (S. et O.), France. Reports numbered 2200 and above are available from La Documentation Francaise, 16 Rue Lord-Byron, Paris VIII, France.

Service Central de Protection contre les Rayonnements Ionisants. Copies are available from Ministère de la Santé Publique, Service Central de Protection contre les Rayonnements Ionisants, B. P. n° 35—LE VESINET (S. et O.), France.

GERMANY

Deutsches Elektronen-Synchrotron DESY. Copies are available from Deutsches Elektronen-Synchrotron Desy, Dokumentation, 2000 Hamburg-Gr. Flottbek 1, Notkestieg 1, Germany.

Gesellschaft für Kernforschung mbH (KFK). Copies are available from Gesellschaft für Kernforschung mbH, 75 Karlsruhe, Postfach 947, Germany. Copies are also deposited in many national nuclear centers in the world.

Kernforschungsanlage. Copies may be ordered from Zentralbibliothek der Kernforschungsanlage Jülich, Jülich, Bundesrepublik Deutschland.

Hahn-Meitner-Institute für Kernforschung. Available without charge from Hahn-Meitner-Institute für Kernforschung Berlin, Bibliothek, Glienicker Strasse 100, 1 Berlin

39, Germany. Copies are deposited in many national nuclear centers in the world.

Johann-Wolfgang-Goethe Universität, Frankfurt Am Main, Institut für Kernphysik, (IKF). Copies are available from Gmelin Institut, 40-42 Varrentrappstrasse, Frankfurt (Main), West Germany.

ISRAEL

Israel Atomic Energy Commission. Available without charge from Ministry of Defence/Atomic Energy Commission, Soreq Research Establishment, Yavne, Israel. Copies are deposited in libraries in Israel and in other countries.

ITALY

Centro Informazioni Studi Esperienze (CISE). For sale at CISE Press Office, Casella Postale 3986, Milano, Italy. Copies are deposited in libraries in Italy.

Comitato Nazionale per l'Energia Nucleare. Copies are available from Comitato Nazionale per l'Energia Nucleare, Divisione Affari Internazionali e Studi Economici, Ufficio Pubblicazioni, Via Belisario, 15, Roma, Italy.

JAPAN

Japan Atomic Energy Research Institute (JAERI). Available from the Staff Supply Cooperative of Japan Atomic Energy Research Institute (JAERI), 1-1 Tamura-Cho, Shiba, Minato-Ku, Tokyo, Japan. Copies are deposited in depositories in Tokyo, Nagoya, and Osaka.

Nagoya University. Copies are available from Research Information Center, Institute of Plasma Physics, Nagoya University, Nagoya, Japan.

University of Tokyo. Available free of charge from Institute for Nuclear Study, University of Tokyo, Tanashi-Machi, Kitatama-gun, Tokyo, Japan.

NETHERLANDS

Reactor Centrum Nederland. For sale by Reactor Centrum Nederland, 112 Scheveningseweg, 's-Gravenhage, The Netherlands. Copies are deposited in university libraries in Holland and in many national nuclear centers in the world.

NEW ZEALAND

Institute of Nuclear Sciences. Copies are available from Librarian, Institute of Nuclear Sciences, D.S.I.R., Private Bag, Lower Hutt, New Zealand. Copies are deposited in other countries.

NORWAY

Forsvarets Forskningsinstitutt. Copies available from Norwegian Defence Research Establishment, Library, P. O. Box 25, Kjeller, Norway.

Institutt for Atomenergi. "KR" reports are available on an exchange basis from the Library, Institutt for Atomenergi, Box 40, Kjeller, Norway. Other series are not generally available to the public.

Norwegian Reactor School. Copies are available from The Library, Institutt for Atomenergi, P. O. Box 40, Kjeller, Norway.

PAKISTAN

Atomic Energy Center. Copies are available from Atomic Energy Center, P. O. Box 658, Lahore, (West Pakistan).

POLAND

Reports of the Polish nuclear institutes are published by the Nuclear Energy Information Center of the Government Commissioner for Use of Nuclear Energy. Copies are available from Ośrodek Informacji o Energii Jądrowej, Warszawa, PKiN, Poland.

SPAIN

Junta de Energia Nuclear. "JEN" reports are available without charge from Servicio de Documentation, Junta de Energia Nuclear, Ciudad Universitaria, Madrid (3), Spain.

SWEDEN

Aktiebolaget Atomenergi. "AE" reports are for sale from Aktiebolaget Atomenergi, Library Section, Box 43041, Stockholm 43, Sweden. Bibliographies and literature surveys of the VDDIT- series may be obtained from Aktiebolaget Atomenergi, Information Office, Scientific and Technical Information, Box 43041, Stockholm 43, Sweden. Other series are not generally available to the public. Organizations in the atomic energy field may obtain copies from Aktiebolaget Atomenergi. Microcopy of AE reports is available from the International Documentation Centre, Tumba, Sweden.

SWITZERLAND

CERN European Organization for Nuclear Research. Available without charge from CERN European Organization for Nuclear Research, Geneva 23, Switzerland. Copies are deposited in libraries in 13 countries.

Eidgenössisches Institut für Reaktorforschung. "EIR" reports are available from Eidgenössiches Institut für Reaktorforschung, c/o Bibliothek, Würenlingen/Ag, Switzerland.

TURKEY

Turkish Atomic Energy Commission. Copies are available free of charge from T.A.E.C., Çekmece Nuclear Research Center, P. O. Box 1, Airport, Istanbul, Turkey.

UNITED KINGDOM

United Kingdom Atomic Energy Authority. Some reports are for sale in the United States by the British Information Service (BIS), 845 Third Avenue, New York, N. Y. 10022. United Kingdom reports generally may be purchased from Her Majesty's Stationery Office, London. Copies not for sale by Her Majesty's Stationery Office may be purchased in microcopy form from Micro Methods Limited, East Ardsley, Wakefield, Yorks, England. Report copies are deposited in a large number of libraries in England, depositories of the USAEC in the United States and abroad, and in most national nuclear centers throughout the world.

Conferences

Published conference proceedings as well as individual unpublished papers from conferences are included in this index. A CONF number is assigned to the conference if published proceedings are received and also if only a single paper is received. The base number used is year-month-sequence. Thus, the number CONF-650101 would indicate that the conference was held in 1965, in January, and that this was the first January 1965 conference so received. This number would be assigned to complete published proceedings, or if individual papers are received, the base number would be extended to include a paper number, i.e., CONF-650101-1. As additional papers are received, they will be assigned consecutive numbers in the series, CONF-650101-1, 2, 3, 4, etc. This numbering system ensures that all papers received from a conference will be associated with that conference in this index.

If published proceedings are received after the receipt of individual papers, the complete proceedings will be abstracted and the abstract number will appear in this index with the base CONF number.

Abbreviations Used in Availability Column

AECL	For sale by Atomic Energy of Canada Ltd., Chalk River, Ontario, Canada.
BIS	For sale by British Information Service, 845 Third Avenue, New York, N. Y. 10022
CFSTI	For sale by the Clearinghouse for Federal Scientific and Technical Information, U.S. Department of Commerce, Spring-

field, Virginia 22151. The symbol "cy" indicates that the format of the item sold may be either a printed document or a photographic reproduction (two-thirds of original size) depending upon the availability of printed stock. The indicated price is for either format. The symbol "mn" is used to indicate that copy is also available in the form of micronegatives (microfiche).

Dep. — AEC reports: Full-size copy is on deposit in the depository libraries both inside and outside the United States. These reports are also for sale by Microcard Editions, Inc., Accounting and Shipping Department, West Salem, Wisconsin 54669.

Non-AEC reports: Full-size copy on deposit in the depository libraries in the United States only.

Dep.(mc) — Same as for Dep., except copy is in Microcard form.

Dep.(mn) — Same as for Dep., except copy is in micronegative (microfiche) form.

DSIR — For sale by the National Lending Library for Science and Technology (D.S.I.R.), Boston Spa, Yorkshire, England.

DTI Extension — Available from the U. S. Atomic Energy Commission, Division of Technical Information Extension, P. O. Box 62, Oak Ridge, Tennessee 37830.

EM — Blueprints and microcopy of AEC engineering drawings are available from Clearinghouse for Federal Scientific and Technical Information, U. S. Department of Commerce, Springfield, Virginia 22151. Current prices of the CAPE- packages may be obtained from this address. TID-4100, available from the Division of Technical Information Extension, P. O. Box 62, Oak Ridge, Tennessee 37831, contains information on all the CAPE- packages for sale.

Gmelin — Available at a nominal charge and under the AED- number shown from Atomic Energy Documentation Center, Gmelin Institute, 40-42 Varrentrappstrasse Frankfurt (Main), West Germany.

GPO — For sale by the Superintendent of Documents, Government Printing Office, Washington, D. C. 20402.

HMSO — Her Majesty's Stationery Office, London.

IAEA — Available from the International Atomic Energy Agency, Vienna, Austria, and from its sales agencies in various countries throughout the world. A list of these agencies is found in each STI/DOC and STI/PUB publication.

JCL — For sale by the Special Libraries Association Translation Center, John Crerar Library, 35 West 33rd Street, Chicago, Illinois 60616.

LC — For sale by the Library of Congress, Photoduplication Service, Washington, D. C. 20540.

NAS — National Academy of Sciences, National Research Council, Washington, D. C. 20418.

NRC — For sale by the National Research Council of Canada, Ottawa, Ontario, Canada.

ORAU — Available on interlibrary loan from the Library, Oak Ridge Associated Universities, Post Office Box 117, Oak Ridge, Tennessee 37830.

ORINS — See ORAU.

UKAEA, London — Available from United Kingdom Atomic Energy Authority, 11 Charles II Street, London, S. W. 1.

UN — United Nations Bookshop, United Nations Headquarters, New York, New York.

USGS — Available free of charge from the U. S. Geological Survey, Washington, D. C. 20242.

ZLDI — Zentralstelle Für Luftfahrtdokumentation Und-Information, Maria-Theresia-Strasse 21, Munich 27, Germany.

[The symbols "ph," "mf," and "fs" are used to designate that copy is available only in photostat, microfilm, or facsimile form. The symbol "mn" is used to designate that copy is available in micronegative (microfiche) form. The symbol "cy" is used to designate full size or photographically enlarged copy (two-thirds of original size).]

Report No.	Abstract No.	Availability
ACNP–	**(Misc.)**	
63562	20-40374	Dep. mn. CFSTI $1.00 cy, $0.50 mn
AD–	**(Misc.)**	
624997	20-39328	CFSTI $2.00 cy, $0.50 mn
629422	20-38603	CFSTI $1.00 cy, $0.50 mn. JCL $1.10 fs, $0.80 mf
632957	20-39124	CFSTI $2.00 cy, $0.50 mn
634746	20-40293	CFSTI $1.00 cy, $0.50 mn
635198	20-39273	CFSTI $1.00 cy, $0.50 mn
635596	20-39378	CFSTI $1.00 cy, $0.50 mn
635655	20-38937	CFSTI $1.00 cy, $0.50 mn
636091	20-40485	CFSTI $7.00 cy, $1.75 mn
636185	20-39476	CFSTI $1.00 cy, $0.50 mn
636206	20-39192	CFSTI $2.00 cy, $0.50 mn
636533	20-39576	CFSTI $3.00 cy, $0.75 mn
636542	20-40454	CFSTI $4.00 cy, $0.75 mn
636736	20-39193	CFSTI $1.00 cy, $0.50 mn
636914	20-39007	CFSTI $6.00 cy, $1.25 mn
636927	20-39167	CFSTI $1.00 cy, $0.50 mn
636947	20-39146	CFSTI $3.00 cy, $0.75 mn
637125	20-40284	CFSTI $3.00 cy, $0.75 mn
637710	20-40165	CFSTI $2.00 cy, $0.50 mn
637711	20-40166	CFSTI $2.00 cy, $0.50 mn
638137	20-39194	CFSTI $2.00 cy, $0.50 mn
AE–	**(Non-AEC)**	
232	20-38994	Dep. mn
235	20-39195	Dep. mn
236	20-39196	Dep. mn
AECD-EP–	**(Pakistani)**	
11	20-39096	Dep. mn
AECL–	**(Canadian)**	
2432	20-39329	Dep. mn. AECL $0.50
2453	20-39379	Dep. mn. AECL $0.50
2564	20-39446	Dep. mn. AECL $1.50
2565	20-39197	Dep. mn. AECL $0.50
2570	20-39380	Dep. mn. AECL $0.50 mn
2581	20-39447	Dep. mn. AECL $0.50
2585	20-39381	Dep. mn. AECL $1.00
2598	20-39623	Dep. mn. AECL $2.00
AED-C–	**(Non-AEC)**	
06-14	20-39168	Dep. mn
22-06	20-40444	Dep. mn
AEEW-M–	**(British)**	
631	20-40398	Dep. BIS $1.10. HMSO 5s. 6d.
650	20-39045	Dep. BIS $1.40. HMSO 7s. 0d.
654	20-40399	Dep. BIS $0.50. HMSO 2s. 6d.
AEEW-R–	**(British)**	
473	20-39382	Dep. BIS $0.80. HMSO 4s. 0d.
477	20-39046	Dep. BIS $0.80. HMSO 4s. 0d.
AERE-M–	**(British)**	
1739	20-39047	Dep. BIS $2.60. HMSO 13s. 0d.
AERE-R–	**(British)**	
4955	20-38554	Health Phys., 12: 1129-38(1966)
AERE-Trans–	**(British)**	
1053	20-39582	Dep. BIS $0.90. HMSO 4s. 6d.
AERE-X–	**(British)**	
PR-2596-9	20-39448	Dep. mn
AFCRL–	**(Non-AEC)**	
66-161	20-40166	See AD-637711
66-204	20-40165	See AD-637710
AFRRI-CR–	**(Non-AEC)**	
66-2	20-40454	See AD-636542
AFRRI-TN–	**(Non-AEC)**	
66-5	20-39476	See AD-636185
AMRA-TR–	**(Non-AEC)**	
66-10	20-39378	See AD-635596
ANL–		
7228	20-40353	Dep. mn. CFSTI $3.00 cy, $0.75 mn
ANL-Trans–		
344	20-39407	Dep. mn. CFSTI $1.00 cy, $0.50 mn. JCL $1.60 fs, $0.80 mf
AP-Note–	**(Misc.)**	
393	20-40354	ORAU
APDA-TPI–		
1	20-40355	Dep. mn. CFSTI $3.00 cy, $0.75 mn
ARL–	**(Non-AEC)**	
66-0072	20-39167	See AD-636927
ATD–	**(Non-AEC)**	
65-109	20-39328	See AD-624997
BAW–	**(Misc.)**	
1225	20-40445	Dep. mn. CFSTI $6.00 cy, $1.25 mn
BLG–	**(Belgian)**	
357	20-39156	J. Pharm. Belg., Nos. 3-4, 137-45(1965)
BM-RI–	**(Misc.)**	
6809	20-38995	
6817	20-39352	Bureau of Mines Free
BMwF-FBK–	**(German)**	
65-05	20-39106	Dep. mn
66-01	20-40065	Dep. mn
66-07	20-39353	Dep. mn
66-08	20-39383	Dep. mn
66-09	20-39354	Dep. mn
66-15	20-40066	Dep. mn
BNL–		
962	20-39330	Dep. mn. CFSTI $2.00 cy, $0.50 mn
9435	20-38624	Health Phys., 12: 1007-20(1966)
9624	20-38986	Int. J. Appl. Radiat. Isotop., 17: 427(1966)
9951	20-38907	J. Phys. Chem., 70: 2517-23(1966)
10111	20-38912	J. Phys. Chem., 70: 2705-7(1966)
10350	20-38855	Dep. mn. CFSTI $1.00 cy, $0.50 mn
10372	20-38856	Dep. mn. CFSTI $1.00 cy, $0.50 mn
10376	20-39478	Dep. mn. CFSTI $1.00 cy, $0.50 mn
10454	20-40455	Dep. mn. CFSTI $1.00 cy, $0.50 mn
10495	20-39479	Dep. mn. CFSTI $1.00 cy, $0.50 mn
10508	20-39480	Dep. mn. CFSTI $3.00 cy, $0.75 mn
BNWL–		
235-3	20-38857	Dep. mn. CFSTI $3.00 cy, $0.75 mn
236	20-40285	Dep. mn. CFSTI $4.00 cy, $1.00 mn
244	20-40400	Dep. mn. CFSTI $2.00 cy, $0.50 mn
250	20-39198	Dep. mn. CFSTI $1.00 cy, $0.50 mn
263	20-39384	Dep. mn. CFSTI $3.00 cy, $0.50 mn
265	20-38795	Dep. mn. CFSTI $1.00 cy, $0.50 mn
267	20-40476	Dep. mn. CFSTI $2.00 cy, $0.50 mn
BNWL-SA–		
272	20-39449	Dep. mn. CFSTI $1.00 cy, $0.50 mn
BRL-MR–	**(Non-AEC)**	
1753	20-39194	See AD-638137
BRL-R–	**(Non-AEC)**	
1312	20-38937	See AD-635655
CALT–		
68-72	20-39903	Phys. Rev. Lett., 17: 340-3(1966)
68-92	20-39743	Dep. mn. CFSTI $2.00 cy, $0.50 mn
CAPE–		
1342	20-40373	EM
1363	20-40424	EM
1368	20-39259	EM
1370	20-39262	EM
1375	20-39263	EM
1377	20-39258	EM
1380	20-39264	EM
1389	20-39185	EM
1391	20-39257	EM

Report No.	Abstract No.	Availability
1393	20-38546	EM
1394	20-39186	EM
1398	20-39256	EM
1401	20-39506	EM
1406	20-40246	EM
1407	20-39507	EM
1408	20-39260	EM
1409	20-39164	EM
1410	20-39253	EM
1411	20-38835	EM
1412	20-39265	EM
1413	20-39036	EM
1414	20-39502	EM
1415	20-39030	EM
1416	20-39267	EM
1417	20-38545	EM
1419	20-39254	EM
1420	20-39503	EM
1423	20-39188	EM
1424	20-39184	EM
1426	20-39037	EM
1427	20-39183	EM
1428	20-39268	EM
1429	20-39269	EM
1430	20-39034	EM
1431	20-39033	EM
1433	20-39505	EM
1434	20-39504	EM
1435	20-39255	EM
1436	20-39261	EM
1437	20-40425	EM
1439	20-39182	EM
1443	20-39340	EM
1445	20-39035	EM
1446	20-39187	EM
1447	20-39038	EM
1449	20-39266	EM
1450	20-39032	EM
1451	20-39031	EM
1453	20-39508	EM
1458	20-39270	EM
CEA-R–	**(French)**	
2788	20-39633	Dep. mn
2852	20-39385	Dep. mn
2895	20-38859	Dep. mn
2905	20-39386	Dep. mn
2909	20-38587	Dep. mn
2947	20-39387	Dep. mn
2956	20-39388	Dep. mn
2963	20-39450	Dep. mn
2968	20-38796	Dep. mn
2973	20-39389	Dep. mn
3003	20-39390	Dep. mn
CEAL–		
1031	20-39481	Dep. mn. CFSTI $1.00 cy, $0.50 mn
CEND–	**(Misc.)**	
259	20-40401	Dep. mn. CFSTI $5.00 cy, $1.00 mn
3107-267	20-40382	Dep. mn. CFSTI $1.00 cy, $0.50 mn
CERN–	**(European Organization for Nuclear Research)**	
66-18	20-39744	Dep. mn
66-20	20-39482	Dep. mn
66-21	20-39483	Dep. mn
66-22	20-39745	Dep. mn
66-24	20-39746	Dep. mn
CONF-384–	**20-38836**	**(Symposium on Radioactivation Analysis and Its Application to the Biological Sciences, Saclay, France, Sept. 1963) Paris, Presses Universitaires de France, 1964**
CONF-564–	**20-40255**	**(Colloquium on Interaction Between Electromagnetic Waves and Plasma, Saclay, France, Sept. 1964) Paris, Presses Universitaires de France, 1965**
CONF-758–	**(American Physical Society Meeting, New York, Jan. 22–25, 1965)**	
61	20-40047	ORAU. Gmelin, AED-CONF-65-003-131
CONF-610602–	**20-40051**	**(American Society for Testing and Materials, 64th Annual Meeting, Atlantic City, N. J., June 27–28, 1961) Amer. Soc. Test. Mater., Spec. Tech. Pub., No. 302, 1-245(1962)**
CONF-630405–	**20-39166**	**(3rd Scientific and Working Conference on Radiation Protection, Leningrad, April 16–20, 1963) Leningrad, Leningrad Scientific Research Inst. on Radiation Protection, 1963**
CONF-641116–	**20-39338**	**(Conference on the Role of Grain Boundaries and Surfaces in Ceramics, Raleigh, N. C., Nov. 16–18, 1964) $22.50**
CONF-641134–	**(Symposium on Water Problems in Nuclear Reactors, Rossendorf, Germany, Nov. 10–13, 1964)**	
1	20-40464	See UJV-1180/64
2	20-40465	See UJV-1181/64
CONF-650220–	**(American Physical Society, Southwest Meeting, Norman, Okla., Feb. 25–27, 1965)**	
5	20-40248	ORAU. Gmelin, AED-CONF-65-022-9
7	20-39619	ORAU
CONF-650452–	**(2nd Conference on Industrial Carbon and Graphite, London, England, Apr. 7–9, 1965)**	
1	20-39439	ORAU
CONF-650570–	**(48th Canadian Chemical Conference and Exhibition, Montreal, Canada, May 31–June 2, 1965)**	
1	20-40149	ORAU. Gmelin, AED-CONF-65-237-2
CONF-650578–	**20-40486**	**(5th National Conference on the Peaceful Uses of Space, St. Louis, Mo., May 26–28, 1965) See NASA-SP-82**
CONF-650606–	**20-40383**	**(EURATOM Symposium on Fuel Cycles of High-Temperature Gas-Cooled Reactors, Brussels, June 10–11, 1965) See EUR-2780.e**
CONF-650653–	**(American Physical Society, Summer Meeting, New York, June 23–25, 1965)**	
28	20-40148	ORAU. Gmelin, AED-CONF-65-170-68
CONF-650664–	**(Canadian Assn. of Physicists Congress, Vancouver, B. C., June 9–12, 1965)**	
8	20-39122	ORAU. Gmelin, AED-CONF-65-288-10
CONF-650710–	**19-43507**	**(American Nuclear Society, Meeting on Reactor Operating Experience, Jackson Lake Lodge, Wyo., July 28–30, 1965)**
3	20-40457	See DP-1049, pp 1-19
CONF-650809–	**(Society for Applied Spectroscopy, 4th National Meeting, Denver, Aug. 30–Sept. 3, 1965)**	
2	20-38853	ORAU. Gmelin, AED-CONF-65-229-3
CONF-650813–	**(6th Biennial Gas Dynamics Symposium, Evanston, Ill., Aug. 27, 1965)**	
3	20-40292	ORAU. Gmelin, AED-CONF-65-216-10
CONF-650826–	**20-39644**	**(International Conference on Energetics, Rochester, N. Y., Aug. 18–20, 1965) New York, American Society of Mechanical Engineers, 1965**
CONF-650833–	**20-17288**	**(4th International Conference on the Physics of Electronic and Atomic Collisions, Quebec, Canada, Aug. 3–7, 1965) New York, Science Bookcrafters, Inc.**
3	20-39620	ORAU. Gmelin, AED-CONF-65-315-50
4	20-40247	ORAU. Gmelin, AED-CONF-65-315-48
CONF-650902–	**(American Chemical Society, 150th National Meeting, Atlantic City, Sept. 12–17, 1965)**	

Report No.	Abstract No.	Availability
35	20-39299	ORAU. Gmelin, AED-CONF-235-81
36	20-38928	ORAU. Gmelin, AED-CONF-65-235-91
CONF-650929–	20-39339	(International Conference on Optical and Electronic Properties of Metals and Alloys, Paris, Sept. 13–16, 1965) $18.50
CONF-650932–	20-34803	(Symposium on the Inelastic Scattering of Neutrons by Condensed Systems, Upton, N. Y., Sept. 1965) See BNL-940
4	20-40344	ORAU. Gmelin, AED-CONF-65-292-6
8	20-39946	ORAU. Gmelin, AED-CONF-65-292-8
CONF-650962–		(6th Electrical Insulation Conference, New York, Sept. 13–16, 1965)
2	20-38971	ORAU. Gmelin, AED-CONF-65-240-3
CONF-650974–		(15th Brazilian Congress, Rio de Janeiro, Sept. 19–25, 1965)
2	20-40070	See IEA-111
CONF-650976–	20-40440	(2nd Foratom Congress, Frankfurt on Main, Germany, Sept. 29–Oct. 1, 1965) Bonn, Deutsches Atomforum e. V., 1965
CONF-651004–		(9th Conference on Analytical Chemistry in Nuclear Technology, Gatlinburg, Tenn., Oct. 12, 1965)
16	20-38854	ORAU. Gmelin, AED-CONF-65-287-3
CONF-651005–		(1st International Symposium on Water Desalination, Washington, D. C., Oct. 3–9, 1965)
5	20-40439	ORAU
7	20-40438	ORAU
CONF-651049–		(IEEE Thermionic Conversion Specialist Conference, San Diego, Calif., Oct. 25–27, 1965)
21	20-39642	ORAU. Gmelin, AED-CONF-65-324-23
CONF-651063–		(Canadian Electronics Conference, Toronto, Oct. 4–6, 1965)
1	20-40437	ORAU. Gmelin, AED-CONF-65-330-1
CONF-651067–		(12th Annual Air Force Science and Engineering Symposium, Brooks AFB, Tex., Oct. 12–14, 1965)
1	20-39992	ORAU. Gmelin, AED-CONF-65-351-1
CONF-651074–		(Optical Society of America, Fall Meeting, Philadelphia, Pa., Oct. 6–8, 1965)
1	20-39468	ORAU
CONF-651078–	20-39016	(Deep Lab Conference, Johannesburg, South Africa, Oct. 12, 1965) See COO-818-94
CONF-651101–	20-3647 20-9102	(American Nuclear Society, Winter Meeting, Washington, D. C., Nov. 15–18, 1965) (Revised 11-8-65)
52	20-40481	See WAPD-T-1851
CONF-651108–		(Symposium on Isotope Techniques, Urbana, Ill., Nov. 10–12, 1965)
3	20-39123	ORAU. Gmelin, AED-CONF-65-347-8
4	20-39141	ORAU. Gmelin, AED-CONF-65-347-5
5	20-39142	ORAU. Gmelin, AED-CONF-65-347-10
CONF-651213–		(American Physical Society, Winter Meeting in the West, Los Angeles, Dec. 20–22, 1965)
4	20-40249	ORAU. Gmelin, AED-CONF-65-400-12
13	20-40147	ORAU. Gmelin, AED-CONF-65-400-34
CONF-660107–		(American Physical Society Meeting, New York, Jan. 26–29, 1966)
49	20-40152	ORAU. Gmelin, AED-CONF-66-003-104
50	20-40154	ORAU. Gmelin, AED-CONF-66-003-108
61	20-39914	ORAU. Gmelin, AED-CONF-66-003-141
62	20-40252	ORAU. Gmelin, AED-CONF-66-003-143
64	20-40045	ORAU. Gmelin, AED-CONF-66-003-152
CONF-660204–		(American Nuclear Society Meeting, San Diego, Calif., Feb. 7–9, 1966)
18	20-40380	ORAU. Gmelin, AED-CONF-66-017-16
20	20-40146	ORAU. Gmelin, AED-CONF-66-017-13
CONF-660206–		(Symposium on Neutron Noise, Waves, and Pulse Propagation, Gainesville, Feb. 14–16, 1966)
19	20-40064	ORAU. Gmelin, AED-CONF-66-014-23
CONF-660209–		(Conference on Intermediate Energy Physics, Williamsburg, Va., Feb. 9–11, 1966)
2	20-40151	ORAU. Gmelin, AED-CONF-66-023-2
CONF-660217–		(Symposium on Interdisciplinary Aspects of Radiative Energy Transfer, Philadelphia, Feb. 24–26, 1966)
6	20-39570	ORAU. Gmelin, AED-CONF-66-013-13
CONF-660220–		(American Nuclear Society, Canadian Nuclear Assn., Nuclear Energy Resources Meeting, Toronto, Canada, Feb. 1, 1966)
2	20-39145	ORAU. Gmelin, AED-CONF-66-022-1
CONF-660303–		(American Physical Society, Conference of Neutron Cross Section Technology, Washington, D. C., Mar. 22–24, 1966)
47	20-40063	ORAU. Gmelin, AED-CONF-66-034-38
CONF-660304–	20-33646	(Institute of Electrical and Electronics Engineers, Scintillation and Semiconductor Counter Symposium, Washington, D. C., Mar 2–4, 1966) Trans. Nucl. Sci., NS-13: No. 3, 1-601(1966)
8	20-39271	ORAU. Gmelin, AED-CONF-66-020-2
CONF-660305–		(American Nuclear Society, Topical Meeting, Augusta, Ga., Mar. 21–23, 1966)
Vol.1	20-39275	See DP-1066(Vol.1)
Vol.2	20-39278	See DP-1066(Vol.2)
CONF-660324–		(26th Annual Conference on Physical Electronics, Cambridge, Mass., Mar. 21–23, 1966)
4	20-39641	ORAU. Gmelin, AED-CONF-66-036-8
CONF-660326–		(7th Symposium on Engineering Aspects of Magnetohydrodynamics, Princeton, N. J., Mar. 30–Apr. 1, 1966)
4	20-39640	ORAU.
5	20-39639	ORAU. Gmelin, AED-CONF-66-047-8
CONF-660327–		(American Physical Society Meeting, Durham, N. C., Mar. 28–31, 1966)
5	20-40343	ORAU. Gmelin, AED-CONF-66-050-16
7	20-40046	ORAU. Gmelin, AED-CONF-66-050-23
8	20-40346	ORAU. Gmelin, AED-CONF-66-050-19
CONF-660401–		(American Meteorological Society, American Geophysical Union, Annual Joint Meeting, Washington, D. C., Apr. 19, 1966)
5	20-39572	ORAU. Gmelin, AED-CONF-66-061-14
6	20-39147	Dep. mn. CFSTI $1.00 cy, $0.50 mn
10	20-39991	ORAU. Gmelin, AED-CONF-66-061-17
CONF-660411–		(American Physical Society Meeting, Washington, D. C., Apr. 25–28, 1966)
7	20-40153	ORAU. Gmelin, AED-CONF-66-060-33
16	20-39569	ORAU. Gmelin, AED-CONF-66-060-65
20	20-40342	ORAU. Gmelin, AED-CONF-66-060-66
21	20-39621	ORAU. Gmelin, AED-CONF-66-060-69
24	20-40341	ORAU. Gmelin, AED-CONF-66-060-50
29	20-39571	ORAU. Gmelin, AED-CONF-66-060-63
43	20-39618	ORAU. Gmelin, AED-CONF-66-060-117
49	20-39617	ORAU. Gmelin, AED-CONF-66-060-101
50	20-40150	ORAU. Gmelin, AED-CONF-66-060-94
CONF-660412–		(Symposium on Accidental Irradiation at Place of Work, Nice, France, Apr. 25–29, 1966)
2	20-38593	See ORNL-P-2175
CONF-660414–		(2nd International Conference on Electron and Ion Beam Science and Technology, New York, Apr. 17–20, 1966)
3	20-40253	ORAU. Gmelin, AED-CONF-66-119-1
5	20-40345	ORAU. Gmelin, AED-CONF-66-119-9
8	20-40347	ORAU. Gmelin, AED-CONF-66-119-10
CONF-660421–		(18th Annual Southwestern IEEE Conference and Show, Dallas, Apr. 20–22, 1966)
1	20-40254	ORAU. Gmelin, AED-CONF-66-065-1

Report No.	Abstract No.	Availability
CONF-660423–		(International Symposium on Lymphocyte in Immunology and Haemopoiesis, Bristol, England, Apr. 12–16, 1966)
1	20-38592	See ORNL-P-2158
CONF-660429–		(American Power Conference, 28th Annual Meeting, Chicago, Ill., Apr. 26–28, 1966)
3	20-40436	ORAU. Gmelin, AED-CONF-66-098-1
CONF-660438–		(International Quantum Electronics Conference, Phoenix, Ariz., Apr. 12–15, 1966)
1	20-40251	ORAU. Gmelin, AED-CONF-66-078-6
CONF-660439–		(Conference on Ground-Based Aeronomic Studies of the Lower Ionosphere, Ottawa, Ontario, Canada, Apr. 11–15, 1966)
1	20-39994	ORAU. Gmelin, AED-CONF-66-063-3
3	20-39995	ORAU. Gmelin, AED-CONF-66-063-4
CONF-660443–		(International Scientific Radio Union, Washington, D. C., Apr. 18–21, 1966)
1	20-39996	ORAU. Gmelin, AED-CONF-66-142-2
2	20-39993	ORAU. Gmelin, AED-CONF-66-142-5
CONF-660505–	20-27419	(American Ceramic Society Meeting, Washington, D. C., May 7–12, 1966)
1	20-39438	ORAU. Gmelin, AED-CONF-66-103-7
8	20-39437	ORAU. Gmelin, AED-CONF-66-103-9
9	20-39367	ORAU. Gmelin, AED-CONF-66-103-13
10	20-39638	ORAU. Gmelin, AED-CONF-66-103-12
CONF-660507–		(Symposium for the Disposal of Radioactive Wastes into Seas, Oceans, and Surface Waters, Vienna, May 17, 1966)
33	20-40479	See ORNL-P-2328
CONF-660510–	20-39510	(International Conference on Isochronous Cyclotrons, Gatlinburg, Tenn., May 2–5, 1966) Trans. Nucl. Sci., NS-13: No. 4, 1-531(1966)
CONF-660524–		(2nd International Thorium Fuel Cycle Symposium, Gatlinburg, Tenn., May 3–6, 1966)
9	20-39006	ORAU. Gmelin, AED-CONF-66-104-10
10	20-40385	See ORNL-P-2327
CONF-660528–		(9th Modulator Symposium, Fort Monmouth, N. J., May 12, 1966)
5	20-39493	See LA-DC-7776
CONF-660531–		(22nd High Temperature Fuels Committee Meeting, Pittsburgh, May 1966)
1	20-40387	See WAPD-T-1939
CONF-660537–		(14th Annual Conference on Mass Spectrometry and Allied Topics, Dallas, Tex., May 23–27, 1966)
1	20-38875	See UCRL-14703-T
CONF-660540–		(Conference on Non-Compact Groups in Particle Physics, Milwaukee, Wis., May 4–6, 1966)
4	20-39915	ORAU. Gmelin, AED-CONF-66-113-5
5	20-39916	ORAU. Gmelin, AED-CONF-66-113-4
CONF-660547–		(Virginia Academy of Science, 44th Annual Meeting, Harrisonburg, Va., May 4–7, 1966)
3	20-40050	ORAU. Gmelin, AED-CONF-66-122-3
CONF-660606–	20-34872	(American Nuclear Society Meeting, Denver, June 19–23, 1966) Trans. Amer. Nucl. Soc., 9: 1-322(1966)
14	20-40360	See WAPD-T-1890
CONF-660609–		(International Symposium on Food Irradiation Meeting, Karlsruhe, Germany, June 6–10, 1966)
7	20-39301	ORAU
9	20-39165	ORAU
10	20-39297	ORAU
23	20-39303	ORAU
26	20-39302	ORAU
28	20-39300	ORAU

Report No.	Abstract No.	Availability
CONF-660610–		(3rd International Congress of Radiation Research, Karlsruhe, Germany, June 22–July 2, 1966)
1	20-39289	See UCD-34P73-9
CONF-660611–		(Society of Applied Spectroscopy Meeting, Chicago, June 14–15, 1966)
5	20-39298	ORAU. Gmelin, AED-CONF-66-172-3
CONF-660614–		(3rd International Congress on Radiation Research, Cortina, Italy, June 1966)
2	20-38575	See ORNL-P-2267
CONF-660621–		(Health Physics Society, 11th Annual Meeting, Houston, Tex., June 27–30, 1966)
14	20-39272	ORAU. Gmelin, AED-CONF-66-103-9
CONF-660627–		(American Society for Testing and Materials, 69th Annual Meeting, Atlantic City, N. J., June 27–July 1, 1966)
2	20-39406	See WAPD-T-1864
CONF-660628–		(International Inst. of Refrigeration Commission I Meeting, Boulder, Colo., June 16–18, 1966)
5	20-40048	ORAU. Gmelin, AED-CONF-66-173-5
6	20-40049	ORAU. Gmelin, AED-CONF-66-173-10
7	20-39643	ORAU. Gmelin, AED-CONF-66-173-11
CONF-660629–		(5th National Congress of Applied Mechanics Meeting, Minneapolis, Minn., June 14–17, 1966)
1	20-39391	Dep. mn. CFSTI $1.00 cy, $0.50 mn
CONF-660632–		(American Inst. of Aeronautics and Astronautics, 4th Aerospace Sciences Meeting, Los Angeles, Calif., June 27–29, 1966)
2	20-40250	ORAU
3	20-40291	ORAU
7	20-39573	ORAU
CONF-660704–		(Magnetohydrodynamic Electrical Power Generation, 2nd International Symposium, Salzburg, July 4–8, 1966)
2	20-39653	ORAU
3	20-39654	ORAU
4	20-39655	ORAU
5	20-39656	ORAU
6	20-39657	ORAU
7	20-39658	ORAU
8	20-39659	ORAU
9	20-39660	ORAU
10	20-39661	ORAU
11	20-39662	ORAU
12	20-39663	ORAU
13	20-39664	ORAU
14	20-39665	ORAU
15	20-39666	ORAU
16	20-39667	ORAU
17	20-39668	ORAU
18	20-39669	ORAU
19	20-39670	ORAU
20	20-39671	ORAU
21	20-39672	ORAU
22	20-39673	ORAU
23	20-39674	ORAU
24	20-39675	ORAU
25	20-39676	ORAU
26	20-39677	ORAU
27	20-39678	ORAU
28	20-39679	ORAU
29	20-39680	ORAU
30	20-39681	ORAU
31	20-39682	ORAU
32	20-39683	ORAU
33	20-39684	ORAU
34	20-39685	ORAU
35	20-39686	ORAU
36	20-39687	ORAU
37	20-39688	ORAU
38	20-39689	ORAU
39	20-39690	ORAU
40	20-39691	ORAU
41	20-39692	ORAU
42	20-39693	ORAU
43	20-39694	ORAU
44	20-39695	ORAU
45	20-39696	ORAU

Report No.	Abstract No.	Availability
46	20-39697	ORAU
47	20-39698	ORAU
48	20-39699	ORAU
49	20-39700	ORAU
50	20-39701	ORAU
51	20-39702	ORAU
52	20-39703	ORAU
53	20-39704	ORAU
54	20-39705	ORAU
55	20-39706	ORAU
56	20-39707	ORAU
57	20-39708	ORAU
58	20-39709	ORAU
59	20-39710	ORAU
60	20-39711	ORAU
61	20-39712	ORAU
62	20-39713	ORAU
63	20-39714	ORAU
64	20-39715	ORAU
65	20-39716	ORAU
66	20-39717	ORAU
67	20-39718	ORAU
68	20-39719	ORAU
69	20-39720	ORAU
70	20-39721	ORAU
71	20-39722	ORAU
72	20-39723	ORAU
73	20-39724	ORAU
74	20-39725	ORAU
75	20-39726	ORAU
76	20-39727	ORAU
77	20-39728	ORAU
78	20-39729	ORAU
79	20-39730	ORAU
80	20-39731	ORAU
81	20-39732	ORAU
82	20-39733	ORAU
83	20-39734	ORAU
84	20-39735	ORAU
85	20-39736	ORAU
86	20-39737	ORAU
87	20-39738	ORAU
88	20-39739	ORAU
89	20-39740	ORAU
90	20-39741	ORAU
91	20-39742	ORAU
CONF-660708–	**(Institute of Electrical and Electronics Engineers, Summer Meeting, New Orleans, La., July 1966)**	
4	20-40452	ORAU
6	20-40453	ORAU
CONF-660712–	**(International Conference on the Alkali Metals, Nottingham, England, July 19–22, 1966)**	
1	20-38856	See BNL-10372
2	20-39392	See CU-2660-29
CONF-660805–	**(International Conference on Solvent Extraction, Goteborg, Sweden, Aug. 27–Sept. 1, 1966)**	
1	20-38855	See BNL-10350
CONF-660808–	**(13th International Conference on High Energy Physics, Berkeley, Calif., Aug. 31–Sept. 7, 1966)**	
5	20-39766	See ORO-3065-10
6	20-39748	See COO-881-76
7	20-39749	See COO-881-77
8	20-39747	See COO-881-75
CONF-660902–	**(American Society of Mechanical Engineers Symposium, Pittsburgh, Pa., Oct. 3–5, 1966)**	
1	20-39020	See K-1632(Pt.2)
CONF-660904–	**(9th Air Cleaning Conference, Boston, Mass., Sept. 13–16, 1966)**	
4	20-39018	See DP-MS-66-46
CONF-660906–	**(International Conference on Nuclear Physics, Gatlinburg, Tenn., Sept. 12–17, 1966)**	
2	20-40079	See ORO-3346-2
3	20-40080	See ORO-3346-3
5	20-40077	See MIT-2098-256
6	20-40076	See MIT-2098-255
10	20-40074	See LA-DC-8069
11	20-40072	See LA-DC-8061
12	20-40073	See LA-DC-8065
CONF-660914–	**(Seminar on Intense Neutron Sources, Los Alamos, N. Mex., Sept. 9, 1966)**	
1	20-40455	See BNL-10454
CONF-660915–	**(2nd International Powder Metallurgy Conference, Starý Smokovec-Vysoké Tatry, Czechoslovakia)**	
1	20-39359	See RISO-113
CONF-660916–	**(1st Nonconventional Energy Conversion Applications Conference, Los Angeles, Calif., Sept. 26–28, 1966)**	
1	20-39026	See UCRL-14660(Rev.1)
COO–		
38-351	20-40317	Mater. Sci. Res., 3: 131-48(1966)
264-304	20-39893	Phys. Rev., 148: 1424-7(1966)
264-305	20-39802	Phys. Rev., 148: 1431-6(1966)
264-306	20-39898	Phys. Rev., 148: 1537-8(1966)
818-94	20-39016	Dep. nn. CFSTI $2.00 cy, $0.50 mn
881-65	20-39801	Phys. Rev., 148: 1428-30(1966)
881-72	20-39784	Phys. Lett., 22: 347-9(1966)
881-75	20-39747	Dep. nn. CFSTI $1.00 cy, $0.50 mn
881-76	20-39748	Dep. nn. CFSTI $1.00 cy, $0.50 mn
881-77	20-39749	Dep. nn. CFSTI $1.00 cy, $0.50 mn
1105-117	20-39199	Dep. nn. CFSTI $1.00 cy, $0.50 mn
1105-118	20-39200	Dep. nn. CFSTI $1.00 cy, $0.50 mn
1109-22	20-38861	Dep. nn. CFSTI $7.15 cy, $2.00 mn
1198-355	20-40311	J. Chem. Phys., 45: 1057-61(1966)
1198-364	20-40012	Dep. nn. CFSTI $4.00 cy, $1.00 mn
1297-6	20-38860	Dep. nn. CFSTI $1.00 cy, $0.50 mn
1371-29	20-39814	Phys. Rev., 148: 1579-?(1966)
1400-10	20-38588	Dep. nn. CFSTI $1.00 cy, $0.50 mn
1528-4	20-38950	J. Phys. Chem., 70: 2529-34(1966)
CRGP–	**(Canadian)**	
1237	20-39197	See AECL-2565
1239	20-39623	See AECL-2598
CU–	**(Misc.)**	
2660-29	20-39392	Dep. nn. CFSTI $2.00 cy, $0.50 mn
18-65-AF-2461-EE	20-40165	See AD-637710
D–	**(Misc.)**	
1-82-0529	20-39624	
DASA–	**(Misc.)**	
1688(Suppl.)	20-39192	See AD-636206
DF–	**(Misc.)**	
65-CAP-31	20-39379	See AECL-2453
DOCKET	**(Misc.)**	
50-247(Exh.B)	20-40406	See NP-16181(Exh.B)(Vol.1)
50-247(Exh.B) (Vol.2)(Pt.A)	20-40407	See NP-16181(Exh.B)(Vol.2)(Pt.A)
50-247(Exh.B) (Vol.2)(Pt.B)	20-40408	See NP-16181(Exh.B)(Vol.2)(Pt.B)
DP–		
1031	20-40375	Dep. nn. CFSTI $3.00 cy, $0.75 mn
1049	20-40456	Dep. nn. CFSTI $2.00 cy, $0.50 mn
1053	20-39017	Dep. nn. CFSTI $2.00 cy, $0.50 mn
1066(Vol.1)	20-39275	Dep. nn. CFSTI $7.00 cy, $1.50 mn
1066(Vol.2)	20-39278	Dep. nn. CFSTI $7.00 cy, $1.25 mn
DP-MS–		
66-46	20-39018	Dep. nn. CFSTI $1.00 cy, $0.50 mn
DUBNA REPORTS	**(Russian)**	
See JINR (Russian)		
EANDC(E)–	**(European-American Nuclear Data Committee)**	
66(U)	20-40069	Dep. nn
ECOM–	**(Non-AEC)**	
01520-3	20-39273	See AD-635198
EFINS–	**(Misc.)**	
66-12	20-39893	See COO-264-304

Report No.	Abstract No.	Availability
66-16	20-39898	See COO-264-306
66-23	20-39802	See COO-264-305
EGG–		
1183-2009	20-39487	Dep. mn. CFSTI $2.00 cy, $0.50 mn
1183-2027	20-39488	Dep. mn. CFSTI $1.00 cy, $0.50 mn
1183-2050	20-39489	Dep. mn. CFSTI $1.00 cy, $0.50 mn
1183-2051	20-39490	Dep. mn. CFSTI $1.00 cy, $0.50 mn
EUR–	**(European Atomic Energy Community)**	
2389	20-40403	See EURAEC-1464
2761.f	20-38589	Dep. mn
2780.e	20-40383	Belgian American Bank and Trust Co., New York, $12.00
2842	20-40356	See EURAEC-1644
2853	20-40384	See EURAEC-1660
2968.e	20-39451	Dep. mn
2981.f	20-39452	Dep. mn
2988.f	20-39355	Dep. mn
2993.d	20-40402	Dep. mn
2997.e	20-39344	Dep. mn
2999.e	20-39201	Dep. mn
3054.e	20-39453	Dep. mn
3055.e	20-39454	Dep. mn
3056.e	20-39455	Dep. mn
EURAEC–		
1464	20-40403	Dep. mn. CFSTI $7.00 cy, $2.25 mn
1626	20-39456	See GEAP-5100-1
1638	20-40382	See CEND-3107-267
1644	20-40356	Dep. mn. CFSTI $4.00 cy, $1.00 mn
1654	20-39356	See GEAP-5134
1656	20-39019	See GEAP-5149
1660	20-40384	Dep. mn. CFSTI $6.00 cy, $1.25 mn
1681	20-39457	See GEAP-5100-9
FTD-TT–	**(Non-AEC)**	
65-1682	20-38603	For translation see AD-629422
GA–	**(Misc.)**	
5781	20-39310	Dep. mn. CFSTI $4.00 cy, $1.00 mn
6511	20-39148	Dep. mn. CFSTI $3.00 cy, $0.75 mn
GEAP–	**(Misc.)**	
4496	20-40404	Dep. mn. CFSTI $6.00 cy, $1.50 mn
4831	20-39345	Dep. mn. CFSTI $4.00 cy, $0.75 mn
4878	20-39393	Dep. mn. CFSTI $1.00 cy, $0.50 mn
5100-1	20-39456	Dep. mn. CFSTI $3.00 cy, $0.75 mn
5100-9	20-39457	Dep. mn. CFSTI $2.00 cy, $0.50 mn
5115	20-39048	Dep. mn. CFSTI $1.00 cy, $0.50 mn
5134	20-39356	Dep. mn. CFSTI $1.00 cy, $0.50 mn
5149	20-39019	Dep. mn. CFSTI $3.00 cy, $0.75 mn
GEMP–	**(Misc.)**	
152	20-40459	Dep. mn. CFSTI $3.00 cy, $0.50 mn
415	20-39394	Dep. mn. CFSTI $3.00 cy, $0.50 mn
HEPL–	**(Misc.)**	
236	20-39750	ORAU
HIT–		
3583-27	20-40405	Dep. mn. CFSTI $2.00 cy, $0.50 mn
HW–		
80056	20-40477	Dep. mn. CFSTI $1.00 cy, $0.50 mn
IA–	**(Non-AEC)**	
1074	20-38938	Dep. mn
IAE–	**(Non-AEC)**	
1028	20-39395	Dep. mn
IAEA–	**(International Atomic Energy Agency)**	
3173-5	20-38708	Dep. mn. CFSTI $1.00 cy, $0.50 mn
IBJ–	**(Polish)**	
See INP		
IC–	**(Misc.)**	
65/90	20-40167	Dep. mn
66/77	20-39850	Dep. mn
66/96	20-39851	Dep. mn
IDO–		
17191	20-40460	Dep. mn. CFSTI $3.00 cy, $0.50 mn
IEA–	**(Brazilian)**	
111	20-40070	Dep. mn.
IFA-PN–	**(Rumanian)**	
17	20-39202	Dep. mn
IFJ–	**(Polish)**	
See INP		
IN–		
1011	20-40478	Dep. mn. CFSTI $2.00 cy, $0.50 mn
INP–	**(Polish)**	
476/PL	20-39203	Dep.
480/PL	20-39852	Dep.
INR–	**(Non-AEC)**	
694/III/PL	20-39204	Dep.
703/III/PL	20-39205	Dep.
INSJ–	**(Japanese)**	
99	20-39206	Dep. mn
IS–		
1126	20-38819	Progr. Nucl. Energy, Ser. IX, 6: 95-146 (1966)
1290	20-38906	J. Phys. Chem., 70: 2450-5(1966)
1291	20-38903	J. Phys. Chem., 70: 2423-9(1966)
1292	20-38905	J. Phys. Chem., 70: 2440-9(1966)
1294	20-38904	J. Phys. Chem., 70: 2430-40(1966)
1306	20-40110	Nucl. Phys., 82: 372-84(1966)
1356	20-38870	Dep. mn. CFSTI $5.00 cy, $1.00 mn
IS-T–		
60	20-39396	Dep. mn. CFSTI $4.00 cy, $0.75 mn
84	20-40013	Dep. mn. CFSTI $4.00 cy, $1.00 mn
ISS–	**(Italian)**	
66/17	20-39169	Dep. mn
66/18	20-39207	Dep. mn
JEN–	**(Spanish)**	
157-DF/I-48	20-39853	Dep. mn
JINR–	**(Russian)**	
E-2738	20-39751	Dep. mn
E-2754	20-39854	Dep. mn
E-2765	20-39752	Dep. mn
E-2771	20-39855	Dep. mn
E-2774	20-40071	Dep. mn
E-2826	20-39856	Dep. mn
E-2827	20-39753	Dep. mn
E-2858	20-39754	Dep. mn
E-2876	20-39857	Dep. mn
P-2705	20-39208	Dep. mn
P-2728	20-39209	Dep. mn
P-2732-1	20-39491	Dep. mn
P-2736	20-39755	Dep. mn
P-2742	20-39756	Dep. mn
P-2745	20-39210	Dep. mn
P-2758	20-39997	Dep. mn
P-2760	20-39858	Dep. mn
P-2761	20-39859	Dep. mn
P-2763	20-39757	Dep. mn
P-2773	20-39758	Dep. mn
P-2776	20-39759	Dep. mn
P-2790	20-39860	Dep. mn
P-2791	20-39577	Dep. mn
P-2802	20-39760	Dep. mn
P-2807	20-39578	Dep. mn
P-2809	20-39761	Dep. mn
P-2811	20-39492	Dep. mn
P-2821	20-39861	Dep. mn
P-2838	20-39579	Dep. mn
P-2842	20-39211	Dep. mn
P-2849	20-39762	Dep. mn
P-2850	20-39763	Dep. mn

Report No.	Abstract No.	Availability
JPL–	**(Non-AEC)**	
32-946	20-39634	
JPRS–	**(Non-AEC)**	
35594	20-38877	CFSTI $1.00 cy, $0.50 mn
K–		
1632(Pt.2)	20-39020	Dep. mn. CFSTI $3.00 cy, $0.75 mn
1665	20-39021	Dep. mn. CFSTI $5.00 cy, $1.00 mn
KAPL–		
3147	20-39998	Dep. mn. CFSTI $6.00 cy, $1.25 mn
KLX–	**(Misc.)**	
1876	20-39287	Dep. mn. CFSTI $2.25 cy, $1.25 mn
LA–		
3362	20-39327	Dep. mn. CFSTI $3.00 cy, $0.75 mn
3453	20-39469	Dep. mn. CFSTI $3.00 cy, $0.75 mn
3488	20-39346	Dep. mn. CFSTI $2.00 cy, $0.50 mn
LA-DC–		
7546	20-39940	Physica, 32: 1001-18(1966)
7747	20-38911	J. Phys. Chem., 70: 2703-5(1966)
7776	20-39493	Dep. mn. CFSTI $1.00 cy, $0.50 mn
7854	20-39242	Phys. Today, 19: No. 7, 79-84(1966)
8019	20-38898	Inorg. Nucl. Chem. Lett., 2: 211-14(1966)
8061	20-40072	Dep. mn. CFSTI $1.00 cy, $0.50 mn
8065	20-40073	Dep. mn. CFSTI $1.00 cy, $0.50 mn
8069	20-40074	Dep. mn. CFSTI $1.00 cy, $0.50 mn
LNF–	**(Italian)**	
66/15	20-39494	Dep. mn
66/22	20-39495	Dep. mn
66/30	20-40075	Dep. mn
MAB–	**(Non-AEC)**	
212A-M	20-39357	CFSTI $1.00 cy, $0.50 mn
MIT–	**(Misc.)**	
2098-235	20-39900	Phys. Rev., 148: 1551-2(1966)
2098-253	20-39811	Phys. Rev., 148: 1542-51(1966)
2098-255	20-40076	Dep. mn. CFSTI $1.00 cy, $0.50 mn
2098-256	20-40077	Dep. mn. CFSTI $1.00 cy, $0.50 mn
2098-257	20-39787	Phys. Lett., 22: 354-7(1966)
MLM–		
1311	20-39320	Dep. mn. CFSTI $2.00 cy, $0.50 mn
1312	20-39321	Dep. mn. CFSTI $2.00 cy, $0.50 mn
MND–	**(Misc.)**	
3264-3	20-39273	See AD-635198
MND-SR–		
2586	20-39311	Dep. mn. CFSTI $2.00 cy, $0.50 mn
MSAR–	**(Misc.)**	
66-150	20-38797	Dep. mn. CFSTI $2.00 cy, $0.50 mn
N–	**(Misc.)**	
66-14700	20-39328	See AD-b24997
66-18175	20-39274	CFSTI $2.00 cy, $0.50 mn
NAA-SR–		
11766	20-40357	Dep. mn. CFSTI $3.00 cy, $0.75 mn
11879	20-40446	Dep. mn. CFSTI $3.00 cy, $0.75 mn
11913	20-40447	Dep. mn. CFSTI $1.00 cy, $0.50 mn
11943	20-39022	Dep. mn. CFSTI $3.00 cy, $0.75 mn
11952	20-39023	Dep. mn. CFSTI $3.00 cy, $0.75 mn
NASA-CR–	**(Misc.)**	
389	20-39274	See N-66-18175
559	20-40168	CFSTI $1.00 cy, $0.50 mn
NASA-SP–	**(Misc.)**	
82	20-40486	GPO $1.50
NASA-TM–	**(Misc.)**	
X-1252	20-39397	CFSTI $1.00 cy, $0.50 mn
NASA-TN–	**(Misc.)**	
D-3527	20-39398	CFSTI $2.00 cy, $0.50 mn
D-3528	20-39399	CFSTI $2.00 cy, $0.50 mn
D-3531	20-39400	CFSTI $1.00 cy, $0.50 mn
D-3552	20-40461	CFSTI $2.00 cy, $0.50 mn
D-3595	20-40169	CFSTI $1.00 cy, $0.50 mn
NDL-TR–	**(Non-AEC)**	
71(Suppl.)	20-39192	See AD-636206
NIJS-R–	**(Yugoslavian)**	
465	20-38798	Dep. mn
474	20-40462	Dep. mn
483	20-38997	Dep. mn
NLCO–		
980	20-38799	Dep. mn. CFSTI $2.00 cy, $0.50 mn
NP–	**(AEC File No. for Non-AEC Reports)**	
16181(Exh.B) (Vol.1)	20-40406	Dep. mn. CFSTI $6.00 cy, $1.50 mn
16181(Exh.B) (Vol.2)(Pt.A)	20-40407	Dep. mn. CFSTI $6.00 cy, $1.25 mn
16181(Exh.B) (Vol.2)(Pt.B)	20-40408	Dep. mn. CFSTI $7.00 cy, $1.50 mn
16203	20-40078	Dep. mn
16217	20-40448	Dep. mn
16225	20-39458	
16229	20-40487	Dep. mn
16230	20-40409	Dep. mn
16232	20-39764	Dep. mn. Inst. of Mathematical Sciences, Madras-20, India $1.00
16239	20-39347	Dept. of Mines and Technical Surveys, Ottawa, $0.50
16242	20-39862	Dep. mn
16251(Vol.1)	20-40410	Dep. mn. CFSTI $7.00 cy, $1.75 mn
16251(Vol.2)	20-40411	Dep. mn. CFSTI $6.00 cy, $1.50 mn
NP-tr–	**(AEC File No. for Non-AEC Translations)**	
1394	20-39214	Dep. mn. CFSTI $1.00 cy, $0.60 mn. JCL $1.60 fs, $0.80 mf
NSJ-tr–	**(Japanese)**	
46	20-39408	Dep. mn. JCL $1.60 fs, $0.80 mf. JAERI
NYO–		
28	20-39149	Dep. mn. CFSTI $4.00 cy, $1.00 mn
NYO–		
918-15	20-38547	Dep. mn. CFSTI $1.00 cy, $0.50 mn
1704-13	20-38735	Dep. mn. CFSTI $3.00 cy, $0.75 mn
1769-54	20-38871	Dep. mn. CFSTI $4.00 cy, $0.75 mn
1769-68	20-38872	Dep. mn. CFSTI $3.00 cy, $0.75 mn
1932-109	20-39810	Phys. Rev., 148: 1520-7(1966)
1932-108	20-39891	Phys. Rev., 148: 1385-1404(1966)
1979-13	20-38590	Dep. mn. CFSTI $2.00 cy, $0.50 mn
2262-112	20-39807	Phys. Rev., 148: 1501-14(1966)
2269-9	20-38873	Dep. mn. CFSTI $4.00 cy, $0.75 mn
2391-31	20-40030	Phys. Lett., 22: 276-7(1966)
2668-13	20-38939	Dep. mn. CFSTI $1.00 cy, $0.50 mn
2753-4	20-39150	Dep. mn. CFSTI $2.00 cy, $0.50 mn
3000-11	20-39428	Platinum Metals Rev., 10: 20-3(1966)
3267-3	20-38745	Dep. mn. CFSTI $1.00 cy, $0.50 mn
3364-19	20-38746	Dep. mn. CFSTI $1.00 cy, $0.50 mn
3410-2	20-38940	Dep. mn. CFSTI $3.00 cy, $0.75 mn
3421-7	20-39212	Dep. mn. CFSTI $1.00 cy, $0.50 mn
3445-7	20-38591	Dep. mn. CFSTI $2.00 cy, $0.50 mn
3449-1	20-38574	Dep. mn. CFSTI $1.00 cy, $0.50 mn
3504-6	20-40295	Appl. Phys. Lett., 9: 171-3(1966)
ORNL–		
3924	20-39470	Dep. mn. CFSTI $5.00 cy, $1.00 mn
3957	20-40488	Dep. mn. CFSTI $2.00 cy, $0.50 mn
3958	20-38998	Dep. mn. CFSTI $3.00 cy, $0.75 mn
3963	20-39401	Dep. mn. CFSTI $2.00 cy, $0.50 mn
3979	20-39402	Dep. mn. CFSTI $2.00 cy, $0.50 mn
3983	20-39358	Dep. mn. CFSTI $2.00 cy, $0.50 mn
3989	20-40170	Dep. mn. CFSTI $5.00 cy, $1.00 mn
ORNL-NSIC–		
17	20-40358	Dep. mn. CFSTI $4.00 cy, $0.75 mn
ORNL-P–	**(Misc.)**	
1081	20-38669	Photochem. Photobiol., 5: 189-200(1966)

Report No.	Abstract No.	Availability
1387	20-39590	J. Catalysis, 5: 218-23(1966)
1542	20-38612	Cancer Res., 26: 1211-20(1966)
1620	20-40023	J. Appl. Phys., 37: 3361-6(1966)
1673	20-38649	Mutat. Res., 3: 237-48(1966)
1674	20-40225	Surface Sci., 4: 234-40(1966)
1764	20-38543	Int. J. Appl. Radiat. Isotop., 17: 417-23 (1966)
1850	20-39221	Health Phys., 12: 1141-2(1966)
2057	20-39366	Weld. J. (N. Y.), 45: 250s-7s(1966)
2158	20-38592	Dep. mn. CFSTI $2.00 cy, $0.50 mn
2175	20-38593	Dep. mn. CFSTI $1.00 cy, $0.50 mn
2197	20-39462	Amer. Soc. Metals, Trans. Quart., 59: 568-70(1966)
2205	20-40185	Appl. Phys. Lett., 9: 77-9(1966)
2267	20-38575	Dep. mn. CFSTI $1.00 cy, $0.50 mn
2277	20-39602	Phys. Rev. Lett., 17: 285-7(1966)
2327	20-40385	Dep. mn. CFSTI $2.00 cy, $0.50 mn
2328	20-40479	Dep. mn. CFSTI $2.00 cy, $0.50 mn
ORNL-TM-		
497	20-40412	Dep. mn. CFSTI $2.00 cy, $0.50 mn
1268	20-39024	Dep. mn. CFSTI $3.00 cy, $0.75 mn
1450	20-39403	Dep. mn. CFSTI $1.00 cy, $0.50 mn
1540	20-38874	Dep. mn. CFSTI $7.00 cy, $1.50 mn
1578	20-39213	Dep. mn. CFSTI $1.00 cy, $0.50 mn
1598	20-40015	Dep. mn. CFSTI $3.00 cy, $0.75 mn
ORNL-tr-		
1257	20-38878	Dep. mn. CFSTI $1.00 cy, $0.50 mn. JCL $1.60 fs, $0.80 mf
ORO-		
636	20-39288	Dep. mn. CFSTI $2.00 cy, $0.50 mn
2066-10	20-38594	Dep. mn. CFSTI $2.00 cy, $0.50 mn
2410-1	20-38548	Dep. mn. CFSTI $2.00 cy, $0.50 mn
2504-91	20-39765	Dep. mn. CFSTI $3.00 cy, $0.75 mn
2980-12	20-39025	Dep. mn. CFSTI $3.00 cy, $0.75 mn
3065-10	20-39766	Dep. mn. CFSTI $1.00 cy, $0.50 mn
3295-2	20-38595	Dep. mn. CFSTI $1.00 cy, $0.50 mn
3346-2	20-40079	Dep. mn. CFSTI $1.00 cy, $0.50 mn
3346-3	20-40080	Dep. mn. CFSTI $1.00 cy, $0.50 mn
PAEC(C)RE-	**(Philippines)**	
652	20-38800	Dep. mn
PAEC(D)IS-	**(Philippines)**	
652	20-38982	Dep. mn
653	20-40081	Dep. mn
PAN-	**(Polish)**	**(This series of reports was terminated in 1965. Subsequent reports are identified by the code INR)**
PATENTS	**(British)**	**(4s. 6d. each, U. K. Patent Office)**
1,033,143	20-39376	
1,033,201	20-39368	
1,033,207	20-39369	
1,033,223	20-39342	
1,033,246	20-39377	
1,033,391	20-39343	
1,033,393	20-40395	
1,033,641	20-40365	
1,034,227	20-39443	
1,034,424	20-39444	
1,034,654	20-39370	
1,035,057	20-39040	
1,035,087	20-40396	
1,035,116	20-39296	
1,035,129	20-40366	
1,035,134	20-40367	
1,035,480	20-39249	
1,035,487	20-40397	
PATENTS	**(Canadian)**	
735,586	20-39350	
PATENTS	**(Japanese)**	
1965-9966	20-38977	
1965-17150	20-38978	
1965-17662	20-38979	
1965-18430	20-38980	
1965-19192	20-38981	
PATENTS	**(U. S.)**	**($0.50 each, U. S. Patent Office)**
3,252,916	20-38993	
3,253,152	20-39371	
3,253,191	20-39372	
3,254,485	20-39013	
3,254,939	20-38975	
3,254,949	20-38929	
3,255,083	20-40368	
3,255,084	20-40432	
3,255,085	20-40369	
3,255,088	20-40433	
3,256,732	20-39012	
3,257,009	20-39041	
3,257,285	20-40434	
3,257,286	20-40370	
3,257,287	20-40371	
3,257,557	20-39137	
3,257,558	20-39250	
3,257,561	20-39042	
3,258,317	20-39373	
3,258,402	20-39509	
3,258,403	20-40372	
3,258,404	20-38972	
3,258,405	20-40435	
3,258,412	20-38974	
3,258,593	20-39136	
3,261,696	20-39375	
3,262,882	20-38973	
3,263,077	20-39189	
3,263,080	20-39251	
3,263,081	20-39252	
3,263,083	20-39139	
3,263,415	20-39095	
3,264,147	20-39374	
3,264,202	20-38976	
3,264,219	20-39351	
3,264,224	20-39341	
3,264,477	20-39138	
3,264,501	20-39043	
3,265,540	20-39441	
3,265,626	20-39442	
3,265,893	20-39140	
3,265,894	20-39190	
3,265,897	20-39044	
3,265,910	20-39637	
3,265,918	20-39039	
3,266,203	20-39053	
3,266,890	20-39440	
3,266,892	20-39445	
3,267,282	20-39191	
PG-Report-	**(British)**	
729	20-38801	Dep. BIS $0.30. HMSO 1s. 3d.
PPAD-		
589-E	20-39794	Phys. Rev., 148: 1315-26(1966)
PUC-		
937-208	20-39901	Phys. Rev., 148: 1553-5(1966)
R-	**(Misc.)**	
3	20-40181	See TID-23307
183	20-39347	See NP-16239
463	20-39007	See AD-636914
RHEL/R-	**(British)**	
117	20-39496	Dep. mn. BIS $2.60. HMSO 13s.
RISO-	**(Danish)**	
113	20-39359	Dep. mn
RISO-M-	**(Danish)**	
423	20-39170	Dep. mn
RRL-		
2310-182	20-38941	Dep. mn. CFSTI $1.00 cy, $0.50 mn
SAN-		
590-1	20-38596	Dep. mn. CFSTI $1.00 cy, $0.50 mn
650-1	20-40449	Dep. mn. CFSTI $2.00 cy, $0.50 mn

Report No.	Abstract No.	Availability
SC-CR-		
66-2044	20-39312	Dep. mn. CFSTI $6.00 cy, $1.25 mn
SC-DC-		
66-1118	20-40489	Dep. mn. CFSTI $3.00 cy, $0.75 mn
SGAE-CH-	(Austrian)	
33/1966	20-40386	Dep. mn
SGAE-SS-	(Austrian)	
3/1966	20-38983	Dep. mn
SIT-	(Misc.)	
187	20-40178	See SIT-2582-19
2582-19	20-40178	Dep. mn. CFSTI $6.00 cy, $1.25 mn
SLAC-		
65	20-39497	Dep. mn. CFSTI $3.00 cy, $0.75 mn
SLAC-PUB-		
165	20-39896	Phys. Rev., 148: 1467-78(1966)
169	20-39804	Phys. Rev., 148: 1452-67(1966)
SM-	(Misc.)	
72/3	20-40479	See ORNL-P-2328
STI-PUB-	(International Atomic Energy Agency)	
119	20-40480	IAEA: $2.00; S42.-; 12/-stg; F Fr 8,-; DM 6,40
SU-IPR-	(Misc.)	
49	20-40179	Dep. mn. CFSTI $6.00 cy, $1.25 mn
69	20-40180	Dep. mn. CFSTI $2.00 cy, $0.50 mn
SWRI-		
1228-4-20	20-39404	Dep. mn. CFSTI $3.00 cy, $0.75 mn
1228-8-24	20-39008	Dep. mn. CFSTI $2.00 cy, $0.50 mn
TID-		
8200(13th Rev.)	20-40359	Dep. mn. CFSTI $1.00 cy, $0.50 mn
21529	20-38821	Progr. Nucl. Energy, Ser. IX, 6: 181-211 (1966)
22103	20-38576	Dep. mn. CFSTI $1.00 cy, $0.50 mn
22724	20-40112	Nucl. Phys., 86: 509-27(1966)
22761	20-40333	Solid-State Electron., 9: 615-17(1966)
22933	20-40119	Nucl. Phys., 86: 611-24(1966)
22955	20-38598	Dep. mn. CFSTI $1.00 cy, $0.50 mn
22968	20-38599	Dep. mn. CFSTI $3.00 cy, $0.50 mn
23034	20-38600	Dep. mn. CFSTI $1.00 cy, $0.50 mn
23057	20-38597	Dep. mn. CFSTI $1.00 cy, $0.50 mn
23184	20-39014	Dep. mn. CFSTI $1.00 cy, $0.50 mn
23229	20-38999	Dep. mn. CFSTI $1.00 cy, $0.50 mn
23257(Vol.1)	20-40413	Dep. mn. CFSTI $4.00 cy, $1.00 mn
23257(Vol.2)	20-40414	Dep. mn. CFSTI $2.00 cy, $0.50 mn
23257(Vol.3)	20-40415	Dep. mn. CFSTI $2.00 cy, $0.50 mn
23264	20-38930	Dep. mn. CFSTI $5.00 cy, $1.00 mn
23278	20-39767	Dep. mn. CFSTI $1.00 cy, $0.50 mn
23307	20-40181	Dep.
TIM-	(Misc.)	
911	20-40450	Dep. mn. CFSTI $2.00 cy, $0.50 mn
TRG-Report-	(British)	
1255	20-39360	Dep. BIS $0.30. HMSO 1s. 9d.
1278	20-39459	Dep. mn
TT-	(Canadian)	
66-32029	20-38877	See JPRS-35594
UCD-		
34P73-9	20-39289	Dep. mn. CFSTI $1.00 cy, $0.50 mn
UCD-CNL-		
45	20-40114	Nucl. Phys., 86: 535-44(1966)
UCLA-		
12-567	20-38601	Dep. mn. CFSTI $1.00 cy, $0.50 mn
12-592	20-38549	Dep. mn. CFSTI $1.00 cy, $0.50 mn
34P60-1	20-38602	Dep. mn. CFSTI $3.00 cy, $0.75 mn
UCRL-		
11100(Rev.1)	20-39768	Dep. mn. CFSTI $2.00 cy, $0.50 mn
14413	20-40463	Dep. mn. CFSTI $2.00 cy, $0.50 mn
14571-T	20-38909	J. Phys. Chem., 70: 2639-5(1966)
14579(Rev.1)	20-39423	J. Phys. Chem. Solids, 27: 1201-4(1966)
14660(Rev.1)	20-39026	Dep. mn. CFSTI $1.00 cy, $0.50 mn
14700	20-39107	Dep. mn. CFSTI $2.00 cy, $0.50 mn
14703-T	20-38875	Dep. mn. CFSTI $1.00 cy, $0.50 mn
14754	20-39049	Dep. mn. CFSTI $5.00 cy, $1.00 mn
14877	20-39015	Dep. mn. CFSTI $2.00 cy, $0.50 mn
14944	20-39009	Dep. mn. CFSTI $1.00 cy, $0.50 mn
16535	20-39050	Dep. mn. CFSTI $6.00 cy, $1.25 mn
16597	20-39806	Phys. Rev., 148: 1491-1501(1966)
16655	20-39769	Dep. mn. CFSTI $3.00 cy, $0.75 mn
16699	20-39635	Dep. mn. CFSTI $3.00 cy, $0.50 mn
16720	20-39789	Phys. Rev., 148: 1280-1(1966)
16749	20-39791	Phys. Rev., 148: 1289-96(1966)
16750	20-39792	Phys. Rev., 148: 1297-1302(1966)
16788	20-39770	Dep. mn. CFSTI $4.00 cy, $0.75 mn
16809	20-39498	Dep. mn. CFSTI $1.00 cy, $0.50 mn
16844	20-39405	Dep. mn. CFSTI $2.00 cy, $0.50 mn
16923	20-39771	Dep. mn. CFSTI $2.00 cy, $0.50 mn
16959	20-39499	Dep. mn. CFSTI $2.00 cy, $0.50 mn
17007	20-39772	Dep. mn. CFSTI $3.00 cy, $0.50 mn
UCRL-Trans-		
1325	20-38879	Dep. mn. CFSTI $1.00 cy, $0.50 mn. JCL $1.10 fs, $0.80 mf
10029	20-38542	Dep. mn. CFSTI $3.00 cy, $0.75 mn. JCL $8.60 fs, $3.02 mf
10044	20-39331	Dep. mn. CFSTI $2.00 cy, $0.50 mn. JCL $2.60 fs, $1.10 mf
UCSD-		
34P84-2	20-39133	Progr. Oceanogr., 3: 173-7(1965)
UJV-	(Czechoslovakian)	
1180/64	20-40464	Dep. mn
1181/64	20-40465	Dep. mn
1457	20-38942	Dep. mn
1598	20-38876	Dep. mn
USNRDL-TR-	(Misc.)	
1034	20-39193	See AD-636736
WAPD-	(Misc.)	
305	20-39361	Dep. mn. CFSTI $3.00 cy, $0.50 mn
WAPD-T-		
1851	20-40481	Dep. mn. CFSTI $2.00 cy, $0.50 mn
1864	20-39406	Dep. mn. CFSTI $1.00 cy, $0.50 mn
1890	20-40360	Dep. mn. CFSTI $2.00 cy, $0.50 mn
1939	20-40387	Dep. mn. CFSTI $2.00 cy, $0.50 mn
WAPD-TM-	(Misc.)	
514(Add.1)	20-39460	Dep. mn. CFSTI $1.00 cy, $0.50 mn
577	20-39362	Dep. mn. CFSTI $3.00 cy, $0.50 mn
WCAP-	(Misc.)	
2222-P	20-40416	Dep. mn. CFSTI $4.00 cy, $0.75 mn
6074	20-39461	Dep. mn. CFSTI $3.00 cy, $0.50 mn
WERL-	(Misc.)	
2823-21	20-39098	Dep. mn. CFSTI $3.00 cy, $0.50 mn
WWO-	(Misc.)	
16-R92	20-40356	See EURAEC-1644
Y-		
1483	20-40490	Dep. mn. CFSTI $4.00 cy, $0.75 mn
Y-DA-		
1287	20-39027	Dep. mn. CFSTI $1.00 cy, $0.50 mn

DEPOSITORIES OF USAEC REPORTS

In Countries Other than the U.S.

ARGENTINA
Buenos Aires, Comisión Nacional de Energía Atómica
AUSTRALIA
Canberra, Australian National Library
Sutherland, New South Wales, Australian Atomic Energy Commission
AUSTRIA
Vienna, Zentral Bibliothek der Physikalischen Institute der Universität
BELGIUM
Mol-Donk, Centre d'Etude de l'Energie Nucleaire
BOLIVIA
La Paz, Comisión Nacional de Energía Nuclear
BRAZIL
Rio de Janeiro, Instituto Brasileiro de Bibliografia e Documentacao
São Paulo, Instituto de Energia Atomica, Cidade Universitaria São Paulo
BURMA
Rangoon, Union of Burma Applied Research Institute, Atomic Energy Center Library
CANADA
Hamilton, McMaster University
Ottawa, National Research Council Library
Vancouver, University of British Columbia
CHILE
Santiago, Departamento de Fisica, Universidad de Chile
CHINA
Hsinchu, Taiwan, Free China, National Tsing Hua University
COLOMBIA
Bogota, Instituto De Asuntos Nucleares
COSTA RICA
San Pedro, University of Costa Rica Library
DENMARK
Risö, Danish Atomic Energy Commission
ECUADOR
Quito, Escuela Politécnica Nacional
EL SALVADOR
San Salvador, Universidad de El Salvador, Biblioteca de Energia Nuclear
FINLAND
Helsinki, Teknillisen Korkeakoulun Kirjasto
FRANCE
Gif-sur-Yvette, Centre d'Etudes Nucléaires de Saclay
Paris, Académie des Sciences
GERMANY
Berlin, Hahn-Meitner-Institut für Kernforschung Berlin
Frankfurt/Main, Gmelin-Institut
Munich, Technische Hochschule, Bibliothek
GHANA
Accra, University College of Ghana
GREECE
Athens, Nuclear Research Center "Democritus"
GUATEMALA
Guatemala, Comisión Nacional de Energía Nuclear
INDIA
Bombay, Department of Atomic Energy
IRAN
Tehran, Tehran University Nuclear Centre
IRAQ
Baghdad, Iraqi Atomic Energy Commission
IRELAND
Dublin, University College
ISRAEL
Rehovoth, Israel Atomic Energy Commission
ITALY
Rome, Centro di Studi Nucleari della Casaccia
Rome, Comitato Nazionale per l'Energia Nucleare
JAPAN
Tokyo, National Diet Library
KOREA
Seoul, Office of Atomic Energy
LEBANON
Beirut, Lebanese National Council for Scientific Research
LUXEMBOURG
Luxembourg, Ministry of Transport and Electricity
MALAYSIA
Kuala Lumpur, University of Malaysia
MEXICO
Mexico, D.F., Comisión Nacional de Energía Nuclear
NETHERLANDS
The Hague, Reactor Centrum Nederland
NEW ZEALAND
Lower Hutt, Institute of Nuclear Sciences
NIGERIA
Ibadan, University of Ibadan
NORWAY
Lillestrøm, Institutt för Atomenergi
PAKISTAN
Lahore, West Pakistan, Atomic Energy Centre
PERU
Lima, Junta de Control de Energia Atomica
PHILIPPINE REPUBLIC
Manila, Philippine Atomic Energy Commission
POLAND
Warsaw, Biura Pelnomocnika Rzadu do Spraw Wykorzystania Energii Jadrowej
PORTUGAL
Sacavem, Junta de Energía Nuclear
REPUBLIC OF SOUTH AFRICA
Pretoria, Atomic Energy Board Library
REPUBLIC OF THE CONGO
Leopoldville, Université Lovanium
SPAIN
Madrid, Junta de Energía Nuclear, Biblioteca Documentación y Publicaciones, Ciudad Universitaria
SWEDEN
Nyköping, Aktiebolaget Atomenergi
SWITZERLAND
Zürich, Eidgenössische Technische Hochschule, Bibliothek
THAILAND
Bangkok, Office of the Thai Atomic Energy Commission, Department of Science
TURKEY
Ankara, Turkish Atomic Energy Commission, Atomic Energy Library
UNITED ARAB REPUBLIC
Cairo, Atomic Energy Commission
UNITED KINGDOM
Birmingham, Central Library
Boston Spa, National Lending Library for Science and Technology
Kingston upon Hull, Central Library
Liverpool, Central Library
London, Central Library, Acton
London, National Reference Library
London, Science Museum Library, South Kensington
Manchester, Central Library
Newcastle upon Tyne, Central Library
Nottingham, Central Library
Sheffield, Central Library
URUGUAY
Montevideo, Comision Nacional de Energia Atomica
VENEZUELA
Ceracas, Instituto Venezolano de Investigaciones Científicas
VIET-NAM
Saigon, Atomic Energy Office
YUGOSLAVIA
Belgrade, Federal Commission for Nuclear Energy

In International Agencies

AUSTRIA
Vienna, International Atomic Energy Agency
BELGIUM
Brussels, La Bibliotheque EURATOM
FRANCE
Paris, European Nuclear Energy Agency, O.E.C.D.
ITALY
Ispra, EURATOM Research Center
SWITZERLAND
Geneva, United Nations Library

UNITED STATES
GOVERNMENT PRINTING OFFICE
DIVISION OF PUBLIC DOCUMENTS
WASHINGTON, D.C. 20402

OFFICIAL BUSINESS

POSTAGE AND FEES PAID
U.S. GOVERNMENT PRINTING OFFICE

TECHNICAL PROGRESS REVIEWS

The Division of Technical Information, U. S. Atomic Energy Commission, also publishes the Technical Progress Reviews, a series of four quarterly journals on nuclear technology. These journals, compiled by specialists and recognized authorities, summarize, evaluate, and reference the progress of development in four important fields.

Isotopes and Radiation Technology P. S. Baker, A. F. Rupp, and associates, Oak Ridge National Laboratory. Reviews AEC-sponsored projects and related significant worldwide developments in radioisotopes and radiation technology.

Nuclear Safety Wm. B. Cottrell, W. H. Jordan, J. P. Blakely, and associates, Nuclear Safety Information Center, Oak Ridge National Laboratory. Covers topics relevant to the analysis and control of hazards associated with nuclear reactors and with operations involving fissionable materials and the products of nuclear fission.

Power Reactor Technology Argonne National Laboratory. Reviews research, development, design practices, and operating experiences associated with power reactors, including aerospace applications.

Reactor Materials E. M. Simons and associates, Battelle Memorial Institute. Covers the properties, behavior, and fabrication processes of materials used in nuclear reactors and associated equipment.

Availability

SUBSCRIPTION RATE: The Technical Progress Reviews may be purchased from the Superintendent of Documents, U. S. Government Printing Office, Washington, D. C. 20402. *Nuclear Safety* at $3.00 per year for each subscription or $1.00 per issue; each of the other journals at $2.50 per year or $0.70 per issue.

POSTAGE: Postpaid within the United States, Canada, Mexico, and all Central and South American countries except Argentina, Brazil, Guyana, French Guiana, Surinam, and British Honduras. For these Central and South American countries and all other countries, add $0.75 for each annual subscription or $0.20 for a single issue.

REMITTANCE: Payment should be by check, money order, or document coupons and MUST accompany order. Remittances from foreign countries should be made by international money order or draft on an American bank payable to the Superintendent of Documents or by UNESCO book coupons.